american society for mass spectrometry

29th

ANNUAL CONFERENCE ON MASS SPECTROMETRY AND ALLIED TOPICS

ABSTRACTS

May 24–29, 1981
Minneapolis

american society for mass spectrometry

29th

ANNUAL CONFERENCE ON MASS SPECTROMETRY AND ALLIED TOPICS

May 24 - 29, 1981
Radisson Downtown Hotel
Minneapolis, Minnesota

TABLE OF CONTENTS

CITATION NOTICE

INTRODUCTION

The "Bound Volume" of ASMS is the official record of the society, containing not only the abstracts of papers presented at the Annual Conference on Mass Spectrometry and Allied Topics, but also reports of workshops, standing and ad hoc committees, special reports (such as the Salary Survey which appears in this volume), minutes of business meetings and other matters of interest to the membership. There having been no substantive changes in the Constitution and By-Laws of ASMS, these are not reproduced in the present volume; they appear in the 1980 Bound Volume.

As retiring editor, I want to thank all the contributors for the care that went into preparing their abstracts and for adherence to the deadlines. Particular thanks are due Henry Fales, Secretary of the Society, and the committee and workshop chairpersons, whose reports had to be prepared in the very short time between the end of the ASMS meeting and press deadline.

Special thanks go to ASTM, and particularly Robert Meltzer and Bruce Vieth, which for the second year is handling the printing and distribution of the Bound Volume, after having done such a fantastically fine job with the 1980 volume.

The deepest expression of gratitude, however, is reserved for Mrs. Judith Watson of the newly formed ASMS office. It was she who, for the first time, assembled the many contributions and added the remaining items needed to transform huge stacks of separate sheets of paper into the volume you are now reading. With Judith doing so much and doing it so well, the job of Editor this year became downright easy.

Wade L. Fite, Editor

The American Society for Mass Spectrometry

President	Burnaby Munson, Department of Chemistry, University of Delaware, Newark, DE 19711
Vice President (Programs)	Catherine C. Fenselau, Department of Pharmacology, Johns Hopkins University, 725 N. Wolfe Street, Baltimore, MD 21205
Vice President (Arrangements)	W. Alan Wolstenholme, VG Instruments, 13840 West Oak Glen Road, Valley Center, CA 92082
Secretary	Henry M. Fales, National Institutes of Health, Building 10, Room 7N322, Bethesda, MD 20205
Treasurer	Margaret A. Frisch, IBM, Thomas J. Watson Research Center, PO Box 218, Yorktown Heights, NY 10598
Chairman ASTM E-14	Mynard Hamming, Conoco, Inc., Research and Development, Ponca City, OK 74601
Directors-at-Large	Wade L. Fite, Extranuclear Laboratories, Inc., PO Box 11512, Pittsburgh, PA 15238
	J. Throck Watson, Department of Biochemistry, Michigan State University, East Lansing, MI 48824
Past President	James A. McCloskey, Department of Medicinal Chemistry, University of Utah, Salt Lake City, UT 84112
ASMS Office	Judith Watson, PO Box 1508, East Lansing, MI 48823

The American Society for Mass Spectrometry is grateful to the following corporate members and sponsors for their support of the 1980 Conference.

BALZERS
8 Sagamore Park Road
Hudson, NH 03051
*Dr. Philip Irving

R. J. BRUNFELDT CO.
P. O. Box 3636
Bartlesville, OK 74003

COMMERCIAL TESTING/ENGINEERING
490 Orchard Street
Golden, CO 80401
*Mr. M. L. Jacobs

CORNELL UNIVERSITY
G-24 Uris Hall
Ithaca, NY 14853
*Mr. Dan Bartholomew

CVC, INC.
525 Lee Road
P. O. Box 1886
Rochester, NY 14603
*Mr. Larry Gilbert

EXTRANUCLEAR LABORATORIES, INC.
100 Beta Drive
P. O. Box 11512
Pittsburgh, PA 15238
*Mr. Michael McKeown

FINNIGAN CORPORATION
845 West Maude Avenue
Sunnyvale, CA 94086
*Mr. Michael Story

FINNIGAN INSTITUTE
11 Triangle Park Drive
Cincinnati, OH 45246
*Dr. Don DeJongh

GALILEO ELECTRO-OPTICS
Galileo Park
Sturbridge, MA 01518
*Mr. P. W. Graves

HEWLETT PACKARD
1601 California Avenue
Palo Alto, CA 94304
*Dr. James Serum

HEYDEN & SON, INC.
247 South 41st Street
Philadelphia, PA 19104
*Mr. Joel Packman

INFICON LEYBOLD-HERAUS
6500 Fly Road
East Syracuse, NY 13057
*Mr. Russ Carr

JEOL, LTD/USA
235 Birchwood Avenue
Cranford, NJ 07016
*Mr. R. S. Martin

KOR ISOTOPES, INC.
56 Rogers Street
Cambridge, MA 02142
*Mr. Joel Bradley

KRATOS SCIENTIFIC INSTRUMENTS
24 Booker Street
Westwood, NJ 07675
*Mr. C. H. Benney

MERCK & CO./ISOTOPES
P. O. Box 2000
Rahway, NJ 07065
*Dr. S. P. Manrao

NIH/EPA CIS
EPA, PM-218
Washington, DC 20460
*Dr. Steve Heller

NICOLET INSTRUMENT CORPORATION
5225 Verona Road
Madison, WI 53711
*Mr. J. J. Christenson

NUCLIDE CORPORATION
642 East College Avenue
State College, PA 16801
*Mr. L. F. Herzog

PERGAMON PRESS
Maxwell House
Pairview Park
Elmsford, NY 10523
*Ms. Dawn Cusumano

PERNICKA CORPORATION
450 East Middlefield Road
Mountain View, CA 94043
*Mr. J. C. Pernicka

RDS/NERMAG, INC.
3064 Scott Blvd.
Santa Clara, CA 95050
*Mr. David Sparkman

SCIENTIFIC GLASS ENGINEERING
2007 Kramer Lane
Austin, TX 78758
*Mr. K. O. Mahler

SCIEX, INC.
55 Glencameron Road, Suite 202
Thornhill, Ontario L3T 1P2
CANADA
*Dr. A. Lovett

SHRADER ANALYTICAL LABORATORIES
3450 Lovett Avenue
Detroit, MI 48210
Dr. S. R. Shrader

TEKNIVENT CORPORATION
10774 Trenton Avenue
St. Louis, MO 63132
*Mr. P. F. Berger

UTI INSTRUMENTS CO.
325 North Mathilda Avenue
Sunnyvale, CA 94086
*Mr. S. Dahle-Fuller

VACUMETRICS, INC.
2261 Palma Drive
Ventura, CA 93003
*Mr. G. Peele

VG INSTRUMENTS
58 Buckingham Drive
Stamford, CT 06902
*Mr. G. L. Kearns

*Representative

PROCEEDINGS OF THE TWENTY-NINTH ANNUAL CONFERENCE

PLENARY LECTURES

INTRODUCTORY LECTURE

GAS CHROMATOGRAPHY/MASS SPECTROMETRY

ION MOLECULE REACTIONS/DYNAMICS & STRUCTURES OF IONS

INSTRUMENTAL TECHNIQUES

BIOMEDICAL AND FORENSIC APPLICATIONS

INDUCTIVELY COUPLED PLASMA MS/INSTRUMENT DESIGN

MASS SPECTROMETRY/MASS SPECTROMETRY

POSITIVE AND NEGATIVE CHEMICAL IONIZATION

DYNAMICS AND STRUCTURES OF GASEOUS IONS

BIOCHEMISTRY

PLENARY LECTURE

THE ISOTOPIC RECORD OF PRECAMBRIAN EVOLUTION; J. M. Hayes; Biogeochemical Laboratories, Depts. Chem. and Geol., Indiana University, Bloomington, IN 47405.

When did life first arise on Earth and how did the various levels of organizational and biochemical complexity subsequently develop? Microfossils and other morphological remains have always seemed to provide the best evidence bearing on the first question (which cannot, in any case, be answered with precision because of the fragmentary nature of the most ancient sedimentary records). If the second question is to be explored, however, chemical evidence must be defined, because one microbe looks much like another after billions of years of burial. It now appears that no significant molecular structures have survived in rocks older than 2.5 billion years, but that substantial and biochemically significant variations in the $^{13}C/^{12}C$ ratios of sedimentary organic materials can be observed in that time interval. While not yet fully interpretable, these variations are consistent with (i) the existence of autotrophs 3.5 billion years before the present, (ii) an early carbon cycle in which methanogens functioned as the only recyclers on an anaerobic earth, and (iii) the subsequent development of aerobiosis more than 600 million years after the first appearance of microfossils. (Work performed at UCLA with J. W. Schopf and other members of the Precambrian Paleobiology Research Group, 1979-1980.)

PLENARY LECTURE

LASER MULTIPHOTON IONIZATION: WRITING AN OPTICAL SIGNATURE ON MASS SPECTROMETRY; RICHARD N. ZARE; Department of Chemistry, Stanford University, Stanford, CA. 94305.

Traditional light sources are so weak that the interaction of radiation with matter usually involves single-photon processes, e.g., absorption or emission. Pulsed laser light sources are so strong that multiple photon processes often readily occur, presenting experimentalists with many novel and exotic phenomena. Multiphoton absorption of infrared light by polyatomic molecules leads to dissociation while multiphoton absorption of visible or ultraviolet light leads to ionization. The latter possibility can serve as an alternative ion source for mass spectrometry with the advantages of high inherent sensitivity and selectivity. Laser multiphoton ionization (MPI) can be used to detect single atoms, to differentiate between isotropic and isomeric species, and to determine structural information on and fragmentation kinetics of excited intermediate states seldom accessible to study by other means. Indeed, MPI may be the "poor man's synchrotron source" for photoionization studies. A general review will be presented of the rapid progress being made in this new field of inquiry.

INTRODUCTORY LECTURE

BASICS OF HYDROGEN REARRANGEMENTS IN ELECTRON IMPACT MASS SPECTRA

Maurice M. Bursey

Department of Chemistry 045 A, University of North Carolina at Chapel Hill,

Chapel Hill, North Carolina 27514

First, to gain an appreciation of where to expect rearrangements, it is important to consider two comparisons of simple cleavages and rearrangements as chemical reactions:

> Because bonds are formed as well as broken in rearrangements, but only broken in simple cleavages, rearrangements cost less energy than cleavages.
>
> Because the two reacting centers have to be brought near each other in rearrangements, rearrangements cost more order (in the activated complex) than cleavages.

So, in general, the appearance potentials of rearrangement reactions are lower than those of simple cleavages (provided there are no complications from symmetry) and, because of the constraints on achieving the activated complex, the ultimate maximum rates for rearrangements -- those achieved at very high energies -- are lower than those for simple cleavages. Therefore there are energy regions where the rates of rearrangements are as fast as, or even faster than, those of simple cleavages: those of low energy (low voltage electron impact, chemical ionization, etc.). There are also conditions of sampling high-energy ions where the rates of rearrangements are so slow relative to those of simple cleavages that they are suppressed (the short-time end of field ionization kinetics, collisional activation). Rearrangements are more competitive with simple cleavages at low internal energies.

Second, rearrangements of hydrogen can be divided into two categories: random rearrangements and specific rearrangements. Random rearrangements most commonly occur in hydrocarbon ions: molecular ions of alkanes and alkenes, and alkyl ions, for example. The origin of scrambling in alkane molecular ions is rooted in the energy of different ion structures. Ethane, with 18 electrons, and diborane, with 16 electrons, have quite different structures; ethane molecular ion, with 17 electrons, has a low-energy excited state of the diborane form, and passing through this form before fragmentation leads to hydrogen scrambling. At least one alkene scrambling mechanism consists of sequential 1,3 hydrogen shifts: the loss of C_2H_4 by a retro-Diels-Alder process of the molecular ion of cyclohexene has been studied at different times after ionization and the formation of different labeled products from a labeled precursor is consistent with this mechanism. These ions, and also alkyl ions, may also scramble by carbon skeletal rearrangements in some cases. The scrambling is most important in the smaller ions in each series.

There are many examples of well understood specific rearrangements. Those mentioned are the McLafferty rearrangement and the elimination of H_2O and HX from alcohols and alkyl halides respectively. The γ hydrogen transfer of the McLafferty rearrangement occurs before the cleavage of the β bond in at least one case, and radical site stability thus explains why secondary H is transferred 10 times faster than primary H. The hydrogen to be transferred must also be no more than 1.8 Å distant from the ketone oxygen, nor more than about 50° above the carbonyl system plane. The preferred geometry for loss of water is also a six-membered ring. In such rings there is a stereochemical preference for loss of water through a chair conformation of the six atoms. In some cyclic systems stereochemical specificity ordains the intermediacy of a boat form for selection of the 4-hydrogen or a hydrogen of a 4-substituent of a 4-alkylcyclohexanol. Loss of HX often passes through a five-membered ring, and some stereospecificity is preserved; when the selectivity is compared to the selectivity of five-membered ring water loss (rare), they are similar.

CURRENT DEVELOPMENT IN TRIPLE STAGE QUADRUPOLE GC/MS/MS/DS; MICHAEL S. STORY, URS STEINER, CHARLES A. BOITNOTT, STEVE SOKOLOW, MARK WEISS and JOHN R.B. SLAYBACK; Finnigan Corporation, 845 W. Maude Ave., Sunnyvale, California 94086

In this paper, we will report on recent advancements in the design and development of a triple stage quadrupole (TSQ) mass spectrometer/data system.
The TSQ hardware consists of a gas chromatograph, an electron impact/chemical ionization source (EI/CI), three tandem quadrupoles, turbomolecular vacuum pumps, dual/independent pulsed positive ion-negative chemical ionization modules, a multiplexer control assembly and a complete interactive data system.
To meet the complexities of TSQ instrument control and data processing, the data system provides convenient, interactive control of all instrument configurations and mass scanning modes during real time operation. This allows the chemist to define a sequence of experiments that will cycle automatically during the acquisition of data, thus maximizing the information obtained from a single sample analysis. The data system also senses analog input values, labels printer and CRT outputs according to the experiment and sorts data which have been acquired from multi-configurational analyses. The unit mass resolution provdied by tandem quadrupole operation allows use of conventional software programs to interpret GC/MS/MS or MS/MS data.

GAS CHROMATOGRAPHY-FOURIER TRANSFORM MASS SPECTROMETRY (GC/FTMS)

ROBERT L. WHITE, E. B. LEDFORD, Jr., C. L. WILKINS, and M. L. GROSS, Department of Chemistry, University of Nebraska, Lincoln, NE 68588

GC/MS/COM systems have greatly simplified the task of multicomponent mixture analysis and have become an important tool for the analytical chemist. It is therefore important to consider the implementation of GC/MS/COM in the evaluation of the analytical capabilities of Fourier Transform Mass Spectrometry (FTMS). Preliminary experiments indicate that GC/FTMS/COM is feasible and may be applicable to complex mixture analysis.[1]

The basic operation of a Fourier Transform Mass Spectrometer is quite different from that of conventional mass spectrometers. In FTMS, ion formation and detection are performed within the same region of the spectrometer. Ion detection is accomplished by applying a radio frequency sweep to opposing sides of the analyzer cell in such a way as to excite the cyclotron motion of ions having resonant frequencies within the bandwidth of the sweep. The excited motion is observed as a damped oscillating voltage on the receiver plates of the analyzer cell. Fourier transformation of the time domain signal results in a frequency spectrum which can then be related to the mass spectrum of the material inside the analyzer cell. Signal damping in FTMS is a consequence of excited ions colliding with neutral molecules within the analyzer cell. This occurance must be minimized in order to obtain high resolution mass data since resolution is directly related to the number of cyclotron orbits that ions are allowed to complete. For GC/FTMS, a separator interface between the gas chromatograph and the analyzer cell is necessary in order to reduce the pressure in the cell to a tolerable level. In the present system, a jet separator is used for the GC interface and pressures as low as 5×10^{-8} torr have been attained at the analyzer cell. At this pressure, a mass resolution of 20,000 (defined as the full width at half peak height) at m/z 156 can routinely be achieved.

In addition to high resolution mass analysis, chemical ionization mass spectra for capillary column eluents can also be obtained using FTMS. By introducing a suitable CI reagent gas into the spectrometer and allowing ion-molecule reactions to occur prior to ion detection, it is possible to obtain a mixed CI/EI mass spectrum of a small quantity of sample material. Because CI reagent pressures are usually only 10-100 times higher than those of samples, some EI components of the sample will often be seen among the CI peaks.

[1] E. B. Ledford, Jr., R. L. White, S. Ghaderi, C. L. Wilkins, and M. L. Gross, Anal Chem, 52, pp 2450-2451 (1980).

Peak switching over large mass ranges can be performed in FTMS by simply changing the radio frequency sweep characteristics in such a way as to detect only selected ions from the total mass spectrum. Preliminary GC/FTMS peak switching results indicate that it is possible to switch from m/z 78 from benzene to m/z 156 from bromobenzene in 300 ms at a mass resolution of 20,000 using a SCOT capillary column. The 300 ms scan times were more than sufficient to provide GC peak profiles for the eluting components.

Evaluation of GC/FTMS sensitivity was accomplished by monitoring m/z 78 from benzene while injecting diminishing quantities of benzene into the gas chromatograph. Figure 1 illustrates the sensitivity of GC/FTMS as a function of the on-column quantity of benzene injected. The experiment was performed by monitoring m/z 78 and using the integrated absolute intensity of the time domain signal as a GC detector response.

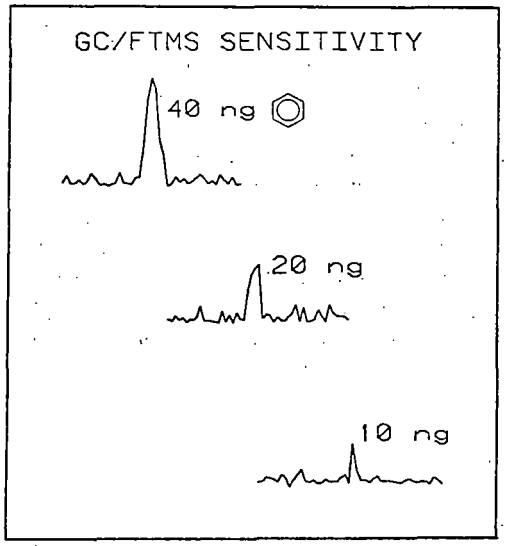

Figure 1

In conclusion, a GC/FTMS/COM system has been constructed and is capable of: rapid scanning, low or high mass resolution, peak switching over arbitrarily wide mass ranges, nanogram range on-column detection limits, chemical ionization of eluting components without instrument modifications, and on-line GC detection using the integrated absolute intensity of the time domain signal as a detector response.

HIGH PRESSURE GC/MS USING 40 μm POROUS LAYER BEAD SMALL PARTICLE PACKED COLUMNS; PAUL VOUROS, B.L. KARGER and D.A. LEWIS; Institute of Chemical Analysis and Department of Chemistry, Northeastern University, Boston, MA 02115

Due to their high efficiencies and low volume flow rates, open tubular capillary columns are finding more wide spread use in the field of GC/MS analyses. Small particle packed columns can also be used as a viable alternative to capillary columns in high resolution GC/MS separations. Based on theoretical expressions[1] total column efficiencies of 30,000 to 50,000 theoretical plates have been obtained with small particle packed GC columns when used in conjunction with elevated inlet pressures[2]. Using a custom built high pressure syringe injector capable of operation at pressures up to 25 atmospheres and 40 μm porous layer beadscolumns, we have succeeded in obtaining GC/MS analyses with efficiencies of 10,000 theoretical plates/meter. Outlet volume flow rates of 5 to 10 ml/min were obtained for these columns. these flow rates can be adjusted somewhat by varying the column tube diameter to accommodate the conductance of the mass spectrometer thus allowing direct MS coupling to the GC without the use of separators. For this work an open split connector using fused silica connecting tubing was used[3].

Due to the packed nature of these columns, sample capacities of 0.5 to 1 μg/meter were possible. This compares to 10 to 100 ng/column capacities typically observed with capillary columns. Sufficiently wide GC peaks were obtained with these columns to allow 3 or more mass spectral scans to be obtained for all but the fastest eluting components with a scan rate of 5 sec/scan (see fig 1). This feature should be of considerable value for GC/high resolution MS applications. Analysis times of <3 min for unretained components were obtained as a result of the small particle diameters used.

Applications of these columns include separation of both low and high molecular weight hydrocarbons, alcohols.fatty acid methyl esters, polychlorinated biphenyls and oxidized steroids as their trimethylsilyl ethers. Based on our initial results, small particle microbore GC columns offer cosiderable advantages for use in GC/MS analyses combining the high efficiencies and low flow rates of capillary columns with the higher sample capacities of conventional packed GC columns.

[1]G. Guiochon, Anal. Chem., 52 (1980) 2002

[2]H.H. Lauer, H. Poppe, and J.F.K. Huber, J. Chromatogr., 132 (1977) 1

[3]W.D. Koller and G. Tressl, H.R.C.&C.C., 3 (1980) 359

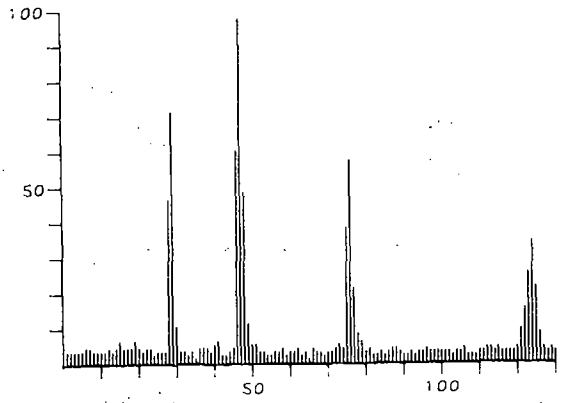

Figure 1 High Temperature/High Pressure Separation of High Molecular Weight Hydrocarbons

Column: 1m x 1mm i.d. with 3% OV-101 on Zipax 37-44 um
Conditions: T= 290°C, P_i= 13.2 atm, carrier gas Helium, flow rate 5.2 ml/min, scan rate 5 sec/scan
Solutes: 1= n-C_{26}, 2= n-C_{28}, 3= n-C_{30}, 4= n-C_{32}

A FUSED-SILICA OPEN-SPLIT INTERFACE FOR CAPILLARY COLUMN GAS CHROMATOGRAPHY-MASS SPECTROMETRY

CHRISTINE N. KENYON and PAUL C. GOODLEY
Hewlett-Packard Company
1601 California Avenue
Palo Alto, CA 94304

Open-split techniques for the coupling of capillary gas chromatography columns to a mass spectrometer appear to offer significant advantages over direct coupling methods which have been widely used in the past (1-3). When the open-split technique is utilized with recently developed fused silica tubing as the GC/MS transfer line, several advantages are realized:

1. Gas chromatography is unaffected by the vacuum system of the mass spectrometer;

2. GC columns can be changed without an isolation valve or venting the vacuum system;

3. The dynamic range of the sample can be greater than the dynamic range of the mass spectrometer because a portion of the GC effluent can be split to vent during elution of highly concentrated components while maintaining a high yield for those components; and

4. The GC column can be operated at any desired flow rate because the purge gas may be used as make-up gas when necessary and because any gas coming through the GC column which is in excess of the capacity of the mass spectrometer pumping system can be vented.

There are, of course, a few disadvantages of this type of an interface:

1. More plumbing connections are required than for a direct connection; and

2. Vacuum leak detection is more difficult.

A modified version of the Scientific Glass Engineering open-split interface has been tested on a 5985B GC/MS system. The interface features an all-fused-silica sample contact area. A diagram of the interface is shown in Figure 1.

HP 5985 OPEN SPLIT GC/MS INTERFACE

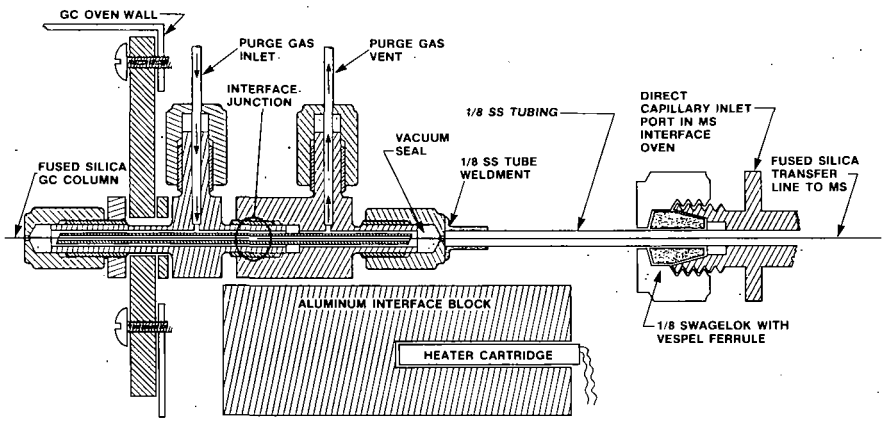

Figure 1

The design incorporates a coaxial helium blanket surrounding the interface region of the GC column outlet and the MS inlet. The design also incorporates a replacement fused-silica scavenge-gas sleeve along with a changeable fused-silica conductance transfer-line to the MS ion source. The highly inert chemical nature of the fused silica environment allows for a wide range of chemical compounds to be transferred to the ion source. The system has been tested for its ability to preserve GC peak resolution and for its chemical inertness. Hydrocarbons from C12 to C42, acids, bases, and diols have been used as test compounds. The results with a series of acids and diamines appear in Figure 2.

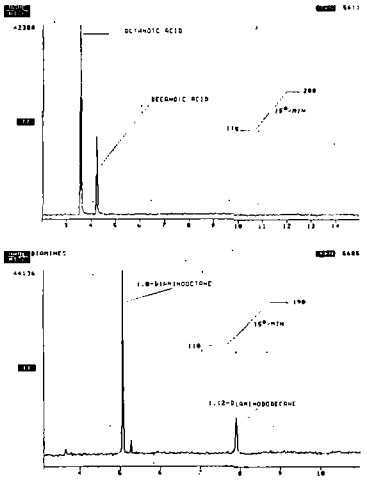

Figure 2. TIC of Organic Acids and Diamines.

Peak shape is excellent for all of the test compounds investigated and is probably only dependent on the quality of the GC columns employed.

The system has also been used for the analysis of acid, base-neutral, and volatile EPA priority pollutant standards as well as for the analysis of polynuclear aromatic compounds in pollutant sample extracts. The total ionization chromatogram from the analysis of a series of pollutant standards and their deuterated internal standard analogues by EPA Methods 1624 and 1625 is illustrated in Figure 3.

Note the excellent peak shape obtained for this analysis of volatiles, acids, and bases on a single 12M SE54 column. It was found that a 12M narrow bore-fused silica column gave equal resolution to that of a 24M column with shorter analysis time and better sensitivity.

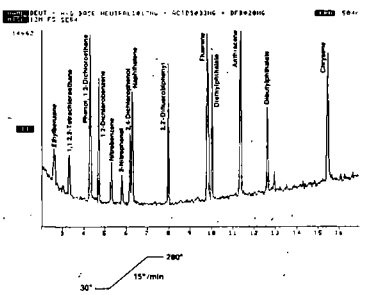

Figure 3. TIC of H- and D- Base Neutrals and Acids.

1. Henneberg, D. et al, Chromatographia 8, 9 (1975).
2. Henneberg, D. et al, J. Chromatogr. 167, 139 (1978).
3. Koller, W.D. and G. Tressl, HRC & CC 3, 359 (1980).

Isotope Cluster Chromatography and its Use in Drug Metabolism Studies, Robert J. Anderegg, Department of Chemistry, University of Maine, Orono, Maine 04469.

In many GCMS analyses, the compounds of interest contain multiple chlorine or bromine atoms, and thus exhibit characteristic isotope clusters in their mass spectra. Pesticides and drug metabolites are two examples. It would be useful to be able to screen a GCMS data set for these isotope clusters in the presence of many non-halogenated species, and so minimize the tedious sorting through vast numbers of mass spectra. A computer program to do such screening has had limited success (1). One difficulty has been to discriminate between a relatively low information-content cluster (such as that produced by a fragment containing one chlorine atom) and random ions occurring in the mass spectra of non-halogenated compounds.

We have overcome this problem by use of a more sophisticated algorithm for searching for the clusters. Our routine calculates the shape of the desired cluster from the number of chlorine and/or bromine atoms present. The unknown spectrum which is to be searched is broken down into parts, each containing exactly as many masses as are present in the cluster. Comparison of the known cluster with each of these spectrum parts is analogous to a library search routine, so we have employed a library search-type algorithm to calculate a similarity index (2) for each of the spectrum parts. The spectrum as a whole is assigned a score based on the weighted sum of these similarity indices and on the intensity of each potential cluster. A normalized plot of these scores vs. scan number in a GCMS experiment results in an "isotope cluster chromatogram" (Figure 1). The program discriminates well between halogenated and non-halogenated compounds, even when only a single chlorine or bromine atom is present. The same algorithm could be applied to sulfur or silicon isotopes, or to artificial isotope clusters generated by stable isotope labeling of the compound of interest (3,4).

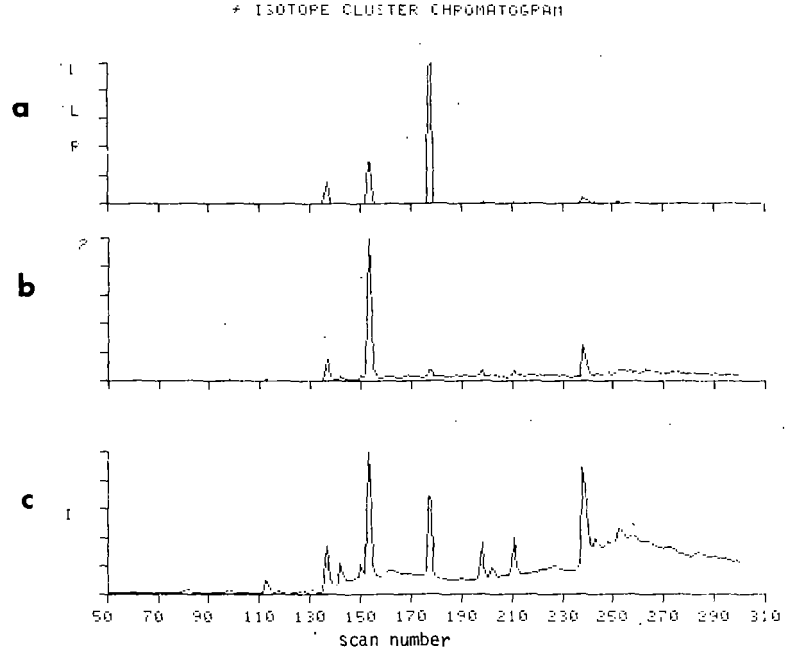

Figure 1. Isotope cluster chromatograms of a urine extract from a lysodren-treated rat, a) Cl_1 cluster, b) Cl_2 cluster, c) total ionization plot. Numbers at the far left indicate maximum score in the chromatogram.

We are currently using the program to search for metabolites of lysodren [1-(o-chlorophenyl)-1-(p'-chlorophenyl)-2,2-dichloroethane], an anticancer drug containing four chlorine atoms, and its analogues.

References:

1. D. C. Canada and F. E. Regnier, J. Chrom. Sci., 14, 149-154 (1976).

2. R. A. Hites, Ph.D. Thesis, Massachusetts Institute of Technology (1968).

3. R. F. Morfin, I. Leav, P. Ofner, and J. C. Orr, Fed. Proc., 29, 247 (1970).

4. K. Clay, W. D. Watkins, and R. C. Murphy, Drug Metab. Disp., 5, 149-156 (1977).

DIETHYLSILYL ETHER DERIVATIVES IN GAS CHROMATOGRAPHY AND GAS CHROMATOGRAPHY-MASS SPECTROMETRY OF HYDROXYPREGNANES

HIROSHI MIYAZAKI, MASATAKA ISHIBASHI,
KOUWA YAMASHITA AND TOSHIHIRO NISHINA*

Research Laboratories of Pharmaceutical Division, Nippon Kayaku, Co.,
3-31 Shimo, Kita-ku, Tokyo 115 and Toranomon Hospital, 2 Aoicho,
Akasaka, Minato-ku, 107 Tokyo*, JAPAN

In previous papers, it was found that dimethylethylsilyl (DMES), dimethyl-n-propylsilyl (DMnPS) and dimethylisopropylsilyl (DMiPS) ether derivatives of hydroxysteroids,[1-4] catecholamines[5] and prostaglandins[6,7] provided excellent GC-MS properties, especially these silyl ether derivatives gave the characteristic ions of $[M-C_2H_5]$ or $[M-C_3H_7]$ as a prominent or base peak in EI mode. In the case of pregnanetriols, it was difficult to find the above advantage of these derivatives. On the other hand, it is known that dimethylsilylating agents, such as dimethyldichlorosilane and dimethyldiacetoxysilane, react with 1,2- or 1,3-diol group of hydroxysteroids to form the thermally stable cyclic silyl ether (siliconide), which gives the molecular ion with high intensity in EI mode. However, the dimethylsilyl ether derivatives have not been used for GC-MS because of their instability. Then, N,O-bis(diethylsilyl)trifluoroacetamide (DEHS-BSTFA) was synthesized as a new silylating agent to investigate the GC and GC-MS properties and stability of the resulting DES-DEHS ether derivatives of hydroxysteroids.

[APPARATUS] A Shimadzu GC-5A with FID and a Shimadzu LKB-9000B GC-MS with GCMSPAC-500 data processing system were employed.
[SAMPLES AND REAGENTS] Pregnanes used in this study were commercially available. Compound number [6],[7],[10],[11] and [12] in table were kindly supplied by Dr. D. K. Fukushima, Institute for Steroid Research,N. Y. and Prof. T. Nambara, Pharmaceutical Institute, Tohoku University, Japan. DEHS-BSTFA was synthesized as follows: Diethylchlorosilane was prepared from trichlorosilane and ethylmagnesium bromide and then was treated with trifluoroacetamide according to the analogous method for preparation of BSTFA. It was obtained as a colorless clear liquid, bp. 95°C/ 48 mmHg.

[RESULTS AND DISCUSSION] GC and GC-MS data of the DEHS ether derivatives of hydroxypregnanes were summarized in table. The hydroxypregnanes DEHS ether derivatives were prepared in the same way as the TMS ether derivatives. The reactivity of DEHS-BSTFA to hydroxypregnanes in pyridine were nearly equal to those of BSTFA. All hydroxypregnanes were easily derivatized at room temperature without formation of by-product and exhibited a sharp, Gaussian peak. The hydroxypregnanes with a sterically hindered 17α-hydroxy group, such as pregnanetriols, were derivatized within 1 hour under the mild

Table Gas chromatographic and mass spectrometric data of the DEHS or DES-DEHS ether derivatives of hydroxypregnanes

Compounds	MU	MW	$\frac{[M]^{+*)}}{a}$	$\frac{[M]^{+*)}}{b}$	$[M-29]^+$	Other fragment ions (%)				
1) 5α-Pregnane-3α,20α-diol	32.29	492	0.2	-	1.0	388(3)	360(2)	233(3)	131(100)	121(2)
2) 5α-Pregnane-3β,20β-diol	32.46	492	0.2	-	1.1	284(9)	283(7)	131(100)	121(5)	103(18)
3) 5β-Pregnane-3α,20α-diol	31.72	492	0.1	-	1.0	284(5)	269(5)	131(100)	121(4)	103(13)
4) 5β-Pregnane-3β,20β-diol	31.05	492	0.2	-	0.5	388(4)	284(5)	283(4)	269(4)	131(100)
5) 5α-Pregnane-3α,17α,20α-triol	31.41	506	-	63.6	1.9	185(100)	171(19)	147(24)	119(11)	103(19)
6) 5α-Pregnane-3β,17α,20α-triol	33.29	506	-	60.6	4.1	185(100)	171(17)	147(19)	119(11)	103(18)
7) 5α-Pregnane-3β,17α,20β-triol	32.73	506	-	92.2	5.1	185(100)	171(23)	147(16)	119(11)	103(18)
8) 5β-Pregnane-3α,17α,20α-triol	31.05	506	-	57.8	-	185(100)	171(23)	147(16)	119(11)	103(19)
9) 5-Pregnene-3β,17α,20β-triol	32.68	504	-	100.0	4.6	400(15)	185(85)	171(27)	147(68)	119(24)
10) 3α,17α,20α-Trihydroxy-5β-pregnan-11-one	32.34	520	-	32.4	3.1	416(17)	185(100)	171(20)	147(20)	103(21)
11) 5β-Pregnane-3α,11β,17α,20α-tetraol	33.68	608	-	19.9	0.4	504(26)	238(17)	185(100)	171(23)	147(24)
12) 5β-Pregnane-3α,11β,17α,20β-tetraol	33.25	608	-	40.5	0.6	504(27)	238(16)	185(100)	171(23)	147(27)
13) 5β-Pregnane-3α,11β,17α,20α,21-pentaol (α-cortol)	37.23	710	-	26.8	1.7	205(100)	175(48)	171(49)	147(62)	103(63)
14) 5β-Pregnane-3α,11β,17α,20β,21-pentaol (β-cortol)	36.65	710	-	27.5	1.0	287(36)	205(100)	175(52)	157(40)	147(60)

*) a : DEHS ether
b : DES-DEHS ether(siliconide)

condition described above, to give their DEHS-17,20-diethylsilyl (DES) ether derivative. The hydrolytic stability was investigated using [8] as a model compound, indicating that the DEHS-DES ether derivative is stable for a week at room temperature.

The mass fragmentation pattern of the pregnanediol DEHS ether derivatives were closely related to that if the corresponding TMS ether derivatives except for 14 mass unit shift per one hydroxyl group. The hydroxypregnanes with 17, 20-diol group gave a molecular ion with prominent intensity due to the formation of 17, 20-DES. None of pregnanes TMS ether derivatives gave a characteristic ion with high intensity in high mass region. The DES ether derivative gave characteristic fragment ion at m/z 185 as a base peak except for [9], which produced by the cleavage of D-ring system and elimination of one proton. Figure 1 shows the mass spectrum of [8] 3-DEHS-17, 20-DES ether derivative. The mass spectra of the reaction products of α- and β-cortols with DEHS-BSTFA provided the molecular ions with prominent intensity at m/z 710, respectively. The structure of these derivatives were identified to be 3,11,21-tris DEHS-17,20-DES ether derivatives.

Figure 2 shows the separation of 15 kinds of the pregnane DEHS, DEHS-DES and MO-DEHS-DES ether derivatives using a SE-30 WCOT glass capillary column. Thirteen compounds except for [3] and [16] could be almost completely separated. This method was applied to the analysis of urinary hydroxypregnanes of the patient with congenital adrenocortical hyperplasia (CAH). Gas chromatography revealed that several peaks were observed in that patient urine. Figure 3 shows the selected ion recording of hydroxy-pregnanes in extracts from the above patient urine monitored at the molecular ions of pregnanetriol (m/z 506), 11-oxopregnanetriol (m/z 520), pregnenetriol (m/z 504) and pregnanetetraol (m/z 608), respectively. Peak 1 and 2 corresponding to the ion of m/z 506 and 520 were estimated to be 5β-pregnane-3α,17α,20α-triol and its 11 oxygenated derivative. The structure of both peaks were confirmed by their mass spectral data in comparison with their authentic compounds.

In conclusion, DEHS-BSTFA reacted smoothly with 1,2-diol and/or 11β-hydroxy group into the DEHS-DES ether derivatives without formation of by-product. The resulting DEHS-17,20-DES ether derivatives may be helpful for the identification of hydroxy-pregnanes and also profitable for the microanalysis of them in biological fluids by selected ion monitoring.

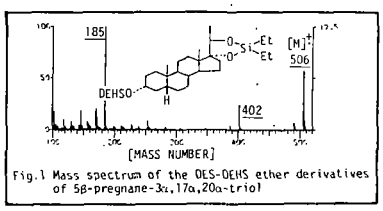

Fig.1 Mass spectrum of the DES-DEHS ether derivatives of 5β-pregnane-3α,17α,20α-triol

[REFERENCES]

1) H. Miyazaki, *et al.*, *Biomed. Mass Spectrom.*, 4, 23 (1977). 2) H. Miyazaki, *et al.*, *Biomed. Mass Spectrom.*, 5 , 469 (1978). 3) H. Miyazaki, *et al.*, *Bimed. Mass Spectrom.*, 6, 57 (1979). 4) J. Yanagisawa, *et al.* *Anal. Biochem.*, 104, 75 (1980). 5) H. Miyazaki, *et al.*, *Chem. Pharm. Bull (Tokyo).*, 29, 796 (1981). 6) H. Miyazaki, *et al.*, *J. Chromatogr.*,153, 83 (1978). 7) H. Miyazaki, *et al.*, *Biomed. Mass Spectrom.*, in press.

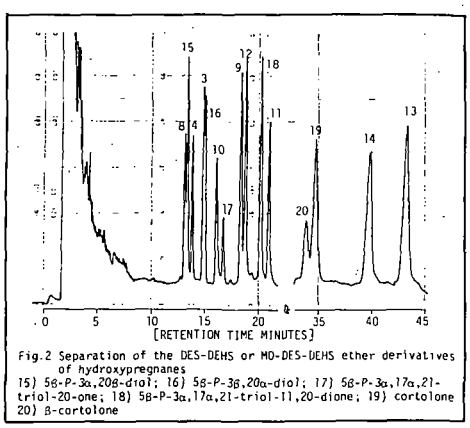

Fig.2 Separation of the DES-DEHS or MO-DES-DEHS ether derivatives of hydroxypregnanes
15) 5β-P-3α,20β-diol; 16) 5β-P-3β,20α-diol; 17) 5β-P-3α,17α,21-triol-20-one; 18) 5β-P-3α,17α,21-triol-11,20-dione; 19) cortolone 20) β-cortolone

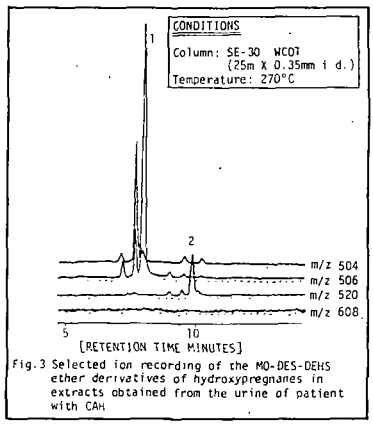

Fig.3 Selected ion recording of the MO-DES-DEHS ether derivatives of hydroxypregnanes in extracts obtained from the urine of patient with CAH

GC/MS OF TRICHOTHECENE HEPTAFLUOROBUTYRATES AND APPLICATION TO GRAIN ANALYSIS, P.-Y. LAU, P.M. SCOTT and S.R. KANHERE, Health and Welfare Canada, Health Protection Branch, Food Research Division, Tunney's Pasture, Ottawa, Ontario, CANADA, K1A 0L2.

Trichothecene mycotoxins are a class of naturally occurring toxin produced by Fusarium and some other species of molds. Under suitable temperature and humidity conditions, these molds are capable of rapid growth during harvest, drying, transport and storage of crops. In the summer of 1980, the Ontario white winter wheat crop was found to be extensively contaminated with pink kernels, later shown to be associated with the presence of Fusarium graminearum. Analysis of an initial 25 samples of the wheat in this laboratory for trichothecenes revealed the presence of deoxynivalenol (vomitoxin, DON) in all samples, while T-2 toxin, HT-2 toxin and diacetoxyscirpenol (DAS) did not appear to be present.

E.I. mass spectra of 10 trichothecenes (deoxynivalenol, diacetoxyscirpenol, HT-2 toxin, T-2 toxin, T-2 triol, T-2 tetraol, neosolaniol, nivalenol, fusarenon-X, 3-acetyldeoxynivalenol) as their heptafluorobutyrate (HFB) derivatives have been recorded. A quantitative determination of DON in various grain products by both electron capture gas chromatography and GC/MS/single ion monitoring (SIM) has been developed in conjunction with an assessment of contamination of wheat in different provinces in Canada. Fifty grams of sample were extracted with methanol-water, treated with ammonium sulfate solution, partitioned into ethyl acetate and then cleaned-up by silica gel column chromatography[1]. The HFB derivative was used for GC/EC and GC/MS/SIM analyses. GC column temperature was 170°C for GC/EC and 180°C for GC/MS.

The relatively strong molecular ion of DON-tris-heptafluorobutyrate (DON-HFB) at m/z 884 under EI conditions was used for single ion monitoring. Because of its high m/z value, this ion offers very high specificity and sensitivity. The detection limit of DON was estimated to be 1-3 pg (S/N=3). This corresponds to low ppb level with the final extract concentration equivalent to 0.1 g of sample/ml. Theoretically, the sensitivity can be improved down to ppt level if a higher concentration of the extract is used.

Forty-five wheat samples from Ontario, Quebec and western provinces in Canada were analyzed for DON by both GC/EC and GC/MS/SIM methods. In general, the results obtained from both methods were in good agreement except interference from Western Canadian wheat samples was observed in the GC/EC analysis. Results indicated that around 98% of the Ontario white winter wheat samples and 100% of the Quebec red spring wheat samples that we analysed were contaminated by DON. Western Canadian wheat was fortunately not a problem.

This method has also been applied to the analysis of DON in corn, barley, soybeans, corn flour, oats flour, corn flakes, corn syrup, corn starch, bran, dried white peas, kidney beans, etc. GC interference from corn flour, corn flakes and bran samples can be eliminated by GC/MS/SIM method.

[1] P.M. Scott, P.-Y. Lau and S.R. Kanhere, submitted to JAOAC (1981) for publication.

Three other trichothecenes, namely, diacetoxyscirpenol (DAS), HT-2 toxin and T-2 toxin were analysed similarly. Their SIM ion, column temperature and detection limit were: m/z 502 [DAS·HFB - HOAc]$^{+}$, 210°C, 13-23 pg; m/z 654 [HT-2 toxin·bis-HFB - HOAc - $(CH_3)_2CHCH_2COOH$]$^{+}$, 220°C, 40-80 pg; m/z 602 [T-2 toxin·HFB - HOAc]$^{+}$, 240°C, 1 ng respectively.

Further studies are underway to assess the extent of trichothecene contamination of various Canadian grains.

ANALYSIS OF TRICHOTHECENES USING CHEMICAL IONIZATION MASS SPECTROSCOPY; J. M. ROTHBERG, J. L. MACDONALD, J. C. SWIMS, and T. R. ROMER; Ralston Purina Co., St. Louis, MO 63188.

An analysis method has been developed for the detection of selected trichothecenes by negative chemical ionization mass spectrometry. Trichothecenes are a class of toxic compounds produced by the mold Fusarium. This class of compounds is important to the food and feed industry because the presence of low levels of trichothecenes will cause feed refusal, a resulting loss of feed efficiency, vomiting, lower white cell counts, and other toxic effects. This analysis technique enables the separation and confirmation of trichothecenes in naturally contaminated grains.

Trichothecenes are closely related in structure (Figure I) consisting of two six membered rings, a five membered ring, and an epoxide bridge. The trichothecenes differ by substitution of hydroxyl groups, acetate esters or isobutyl esters at one of four sites on the molecule. In order to improve their volatility for gas chromatography, a derivatization method, using n-heptafluorobutrylimidazole (HFBI), had been developed for use in GC/EC detection of some trichothecenes (1). Chemical ionization mass spectrometry has been shown to be very useful for the detection of these compounds due to the production of abundant high mass ions (2). Few interferences are seen in the high mass region when samples are analyzed using selected ion monitoring.

Negative chemical ionization improves the sensitivity to these compounds, due to the electronegativity of the heptafluorobutyl (HFB) groups attached to the trichothecenes. NCI chromatograms are similar to the electron capture gas chromatograms of these compounds. The heptafluorobutyl esters are formed at the site of the hydroxyl groups on the trichothecene molecule. Depending on the number of hydroxyl groups, 1, 2, or 3 HFB groups may attach, increasing the molecular weight of the compound by 196 amu with each attachment. This produces relatively high molecular weight compounds in the range of 550-950 amu.

Derivatization is performed by taking the sample to dryness, adding 150 microliters of HFBI and 1 milliliter of toluene. The reaction is performed at room temperature except in the case of the tri-hydroxy compounds, which are heated at 100°C for 10 minutes. The excess HFBI is removed by washing with 5% sodium bicarbonate. The organic layer is removed and injected into the GC/MS.

The NCI spectra are characterized by the molecular ion, loss of HF (M-20) groups, and loss of intact HFB (M-213) groups. Figures I and II show typical NCI-methane spectra of Fusarenon-X and HT-2 Toxin.

A Hewlett Packard 5985B mass spectrometer, operated in the negative chemical ionization mode, was used for the analysis. Methane was the reactant gas and the source temperature was 125° C. Tabulated spectra of six trichothecene standards are shown below. The molecular ion is underlined.

Deoxynivalenol/tri-HFB	213(100), 884(66), 194(63), 885(21), 458(12), 671(7), 884(5), 864(5).
Fusarenon-X/tri-HFB	942(100), 213(80), 194(67), 943(35), 942(8), 902(9), 728(9), 922(5).
Neosolaniol/di-HFB	213(100), 194(67), 692(97), 754(51), 693(24), 774(25), 755(14), 734(9).
HT-2/di-HFB	816(100), 817(36), 233(22), 818(9), 796(7), 583(6), 797(4).
Diacetoxyscirpenol/HFB	480(100), 481(26), 194(24), 482(7), 483(9), 562(2), 542(9), 522(6).
T-2/HFB	580(100), 581(30), 194(25), 583(10), 237(11), 662(4), 642(8), 622(5)

Initial screening of samples is performed by GC with electron capture detection. Confirmation of positive samples is performed by selected ion monitoring (SIM) mass spectrometry using the molecular ion of the derivative. Using SIM, coeluting peaks can be separated and quantitated without difficulty. Figure III shows separation of six trichothecene standards. The GC conditions used in this study were: 6 ft. x 2 mm ID glass column packed with 5% SE-30. The column was temperature programmed from 150°C to 250°C at 8°C/min. The injection temperature was 175°C and the interface temperature was 275°C. A SIM chromatogram from an extract of corn is shown in Figure IV, confirming the presence of DON and HT-2.

(1) Romer, T.R.; Boling, T.M.; MacDonald, J.L.; JAOAC 61(4), 1978, pg. 802-808.
(2) MacDonald, J.L.; Romer, T.R. Proc. 25th Annual Conf. Mass Spec. Allied Topics, Washington, DC (1977).

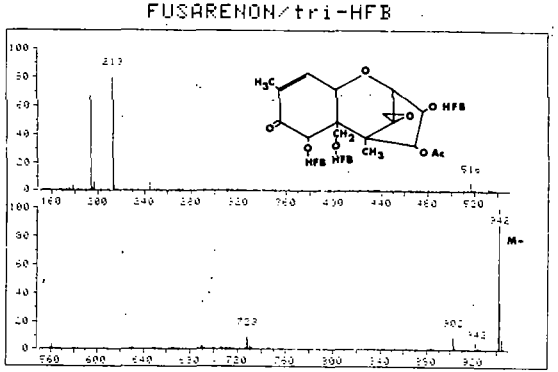

Figure I

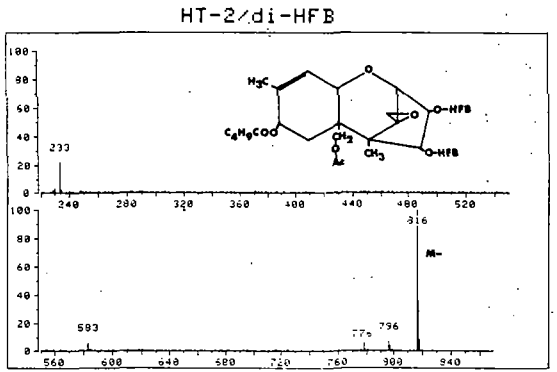

Figure II

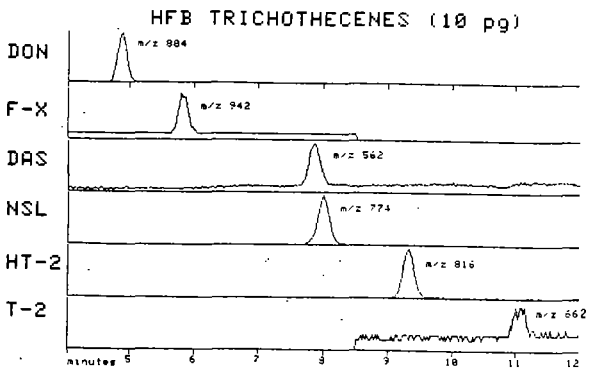

Figure III

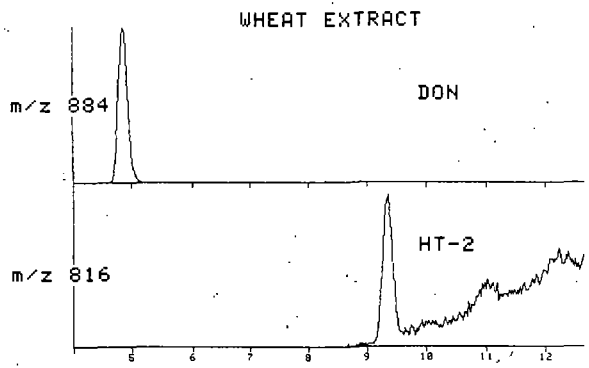

Figure IV

PRECISION AND ACCURACY IN A LARGE MULTI-LABORATORY ENVIRONMENTAL SURVEY USING GC/MS

William L. Budde
Office of Research and Development
U.S. Environmental Protection Agency
26 W. St. Clair Street
Cincinnati, Ohio 45268

During the second half of 1980, the U.S. Environmental Protection Agency conducted a large scale, multi-media, integrated (air, water, soil, sediment, and biota) environmental monitoring program in the vicinity of a closed chemical manufacturing waste disposal site. This program employed, for the organic compound analyses, a massive application of gas chromatography/mass spectrometry (GC/MS). The GC/MS analyses were designed to identify and to measure up to 152 individual target compounds and mixtures of target compounds (product formulations) and to identify up to 20 of the most prominent non-target compounds in each sample. A majority of the sample extracts was submitted to conventional glass capillary or fused silica capillary GC/MS, but some conventional packed column GC/MS was employed. Surrogate quality control compounds were added to each of the original water samples at known levels (5-25 micrograms per liter) to evaluate the performance of the six laboratories that participated in the survey.

Fluorobenzene and p-bromofluoro-benzene were added to each water sample that was submitted to the purge and trap extraction followed by GC/MS analysis with a packed column (EPA Method 624). For 598 measurements of fluorobenzene by six different laboratories in five different types of ambient water (drinking, ground, sump, storm sewer and surface) the mean recovery was 99.7% with a standard deviation of 18.1%. In 588 measurements of p-bromofluorobenzene the mean recovery was 94.3% with a standard deviation of 27.9%. These statistics were utilized in the validation of data from all laboratories that applied Method 624.

2-Fluorophenol, 1-fluoronaphthalene, and 4,4'-dibromooctafluorobiphenyl were added to each water sample that was extracted with methylene chloride and submitted to GC/MS analysis with a 30 meter SE54 fused silica capillary column. 2-Fluorophenol was measured 378 times with a mean recovery of 48.0% and a standard deviation of 30.5%. 1-Fluoronaphthalene was measured 429 times and gave a mean recovery of 55.0% with a standard deviation of 33.2%. 4,4'-Dibromooctafluorobiphenyl was measured 406 times with a mean recovery of 48.2% and a standard deviation of 34.2%.

All of the above statistics were computed after rejection of outliers associated with systematic method errors. Again these statistics were used to validate the data from Method 625. The lower mean recoveries observed with Method 625 are caused by losses during liquid-liquid extraction and concentration of the extract. With Method 624, losses due to extraction inefficiency are automatically corrected by the method of calibration in samples without a matrix effect.

Characterization of Hydrocarbon Emissions from Vehicles on the Road

C. V. Hampton, W. R. Pierson, T. M. Harvey*, W. S. Updegrove, R. S. Marano, D. Schuetzle
Ford Motor Co., Engineering & Research Staff, Dearborn, MI 48121

A GC/MS survey of gas-phase organic compounds generated by motor vehicles in highway operation was conducted in the Allegheny Mountain Tunnel of the Pennsylvania Turnpike.[1] Objectives of the study were primarily to identify not only the exhaust emissions but also the contributions from any other aspect of vehicle operation in the tunnel second, to develop quantitation methodology to resolve components into Diesel and gasoline-powered vehicle contributions; and third, to compare vehicle emission rates generated in an on-road setting with those obtained from tailpipe and evaporative emissions studies.

The Allegheny Tunnel is a well characterized experimental site; environmental tests have been conducted there by this laboratory for the past ten years.[2] Because of the strong diurnal and weekly traffic patterns in the tunnel, samples were obtained in periods dominated by gasoline-powered vehicles as well as periods dominated by Diesel vehicles. In this manner, concentrations for specific components were varied as a function of traffic composition. The traffic composition and traffic volume were determined by visual count in combination with a road-tube axle counter. Tunnel air flow was monitored with an anemometer. By combining these four experimental variables: concentration, air throughput, traffic composition and traffic volume, emission rates for specific components were generated. Linear regression analysis weighted for traffic flow asymmetry, fan speed and tunnel air throughput provided resolution into Diesel and gasoline emission rates. The following relationship was used:

$$\frac{\%G}{100}(E_g - E_D) + E_D = \left[PC_{Tunnel} - (\alpha C_{EFAN} + B\,C_{WFAN})\right]\frac{S}{VL}$$

% G = % Gasoline vehicles
E = emission rate; D-Diesel, G-Gasoline
P = traffic asymmetry factor
α,B = air flow weighting factors
C = concentration
V = total vehicle count
L = length of tunnel
S = tunnel air volume during sampling

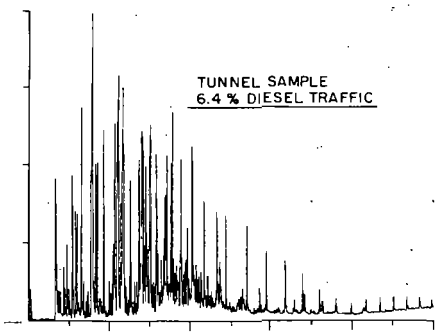

FIGURE 1

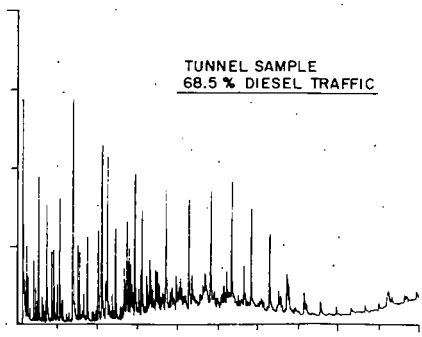

FIGURE 2

Sampling

Samples were collected in cartridges packed with Tenax GC. Tunnel samples were obtained with and without upstream filtering in order to evaluate the contribution of condensed phase material captured in the sampling process. Concurrent sampling of the tunnel air and of the tunnel intake ventilation air permitted discrimination between vehicle-derived and ambient background components. Approximately 40% of the air flow into the tunnel during these experiments entered through the tunnel entrance under the piston action of the traffic and the prevailing wind. The rest of the air inflow was provided by large intake fans located on the east and west side of the mountain above the tunnel portals.

GC/MS Analysis

The samples were analyzed by thermal desorption gas chromatography/mass spectrometry using a VG Micromass MM-16 magnetic sector instrument coupled with a Finnigan 2000 data system. Sample desorption was achieved using an injector port patterned after a design by Zlatkis et. al.[3] connected in series with a liquid-nitrogen-cooled capillary trap.[4] The GC column employed was a 50 m. x 0.25 m.m. i.d. silicone oil SF-96 borosilicate glass capillary, temperature programmed from -20°C to 230°C at a rate of 3°C/minute. Hexafluorobenzene was used as an internal standard.

Results

Comparison of the tunnel samples collected under various traffic compositions shows that 1) the same peaks are always present and 2) the intensities of the peaks vary with traffic composition. This is described by the reconstructed ion chromatograms shown in Figures 1 and 2. Figure 1 describes exhaust gases collected during a period of 6.4% Diesel traffic; Figure 2, gases collected during a period of 68.5% Diesel traffic.

Over three hundred of the four hundred compounds found in the tunnel air have been identified. The major components are homologous series of n-alkanes (C_5-C_{26}), branched alkanes, alkenes, and various alkyl series based on cyclopentane, cyclohexane, benzene, styrene, indene, naphthalene and decalin.

The samples were found to be too complex for adequate species identification by mass spectral analysis alone. Additional criteria were needed to assist in identifications. Advantage was taken of the thermodynamic properties inherent in gas chromatographic data to devise a new version of the classical isothermal relationship between carbon number and logarithm of the retention time. This linear, empirical relationship (reciprocal carbon number versus log retention time) derived for linear programmed temperature chromatography aided in locating compounds within a homologous series. Compounds have been shown to elute from an SF-96 column according to boiling point in a well-defined manner.[5] It was therefore possible to specify for each class of compound a relationship between boiling point and retention time (Figure 3). In this manner, the identifications of isomers exhibiting nonunique mass spectra were resolved.

Good agreement was obtained between emission rates from this study and those obtained from tailpipe and evaporative emission values.[6,7] Table I shows the comparison. Twenty two compounds have been quantitated and resolved into Diesel and gasoline contributions. These will be published at a later date.

COMPARISON OF TAILPIPE EMISSIONS (mg/vmi) WITH CALCULATED EMISSIONS FOR GASOLINE VEHICLES IN THE ALLEGHENY EXPERIMENT

	OCTANE	NONANE	N-PROPYL BENZENE	TOLUENE
ALLEGHENY	10.2 ± 1.2	5.2 ± < 1	3.1 ± 2	56.4 ± 9.2
EPA [a] BLACK & HIGH	4.8	1.2	1.8	75.6 [c]
EPA [b] BLACK & HIGH	5.2	1.4	0.8	62.3 [c]

a. VALUES AVERAGED FROM TAILPIPE AND EVAPORATIVE EMISSIONS OBTAINED FROM FOUR GASOLINE VEHICLES AND FOUR FUEL BLENDS

b. VALUES AVERAGED FROM 22 GASOLINE VEHICLES

c. VALUE IS FOR A COMBINATION OF TOLUENE PLUS 2,3 DIMETHYL HEXANE

TABLE I

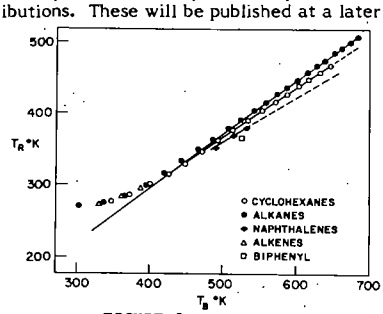

FIGURE 3

References

1) C. V. Hampton, W. R. Pierson, T. M. Harvey, W. S. Updegrove and R. S. Marano, "Hydrocarbon gases emitted from vehicles on the road, I. A qualitative GC/MS survey," submitted to Environmental Science and Technology.
2) W. R. Pierson and W. W. Brachaczek, SAE Paper 760039 (1976) (and references therein).
3) A. Zlatkis, H. A. Lichtenstein, and A. Tishbee, Chromatographia 6, 67-70 (1973).
4) E. D. Pellizzari, B. H. Carpenter, J. E. Bunch, and E. Sawicki, Environ. Sci. Technol. 9, 556-560(1975).
5) F. T. Eggertsen, S. Groennings, and J. J. Holst, Analytical Chem. 32, 904-909 (1960).
6) F. M. Black and L. E. High, SAE Paper 770144 (1977).
7) F. M. Black and L. E. High, EPA-600/2-80-085 (1980); J. Air Pollut. Control Assoc. 30, 1216-1221 (1980).

*Present Address: Chemistry Dept., U. of Virginia
Charlottesville, VA 22901

RESONANCE ENCHANCED MULTIPHOTON IONIZATION AND FRAGMENTATION OF POLYATOMIC MOLECULES, THOMAS E. CARNEY and Tomas Baer; Department of Chemistry, University of North Carolina, Chapel Hill, North Carolina.

A new form of mass spectrometry has emerged in the past two years, known as multiphoton ionization (MPI) mass spectrometry. The technique usually employs pulsed visible dye or UV lasers to ionize molecules by the absorption of a minimum of 3 or 4 photons. The ionization efficiency may be enhanced by several orders of magnitude by tuning the laser to a resonant state at the 2 or 3 photon level of the neutral molecule, thus the term resonance enhanced multiphoton ionization, or REMPI. The REMPI mass spectra of most polyatomic molecules exhibit considerably more fragmentation than is observed by conventional electron impact or UV photoionization methods. With benzene, for example, the most abundant fragment is C^+, while parent ions are completely absent. The abundance of small, high energy fragments implies the absorption of many visible photons. There is currently considerable interest in elucidating the absorption and fragmentation pathways in the REMPI process.

Our experiment consists of a nitrogen laser pumped dye laser, the output of which is focused into the ionization/acceleration region of a 30 cm long time-of-flight (TOF) mass spectrometer. A small portion of the laser pulse is split to a fast photo-diode which provides the start signal to a time-to-amplitude converter, while detected ions produce stop pulses. The TOF spectrum is then displayed on a multichannel analyzer. With this apparatus we can collect ion TOF distribution at fixed laser wavelengths, or we can scan the laser wavelength and collect mass analyzed ions.

Two basic mechanisms have been proposed for the absorption pathways in the REMPI process. One possibility involves absorption of photons by an autoionizing "ladder" of states of the neutral molecule. At some point autoionization will be faster than photon absorption and the molecule will ionize and "explode" into fragments. Alternatively, parent ions may first be formed via the lowest energy ionization pathway. These parent ions may then absorb photons up a ladder of ionic states, again resulting in "explosion" of the parent ion. We have observed direct evidence of the ionic ladder process with the molecule 2,4-hexadiyne,[1] a linear benzene isomer, and with toluene. In each case a dramatic change in the mass spectrum was observed upon changing the laser wavelength over a small range in the green legion. At longer wavelengths only parent ions were observed. At slightly shorter wavelengths severe fragmentation occurs, with very few parent ions remaining. This change in wavelength correlates exactly with the ability to pump the $\tilde{X}$ to $\tilde{A}$ transition in the parent ion with one photon. Thus the one photon transition from the ground state of the parent ion acts as a bottleneck for further absorption and fragmentation.

We have also studied fragmentation patterns as a function of laser power. In agreement with other workers[2,3] it was found that each fragment exhibits a difference laser power dependence. In addition, the dependence on laser power is a linearly decreasing function of the number of carbon atoms in the fragment ion.

We have confirmed the results of Zandee and Bernstein[4] which showed that all benzene fragments exhibit the same laser wavelength spectrum. That is, all spectroscopy is determined by the resonant states of the neutral parent molecule. Such observations serve as the basis for selective ionization and fragmentation of molecules in a mixture by tuning the laser to appropriate resonances.

REFERENCES

1. T. Carney and T. Baer, J. Chem. Phys. 75, XXXX (1981).

2. L. Zandee and R. B. Bernstein 71, 1359 (1979).

3. J. P. Reilly and K. L. Kompa, J. Chem. Phys. 73, 5468 (1980).

4. L. Zandee and R. B. Bernstein, J. Chem. Phys. 70, 2574 (1979).

The Role of Thermally Produced Ions in Mass Spectrometric Desorption Methods

Robert J. Cotter
Middle Atlantic Mass Spectrometry Facility
The Johns Hopkins University
Baltimore, MD 21205

Alfred L. Yergey
National Institutes of Health
Bethesda, MD 20205

In addition to molecular ions (M^+), the field desorption technique often produces cationized ($M+Na^+$) and protonated (MH^+) molecular species. The cationized species, in particular, are easily formed at reduced fields, or using untreated wires (1), conditions which suggest a greater role for the temperature (emitter current) in the actual ion formation process. In addition, many organic salts, such as quaternary ammonium and phosphonium halides (MX), produce molecular cations (M^+) under similarly relaxed field conditions (2). Laser desorption, using wavelengths in the infra-red region, has been shown by a number of investigators to also desorb these more easily formed cationized molecules and molecular cations (3-5).

As a demonstration of the importance of temperature in the desorption process, mass spectra of glucose and several quaternary ammonium salts have been obtained, using an ionization technique which is purely thermal. The instrumental configuration is shown in Figure 1. The source is an electron impact source; however, no electron beam is used in the experiments, and the ions are formed solely by heating the probe tip, onto which the sample has been previously coated. Figure 2 shows a spectrum of glucose obtained by this technique, in which cationized species are observed, along with sodium and potassium ions.

Figure 3 is a thermal desorption spectrum of tetramethyl ammonium chloride. In addition to the molecular cation, a decomposition peak at mass 58 is observed and results from the loss of neutral methane to reform an imminium ion which retains a tetravalent nitrogen. This even electron species is different from that expected in EI or CI spectra, where loss of methyl halide produces volatile neutral tertiary amines, which are subsequently ionized or protonated to give peaks at mass 59 and 60 respectively.

Tetra n-butyl ammonium chloride shows similar imminium ion formation (Figure 4), and in this respect the spectra resemble those obtained by field desorption (FD), fission fragmentation induced desorption (FFID) and laser desorption (LID) (6). Recent results in our laboratory in the analysis of long chain quaternary amines by fast atom bombardment (FAB) indicate that similar processes are occurring. (7)

(1) F.W. Röllgen and H.-R. Schulten, Org. Mass Spectrom., 10, 660 (1975)

(2) F.W. Röllgen, U. Geissmann, H.J. Heinen and S.J. Reddy, Int. J. Mass Spectrom. Ion Phys., 24, 235 (1977)

(3) M.A. Posthumus, P.G. Kistemaker, H.C.C. Meuzelaar, and M.C. Ten Noever de Brauw, Anal Chem., 50, 985 (1978)

(4) R. Stoll and F.W. Röllgen, Org. Mass Spectrom., 14, 642 (1979)

(5) R.J. Cotter, Anal. Chem., 53, 719 (1981)

(6) B. Schueler and F.R. Krueger, Org. Mass Spectrom., 14, 439 (1979)

(7) R.J. Cotter, G. Hansen and T. Jones, RPA7, 29th ASMS, 1981

(8) R. Stoll and F.W. Röllgen, J. Chem. Soc., Chem. Commun., 789 (1980)

(9) R.J. Cotter and A.L. Yergey, J. Am. Chem. Soc., 103, 1596 (1981)

FINNEGAN 4021 MASS SPECTROMETER
WITH THERMAL DESORPTION PROBE

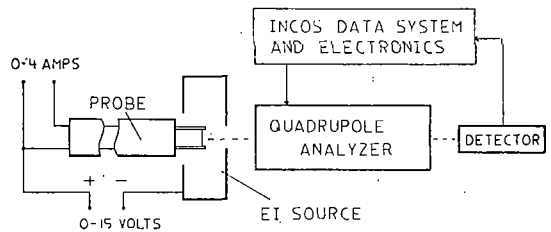

A.L. YERGEY, N.E. VIEIRA, J.W. HANSEN, ANAL CHEM, 52, 1811 (1980)

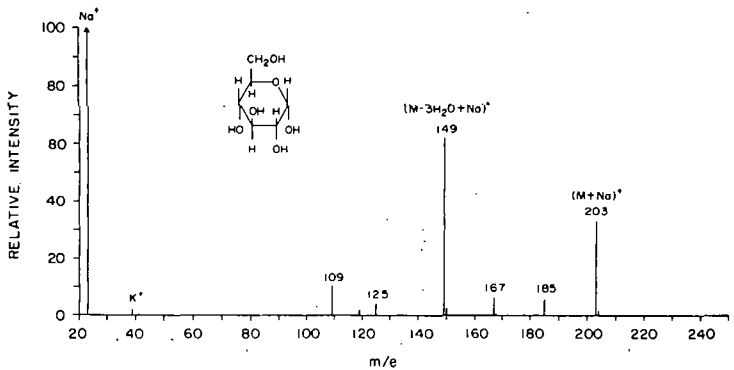

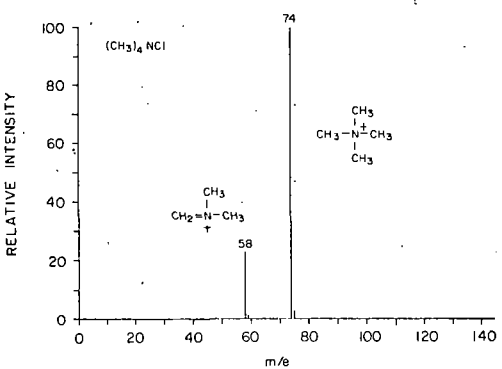

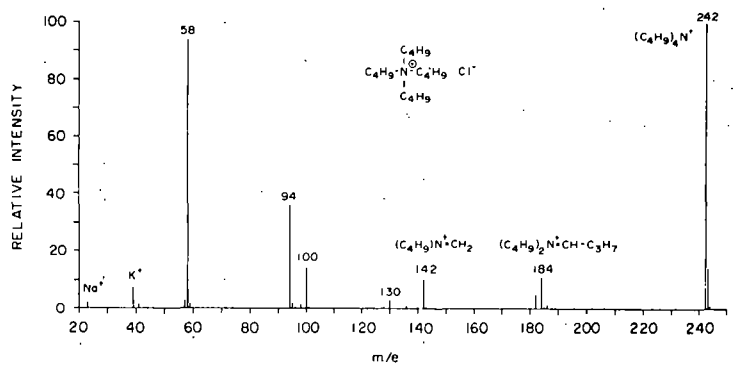

ION FORMATION FROM ORGANIC SOLIDS BY LASER OR SWIFT ION IRRADIATION, RELATED TO THEIR ACIDITY AND BASICITY SCALE

FRANZ R. KRUEGER

Institut für Biophysik -Physik für Mediziner- Universität Frankfurt/Main, Haus 74, Th.-Stern-Kai 7, D-6000 Frankfurt/Main 70, West Germany

By means of the LAMMA method negative and positive ions can be obtained from solid organic substances via Q-switched UV-laser induced desorption (Q-LD) [1]. A laser beam is focused on to an about 1 µm Ø spot of the surface of the organic bulk. Typical fluxes are about some 10^7 Wcm^{-2} for some tens of nanoseconds. The instantaneously produced ions are detected by a time-of-flight technique (TOF). The obtained mass spectra are similar to those produced by 252-Cf fission-fragment induced desorption (FFID) [2,3] measuring secondary ions produced from an organic bulk surface when penetrated by 100 MeV fission fragments also detected by TOF. The molecular mass spectra are also similar to those obtained by SIMS adopted to TOF [4]. Magnetic spectrometers, however, measure also the ions evaporated up to microseconds after the primary event (laser shot, fast ion traversion). These ion types may be of similar kind, as observed with SIMS [5], but also may differ, as observed with LD [6]. Here we deal only with the instantaneously produced ions.

As a rule, all these ions are produced via a very rapid energy transfer to the organic lattice, thus depositing suddenly the energy necessary for a phase transfer from the solid into the gaseous state. In order to predict the ion types being produced by these fast processes, first of all we have to obey the ranking of the typical relaxation frequencies:

$$\omega_{electron} > \omega_{proton} > \omega_{sceletal}$$
$$\sim 10^{16}\ s^{-1} \qquad \sim 10^{14}\ s^{-1} \qquad \sim 10^{12}\ s^{-1}$$

As it is energetically more favorable to produce ions via proton transfer than via electronic ionization in the condensed phase, and as the electronic relaxation is very fast, we expect non-radical species except with aprotic substances like such unpolar species as paraffines, some steroids, condensed homocyclic aromatics, graphite, and so on.
In the mass spectra we will expect the charged acids A^+ and bases B^- from the reactions

$$A \longleftrightarrow B^- + H^+ \quad ; \quad A^+ \longleftrightarrow B + H^+ \quad ,$$

if A^+ and B^- are weak acids or bases, respectively, in the condensed phase. Otherwise stating, the neutral A or B should be strong acids or bases, respectively. The $A^{(+)}$ and $B^{(-)}$ may either be molecular species or sufficiently polar order structures of the lattice or the surface.

As the sceletal relaxation is slow compared with the energy transfer and protic ionization of neutrals, the instantaneous "evaporation" is a Franck-Condon-type process: a non-adiabatic transition from the electronic hypersurface forming the bound states into quasifree states, as it is depicted in the figure on the next page.
Also preformed "cluster" ions like kationized bases or even anionized acids are suddenly evaporated, thus forming ions of the type $(B+Alkali)^+$; $(A+Halid)^-$

Generally, one is able to say that clusters of the order n can be formed by the decay of larger surface areas, which are of the type $(b_n a_{n-1})^-$ and $(a_n b_{n-1})^+$ clusters with $b_1, b_2, b_3, \ldots$ being any charged bases or even negative sites in zwitter ions ($-COO^-$) etc., and $a_1, a_2, a_3, \ldots$ being any charged acids or positive sites ($-NH_3^+$).
The dynamics of forming such clusters have been prooved to be in Q-LD dependent only on the alkali-basicity and halide-acidity of alkali halide clusters in the solid state [7], whereas in FFID kinetic relaxation phenomena alter the picture.
Also with organic ionics the ion production yields seem to be mainly dependent on the acidity and basicity of the clusters, molecules, and polar substructures in that sense, that neutral bases being strong in the condensed phase form weak charged acids as kations, and neutral acids being strong in

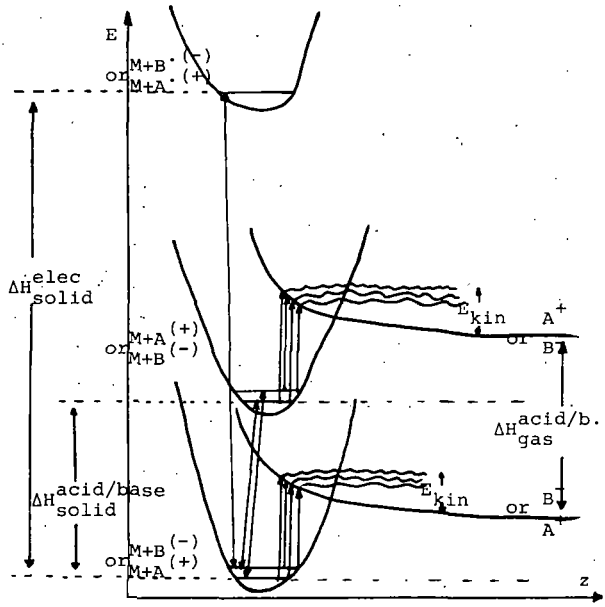

Examples of

weak charged acids	strong neutral bases / acids	weak charged bases
NH_4^+	NH_3	
(H_3O^+)	(H_2O)	(OH^-)
	H_2S	SH^-
$C_3H_3^+$		
$H_3C-S^+=CH_2$	HNO_2	NO_2^-
$R_2-\overset{R_1}{\underset{R_4}{N^+}}-R_3$	HCNO	CNO^-
	HCNS	CNS^-
$R-\overset{H}{\underset{+NH_2}{C}}-H$ $(M-45)^+$ with amino acids	$HS-CH_3$	CH_3S^-
		$R-S-S^-$
		J^- (Br^-)
$R_1^+-COO^-\cdot Alk^+$	$R_1^+-X-R_2^-$	$R_2^--\overset{R}{\underset{H}{N^+}}-H \cdot Hal^-$
$(M+1)^+$ $(M+Kat)^+$	M	$(M-1)^-$

the condensed phase form weak charged bases as anions. Kations of the onium type, which are not able to loose a proton as certain quaternary ammonium or tertiary sulfonium ions are the strongest lines measured in the mass spectra.

On the other hand, the production of clusters via gas phase reactions could be excluded experimentally, as well as proton transfer in the gas phase. A neutral evaporation and subsequent ionization has been falsified by exact TOF-analysis in FFID. In the table thus favored ion species are given.

Due to the fact that non-preformed ions mostly have to be formed via rapid proton transfer, strong kinetic H/D-isotope effects are expected. They have been observed in a hindrance of ion formation from deuterated substances in Q-LD and FFID (e.g. by a factor of 4 with amino acids in FFID).

It is worthwile to notice, that the observed kinds of ions do not depend strongly on the kind of primary lattice perturbation rather than of the rate of energy transfer. Irradiation into UV-resonances of molecules (e.g. λ=265 nm with aromatics) do not alter the mass spectra significantly, compared with non-resonant irradiation. However, the mass spectral background is altered systematically but unspecifically with wave length and pulse duration (psec-measurements [8]). In FFID is no fragmentation dependence on primary ion LET, being in good agreement with the diabatic desorption model. [9]

References:

(1) H.J.Heinen, S.Meier, H.Vogt, R.Wechsung, Adv.in Mass Spectr.8,(1980),942
(2) R.D.Macfarlane, D.F.Torgerson, Science 191,(1976), 920
(3) F.R.Krueger, B.Schueler, Adv.in Mass Spectr. 8,(1980),918
(4) K.G.Standing, in: Ion Formation from Organic Solids, Münster (in press)
(5) A.Benninghoven, W.Sichtermann, Org. Mass Spectr. 12,(1977), 595
(6) F.Heresch, E.R.Schmid, J.F.K.Huber, Anal. Chem. (Oct. 1980)
(7) B.Jöst, Diploma thesis (Frankfurt 1981)
(8) F.Hillenkamp, private communication
(9) P.Dück, W.Treu, H.Fröhlich, W.Galster, H.Voit, Surf. Science 95,(1980),603

LASER DESORPTION MS/MS OF SUCROSE AND THE MECHANISM OF DESORPTION IONIZATION, Don Zakett, Alan E. Schoen, R. Graham Cooks, Dept. of Chem., Purdue Univ., West Lafayette, IN 47907 and Philip H. Hemberger, Union Carbide Corp., Nuclear Div., Oak Ridge Y12 Plant, Oak Ridge, TN 37830

A combined LD/CI/EI source has been constructed and put into operation on the Purdue MS/MS (MIKES) instrument. Preliminary results have been obtained for LD of sucrose. The LDMS of sucrose has been obtained using a pulsed source combined with conventional scanning techniques and shows a striking resemblance to that previously obtained by SIMS (1). The LDMS/MS spectrum of silver cationized sucrose (S), (^{107}Ag+S) = m/z 449, has also been obtained and displays several structurally significant fragmentations which again parallel SIMS processes. Temporal studies of the ion desorption resulting from a 10 nsec laser pulse have been conducted and indicate that ion production occurs for periods of 200 μsec - 1.5 msec following the laser pulse and is dependent upon CI source pressure.

Desorption ionization methods such as field desorption(2), fission fragment desorption(3), secondary ion mass spectrometry(4) and laser desorption(5) have increased the number of types of compounds which can be studied by mass spectrometry. Additional structural information can often be obtained by combining conventional mass analysis with collision-induced dissociation (CID) of a mass selected ion and subsequent fragment ion mass analysis. The technique of MS/MS has been successfully applied using FD ionization(6) and, as expected, increased the amount of structural information from the analysis.

We report here the first successful combination of LD with MS/MS. A Quanta Ray DCR-1A (Mountainview, CA) pulsed Q-switched Nd:YAG laser with harmonic generator crystals was used in these studies. Only the 1064 nm output was actually used and the laser was typically operated at 10 Hz set to deliver 0.1 J/pulse. The Q-switched pulse width was approximately 10 nsec and with a focussed spot size of 2 mm., the power density at the sample surface was approximately 10^9 W/cm^2.

Figure 1 shows the LDMS of sucrose supported on a silver foil extension to the mass spectrometer solids probe. The sucrose was mixed with ammonium chloride and silver powder and deposited on the foil from aqueous solution. The mass spectrum was obtained by slowly scanning the magnet (ca. 1 amu/sec) while repetitively pulsing the laser at 10 Hz. Analog signal detection (Keithley #640 electrometer) was used to record the LDMS. The long time constant of this electrometer effectively smoothed the pulsed character of the mass spectrum (10 laser shots across a mass peak).

The laser irradiation was observed to produce an intense silver cation beam (m/z 107/109) from the silver foil sample support which cationized the intact, laser desorbed, sucrose molecules resulting in pseudomolecular ions at m/z 449/451. Only minor peaks corresponding to $(S+Na)^+$ and $(S+K)^+$, S=sucrose, were observed at m/z 365 and m/z 381 respectively. Thermal generation of NH_3 (from the NH_4Cl) resulted in formation of $(AgNH_3)^+$ and $(Ag(NH_3)_2)^+$ which with Ag^+ were the dominant low mass ions observed in the mass spectrum. As shown in Figure 1 the major fragmentations of $(S+Ag)^+$ and $(S+AgNH_3)^+$ are centered about the glycosidic linkage with only minor amounts of water loss from the molecular ion.

The LDMS of sucrose is strikingly similar to that obtained by SIMS shown in Figure 2. Here sucrose mixed with ammonium chloride supported on silver foil was ionized by bombardment with a high energy ion beam. The silver cationized molecule, pseudomolecular ion minus water, and glycosidic cleavage ions are again present. The thermally related ammonia containing ions are not observed in the SIMS spectrum suggesting that bulk heating is more prevalent in LD. The sucrose fragment ion peaks are of similar relative intensities in both LD and SIMS suggesting that these peaks result from unimolecular fragmentation of the intact silver cationized sucrose molecule as a consequence of the exothermicity of the cationization process and energy deposited in the desorption event. If so, this implies that most molecules are desorbed intact and; subsequently cationized by silver. There is no evidence for desorption of neutral fragments.

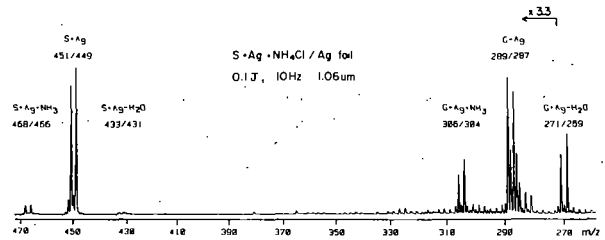

Figure 1. Laser-desorption mass spectrum of sucrose (S), admixed with NH_4Cl and silver powder and supported on silver foil (analog output of a single scan).

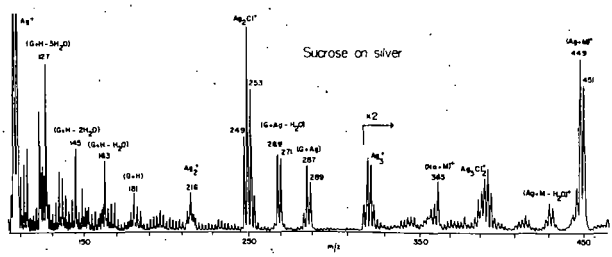

Figure 2. Secondary ion mass spectrum of sucrose, admixed with NH_4Cl and supported on silver foil.

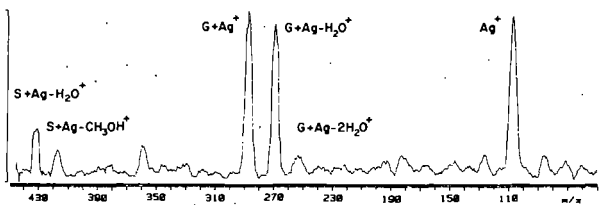

Figure 3. MS/MS spectrum of the $^{107}Ag^+$ adduct of sucrose generated by laser desorption.

References:

(1) L.K. Liu, K.L. Busch, and R.G. Cooks, Anal. Chem. (1981) 53, 109.
(2) H.R. Schulten, Int. J. Mass Spectrom. Ion Phys. (1979) 32, 97.
(3) R.D. MacFarlane and D.F. Torgeson, Science (Washington, DC)(1976) 191, 920.
(4) R.J. Day, S.E. Unger, and R.G. Cooks, Anal. Chem. (1980) 52, 557A.
(5) R.J. Conzemius and J.M. Capellen, Int. J. Mass Spectrom. Ion Phys. (1980) 34, 197.
(6) H.J. Veith, in "Advances in Mass Spectrometry", (A. Quayle Ed.), Vol. 8A, 768, Heyden and Son, London (1980).

LASER IONIZATION MASS SPECTROMETRY OF NONVOLATILE MOLECULES; E. D. HARDIN and M. L. VESTAL; Dept. of Chem., Univ. of Houston, Houston, TX 77004

A new laser ionization mass spectrometer has been developed which employs a moving stainless steel belt onto which the sample is either electrosprayed or thermosprayed for continuous sample introduction. Ionization is produced by focusing the output of a tunable dye laser onto the moving belt. The dye laser is pumped by a pulsed N_2 laser and the output is typically 400 microjoules in 5-7 nsec pulses at 25 hz focused to a spot diameter of 0.1-1mm. Except for the use of a gated boxcar integrator to process the pulsed ion signal, the mass spectrometer is a conventional quadrupole. Mass spectra have been recorded for a number of nonvolatile biomolecules including saccharides, amino acids, peptides, nucleosides, and nucleotides. Generally, these spectra show intense cationized molecular ions, often including multiple alkali addition, and little fragmentation. Protonated molecular ions are also observed and are particularly intense for basic samples such as guanosine, adenosine, arginine and histidine.

Time-of-flight distributions have been measured on selected ions which show that ions produced by laser desorption/ionization have broad kinetic energy distributions. Typically, most probable kinetic energies are about 6 eV with high energy tails extending beyond 25 eV. Analysis of the TOF spectra show that a substantial fraction of the observed ions are formed by metastable decomposition of larger clusters in flight and often only a small fraction of the observed ions are formed directly at or near the surface. The size of the precursor clusters is dependent on the surface coverage and the laser power density. A model of the laser desorption/ionization process is proposed which accounts qualitatively for the observed effects.

MECHANISMS IN MOLECULAR SIMS AND OTHER FORMS OF DESORPTION IONIZATION (DI); K.L. BUSCH, S.E. UNGER, and R.G. COOKS; Department of Chemistry, Purdue University, West Lafayette, IN 47907.

Molecular SIMS is concerned with identification and quantitation of bulk organic materials supported on heterogeneous substrates. Desorption of ions from surfaces occurs as a result of energy deposition by impact of a primary ion. The ejected secondary ions arise by three common processes: direct desorption of precharged ions from the solid matrix, cationization (and anionization), and electron ionization. Of these, the first two differentiate SIMS from gas phase ionization techniques such as EI and CI, and bind it most strongly to other desorption ionization techniques -- FD, PD, LD, and EHD. The use of these techniques has made possible the analysis of thermally fragile, nonvolatile, and high molecular weight compounds.

DIRECT DESORPTION - When the sample itself is precharged, then the desorption efficiency, and both specificity and sensitivity, are optimized. Samples can be analyzed from such diverse matrices as plant tissue[2], chromatography media[3], or vacuum compatible liquid phases[4]. The neutral matrix can be essentially transparent to the desorption process. Derivatization reactions can be used to convert neutral samples to precharged forms (reverse derivatization) with concomitant spectral enhancement[5]. An example of this is shown in Figure 1, where p-toluenesulfonic acid was used to convert the neutral zwitterionic compound into its precharged protonated form.

CATIONIZATION - Cationization is an ionization process; the creation of a stable species (C+M) is controlled by many experimental factors. As in FD and LD, addition of alkali salts promotes the formation of the appropriate cationized species in SIMS. Cationization with metals such as silver, commonly observed in SIMS, has now been observed in LD experiments[6], specifically in the case of sucrose, from which $(Ag+M)^+$ can be formed. Cationization promises to become a general method of ion formation in desorption ionization mass spectrometry.

COMPARISONS WITH OTHER DESORPTION IONIZATION METHODS - The recurrent similarity in spectra of complex organic molecules obtained by SIMS, FD, PD, LD, and EHD suggests close relationships between them. Comparisons between SIMS and other methods have been made for biological[6,7] and for organometallic compounds[8]. Using the same quadrupole mass spectrometer and ion optics, a direct comparison between SIMS and LD has been made[9]. The LD spectrum of thiamine hydrochloride is very similar to that obtained by SIMS and other techniques. The spectra of complex quaternary salts can also be compared (Figure 2); similarities are evident, as are some differences (vide infra). The reverse derivatization effect operates in FD[10], as well as in LD[5] and SIMS[5].

A MODEL FOR DESORPTION IONIZATION - Figure 3 summarizes several key elements in a general model of desorption ionization: (i) isomerization of energy deposited at a surface, (ii) a low energy desorption event for preformed ions, (iii) a separate ionization event of variable efficienty for desorbed neutrals, (iv) separability of desorption and ionization from dissociation processes of metastable ions, the major source of fragment ions. Similarities in spectra arise because of the propensity to desorb preformed ions (ii) and the similarities in the metastable ion fragmentations after various DI processes. Differences arise because of different instrumental factors (iv), sample preparation methods (iii), and especially because of a different total energy input (i). Practically, then, for these methods of desorption ionization, the question is not "how" applied energy acts to desorb ions, but rather "how much" energy is applied, and with what spectral effects.

This DI model suggests that desorption is followed by chemical reactions of two types occurring in two distinct regions. First, in the selvedge, fast ion/molecule reactions or electron ionization can occur. Second, in free vacuum, unimolecular dissociations occur, governed by the internal energy of the parent ion, the characteristic time scale of the instrument, and the particular gas phase structure of the ion. These metastable transitions are analogous to those observed in those other forms of mass spectrometry which sample gas phase dissociations. The interaction between the incident primary ion and bulk organic molecules at the surface can be considered as an extension of keV ion-molecule interaction processes which form the basis of the collision induced dissociation process. Thus, the model would suggest that the collision results in an electronic excitation of surface species, followed by a very rapid (10^{-11} sec) isomerization of energy into vibrational modes of excitation.

References

(1) R.J. Day, S.E. Unger, and R.G. Cooks, Anal. Chem., 52, 557A (1980).
(2) S.E. Unger, A. Vincze, R.G. Cooks, R. Chrisman, and L.D. Rothman, Anal. Chem., (in press)
(3) S.E. Unger, T.M. Ryan and R.G. Cooks, Surf. Int. Anal., 3, 12 (1981).
(4) K.L. Busch and R.G. Cooks, submitted.
(5) K.L. Busch, S.E. Unger, A. Vincze, R.G. Cooks, and T. Keough, submitted.
(6) D. Zakett, A.E. Schoen, R.G. Cooks, and P.H. Hemberger, J. Amer. Chem. Soc., 103, 1295 (1981).
(7) L.K.Liu, K.L. Busch, and R.G. Cooks, Anal. Chem. 53, 109 (1981).
(8) J. Pierce, K.L. Busch, R.A. Walton, and R.G. Cooks, J. Amer. Chem. Soc. (in press).
(9) S.E. Unger, K.L. Busch, A. Vincze, and R.G. Cooks, submitted.
(10) T. Keough and A.J. Destefano, Anal. Chem., 53, 25 (1981).
(11) K.L. Busch, S.E. Unger, and R.G. Cooks in A. Benninghoven, ed. "Proceedings of the Conference on Ion Formation from Orgamic Solids, University of Münster, 1980," Springer-Verlag, to be published.

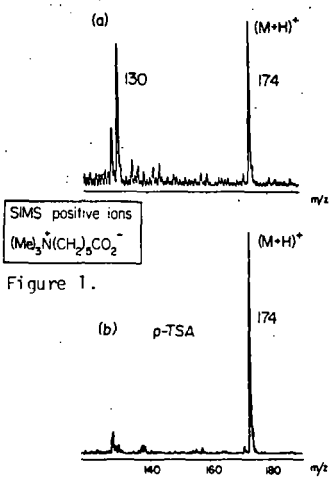

Figure 1.

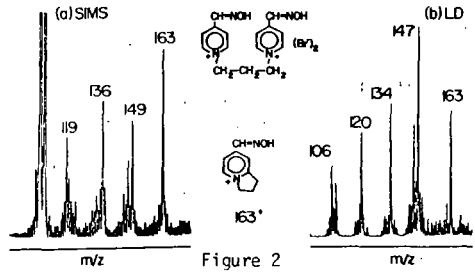

Figure 2

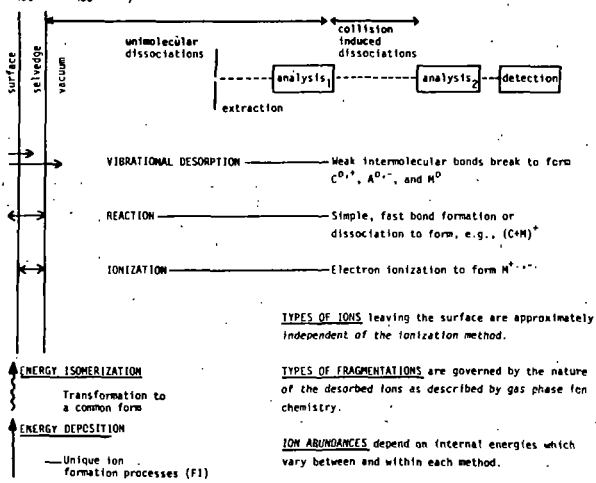

Figure 3

Effect of Energetic Electrons on Breakdown Graphs Determined by Threshold Photoelectron - Coincident Photoion (TPE - CPI) Mass Spectrometry, J. P. Gilman, T. Hsieh and G. G. Meisels Dept. of Chem., Univ. of Nebraska, Lincoln, Nebraska 68588.

The understanding of ion fragmentation processes has been greatly enhanced by TPE-CPI mass spectrometry. This technique permits the study of the chemical fates of ions produced in specifically selected internal energy states; this leads directly to breakdown graphs, which reflect the extent to which competitive ion fragmentation pathways occur as a function of internal energy. In addition, breakdown curves also provide exact branching ratios of all competing fragmentations at a given internal energy; those have been used as a stringent quantitative test of Q.E.T. theory.

In TPE-CPI MS, breakdown curves are usually obtained by time-of-flight analysis of ions that are formed in coincidence with their corresponding zero kinetic energy (ZKE) electrons. Our threshold photoelectron (TPE) detector consists of a collimated hole structure which efficiently transmits ZKE electrons while filtering out most of the energetic ones due to their non-zero transverse velocity component.[1] However, a small but significant number of these non-thermal electrons is still transmitted. If not accounted for these non-ZKE electrons can distort breakdown graphs and lead to false interpretations.

We report here a method to correct breakdown graphs for the false coincidences caused by the transmission of energetic electrons; it relies on convoluting the internal energy distribution of the molecular ion with the transmission function of the TPE detector and the postulated breakdown curve until the experimental and calculated curve match. The internal energy distribution can be represented by the photoelectron spectrum if the energy dependent transmission function of the electron analyzer is narrow. Usually PE Spectrometers using retarding field and deflection analyzers with preacceleration (except for very low energy electrons)[2] show little energy discrimination. The transmission function of the TPE detector has been determined[3], the HeI PES truncated at the photon energy was used to estimate the internal energy distribution.

$$F(E)_{Exp} = \frac{\int_{E'}^{E} P(x)F(x)_{post}\, T(E-x)dx}{\int_{E'}^{E} P(x)T(E-x)dx} \qquad (1)$$

$x = E' \leq x \leq E$; $P(E)$ = photoelectron spectrum; $F(E)_{post}$ = postulated breakdown graph; $T(E)$ = the TPE transmission function; and $F(E)_{Exp}$ = the experimental breakdown graph.

The result of the convolution is shown in figure 1 and the resulting corrected breakdown curves are consistent with those reported by Stockbauer and Inghram[4].

Application of this method to the C_4H_8 isomers are shown in figures 2-4 where the dashed lines indicate the uncorrected breakdown curves and the solid lines indicate the curves corrected for the energetic electrons transmitted. The energy scale is given in terms of the excess energy above the most stable ionic isomer E* where

$$E^* = h\nu + [\Delta H_{X^+} - \Delta H_{B^+}] - IP_X \qquad (2)$$

the enthalpy term refers to the energy released when the ground state isomer X^+ rearranges to the most stable ionic structure B^+ (2-butene).

The corrected breakdown graphs indicate that the four olefinic C_4H_8 isomers (fig. 2) are indistinguishable from each other suggesting that these isomers have completely equilibrated to a mixture of interconverting structures before fragmentation.

However, breakdown graphs of methlcyclopropane (MCP) and cyclobutane (CB) are similar to the olefinic isomers only in a narrow energy region (from onset of $C_3H_5^+$ to 2.6 eV). At higher internal energies, the behavior of MCP and CB is interpreted as a competition between rearrangement to the olefinic structure and fragmentation through a different intermediate.[5]

The results demonstrate that in these cases the energetic electrons transmitted through the TPE detector have a significant contribution on the uncorrected breakdown graphs.

Conversely, if the breakdown graph transmission function and PES curve are known, one can construct a derived PES in the same manner as the corrected breakdown graph. Although similar to a threshold PES, this derived PES represents an integrated PES up to a fixed energy but below the HeI resonance energy (21.21 eV). If the threshold function for the production of two or more states are not step functions, the intensities in the derived PES and HeI PES will be different. A simple model (fig. 5) shows two transitions and the relation between the threshold law, TPES, and the PES.

A derived PES was constructed for CF_3I in the photon energy region 10.00 eV to 11.80 eV (fig. 6) by using known breakdown graphs, PES[6] and again matching the calculated curves with our experimental breakdown curves (fig. 7) by this convolution technique. The intensity of the lowest transition in the derived PES is less than in the HeI PES and greater than in the TPES. Corrections to the HeI PES based on the kinetic energy discrimination in the analyzer (1/E) [2,7] produce only a small change on the spectrum and cannot account for the difference observed between the HeI and the derived PES. This change in intensities is not observed in either propane or the butene isomers which suggests that the difference between the HeI and derived PES in CF_3I may arise from a substantial deviation of threshold behavior from a step function. Therefore, a PES with a photon source below that of the HeI resonance energy and the HeI PES should show a marked intensity difference in the two lowest energy transitions.

We are grateful for the support of the Department of Energy under Contract #DE-AS02-76ER02567 and thank Mr. Pradip R. Das for his assistance in drawing the graphs and Professor J. L. Beauchamp for his suggestions on the CF_3I system.

1. (a) C. F. Batten, J. A. Taylor, G. G. Meisels, J. Chem. Phys. 65, 3316 (1976). (b) C. F. Batten, J. A. Taylor, B. P. Tsai, and G. G. Meisels, J. Chem. Phys. 69 2417 (1978). 2. (a) J. Wayne Rabalais, "Principles of Ultraviolet Photoelectron Spectroscopy", Wiley and Sons, New York, 1977. (b) J. A. D. Eland, "Photoelectron Spectroscopy", Butterworths, London, 1974. 3. T. Hsieh, J. P. Gilman, M. J. Weiss, G. G. Meisels, and P. M. Hierl, Int. Journ. of Mass. Spect. and Ion Phys., 36, 317 (1980). 4. R. Stockbauer and M. G. Inghram, J. Chem. Phys., 65, 4081 (1976). 5. T. Hsieh, J. P. Gilman, M. J. Weiss and G. G. Meisels, J. Phys. Chem. submitted for publication. 6. L. R. Thorne, J. L. Beauchamp, private communication. 7. J. L. Gardner and James R. Samson, Journ. of Electron Spectroscopy & Related Phenomena, 6, 53 (1975).

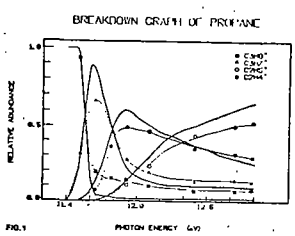

FIG.1

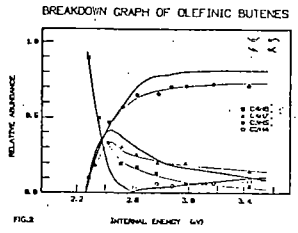

FIG.2

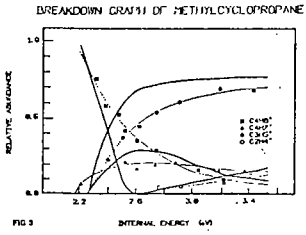

FIG.3

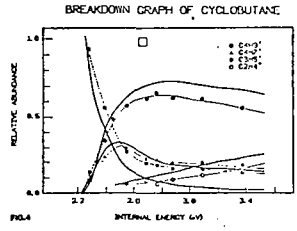

FIG.4

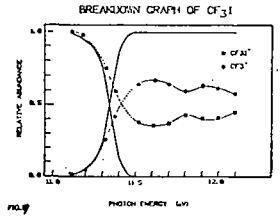

FIG.7

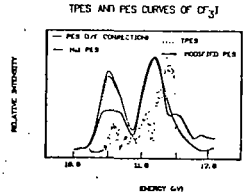

FIG.6

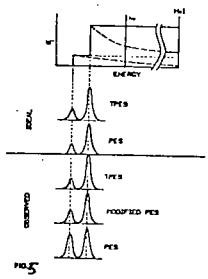

FIG.5

Coincidence Spectrometry Yields an Energetic Model for the Stereoselective Elimination of Acetic Acid in Mass Spectrometers.

Mark M. Green, Department of Chemistry, Polytechnic Institute of New York, Brooklyn, N.Y.; Richard McCluskey, Department of Chemical Engineering, Clarkson College of Technology, Potsdam, N.Y.; JÜrgen Vogt, Physikalisch-Chemisches Institut, Universität Basel, Switzerland.

The rearrangement loss of acetic acid from 2-butyl acetate cation radical exhibits a conformationally reasonable stereoselectivity which parallels the thermal process.(1-6) Figure 1 shows the photoelectron photoion coincidence spectrum for 2-butyl acetate (7-9) for the processes forming m/e 56 (M-HOAc) and m/e 43. (10-12) The data are qualitatively consistent with expectations from theory. (13,14) The literature supports a close correspondence between the nonbonding region of a photoelectron spectrum and the energy deposition on electron impact in that energy region (15-19,20). The thermal energy has been taken into account by convolution of the Boltzmann distribution of s-butylacetate at various ion source temperatures with the breakdown graph for m/e 56 (21-24). Figure 2 shows the ion average energies (Δ) for the various ion source temperatures (0)between 300 and 600 K . Figure 3 shows the energy distribution corresponding to an ion source temperature of 500 K; also plotted is a Boltzmann distribution for neutral 2-butylacetate at 950 K (which has the same average energy) (25,26).

References

1. M.M. Green, J.M. Moldowan, D.J. Hart and J.M. Krakower, J. Amer. Chem. Soc., 92, 3491 (1970); M.M. Green, J.M. Moldowan and J.G. McGrew, II, J. Org. Chem., 39, 2166 (1974). Acetates of varied structure have been the subject of stereochemical investigation: R.N. Rej, C. Taylor and G. Badon, J. Org. Chem., 45, 126 (1980) and early papers in that series.
2. Secondary butylacetate was an early molecular subject for high resolution mass spectrometry. See: J.H. Beynon, R.A. Saunders and A.E. Williams, Anal. Chem., 33, 221 (1961).
3. This regio and stereoselectivity parallels the thermal elimination. See: D.Y. Curtin and D.B. Kellom, J. Amer. Chem. Soc., 75, 6011 (1953); P.S. Skell and W.L. Hall, J. Amer. Chem. Soc., 86, 1557 (1964).
4. E.L. Eliel, N.L. Allinger, S.J. Angyal and G.A. Morrison, Conformational Analysis, Interscience Publ., N.Y., 1965.
5. The idea of utilizing stereochemical observations as a probe of ion structure is discussed in: R.G. Cooks, J.H. Beynon, R.M. Caprioli and G.R. Lester, Metastable Ions, Elsevier Publ., N.Y.p. 206-210.
6. There is a large literature of stereoisomeric observations in mass spectrometry. See: M.M. Green, Topics in Stereochemistry, (Edited by N.L. Allinger and E.L. Eliel) Vol. 9, pp. 35-110, Interscience, N.Y. 1976; A. Mandelbaum, Handbook of stereochemistry (Edited by J. Kagan), Vol. 1, Thieme Verlag, Stuttgart, 1978.
7. B.Brehm and E. von Puttkamer, Z. Naturforsch. 22a, 8 (1967); ibib., Advances in Mass Spectrometry, 4, 591 (1968); J.H.D. Eland, Int. J. Mass. Spec. Ion Phys., 8, 143 (1972); C.J. Danby and J.H.D. Eland, ibid., 153 (1972). See also: J.H.D. Eland, "Specialist Periodical Reports, Mass Spectrometry", Vol.5, The Chemical Society, 1979, Ch. 3; H.M. Rosenstock, R. Stockbauer and A.C. Parr, J. Chem. Phys., 71, 3708 (1979); A.S. Werner and T. Baer, J. Chem. Phys., 62, 2900 (1975): C.F. Batten, J.A. Taylor and G.G. Meisel, J. Chem. Phys., 65, 3316 (1976); R. Stockbauer and M.G. Inghram, J. Chem. Phys.,62,4862 (1975).
8. The coincidence spectrometer utilized here has been described. See: J. Dannacher and J. Vogt, Helv. Chim. Acta, 61, 361 (1978). The branching ratios for m/e 56 and m/e 43 (Figure 1) are closely reproduceable on a threshold photoelectron photoion coincidence spectrometer (unpublished data taken at the National Bureau of Standards). See: A.C. Parr, A.J. Jason and R. Stockbauer, Int. J. Mass Spectrom. Ion Phys., 33, 243 (1980) for leading references and descriptions of this instrument.
9. D.A. Sweigart and D.W. Turner, J. Amer. Chem. Soc., 94, 5592 (1972).
10. The fragmentation mechanism of this molecule cation radical is discussed in: F.W. McLafferty, "Interpretation of Mass Spectra," Second Edition, Benjamin Publishers, 1973, p. 132-135.

11. K. Levsen, Fundamental Aspects of Organic Mass Spectrometry, Verlag Chemie, N.Y., 1978, p. 12-17 and references therein.
12. The electron impact appearance potential for m/e 56 in the mass spectrum of 2-butylacetate is below all other fragments: ca .3 eV (see ref. 13 below), while m/e 43 is the base peak at 70 eV. Thermochemical calculations for: 2-butyl Acetate→acetic acid+$C_4H_8^+$yield ΔH=9.74 eV which is very close to the adiabatic ionization potential. Necessary data from: H.M. Rosenstock, K.Draxal, B.W. Steiner and J.T. Herron, J. Phys. Chem., Ref. Data, 6, Suppl. 1 (1977); S.W. Benson, F.R. Cruickshank, D.M. Golden, G.R. Hangen, H.E. O'Neil, A.S. Rodgers, R. Shan and R. Walsh, Chem. Revs., 69, 279 (1969).

13. M.M. Green, T.J. Mangner, S.P. Turner and F.J. Brown, J. Amer. Chem. Soc. 98, 7082 (1976).

14. These ideas are well discussed in: D.H. Williams and I. Howe, "Principles of Organic Mass Spectrometry," McGraw-Hill, London, 1972, Ch. 4; F.W. McLafferty, "Interpretation of Mass Spectra," 2nd ed., Benjamin, Reading, Mass. 1973, Ch. 8.
15. G.G. Meisels, C.T. Chen, B.G. Giessner and R.H. Emmel, J. Chem. Phys., 56, 793 (1972); G.G. Meisels and R.H. Emmel, Int. J. Mass Spectrom Ion Phys., 11, 455 (1973).
16. A. Katrib, T.P. Debies, R.J. Colton, T.H. Lee and J.W. Rabalais, Chem. Phys. Lett., 22, 196 (1973).

17. S. Trajmar, Acc. Chem. Res., 13, 14 (1980) and references therein.
18. See reference 15 above and M. Inokuti, Rev. Mod. Phys., 43, 297 (1971).
19. See: W.C. Tam and C.E. Brion, J. Electron Spectrosc. Rel. Phenom., 3, 467 (1974); ibid., 4, 139 (1974).
20. Although the overall photoelectron spectrum in Fig. 1 could not be quantitatively correlated with the 70 eV energy deposition function over all ionizing energies. See reference 11 above and: B.N. McMaster, Specialist Periodical Reports, Mass Spectrometry, Vol. 3,The Chemical Society, 1975, p.10-14.
21. W.A. Chupka, ibid. 54, 1936 (1971); 30, 191 (1959); Effective use has been made of the procedures by: F.W. McLafferty, T. Wachs, C. Lifshitz, G. Innorta and P. Irving, J. Am. Chem. Soc., 92, 6867 (1970); D.J. McAdoo, P.F. Bente, III, M.L. Gross and F.W. McLafferty, Org. Mass Spectrom. 9, 525 (1974); P.F. Bente, III, F.W. McLafferty, D.J. McAdoo, and C. Lifshitz, J. Phys. Chem. 79, 713 (1975).
22. All the fundamental frequencies for 2-butylacetate are available in the literature and were treated as harmonic oscillators. See: J.E. Saunders, J.J. Lucier and F.F. Bentley, Applied Spectroscopy, 22, 697 (1968): "CRC Atlas of Spectral Data and Physical Constants of Organic Compounds," J.G. Grasselli and W.M. Ritchey, Eds., 2nd Ed., (1975); L.J. Bellamy, "The Infrared Spectra of Complex Molecules," John Wiley, N.Y., 1958. The density of states calculation followed the algorithm of: T. Beyer and D.F. Swinehart, "Number of Multiply Restricted Partitions," Commun. Assoc. Comput. Machin, 16, 379 (1973). The Boltzmann distributions were calculated for the ion source temperatures reported in reference (13) above and also for various temperatures between 800°K and 1200°K (see below). See W. Forst, "Theory of Unimolecular Reactions" Academic Press, N.Y., 1973, p. 153 for these procedures.
23. W. Forst, "Theory of Unimolecular Reactions," Academic Press, N.Y., 1973, p. 308.
24. The breakdown curve (m/e 56, Fig. 1b) was terminated at 13.0 eV and the branching ratios of m/e 56 (Fig. 1b(o) were multiplied by the corresponding relative intensity of the photoelectron spectrum (Fig. 1a). This yields the ionization deposited internal energy spectrum of the m/e 56 precursors.
25. M.M. Green is grateful to the National Institutes of Health General Medical Sciences and the Petroleum Research Fund administrated by the American Chemical Society for the financial support for this work. We are indebted to T. Mukhopadhyay, and M. Vairamani and L. Bumm for technical help with the experiments.
26. The work in Basel has been supported by the Schweizweischer Nationalfonds zur Förderung der wissenschaftlichen Forschung, Part C 17 of Project No. 2. 212-0.79. Financial support by Ciba-Geigy SA, Hoffman-La Roche & Cie SA, and Sandoz SA, Basel, is gratefully acknowledged.

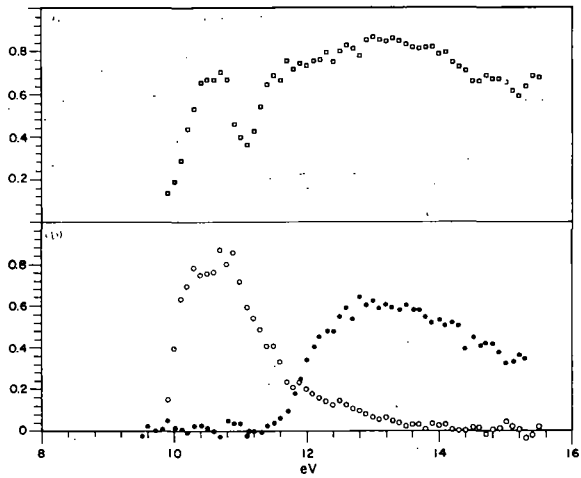

Fig.1 (a) Photoelectron spectrum of 2-butyl acetate measured under same conditions as for the branching ratios in part (b);
(b) Branching ratios for m/e 56 and m/e 43 from 2-butyl acetate. See references 7 and 8 in the text.

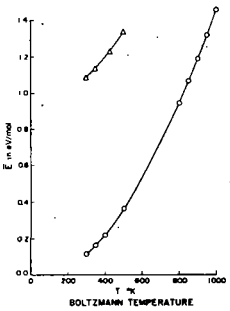

Fig. 2 Average vibrational energy $\bar{E}$ vs. temperature in K. (v) corresponds to computed 2-butyl acetate cation radical energy at various ion source temperatures (see text) and (o) to computed thermal average energies for 2-butyl acetate at various temperatures.

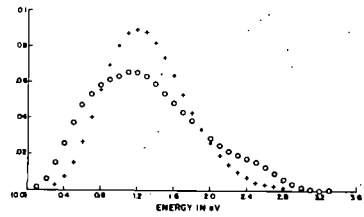

Fig. 3 For both curves: relative probability versus vibrational internal energy (eV on abscissa). (o) corresponds to 2-butyl acetate cation radical in the mass spectrometer ion source[4] held at 500 K and (+) to a thermal distribution of 2-butyl acetate at 950 K. See the text.

MAMOB9

Para-Isotoluene. A New Entry into the $C_7H_8^+/C_7H_7^+$ System. J.J.Gajewski and J.E.Bartmess
Department of Chemistry, Indiana University, Bloomington, IN 47405

Various C_7H_8 isomers have been shown by use of ion-molecule reactions[1] and photodissociation[2] to give non-interconverting radical cations after the primary electron impact event. The $C_7H_7^+$ fragment ion is a mixture of benzylium and tropylium cations, the ratio being a function of the isomer and electron energy. We report here a new C_7H_8 isomer, para-isotoluene, I, synthesized via the scheme.

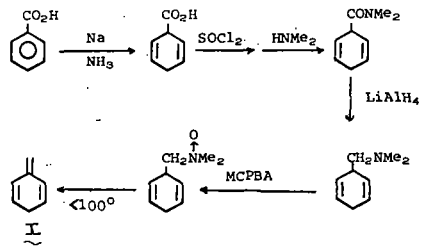

I

An electron impact IP of 8.6 ± .1 eV is found for I. The 70 eV mass spectrum is similar to that of toluene, but with greater fragment ion abundance. The ΔH_f° for I is found by reacting it with successively stronger bases as in reaction 1. The onset for 91^-

$$A^- + \text{isotoluene} \rightarrow AH + 91^- \qquad (1)$$

production in the ICR is at $nPrS^-$ as base, making it 23.5 ± 2 kcal/mole higher in energy than toluene. The 91^- exchanges two protons with D_2O, consistent with the benzyl anion structure. These results put the radical cation of para-isotoluene 15 ± 4 kcal/mole higher in energy than that of toluene, and comparable to that of cycloheptatriene. The lack of reactivity of 92^+ with alkyl nitrates indicates that it is not the toluene radical cation.

The $C_7H_7^+$ formed on electron impact reacts with isotoluene to give 105^+. Using the criteria that the reactive fraction of $C_7H_7^+$ is of the benzyl structure, while the non-reactive part is tropylium,[3] we find that 91^+ here is ca. 96% benzylium at 20 eV electron energy with a slight increase in tropylium at lower energies. This contrasts with 91^+ from toluene which is only 60% benzyl ion under comparable conditions.[3]

The chemistry of the neutral is also different from toluene: isotoluene is protonated by its radical cation readily ($k = 2.2 \times 10^{-10}$ cc-molec^{-1}s^{-1}), while the more stable tautomer is unreactive. Numerous higher mass reaction products are also observed.

(1) Hoffman, M. K.; Bursey, M. M.; Tetrahedron Lett., 1971, 2539-2542.
(2) Dunbar, R. C.; Fu, E.; J. Am. Chem. Soc., 1971, 93, 4354.
(3) Jackson, J. A.; Lias, S. G.; Ausloos, P.; J. Am. Chem. Soc., 1977, 99, 7515-7521.

CHEMICAL PROPERTIES OF THE GAS-PHASE BENZVALENE RADICAL CATION AND OTHER SELECTED C_6H_6 RADICAL CATIONS

D.L. MILLER and M.L. GROSS
Department of Chemistry
University of Nebraska-Lincoln
Lincoln, NE. 68588

The ion structure and chemical properties of the benzvalene (I) radical cation have been investigated using the techniques of Fourier

Transform Mass Spectrometry (FT-MS) and collision spectroscopy (CID). The radical cation reacts with selected reagent neutrals (1,3-butadiene, methyl vinyl ether, etc.), and the resulting ion-molecule reactions have been compared to those produced by reaction of the neutrals with the C_6H_6 radical cations from other sources. Several of these characteristic reactions are shown below. The results of these

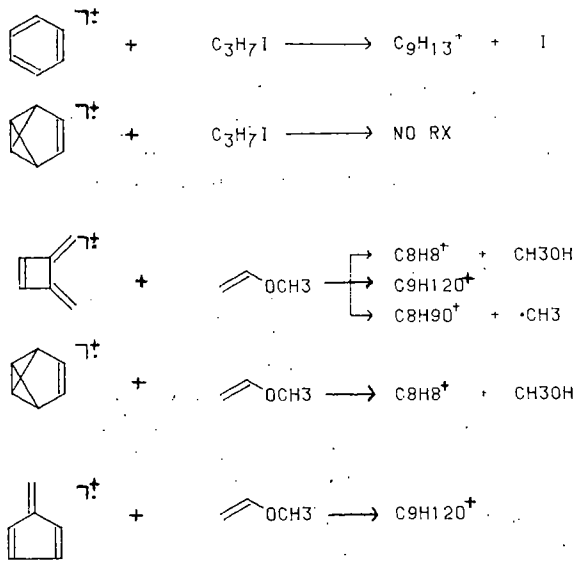

experiments are consistent with the concept that the benzvalene radical cation possesses a unique ion structure at ionizing energies close to the threshold.

The mechanism of one of the characteristic reactions, that with 1,3-butadiene, has been investigated using both C-13 and H-2 labeling. The following reaction mechanism is proposed based on the results of these preliminary studies:

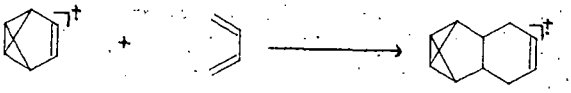

Further labeling studies are underway to confirm the mechanism.

The high energy collisional activation spectra have been taken for benzvalene, benzene, 3,4- dimethylenecyclobutene, and several acyclic C_6H_6 isomers and the spectra compared. Differences are observed which correlate with the low energy ion-molecule reactivities but distinctions are less dramatic as seen in the table.

PARTIAL CA SPECTRA

SOURCE	M/Z							
	63	62	61	52	51	50	39	37
BENZENE	4.4	2.7	1.9	16	28	23	9.0	4.8
2,4-HEXADIYNE	6.9	7.6	5.7	17	24	19	5.8	4.8
DMCB	7.0	3.8	2.4	20	25	19	9.2	4.3
BENZVALENE	1.6	2.8	3.3	37	29	8	2.2	7.0

Finally, the structure of the collision complex produced by reaction of ionized benzene with 2-propyl iodide in the FT-MS was investigated by producing the complex in the chemical ionization source of the MS50-TA and acquiring the high energy collisional activation spectrum of the complex. Comparision of the spectrum of the complex with the spectra of model compounds such as protonated isopropylbenzene, n-propylbenzene, 1,3,5-trimethylbenzene and other isomers show that the complex appears to possess the structure of protonated isopropylbenzene.

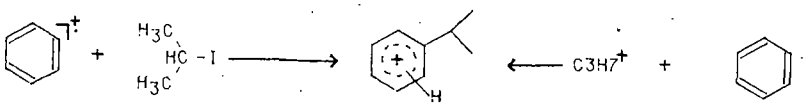

FRAGMENTATION OF THE 2-METHYL-2-PENTENE AND 4-METHYL-2-PENTENE MOLECULAR IONS

A. G. Harrison and K. R. Laderoute

Department of Chemistry
University of Toronto
Toronto, Canada

The 70 eV electron impact mass spectra of 2-methyl-2-pentene and 4-methyl-2-pentene are essentially identical. In addition, both molecular ions show the same metastable fragmentation reactions (90% loss of CH_3, 10% loss of C_2H_4) with identical kinetic energy releases.

In a study of the metastable loss of methyl we have obtained the results for deuterium labelled compounds presented in the Table. The labelled compounds differing only by double bond position show identical behaviour. The major fragmentation reactions in the metastable ion domain involve loss of CH_3 and loss of CD_3 with only a minor loss of the mixed methyls CH_2D and CHD_2. If only intact methyl groups are lost, the loss of CH_3 from the d_3 labelled molecules should equal the loss of CD_3 from the d_6 molecules while the loss of CD_3 from the d_3 compounds should equal the loss of CH_3 from the d_6 compounds. That this is not so can be attributed in part to a kinetic isotope effect; however, the metastable ions for $CD_3CH_2CH{=}C(CD_3)_2$ showed only 70% loss of CD_3 and, surprisingly, 17% loss of CH_3 with 13% loss of mixed methyls. From these results, ignoring the small amount of isotopic scrambling, we derive k_{CH_3}/k_{CD_3} 1.7 and the relative importances of the methyl loss processes, as follows.

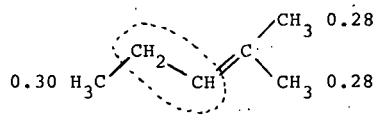

0.15

The equivalence of the two double bond isomers can be rationalized in terms of interconversion through the 1,1,2-trimethylcyclopropane molecular ion intermediate as indicated in the Scheme. This mechanism is supported by preliminary studies of deuterium labelled trimethylcyclopropanes which show metastable ion intensities in agreement with those obtained for the acyclic isomers.

TABLE

Metastable Fragmentation of Labelled C_6H_{12} Isomers

	Methyl lost %			
	CH_3	CH_2D	CHD_2	CD_3
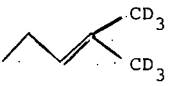	50.3	7.7	7.0	35.0
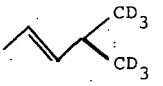	50.3	6.1	8.0	35.6
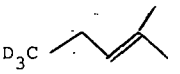	71.4	7.3	4.3	17.1
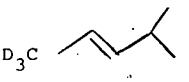	72.6	6.8	4.0	16.5

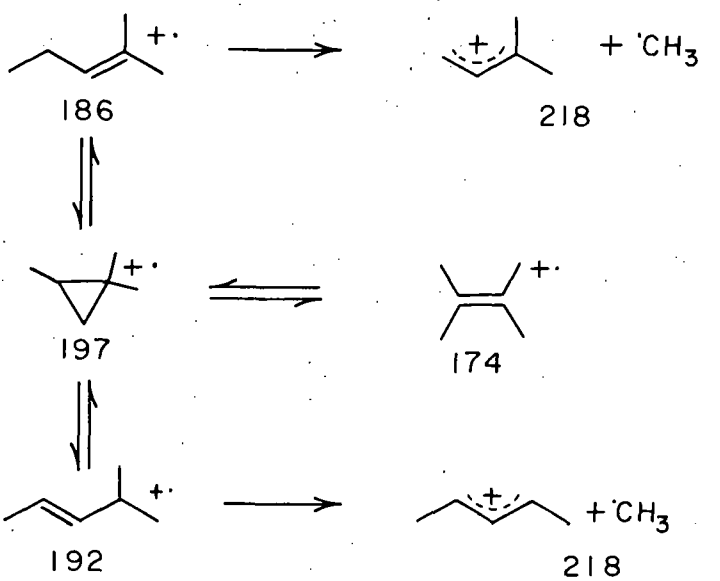

SOME NEW DEFINITIONS OF HIGH TEMPERATURE MASS SPECTROMETRY. RICHARD F. PORTER, Dept. of Chemistry, Cornell University, Ithaca, N.Y. 14853.

Over the past 25 years mass spectrometry has clearly demonstrated its value as an analytical tool for characterization of high temperature chemical reactions. No other technique has been as generally useful for identification of gaseous reaction products and for measurement of their thermodynamic properties. In the first part of this lecture, I will attempt to cite some of the important historical highlights that led to the development of this area of research. In the second part, I will describe some recent investigations in our laboratory which include high temperature ion-molecule reactions, proton transfer reactions involving metal atoms and "high temperature molecules" generated by ion neutralization techniques. Transient neutral species formed in various states of electronic excitation by the reaction

$$RH^+ + M(g) \rightarrow RH^* + M^+ \quad (M = K, Na, Mg \text{ or } Zn)$$

may undergo radiative transition or release internal energy by fragmentation. From measurement of fragmentation energies vertical electron affinities of ions may be obtained. Results for CH_n^+ ions (n = 1-5) will be discussed.

THERMODYNAMIC STUDIES AT HIGH TEMPERATURES BY THE MASS SPECTROMETRIC KNUDSEN CELL METHOD

J. DROWART
Laboratorium voor Fysische Chemie
Vrije Universiteit Brussel
Pleinlaan 2, B-1050 Brussels, Belgium.

Mass spectrometric studies characterizing the gaseous species vaporizing from surfaces or effusing from Knudsen cells were initiated almost thirty years ago. The method has since been applied to the investigation of numerous elemental, binary, ternary and more complex systems in order to identify the components of the gas phase, to measure their partial pressures and to calculate there from either the thermodynamic properties of the gaseous molecules or those of the condensed phases.

Through such investigations, mass spectrometry has contributed much to the quantitative knowledge and to the understanding of chemical bonding, to the elucidation of vaporization processes and of phase relations and to the solution of practical thermochemical problems at high temperatures.

Extended descriptions and discussions of the method have already been given (1-4), while many of the results are included in compendia of thermochemical properties. Reference is made to these publications for details.

Recent studies in the author's laboratory are summarized as follows.

The investigation of the As-O system involved the study of As_4O_6 (arsenolite), of $As_2O_4(s)$, $As_2O_5(s)$, of meta-, pyro- and ortho-uranylarsenate, placed in quartz cells and of mixtures of $PbO(s)$, $Bi_2O_3(s)$ or $Fe_2O_3(s)$ with $As_2O_5(s)$ or ortho-uranylarsenate placed in stainless steel cells. Temperature ranged from 375 K for $As_4O_6(s)$ to 1250 K for the last cited systems. The molecules characterized are $As_4O_6(g)$ above $As_4O_6(s)$ and $As_4O_6(g)$ through $As_4O_{10}(g)$ and O_2, in varying proportions, above the different arsenates. $As_2O_3(g)$, $AsO_2(g)$ and $AsO(g)$ were observed at the highest temperatures. Thermodynamic functions were calculated from known (As_4O_6,g) or estimated molecular parameters; for $As_2O_3(g)$, a trans rather than a eis or a bipyramidal structure was retained. Absolute pressure determinations by quantitative vaporization of weighed amounts of the various initial compositions and metathesis reactions were used to determine reaction enthalpies. The 0 K values, in kcal·mol^{-1} are, for the reactions $As_4O_{6+n}(g) + As_4O_{6+n+2}(g) = 2\ As_4O_{6+n+1}(g)$, for n = 0, -3.6 ± 0.2 and -3.4 ± 0.2; for n = 1, -3.6 ± 0.1 and -3.6 ± 0.2; for n = 2, -4.6 ± 0.4 and -4.0 ± 0.2 by the 2nd and 3rd law respectively; for $As_4O_6(g) + 1/2\ O_2(g) = As_4O_7(g)$, 22.7 and 22.6 ± 0.7; for $As_4O_6(g) + MO(g) = As_4O_7(g) + M(g)$, with M = Bi, 0.0 and with M = Pb, 7.0 by the 3rd law. For the reaction $2\ As_2O_5(s) = As_4O_{10}(g)$, the enthalpy difference at 298 K equals 82.8 and 84.5 kcal·mol^{-1}. The, again 0 K values, are, for $As_4O_6(g) + AsO_2(g) = As_4O_7(g) + AsO(g)$, 1.8 (3rd law), for $As_4O_6(g) = 2\ As_2O_3(g)$, 109.2 (2nd) and 106.6 (3rd law) and for $As_2O_3(g) = AsO(g) + AsO_2(g)$, 86.4 (3rd law) kcal·mol^{-1}. These data lead to $D^\circ_0(O\text{-}As_4O_{6+n}) = 81.6$, 79.8 and 76.0 ± 1.5 kcal·mol^{-1} for n = 0 to 3 respectively. With $D^\circ_0(AsO) = 114.8 \pm 1$ kcal·mol^{-1}, the last three reactions yield 905.4 ± 3 kcal·mol^{-1} for the atomization energy of $As_4O_6(g)$, compared to 908.6 ± 2 kcal·mol^{-1} calculated from the vapor

pressure and the enthalpy of formation of As_4O_6 (arsenolite). The atomization energies for $AsO_2(g)$ and $As_2O_3(g)$ are respectively 198.2 ± 2 and 399.4 ± 3 kcal·mol^{-1}.

The $As_4O_{6+n}^+$ ions undergo metastable transitions, hitherto rarely observed in high temperature mass spectrometry. Their fragmentation is further temperature dependent. For $As_4O_6(g)$ e.g., the parent to $As_3O_4^+$ fragment ion intensity ratio, R, at 20 eV, decreases approximately exponentially from 3.9 at 400 K to 0.9 at 1200 K; $AP(As_3O_4^+)$ varies from 12.7 eV at 400 K to 11.5 eV at 1080 K, but $IP(As_4O_6,g)$ is, within experimental uncertainty, constant at 9.4 ± 0.3 eV. These observations can be interpreted in terms of the theory of unimolecular reactions of positive ions (5), under the assumption that the thermal vibrational energy distribution, P(E), in the neutral molecule is quantitatively transferred during the ionization process and that the energy deposition function, D(y), is, except for its dependence on energy under electron impact, basically given by the photo-electron spectrum (6). To calculate R, the internal energy distribution in the molecular ion, calculated by convolution of D(y) with P(E) was integrated respectively below and above an effective cut-off energy of 13.2 eV, estimated from $AP(As_3O_4^+)$ at 400 K and P(E) at the same temperature. The simplifying assumptions described above, which imply that auto-ionization is not very pronounced, are critically discussed during the lecture. General conclusions are drawn also with respect to the mass spectrometric determination of the thermodynamic properties of complex molecules studied in a wide temperature interval.

In the system Gd-S, known compositions near stoichiometry, mixtures thereof with Gd metal, $Gd_3S_4(s)$ and $Gd_2S_3(s)$, all placed in tungsten cells, were investigated between 1500 and 2400 K. By preferential effusion of Gd(g), the two phase system Gd(l) + GdS(s) changes monovariantly in composition until the hypostoichiometric phase limit, $GdS_{0.75}$, is reached; next the composition moves bivariantly through the $GdS_{1\pm x}$ homogeneity range towards the congruently effusing composition, $GdS_{1.08\pm0.02}$ at 2320 K, where the gas phase is made up of comparable amounts of Gd(g), GdS(g) and S(g). $Gd_2S_3(s)$ effuses preferentially towards $S_2(g)$ at low temperatures, with evolution in composition towards $Gd_3S_4(s)$, which also effuses congruently at 2320 K. At lower temperatures, vaporization of $Gd_3S_4(s)$ is noncongruent and is concluded to lead towards formation of $GdS_{1+x}(s)$, after traversing the $Gd_3S_4(s)$ + GdS(s) two-phase region. Absolute pressures were determined by quantitative vaporization of samples of known weight and composition, which as in an earlier study of EuS(s) (7), made possible i) the determination of the ionization cross section ratios $\sigma(Gd)/\sigma(S)$ and $\sigma(GdS)/\sigma(Gd)$; ii) the calculation of pressures as a function of composition; iii) the determination of the composition at phase limits and at congruency; iv) the measurement of enthalpies of formation and dissociation, in particular $D_0^\circ(GdS)$ = 122.8 ± 1.7 kcal·mol^{-1}. $\sigma(GdS)/\sigma(Gd)$ = 0.65 ± 0.05 at 20 eV indicates, as for several homonuclear and binary diatomic oxide molecules, substantial departure from the additivity of the atomic cross sections.

In view of the particular importance of cross section ratios in thermochemical studies by mass spectrometry, the dependence of this parameter on the nature of the heteroatom was measured for the chalcogenides PbS(g), PbSe(g) and PbTe(g). The results are $\sigma(MX)/\sigma(M)$ = 0.83, 1.03 and 1.46 for X = S, Se and Te respectively.

The reaction SeO(g) + SeS(g) = SO(g) + $Se_2(g)$ was investigated between 1300 and 1800 K to establish the dissociation energy for an oxide in the vicinity of 100 kcal mol^{-1}, to be

used in other metathesis reactions. The reaction enthalpy for the above equilibrium equals -12.7 ± 0.4 (2nd) and -12.6 ± 0.2 (3rd law) and leads, with $D_0^\circ(SO)$ = 123.6 ± 0.1, $D_0^\circ(Se_2)$ = 78.65 ± 0.06 and $D_0^\circ(SeS)$ = 87.7 ± 1.6 to $D_0^\circ(SeO)$ = 101.94 ± 1.5 kcal mol^{-1}. Since a system consisting initially of MnSe(s), EuS(s) and Fe_2O_3(s) was retained for this study, the molecules FeO(g) and MnO(g) were also observed. For the reaction FeO(g) + Se(g) = Fe(g) + SeO(g), the enthalpy difference, at 0 K, equals -5.9 ± 1.2 (2nd) and -5.7 ± 0.2 (3rd law) and yields $D_0^\circ(FeO)$ = 95.9 ± 1.8 kcal mol^{-1}. The 2nd-3rd law agreement could only be obtained with a $X^5\Delta$ electronic state as is at present spectroscopically established (8). The enthalpy difference for the reaction MnO(g) + Fe(g) = Mn(g) + FeO(g) is -8.5 ± 0.4 (2nd) and -7.9 ± 0.2 (3rd law) and gives $D_0^\circ(MnO)$ = 88.0 ± 1.8 kcal mol^{-1}, based on a $X^6\Sigma$ state.

Acknowledgements. The author wishes to express his gratitude to H. Barten and E. Cordfunke (E.C.N., Petten, The Netherlands) and S. Smoes (As-O system); M. De Decker and S. Smoes (monomolecular decomposition of $As_4O_6^+$), K. Reichelt (K.F.A., Juelich, G.F.R.), S. Smoes and A. M. Vander Auwera-Mahieu (Gd-S system), A. Kalashnikov (I.E.T., Moscow, U.S.S.R.) and S. Smoes (PbX systems) and S. Smoes (D_0°(SeO;FeO; MnO)). The author also wishes to thank the Belgian National Fund for Scientific Research (NFWO) for support.

References

1. M. G. Inghram and J. Drowart, in "High Temperature Technology," McGraw-Hill, New York, 1959, p. 219.
2. J. Drowart and P. Goldfinger, Angew. Chem. Int. Ed., 6, 581 (1967).
3. C. Chatillon, A. Pattoret and J. Drowart, High Temp., High Presssures 7, 119 (1975).
4. E. D. Cater, in "Characterization of High Temperature Vapors and Gases," J. W. Hastie, Ed., NBS Special Publ. 561, 1979, p 3.
5. W. Forst, "Theory of Unimolecular Reactions," Academic Press, New York, 1973.
6. E. Diemann, Inorg. Chimica Acta 24, L27 (1977); P. H. Cannington and H. J. Whitfield, J. Electron. Spectrosc. Relat. Phenom. 10, 45 (1977); R. G. Egdell, M. H. Palmer and R. H. Findlay, Inorg. Chem. 19, 1314 (1980).
7. S. Smoes, J. Drowart and J. M. Welter, J. Chem. Thermodynamics, 9, 275 (1977).
8. A. S. Cheung, R. M. Gordon and A. J. Merer, J. Mol. Spectr., in press.

ION BEAM AND ION CYCLOTRON RESONANCE STUDIES OF HIGH TEMPERATURE SPECIES; J. L. BEAUCHAMP, P. B. ARMENTROUT and L. F. HALLE; Dept. of Chem., Calif. Inst. of Tech., Pasadena, CA 91125

An examination of thresholds for endothermic reactions of atomic metal ions with small molecules yields bond dissociation energies for diatomic metal hydride, halide, oxide, nitride and carbide ions. These data are related to bond dissociation energies in the corresponding neutrals by adiabatic ionization potentials for the latter. Metathesis reactions of small metal containing ions studied using ion beam techniques and ion cyclotron resonance spectroscopy provide additional insights into the thermochemical properties and reactivity of these high temperature species. Available data will be summarized and discussed with an emphasis on periodic trends in reactivity and bond energies and their relationship to electronic structures.

MASS SPECTROMETRIC STUDIES OF COMBUSTION PROCESSES; FRED J. KOHL; National Aeronautics and Space Administration, Lewis Research Center, Cleveland, OH 44135

The role of the mass spectrometer in the determination of the reactants and products of various combustion processes is discussed. Most combustion processes take place at near-atmospheric or higher pressures. Because mass spectrometers are inherently low pressure devices, a sample must be extracted from the system under study and transferred to the mass spectrometer for analysis. The transfer must be made in such a way that the chemical integrity of the sample is not altered by the sampling process. Classical methods of sampling have long been employed to determine the concentrations of the major products of combustion--species which are usually permanent gases. More recently, free jet expansion molecular beam sampling has come into wide use. This technique allows the detection and measurement of free radicals, intermediate molecules, ions, condensible high temperature molecules, and other reactive species. Combustion-type applications now have been extended to include studies of rocket propellant systems, internal combustion engines, pollutant formation, coal-dust flames, and chemically inhibited flames. Advances have also been made in the direct sampling of thermal and laser-induced pyrolysis processes. Flames have been used as wall-less containers for the study of chemical equilibria and for the derivation of thermodynamic properties for metal-containing molecules. Considerable effort has been devoted to the sampling of ions in flames in which ion-extraction and focusing present additional complications to the experimental technique. Illustrative examples of the use of free jet expansion molecular beam sampling are given for hydrocarbon flames, metal-containing systems, and special applications.

MAMOC5 PHOTODETACHMENT SPECTROSCOPY; W. C. LINEBERGER, Department of Chemistry and Joint Institute for Laboratory Astrophysics, University of Colorado and National Bureau of Standards, Boulder, Colorado.

The availability of intense tunable and fixed frequency lasers has increased enormously the variety of species which can be studied in cross photon beam-ion beam experiments. Two major experimental approaches have been developed for the study of negative ions: fixed frequency negative ion photoelectron spectroscopy and tunable laser photodetachment/photodissociation spectroscopy. The former technique is best suited for determinations for electron affinities and structural properties of ions and radicals, while the latter provides extremely accurate electron affinities and dynamical information on electron molecule interactions. Utilizing either sputter negative ion sources or electrical discharges in volatile transition metal complexes, we have been able to study a number of transition metal anions, their hydrides and oxides. Results on these high temperature species will be reviewed.

CHIRAL CAPILLARY ANALYSIS OF FREE AND PHOSPHORYLATED CARBOHYDRATES. William R. Sherman and Alan L. Leavitt, Dept. of Psychiatry, Washington University School of Medicine, St. Louis, MO 63110.

Previously reported chromatographic separations of carbohydrate enantiomers have been performed with diastereoisomers prepared with a pure optical isomer of a chiral substance and then separated by conventional GC on packed or capillary columns. A more attractive alternative is the use of GC derivatives chromatographed on a chiral phase since many derivative types are available which form in quantitative yield and the mass spectra of which have been evaluated. Our laboratory wished to determine the chiral composition of the myo-inositol 1-phosphate (MIP) elevated in cerebral cortex of rats upon administration of lithium, a drug used to treat mania. The importance of the chiral analysis lay in the fact that L-MIP is the product of de novo inositol biosynthesis and D-MIP is a product of lipid metabolism, and likely to be meaningful in terms of neural function.
We found that, while hepta-(trimethylsilyl)-DL-MIP was not resolved, penta-(trimethylsilyl) myo-inositol-1-dimethylphosphate was well-separated by capillary GC on the commercially-available Chirasil-Val of Frank, Nicholson and Bayer (e.g., J. Chromatog. 146 197, 1978). Quantitative analysis on the chiral capillary column with a flame photometric detector revealed that lithium, at several dose levels, elevated both enantiomers of MIP, however, the D-isomer was always affected to a much greater degree. This was confirmed by ion monitoring using NH_3 CI GC/MS.
We have found that per-(heptafluorobutyric) esters are the most generally useful for separations of simple sugar enantiomers. DL-Arabinose, -fucose, -xylose, -mannose and -chiro-inositol were all well-resolved in this form by a 20 meter column. DL-Glucose was best separated as the methaneboronate-TMS derivative. However, in general, alkaneboronates, (with trimethylsilyl or acetyl coderivatization, as necessary, were less effective.
Supported by NIH Grants NS-05159 and RR-00954.

THE APPLICATION OF HIGH RESOLUTION GAS CHROMATOGRAPHY/HIGH RESOLUTION MASS SPECTROMETRY TO ENVIRONMENTAL ANALYSIS; J.R. Hass, T.W. COCHRAN and M.-J. Bobenrieth; N.I.E.H.S., P.O. Box 12233, Research Triangle Park, NC 27709

There is at present little argument concerning the advantages of high resolution capillary gas chromatographic columns in comparison to lower resolution packed columns for the analysis of environmental matrices. In contrast, a number of environmental laboratories contend that low resolution mass spectrometers are adequate, especially in combination with high resolution gas chromatography. In this paper we present the results for the analysis of complex samples using high resolution gas chromatography in combination with mass spectrometry at various resolutions ranging from "unit" on a quadrupole instrument to 10,000 on a double-focusing mass spectrometer. The results are critically compared on the basis of reliability of identifications, sensitivity, dynamic range, and the reliability of quantitative results.

ADVANTAGES OF THICK FILM CAPILLARY COLUMNS IN VACUUM OUTLET GC/MS

P.A. LECLERCQ, G.J. SCHERPENZEEL and C.A. CRAMERS
Laboratory of Instrumental Analysis
Eindhoven University of Technology
P.O. Box 513, 5600 MB Eindhoven, Netherlands.

It was recently shown [1,2] that the use of thin-film capillary columns at vacuum outlet has many advantages over the normal operation at atmospheric outlet pressure. It was derived theoretically and confirmed by experiments that the direct insertion of glass or fused silica columns into the ion source of a mass spectrometer can cause an appreciable gain in speed of analysis (inversely proportional to the inlet pressure) without significant loss in separation power under optimum chromatographic conditions.
This paper deals with the application of thick-film columns for vacuum outlet GC/MS. These columns show enhanced resolution and less adsorption, and have higher sample capacity than thin-film capillaries. Drawbacks are that the optimum plate height and the analysis time are increased. It will be shown, however, that the latter drawback, which is solely caused by the increased resistance to mass transfer in the liquid phase, is compensated by the gain in speed of analysis by vacuum outlet operation.

Theory

Band broadening in capillary columns is satisfactorily described by the Golay equation, extended to situations of appreciable pressure drop by Giddings et al. [3-5]. By differentiating this equation with respect to the gas velocity, the minimum value of the plate height, H, and the optimum value of the gas velocity, $\bar{v}$, are found [6].
From these equations for the optimum gas chromatographic conditions, the following equation for the hold-up time, t_o, of the carrier gas can be derived for optimum vacuum outlet conditions [7]:

$$t_o = \frac{3}{2} N \left[C_m \frac{P_i}{P_1} + C_s \right] \qquad (1)$$

In eq. 1 the following symbols are used:
- N is the plate number; N = L/H
- L is the column length
- C_m is the term describing the resistance to mass transfer in the mobile (gas) phase, which is a function of k, r, and D_m [6]
- k is the capacity ratio of a solute
- r is the column radius
- D_m is the diffusion coefficient of a component in the carrier gas at atmospheric pressure

- P_i is the optimum inlet pressure at vacuum outlet operation
- P_l is the atmospheric pressure
- C_s is the term describing the resistance to mass transfer in the stationary (liquid) phase, which is a function of k, d_f, and D_s [6]
- d_f is the film thickness
- D_s is the diffusion coefficient of a component in the liquid phase

Using eq. 1, thick film ($C_m \approx C_s$) and thin film columns ($C_m >> C_s$) can be compared under vacuum outlet conditions. Assuming N and C_m constant (meaning $L_{thick} > L_{thin}$ for a column with r constant, and k is constant, implying operation of the thick film column at a higher temperature than the thin film one) it can be derived that

$$\frac{t_{thick}}{t_{thin}} = \frac{P_{i,thick}}{P_{i,thin}} + \frac{C_s}{C_m}\frac{P_l}{P_{i,thin}} \qquad (2)$$

where t stands for either t_o or the retention time, t_R, of a component: $t_R = t_o(1 + k)$.

By combining the well known Poiseuille equation for viscous flow with the equation for the minimum plate height, it can be derived that

$$P_{i,thin} = P_{i,thick}\sqrt{\frac{\frac{C_m}{C_s}\frac{P_{i,thick}}{P_l} + \frac{2}{3}}{\frac{C_m}{C_s}\frac{P_{i,thick}}{P_l} + 1}} \qquad (3)$$

under optimum vacuum outlet conditions.
A direct comparison of vacuum outlet vs. atmospheric pressure outlet operation of a thick film column is very complicated. However, vacuum outlet operation of a thick-film column can easily be compared with atmospheric outlet pressure operation of a thin-film column.
The gain in speed of analysis for a given thin-film column, operated under vacuum outlet conditions as compared to atmospheric outlet conditions, has been shown to equal [1,2]

$$G = \frac{\bar{v}_{vac}}{\bar{v}_{atm}} = \frac{(P_{i,thin}^2 + P_l^2)^{3/2} - P_l^3}{P_{i,thin}^3} \qquad (4)$$

where $\bar{v}$ is the optimum linear gas velocity: $\bar{v} = L/t_o$.
Theoretically, a loss in column efficiency up to 12.5% can be expected in this case. For a given separation problem, requiring N theoretical plates, the column should be 9/8 longer under vacuum outlet conditions. The gain in analysis time is therefore reduced:

$$\frac{t_{thin,vac}}{t_{thin,atm}} = \frac{9}{8\ G} \qquad (5)$$

Keeping the carrier gas, r, k and N constant (L and the temperature are different) the ratio of retention times for optimum chromatographic conditions is therefore:

$$\frac{t_{thick,vac}}{t_{thin,atm}} = \frac{t_{thick,vac}}{t_{thin,vac}} \times \frac{t_{thin,vac}}{t_{thin,atm}} = \frac{t_{thick,vac}}{t_{thin,vac}} \times \frac{8}{9\ G} \qquad (6)$$

This ratio can be calculated using eqs. 2, 3 and 4.

Results and discussion

Vacuum outlet operation of capillary columns always results in a gain in speed of analysis as compared to the normal use at atmospheric outlet pressure. This is valid, under optimum chromatographic conditions, for both thick and thin-film columns.

The gain in speed of analysis is particularly pronounced for low pressure drop columns with subatmospheric optimum inlet pressures. The use of wide bore and/or short capillaries is therefore recommended.

Vacuum outlet operation of low pressure drop thick-film columns practically always yields even shorter analysis times than atmospheric outlet pressure operation of thin-film columns (N and k constant). It can be calculated that even very thick film columns ($C_m = C_s$) yield such gain if $P_i < 0.6$ bar; if $C_m/C_s = 2$, a gain is already obtained if $P_i < 1$ bar.

As with thin-film columns, the optimum inlet pressures and hence the gain factors of thick-film columns are carrier gas dependent [2].

Experimental data show the validity of the theory. In Fig. 1 the behavior of a thick-film ($C_m/C_s = 5$) and a thin film ($C_m/C_s = 80$) column are compared. It can be seen that the optimum carrier gas velocities of the thick-film column are slightly lower than those of the thin-film one. The expected increase in plate height of the former column is actually a decrease, due to better coating efficiency. Taking this advantageous effect into account, the calculated values of inlet pressure and retention time ratios (eqs. 3, 2 and 6) agree very well with the measured data.

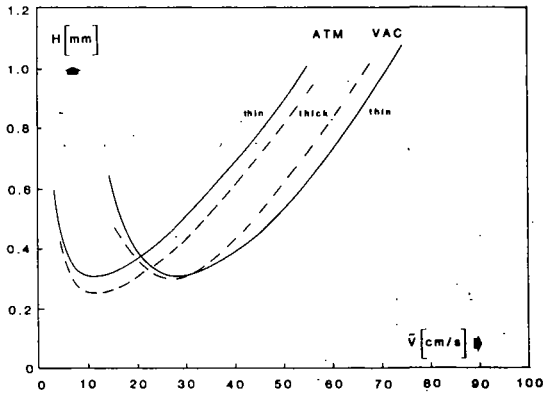

Fig. 1. H. vs. $\bar{v}$ curves of thick (1 µm) and thin (0.4 µm) film SE-30 glass capillary columns (0.4 mm i.d., length 34 m and 30 m, respectively). Carrier gas: N_2. Curves for n-dodecane at 149°C and 127°C, respectively (k = 2.0). Outlet pressures as indicated.

References

1. P.A. Leclercq, G.J. Scherpenzeel and C.A. Cramers, presented at the 28th Annual Conference on Mass Spectrometry and Allied Topics, New York, N.Y., May 25-30, 1980 (Abstracts p. 123).
2. C.A. Cramers, G.J. Scherpenzeel and P.A. Leclercq, J. Chromatogr., 203 (1981) 207.
3. M. Golay, in "Gas Chromatography, 1958", D.H. Desty, ed., Butterworth, London, 1959, p. 36.
4. J.C. Giddings, S.L. Seager, L.R. Stucki and G.H. Stewart, Anal. Chem., 32 (1960) 867.
5. J.C. Giddings, Anal. Chem., 36 (1964) 741.
6. C.A. Cramers, F.A. Wijnheijmer and J.A. Rijks, J. High Res. Chrom. & Chrom. Comm., 2 (1979) 329.
7. C.A. Cramers, G.J. Scherpenzeel and P.A. Leclercq, to be published in J. Chromatogr.

THIS PAGE LEFT
INTENTIONALLY BLANK

POLYCHLORODIBENZODIOXINS AND POLYCHLORODIBENZOFURANS IN ENVIRONMENTAL SAMPLES;
H.R. BUSER; Swiss Federal Research Station, CH-8820 Wädenswil, Switzerland

High-resolution gas chromatography (HRGC) in combination with mass spectrometry (MS) was used to separate and identify polychlorodibenzodioxin (PCDD) and polychlorodibenzofuran (PCDF) isomers, including the extremely toxic 2378-tetra-substituted compounds. Glass capillary and fused silica columns with different stationary phases (OV-101, OV-17, silar 10c) and lengths of up to 50 meters were used. Glass capillary columns were connected to the MS via a platinum or a fused silica interface; fused silica columns were connected directly with the column and leading into the ion source. The quadrupole MS was operated in the electron-impact (EI) or negative ion chemical ionization (NCI) mode. Complete or partial mass spectra were recorded using a data system. Mass specific detection was carried out in the analog mode. These analytical techniques were used to study the separation and occurrence of all 22 tetrachlorodibenzodioxins (TCDDs) and other PCDDs and PCDFs at parts-per-trillion (ppt) levels in a variety of samples including fish tissue samples from several American rivers, human tissue and human blood samples as well as environmental samples from known contaminated areas.

HIGH RESOLUTION GAS CHROMATOGRAPHY - NEGATIVE CHEMICAL IONIZATION MASS SPECTROMETRY OF INDOLEAMINES. P. L. Taylor and S. P. Markey. Laboratory of Clinical Science, National Institute of Mental Health, Bethesda, Maryland 20205

The theoretical advantages of capillary columns for GCMS analysis of biological compounds are well known. The increased resolution and low sample adsorption of these columns should provide a significant improvement in performance compared with that of packed columns. In practice, however, the fragility of glass columns and the difficulties encountered in interfacing with existing GCMS systems has precluded their widespread adoption by the analytical community. The recent introduction of flexible fused silica columns has considerably simplified problems of handling and interfacing, and we are now able to report our experiences in the adaptation of three assays, previously performed on packed columns to high resolution capillary chromatography.

The three compounds which we wish to analyze are the putative pineal hormone melatonin, its urinary metabolite 6-hydroxymelatonin, and the neurotransmitter serotonin. The extraction and derivatization procedures for the assay of these compounds by negative chemical ionization GCMS have been described previously (1-3). The three analytes show circadian rhythms, and in order to investigate the phase relationships between these rhythms it is frequently necessary to analyze large numbers of samples from a single subject. In the cases of melatonin and serotonin extremely low levels (1-10 pg/ml) are present at some parts of the cycle, and in addition very limited amounts of biological fluids such as human cerebrospinal fluid are available. A suitable analytical method should therefore be able to detect < 1 pg per sample. Interference from other compounds present in the biological matrix is a persistent problem, and although the specificity conferred by the existing NCI-GCMS method is excellent, further improvement would be useful. The general requirements for the method are therefore as follows:

1. High sensitivity - minimum sample loss.
2. High resolution - ability to discriminate against interfering compounds.
3. Short retention time - high throughput.
4. Constant retention time - certainty of peak identification.

The configuration which we adopted initially is shown in Fig. 1. The requirement for minimum sample loss precluded the use of an inlet splitter, and the requirements for a short and constant retention time implied the use of high temperature isothermal column operation. This in turn ruled out the use of on-column injection. We therefore adopted a solid injection system of the dropping needle type. The rejection of the injection solvent provided by this technique simplified the problems of interfacing at the downstream end of the column, which was inserted directly into the MS source via a 1/8" dia stainless steel tube equipped with a T joint through which the methane reagent gas was coaxially introduced. The Finnigan 1015 quadrupole mass spectrometer was operated in the NCI mode under conditions similar to those described previously (1-3).

Initial results obtained with this system were disappointing, in that isothermal operation of the column at high temperatures gave poor peak shapes with severe tailing, although results were good when temperature programming was employed. In addition, further deterioration of performance occurred as the needle became dirty and the fragile tip chipped. The injection system was therefore modified to incorporate the principle of thermal focussing, by raising the whole assembly clear of the column oven, leaving a 50 mm length of the column exposed to the air. A moveable heater was fitted as shown in Fig. 2. The injection sequence with this apparatus is as follows. With the needle and heater raised, sample (1-10 µl) is injected onto the tip of the needle. Solvent evaporates and is carried away by the carrier gas via the restriction at the top (Fig. 2,1).

The needle is then lowered into the heated area (Fig. 2,2) and the sample evaporates and condenses in the unheated section of the column. The heater is then lowered, heating the cold trap rapidly and releasing the sample onto the rest of the column (Fig. 2,3). This system gave excellent peak shapes at all column temperatures, and was completely indifferent to the condition of the needle tip.

The properties of three commercially available columns have been investigated in this system, and the plot of N against inlet pressure (Fig. 3) with serotonin-acetate/PFP derivative as the analyte shows the results. Practical retention times ranged from 2 to 7 minutes depending on column and analyte. In general, the wider bore

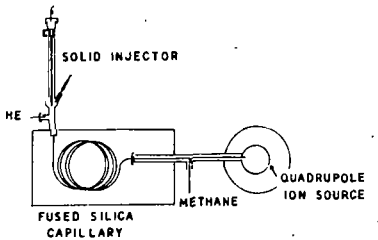

Figure 1

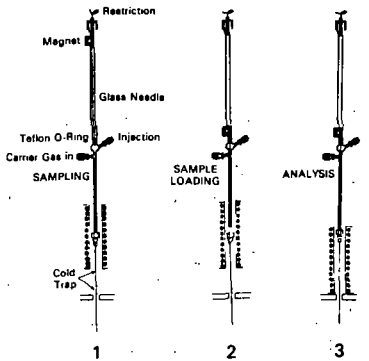

Figure 2

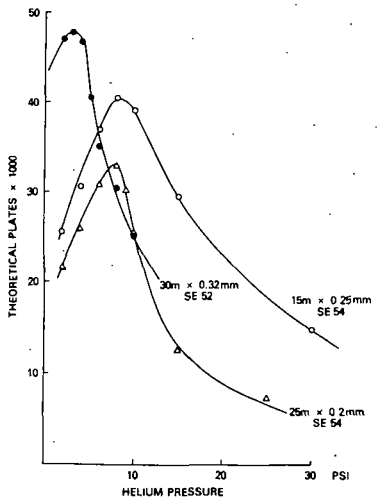

Figure 3

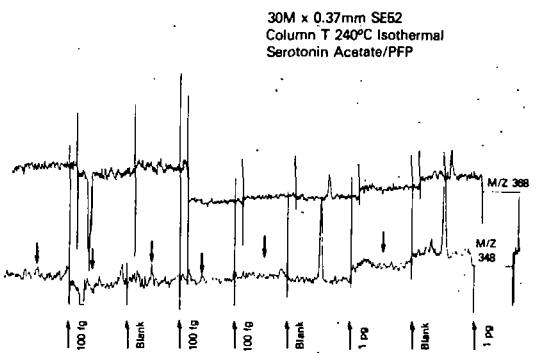

Figure 4

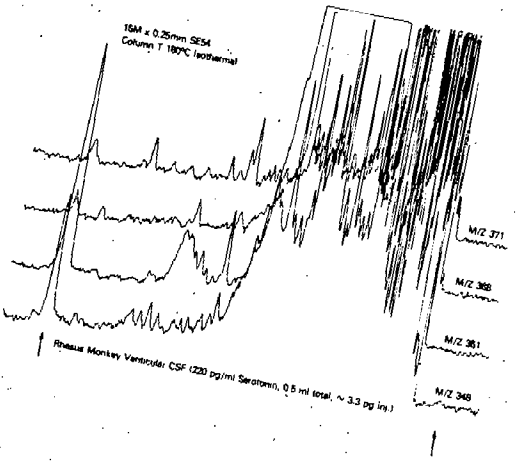

Figure 5

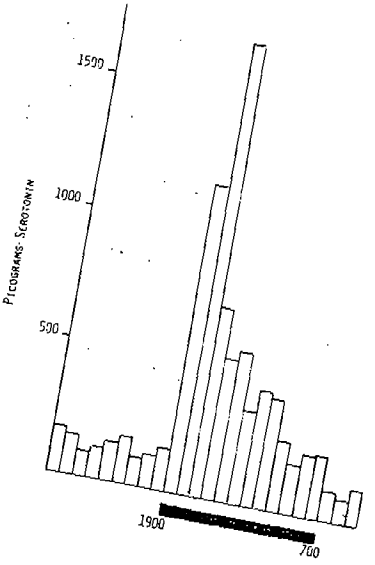

Figure 6

column gave the best results, with regard to both high resolution and low retention time, although some problems were encountered with the inlet system when operating at very low pressures, as the dropping needle injector requires a positive flow of helium upwards to remove the solvent and prevent air entering through the vent. This problem also ruled out the use of hydrogen as the carrier gas, as in this case negative inlet pressures would be required for optimum resolution.

Maximum resolution obtainable under these conditions is considerably lower than that claimed by the column manufacturers, partly because of the nature of the analyte and partly because the tail end of the column was operated under vacuum. We have investigated the use of an open split interface (4) to overcome the latter problem, and although this device increased the available resolution by about 20%, sensitivity under optimum conditions was reduced by 70% compared to that obtained with the direct connection.

Experience with these compounds using packed columns suggests that best results are obtained using "medium polarity" stationary phases such as OV17 and OV225. Unfortunately, fused silica columns with these phases are not available at present, and the SE52 and SE54 phases which we have been using have proved inadequate to separate melatonin from interfering compounds present in human blood extracts. Although the minimum detectable quantity of melatonin was 2-5 times lower on the high resolution capillary system than with a packed column, plasma samples could not be satisfactorily analyzed on the capillary column due to the quantity of plasma extract which had to be applied, and the deleterious effect of that mass of material on the resolution of the column. In contrast, a long (5 M x 2mm) conventional column packed with 1% OV225 could easily provide the separation and capacity required for melatonin analysis. In the case of 6-OH-melatonin in human urine the high levels of the analyte and relative freedom from interfering compounds simplify the chromatography, and while capillary columns gave excellent results there was no clear evidence of improvement compared with results obtained from the packed column. The technique has proved most useful in the measurement of serotonin in human and Rhesus monkey cerebrospinal fluid. Ultimate sensitivity towards serotonin is high, as shown in Fig. 4, where successive injections of standard of 1 pg or 100 fg interspersed with blanks were made. Ions were monitored at two masses, M/z 348 and 368 corresponding to M^- - HF and M^- - 2HF. In Fig. 5 a biological sample is shown. Here, ions corresponding to the deuterated internal standard were also monitored. Using this technique we have demonstrated the presence of a marked diurnal variation in serotonin levels in Rhesus monkey cerebrospinal fluid (Fig. 6).

In summary, the improvement in performance expected from the substitution of high resolution capillary columns for packed columns in the GCMS measurement of indolealkylamines has only been obtained in one out of three assays studied. Further improvements may, however, be expected as the range of stationary phases available from the manufacturers of the columns is extended.

References

1. Lewey, A.J. and S.P. Markey, Science 201, 741 (1978).
2. Tetsuo, M., S.P. Markey, R.W. Colburn and I.J. Kopin, Anal. Biochem. 110, 208 (1981).
3. Markey, S.P., R.W. Colburn and J.N. Johannesson, Biomed. Mass Spectrom. in press (1981).
4. Henneberg, D., U. Henrichs, H. Husmann and G. Schomburg, J. Chromatog. 167, 139 (1978).

APPLICATION OF CAPILLARY COLUMN GCMS WITH LOW RESOLUTION ACCURATE MASS MEASUREMENT TO THE ANALYSIS OF HUMIC ACID DEGRADATION PRODUCTS.

D. S. Millington and D. Norwood
Department of Environmental Sciences and Engineering
University of North Carolina
Chapel Hill, N.C. 27514

Humic substances are believed to be the end-products of a general, natural metabolic process involving oxidation and polymerization of biologically degraded lignin. As they occur in aquatic systems, these substances, which account for most of the organic content (both natural and anthropogenic), can be broadly subdivided into two subcategories: a combined humic-hymatomelanic acid (HA) fraction that precipitates at pH 2 and a soluble fulvic acid (FA) fraction, which forms the bulk of the dissolved humic material. Our studies have centered on the isolation, purification and controlled oxidative degradation of HA and FA and on the identification of the products, using GC/MS as the primary analytical tool. The major goals are to provide a background of data for assessment of possible health hazards due to the treatment of drinking water and to shed more light on the chemical nature of humic substances.

Experimental

The procedures for isolation of humic material from a natural source (Black Lake, Elizabethtown, N.C.) and its reaction with chlorine and permanganate have been described previously.[1,2] After methylation using distilled ethereal diazomethane, oxidation products were analyzed by GC/MS using a HP-5710A gas chromatograph/VG-Micromass 7070F double focussing MS/VG-Datasystems 2035 Computer Combination. Separations were performed on either a 50m Applied Science "Quadrex" glass OV-17 coated capillary column or a 25m Hewlett-Packard "fused-silica" SP2100 column. A grob-type injector was employed, operated usually in "split" mode. The reactant gas used for CI was isobutane. Accurate mass determinations (around ±15 ppm RMS) were performed at a scan rate of 1.5s/decade and a resolution of ~1500 using tetraiodoethylene as the internal calibrant, by a technique previously published.[3]

Results and discussion

The TIC chromatogram from an exhaustive permanganate oxidation of HA is shown in Figure 1. The main compounds identified are straight (and some branched) chain fatty acid methyl esters, a series of aliphatic diesters with terminal carboxyl groups and a large number of one-ring aromatic esters. All isomers of benzene mono, di, tri, tetra, penta and hexacarboxylic esters were identified. Most of these have been verified by comparison of GC retention and MS data with those of authentic samples. Another prominent series of aromatic esters, indicated by the ? symbol in Figure 1, was also observed and interpreted as derivatives of mono-α-keto benzenecarboxylic acids. The lowest molecular weight member has been positively identified as phthalonic acid dimethyl ester. Interpretation of these structures was greatly aided by the CI spectra (see Figure 2) and by prior knowledge that $KMnO_4$ plus napthalene gives phthalonic acid in high yield.[4] These compounds have not been previously reported as oxidation products of humic material and constitute the first evidence for the possible existence of fused-ring structures in the humic acid macromolecule.

Chlorine has also proved to be an effective degrader of humic acid, producing a

Figure 1. DEGRADATION PRODUCTS OF HUMIC ACID ANALYZED BY GC-MS

o monobasic aliphatic ester series

▼ ω-dibasic aliphatic ester series

shaded peaks - aromatic esters

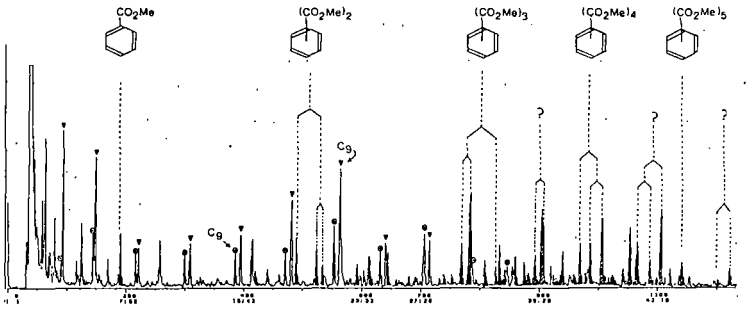

similar distribution of compound types to those generated by permanganate oxidation plus a number of chlorinated aliphatic acids. The TIC chromatogram of components separated on SP2100 is shown in Figure 3. The major products, eluting early in the chromatogram, are dichloro- and trichloroacetic acid methyl esters. Other prominent components are dichlorosuccinic, maleic and fumaric acids. These were easily identified from the CI and accurate mass data (see Figure 4 for example). A complete list of the degradation products will be published,[5] showing the status of component identification to be about 80% complete, most of the remainder being minor components.

Figure 2.

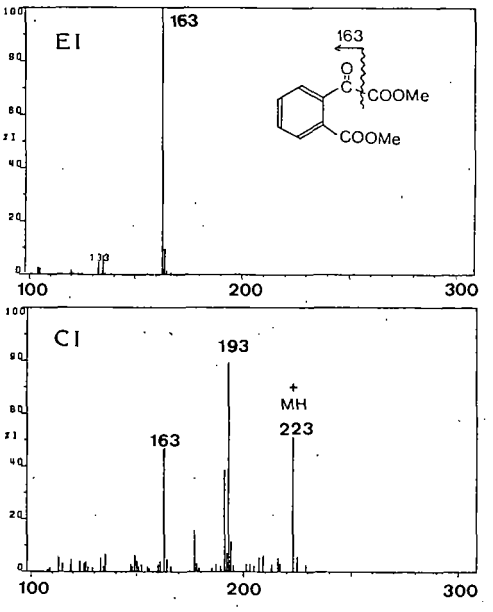

Conclusions

A powerful analytical technique for analysis of degradation products of humic material has been developed. Three major factors have contributed to the success of this method

Figure 3.

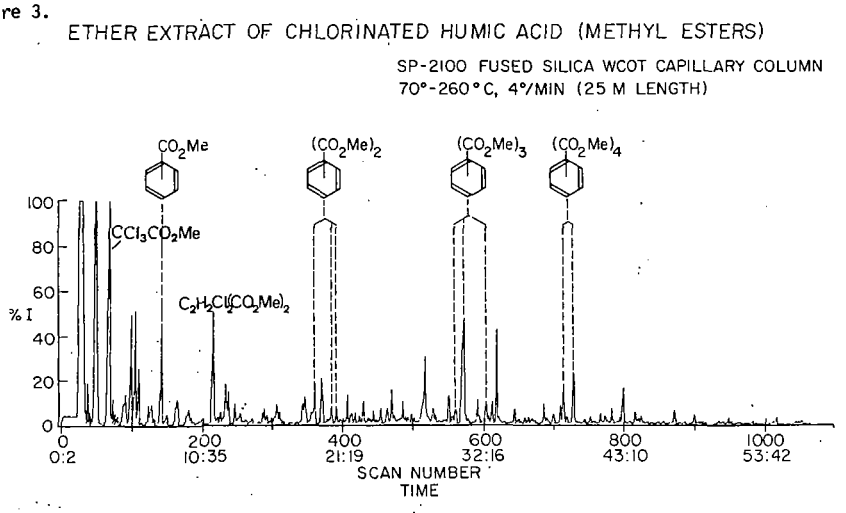

Figure 4.

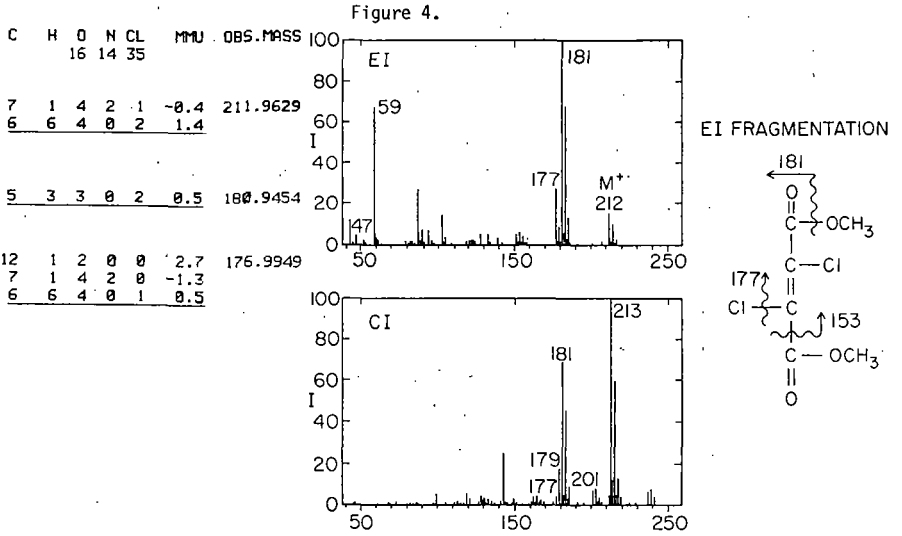

for component identification:

(1) The use of fused-silica capillary GC columns, replacing the standard packed columns employed in an earlier study, has more than trebled the number if identifiable products (Table 1).

Table 1. SUMMARY OF COMPONENTS DETECTED BY GC/MS

	Packed	Capillary
Aliphatic mono-esters	5	21
Aliphatic di-esters	5	11
Aromatic esters	15	24
Chlorinated compounds	15	15[1], 36[2]
Others	0	38[2]

[1] OV-17

[2] SP-2100

(2) The ability to employ scan rates compatible with the sharp elution profiles of the capillary GC peaks using a double focussing MS has enabled realization of the full potential of the equipment.

(3) The routine acquisition of accurate mass data without compromise to the sensitivity or scan speed, made possible by the low resolution technique, enables the determination of elemental composition of components. This vital additional information has been the most valuable interpretative aid, enabling the identification of many more components with greater confidence than is currently feasible using nominal mass spectral data with library search techniques.

References

1. R. F. Christman, J. D. Johnson, F. K. Pfaender, D. L. Norwood, M. Webb, J. R. Hass and M. J. Bobenreith, "Water Chlorination: Environmental Impact and Health Effects," Vol. 3, R. J. Jolley et al., eds., Ann Arbor Science Pub., Ann Arbor, 1980, 75-83.

2. R. F. Christman, W. T. Liao, D. S. Millington and J. D. Johnson, ACS Symposium, Las Vegas, 1980 (to be published).

3. P. Powers, P. H. D'Arcy, J. C. Bill and M. J. Wallington, Proceedings of the 26th ASMS Conference, St. Louis, 1978, p. 480.

4. J. H. Gardner and C. H. Naylor, Org. Syn. Coll. 2, 523 (1943).

5. J. D. Johnson, R. F. Christman, D. L. Norwood and D. S. Millington, Health Effects Symposium, Cincinnati, 1981 (to be published).

MASS SPECTROMETRIC OBSERVATIONS OF THE OXIDATIVE FATE OF CARBON COMPOUNDS OVER HEATED COPPER (II) OXIDE; George M. Wood, Billy T. Upchurch*, Ronald F. Hoyt, Patricia A. Paulin, and Edwin L. Wildner**; NASA, Langley Research Center, Hampton,VA 23665

The use of copper (II) oxide for the oxidation of organic compounds and the subsequent determination of their carbon, nitrogen, and hydrogen composition dates to Gay-Lussac and Thenard in 1811[1]. Historically, these oxidative processes have been carried out under high temperature conditions which assured complete oxidation of almost any organic compound[2]. We have observed the oxidative process for a number of compounds as a function of temperature ranging from ambient to that necessary for complete oxidation. Additionally, we have used isotopic labeling of the reaction products to examine the oxidation process for several saturated and unsaturated low molecular weight compounds; to observe the decarbonization process in stainless steel; and to study the exchange of oxygen atoms between those of copper (II) oxide and of carbon monoxide, carbon dioxide, and labeled oxygen.

These measurements were obtained by flowing gas mixtures through a packed heated quartz or stainless steel tube, with the effluent directly input through a capillary inlet into the ion source region of a modified CEC 21-104 mass spectrometer[3]. Isotope exchange studies with the labeled oxygen on the copper (II) oxide revealed that oxygen exchange between the CuO^* and gaseous oxygen did not proceed below 775°C, the temperature around which CuO begins to be transformed to Cu_2O with the evolution of oxygen[4]. It was further observed that the oxygen in carbon dioxide did not exchange with the labeled CuO^* below approximately 500°C. Oxidation of carbon monoxide on the other hand was observed to result in complete transformation of CO to monolabeled CO_2^* at temperatures near 225°C (fig. 1). Isotopic scrambling of the CO_2^* composition was observed at temperatures above 500°C; however, it has not yet been determined if part or all of this results from instrumental artifacts.

The oxidation of a series of low molecular weight alkanes was accomplished on unlabeled CuO by passing a mixture of the alkane and an inert gas over the heated substrate at a fixed mass flow rate. By monitoring the alkane depletion and the CO_2 evolved, the conversion to CO_2 and H_2O was mass spectrometrically determined as a function of temperature. It was found methane was not completely oxidized until the temperature exceeded approximately 750°C (fig. 2). Oxidation of the remaining C_1-C_6 alkanes show a progressively decreasing temperature for complete oxidation with increasing carbon number (Table 1). Several alkenes, alkynes, and benzene were also tested with CuO. Single mass monitoring demonstrated a desorption of the alkene from the substrate as the temperature was increased. Desorption was essentially completed prior to the onset of oxidation, which then proceeded in a manner similar to the alkanes (fig. 3). The alkynes and the benzene desorption bulge was more pronounced, but was also completed prior to the onset of oxidation to CO_2, with maximum evolution occurring at considerably lower temperatures than for the corresponding alkanes. The oxidative conversion efficiency to CO_2 was observed to decrease with further increases in temperature (fig. 4), while at the same time the alkyne or benzene concentration continued to decrease towards zero. This suggests that decomposition and/or polymerization processes are effected at the higher temperature, yielding products, such as methane or ethane, that are less efficiently converted to CO_2. The apparent lack of a clear temperature-carbon number relationship also suggests that the conversion processes for unsaturated hydrocarbons on CuO are more complex than for the saturated.

CONVERSION TEMPERATURES FOR OXIDATION TO CO_2 OVER CuO, °C

Carbon #	ALKANES		ALKENES		ALKYNES		OTHER		
	10%	100%	10%	100%	10%	100%	10%	100%	
1	575	760					135	225	Carbon Monoxide
2	455	630	225	425	200	325			
3	365	550	250	350	310	425			
4	330	525	260	360					
5	310	475							
6	225	450					220	310	C_6H_6

TABLE 1

1. Wilson, N. H., "An Approach to Organic Chemical Analysis," Pergamon Press, NY (1966)
2. Nierderl, J. B. and Nierderl, V., "Org. Quantitative Microanal.," John Wiley, NY (1938)
3. Wood, G. M., Upchurch, B. T. and Hughes, D. B., Paper H-10S, 23rd An. Conf. Mass Spec., Houston (1975)
4. Haag, G., "Gen. and Inorg. Chem," John Wiley, NY (1969); pp. 218, 753

* Old Dominion Univ., Norfolk, VA 23508; **Consultant, 4 Merry Terrace, Newport News, VA 23606

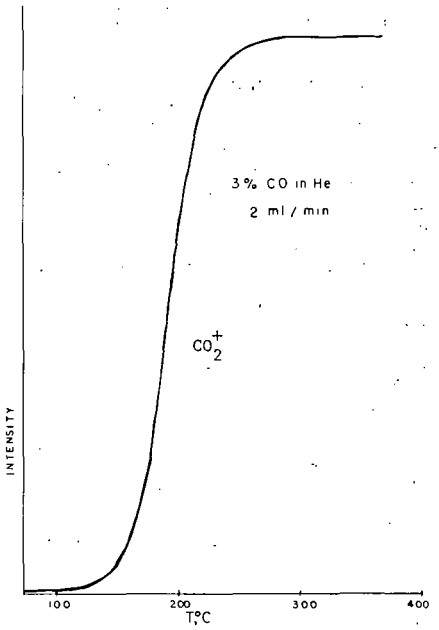

1. OXIDATION OF CARBON MONOXIDE ON CuO

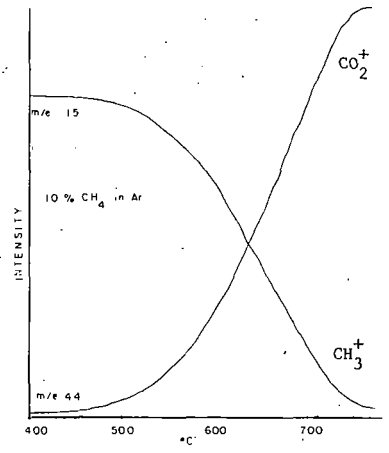

2. OXIDATION OF METHANE ON CuO

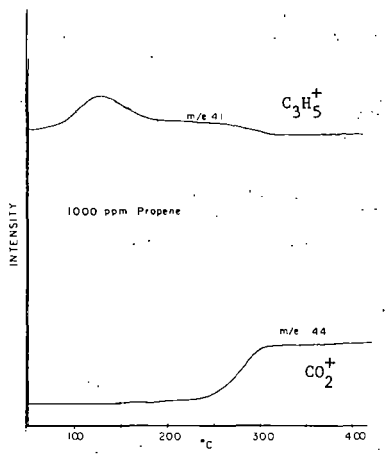

3. OXIDATION OF PROPENE ON CuO

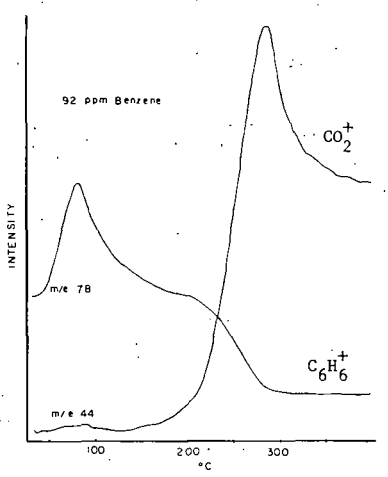

4. OXIDATION OF BENZENE ON CuO

GAS PHASE NITRATION AND NITROSATION OF AROMATIC RADICAL CATIONS

Robert J. Schmidt, D. S. Ross and S. E. Buttrill, Jr.
Mass Spectrometry Development Program
SRI International Menlo Park, CA 94025

The mechanism of aromatic nitration in solution is generally thought to involve the following five steps:

$$H^+ + HNO_3 \rightleftarrows H_2NO_3^+$$

$$H_2NO_3^+ \rightleftarrows NO_2^+ + H_2O$$

$$NO_2^+ + ArH \rightarrow ArHNO_2^+(\pi)$$

$$ArHNO_2^+(\pi) \rightarrow ArHNO_2^+(\sigma)$$

$$ArHNO_2^+(\sigma) + B \rightarrow ArNO_2 + BH^+$$

Recently Perrin[1] has suggested that the nitration itself involves the initial oxidation of the aromatic (ArH) by NO_2^+ to an aromatic radical cation followed by the reaction of the radical cation with neutral NO_2.

$$NO_2^+ + ArH \rightarrow ArH^{+\cdot} + NO_2 \qquad ArH^+\cdot + NO_2\cdot \rightarrow ArHNO_2^+(\sigma)$$

This reaction is postulated to produce directly a sigma complex which subsequently looses a proton to a convenient base (e.g. a solvent molecule). Perrin's mechanism bypasses the formation of an intermediate π-complex. From the point of view of gas phase ion chemistry, it is quite reasonable, since the ionization potentials of all aromatic hydrocarbons are less than the ionization potential of nitrogen dioxide.

Additional interest in the mechanism of gas phase aromatic nitration is aroused by the recent results of Reents and Freiser[2] on the gas phase nitrosation of benzene. They formed a benzene-NO^+-complex by each of the following reactions:

$$CH_3ONO^+ + C_6H_6 \rightarrow CH_2O + C_6H_6NO^+$$

$$CH_3ONONO^+ + C_6H_6 \rightarrow CH_3ONO + C_6H_6NO^+$$

$$C_6H_6^+\cdot + CH_3ONO \rightarrow C_6H_6NO^+ + CH_3O\cdot$$

They demonstrated on the basis of its photodissociation spectrum and ion chemistry that the $C_6H_6NO^+$ product of these reactions was a π-complex and was distinctly different from the ion formed by protonating authentic nitrosobenzene.

We have used the apparatus described in Paper PAMOC5 of this conference to study the mechanism of the gas phase nitrosation and nitration of aromatic radical cations. In a mixture of benzene and NO which is ionized by the pulsed argon resonance lamp to produce only benzene molecular ions and NO^+, the dominant product at long reaction time is $C_6H_6NO^+$ formed by the reaction

$$(C_6H_6)_2^+ + NO \rightarrow C_6H_6NO^+ + C_6H_6$$

A trace amount of pyridine added to the reaction mixture leads to the results shown in Figure 1. The $C_6H_6NO^+$ ion does not transfer a proton to pyridine, even at the longest reaction times. This result demonstrates that even in the high pressure mass spectrometer with tens of thousands of collisions, the π-complex does not rearrange to a sigma bonded structure. Our results simply confirm and extend those of Reents and Frieser by shown that the benzene NO^+ complex formed directly from NO at high pressures has the same structure as the ion which they formed by bimolecular processes at the much lower pressures of their ICR mass spectrometer.

The results for the gas phase nitration of aromatic radical cations are completely different from the nitrosation case. Previously Dunbar, et al.[3] showed that NO_2^+ could be transferred to neutral aromatic molecules by the following reaction.

$$CH_2ONO_2^+ + ArH \rightarrow ArHNO_2^+ + CH_2O$$

No attempt was made to determine the structure of the ion product formed. Ausloos and Lias[4] observed the formation of this ion by NO_2^+ transfer from ethyl nitrate. In addition, they found that NO_2^+ reacted directly with aromatic hydrocarbons by transferring an oxygen aromatic ion in the low pressure ICR mass spectrometer.

In the pulsed photoionization high pressure mass spectrometer, we have confirmed the oxygen ion transfer reaction for several aromatic hydrocarbons including benzene, toluene, and xylene. However, we find that the gas phase oxidation (charge transfer) of aromatic hydrocarbons by NO_2^+ is always much faster than the O+ transfer reaction.

Figure 2 shows the results of a time resolved study of a mixture of benzene-d_6, nitrogen dioxide, and a trace amount of pyridine in a 10 torr helium carrier gas. This mixture is photoionized by the pulsed argon resonance lamp so that the only ions produced initially are the benzene radical cation and a small amount of NO_2^+.

In a π-complex between $C_6H_6^{+\cdot}$ and NO_2 the aromatic character of the hydrocarbon is retained; none of the ring hydrogens becomes acidic. In constrast, formation of a sigma complex in which nitrogen is bound to carbon results in one of the ring hydrogens becoming acidic. The least acidic sigma complex would be the one with the most stable structure, protonated nitrobenzene. Therefore, any sigma complex should be capable of transferring a proton to substances more basic than nitrobenzene. The observation of D^+ transfer from the complex formed between the benzene-d_6 radical cation and NO_2 to pyridine shows that this species is a sigma bonded structure.

There is a striking difference between the gas phase reactions of aromatic radical cations with NO and NO_2. The gas phase nitrosation product is formed exclusively as a π-complex, even when both reactants are initially radical species! In constrast, the reaction of aromatic radical cations with NO_2 appears to lead exclusively to a sigma bonded product. The complete disappearance of the $C_6D_6NO_2^+$ products shown in Figure 1 provides no evidence that even a small fraction of this ion retains the π-complex structure. Both these results strongly support Perrin's suggestion that aromatic nitration involves the oxidation of the aromatic hydrocarbons by NO_2^+ and the subsequent reaction of the aromatic cation with NO_2.

Refererences

1. C. L. Perrin, J. Am. Chem. Soc. 1979, 99, 5516.
2. W. D. Reents and B. S. Freiser, J. Am. Chem. Soc., 1980, 102, 271.
3. R. C. Dunbar, et al, J. Am. Chem. Soc., 1972, 93, 6863.
4. P. Ausloos and S. G. Lias, Int. J. Chem. Kin., 1978, 657.

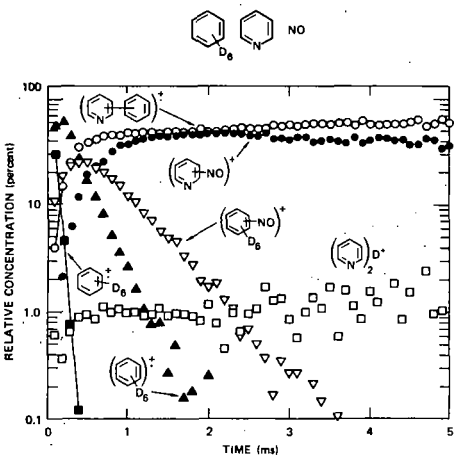

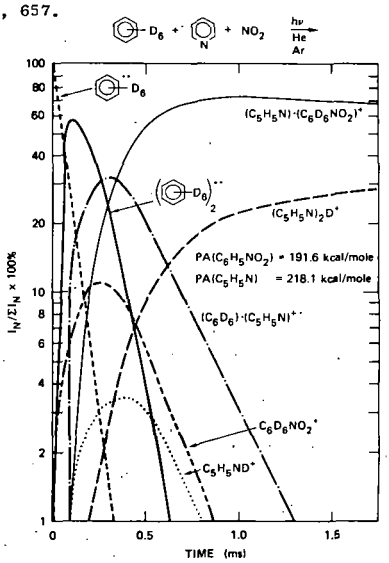

ANALYSIS OF COAL LIQUIDS

Thomas Aczel
Exxon Research and Engineering Company
Baytown Analytical Research Division
Baytown, Texas

Detailed mass spectrometric characterization of coal liquids has been one of the major activities of our laboratory over the past 15 years. This presentation will review the methodology developed in this period, the reasoning used in selecting particular options among the available analytical procedures and illustrate the capabilities of our approach with examples taken from the high resolution, low voltage MS analyses of mild pyrolyzates of chemically treated and untreated coals.

The methodology developed is summarized in Slides 1-3.

Differentiation between neutral and acidic oxygen types, such as aromatic furans and hydroxyaromatics requires separated fractions. Differentiation between basic, pyridinic, and neutral, pyrrolic type nitrogen compounds also requires physical separation of the two classes.

Decisions on what particular methodology to use on a given sample or set of samples are based on a variety of factors, including sample characteristics, budget and time constraints and a realistic view of the importance of the analytical data in a given case.

Capabilities of this analytical methodology, and in particular of the high resolution MS can be illustrated with recent work on the composition of organics in coal.[1] In this case, our interest was focused on the nature of cleavable etheric bonds and the adjacent aromatic moieties that might yield phenols during coal liquefaction and pyrolysis.[2] MS data obtained on the pyrolyzates of a large number of model compounds indicated that the bonds most likely to be cleaved are of the type Ar-O-CH_2-Ar. This type of etheric bridges are widely believed to be present in coal structures, although there is no definite information available in the literature on the nature of the aromatic structures adjacent to these bridges. We gained an insight into the average distribution of these aromatic structures by pyrolyzing untreated coal samples and coal treated with KOH and by the high resolution MS identification of the very complex pyrolyzates obtained.

Treatment with KOH selectively blocks the phenol functions existing in the coal structure. Pyrolyzates from untreated coals thus contain phenols derived both from ether cleavage and phenols that existed as such in the original coal structure; pyrolyzates from treated coals contain only phenols derived from ether cleavage. Detailed MS comparison of the pyrolyzates can thus lead to the differentiation of these two types of phenols.

The complexity of the MS spectra is illustrated in Slide 4.

Summary data on the characterization are shown in Slides 5-7. Major conclusions that can be deduced from these data are summarized below:

- One ring phenols are mostly formed during pyrolysis.
- Hydroxy-groups in coal are located mainly on multiring aromatics.
- Cleavable etheric bonds are not directly attached to furanic or thiophenic structures.
- Polyether units are ordered tail to tail.

[1]Siskin, Michael and Aczel, Thomas, "Pyrolysis Studies on the Structure of Ethers and Phenols in Coals" to be presented at the International Conference on Coal Science in Dusseldorf, West Germany, September 7-9, 1981.

[2]Aczel, Thomas, Williams, R. B., Brown, R. A., and Pancirov, R. J., "Chemical Characterization of Synthoil Feeds and Products", Chapter 17, Academic Press, Inc., 1978.

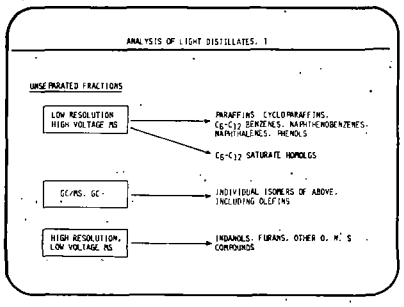
ANALYSIS OF LIGHT DISTILLATES. 1
UNSEPARATED FRACTIONS
LOW RESOLUTION HIGH VOLTAGE MS
PARAFFINS. CYCLOPARAFFINS. C6-C12 BENZENES. NAPHTHENOBENZENES. NAPHTHALENES. PHENOLS
C6-C12 SATURATE HOMOLOGS
GC/MS. GC -
INDIVIDUAL ISOMERS OF ABOVE. INCLUDING OLEFINS
HIGH RESOLUTION. LOW VOLTAGE MS
INDANOLS. FURANS. OTHER O. N. S COMPOUNDS

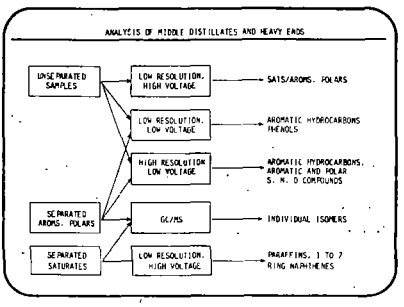
ANALYSIS OF MIDDLE DISTILLATES AND HEAVY ENDS
UNSEPARATED SAMPLES
LOW RESOLUTION. HIGH VOLTAGE
SATS/AROMS. POLARS
LOW RESOLUTION. LOW VOLTAGE
AROMATIC HYDROCARBONS PHENOLS
HIGH RESOLUTION LOW VOLTAGE
AROMATIC HYDROCARBONS. AROMATIC AND POLAR S. N. O COMPOUNDS
SEPARATED AROMS. POLARS
GC/MS
INDIVIDUAL ISOMERS
SEPARATED SATURATES
LOW RESOLUTION. HIGH VOLTAGE
PARAFFINS. 1 TO 7 RING NAPHTHENES

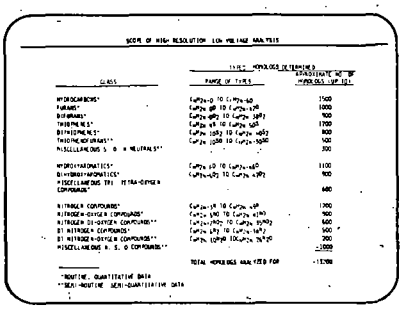
SCOPE OF HIGH RESOLUTION LOW VOLTAGE ANALYSIS
CLASS
TYPES - HOMOLOGS DETERMINED
RANGE OF TYPES
APPROXIMATE NO. OF HOMOLOGS PER TYPE
HYDROCARBONS*
FURANS*
BENZOFURANS*
THIOPHENES*
BENZOTHIOPHENES*
THIOPHENOPHENANES**
MISCELLANEOUS S. O. N NEUTRALS**
HYDROXYAROMATICS*
DIHYDROXYAROMATICS*
MISCELLANEOUS TRI- TETRA-OXYGEN COMPOUNDS*
NITROGEN COMPOUNDS*
NITROGEN-OXYGEN COMPOUNDS*
NITROGEN DI-OXYGEN COMPOUNDS**
DI NITROGEN COMPOUNDS*
DI NITROGEN-OXYGEN COMPOUNDS**
MISCELLANEOUS N. S. O COMPOUNDS**
TOTAL HOMOLOGS ANALYZED FOR
*ROUTINE. QUANTITATIVE DATA
**SEMI-ROUTINE SEMI-QUANTITATIVE DATA

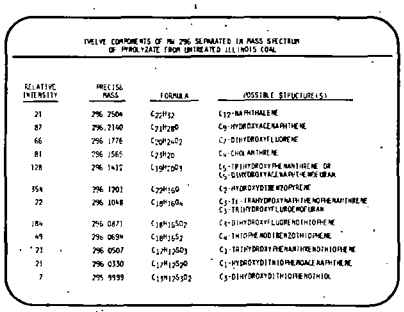
TWELVE COMPONENTS OF PM 296 SEPARATED IN MASS SPECTRUM OF PYROLYZATE FROM UNTREATED ILLINOIS COAL
RELATIVE INTENSITY
PRECISE MASS
FORMULA
POSSIBLE STRUCTURE(S)
21 296.2504 C22H32 C12-NAPHTHALENE
87 296.2140 C21H28O C8-HYDROXYACENAPHTHENE
66 296.1776 C20H24O2 C7-DIHYDROXYFLORENE
81 296.1565 C21H20 C16-CHOLANTHRENE
128 296.1432 C19H20O3 C5-TRIHYDROXYPHENANTHRENE OR C5-DIHYDROXYACENAPHTHENOFURAN
356 296.1201 C22H16O C12-HYDROXYDIBENZOPYRENE
22 296.1048 C19H16O4 C4-TETRAHYDROXYNAPHTHENONAPHTHENE OR C3-TRIHYDROXYFLUORENOFURAN
184 296.0871 C18H16O3 C6-DIHYDROXYFLUORENOTHIOPHENE
49 296.0694 C18H14O2 C16-THIOPHENOBENZOTHIOPHENE
21 296.0507 C17H12O3 C3-TRIHYDROXYPHENANTHRENOTHIOPHENE
21 296.0330 C17H12S2O C1-HYDROXYDITHIOPHENOACENAPHTHENE
7 295.9999 C15H12S2O2 C3-DIHYDROXYDITHIOPHENOTHIOL

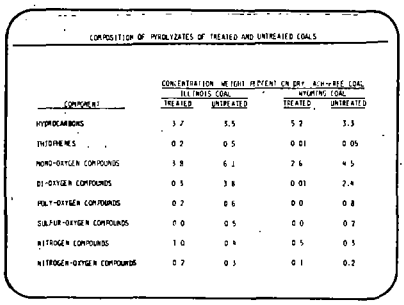
COMPOSITION OF PYROLYZATES OF TREATED AND UNTREATED COALS
CONCENTRATION WEIGHT PERCENT ON DRY ASH-FREE COAL
ILLINOIS COAL
WYOMING COAL
COMPONENT
TREATED
UNTREATED
TREATED
UNTREATED
HYDROCARBONS 3 7 5 5 5 2 3 3
THIOPHENES 0 2 0 5 0 01 0 05
MONO-OXYGEN COMPOUNDS 3 8 6 1 2 6 4 5
DI-OXYGEN COMPOUNDS 0 5 3 8 0 01 2 4
POLY-OXYGEN COMPOUNDS 0 2 0 6 0 0 0 8
SULFUR-OXYGEN COMPOUNDS 0 0 0 5 0 0 0 2
NITROGEN COMPOUNDS 1 0 0 4 0 5 0 5
NITROGEN-OXYGEN COMPOUNDS 0 2 0 3 0 1 0 2

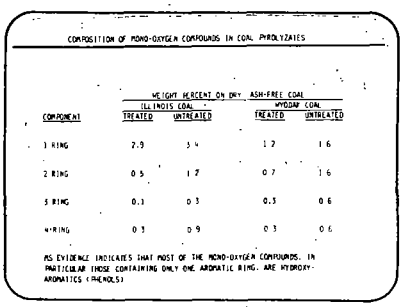
COMPOSITION OF MONO-OXYGEN COMPOUNDS IN COAL PYROLYZATES
WEIGHT PERCENT ON DRY ASH-FREE COAL
ILLINOIS COAL
WYODAK COAL
COMPONENT
TREATED
UNTREATED
TREATED
UNTREATED
1 RING 2 9 3 4 1 2 1 6
2 RING 0 5 1 7 0 7 1 6
3 RING 0 1 0 3 0 3 0 6
4+RING 0 1 0 9 0 3 0 6
AS EVIDENCE INDICATES THAT MOST OF THE MONO-OXYGEN COMPOUNDS. IN PARTICULAR THOSE CONTAINING ONLY ONE AROMATIC RING. ARE HYDROXY-AROMATICS (PHENOLS)

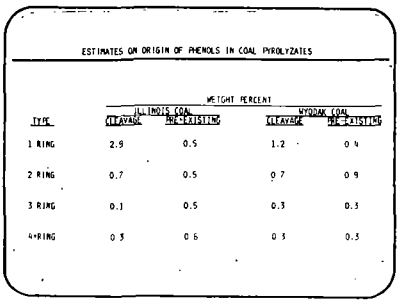
ESTIMATES ON ORIGIN OF PHENOLS IN COAL PYROLYZATES
WEIGHT PERCENT
ILLINOIS COAL
WYODAK COAL
TYPE
CLEAVAGE
PRE-EXISTING
CLEAVAGE
PRE-EXISTING
1 RING 2.9 0.5 1.2 0 4
2 RING 0.7 0.5 0 7 0 9
3 RING 0.1 0.5 0.3 0.3
4+RING 0 3 0 6 0 3 0.3

STRATEGIES FOR THE IDENTIFICATION OF GENOTOXIC CONSTITUENTS IN HEAVY-END COAL LIQUIDS

Bary W. Wilson and Richard A. Pelroy
Battelle Pacific Northwest Laboratory, Richland, Washington

Milton L. Lee and Douglas W. Later
Department of Chemistry
Brigham Young University, Provo, Utah

The induction of microbial mutation in the Ames assay and skin carcinogenesis in mice by SRC-I and SRC-II coal liquids appears to be restricted to the heavy-end fractions of these materials[1]. Fractional distillation of full boiling range SRC process solvent and other coal liquid source materials shows, for example, that mutagenic activity of intact 50°F boiling point cuts is expressed by those materials which distill above 700°F for SRC-II, and above 750°F for SRC-I. A number of specific mutagens and/or carcinogens have been identified in these full boiling range liquids by GCMS following chemical fractionation and chromatographic separation of the raw materials[2]. The most mutagenically active constituents of the full boiling range materials in general are primary aromatic amines which are concentrated in moderately polar or basic fractions. Heavy-end materials exhibit mutagenicity in their highly polar fraction as well as in the moderately polar ones where the simple primary aromatic amines are concentrated. However, the high polarity and/or molecular weight of a substantial number of the compounds comprising the heavy ends precludes GC and, hence, GCMS as a method for the general analysis of these materials. We have developed a strategy involving several direct inlet mass spectrometric techniques including high resolution, field desorption and metastable ion analysis to characterize a number of heavy-end coal refining products including both liquid and solid phase materials.

Mutagenically active fractions of the heavy-end materials were submitted to high resolution mass spectral analysis to obtain elemental compositions of the major components. The moderately polar fractions yielded elemental compositions containing one or two nitrogens and essentially no oxygen, and the highly polar fractions contained compounds having oxygen as heteroatoms with some which contained both oxygen and nitrogen. In order to ascertain the functionality of the heteroatoms observed in the active fractions, second field free region metastable ion energy analyses were performed with a VGMM ZAB1F double-focussing mass spectrometer. Figure 1 compares the metastable ion spectra of a putative aminobenzo[a]pyrene (m/e 267) in a moderately polar active fraction to authentic aminobenzo[a]pyrene which was synthesized for comparison. (Both the 6- and 7-amino isomers of this compond exhibited mutagenic activity.) Note that the M-17 transition ions appear to be extremely useful in detecting primary amino functionalities in complex nitrogen-rich fractions by metastable ion analysis. Figure 2 illustrates a metastable scan from a more highly polar region of the m/e 271 ion with elemental composition $C_{19}H_{13}NO$ which was the only ion reported at that nominal mass. (An analogous spectrum was obtained from m/e 257; however, HRMS showed that there was a component of a C_1-azabenzanthracene also present at that m/e value.) Although the compounds cannot be positively identified from these data, it is clear from HRMS and metastable ion analysis that they contain primary amino as well as hydroxyl functionality and structures have been proposed based upon the most probable PAH parent compound[3]. Since the mutagenic activity for this particular fraction was eliminated after treatment with nitrous acid, which selectively converts primary amines to their corresponding phenols, the hydroxylated primary amines identified are considered good candidates as genotoxins in these more polar fractions.

In order to confirm metastable ion data which indicated the presence of amine functionality on parent ring structures already containing nitrogen such as quinolines, phenanthridines, or higher benzologs, a specific fractionation and derivitization procedure was developed[4]. The extraction step yields a highly enriched amine fraction which is then derivitized with pentafluoro proprionic anhydride. The PFP derivitives of the amines are easily distinguished by HRMS from any non-derivitized aza components present, due in part to the relative mass deficiency conferred by the five fluorine atoms as well as the overall increase in mass. This method has been used to confirm the presence of aza amines as well as primary aromatic amines and their C_1-C_4 alkyl homologs having from 1 to 7 rings in moderately polar mutagenic fractions by HRMS[5], and is currently being developed for the identification and quantitative estimation of primary amine content in coal-derived products by negative ion CI at low resolution.

Finally, from molecular weight data obtained from high pressure dextran size exclusion chromatography, it appeared that EI and even CI ionization modes discriminated against higher molecular weight components in the heavy-end materials leading to underestimation of their actual molecular weight range by MS analysis. Field desorption was thus applied as a method for more accurately estimating the molecular weight of these materials, many of which are solids or extremely viscous at room temperature. SRC-I solid product, for example, which appeared to contain no compounds above mass 800 to 850 by EI or CI, yielded peaks in excess of m/e 1400 by FD. The limiting factor in the former methods is probably failure to evaporate the high molecular weight components from the probe rather than fragmentations which occur subsequent to ionization.

In summary, high performance mass spectrometric techniques have been applied to characterize SRC materials and to identify higher molecular weight primary aromatic amines as well as their hydroxylated and aza analogs in genotoxic fractions from the heavy-ends.

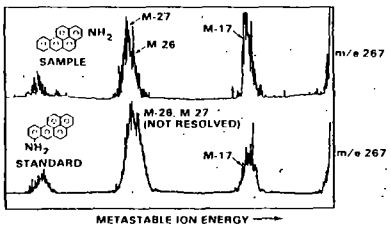

Fig 1. Metastable ion energy scan (upper) of the m/e 267 ion (elemental composition $C_{20}H_{13}N$) from SRC-II heavy distillate compared to the spectrum of authentic 7-amino-benzo[a]pyrene (lower).

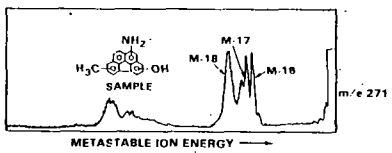

Fig. 2 Metastable ion energy spectrum of m/e 271 from SRC-II heavy distillate. M-16, M-17 and M-27 ions arise from losses involving the amine group, while the M-18, M-28, and M-29 ions arise from oxygenated losses.

References

1. PNL-3787, Fractional Distillation as a Strategy for Reducing the Genotoxic Potential of SRC-II Coal Liquids: A Status Report, R. A. Pelroy and B. W. Wilson, eds., NTIS (1981).

2. Wilson, B. W., and Pelroy, R. A., Mutation Res. 79, 193-202 (1980).

3. Wilson, B. W., et al., Identification of Genotoxic Constituents in Heavy-End Coal Liquids by Coupled High Resolution and Metastable Ion Mass Spectral Analysis, Anal. Chem. (submitted for publication 1981).

4. Later, D. W., et al., Rapid Chemical Class Separation and Detailed Characterization of Organic Compounds in Synthetic Fuels, Anal. Chem. (accepted for publication 1981).

5. Later, D. W., et al., Selective Detection of Amino Polycyclic Aromatic Hydrocarbons in Solvent Relfined Coal, Anal. Chem. (submitted for publication 1981).

PYROPROBE/GC/MS ANALYSIS OF SELECTED COALS

R. J. PANCIROV AND T. R. ASHE
EXXON RESEARCH AND ENGINEERING COMPANY
LINDEN, NEW JERSEY 07036

A series of eight coals were examined by pyrolysis gas chromatography mass spectrometry (Py/GC/MS). The coals were specifically chosen to cover a wide range of different ranks and oxygen contents. The scope of the study was to see if Py/GC/MS could provide data that would be characteristic for the different coals. Along with the data that related to the oxygen contents of the coals, there was the possibility that the data obtained from this study could provide information on the processabiltiy of coals. This aspect of the data is outside the scope of the present study for neither the time nor the additional information required to fully evaluate this phase of the work was available.

The analysis was carried out using a Chemical Data Systems (CDS) 120 Pyroprobe, the GC was a Perkin-Elmer 900, and the mass spectrometer a duPont 21-491. The pyrolyses were performed at 600, 800, and 1000°C. The pyrolysate was passed through a 10 ft 10% SP2100 column programmed from 60 to 320°C at 8°C/min. The pyrolysis conditions were a heating rate of 10,000°C/sec and a hold time of 20 sec at the upper temeprature. The coals were run as received. Though these were the upper limits set for the probe, the actual temperature of the pyrolysis was somewhat lower. Tests showed that the actual pyrolysis temperature was about 200°C lower than the limit set on the probe. However, all data will be reported at the temperature reading of the probe.

Characterization of polycyclic Aromatic Hydrocarbons in Solvent Refined Coal and Diesel Particulates by Mass Spectrometry/Mass Spectrometry, Karl V. Wood, J. D. Ciupek, D. Zakett and R. G. Cooks.

Mass spectrometry/mass spectrometry (ms/ms) can be used for the analysis of compounds of interest in complex mixtures like solvent refined coal (SRC) and diesel engine particulates. Of particular interest is the selectivity and specificity of ms/ms for differentiating compounds having the same molecular weight. Nitrogen containing compounds are of special interest in SRC because of the high concentration of nitrogen relative to that found in petroleum, and the toxicity of some of these compounds.

The differences observed in methane chemical ionization ms/ms for isomeric amino-PNAs and methyl-aza-PNAs will be described. Protonated amino-PNAs tend to fragment by loss of NH_2 (16) and NH_3(17) while methyl-aza-PNAs lose CH_3(15) and CH_4(16). For example, in Figure 1 these mass loss differences along with differences in fragment ion intensities allow differentiation of these two compound types. (Amino-PNA, 1-amino anthracene, MW 193; Methyl-aza-PNA, 2-methyl benzoquinoline, MW 193,) As the number of fused rings increases past three the differences in the ms/ms spectra of these two compound types becomes less well-defined.

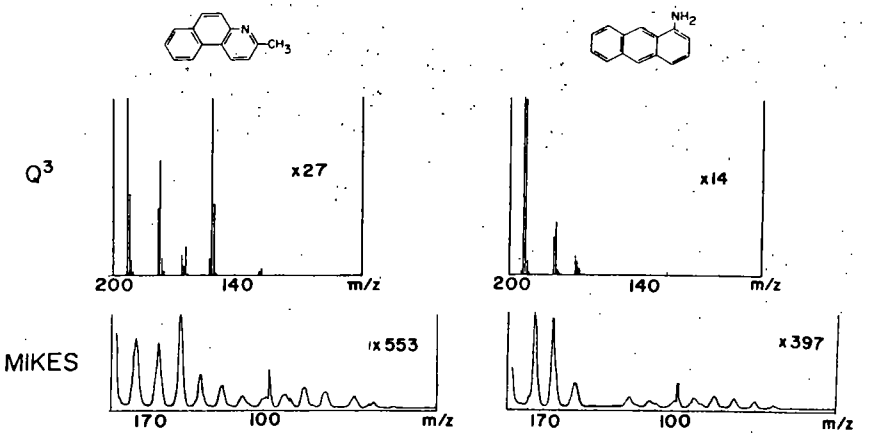

Figure 1

When using ms/ms for the analysis of nitrogen containing constituents in SRC it is necessary to correct for the ^{13}C isotopic contribution from the peak one mass less than the nitrogen containing peak of interest. When using the direct insertion probe this contribution can usually be separated by comparing the time/ion intensity profile of the ion of interest with profile of the lower mass ion. This procedure was used to show that the predominant nitrogen containing species at m/z 144 is methyl quinoline isomer(s) and at m/z 182 is methyl carbazole isomer(s)

The ms/ms procedure for nitrogen containing PNA's might be facilitated by using NH_3 chemical ionization for preliminary compound separation via specific ionization. Similarly a simple acid/base/neutral separation might help provide a more definitive analysis as to the presence of mutagenic amino-PNAs. Both these avenues are being examined.

In conclusion it is worth emphasizing that ms/ms done with high energy collisions (MIKES) gives substantially different spectra to that done with low energy collisions (triple quadrupole). Examples of this comparison will be made for some representative compounds including 4-methyl quinoline/1-amino naphthalene (MW 143), 5-methyl carbazole/2-amino fluorene (MW 181) and the previously mentioned MW 193 compounds. An example of the variation of ms/ms spectra with collision energy in the low energy regime will be discussed. It is evident that collision energy controls the degree of fragmentation and is a valuable structural diagnostic.

NON-CONVENTIONAL USES OF GC/MS IN THE ANALYSIS OF REFINERY STREAMS AND SYNFUELS

S. G. Colgrove and Thomas Aczel
Exxon Research and Engineering Company
Baytown Analytical Research Division
Baytown, Texas
81AN T0216

GC/MS techniques play a significant role in the detailed characterization of refinery streams and synfuels. In our laboratories GC/MS constitutes a part of an integrated analytical approach that often includes such techniques as liquid-liquid separations, ultra-high resolution low voltage MS, low resolution MS, and chemical analyses. This presentation will emphasize some of these procedures including the integration of GC/MS and high resolution low voltage MS data, the use of GC/MS to determine compound type and chemical class distribution as a function of boiling range and the proposed use of GC/MS data as calibration for MS distillation.

The need for integrating GC/MS and ultra-high resolution MS data stems from the complementary nature of these techniques. Ultra-high resolution, low voltage MS determines all volatile components in a synfuel or refinery stream, including aromatic hydrocarbons, sulfur, nitrogen, and oxygen compounds; but it is restricted to an empirical formula analysis, with no possibility of determining the isomeric distribution within carbon number homologs.

This function can be readily assumed by GC/MS for a large number of homologs. Relative concentrations of individual isomers of a given carbon number homolog determined by GC/MS, are normalized to the concentration of the latter, as obtained by high resolution MS.

This procedure is justified by the good agreement observed between GC/MS and by low voltage MS either in the low or high resolution mode. This agreement is illustrated by Slides 1-2 for sets of alkyl-benzenes and hydroxy-benzenes.

Another important task of GC/MS is to determine the relative concentrations of various classes of components as a function of boiling point. This is feasible with the availability of a good boiling point type GC column. We generally use 30-60 meter fused silica capillary columns, coated with polymethylsiloxane phases such as SE30, OV101, or DB-1 (J & W Scientific).

Determination of the relative concentrations of the various classes are carried out using fragment peak summations in a priori designated boiling point/retention time intervals (Slide 3).

Availability of a good boiling point/retention time correlations, combined with MS fragmentation patterns are also helpful in the identification of components that are not included in the GC/MS library or that cannot be unequivocably identified. In addition, the correlation can also be used to determine the boiling points of components for which no reliable boiling points are available in the literature. These boiling points, as well as average boiling points for carbon number homologs, calculated from the boiling point of the individual isomers, and weighted for the isomeric distribution, can be used for calibration data for our MS distillation procedure.[1]

In conclusion, we have found the GC/MS has a definitive role in our overall analytical study for synfuels and refinery streams. This role is not limited to the conventional identification approach, as important as this function is, but it can be extended to improve and to complement our other procedures.

[1]Thomas Aczel and Lumpkin, H. E., Proceedings, The 18th Annual Conference on Mass Spectrometry, San Francisco, California, May 1970, Pages B37-B39.

COMPARISON OF HIGH RESOLUTION MS AND GC/MS DATA ON ALKYL-BENZENES

COMPONENT	RELATIVE WEIGHT PERCENT SAMPLE A MS	SAMPLE A GC/MS	SAMPLE B MS	SAMPLE B GC/MS	NO. OF ISOMERS BY GC/MS A	B
C_8-BENZENES	8 3	6.7	2.7	1 5	4	4
C_9-BENZENES	45 5	53 4	7 2	8 3	7	7
C_{10}-BENZENES	36 8	32 9	34.2	38 6	19	17
C_{11}-BENZENES	8 8	6 5	39.6	36 8	19	19
C_{12}-BENZENES	0 6	0.1	16.3	14 8	14	26
	100 0	100.0	100 0	100 0	63	73

COMPARISON OF MS AND GC/MS DATA ON PHENOLS

COMPONENT	RELATIVE WEIGHT PERCENT MS	GC/MS	NO. OF ISOMERS BY GC/MS
PHENOL	68 9	65 4	1
CRESOLS	25 5	27 8	2
XYLENOLS AND ETHYLPHENOLS	5 6	6 8	9
	100 0	100 0	12

DETERMINATION OF SATURATES/AROMATICS IN NARROW BP RANGES

BOILING RANGE, °F	WEIGHT PERCENT TOTAL SAMPLE	SATURATES	AROMATICS	RELATIVE PERCENT SATS	AROMS
250 - 300	5 9	5 2	0 7	88	12
300 - 350	47 4	37 9	9 5	80	20
350 - 400	40 8	29 7	11 1	73	27
400 - 500	5 9	3.4	2 5	58	42

* SATURATES/AROMATICS DISTRIBUTION DETERMINED BY MS FRAGMENT PEAK SUMMATIONS ON TOTAL SAMPLE. DATA CORROBORATED BY GC/MS DISTILLATION OF SEPARATED FRACTIONS

Di- and Tricyclic Hydrocarbons as Indicators of Higher Terrestrial Input In A Salawati (Indonesia) Reservoir, By: J. Stuart Richardson and Denis E. Miller, Phillips Petroleum Company, Bartlesville, Oklahoma 74004

This work describes the computerized GC/MS analysis of the saturate fraction of a primarily terrestrially derived oil from a Salawati reservoir. Our attention focussed upon certain polycyclic terpanes which might be used as unambiguous indicators of terrigenous input to the oil source sediment. Tentative structures of four dicyclic and eleven tricyclic terpanes present in the extract are based upon possible biological precursors and mass spectral data.

An m/z 123 mass chromatogram, Figure 1, was used to initially detect the possible presence of dicyclic terpanes. Two isomers of 208 molecular weight and two of 222 molecular weight were found as Compounds 1, 2, 3, and 4, respectively. Figure 2 shows the mass spectrum of Compound 1 with its proposed structure (I). Structures of possible precursors onocerin, ambrien, manoöl and agathic acid, all natural products found in terrestrial plants, are given in Figure 3. Agathic acid is produced by members of the genus Agathis, a group of conifers found in the land areas between New Zealand and Malaysia.

Mass chromatograms of m/z 163 (Figure 4), 177, and 191 (fragments characteristic of tricyclic terpanes) were used to detect the presence of the eleven tricyclic terpane skeletal structures.

Figure 5 gives the mass spectrum and proposed structure (II) of Compound 5. Presumably, the prominent m/z 163 fragment arises from the dual fragmentations illustrated by the following:

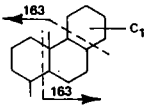

Extrapolation of this fragmentation scheme gives skeletal structures of the remaining tricyclic terpanes. They occur in four distinct structural types (III, IV, V, and VI) and range in molecular weight from 234 to 346. Table I shows their arrangement according to molecular weight and structure type. Structure Types IV, V, and VI are exclusively associated with molecular weights at or below 276. Structure Type III is exclusively associated with molecular weights at or above 304. Precursors of terpanes with structure Types IV, V, and VI are probably abietic and/or pimaric acids (Figure 6). Both of these are exclusively associated with higher plants. Products from their thermal alteration can thus serve as unambiguous terrestrial biomarkers. Terpanes with structure Type III arise from the cyclization of squalene, or squalene-like compounds (Figure 6). The R substitution is a C_1-C_{11} alkyl group. Squalene occurs in both higher plants and marine environments. This latter group of tricyclic terpanes may not be used as unambiguous terrestrial biomarkers.

Acknowledgment: Our thanks go to J. A. Lytle for his help in obtaining much of the mass spectral data.

References: 1) Anders, D. E. and Robinson, W. E., Geochim. Cosmochim. Acta. 35, 661 (1971); 2) Bendoraitis, J. G., Adv. Org. Geochem. 1973, 209 (1974); 3) Douglas, A. G. and Grantham, P. J.., Adv. Org. Geochem. 1973, 261 (1974); 4) Eglinton, G. and Murphy, M. T. J., Organic Geochemistry, Springer-Verlag Co., 602 (1969); 5) Gallegos, E. J., Anal. Chem. 43, 1151 (1971); 6) Geisman, E. A. and Crout, D. H. G., Organic Chemistry of Secondary Plant Metabolism, Freeman Cooper & Co., 291 (1969); 7) Reed, W. E., Geochim. Cosmochim. Acta. 41, 237 (1977); 8) Simoneit, B. R. T., Geochim. Cosmochim. Acta. 41, 463 (1977).

A more detailed description of this work will be submitted for publication in Analytical Chemistry.

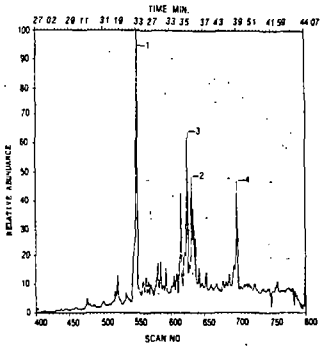

Figure 1. M/Z 123 Mass Chromatogram Showing Distribution Of Dicyclic Terpanes.

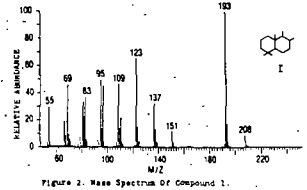

Figure 2. Mass Spectrum Of Compound 1.

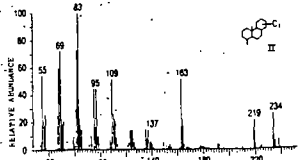

Figure 5. Mass Spectrum Of Compound 5.

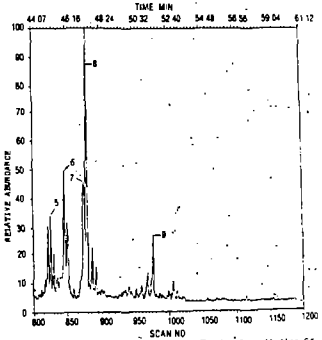

Figure 4. M/Z 163 Mass Chromatogram Showing Distribution Of Tricyclic Terpanes Having Prominent M/Z 163 Fragments.

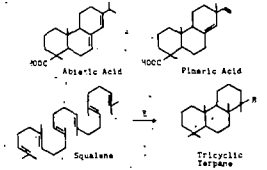

Figure 6. Structures of Probable Precursors of Tricyclic Terpanes.

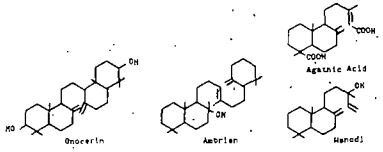

Figure 3. Structures of Probable Precursors of Dicyclic Terpanes.

TABLE I
BASE SKELETAL STRUCTURES OF TRICYCLIC TERPANES
SKELETAL TYPE

MOLECULAR WEIGHT	IV	V	VI	III
234	C_1 5	*	*	*
248	C_1 ± 6a 7a	C_2 8	C_1 ± 6b 7b	*
262	*	*	C_3 10	*
276	*	C_4 9	C_3 11	*
290	*	*	*	*
304	*	*	*	C_4 12
318	*	*	*	C_5 13
332	*	*	*	C_6 14
346	*	*	*	C_7 15

± ALTERNATE POSSIBILITIES

IDENTIFICATION OF CRUDE OILS BY SELECTIVE CHEMICAL IONISATION MASS SPECTROMETRY

R.P. Morgan and C.A. Gilchrist

Shell Research Limited, Thornton Research Centre, P.O. Box 1, Chester, CH1 3SH, U.K.

P.D. Burke and K.R. Jennings

Department of Chemistry, University of Warwick, Coventry, U.K.

A large amount of effort has been devoted to the analysis and characterisation of crude oils. Unfortunately, no single technique exists which is sufficient for the unambiguous identification of an oil and hence a number of complementary techniques must be used. Consequently, the identification becomes time consuming and thus expensive. We are attempting to develop a rapid mass spectrometric technique, which is capable of automation, to identify all types of oils and their precursors.

OH^- chemical ionisation ionises selectively the aromatic portion of an oil (1). We have utilised this to obtain simple, low resolution mass spectra of crude oils which are similar in character to those obtained by Sieck (2) using photoionisation. A typical spectrum is shown in the figure.

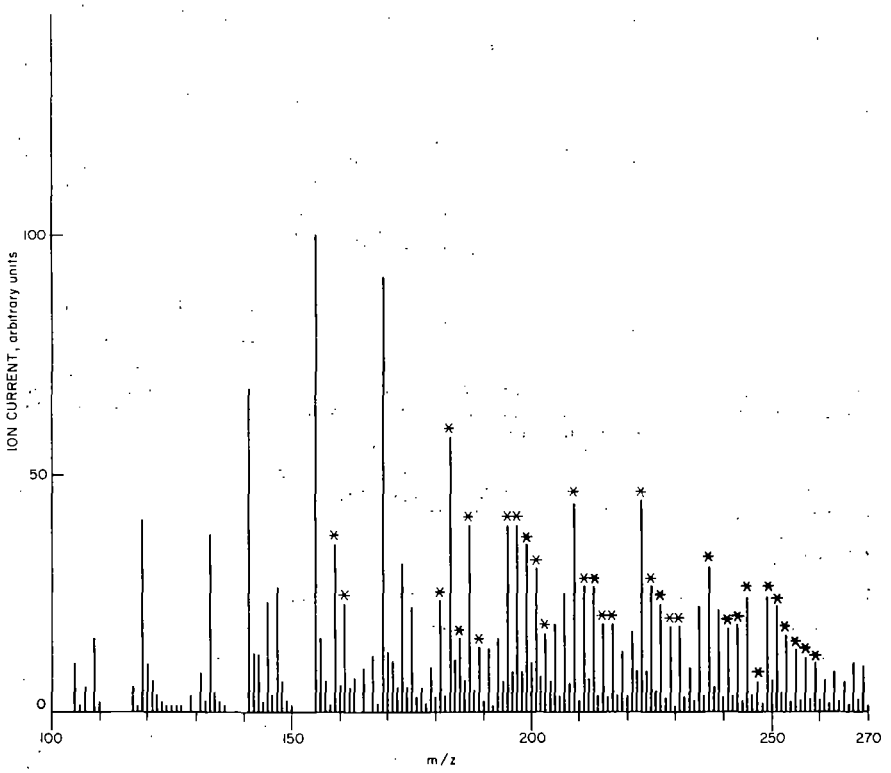

FIG. 1 – Typical OH^- chemical ionisation mass spectrum of a crude oil

Each reference crude oil spectrum is reduced to the thirty-three peaks noted in the figure by asterisks and this fingerprint spectrum is then stored in a computer library. Unknown spectra are then mathematically compared with the library spectra by a least squares routine and the results outputted to a line-printer. Typical results from a crude oil sample which is in the library and from a crude oil sample not represented in the library are shown in Table 1 and Table 2 respectively. (The letters A, B, C etc. denote geographical areas while the subscripts 1, 2, 3 etc. denote different fields within geographical areas.)

Table 1

Top ten mismatches of unknown I (C_2) with the reference library of spectra

Crude oil	Mismatch
C_2	1.0
B_4	4.2
B_2	5.3
B_3	5.5
C_1	5.6
B_5	5.7
B_1	6.1
A_4	6.6
A_5	6.7
A_2	7.4

Table 2

Top ten mismatches of an oil (II) from outside the reference library of spectra

Crude oil	Mismatch
A_5	4.2
A_2	4.6
A_1	5.5
A_4	5.8
B_2	5.8
A_8	5.9
B_5	6.8
A_6	7.1
D_1	7.6
A_3	7.6

The results show that the method can be used to identify individual fields where the unknown oil is present in the library and can identify the geographical area of origin of an oil when it is not represented in the reference library.

Extension of this method to distillate derived oils and weathered crudes has not proved entirely satisfactory, but the use of B/E CA spectra, combined with this method, shows promise of providing an automated oil analysis technique.

References

1. A.L.C. Smit and F.H. Field, J. Amer. Chem. Soc. 99, 6471 (1977).

2. L.W. Sieck, Anal. Chem. 51, 128 (1979).

PYROLYSIS GC-MS-C AND ^{13}C FT NMR ANALYSIS OF ARABIAN HEAVY AND IRANIAN LIGHT ASPHALTENES

E. J. GALLEGOS AND D. M. WILSON
CHEVRON RESEARCH COMPANY
RICHMOND, CALIFORNIA 94802

Py-GC/MS-C and FT NMR were used in the analysis of asphaltenes from Arabian Heavy and Iranian Light crudes. Both show release of volatile components at a peak temperature of ~490°C as measured by thermal gravimetric analysis.

Py-GC/MS-C revealed the presence of a homologous series of n-alkanes, branched alkenes, alkenes and/or monocyclic alkanes, alkylbenzenes, acenaphthenes, and acenophthylenes in the carbon range from $\sim C_{10}$ to C_{35}. Also identified were benzothiophenes, dibenzothiophenes, naphthalenes, phenanthrenes, pyrenes, and higher polynuclears along with the well-known "biomarkers" hopanes, hopenes, and steranes from C_{27} through C_{35}. These data are consistent with that obtained from ^{13}C FT NMR.

Molecules are pyrolytically released, through chemical bond clearage, from large complex macromolecular systems. The release of these molecules is similar to the release of many similar components in the pyrolysis of kerogens and coals. The relationship of these various complex systems is discussed.

HYDRODESULFURIZATION OF DIBENZOTHIOPHENE STUDIED BY GC/MS

C. S. HSU, T. R. ASHE AND T. A. PECORARO
EXXON RESEARCH AND ENGINEERING COMPANY
LINDEN, NEW JERSEY 07036

Combined gas chromatography-mass spectrometry has been used to elucidate the complexity of the hydrodesulfurization (HDS) of dibenzothiophene (DBT). With an active system, many new products were produced. Only through detailed mass spectral interpretation can these materials be identified.

In the 70-ev EI spectra, the predominant fragmentation pathway for the hydrogenated sulfur compounds, such as tetrahydrodibenzothiophene and octahydrodibenzothiophene, appeared to be via a retro-Diels-Alder mechanism. The fragmentation of the hydrogenolyzed DBT, such as benzylcyclopentane and cyclopentylcyclohexylmethane, exhibited a rearrangement via a four-centered intermediates.

Through the characterization of the products, HDS was found to be a very complex process. Quantitation by GC/MS was applied when there were unresolved materials present in the gas chromatographic (GC) analysis.

Better resolution of the HDS products of DBT was obtained by using a SP2250 column or its equivalent rather than a methyl silicone column conventionally used. A SP2250 column resolves not only tetrahydrodibenzothiophene from dibenzothiophene, but also the materials isomeric with cyclohexylbenzene from those of bicyclohexyl. If a whole group of isomers rather than individual isomers is of interest, GC quantitation can be done by integrating the peak areas of all the components in the isomer region.

MASS SPECTROMETRIC MEASUREMENT OF THE THERMOCHEMICAL PROPERTIES OF GASEOUS CaOH and SrOH

By

Edmond Murad
Air Force Geophysics Laboratory, Hanscom AFB, MA 01731

Four gaseous equilibria

$$Ca(g) + H_2O(g) = CaOH(g) + H(g)$$
$$Ca(g) + H_2O(g) = CaO(g) + H_2(g)$$
$$Sr(g) + H_2O(g) = SrOH(g) + H(g)$$
$$Sr(g) + H_2O(g) = SrO(g) + H_2(g)$$

were measured over the temperature range 1896 - 2001K when $H_2O(g)$ was passed over a Knudsen cell containing CaO(s) and SrO(s). These gaseous species were measured in a 30.5 cm radius of curvature, 60°- sector mass spectrometer. The Knudsen cell was made of molybdenum and was heated radiatively by a tantalum heater. The effusing gaseous species were ionized by electron impact, and the appearance potentials were measured using a digitally-scanned electron energy control and a multichannel analyzer. The apparatus has been described in detail previously.[1] The heats of reaction were measured and found to be $\Delta H_1(OK) = 26.0 \pm 4$, $\Delta H_2(OK) = 21.9 \pm 5$, $\Delta H_3(OK) = 26.2 \pm 4$, and $\Delta H_4(OK) = 20.6 \pm 3$ kcal/mol. These heats of reaction to $D_0^0(Ca\text{-}OH) = D_0^0(Sr\text{-}OH) = 92 \pm 4$ kcal/mol. Comparison of $D_0^0(CaO)$ and $D_0^0(SrO)$ derived from this work with previous determinations[2,3] leads to $D_0^0(CaO) = 94 \pm 3$ kcal/mol and $D_0^0(SrO) = 98 \pm 3$ kcal/mol. In addition to the dissociation energies, the following appearance potentials were measured: $AP(CaO^+) = 7.6 \pm 0.5$ eV, $AP(CaOH^+) = 5.5 \pm 0.2$ eV, $AP(SrO^+) = 7.0 \pm 0.2$ eV and $AP(SrOH^+) = 5.1 \pm 0.2$ eV.

REFERENCES

1. E. Murad, J. Chem. Phys., 73, 1381 (1980)
2. R. Colin, P. Goldfinger and M. Jeunehomme, Trans Faraday Soc., 60, 306 (1964)
3. J. Drowart, G. Exsteen and G. Verhaegen, Trans. Faraday Soc., 60, 1920 (1964)

MPMOC2 **A THERMODYNAMIC STUDY OF THE THULIUM-TELLURIUM SYSTEM**; MARGARET A. FRISCH; IBM Research Center, PO Box 218, Yorktown Heights, NY 10598

The vaporization behavior of single crystal TmTe, heated in a tungsten Kundsen cell, was studied over the temperature range 1000 to 1800°K. The temperature was cycled up and down many times until the entire sample was vaporized. The time-temperature dependence of the vapor pressure was measured by a quadrupole mass spectrometer, using beam modulation and ion counting techniques. An IBM S/7 computer was employed for measurement and control of the temperature, for control of the mass spectrometer and ion source and for measurement of the ion signals. The ion signals for Tm and Te were integrated and equated to the sample mass for absolute pressure calibration.

During the initial heating, Tm was preferentially vaporized until a composition of about $Tm_{0.765}Te$ was reached at 1600°K. However, the composition at congruency was found to be a function of the temperature. At 1800°K the composition is about $Tm_{0.80}Te$. The enthalpies for removal of Tm and Te from the lattice also reflect this observation. For the 1:1 composition the ΔH is 306 kJ $mole^{-1}$ for Tm and 329 kJ $mole^{-1}$ for Te. These reaction enthalpies gradually change to 279 and 361 kJ $mole^{-1}$, respectively, as the composition moves to 0.77. However, the ΔH for the reaction TmTe(s) = Tm(g) + Te(g) is a constant over the entire composition range, being 636±6 kJ $mole^{-1}$. In addition to Tm and Te, the diatomic molecules TmTe and Te_2 were also observed and their dissociation energies measured. The thermodynamic details of these and other equilibrium reactions will be presented.

MASS SPECTROMETRIC DIFFERENTIAL ANALYSIS OF IONIZATION AND FRAGMENTATION PATTERNS OF GASEOUS TITANIUM OXIDE SPECIES

Serge BANON, Christian CHATILLON, and Michel ALLIBERT

Laboratoire de Thermodynamique et Physico - Chimie - Metallurgiques, Associé au CNRS LA 29,
E.N.S.E.E.G., B.P. 44, 38401 SAINT MARTIN D' HERES, FRANCE

The dissociative ionization of TiO and TiO_2 gas into Ti^+ and TiO^+ has been studied by use of either a single conventional effusion cell or a multiple effusion cell, coupled with a mass spectrometer. The ionization efficiency curves of Ti^+ and TiO^+ are simultaneously recorded for molecules vaporizing from different samples, through the partial vaporization reactions:

$$Ti(s) \rightleftarrows Ti(g) + \text{very small } TiO(g) \text{ from O impurity} \qquad (a)$$

$$Ti_3O_5(s) \rightleftarrows Ti(g) + TiO(g) + TiO_2(g) + - - - \qquad (b)$$

$$TiO(s) \rightleftarrows Ti(g) + TiO(g) \qquad (c)$$

$$TiO_{2-x}(s) \rightleftarrows TiO(g) + TiO_2(g) \qquad (d)$$

The comparative recordings of the ionization of Ti gas from (a) and (c) (Fig. 1) show that Ti^+ is mainly parent ion. In fact, a slight departure from the pure Ti curve indicates that there is a small fragment contribution since Ti and TiO gaseous species are simultaneously present in comparable amounts above TiO solid. To get better conditions for the observation of a possible dissociative ionization of TiO gas, a Ti_3O_5 sample was heated (reaction (b)) at 2290 K in a conventional single molybdenum cell, and the ionization efficiency curves were recorded. (Fig. 2 for Ti^+)

The comparative recordings (Fig. 3) of Ti^+ and TiO^+ from (c) and (d) show that Ti^+ and TiO^+ from $TiO_{1.965}$ are fragment ions. The first fragmentation thresholds correspond to the following processes:

$$TiO + e^- \rightarrow Ti^+ + O + 2\ e^- \qquad 12.8 \pm 0.4 \text{ eV observed}$$

$$TiO_2 + e^- \rightarrow + O_2 + 2\ e^- \qquad 14.6 \pm 0.5 \text{ eV} \quad "$$

$$TiO_2 + e^- \rightarrow TiO^+ + O + 2\ e^- \qquad 13.7 \pm 0.5 \text{ eV} \quad "$$

The first fragmentation threshold for TiO_2 into Ti^+ shows a shift towards lower energies meaning that the value of the dissociation energy of the TiO_2 molecule has to be decreased by 8.5 (±2) kcal/mol. The fragmentation to ionization cross-section ratios are estimated at 30 eV and 70 eV as follows:

$TiO_2 \rightarrow Ti^+$ $\sigma^f/\sigma = 0.046$ (30 eV), 1.135 (70 eV)

$TiO_2 \rightarrow TiO^+$ $\sigma^f/\sigma = 0.262$ (30 eV), 1.254 (70 eV)

$TiO \rightarrow Ti^+$ $\sigma^f/\sigma = 0.006$ (30 eV).

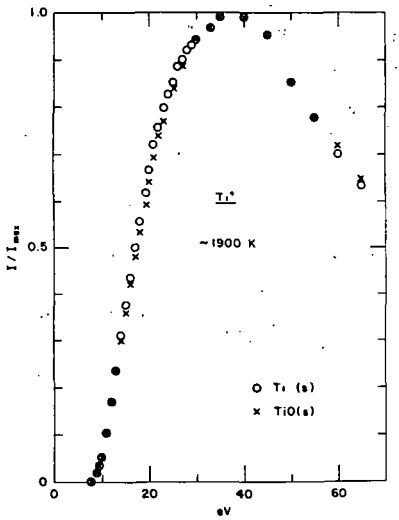

Fig. 1. Simultaneous recordings of Ti^+ efficiency curves obtained when vaporizing pure Ti(s) and TiO(s).

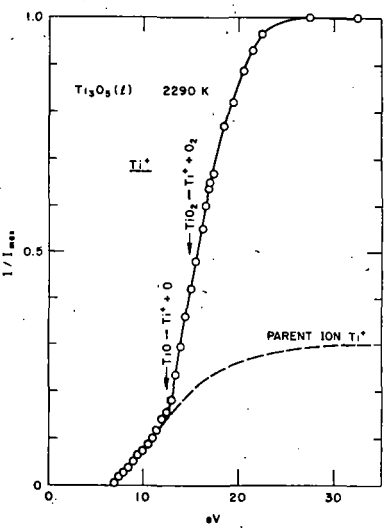

Fig. 2. Ti^+ ionization efficiency curve obtained when vaporizing Ti_3O_5 liquid.

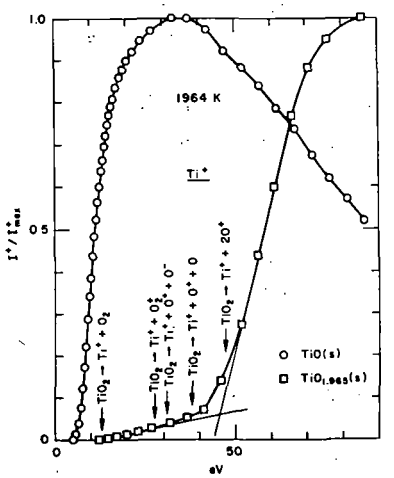

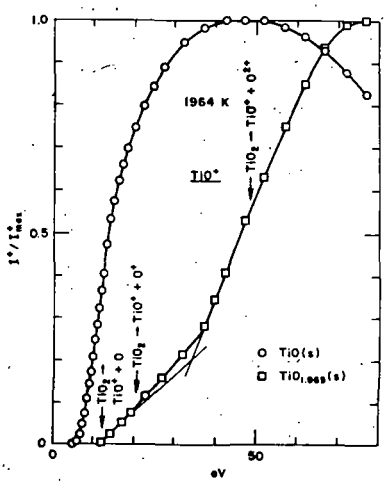

Fig. 3. Simultaneous recordings of Ti^+ and TiO^+ efficiency curves obtained when vaporizing TiO(s) and $TiO_{1.965}$(s).

MASS SPECTROMETRIC STUDIES OF THE BERKELIUM-249 AND PROTACTINIUM-231-OXYGEN SYSTEMS†

P. D. Kleinschmidt and J. W. Ward
Los Alamos National Laboratory
Los Alamos, New Mexico 87545

We have measured the pressures of ^{249}Bk (half life 320 days) and of the ^{231}Pa-$^{231}PaO_2$ (half life 32,800 years) systems using Knudsen effusion mass spectrometry. The mass spectrometer is an Extranuclear quadrupole. In addition, effusing material can be collected on a target and analyzed for alpha and beta activity.

The vapor pressure of ^{249}Bk metal was measured over the range of 1100 to 1500 K. The vapor pressures are described by the equations:

$$\text{Log}_{10}P(\text{atm}) = -(15{,}753\pm264)/T + 5.84\pm0.22 \quad \text{[solid, 1107 to 1319 K]}$$

$$\text{Log}_{10}P(\text{atm}) = -(15{,}047\pm203/T + 5.27\pm0.14 \quad \text{[liquid, 1345 to 1528 K]}$$

from which are obtained the heats of vaporization:

$$\Delta H^\circ_{298}(\text{2nd Law}) = 74{,}586\pm1192 \text{ cal./mole [solid points]},$$

$$\Delta H^\circ_{298}(\text{2nd Law}) = 73{,}331\pm891 \text{ cal./mole [liquid points]}.$$

The third law value is:

$$\Delta H^\circ_{298}(\text{3rd Law}) = 74{,}168\pm60 \text{ cal./mole [all points]}.$$

From the change in slope of the pressure equation a heat of melting of 3,200 cal./mole and an entropy change of 1.9 cal./deg.-mole was obtained. We have arbitrarily chosen 1050±100°C as the melting point. (Early work indicates it is to be 986°C [1] but recent results indicate it may be higher [2].) From the data a boiling point of 2860±50 K is calculated. The sample of seven milligrams of high-purity metal was vaporized from a single crystal tungsten cup in a molybdenum effusion cell. Initially the vapor contained a large amount of the more volatile Cf^{249} which upon further vaporization decreased to a small percentage of the ^{249}Bk intensity. Appropriate corrections were made to the mass 249 intensity. (^{249}Cf is the decay product of ^{249}Bk.) Electronic energy levels from Conway, et al. [3] were used to calculate the gas phase free-energy function. From the correlation of Ward and Hill [4], the crystal entropy was estimated to be 18.7±0.3 cal./deg.-mole. Neodymium was used as the model and the magnetic entropy was calculated for a f^8 trivalent ground state.

The vapor pressure of ^{231}Pa metal was measured over the range 2000 K to 2400 K. The vapor pressure is described by the equation:

$$\text{Log}_{10}P(\text{atm}) = -(28{,}181\pm1{,}157)/T + 6.48\pm0.54$$

from which is obtained the heat of vaporization:

$$\Delta H^\circ_{298} = 136{,}400\pm5{,}300 \text{ cal./mole}.$$

Using the thermodynamic functions given in Oetting, Rand and Ackermann [5], the third law value is:

$$\Delta H^\circ_{298} = 135{,}920\pm810 \text{ cal./mole}.$$

The presence of the PaO_2 and PaO molecules in the vapor indicated an oxide to be present. Crystallography of the residue in the single crystal tungsten cup and the tungsten effusion cell indicated it to be $PaO_{1.98}$. However, by analogy with UO_2 the stoichiometry could be as low as $PaO_{1.6}$ [6] at 2200 K. The PaO can come from a congruently vaporizing substoichiometric compound and from the reduction of the oxide by the metal. Of the two samples used in this study, the first had only oxides present in the vapor and the second had Pa present along with the oxides. After depletion of the metal the intensities and slopes of PaO_2 and PaO were

T(K)	P(atm)	ΔH^{o}_{298} (cal./mole)
Solid		
1107	4.02×10^{-9}	74,120
1124	6.62×10^{-9}	74,113
*1128	8.54×10^{-9}	73,798
1155	1.44×10^{-8}	74,315
1159	1.66×10^{-8}	74,238
1176	2.85×10^{-8}	74,031
1219	9.04×10^{-8}	73,852
1254	1.95×10^{-7}	73,978
*1282	4.01×10^{-7}	73,728
1319	7.04×10^{-7}	74,287
Liquid		
1345	1.24×10^{-6}	74,168
1371	1.87×10^{-6}	74,412
1380	2.44×10^{-6}	74,145
*1421	4.70×10^{-6}	74,367
1443	7.09×10^{-6}	74,263
1528	2.59×10^{-5}	74,400

*denotes target point

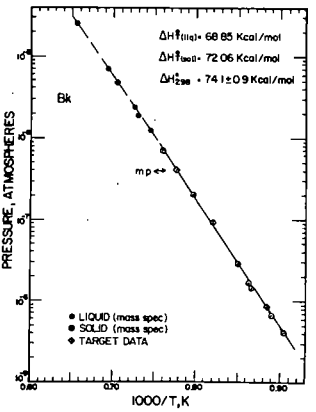

almost the same as in the previous sample. For PaO_2 we obtained:

$$\text{Log}_{10}P(\text{atm}) = -(28{,}365 \pm 281)/T + 7.51 \pm 0.13 \text{ [1st sample]}$$

$$\text{Log}_{10}P(\text{atm}) = -(27{,}585 \pm 733)/T + 6.76 \pm 0.33 \text{ [2nd sample]}$$

from which:

$$\Delta H^{o}_{2173} = 129{,}800 \pm 1{,}300 \text{ cal./mole [1st sample]}$$

$$\Delta H^{o}_{2168} = 126{,}200 \pm 3{,}400 \text{ cal./mole [2nd sample].}$$

Estimating spectroscopic constants for $PaO_2(g)$ by comparison with other actinides and estimating the heat capacity of $PaO_2(s)$ by using that of $UO_2(s)$ we obtain a heat of sublimation of $PaO_2(s)$ at 298 K of 142,200 for sample 1 and 138,600 cal./mole for sample 2. These values are similar to that obtained for UO_2. The ionization potential of PaO_2 is 0.5 eV lower than that for PaO. This is different in ThO_2 where the ionization potential of the ThO_2 is 3 eV higher than that of ThO. We believe this effect is due to the first 5f electron which is delocalized in the metal.

†Work performed under the auspices of the U. S. Department of Energy, Office of Basic Energy Sciences, Chemical Sciences Division.

1. J. A. Fahey, J. R. Peterson and R. D. Baybarz, Inorg. Nucl. Chem. Letters 8 (1972) 101.

2. R. G. Haire, private communication.

3. J. G. Conway, E. F. Worden, J. Blaise, P. Camus and J. Verges, Spectrochimica Acta 32B (1977) 101.

4. J. W. Ward and H. H. Hill in Heavy Element Properties, eds. W. Muller and H. Blank, North Holland/American Elsevier, New York, 1976, p. 65.

5. F. Oetting, M. Rand, and R. J. Ackermann, eds. The Chemical Thermodynamics of Actinide Elements and Compounds, Part I: The Actinide Elements, IAEA, Vienna, 1976.

6. P. Kofstad, Nonstoichiometry, Diffusion, and Electrical Conductivity in Binary Metal Oxides, Wiley-Interscience, New York, 1972, p. 301.

Vaporization Kinetics of Molten Selenium

Yun-Kuang Huang, J. Edward Bennett and Paul W. Gilles

Department of Chemistry
University of Kansas
Lawrence, Kansas 66045

Selenium is known to consist of long chain molecules (10^4 atoms per chain) in thermodynamic equilibrium with about 40 wt % of Se_8 rings in the molten state at about 500 K. Selenium vapor consists of about 44% Se_6, 33% Se_5, 13% Se_7 and only 1% Se_8, the rest being Se_2, Se_3 and Se_4. Two of these gaseous molecules, Se_5 and Se_6, are rings, and the others are generally believed to be rings also. Since the structures of the liquid and the gaseous molecules are seemingly so different, one can suspect that the vaporization of molten selenium might be a retarded process; *i.e.*, with the vaporization coefficient being less than unity. Also, it is puzzling that the concentration of Se_8 in the vapor is so low despite the fact that its concentration in the liquid is so high and that Se_8 has the highest atomization energy per atom. This research was carried out (A) to seek answers to these problems, (B) to determine the vaporization coefficient, the activation enthalpy and the activation entropy of vaporization for each vapor species, (C) to investigate whether non-equilibrium vaporizations give different vapor compositions from equilibrium vaporizations, (D) to ascertain whether changing the structure of liquid selenium will affect the rate of vaporization and the vapor composition, and (E) to reveal the fundamental mechanism of the vaporization reaction.

The experiments involve both Knudsen (equilibrium) and Langmuir (non-equilibrium) types of vaporization from pyrex glass crucibles. An EAI QUAD 200 quadrupole mass spectrometer and its HP 2116B minicomputer-based data acquisition and equipment control system was used to measure the vapor compositions, and a Cahn RG 2000 vacuum microbalance was used to measure the rate of weight loss, both as a function of temperature. A complementary experiment was also performed in which the liquid was changed by doping it with various concentrations of thallium, and the resultant samples were subjected to the same vaporization studies.

The experimental results are expressed in terms of Knudsen and Langmuir pressures; equilibrium and activation enthalpies, entropies and free energies of vaporization; vaporization coefficients; and mol percent of each vapor species. These results indicate that (A) the vaporization of molten selenium is indeed a retarded reaction with a vaporization coefficient of about 0.1 at 500 K for all vapor species and for all samples, pure and doped; (B) the vapor compositions under equilibrium and non-equilibrium conditions are about the same; (C) the activation enthalpy and entropy of vaporization for each species are lower than the equilibrium enthalpy and entropy of vaporization in all samples, whereas the activation free energy of vaporization for each species is higher than the equilibrium free energy of vaporization in all samples by about 2 Kcal/mol at 500 K.

A mechanism for the vaporization of molten selenium based on the transition-state theory is postulated in which the rate-limiting step is proposed to be the formation of short chain molecules lying on the liquid surface but still weakly bonded to long chains buried in the bulk. These short chains contain the same number of atoms as the gaseous ring molecules they form. Besides being able to explain the experimental observations, this mechanism indicates that Se_8 rings in the liquid do not vaporize directly to form Se_8 gaseous ring molecules. They are in equilibrium with long chain molecules in the liquid, which, in turn, have to form the weakly bonded short chain activated complexes on the liquid surface before vaporizing. A critical test of this mechanism is proposed, which also suggests an important alternate route to prepare high purity single crystals of trigonal selenium.

The microbalance experiments were performed at Arkansas State University. Financial support came from the U. S. Department of Energy under contract E(11-1)-1140 and from the University of Kansas General Research Fund.

STUDIES OF MOLECULAR SPECIES IN THE ARSENIC-OXYGEN SYSTEM

R. D. Brittain, K. H. Lau, and D. L. Hildenbrand

Materials Research Laboratory
SRI International
Menlo Park, CA 94025

In previous studies of the As-O system, the gaseous molecules As_4O_6 and AsO were identified, the former from electron diffraction and vapor density measurements on the saturated vapor over $As_2O_3(s)$, and the latter from the electronic band spectrum produced by a discharge source containing As_2O_3. By analogy with the N-O and P-O systems, it seems reasonable that polyatomic species such as As_2O_3, AsO_2, and others might play a significant role in the chemistry of the As-O system, but detailed studies have not been reported to date. We are investigating the gaseous arsenic oxides by mass spectrometry using a molecular effusion beam source; both quadrupole and magnetic sector instruments are being used.

In the mass spectrum of the saturated vapor over $As_2O_3(s)$ at about 370 K, the ions $As_4O_6^+$, $As_4O_5^+$, $As_3O_4^+$, and $As_2O_3^+$ were observed with threshold appearance potentials (AP) of 10.3, 15.5, 13.0, and 18.0 eV, all $\pm$ 0.3 eV. $As_4O_6^+$ is clearly a parent ion, in agreement with earlier studies, and the other ions are fragments. On superheating the vapor to 1000 K during passage through a second chamber, the AP's of $As_4O_5^+$, $As_3O_4^+$, and $As_2O_3^+$ dropped to 9.0, 11.5, and 10.0 eV, while AsO^+ appeared at 9.0 eV, signifying the presence of neutral As_4O_5, As_2O_3, and AsO. The AP of $As_3O_4^+$ dropped to 10.5 eV on heating the unsaturated vapor to 1200 K, and the new ion $As_4O_4^+$ appeared at 8.9 eV, indicating the latter to be a parent. In going one step further and superheating the vapor over a mixture of As_2O_3 and CaO to about 1500 K, AP($As_3O_4^+$) decreased to ~9.3 eV and the additional ions $As_4O_3^+$, $As_3O_3^+$, and AsO_2^+ not observed under other conditions appeared at 8.8, 11.0, and 10.8 eV.

The results indicate a surprising degree of complexity in As-O vapor, and point up the need for careful AP determinations in the identification process. Note that the ion $As_3O_4^+$ appears at four distinct threshold energies. Thus far, the stable gaseous species As_4O_6, As_4O_5, As_4O_4, As_4O_3, As_3O_4, As_2O_3, AsO_2, and AsO have been positively identified, and thermochemical studies of all but As_3O_4 and As_4O_3 have been carried out. The data for As_4O_6 agree closely with previous mass effusion rate measurements, while the results on AsO yield a dissociation energy within 0.06 eV of a value derived from a predissociation in the B state of AsO.

Thermodynamic Study of Gaseous Rare Earth - Iridium Carbides

K.A. Gingerich, B.M. Nappi, R. Haque and M. Pelino
Department of Chemistry, Texas A&M University
College Station, Texas 77843

The existence of stable mixed transition metal dicarbides and monocarbides has been established by high temperature mass spectrometric studies in a number of investigations (1-5). Here we present new examples from the lanthanum and yttrium mixed carbides with iridium.

The graphite effusion cell containing a lanthanum-iridium or yttrium-iridium sample was inserted into an outer tantalum Knudsen cell to minimize the loss of carbon at the high temperature of investigation. Excess graphite was added to insure unit activity of carbon in the condensed system. Each series of experiments was preceded by a pressure calibration using gold as a standard. The instrument and the experimental procedure used have been described previously (6). The mixed carbides were observed in connection with the investigation of gaseous LaIr (7) and IrY (8) and reference to these two papers is made for additional experimental details. The new mixed carbides observed and measured were IrLaC, $IrLaC_2$, $IrLaC_3$, IrYC and $IrYC_2$.

Information concerning the bond energies of the $IrMC_n$ molecules was derived from the third law evaluations of the reactions

$$Ir(g) + M(g) + nC \text{ (graph)} = IrMC_n(g)$$

The necessary thermal functions were taken from literature for the elements (9). For the new carbide molecules they were calculated from estimated molecular parameters by standard statistical thermodynamic procedures. The geometries considered were: MIrC (linear), IrMC (linear), MCIr (linear) and MCIr (bent) for the the monocarbdies; $IrMC_2$ (linear) and IrC_2M (linear) for the dicarbides and IrC_3La (linear) for the tricarbide. The partial pressures were obtained from the measured ion currents on the basis of a calibration utilizing the known $Au_2(g) = 2\ Au(g)$ (10) equilibrium. In Table I the selected third law reaction enthalphies are given for IrMC(g) and $IrMC_2(g)$.

Table I: Selected enthalpies for the reaction $Ir(g) + M(g) + nC(graph.) = IrMC_n(g)$ and derived atomization energies and heats of formation of the molecules $MIrC_n$. Values are in kcal mol^{-1}.

Molecule	ΔH°_0	$\Delta H^\circ_{298.15}$	D°_0	$D^\circ_{298.15}$	$\Delta H_{f,298.15}$
YIrC	-67.6±8	-67.9±8	238±8	240±8	194±8
$YIrC_2$	-61.4±8	-61.6±8	401±8	404±8	200±8
LaIrC	-78.6±8	-78.8±8	249±8	250±8	184±8
$LaIrC_2$	-95.4±15	-95.3±15	435±15	438±15	168±15
$LaIrC_3$	-52.7±15	-52.6±15	563±15	566±15	210±15

They were obtained as the respective average of the various assumed geometries. Also included are the derived atomization energies, D°_0 and $D^\circ_{298,15}$, and the standard heats of formation obtained for these gaseous molecules from the selected reaction enthalpies and from the heats of sublimation given by Hultgren et.al. (9). For $IrLaC_2$ the selected value for the reaction enthalpy corresponds to the average of the 2nd and 3rd law results obtained for each of the two assumed geometries. The error terms correspond to estimated overall uncertainties. The results for $LaIrC_3$ are based on only two data sets for which the respective reaction enthalphy disagrees by 7 kcal. We consider the results for $LaIrC_2(g)$ and $LaIrC_3(g)$ presented here as tentative.

Table II: Atomization energies, D_0°, of mixed rare earth - platinum metal carbides (values are in kcal mol^{-1}).

Molecule	D_0°	Ref.	Molecule	D_0°	Ref.
ScRhC	239±7	(4)	$RhScC_2$	386±10	(4)
CeRhC	242±10	(3)	$RhYC_2$	399±10	(4)
CeRuC	261±10	(3)	$RhCeC_2$	400±12	(1)
LaIrC	249±10	This inv.	$PtCeC_2$	405±12	(1)
YIrC	238±10		$YIrC_2$	401±10	This inv.

Tentative values (in kcal mol^{-1}) from this investigation:
$LaIrC_2$, 435±16 ; $LaIrC_3$, 563±16.

In Table II the atomization energies for the known mixed gaseous rare earth - platinum metal carbides are summarized. For either the monocarbides or the dicarbides the atomization energies are quite similar. The small trends that may be noted reflect the trend in the respective binary compounds. Thus the atomization energies of the mixed rhodium dicarbides with scandium, yttrium, and apparently cerium reflect the stability trend of the corresponding rare earth dicarbides. For the mixed cerium carbides with rhodium and platinum the difference in atomization energies reflects the difference in the dissociation energies of RhC and PtC. In general, the bond additivity concept appears to be applicable. But it may not be confidently applied to obtain information concerning the geometry or electronic partition function of a given molecule. There are too many variations possible in the individual component properties that may act differently in different molecules. For the application of the bond additivity concept reliable values for the dissociation energies of the diatomic rare earth carbides would also be needed, which are lacking. There is an urgent need for experimental spectroscopic data of such molecules. Such data are completely lacking. For the scandium compounds theoretical calculations of the molecular and electronic structure may also be possible.

Acknowledgement: The authors thank the National Science Foundation for the suppport given this work under Grant No. CHE-8007549.

References

1. K.A. Gingerich, J. Chem. Phys. 60, 3703 (1974).

2. S.K. Gupta and K.A. Gingerich, J. Chem. Soc. Faraday Trans. II, 74, 1851 (1978).

3. K.A.Gingerich and K.L. Cocke, Inorg. Chimica Acta 33, L107 (1979).

4. R. Haque and K.A. Gingerich, J. Chem. Soc. Faraday Trans. I, 75, 985 (1979).

5. S.K. Gupta and K.A. Gingerich, High-Temp. High-Press., 12, 273 (1980).

6. K.A. Gingerich, in NBS Special Publication 561, 1979,pp. 289-300.

7. R. Haque, M. Pelino and K.A. Gingerich, J. Chem. Phys. 71, 3072 (1979).

8. R. Haque, M. Pelino and K.A. Gingerich, J. Chem. Phys. 73, 4045 (1980).

9. R. Hultgren, P.D. Desai, D.T. Hawkins, M. Gleiser, K.K. Kelly, and D.D. Wagman, "Selected Values of the Thermodynamic Properties of the Elements." (American Society for Metals, Metals Park, Ohio, 1973).

10. J. Kordis, K.A. Gingerich and R.J. Seyse, J. Chem. Phys. 61, 5114 (1974).

High Temperature Photoelectron Spectroscopy of Small Molecules

by J. M. Dyke, G. D. Josland, R. A. Lewis, A. Morris and A. M. A. Ridha
Department of Chemistry, The University, Southampton SO9 5NH, U.K.

In recent studies, both ground and excited states of atoms have been observed by photoelectron spectroscopy (1, 2). For germanium and tin (1), bands associated with ionization from the outermost p orbital have been recorded from the ground (J=0) state as well as from the two lowest excited states (J=1 and J=2). Also bromine atoms in their first excited ($J=\frac{1}{2}$) state have been generated via the rapid reaction F + HBr (2).

As a continuation of these studies, the vacuum ultraviolet photoelectron spectrum (u.v.p.e.s.) of gallium has been recorded. This element was chosen for study as the ground state configuration of gallium is $4s^24p^1$ and the separation of the lowest $J=\frac{1}{2}$ and $J=\frac{3}{2}$ states is 0.102 eV. The first band of gallium (obtained by evaporating the metal at 1720 K) recorded with NeI radiation shows two peaks corresponding to the ionizations Ga^+ ($4s^2$, J=0) $\longleftarrow$ $Ga(4s^24p^1, J=\frac{3}{2})$ and Ga^+ ($4s^2$, J=0) $\longleftarrow$ Ga ($4s^24p^1$, $J=\frac{1}{2}$). The relative intensities of these bands for ionization from the $J=\frac{3}{2}$ and $J=\frac{1}{2}$ states is measured as (0.69 ± 0.07):1 giving an effective temperature of excited gallium of (1100 ± 150)K. The corresponding intensity ratio observed in the HeI spectrum of gallium is (5.0 ± 0.8):1. This result can be explained in terms of autoionization in the excited $J=\frac{3}{2}$ state. The 21.217 eV HeI photon excites a transition $Ga^*3d^94s^24p^2 \longleftarrow Ga3d^{10}4s^24p^1$, $J=\frac{1}{2}$, and the excited state, Ga*, then autoionizes to give states of Ga^+. No such resonance transition is possible from the gallium ground state (... $3d^{10}4s^24p^1$, $J=\frac{1}{2}$) with HeI radiation. Bands associated with the $(4s)^{-1}$ ionization of gallium have also been observed with HeI radiation and show clear evidence of an autoionization process involving the $Ga3d^{10}4s^24p^1$, $J=\frac{3}{2}$ state.

As an example of an unstable species generated by high temperature pyrolysis we cite the dimethylsilaethylene molecule. The band which we associate with the first ionization potential of dimethylsilaethylene, obtained from pyrolysis of dimethylsilacyclobutane at ∿ 970 K is shown in Figure 1.

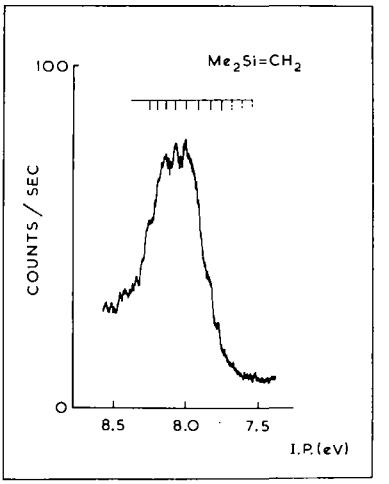

Figure 1: the band associated with the first ionization potential of dimethylsilaethylene

Ethylene was also observed as a pyrolysis product and when the area of the first band of ethylene and the first band of dimethylsilaethylene are plotted against temperature (measured ∿2 mm outside the furnace), the dimethylsilaethylene intensity showed a clear maximum at ∿970 K, whereas the ethylene signal increased steadily from 850 K, in agreement with a mass spectrometric low-pressure pyrolysis study of 1,1 dimethyl 1-silacyclobutane. The vertical and adiabatic ionization potentials of dimethylsilaethylene determined in this study are (8.00 ± 0.01) eV and (7.50 ± 0.05) eV respectively. Figure 1 also shows some resolvable, regular vibrational structure, measured as (600 ± 50) cm^{-1}, assigned tentatively to excitation of the Si-C stretching vibration in the ion reduced from the neutral molecule value of 1001 cm^{-1}.

As a continuation of our interest in diatomic metal and non-metal oxides such as CO, SiO and GeO, we have recently recorded the u.v.p.e.s. of SnO by vapourizing SnO_2(s) from an alumina lined carbon furnace at 1150 K. In molecules of this type, an important requirement is to use a theoretical method which accurately predicts vertical ionization potentials and this series provides a suitable test for such a method. For example, comparison has been made between experimental ionization potentials and ionization potentials predicted via the transition state approximation with the MSXα method (with sphere radii determined via Norman's criterion and overlapped by 30%) and *Hartree-Fock-Slater calculations using STO basis functions of double-zeta quality.* The agreement between experimental and computed vertical ionization potentials obtained via the Hartree-Fock-Slater method is very satisfactory whereas the MSXα predictions are poor, probably because molecules of this type have a relatively large inter-sphere region where the potential is assumed constant (3).

References

1. J. M. Dyke, N. K. Fayad, G. D. Josland and A. Morris
   Molecular Physics 41, 1980, 1051

2. J. M. Dyke, N. Jonathan, A. Morris and M. J. Winter (unpublished data)

3. J. M. Dyke, A. Morris and A. M. A. Ridha (unpublished date)

MASS SPECTROMETRIC STUDY OF THE GAS SPECIES IN THE GERMANIUM-LITHIUM SYSTEM; C.H. Wu, H. R. Ihle, KFA Jülich, Institut für Chemie, Germany

In earlier studies of the gaseous lithium-group IVa-compounds the dissociation energies of SiLi[1] and PbLi[2] have been measured. This work was continued and extended by an investigation of the gaseous lithium-germanium molecules. Dimers and polymers of germanium and lithium have previously been observed and the atomization energies of the following species have been determined: Ge_2[3], Ge_3 to Ge_7[4], Li_2[5] and Li_3[6]. In the present study we have analyzed the vapor composition over Ge-Li alloys by Knudsen effusion mass spectrometry. From the measurements the dissociation energy of GeLi and the atomization energy of $GeLi_2$ were derived.

EXPERIMENTAL

The experimental arrangement used for this work has been described in detail earlier[7]. Briefly, it consists of a quadrupole mass filter (Quad. 250B, EAI, Palo Alto, CA) and a molybdenum Knudsen cell heated by a rf generator as source for the moleculer beam enclosed in the ultra high vacuum chamber. A base pressure $< 10^{-11}$ Torr is maintained during measurements.

A shutter between the orifice of the Knudsen cell and the ion source enables a distinction between residual background and signals due to molecules effusing from the cell. The sensitivity is such, that the vapor pressure of lithium at its triple point ($\approx 7 \times 10^{-11}$ Torr) leads to an ion current of 3.5×10^{-16} A. Samples of the alloy were prepared in situ by melting together the constituents in about equal quantities.

The relative intensities of the ions detected during vaporization at 1370K are shown in Table I.

Table I: Relative ion intensities at 1370K and composition Ge/Li = 1

Ion	Li^+	Li_2^+	Ge^+	Ge_2^+	
Intensity	1.0	2.0×10^{-4}	2.0×10^{-4}	5.0×10^{-6}	
Ion	$GeLi^+$	$GeLi_2^+$	$GeLi_3^+$	$GeLi_4^+$	$Ge_2Li_2^+$
Intensity	1.3×10^{-4}	1.2×10^{-5}	8.0×10^{-6}	1.0×10^{-6}	8.0×10^{-7}

The species were identified by their m/e ratio, their isotopic composition, and their complete shutterability. The ion abundancies of $GeLi_3^+$, $GeLi_4^+$ and $Ge_2Li_2^+$ were too low to permit the evaluation of atomization energies. From the measured ion intensities I_i and from ionization cross sections of molecules estimated to be $0.75 \Sigma \sigma_i$[8], constants of gas equilibria were calculated from which the dissociation energy of GeLi and the atomization energy of $GeLi_2$ were determined.

The ion intensities were measured at an electron energy 2.5 eV above the appearance potentials of the ions to avoid dissociative ionization of molecules. Values of the free energy function $-(G_T^\circ - H_0^\circ)/T$ for the monatomic species were taken from Stull and Sinke[9], for Ge_2 from ref. [10, 11] and those for Li_2 from JANAF tables [12]. The equilibrium distance for GeLi was calculated as the sum of the metallic single bond radii according to Pauling[13]. The same internuclear distance has been assumed for Ge-Li in linear $GeLi_2$. The vibrational frequency for GeLi was calculated using the Guggenheimer relation[14] for polar bonded diatomic molecules and the frequencies for $GeLi_2$ were estimated from the relation suggested by Herzberg[15]. The electronic contribution to the free energy function was computed using a ground state degeneracy $g_i = 2$ for GeLi(g) and $g_i = 3$ for $GeLi_2$(g). The results for the calculation of the enthalpies of the reaction GeLi(g) + Ge(g) → Ge_2(g) + Li(g) and the dissociation energy D_0°(GeLi) are given in Table II.

Table II: Third law enthalpies for the reaction GeLi(g) + Ge(g) → Ge_2(g) + Li(g)

T	K	$-\Delta[(G_T^\circ - H_0^\circ)/T]$	ΔH_0°
(K)		(cal mol^{-1} K^{-1})	(kcal/mol)
1403	4.75×10^2	0.72	-18.19
1413	2.19×10^2	0.72	-16.15
1393	1.73×10^2	0.72	-15.27
1428	3.88×10^2	0.72	-17.94
1369	1.88×10^2	0.73	-15.24
			-16.56

D_0°(GeLi) = 48.3 kcal/mol using $D_0^\circ(Ge_2)$ = 64.9 kcal/mol

The measured stabilities of the group IVa-lithides are compared with values calculated according to Pauling's rule: $D(A-B) = 1/2[D(A-A) + D(B-B)] + 23(x_A - x_B)^2$ kcal/mol in Table III.

Table III: Stability of group IVa - lithides

Molecule	$D^{\circ}_{0,obs.}$ (kcal/mol)	$D^{\circ}_{0,Pauling}$ (kcal/mol)	$D^{\circ}_{0,obs.} - D^{\circ}_{0,Pauling}$ (kcal/mol)
SiLi	67.0	63.0	+ 4.0
GeLi	48.3	59.9	-11.6
PbLi	17.9	36.2	-18.3

With higher Z a decrease of the measured $D^{\circ}_0(MLi)$ relative to the calculated value is observed. From the enthalpies of the reactions: $GeLi_2(g) + Ge_2(g) \rightarrow Ge_2(g) + Li_2(g)$ and $GeLi_2(g) + Ge(g) \rightarrow 2GeLi(g)$ as given in Tables IV and V an atomization energy $D^{\circ}_0(GeLi_2)$ = 106.8 kcal/mol is obtained.

Table IV: Third law enthalpies for the reaction $GeLi_2(g) + Ge(g) \rightarrow Ge_2(g) + Li_2(g)$

T (K)	K	$-\Delta[(G^{\circ}_T - H^{\circ}_0)/T]$ (cal mol^{-1} K^{-1})	ΔH°_0 (kcal/mol^{-1})
1428	1.38×10^{-2}	1.99	14.99
1413	2.72×10^{-2}	2.00	12.96
1370	1.39×10^{-2}	2.03	14.42
1343	2.00×10^{-2}	2.05	13.19
			13.89

$D^{\circ}_0(GeLi_2)$ = 104.3 kcal/mol

Table V: Third law enthalpies for the reaction $GeLi_2(g) + Ge(g) \rightarrow 2GeLi(g)$

T (K)	K	$-\Delta[(G^{\circ}_T - H^{\circ}_0)/T]$ (cal mol^{-1} K^{-1})	ΔH°_0 (kcal/mol)
1307	2.22×10^{-2}	2.09	12.62
1370	7.37×10^{-2}	2.03	9.88
1413	1.16×10^{-2}	2.01	15.43
			12.64

$D^{\circ}_0(GeLi_2)$ = 109.3 kcal/mol $\quad D^{\circ}_{0,av.}(GeLi_2)$ = 106.8 kcal/mol

REFERENCES:

[1] H. R. Ihle, C. H. Wu, M. Miletic, and K. F. Zmbov, Advances in Mass Spectrometry, Vol.7A, p. 670 (Heyden, London, 1976)
[2] A. Neubert, H. R. Ihle and K. A. Gingerich, J. Chem. Phys. 73, 1406 (1980)
[3] J. Drowart, G. De Maria, A. J. H. Boerboom and M. G. Inghram, J. Chem. Phys. 30, 308 (1959)
[4] A. Kant and B. H. Strauss, J. Chem. Phys. 45, 822 (1966)
[5] W. C. Stwalley, J. Chem. Phys. 65, 2038 (1976)
[6] C. H. Wu, J. Chem. Phys. 65, 3138 (1976)
[7] H. R. Ihle and C. H. Wu, J. Chem. Phys. 63, 1605 (1975)
[8] B. Mann, J. Chem. Phys. 46, 1646 (1967)
[9] D. R. Stull and A. C. Sinke, Advan. Chem. Ser. 18, 96 (1958)
[10] A. Kant, J. Chem. Phys. 44, 2450 (1966)
[11] J. Drowart and R. E. Honig, J. Phys. Chem. 61, 980 (1957)
[12] JANAF Thermochemical Tables 2nd edition, NSRDS - NBS 37 (1971)
[13] L. Pauling, The Nature of the Chemical Bond (Cornell University, Ithaca, 1960), 3rd edition
[14] K. M. Guggenheimer, Proc. Phys. Soc. London 58, 456 (1946)
[15] G. Herzberg, Molecular Spectra and Molecular Structure II, Infrared and Raman Spectra of Polyatomic Molecules, D. van Nostrand Co, Inc. Princeton, N.J.

TEMPERATURE DEPENDENT ELECTRON IMPACT FRAGMENTATION IN HIGH TEMPERATURE MOLECULAR BEAMS

D. W. Bonnell and J. W. Hastie
Chemical Stability and Corrosion Division
National Bureau of Standards
Washington, DC 20234

High temperature mass spectrometry normally assumes the electron impact process to be temperature independent, since kT << eV. For the alkali halides, where fragmentation is extensive, the M^+/MX^+ ratio is normally temperature insensitive by Knudsen Effusion Mass Spectrometry (KMS). However, in one known exception, Akishin et al. (1) reported the observation of a 20 percent variation in the ratio $Cs^+/CsCl^+$ over the temperature range 800 K to 900 K. This effect can be explained in terms of Franck-Condon overlap for the molecule → molecule-ion transition. Bloom et al. (2), in explaining extended curvature in the toe region of ionization efficiency curves of alkali metal fragment ions invoked the Franck-Condon principle to postulate approximate functions for various states of CsCl leading to ionization. They suggested that the Franck-Condon region of vertical transition overlap for ground state CsCl intersected the repulsive edge of the lowest bound state for the molecule-ion. More recently, Dronin and Gorokhov (3) modeled the CsCl ionization process and obtained good agreement with the experimental results (1), but, unfortunately, the details of the calculation (4) are unavailable in this country in any form except abstract. They argue that, at the vaporization temperature, the alkali halide molecules have a substantial population of excited vibrational and rotational states. Typically, for CsCl at 800 K, only 32 percent of the molecules are in the v = 0 state, and the rotational population peaks in a broad maximum near J = 60. This temperature-sensitive thermal population of upper states affects the extent of Franck-Condon overlap and hence the degree of fragmentation as a function of temperature. However, there are no other reports in the literature, to our knowledge, of an observed temperature dependent fragmentation in alkali halide systems. Feather and Searcy (5) reported no detectable temperature dependence in the ratio $Na^+/NaCl^+$ over the temperature range 850 to 1050 K. Table 1 summarizes fragmentation ratio data for some alkali chlorides.

In the application of Transpiration Mass Spectrometry (TMS) to alkali halide systems, anomalously high ratios for M^+/MX^+ are observed (6). This can be interpreted in terms of the above model by noting that the source temperature is not a good description of the final state of the expansion. In addition to translational cooling, both rotation and, in many cases, vibration, relax to the temperature of the isentropic expansion. Thus the true temperature of molecules in the beam is very low. Using this argument, and calculating expansion temperature from source pressures using the sudden freeze approximation (6, 7), a comparison of the TMS and KMS data can be made. Typical results for NaCl are given in Figure 1. Note the smooth transition from low (TMS) to high (KMS) temperatures. The curve is qualitatively very similar to that obtained for the ratio of v = 0 to vibrationally excited states from a thermal Boltzmann distribution. On the other hand, Table 1 entries for K^+/KOH^+ show that TMS and KMS values are in reasonable agreement, and a pressure dependence plot shows only minimal dependence even at low temperatures, indicating good v = 0 state overlap.

It is still uncertain whether thermodynamic data obtained via KMS is significantly influenced by this effect. Future applications of the TMS method will need careful attention to this effect; however, it should be possible to extract more detailed information about molecule and molecule-ion potential functions from TMS experiments.

REFERENCES

1. P. A. Akishin, L. N. Gorokhov, and L. N. Sidorov, Proc. Acad. Sci. USSR, [Dok. Phys. Chem.] 135 [1], 1001 (1960).
2. H. Bloom, J. W. Hastie, and J. D. Morrison, J. Phys. Chem. 72, 3041 (1968).
3. A. A. Dronin and L. N. Gorokhov, Teplofiz. Vys. Temp. 10, 49 (1972).
4. A. A. Dronin and L. N. Gorokhov, Zh. Fiz. Khim. 49, 798 (1975).
5. D. H. Feather and A. W. Searcy, High Temp. Sci. 3, 155 (1971).
6. D. W. Bonnell and J. W. Hastie, Proc. 10th Matls. Symp. 1, 357 (1979).
7. C. A. Stearns, F. J. Kohl, G. C. Fryburg, and R. A. Miller, Proc. 10th Matls. Symp. 1, 303 (1979).
8. J. Berkowitz and W. A. Chupka, J. Chem. Phys. 29, 653 (1958).
9. T. A. Milne and H. M. Klein, J. Chem. Phys. 33, 1628 (1960).
10. H. Bloom and J. W. Hastie, Aust. J. Chem. 19, 1003 (1966).

11. H. Bloom and J. W. Hastie, J. Chem. Phys. 49, 2230 (1968).
12. A. V. Gusarov and L. N. Gorokhov, Zh. Fiz. Khim. 42, 860 (1968).
13. R. C. Schoonmaker and R. F. Porter, J. Chem. Phys. 31, 830 (1959).
14. J. W. Hastie and J. L. Margrave, High Temp. Sci. 1, 481 (1969).

Table 1
Fragmentation Ratios of Selected Alkali Halides/Hydroxides

Molecule	$R = M^+/MX^+$ [a]	Temperature K	eV	Comments
NaCl	1.7	~ 950	75	(8)
	1.4	~ 940	20	(9)
	1.0 and 0.8	850 to 1050	70	(5)
	1.5	952	30	(6)
	25 to 33	1090 to 1440[b]	30	This work
KCl	6.0	~ 900	75	(8)
	60 to 85	990	30	This work
CsCl	86	~ 830	75	(8)
	154	861	50	(10)
	110	850	20	(11)
	86; 70; 67	800; 828; 900	90	(1)
	310 to 135	980 to 1440[b]	30	This work
KOH	0.43	623 to 670	50	(12)
	1.1	650 to 950	100	(13)
	2.0 ± 0.3	990[b]	30	This work

[a] Assumes no contribution to M^+ or MX^+ from M_2X^+ or higher polymers; for X = halide and M > Li, it has been concluded (14) that M^+ and MX^+ have the same molecular origin. Literature data are from KMS experiments where $T_{beam} = T_{source}$. In present study, with supersonic expansion conditions $T_{beam} << T_{source}$.

[b] Sample temperature. Calculated beam temperature < 100 K due to expansion.

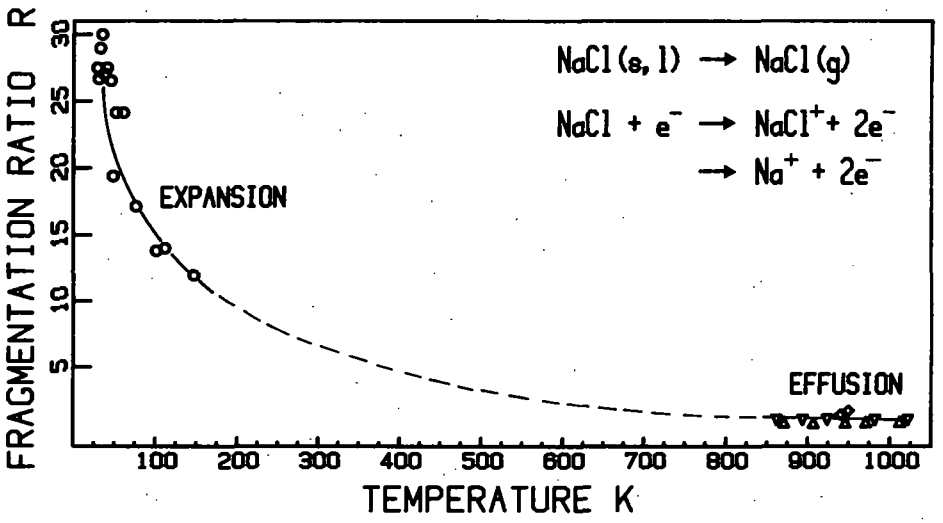

Fig. 1. Dependence of fragmentation ratio $R = Na^+/NaCl^+$ on expansion (TMS, this work) or effusion (KMS, see Table 1) temperature.

UPDATING OF AN AEI-MS9 MASS SPECTROMETER, AN IN-HOUSE CONVERSION: G. K. EIGENDORF, D. CATT and M. VAGG, Department of Chemistry, University of British Columbia, Vancouver, B.C., Canada V6T 1Y6

An AEI-MS9 mass spectrometer, vintage 1964, has been overhauled extensively.

All components of the control console, except for the original UV chart recorder, have been replaced. A new console was constructed from three 19 inch rack-mount cabinets with desk front.

Wherever possible, electronic components manufactured in North America were utilized. In addition a hexapole and y-lens kit were obtained from KRATOS.

The analyzer section was also reconstructed. Rotary pumps were placed in a cubicle separate from the analyzer. New ion gauges and thermocouples with controls and protection features were added. A new inlet system for gaseous and liquid samples and a multiple reference inlet system have been added.

Controls for baking heaters, probes and interface heaters are located in a separate small cabinet.

The feed through plate at the ESA box which carries the leads for the ESA plates, the y and z lenses and the monitor has also been replaced. A KRATOS MS50 magnet has been used to replace the old magnet.

UPGRADING 21-110 MASS SPECTROGRAPHS

L.F. Herzog, T.J. Eskew, D.J. Marshall, and K.H. Underwood,
NUCLIDE CORP, 642 E. College Ave, State College, PA 16801

There are a substantial number of CEC/du Pont 21-110 mass spectrographs in the field, but many are not in use – due to failures in electronics, decreased resolution, loss of sensitivity, and/or loss of ability to measure trace-abundance species due to increases in background-spectrum levels and/or in "fogging", coupled with the fact that the manufacturer no longer provides assistance in solving such problems.

The ion-optics of the "110" are, however, fundamentally sound, and the materials used in its high vacuum system, and the methods of joining and gasketing used, and so on, are compatible with the attainment of ultra-high vacuum. Hence, in the hands of persons who have the in-house expertise to keep it running, it still has the capability to be an exceptionally useful ion analyzer – as papers given at this Conference demonstrate. Hence, updating and upgrading an idle 21-110 and adding mechanisms to keep it in good alignment more easily is, we felt, well worth considering – since today such an instrument, new, costs at least $500,000.

We have therefore worked out a complete program for upgrading 21-110s which can (if the budget so dictates) be executed piecemeal, with each change improving some aspect of performance. We also made it an objective to make it convenient to add later-developed accessories such as ion, laser and field desorption probes, and EOID or other multi-channel electrical detector arrays, and to automate operation.

Fortunately, many electronic components used in Nuclide's GRAF III spectrographs can be used without change in the 110, simplifying both upgrading and later servicing; this also helps keep costs down. (Incidentally, these components can also be fitted to existing mass spectrographs of other manufacture, in many cases.)

Two magnet regulators are offered – one regulates coil current only (with very high stability) while the other can regulate magnetic field as well. The current-only regulator is offered, even though the ability to precisely set magnet field rather than current is essential to monitoring selected ions by stepping among the magnetic field values that bring desired species into focus onto a detector at a fixed radius, because this capability is not required for photoplate detection only. Also, there is a serious problem in implementing field control, in that most 110 magnets do not provide any space in the magnet-gap in which to mount a field sensor. Sensing field in an auxiliary gap created in series with the main gap by raising the top yoke piece by 0.040" is recommended – reasons for this choice and the use of a temperature-compensated Hall probe being given.

The original electronics of the 110 are not packaged in standard-width electronic racks, while the GRAF III's are. To keep down cost we decided to use them "as is", mounted in a new 2-bay console. This yields a fringe-benefit: some of the new pumps recommended can be added in locations originally filled with electronics.

Automated MS control and data processing systems developed for GRAF III (e.g., PC-SIM and DACS-III) transfer and analyze photoplate-collected spectra, and collect and analyze data taken using electrical ion detection by scanning or peak-stepping.

Improving Ion Transmission and Focusing

The 21-110 has a 25 inch radius cylindrical electrostatic analyzer, which gives it the capability of resolution as high as 50,000. As delivered, it has no ion-optical elements for deflecting or focusing the beam in the Z-direction, although it does have mechanical provision for adjusting the positions of various parts relative to each other. Since gains in sensitivity of up to X1000 are often possible (depending on how

good alignment was before), Nuclide especially recommends that electrical beam-steering and focusing be added. The GRAF III's FEA-1 control provides the voltages necessary to deflect the beam and to touch-up its focus via an einzel lens.

Spark Source 21-110

The complete upgrading program additionally includes thoroughly cleaning and degreasing the system, and replacing the original hivac "oil" diffusion pumps with much higher speed pumps of other types, to eliminate "oil" hydrocarbon spectrum buildup, reduce all background spectrum intensities, and substantially decrease pumpdown time to operating vacuum levels after changing samples.

A GRAF III source housing with a high-conductance pumping lead replaces the original; it connects to a new drift-tube housing in which ion lens elements not present in the original facilitate maximizing beam transmission and focus without the need to make tedious mechanical adjustments. With the GRAF III source housing installed, accessories designed for it such as ion, laser and electron-beam probes can be added as easily as on the Nuclide spectrograph.

The new source housing also has ports on both sides on which to mount electrode motion mechanisms. This makes it possible to add a system for precise automatic control of the location of the spark with respect to the ion-optical axis, of the type H. Svec and R. Conzemius added to a Nuclide GRAF-II.

The original "final amplifier" of the R-f spark-forming circuit is retained because neither the technology nor the components available has changed appreciably.

The 21-110's original pumping system had three oil diffusion pumps. Estimated speeds at these ports are given in a table; all are quite low. In comparison, the new pumping system installed on a Spark-110 that is the basis of an analytical service is as follows: the replacement GRAF III source housing has a 6-inch pumping port, with a 1500 L/S turbopump and 6-inch valve; speed at the source port is now over 700 L/S, a more than tenfold increase.

The replacement drift tube housing also has a higher-conductance source-isolation valve and a much larger pumping port with 150 L/S ion pump.

A valved 270 L/S turbo was added to pump the magnetic analyzer using one of the photoplate access ports. The original "short circuit" in the pumping systems of ESA and magnetic analyzer was eliminated and 150 L/S getter-ion pumps installed on both ports.

"Organic" (EB Source) 21-110s

The upgrading program for EB-source ("organic") 21-110s is identical in most particulars. However, if it will have to cope with very high gas flow rates, as in GC/MS or "chemical" ionization, and trace-species detection is not important, a very large (e.g. 6") source diffusion pump may be recommended. New capabilities are offered for the EB-110 also — for example, the field desorption probe we described at this Conference in 1980.

Summary:

The changeover to the GRAF III's source housing, increases in pumping speed, elimination of the possibility of oil contamination, addition of electrical beam-steering and focusing, and the replacement of the original electronics with modern Nuclide units not only brings the 110 spectrographs up to modern standards but restores them and their owners to a relationship with a MS manufacturer who will accept responsibility for servicing them, and who has an ongoing development program for mass spectrographs, the results of which will thereafter be directly applicable to the modified 110s.

GAS-PHASE REACTIONS OF Fe^+ WITH KETONES AND ETHERS

R.C. Burnier, G.D. Byrd, and B.S. Freiser

Department of Chemistry
Purdue University
West Lafayette, Indiana 47907

A pulsed laser has been used in conjunction with an ICR spectrometer to generate and study the gas phase ion-molecule reactions of Fe^+ with simple carbonyls and ethers. Some examples of these reactions are presented in Table I. In both systems initial interaction generates a chemically activated species which can then undergo the sequential processes of oxidative addition, rearrangement, and reductive elimination.

For ketones, decarbonylation by Fe^+ is an important reaction channel only for the smaller ketones such as acetone and 2-butanone. With larger ketones facile β-hydride shifts compete effectively with the alkyl recombination. No evidence for metal-carbene complexes formed by α-elimination is observed.

For large aliphatic ketones a number of competitive initial dissociation processes may exist. In particular, rather extensive dehydrogenation occurs for ketones with long unbranched alkyl groups and for alkyl groups branched at the α-carbon loss of CH_4 dominates. Thus, interaction with the alkyl portion of the ketone becomes more important as the ketone increases in size.

For ethers, the oxidative addition of Fe^+ across the C-O bond produces a metal alkoxide which undergoes β-elimination with neutral alkane or alcohol loss.

In general, the direct cleavage of C-C, C-H, and C-O bonds produces alkyl, acyl, and alkoxide Fe^+ intermediates whose kinetic labilities should be strongly influenced by the extent of coordinative saturation of the metal. The absence of other coordinating ligands provides the ideal environment for β-elimination.

More details of this work will be printed in the Journal of American Chemical Society.

Table I

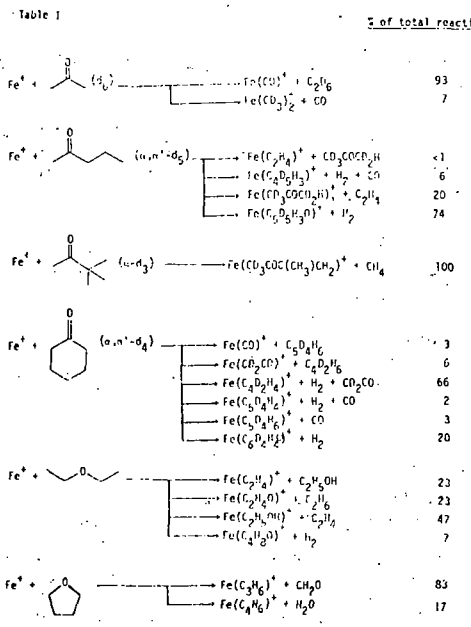

Interactions Of Transition Metal Ions With Ketones In The Gas Phase

Kevin A. Kalmbach and Douglas P. Ridge
University of Delaware, Newark, De. 19711

Fragmentation and condensation are two reactive channels available to a transition metal-ketone complex. All metal ions studied form the stabilized condensation product. The observed collision complex must have a lifetime of at least a millisecond in order to be observed with drift mode Ion Cyclotron Resonance Spectroscopy. Stabilization can occur by a radiative process or collision with a neutral.

$$M^+ + \text{Ketone} \longrightarrow [\text{M-Ketone}]^{+*} \xrightarrow{+N} [\text{M-Ketone}]^+ + N^*$$

$$[\text{M-Ketone}]^{+*} \longrightarrow [\text{M-Ketone}]^+ + h\nu$$

The pressure dependence of the M^+ double resonance in several systems indicates a radiative stabilization of the collision complex, probably through infrared emmision by the carbonyl chromophore.

While Mn^+ and Cr^+ form the condnsation product exclusively, ketone complexes with Fe^+, Co^+ and Ni^+ can undergo fragmentation reactions with cyclic ketones. The reactions of Fe^+ with cyclohexanone[1] are shown below.

$$Fe^+ + C_6H_{10}O \longrightarrow FeC_6H_6^+ + CH_2CO + H_2$$

$$C_6H_{10}O \longrightarrow FeC_6H_8O^+ + H_2$$

In addition, reactions of Co^+ and Ni also produce a metal-ketene complex ion. Deuterium labeling, study of the 2-cyclohexen-1-one and norcamphor systems suggest an electrocyclic reversion mechanism.

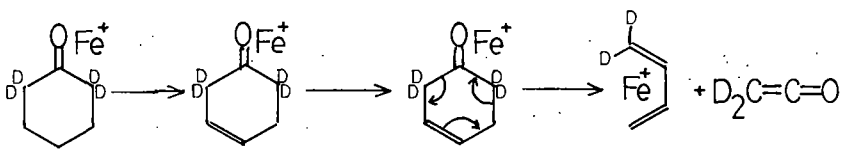

Reaction of Fe^+ with cycloheptanone and 2-cyclohepten-1-one produce similar products including dehydrogenation, loss of ketene or methyl ketene neutral.

1) Allison, John; Ph.D. Thesis (1977)
University of Delaware; Newark, De. 19711

An interesting synthetic technique to produce odd-carbon cyclic ketones has been recently reported[2].

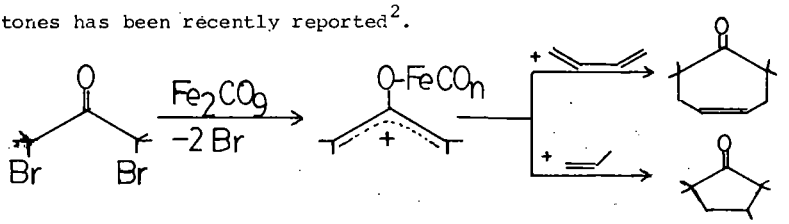

The proposed intermediate, an iron oxy-allyl complex ion (Noyori Reagent) is believed to add electrocyclicly to a diene or olefin producing the ketone product.

The $(Fe\text{-}C_3H_4O)^+$ product ion, which has the same stoichiometry as the Noyori reagent ion, is observed from reaction of Fe^+ and ^{18}O-cyclopentanone. Further study to determine the exact structure,

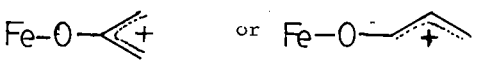

, is required.

These studies suggest that electrocyclic processes occur in the fragmentation of cyclic ketones by transition metal ions. This similarity to the Noyori reaction may indicate that similar synthetic routes are possible utilizing metal ions to activate ketene for electrocyclic addition.

2). Noyori, Ryoji; Accounts of Chemical Research
Volume 12,2(1979) p.61

Proton Transfer and Isotopic Exchange Reactions of Ar H^+

J.H. FUTRELL*, W. LINDINGER, H. VILLINGER and F. HOWORKA

Inst. f. Experimentalphysik der Universität Innsbruck, Abt. f. Atom- und Molekülphysik, Karl Schönherrstrasse 3, A 6020 Innsbruck, Austria

The proton transfer reactions from ArH^+ to H_2, D_2, CH_4, N_2, O_2, CO and CO_2 and the corresponding deuteron transfer reactions of ArD^+ with H_2 and D_2 as well as several isotopic exchange reactions of the type

$$XH^+ + D_2 \rightarrow XD^+ + HD$$

have been investigated in a drift experiment. The apparatus used for these investigations is a slow flow drift tube like the one described by Lindinger et al.[1], but with the addition of a venturi inlet similar to the disign of Smith and Adams[2] through which ions, preselected by a quadrupole mass filter, enter the drift chamber. From the decline of the reactant ion signal with addition of reactant gas to the buffer, reaction rate coefficients are obtained in the usual way[3], and as such measurements are performed at drift conditions of various E/N values (E denoting the electric field strength and N the number density of the buffer gas), rate coefficients are obtained as a function of the relative kinetic energy KE_{cm}, between the reactants[1,3]. Helium was used as a buffer gas; in some cases argon was used.

The proton transfer reactions of $ArH\ (D)^+$ with $H_2(D_2)$ all proceed fast at room temperature (the values of the rate constants being in the range from 8 to 5 x 10^{-10} $cm^3\ sec^{-1}$) and show a decline of the rate coefficients by nearly a factor of 2 when KE_{cm} is increased up to a few tenths of an eV. Besides the fast proton transfer, no isotopic exchange is observed in these reactions. In Ar - H_2 mixtures, equilibrium between ArH^+ and H_3^+ is easily obtained, and a Van't Hoff plot, obtained from the equilibrium constants, at various E/N values, a difference in the proton affinities ΔPA = 0.55 eV is calculated, which is in agreement with the accepted values of the proton affinities of Ar and H_2.

The reactions of ArH^+ with CH_4, N_2, O_2, O_2, CO and CO_2 were investigated in the energy regime from thermal to a few eV, KE_{cm}. All these reactions proceed rapidly with rate coefficients close to the theoretical limits[4]; no kinetic energy dependences of these rate coefficients were observed.

While in the reaction of ArH^+ with D_2 no isotopic exchange to produce ArD^+ was observed, isotopic exchange is fast in the reaction of H_3^+ with D_2 and of N_2H^+ with D_2. Further tests seem to indicate that isotopic exchange does not occur, in reactions of XH^+ with D_2, when it has to compete with an exoergic, and therefore fast proton transfer channel, i.e., when $PA(D_2) > PA(X)$. In cases where the proton transfer channel is endoergic, the complexes XH^+-D_2 seem to have a lifetime long enough to allow for the isotopic exchange to produce XD^+.

A more detailed discussion on the kinetics of the proton transfer reactions of ArH^+ with the molecules listed above will be given in a forthcoming paper.[5]

*Fulbright Fellow 1980/81 on leave from Dept. Chem. Univ. Salt Lake City, Utah 84112, USA

1. W. Lindinger, E. Alge, H. Störi, R.N. Varney, H. Helm, P. Holzmann and M. Pahl, Int. J. Mass Spectrom. Ion Phys. 30, 251 (1979)
2. N.G. Adams and D. Smith, Int. J. Mass Spectrom. Ion Phys. 21, 349 (1976)
3. M. McFarland, D.L. Albritton, F.C. Fehsenfeld, E.E. Ferguson and A.L. Schmeltekopf, J. Chem. Phys. 59, 6620 (1973)
4. T. Su and M.T. Bowers, Int. J. Mass Spectrom. Ion Phys. 12, 347 (1973)
5. H. Villinger, J. Futrell, F. Howorka, N. Duric and W. Lindinger, to be published

Generation of Transition Metal Polysulfide Ions in the Gas Phase by Sequential Reactions of Metal Ions with Ethylene Sulfide

T.J. Carlin, M.B. Wise, and B.S. Freiser

Department of Chemistry
Purdue University
West Lafayette, Indiana 47907

Sequential reactions of some atomic metal ions with ethylene sulfide in the gas phase lead to the formation of metal polysulfide ions. V^+ was found to attach at least eight sulfur atoms by the reaction

$$VS^+_{n-1} + \text{ethylene sulfide} \rightarrow VS^+_n + C_2H_4 \quad (n = 1 \rightarrow 8).$$

Similarly Co^+ and Ti^+ were observed to attach at least five sulfurs and Fe^+ at least six. Al^+ and Cu^+ show only direct attachment of ethylene sulfide. At higher pressures additional reaction products are observed and postulated as corresponding to "dithiolene" ions. All the masses observed in the V^+-ethylene sulfide system can be fit to the general formula

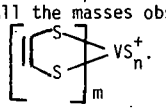

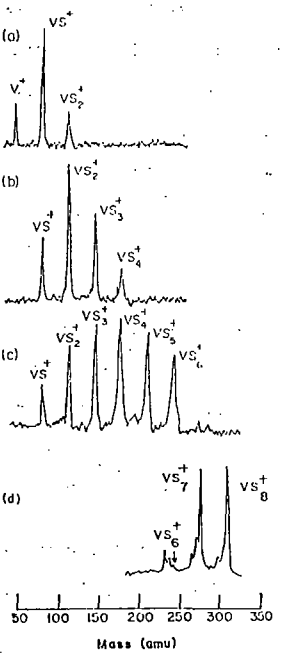

V^+ chemical ionization mass spectra of ethylene sulfide at neutral gas pressures of approximately (a) 1×10^{-7} torr (b) 2×10^{-7} torr (c) 5×10^{-7} torr and (d) 5×10^{-6} torr. Other conditions were a trapping time of 250 ms and an observing frequency of 65.2 kHz.

REACTIONS OF METAL DIMER IONS IN THE GAS PHASE

R. B. Freas and D. P. Ridge, University of Delaware, Newark, De. 19711

Recent investigations in our laboratory have been done utilizing the technique of ion cyclotron resonance spectroscopy (ICR) to explore the chemistry of metal cluster ions and their reactions with simple organic neutrals. The objective has been to study these reactions to gain knowledge concerning the mechanisms and structures of the species involved, as well as to provide an insight as to the relationship of catalytic processes.

The metal dimer ions Mn_2^+ and Co_2^+ are major peaks in the fragmentation spectrum produced in the ICR by 70 eV electron impact upon the corresponding binuclear carbonyls, dimanganesedecacarbonyl, $Mn_2(CO)_{10}$, and dicobaltoctacarbonyl, $Co_2(CO)_8$. The organic species studied included simple alkanes, alcohols and alkyl halides. Precursors of the product ions were unambiguously identified by the double resonance technique.

Considerable interest has arisen concerning the activation of carbon-carbon bonds in simple alkanes and recent literature[1] reports the cleavage of pentane by small clusters of metal atoms cocondensed at 77K. Although the monometallic Co^+ ion has been observed to react[2], in contrast to the literature neither of the dimer ions have been observed to react with alkanes.

With any alcohol, the only reaction of the Mn_2^+ ion that has been observed is the same as that of the reaction with methanol shown in [1], that is, cleavage of the Mn-Mn$^+$ bond and formation of an $MnROH^+$ product ion.

$$Mn_2^+ + CH_3OH \longrightarrow MnCH_3OH^+ + Mn \qquad [1]$$

The reaction of the dimanganese ion with isopropyl bromide is shown below, and is representative of the reaction with any alkyl bromide.

$$Mn_2^+ + i\text{-}C_3H_7Br \xrightarrow{10} MnC_3H_7Br^+ + Mn$$
$$\xrightarrow{58} Mn_2Br^+ + C_3H_7 \qquad [2]$$
$$\xrightarrow{32} Mn_2HBr^+ + C_3H_6$$

In the reaction with the alkyl bromides the reaction channnel to produce the MnRBr+ product is a significantly less important pathway than in the analogous reactions with the alkyl chlorides and the alcohols. With ethyl iodide, $MnC_2H_5I^+$ is not observed as a reaction product.

The reactions of the dimanganese ions are perceived to proceed through insertion of one end of the manganese dimer ion into the R-X bond analogous to the reactions of monometallic ions with these organics[3]. The proposed reaction scheme is shown below.

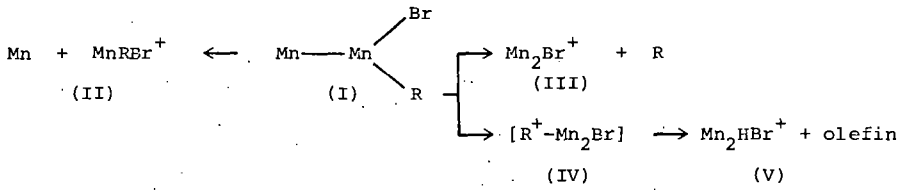

Insertion into the R-Br bond produces intermediate (I). If cleavage of the Mn-Mn bond occurs, the products shown in (II) are observed. If cleavage of the Mn-R bond in (I) occurs, then the products are those in (III) and (IV). (IV) reacts via proton transfer to give the products observed in (V).

In contrast to the dimanganese ion, the cobalt dimer has not been observed to react to cleave the Co-Co bond. Also the dicobalt ion reacts with alcohols and alkyl halides to eliminate HX forming $Co_2(olefin)^+$ as a product. A typical reaction, that with isopropyl bromide is shown in [3].

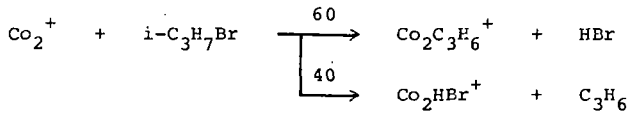

[3]

Again a proton transfer is most likely responsible for the formation of the Co_2HBr^+ product as in (IV).

In general, the metal dimer ions so far observed are less reactive than their monometallic counterparts, although interesting reactivity is seen and needs to be studied more thoroughly.

[1] S.C. Davis and K.J. Klabunde; J. Am. Chem. Soc., 100, 5973(1978).

[2] R.B. Freas and D.P. Ridge; J. Am. Chem. Soc., 102, 7129(1980).

[3] J. Allison and D.P. Ridge; J. Am. Chem. Soc., 98, 7445(1976).

THE DEPENDENCE OF ABSOLUTE BIMOLECULAR ION-MOLECULE CONSTANTS AND BRANDING RATIOS ON INTERNAL ENERGY IN THE REACTANT ION; P. R. KEMPER and M. T. BOWERS; Dept. of Chem., Univ. of Calif., Santa Barbara, CA 93106

In recent years beautiful experiments have been done using coincidence techniques to measure the dependence of absolute unimolecular rate constants on the internal energy of the reactant ion. Only a few bimolecular studies have been done, however, due to the difficult task of forming the reactant in a known energy state under noncoincidence conditions and often these studies required the reactant ion have significant kinetic energy. In this paper we report the first results obtained on the UCSB Tandem ICR. In this instrument reactant ions are formed in a temperature variable high pressure source, extracted and accelerated, Dempster Mass analyzed, deaccelerated and injected through a miniature Wein filter into a differentially pumped ICR cell. Vibrationally excited ions are formed in the source by charge transfer. The amount of internal energy is determined by measuring the kinetic energy release of the charge transfer reaction and invoking energy conservation. It will be shown NH_3^+ ions can be conveniently formed with known amounts of internal enrgy between 0-5 eV. These ions are then injected into the ICR cell at kinetic energies $\leq$0.2 eV and absolute and relative rate constants measured. A number of systems will be reported.

COLLISIONAL DISSOCIATION OF CLUSTERED NEGATIVE IONS, $OH^-(H_2O)n$, (n=1-4)

Richard L.C. Wu and Thomas O. Tiernan
Brehm Laboratory, Wright State University
Dayton, Ohio 45435

Studies of ion-molecule clustering reactions advance our understanding of the ionized species present in the upper atmosphere, and are also useful in elucidating the basic theory of nucleation phenomena. Thermodynamic data, such as dissociation energies, are important in determining the stability of such clusters. Thus far, these data have been derived only from high pressure mass spectrometer measurements. It is desirable, however, to verify the latter results by obtaining bond energy data for ion clusters by using different techniques. The present study entails measurements of the energy thresholds for collision-induced dissociation (CID) reactions of cluster ions obtained with a tandem mass spectrometer. Such methods have previously been applied in several studies reported from our laboratory.

The apparatus used in the present study has been previously described. The projectile ions, $OH^-(H_2O)n$, (n=1-4), were produced by electron impact on a gaseous mixture of H_2O and N_2O at elevated pressure (~>0.1 torr) and ambient temperature. The projectile ions are apparently produced by a sequence of processes which involve, initially, dissociative electron attachment, followed by appropriate negative ion-molecule reactions yielding the clustered species of interest, $O^- + H_2O \rightarrow OH^- + OH$, and $OH^- + n\ H_2O \rightarrow OH^-(H_2O)_n$, n=1-4. The measured translational energy thresholds were corrected in order to take account of the incident ion energy distribution and the Doppler motion of the neutral target.

Typical excitation functions for $OH^-(H_2O)/Ar$ and $OH^-(H_2O)_2/Xe$ reactions are shown in Figures 1 and 2, respectively. Table 1 summarizes the translational energy thresholds derived from these excitation functions, and from similar data obtained using $OH^-(H_2O)_3$ and $OH^-(H_2O)_4$ as the projectile ions. The uncertainty in the values of E_o is ±0.1 eV (CM), which is estimated from the ranges of E_o values which yield a good fit to the experimental data. The high pressure mass spectrometric equilibrium data of Kebarle and co-workers are also shown in Table I. Within experimental error, the present results are in excellent agreement with the previously reported data which are available.

Acknowledgement

This work was supported in part by U.S. DOE contract No. DE-AC02-80ER-10668 with Wright State University.

Table 1. Bond Dissociation Energy Data For Negative Cluster Ions

Species Studied	Method of Formation	Bond Dissociation Energy (eV) This Study	Lit.
$OH^- \cdot H_2O$	$N_2O + H_2O + e$	$D_0^\circ(OH^- - H_2O)=1.0 \pm 0.1$	1.08 [a]
	$H_2O + e$ + trace H_2O_2		
$OH^- \cdot (H_2O)_2$	$N_2O + H_2O + e$	$D_0^\circ(OH^- \cdot H_2O - H_2O)=0.7 \pm 0.1$	0.71 [a]
		$D_0^\circ(OH^- - 2H_2O)=1.7 \pm 0.1$	--
$OH^- \cdot (H_2O)_3$	$N_2O + H_2O + e$	$D_0^\circ(OH^- \cdot 2H_2O - H_2O)=0.7 \pm 0.1$	0.65 [a]
$OH^- \cdot (H_2O)_4$	$N_2O + H_2O + e$	$D_0^\circ(OH^- \cdot 3H_2O - H_2O)=0.65 \pm 0.1$	0.62 [a]

[a] J.D. Payzant, R. Yamdagni, and P. Kebarle, Can. J. Chem. 49, 3309 (1971).

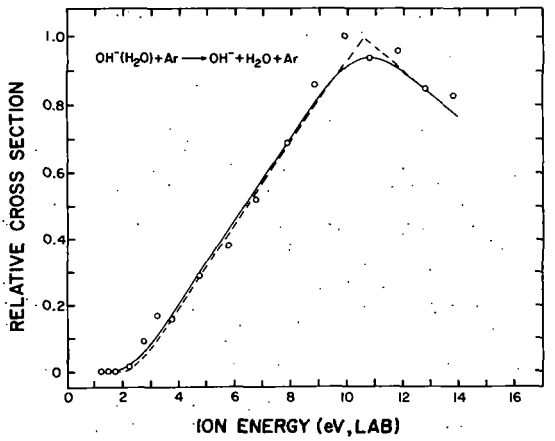

Fig. 1. Cross section for the reaction $OH^-(H_2O) + Ar \rightarrow OH^- + H_2O + Ar$ as a function of translational energy. Solid line is the calculated "best fit" excitation function.

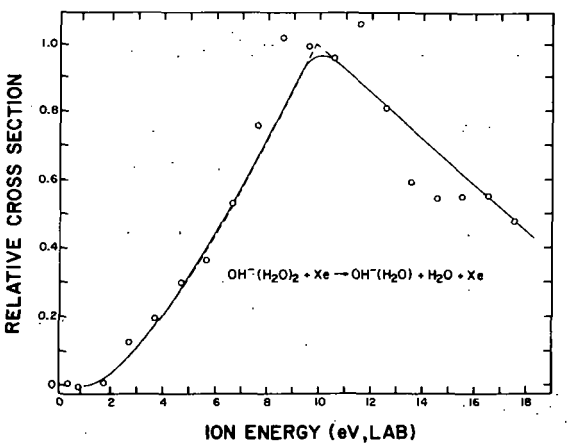

Fig. 2. Cross section for the reaction $OH^-(H_2O)_2 + Xe \rightarrow OH^-(H_2O) + H_2O + Xe$ as a function of translational energy. Solid line is the calculated "best fit" excitation function.

MOBILITY OF NEGATIVE HALOGEN IONS

T. Fujii* and G.G. Meisels
Department of Chemistry, University of Nebraska, Lincon, NE 68588

Knowledge of the mobilities of negative halogen ions is important to a quantitative understanding of plasma, laser and electrical discharge physics and radiation chemistry in atmospheres containing halogenated compounds, and to the measurement of ion-molecule reaction rate constants in negative chemical ionization as well as their application to analytical negative chemical ionization. The energy or temperature dependence of drift properties may also be used to derive ion-molecule interaction potential (1). However, only little information about mobilities of negativities is available.

The mobilities of SF_6^- in He and of F^-, Cl^-, Br^- and I^- in Ar, Xe, H_2, N_2, CO, CH_4 have been investigated at 298°K over the field strength (E/P) range of 5 to 25 V/cm Torr using time-resolved high pressure mass spectrometry and an ion source with coaxial electron entrance and ion drift fields. The reduced mobilities obtained by this method are in good agreement with those obtained in drift tubes when comparison is possible. Results are compared with "Langevin" polarization limits and with the drift properties of isoelectronic positive alkali ions measured previously.

APPARATUS. Measurements were conducted using a pulsed high pressure mass spectrometer described previously (2). Briefly the electron entrance aperture and ion exit slit are coaxial, the parallel equipotential lines are parallel throughout the entire drift region, and the electron gun is pulsed by unblocking 0.1 ∿ 0.2 μsec at ca. 1 kHz. A new detection system for negative ion is employed.

MOBILITY OF SF_6^- IN He. Figure 1 shows a typical arrival time distribution of SF_6^- in He at the extraction potential E of 7.5 V/cm in the limit of low electron energy (16 eV nominal) and high ion source pressure (1.0 Torr). The points are experimental and the solid line is the calculated distribution (3).

Figure 2 shows the variation of the measured drift velocities (v_d) for SF_6^- in He with increasing E/P at a source pressure of 1.0 Torr. v_d varies linearly with E/P throughout the entire range studied, as expected for E/P < 30 V/cm/Torr. The slope leads to a measured mobility of SF_6^- in He $K_0(SF_6^-/He, 298°K) = 12.0 \pm 0.2$ $cm^2/V \cdot sec$, in good agreement with the value 12.2 $cm^2/V \cdot sec$ obtained using a drift tube mass spectrometer.

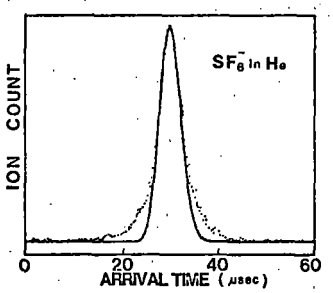

Figure 1: Arrival time distribution of SF_6^- in He. E/p was 7.5 V/cm Torr and T was 298°K. The solid curve is the calculated distribution.

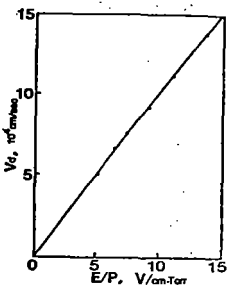

Figure 2: Dependence of drift velocities of SF_6^- in He on E/P. P(He) = 1.0 Torr, T = 298°K, 16 eV electrons.

TABLE I.

Low Field Mobilities of Negative Halogen Ions in Ar at 298°K.

Ion	$K_o(cm^2/V \cdot sec)$ This work	Literature
F^-	3.56 ± 0.08	3.33 ± 0.17
Cl^-	2.89 ± 0.06	2.87 ± 0.14
Br^-	2.46 ± 0.02	2.40 ± 0.12
I^-	2.28 ± 0.07	2.27 ± 0.11

*Visiting Research Scientist from the National Institute for Environmental Studies in Japan.

MOBILITIES OF F^-, Cl^-, Br^- AND I^- IN Ar. Measurements of low-field mobility of F^-, Cl^-, Br^- and I^- in Ar were made at 298°K (Table I). The comparison between this work and literature values indicates excellent agreement except for F^-. Even for F^-, however, the discrepancy is still within the combined error limits of the two methods.

Table II compares experimental and theoretical mobility (Langevin polarization limit, $K_{o,t}$) in terms of the ratio $K_o/K_{o,t}$ for a number of negative halogen ions and their positive, isoelectronic alkali ion analogues in Ar. Although the measured F^-, Cl^-, Br^- and I^- mobilities decrease with increasing ionic mass as predicted, measured values are consistently 16 to 18% higher than calculated values; this has been observed frequently. The ratios of $K_o/K_{o,t}$ for all the negative ions are virtually identical; similarly, $K_o/K_{o,t}$ values are essentially the same for all alkali ions.

The differences in these ratios must be ascribed to the larger ionic radius of negative ions, suggesting that failure of the point charge approximation inherent in Langevin theory is a primary cause of the deviation of $K_o/K_{o,t}$ from unit.

MOBILITIES OF Cl^- IN Ar, Xe, H_2, N_2, CO AND CH_4. Mobilities of the Cl^- ions in several gases have also been measured. No other such measurements have been reported to date for halide ion drift in the molecular gases.

Our results, including those reported previously for K^+ ions, are shown in Table III and compared with the polarization limit, again in terms of $K_o/K_{o,t}$. $K_o/K_{o,t}$ for Cl^- in H_2 is about the same as that for all the halide ions in Ar. It is less than unity for Xe and the other molecular gases.

A comparison of the mobilities of the Cl^- ions with those of its positive, isoelectronic counterpart, K^+ (Tables II and III), shows no obvious correlation. We believe that this indicates the need to consider all compoents of the intermolecular potential and that the observed differences at a single temperature only reflect an accidental combination of terms which determine the dependence of zero-field mobilities on temperature.

ACKNOWLEDGEMENTS: We are grateful for the support of this research by the Department of Energy, Contract Number DE-AS02-76ER02567.A005.

LITERATURE CITED. 1. E.W. McDaniel and E.A. Mason, "The Mobility and Diffusion of Ions in Gases", Wiley, New York, 1973. 2. A.J. Illies and G.G. Meisels, Anal. Chem., 52, (1980) 325. 3. C. Chang, G.J. Sroka, G.G. Meisels, Int. J. Mass Spectrom. Ion Phys., 11 (1973) 367.

TABLE II.

Ratios of Measured Mobilities (K_o) to Those in Polarization Limits ($K_{o,t}$) for a Number of Ions in Ar Gases

This work			Literature		
Ion	K_o(cm²/V·sec)	K_o/K_p	Ion	K_o (cm²/V·sec)	$K_o/K_{o,t}$
F^-	3.56	1.18	Na^+	3.02	1.07
Cl^-	2.89	1.16	K^+	2.66	1.09
Br^-	2.46	1.18	Rb^+	2.25	1.09
I^-	2.28	1.17	Cs^+	2.10	1.08

TABLE III.

Reduced Mobilities of Cl^- and K^+ Ions in Several Gases at 298°K.

	Cl^- This work		K^+ Literature	
Neutral gas	K_o(cm²/V·sec)	$K_o/K_{o,t}$	K_o(cm²/V·sec)	$K_o/K_{o,t}$
Ar	2.89 ± 0.06	1.16	2.66	1.09
Xe	1.27 ± 0.05	0.98	1.35	1.08
H_2	12.93 ± 0.5	11.5	12.75	11.5
N_2	2.52 ± 0.04	0.95	2.55	0.99
CO	2.37 ± 0.03	0.95	2.30	0.94
CH_4	2.12 ± 0.094	0.82	—	—

The Effect of Monosolvation on Negative Ion Basicity. G. W. Caldwell and J. E. Bartmess, Department of Chemistry, Indiana University, Bloomington, IN 47405

We have measured the gas-phase equilibrium constants for reaction (1) using pulsed

$$RO^-..HOR' + R''OH \rightleftarrows RO^-..HOR'' + R'OH \qquad (1)$$

ion cyclotron resonance spectroscopy (ICR). Results of all measurements are listed in Table I. Entropy changes, ΔS°_{calc}, are calculated from ratios of symmetry numbers of reactants and products. Our results are in agreement with previously reported equlibrium constants.[1]

Table I

Reaction (1)[a]	ΔG°[b]	ΔH°[c]
$1^-,1 \rightleftarrows 2^-,1$	-1.6(-1.2)[d]	-1.2
$1^-,1 \rightleftarrows 3^-,1$	-2.7	-2.3
$1^-,1 \rightleftarrows 4^-,1$	-3.0	-2.6
$2^-,2 \rightleftarrows 2^-,1$	.8(.4)[d]	1.2
$2^-,2 \rightleftarrows 3^-,2$	-1.1	-.7
$2^-,2 \rightleftarrows 4^-,2$	-1.6	-1.2
$3^-,3 \rightleftarrows 3^-,1$	.8	1.2
$3^-,3 \rightleftarrows 3^-,2$	.1	.5
$3^-,3 \rightleftarrows 4^-,3$	-.6	-.2
$3^-,3 \rightleftarrows 5^-,3$	-2.6	-2.2
$4^-,4 \rightleftarrows 4^-,1$	1.7	2.1
$4^-,4 \rightleftarrows 4^-,2$	.7	1.1
$4^-,4 \rightleftarrows 4^-,3$	.5	.9
$4^-,4 \rightleftarrows 5^-,4$	-2.2	-1.8

[a] Nomenclature: 1 = MeOH, 2 = EtOH, 3 = nPrOH, 4 = tBuOH and 5 = $tBuCH_2OH$. Thus, $MeO^-...HOMe$ is $1^-,1$.

[b] T = 300 K, kcal/mole.

[c] Uncertainties are ± .3 kcal/mole; $T\Delta S$ = 0.4 kcal/mole.

[d] Reference 1.

For the alcohols studied, monosolvation results in a decrease in basicity (reaction 2) relative to the free anion. The stronger the acid (H bond donor), the smaller the

$$RO^-...HOR' + H^+ \rightarrow ROH + R'OH \qquad (2)$$

decrease is. The relative hydrogen bonding strengths of the cluster ions can be calculated via a thermochemical cycle. These are shown in the Figure vs ΔH°_{acid}: the bond strengths appear to be linearly related to the acid/base properties of the alcohols, but lack of an absolute value to anchor these relative numbers with prevents derivation of an equation analogous to that of Yamdagni and Kebarle.[2] The linearity and relative insensitivity of the symmetrical cases to changing structure is analogous to the corresponding positive ion clusters.[3]

The deviation of the C_5 carbon alcohols from the lines in the figure is attributable to a perturbation on equilibrium 1, arising from bimolecular clustering of the larger alcohols at low pressures.[4] We are in the process of correcting the data for this effect.

(1) McIver, R. T., Jr.; Scott, J. A.; Riveros, J. M.; J. Am. Chem. Soc., 1973, 95, 2706.

(2) Yamdagni, R.; Kebarle, P.; ibid.; 1971, 93, 7139.

(3) Bomse, D. S.; Beauchamp, J. L.; J. Phys. Chem., 1981, 85, 488.

(4) Bartmess, J. E.; Caldwell, G. W.; 28th Conf. on Mass Spec.; Allied Topics, New York, 1980 Paper RPM003; submitted, J. Phys. Chem.

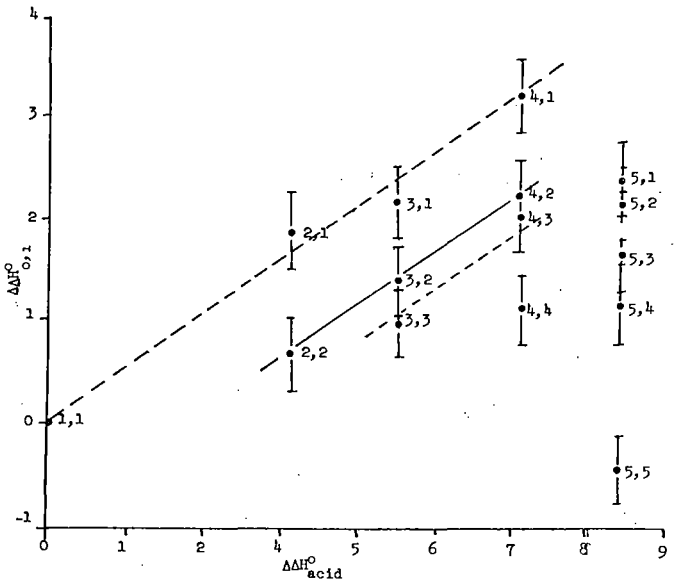

MPA11

Compilation of Gas Phase Negative Ion Thermochemistry. John E. Bartmess, Department of Chemistry, Indiana University, Bloomington, IN 47405

A comprehensive search of the literature for data pertaining to the heats of formation of negative ions in the gas phase is described. Using thermochemistry derived from the gas phase equilibrium acidity scale as a framework, thermochemical limits can be placed on many negative ions, based on the occurance of ion-molecule reactions. The data are checked for internal consistency in terms of structural effects on acidity and electron affinities. Error limits are assigned.

One of the chief problems in such an assignment of thermochemistry is the lack of suitable heats of formation for neutral compounds. Those cases where a single neutral heat would support several pieces of gas phase data are noted.

QUANTITATIVE STUDIES OF THE KINETICS OF ION DISSOCIATION AND ION MOLECULE DECLUSTERING USING A TRIPLE QUADRUPOLE. P.H. Dawson, National Research Council, Physics Division, Ottawa, K1A 0R6; and D.J. Douglas, SCIEX INC., 55 Glencameron Rd., Thornhill, Ontario, Canada, L3T1P2.

Triple quadrupole MS/MS systems are being applied to a rapidly growing variety of analytical tasks. Since little discussion of the fundamentals of collision induced dissociation (CID), central to these instruments, has appeared, the optimization of these instruments has been largely empirical. To gain a better understanding of the basic CID process we have (1) studied the effect of collision energy on fragment yields, (2) measured fragment ion energies, and (3) investigated the dependence of fragment yields on target gas density. The results we report here show that CID occurs through an efficient activation step followed by unimolecular dissociation and that relative fragment yields can be understood in conventional kinetic terms.

All experiments were performed on a prototype TAGA™ 6000 triple quadrupole MS/MS system. A unique feature of this instrument is the use of close coupled quadrupoles. Ion lenses, which can introduce strong energy- or mass-dependent transmission between quads, are not used. Close coupled quads assure a high ion transmission over a broad range of ion energy and mass, facilitating quantitative measurement of the energy dependence of reaction cross sections and fragment energy distributions.

Figure 1 shows the cross section for fragmentation of $C_6H_5Br^+$ on a nitrogen target plotted against LAB and centre of mass collision energy. The threshold expected from the published bond strengths (2 determinations) are shown by arrows "a" and "b". The threshold allowing for a kinetic shift due to the residence time in quadrupole 2 is shown by the arrow "c". This kinetic shift is largely masked by thermal motion of the target. From threshold the cross section rises to a maximum (σ_{max}>100 Å^2) over an energy range of a few volts (centre of mass), implying an efficient use of translational energy to promote reaction. Also shown are two model cross sections. The first, (I), is that predicted by a line of centres model, widely used to describe endothermic processes. The second, (II), was calculated assuming that the parent ion and target form a collision complex leading to randomization of the centre of mass energy in the parent ion. While the efficiency of the CID process is high (greater than (I)), it is not so great as predicted by model II. Evidently, if a collision complex is formed, not all the energy randomizes in the available degrees of freedom of the organic ion.

The form of the fragmentation cross section has also been studied for $C_6H_5Cl^+$ ions incident on N_2 and Ar targets. The maximum cross section was 56 Å^2 in each case, and furthermore, the shape of the cross sections, when plotted against centre of mass energy, were the same, indicating that N_2 vibration and rotation do not participate appreciably in the fragmentation process. The results obtained on these simple compounds were found to apply to the fragmentation of a complex organic ion, protonated dimethyl-morpholino- phosphoramidate (DMMPA) of mass 196 (see paper RPC6). Despite the complexity of the many sequential and competing dissociation pathways of this ion, the overall fragment yield showed similar behavior to that of Figure 1, reaching a maximum at 8 eV (centre of mass) [64 eV (LAB)].

The detailed mechanism of the CID of polyatomic ions in this energy range has received little discussion. It has often been assumed that the process occurs by a two step mechanism: an activation step followed by unimolecular fragmentation. The evidence to date has been largely inferential. Direct evidence for this mechanism is provided by the fragment ion energies. These are conveniently measured on the TAGA™ 6000 by changing the rod offset of quadrupole 3 to obtain a stopping curve. An example of this is shown in Figure 2 which records the energy distribution of the $C_6H_5^+$ fragment from dissociation of $C_6H_5Cl^+$ on an argon target at 25 eV energy (LAB). The arrows show the energy calculated assuming the fragmentation occurs through an activation step in which the parent loses some kinetic energy, followed by a unimolecular dissociation with minimal kinetic energy release. The angles refer to the scattering angle (in centre of mass co-ordinates) occuring in the activation step. There is good agreement between the calculated and measured energies. Fragment ions have less energy than parents, and acquire a spread in energy from the range of scattering angles possible in the activating collision. Also shown (by the dashed line) is the parent energy distribution shifted by the ratio of the fragment to parent mass (77/112). This is the energy fragment ions would have if they moved at the same speed that the parent has before the collision. Since parent ions lose an appreciable fraction of their LAB energy in the activation step, fragment ions are shifted to somewhat lower energies.

For the case of a heavy parent incident on a light target, the fragment energies conform more closely to $E_f = (m_f/m_p)E_p$ where subscripts "p" and "f" refer to parent and fragments respectively. This has been observed for the fragments of DMMPA (mass = 196) with an N_2 target. Fragment energies were found to be proportional to fragment mass, essentially because all fragments move with the speed of the centre of mass of the collision partners, and this is (approximately) the speed of the parent.

The dependence of fragment yield on target gas pressure has received only qualitative description in the literature. In fact, relative fragment yields can be understood in conventional terms of the reaction kinetics for sequential and competing reactions. Figure 3 illustrates this by showing the fragment yields from the declustering of $H(H_2O)_3^+$ (mass = 55) on an argon target (parent energy 35 eV). Loss of one to three water molecules is possible. Yields are plotted against target thickness (number density x length; units of 10^{15} cm^{-2}) since it is only this product which enters the solution to the rate equations. The solid lines in Figure 3 were calculated by solving the rate equations describing the following kinetic scheme:

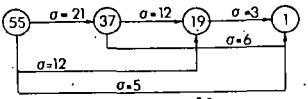

Cross sections (σ) for each step are shown in $Å^2$. The fit to the data is good, indicating that the rate equations can quantitatively describe the pressure dependence. No mass dependent corrections to the ion transmission were used. Furthermore, it was not necessary to include scattering losses in the kinetics indicating that the RF only quadrupole is highly efficient in retaining fragment ions. Again, the salient features of this study on a simple system were found to apply to the fragmentation of DMMPA. Modelling the pressure dependence of the fragmentation of DMMPA shows fragments resulting from up to four collisions of precursor ions. Scattering losses were again found to be small (<5%) for a wide range of fragment masses. The sequential formation of daughter and granddaughter ions could be observed, and was of use in determining the fragmentation pathways of this complex ion.

The results reported here show that while the development of triple quadrupoles has been prompted by their analytical capabilities, these instruments will also be useful for the exploration of the dynamics of ion molecule interactions.

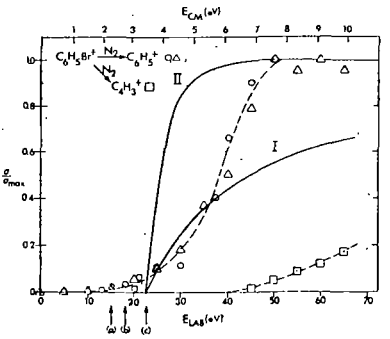

FIGURE 1

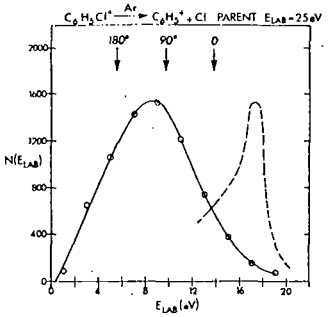

FIGURE 2

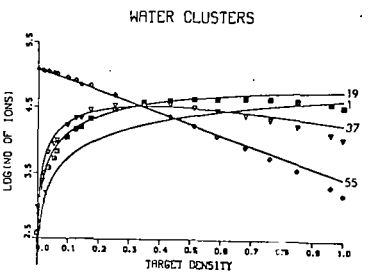

FIGURE 3

TWO LASER MULTIPHOTON DISSOCIATION OF IONS IN THE ICR SPECTROMETER; N.B. LEV, J.P. HONOVICH, and R.C. DUNBAR, Chemistry Department, Case Western Reserve University Cleveland, OH 44106.

Two photon dissociation of iodobenzene cations by visible light at 6100 Å has been shown to be enhanced by simultaneous irradiation with infrared photons from a low power cw CO_2 laser. In studies of other ions which undergo visible two photon dissociations, adding infrared irradiation enhances the visible dissociation in some cases (e.g., bromobenzene at 5145 Å), but not in others (e.g., 1- and 2-methylnaphthalene at 6100 Å). Computer simulation of the two laser multiphoton experiment shows that collisional deactivation of the excited ions produced by absorption of one visible photon is the main relaxation process competing with the absorption of additional photons. Varying the efficiency of the collisional deactivation process by using bath gases other than the parent neutrals provides further information about the rates of the competing processes.

DISSOCIATION RATES FOR THE *n*-BUTYLBENZENE MOLECULAR ION DERIVED FROM PHOTODISSOCIATION ION KINETIC ENERGY SPECTRA. I.W.Griffiths, E.S.Mukhtar, F.M.Harris and J.H.Beynon, Royal Society Research Unit, University College of Swansea, Singleton Park, Swansea SA2 8PP, U.K.

A simple form of the quasi-equilibrium theory (QET) is applied in the calculation of photodissociation fragment-ion currents for competing reactions of the positive molecular ion of n-butylbenzene. Previous experimental results[1] have shown that dissociation of the molecular ions gives mainly fragment ions of masses 91 u and 92 u the relative abundances being governed by the photoexcitation energy. The object of the calculations is to determine the ratio R for $[91^+/92^+]$ currents and adjust two of the parameters in the equations used to bring the calculated and experimental values of R into agreement.

The method is one which was applied initially to calculate the effect of competing dissociation reactions for excited molecular ions of nitrobenzene.[2] Rate constants are needed and their dependence on the internal energy E of the ion is approximated by the simple QET equation

$$K(E) = \nu \left[\frac{E - E_c}{E}\right]^{S-1} \qquad (1)$$

where E_c is the critical energy for a given dissociation and S is a constant which has been described as an 'effective number of oscillators'. Each dissociation reaction will have its corresponding rate equation.

Highly excited ions formed by electron-impact ionization in the source dissociate unimolecularly very rapidly with the result that the majority of ions which reach the second field-free region of a ZAB-2F spectrometer have internal energies less than the lowest critical energy for dissociation. These stable ions are irradiated in the second field-free region with monochromatic radiation from an argon-ion laser and a fraction of them are photoexcited by an amount ϵ, the photon energy.

The calculation monitors the fate of ions formed in the source which subsequently reach and pass through the interaction region. For this an initial internal energy distribution has been used which is estimated from the photoelectron spectrum of the molecule.[3] The probabilities of the ions that are photoexcited fragmenting to give 91^+ and 92^+ ions is governed by the rate constants for the two reactions. These depend on the photoexcitation energy given to the ions and thus lead to a prediction of the dependence of R on wavelength.

The critical energies have been taken from previous work[4] and the frequency factor for the formation of 91^+ is assumed to be 3×10^{13} s^{-1} i.e. of the order of a molecular vibrational period. The frequency factor ν_0 for 92^+ formation, and S, were considered to be adjustable parameters. The calculations resulted in the derivation of two equations,

(a) for the formation of 92^+

$$K_0(E) = 6\times10^9 \left[\frac{E - 1.4}{E}\right]^{17} \qquad (2)$$

(b) for the formation of 91^+

$$K_1(E) = 3\times10^{13}\left[\frac{E - 2.6}{E}\right]^{17} \qquad (3)$$

with the internal energy E in units of eV. The values of R calculated are shown in Table 1 together with the measured values for four photoexcitation energies. It can be seen that the measured values agree with the experimental data within the experimental error.

Table 1 Relative abundances of the photo fragment ions 91^+ and 92^+ for various photoexcitation energies.

Wavelength (nm)	Photoexcitation energy (eV)	Ratio $[91^+/92^+]$ Experimental	Calculated
514.5	2.41	1.02±0.05	1.02
488.0	2.54	1.30±0.05	1.25
457.9	2.71	1.69±0.05	1.70
357	3.47	6.90±0.30	6.90

Relatively small changes in S and ν_o take the calculated values out of agreement with the experimental data. Thus, the errors in S and ν_o are judged to be ±1 and $\pm 1 \times 10^9$ respectively.

Because of uncertainties in the initial internal energy distribution of the parent ions, in the dependence of the probability of photoexcitation on internal energy and in the critical energies for the two dissociation reactions, the use of a more sophisticated rate equation in the calculations does not seem justified. The simple equation seems to be adequate since the rate equations (2) and (3) satisfactorily predict the photodissociation pattern of the n-butylbenzene molecular ion observed in practice.

References

1. E.S.Mukhtar, I.W.Griffiths, F.M.Harris and J.H.Beynon, Int.J.Mass Spectrom.Ion Phys. 37, 159, 1981.
2. I.W.Griffiths, F.M.Harris, E.S.Mukhtar and J.H.Beynon, Int.J.Mass Spectrom.Ion Phys. 38, 127 1981.
3. E.Nagy-Felsobuki and J.B.Peel. J.Electron Spectroscopy and Related Phenomena. 16, 397, 1979.
4. P.Brown. Org.Mass Spectrom. 3, 1175, 1970.

ISOMERIZATION OF PHENOL TO CO ELIMINATION

H.J. WALTHER, H. EYER and U.P. SCHLUNEGGER
Institute of Organic Chemistry, University of Berne, Switzerland and
C.I. PORTER, E.A. LARKA and J.H. BEYNON
Royal Society Research Unit, University College of Swansea,
Great Britain.

Phenol has been suggested to isomerize prior to the well known CO elimination. Maquestiau et al. proposed an unsaturated openchained aldehyde as the isomeric structure, but without any experimental proof.

In this work, five possible openchained isomeres of phenol have been synthesized and compared with phenol by MIKES, CID/MIKES, "kinetic energy release" measurements and FI-CID/MIKES: CH_3-C≡C-C≡C-CH_2-OH (I), CH_3-C≡C-CH=CH-CHO (trans: II; cis: III) and CH_3-CH=CH-C≡C-CHO (trans: IV; cis: V).

All of them show a loss of 28 mass units in the MIKE spektra of the molecular ion. The corresponding metastable peak shapes of II and III are almost identical and very similar to that of phenol, while I, IV and V are significantly different. The kinetic energy releases ($T_{0.5}$) by MIKES are the same for II and III and slightly different to phenol. The CID/MIKE spectra of the molecular ions of II and III show small differences in the ion abundances. They are most similar to that of phenol-measured on a modified MAT CH5-DF and a VG Micromass ZAB-2F mass spectrometer.

It has been suggested that the remaining differences could originate from an incomplete isomerization of the phenolic ion. Therefore the FI-CID/MIKE spectra of II, III and phenol have been recorded. The comparison with the EI-CID/MIKE spectra shows differences only for phenol.

The results imply that phenol partially isomerizes prior to the loss of CO. An isomerization of about 40 % to the structure of cis 2-hexen-4-yn-1-al is in good accordance with the spectral data.

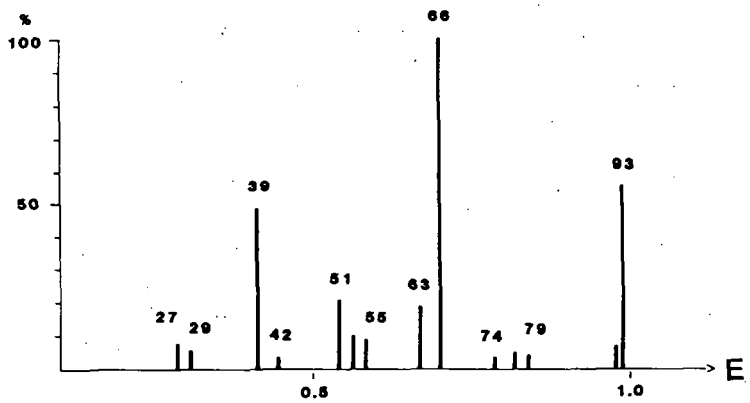

Composed spectrum of the FI-CID/MIKE spectra of M^+

60% phenol , 40% cis-2-hexen-4-yn-1-al

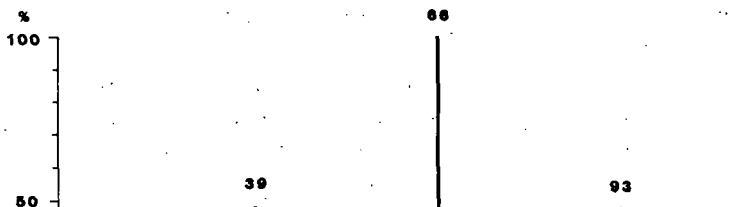

EI-CID/MIKE spectrum of M^+ of phenol

Loss of Hydroxyl from Ionized Acetic Acid Enol

Charles E. Hudson and David J. McAdoo
Marine Biomedical Institute
The University of Texas Medical Branch
Galveston, Texas 77550

In 1980 Holmes and Lossing reported that the title ion gives a metastable peak for loss of OH which is not of Gaussian shape.[1] From thermochemical measurements they concluded that the daughter is the acetyl ion, whose production requires the transfer of a hydrogen atom from O to C. They proposed that the peak shape be explained by a superposition of two processes: (1) A low energy mechanism with a narrow peak having stepwise O to C hydrogen transfer and fragmentation and (2) A high energy process giving a wider peak in which the hydrogen rearrangement is concerted with fragmentation.

In a reinvestigation of the problem using the MS 50 triple analyzer at the Midwest Center for Mass Spectrometry, we have obtained data (Table 1) that generally agrees with reference 1. However, we suggest a different interpretation.

Table 1

Precursor	Ion	Metastable Peak Height Ratio -OD/-OH	$T_{0.5}$ (meV) -OH	-OD
CH_3CO_2H	$CH_3C(=\overset{+}{O}\cdot)OH^{+\cdot}$ (1)	0	7.4	
CH_3CO_2D	$CH_3C(=\overset{+}{O}\cdot)OD^{+\cdot}$ (2)	14	15	7.0
$CH_3CH_2CH_2CO_2H$	$CH_2=C(OH)_2^{+\cdot}$ (3)	0	19	
$CH_3CH_2CH_2CO_2D$	$CH_2=C(OH)OD^{+\cdot}$ (4)	2.7	33	21
$CD_3CH_2CH_2CO_2H$	$CH_2=C(OD)OH^{+\cdot}$ (4')	2.7	36	18
$CD_3CH_2CH_2CO_2D$	$CH_2=C(OD)_2^{+\cdot}$ (5)	5.7	29	35

The -OD/-OH ratio is approximately that expected from an isotope effect on single hydrogen transfer reaction.

Since the stepwise and concerted mechanisms would involve essentially the same atomic motions we did not see how they could be distinct, competing reactions. Also both $CH_3C(=\overset{+}{O}\cdot)OD$ and $CH_2=C(OD)_2^{+\cdot}$ lose OH with energy releases larger than for the undeuterated ions, demonstrating that the acid and enol structures which interconvert also have elevated energy releases, i.e. increased energy releases follow stepwise hydrogen transfers.

The peak for loss of OH from 4 and 4' is less intense and wider than the peak for loss of OD. From 5 both peaks are wide. The loss of OH from 4 and 4' and the OD loss from 5 both require a transfer of D from O to C. If the energy of this process is raised by an isotope effect then it should be suppressed. Assuming that the isotope effect raises the transition state energy by 1.5 kcal/mole or less[2], then at least 21% of the excess energy is converted into translational energy of fragmentation. The analysis is applicable to $CD_3CH(CH_3)CO_2H$ also. It fragments as follows:

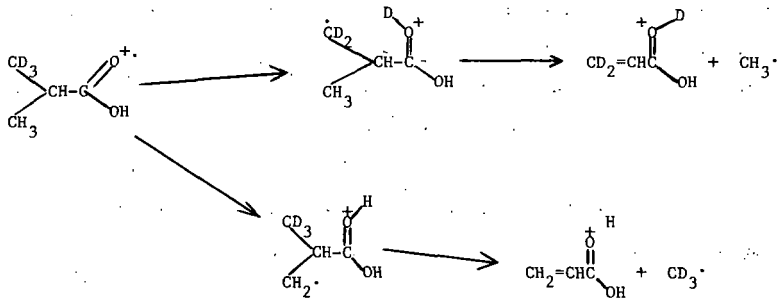

Table 2 gives the data for this compound.

Table 2

Relative Peak Height	$T_{0.5}$ (meV)	
$M-CD_3/M-CH_3$	$M-CD_3$	$M-CH_3$
2.7	17.6	25.4

Thus a surprisingly large fraction of the increased activation energy due to the deuterium isotope effect on hydrogen transfer in one part of an ion can be released in subsequent fragmentation in another part of the ion. Supported by Robert A. Welch Foundation Grant H-609.

1. J.L. Holmes and F.P. Lossing, J. Amer. Chem. Soc., 102: 3732 (1980.

2. K.B. Wiberg, Chem. Rev., 55: 713 (1955).

COMPARISON OF LOW AND HIGH ENERGY COLLISION INDUCED DISSOCIATION FRAGMENTATION OF SELECTED METHYL KETONES. J.A.Nyström,[1,2] D.J.Harvan,[2] R.D.Voyksner,[1,2] W.L.Grady,[1] R.L.Cerny,[1] J.Yinon,[1,3] M.M.Bursey,[1] M.W.Siegel,[4] J.R.Hass[2]
1. William Rand Kenan, Jr.-Laboratories of Chemistry, The University of North Carolina, Chapel Hill, NC 27514.
2. Laboratory of Environmental Chemistry, N.I.E.H.S., PO Box 12233, Research Triangle Park, NC 27709
3. The Weizmann Institute of Science, Rehovot, Israel
4. Extranuclear Laboratories, Inc., PO Box 11512, Pittsburgh, PA 15238

The recent development of quadrupole mass filters for the analysis with collision-induced decomposition (CID) or mass spectrometry/mass spectrometry (MS/MS) offers an alternative to the older CID mass analyzed ion kinetic energy spectrometry (MIKES) technique. CID/MIKES employs first momentum and then kinetic energy analysis in a double focussing mass spectrometer. Both different modes and levels of ion excitation are observed in each technique. The tandem quadrupole methodology is based upon energy conversion (via momentum transfer) in relatively low-energy collisions (0-100eV acceleration) while the CID/MIKES technique is based upon high-energy collisions (2000-8000eV acceleration) with electronic excitation occuring in the glancing collisions. The study of several simple methyl ketones was undertaken in order to compare the differences in the MS/MS spectra.

Table 1. (intensities corrected for metastables observed) compares the CID spectra of the stable molecular ions obtained with a tandem quadrupole (Extranuclear Laboratories, Inc.) with those obtained with a double focussing instrument (VG Micromass ZAB/2F). The compounds studied are acetone, 2-butanone, cyclopropyl methyl ketone, and 3-methyl-2-pentanone. Collision gases used were He and N_2 in the tandem quadrupole (QQ) and He in the ZAB/2F instrument. The QQ spectra show less fragmentation but the fragments obtained carry more of the initial primary ion intensity than do the fragment ions of the sector instrument. The QQ fragments (detection of peaks above 1%) further show greater structural significance while the additional CID-MIKES ions add little structural information.

Literature cites several studies concerning the appearance energy (AE) of several acetone fragment ions. By looking at the ions observed, one can suggest possible ranges of energy transfer in the QQ instrument. Acetone has an ionization potential (IP) equal to 9.7eV (935kJ/mol). The QQ spectra show primarily the acyl ion, CH_3CO^+ (AE = 10.4eV or 67kJ/mol above the IP of acetone). The high-energy CID/MIKES spectrum shows the presence of several other ions whose AEs are known. These ions include $C_2H_2O^+$ (96kJ/mol above acetone's IP), $C_2H_3^+$ (695kJ/mol above acetone's IP), and CH_2^+ (probably has a higher AE than $C_2H_3^+$). In the QQ spectra, the acyl ion carries 94-100% of the daughter ion current while the CID/MIKES shows only 80%. In the case of direct mixture analysis, the low intensity daughter ions could easily lead to misidentification of mixture components. These low intensity fragments hence would only be useful for fingerprinting the spectra.

In the case of 2-butanone, QQ spectra contain two acyl ions (95-97% total fragment current) as well as the $C_2H_5^+$ ion (325kJ/mol above the IP of 2-butanone). The CID/MIKES spectrum also contains these two acyl ions (88%) as well as a wealth of ions which are products typical of higher energy processes (again only useful in fingerprinting spectra).

For cyclopropyl methyl ketone on the QQ, one sees the structurally informative acyl ions (98-100% total daughter ion current) but also the cyclopropyl cation ($C_3H_5^+$). The CID/MIKES spectrum has the above three ions (acyl ions, 94%) as well as the fingerprinting $C_5H_7O^+$ and $C_3H_3^+$ ions.

For both the QQ and the CID/MIKES spectra, 3-methyl-2-pentanone's major ion is the McLafferty rearrangement ion (QQ, 56-76%; CID/MIKES, 77%). The QQ carries the remainder of its fragment current in the two acyl ions. The two acyl ions and the McLafferty rearrangement ion fragments yield 92% of the total ion current in CID/MIKES spectra.

In conclusion, the use of He as a low-energy collision gas produces spectral information sufficient to characterize and identify compounds of this class. The use of N_2 as a low-energy collision gas produces more fragmentation but not necessarily more useful information. Additional peaks found in the high-energy CID/MIKES are primarily beneficial for

fingerprinting spectra. In direct mixture analysis, the use of low-energy He CID would give simple ions which are not complicated by structurally uninformative ions.

EXPERIMENTAL:

The methyl ketones were commercial samples with no impurities detectable by mass spectrometric survey. Ketones were used as obtained.

High energy CID/MIKES measurements were made on the reverse geometry Nier-Johnson mass spectrometer, VG Micromass ZAB/2F. Samples were run with a source pressure of 5×10^{-7} torr, a source temperature of 200 C, and an accelerating voltage of 7 kV. He was used as a collision gas at a pressure of 2×10^{-7} torr gauge (5×10^{-3} torr in the collision cell). The collision cell pressure yielded a 50% reduction of the main beam intensity.

Low energy CID measurements were made on a tandem quadrupole system containing a quadrupole field collision cell developed by Extranuclear Laboratories, Inc. This cell system allows the use of two sets of quadrupole rods instead of three sets with an R.F. only collision region within the field cell. The collision cell may be biased so that the primary ion beam in the cell differs from that imposed by the ion source potential, and an axial field (focussing, collecting) can be imposed. Both He and N_2 were introduced into the collision cell. Collision gas pressure was adjusted to yield maximum fragmentation of the main ion beam. Source pressure and temperature were comparable to those of the ZAB/2F.

TABLE 1

ACETONE

QQ	(He)	(N_2)	ZAB-2F	(He)
43	100	100	57	0.7
15	--	6	43	100.
			42	12.
			41	1.8
			39	1.4
			38	0.7
			37	0.5
			29	1.8
			27	1.8
			26	0.8
			15	2.4
			14	0.7

2-Butanone

QQ	(He)	(N_2)	ZAB-2F	(He)
57	100	26	71	3.1
43	59	100	57	100.
29	8	2	56	1.8
			55	0.9
			53	1.0
			43	90.
			42	5.4
			41	1.7
			39	1.2
			29	4.9
			28	0.9
			27	3.5
			26	0.8
			15	0.7

Cyclopropyl Methyl Ketone

QQ	(He)	(N_2)	ZAB-2F	(He)
69	44	100	83	5.4
43	100	100	69	100.
41	--	3.5	43	44.
			41	2.4
			39	1.9

3-Methyl-2-Pentanone

QQ	(He)	(N_2)	ZAB-2F	(He)
85	31	46	85	14.
72	100	100	72	100.
43	--	32	71	1.7
			57	2.6
			56	1.3
			55	0.7
			53	1.0
			43	6.3
			39	0.7
			29	0.7
			27	0.5

SELECTED METASTABLE ION MONITORING USING DEUTERIUM LABELLED INTERNAL STANDARDS: QUANTIFICATION OF m- AND p-HYDROXYPHENYLACETIC ACID IN A SINGLE RAT CAUDATE NUCLEUS: DAVID A. DURDEN: Psychiatric Research Div., University Hospital, Saskatoon, Sask., Canada, S7N OXO.

Selected metastable ion monitoring (SMIM) of fragment ions using linked magnetic (B) and electric sector (E) at constant accelerating voltage (V) of a double focussing mass spectrometer has proven to be a sensitive and specific method in nature for quantifying biogenic products at the picomole level (1,2). The procedures first reported (1,2) used only one value for the constant E/B and thus the internal standard was limited to one which underwent the same fragment loss as the unknown. This obviated the use of a stable isotope labelled internal standard.

In this report is described a simple modification to a VG 70-70 mass spectrometer which allows two values of E/B to be set up using analog circuitry in conjunction with a multiple ion detector controller (DIGMID).

For the two compounds, the protonated parent ion M_1 and the deuterated parent ion M_3 and fragment ions M_2 and M_4 the following conditions apply. Parent ion M_1 formed in the ion source is detected unchanged in the normal operating mode at E_1 and V by manually selecting B_1. Ion M_2, resulting from decomposition of metastable ions M_1 in the first field free region between the ion source and the electric sector, is detected at V, E_2 and B_2 where:

$$B_2 = (M_2/M_1) \cdot B_1 \ , \ E_2 = (M_2/M_1) \cdot E_1 \text{ and } K_1 = E_1/B_1$$

Stable isotope labelled parent ion M_3 is detected at V, E_1 and B_3 where:

$$B_3 = \sqrt{M_3/M_1} \cdot B_1 \ , \qquad K_2 = E_1/B_3 = K_1 \cdot \sqrt{M_1/M_3}$$

Ion M_4, from decomposition of metastable M_3 ions is detected at V, B_4 and E_4 where:

$$B_4 = B_1 \ (M_4/M_3) \cdot \sqrt{M_3/M_1} \text{ and } K_2 = K_1 \cdot \sqrt{M_1/M_3}$$

These values are shown schematically on Figure 1. The line at constant E_1 represents the condition of normal magnetic scan analysis of ions formed in the ion source. The lines of K_1 and K_2 passing through the origin and B_1 and B_2 at E_1 represent the conditions for detection of metastable peaks from ions formed in the first field free region.

Figure 2a illustrates the interconnections required for monitoring a metastable transition at one value of E/B. In the modified circuit 2b, the output of the variable amplifier which sets K_1 may be reduced by the factor $\sqrt{M_1/M_3}$ by the "metastable ratio amplifier" depending upon the DIGMID channel setting. The metastable ratio amplifier (Figure 3) is a precision amplifier with an adjustable gain of 1.00000 (channel 1 or 2) or a lower value (channel 3 or 4) which operates in a manner similar to a mass measurement decade amplifier. If all four channels are selected in sequence, then both parents and both metastable peaks can be detected. For SMIM quantitation only the metastable peaks M_2 and M_4 were selected.

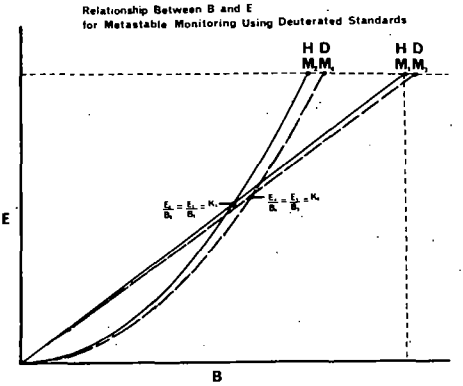

Figure 1.

Figure 2.

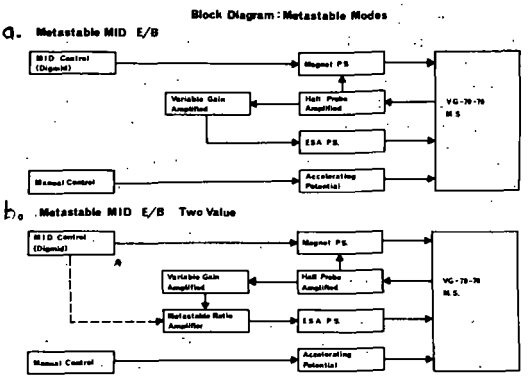

Figure 3.

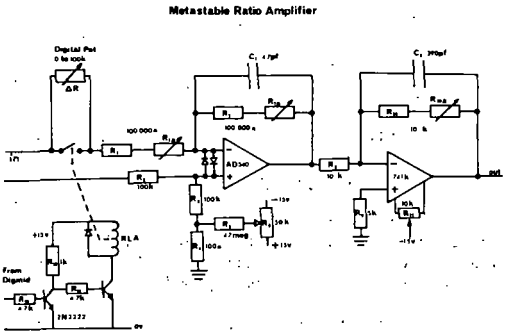

An example of use of SMIM is the quantitation of m- and p-hydroxyphenylacetic acids in a single caudate nucleus using di-deuterated internal standards. The acids were extracted, derivatized with pentafluoropropionic anhydride and trifluoroethanol and separated on a SCOT OV-101 capillary column. The metastable transitions observed were loss of $CO_2CH_2CF_3$ from the molecular ions M_1 = 380 and M_3 = 382, i.e. $M_1 \rightarrow M_2$ = 380 → 253 and $M_3 \rightarrow M_4$ = 382 → 255. It was found that the concentrations of meta and para hydroxyphenylacetic acid, determined by MSIM corresponded to values obtained with regular high resolution SIM of a pool of ten caudates.

Table 1. Concentrations of m- and p-hydroxyphenylacetic acids in rat caudate nucleus.

Method and amount of internal standard	m-HPAA (ng/g)	p-HPAA (ng/g)
SMIM, single C.N. 800 resolution 1.0 or 2.5 ng I.S.	9.7 ± 1.7	40 ± 3.6
SIM, pooled 10 C.N. 5000 resolution 100 ng I.S.	9.4 ± 1.2	43 ± 3.9

1. Gaskell, S.J. and Millington, D.S., Biomed. Mass Spectrom. 5 (1978) 557-8.
2. Harvey, D.J., Leuschner, J.T.A. and Paton, W.D.M., J. Chromatogr. 202 (1980) 83-92.

Supported by Saskatchewan Health and the Medical Research Council of Canada.

A LINEAR, BI-POLAR, 6½ DECADE CURRENT-TO-FREQUENCY CONVERTER

BY JAMES L. LAWRENCE, JR., and DAVID L. RAYMOND, Analog Technology Corp. 15859 E. Edna Place, Irwindale, CA 91706

The scientist's requirement for increased utility, quantitative accuracy and resolution in various spectrometric measurements has led to the proliferation of microprocessors for interactive control of the spectrometer and processing of the low-level resolved ion or photon current signal. Nevertheless, fast quantization of these low-level signals is particularly difficult and presents a limitation on system performance when the currents vary over a 10^7 dynamic range and when high accuracy must be maintained for small currents on the order of 10^{-14}A. Time-honored electrometer techniques (current-to-voltage converters), whether range switched amplifiers followed by analog-to-digital converters or single-range systems followed by voltage-to-frequency converters, do not possess the desired composite qualities of speed, accuracy, and wide dynamic range. Limitations of electrometers and other low-level current-measuring techniques when integrated with data systems are discussed.

This paper describes a unique, closed-loop, current-to-frequency (I/F) converter which stems from space technology in which a succession of small charge feedback pulses is selectively generated to null the input current. An early generic relation to the ATC I/F used resistive feedback to form the charge pulses but suffered poor low end linearity and lacked comparable dynamic range due to the inability to precisely control the width and amplitude of the voltage pulse driving the resistor. (1) An ATC design of that period used capacitive charge feedback and offered superior performance, but also required autozeroing and the cooperation of a host processor for its operation.(2) In this new I/F converter, feedback pulses are generated by applying voltage pulses of precisely controlled magnitude to a precision capacitor to produce pulses of precisely determined charge content.(3) These pulses are then applied to a charge dividing circuit including a matched pair of bi-polar transistors. The charge dividing circuit bypasses the bulk of the charge in each pulse, while applying only a fraction of each pulse as the feedback current. This transfer function is temperature compensated. In essence, since this I/F converter is a nulling device which works on the integral of the charge signal, it is independent of the threshold variations encountered in pulse counting and other I/F systems. Since the charge per pulse is accurately controlled and the output pulse repetition rate is exactly proportional to input current, an interface data system may be readily programmed to calculate average current for selectable counting intervals or, alternatively, the total charge into the I/F converter.

Linearity and noise measurements on production converters at charge feedback sensitivities ranging from 10^{-14} to 10^{-12} C/pulse and at varying integration periods are presented. Worst-case integral nonlinearity of 0.1% between the 1Hz and 2MHz operating points with a noise figure less than 10^{-14}A is demonstrated.

References:

(1) Woodruff and Malmstadt, "High speed charge to current data domain converter for Measurement Systems", Analytical Chemistry, Vol. 46, No. 9, August 1974, pg. 1162

(2) J. H. Marshall III, A Proposal for a Miniature Radiac Device, ATC Proposal 73-716, pg. 12, April 1973

(3) David L. Raymond, Current-to-Frequency Converter, U.S. Patent #4,109,168

A Frequency Swept Detector for Ion Cyclotron Resonance Mass Spectrometers

CHEM. DEPT., UNIV. OF DELAWARE, NEWARK, DE. 19711
J. Wronka and D. P. Ridge

A frequency swept bridge detector with a frequency range of 30 KHz to 1.5 MHz for use with Ion Cyclotron Resonance Mass Spectrometers (ICR-MS) has been constructed and demonstrated. A detector of this type has several advantages which greatly increase the abilities and versatility of ICR-MS. Such a detector allows a much greater mass range, as determined by the formula $m = qH/\omega c$. This increase can be accomplished by the use of lower radio frequencies allowed by the bridge, and superconducting magnets which increase the magnetic field strength (H). The use of a higher field also facilitates trapping experiments thereby allowing the longer observation time required for high resolution work.

The detector has a faster response time than previous detectors which facilitates pulsed ICR-MS experiments. The decreased response time also allows rapid scan ICR-MS that would be necessary for rapid acquisition of data needed for small sample sizes or GC-ICR-MS. This ability to do rapid scan makes it possible to use computer interfacing and signal averaging techniques.

The ability to sweep frequency greatly increases the ability of ICR mass spectrometry to elucidate ion molecule chemistry. One variation on the traditional double resonance experiment is particularly useful in determining all of the daughter (product) ions from any given parent (reactant) ion. A reactant is

irradiated at its cyclotron frequency with a signal that is amplitude modulated at some audio frequency. Phase sensitive detection at this modulation frequency yields a single spectrum of all the daughters of a given parent. Both endothermic and exothermic reactions may be observed.

Special features of the bridge detector include the use of a ninety degree sync output available on many inexpensive commercial voltage controlled signal generators, and characterization and simple automatic correction of phase shift to allow broadband detection. Any high quality broadband (video) amplifier or transformer has a phase shift proportional to frequency so that a composite signal is not distorted when it is amplified. The phase shift is the result of a constant (frequency independent) signal delay in the amplifier or transformer. This phase shift is kept to a minimum in the detector by limiting the number of amplifiers and may be compensated for by a delay line in the reference signal. A simple radio frequency phase sensitive detector based on a balanced modulator demodulator is included in the bridge detector.

The detector is simple to construct and implement since the phase sensitive detector eliminates the need for signal modulation schemes used in the past. Performance of this detector is excellent as shown by the attainment of a resolution of greater than 20,000 at mass 262. The detector may be used at constant field or constant frequency with no adjustments other than the initial setting of the radio frequency level applied.

Equilibrium and Double resonance in the Unquenched Mode in Trapped ICRvSpectrometry

John E. Bartmess and Gary Caldwell, Department of Chemistry, Indiana University, Bloomington IN 47405

If the quench pulse in a McIver-type trapped ICR cell is turned off, the ion density increases until some ballance is achieved between ion production and collisional ion loss to the walls. This unquenched continuous mode of operation has been shown to give greater sensitivity for detection of small samples with chemical ionization.[1] These previous studies have dealt only with the simple case of a single reagent ion and a single sample. Can the unquenched mode provide information regarding ion-molecule kinetics and equilibria? For a typical equilibrium scheme

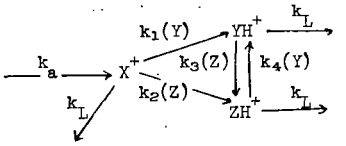

k_a is the primary ion appearance rate from electron impact, and k_L is the constant magnetic field collisional loss rate constant (ca. 10^{-12} cc-molec^{-1}-s^{-1}). Let $S_1 = k_1(Y)$, $S_2 = k_2(Z)$, etc. Then the steady state solution to the normal kinetic expression for the above scheme is

$$\frac{X^+_{ss}}{T^+_{ss}} = \frac{S_L}{(S_1+S_2+S_L)} \qquad \frac{YH^+_{ss}}{T^+_{ss}} = \frac{(S_1+S_2)S_4+S_1S_L)}{S_L(S_1+S_2+S_L)(S_3+S_4+S_L)}$$

$$K_{eq} = \frac{(Z)\ S_4}{(Y)\ S_3} \qquad K_{app} = \frac{(Z)\ ((S_1+S_2)S_4+S_1S_L)}{(Y)\ ((S_1+S_2)S_3+S_2S_L)}$$

where T^+ is the total ion current, K_{eq} is the true equilibrium constant, and K_{app} is the apparent one based on the steady state abundances. For proton transfer between n-donor bases, k_1-k_3 is ca. 5×10^{-10}cc-molec^{-1}s^{-1} and we find:

Base	$\Delta\Delta G^o_{base}$ [2]	$\Delta\Delta G^o_{obs}$	$\Delta\Delta G^o_{calc}$
HCO_2Et	(0)	(0)	(0)
HCO_2Pr	1.0	1.3	1.0
HCO_2Bu	1.6	1.9	1.6
Me_2CO	3.5	3.2	3.2
$MeCO_2Et$	7.1	3.2	3.3
Et_2S	11.9	3.2	3.3

The theory predicts and we observe (1) equilibria are always in the right direction compared to the true equilibria (2) they are independent of total pressure and base ratio up to 10^{-5} Torr (3) when k_4 approaches k_L the apparent equilibria level off. For anions, where k_3 and k_4 may be comparable to k_L the K_{app} may represent only the kinetic partioning of the primary anion signal. Unquenched double resonance between XH^+ and YH^+ can be near baseline if the rates are fast. For $k_4 = k_L$ 50% decrease is seen.

Even for k_4 less than k_L some decrease is senn in double resonance.

The theory also predicts that all intermediates, forming and reacting bimolecularly will be seen even if they form slowly and react rapidly. The unquenched abundances represent neither short nor long times but the integral over all times. The time-dependent theory predicts that the half life for establishing or ejecting the steady state is directly related to k_L; terms in the other rate constants are of negligible importance at microtorr pressures.

(1) Hunter, R.L., McIver, R.T.,Jr., Anal.Chem. 1979,51,699-704

COMPUTER CONTROLLED ELECTRON IONIZATION - FLASH DESORPTION MASS SPECTROMETRY WITH ELECTRO-OPTICAL ION DETECTION

H.G. Boettger and C.E. Giffin
Jet Propulsion Laboratories
Pasadena, California 91103

T.D. Lee, W.R. Anderson, Jr., and G. Doyle Daves, Jr.
Department of Chemistry and Biochemical Sciences
Oregon Graduate Center, Beaverton, Oregon 97006

Electron ionisation - flash desorption mass spectrometry[1,2] is characterized by rapid ($\sim$ 50 ms) desorption of the sample requiring simultaneous collection of the resulting ions. The increased sensitivity ($\sim 10^3$) of electro-optical ion detection[3] (EOID) over that of photoplate detection has resulted in a reduction of the sample size and an increase in the molecular weight range for which complete spectra can be obtained.

Efficient use of the EOID with the EI-flash desorption technique has been accomplished by computer coordination of operation of the spectrometer and sample probe control unit. (Figure 1) A signal from the computer activates a circuit which counts end of scan signals (EOS) from the detector. After a set number of EOS, the probe is fired and the sample desorbed. Ion production is then terminated using a beam switch with a variable delay. The beam switch eliminates unwanted ions due to background and secondary products. It also ensures that ion production does not occur during computer readout of the detector.

References

1. T.D. Lee, W.R. Anderson, Jr., and G.Doyle Daves, Jr., Anal. Chem. 53, 304 (1981)

2. G.D. Daves, Jr., T.D. Lee, W.R. Anderson, Jr., D.F. Barofsky, G.A. Massey, J.C. Johnson and P.A. Pincus, Adv. Mass Spectron, 8, 1012 (1980).

3. H.G. Boettger, C.E. Giffin, D.D. Norris, W.J. Dreyer and A. Kuppermann, Adv. Mass Spectron, Biochem. Med., 2513 (1977).

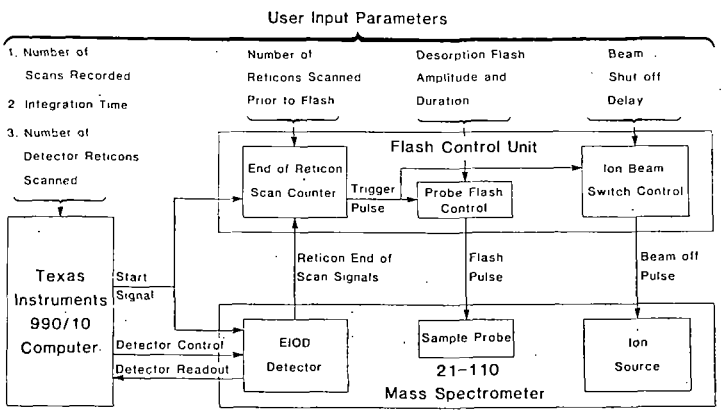

Figure 1

A THIN LAYER CHROMATOGRAM SCANNER COUPLED TO A MASS SPECTROMETER FOR TLC-MS

L. RAMALEY and M. E. NEARING, Department of Chemistry,
Dalhousie University, Halifax, N.S., Canada, B3H 4J3

W. D. JAMIESON Atlantic Research Laboratory, National Research Council of Canada
1411 Oxford Street, Halifax, N.S., Canada, B3H 3Z1

R. G. ACKMAN, Technical University of Nova Scotia,
Halifax, N.S., Canada, B3J 2X4

A device which couples directly to a Finnigan 4000 quadrupole mass spectrometer through the direct probe inlet and allows scanning of 1X10 cm TLC plates has been described previously (1). Thermal energy from a 150 W tungsten incandescent lamp desorbs samples from the plate. These are swept into the ion source through a heated transfer line by CI reagent gas which continuously flows over the plate. This scanner has the advantage that it requires no modification of the mass spectrometer and can be inserted or removed in a matter of minutes, making changeover from one method of sample introduction to another very simple. Tests showed (1) that good sensitivity (10 ng; 2s sweep scan; 80-250 m/z) could be obtained for thermally stable compounds such as phenanthrene and benzophenone. However, on a relative basis peaks were twice as wide as the spots on the plate. This degradation of spatial resolution was attributed to retention of heat by the plate, resulting in continued sample desorption after passing the heated area and to a memory effect in the plate chamber. For less stable compounds results were somewhat disappointing. Cholesterol produced only fragment ions with m/z less than 120 and methyl stearate produced no ions at all above m/z 80 (the lower mass scan limit used).

In an attempt to improve the scanner performance, the incandescent energy source was replaced with a small, pulsed CO_2 laser designed and built by the Physics Division of the National Research Council of Canada (NRCC). The laser produces 20 mJ pulses at 10.6 μm at rates from 1.5 to 6 pulses per second (pps). Above 6 pps the energy per pulse falls off markedly. The energy is focused to a 1.0 cm long line on the plate by a 15 cm focal length cylindrical lens. All transmission optics are NaCl. No changes were made to the scanning chamber itself. The laser and its power supply must be well shielded to prevent rf interference.

Tests were performed both by spotting compounds on E Merck Silica Gel 60 TLC plates (no indicator) to simulate chromatograms and by chromatographing actual mixtures. Background was due to CI reagent gas, usually methane, with major contributions at m/z 249 and 251 attributed to oxidation of the filament to ReO_4^+ by water vapor. Polar components in solvents, e.g. acetone or water, were found to also contribute to the background due to incomplete desorption from the plate surface prior to the scan. With respect to reproducibility of peak height (about 20%), linearity (ion counts increase more rapidly than amount of sample in the spot) and reproducibility of R_f values (very good), lamp and laser desorption produced the same results.

For thermally stable compounds such as phenanthrene and benzophenone laser desorption produced no increase in spatial resolution, yet gave about a factor of ten less sensitivity. Since laser desorption produces no bulk heating of the plate, the loss of resolution was attributed to the dead-volume in the plate chamber. Modifications are presently underway in an attempt to correct this problem. Sensitivity appears to be a function of both laser pulse rate and pulse energy. Sensitivity increases up to 6 pps but declines rapidly after that as laser pulse energy decreases, even though the total energy supplied to the plate does not change significantly. Laser pulse energy cannot be increased indefinitely because the silica gel layer itself evaporates at sufficiently high energies. Studies are presently underway to determine the optimum relation between sensitivity, energy per pulse and pulse rate.

Laser desorption proved far superior to lamp desorption for more thermally sensitive compounds. Cholesterol (base peak, m/z 369) and methyl stearate (base peak, m/z 299) were both readily detectable. The sensitivity was about a factor of five less than

for more stable compounds. Neither lamp nor laser desorption removed all the material from the plate. Plates could be rerun or subjected to other methods of detection after an initial scan.

In general with the present apparatus lamp desorption is simpler and more sensitive for compounds of moderate thermal stability. Laser desorption provides much better results for less stable compounds.

ACKNOWLEDGEMENTS

This work was supported by NRCC Contract No. 080-155/0-6314. The authors wish to express their thanks to E. Lewis, N. H. Burnett, B. Avery and F. Mason of the NRCC for their kind help with various aspects of this project.

REFERENCES

1. L. Ramaley, W. D. Jamieson and R. G. Ackman, 28th Annual Conference on Mass Spectrometry and Allied Topics, New York, N.Y., May 25-30, 1980, paper TPMP3.

MPB9 APPLICATION OF LANTHANUM HEXABORIDE CATHODES IN MASS SPECTROMETRY

L. Kelner, H. M. Fales, S. P. Markey, National Institutes of Health, Bethesda, Maryland 20205, and
C. K. Crawford, Kimball Physics, Inc., Wilton, NH 03806

We report here preliminary data on the possible application of polycrystalline and single crystal lanthanum hexaboride (LaB_6) as an electron emitter for EI and CI analytical ion sources. LaB_6 is a refractory compound with a low work function (2.6 eV) and over the last few years it has been developed into a valuable thermoionic electron emitter for use in electron probe instrumentation. Surprisingly, LaB_6 has not found much application in mass spectrometry except as mentioned by Buckingham (1) and as used in the Omegatron (2).

Polycrystalline (sintered) and single-crystal LaB_6 cathodes were mounted on standard filament assemblies of Finnigan 3000, AEI MS-9, LKB-9000 and LKB-2091 mass spectrometers. Polycrystalline cathodes were made of lanthanum hexaboride powder deposited on an outgassed 50 um thick carbon strip which was in turn mounted on metal (Ta) holders. Single-crystal cathodes were made of a precision-machined grain-of-sand sized lanthanum hexaboride block mounted on a precision-etched 50 um thick arch-shaped carbon strip, which was in turn mounted in refractory metal holders. The emitting surface was oriented in the (100) direction. Details of mounting procedures are discussed thoroughly (by CKC) elsewhere (3). The cathodes are directly heated by I^2R heating using the original equipment power supplies. Typical operating parameters were 2.5-4 V and 1.1-2.0 A. Actual parameters depend upon cathode dimensions, emission current required, and desired life. Chemical and mechanical stability of the cathodes are good, and they are not harmed by repeated exposure to the ambient atmosphere when cold.

We estimated the equilibrium source temperature when using Re and LaB_6 filaments on three different instruments: LKB-9000, LKB-2091 and Finnigan-3000 (Table I). Differences in temperatures between instruments are mainly due to the differences in the thermal masses of their sources along with thermal transfer variations within the vacuum system. Because of its lower power requirements use of LaB_6 resulted in lower ion source temperatures especially on the Finnigan-3000.

We have also compared the ionization efficiency of ion sources with LaB_6 and rhenium filaments. In electron ionization sources (LKB-9000 and LKB-2091) similar efficiencies for ionization were observed using the same emission current derived from Re and LaB_6 cathodes (50-60 uA) for both methyl stearate and N-(2,3-epoxypropyl)phthalamide (2,3-EPP). However, in the chemical ionization (CI) mode using the Finnigan-3000 more efficient ionization by LaB_6 cathodes at the same emission (1.57 mA) has been observed in both positive and negative ion detection (Table II). At lower emission current the advantage of LaB_6 is even greater: close to the order of magnitude difference was observed, when detecting ion m/z 299 (methyl stearate) in positive CI at .4mA of the emission current.

Thus, application of the lanthanum hexaboride cathode may offer better performance in terms of ion current output per sample introduced, as well as being useful in analyzing thermally unstable compounds. The lifetime of LaB_6 in mass spectrometers will be investigated in the near future.

1. J. D. Buckingham, Brit. J. Appl. Phys. 16, 1821 (1965).

2. W. Steckelmacher and J. D. Buckingham, Nuovo Cim., Suppl. #2, Ser.1,1,418 (1964).

3. C. K. Crawford, SEM/1979/I, SEM, Inc., AMF O'Hare, IL 60666, 19-30

TABLE I. Equilibrium temperature(°C) of the ion source with no heating other than filament

	LKB-9000 I em = 60 μA	LKB-2091 I em = 60μA	Finnigan-3000 I em = 1.5 mA
Re filament	260	217	150
LaB_6 polycryst.	230	-	-
LaB_6 single-crystal	-	187	80

TABLE II. Relative efficiency of ionization in the Finnigan CI ion source.

	Re	Single crystal LaB_6	Polycrystalline LaB_6
203 (neg. CI)	1	2	3
204 (pos CI)	1	5	3

Application of Dynamic Emittance Matching to Secondary Ion Mass Spectrometry

J. R. Wyatt, T. M. Barlak, J. E. Campana
R. J. Colton, and J. J. DeCorpo

Code 6110
Naval Research Laboratory
Washington, D. C. 20375

Recently, we described a high-performance SIMS instrument which is based on a double-focusing mass spectrometer.[1] In that report we described an experiment to determine the viewing area, where the primary beam was rastered over a molybdenum wire grid as the secondary ion beam deflectors were manually swept. The results of this experiment suggested it should be possible to increase the viewing area of the instrument by synchronously rastering the secondary ion beam and the primary beam.

This method was theoretically and conceptually described by Liebl[2] and is termed dynamic emittance matching (DEM). This method optimizes the transmission of the secondary ion beam (when the primary ion beam is rastered) by matching the emittance of the sputtered ion beam with the acceptance of the mass spectrometer. In DEM the primary and secondary ion deflectors are synchronously rastered so as to deflect secondary ions emitted from the larger viewing area onto the object slit. Liouville's theorem can be invoked to show that the net effect of DEM is to decrease the divergence of the secondary ion beam so that it is nearer the acceptance angle of the mass spectrometer at the object slit.

The Figure illustrates DEM as incorporated into our SIMS instrument. The optics between the first set of secondary ion deflectors and object slit have been omitted for simplicity as shown in the inset. Both x and y deflectors are included in our system; however, the figure represents only the y-deflector system. The dotted lines depict secondary ions resulting from a given sample origin and focused on the object slit. As the primary ion beam is moved, all other instrumental conditions remaining the same, the secondary ions will have trajectories significantly divergent from the former. These ion trajectories would continue in a linear fashion at the exit of the acceleration portion of the beam transfer optics and actually miss the object slit of the spectrometer. DEM directs these divergent ions onto the object slit as depicted by the broad lines in the Figure.

Results and Discussion

The experiment with a molybdenum grid described previously[8] was repeated with the DEM system. The most dramatic difference between the two experiments is the number of wires which can be actually viewed. Thirty to forty wires can be counted in the DEM traces obtained. This result indicates a x-axis view of 0.75-1 cm as compared to our previous result obtained without the DEM of 0.025 cm. The second observation is the increased spacial resolution of the signal which is less than the grid spacing (.025 cm). This improvement in spacial resolution compared to our previous experiments is due to our ability to dynamically tune the ion optics with the aid of the oscilloscope image and the use of a more sharply focused primary ion beam.

The improvement in ion transmission under full primary ion beam raster conditions (1 cm^2) with DEM was evaluated by measuring the signal of a high mass cluster ion ^{32} of CsI at m/z 1432. A series of measurements gave a range of ion transmission factors from a low of 7 to a high of 30 times greater than the signal obtained without DEM. These transmission factors were dependent on how carefully the ion optics were adjusted between each measurement.

The concept of DEM has been incorporated into our SIMS instrument. This feature has resulted in notable increases in the viewing area and ion transmission of the SIMS instrument. Under full primary ion beam raster conditions the viewing area and ion transmission have increased at least a factor of ten. These positive attributes of the DEM system permit a more average analysis of the surface under study and better instrumental sensitivity in the molecular SIMS mode. Additionally, this feature has added an imaging capability to our system, a feature not available on conventional SIMS instruments.

References

1. R. J. Colton, J. E. Campana, T. M. Barlak, J. J. DeCorpo, J. R. Wyatt, Rev. Sci. Instrum., 1980, 51, 1685-1689.

2. H. Liebl in (N. R. Daly, ed.) Adv. Mass Spectrom., Vol. 7A, Heyden & Son Ltd., London, 1978, pp. 751-757; H. Liebl in (K. G. Stephens, I. H. Wilson, J. L. Moruzzi, eds.), "Low Energy Beams, 1977," Conference Series, Number 38, The Institute of Physics, Bristol and London 1978; pp. 266-281.

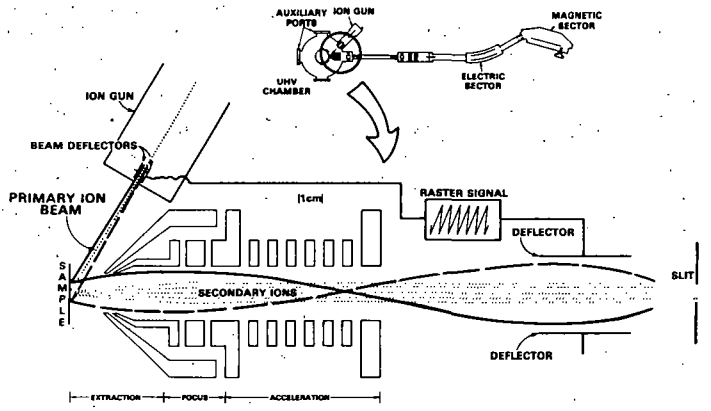

DYNAMIC EMITTANCE MATCHING

DESIGN AND PERFORMANCE OF A MODULAR PYROLYSIS MASS SPECTROMETRY SYSTEM; HENK L. C. MEUZELAAR, JOE H. TOMLINSON, DONNA J. IWAMOTO AND DAVID L. POPE, Biomaterials Profiling Center, Univ. of Utah, Salt Lake City, UT 84108.

Pyrolysis mass spectrometry (Py-MS) is a relatively young field. The Py-MS instrumentation described in the literature thus far is very heterogeneous and includes filament, direct probe and laser pyrolysis techniques in combination with different ionization techniques such as (low voltage) EI, CI, FI and FD, as well as totally different mass spectrometers, e.g. quadrupoles, TOF instruments and single and double focussing magnetic spectrometers. In order to enable the comparison of different pyrolysis methods under standardized experimental conditions, a modular Py-MS system was designed based on an Extranuclear quadrupole mass filter equipped with an open cross-beam type EI source surrounded by a LN_2 cooled screen, which combines filament (Curie-point), direct probe and laser pyrolysis capabilities. In addition the system features fully automated sample introduction, time-resolved recording of pyrolysis events and capabilities for identification of individual pyrolysis products by collisional activation MS. The Py-MS system is connected to a HP 21MX data system through an Extranuclear (Interlink) interface with fast ions counting channel. Specially developed computer programs enable signal averaging, mass peak identification, as well as operator-interactive spectrum normalization and feature selection operations. Final evaluation of Py-MS patterns is performed with the ARTHUR program package for multivariate statistical analysis. Applications investigated thus far include classification of cells and tissues, characterization of coals and shales, identification of drugs and metabolites in body fluids, and mechanisms and kinetics of polymer degradation.

A PYROLYSIS - MASS SPECTROMETRY STUDY OF THE ROLE OF ORGANIC RELEASING AGENTS IN GRAPHITE FURNACE ATOMIC ABSORPTION SPECTROSCOPIC ANALYSIS OF SEA WATER*

C. G. FLINN, R. GUEVREMONT and W. D. JAMIESON
Atlantic Research Laboratory, National Research Council of Canada
1411 Oxford Street, Halifax, N.S., Canada, B3H 3Z1

Severe interferences resulting from volatilization of the salt matrix has made direct graphite furnace atomic absorption spectrometry (GFAAS) impractical for determination of trace metals in seawater. These difficulties can be alleviated for several elements by adding EDTA or citric acid to the seawater. Detection limits of 0.01 and 0.12 µg/L for cadmium and zinc in seawater, using these "releasing agents" or "matrix modifiers", have been reported (1,2). Extension to determination of Cu, Fe, and Mn is being investigated. The physical and chemical processes relevant to such matrix modification are important in selection of reagents.

Sea salt pyrolysis experiments were performed with a CDS-Pyroprobe (model 120-382, direct introduction Pt filament probe) and a Finnigan 4000 mass spectrometer interfaced to an INCOS data system. The system studied, for the most part, was Zn in 50% sea water with 10 mg/mL citric acid as matrix modifier; 5 µℓ samples were deposited on the filament. Sample pyrolysis emulated graphite furnace operation. Desolvation: ramp at 300°/min to 100°, total 4 min. Char (optional for PY-MS): ramp at 200°/sec to <500°, total 20 sec. Atomize: ramp at 100° or 200°/sec to ≤1400°, total 20 sec. Temperatures were checked by optical pyrometry. Mass spectral conditions: electron impact ionization, electron energy = 16 eV, source temperature = 150°, scan frequency = 2 or 10 Hz, low mass ≥ m/z 11, high mass < m/z 300. Use of a modified version of the INCOS STABility program helped detect ionic multiplets and aided in mass assignment procedures.

Mass spectra obtained at 16 eV selectively enhanced metal atom ion counts and reduced the complexity of the spectra. Profile data allowed assessment of source defocusing during the initial burst of pyrolysis products. Species identified tentatively as present during the pyrolysis included: H_2O, S_2, H_2S, HCl, C_{2-6} H_{2-8} O_{0-7} (<200°); CO_2, $C_2H_4O_2$, CS_2 (200-350°); CS_2, Zn (>400°); C(1300°).

A memory effect complicated determination of analytical sensitivity and effect of sample size. Cleaning the filament with dilute HNO_3 reduces this memory effect. Sample composition was varied to include Cd and Hg. Ascorbic, tartaric, malonic and succinic acids were evaluated as matrix modifiers. Cd and Hg were successfully volatilized from the salt matrix. Citric and tartaric acids were very effective; others less so.

From this preliminary investigation: strongly reducing conditions exist in the solid phase at relatively low temperatures; no gaseous organometallic compounds were observed; several derivatives of seawater components were identified (e.g. HCl, H_2S, $S_2(SO_2?)$, CS_2); there is evidence of ion-molecule reactions during the initial burst of pyrolysis products. Isotope dilution analyses by PY-MS are possible, depending on the memory effect.

REFERENCES

1. R. Guevremont, R. E. Sturgeon, S. S. Berman, Anal. Chim. Acta., 1980, 115, 163-70.

2. R. Guevremont, Anal. Chim., 1981, 53, 911-14.

*NRCC No. 19062

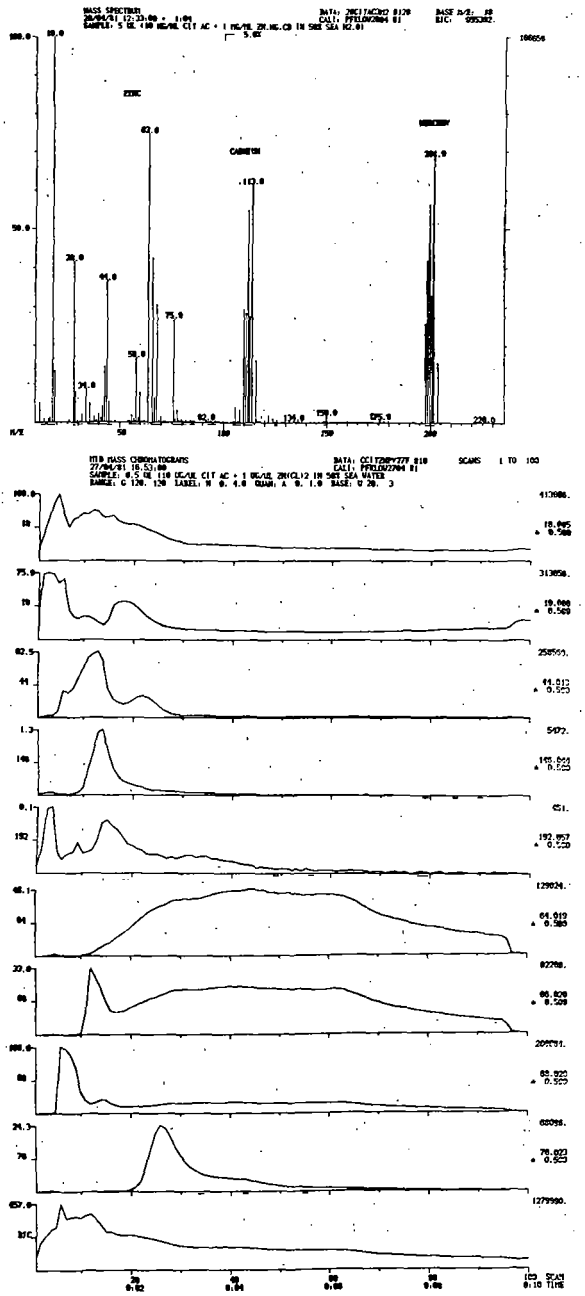

POSITIVE IONS OBSERVED IN SPARKED SF_6 AND SF_6-CONTAINING MIXTURES AT 40 kPa*

L. C. Frees, I. Sauers, L. G. Christophorou,† and H. W. Ellis‡
Atomic, Molecular and High Voltage Physics Group
Health and Safety Research Division
Oak Ridge National Laboratory
Oak Ridge, Tennessee 37830

Because of its high dielectric strength, SF_6 is finding increasing acceptance by industry as an insulator in high voltage equipment. Although SF_6 itself is inert and nontoxic, some of the products of its decomposition under electrical stress are highly reactive and toxic. The decomposition of SF_6 has been studied for nearly 30 years but is still not well understood. We have assembled a mass spectrometer with a high pressure spark ion source in order to study the decomposition of SF_6 and other dielectric gases.[1]

The apparatus consists of a spark ion source, operable at pressures up to 100 kPa, coupled to a quadrupole mass spectrometer equipped with an appropriate ion-focusing lens assembly. The ion source houses a pair of tungsten electrodes (0.8-mm-diameter rods with rounded ends) spaced ∿1 mm apart and mounted on a linear motion feedthrough so that the distance between the electrodes and the entrance aperture can be varied from 0.5 to 20 mm. The aperture, fashioned from 25-μm-thick-electroformed nickel, has a hole diameter of 30 μm. The mass spectrometer is also equipped with an electron impact ionizer so that neutral species produced as a result of the spark can also be observed.

The spark was produced with a positive high voltage pulse applied to one of the electrodes. The other electrode and the aperture were at ground potential. The high voltage pulse had a duration of 2 μs and a repetition rate of 100 Hz. The spark current was typically 1 A.

The mass spectrum of positive ions produced in the spark ion source with dielectric grade SF_6 (99.6% purity, by volume) at 40 kPa was dominated by ions containing impurities.[2] The most intense ions, $N_2O_2F^+$, $S_2NF_4^+$, $SO_2F_5^+$, $S_2NOF_4^+$, and $S_2NO_2F_4^+$, have been identified by their isotope ratios. Among the less intense ions are $H_2SOF_2^+$, $N_2F_4^+$, $S_2F_7^+$, $S_2NF_8^+$, and $S_4NF_6^+$. The addition of 1% O_2 to SF_6 greatly intensified the $SO_2F_5^+$ peak, while the addition of 1% N_2 resulted in enhanced intensities for the $N_2O_2F^+$, $S_2NF_4^+$, $S_2NOF_4^+$, $S_2NO_2F_4^+$, $S_2NF_8^+$, and $S_4NF_6^+$ ions. The addition of D_2O to the SF_6 resulted in new peaks in the mass range 89 through 92 u, confirming the assignment of the 88 u peak to $H_2SOF_2^+$.

When a fresh sample of SF_6 was sparked, the most intense ions were $S_2NF_4^+$ and $S_2NF_8^+$. After ∿1/2 hour of sparking, however, $SO_2F_5^+$, $S_2NOF_4^+$, and $S_2NO_2F_4^+$ became the most intense peaks, indicating that these ions are the result of reactions involving the products of previous sparking.

In order to minimize the effect of impurities, the ion source and gas handling lines were baked out overnight at 300°C, resulting in a much lower background pressure and water content. Several cycles of a freeze-pump-thaw purification procedure (at liquid N_2 temperature) significantly decreased the impurity contentrations in the SF_6 (to <20 ppm N_2 and <5 ppm O_2).

For the purified SF_6 at 40 kPa, the most intense ion was $S_2F_7^+$ (confirmed by isotope ratio measurements). There was a moderate intensity of SF_3^+ and traces of SOF_3^+, $SO_2F_3^+$, S_4F^+, $S_3F_3^+$, $S_2OF_5^+$, $S_4F_7^+$, and $S_3OF_9^+$, indicating that even these low levels of impurities can have an observable effect on the ion chemistry of the discharge.

At a pressure of 13 kPa, over 70 ion species of the form $S_xF_y^+$ (x = 2-16, y = 0 or an odd integer from 1 to 11) were observed. These ions were all deficient in fluorine, relative to SF_6, suggesting that they were formed in the rapidly cooling plasma after the spark pulse. They could not have been formed in subsequent ion-molecule reactions between

---

*Research sponsored by the Division of Electric Energy Systems, U.S. Department of Energy, under contract W-7405-eng-26 with the Union Carbide Corporation.

†Also Department of Physics, The University of Tennessee, Knoxville, Tennessee 37916.

‡Permanent address: Department of Natural Sciences, Eckerd College, St. Petersburg, Florida 33733.

precursor ions and residual SF_6 molecules while drifting from the spark region to the aperture because reactions increasing only the sulfur content of the ion would require breaking 6 sulfur-fluorine bonds, requiring collision energies in excess of 20 eV.

The spark color was a light blue at 13 kPa, changing to pale red at 40 kPa, indicating lower spark temperatures at higher pressures, for a constant power in the spark. This temperature difference is probably the reason for the difference in mass spectra.

At 40 kPa, mixtures of purified SF_6 with O_2, at concentrations of 500, 5,000, and 50,000 ppm O_2, resulted in the appearance of SOF_3^+, $SO_2F_3^+$, $SO_2F_5^+$, $S_2OF_5^+$, and $S_3OF_7^+$. At the 50,000 ppm O_2 level, SOF_3^+ and $S_3OF_7^+$ were the dominant ions. The $S_2F_7^+$ was almost absent, and the overall ion intensity had decreased by a factor of 8.

Mixtures of purified SF_6 with N_2, at a concentration of 500 ppm, resulted in the appearance of $S_2NF_8^+$ as the most intense peak, followed by $S_2F_7^+$, $SNOF_4^+$, and $N_2O_2F^+$. At a level of 20,000 ppm N_2, $N_2O_2F^+$, and $S_2NOF_4^+$ were the dominant ions. There was little $S_2F_7^+$ and the overall ion intensity was less than half that for purified SF_6.

Since the addition of impurities at levels as low as 500 ppm has such a large effect, the impurity-containing ions are probably the result of ion-molecule reactions between precursor ions, such as $S_2F_7^+$, and impurity-containing molecules as the ions drift toward the aperture.

When first sparked, a mixture of purified SF_6 and 5,000 ppm H_2O resulted in a mass spectrum consisting entirely of water clusters of the form $H^+(H_2O)_n$ (n = 2-5; for 10,000 ppm of H_2O, n = 2-6) with traces of $H_2SOF_3^+$ and, possibly, HSO_4^+. After the gas had been sparked for 1 hour, the water clusters were absent, and the spectrum was essentially that of purified SF_6 with the addition of SOF_3^+ and $H_2SOF_3^+$, indicating that the H_2O had been consumed in reactions with decomposition products (e.g., with SF_4 which has been detected using the electron impact ionizer).

Mixtures of 1% 2-C_4F_8 in SF_6 behaved differently. The $S_2F_7^+$ intensity was only decreased by a factor of 4, while $SC_4OF_{11}^+$ (confirmed by sulfur and carbon isotope ratios) became the most intense peak. A moderately strong peak appeared, confirmed by isotope ratios to be $S_2CF_5^+$, in addition to many smaller peaks 200 u higher in mass than other ions present in both pure SF_6 and SF_6 + 2-C_4F_8 spectra, suggesting the formation of clusters or complexes of 2-C_4F_8 with some of the ions.

The general effect of impurities or the additives studied so far on the spark ion spectrum of SF_6 is to decrease the overall ion intensity and to dominate the ion chemistry. This can have important effects in applications such as alternating current circuit breakers where SF_6 is used to quench the arc produced when the circuit is broken. The ability of the gas to withstand the voltage rise on the next cycle of power is directly related to the number density of ions present after the arc ceases. These results also help to explain the effects that impurities have on the decomposition products of SF_6.

[1]L. C. Frees, L. G. Christophorou, H. W. Ellis, and I. Sauers, *28th Annual Conference on Mass Spectrometry and Allied Topics*, New York, 1980, p. 197.

[2]L. C. Frees, I. Sauers, H. W. Ellis, and L. G. Christophorou, *J. Phys. D: Appl. Phys.* (in press).

A METHOD FOR MEASURING THE GAIN OF AN ELECTRON MULTIPLIER; WILLIAM J. FIES, JR.; Finnigan Corporation, 845 W. Maude Avenue, Sunnyvale, CA 94086

This paper presents a method for measuring the gain of an electron multiplier that does not require direct measurement of the input current. The method is based on the relation between the DC current and the RMS noise current at the input to the electron multiplier. Errors also arise if shot noise is not the dominant noise source in the system. However, methods for evaluating these errors are presented. The method offers a means for comparing the quality of various devices that use electron multipliers and also for judging the relative degradation over the life of an electron multiplier.
Experimental results are presented that were obtained from measurements on various types of electron multipliers installed in a quadrupole mass spectrometer. The method is particularly suitable for implementation in the computerized data systems in common use with mass spectrometers.

STUDIES OF ELECTRONIC TRANSITIONS AND EXCITED STATE CHEMISTRY BY ION KINETIC ENERGY SPECTROMETRY; A. J. ILLIES and M. T. BOWERS; Dept. of Chem., Univ. of Ca., Santa Barbara, CA 93106

Ion-atom collisions occuring at high energies (8 KV) involve electron-cloud interactions with relatively small momenta exchange. During these collisions translational energy of the ion (the fast particle) may be converted into internal energy of the system and vice versa, leading to a form of kinetic energy spectrometry. We have used the ZAB-2F in two different types of experiments, both involving the study of excited states using the collision cell.

In the first type of experiment use has been made of the fact that the ground state and excited states of ions may have different kinetic energy releases after a collision. This allows one to study reactions of electronic excited states in the ion source. We have already demonstrated that an excited state of NO^+ can be collisionally stablized and are in the process of measuring self stablization efficiencies.

The second experiment involves the use of high translational energy resolution (>40,000 FWHM) to study electronic transitions in the collision itself. For example the following reactions with Kr^+ are observed by the energy gain and loss of the main beam.

$Kr^+(^2P_{3/2}) \rightarrow Kr^+(^2P_{1/2})$ $\quad \Delta H = +0.67$ eV

$Kr^+(^2P_{1/2}) \rightarrow Kr^+(^2P_{3/2})$ $\quad \Delta H = -0.67$ eV

This experiment can therefore be used to study both the energies of electronic states of ions and as a specific probe for individual states as in part 1. As an example of the latter experiment we have shown that the two electronic states of Kr^+ react with N_2O at different rates. Quantitative measurement of these rates will be attempted in order to compare our results with the known published rates, and to establish the technique. Data on a number of molecular systems will be presented as well.

A STUDY OF DOUBLY-CHARGED ORGANIC IONS BY THE CHARGE-STRIPPING TECHNIQUE. T. Ast, C.J. Porter, C.J. Proctor and J.H. Beynon, Royal Society Research Unit, University College of Swansea, Singleton Park, Swansea SA2 8PP, U.K.

Charge-stripping reactions : $m_1^+ + N \rightarrow m_1^{2+} + N + e^-$, where N represents an atom or molecule of a neutral collision gas, have been studied in a collision cell located in the second field-free region of a double-focusing mass spectrometer of reversed geometry. Charge-stripping takes place in an isolated system in which the ion m_1^+ provides, through its translational energy, the source of electronic energy to drive the reaction. The translational energy loss can be measured by passing the product m_1^{2+} ions through an electric sector analyser[1] and, provided certain conditions are met[2], the translational energy loss will equal the ionization energy of m_1^+. This constitutes a useful and generally applicable method for determination of double-ionization energies; it overcomes most of the problems associated with the commonly employed electron impact threshold measurements. An accuracy of ± 0.5 eV is typically achieved; the method is fast and straightforward and the sensitivity adequate for most species studied.

A typical charge-stripping peak is shown in Figure 1(a). It represents the process $C_7H_8^+ \cdot \rightarrow C_7H_8^{2+}$ in toluene, using nitrogen as collision gas. Figure 1(b) shows the peak due to the main beam of stable $C_7H_8^+ \cdot$ ions plotted under identical conditions so that the two can be compared. In order to obtain the translational energy loss Qmin in the charge-stripping process (the translational energy difference between singly- and doubly-charged ions), the high energy side of the charge-stripping peak is extrapolated to the baseline and its position corrected for the initial energy spread of the m_1^+ ions. Therefore, the peak onset represents the m_1^+ ions which have lost minimum translational energy in becoming m_1^{2+} ions; any other processes involving additional translational energy loss contribute to the peak broadening on the low energy side.

Good agreement with literature values was found for a number of organic compounds (Table 1). Results for a number of monosubstituted-benzene molecular ions are shown in Table 2.

Experiments were performed with a number of different collision gases; significant changes in peak abundances and widths were observed, but the position of the peak onset remained constant. The results of these experiments are shown in Table 3 which suggest oxygen to be the most efficient collision gas for charge-stripping. Helium collision gas causes considerable broadening of the charge-stripping peaks, which become almost twice as wide as the main beam as shown in Figure 2.

Significant differences have been observed for production of doubly-charged ions from neutral molecules in the source by electron impact, and from singly-charged ions by the charge-stripping process. Thus, nitrobenzene gives an abundant doubly-charged molecular ion in the source but an extremely weak charge-stripping peak. On the other hand, methane shows no trace of the doubly-charged molecular ion in the source, but gives an abundant CH_4^{2+} ion by charge-stripping process[3].

References

1. R.P. Morgan, J.H. Beynon, R.H. Bateman, B.N. Green, Int.J.Mass Spectrom. Ion Phys., 28, 171 (1978).

2. T.Ast, C.J. Porter, C.J. Proctor and J.H. Beynon, Bull.Soc.Chem.Beograd, 46, 135 (1981).

3. T.Ast, C.J. Porter, C.J. Proctor and J.H. Beynon, Chem.Phys.Letts., 78, 439 (1981).

TABLE 1. Comparison of experimental and literature values of ionization energies of some organic molecular ions.

Compound	IE(m^+), eV[a]	IE(m^+), eV[b]
Benzene	16.8	16.9
Toluene	15.7	15.7
Benzonitrile	16.9	16.9
Naphthalene	15.0	14.7
Biphenyl	13.3	13.6
Anthracene	14.0	14.0

a This work.
b Literature value

TABLE 2. Ionization energies of some monosubstituted benzene molecular ions $C_6H_5X^{+\cdot}$

Substituent	IE($C_6H_5X^{+\cdot}$), eV	IE(C_6H_5X)[a], eV	Substituent	IE($C_6H_5X^{+\cdot}$), eV	IE(C_6H_5X)[a], eV
$COOCH_3$	12.8	9.35[b]	CH_3	15.7	8.82
COC_2H_5	13.2	9.27[b]	Br	15.7	8.98
CH_2NH_2	13.7	8.64[b]	OH	16.1	8.50
NHC_2H_5	13.9	7.56[c]	Cl	16.2	9.07
$N(CH_3)_2$	14.5	7.14	CN	16.7	9.71
I	14.9	8.72	H	16.8	9.24
NH_2	15.4	7.70	F	17.2	9.20
CHO	15.7	9.53			

a All values obtained by photoionization method, unless specified otherwise.
b Electron impact method. c Charge transfer method.

TABLE 3. Effect of different collision gases on the charge-stripping process $C_7H_8^{+\cdot} \rightarrow C_7H_8^{2+}$ in toluene.[a]

Collision gas	$C_7H_8^{+\cdot}$ peak width at half-height, eV	$C_7H_8^{2+}$ peak width at half-height, eV	Abundance ratio $C_7H_8^{2+}/C_7H_8^{+\cdot}$
Ar	3.79	5.01	6.2×10^{-7}
CH_4	3.92	5.47	9.9×10^{-7}
CO_2	3.84	5.31	3.0×10^{-6}
He	4.03	7.79	5.3×10^{-6}
CO	3.84	4.67	2.2×10^{-5}
N_2	3.87	4.46	3.9×10^{-5}
O_2	3.83	4.11	4.6×10^{-4}

a The pressure of the collision gas was adjusted in each case so as to effect an 80% attenuation of the main beam.

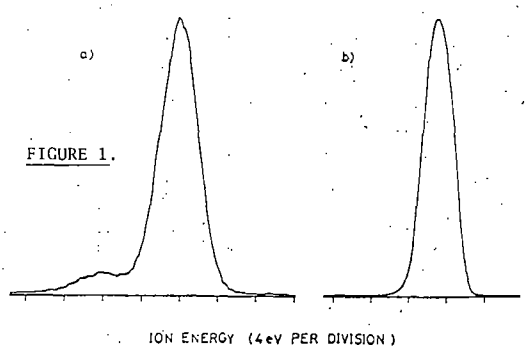

FIGURE 1.

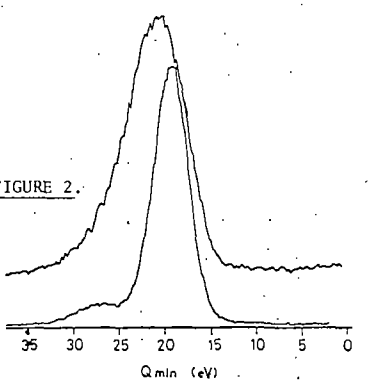

FIGURE 2.

FIGURE 1. Comparison of peak widths a) for the $C_7H_8^{2+}$ peak from the charge-stripping process $C_7H_8^{+\cdot} \rightarrow C_7H_8^{2+}$ and b) for the main beam of stable $C_7H_8^{+\cdot}$ ions in toluene.

FIGURE 2. The peak due to the charge-stripping process $C_7H_8^{+\cdot} \rightarrow C_7H_8^{2+}$ in toluene obtained with nitrogen collision gas (lower trace) and helium collision gas (upper trace).

MASS SPECTROMETRIC INVESTIGATION OF THE KINETICS AND ENERGETICS OF THE IONIZATION OF VAN DER WAALS CLUSTERS

J. H. Futrell
Dept. Chemistry, University Utah, Salt Lake City, Utah 84112, USA
K. Stephan, T. D. Märk
Kernphysik und Gaselektronik, Institut für Experimentalphysik
Leopold Franzens Universität, A 6020 Innsbruck, Austria
K. I. Peterson, A.W. Castleman, Jr.
Dept. Chemistry, University Colorado, Boulder, Colorado, 80309, USA
N. Djurić
Institute of Physics, 11001 Beograd, Jugoslavien

The formation and investigation of the physical and chemical properties of Van der Waals cluster molecules is a topic of considerable current interest. Little information exists on kinetics parameters for the formation of these species and for their electron impact ionization and subsequent decomposition mechanisms. Accordingly, we have used our molecular-beam-deflection-mass-spectrometer-technique /1,2/ to investigate the cluster systems $(CO_2)_x$ and $(NH_3)_x$ with x up to 10. For both neat and seeded beams we have investigated the kinetic energy distributions of the neutral species, the electron impact ionization appearance potentials of the respective ionic clusters, the energy profiles of fragment cluster ions and the in-flight decomposition processes (both unimolecular and collision induced) for Van der Waals and proton bound cluster ions /3-5/.

The experimental apparatus used in the present study consists of a 10^{-5} m aperture molecular beam source and a reversed geometry double focussing mass spectrometer. The expansion chamber is pumped by a 500 l/s turbomolecular pump. The supersonic jet is sampled transversely by an electron impact ion source and an ion optical system described in detail in Ref. 1 and 2. The transverse sampling of the supersonic beam results in ions originating from the beam having a significantly different velocity distribution than ions originating from the stagnant background gas. Application of a deflection voltage allows the separation of beam components from the background gas. Moreover, we have used the general utility of the high resolution mass spectrometer in order to positively identify and analyze certain cluster ions. In the ammonia system, for example, the NH_4^+ produced by electron impact ionization of $(NH_3)_2$ at m/z = 18 is contaminated, under certain circumstances, with $^{15}NH_3$, $^{16}OH_2$, $^{18}O^+$ and with NH_4^+ produced in the background gas via reaction $NH_3^+ + NH_3 \rightarrow NH_4^+$.

The present results include appearance potentials of the following ions: $(CO_2)_2^+$, $(CO\ CO_2)^+$, $(Ar\ CO_2)^+$, NH_4^+, $(NH_3)_2^+$, $(NH_3)_2H^+$, $(NH_3)_3^+$, $(NH_3)_3H^+$ and $(NH_2\ NH_3)^+$. Using a thermodynamic cycle the exothermicity of the reaction of CO_2^+ with CO_2 to form $(CO_2)_2^+$ was found to be 17.5 $\pm$ 3 kcal/mole in good agreement with previous high pressure mass spectrometry determinations /6,7/, thus resolving previous discrepancies between ionization and ion molecule studies. Unfortunately in case of ammonia not all of the existing discrepancies could be resolved. In both cases it was possible to detect the fragment

ions $(NH_2\ NH_3)^+$ and $(CO\ CO_2)^+$ and measure their appearance potential in good agreement with values derived from the respective monomer fragmentation.

The present apparatus was also used to investigate the dissociation of ion clusters as a function of time after ionization, using the well established technique of decoupling the acceleration and deflection electric fields /8/. The reliability of the technique was demonstrated by a study of well-characterized metastable ions in propane which corrobates and extends previous measurements, lending credence to the presently reported metastable cluster ions. Our tentative conclusion is that small cluster ions should be described by a loosely-coupled mode. The simple dissociations of $(CO_2)_2^+$, $(NH_3)_2^+$ and $(NH_3)_2H^+$ are all collision-induced, supporting this model. On the other hand, the observation of true (unimolecular decay) metastables for the rearrangement decay of the ammonia dimer ion to NH_4^+ and for the dissociation of the proton bound trimer to the proton bound dimer ion suggest strongly-coupled oszillators which are most appropiately treated by a statistical model such as the QET. Molecular complexity, the availability of a rearrangement decomposition channel, and the strength of bonding in the cluster are relevant factors which affect the transition from short-lifetime to long-lifetime cluster ions.

A full account of this work will be submitted for publication, see Ref. 3-5

Acknowledgements

Work partially supported by the Österreichischer Fonds zur Förderung der wissenschaftlichen Forschung under Projekt S-18/05 and S-18/08.

References

/1/ H. Helm, K. Stephan and T.D. Märk, Phys. Rev. A 19 (1979) 2154

/2/ K. Stephan, H. Helm and T.D. Märk, J. Chem. Phys., 73 (1980) 3763

/3/ K. Stephan, J.H. Futrell, K.I. Peterson, A.W. Castleman Jr., and T.D. Märk An electron impact study of carbon dioxide dimers in a supersonic molecular beam: appearance potential of $(CO_2)_2^+$, $(CO\ CO_2)^+$ and $(Ar\ CO_2)^+$, to be published in J. Chem. Phys.

/4/ K. Stephan, J.H. Futrell, K.I. Peterson, A.W. Castleman, Jr., H.E. Wagner, N. Djurič and T.D. Märk, An electron impact study of ammonia clusters in a supersonic molecular beam: appearance potentials of NH_4^+, $(NH_3)_2^+$, $(NH_3)_2H^+$, $(NH_3)_3^+$, $(NH_3)_3H^+$ and $(NH_2\ NH_3)^+$, to be published in Int. J. Mass Spectrom. Ion Phys.

/5/ J.H. Futrell, K. Stephan and T.D. Märk, The metastable and collision induced dissociation of propane, CO_2-clusters and NH_3-cluster ions, to be published in J. Chem. Phys.

/6/ M. Meot-Ner (Mautner) and F.H. Field, J. Chem. Phys., 66 (1977) 4527

/7/ J.V. Headley, R.S. Mason and K.R. Jennings, presented at 28th Annual Conference on Mass Spectrometry and Allied Topics, New York, May 25-30, 1980

/8/ R.G. Cooks, J.H. Beynon, R.M. Caprioli and G.R. Lester, Metastable Ions, Elsevier Publishing Company, Amsterdam, 1973

UNIMOLECULAR FRAGMENTATION OF IONS: COMPETITION BETWEEN STATE SPECIFIC AND ENERGY RANDOMIZED PATHWAYS

J.P. Gilman, T. Hsieh and G.G. Meisels, Dept. of Chem., Univ. of Nebraska, Lincoln, NE 68588

The fragmentation of gaseous ions is generally interpreted in terms of the widely accepted quasiequilibrium theory of mass spectra (QET). It is usually applied by assuming that molecular ions are formed in a distribution of electronically and vibrationally excited states which rapidly convert to vibrationally excited states of the ground electronic state of the ion. Fragmentation is then described by a series of consecutive and competitive fragmentation processes from an energy randomized intermediate. That is, energy randomization over all vibrational and rotational degrees of freedom is normally assumed to occur entirely within the ground electronic state.

"Isolated" (non-interconverting) electronic states have been revoked repeatedly to explain unexpected results in organic mass spectrometry, however, unambiguous verification of the existence of "isolated" states is difficult at best.

We have recently presented evidence that the assumption of conversion to the ground state and randomization may not hold for methylnitrite ion (CH_3ONO^+). The fragments NO^+ (30) and CH_3O^+ (m/e 31) are formed non-competitively and we have postulated that they come from different electronic surfaces of the parent ion, possibly involving a curve crossing in the formation of CH_3O^+ (1). This unique behavior may be associated with the -ONO group where the lone pair electrons may play an important role. The relatively small size of this molecule may also be of significance. We report here on our investigation of these factors using threshold photoelectron-coincident photoion (TPE-CPI) mass spectrometry (2) of the higher homologues of methylnitrite; ethylnitrite (C_2H_5ONO), deuterated ethylnitrite (C_2D_5ONO), and n-propylnitrite (n-C_3H_7ONO).

Ethylnitrite and deuterated ethylnitrite were synthesized by dripping diluted sulfuric acid into a cold, aqueous solution of ethanol (or C_2D_5OD) and sodium nitrite. The escaping gas was passed through a conc. solution of NaOH to remove NO_2 and through a drying tube containing $CaCl_2$, and collected at 0°C. Trap-to-trap distillation was repeated several times before the product was stored in a dry ice-acetone cold bath. n-Propylnitrite was obtained from Frinton laboratories and was further purified by vacuum distillation.

Asymmetric peak broadening of m/e 31 (CH_3O^+) but not of m/e 30 (NO^+) in the TOF curve (Fig. 1) from TPE-CPI of methylnitrite is the principal evidence supporting that these ions arise from separate non-interconverting electronic states of CH_3ONO^+. In propylnitrite, the peak analogous to CH_3O^+ is the $C_3H_7O^+$ ion (m/e 59) but it is not observed in the TOF curve (Fig. 2). Mass resolution in the TPE-CPI apparatus in the TOF mode is approximately 30 and is not sufficient to resolve m/e 59 from m/e 60 (CH_3ONO^+). However, low and high energy electron impact mass spectra indicate that $C_3H_7O^+$ is not a major fragmentation pathway in the decomposition of n-propylnitrite, unlike the processes leading to CH_3O^+ and $C_2H_5O^+$ in methyl and ethylnitrite, respectively. In addition, no metastable ions from n-propylnitrite ion were observed in the 3rd field-free region of the triple sector mass spectrometer (EBE; Kratos MS50TA) but this may be due to the very weak parent ion intensity (~0.3% of base peak intensity in 70 eV EI mass spectrum). Collision-induced dissociation (CID) also produced no peaks corresponding to m/e 59 (Fig. 7) indicating that $C_3H_7O^+$ is not a significant fragmentation product ion. Evidence obtained from the metstable, CID and TPE-CPI studies suggest that the fragmentation of n-$C_3H_7ONO^+$ to $C_3H_7O^+$ ion does not involve dissociation from different electronic states and that its fragmentation behavior is statistical in nature.

In the fragmentation of ethylnitrite, a fragment is observed at m/e 45 (Fig. 1); it includes two unresolved ions, $C_2H_5O^+$ and CH_3NO^+. The corresponding ions in deuterated ethylnitrite are CD_3NO^+ (m/e 48) and $C_2D_5O^+$ (m/e 50) (Fig. 2). The TPE-CPI mass spectra do not permit a conclusive elimination of asymmetric peak broadening of $C_2D_5O^+$. However, a metastable peak (MIKES scan of 3rd field-free region) was observed for $C_2D_5O^+$ (Fig. 6) suggesting that the lifetime of $C_2D_5ONO^+$ (and correspondingly $C_2H_5ONO^+$ (Fig. 7)). Although CD_3NO^+ was also observed as a metastable it probably arises from collision-induced dissociation as is the case with NO^+ from methylnitrite ion. (1). Breakdown graphs constructed from TOF curves (Figs. 3-5; not corrected for false coincidences due to the transmission of energetic electrons through the TPE detector, see MAMOB7) suggest similarity in their fragmentation processes leading to CH_3O^+ from CH_3ONO^+ and $C_2D_5O^+$ from $C_2D_5ONO^+$. These studies indicate that ehtylnitrite may be non-statistical in its fragmentation behavior and further work using a quadrapole mass analyzer to improve resolution in the TPE-CPI results is underway.

This investigation was supported in part by the U.S. Department of Energy under contract DE-A502-76ER02567 and the National Science Foundation through the regional facility in mass spectrometry at the University of Nebraska. We also wish to thank Mr. Pradip R. Das for his assistance in preparing this manuscript.

REFERENCES

1. G.G. Meisels, T. Hsieh and J.P. Gilman, J. Chem. Phys., **73**, 4126 (1980). 2. C.F. Batten, J.A. Taylor, B.P. Tsai, and G.G. Meisels, J. Chem. Phys.., **69**, 2417 (1978).

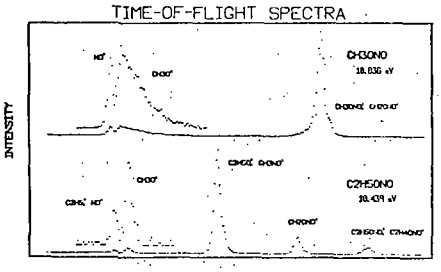

FIG. 1

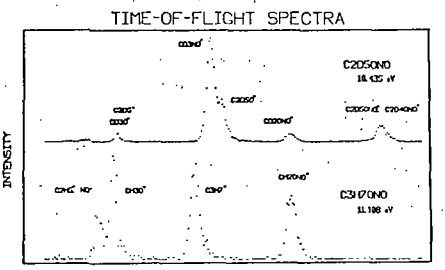

FIG. 2

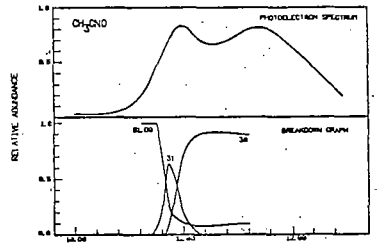

FIG. 3

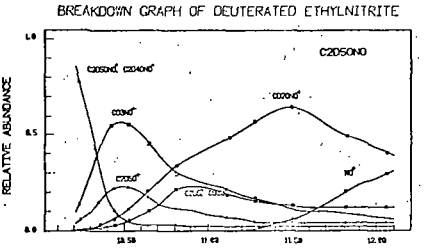

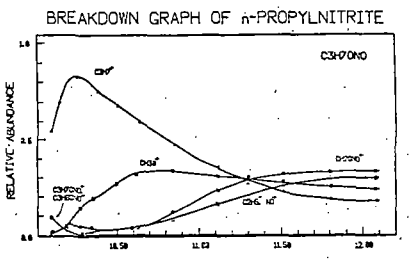

FIG. 5

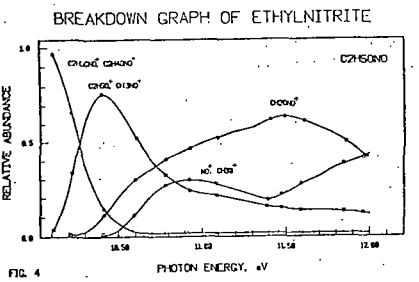

FIG. 4

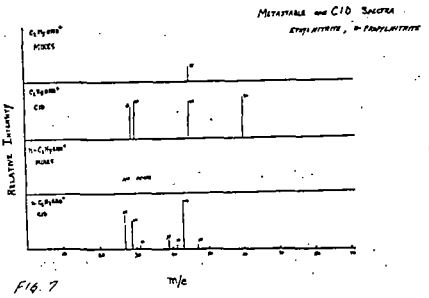

FIG. 7

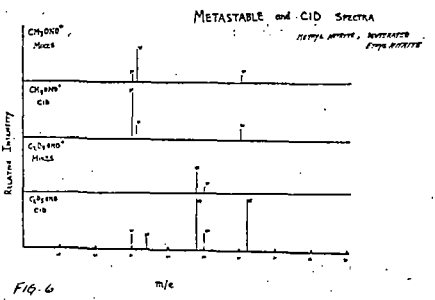

FIG. 6

NEUTRAL FRAGMENT SPECTRA OF THE TETRAMETHYL DERIVATIVES OF THE GROUP IVA ELEMENTS

Gerald D. Flesch and Harry J. Svec
Ames Laboratory-USDOE and Dept. of Chemistry
Iowa State Univ., Ames, Iowa 50011

A neutral fragment mass spectrometer capable of simultaneous mass analysis of positive ions and neutral fragments resulting from interactions of electrons and molecules has been used to characterize the unimolecular decompositions of the title compounds. Neutral species are produced in the primary chamber of the dual-chambered ion source using 200 μa pulses of 50 eV electrons. The neutral species diffuse into the secondary chamber. Ions formed there are characterized by mass spectra and ionization efficiency plots.

A "normal" mass spectrum is obtained when the 30 μa, 15 eV, secondary chamber electron beam is "on". An "autoionizing" spectrum is obtained when the secondary chamber electron beam is "off". Residual oxygen is used to calibrate the energy scale for the ionization efficiency plots.

Mass Spectra. The two quadrupole mass filters were adjusted to obtain the maximum sensitivity at the lowest resolution compatible with obtaining good data. Ions obtained in the "normal" spectrum could result from simple ionization or from dissociation ionization. Ionization efficiency studies usually permit differentiation between the two possibilities. CH_3^+, $C_2H_2^+$, and $C_2H_4^+$ are formed in low abundance in the secondary chamber by simple ionization of neutral fragments in or near their ground states. Except for $C(CH_3)_3^+$, $M(CH_3)_3^+$ is formed by dissociative ionization of slightly excited $M(CH_3)_4^*$. This excited species accounts for >90% of the neutral species observed. Other metal-containing fragments are observed in low abundance. Spectra obtained at higher resolution indicate that the neutral fragments tend toward three-ligand species.

Abundances of "auto" ions are very low. All ions $M(CH_3)_n^+$ (n=0-3) are observed except C^+. The abundances of both "normal" and "auto" ions vary linearly with pressure.

Ionization Efficiency. Ionization efficiency data are good for CH_3, C_2H_2, and C_2H_4 and ionization energies with ±0.15 eV uncertainties are obtained. Comparison to literature values indicates that C_2H_2 and C_2H_4 are formed in the ground state and that CH_3 is formed with 0.29 eV excitational energy, corresponding to symmetric stretch (0.34 eV).

Ionization and appearance energies for the metal-containing fragments are reproducible to ±0.5 eV. $M(CH_3)_3^+$, except for $C(CH_3)_3^+$, result from dissociative ionization of $M(CH_3)_4^*$. Most of the other ions $M(CH_3)_n$ (n=0,1,2) result from ionization of neutral fragments.

Summary. At least four kinds of neutral species are produced: 1) fragments containing only ligands; 2) fragments containing the central atom; 3) slightly excited molecular species, e.g. $M(CH_3)_4^*$; and 4) highly excited molecular species, e.g. $M(CH_3)_4^{**}$.

The CH_3 fragment is produced in a vibrationally excited state, and C_2H_2 and C_2H_4 in their ground states.

The most abundant product of electron - $M(CH_3)_4$ interactions is $M(CH_3)_4^*$.

This research is described fully in the issue of the International Journal of Mass Spectrometry and Ion Physics dedicated to the 60th birthday of Professor Doctor H. D. Beckey.

THERMAL IONIZATION SPECTRA OF ORGANIC CATIONS

Alfred L. Yergey
National Institute of Child Health and Human Development
National Institutes of Health, Bethesda, MD 20205

Robert J. Cotter
Middle Atlantic Mass Spectrometry Facility
Baltimore, MD 21205

Thermal ionization mass spectra of a wide variety of alkyl and alkyl/aryl ammonium, phosphonium and sulfonium, choline and its derivatives and more complex quaternary salts have been recorded. The spectra exhibit substantial molecular cation peaks, M^+, (from the salt, MX) as well as fragment ions that are principally even electron species. These spectra are qualitatively similar to those produced by field desorption/collisional activation (FDCA), by laser induced desorption, and by other new techniques for the mass spectrometry of non-volatile materials, but the process giving rise to our spectra is a purely thermal one. No auxilliary ionization means are employed to produce ions; we merely heat salt coated filaments inside the ion source.

A Finnigan 4000 quadrupole with an INCOS data system was used in conjunction with a solids probe designed for thermal ionization. The probe, filaments and instrument modifications are described elsewhere in detail[1]. Samples of salts were dissolved in water at concentrations of about 100 ng/µl. Filaments were prepared by placing 10 µl of a salt solution on the surface and drying the solvent under a heat lamp. Dried filaments were inserted into the ion source on the end of the solids probe and heated using current pulses that were adjusted for best spectra. Typical operating conditions involved pulses of 1.1 sec in a 2.4 sec cycle; the pulses had plateau current levels of about 2 amperes. Independent filament temperature measurements show that at temperature <900°C, M^+ ions are at a maximum and at temperature >1000°C fragment ions intensities are maximized.

From the present work it cannot be determined whether the ions observed are produced on the surface and desorbed, or whether they are the product of gas phase decomposition after volatilization of the salt. In any case, at filament temperatures below about 1100°C, the ions observed are almost exclusively even electron species. Based on earlier studies using MIKES[2] and FDCA[3], we suggest that the mechanisms leading to the observed fragments involve a series of α-cleavages and hydrogen rearrangements to yield a series imminium (or phosphinium or sulfininium) ions for salts that have alkyl substituents,e.g.

$$R_4\overset{+}{N} \rightarrow R_2\overset{+}{N}{=}CHR^1, \quad R'CH{=}\overset{+}{N}{=}CHR^1, \text{ etc,}$$

for tetraalkyl ammonium salts. For salts with some aromatic substituents, few if any imminium ions are seen, rather there are successive losses of one or 2 molecules of hydrogen at temperatures just above the temperatures where M^+ is seen, and then at higher temperatures, hydrocarbon fragments are observed.

1. A.L. Yergey, N.E. Vieira and J.W. Hansen, Anal. Chem., 52, 1811 (1980).

2. M.L. Sigsby, R.J. Day and R.G. Cooks, Org. Mass Spect., 14, 556 (1979).

3. H.H. Gierlich, F.W. Rollgen, F. Borchers and K. Levsen, Org. Mass Spect., 12, 387 (1977).

CHARACTERIZATION AND OPTIMIZATION OF THERMOSPRAY IONIZATION; J. J. CARMODY, C. R. BLAKLEY, and M. L. VESTAL; Dept. of Chem., University of Houston, Houston Texas 77004.

Recently we discovered a new ionization technique which appears widely applicable to mass spectrometry of nonvolatile molecules. This new technique, which we are tentatively calling the thermospray process, generally provides spectra which are similar to those obtained by field desorption or plasma desorption without some of the disadvantages. In particular, the new technique is compatible with on-line LC; it is fast, sensitive, relatively simple, and inexpensive. This new ionization technique employs apparatus developed for on-line LC-MS coupling. While the mechanism of the ionization process is not yet fully known, it appears that ions are produced by a combination of partial vaporization by very rapid heating of a liquid solution containing the sample and final vaporization by impact of an aerosol containing the sample on a heated metal plate. No ionizing source such as an electron beam or strong electric field is required. We have recently undertaken a series of studies aimed at establishing the dependence of this ionization process on critical parameters such as vaporizer temperature and geometry, liquid flow rate, and solvent composition. The results of these studies are presented together with a discussion of their implications concerning the mechanism of the process. Procedures for optimizing the performance of the thermospray ionization process are described.

EFFECT OF ^{63}Ni BETA PENETRATION DEPTH ON THE ELECTRON CAPTURE DETECTOR AND THE ATMOSPHERIC PRESSURE IONIZATION MASS SPECTROMETER

M. J. Connally, S. W. Warden, and E. P. Grimsrud, Department of Chemistry, Montana State University, Bozeman, Montana 59717.

The typical geometry of the Electron Capture Detector (ECD) or the Atmospheric Pressure Ionization (API) mass spectrometer ion source is cylindrical where the beta emitter, ^{63}Ni (embedded onto Pt foil), forms the entire cylindrical wall. We would like to determine the density of ionization caused by the beta flux within these cells as a function of distance from the cell walls.

An APIMS was used with two different ion sources. In ion source A ionization is caused by a small disk containing 0.20 mCi of ^{63}Ni. The disk is movable so that the distance, d, between the disk and the ion-sampling aperture is continuously variable. Ion source B has a large 15-mCi ^{63}Ni foil forming the cell wall in addition to the small movable disk. The total positive ion signal is measured as a function of d for each cell.

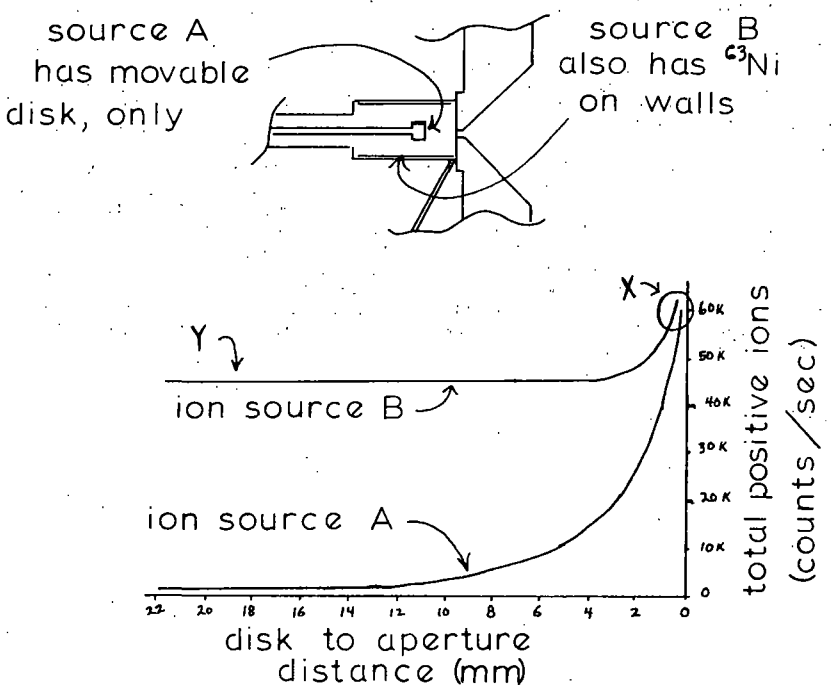

The results shown above are for air carrier gas at ambient temperature and pressure. For these conditions, total negative ion signals varied with d in exactly the same manner. At higher source temperatures, the total positive ion signals are consistently lower (most likely due to the reduced mass density), but are dependent on d in a proportionately similar manner as the data shown above.

The ion signals observed are thought to reflect the ionization density caused by ^{63}Ni beta radiation in a small portion of the source immediately adjacent to the sampling aperture. The most striking feature of the data is the relatively large signals observed

when the disk is very close ($d \approx 1$ mm) for both sources (see region marked "X" on figure). This result is somewhat unexpected in that the "average" ^{63}Ni beta is calculated to travel about 13 mm in one atmosphere of air, and should cause somewhat greater ionization per path length as the beta loses energy during its flight. The increased ion density observed near the foil surface is due to low energy betas and those which are backscattered from the Pt foil on which the ^{63}Ni is embedded. (Obviously, $\frac{1}{2}$ of all betas are initially directed backwards into the Pt foil. Because of the large atomic mass of Pt a significant fraction of these will backscatter with reduced energy into the source.)

We are presently attempting to transform the data shown above so that the ionization density thoughout any imagined cell design can be precisely predicted. While this work is is not yet complete, a qualitative prediction for the 10-mm cell is readily obtained from the data shown in the above figure. This data suggests that the ionization density near the wall of a 10-mm cell will be significantly greater than that in more central regions of the cell.

This conclusion is drawn by considering two small volumes within the 10-mm cell. Let one volume, x, be near the cell wall and another, y, be near the axis of the cell. The relative ionization density at point y is estimated from the data in the figure in the region marked "Y". This measurement (45K) is proportional to the ion density at a point on the axis and at the end of the cylinder. The ion density at a point on-axis and at the center of the cylinder may be up to twice this value (proportional to 90K). At point x, ionization from long-range betas should be similar in magnitude to that seen at point y. However, point x also experiences considerable addition ionization from short range effects (see region "X" of the figure). The curvature of the cylindrical foil will further enhance the short range effects. Thus, we expect ionization density near the wall of the 10-mm cell will be at least 2x greater than that near the axis of the cell.

Significance for APIMS and ECD. In optimizing the ^{63}Ni API source, the most important consideration is to cause maximum ionization near the sampling aperture. Our data suggests that a cylindrical source of smaller dimensions than the 10-mm source used here will provide greater total ion signals even though its net activity will be less.

Recent developments in the theory of the ECD indicate that positive ions will contribute (subtract from) the normal ECD response to sample. The magnitude of this positive ion contribution will depend on the penetration depth of the ionizing radiation relative to the size of the cell. In our present studies of Gas Phase Coulometry, we have taken advantage of this knowledge by designing ECDs which are affected minimally by the positive-ion contribution to the response.

AN IMPROVED FI/FD/EI ION SOURCE FOR USE ON A MODIFIED AEI MS9 MASS SPECTROMETER.

A. M. Hogg & J. D. Payzant; Department of Chemistry, University of Alberta, Edmonton, Alberta, Canada T6G 2G2

An FI/FD/EI ion source has been in use in our laboratory for about 5 years. It was described at the 1977 ASMS meeting and later in the literature (A.M. Hogg & J.D. Payzant, Int. J. Mass Spectrom. Ion Physics 27 (1978) 291). It has been used on a routine basis for hydrocarbon analysis in the FI mode and to a lesser extent for FD analysis of organic and organometallic compounds which could not be handled by EI and CI. Some limitations in the design have become apparent over the years and an improved version is now in use which incorporates several modifications. These changes, while relatively minor, have made routine day-to-day operation much more satisfactory.

Sensitivity in the FI/FD mode is always less than ideal and the following modifications have been made to improve it.

a) A narrower more gas-tight ionization chamber gives a higher loeal sample pressure around the emitter particularly in GC/FIMS operation.

b) The use of a high negative voltage (~-1700 V) on the MS9's Y deflection plates (mean Y voltage) has been found to give a gain of X4 on our instrument when operated at a resolution of ~1000 with wide slits.

c) An integrating input before the normal interface of our KRATOS DS50 data system give much better results where FI peaks are a collection of single ion peaks in close succession.

It has been found that performance can deteriorate and discharges occur which can only be cured by cleaning the counter electrode slit (sometimes this may be due to a broken emitter wire becoming lodged in the slit). Modifications in the new source allow the beam centering plates, the counter electrode and even the ion chamber walls to be removed quickly without disturbing the rest of the source. Reassembly and rejigging is very simple and the source can be removed, the counter electrode cleaned and the system put back in operation again in less than 1/2 hour.

A new ionization chamber geometry is now used which is very similar to that of the standard EI source but only 1/3 of the width. A standard KRATOS filament and trap are used and higher-field collimating magnets have been installed. 500μA trap current can be maintained and sensitivity, using the repeller probe, is indistinguishable from the standard source. High resolution EI scans can be interspersed with FI work without changing sources. For calibration purposes between FI runs it is only necessary to withdraw the emitter probe slightly, sensitivity is adequate without the use of a repeller.

Unlike the original design the new source uses standard KRATOS spacers and the heater wells in the new heater block accommodate Vacumetrics MS9 heaters (or the original KRATOS heaters). Jigging is simple using the standard MS9 source jig and rods.

A floating variable voltage supply is needed to provide heating current for the emitter. Because high voltage arcs are a constant hazard, regulated supplies especially ones which incorporate feedback from a total emission monitor, have been found to be troublesome. A very primative supply using an alkaline D-cell (which lasts for several months of normal use) together with a simple current limiting circuit on the high voltage feed to the emitter is now used and has proved to be completely trouble free.

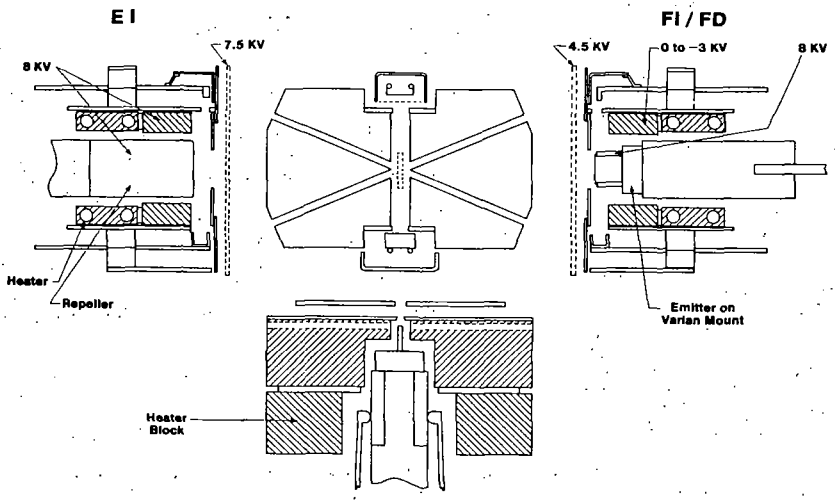

Simplified Emitter Heating and Spark Supression Circuit

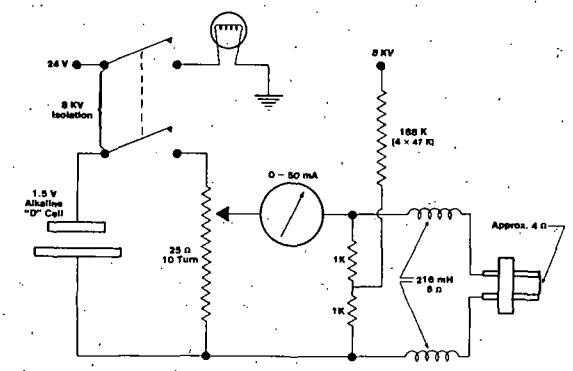

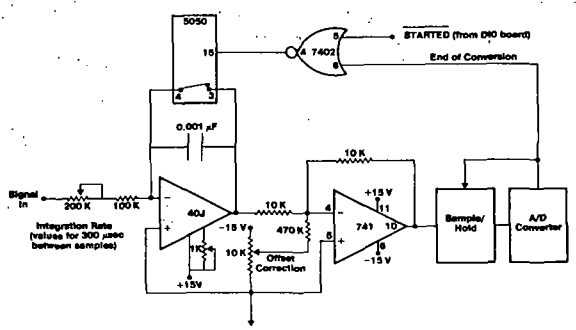

Integrator Input for DS50 Data System

SIMPLE MASS SPECTROMETRIC ASSAY OF CARBON 14 FOR BIOMEDICAL STUDIES

R.C. Abbott, M. Anbar and J.H. McReynolds
Department of Biophysical Sciences
School of Medicine
SUNY/Buffalo, New York 14214

The possibility of mass spectrometric assay of very small amounts of ^{14}C was conceived in 1969 by M. Anbar. The first experimental attempts along this line were reported in 1974 (1). The objective of these early experiments was to assay $^{14}C/^{12}C$ isotopic ratios in the form of CN^- ions down to 10^{-16} to facilitate more sensitive carbon dating. This goal, which was not reached at that time because of background interference ($^{29}Si^-$, $^{28}SiH^-$) (2,3,4), has since been achieved by much more elaborate instrumentation involving accelerator generated C^- ions (5,6).

Compared with carbon dating, biomedical tracer studies require a lower sensitivity of detection of ^{14}C atoms by about 8 orders of magnitude. Consequently we concentrated our efforts to develop a simple mass spectrometric technique which will meet the biomedical needs without a prohibitive cost of instrumentation. Our goal has been to assay ^{14}C with a sensitivity of 10^4 higher than that achieved by routine scintillation counting, thus allowing clinical tracer studies with a total body radiation dose of the order of 0.1 mrad. We aimed at a mass spectrometric assay of 3×10^{-15} Ci (3×10^7 ^{14}C atoms), at specific activities of the order of 6×10^{-5} Ci/mole, in less than 1 min. At this specific activity 3×10^{-15} Ci ^{14}C would constitute 5×10^{-11} moles or 3×10^{13} ^{12}C atoms, giving a $^{14}C/^{12}C$ ratio (R) of $3 \times 10^7/3 \times 10^{13} = 10^{-6}$. This would require an overall ionization and detection efficiency of about 3×10^{-5} ions/^{14}C atom, an abundance sensitivity m/z 14/13 of $\leq 10^{-7}$ (allowing assay of $R \leq 10^{-9}$) and a background of $R \leq 10^{-9}$. These three objectives have been achieved in a simple mass spectrometric system.

The production of C^- ions at a high yield was achieved in a small cold cathode discharge source in which CO_2 is diluted in an overwhelming excess of He in the presence of Cs vapor. The pressure in the source is estimated at 0.5 Torr, the partial pressure of CO_2 10^{-6} to 10^{-4} Torr; cathode potential - 2500V; source temperature 100 to 150°C; partial pressure of Cs about 10^{-3} Torr. A detailed description of the complex set of reactions taking place in the ionization source under these conditions is beyond the scope of this communication. In a very simplified manner it can be said that excited helium atoms produce from CO_2 C atoms and C^+ ions and that these are converted to C^- ions by reaction with Cs atoms.

Under the conditions described above we can detect one C^- ion for every 1.25×10^4 CO_2 molecules entering the source diluted with 5×10^9 He atoms, with the yield of C^- decreasing with the square root of its partial pressure in He. This change in sensitivity of detection of C^- does not affect, however, the ratio R, which depends on the ratio of $^{14}CO_2$ to $^{12}CO_2$ in the feed.

The two species that can interfere with our assay are $^{13}CH^-$ ($+^{12}CD^-$) and $^{12}CH_2$. These species could be formed from organic contaminants and especially from H_2O in the feed gas. Organic contaminants can be quantitatively removed by oxidation over CuO, but the partial pressure of the water thus produced cannot be readily reduced below 10^{-8} torr without

a chemical conversion train (3). To check on the yield of CH^- and CH_2 formed from CO_2 and H_2O we deliberately added overwhelming amounts of H_2O to the feed gas (H_2O/CO_2 = 30). We then observed at 4 torr H_2O a significant increase in the m/z 13/12 ratio by about 0.03 while R increased by $< 7 \times 10^{-3}$. We then measured the yield of CH^- in the form of CD^- by adding D_2O (98 percent D) to the gas feed. ΔR was proportional to the partial pressure of D_2O. At a partial pressure of 3000 ppm D_2O and 98 ppm CO_2 we observed $\Delta R = 0.013$. From this value we can calculate the yields of CH^- and CH_2 formed from CO_2 and H_2O under the expected routine operating conditions. Under the latter conditions we expect a partial pressure of $< 10^{-8}$ torr H_2O in the feed gas, thus the contribution of $^{12}CH_2$ to m/z 14/12 would be $< 0.007 \times 10^{-8}/4 = 18 \times 10^{-11}$. The contribution of $^{12}CH^-$ to m/z 13/12 would be $< 0.03 \times 10^{-8}/4 = 7.5 \times 10^{-11}$ and therefore the expected contribution of $^{13}CH^-$ to R would be $< 10^{-12}$. Remembering that the CH_2 and CH^- background due to hydrocarbon contamination can be quantitatively removed ($< 10^{-10}$) by passing over CuO (3), we conclude that the projected background at m/z 14 due to $^{13}CH^-$ (plus $^{12}CD^-$) and $^{12}CH_2$ is $< 10^{-10}$, as required by our rather ambitious design parameters. The requirement of abundance sensitivity of $< 10^{-7}$ is readily achievable between m/z 13 and 14 with a magnetic sector (1).

We have thus proven the feasibility of the mass spectrometric assay of ^{14}C at sensitivities which exceed routine scintillation counting by over 4 orders of magnitude. We are now designing a gas chromatographic preseparator followed by a CuO combustion furnace and a chemical water removal system (3) (7) to allow handling of a variety of ^{14}C labelled compounds.

Acknowledgement. This research has been sponsored by a grant from NIGMS NIH number 15768.

References:

1. R. Schnitzer, W.A. Aberth, H.L. Brown and M. Anbar, Proc. 22nd Annual Conference American Society Mass Spec. Allied Topics, Philadelphia, May, 1974, pp. 64-69.

2. R. Schnitzer, W.A. Aberth and M. Anbar, Proc. 23rd Annual Conference American Mass Spec. Allied Topics, Houston, May, 1975, pp. 479-481.

3. R. Schnitzer and M. Anbar, Proc. 24th Annual Conference American Society Mass. Spec. Allied Topics, San Diego, May, 1976, pp. 361-366.

4. M. Anbar, Proc. First Conference on Radiocarbon Dating with Accelerators, Rochester, April, 1978, pp. 152-156.

5. L.H. Shea et al., Radiocarbon 22, 830 (1980).

6. R.E.M. Hedges, Archaeometry 23, 3 (1981).

7. D.E.M. Matthews and J.M Hayes, Analytical Chemistry 50, 1465 (1978).

A NOVEL EI/CI ION SOURCE FOR A QUADRUPOLE MASS SPECTROMETER;

GEORGE C. STAFFORD, DONALD C. BRADFORD, and DAVID R. STEPHENS
Finnigan MAT Corp., 845 W. Maude Avenue, Sunnyvale, CA 94086

The object of this research program is to develop an improved ion source for a quadrupole mass spectrometer with optimized performance in both EI and CI operation. A main consideration is the reduction of ionizer contamination so that we can maintain high sensitivity and extend the operating period between routine cleaning. A final goal was to incorporate into the ion source design an electric discharge as an alternative to the conventional filament.

We have observed operation of an ion source under CI conditions quickly contaminates the inside of the ionization chamber (ion volume). Although this contamination does not seriously reduce performance in the CI mode, ionizer sensitivity in the EI mode is drastically reduced by ion chamber contamination. Therefore, an ionizer designed to be operated in EI and CI should have separate ion chambers to eliminate cross contamination between these two modes of operation.

To allow for separate EI and CI ion chambers, we designed an ion source with interchangeable ion chambers which can be removed through the solid probe vacuum lock. This exchange is accomplished with a special probe and without loss of the manifold vacuum. Both the EI and CI ion chambers were designed to give optimum performance in their respective mode of operation. The EI chamber has a relatively large electron entrance aperture to allow a high electron current inside the ion volume in order to increase ionizer sensitivity. Also the EI ion exit aperture is very open so that ions can be efficiently extracted by the lens system and injected into the quadrupole filter (see the EI configuration diagram).

On the other hand, both the electron entrance and the ion exit aperture are much smaller in the CI ion chamber. These smaller apertures reduce the conductance of the ion chamber and allow for the high reagent gas pressure ($\sim$1 torr) necessary for CI operation (see the CI configuration diagram).

The new ionizer design also incorporates a low current electric discharge as an alternative to the conventional filament. The cup electrode opposite the filament (see diagrams) functions as a conventional electron beam trap under normal EI operation, however, this cup electrode is also used as the discharge cathode under CI conditions. Under CI pressures of approximately 1 torr, a potential of 1 to 2 KV will produce a low current (100 uA) stable gaseous discharge inside the hollow cathode electrode. The discharge will inject energetic electrons into the ion chamber causing ionization of reagent gas and sample molecules. Ion source sensitivity with the electric discharge is comparable to CI operation with the filament. The electric discharge will be most useful when corrosive or oxidizing CI reagent gases are used that would normally adversely effect filament longevity.

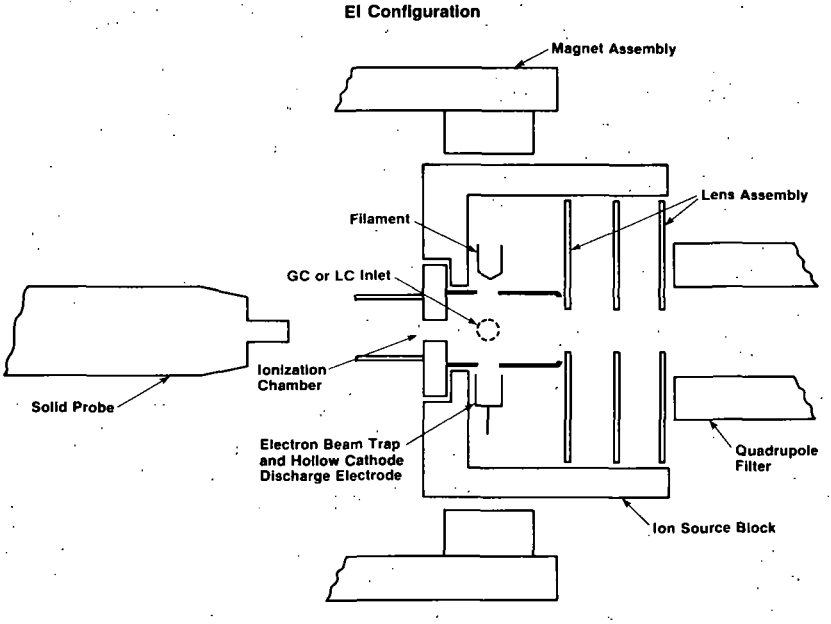
EI Configuration
Magnet Assembly
Lens Assembly
Filament
GC or LC Inlet
Ionization Chamber
Solid Probe
Electron Beam Trap and Hollow Cathode Discharge Electrode
Quadrupole Filter
Ion Source Block

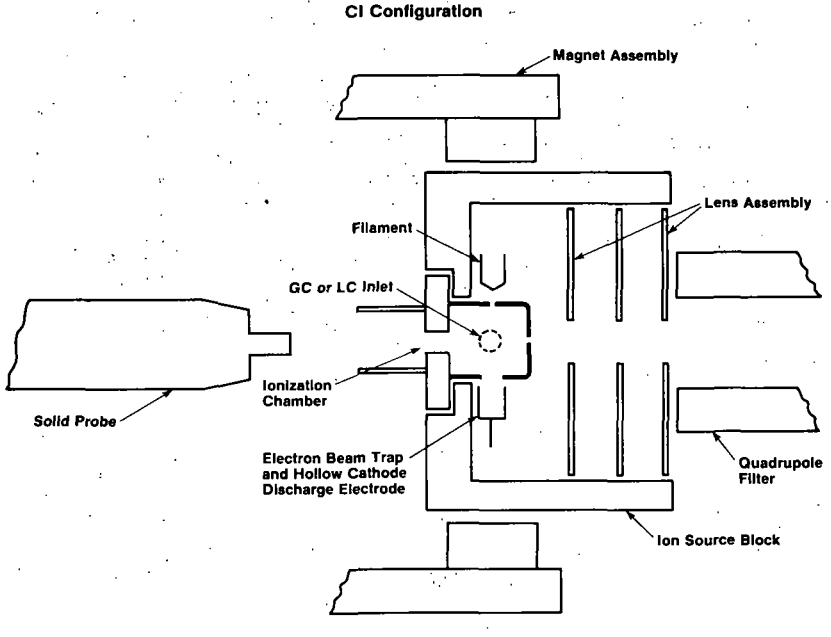
CI Configuration
Magnet Assembly
Lens Assembly
Filament
GC or LC Inlet
Ionization Chamber
Solid Probe
Electron Beam Trap and Hollow Cathode Discharge Electrode
Quadrupole Filter
Ion Source Block

DESIGN AND DEVELOPMENT OF A NEW LC-MS USING SIMS AND COLLISION INDUCED DISSOCIATION

Richard D. Smith
Physical Sciences Department
Pacific Northwest Laboratory
Richland, Washington 99352

At the ASMS meeting last year we reported the initial results obtained using a new LC-MS interface. The LC-MS designed in this work utilizes a moving ribbon interface for evaporation of the mobile phase (from a Spectra Physics 8700 HPLC), sample storage, and transfer to the analysis section. In the SIMS mode the solid residue is bombarded with high energy ions and emitted secondary ions are energy selected and analyzed using a quadrupole mass spectrometer. Alternatively, the ribbon is heated rapidly and desorbed species are ionized using electron impact. Figure 1 gives and overall schematic illustration of the apparatus.

In the development of a new LC-MS instrument using secondary ion emission, we have attempted to maximize both sensitivity and selectivity. The thermal desorption/electron impact mode of operation was included to allow conventional mass spectrometric analysis for comparison with the SIMS mode without degrading its performance. The instrument includes a triple quadrupole analyzer to allow the application of collision induced dissociation (CID) techniques for enhanced selectivity. Novel features of this instrument include aerosol deposition of the LC mobile phase for more efficient evaporation[1], ribbon storage[2] and clean-up techniques[3]. Figure 2 demonstrates the application of ribbon storage techniques to a complex fuel sample showing the reconstructed ion chromatograms for ribbon passages at three different temperatures. Figure 3 gives results of a calibration experiment obtained in the SIMS mode of operation demonstrating detection limits in the 10 pg. range for arginine while scanning.

Our experience with LC-MS using electron impact and SIMS ionization methods in conjunction with ribbon storage capabilities indicates significant promise. The major findings on the basis of these studies may be summarized as follows:

1. Ribbon storage techniques offer extended analytical capabilities for both TD/EI and SIMS methods. In the TD/EI mode the separated chromatographic material may be examined repeatedly at increasing temperatures while in the SIMS mode only minor sample amounts are consumed in each subsequent analysis under the relatively high primary ion currents. In the TD/EI mode the ribbon storage technique allows several advantages over the conventional approach including the selectivity from multiple passes at increasing temperatures, the potential of decoupling the moving ribbon speed for LC deposition from the speed through the flash heater, and removal of the requirement to optimize the flash heater temperature for each compound of interest.

2. The SIMS ionization mode offers an effective and sensitive method for the detection and identification of many, particularly thermally labile, highly polar compounds. Initial results indicate that quantitation is possible by adjustment of ribbon speed, or sample flow to the ribbon, to limit material to less than a monolayer on the ribbon surface. At higher concentrations response becomes nearly independent of concentration while very thick layers may act as an insulator and cause a suppression of ionization. The suppression might be avoided by use of fast atom bombardment.

3. Ribbon cleaning using silver vapor deposition offers an effective mechanism for reduction of background due to impurities, ribbon contamination, and residual material from previous analyses. The combination of TD/EI and SIMS may prove to be a particularly effective combination, particularly in conjunction with ribbon storage techniques. In such a dual source, for example, the first ribbon pass can be in the SIMS mode which results in only minor sample consumption while subsequent ribbon passes could use the TD/EI mode. The combined approach offers the possibility of a greatly enhanced ability for identification of complex samples while reducing to a minimum compounds which might not be responsive to one of the methods.

References:

1. R. D. Smith and A. L. Johnson, Anal. Chem., 53, 739 (1981).

2. R. D. Smith and A. L. Johnson, Anal. Chem., in press.

3. R. D. Smith, J. E. Burger, and A. L. Johnson, Anal. Chem., to be published.

Prepared for the U.S. Department of Energy under Contract DE-AC06-76RLO 1830.

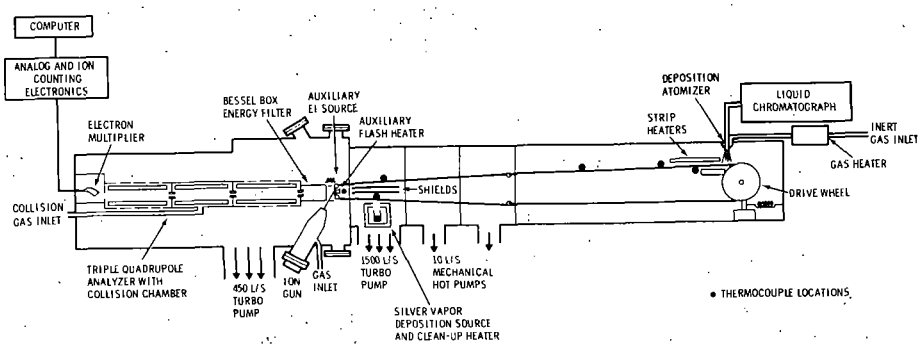

FIGURE 1. Schematic illustration of the LC-MS using electron impact and SIMS ionization. Not illustrated is the water-cooled copper shield for the upper ribbon path to the analysis region to prevent heating in the "clean-up" region.

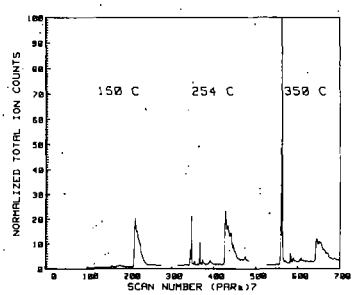

FIGURE 2. Normalized total ion counts as a function of scan number for a LC-MS analysis of methanol soluble fraction from a Sephadex LH-20 column separation of a retorted shale oil. The reconstructed ion chromatograms were obtained in the TD/EI mode and represent three passes of the separated material from a single injection through the analysis region at the indicated temperatures.

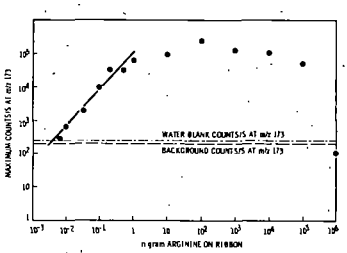

FIGURE 3. Mass spectrometric response at m/z 173 for samples spanning eight orders of magnitude in concentration (10 pg to 1 mg). Samples were placed in uniform spots on the ribbon and the maximum count rate plotted versus sample size. Also indicated are the background count rates for a clean ribbon and a water "blank."

THE DESIGN OF A TOTALLY-COMPUTER-AUTOMATED ECLECTIC TRIPLE QUADRUPOLE MS/MS*

Carla M. Wong, Richard W. Crawford, Victor C. Barton
James E. Bowman and Hal R. Brand

Lawrence Livermore National Laboratory
P.O. Box 808, L-310
Livermore, California 94550

The triple quadrupole mass spectrometer as an unique analytical instrument has been previously described by Yost and Enke. At Lawrence Livermore National Laboratory, a need for this instrument has been clearly noted due to the variety and complexity of sample types and the urgency with which some analyses are needed. Additionally, much of our data have to be transportable to the large systems computers such as the CDC7600 or the CRAY for modeling studies.

Given these constraints, we decided to build a completely automated system using two LSI-11/23 computers, one to control data manipulation and storage and the other one to handle data acquisition and control of all of the mass spectrometer hardware.

All ionization voltages, source elements, axial energy and interquad lenses are designed to be under computer control. This enables us to perform such functions as automatic tuning procedures, switching the source from EI to CI or from positive to negative ions.

The quads are set up to scan rapidly, with one or both under "firmware" or "software" scan control. The resolution, DC on/off, CID chamber pressure and gas type are computer controlled.

The detector high voltage and positive/negative ion current measurements are under computer control.

The system is differentially pumped by three turbo molecular pumps and will have a direct inlet solid probe, gas chromatograph, and gas and pyroprobe inlets.

*Work performed under the auspices of the U.S. Department of Energy by the Lawrence Livermore National Laboratory under contract number W-7405-ENG-48.

ION DYNAMICS OF AN RF-ONLY MASS FILTER

Donald M. Mintz, Charles A. Boitnott, and Urs Steiner

FINNIGAN-MAT
845 W. Maude Ave.
Sunnyvale, CA 94086

The performance of a quadrupole mass filter operated in the RF-only mode has been modeled by two independent methods. The first is a multi-particle trajectory outcome survey. The second method employed a phase space approach, whereby transmission was taken to be the acceptance of an RF-only mass filter, averaged over initial RF phase. The goal was to characterize the dependence of transmission, path length, and transverse kinetic energy on operating parameters of the RF-only mass filter.

By the first method, ions are injected into a mass filter from a parallel beam source with established axial energy. The initial transverse velocity was taken to be zero in all cases. It was assumed that the beam source filled an entrance aperture uniformly in regard to position and initial RF phase. Path length through the filter could be calculated along the trajectories by summing contributions from each integration step (1/600th of an RF cycle). Average transverse kinetic energy was noted by calculating values at each integration step, summing, and, finally, averaging over both the number of steps and over all of the trajectories surveyed (approximately 100). The exit aperture was taken to have a radius of r_o, that of the circle inscribed in the quadrupole rods.

By the phase space method, on the other hand, the range of initial velocities could be that which would be limited by the exit aperture (in this case, 0.127 cm radius). High RF voltages and high particle masses may permit ions having enormous amounts of transverse kinetic energy (exceeding 100 eV) to enter and be transmitted. Experimentally, the initial transverse kinetic energy, especially for particles which have passed through lens apertures before entering the RF-only mass filter, should not exceed a few eV.

The two methods thus differ in their selected range of initial transverse velocities. The actual emittance of the first mass filter of a triple quadrupole instrument, as transformed by exit lenses, has not been characterized. As a result, it was felt that the two methods outlined above would serve as useful limits to the actual device performance. The calculations were performed using parameters of a commercial mass filter having r_o = 0.275 cm, a length of 14 cm, and operated at 1.492 MHz RF frequency.

The dependence of ion transmission and transverse kinetic energy on RF voltage for the multi-particle calculation are displayed in figures 1 and 2, respectively. The quantity labelled m_{CUT}/m is a measure of peak to peak RF voltage V, where m_{CUT} is the minimum mass transmitted at a given RF voltage. That is, at cutoff,

$$q = 0.908 = \frac{2eV}{m_{CUT}\omega^2 r_o^2}$$

where $\omega = 2\pi f$ furnishes the RF frequency. The prediction of the phase space method for the dependence of ion transmission on RF voltage is shown here in figure 3 for m = 40.

The two methods differ somewhat in their dependence of transmission on RF voltage. In the low RF voltage range, the principle limitation (phase space) comes from an inability to contain ions having even thermal off-axis velocity components. This is an ignored issue in the multi-particle calculation, so that the phase space method is probably accurate. Similarly, oscillations of transmission with RF voltage, which arise in the phase space calculation from the presence of an exit aperture, are expected to be realistic.

In the high RF voltage regime, near cutoff, a substantial amount of energy is pumped into transverse ion motion. As seen in figure 2, the quantity $E_\perp$ for m = 400 AMU is roughly 10 times that for m = 40 AMU. That is, ions injected into a $\perp$ mass filter of a given value of m_{CUT}/m with no initial transverse velocity assume roughly the same average value of transverse velocity over the course of 20-120 cycles in the filter. At the same time, the multi-particle calculation predicts that a smaller range of starting positions may be transmitted as m_{CUT}/m approaches 1. That the transmission goes to zero as $m_{CUT}/m \to 1$ makes sense, since trajectories for $m < m_{CUT}$ lie outside the region of stability for a mass filter. This result is more reasonable than that of the phase space calculation, where the transmission oscillates about a continuous rise as $m \to m_{CUT}$. This is probably an artifact of permitting the initial transverse energy to assume any arbitrary large value. The plateau in the lower trace of figure 3 demonstrates the effect of even a fairly large upper limit (1 eV) to the initial transverse kinetic energy.

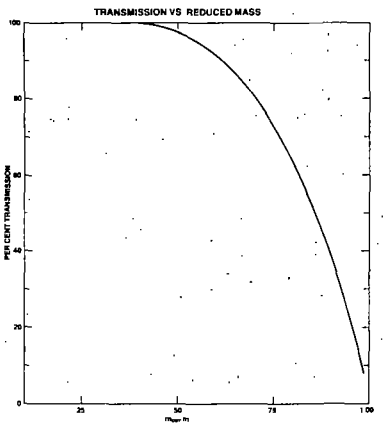

Figure 1

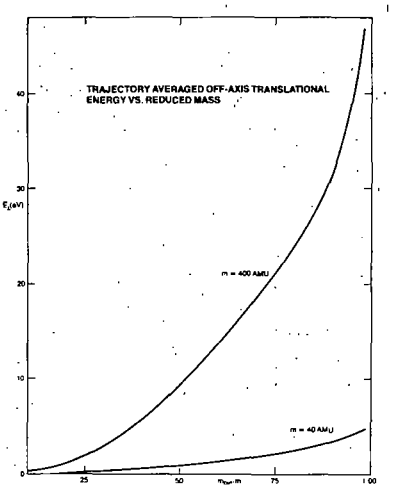

Figure 2

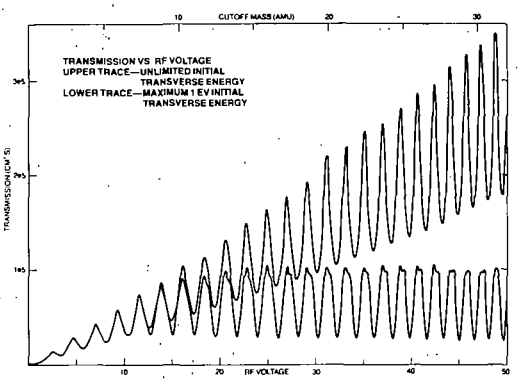

Figure 3

An Improved Time of Flight Mass Spectrometer

By A. Kornel, E. Younginger and R. A. Day, University of Cincinnati, Chemistry Department, Cincinnati, Ohio 45221

The Time of Flight Mass Spectrometer (TOFMS) in our laboratories (Bendix Model 12-101) had been modified to give a resolution of 500-700 (M/ΔM) and a sensitivity of 0.37 X 10^{-4} S tor^{-1} l^{-1} (Ref. 1). This resolution and sensitivity are suitable for modification to a capillary GCMS system, however, the original analog scanner and electrometer circuits could not withstand the faster scanning rates required by the use of capillary GC columns. Therefore, it was decided to improve upon these circuits and to further improve the ion source geometry (for sensitivity) such that the TOFMS could be interfaced with a capillary GC.

The ocilliscope had been generally used as the TOFMS output device. Since this output is acquired at the rate of 10,000 spectra per second, it does not lend itself to direct interface with a data system. The analog scanner must be used to interface to a data system. Since the original scanner and electrometer circuits were of vacuum tube design, they were not suitable for the following reasons: (1) loss of resolution, (2) loss of sensitivity, and (3) an increase in background noise (all compared to the ocilliscope output). Also, the scanner output being proportional to the square root of the mass ($t = \sqrt{KM}$) presented a problem in interfacing to the available VG2000 Data System. This was due to software only being available for either linearly or exponentially acquired scans.

The new electrometer and scanner circuits were designed using state of the art integrated circuitry. The electrometer (Analog Devices AD 515KH) was redesigned to minimize all capacitances (i.e. time constants), was built on a P.C. board small enough to fit into the original analog electrometer (thus totally shielded) range switch, and this unit was mounted on an aluminum plate bolted directly to the detector header (thereby keeping all lines to a minium). This arrangement proved very satisfactory for sensitivity, speed, and reduction of noise. The solid state analog scanner was built into the original scanner console (a new console is being designed) and consists basically of a dual integrator. This arrangement presents the mass output linearly with respect to time ($t = KM$). The scan rate over the range of 500 to 17 AMU is 4 seconds.

After completing and testing the efficiency of the electronic changes, the ion source was further modified. The modifications consisted of enlarging the first ion grid to 0.5 inches for increased ion throughput and, thus, increased sensitivity and enlarging the electron beam exit from 1/16 inch to 1/8 inch, thus improving the trap current. Further, the ion source inlet tube was modified such that a gas inlet system and a capillary GC interface could be used, either simultaneously or separately.

The resulting TOFMS is suitable for interfacing to a capillary GC system. It can be scanned rapidly (4 sec., 500-17 AMU), has a linear mass output ($t = KM$) and has exceptionally high sensitivity. This makes the TOFMS an instrument relatively simple to operate and adequate for organic capillary GCMS analysis.

Ref. 1. J. Lehman, E. Younginger, Inter. J. Mass Spectrum and Ion Physics, 33, (1980) 95-98.

THE DEVELOPMENT OF A NEW HIGH PERFORMANCE MAGNET FOR THE KRATOS MS80

S. Evans, L.C.E. Taylor, D.R. Denne, H.J.M. Fitches, C.J. Wakefield,
K.R. Compson, Kratos Limited, Barton Dock Road, Urmston, Manchester, England

Most commercial mass spectrometers are based upon the ion optical equations developed by Hintenberger and Konig. These equations, however, make a number of assumptions which restrict their value for modern mass spectrometer design. Thus:

1. Fringing fields are ignored and all magnetic fields are assumed to be homogeneous.
2. All aberration terms higher than second order are assumed to be small and are therefore ignored.
3. The theory is confined to the radial plane and Z-direction defocussing effects are not considered.

The computer program TRIO(1) enables third order terms and non ideal fringe fields to be considered. These methods have been extended by us to include the use of hexapole lenses, which in advanced mass spectrometer designs contribute significantly to maximising sensitivity at high resolving power.

Applying these computer treatments to existing mass spectrometer designs reveals that many geometries, including the so called zero-alpha-beta instruments, have finite second order aberrations and third order terms which in some cases are large and virtually uncorrectable.

More complex magnet designs are now possible. The relative sizes of electrostatic and magnetic analysers and their associated field free regions are now seen to be less rigidly defined. For example, a dramatic reduction in size of the ion optical system for a given performance is now possible. Furthermore, careful optimization of the construction of the magnet can also radically improve its scanning capabilities. A magnet incorporating all these benefits has been fitted to a Kratos MS80 mass spectrometer.

Fomblin and P.F.K, materials frequently used as reference compounds in mass spectrometry, are used here to demonstrate the major advantages of the new magnet design. All the data presented here has been acquired via a Kratos DS55 data system.

Figure 1 illustrates the mass range now available at full ion accelerating potential, formerly 1000 amu, this has now been more than doubled. The spectrum was obtained using Fomblin.

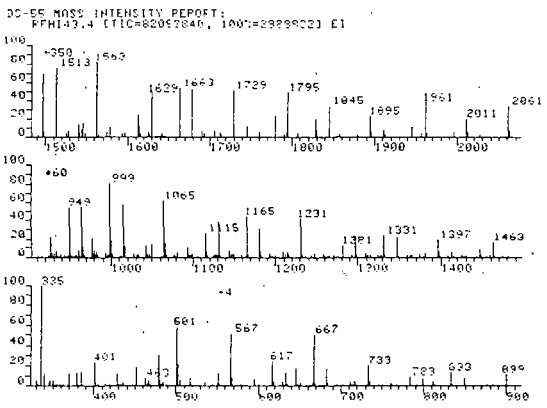

Figure 1

The exceptional scanning capability is demonstrated in figure 2 which depicts the interscan reports for successive scans of the spectrum of PFK. The scans, covering more than a decade in mass, were obtained at a 1000 resolving power, 0.1 second per decade scan rate and a reset time of less than 0.2 of a second. The successive times recorded in the fifth column confirm the overall cycle time of better than 0.3 seconds.

MINI-DLIST INTERSCAN REPORT, RUN: RFM7

SCAN NO	#PKS	TIC	BASE INTEN	RETN TIME	#NSE
1	367	2813696	971456	0:00	74
2	374	2898112	989776	0:00	73
3	380	2901504	981776	0:00	86
4	384	2910080	991952	0:01	61
5	384	2922176	996112	0:01	100
6	394	2992448	1037328	0:01	71
7	384	2906240	1006240	0:02	63
8	383	2925568	1029856	0:02	69
9	403	2938192	1016656	0:02	71
10	417	2902688	971552	0:03	82
11	377	2862976	1010224	0:03	85
12	391	2965064	1033696	0:03	83
13	386	2915584	1029168	0:03	92
14	400	2895232	1033984	0:04	90
15	398	2910720	1015344	0:04	80
16	397	2918912	1030784	0:04	82
17	399	2853312	990896	0:05	80

P

Figure 2

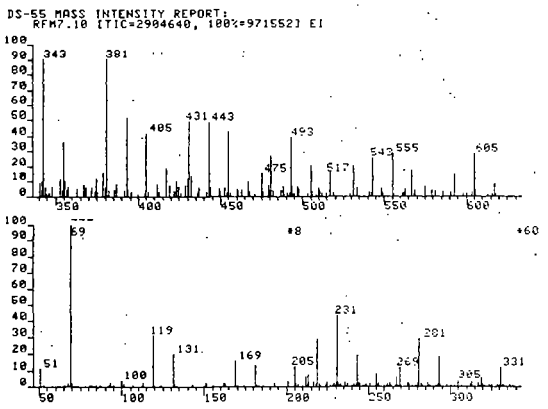

Figure 3

The consistency of the spectrum obtained under these scanning conditions is illustrated in figures 3 and 4 which show plots of the spectrum recorded during consecutive scans of the magnet

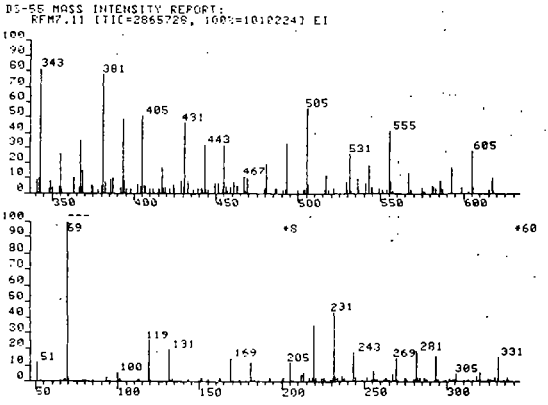

Figure 4

(1) Matsuo T; Matsuda H; Fujita Y; Wollnik H. Mass Spectroscopy (Japan)Vol 24 No 1 Mar '76 pp 19-61

STABLE CHANNEL ELECTRON MULTIPLIERS

P. Henkel and J. Gray; Galileo Electro-Optics Corporation, Sturbridge, MA 01518

Significantly smaller gain degradation has been observed with a new Channeltron® detector incorporating a preamplified Spiraltron configuration and specially engineered materials.

The glass surface of Channeltron electron multipliers widely used in mass spectrometers are inherently stable in air; however, changes in gain during operation occur due to the electron cascade within them in combination with environmental factors. Normally, the greatest change occurs during the initial period of use when layers of gases adsorbed on the surface are being removed. Large degradation in Channeltron gain may be induced after this period of desorption by exposure to organic substances or operation at pressures greater than 10^{-6} torr - conditions prevalent in organic mass spectrometry.

It was hypothesized that both the desorption period and the magnitude of post-desorption gain degradation may be dependent upon multiplier material and/or configuration. Experiments were conducted in a cryogenically roughed, ion pumped, stainless steel and glass bell jar. Standard 4700 Series Channeltrons were used as a control. All detectors were operated simultaneously under identical conditions at 3000V and an output count rate of 50,000 cts/sec. Although these conditions are not representative of environments encountered in organic mass spectrometry, in our opinion the relative test results (indicated below) are valid.

The improved stability of the new Channeltron is particularly evident after the period of desorption as shown in the table. The period of desorption was substantially the same as had previously been observed for Series 4700 detectors. The rapid degradation of the standard detectors observed in our experiments is not a common phenomenon in the field and is, we believe, indicative of some form of harsh environment in our test chamber (quite possibly the proximity of hot filaments used to excite the detectors). The new Channeltrons were not similarly affected.

The new detectors have been designated 5000 Series Channeltrons®. Future work will include evaluation under actual organic mass spectrometry conditions through cooperative efforts with manufacturers and individual users of mass spectrometers.

COMPARATIVE GAIN OF NEW AND STANDARD CHANNELTRONS® AFTER DESORPTION

AS A PERCENT OF ORIGINAL GAIN

Detector	Gain After $1x10^9$ Counts / Original Gain	Gain After $2x10^{10}$ Counts / Original Gain
New Channeltron #1	60%	65%
New Channeltron #2	45%	45%
New Channeltron #3	62%	66%
Standard 4700 #1	10%	*Not measured
Standard 4700 #2	22%	*Not measured
Standard 4700 #3	13%	*Not measured
Standard 4700 #4	44%	4%
Standard 4700 #5	35%	5%
Standard 4700 #6	60%	13%

*Due to the common high voltage configuration used in this test, we were unable to adjust for the increasing difference in gain between the new Channeltrons and the standard Channeltrons. The pulse amplitude range capability of our counting electronics was exceeded and testing of the standard Channeltrons was terminated at 10^9 counts with their gain $\sim 6x10^5$.

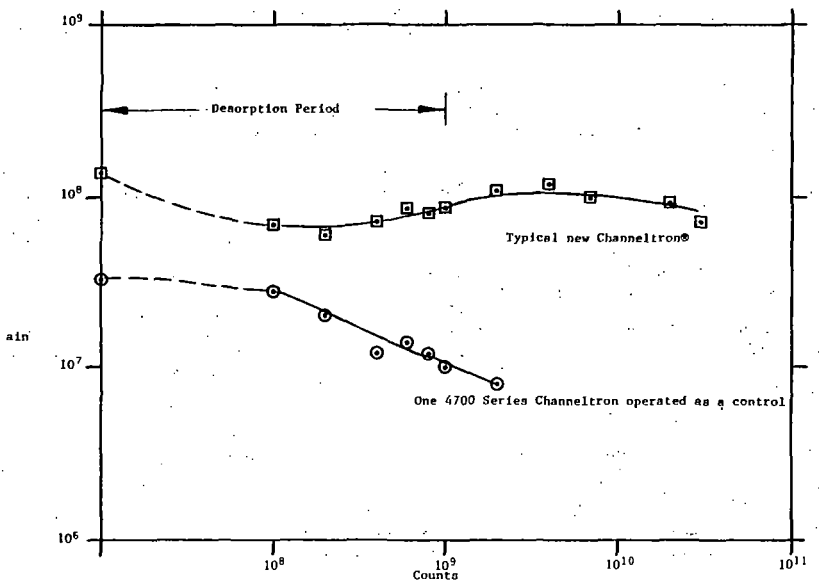

Channeltron Gain vs. Accumulated Output Counts

ADVANCES IN ISOTOPE RATIO MEASUREMENTS IN GEOCHEMISTRY; S. S. GOLDICH, Branch of Isotope Geology, U.S. Geological Survey, Federal Center, Denver, CO. 80225

Advances in isotope ratio measurements are very evident in many areas of geochemistry within recent years. The ^{147}Sm-^{143}Nd decay system is now firmly established as a useful tool in geochronology, and, similarly, the ^{176}Lu-^{176}Hf system shows great promise. U-Pb and Th-Pb ratio measurements have been extended to very small samples, and precise measurements have advanced not only age determinations but also understanding of geologic processes and of geologic history. Precise measurements of the isotopes of Sr, Pb, Nd, and, now, Hf provide a principal mode of attack on the fundamental but difficult problems of crustal and mantle evolution. Improvements in isotope ratio measurements stem from three major sources: (1) improvements in mass spectrometers and related instrumentation, (2) refinements in chemical preparation procedures, and (3) progress in the use of data acquisition systems. Advances in measuring of light-stable isotope ratios have greatly increased the volume and quality of the data with applications becoming increasingly important in volcanology, climate research, underground water derivation and movements, geothermal development, ore genesis, and rock alteration. As the volume of analytical data obtained by instrumental methods in geochemistry increases there is a constant and pressing need for maintaining standards of precision and accuracy. Isotope-dilution mass-spectrometric determinations of minor and trace elements best fill this need for reliable standard reference materials.

THE COMPOSITION OF PLANETARY ATMOSPHERES;
M.B. McELROY; Center for Earth and Planetary Physics, Harvard University, Cambridge, MA 02138

The elemental and isotopic composition of the Martian atmosphere was studied with mass spectrometers carried on the U.S. spacecraft Viking. Similar data are available for Venus from experiments on the U.S. Pioneer and Soviet Venera probles. In combination with more extensive information for the Earth and meteorites, these data provide invaluable clues to the nature of the origin and early evolutionary history of the planets. Present understanding of these issues is reviewed. It is argued that condensation in the early solar nebula may have proceeded more rapidly at the orbit of Mars, less rapidly at Venus. The pre-Venus material may have acquired significant concentrations of noble gases from the early solar wind while pre-Mars material may have differentiated losing volatiles during the first 10^7 years. Biological transformations influenced the composition of the terrestrial atmosphere from an early time and are presently dominant for important gases as N_2, O_2, CO_2 and CH_4.

A FRACTIONATION MODEL FOR THERMAL IONISATION

by K. Habfast, Finnigan MAT GmbH, Bremen (F.R.G.)

Due to fractionation, the observed isotope ratio from a multiple filament thermal ionisation source normally is not the "true" isotope ratio of the sample. The true ratio has to be calculated from the measured data by application of (1) standard samples or internal standards of known isotopic composition and (2) a theoretical model which predicts, how fractionation depends on the different experimental parameters.

The model presented here is based on a proposal of Kanno and assumes (a): Langmuir type evaporation and complete mixing of the (solid) sample at any time, (b): partial decomposition of the sample into two chemically different isotopic species during evaporation and (c): different ion yields for the different evaporating species.

By application of some meaningful approximations to the exact mathematical solution of the generalized Ralleigh distillation equation, which is appropriate for the problem, one can deduce an explicit expression for the observed isotope ratio r_{obs} of a sample, having the "true" ratio R_o:

$$\frac{r_{obs}}{R_o} = \frac{\alpha + k \cdot j \cdot \beta}{1 + k \cdot j}\left[1 + \left(1 - \frac{1 + k}{\alpha + k \cdot \beta}\right) \ln q\right] \qquad (1)$$

The two species have the evaporation rates dA/dt resp. dB/dt and the resp. ion yields Ya and Yb. Moreover, we define:

α, β = SQR (heavy/light mass) of the two species

q = relative amount of undecomposed sample on the filament

k = dB/dA ; j = Yb/Ya

By integration of the ion current/time profile i (t), the time dependence of r_{obs} can be calculated, because

$$q(t) = 1 - \frac{M_o}{F \cdot Q_o} \cdot \frac{1 + k}{Y_a + k Y_b} \int_0^t i(t) \cdot dt \qquad (2)$$

where M_o : Molecular weight of the sample; F = 96522 A · s/mol

Q_o : loaded sample weight in grams.

Some important consequences are as follows:

(1) $$\int_0^1 r_{obs}\,dq = \left(\frac{1+k}{1+j\cdot k}\right)\left(\frac{\alpha+k\,j\,\beta}{\alpha+k\,\beta}\right)\cdot R_o\,; \quad \left(= R_o \text{ if } Y_a = Y_b\right)$$

(2) $r_{obs} = R_o$ for $q = e^{-1} \approx 0{,}37$, only if Ya = Yb

(3) for an <u>exponentially decaying</u> ion current $i = i_o \cdot \exp(-\mu \cdot t)$ (i.e. for a constant evaporation temperature) and under the assumption that only one species evaporates (k = 0):

a) the fractionation pattern is linear with time:

$$\frac{r_{obs}}{R_o} = \alpha - \frac{(\alpha-1)\cdot M_o}{F}\cdot\frac{i_o\cdot t}{Y_a\cdot Q_o} \qquad (3)$$

b) the fractionation per mass difference ΔM is given by

$$\frac{r_{obs}}{R_o} \approx 1 + \frac{\Delta M}{2M}\left(1 - \frac{M_o}{F}\cdot\frac{i_o\cdot t}{Y_a\cdot Q_o}\right) \qquad (4)$$

c) the measuring error between two identical samples which are measured with different sample weight (ΔQ), ion currents (Δi), ion yields (Δy) and at different measuring times (Δt) is

$$\frac{\Delta r_{obs}}{r_{obs}} \approx \frac{\Delta M\cdot M_o\cdot t\cdot i_o}{2\,M\cdot Y_a\cdot Q}\sqrt{\left(\frac{\Delta t}{t}\right)^2+\left(\frac{\Delta i_o}{i_o}\right)^2+\left(\frac{\Delta Y_a}{Y_a}\right)^2+\left(\frac{\Delta Q}{Q}\right)^2}$$

(4) the slope of the fractionation curve may be positive, negative or even zero, depending on an eventual change of k and/or j with time during evaporation.

If, for a multi isotope system, equation (1) is applied twice for two ratios r_{obs1} resp. r_{obs2}, q can be eliminated and a general equation for the <u>normalization to an internal standard</u> ratio (R_{o2}) is obtained:

$$\frac{r_{obs1}}{R_{o1}} = (1-\varphi) + \varphi\,\frac{r_{obs2}}{R_{o2}} \qquad (5)$$

$$\varphi = \frac{(\alpha_1+k\,j\,\beta_1)(\alpha_2+k\beta_2)(\alpha_1+k\,\beta_1-1-k)}{(\alpha_2+k\,j\,\beta_2)(\alpha_1+k\beta_1)(\alpha_2+k\,\beta_2-1-k)}$$

The maximum normalization error (if the chemical form which evaporates is not known) is thus given by

$$F_m = \left(\frac{\Delta R_{o1}}{R_{o1}}\right) \approx \frac{(R_\alpha - R_\beta) \cdot \Delta M_1}{2(M_{L1} + N) - R_\alpha \cdot \Delta M_1} \; ; \quad R_\alpha = \frac{M_{L2}}{M_{L1}} \; ; \; R_\beta = \frac{M_{L2} + N}{M_{L1} + N}$$

M_{L1}, M_{L2} : Lower masses of the ratios

N : excess mass of the heavier chemical species

We get $F_m = 0$, if the lower masses of both ratios are equal.

If a sample (R_{o1}) and a standard (R_{o2}) of a two isotope system are measured, assuming k = 0 and identical sample weights, but different ion current/time profiles i(t), then their measured and true ratios are related as follows for an external normalization:

$$\frac{r_{obs1}(t)}{R_{o1}} = \alpha + (\alpha - 1) \ln \left[1 - \left(1 - e^{F_2}\right) \frac{\int_0^t i_1(t) \cdot dt}{\int_0^t i_2(t) \cdot dt} \right] \qquad (6)$$

and

$$F_2 = \frac{\frac{r_{obs2}(t)}{R_{o2}} - \alpha}{\alpha - 1}$$

This equation reduces to the well-known:

$$\frac{r_{obs1}(t)}{R_{o1}} = \frac{r_{obs2}(t)}{R_{o2}} \qquad (7)$$

if the ion current/time profiles of both runs are identical.

OZONE MEASUREMENT IN THE STRATOSPHERE; K. MAUERSBERGER; School of Physics and Astronomy, University of Minnesota, Minneapolis, MN 55455

A gas expansion system, combined with a mass spectrometer, has been tested and flown successfully in the stratosphere. In this arrangement, neutral gas particles are formed into a molecular beam which traverses the ion source of the mass spectrometer without wall interactions. Vertical profiles of constituents such as H_2O, CO_2, O_3 and others have been measured. Before each flight the mass spectrometer system is calibrated in the laboratory for many gases of interest, including ozone. Ozone mixing ratios determined in recent flights have accuracies of better than 5%.
The sensitivity of the mass spectrometer system is sufficiently high to also measure the heavy isotope of ozone at 50 amu. A large, unexpected variation in the 50/48 ratio has been found, always exceeding the theoretical value of 6.1×10^{-3}. During a day flight the ratio was almost three times higher than the theoretical value at 40 km. During night flights ratios of 8×10^{-3} have been measured, indicating a pronounced diurnal variation in the 50/48 ozone ratio. An enhancement of heavy ozone in the upper stratosphere has been recently predicted by Cicerone and McCrumb (1980).*

*R. J. Cicerone and J. L. McCrumb, Geophys. Res. Lett. 7, 251, 1980.

HIGH SENSITIVITY MASS SPECTROMETRY; W. R. Shields & Associates, Los Alamos National Laboratory

High sensitivity mass spectrometry should be defined, at least for the purposes of this discussion, as the measurement of a very small number of ions. The sample size's for the measurements described are all rather large and range from 10^{-6} to 10^{-10} grams; the ratios range from 1:1 to $1:10^{12}$. In every case the bottom detection limit is at the attogram level. The instruments used to make these measurements were all equipped with modified "Nier" linear thin lens sources, and collectors and measuring systems optimized at Los Alamos National Laboratory. The instruments are in no way unique but the methods used to eliminate isobaric interferences warrants the discussion.

Samples and measurements to be discussed:

U^{233}, 4-9's pure	235-238 atom ratio
Pu^{244}	239-244 atom ratio
Bi 205, 206, 207, 208, 209 etc.	
$C^{13}D_4$	

ISOTOPE RATIO MEASUREMENTS OF IRON, ZINC, AND COPPER IN BLOOD, URINE, FECES, AND SWEAT OF MEN GIVEN STABLE ISOTOPE TRACERS

Phyllis E. Johnson and Glenn I. Lykken

USDA/SEA, Human Nutrition Research Center
and
Department of Physics, University of North Dakota
Grand Forks, ND, 58202

The use of radioisotopes in research with human subjects is often ethically contraindicated, or, as in the case of copper, not practical due to the short half-lives of the radioisotopes available. As research in trace metal metabolism and nutrition has increased, so has the need for the use of stable isotopes in humans, and for methods of analyzing them.

There are various published methods for EI/MS of metal chelates which have been applied to the analysis of metal isotopes in plasma, urine, and brain tissue. We found that problems arose when other samples of biological origin, such as feces, were used, due to the different matrix. We report here an adaptation of the method of Hui and Boulton (1) for the analysis of isotopes of iron, zinc and copper as their tetraphenylporphyrin chelates with samples derived from plasma, red cells, urine, feces, and sweat of men, and from plants.

Samples of tissue and excreta were ashed in a low temperature asher, followed by treatment with 50% H_2O_2. The ash was dissolved in 12 N HCl and the iron, zinc, and copper separated as the complex anions on Dowex-1-Cl, with a step gradient of 4 M, 2.5 M, 0.5 M, and 0.005 M HCl. Samples were evaporated to dryness and derivatized with meso-tetraphenylporphyrin (TPP) in refluxing dimethylformamide. Solvent was removed by heating.

Each sample was dissolved in $CHCl_3$, and 5-25 µl of the resulting solution was placed on the direct probe of a Dupont DP-102 mass spectrometer. Analyses were done in the electron impact mode, with the source at 220° and the probe at a constant temperature of 275°. Repetitive scans of the mass region of the molecular ion were made, and ratios of ion intensities were computed after 200-500 scans. Masses scanned were m/e 664-672, 675-685, and 674-682 for Fe TPP, Zn TPP and Cu TPP, respectively.

Calibration curves were prepared using standards of 1% to 40 atom % excess of ^{54}Fe, ^{57}Fe, ^{67}Zn, ^{70}Zn, and ^{65}Cu, and the theoretical and measured isotope ratios were compared. Eight levels of enrichment were used for each isotope. Levels of enrichment were measured with about 2.5% accuracy.

This procedure is sufficiently quick and accurate for the routine measurement of enrichment factors in blood, urine, feces, and sweat from human subjects given stable isotopes as tracers. Absorption of an isotope dose can be measured by the method of fecal monitoring (2), or total dietary absorption of the metal in question can be measured after an equilibration period, using isotope dilution (3). Using isotope dilution, serial absorption measurements can be made on the same subject after only one isotope dose.

Using the former method, a man on a low copper diet was found to absorb 69% of a 2 mg dose of ^{65}Cu, while he and another subject on a diet adequate in copper absorbed 70% and 85% of the 2 mg ^{65}Cu dose, respectively.

Using the latter method, two men on a diet low in zinc were found to absorb 64% and 83% of dietary zinc before being depleted of zinc, and 75% and 100% of dietary zinc after two months of depletion.

It was possible to detect ^{54}Fe and ^{67}Zn in the sweat of these men 10 weeks after they ingested the isotopes, as shown in Table I.

Intrinsically labelled foodstuffs can be produced by injection of stable isotopes into plants grown in soil in a conventional manner. Corn, wheat, and sunflowers were labelled

Table I. Sweat of Men Given ^{54}Fe and ^{67}Zn

m/e	666/668 (^{54}Fe)	679/676 (^{67}Zn)
Unenriched standard	.064	.394
Blank	.067	.384
Volunteer 1	.121	.421
Volunteer 2	.163	.428

with ^{54}Fe, ^{67}Zn or ^{65}Cu at the pollination stage. The metal oxides were dissolved in HCl and then buffered at pH 6-7 with 0.1 M citrate-phosphate buffer before injection into the plants just below the heads or flowers. Copper enrichment was measured by both mass spectrometry and neutron activation analysis (Table II). Enrichment values vary somewhat between the two techniques because of the heterogeneity of the samples; grains were sampled as kernels rather than ground.

Table II. ^{65}Cu Enrichment in Wheat and Corn

	Cu, μg/g	atom % ^{65}Cu NAA	atom % ^{65}Cu MS
Corn	0.13	25	35
Wheat	3.30	68	79
Wheat	2.58	72	77
Wheat	2.82	74	76
Wheat	1.49	21	34

References

1. Hui, K.D., Davis, B.A., and Boulton, A.A., Neurochem. Res. 2, 495-506 (1977).
2. Janghorbani, M., and Young, V.R., Am. J. Clin. Nutr. 33, 2021-2030 (1980).
3. Weigand, E., and Kirchgessner, M., Nutr. Metab. 20, 314-320 (1976).

THE RELATIVE BIOAVAILABILITY OF CARPROFEN TABLETS DETERMINED BY THE SASIV* TECHNIQUE

W.A. Garland,[a] W.G. Crouthamel,[b] S.V. Givens,[c] I. Patel,[b] J.J. Konikoff,[d] B.J. Miwa,[a] F. Rubio,[a] T. Crews,[a] G. Woo,[a] A. Holazo,[b] and H.P. Blumenthal.[d] Departments of Biochemistry and Drug Metabolism, ([a]) Pharmacokinetics and Biopharmaceutics ([b]), Biostatistics ([c]), and Clinical Pharmacology ([d]), Hoffmann-La Roche, Inc., Nutley, N.J. 07110.

The relative bioavailability of tablets containing the new antiinflamatory agent, carprofen, was determined by co-administering to volunteers the tablet containing unlabeled drug and an aqueous solution containing an equivalent amount of ^{13}C-Carprofen. Nine volunteers were given a 50 mg tablet, 9 volunteers were given a 100 mg tablet and 9 volunteers were given a 150 mg tablet. Serial plasma samples were obtained and analyzed by GC/CIMS/SIM (1) for ^{12}C-carprofen and ^{13}C-carprofen. $^{2}H_3$-Carprofen was used as the internal standard in the assay. The procedure of Dutcher et al (2) was used to correct for isotope overlap. No difference was found between the elimination rate constants of ^{13}C-carprofen and ^{12}-C-carprofen. As expected, the aqueous solution of carprofen showed higher maximum plasma concentrations and shorter times to reach maximum plasma concentrations than the tablet. Virtually no difference was found between the areas under the plasma concentration-time curves of the solution and tablet confirming a comparable extent of absorption of carprofen given in the tablet or aqueous solution. Statistical power calculations for the AUC measurements indicated that the number of subjects required for 80% power with a 25% difference at the α=0.05 level would be 4, 7, and 3 subjects, respectively, for the groups that ingested the 50, 100, and 150 mg tablets.

*Simultaneous administration of a stable isotope variant

1. B.J. Hodshon, W.A. Garland, C.W. Perry, G.J. Bader, BMS, 6, 325, (1979)

2. J.S. Dutcher, J.M. Strong, W.K. Lee, A.J. Atkinson, Proceed. 2nd Intntl. Conf. on Stable Isotopes, U.S. Gov't Printing Office, Wash. D.C., 1976, P 186

A SIMPLE METHOD FOR THE QUANTIFICATION OF FREE FATTY ACID TURNOVER USING [16,16,16-$^{2}H_{3}$]HEXADECANOIC ACID. KOU-YI TSERNG, CAROL GILFILLAN and SATISH C. KALHAN, Division of Pediatric Metabolism, Case Western Reserve University at Cleveland Metropolitan General Hospital, Cleveland, Ohio, 44109

A safe, stable isotopic method for the measurement of free fatty acid turnover in humans has been developed using [16,16,16-$^{2}H_{3}$]hexadecanoic acid (palmitic acid) and gas-chromatography mass spectrometry. The plasma sample (50 µl) was treated with 1 ml 2,2-dimethoxypropane (DMP) and 25 µl concentrated hydrochloric acid. DMP serves as water scavenger, deproteinizing agent and as a methylating agent. Complete methylation of free fatty acids occurred in 15 minutes at room temperature. Transmethylation of esterfied fatty acids in plasma (triglycerides, phospholipids, etc) was negligible, thus eliminating the need for their pre-removal by thin-layer chromatography. A 10 meter wall coated glass capillary column (SP-2100) and splitless injection mode, were used for gas-chromatographic analysis. Electron impact at 70 eV was used for ionization of samples. The molecular ions of palmitic acid methyl ester (m/e 270) and that of the tracer (m/e 273) were monitored. The amount of palmitic acid required was only 1.5 µg and enrichment as low as 0.1% could be easily detected.

The procedure was evaluated in 3 mongrel dogs by simultaneously infusing deuterium and [1-^{14}C] labelled hexadecanoic acid, according to the prime-constant rate infusion technique. Similar turnover rates of palmitic acid were observed by both tracer techniques.

1,2,3-PROPANETRIOL,TRIACETATE ISOTOPE RATIOS

M. Wolfe; Dept. of Surgical Research,
Harvard Medical School, M.G.H.-S.B.I.
51 Blossom St., Boston, Mass.02114

The MGH-SBI Mass Spec Lab is a Consortium facility shared by the Harvard Medical School Dept. of Surgical Research and the M.I.T. Dept. of Nutritional Biochemistry. The lab is involved almost exclusively with measuring regulators of human metabolism by means of stable isotope tracers. One of several current interests is fat metabolism, and in that context it is important to be able to measure the rate of glycerol flux.

"Flux" is defined as the rate of infusion of a labelled molecule divided by the percent excess of that molecule in the physiological matrix at a later time. Glycerol flux serves as an index of lipolysis in the fat cell, since glycerol is not synthesized in the body, and glycerol released within the fat cell cannot be reincorporated into triglycerides. Fatty acids, on the other hand, can either be released into the plasma or re-esterified. Thus, the rate of glycerol flux expressed in relation to free fatty acid flux gives an index of the relative rates of lipolysis and re-esterification. We presented the method for measuring FFA flux at the 1979 ASMS Conf., in Seattle.

The method for measuring glycerol flux involves giving a large priming dose of the perdeuterated glycerol to rapidly achieve an enrichment plateau, followed by a constant infusion of the labelled molecule in tracer amounts. We then measure the dilution of the labelled molecule by the appearance of the unlabelled molecule in the plasma. We are not, in this case, tracing the metabolic pathway of the label itself, which is subject to isotope effects.

One of the several factors to be considered in the analysis of plasma glycerol is the fact that there might be as little as 50 ul of plasma to work with. This is the case for small or premature infants, small laboratory animals, or adults where larger samples may be taken, but must be split into several small aliquots for different analyses. In this amount of plasma there are about 4 nanomoles of available glycerol. The enriched portion to be measured makes up about 1% of the total, or about 40 picomoles. This is adequate for measurements both of enrichment and total amount, but it would be preferable not to split the sample further for analysis of other substances.

One such other molecule is glucose. Deuterated glucose is frequently administered simultaneously with glycerol to facilitate the measurement of glucose flux. In most cases, glucose would be the more important measurement, and therefore, the best sugar derivatives are applied to the combined glucose, glycerol plasma extract.

Of the several derivatives which can be applied, the two that nicely exemplify the isotope effect are the triacetate and tri-TMS derivatives. Both of these would be considered excellent glycerol derivatives; they are easy to make, stable, separate well on GC, have well characterized mass spectra, can be quantitated on GC-FID, give reproducible response factors, and are sensitive at the levels of enrichment being measured. However, the triacetate derivative is inferior because it yields no ion in E.I. or C.I. which is not affected by the presence of the isotopes being measured. This is not the case for the tri-TMS derivative.

In the E.I. spectrum, rearrangement ions as well as fragment ions occur at masses 103 and 145. Since the pressure dependence of the rearrangement ions is so different from that of the fragment ions, these ions cannot be used for quantitation. The other major ions, at 115 and 116, shift upward to 119 and 120, respectively, for the perdeuterated glycerol. The relative abundances in the labelled and unlabelled spectra differ. The methane C.I. spectra are primarily the result of the loss of acetic acid, and also display relative abundance differences in the labelled and unlabelled molecule.

We have defined this relative ion abundance effect as "rho". An isotope effect or an inverse isotope effect occurs if rho is less than or greater than 1, respectively. Rho is measured by the ratio of the relative ion abundances of the labelled and unlabelled fragments to the theoretical value. All ions are 'plus' 3,4, or5 - type, so there is no labelled-unlabelled ion overlap. Theoretical values are cross checked on Nuclide 3-60 isotope ratio mass spec whenever possible.

This is valuable shorthand notation in biomedical SIM measurements of low level enrichment. It is distinguished from statistical effects of labelled-unlabelled fragment overlap, and from other terms which have been used to refer to specific isotope events such as probability of breaking a primary or secondary bond with deuteration. The triacetate derivative yields some ions (esp115/119) whose rho value is greater than one, and several ions whose rho value is less than one. The tri-TMS derivative would be more suitable if it could be used because it yields several ions whose rho values are 1.

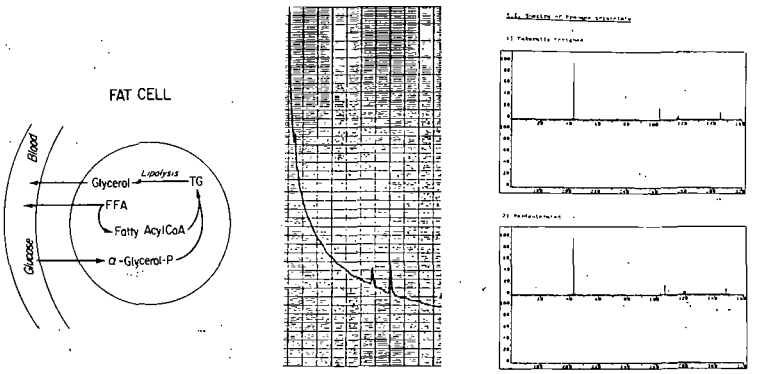

(a) (b) (c)

(a) Fat Cell showing rationale for glycerol turnover.
(b) Separation from internal standard and quantitation by GC-FID
(c) Glycerol triacetate natural and deuterated E.I. mass spectra; values for ρ must be used when different from 1.

This paper has been submitted with more detail to Biomedical Mass Spectrometry.

STATISTICAL EVALUATION OF THE NON-LINEARITY OF STANDARD CURVES IN ID-MS

J.A.A. Jonckheere and A.P. De Leenheer

Laboratoria voor Medische Biochemie en voor Klinische Analyse, De Pintelaan 135, 9000 GENT, BELGIUM

The fundamental principles of isotope dilution mass spectrometry (ID-MS) indicate that a linear relationship between isotope ratio and mole ratio exists only under particular circumstances. Departure from linearity depends on the actual values of p_j and q_i in the equation (1) :

$$R_m = \frac{\frac{x\ p_i}{y\ E} + \frac{q_i}{F}}{\frac{x\ p_j}{y\ E} \quad \frac{q_j}{F}} \qquad \text{(Eq.1)}$$

Several data handling procedures have been proposed to deal with the possible non-linearity (e.g. inverse ratio's, atom % excess, weighted linear regression) (2). Instead of artificially transforming the data to a linear model, we report the use of weighted polynomial regression with model-testing to describe the possible curvature of standard curves. In terms of matrix mathematics the minimization of weighted square deviations of any polynomial (i.e. including the linear equation) is expressed as :

$$A = \left[X^{-1}\ P\ X\right]^{-1} \quad X\ P\ Y$$

where

$$A = \begin{bmatrix} a_1 \\ a_2 \\ \vdots \\ a_n \end{bmatrix} \qquad X = \begin{bmatrix} 1 & x_1 & x_1^2 & x_1^3 & \cdots & x_1^n \\ 1 & x_2 & x_2^2 & x_2^3 & \cdots & x_2^n \\ & & \vdots & & & \\ 1 & x_n & x_n^2 & x_n^3 & & x_n^n \end{bmatrix} \qquad Y = \begin{bmatrix} y_1 \\ y_2 \\ \vdots \\ y_n \end{bmatrix} \qquad P = \begin{bmatrix} p_1 & \cdots & 0 \\ & p_2 & \\ & & \ddots \\ 0 & \cdots & p_n \end{bmatrix}$$

and y stands for the mole ratio, x for the isotope ratio, A being the coefficient matrix and P the square matrix of the weighting factors. These factors are the inverse of the variances, determined by replicate analysis of each standard mixture. The computer program calculates the different polynomials (up to a fifth degree) and the residuals around the curves are used in a F-test for significance to select the best fitting polynomial. The unknown x values are calculated by an iteration procedure.

The present method has been applied to experimental data of two published ID-MS studies (3)(4). In both cases a higher degree polynomial was selected.

The figures show the deviation from the theoretical values for both a weighted linear (●) and a weighted polynomial (o) regression. As can be seen, the F-test indicated that, although a very high correlation may be found for the linear model, the higher degree polynomial is the better choice.

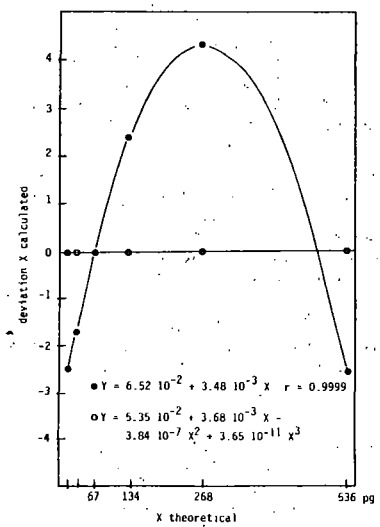

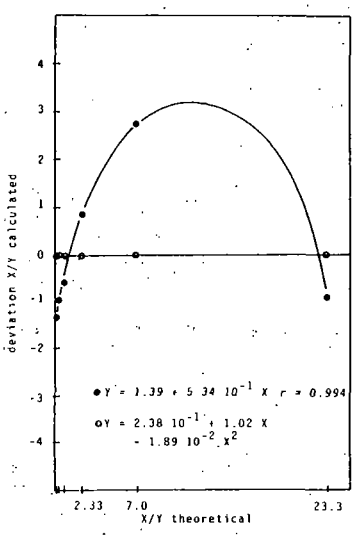

This study proves that the eventual curvature of ID-MS calibration lines can be described very accurately by means of higher degree polynomials. The ability to check different models allows one to adapt the same calculating procedure regardless of the degree of labeling (q_j value).
The applicability of this method is even wider in view of the fact that any chromatographic separation of the internal standard, due to high resolution capillary columns or polydeuterated compounds, destroys the validity of the basic ID-MS equation (Eq. 1) and subsequent calculating procedures based on this formula.

Programs are available in both Fortran IV and HPL Basic.
This work was supported by a NFSR grant to the first author.

References :

(1) Pickup, J.F. and Mc Pherson, K., *Anal. Chem.*, 48, 1885 (1976).
(2) Schoeller, D.A., *Biomed. Mass Spectrom.*, 3, 265 (1976).
(3) Jonckheere, J.A.A., Thienpont, L.M.R., De Leenheer, A.P., De Backer, P., De Backere, M. and Belpaire, F.M., *Biomed. Mass Spectrom.*, 7, 582 (1980).
(4) Colby, B.N. and Mc Caman, M.W., *Biomed. Mass Spectrom.*, 6, 225 (1979).

A PORTABLE MS DESIGNED FOR LOCAL CEREBRAL BLOOD FLOW AND BRAIN TISSUE METABOLISM STUDIES BY COMPUTER-ASSISTED TOMOGRAPHY, USING INHALED STABLE XENON AS TRACER. L.F. HERZOG, D.J. MARSHALL, AND T.J. ESKEW, Nuclide Corporation, 642 E. College Ave., State College, PA 16801

Introduction:

Combining continuous mass spectrographic analysis of a subject's breath with x-ray scans by computer-assisted tomography (CT) provides a non-invasive technique for measuring local cerebral bloodflow (LCBF).

CT reveals the distribution, in tissue, of substances which strongly absorb x-rays, such as the heavy, inert gas xenon — with a spatial resolution (for present generation CTs) of ∿ 0.5 cm. The role of the mass spectrometer is to provide continuously, during the experiment, accurate data on the concentration of Xe in the subject's blood. This can be done very conveniently by measuring the Xe concentration in breath, since it has been shown that the Xe in breath and blood are in equilibrium at the end of an expiration. Since equilibrium exists only at this "end tidal" point, the MS (or other Xe-detector) must be able to provide many — say, 10 or more — accurate Xe measurements during a single breath.

Mass spectrometric monitoring of the changing concentration of xenon in the breath of a subject during uptake and washout also provides needed information as to the optimal times at which to make x-ray scans, so that x-ray exposure can be minimized. Thus the inherent advantages of using xenon for these 3-dimensional studies in humans can be realized — i.e., that it is inert, diffusable, soluble in body fats, absorbs x-rays strongly, is only mildly anaesthetic, and can be administered by inhalation.

An important advantage of using a mass spectrometer for LCBF — Xe measurements is that the instrument can also be used for other medical MS analyses such as studying numerous other constituents of breath or blood, with each gas species' concentration being measured several times during a single breath.

Mass Spectrometer:

A Nuclide 3-60-Sectorr mass spectrometer, equipped with a fast "flowby"-type inlet is now being used for CT/MS-Xe studies by Dr. David Rottenberg and colleagues C. Ray, J. Conti and V. Dhawan at The Memorial Sloan Kettering Cancer Center. This instrument uses a permanent magnet as the ion analyzer; the species being monitored is selected by changing the ion accelerating voltage. Turbomolecular pumping was selected because tubos pump xenon as well as air gases and require no cold trap or cooling water. The inlet, analyzer and pumping system are all mounted on or in a small, mobile cart. This resides in the CT room while the electronics are in the adjoining room with the CT's controls and computer.

The high voltage supply of the MS, which is used to set mass, is controlled by a Hewlett-Packard 9825T programmable calculator via a DAC-16 D/A converter, for monitoring selected ions or scanning; the PC also accepts MS output signals digitized by an IR3A IDVM, and processes them to calculate the relative abundances of the selected species. (The IR3A's denominator provides the time base). This data is then relayed to the CT's own major (remote) data-processing computer for correlation with x-ray scan data, etc.

Sampling of the subject's breath is continuous via the "flow-by" inlet, which provides rapid response to changes in sample composition with minimal blurring. It has a microvalve at its distal end, which is attached to a mask worn by the subject. A small vacuum pump pulls gas through this sampling-valve, through a long plastic tube (at a rate of approximately 3 ml per minute), past an orifice containing a fixed-conductance gold "leak," which admits a very small portion, ∿ 0.1 ml/min, into the MS's ionization chamber. After a step-change in sample gas composition the lag until the MS records it is only a few seconds. More importantly, the response time (RC) of the inlet-plus-MS after the lag is only ∿ 100 ms for Xe (and substantially less for substantially lighter species).

All breathing mixtures are formulated to contain approximately 1% argon — it's concentration in the terrestrial atmosphere, so that the intensities of all other species can be ratioed to argon as an internal-calibration standard.

Calibrations made using 20 to 80% Xe showed that the intensity of the m/e 68 peak varied linearly with Xe concentration. (Doubly-charged xenon 136, at m/e 68, is used when the electron multiplier is used, since this doubles the ion's energy, when HV mass-selection is used, and improves precision.)

Xenon level changes in breath recorded during a typical experiment are shown in Fig 1. When Xe adminstration is commenced, Xe begins to increase — but the level rises and falls cyclically as the subject breathes; the minima are the end-tidal values. After a few minutes the average level becomes constant — saturation has taken place. Then, the xenon is replaced by air (or oxygen), and the Xe level starts to fall again, cycling as the patient breathes — but now the end-tidal values are the maxima. The shape of this "minmax" curve corresponds well with theory.

During the Xe analysis data on other breath constituents such as Ar, N_2, O_2, or CO_2, can also be obtained, by peak stepping; if (e.g.,) only CO_2 and Xe are monitored, the MS monitors each for 20 milliseconds every 40 ms.

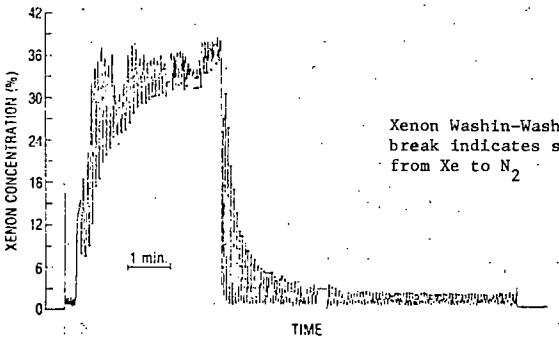

Xenon Washin-Washout Study — break indicates switchover from Xe to N_2

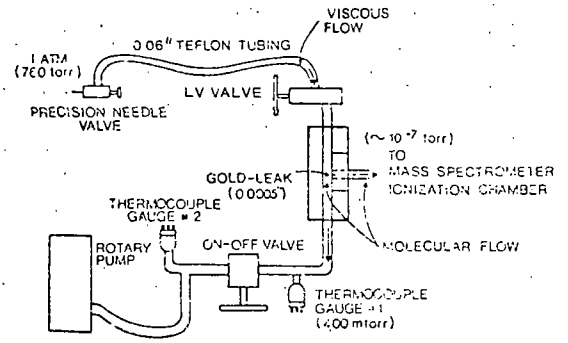

"Flowby" Inlet System

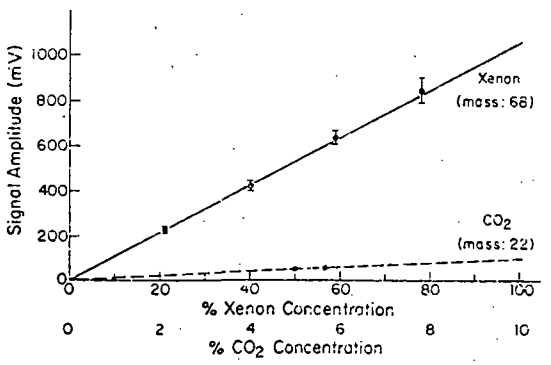

Xe and CO_2 Calibration Analyses

THE USE OF A MOBILE ATMOSPHERIC PRESSURE CHEMICAL IONIZATION MASS SPECTROMETER IN THE DETECTION OF ILLICIT DRUGS

Lyal V.S. Hood, United States Customs Service,
1301 Constitution Avenue, N.W. Washington, D.C.,
William R. Davidson and Sabatino Nacson, SCIEX INC.,
55 Glencameron Road, Thornhill, Ontario Canada L3T IP2

The illegal importation of cocaine and heroin is a serious problem in most western countries. During the past decade U.S. Customs has employed trained dogs in the examination of cargo and conveyances for concealed drug contraband, and has been keenly interested in complementary instrumental approaches to drug detection. One technique which has shown potential in detecting these drugs in a non-invasive manner is atmospheric pressure chemical ionization mass spectrometry (APCI/MS), the preliminary use of which is described in this paper.

A Sciex Inc. Mobile TAGA^{TM} 3000 API/MS system was used to characterize the volatile constituents associated with illicit drugs and was employed as a detection device in practical laboratory exercises. This instrumentation has been previously described in detail. (1) Briefly the system incorporates a corona discharge APCI source, a cryovacuum pumping system, appropriate ion optics, and a quadrupole mass filter all under computer control and fully integrated in a mobile van. Vapor sampling was performed using a direct inlet in realtime, and a wire probe coated with OV-17 for short term (up to 1 minute) concentration with subsequent thermal desorption and analysis.

Seizure samples of heroin and cocaine were analyzed by the APCI/MS technique to characterize the drug principals and the associated volatile impurities such as solvents, decomposition products, diluents and by-products. Detectibility limits were determined for these common constituents and are shown in the Table. Positive ion spectra were determined for most of the compounds with detectibility measurements made in a single ion monitoring mode for MH^+ ions; for acetic acid negative ion spectra were obtained with detectiblity limits measured for $(M-H)^-$ ions. Studies were also done of detectibility as a function of chemical background in the environment. For the volatile constituents such as acetone, acetic acid, and methyl benzoate, environmental background was extremely variable and could reduce practical detectibility limits by as much as several orders of magnitude. For the less volatile drug diluents ($m/z > 190$), background levels observed at the ions of interest (MH^+) were still significant, reducing practical detection limits for these compounds from several fold to one order of magnitude. Background levels in the mass range of heroin and cocaine, ($m/z > 300$) in most environments did not affect detectibility limits significantly.

APCI/MS DETECTIBILITY LIMITS
FOR DRUGS, DILUENTS,
DECOMPOSITION PRODUCTS,
AND SOLVENTS

Compound	m/z	Detectibility Limit (PPT)
Heroin	370	19
6-Monoacetylmorphine	328	0.9
Acetylcodeine	342	2
Cocaine	304	2
Benzoylecgonine	290	3
Ecgonine	186	7
Methyl Benzoate	137	10
Procaine	237	2
Lidocaine	235	4
Caffeine	195	0.5
Acetone	59	38
Acetic Acid	59	17

Practical laboratory exercises were conducted in which the APCI/MS was used for detection of drugs as articles of luggage containing samples passed through a baggage examination system (2), or as people carrying samples were examined using an air curtain. The volatile constituents were easily detected in realtime using these procedures as shown in Figure 1 for acetic acid. Due to sampling line losses, nonvolatile compounds such as heroin and cocaine themselves, were not detected in realtime. A probe concentrator was used for near realtime analysis (1 minute sample collection) for the nonvolatile drugs in luggage, on people, or in conveyances. The thermal desorption profile for a sample of cocaine is shown in Figure 2.

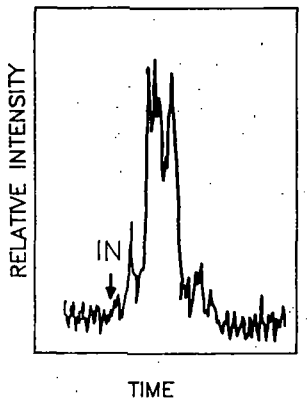

Figure 1. Realtime detection of acetic acid at m/z=59: person under air curtain holding a brief case.

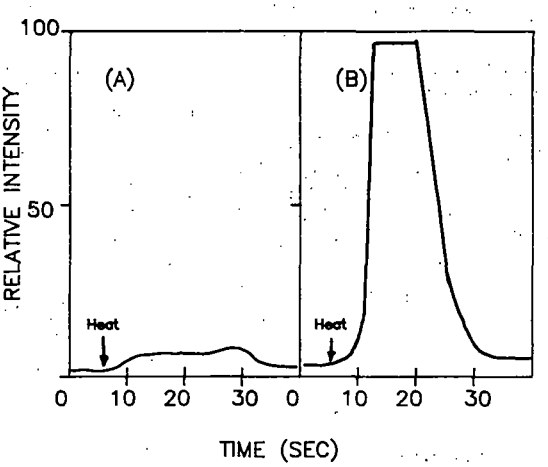

Figure 2. 1 min probe concentrator response for cocaine at m/z=304:(A) background (B) person carrying cocaine sample.

Field exercises were also conducted using the mobile system in the real-life circumstances found at a seaport and airport. The practical use of this approach for drug detection is being further studied in additional tests now in progress.

REFERENCES

1. N.M. Reid, J.A. Buckley, C.C. Poon, and J.B. French, Advances in Mass Spectrometry, Volume 8, B (1979) 1843: TAGA™ 3000: A New Multipurpose Digitally Controlled Atmospheric Pressure Chemical Ionization Mass Spectrometer Based System.

2. M. Lerner and R. Ericson, U.S. Patent 4,111,049 September 5, 1978, Apparatus for Securing Vapor Samples.

GLYCEROL TRIETHERS: SYNTHESIS, CHARACTERIZATION BY MASS SPECTROMETRY, AND USE AS NONABSORBABLE MARKERS IN INTESTINAL ABSORPTION STUDIES, V. J. Feil, C. J. Lamoureux, and C. B. Struble, Metabolism and Radiation Research Lab and NDSU Animal Science Dept., State University Station, Fargo, ND 58105

Tritium labeled glycerol triethers have been proposed as nonabsorbable markers for study of intestinal absorption and metabolism.[1] Their synthesis was accomplished by following sequence: alkylation of 1,2-isopropylidene glycerol with an unsaturated alkyl methanesulfonate, (2) hydrolysis, (3) alkylation with a saturated alkyl methane sulfonate, (4) catalytic reduction with tritium. We prepared our glycerol triethers from an isomer of 1,3-benzylidene glycerol because we were able to prepare it in greater purity than 1,2-isopropylidene glycerol.

Purification of the glycerol triethers was accomplished by chromatography and/or recrystallization. Dialkyl ethers formed in the alkylation reactions could be removed only with difficulty by chromatography. Differential refractive index monitoring of column chromatographic effluents showed "base line" separation of dialkyl ethers and glycerol triethers; however, the glycerol triether fractions usually contained dialkyl ethers when analyzed by chemical ionization mass spectrometry. Although repeated chromatography ultimately yielded product of acceptable purity, recrystallization yielded higher quality material.

The electron impact spectra of glycerol triethers and dialkyl ethers are characterized by the following:

CH_2-O-$C_{12}H_{25}$ CH-O-$C_{18}H_{37}$ CH_2O-$C_{12}H_{25}$	No $M^{+\cdot}$ or weak $M^{+\cdot}$ $C_{12}H_{25}]^+$ 169 $C_{18}H_{37}]^+$ 253 $C_{12}H_{25}O$-CH=CH-O$C_{18}H_{37}$ $^{+\cdot}$ 480
$C_{12}H_{25}$-O-$C_{12}H_{25}$	No $M^{+\cdot}$ or weak $M^{+\cdot}$ $C_{12}H_{25}]^+$ 169

Chemical ionization spectra with isobutane show large molecular ions with very little fragmentation.

Intestinal absorption studies indicated that 1,3-dibutyl-2-decyl-9,10-$^3H_2$ glycerol was extensively absorbed and/or metabolized whereas 1,3-didodecyl-2-octadecyl-9,10-$^3H_2$ glycerol was much less absorbed and/or metabolized.

	BILE FISTULATED RATS	
Triether	4-10-4	12-18-12
Bile	5.5%	0.3%
Urine	16.5	0.23
Feces	64.9	83.3

RATS

BILE FISTULATED BLADDER CATHETER 1 mg 12-18-12 (15 μCi) 5 g Simulated Meal		BLADDER CATHETER 1 mg 12-18-12 (20 μCi) 1 ml Triolein	
Bile	0.27% ± 0.04		
Urine	0.23 ± 0.13	Urine	2.67% ± 1.22
Feces	83.3 ± 15.8	Feces	88.98 ± 2.43
GI + Contents	9.56 ± 8.54	GI + Contents	0.09 ± 0.04
Liver	0.009 ± 0.006	Liver	0.13 ± 0.03
Kidney	0.004 ± 0.004	Kidney	0.01 ± 0.005
Carcass	0.68 ± 0.71	Carcass	0.81 ± 0.09
Recovery	93.9 ± 12.2	Recovery	92.7 ± 2.2

Approximately 80% of the tritium activity in the urine of rats dosed with 1,3-didodecyl-2-octadecyl-9,10-$^3H_2$ glycerol was volatile and appeared to be tritiated water. Thus, even the high molecular weight triethers appear to be metabolized to a small extent. Their use as nonabsorbed markers in absorption and metabolism studies is questioned.

[1] R. G. H. Morgan and A. F. Hofmann, J. Lipid Res., 11, 223 (1970).

THE SYNTHESIS OF ^{18}O LABELED ANALOGS OF PYRIMIDINE NUCLEOSIDES

R. THOMAS SOLSTEN and K.H. SCHRAM
DEPARTMENT OF PHARMACEUTICAL SCIENCES, UNIVERSITY OF ARIZONA
TUCSON, ARIZONA 85721

INTRODUCTION

The use of pyrimidine nucleosides as anti-neoplastic and anti-viral agents has increased dramatically in recent years. The ability to monitor plasma levels of these drugs and their metabolites aids clinicians in designing dosage schedules for maximal therapeutic effects with minimal toxicity. Quantitation of drugs and metabolites in biological fluids by GC-MS is best accomplished with internal standards and isotopically labeled analogs have proven to be superior internal standards.(1) Therefore, a general synthetic scheme for the preparation of these internal standards should be of significant value in metabolic and clinical studies of the pyrimidine nucleosides. We have devised such a scheme for the preparation of highly enriched ^{18}O labeled analogs of these therapeutically useful compounds.

SYNTHESIS

Treatment of 2',3'-O-isopropylidene uridine with triphenylphosphine and diethyl azodicarboxylate affords the corresponding $O^2,5'$ anhydro nucleoside in ca. 75% yield.(2) Ring opening with $Na^{18}OH$ will introduce the label into the base portion of the nucleoside in a quantitative manner. Subsequent reclosure and a second opening with either $Na^{18}OH$ or $Na^{16}OH$ followed by de-blocking gives one the free nucleoside labeled in the base, the sugar, or both portions. The TMS derivatives were made for each compound and the isotopic purity measured for the M-15 ion.

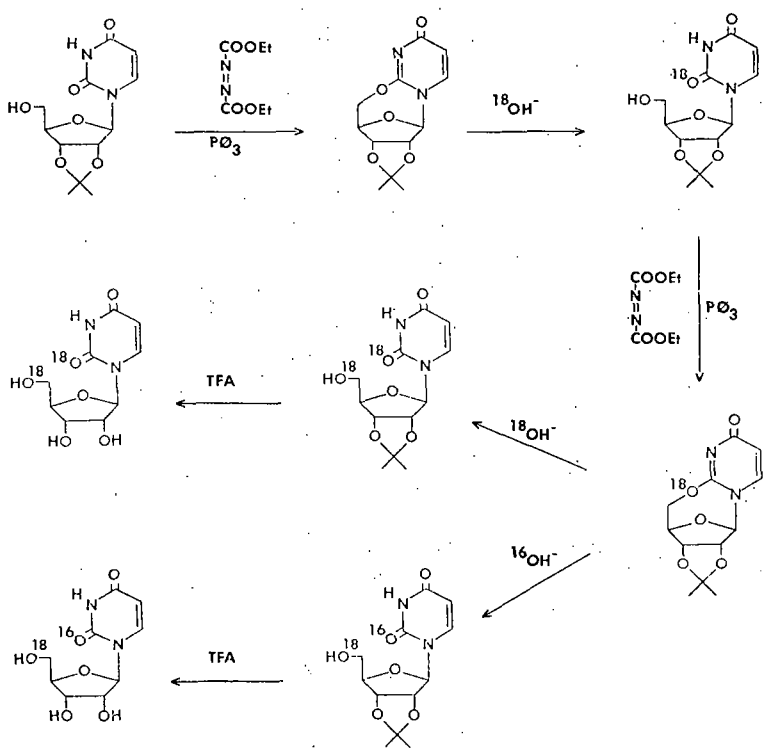

In all cases the isotopic purity was found to be greater than 97% when 99% $Na^{18}OH$ was used for the anhydro opening reaction.

MASS SPECTRA

The purity of the isotopic label is evident in the M-15 region (m/z 517) of the mass spectra shown below. The location of the label in either the sugar or the base is indicated by the ion at m/z 348 (350) formed by cleavage of the glycosidic bond.

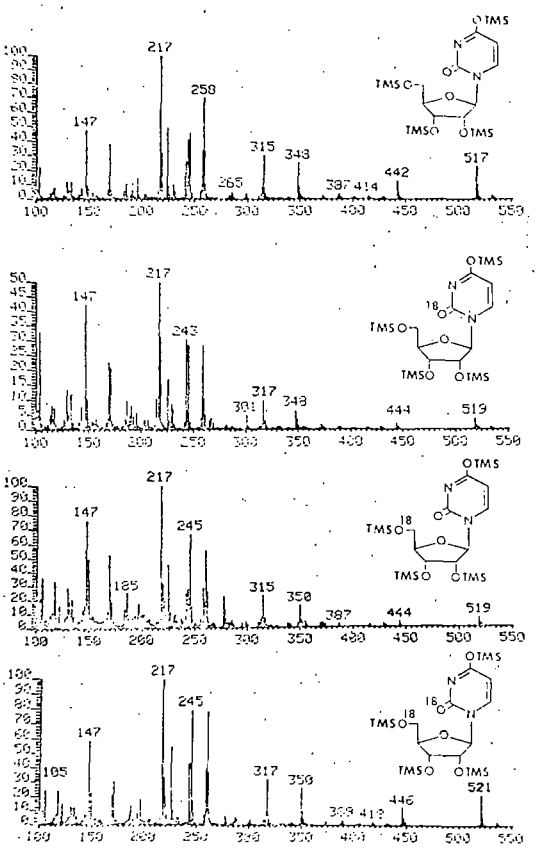

REFERENCES

1. B.J. MILLARD, "QUANTITATIVE MASS SPECTROMETRY" Heyden and Sons Ltd., 1978, Chapters 3, 4 and 6.

2. M. WADA and O. MITSUNOBU, TETR. LETT., 13, 1279 (1972).

MASS SPECTROMETRIC ANALYSIS OF SOLUTIONS WITH AN INDUCTIVELY COUPLED PLASMA ION SOURCE; R. S. Houk, H. J. Svec, and V. A. Fassel; Ames Lab., U.S. Dept. of Energy and Dept. of Chem., Iowa State Univ., Ames, IA 50011

Inductively coupled plasmas (ICP's) are widely used as excitation sources for elemental determinations at all concentration levels by optical emission spectrometry. Solution aerosols are directly and continuously introduced into ICPs, hence samples can be changed in 1-2 minutes. Most elements are extensively ionized in ICPs. Thus, rapid sample throughput and efficient analyte ionization make ICPs potentially useful as ion sources for rapid, direct elemental and isotopic analysis of solutions (1).
Because the ICP operates at 1 atm and ~6000 K, an interface between the ICP and the mass spectrometer is necessary. Plasma particles (ions, electrons, and neutral species) are sampled through a 50-70 μm diameter orifice into the first stage of a differentially pumped vacuum system. Ions are collected from the resulting supersonic jet by an electrostatic ion lens. The lens focusses the ions into the second stage of the vacuum system. Here the ions are m/z-resolved by a quadrupole mass spectrometer and detected by a *Channeltron electron multiplier*.
Our prototype inductively coupled plasma-mass spectrometer (ICP-MS) has been described (1). In the present paper improvements to the ion sampling, focussing, mass analysis, and data acquisition functions are described. Analytical figures of merit such as detection limits, accuracy, and precision obtained for trace elemental and isotopic analysis by ICP-MS are given.

(1) Houk, R. S.; Fassel, V. A., Flesch, G. D.; Svec, H. J., Gray, A. L.; and Taylor, C. E. Anal. Chem. 1980, 52, 2283-2289.

APPLICATION OF MASS SPECTROMETRY TO STUDY OF ION AND NEUTRAL DIFFUSION THROUGH ALUMINA; VINCENT D. MEYER AND PAUL FORTUCCI, GTE Lighting Products, Danvers, MA 01923.

A mass analyzer has been used to detect ions and neutrals which have permeated through the alumina arc tube of high pressure sodium, HPS, lamps. In this paper a description of the method and apparatus is given, and the results of measurements as a function of time, position on the arc tube and bias voltage are reported.

The HPS lamp consists of a polycrystalline alumina arc tube in an evacuated outer jacket. The arc tube is charged with a sodium amalgam and a rare gas fill. A discharge across the electrodes produces pressure broadened sodium resonance radiation, $^2P \rightarrow ^2S$, centered in the yellow region of the visible spectrum. During operation the wall of the arc tube can reach 1500°K. In some rare cases HPS lamps develop darkened outer jackets. Surface analyses of darkened outer jackets have detected high concentrations of sodium, indicating sodium loss through the arc tube.

To confirm the sodium leakage a quadrupole mass analyzer and an operating arc tube, separated by a slit, were placed in an ultra-high vacuum system. A slide mechanism coupled to feedthroughs permitted linear and rotary motion of the arc tube. This arrangement, shown in figure 1, makes it possible to position any point on the arc tube in front of the slit. With the filaments in the ionization chamber of the mass analyzer

Figure 1

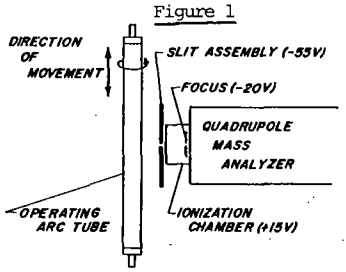

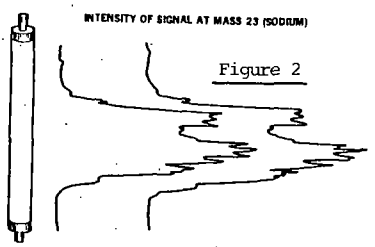

Figure 2

turned on, both ions and neutrals which make their way into the ionization chamber are detected. But with the filaments turned off, only those species which are already ionized can be detected. Sodium ions and neutral sodium atoms from operating arc tubes have been detected. In addition potassium and lithium ions and, in one case, mercury atoms were detected. Figure 2 shows the signal at mass 23 as a function of position along the arc tube and a second measurement is shown to demonstrate the repeatability. The signal in this case represents both ions and neutrals since the filaments were on. A reduction in signal occurs when the filaments are turned off. Over short periods of time the results are repeatable, but the nature of sodium permeation changes with time. Data accumulated over the life of an arc tube showed that initially leakage is by ions; as the tube ages neutrals are detected, and toward the end of life neutrals are the dominant species.

Figure 3 shows the waveform of the voltage on the arc tube and of the signal at mass 23 with the filaments both on and off. The detection of both ions and neutrals is demonstrated by the reduction in signal when the filaments are turned off, and by the shape of the waveforms. The charged species, sodium ions, follow the AC voltage on the arc tube but the neutral species, sodium atoms, are not affected by the voltage.

By monitoring the signal as the lamp was turned off, it was found that the decay of the sodium ions is much more rapid than that of sodium atoms. Another property of sodium permeation is demonstrated in figure 4. The signal at mass 23 is recorded as the lamp is turned off. The sodium ion signal disappears very rapidly, but when the voltage is reapplied the signal at mass 23 reappears even though the lamp remains extinguished. The signal does not reappear if the voltage is reapplied after a long time. These results indicate that sodium permeation is a function of the temperature of the arc tube. As the tube cools, permeation decreases.

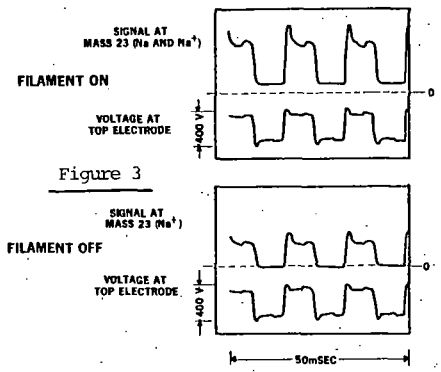

Figure 3

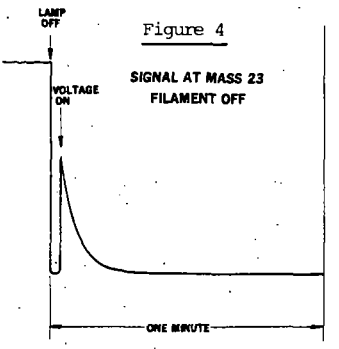

Figure 4

An additional type of measurement was made by electrically isolating the arc tube and varying the voltage (bias) between the slit and the arc tube. This type of measurement establishes the threshold voltage necessary to extract positive sodium ions from the operating arc tube. Figure 5 shows this threshold voltage as a function of position on the arc tube. The change with position reflects the voltage drop across the arc tube.

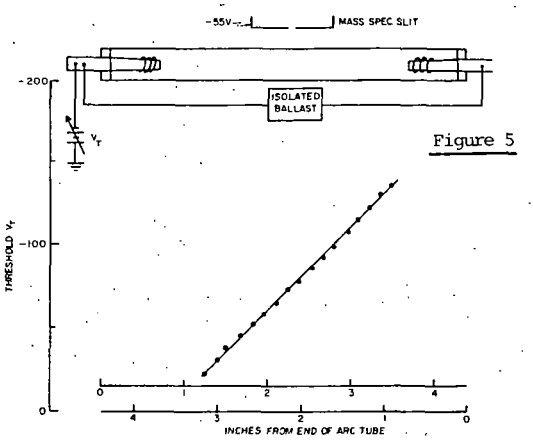

Figure 5

Measurements as a function of the distance between the slit and the arc tube have shown that the signal varies inversely with distance, but the threshold voltage is independent of this distance. These results demonstrate that the extraction of sodium ions requires a voltage bias to overcome a barrier; either to pass ions through the arc tube or to remove ions bound to the arc tube exterior.

The suggestions and cooperation of E. Wyner and D. Dugger are acknowledged.

IONIC MASS SPECTRA FROM Ar/H_2 PLASMAS IN A PLANAR MAGNETRON SPUTTERING DEVICE

K. Hoefler, G. Rettinghaus, BALZERS AG, FL-9496 Balzers, Liechtenstein
and P. Irving, BALZERS, Hudson, NH 03051

Introduction

Studies of sputtering in dc diode systems have shown that small impurities of H_2 in Ar drastically reduce the deposition rate (1). For sputtering in a planar magnetron system however, Maniv and Westwood (2) found no change in the deposition rate even with H_2/Ar ratios of up to 1.0 (Ar pressure constant). The reason for this different behavior was assumed to be the tendency to convert hydrogen ions to ArH^+ in the magnetron plasma (ArH^+ has the same sputtering yield as Ar^+), so that H^+ and the H_2^+, with their smaller sputtering yields, would not substantially contribute to the discharge current. Until now it was not clear to what extent ArH^+ is formed, since there are no experimental data for the low pressure region ($\approx$0.2 Pa) typical of magnetron discharge. The aim of our experiment was to identify the ionic species existing in an Ar/H_2 magnetron plasma and to determine their abundance as a function of the mixing ratio.

Experimental

The experimental setup consists of a 12.7 cm x 38.1 cm planar magnetron with Cu-cathode operated at a constant current of 4A (ca. 600 VDC) and a differentially pumped Quadrupole Mass Analyzer (BALZERS QMA 150) setup for the analysis of ions from plasmas. The ions are sampled through an electrically isolated aperture and focussed to the entrance aperture of the rod system by ion optics. After passing through the mass filter, the ions are deflected by 90° to the conversion dynode of the off-axis SEM. The SEM signal goes to an electrometer amplifier for current measurement.

Special attention was paid to the avoidance of artifacts occasionally resulting from secondary processes in the plasma sheath or in the orifice region (3). To ensure minimum disturbance of the plasma by the sampling device, the ion intensity was recorded as a function of the extraction voltage (giving probe characteristics) to find a convenient extraction mode. To get additional information about the plasma properties Langmuir probe measurements were made.

The discharge was first operated in pure argon at 0.2 Pa and then (with Ar flow fixed) the total pressure was increased by admitting H_2 up to the desired mixing ratio.

Results and Discussion

The Langmuir probe measurement yielded a plasma potential of V_{pl}= +3V, compared to the grounded vacuum vessel. The ionic mass spectra were recorded with the sampling orifice at floating potential ($V_{fl} \approx -9V$). The extraction voltage relative to the plasma was therefore about 12V.

Figure 1 summarizes some of the results obtained with different H_2/Ar ratios, R. The main features in the spectrum for $R \leq 0.01$ occur at the mass numbers 20, 40, 63 and 65. These originate from the ions Ar^{++}, Ar^+, and Cu^+ respectively. At larger ratios, there is a spectacular increase of the peaks at m/e = 41 (ArH^+) and m/e = 2, 3 (H_2^+, H_3^+), while the intensity of the Ar^+ ion decreases. The Cu^+ ion intensity remains constant. For ratios $R \geq 0.56$ the total ion intensity decreases whereby the gradient is different for different species.

From the overall behavior of the spectra, it is clear that the ArH^+ ion plays an important role in the magnetron sputtering plasma as was assumed by Maniv and Westwood (2). Most of the Ar^+ ions are converted to ArH^+. But the intensities of the light ions, especially H_3^+, are not negligible. It is difficult to see why they should not contribute to the discharge current, thus reducing the overall sputtering rate. On the other hand, the Cu^+ intensity is constant up to R = 0.28 and the decrease for $R \geq 0.56$ does not contradict the result of a constant deposition rate seen by Maniv and Westwood. This general decrease may be caused by a reduction of the ionization efficiency, because of the lower electron temperature in the case of H_2 present in the discharge. (The Langmuir probe measurement showed a decrease of the electron temperature by about 50% from $R \leq 0.01$ to R = 0.56).
The discrepancy above may be explained by the possibility of different plasma chemistry inside the dense zone of the magnetically confined plasma just in front of the cathode. Therefore it appears necessary to analyze the ionic species actually hitting the cathode.

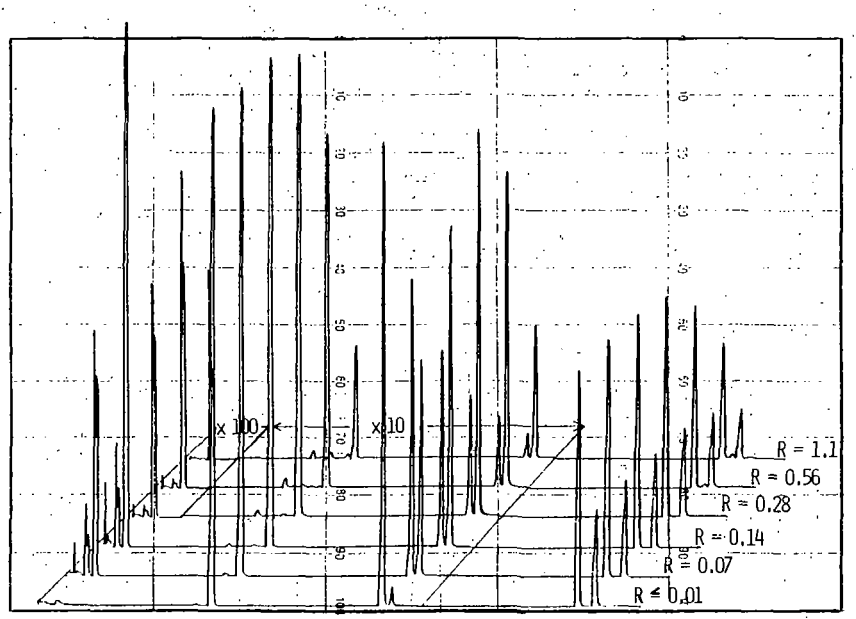

Fig. 1: Ionic Mass Spectra as a Function of H_2/Ar Mixing Ratio R

References

1. W.D. Westwood and R.J. Boynton, J. Appl. Phys., 44 (1973) 2610
2. S. Maniv and W.D. Westwood, J. Vac. Sci. Technol., 17 (1980) 403
3. H. Helm, T.D. Märk, and W. Lindinger, Pure Appl. Chem., 52 (1980) 1739

AN ATMOSPHERIC PRESSURE PLASMA/QUADRUPOLE MASS SPECTROMETER SYSTEM FOR ELEMENTAL ANALYSIS.
D.J. Douglas, E.S.K. Quan and R.G. Smith. SCIEX INC., 55 Glencameron Rd., Thornhill, Ontario, Canada, L3T1P2; and J.B. French, University of Toronto Institute for Aerospace Studies, 4925 Dufferin St., Downsview, Ontario, Canada.

Introduction

Work is progressing in this lab[1] and others[2] on the coupling of atmospheric pressure argon plasmas to quadrupole mass spectrometers for elemental analysis. Both microwave induced plasmas (MIP) and inductively coupled plasmas (ICP) are currently under development here. In these instruments solutions are nebulized and carried into the plasma where the dissolved solids are vapourized, dissociated and ionized. The resulting ions are extracted into the quadrupole vacuum system (either TAGA™ 3000 or TAGA™ 6000) through a differentially pumped region. Results of the analysis of some NBS reference materials with an MIP source will be reported here.

Since the initial report on this work,[1] a number of improvements have been made to the plasma system. A new torch design, incorporating separate plasma and nebulizer gas flows is now in use.[3] This torch uses swirl in the plasma gas to centre the plasma in the discharge tube (I.D. 4mm). The sample is injected on the centreline and directed at the plasma. (The torch is analogous to an ICP torch in this respect, although a toroidal plasma is not formed.) Microwave power is coupled to the resonant cavity through the electric field, rather than the magnetic field as used in the original work with a Beenaker cavity. This gives a better impedance match and a hotter plasma. A shield gas (N_2) has been added to sheath the plasma and prevent entrainment of air in the tail flame. This has greatly reduced the formation of NO which limits the sensitivity of the instrument to elements of high ionization potential. Lastly, a cross flow pneumatic nebulizer is now in use and this produces a more stable signal than the ultrasonic nebulizer used previously. Although the pneumatic nebulizer produces less aerosol, the detection limits are not degraded because of the other improvements in the plasma system. All sample handling is at atmospheric pressure and the response time of the system is a few seconds, permitting the rapid direct analysis of solutions for trace elements. Detection limits are comparable to or improve on those of the best atomic emission instruments.

Results

(a) NBS Orchard Leaves (SRM 1571)

Table I shows the results of analysis of NBS orchard leaves for four elements at the minor and trace level. Orchard leaves were ashed at 550°C. Following addition of concentrated HCl and a few drops of HNO_3, the sample was warmed to dissolve the residue and, after cooling, diluted to volume. This work-up gave a 100X dilution of the trace element concentrations (W/W). Each element was determined by simple calibration of the instrument with dilute solutions of the element, and also by standard addition. Copper was also determined by isotope dilution. Of these elements, only Sr showed a matrix effect. Chromium suffered a background peak at ^{52}Cr, but this was overcome by measuring ^{53}Cr. The slightly high value obtained in the Cr determination can most likely be attributed to contamination of the sample digest by a few ppb of chromium. Other elements were readily detected but were not quantified in this preliminary study.

(b) NBS Standard Water (SRM 1643a)

NBS standard water was analyzed directly with no work-up and the results are shown in Table II. Several elements showed a matrix effect and some showed interferences from the oxide or hydroxide of Ca (e.g., CaO^+ interferes with ^{56}Fe). The matrix effect was overcome by using standard addition. Isotope dilution could also be used to overcome matrix effects for each of these elements and would also provide greater precision. Interfering peaks were circumvented by measuring alternate isotopes and in some cases, by matrix matching the blank and subtracting this background. Thus some care in the analysis is necessary, but if this is done, a wide range of trace elements can be determined.

(c) NBS Uranium Isotopic Standards

The MIP/TAGA™ system is suited to the direct measurement of isotope ratios of elements in solution. Table III illustrates this with the determination of isotope ratios of

several NBS uranium standards. Solutions of 5 or 10 ppm concentration were used and the measurement time was 1 to 2 minutes per sample. Since the sample uptake rate was approximately 1.5 ml min^{-1}, this corresponds to 7.5 - 30 g of uranium per determination. The precision and accuracy of this initial data is 1.5% or better. As the sources of noise and uncertainty are identified through continued development, the precision will improve and is expected to be in the 0.1 to 1% range for all samples. Thus isotope ratios of moderate precision with rapid sample throughput will be possible.

Conclusion

The results reported here illustrate the use of a microwave plasma/quadrupole system for elemental analysis and isotope ratio determinations. A program is now underway to add this elemental analysis capability (both MIP and ICP) to the commercially available TAGA™ 3000 and TAGA™ 6000 quadrupole systems.

References

(1) D.J. Douglas and J.B. French, Anal. Chem. 53, 37, 1981.

(2) For a report on the use of an ICP/quad system see (a) R.S. Houk, V.A. Fassel, G.D. Flesch, H.J. Svec, A.L. Gray and C.E. Taylor, Anal. Chem. 52, 2283, 1980 (b) paper TAMOCI, this conference.

(3) A. Bollo-Kamara and E.G. Codding, 1981 Pittsburgh Conference on Analytical Chemistry and Applied Spectroscopy, paper 512.

Table 1. Detection Limits for some elements in aqueous solution (ng/ml).

Element	MIP/TAGA™	ICP/AES	AAS
Ag	0.1	6	5
Cd	1	3	1
Cu	0.2	1.5	2
Pb	1	12	10
Tl	1	300	30
U	1.5	45	—

TABLE II

DETERMINATION OF TRACE ELEMENTS IN NBS STANDARD WATER (SRM 1643a) CONCENTRATIONS IN ng/ml (ppb)

Element	MIP/TAGA™	Certified
Sr	212±15	239±5
Zn	62±6	72±4
Ni	48±3	55±3
V	70±12	53±3
Ba	41±4	46±2
Cr	19±3	17±2
Cd	11±1	10±1
Ag	3.9±0.5	2.8±0.3

TABLE III

ISOTOPE RATIOS OF NBS URANIUM STANDARDS

SAMPLE	MIP/TAGA™	CERTIFIED
U-005	$(4.95\pm0.03)\times10^{-3}$	4.92×10^{-3}
U-010	$(9.95\pm0.15)\times10^{-3}$	10.14×10^{-3}
U-500	$0.9981\pm.004$	0.9997
U-930	17.30 ± 0.15	17.348
common U	$(7.24\pm0.05)\times10^{-3}$	7.202×10^{-3}

PULSED PHOTOIONIZATION LIGHT SOURCE FOR TIME RESOLVED HIGH PRESSURE MASS SPECTROMETRY

S. E. Buttrill, Jr., R. J. Schmidt and D. S. Ross
Mass Spectrometry Development Program
SRI International, Menlo Park, CA 94025

At the 1979 ASMS Meeting in Seattle, we described a high pressure flow discharge mass spectrometer system for monitoring low concentrations of organic compounds in ambient air.[1] Recently, we modified this system in order to carry out studies of the ion molecule chemistry involved in gas phase nitration and nitrosation of aromatic radical cations (see paper MPMOB3 of this conference). Data collection is now carried out using a PDP11/2 Computer System connected to the ion counting electronics via an ion counting interface. The system operates as a pulsed high pressure mass spectrometer, and allows us to record the time dependence of the ion concentrations within the source following the ionization pulse. This paper describes a new pulsed photoionization light source which is extremely simple, efficient, and selective.

Figure 1 shows a schematic of the flow discharge ion source. The rapid gas flow through the inner 0.5 inch tube rapidly carries ions to the ion exit aperture. For operation up to 50 torr, this aperture is a 0.004 inch hole. Almost all of the gas is pumped away through the annular space between the inner and outer tubes which comprised the ion source. The mass spectrometer vacuum system must only contend with those gas molecules which exit the source together with the ions. The pulsed photoionization source is shown schematically in Figure 1 approximately 1.5 inches behind the ion exit aperture. We find that the source can operate with the light source anywhere from 1.0 to 4.5 inches back.

The pulsed field ionization light source consists of an electrical discharge within a flow of pure argon confined within a 1/8th inch glass tube. Figure 2 shows a scale drawing of the construction of the discharge region. Argon (or other suitable gas) flows between the 1/16th inch ceramic insulator and the inside of the glass tube. The ceramic insulator is a standard thermocouple shield which contains two molybdenum wires. A high voltage pulse applied to these wires causes a short (approximately 10 microseconds) discharge in the pure argon. The discharge produces argon ions, electrons, and excited argon atoms. Although the argon gas is constantly flowing through the pulsed lamp, the flow rate is so low that argon ions and electrons do not escape into the ion source itself. Only the argon resonance radiation at 11.83 and 11.62 eV leaves the discharge lamp. These vacuum UV photons produce a nearly uniform ionization of organic molecules throughout the ion source downstream of the pulsed lamp.

Typical operating conditions for the flow discharge ion source using argon in the pulsed lamp are 10 torr helium carrier gas, 0.7 torr argon, and less than 50 microns organics. Flow velocity within the ion source is variable, but is typically approximately 200 cm/s. The ion source has been operated from 30 up to 200°C.

The use of argon resonance radiation allows a large number of organic compounds to be ionized with little or no fragmentation. Benzene, toluene, xylene, acetaldehyde, pyridine, furan, naphthalene, ethyl ether, the fluorobenzenes, ethyl nitrate, anisole, THF, NO, and NO_2 have all been ionized. Compounds which are not ionized include oxygen, hydrogen, nitrogen, argon, water and helium. As would be expected, when helium is used as the discharge lamp gas, extensive ionization of these compounds is produced because of the much higher energy of the helium resonance radiation. Other carrier gases may be used in the ion source and other discharge gases may be used within the pulsed lamp, but care must be taken to assure that the gases utilized are compatable. In general, molecular gases are not suitable as carriers because they absorb the vacuum uv radiation. In this case, the ion signal at short times is very

weak and rises to a large value when the gas originally present near the lamp exit reaches the ion sampling orifice. A possible suitable combination would be hydrogen in the lamp together with argon as a carrier gas. The carrier gas must be of extremely high purity because reaction of organic ions with trace impurities can compete effectively with the ion molecule chemistry of interest.

The new pulsed high pressure mass spectrometer system was tested by measuring the equilibrium constant for the benzene dimerization reaction.

$$C_6H_6^{+\cdot} + C_6H_6 \rightleftarrows (C_6H_6)_2^{+\cdot}$$

A van't Hoff plot of the equilibrium constant versus 1/T yielded a value of $\Delta H = -14.70$ kcal/mol and a value of $\Delta S = 22.5$ eu. For comparison, other literature values for these quantities are 15.03 kcal/mol and -23.2 eu.[2]

Further details of this light source will be reported in a full publication to be submitted to the International Journal of Mass Spectrometry and Ion Physics.

References

1. S. E. Buttrill, Jr., Paper FAMP-12 Presented at the 27th Annual Conference on Mass Spectrometry and Allied Topics, Seattle, WA, June 3-8, 1979.
2. J. M. Janski, R. N. Rosenfeld, D. M. Golden, and J. I. Brauman, J. Am. Chem. Soc. 101, 2259 (1979).

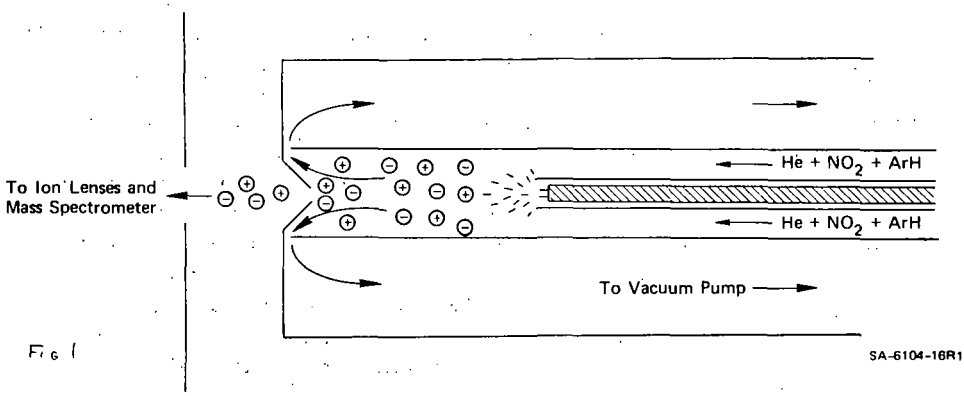

Fig 1

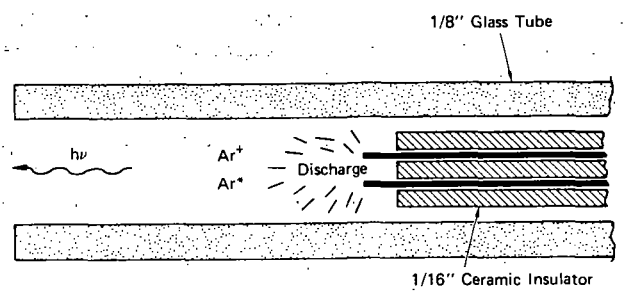

Fig 2

CHEMISTRY OF MICROWAVE INDUCED REACTIONS IN HYDROCARBONS.

I. PLATZNER and P. MARCUS, Dept. of Chem., Nuclear Research Centre-Negev, Beer-Sheva POBox 9001, ISRAEL.

The glowing plasma of pure hydrocarbons and their mixtures with Ar, Kr, O_2 or N_2 was directly sampled with a TOF-MS at the following conditions: a) gas flow rates (through a 16 mm OD quartz tube with a 0.05 mm axially located pinhole) : 0.3-2 lit/h, b) total pressure: 0.5-5 torr, c) MW power at 2540 MHz : 20-160 watt. Low electron energy spectra, (15 eV) were recorded.

In the methane discharge, mainly unsaturated molecular species with 2 to 6 carbon atoms were identified. The more important reactions besides the formation of C_1 radicals and ions are believed to be: a) radical and ion-molecule reactions of CH_3, CH_2 radicals and of hydrogen deficient ions, CH_2^+, CH^+ , with methane; b) further condensation reactions of C_2 ions, mainly $C_2H_2^+$ and $C_2H_3^+$ with methane and C_2 neutrals. In the presence of argon or krypton an increased rate of polymerization is observed. This is attributed to an efficient primary process Ar^* (or Kr^*) + $CH_4 \rightarrow$ Ar (or Kr) + CH_2 + H_2 followed by electron impact ionization of the CH_2 radical, rather than to dissociative charge transfer $Ar^+ + CH_4 \rightarrow Ar + CH_2^+ + H_2$, which for Kr^+ ions and ground state methane is not known.

Detailed experiments were carried out to study the polymerization process in methane (1) acetylene(2) and propylene. The reactivity of n-hexane, cyclo-hexane, several partially unsaturated hexanes and benzene in the microwave discharges was also qualitatively studied. Only polyacetylenes of the general formula $H-(C\equiv C)_n-H$ (n = 1,2,3, ...) were identified in the plasma of pure acetylene. The $C_2H_2^+$ ions and $C_2H^\cdot$ radicals are assumed to be the reaction precursors. Calculation based on known reaction rate constants for the ions and radicals with acetylene show that even relatively low ion concentrations may contribute significantly to the polymerization processes. Ions were identified in a RF plasma of acetylene (3). Besides polyacetylenes, oxidation products as CO, CO_2, C_2H_2O and CH_2O , and the following nitrogen containing molecular species: $H-(C\equiv C)_n-CN$ (n = 0, 1, 2 ...) were observed in the presence of oxygen and nitrogen. Argon does not change essentially the chemical behaviour of the acetylene plasma.

In propylene a more complex behaviour is observed, indicating several reaction channels. The dominant products are C_2H_2 and C_2H_4 followed by unsaturated C_4 hydrocarbons, C_6H_6 and C_7H_8. Among the C_6 compounds only benzene shows a strong tendency towards condensation. In its spectrum C_2H_2, C_4H_2, C_2H_4 and C_3H_4 are the fragmentation products. About ten significant peaks are present in the 80-200 mass range, among them (in decreasing intensities): $C_6H_5.CH_3$, (or probably cyclic C_7H_8), $C_6H_5.C_6H_5$, $C_6H_5.C_3H_3$, $C_6H_5.C_2H$, naphtalene, $C_6H_4.CH_2.C_6H_4$ and $C_6H_5.C_2H_3$. Low yields of polymerization products were observed in 1-hexine, trans 2-hexene and cyclo-hexane. No high molecular weight products were formed in cis 2-hexene, 1-hexene and n-hexane, the last being almost inert towards MW irradiation. C_2H_4 and C_2H_2 are the major fragments, contributing to di and triacetylene and others in trace quantities.

1) P. Marcus and I. Platzner : Int. J. Mass. Spectrom. Ion Phys., 32, (1979) 77.

2) I. Platzner and P. Marcus to be published.

3) M.J. Vasile and G. Smolinsky, Int. J. Mass. Spectrom. Ion Phys., 24 (1977) 11.

HIGH VOLTAGE, LOW CURRENT DUAL CATHODE GLOW DISCHARGE FOR ATOMIC MASS SPECTROMETRY, T. J. Loving, P. J. Savickas, and W. W. Harrison, Department of Chemistry, University of Virginia, Charlottesville, Virginia 22901

A review of the literature shows a continuing increase in the use of glow discharges in analytical spectroscopy. These applications include the area of atomic emission, atomic absorption, atomic fluorescence, and mass spectrometry. In recent years, we have studied the glow discharge in several different configurations, most of which have involved relatively large cathodes in low voltage, high current applications. By restricting the size (surface area) of the cathode, it is possible to achieve satisfactory current density at small currents with an attendant high voltage which promotes cathodic sputtering. This study describes the use of two such mini-electrodes, both serving as cathodes in a DC glow discharge.

Experimental

Our glow discharge chamber was designed to accommodate numerous cathode geometries while offering the possibility of simultaneous atomic absorption and mass spectrometric analysis. (Figure 1) The rest of the experimental arrangement has been described previously.[1,2]

1x7mm dual pin cathodes similar in geometry to those used in spark source mass spectrometry were used throughout this work, and have performed favorably compared to our previous cathode geometries[3]. The entire vacuum housing acts as the anode in this configuration.

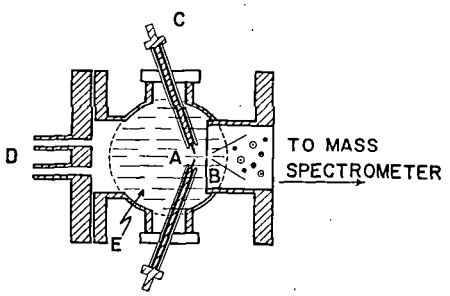

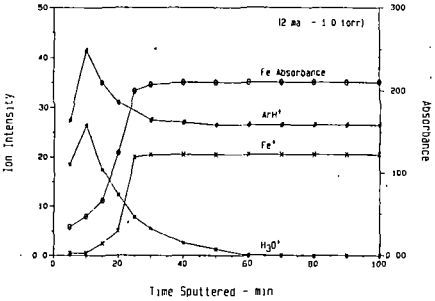

Figure 1. (A) Dual pin cathodes in stainless steel holders, (B) Ion exit orifice leading to high vacuum chamber for quadrupole mass filter, (C) Electrical feedthru-cathode holder assembly, (D) Gas inlet and pumping port, (E) Quartz window for atomic absorption measurements.

Figure 2. Start up performance of pin type cathodes. SS -304 sample - Ar discharge.

Results and Discussion

The dual pin cathode geometry has several advantages compared to previous designs. Th cathode site is smaller, thus making more efficient use of the sample material, while allowing lower discharge currents. This leads to a resultant decrease in power dissipation at comparable experimental conditions, which keeps the rate of desorption of gases off the chamber walls to a minimum.

Following the atomic and ionic populations simultaneously allows us to study the effec of changing various experimental parameters. A plot of time vs. atomic absorption and ion intensities of several discharge species for a stainless steel #304 sample is shown in Figure 2.

When the discharge is initiated, a pre-equilibrium period occurs where a significant amount of water is seen in the mass spectrum. We have duplicated this pre-equilibrium situation artificially by introducing water vapor into the discharge, and have observed comparable effects, i.e., a decrease in elemental ion and absorbance intensity, coupled

with an increase in discharge voltage, at constant current. This is believed to be caused by a decrease in sputter yield and ionization efficiency in the discharge due to the presence of water.[4] Upon discontinuation of the flow of water vapor into the discharge, a relatively short amount of time is needed to re-establish equilibrium.

The sputtered atomic population[5] is seen in Figure 3 to be concentrated around the ion exit orifice.

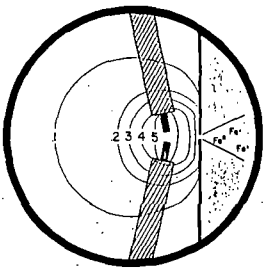

Figure 3. Atomic absorption profile of Fe in a SS #304 sample - 2.0 ma - 1.0 Torr

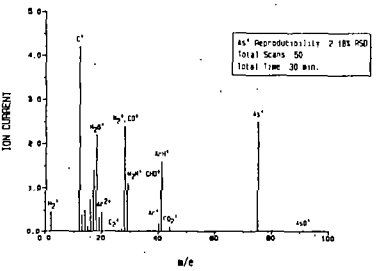

Figure 4. Mass spectrum of 10% arsenic, 90% carbon pressed pin cathodes.

We have found this condition to be related to a more favorable Fe to Ar ion ratio. The observed increase in this ratio is attributed to a greater distribution of more efficient sputtering angles and less redeposition onto the cathode surface, because of the smaller cathode diameter.

An additional use of this cathode geometry involves the pressing of non-conducting or conducting powdered samples into a conducting graphite matrix cathode whose make up is similar to those used in spark source mass spectrometry. Figure 4 shows a mass spectrum of an arsenic doped graphite pin cathode.

The good reproducibility of the As ion current over a number of scans shows that the sample is homogeneous; hence this should be a good method for analysis of mixtures. Water is persistent in this spectrum, constantly being introduced into the discharge from the cathode material, as no special handling or drying procedures were taken.

References

1. B. L. Bentz, C. G. Bruhn, W. W. Harrison, Int. J. Mass. Spec. Ion Phys., 28, 409 (1978).

2. B. L. Bentz, C. G. Bruhn, W. W. Harrison, Anal. Chem., 51, 673 (1979).

3. W. A. Mattson, B. L. Bentz, W. W. Harrison, Anal. Chem. 48, 489 (1976).

4. W. Lindinger, Phys. Rev. A., 7, 328 (1973).

5. A. J. Sterling, W. D. Westwood, J. Appl. Phys., 41, 742 (1970).

OPTICAL AND MASS SPECTROMETRY OF INERT AND REACTIVE GLOW DISCHARGE SPUTTERING OF DISC CATHODES, S. L. Tong, R. B. Keefe, and W. W. Harrison, Department of Chemistry, University of Virginia, Charlottesville, Virginia 22901

To better understand atomization and ionization phenomena in glow discharges, it is useful to determine the effects of discharge gases and discharge parameters on various species. We have designed a source which can be monitored optically for neutral atoms (ground state and excited) and by mass spectrometry for ionic populations. The inert discharge atmosphere of argon was altered by systematically introducing increasing percentages of oxygen while observing the changes in atomic and ionic populations. Our long term goal in these studies is the application of glow discharge mass spectrometry to trace element analysis.[1,2]

Experimental

The water-cooled disc cathode discharge source coupled to a quadrupole mass filter which allows simultaneous atomic absorption profile measurements and ion analysis is shown in Figure 1.

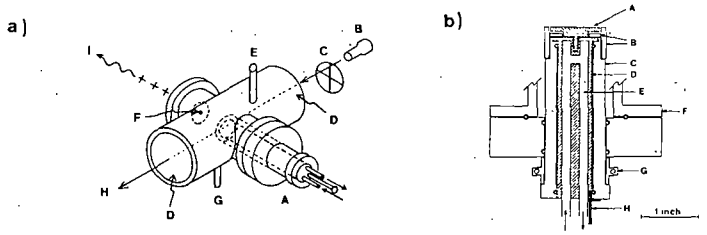

Figure 1. (a) Diode glow discharge source for optical and mass spectrometry. (A) Water-cooled cathode holder, (B) Hollow cathode lamp, (C) Chopper, (D) Quartz windows, (E) Gas inlet, (F) Anode plate and ion exit orifice, (G) Pump port, (H) To spectrophotometer, (I) To quadrupole mass filter.

(b) Cross-sectional view of the water-cooled cathode holder. (A) Disc cathode, (B) Macor shield, (C) Macor cylinder body, (D) Aluminum cylinder, (E) Cooling water, (F) To glow discharge chamber, (G) Adjustable collar, (H) Cathode lead.

Thin disc cathodes of chromium, copper and niobium have been used. Argon, and a mixture of oxygen and argon from very low to high percentages served as discharge gases. Typical source pressure varies from 0.3-1.2 Torr with discharge currents up to 20 mA, and voltages of 400-1200 V.

Results and Discussion

Figure 2 shows typical atomic density profiles for a chromium cathode in an argon discharge. The general trends and the maxima at the boundary of the cathode dark space and the negative glow are consistent with those reported at lower pressure discharges.[3] The relative atomic density maxima vary in location as a function of pressure, as does the rate of decrease in atomic density with distance from the cathode surface. Figure 3 compares the effect of discharge pressure on atomic density adjacent to the exit orifice and the extracted ion current from this location. Plots are shown for three different cathode-anode distances. Higher pressure tends to decrease ion current at large cathode-anode distances, an effect which is also observed to a less dramatic degree with the atomic densities.

Abrupt changes in the sputtering rates on introducing a small percentage of O_2 in an inert atmosphere discharge often have been known in the range of ~0.5-1%[3,4]. Our results from optical studies in Figure 4 show: (1) With the careful control of the discharge conditions, in particular the discharge voltage, high sputtering rates were attained at even higher levels of O_2 (up to 5%). (2) While maintaining the discharge above a certain critical voltage as shown, the sputtering rates were significantly enhanced as compared to a pure argon discharge.

Mass spectrometric measurements under similar conditions confirm the optical results and show no detectable or very low signal levels of O^+ and O_2^+ at O_2 partial pressures up to 5%. On increasing the O_2 level in Ar to the range of 5-100%, Ar^+ drops by a factor of 10 and Cr^+ decreases by as much as 200x, while O_2^+ and O^+ become the predominant ion species. Only CrO^+ and CrO_2^+ are observed in contrast to a previous report where greater abundance of the higher oxides in the negative ion sampling mode were observed[5]. The ratio of MO^+/M^+ has a value of ~0.01 initially and increases at higher percentages of O_2.

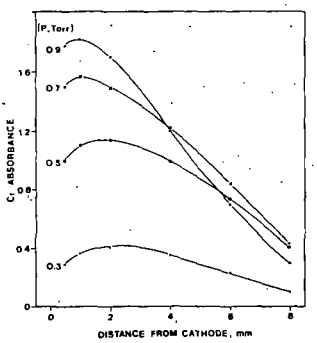

Figure 2. Atomic density profiles for chromium in an argon discharge using a chromium disc cathode.

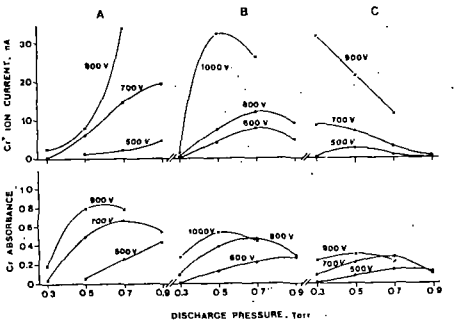

Figure 3. Sputtered chromium absorbance and ion current (Cr^+) as a function of discharge pressure and voltage. Cathode-anode distance: A = 6 mm, B = 9.5 mm, C = 13 mm.

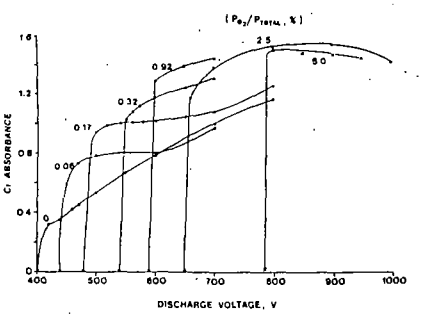

Figure 4. Sputtered chromium absorbance as a function of discharge voltage for different percentages of O_2 in Ar. Ptotal = 0.60 Torr.

References

1. B. L. Bentz, C. G. Bruhn, and W. W. Harrison, Int. J. Mass. Spect. Ion Phys., 28 409 (1978).
2. C. G. Bruhn, B. L. Bentz, and W. W. Harrison, Anal. Chem., 51 673 (1979).
3. W. D. Westwood, Prog. Surf. Sci., 7, 71 (1976).
4. A. H. Eltaukhy, B. R. Natarajan, J. E. Greene, and T. L. Barr, Thin Solid Films, 69, 219 (1980).
5. B. L. Bentz and W. W. Harrison, Int. J. Mass. Spect. Ion Phys., 37 167 (1981).

CHEMICAL IONIZATION WITHOUT DIFFERENTIAL PUMPING

DAVID P. BEGGS and STUART D. LERNER
Hewlett-Packard Company
1601 California Avenue
Palo Alto, CA 94304

Previously chemical ionization sources have been constructed in differentially pumped vacuum systems. This was necessary because of the need to maintain a relatively high pressure inside the ion source, a relatively low pressure just outside the ion source, and an even lower pressure in the analyzer and detector regions. The differentially pumped system was designed to evacuate the source region with one pump and the analyzer and detector regions with another pump. These differentially pumped systems include a large high vacuum pump in the source region (~1000 L/sec) and a smaller high vacuum pump in the analyzer region (~150 L/sec). The two pumping regions are separated by a baffle which allows transmission of the ion beam but restricts gas flow between the two pumping regions. The pressure in the ion source is usually 1 Torr, while the pressure just outside the source is 10^{-3} Torr. This pressure is too high for effective operation of the analyzer, hence the need for a differentially pumped system which allows the analyzer pressure to stay below 1×10^{-4} Torr.

A new chemical ionization source has been designed which will operate with only one small high vacuum pump servicing the complete vacuum system. The successful operation of this ion source in the chemical ionization mode is achieved through the combination of several design factors. A 110 L/sec turbo-molecular pump was used as the high vacuum pump. This pump situated in the middle of the vacuum chamber provides good pumping efficiency and excellent performance over a wide range of pressures. The use of a quadrupole mass filter provides an analyzer which has a high tolerance to increased analyzer pressures. The source is designed to minimize extraneous gas flow out of the ion source. The sample inlet line is sealed from the vacuum system via a spring-loaded polymeric sealing interface. The inlet line and the ion source chamber are mechanically contiguous. The ion exit and electron inlet holes are the only apertures in the ion source. These holes have been reduced in size to provide an optimum gas flow/sample sensitivity design for this system.

The performance of this new source compares favorably with the performance of other chemical ionization sources now in use. A typical reagent spectrum obtained with this source is shown below.

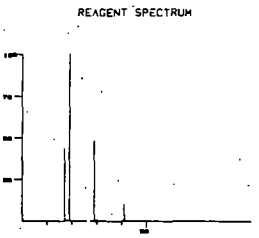

The methane reagent spectrum shows very reasonable abundances of $C_2H_5^+$ and $C_3H_5^+$. The presence of water in the reagent gas contributes the H_3O^+ at m/e 19. Static pressure measurements as well as measurement of the relative abundance of $C_3H_5^+$ have shown the ion source pressure to lie between 0.5 and 1.0 Torr.

A large number of different compounds, representing various functional groups, have been analyzed with the source. The resulting spectra show excellent quality. No indication of fragmentation has been observed. This indicates that collision induced dissociation outside the source, or low pressure fragmentation inside the source is not occurring. Representative sample spectra will be shown and discussed.

1. F.H. Field, M.S.B. Munson, I.A.C.S., 87, 3289 (1965).

AUTOMATED MULTIMODE MASS SPECTROMETRY (AMMS): II. DISCUSSION OF SEVERAL INNOVATION CONCEPTS.

C. CHANG, Brehm Lab. and Dept. of Chem., Wright State University, Dayton, Ohio 45435.

In a GC-MS system in order to provide a more comprehensive chemical analysis it is desirable that the sample be analyzed under various mass spectrometric operating modes including variations of ionization modes (EI, CI, etc.), ion charge polarities (positive/negative ion CI, etc.) and CI reagent gases. Automated multimode mass spectrometry (AMMS)[1,2] is a mass spectrometric technique in which two or more different operating modes are conducted either simultaneously or sequentially in rapid succession with the cycle for each period short in comparison with the sample residence time within the ion source. Presented in the following are several innovation concepts for achieving a better design of AMMS.

Concept 1: Simultaneous Positive Ion and Negative Ion CI (SPINICI). Simulatneous positive ion and negative ion EI has been known for some time[3] but was not widely adopted due to its limited analytical capability. On the other hand, the negative ion CI has been a well established analytical technique.[4] This simultaneous detection of both positive ions and negative ions in a CI source represents the best choice, and probably the only choice if one is interested in obtaining both EI and CI within a single GC run. It allows for the most efficient utilization of the sample materials and analysis time.

Fig. 1 is the schematic of an ion source for simultaneous PICI and NICI analysis. An electron beam is entering the source along the center line. With the sample and CI reagent gas introduced into the source both positive ions and negative ions of the sample will be formed simultaneously under favorable condition. The electrostatic potential field shown in the figure is reproduced from a previous calculation[5] which shows that a favorable field can be achieved for extracting both positive ions and negative ions with high collection efficiency. This is especially true during an EI operation because of less frequent ion-molecule collisions.

Concept 2: Variation of Ion Source Conductance Through Reversible Gaseous Flow. In order to individually optimize the operating conditions of CI and EI and to facilitate the rapid CI/EI or CI/CI switching the ion source conductance should be made variable. However, due to the delicate nature of the ion source assembly no conventional design has been made practical to effect rapid and repetitive variation of the ion source conductance without severely deteriorating the operation of CI or EI. In the present approach the variation of the effective ion source conductance is achieved without changing the ion source configuration. For the purpose of illustration a simplified schematic of the present design is shown in Fig. 2 (A and B). In this figure a three-way valve is shown which is placed in the close vicinity of the source and in communication with the ion source using a short flexible tubing. The second port of the valve is connected to a CI reagent gas source while the third port is constantly exposed to the mass spectrometer vacuum housing. During a CI operation the CI reagent gas is flowing into the ion source as shown in Fig. 2 (A). At the completion of the CI operation the valve is switched to a new position as shown in Fig. 2 (B). Instead of being idle and acting as a dead volume the flexible tubing is seen to provide a new pumping route for the ion source. The gaseous flow in this tubing is reversed and the residue gaseous content of the ion source will be rapidly pumped away. The effective ion source conductance will also be substantially increased during the subsequent EI operation.

Concept 3: Elimination of Dead Volume in the CI Reagent Gas Inlet System. In the conventional single source mass spectrometers capable of CI/EI or CI/CI switching a relative long waiting time is normally required for each mode switching. The root of the problem is to a large extent due to the undesirable CI reagent gas inlet system design in which a large dead volume inevitably exists. During each mode switching the gas that is trapped within the volume must be pumped away which can cause a time delay at least in the order of several sec.

However, under closer examination it is found that this large dead volume is really not necessary, and can be eliminated if a better CI reagent gas inlet system can be divised. This concept is schematically represented by a 4-way valve design shown in Fig. 2 (C, D and E). Only one of the three ports at a time as shown (C, D or E) is in communication with the fourth port which is connected to the ion source. The most unique feature of this valve is that each CI reagent gas inlet port is equipped with a built-in flow restrictor. This flow restrictor serves the function of a conventional metering valve for regulating the flow rate of the CI reagent gas. The restrictor shown here is in the form of a porous element. Many other possible forms of the flow restrictor, such as a single or multiple capillary passages or adjustable needle, etc. can also be employed. Since the flow restrictor is placed in the close vicinity of the valve aperture there is practically no dead volume and instant CI/EI or CI/CI switching can be achieved.

For the purpose of evaluation the ion source gas pressure profiles during a typical

operation cycle in a design based on these concepts are calculated. For simplicity a cyclic operation with a format of [± CI/± EI] is chosen for the present calculation. Assume that the mass spectrometer is interfaced with a capillary GC column with its effluent (containing a sample of M.W. of 256 and concentration of 0.01%) directly introduced into the ion source continously. He is used as the GC carrier gas (1 cc-atm/min) and CH_4 is the CI reagent gas independently introduced into the ion source during the CI operation (2 cc-atm/min). The ion source is assumed to have a volume of 0.5 cc and have two ion exit aperture of 0.5 mm dia. each. The flexible tubing is assumed to have an ID of 0.48 cm and length of 2 cm.

The results of this calculation are shown in Fig. 3 which shows the time profiles of the pressures of CH_4, He, sample and the total mixture during one complete operation cycle. The results clearly indicate that a switching period of 0.1 sec is more than adequate allowing for ion source rejuvenation and pressure stabilization in a cyclic EI/CI or CI/CI operation.

The above three innovation concepts are based on sound physical principle and can be economically implemented without much engineering difficulties. It forms the basis of a new automated multimode mass spectrometer system (Fig. 4) which is currently in progress. This offers a promise of more complete sample analysis without sacrifice of either spectra quality or detection sensitivity, with a saving of sample material, analysis time and labor.

1. C. Chang, Amer. Lab. 12 (11), 49 (1980). 2. C. Chang, 28th Annual Conference on Mass Spect. and Allied Topics, (1980) p. 34. 3. H.J. Svec and G.D. Flesch, Int. J. Mass Spect. Ion Phys., 1 (1968) pp. 41-52. 4. Hunt, D.F., et al, Anal. Chem. 48, 2098 (1976). 5. C. Chang, G.J. Sroka, and G.G. Meisels, Int. J. Mass Spect. Ion Phys., 11 (1973) p. 367.

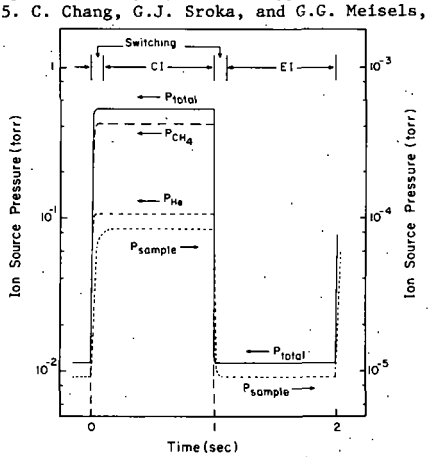

Fig. 3. The ion source pressure profiles for CH_4, sample, He and the total mixture during one CI/EI operation cycle.

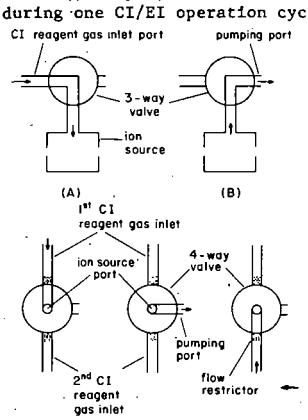

Fig. 2. The schematic representation of a 3-way valve (A and B) and a 4-way valve for CI/EI and multiple CI operation.

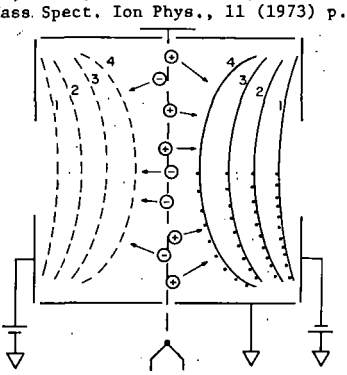

Fig. 1. The schematic of an ion source for SPINICI. The solid curves 1, 2, 3 and 4 are calculated equipotential lines[5] corresponding to 20, 40, 60 and 80%, respectively, of the extraction potential (in the positive ion side). The solid points are the measured values. The dash curves are the estimated equipotential lines in the negative ion side.

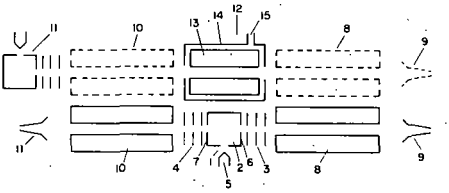

Fig. 4. Schematic illustration of a mass spectrometer design for AMMS application. The quadrupole mass filters 8 and 10 and the electron multiplier 9 are mounted on a rotatable shaft. The shown position corresponds to SPINICI operation. When they are swung to the new position (dash line) the mass spectrometer becomes capable of MS/MS operation (triple-quadrupole MS).

IDENTIFICATION OF NITROAROMATICS IN DIESEL EXHAUST PARTICULATE BY GC/NICIMS; K. B. TOMER, M. D. ERICKSON, D. L. NEWTON, P. R. GENTRY, and E. D. PELLIZZARI, Analytical Sciences Division, Research Triangle Park, NC 27709 and R. B. ZWEIDINGER, Mobile Source Emissions Research Branch, Environmental Sciences Research Laboratory, U.S.E.P.A, Research Triangle Park, NC 27711.

Diesel exhaust particulate extracts have been found to be mutagenic in the Ames microbial assay.[1] This mutagenicity has generated much concern about health effects from exposure to diesel exhaust particulate. The importance of identifying mutagenic organic components in diesel exhaust particulates and complexity of the organic material has led to separation of extracts into less complex fractions. One semipolar fraction, which exhibited high mutagenicity, was selected for intensive characterization.

To identify components, the fraction was initially analyzed by glass capillary/negative ion chemical ionization mass spectrometry (GC/NICIMS). The NICIMS analyses were performed using methane as a moderating gas, with negative ion formation by capture of thermal electrons. The reconstructed gas chromatogram (RGC) is shown in Fig. 1. For comparison the electron impact GC/MS analysis was also performed, with the RGC also shown in Fig. 1. As expected, the NICIMS analyses showed much less interference from hydrocarbons in the spectra. Figs. 2 and 3 show the NICI mass spectrum of two components (Peaks No. 53 and 80) identified as nitroanthracene and nitropyrene by comparison of elution times and spectra with standards. NICI mass spectra of authentic materials are shown in Figs. 4 and 5. In addition to the excellent spectral agreement the retention times agreed. In the absence of a complete series of standards the exact position of the nitro substituent on the ring as well as the configuration of the aromatic nucleus cannot be unambiguously specified. Nitropyrene has been characterized as a direct mutagen. Therefore confirmation of its identity was a primary concern. High resolution mass spectral analysis of the extract gave $C_{16}H_9NO_2$ as the composition of the m/z 247 ion. GC/FTIR was also used for confirmation. The standard spectra of nitropyrene and the unknown spectra are shown in Fig. 6. Again, an excellent correlation was observed with major absorbance peaks occurring at identical wave numbers (± 4 cm^{-1}).

Thus nitropyrene/fluoranthene and nitroanthracene/phenanthrene were identified in mutagenic diesel exhaust particulate extracts with a high degree of certainty.

This work was supported by EPA Contract No. 68-02-2767.

[1]Ames, B. N., J. McCann, E. Yamasaki, Mutation Res., 31, 347 (1975)

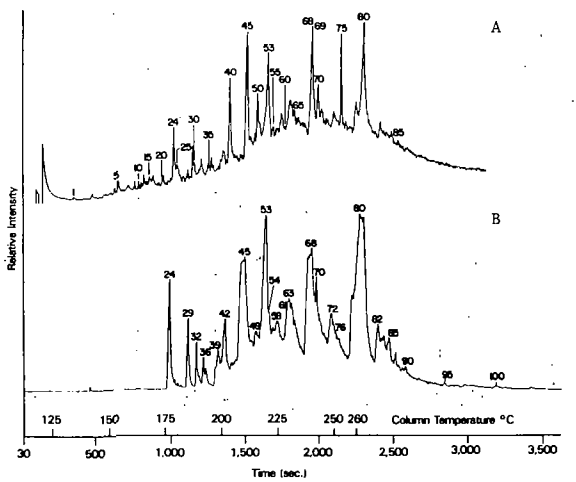

Fig. 1. A) RGC of NICI analysis; B) RGC of EI analysis.

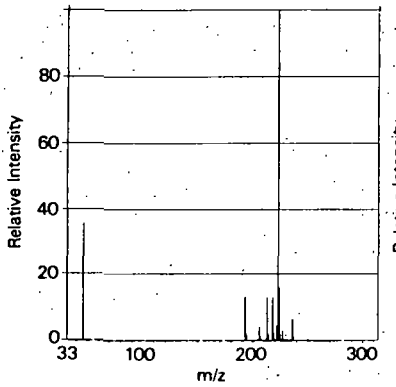

Fig. 2. NICI spectrum of eluant 53.

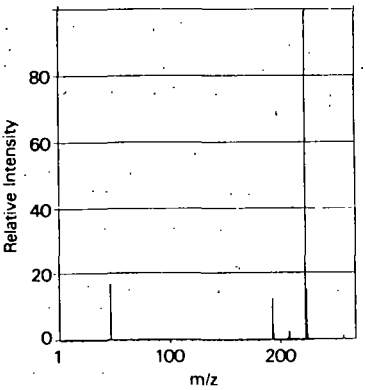

Fig. 3. NICI spectrum of 9-nitroanthracene.

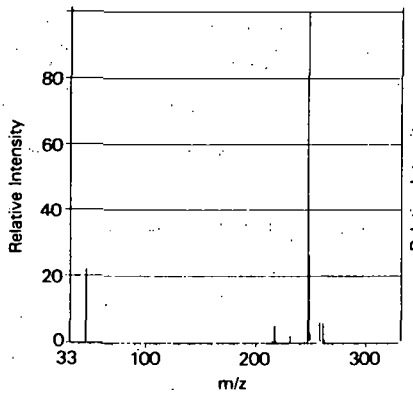

Fig. 4. NICI spectrum of eluant 80.

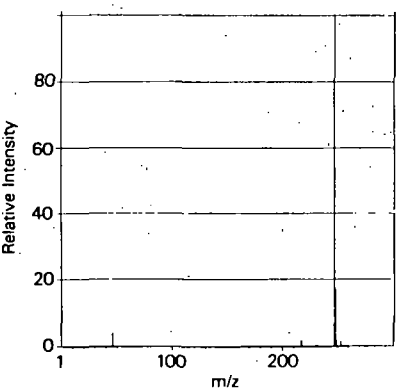

Fig. 5. NICI spectrum of nitropyrene.

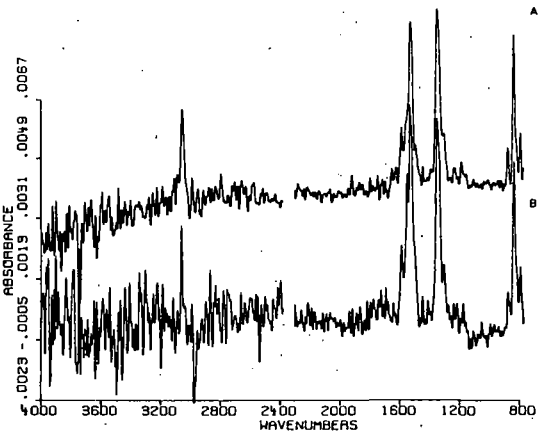

Fig. 6. A) GC/FTIR spectrum of analyte; B) GC/FTIR spectrum of 3-nitropyrene.

GC/MS INVESTIGATIONS OF PARTICULATE ORGANIC MATTER FOUND IN THE ENVIRONMENTAL SAMPLES; R.C. Lao, M. Lanoy, R. S. Thomas and S. W. Lee; Chemistry Division, Air Pollution Control Directorate, Environment Canada, Ottawa, Canada, K1A 1C8

The compounds of particulate organic matter (POM) are found throughout the biosphere as trace pollutants. Although often present only in trace concentrations, these compounds are the source of much concern since many of them have shown biological activities. Sharp increases in cost of the petrochemical fuels used for conventional heating systems stimulated a corresponding interest in renewable resource fuels and wood burning stoves as alternative domestic heating sources, this type of heating may increase substantially the existing POM and other toxic organic pollutants into the environment.

In this study, high resolution capillary GC is used for the analysis of organic pollutants and confirmation is made by quadrupole GC/MS. Negative ion spectra are obtained with CI source for the identification of many compounds found in the samples. Results will be given for the samples of wood burning stove emissions, incinerator exhaust and other environmental contaminated sources.

BREATH ANALYSIS BY APCI/MS - A STUDY OF HUMAN EXPOSURE TO ORGANIC VOLATILES.

F.M. Benoit, Health and Welfare Canada, Ottawa, Canada, K1A 0L2, W. Davidson, A. Lovett, S. Nacson and A. Ngo, Sciex Inc., Thornhill, Canada, L3T 1P2

Real time breath analysis by direct exhalation into a TAGA 3000 via a specially designed inlet system has been used to study the human uptake and elimination of some organic volatiles via the respiratory system. The technique of APCI/MS permits the extraction of volatiles directly from the exhaled gaseous matrix by high pressure chemical ionization, thus eliminating the conventional chemical workup which usually must precede the analysis of exhaled breath by GC/MS.

In a series of experiments to test the feasibility of breath analysis by APCI/MS, a TAGA 3000 was equipped with an inlet system which was designed to allow a controlled and measurable amount of breath into the ion chamber. This was accomplished by inserting a removable capillary tube of known bore and length between the mouthpiece and a mixing chamber into which a carrier gas (zero air) was flowing at a known rate. The quantity of breath introduced into the ion chamber was determined by the pressure drop across the capillary at constant carrier gas flow. The pressure drop across the capillary was measured with a magnehelic manometer which was in view of the subject. The subject was asked to breathe into the mouthpiece such as to maintain a constant pressure on the magnehelic gauge. An adjustable by-pass valve opening to the atmosphere was used to dump the excess breath.

Two problems which caused difficulties were saturation of the ion signal and interferences from compounds of high proton affinities, both of which occurred at higher inlet pressures. The response curves for each solvent studied (methanol, toluene and tetrachloroethylene), obtained by introducing known quantities of the vapour into the system, showed a linear portion at concentrations in the low ppm and below range and a curved portion at concentrations in the high ppm and above range. In order to obtain precise quantitative estimations all the results in present study were obtained at ion chamber concentrations ocrresponding to the linear portion of the responses curves. Interference from volatiles of higher proton affinity than the compound of interest occurred when the concentrations in the ion chamber were sufficiently high that collisions between the protonated exposure compound and a compound of higher proton affinity were likely. This served to deplete the ion signal of the exposure compound and the quantitative response factor, determined in the absence of interferences, was no longer valid. This problem was eliminated by dilution of the breath sample. It was found that at a pressure differential of ~ 0.2 inches of water across a capillary of bore 0.5 mm and length 5 cm, the problems of saturation and interference were eliminated and good sample sensitivity was maintained. Under such conditions a dilution factor of 1000:1 was achieved.

Under medical supervision, human subjects were exposed to artificially contaminated atmospheres containing low levels of methanol (~ 100 ppm), toluene (~ 50 ppm) or tetrachloroethylene (~ 100 ppm) for a period of ~ 90 min. in an enclosed chamber. The exposure levels were selected to be one half the recommended TLV-TWA for each compound. The exposure compound was loaded by bleeding bottled air, which had been bubbled through the selected solvent, into an airstream from outdoors. During the exposure experiment, the level of the exposure compound in the exposure chamber was monitored continuously by FID. The subject's breath was monitored during (in some cases) and after (in all cases) the exposure period for a selected ion, characteristic of the exposure compound (methanol: MH^+, m/e 33, toluene: $(M-H)^+$, m/e 91 and tetrachloroethylene: Cl^-, m/e 35).

The instrument response to the subject's breath was virtually instantaneous; at the beginning of each exhalation the ion signal rose sharply and at the end of each exhalation dropped sharply to background levels with little or no tailing. Cross contamination of the system from one breath to another was not observed.

The levels of the exposure compound on a subject's breath was observed to be an average of 18% for methanol, 17% for toluene and 13% for tetrachloroethylene of the levels in the air of the exposure chamber. These results indicate that a substantial amount of the organic volatile was retained by the subjects. The fate of the retained materials has not been determined. It is noteworthy, however, that no metabolic products of the exposure compound could be identified unambiguously in the

breath of exposed subjects.

The disappearance of the exposure compound from the subject's breath following exposure was exponential and followed first order kinetics. The half life varied from subject to subject and from compound to compound. Average half life values for the disappearance of the exposure compound from breath were 24 min. for methanol, 27 min. for toluene and 79 min. for tetrachloroethylene, indicating a fairly rapid clearout of the respiratory system following exposure. However, we must be cautious in the interpretation of this result because the disposal route of the exposure compound is unknown. It could well be that the disappearance of the exposure compound occurs by absorption into the body rather than by emission into the exhaled breath.

These preliminary results demonstrate the viability of APCI/MS for the real time monitoring of volatile compounds on the breath of human subjects.

ATMOSPHERIC PRESSURE IONIZATION MASS SPECTROMETRY: THE ISOMER SPECIFIC DETERMINATION OF TRACE LEVELS OF 2,3,7,8-TCDD IN THE PRESENCE OF CONTAMINANTS

R. K. Mitchum, W. A. Korfmacher and G. F. Moler
DHHS/FDA/National Center for Toxicological Research
Jefferson, Arkansas 72079

The distribution of chlorinated hydrocarbons in the environment and food chain has been a concern of regulatory agencies for many years and will continue to be one of the prime regulatory and research areas in the federal and industrial sector. Of the numerous chlorinated aromatic hydrocarbons the most toxic and persistent class of compounds is represented by the tetrachlorodibenzo-p-dioxins (TCDDs). The 2,3,7,8-tetrachlorodibenzo-p-dioxin (2,3,7,8-TCDD) isomer has been found to be the most potent chemical toxicant of this group. The analytical methods which have been utilized for the determination of TCDDs include electron capture gas chromatography, GC-low resolution mass spectrometry, GC-high resolution mass spectrometry, metastable ion monitoring, and low and high pressure negative chemical ionization mass spectrometry. Several interferences exist which preclude determination by several of these analytical techniques. These include contaminants such as p,p'-DDE, a minor component of toxaphene, PCBs, benzylphenylethers and tetrachloromethoxybiphenyls which interfere with the analysis by having similar gas chromatographic retention indices and/or interfering mass ions.

The variation in the biological activity of the TCDD isomers and the finding of several TCDD isomers in environmental samples has led to the need for an isomer-specific method for the determination of 2,3,7,8-TCDD. The synthesis of the 22 TCDD isomers has recently been reported. Lamparski and Nestrick(1) have reported an isomer-specific method for 2,3,7,8-TCDD based on extensive HPLC fractionation combined with LR/GC and low resolution electron impact mass spectrometry. Buser and Rappe(2) have recently reported an isomer-specific method for 2,3,7,8-TCDD using HR/GC combined with low resolution electron impact mass spectrometry.

The negative ion chemical ionization mass spectrometry of the TCDD isomers in an oxygen-rich plasma has been proposed(3) to be specific for the 2:2 chloro-substituted TCDD isomers based upon both the formation of a unique ion, the 4,5-dichloro-1,2-benzoquinone radical anion, and the phenoxide ion resulting from oxygen substitution with loss of chlorine. This paper reports the investigation of the reactions of the 22 TCDD isomers in an oxygen-rich plasma at atmospheric pressure and demonstrates the selectivity of this methodology for the 2,3,7,8-TCDD isomer when coupled with high resolution capillary gas chromatography.

Dissociative electron capture to form Cl^- is the predominant pathway for all 22 TCDD isomers. Associative electron capture occurs for a limited number of the TCDD isomers. All of the 2:2 substituted TCDD isomers form molecular anions except for the 1,3,7,8- and 2,3,7,8-isomers. The 1:3 TCDD isomers substituted in the 1,2,4,6 and 1,2,4,9 positions also form molecular anions.

The formation of the oxygen-substituted phenoxide ion corresponding to the M-19 anion (M-Cl+O) is shown to occur for all of the 2:2 chloro-substituted TCDD isomers. This observation is contrary to the general scheme proposed by Hass(3), albeit under different conditions, that only TCDD isomers having chlorine in the peri position could form the phenoxide anion and that the 2,3,7,8-TCDD isomer does not form this ion-molecule product.

The formation of the dichlorobenzoquinone anion, m/z 176, is shown (Figure 1) to occur for all 2:2 chloro-substituted isomers. The 1:3 and 0:4 chloro-substituted isomers did not form m/z 176; this result agrees with previous predictions (3).

A high resolution gas chromatogram of the 22 TCDD isomers (Figure 1) was obtained by monitoring m/z 35. Since all 22 TCDD isomers undergo dissociative electron capture to form Cl^-, this high resolution chromatogram would analogously correspond to a typical analysis using electron impact and monitoring the molecular ion, m/z 320. The selectivity of the ion molecule reaction to form m/z 176 is shown in Figure 1. Three TCDD isomers failed to separate completely from 2,3,7,8-TCDD when monitoring m/z 35: 1,2,3,7-, 1,2,3,8- and 1,2,3,9-TCDD. These isomers were shown not to interfere with 2,3,7,8-TCDD when the dichlorobenzoquinone anion, m/z 176, was monitored. Therefore, baseline resolution of the 2,3,7,8-TCDD isomer is obtained in the presence of isomers which co-

elute chromatographically. Application of both this ion-monitoring scheme and the capillary chromatography is straightforward and the technique allows for an isomer-specific determination of the 2,3,7,8-TCDD isomer.

The investigation of compounds which are known to interfere with low resolution electron impact analysis was performed on a mixture consisting of p, p'-DDE, PCB's (Arochlors 1242, 1254 and 1260), toxaphene, and a commercial pesticide mixture (Alltech PE-Mix-A, containing several chlorinated pesticides) to determine the extent of any interference. Even though this mixture represents a worst-case example (i.e., very little sample cleanup) the results (Figure 2) indicated that no interference with 2,3,7,8-TCDD determination existed when the methodology described here was used. This lack of interference, coupled with the capacity for baseline resolution of the 2,3,7,8-TCDD isomer in the presence of other interfering TCDD isomers, is of significant analytical value.

(1) Lamparski, L. L.; Nestrick, T. J. Anal. Chem. 1980, 52, 2045-2054.

(2) Buser, H. R.; Rappe, C. Anal. Chem. 1980, 52, 2257-2262.

(3) Hass, J.R.; Friesen, M.D.; Hoffman, M.K., Org. Mass Spectrom., 1979, 14, 9-16.

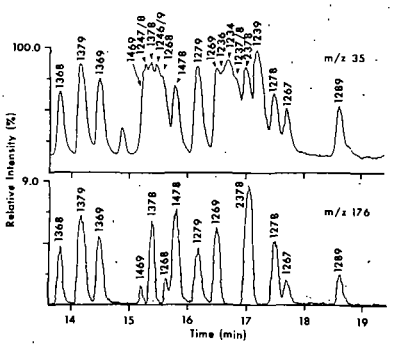

Figure 1
Chromatogram of the 22 isomeric TCDDs.

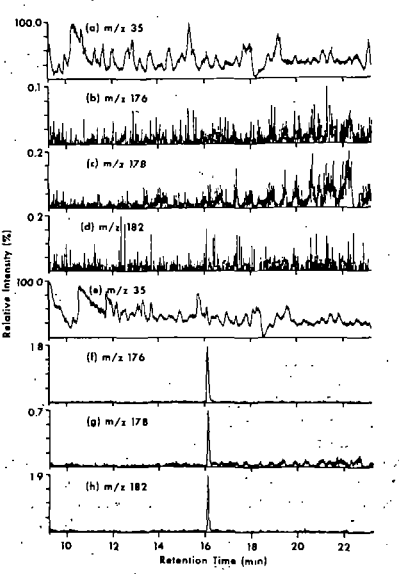

Figure 2
Traces a-d: Chromatogram of mixture of interferring compounds. Traces e-h: Chromatogram of mixture plus .3 ng each ^{12}C and ^{13}C 2,3,7,8-TCDD.

APPLICATIONS OF GC-MS FOR DETERMINATION OF CHLORINATED DIBENZO-p-DIOXINS AND CHLORINATED DIBENZOFURANS IN THE PRODUCTS FROM INCINERATION OF CHEMICAL WASTES

T.O. Tiernan, J.H. Garrett, J.G. Solch, G.F. VanNess and M.L. Taylor
Brehm Laboratory and Depts. of Chemistry and Pharmacology/Toxicology
Wright State University, Dayton, Ohio 45435

A comprehensive analytical scheme has been developed for quantitative determination of the entire series of chlorodibenzo-p-dioxins (CDDs) and Chlorodibenzofurans (CDFs) in stack effluents and other products resulting from combustion of chemical wastes. Samples are initially extracted and fractionated as indicated by the flow chart in Figure 1.

Figure 1. FLOW DIAGRAM SHOWING SEQUENCE OF OPERATIONS IN PREPARATION OF COMBUSTION PRODUCT SAMPLES FOR ANALYSES OF CHLORINATED DIBENZO-p-DIOXINS (CDDs) AND DIBENZOFURANS (CDFs)

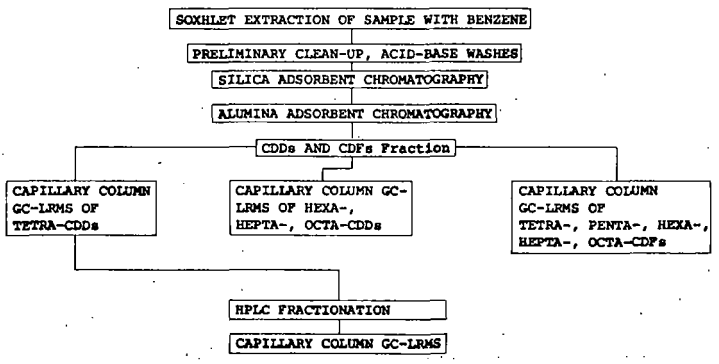

The resultant extracts are analyzed using both capillary column GC-low resolution MS (Perkin Elmer Sigma III GC coupled to a Kratos MS-25 MS) and capillary column GC-high resolution MS (Varian 3700 GC, coupled to an AEI MS-30 MS). Several different capillary GC columns (50-meter) are utilized, including OV-101, Silar 10C and new mixed phase, Silov-82. Selected ion monitoring MS is used to detect and quantitate CDDs and CDFs. At least one CDD and CDF isomer of each chlorinated class (Cl through Cl_8) is used for instrument calibration. Typical results from the analysis of one sampling train sample, collected during incineration of chlorinated chemical wastes, are shown in Table 1. The use of capillary GC columns in the GC-MS analyses permit the determination of individual TCDD isomers in the combustion products. All 22 TCDD isomer standards are available for calibration purposes. Typical results of TCDD-isomer analyses are shown in Table 2. Similar results for other chemical waste combustion studies will be presented, along with a more detailed description of the analytical procedures.

TABLE 1. HIGH RESOLUTION GAS CHROMATOGRAPHIC-LOW RESOLUTION MASS SPECTROMETRIC DATA ON TOTAL CDDs AND CDFs (TETRACHLORINATED THROUGH OCTACHLORINATED) IN PROBE WASH SAMPLE FROM INCINERATION TESTS AT ROLLINS ENVIRONMENTAL SERVICES, DEER PARK, TEXAS.

CDD/CDF[a]	NUMBER OF APPARENT ISOMERS	QUANTITY OF TOTAL CDD/CDF DETECTED IN TOTAL SAMPLE (ng)[b]	MINIMUM DETECTABLE QUANTITY (ng)	% RECOVERY[c]
TCDD	7	3.8	0.4	100
PCDD	4	4	0.3	--
HxCDD	2	1	0.5	--
HpCDD	1	2	2	100
OCDD	1	5	3	--
TCDF	7	5	0.2	--
PCDF	6	30	0.3	--
HxCDF	4	25	0.5	--
HpCDF	2	12	2	--
OCDF	1	10	3	--

a. Prefix designations are: T = tetra-; P = penta-; Hx = hexa-; Hp = hepta; O = octa-.

b. Results corrected for recovery on the basis of recovery of added internal standards.

c. Recoveries for the CDDs were estimated on the basis of recovery of two internal standards added to the samples prior to processing. These standards are $^{37}Cl_4$-2,3,7,8-TCDD, the recovery of which was assumed to be indicative of the recoveries of native PCDDs and lower chlorinated CDDs (that is, mono- through penta- CDDs), and $^{37}Cl_4$-1,2,3,4,6,7,8-HpCDD, the recovery of which was assumed to be indicative of the recoveries of native HxCDDs and higher chlorinated CDDs (that is, hexa- through octa- CDDs). No isotopically-labelled CDFs were available, and so the recoveries of CDFs could not be directly assessed. However, recoveries of CDFs are probably on the same order as the corresponding CDDs.

TABLE 2. TCDD ISOMERS DETERMINED IN COMBUSTION PRODUCT SAMPLES FROM INCINERATION OF VARIOUS CHEMICAL WASTES

SAMPLE DESIGNATION	ORIGIN	TCDD ISOMERS DETECTED	% OF TOTAL TCDDs
6-0606	Rollins Environmental Services - Chlorinated Waste Incineration Stack Effluent	1,3,6,8-	25
		1,3,7,9-	22
		1,3,6,9-	9
		1,2,7,9-[a]	9
		Others	35
6-0606	ENSCO - Chlorinated Waste Incineration Stack Effluent	1,3,6,8-	20
		1,3,7,9-	18
		1,3,6,9-	3
		1,2,7,9-[b]	5
		Others	54
80-07-027-44	Acurex - PCP Waste Incineration - Ash	1,2,7,9-	--
		1,3,6,8-	--
		1,3,7,9-[c]	--
		Others	--

a. TCDDs are also observed at retention times corresponding to the 1,3,7,8-; 1,2,6,8-; and 1,2,6,9- isomers, but these isomers are apparantly no completely resolved from several other TCDD isomers which could also account for these peaks.

b. TCDDs are also observed at retention times corresponding to the 1,3,7,8-; 1,2,6,8-; and 1,2,3,4- isomers, but these peaks may also be accounted for by several other isomers.

c. TCDDs are also observed at retention times corresponding to the 1,3,7,8- and 1,2,3,4-TCDD isomers, but these isomers are not uniquely resolved from other TCDD isomers under the conditions of these analyses.

GC-MS PROCEDURES FOR DETERMINATION OF CHLORINATED DIBENZO-p-DIOXIN ISOMERS IN PARTICULATES FROM COMBUSTION SOURCES

J.G. Solch, T.O. Tiernan, G.F. VanNess, J.H. Garrett and M.L. Taylor
Brehm Laboratory and Depts. of Chemistry and Pharmacology/Toxicology
Wright State University, Dayton, Ohio 45435

The efficacy of several different capillary gas chromatographic columns for separating the 22 isomers of tetrachlorodibenzo-p-dioxin (TCDD), and for quantitative measurements of these using GC-MS, has been determined. The GC columns evaluated include 50-meter OV-17, OV-101, and Silar 10C columns, which have been previously utilized in various laboratories, as well as a new mixed-phase 50-meter column, Silov-82, developed to our specifications. These studies indicate that the latter column is superior to those previously employed (see Table 1 and Figure 1) for TCDD isomer determinations, and exhibits excellent sensitivity (picogram-level) analytical reproducibility, and stability.

The Silov-82 column has been used in a Perker-Elmer Sigma III Gas Chromatograph coupled to a Kratos MS-25 Mass Spectrometer which is controlled by a DS-50SM Computer system, for analyses of TCDD isomers in a variety of combustion products.

TABLE 1. TCDD ISOMERS UNIQUELY RESOLVED ON DIFFERENT CAPILLARY GC COLUMNS

Column Coating	Number of TCDD Isomers Resolved
OV-17	7
OV-101	9
Silar 10C	11
Silov 82	14

These solid samples were first extracted in a Soxhlet apparatus, generally using benzene, and the extracts were subjected to a sequence of washings with dilute base, concentrated acid and water. The organic extracts were next separated preliminarily by liquid column chromatography using a combination acid and base-treated silica gel and highly activated basic alumina. The extracts were further fractionated using reverse phase High Performance Liquid Chromatography. Finally, these extracts, containing the TCDDs, were subjected to GC-MS analysis, as described above. Some extracts were also analyzed by GC-high resolution mass spectrometry using a Varian 3740 Gas Chromatograph coupled to an AEI MS-30 Mass Spectrometer.

The results of analyzing extracts of fly ash from a municipal refuse incinerator are shown in Figure 2. At least eighteen TCDD isomers were detected, the 1,3,6,8-, 1,3,7,9-, and 1,3,7,8- isomers being the major species, while 2,3,7,8-TCDD is present only at very low concentrations. Figure 3 shows similar results for soot collected from the chimney of a wood-burning fireplace. In this case, at least 15 distinct isomers are present, and again, the major isomer components are 1,3,6,8- and 1,3,7,9-TCDD. The results of similar analyses of other combustion products will also be discussed.

Figure 1. Selected Ion Mass Chromatograms For Silov-82 Capillary Column GC-MS Analysis Of A Mixture of 22 TCDD Isomers.

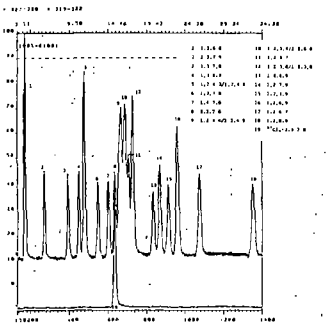

Figure 2. Selected Ion Mass Chromatograms For Silov-82 Capillary Column GC-MS Analysis Of An Extract Of Fly Ash From A Municipal Refuse Incinerator.

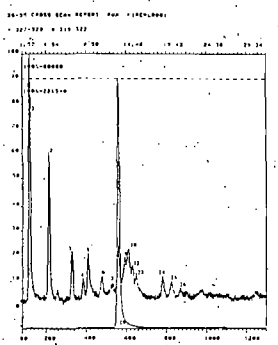

Figure 3. Selected Ion Mass Chromatograms For Silov-82 Capillary Column GC-MS Analysis Of Soot From a Wood-Burning Fireplace.

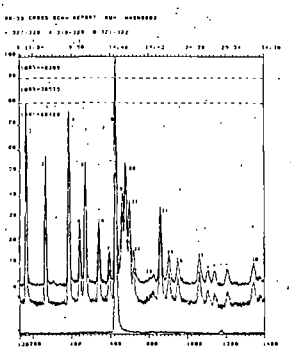

QUANTITATIVE HRGC - HRMS: STUDY ON THE USE OF A NON - ISOTOPICALLY LABELLED INTERNAL STANDARD IN THE ANALYSIS OF 2,3,7,8-TCDD IN MILK.

Yves Tondeur, J. Ronald Hass, Phillip W. Albro, Joanna L. Schroeder and Kun Chae

NIEHS, P.O. Box 12233, Research Triangle Park, NC 27709

Introduction

A high resolution glass capillary column gas chromatograph coupled to a high resolution mass spectrometer has proven itself useful as an analytical tool in meeting the requirements to identify, confirm and quantitate trace levels of TCDD (1). During the past few years, specific qualitative criteria have been developed. Quantitative analysis usually involves the use of an internal standard which is typically an isotopic variant of TCDD added to compensate for sample handling losses. By using selected ion monitoring techniques, the limitations of the use of a non - isotopically labelled internal standard (2) are evaluated.

Instrumentation

GC: HP - 5700 gas chromatograph with a 20 m fused silica OV 1 column (i.d. 0-2 mm; coupled directly into the MS source) is programmed from 150°C to 220°C at 8°C/min.

MS: Reversed geometry ZAB-2F VG Micromass coupled to a Finnigan/Incos 2300 Data System is operated in the EI mode (70 eV). The exact masses monitored are m/z 321.8935 for TCDD and m/z 339.8841 for (2). The lock mass is a fragment ion from C_2I_4 at m/z 277.8093. Usually, the corresponding dwell times are 0.5, 0.5 and 0.2 sec respectively. The resolution is 10,000 (5% valley) and the accelerating voltage is 8 KV. The window size of the scanning ESA voltage is 200 ppm (see fig. 2) allowing one to visualize the peak profile centered in the channel.

Results and Discussion

As a part of the development of a validated procedure for the analysis of TCDD (ppt level) in human milk, a GC-MS evaluation of the utility of 1,2,3,4-tetrachloro-7-fluoro-dibenzo-p-dioxin (2) as an internal standard is being conducted. The two compounds 1 and 2 do not coelute (ΔR_t = 46 sec; RSD = 1.6%; N = 6) and produce ions at different m/z.

Evaluation of the GC-MS system: In the range of the concentrations envisaged (i.e. from 10 to 100 pg/µl), the variation of the latter has been found to have no significant effect upon the area ratio measurements, although the ratio is significantly affected by the dwell times (0.2; 0.5; 1 sec). Neither parameter affects the precision on the area ratio evaluations. A minimum variance is observed when the amounts of TCDD and F-TCDD (2) are equal and does not exceed unreasonable values when the weight ratio ranges from 0.3 to 12 (fig. 4). Data obtained over a period of 4 days show a significant variation for the area ratios indicating the need of a better control of the mass spectrometer parameters. For example, one notices that the ratio value increased when the absolute intensity of the lock mass decreased.

Evaluation through the procedure: Goat milk (lipid content = 25 mg/ml; RSD 1.3%; N = 3), used in these exploratory experiments, is spiked followed by an hydrolysis, extraction and two clean-up steps. The first step in the clean-up (removal of the bulk of the lipids and aliphatic compounds) is definitely not sufficient by itself, as evidenced by (1) chemical noise (fig.3), (2) the presence of an "quantitative interference", i.e. an unidentified component in the mixture which co-elutes with TCDD, affecting the sensitivity. The difference between the measured area ratio of the sample and the one obtained from the standard mixture on the same day is 70 times the standard deviation of the latter. The response obtained from the control milk spiked after clean-up and prior GC-MS is within one σ. The second clean-up step (removal of traces of lipids, PCB's and other potential chlorinated interferences) is fully justified as exemplified by the elimination of the previously mentioned "quantitative interference" and by the net reduction in chemical noise. Although the data in fig. (5) are indicating that the 2 compounds are not recovered to the same extent, it would be at this moment premature to decide whether or not 2 is a suitable internal standard.

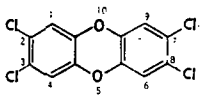

1

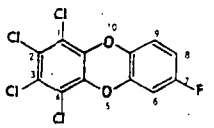

2

Fig. 1

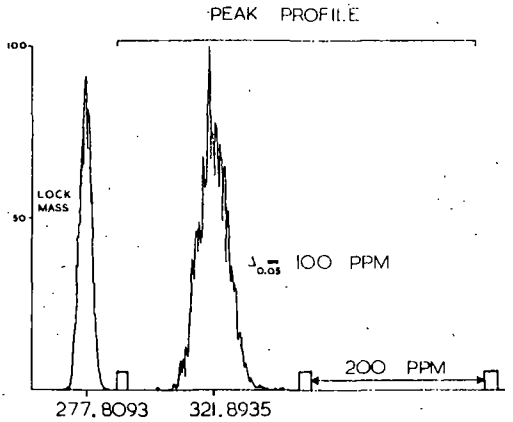

Fig. 2

Fig. 3

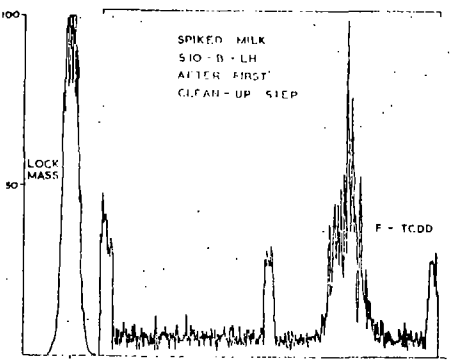

Fig. 5

INFLUENCE OF CONCENTRATION RATIOS

UPON PRECISION OF AREA RATIO MEASUREMENT

CONCENTRATION RATIOS*	CV(%; N = 3)
12	7.4
3	4.5
1.2	2.0
0.3	18.7

*AMOUNT OF P-TCDD IS HELD CONSTANT AT 10PG.

Fig. 4

QUANTITATIVE DATA

AFTER SECOND CLEAN-UP STEP

1 PPB LEVEL(TCDD): DUPLICATE EXP. CV = 14.9%

(AMOUNT OF P-TCDD HELD CONSTANT)

N=3	RSD A TCDD	RSD AF-TCDD	RSD A.R.	MEANS AREA RATIOS
STANDARD MIXTURE	5.0	7.4	11.9	0.1268
S10-B-LH-A_{540}	13.4	21.5	8.8	0.0888*
S10-C-LH-A_{540}	14.2	7.4	19.0	0.0719*
CONTROL + SPIKE (N=1)	-	-	-	0.1201

Mass Spectral Identification of Chemical Residues Encountered in the Total Diet Program

David L. Heikes
U. S. Food and Drug Adm.
Total Diet Research Center
Kansas City, MO 64106

The Total Diet Program of the Food and Drug Administration consists of the surveillance of residue levels of pesticides and industrial chemicals in processed foods. Each sample, or market basket, represents the food consumed by a 16-19 year-old male in two weeks. The various items of each market basket are divided into twelve composites, and analyzed by procedures found in the Pesticide Analytical Manual of the FDA. Frequently, residues of tetrachloronitrobenzene (TCNB) and related compounds have been found in the composite of potatoes. TCNB (Fusarex®, Tecnazene®) is used as a post-harvest sprout suppressant on potatoes. The recommended application rate for Fusarex®(6% TCNB) is 1.0 lb. for each 600 lbs. of potatoes.

A sample of Fusarex® was assayed using gas chromatography with electron capture detection and mass spectral confirmation.

TABLE 1
Assay of Fusarex®

Identity	ppm
Tetrachloronitrobenzene (TCNB)	58,300 (5.83%)
Trichloronitrobenzene	570
Tetrachlorobenzene	383
Pentachloronitrobenzene (PCNB)	280
Pentachlorobenzene (QCB)	14

In addition to the impurities found in Fusarex®, several other residues found in potatoes were identified by mass spectrometry. Gas chromatographic comparison of these residues with available or synthesized standards, showed the tetrachlorinated compounds found to be the 2,3,5,6-isomers. TABLE 2 lists the compounds identified in potatoes with GLC retention data relative to pentachlorobenzene (QCB).

TABLE 2
Compounds Found in Potatoes

Identity	relative retention (QCB = 1.00; 6.5 min) 3% OV-1, 130°
Tetrachlorobenzene	0.40
Trichloronitrobenzene	0.86
2,3,5,6-Tetrachloroanisole	1.02
Tetrachloronitrobenzene (TCNB)	1.37
Tetrachloroaniline (TCA)	1.50
Tetrachlorothioanisole (TCTA)	2.72
Pentachloronitrobenzene (PCNB)	2.98
Tetrachloro-p-nitroanisole	3.45
Trichloronitrothioanisole	3.60
Tetrachloro-p-anisidine	3.63

Tetrachloro-p-nitroanisole, tetrachloro-p-anisidine and trichloronitrothioanisole are previously unreported metabolites of TCNB. Their mass spectra are represented in Figures 1 to 3, respectively.

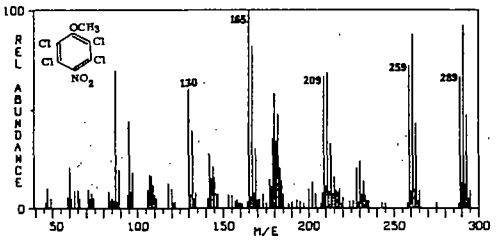

Figure 1 - Electron impact mass spectrum of tetrachloro-p-nitroanisole.

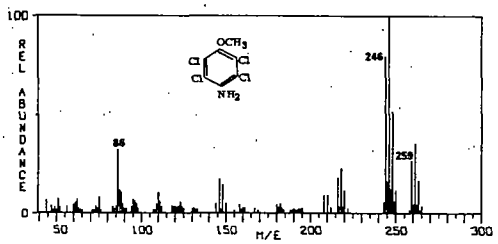

Figure 2 - Electron impact mass spectrum of tetrachloro-p-anisidine.

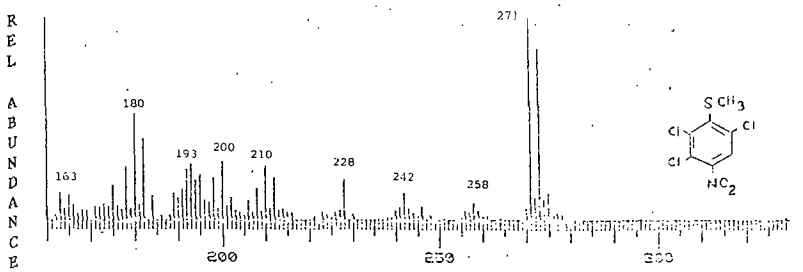

Figure 3 - Electron impact mass spectrum of trichloronitrothioanisole.

IDENTIFICATION AND QUANTITATION OF POLY-CHLORINATED DIBENZOFURANS IN ENVIRONMENTAL SAMPLES; L.M. SMITH, J.L. JOHNSON, D.L. STALLING, J.D. PETTY, G.R. DUBAY; Columbia Nat'l. Fishery Res. Lab; RR 1, Columbia, MO 65201

High resolution (HR) GC/negative ionization (NI)-MS was used to identify polychlorinated dibenzofurans (PCDFs) in processed fish tissue samples. The most abundant tetrchloro-dibenzofuran (TCDF) found in the tissues has the same retention time as 2,3,7,8-TCDF which is very similar in structure and toxicity to 2,3,7,8-TCDD. The level of contamination in most samples measured as total PCDF residues ranged from 25 to 250 ppt. A composite fish sample from an area of extremely high PCB contamination was found to have a total furan contamination of 2000 ppt (2 ppb) including 1 ppb of the component which matched 2,3,7,8-TCDF in retention time and NIMS spectrum. Detection of PCDF residues at 1 ppt (per component) and below was possible by means of multiple ion detection (MID) NIMS; the practical limit of sensitivity was 100 femtograms for individuals components.

A specially developed procedure, which was a critical element of this study, permitted quantitative removal of PCBs and other interferences from planar aromatic residues each as those of PCDFs. Recent improvements in the application of carbon adsorbants to the enrichment of planar aromatic compounds has allowed the removal of a wide variety of non-planar compounds which are known to interfere with the analysis of chlorinated-dibenzofurans and -dibenzodioxins.

Both electron-impact and NIMS were tested for the analysis of PCDF and NIMS was demonstrated to be more sensitive than EIMS. The extent of sensitivity enhancement for NI with respect to EI was observed to be dependent on the extent and position of chlorine substitution. Pentachlorodibenzofurans with different substitution patterns showed significantly different increases in response in NIMS. Thus, a large number of standards are required to determine the concentration of individual PCDF components. The sensitivity of components was increased by using MID of the four most intense ions within the molecular ion cluster of all PCDF.

THE CHARACTERIZATION AND ENVIRONMENTAL IMPACT OF COMPOUNDS FORMED IN THE PHOTODEGRADATION OF POLYBROMINATED BIPHENYL CONGENERS

D. G. Patterson, D. L. Orti, L. W. Yert, R. H. Hill, Jr., J. Lee, J. S. Holler, and L. L. Needham
Department of Health and Human Services, Public Health Service, Centers for Disease Control, Center for Environmental Health, Clinical Chemistry Division, Atlanta, Georgia 30333

In 1973 and 1974, a segment of Michigan's population was exposed to grain, meat, dairy, and poultry products that had been contaminated with Firemaster FF-1, a polybrominated biphenyl (PBB) mixture consisting primarily of hexabrominated biphenyl (see Figure 1). PBBs have low acute toxicity, but are fat-soluble, biologically persistent, and capable of causing chronic injury to the liver, kidneys, skin, and lymphatic tissue. In addition, PBBs have been found in chronic rat-feeding studies to induce neoplastic liver nodules.

Purpose

Degradation of PBBs in the environment can occur by metabolic as well as photochemical pathways. We have undertaken the study of PBB photochemistry in order to assess the environmental significance of this nonbiological degradation pathway.

Results and Discussion

Gas chromatography, nuclear magnetic resonance, and gas chromatography/mass spectrometry (GC/MS) analyses have been used to determine major photodegradation products from a number of important congeners occurring in the commercial polybrominated biphenyl mixture (see Figures 4-8). Rabbit-ear testing was used to examine concurrent changes in biological activity under photolytic conditions. The major component in Firemaster, the inactive hexabromobiphenyl PBB-4 (see Figure 1), is observed to photodegrade to a biologically active mixture of lower brominated biphenyls (see Figure 5). The evidence for the structural assignments for the various decomposition products will be reviewed. Structural identification of isomeric PBBs is assisted by hydride reduction of higher brominated homologues. This reduction when conducted using deuterium reducing agents, can generate isotopically labeled materials for use in quantitative analyses.

Because of this severe activity generated in the photodegradation of PBB-4 (see Figure 5), several soil samples from a manufacturing plant site have been examined for PBB residues. The results suggest that significant degradation has occurred (see Figure 2). Samples with very low levels of PBB were analyzed by negative ion chemical ionization mass spectrometry which provided increased sensitivity (see Figure 3).

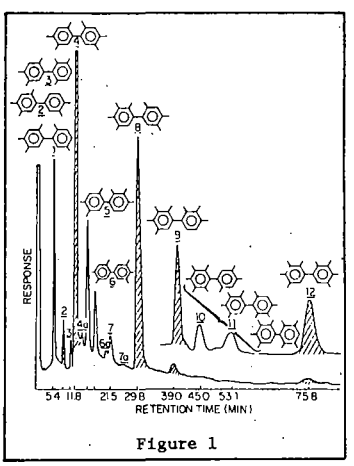

Figure 1

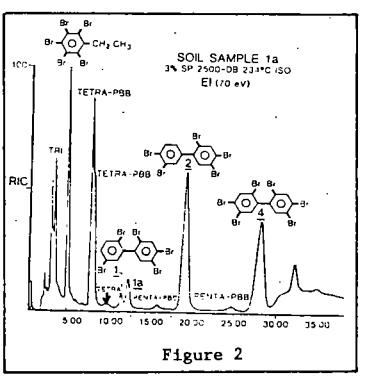

Figure 2

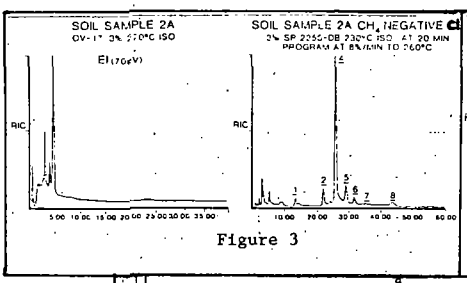

Figure 3

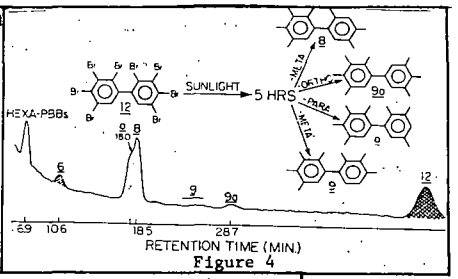

Figure 4

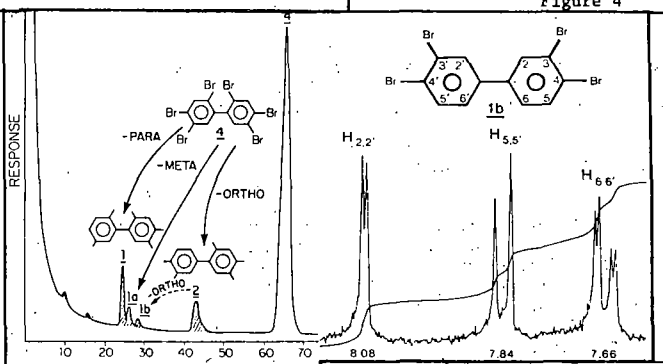

Figure 5

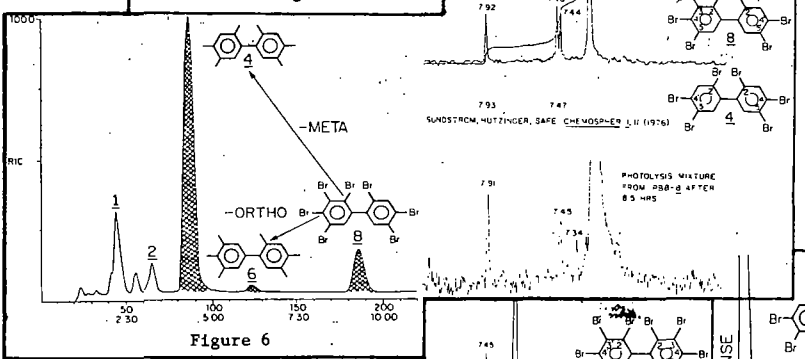

Figure 6

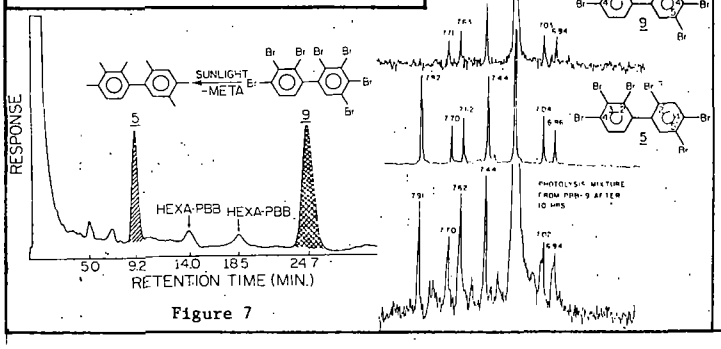

Figure 7

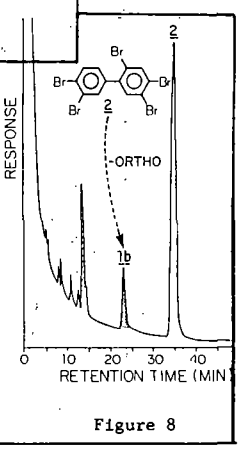

Figure 8

CHEMICAL IONIZATION MASS SPECTROMETRY OF N-NITROSOUREAS

Gary A. McClusky, Shing-Kwan Huang, and William Lijinsky

Chemical Carcinogenesis Program
Frederick Cancer Research Center
Frederick, MD 21701

Many N-nitrosoureas are carcinogens and mutagens, and are important compounds in the drug and agricultural chemical industries. A more thorough investigation of the mass spectrometry of N-nitrosoureas would facilitate the analysis and characterization of this class of compounds. Electron impact ionization of these thermally sensitive compounds generally results in weak intensity or no molecular ions. Enhancement of the molecular ion region eases compound identification and detection by improving the chemical signal to noise ratio for direct mass spectrometric analysis or the MS/MS technique of CID/MIKES.

The chemical ionization of monosubstituted nitrosoureas resulted in formation of $(M+H)^+$ ions with a 10-100 fold enhancement over electron impact ionization. The base peak was derived from the $(M+H)^+$ ion by loss of hydrogen isocyanate to form a protonated diazotic

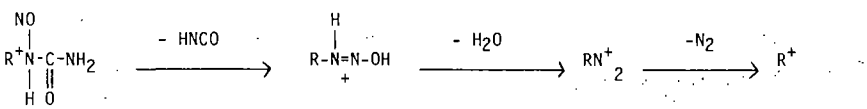

acid ion. Subsequently, the loss of H_2O can occur to produce a diazonium ion followed by loss of N_2 to generate a carbenium ion. The presense of an ion at $(M-28)^+$ was indicative of the corresponding urea as an impurity in the nitrosourea.

As the number of substituent groups is increased, the chemical ionization of di- and trisubstituted nitrosoureas produced substituted isocyanate cations with much greater relative intensity. In addition, when R_1 has a ß-activating substituent as in BCNU, the

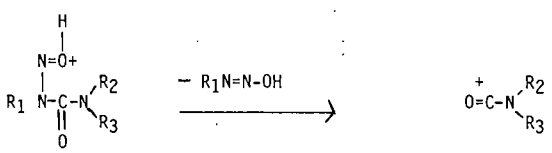

nitroso and activating group can be loss to give an intense fragment ion with the following proposed structure.

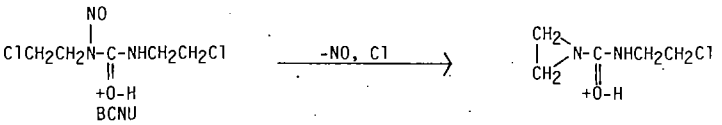

The negative chemical ionization of monosubstituted nitrosoureas resulted in the formation of intense $(M-H)^-$, $(M-30)^-$, diazotate, and isocyanate ions. In addition, there were novel ions appearing at $(M+13)^-$ and $(M+42)^-$. These novel ions are proposed to be formed from an ion molecule reaction between hydrogen isocyanate, $(M-30)^-$ and $(M-H)^-$. The CID/MIKE spectrum indicated that these ions are not just hydrogen bonding adducts but are covalently bonded adducts.

This work was supported by Contract No. N01-CO-75380 with the National Cancer Institute, NIH, Bethesda, MD 20014.

ISOTOPE DILUTION SPARK SOURCE MASS SPECTROMETRIC DETERMINATION OF SULFUR IN NBS IRON BASE ALLOYS.

P. J. PAULSEN and R. W. BURKE; Center for Analytical Chemistry National Measurement Laboratory, National Bureau of Standards, Washington, DC 20234

The sulfur content of iron base alloys needs to be controlled at or below specific concentrations depending on the end use of the alloy. At the same time, routine laboratory methods for measuring sulfur need to be rapid, accurate and low cost. The instrumental techniques currently used are fully capable of meeting these criteria provided standards of proven accuracy are available. In response to recent discrepancies reported for sulfur in steels, a procedure has been developed at NBS utilizing spark source mass spectrometry (SSMS) isotope dilution for the determination of sulfur in iron base Standard Reference Materials (SRM). This method is 10 to 100 times more sensitive than the chemical techniques used previously to certify sulfur in iron SRM's and has the advantage of being a definitive method. Samples, spiked with ^{34}S, are dissolved in a HNO_3-HCl mixture by heating at 180°C in a sealed glass tube. This dissolution technique prevents the loss of any sulfur prior to the equilibration of the natural and spike isotopes. The equilibrated solution is evaporated several times with HCl to remove all traces of HNO_3. The sulfur compounds are then reduced to H_2S using a mixture of hypophosphorus, hydroiodic, and hydrochloric acids. The H_2S is collected as Ag_2S by passing the H_2S through a $AgNO_3$ solution. The dried Ag_2S is mixed with 6-9's pure gold powder, pressed into electrodes and analyzed in the SSMS. The altered sulfur isotopic ratios are measured on the S^{+1} ion using electronic detection SSMS. Sulfur blanks below 1 µg are obtained by use of pure acids and by evaporating the sample under a nitrogen gas atmosphere.

NEGATIVE ION FORMATION FROM SF_6 ON HOT SURFACES

J. E. DELMORE

Exxon Nuclear Idaho Co. Inc.
Box 2800
Idaho Falls, Idaho 83401

Positive surface ionization is a widely used technique for the isotopic analysis of a number of elements. The corresponding negative ion technique has found much less use. One of the main reasons is that hot filaments emit electrons, which are accelerated by the potentials on the negative ion lens, and repulsed by the potentials on the postive ion lens. Negative surface ionization (NSI) must then be limited to conditions under which the resulting electron current does not become large enough to disrupt the operation of the lens due to arcing, charge density defocusing or heating of the focus plates.

Hot filaments operated in the negative ion mode have the potential of ionizing not only by NSI, but also by electron attachment. Many molecules attach thermal electrons (<0.5 volts) to form negative ions. The electron attachment rate drops off very rapidly at electon energies above 0.5 volts. The region in a surface ionization source where electrons have such low energy is limited to just in front of the filament.

Electron emission (EE) is governed by the temperature and by the work function (ϕ) of the surface, and is described by the Richardson equation:

$$EE \propto T^2 \exp(-\phi/kT)$$

If the ionization mechanism were electron capture, ion intensity should be proportional to EE.

Surface ionization rates can be estimated with reasonable accuracy for only a few simple atoms. Molecules, particularly if a decomposition is involved, do not fit a simple theory. The theory, where it does apply, predicts that lowering ϕ improves the ion to electron ratio.

A method for differentiating between NSI and electron attachment is to measure relative ionization efficiency on several filament materials with widely differing work functions. If the ionizaton mechanism is electron capture the ionization process will be similar on all ionizers for a constant electron flux. NSI will give different ionization efficiencies under constant electron flux.

The hexafluorides are a group of molecules that are of considerable interest for this type of ion source. Hexafluorides of S, Se, Te, Mo, W, Re, Ir, Pt, Os, Au and U readily form negative ions. All except SF_6 (ea <0.5 volts) have high electron affinities (3 to 10 volts), and SF_6 has a high thermal electron attachment rate. Thus SF_6 will form negative ions from an electron attachment process, while the others will form negative ions from an NSI process.

UF_6 and SF_6 are already widely used for the isotopic analysis of U and S respectively, using electron bombardment positive ionization. As these molecules readily form negative ions, the investigation of the possibility of performing isotopic analyses of these molecules using the negative ion technique described earlier is a logical step. SF_6 was chosen for the initial experiment due to its non-corrosive nature.

An experiment was set up with a gas inlet connected by a variable leak to the source housing of a NBS 12-90 surface ionization isotope ratio mass spectrometer. Single filaments of LaB_6, ZrC, Hf, W and Re were tested sequentially. The source was pumped to $2 \cdot 10^{-8}$ torr, and SF_6 gas introduced to give $\sim 6 \cdot 10^{-7}$ torr. SF_6^- was the major ion, giving 10^{-11} amp at the collector. Peak shapes and baselines were good. A temperature plateau ($\sim$20°) was observed over which little change ($\sim$0.25%) in ion intensity occurred.

SF_6^- reached a maximum and approximately constant intensity at a constant electron flux for all 5 ionizers. This supports an electron attachment mechanism, as would be predicted from the ea and the electron attachment rate. The drop in intensity when exceeding this optimum electron flux is probably due to defocusing in the ion lens from charge density.

The use of a variable leak precluded high accuracy measurements on sulfur isotope ratios. A viscous flow dual gas inlet would be required to check out this aspect of the measurement. Precision within a measurement, however, is a prerequisite for high accuracy, and this could be checked. A peak stepping data system with a single deep faraday collector was used. All five ionizers gave precisions of better than 0.02% under most circumstances. When attention was paid to operating on the more favorable portion of the ionization curve, and intensity kept below the point where secondary electrons became a problem, LaB_6 produced precisions of better than 0.005% in the $32/34$ sulfur ratio. This precision approaches the limit for the mass spectrometers data system.

The next question to ask is why this type of ion source might be preferred to the electron bombardment sources that are already in wide use for sulfur isotope ratio measurements. The answer is in the mechanical and electronic simplification. The electron trap and all that is required to support it is replaced with a simple filament aligned with the lens, and a simple power supply to heat this filament A strong potential also exists for improved sensitivity due to the high ionization efficiency.

CORRELATIONS BETWEEN THE MASS DISCRIMINATION FACTORS OF URANIUM AND PLUTONIUM,
D. W. Crawford and M. A. Legel, U.S. Department of Energy, New Brunswick Laboratory, Argonne, IL 60439

Calibrated synthetic mixtures of ^{239}Pu and ^{242}Pu isotopes were analyzed by triple-filament thermal ionization mass spectrometry to determine the mass discrimination factor of plutonium relative to that of uranium. This comparison is significant since previous mass discrimination factors for plutonium have been based upon the mass discrimination of uranium. Recent availability of calibrated plutonium standards have made this study possible.

Five synthetic mixtures of plutonium were obtained from the Savannah River Plant. The mixtures were prepared by mixing solutions of National Bureau of Standards (NBS) 949b metal of high ^{239}Pu content with SRP production metal 018A of high ^{242}Pu content. Both "parent" solutions have well-characterized isotopic and assay values and were independently analyzed. Weighed aliquants from one liter stock solutions of the parents were mixed to yield $^{242}Pu/^{239}Pu$ values of approximately 1, 0.1, 10, 0.25, and 4 with prepared uncertainties of ± 0.10%.

These solutions were analyzed concurrently with a series of five calibrated uranium isotopic standards with $^{238}U/^{235}U$ ratios corresponding to the $^{242}Pu/^{239}Pu$ ratios. The high purity NBS U_3O_8 isotopic standard reference material was dissolved in 1:1 HNO_3, and evaporated to dryness. The residues were dissolved and 5% HNO_3 and uranium the concentration adjusted to 1 g/l. Table I lists the $^{242}Pu/^{239}Pu$ ratios in the Pu mixtures and the corresponding $^{238}U/^{235}U$ ratios in the uranium solutions.

TABLE I

RATIO VALUES FOR CALIBRATED SOLUTIONS USED

PLUTONIUM[1]		NBS URANIUM ISOTOPIC STANDARDS	
Mixture	$^{242}Pu/^{239}Pu$	Standard	$^{238}U/^{235}U$
SRP #1	0.9144 ± 0.10%	SRM U-500	1.000302
SRP #2	0.0859_2	SRM U-900	0.096379
SRP #3	8.2903	SRM U-100	8.803140
SRP #4	0.2436	SRM U-800	0.234432
SRP #5	3.7071	SRM U-200	3.979963

[1]Values for January 1981

Ampoules containing aliquants of plutonium mixtures were opened and the solution quantitatively separated from its decay products and other impurities by a HNO_3 anion exchange. The concentration of the resulting clean plutonium solution was adjusted to 1 mg Pu/ml in 5% HNO_3.

A Nuclide 12"90° thermal ionization mass spectrometer was used for the analysis. A triple-filament assembly, consisting of two rhenium sample filaments and a central rhenium ionizing filament, was used as the ion source. Approximately 7 µl of the sample solution was evaporated onto each of the sample filaments and, by passing an electrical current through the filaments, was further heated to form the metal oxide by passing an electrical current through the filament. The assembly was inserted into the source of the mass spectrometer. At a source pressure of 5×10^{-7} torr, the filaments were "flashed" to a specific temperature for 15 seconds, or until the pressure began to drop, to drive off any volatile components (but not the oxide) prior to the beginning of the analysis. The measurement was begun when the pressure in the source had dropped to the low end of the 10^{-7} torr range. The ionizing filament temperature was increased to a temperature of approximately 2100°C and controlled by $^{187}Re^+$ intensity monitoring. Current to a single sample filament was increased to yield a total M^+ intensity of 1V (1×10^{-11} A) for five minutes, a total 3V signal for ten minutes, and readjusted, if necessary, to a 3V intensity at about 15 minutes. The ionizing filament intensity was rechecked and if a stable M^+ intensity existed at typical filament currents with source and analyzer tube pressures of 10^{-7} and 10^{-8} torr, respectively, data acquisition was begun. Sets of

isotope ratio measurements were taken until approximately 45 minutes, at which time the analysis was terminated. This resulted in an average burntime of approximately 30 minutes for each filament run.

Each set of ratios consisted of a total of five scans of the reference peak and the peak being measured (i.e. ^{239}Pu and ^{242}Pu; ^{235}U and ^{238}U) to yield a total of nine ratios. When applicable, any individual ratio in a set which was determined to be a statistical outlier was deleted and a new average determined accordingly. An internal precision statement (relative standard deviation) was calculated for each set and for the mean of all sets for one filament loading. Table II shows the results of the measurements of the plutonium and uranium in terms of mass discrimination factors.

TABLE II

Mixture	Plutonium $^{242}Pu/^{239}Pu$ C.F.[2]	RSD for n Filament Ldgs.		SRM#	Uranium $^{233}U/^{235}U$ C.F.	RSD for n Filament Ldgs.	
SRP #1	1.001971	0.02%	n=5	U-100	1.001995	0.04%	n=4
SRP #2	1.001357	0.03%	n=5	U-200	1.001609	0.03%	n=4
SRP #3	1.001884	0.03%	n=4	U-500	1.001789	0.03%	n=6
SRP #4	1.001590	0.03%	n=5	U-800	1.001637	0.04%	n=4
SRP #5	1.001423	0.04%	n=5	U-900	1.001461	0.01%	n=5
MEAN	1.001645	0.02%		MEAN	1.001698	0.02%	
NBS-SRM-947	1.001661	0.03%	n=5				

[2]Prepared/measured ratio

To observe the fractionation pattern as a function of the rate of change of the correction per unit time, the individual sets of values were plotted on a graph of correction vs. burntime. The slope of the correction curve (theoretically, a straight line) was determined for each filament loading and the average of all loadings per sample calculated. Table III shows these results.

TABLE III
OBSERVED FRACTIONATION PATTERNS OF PLUTONIUM AND URANIUM

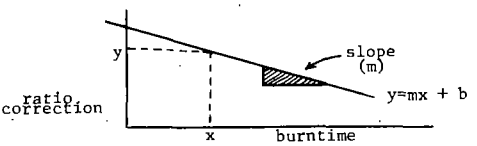

Mixture	Plutonium Slope	Standard	Uranium Slope
SRP #1	-3.0×10^{-5} minutes^{-1}	SRM U-100	-2.3×10^{-5} minutes^{-1}
SRP #2	-3.2×10^{-5}	SRM U-200	-3.3×10^{-5}
SRP #3	-2.8×10^{-5}	SRM U-500	-3.7×10^{-5}
SRP #4	-4.7×10^{-5}	SRM U-800	-3.7×10^{-5}
SRP #5	-3.0×10^{-5}	SRM U-900	-4.9×10^{-5}
MEAN	-3.3×10^{-5}		-3.6×10^{-5}

The study concludes that the mass discrimination corrections due to fractionation are very similar for uranium and plutonium while undergoing thermal ionization.

A PRECISE METHOD FOR THE MASS SPECTROMETRIC DETERMINATION OF LITHIUM ISOTOPE RATIOS.

E. MICHIELS* and P. DE BIEVRE, University of Antwerpen, Central Bureau for Nuclear Measurements, Geel, Belgium.

A mass spectrometric method has been developed for the determination of precise ratio measurements on lithium. The method yields an external reproducibility of better than 1 part in 10^3 (s.d.) on 1 microgram samples. We have applied our method to a first system calibration by means of synthetic mixtures. An absolute value for the isotope abundances of a natural Li sample has been established as well as an atomic weight.

The samples were loaded on the Re filaments of a triple filament thermal ionization source as lithium iodide in 1 $\mu g/\mu l$ solution. The droplets were dried at room temperature in approximately 20 minutes in an exsiccator under a lowered pressure of 0.5 atm. It is believed that in this way more uniform and reproducible sample layers are obtained than is the case with sample drying using resistance heating. To avoid cross contamination during the drying process each sample was put in a little plastic box with a few holes in the upper side.

The mass spectrometric analysis was accomplished at an ionizing filament temperature of 860 °C, determined with a pyrometer. The ionizing filament temperature proved to be an extremely critical parameter which had to be controlled very carefully. Reproducible changes in temperature of a few tens of degrees resulted in more than one percent reproducible changes in the observed isotope ratio. To eliminate erroneous filament temperature setting due to changes in resistance of the filament with temperature, readjustment to 860 °C was made after two minutes. The 'external' reproducibility of these temperatures was well within 5 °C.
The temperature of the evaporation filaments is equally critical. Therefore a measurement pattern (sum of the two isotope signals vs time) had to be followed ridgidly.

Due to isotopic fractionation, the isotope ratio changes with time. Both 'normal','reverse' and 'zero' fractionation were observed during the first part (45 minutes) of the measurement. In all cases the isotope ratio came to the same value and remained almost constant (to within ± 0.01 %) for at least two hours. Data were taken (digital voltmeter readings) between 50 - 70 minutes, when the change with time of the isotope ratio was negligible.

As a result of careful control of the sample drying and instrumental analysis parameters single internal standard deviations better than 0.01 % have been obtained consistently.

The method has been applied to a first rough system calibration with the aid of synthetic isotope mixtures of ^{6}Li (^{6}Li/Li = 0.99) and ^{7}Li (^{7}Li/Li = 0.9999) the ratios of which were known to better than 0.03 % and prepared previously (1). Mixtures were used at 2 - 7 - 7.5 - 8 - 20 - 50 - 80 - 92 % ^{6}Li. The absolute natural isotope ^{6}Li/^{7}Li isotope ratio derived is :

$$^6\text{Li}/^7\text{Li atom ratio} = 0.08140 \pm 0.00014 \ .$$

The absolute isotopic composition of natural Li consequently is :

$$^6\text{Li} = 7.528 \pm 0.012 \ \text{atom \%}$$
$$^7\text{Li} = 92.472 \pm 0.012 \ \text{atom \%} \ .$$

The relative atomic weight of natural Li is therefore :

$$6.94067 \pm 0.00012.$$

These values can be compared to those obtained by Flesch (2) and Callis (3).

A more extensive system calibration and a thorough error analysis will still be performed and published elsewhere.

* this work was made possible by the allocation of a grant from the Commission of the European Communities.

Table 1 : Lithium System Calibration (20 - 27th April 1981).

mixture	$q = \frac{N_A}{N_B}$	$R_{obs.}$ ($\bar{s}_{int.}$)	$K = \frac{R_{true}}{R_{obs.}}$	R_{true}
A 202	0.021359	1) 0.021551 (0.018%) 2) 0.021526 (0.019%) 3) 0.021572 (0.019%)	0.9869 0.9880 0.9860	0.021267
A 207	0.072925	0.073397 (0.023%)	0.9851	0.0723025
A 208	0.087357	0.08786 (0.011%)	0.9854	0.0865775
A 220	0.24700	1) 0.24776 (0.0081%) 2) 0.24758 (0.011%)	0.9857 0.9864	0.24422
A 250	1.01657	1) 1.01260 (0.012%) 2) 1.01216 (0.011%)	0.9851 0.9855	0.99749
A 280	4.01949	1) 3.8928 (0.014%) 2) 3.89029 (0.012%)	0.9852 0.9859	3.8353
A 292.5	12.6056	1) 11.319 (0.0096%) 2) 11.300 (0.010%) 3) 11.315 (0.011%)	0.9852 0.9870 0.9856	11.1515

A 201 : R_A = 105.77 ± 0.05 (that is 0.05%) (99.06 % ^{6}Li).

A 299 : R_B = 0.0001145 ± 0.00000286 (that is 2.5%) (99.99 % ^{7}Li).

K = 0.98593 ± 0.00012 that is 0.087 %.

Table 2 : ^{6}Li/^{7}Li isotope ratio of a natural lithium sample (March 1981).

$R_{obs.} = \frac{^6Li}{^7Li}$	$\bar{s}_{int.}$
0.08250	0.0088%
0.08248	0.0077%
0.08249	0.0072%
0.08273	0.011%
0.08248	0.011%
0.08271	0.0071%

n = 6 $R_{obs.}$ = 0.082565 ± 0.00012

R_{true} = 0.08140 ± 0.00014

References :

(1) J. Pauwels, K.F. Lauer, Y. Le Duigou, P.J. De Bièvre and G.H. Debus, The preparation of precisely defined Lithium Isotope Mixtures, Anal. Chim. Acta 43 (1968) 211 - 220.

(2) G.D. Flesch, A.R. Anderson and H.J. Svec, Int. J. Mass Spec. Ion Phys. 12 (1973)

(3) E.L. Callis, A.E. Essling, G. Reedy, R.J. Meyer, Proc. 28th Ann. Meeting ASMS, 1980.

THE DETERMINATION OF B AND LI IN NUCLEAR MATERIALS BY SECONDARY ION MASS SPECTROMETRY*

R. E. Eby and W. H. Christie
Analytical Chemistry Division
Oak Ridge National Laboratory
Oak Ridge, Tennessee 37830

We have used secondary ion mass spectrometry (SIMS) to perform mass and isotopic analysis for B and Li in samples that are not readily amenable to more conventional mass spectrometric techniques (e.g., surface ionization, electron impact, etc.). In this paper three specific applications of SIMS analysis to nuclear materials will be discussed: first, the quantitative determination of B and its isotopic composition in borosilicate glasses; second, the determination of the isotopic composition of B and Li in irradiated nuclear-grade aluminum oxide/boron carbide composite pellets, and, lastly, the quantitative and isotopic determination of B and Li in highly radioactive solutions of unknown composition.

In the SIMS technique it is well known that some method of surface charge compensation must be employed in the analysis of insulator materials. It is also recognized that samples to be analyzed must be presented as reasonably flat, smooth surfaces. In our analysis technique we have met both of these criteria by distributing pulverized samples as a thin film on a flat conducting substrate. Solid samples are typically prepared by grinding in a mortar. The powdered material is placed in a small plastic vial and enough water added to create a suspension after shaking. The suspension is allowed to settle briefly and a 1 µl pipet is inserted into the top of the solution in order to withdraw a µl or less of suspended sample fines out for analysis. This suspension is deposited on a conducting substrate, dried and loaded into the SIMS instrument for analysis.

We have studied the effect of analyzing borosilicate glasses, prepared in the above mentioned fashion, using both O^- and O_2^+ primary beams and have established that statistically equivalent results are obtained with either beam. Since O_2^+ beams are more readily generated in our duoplasmatron ion source, we used this beam for all analyses. All analytical results in this study were corrected for counting system dead time and bias due to isotopic fractionation by calibration with standards of known composition. Table I presents the results of SIMS isotopic analysis for B in a series of borosilicate glasses containing natural B.

Table II presents the results of SIMS quantitative analysis for B in five borosilicate glass samples. The samples were ground, weighed, dissolved in dilute HF and spiked with a known solution containing enriched ^{10}B. The quantitative results obtained are compared to results for the same samples analyzed by conventional atomic absorption methods.

Irradiated Al_2O_3/B_4C composite pellets, used as reactor control rods, were analyzed using SIMS in a manner analogous to that described for borosilicate glasses. Using 1 µl of an aqueous suspension of this material reduced the radioactivity handled to a few milliroentgen of radiation for each sample. We were able to determine isotopic values for both Li and B in this type sample.

The application of SIMS to the quantitative determination of B and Li in solutions of unknown composition was examined by analyzing a radioactive liquid generated in the Three-Mile Island nuclear reactor accident. The original sample consisted of a highly radioactive aqueous solution that indicated about 1 $Rh^{-1}mL^{-1}$ of β, γ activity on contact with the sample vial surface. These samples were diluted and spiked with enriched ^6Li and ^{10}B standards. This resulted in a sample that gave a combined α, β activity of approximately 1 $mR^{-1}h^{-1}$. These samples were then analyzed via SIMS to provide quantitative and isotopic information for Li and B. An advantage of the SIMS method for

*Research sponsored by the U. S. Department of Energy, Division of Basic Energy Sciences, under contract W-7405-eng-26 with the Union Carbide Corporation.

this kind of analysis is the fact that very low levels of radiation were actually handled because of the ultrahigh sensitivity of the method for Li and B. A detailed account of this work has been published.(1)

Table I. SIMS Isotopic Analysis of Borosilicate Glass Powders

sample no.	atom ratio $^{10}B/^{11}B$ av	SD[a]	% RSD[b]	n[c]	% abs error $100(y - x)/y$[d]
1	0.2469	0.0005	0.20	10	0.00
1	0.2468	0.0005	0.20	10	-0.04
2	0.2495	0.0019	0.76	10	1.05
2	0.2472	0.0007	0.28	10	0.12
3	0.2469	0.0013	0.53	10	0.00
3	0.2478	0.0013	0.52	10	0.36
4	0.2467	0.0008	0.32	10	-0.08
4	0.2497	0.0006	0.24	10	0.41
5	0.2456	0.0008	0.33	10	-0.53
5	0.2474	0.0006	0.24	10	0.20
6	0.2457	0.0009	0.37	8	-0.49
6	0.2467	0.0009	0.36	10	-0.08
7	0.2455	0.0016	0.65	10	-0.57
7	0.2465	0.0009	0.25	10	-0.16
8	0.2470	0.0006	0.24	10	0.04
8	0.2463	0.0005	0.20	10	-0.24
9	0.2469	0.0010	0.41	10	0.00
9	0.2463	0.0006	0.24	10	-0.24
av	0.2469	0.0009	0.35		-0.01
SD	0.0009				0.34

[a] SD = standard deviation. [b] % RSD = percent relative SD. [c] n = number of replicates. [d] $x = {}^{10}B/{}^{11}B$ average, natural $^{10}B/^{11}B$ taken as 0.2469 ≡ y.

Table II. Comparative Quantitative Analysis of Boron

sample no.	isotope dilution SIMS wt % B	atomic absorption wt % B
1	3.94	3.91
2	3.88	3.90
3	3.98	3.92
4	3.87	3.90
5	3.94	3.88

(1) W. H. Christie, R. E. Eby, R. J. Warmack, and L. Landau, Anal. Chem. 53, 13 (1981).

A SIMS Study of the Resin Bead as a Thermal Ion Source*

David H. Smith, W. H. Christie, and R. E. Eby
Analytical Chemistry Division
Oak Ridge National Laboratory
Oak Ridge, Tennessee 37830

Using a single anion resin bead as a vehicle for introducing uranium samples into a mass spectrometer for thermal emission isotopic analysis was first suggested by workers at NBS.[1] Its application was extended to separation of uranium and plutonium from highly radioactive solutions by Walker et al. of this laboratory.[2] The principal advantages of using this method are: (1) simplified chemical preparation (only adjustment of acid strength and uranium concentration is required); (2) reduced transportation costs; (3) improved ionization efficiency; (4) reduced loss of sample as oxide species. It was decided to investigate the bead-sample-filament system using secondary ion mass spectrometry (SIMS).

Beads were prepared in a way to simulate actual sample treatment as closely as possible. They were mounted on flat Re filaments and heated for varying lengths of time (2 min to 2 hours) at 1700°C.

The beads were examined after this treatment by optical and scanning electron microscopy. This revealed that, even after the longest burns, the beads retained their integrity. The beads slowly evaporate and dissolve into the Re filament, leaving hemispherical carbon skeletons.

SIMS investigations revealed that carbon had penetrated through the thickness of the Re filament, while uranium had not left the bead in detectable quantities, even along grain boundaries. Uranium penetration of the bead is essentially complete, even though loading is only about 1%.

We conclude that ionization occurs at the bead-filament interface, where there is a surface rich in carbon; Re-C composite surfaces are known to have work functions about 0.4 eV higher than that of pure polycrystalline Re.[3] The bead serves as a reservoir of uranium, feeding sample to the ionization region as the bead dissolves or evaporates and simultaneously serving as a reducing medium, preventing undue loss of sample as oxide species.

Our observations made clear that a bead is small with respect to the size of the individual Re grains of the filament surface. The work functions of these grains will vary with the lattice face aligned with the surface. It would thus be desirable to devise a means of identifying those grains of high work function.

A detailed account of this work has been published.[4]

*Research sponsored by the U. S. Department of Energy, Division of Basic Energy Sciences, under contract #W-7405-eng-26, with the Union Carbide Corporation.

References

1. D. H. Freeman, L. A. Currie, E. C. Kuehner, H. D. Dixon, and R. A. Paulson, Anal. Chem. 42, 203 (1970).
2. R. L. Walker, R. E. Eby, C. A. Pritchard, and J. A. Carter, Anal. Lett. 7, 563 (1974).
3. D. H. Smith, J. Chem. Phy. 55, 4152 (1971).
4. D. H. Smith, W. H. Christie, and R. E. Eby, Int. J. Mass Spectrom. and Ion Phys., 36, 301 (1980).

A Quadrupole Mass Spectrometer for a Mobile Laboratory to Measure Isotope Ratios*

J. R. Walton, D. H. Smith, H. S. McKown and J. A. Carter
Analytical Chemistry Division
Oak Ridge National Laboratory
Oak Ridge, Tennessee 37830

A mobile laboratory has been assembled for the Office of Safeguards and Security to be used for "on-site" inspection of plant operations handling special nuclear materials. The necessary chemistry on the collected sample and a rapid measurement of the isotopic composition, with the use of a quadrupole mass spectrometer, can be performed on uranium, plutonium, and other elements.

The vehicle is a 22-foot long Model G Fleetwood mobile home. It contains all the needs and requirements for the chemical preparation and the isotopic measurements of the samples. The quadrupole and control unit are mounted in two modules which are anchored on a low bench on the left side of the vehicle. A microscope, vortex mixer, and a centrifuge are mounted on a work bench on the right side.

The mobile laboratory has three electrical systems. One provides 115-volt power to operate all 115-volt instruments and appliances. This system is used when power is available from a public utility. A fifty-foot heavy-duty power cord is available to be plugged into any adequate 115-volt power source. A second power source is a self-contained inverter which operates from two heavy-duty 12-volt marine batteries. The output is 1000 volt amperes at 115 volts, with a low distortion sinusoidal wave form. The batteries, which can tolerate many deep discharge cycles, are charged by a 130-ampere generator turned by the vehicle engine. This power is used to keep the quadrupole pumping system functioning while in transit. The inverter will continue to furnish 115-volt power for more than two hours while the vehicle engine is turned off. A third source of power uses an on-board auxiliary battery to provide power for 12-volt lighting, appliances, and accessories.

The mass spectrometer is a Balzers quadrupole mass spectrometer model QMG 311. The instrument was assembled in two modules and adapted for thermal ionization by the J. Pernicka Corporation. The pumping system is comprised of a Pfeiffer turbomolecular pump and Pfeiffer direct drive rotary vane backing pump. Pressures of 10^{-8} torr are routinely maintained. A 0-12 ampere d.c. power supply furnishes current for the thermal ionization filament. The ion measurement system is composed of a 17-stage Cu/Be secondary electron multiplier with a range of 10^{-14} to 10^{-9} amperes and a linear amplifier with an output limit of 10 volts. A Tektronix 31 programmable calculator serves both to control mass scanning and acquire and process data. The information may be recorded on thermal paper tape or bulk storage is available on cassette tapes. These are convenient for storage of different programs and also serves as a long-term storage for mass spectral data. The thermal ion probe is 20 cm long and the barrell is 1.6 cm in diameter. The highly polished surfaces aid in sliding the probe through the "O" rings in the vacuum lock while maintaining vacuum integrity. The filament posts are spaced 6 mm apart by a fused glass insulator. The ends of a "V" shaped rhenium filament are spot welded to the opposite sides of the posts. The end view would show the filament lying diagonally between the two posts. The reason for this configuration is to assure that the sample at the center of the filament would lie on the field axis of the quadrupole. The thermal ion probe vacuum lock is rough pumped by a second Pfeiffer direct drive pump. A sample change may be made and operating pressure obtained in less than four minutes.

---

*Research sponsored by the U. S. Department of Energy, Division of Basic Energy Sciences, under Contract W-7405-eng-26 with the Union Carbide Corporation.

Uranium standards were loaded on resin beads, a technique developed at Oak Ridge National Laboratory several years ago.[1] This involves adjusting the pH of the solution, adding a tracer of an enriched isotope, if needed, and exposing the solution to resin beads by agitating in a vortex mixer for 20 minutes. One bead is selected and mounted at the center of the "V" shaped filament and held in place with collodion. Five minutes at low temperatures (800-1200°C) are required for the destruction of the resin bead and conditioning of the sample for stable ion emission. This technique produces high sensitivity for uranium as well as plutonium. A sample of 1-3 ng of uranium results in a 5 to 8 volt signal which lasted more than one hour. We have successfully measured uranium concentration as low as 10 ppb.

Table 1 shows some results utilizing certified NBS isotopic uranium standards. The statistics shown represent one standard deviation on five separate loadings. All the results agree to better than 1.6 percent. The amount of sample on each bead was from 1-3 ng of the element.

Table 1. Results of NBS Uranium Standards

NBS Number	Certified $^{235}U/^{238}U$	Measured $^{235}U/^{238}U$
U-930	17.3487	17.6259 ± 0.2699
U-750	3.1660	3.2013 ± 0.0090
U-500	0.9997	0.9993 ± 0.0053
U-200	0.2513	0.2474 ± 0.0030
U-100	0.1136	0.1143 ± 0.0015
U-030	0.0314	0.03191 ± 0.00064
U-010	0.01014	0.01025 ± 0.00019
U-950a (natural)	0.007253	0.007240 ± 0.00021

Boron is used as a neutron capturing agent and its concentration in a liquid-cooled nuclear reactor is of utmost importance. Isotope dilution mass spectrometry using enriched ^{10}B as a tracer would be an effective way of making that measurement. Boron isotopic ratios have been determined using less than 100 ng of boron in the form of $Na_2B_4O_7$ on a platinum "V" shaped filament. Ion masses 88 and 89 ($Na_2BO_2^+$) were monitored to determine the $^{10}B/^{11}B$ ratio. These ratios have been determined at less than 1 percent standard deviation. Table 2 shows some results of boron analysis.

Table 2. Boron Analysis

	"Normal" Boron Standard	Quadrupole Analysis
$^{10}B/^{11}B$ ratio	0.2469	0.2501 ± 0.0020
	Sample B	Sample C
$^{10}B/^{11}B$ ratio (^{10}B spiked)	2.167 ± 0.019	1.382 ± 0.010
Measured amt. of B in sample	460 ppm	820 ppm
Spark source isotope dilution	480 ppm	840 (titration) ppm

[1] R. L. Walker, R. E. Eby, C. A. Pritchard and J. A. Carter, Anal. Lett. 7, 563 (1974).

A Portable, Solid Source, Quadrupole MS for Rapid Assay of U and Pu

M. W. Echo, Exxon Nuclear Idaho Co., P. O. Box 2800, Idaho Falls, Idaho 83401

The effective safeguarding of fissionable material at a nuclear plant requires the capability to make frequent analyses of the isotopic composition of such material. For this and other reasons, the Safeguards Development Section at the Idaho Chemical Processing Plant was assigned the task of developing a light weight, transportable mass spectrometer which could be conveniently carried into a nuclear plant and used to perform mass assays on uranium and plutonium.

Target specifications for the instrument were as follows: It should weigh less than 150 kilograms, require only standard electrical power and cooling water, and require not more than one microgram of sample for an analysis. It should determine the isotopic ratio of uranium 235 to uranium 238 with an accuracy of 1% or better for material of 5% or more enrichment, require not more than 20 minutes for an analysis, have a resolution at mass 238 of 300 or better and an abundance sensitivity of 3,500 or better, and its operation should be made as nearly automatic as practical.

Three instruments were selected as candidates; two quardupoles and one magnetic sector machine. From these, a gas chromatograph mass spectrometer built by Hewlett-Packard Company was chosen, their Model 5992A. The gas chromatograph parts of the instrument were of no use and were removed and discarded.

The Hewlett-Packard GCMS is built with the mass filter assembly physically inside of the oil diffusion pump. Access to the entrance lens on the quadrupole assembly is gained through the center of the diffusion pump heater and up through the center of the diffusion pump boiler. The gate valve and lock assembly are affixed at the base of the diffusion pump. The decision was made to use a thermal emission, single filament source. A common glass to metal seal assembly was chosen to hold the filament which is a one by thirty mil Rhenium ribbon. The vacuum lock shaft is a 3/4 inch tube. The filament assembly plugs into a socket in the end of the lock shaft. The filament power is supplied by a regulated and programmable power supply. Accelerating voltage is supplied by the circuitry that was originally used for the sample ionization current. A cold cathode gauge was installed for pressure measurement, but it is not very accurate at operating pressure and is often very difficult to start.

The vacuum lock is carried on another vertical shaft and is raised and lowered manually into and out of the lock assembly. It is indexed by a rail mechanism so that its vertical position is easily controlled. The lock shaft is swung inward and indexed, then raised stepwise through the lock mechanism and gate valve into battery with a docking fixture on the entrance lens. Two ball valves control the connection of the mechanical pump to either the diffusion pump or the vacuum lock or both. About three minutes are normally required to insert a sample and pump down to operating vacuum. The oil diffusion pump produces a vacuum of better than 10^{-7} torr, and will maintain an operating vacuum of about 2×10^{-7} for normal sample frequency. The instrument has no other high vacuum pumping device, nor cold trap. From a cold, secured, shutdown condition, operating vacuum is attained in about 3 hours.

The Model 5992 GCMS is furnished with a model 9825 programmable calculator which controls almost all of the mass spectrometer functions. The basis of this control is a large machine language program which is loaded into memory from a cassette tape. This machine language or binary program recognizes a number of calls by means of which the operation of the mass spectrometer is controlled. This provides a convenient means for very fast program execution but, since the binary cannot be listed or changed, severly limits innovation in programming. Many variations in data collection routines were tried. The final program makes use of a Selected Ion Monitor or "sim" call, which sets up the mass filter to focus the designated mass; sets the mass gain and offset parameters; makes the specified number of discrete observations of collector current; and stores the mean of those observations in a program variable. A Galileo Channeltron infinite dynode multiplier is used in the collector and its output is fed into a logarithmic preamplifier. If a single observation is specified in the "sim" call, the log of the collector current is returned and stored; if more than one, the mean of the antilog is returned and stored. The data collected during a single sample run comprises a total of 1,357,500 discrete measurements of collector current, and takes about 3-1/2 minutes. Figure 1 shows a log plot of NBS SRM-U 750, indicating resolution and peak shape.

Originally, liquid samples were loaded onto the filament. About one microliter, containing about one microgram of uranium, was evaporated to dryness in the center of the filament ribbon. Subsequently an improved technique was developed, whereby a small depression is made in the center of the filament. The depression is about 200 micrometers in diameter and depth.

A resin bead containing the sample is then loaded into the depression and heated. By this means a condition is thought to occur during analysis similar to that of a double filament source, whereby sample ionization takes place on a much hotter surface than for evaporation. A substantial increase in sensitivity has been observed using this technique. Resin beads containing 3 nanograms of uranium have been satisfactorily analyzed using this method. The better results are obtained using beads of 100 micron diameter or smaller. After the filament is loaded into the spectrometer and pumped down, the remainder of the operation is completely automatic. The filament is run up, parameters adjusted for best focus, data taken and reduced, and results printed out, all under calculator control. After the data are taken and reduced, the printout includes the date, sample ID, operating parameters, background, values for each measurement, the final results, the measured ratio, and the percent standard deviation.

The first evaluation program consisted of a series of 30 samples, each of which was run 4 to 6 times. The results of these analyses indicated an accuracy of better than 1 percent. Final modifications to the instrument were then completed, and a second evaluation program was carried out, similar to the first except for the dimpled filament and resin bead loadings, and that somewhat fewer samples were run. All of the target specifications for the spectrometer have been met or exceeded. The accruacy is better than 1 per cent, even for wide ratios, and analyses of 10 nanogram samples can be routinely performed at the rate of 6 or more per hour by persons with little or no technical training. The weight of the instrument is 88 kilograms and of the calculator and printer, about 26 kilograms. If the printer is omitted and the calculator's own printer is used, the weight would drop to about 98 kilograms, total. The spectrometer can be carried short distances reasonably easily by two persons and has been transported in the trunk of a Volkswagen Rabbit.

It is strongly believed that the performance of this instrument could be substantially improved. The log preamp, for example, was designed for GCMS work, and is not ideal for the present usage. Further refinements and adjustments would undoubtedly result in improved performance.

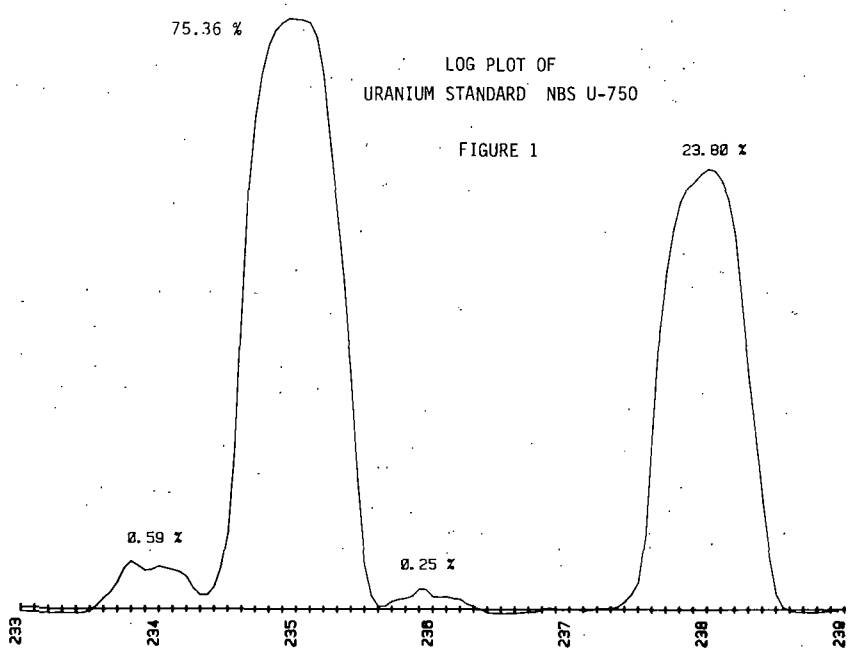

DEVELOPMENTS IN FULLY AUTOMATIC THERMAL IONIZATION - MASS SPECTROMETRY

R.C. Haines - P.J. Turner
VG Isotopes Ltd., Winsford, Cheshire, England

The work described here consists of a more rapid analysis of uranium than previously reported and at a reduced cost. Some small samples of uranium have been analysed using the Daly detector and this will primarily interest those who work with plutonium. All the measurements were made in the fully automatic mode of the Isomass 54E thermal ionization mass spectrometer. The data in the table consists of 15 loadings of NBS U500 Standard. These two microgram samples were loaded onto the tantalum side filaments of triple filament beads. The ionizing filament was rhenium. The average analysis time for these samples was 30 minutes. A mean value of 1.00363 was obtained for the 235/238 ratio and the relative standard deviation was 0.024 percent one sigma. Rejection of one "rogue" value (sample 4) improved the relative standard deviation to 0.020 percent.

NBS U500 - 2 Micrograms - Tantalum Side Filaments

N	MEASURED RAW	BIAS CORRECTED	ERROR %	TRUE	% FROM TRUE	T (MINS)
1	1.003864	.999933	.029	.9997	.02	29
2	1.003858	.999927	.015	.9997	.02	32
3	1.003504	.999574	.014	.9997	-.01	31
4	1.004193	1.000260	.015	.9997	.06	32
5	1.003437	.999507	.015	.9997	-.02	35
6	1.003808	.999957	.008	.9997	.03	29
7	1.003290	.999361	.018	.9997	-.03	30
8	1.003455	.999525	.015	.9997	-.02	35
9	1.003623	.999693	.039	.9997	-.00	30
10	1.003344	.999415	.011	.9997	-.03	31
11	1.003412	.999483	.008	.9997	-.02	30
12	1.003418	.999489	.021	.9997	-.02	30
13	1.003762	.999831	.035	.9997	.01	32
14	1.003656	.999726	.014	.9997	.00	31
15	1.003750	.999819	.025	.9997	.01	30

MEAN = 1.003630

ACCURACY 0.024 PERCENT 1 SIGMA

BIAS .00131 PER AMU

The observed fractionation factor of 1.0039 corresponds to the value expected near the beginning of the fractionation curve, where the observed value approaches the NBS value multiplied by the square root of 238/235 as expected from a simple model of fractionation.

The peak jumping cycle also included the 234 and 236 isotopes. The mean value for the 234/238 ratio was 0.010454 with a relative standard deviation of 0.192 percent one sigma.

For the small uranium samples we have exploited the powers of the Daly detector. The loadings were of two nanograms of NBS U500 standard on single rhenium boat filaments. At the 35 minute point in the analysis the mean 235/238 ratio measured on nine loadings was observed to be 1.011418 with a relative standard deviation of 0.106 percent 1 sigma. At about 50 minutes the standard deviation had improved to 0.08 percent.

NBS U500 - 2 Nanograms - Single Rhenium Filament

N	MEASURED RAW	BIAS CORRECTED	ERROR %	TRUE	% FROM TRUE	T (MINS)
1	1.009505	.997809	.040	.9997	-.19	33
2	1.013228	1.001489	.049	.9997	.18	34
3	1.011646	.999926	.029	.9997	.02	32
4	1.011930	1.000206	.024	.9997	.05	30
5	1.010929	.999217	.019	.9997	-.05	37
6	1.010039	.998337	.037	.9997	-.14	29
7	1.011613	.999893	.036	.9997	.02	35
8	1.011507	.999788	.026	.9997	.01	33
9	1.012362	1.000633	.024	.9997	.09	35

MEAN = 1.011418

ACCURACY 0.106 PERCENT 1 SIGMA

BIAS .00391 PER AMU

To demonstrate the relatively good linearity of the Daly detector system, we have observed the change of the 87/86 ratio with ion beam size in a sample of NBS 987 strontium standard. The change in the 87/86 ratio represents the effect of non-linearity on the 11 to 1 88/86 ratio being superimposed on the 87/86 ratio via the internal fractionation correction. The ion intensities of the strontium 88 beam were in the range 5×10^{-14}A to 9×10^{-13}A. This data indicates that in the normal operating ion current range 5×10^{-14} to 5×10^{-13}A the linearity corrections needed are 0.2% or less. Uncertainty in these linearity corrections would leave a residual error of 0.05% or less, which compares favorably with other measurement errors.

This systematic and predictable behavior of the Daly detector is a consequence of its design principles. It consists of a high voltage electrode operating at about 20KV which attracts the ion beam. The collision of the ions with the electrode is a high gain process, several electrons being produced for each ion. These electrons then strike a scintillator to produce light which passes to a photomultiplier external to the vacuum system. The initial ion-electron conversion on a planar metal surface leads to a very stable gain and one which is essentially constant across the peak top, giving peak top flatness of better than 0.1%. It is these characteristics which make the detector suitable for measurements of the precision described above.

Automated Nitrogen Isotope Ratio Analysis

W. E. Rayford, R. Kleiman, and R. D. Plattner, Northern Regional Research Center, Science and Education Administration, Agricultural Research, U.S. Department of Agriculture, Peoria, IL 61604

Traditionally, isotopic analysis of nitrogen gas has been a labor-intensive operation that requires generating nitrogen gas from ammonium salts under nonatmospheric conditions and injecting it into the mass spectrometer. The analytical procedures most commonly employed are modifications of those developed by Rittenberg et al. (1,2) for tracer investigations involving the use of ^{15}N enriched compounds. Ross and Martin (3), in 1970, developed a conversion system that replaced the Rittenberg tube with throw-away vials and lithium hypobromite reservoir. Later, Porter and O'Deen (4) improved Ross and Martin's conversion system by making it easier to construct and maintain. We now report a computer-controlled system for nitrogen isotope determination following the techniques of Porter and O'Deen.

When totally implemented, this system will allow around-the-clock analysis. The system consists of electrical and mechanical modifications of a commercial gas chromatographic automatic sampler that enables it to generate nitrogen gas from dry ammonium salts under computer control. Computer-controlled valves are installed to control the vacuum and transference of nitrogen gas to the mass spectrometer. ^{15}N enrichment or deletion is determined with a Varian Mat 250 mass spectrometer, which is controlled by a Hewlett-Packard 9815 desktop computer.

Comparison of the Porter and O'Deen conversion system and our automated conversion system is done by analyzing the results of identical enriched and deleted nitrogen samples (Table 1). The results reported by O'Deen and Porter (5) were done following their traditional procedures. Though all the procedures in the comparison are not identical, the results show that the performance of the automatic injection system compares favorably to that of the manual system.

References

1. Rittenberg, D., Keston, A. S., Roseburg, F., and Schoenheimer, R. J. Biol. Chem. 127, 291-299 (1939).
2. Sprinson, D. B., and Rittenberg, D. J. Biol. Chem. 180, 707-714 (1949).
3. Ross, P. J. and Martin, A. E. Analyst (London) 95, 817-822 (1970).
4. Porter, L. K., and O'Deen, W. Anal. Chem. 49, 514 (1977).
5. O'Deen, W., and Porter, L. K. Private communication.

Comparison of Automatic Nitrogen System with Porter and O'Deen System

	Automated N_2-Generated		
Standard[a]	Atom % ^{15}N[b]	Standard Deviation	Porter & O'Deen Atom % ^{15}N[c]
0.01	0.0082	±0.00068	0.0055
0.11	0.1085	±0.00112	0.1059
0.2	0.2076	±0.00102	0.2063
0.5	0.5163	±0.00242	0.5074
1.0	1.0090	±0.00069	1.0123
NH_4Cl	0.3702	±0.00109	0.3684

[a] Supplied by B. B. McInteer, Los Alamos, New Mexico.
[b] Six analyses per sample.
[c] Three analyses per sample.

ENHANCED MASS SPECTROMETRIC SENSITIVITY FOR TRACE METALS IN BIOLOGICAL SYSTEMS

M.A. Bourgeois and F.A. White
Departments of Nuclear Engineering and Engineering Science
Rensselaer Polytechnic Institute
Troy, New York 12181

I. Introduction

The basic problem of trace metal detection in either physical or biological systems differs substantially from the usual mass spectrometric measurements in organic chemistry. In trace metal detection it is often desirable to obtain a mass spectrum which consists solely of an elemental spectra, completely free from the complex molecular spectra which is so essential to structure elucidation and the identification or organic materials and reaction products. Further, it is also desirable to completely suppress the generation of multiply-charged ions in order that only atomic, singly-charged specie reach the detector focal plane.

Two other prerequisites for achieving the ultimate sensitivity in trace metals analysis include (1) high transmission in the mass analyzer and (2) the simultaneous detection of multiple isotopes and elements. We have attempted to address all three of these objectives in the belief that mass spectrometry will ultimately exceed all other analytical methods in determining trace metals in biological systems.

II. Ion Production

The technique that we have proposed and tested for in production is based on previous research that focused on the high temperature diffusion of impurities in metals.[1,2] As a practical technique we are now "encapsulating" a micropipetted sample by a very thin film (~5000°A) of high work function material (rhenium on a rhenium surface ionization filament, Fig. 1). This encapsulation (1) prevents prompt loss of neutral sample atoms, and (2) the diffusion process totally dissociates molecular species so that only atomic ions appear in the mass spectrum. Trace metal atoms (after thin film "encapsulation") will thus emerge from the thin sputtered film as neutrals or ions. The efficiency of ion production is predicted by the Saha-Langmuir relationship:

$$\frac{N^+}{N_\tau} = \frac{1}{1 + A \exp(q(IP - \phi)/kT)}$$

where N^+ is the relative rate of positive ions emitted to N_τ total atoms evaporated from the filament surface, A is a constant assumed to be unity, IP is the ionization potential of the sample atoms, ϕ is the surface work function of the filament or coating and T is the absolute temperature of the filament surface.

As expected, we have found this technique does, indeed, enhance ion production as well as eliminating the molecular spectrum (oxides, etc.) which is usually superposed on the elemental spectrum. Some investigators have suggested that as many as 99% of the sample atoms are lost via the prompt evaporation of neutrals from conventional surface ionization filaments, so that this method of sample conservation/ionization appears to be especially attractive for very small sample assay.

III. Ion Transmission

There is usually a trade-off between ion transmission and mass resolution, and this trade-off imposes serious limitations on the minimum number of sample atoms that can be identified. However, in principle at least, the surface ionization-diffusion source eliminates the need for high resolution in metals analysis inasmuch as only the elemental spectrum is recorded. With unit mass rather than millimass resolution required, it becomes feasible to analyze the heavy metals with a rather wide aperture source and/or detector slits, and with magnetic analyzers of reasonable radii of curvature.

Nevertheless, even large magnets often cost less than sophisticated electronics and data processing equipment, so we are suggesting that magnetic analyzers, either single or sector tandem, have an advantage over other types of mass filters. Specifically, we have recently installed a very high vacuum tube in a previously reported inhomogeneous field

magnet of 30" mean radius[3]. The radial ion optic trajectories of this 255° sector are shown in Figure 2. Because of the inhomogeneous field (0.5 index), ions are focused in both the "z" and radial directions, so that a very high transmission is achievable even for off-axial ions.

Virtually 100% transmission can be expected for a well-designed surface ionization source, since the magnet design was originally conceived to accomodate 5 Mev alpha particles with a radial acceptance angle of ± 15°, and an axial or "z" acceptance angle of ± 2°. Of comparable importance is the substantial unit mass dispersion at the detector focal plane that will permit multiple detectors to simultaneously monitor several isotopes. This very large (75 ton) magnet has also been designed with a 4" pole piece gap and a 270° overall geometry so that both ion source and detector are wholly within the boundaries of the magnet. Consequently, there are no "fringing field" regions to defocus the ion beam.

IV. Ion Detection

If the ultimate sensitivity is ever to be achieved in trace metal analysis, it is clear that "scanning" of the mass spectrum with a single detector is not an option. Only if all mass channels simultaneously record the arrival of multiple ion beams can maximum isotopic/elemental information be obtained.

In the past, this laboratory has introduced the use of reversed biased p-n junctions[4] (with ion-electron converters) to detect ion beams in the 10^{-16} to 10^{-19} ampere range. Because of their small size and independence from magnetic fields, p-n junctions have several advantages over electron multipliers. Now, however, it would appear that the advent of the microchannel plate[5] coupled with photo-diode arrays or charge coupled devices (CCD's)[6] will permit the eventual real-time monitoring of the entire elemental spectrum . It is beyond the scope of this paper and present work to present detail, but microchannel plates are now being fabricated with channel densities approaching 10^6 per cm^2 and CCD's with packing densities of 10^7 per cm^2 are being projected for 1990. Thus we predict the development of a real-time, solid state "photographic plate" with a spatial resolution (mass channel width) of 10 microns or less. And while we have not implemented this system, this laboratory will be reporting shortly an extended focal plane instrument which will accomodate the simultaneous detection of lithium to lead.

V. Conclusion

Collectively, these developments in ion production, transmission, and detection, should greatly enhance research relating to the life sciences.

We have successfully applied the surface ionization-diffusion source to detect heavy metals (e.g., Pb, U, etc.) in the food chain, and we envision further developments that should permit trace assays of many metals in the 10^{-10}g to 10^{-16}g range. At this sensitivity labelled stable isotopes will complement radiotracers in nuclear medicine; new measurements can be made of biological lifetimes, and the role of trace elements can be assessed in metabolism, carcinogenesis, and epidemiological studies. We would even submit that an increased world-wide attempt to correlate trace metal concentrations with the early incidence of cancer, merits a serious and objective reappraisal.

Acknowledgement

It is a pleasure to achnowledge encouragement and assistance from Edward D. Fugo, M.D., F.A.C.S., Dr. W.D. Davis, Dr. R.E. Honig, Dr. G.M. Wood, C.S. Lee, J.L. Mewherter, Dr. J.L. Wiza, W. Eakin and A.B. Strines.

References

1. E.C. Schegler, F.A. White, J. Mass Spectrometry and Ion Physics 1, (1968) 191-208.

2. J.R. Rec, W.G. Myers, F.A. White, Analytical Chemistry 46, p. 1243, Aug. 1974.

3. G.C. Spaniol, T.W. Whitehead, F.A. White, Nuclear Instruments and Methods, 117 (1974) 363-373.

4. F.A. White, Mass Spectrometry in Science & Technology, Wiley, N.Y. 1968 p. 105.

5. J.L. Wiza, Nuclear Instruments and Methods, 162, 1979, pp 587-601.

6. D.F. Barbe, Ed. Charge Coupled Devices, Springer-Verlag, N.Y. 1980.

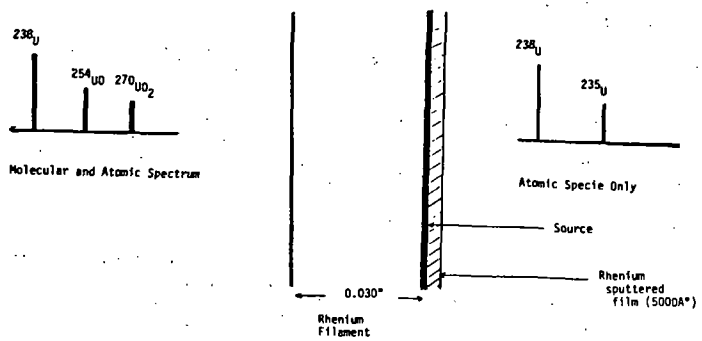

Fig. 1 Schematic of surface ionization-diffusion source, resulting in total dissociation of the molecular specie.

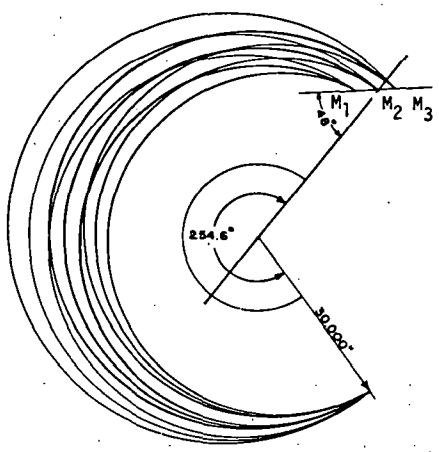

Fig. 2 Trajectories of ions in the 255°, 30-inch radius, inhomogeneous.

MASS SPECTROMETRIC STUDIES OF INTERCALATES

Donald L. Dugger, Daniel W. Oblas, and Sophia Su
GTE Laboratories Incorporated, Waltham, MA 02254

Although intercalated compounds have been known for over 50 years, only recently has considerable interest been shown in these layered compounds. Intercalated compounds are composed of host material, a layered structure such as graphite, interspersed with donor or acceptor elements or compounds called guest species. These layers are arranged in an orderly fashion, and the number of layers of host material between the guest molecules determine the properties of the compound.

Potential applications of intercalated compounds has spurred the current interest in these materials. Most of the suggested uses are based on their conductivity properties. For example, in the fiber form intercalates have been tested as light weight electrical conductors. Other potential applications include superconductivity, battery electrodes, and solid electrolytes. Applications not based on their conducting properties include use as a catalysis, dispensing system, and chemical storage.

Graphite intercalation compounds exhibit several problems and limitations which make them difficult to characterize and effectively limit their use in many applications. Namely, they are generally not stable in air. In some cases this is due to oxidation of the guest material, while in others they deinterlate when removed from the vapor of the guest molecules. Deintercalation often occurs at elevated temperatures, both in air or in a vacuum.

Several methods are currently in use to characterize intercalated compounds. The two most widely used are x-ray diffraction and electrical resistivity. Since the introduction of the guest molecule into the lattice of the host material alters the spacing of the lattice, x-ray diffraction is very sensitive to this change and is used to determine whether or not intercalation has taken place. Other methods which have been employed to a lesser extent are thermal gravimetric analysis and infrared reflectance spectroscopy. This paper reports preliminary data on another technique, thermal desorption mass spectrometry, which could provide valuable information regarding the nature of the species in the lattice. This is important in defining the mechanisms involved in intercalation, which in turn may lead to development of new compounds. The technique involves the thermal desorption of a sample placed in a quartz probe. The probe is 1/2" diameter from Cangal inc., which is inserted into an Hitachi RMS-4 mass spectrometer through a modified inlet port. The probe is resistively heated by ramping a DC power supply using a variable speed motor.

Most of the compounds prepared in the lab used highly oriented pyrolytic graphite (HOPG). Some of the early work involved the use of graphite fibers, while the commercial compounds were made from graphite powders. Four guest molecules were studied; BR_2, HNO_3, $FeCl_3$, and SbF_5. The last two were also obtained commercially as powders and analyzed in a similar manner to the materials prepared in the laboratory.

The results for Br_2 intercalated in HOPG and fibers were the same. This compound is known to be highly unstable once removed from Br_2 vapor. Therefore, in a vacuum with very little heat applied, Br_2 is readily detected. No carbon-bromine compounds were detected even when the sample was heated in vacuum to 900°C. The only other peaks in the mass spectrum were due to HBr which is probably the result of hydrolysis in the mass spectrometer. The commercial $FeCl_3$ intercalate was found to be poor material by both x-ray diffraction and thermal desorption mass spectrometry. The material prepared in the lab however, liberated $FeCl_3$ dimer on heating to 200°C. This was consistent with the TGA results. Some Cl_2 was evolved, but no carbon-chlorine compounds were detected. Again some hydrolysis occurred in the mass spectrometer as evidenced by the presence of HCl in the spectrum. These results do not agree entirely with published literature where reduction of ferric to ferrous at high temperature is reported. Since Fe_2Cl_6 is the dominant species in the vapor phase of pure $FeCl_3$ and the same material is detected coming out of the intercalate upon heating, this suggests that the ferric chloride remains intact in the graphite matrix.

The results obtained for SbF_5 do not support the conclusions given in the literature. The major compound detected during thermal desorption mass spectrometry was SbF_3. A small amount of SbF_5 was also detected. In addition, very small amounts of $SbOF_3$ were found as well as carbon-fluorine compounds. The presence of SiF_4 in the spectrum was due to reaction of HF with the quartz probe. The most complicated results were obtained for HNO_3 in HOPG. There was evidence of extensive oxidation of the graphite and reduction of the nitric acid to NO and NO_2. In addition to the two nitrogen oxides the other major products were CO, CO_2, and H_2O. Due to the complexity of the reactions, the exact nature of the intercalated species is not clear.

In summary, thermal desorption mass spectrometry has demonstrated a usefulness in characterizing intercalated compounds. Moreover, initial studies suggest that additional work is required to identify the intercalated species. This would result in redefining or confirming reaction mechanisms which in turn would be helpful in identifying routes to prepare new intercalated compounds.

S/N ENHANCEMENT USING A SIGNAL AVERAGER; David L. Smith and James A. McCloskey: Dept. of Medicinal Chemistry, University of Utah, Salt Lake City, Utah 84112

Ion signals from a mass spectrometer may be weak because of small sample size or because a low sensitivity mode of operation has been used. Field desorption, high resolution and metastable ion measurements are examples of the latter. These modes of operation are especially useful when low volatility samples are analyzed. The signal-to-noise ratio (S/N) can often be improved by scanning slower and using a lower frequency filter. This approach works well until the scan-time becomes a significant fraction of the duration of the analysis. We, as well as many other workers in mass spectrometry (1), have been using a signal averager to obtain more information from weak signals. This approach permits us to have rapid sampling of changing intensities through fast scanning and still have good S/N. We present here several applications in which we have employed the Nicolet 1170 signal averager and MAT 731 mass spectrometer.

The first example illustrates how the signal averager may be used to scan ion signals obtained by repetitive scanning of the magnetic field over a limited mass range. The purpose of the experiment is to see if the nitrogen atom in the 7-position of guanosine is biosynthetically incorporated into the hypermodified nucleoside Q. Guanosine was synthesized with ^{15}N in the 7-position and incorporated into a growing E. Coli mutant which was unable to synthesize guanosine using normal pathways (2). The tRNA from E. Coli was isolated and enzymatically digested to give free nucleosides which were purified by chromatography. The isolated Q weighing approximately 0.5 µg was derivatized using BSTFA and DMF to give a volatile derivative of molecular weight 1036. Low resolution spectra were acquired by repetitively scanning the magnet over a 10 mass unit range which included the molecular ion. Approximately 50 scans were acquired and integrated for the entire sample. The molecular weight was shown to be 1036 indicating that the nitrogen in the 7-position of guanosine is not used in the synthesis of Q.

In cases where interfering ions are present, isotope ratio measurements may be performed using high resolution. In this case the magnetic field is held constant and the peak matching unit is used to sequentially focus two different mass intervals on the collector. Ion intensities from the two mass intervals are accumulated for the duration of the sample in two quadrants of signal averager memory. This technique was used to analyze a mixture containing approximately 80% guanosine-$^{12}C_{10}$ and 20% guanosine-$^{13}C_{10}$. The objective here was to measure the relative amounts of ^{12}C and ^{13}C guanosine added to the growth medium and in the guanosine isolated from the tRNA. Three aliquots of 1 µg each were analyzed for both the nucleoside substrate and the isolated nucleoside. The resolving power of the instrument was 10,000 and the percent standard deviation for the six measurements was approximately 2. Use of a signal averager in isotope ratio measurements improves the accuracy by properly integrating ion signals for the entire sample, thus minimizing effects due to isotopic fractionation.

The signal averager may also be used with the peak matching unit to improve the accuracy of exact mass measurements in cases where the ion beam is so weak that good peak shapes are not present on the screen for any given scan. Statistical fluctuations in ion intensities are reduced since peaks representative of the entire sample are used for analysis. Futhermore, since the display of the peaks may be made very large using a chart recorder, exact mass measurements may be made using low resolution conditions. This feature is especially useful in field desorption mass spectrometry where ion signals are typically very weak and the presence of ions of different elemental compositions occurring at the same mass is unlikely. Our method of making exact mass measurements using a signal averager is illustrated in Fig. 1 using guanosine. An aqueous solution containing adenosine, N^6-methyladenosine and guanosine was loaded on the emitter wire using the syringe technique. The molecular ion of adenosine, m/z 267, was monitored and stored in quadrant I throughout the experiment, while data in the other three quadrants were acquired sequentially. Quadrant III recorded the molecular ion for N^6-methyladenosine, m/z 281, when the peak match ratio was set to the ratio of exact masses for 267 and 281. Quadrant IV recorded the 281 peak when the peak match ratio was changed by 200 ppm. Quadrant II was used to record the peak of the unknown, m/z 283. Peak profiles from the four quadrants of memory are output to a chart recorder and centroids are determined using triangulation. Differences between the centroids of the 267 and 281 peaks and between the two 281 peaks were used to calibrate the peak match unit and to calibrate the x-axis in terms of ppm of the 267 mass. These are then used to calculate the exact mass of the unknown at m/z 283. When using a resolution of 1,000, the error in the exact mass measurement for the molecular ion of guanosine is usually less than 10 ppm.

In another application we have used the signal averager to increase the S/N when monitoring metastable ions. This mode of operation is highly selective and is particularly

useful for mixture analysis since only ions which are daughters of a specified parent are recorded. The mass spectrometer electronics have been modified so that two different metastable ion transitions may be monitored repetitively. The results given in Fig. 2 illustrates this type of measurement using a sample consisting of 2 μg of adenosine $^{12}C_{10}$ and 25 ng of adenosine $^{13}C_{10}$. The S/N for the 25 ng of adenosine $^{13}C_{10}$ suggests that this can be a sensitive method of analysis.

In conclusion, we find the signal average to be an extremely useful and versatile addition to a mass spectrometer. The primary benefits are the ability to integrate ion signals and to record peak profiles for different masses through the duration of the analysis. Additional advantages include the ability to expand the display of the data, subtract background, correct the baseline and smooth the data.

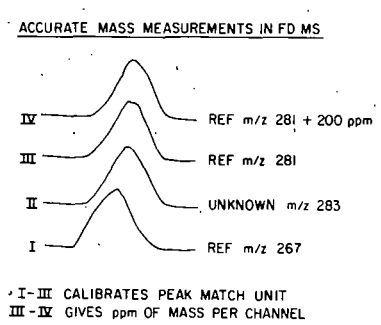

Fig. 1. Illustration of how a signal averager may be used to make accurate mass measurements in low resolution field desorption mass spectrometry.

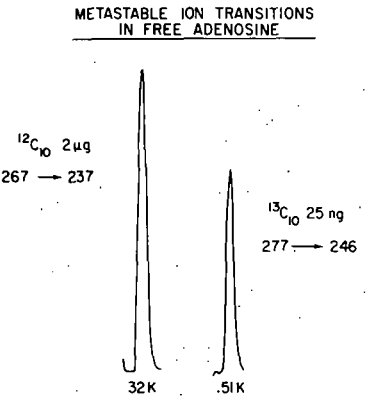

Fig. 2. Illustration of how a signal averager may be used for selected metastable ion transition measurements.

REFERENCES

1. For example, G. L. Peele and D. A. Brent, Biomed. Mass Spectrom. 5, 180 (1978).
2. S. Nishimura, L. B. Townsend and J. A. McCloskey, unpublished experiments.

ELECTROHYDRODYNAMIC IONIZATION MASS SPECTROMETRY OF DYES AND DYE-METAL COMPLEXES.

KELVIN W. CHAN, S.-T. F. LAI[+] and KELSEY D. COOK; School of Chemical Sciences and Materials Research Laboratory, University of Illinois, Urbana, IL 61801

Electrohydrodynamic ionization mass spectrometry (EHMS)[1] has been used as a probe of the chemistry of ion association of metal chelates in glycerol solution, preliminary to direct sampling and observation of dye-metal complexes. This study represents an extension of earlier work where EHMS was found to be useful for characterization of ionic species in glycerol solution, including products of alkali ion association with polymers[2] and other organic compounds, and products of organic and inorganic salt dissociation.[3,4] The present study considers the feasibility of EHMS analysis of transition metal complexes.

Ethylenediaminetetraacetic acid (EDTA, H_4Y) forms stable anionic complexes with a wide range of metals. For example, the EDTA complex of iron(III), $(Fe\text{-}EDTA)^-$, has $K_f > 10^{25}$ in water. Despite this stability, no negative ion corresponding to $(Fe\text{-}EDTA)^-$ (predicted M/Z 344) or to uncomplexed EDTA (H_3Y^-, M/Z 291; H_2Y^{2-}, M/Z 145; HY^{3-}, M/Z 96.3; Y^{4-}, M/Z 72) was observed when a solution of $Fe_2(SO_4)_3$ and EDTA in glycerol was sampled by EHMS. Rather, singly charged positive ions of M/Z 611, 589, 537, 515, 463, 441 and 367 were observed. Reviewing the possible solution chemistry of the system, it became clear that esterification of the carboxylic acid (EDTA) with the alcohol (glycerol) had taken place in the presence of Fe(III), which can act as a Lewis acid catalyst. The observed positive ions can be assigned to the sodiated or protonated tetra-, tri-, di-, and monoesters of EDTA and glycerol (Table 1).

To avoid esterification, solutions of EDTA complexes of weaker Lewis acids (Cu^{2+}, Ca^{2+}) were prepared. In EHMS spectra of these solutions, no ester was detected, but neither was the complex anion nor free EDTA observed. There are at least three possible explanations of this observation: 1) The complexed ion and/or EDTA exist in glycerol solution as neutrals either by "tight" ion pairing with counterions or by protonation by glycerol (deprotonated glycerol was observed); 2) solvent evaporation from sampled ions in the first field-free region may produce "fast" metastable ions which are not detected due to their reduced energy; or 3) complex and EDTA ions may be too highly charged for EHMS sampling. These possibilities are being tested in ongoing experiments.

It should be noted that triply charged cations of the type $[M+3Na]^{3+}$ have been observed in our previous study of polyethylene glycols.[2] Furthermore, doubly negative ions have also been sampled.[4] However, sampling cations is generally simpler, suggesting that several of the aforementioned difficulties may be avoided by employing cationic complexes with simpler solution chemistry.

2,2'-Bipyridine (bipy) forms stable cationic chelates with several metal ions. Fig. 1 and 2 are spectra of two fractions of crystals from a fractional crystallization procedure for the preparation of $Cr(bipy)_3(ClO_4)_2$. Sample 1 (Fig. 1) was labeled as $Cr(bipy)_3^{2+}$, while sample 2 (Fig. 2) was from a fraction that was assumed to be the air oxidation product $Cr(bipy)_3^{3+}$. Surprisingly, $Cr(bipy)_2Cl_2^+$ was the most abundant species in solution1, while only a small amount of $Cr(bipy)_3^{2+}$ and $Cr(bipy)_2Cl^+$ was detected. $Zn(bipy)_2Cl^+$ was also detected, suggesting contamination from Zn(II). Sample 2 was comprised primarily of bipyridyl and chloro complexes of zinc, with virtually no chromium complex. (All ions were identified by their M/Z and isotopic patterns, which agreed well with calculated values.) It was found later that amalgamated zinc was used to reduce Cr(III) chloride to Cr(II) in one of the preparation steps. The Cr(II) was subsequently complexed with bipyridine. Clearly, some of the Zn^{2+} produced during chromium reduction was complexed upon the addition of bipyridine. Furthermore, the ions observed indicated that there was substantial ligand exchange between Cl^- and bipyridine in solution. By contrast, commercially prepared $Ru(bipy)_3^{2+}$ showed no evidence of such exchange (Fig. 3).

Extension of this work to probe the stoichiometry of dye-metal complexes in glycerol solution is in its early stages. Experiments with Indigo Carmine showed that the dye (a disodium salt) underwent partial and complete dissociation. Negative ions $[M\text{-}Na]^-$ and $[M\text{-}2Na]^{2-}$ were observed. In the positive ion spectrum, evidence of extended sodium association ($[M+Na]^+$ and $[M+2Na]^{2+}$) was observed (Table 2). As these and the EDTA studies are extended to observe interactions with wider varieties of ions, they should establish the range of systems for which EHMS can be used to probe the chemistry of ion association in solution.

ACKNOWLEDGMENT:

This work was supported by NIH grant HEW-PHS-GM-19749. The MRL is supported by NSF grant DMR-77-23999.

+Present address: Monsanto Plastics and Resins Co., Indian Orchard, MA 01151.

REFERENCES

1. B. P. Stimpson and C. A. Evans, Jr., J. Electrostatics 5, 411 (1978).
2. S. -T. F. Lai, K. W. Chan, and K. D. Cook, Macromolecules 13, 953 (1980).
3. B. P. Stimpson, D. S. Simons, and C. A. Evans, Jr., J. Phys. Chem. 82, 660 (1978).
4. S. -T. F. Lai and C. A. Evans, Jr., Org. Mass Spectrom. 13, 733 (1978).

Table 1

$Fe_2(SO_4)_3$ (3.0 mole %) + EDTA (3.0 mole %) in Glycerol (100.0 mole %)

M/Z	Relative Intensity (%)	Ion
611	1.0	$Y(OR)_4{}^+Na^+$
589	70.0	$Y(OR)_4{}^+H^+$
537	13.0	$HY(OR)_3{}^+Na^+$
515	100.0	$HY(OR)_3{}^+H^+$
463	0.50	$H_2Y(OR)_2{}^+Na^+$
441	6.0	$H_2Y(OR)_2{}^+H^+$
367	2.0	$H_3Y(OR)^+H^+$

Table 2

Indigo Carmine (0.9 mole %) in Glycerol (100 mole %)

	M/Z	Relative Intensity (%)	Ion
Positive ions	489	26.3	$(M+Na)^+$
	467	10.5	$(M+H)^+$
	256	100.0	$(M+2Na)^{2+}$
Negative ions	443	17.0	$(M-Na)^-$
	256	45.0	$(M-2Na+G)^{2-}$
	210	100.0	$(M-2Na)^{2-}$

Fig 1 Sample 1 + NaCl (4.7 mole %) in glycerol (100.0 mole %)

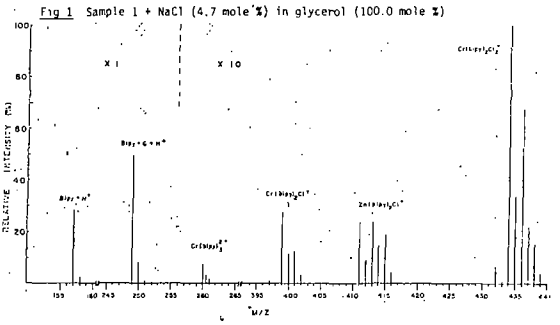

Fig. 2 Sample 2 + NaCl (5.6 mole %) in Glycerol (100.0 mole %)

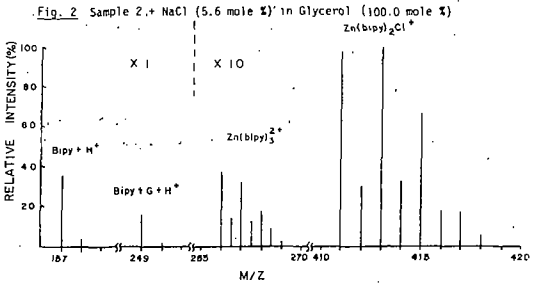

Fig. 3 $Ru(bipy)_3Cl_2$ (1.3 mole %) + NaCl (6.0 mole %) in Glycerol (100.0 mole %)

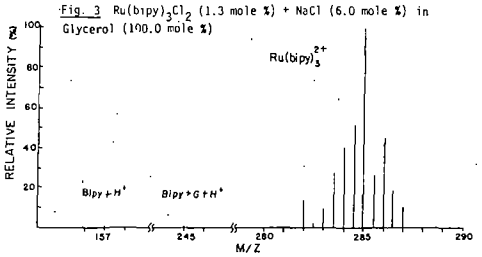

ON THE ORIGIN OF THE BROAD PEAK SHAPES OBSERVED IN CF-252 FISSION FRAGMENT MASS SPECTROMETRY; B.T. CHAIT, and F.H. FIELD, The Rockefeller University, New York, N.Y. 10021

Cf-252 fission fragment mass spectrometry produces significant quasi-molecular (QM) ion yields for large, involatile, and fragile molecules of biological interest.[1] However, broad peak shapes are often observed, especially for QM ions, e.g., the base width of the $(M + Na)^+$ ion peak of β-endorphin (M=3487) is ∿200 daltons[1]. We find that one cause of the broad peak shapes is the metastable decomposition of parent ions in flight. Grid electrodes were placed at the end of the flight tube in front of the ion detector and also at the source end downstream of the sample foil. By applying retarding potentials to the end grids it was possible to separate metastable decomposition products from the parent ions and to investigate the major metastable decay reactions. By applying appropriate potentials to the source grids, the residence time of ions in the acceleration zone could be varied and further information concerning the decomposition reactions and their decay rates could be obtained. Results obtained with ala-ala-ala, guanosine, 5'AMP, erythromycin, and chlorophyll will be discussed. A significant and useful sharpening of the QM ion peaks could be achieved by applying retarding potentials which were large enough to reject all metastable decay products. However, for some of these compounds, only a very small fraction of the QM ions formed survive the flight to the detector. It was further determined that where both a protonated and a sodium cationized QM ion were observed for a given compound, the latter species was formed with substantially less internal excitation.

1. R.D. Macfarlane in Biochemical Applications of Mass Spectrometry, First Supplementary Volume. Edited by G.R. Waller and O.C. Dermer, John Wiley & Sons, Inc. 1980.

TWO-STEP FRAGMENTATION REACTIONS STUDIED IN A CONVENTIONAL DOUBLE-FOCUSSING MASS SPECTROMETER.

R. K. Boyd and B. Shushan, Chemistry Dept., University of Guelph, Guelph, Ontario, Canada, N1G 2W1

The majority of studies of metastable and collisionally activated ions, in double focussing mass spectrometers, involve single-step reactions, i.e., those occurring within the timeframe pertinent to a single field-free region. The present work was devoted to investigating two-step fragmentations, one step in each of two field-free regions:

$$M_1^+ \xrightarrow{\text{1st FFR}} (m_n) + m_2^+ \xrightarrow{\text{2nd FFR}} m_n' + m_3^+$$

The specificity of such processes should be greater than that of single-step reactions. While it should be possible to design instrumentation better suited to such studies, this report is concerned with methods applicable to conventional instruments.

The various scan laws were derived by an adaptation of a general approach described previously[1], and will be given in full elsewhere. Table 1 summarises the more interesting scan laws thus obtained; those requiring changes in the accelerating voltage V were omitted, in view of the resulting detuning of the ion source. (For all cases in Table 1, the apparent mass $m^* = m_3^2/m_1$). As in all linked scans, the problem of artifacts must be faced. In the present context, this has already been fully discussed by Lacey and Macdonald[2,3]. On a two-dimensional ($\rho\mu$) ion intensity map[2], regions of ion current arising from two-step fragmentations are roughly circular, in contrast with the narrow ellipses parallel to the ρ axis which arise from single-step reactions in the first field-free region. Unfortunately, the two-step reactions give signals which are less intense than the single-step "artifacts", by at least one order of magnitude.

Both aspects are illustrated by Figure 1, the result of an experiment using 3-chlorophenol; this test-case was chosen in view of an extensive previous investigation, again due to Lacey and Macdonald[2,3]. The experiment used the first scan law listed in Table 1, (simple B scan, scan line parallel to μ axis), with the electric sector field set (constant ρ) to transmit $(M-CO)^{+\cdot}$ ions formed in the first field-free region from molecular ions of 3-chlorophenol (^{35}Cl). The relative intensities and widths (μ-dimension), of the peaks arising from the one- and two-step fragmentations, are well exemplified by Figure 1.

Clearly, if such experiments are to be of any practical value, some method of discrimination against artifacts is necessary. This might be achieved by introducing an electrically isolable collision cell in each field-free region. Application of a potential, to such a cell, shifts the velocity of fragment ions formed within the cell away from that of similar ions formed outside the cell[4]. If the potential applied to the first collision cell is an a.c. potential (1000 Hz, say), while the second cell potential is at a frequency at least one order of magnitude lower (e.g. 90 Hz), the resulting ion-current signal could be demodulated using two lock-in amplifiers in series, the first tuned to the higher frequency. Such a procedure should transmit only signals modulated at <u>both</u> frequencies, i.e. would discriminate strongly in favour of the two-step reactions.

1. R. K. Boyd and J. H. Beynon, Org. Mass Spectrom. <u>12</u>, 163 (1977).

2. M. J. Lacey and C. G. Macdonald, Org. Mass Spectrom. <u>13</u>, 285 (1978).

3. M. J. Lacey and C. G. Macdonald, Int. J. Mass Spectrom. Ion Phys. <u>30</u>, 359 (1979).

4. J. H. Beynon and R. G. Cooks, Int. J. Mass Spectrom. Ion Phys. <u>19</u>, 107 (1976).

TABLE I. Linked Scan Laws, Connecting V, E, B, for

$$m_1^+ \longrightarrow (m_n) + m_2^+ \longrightarrow m_n' + m_3^+$$

Masses Specified	(V/V_o)	(E/E_o)	B	Scan Law
m_1, m_2	1	(m_2/m_1)	Scan	B only
m_2, m_3	1	Scan	Scan	$B^2/E = (m_3/m_2)(B_3^2/E_o)$
m_1, m_3	1	Scan	$(m_3/m_1)B_1$	E only
m_n, m_3	1	Scan	Scan	$B^2/(1-E/E_o) = (m_3/m_n)^2 B_n^2$

B-scan at $0.7813E_o$

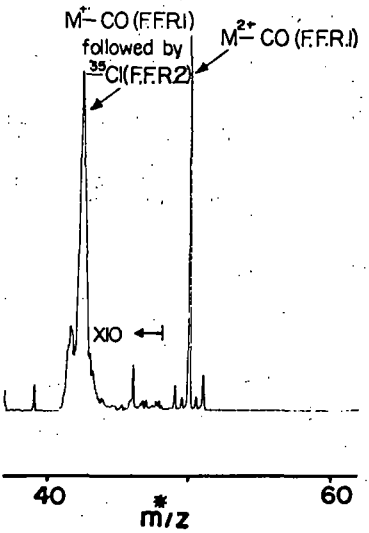

THIS PAGE LEFT
INTENTIONALLY BLANK

A NEW LINKED SCAN AT CONSTANT B^2E; R.K. BOYD, Univ. of Guelph, Guelph, Ontario, Canada N1G 2W1, C.J. PORTER and J.H. BEYNON, Royal Society Research Unit, Univ. Coll. of Swansea, Swansea SA2 8PP, UK.

The simultaneous scanning of two of the fields of a mass spectrometer such that a particular relationship between them is maintained constant has been successfully employed on numerous occasions.[1] These scans are principally those in which the ratio B/E, E^2/V or $[B^2(1-E)]/E^2$ is held constant during the scan, where B represents the magnetic field, V the ion accelerating voltage and E the electric sector voltage. The scans at constant B/E and E^2/V give a spectrum showing all the daughter ions from a pre-selected parent ion, the constant $[B^2(1-E)]/E^2$ scan gives a spectrum showing all parent ions that fragment to lose a pre-selected neutral fragment. In all three scans it is fragmentations in the first field-free region that are studied, and the method has particularly important analytical advantages. For example, the peaks in the spectra are narrower than those that are obtained when only one of the fields is varied. The narrower the peaks, the greater the ability to separate them from one another and to measure their individual heights. Most work in the recent past has been concerned with the linked scan at constant B/E. Its limitations in performance will be discussed and compared with the new linked scan at constant B^2E which partially overcomes some of these limitations and thus results in spectra in which the individual peaks are better resolved, one from another. This scan makes use of fragmentations occurring in the second field-free region and is the first linked scan to do so. It depends for its success on the use of reversed geometry, in which a magnetic sector is used to pre-select a particular reactant ion before its fragmentation is studied and is capable of a mass resolution of several thousand. Like all other linked scans the new linked scan is susceptible to the presence of artefact or interference peaks which will be discussed and shown to be easily distinguishable from the true peaks in the spectrum.

1. R.K.Boyd & J.H.Beynon, Org.Mass Spectrom.12, 163 (1977).

ANALYTICAL APPLICATIONS OF A NEW TRIPLE ANALYZER MASS SPECTROMETER

Edward K. Chess, Michael L. Gross,
Philip A. Lyon, and Frank W. Crow
Department of Chemistry, University of Nebraska
Lincoln, Nebraska 68588

The application of a new triple analyzer mass spectrometer to problems of complex mixture analysis requires high resolution mass selection, high dynamic range, and good transmission for collision-induced decomposition (CID) fragments. Suitable experiments were performed for purposes of evaluating the Kratos MS50-TA, a high resolution triple analyzer mass spectrometer of EBE geometry (1). It was found that reasonable quality full CID spectra can be obtained with moderate signal averaging (50 - 150 scans at 20 sec/scan) for mixture components separated at a mass resolution of 46,000 (10% valley). No interference of one molecular ion was observed in the CID spectrum of the other even under conditions in which a mass resolution of 47,000 is needed to separate $C_{12}H_{14}^{+\cdot}$ (1-phenylcyclohexene) and $C_9H_{18}S^{+\cdot}$ (cyclohexyl-n-propylsulfide).

At moderate mass resolving powers (R=10,000-20,000), a dynamic range of 10^3 was demonstrated using mixture components requiring these resolutions for complete separation. For example, the analysis of 1 ppt pyridine in benzene requires better than 10,000 resolution to separate the pyridine $M^{+\cdot}$ from the isobaric mono-Cl3-containing benzene ion. The dynamic range can be extended to 10^4 to 10^5 in cases requiring only low resolution (R=1,000-3,000). Single reaction monitoring leads to dynamic ranges of better than 10^5 (2).

The transmission of the collision chamber, located in the third field-free region between the magnet and the second electrostatic analyzer, has been shown to be as much as 4% for the ion fragments produced in the CID of methane.

The MS50-TA is well configured for applications of multiple reaction monitoring, wherein the products from an ionic decomposition occurring in the first field-free region (either unimolecularly or collision-induced) are uniquely and unambiguously focussed in the third field-free region where further decompositions (again, unimolecular or CID products) can be monitored. Thus, the structure

of a secondary ion can be studied uniquely, free of isomeric or isobaric interferences which may hinder the study of this ion when formed in the source (3).

Another means of separating components of a mixture is to use a derivatizing reagent ion to selectively react with compounds containing a specific functional group. For example, the o-quinodimethane radical cation (I) was shown to react with neutral styrene (II) through a Diels-Alder type cycloaddition to form 2-phenyltetralin (III). The adduct was identified using unimolecular and CID spectra and labelling experiments. The reaction was carried out at ~1 torr pressure in a CI source using a 4:1 mixture of NO:He as the ionizing gas. The identity of the olefin (styrene, in this case) can thus be deduced from the CID spectrum of the I-M reaction complex.

The evaluation of the triple analyzer and the multiple reaction demonstration will be published in Anal. Chem.. The ionic derivatization study will be submitted to J. Am. Chem. Soc..

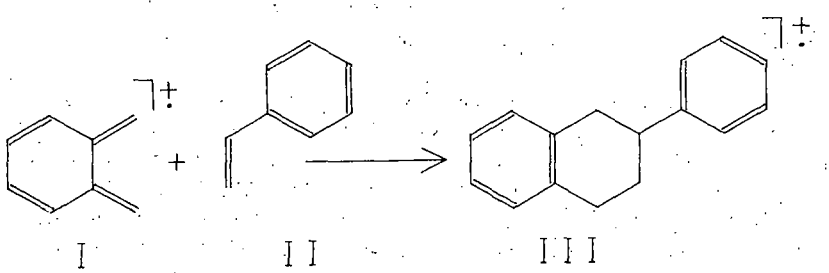

I II III

References

1. M. L. Gross, P. A. Lyon, F. W. Crow, and S. Evans, presented at the 28th Annual Conference on Mass Spectrometry and Allied Topics, New York, N.Y., May 25-30, 1980.
2. E. K. Chess and M. L. Gross, Anal. Chem., 52, 2057 (1980).
3. E. K. Chess, M. L. Gross, D. J. Burinsky, and R. G. Cooks, presented at the 29th Annual Conference on Mass Spectrometry and Allied Topics, Minneapolis, MN, May 24-29, 1981.

GCMS DETECTION OF DISEASE STATES THROUGH QUANTITATION OF URINARY DICARBOXYLIC ACIDS AS THEIR DICYCLOHEXYL ESTERS

EJ NORMAN, HK BERRY, OJ MARTELO AND MD DENTON
DEPT. OF MEDICINE, UNIV. OF CINTI., CINTI., OHIO 45267

We have previously presented a rapid method for the quantitation of urinary methylmalonic acid (MMA) (1). Patients with vitamin B_{12} deficiency have elevated levels of urinary MMA since B_{12} is required for conversion of MMA to succinic acid. MMA levels are a good indication of vitamin B_{12} distribution and function since they are directly related to a B_{12} dependent metabolic pathway.

Efforts to include in this assay measurement of formiminoglutamic acid (FIGLU) were unsuccessful since FIGLU degrades to glutamic acid during the procedure.

Precise determination of urinary MMA has become increasingly important because of reports that the serum B_{12} radioassay can give false values (2). Furthermore, serum B_{12} and B_{12}-binding proteins in some cancer patients have been shown to be abnormally high (3,4) while tissue stores of the vitamin are low. Detection of this functional B_{12} deficiency may only be determined through urinary MMA quantitation.

The past three years 789 patients have been assayed for urinary MMA who had presented with megaloblastic anemia, other anemias, elevated red cell mean corpuscular volume or unexplained neurological disorders. Most patients gave levels < 5.0 µg MMA/ml which we have arbitrarily established as our normal range. A few showed slightly elevated levels between 5.0 and 20 µg MMA/ml urine. We have recently made creatinine measurements on urines with slightly elevated levels of MMA for a better evaluation. Although some patients with 20 µg MMA/ml may have been B_{12} deficient, none to date have been found by their physician to have pernicious anemia as confirmed by the Schilling Test.

Twenty-two patients with clearly elevated levels of urinary MMA (>25. µg MMA/ml) were all found to be B_{12} deficient through the Schilling Test and a clinical response to intramuscular injections of B_{12}. The strikingly abnormal elevated levels of urinary MMA have proven to be more diagnostic of B_{12} deficiency than the serum B_{12} levels. With rapid, reliable quantitation by mass spectrometry urinary MMA measurement is now an extremely useful clinical test.

GCMS was also used for the detection of 3-hydroxy-3-methylglutaryl-CoA lyase (E.C.4.1.3.4.) deficiency in double first cousins (5). This enzyme is in the last step of leucine catabolism and is involved in ketogenesis. To date five other children have been reported with this disorder. However, the children we have diagnosed are the first reported in the United States.

The girl (K) was diagnosed at age 11 months and the boy (B) at age 8 months. The children were hospitalized in different cities for Reye's Syndrome because of their symptoms of lethargy, tachypnea, vomiting, hepatomegaly and hypoglycemia. However, metabolic acidoses led to urinary organic acid screening for K. Elevated levels of 2-hydroxy-3-methylglutaric acid (HMG), 3-methylglutaconic acid (MGT), 3-methylglutaric acid (MG) and 3-hydroxyisovaleric acid (HIV) were found. HMG and MGT were in amounts > 2 mg/ml. Identification of MGT was accomplished by noting prominent ions at m/z 145 and m/z 127, a difference of 18 mass units. This fragmentation pattern suggested a cyclohexyl ester of a dicarboxylic acid with a molecular weight of 144 (1). MGT in the leucine degradation pathway was indicated. Similarly, HMG gave prominent ions at m/z 163 and m/z 145, 18 mass units apart, suggesting a dicarboxylic acid with a molecular weight of 162 (1). Authentic acid standards were then obtained for confirmation. An acid screen on B revealed identical elevated acids.

Dietary restriction of leucine was only partially successful in reducing excretion of the acids. Fat was also shown to contribute to elevated acid levels. Acid quantitation studies suggest that life threatening episodes of hypoglycemia are best prevented on a low protein and low fat diet. Both children are now over two years of age and are developing normally.

REFERENCES

1. Norman EJ, Berry HK, Denton MD: Biomed. Mass Spectrom. 6, 546, 1979.

2. Proc. of 22nd Ann. Mtg. of Am. Soc. of Hema., p. 19, 1979.

3. Saraya AK, Bhaduri S, Clopra SK, Mangalik A: Indian J Med. Res. 71:387, 1980.

4. Carmel R and Eisenberg L: Cancer 40:1348, 1977.

5. Berry HK, Suchy F, Hunt M and Norman EJ. Metabolism and clinical implications of branched chain amino and ketoacids. Eds. Walser, Williamson, Elsevier North Holland, p. 405, 1981.

FATTY ACID PROFILES OF CANDIDA ALBICANS, CANDIDA TROPICALIS, ASPERGILLUS FUMIGATUS, AND ASPERGILLUS NIGER DETERMINED BY CHEMICAL IONIZATION MASS SPECTROMETRY.

JOHN GREAVES, ROBERT SUZUKI, AND JOHN ROBOZ

Department of Neoplastic Diseases
Mount Sinai School of Medicine of the City University of New York
New York, N.Y. 10029

Chemical ionization mass spectrometry (methane) was utilized to determine the fatty acid content to characterize these organisms at the genera and species levels as part of a study to search for metabolic markers for the rapid diagnosis of opportunistic infections in immunosuppressed patients. Pure microorganisms were saponified with 5 % NaOH (in 50 % methanol) by sonification and heating and then taken to pH = 2 with 6 N HCl. Methyl derivatives were formed by heating the samples with 4 ml BCl_3-methanol for 20 min at 80°C. Extraction was made with 8 ml hexane-chloroform (4:1 V/V), repeated 3 times, followed by evaporation with dry nitrogen at room temperature. The derivatives were separated on a 3% SP-2100 gas chromatographic column (Supelco Inc.) using temperature programming (140 - 225°C & 4°/min) and quantified by programmed selected ion monitoring of 5 groups of ions, each group consisting of 3 or 4 masses representing as many as 7 compounds per group. Twenty-three fatty acids were monitored and quantified for each organism. Several ratios were of chemotypic and potential diagnostic importance. The 16:1/16:0 ratio was 10 times larger in the Aspergillus genus than in the Candida genus. The 20:0/19:0 ratio was 20 times larger in A. niger than in A. fumigatus. The ratios of 12:0/14:0 and 16:0/18:1 were reversed in the two Candida species, while cyclic 17:0 was apparently absent in C. tropicalis.

This work was partially supported by Grant CA-15936 from the National Cancer Institute and by the T.J. Martell Memorial Foundation for Leukemia Research.

INCREASED EXCRETION OF GLUTARATE, 3-HYDROXYISOVALERATE AND METHYL-GLUTACONATE DURING CLINICAL EPISODES OF PROPIONIC ACIDEMIA

T. Kuhara, T. Shinka, M. Matsuo° and I. Matsumoto
Research Institute of Medical Mass Spectrometry, Kurume University School of Medicine, Kurume, Fukuoka 830 and
°Kobe Children's Hospital, Kobe, Hyogo, Japan

Propionic Acidemia was first reported in 1961 by Childs et al.. It results from the reduced activity of propionyl CoA carboxylase. Patients with propionic acidemia present with episodic metabolic ketoacidosis, protein intolerance and a remarkably elevated plasma glycine concentration. In patients with propionic acidemia, propionyl CoA undergoes metabolic changes which facilitate transport from mitochondria. The metabolites thus formed are methylcitrate, propionylglycine, 3-hydroxypropionate, 3-hydroxyvalerate, 3-oxovalerate, 2-methyl-3-hydroxyvalerate and 2-methyl-3-oxovalerate[1-4]. We are interested in the factors which affect the profiles of these metabolites and other metabolic intermediates. The factors may be genetic make-up, age, or the patient's clinical/nutritional condition. Here we report comparative studies of two metabolic profiles of different clinical conditions of the same girl with propionic acidemia which provided new perspectives of biological interest.

Forty micrograms of n-heptadecanoic acid was added to the urine volume equivalent of 1 mg of creatinine as an internal standard. Organic acids were extracted with ether at pH 1. As their trimethylsilyl derivatives, the acids were analyzed by combined gas chromatography-mass spectrometry. A 2 mm x 2 m glass column packed with 3 % OV-17 was used for separation. The oven temperature was kept at 80°C for 2 min. and then programmed at 6 °C/min. up to 280°C. Mass spectra were measured repetitively every 5 seconds, stored in a memory disc and treated by a data processing system.

The relative concentrations of 3-hydroxypropionate in normal controls, in the patient under favorable conditions and during a clinical episode, were 0.77, 0.59 and 42.7, respectively; the values being expressed as relative peak ratios to the internal standard. The relative concentrations of 3-hydroxyisovalerate were 0.13, 0.14 and 6.45; glutarate: 0.06, 0.13 and 3.05; and methylglutaconate: 0.05, 0.10 and 3.78, respectively. During a clinical episode the relative concentrations of 3-hydroxypropionate increased 72 times, 3-hydroxyisovalerate increased 46 times and glutarate increased 23 times over those values measured under favorable conditions. 3-Hydroxypropionate is derived from isovaleryl CoA, the catabolic intermediate of leucine. It is known that the formation of 3-hydroxyisovalerate

is enhanced with the decrease in isovaleryl CoA dehydrogenase activity as in isovaleric acidemia. Glutarate is a catabolic intermediate of lysine, hydroxylysine and tryptophan. Normally, glutarate, as its CoA ester, is dehydrogenated to give glutaconyl CoA, the latter usually oxidized to acetyl CoA via acetoacetyl CoA. Increase in glutarate suggests that in a patient during a clinical episode, glutaryl CoA dehydrogenase activity is suppressed. Dehydrogenases of propionyl CoA, isovaleryl CoA and glutaryl CoA are all FAD-dependent flavoproteins. During a clinical episode, propionyl CoA in high concentrations results in the inhibition of isovaleryl CoA and glutaryl CoA dehydrogenase. The inhibitory mechanism may be competitive inhibition by propionyl CoA, acting as product inhibition by acrylyl CoA, or change in mitochondrial redox state induced by the enhancement of β-oxidation of propionyl CoA. As isovaleryl CoA and glutaryl CoA are the precursors of acetyl CoA, the suppression of the catabolism of these intermediates may lead to the decrease in acetyl CoA level in mitochondria.

During a clinical episode, the amount of methylglutaconate increased 38 times over the value measured under favorable conditions. Methylglutaconate is the precursor of acetyl CoA and also the catabolic intermediate of leucine. The urinary excretion of methylglutaconate results in the decrease in the cellular free acetyl CoA level.

We have demonstrated that the catabolism of potent ketogenic amino acids is severely suppressed in the patient with propionic acidemia during a clinical episode. Leucine catabolism is suppressed at two stages. The second stage is immediately before acetyl CoA production. The regulation which causes the decrease in the mitochondrial acetyl CoA level should assist in lowering mitochondrial propionyl CoA levels by preventing the competitive inhibition of acetyl CoA from the metabolism of propionyl CoA, the metabolism of which is analogous to the metabolism of acetyl CoA. This interpretation is supported by the favorable effect of leucine restriction in methylmalonic acidemia (Wada, personal communication) in which propionyl CoA accumulation also takes place[4]. The effect of lysine restriction in patients with propionic acidemia and methylmalonic acidemia is not defined at present.

References

1. T. Ando, K. Rasmussen, W. L. Nyhan and D. Hull, Proc. Natl Acad. Sci. USA 69, 2807 (1972)
2. T. Ando, K. Rasmussen, J. M. Wright and W. L. Nyhan, J. Biol. Chem. 247, 2200 (1972)
3. I. Matsumoto, T. Shinka, T. Kuhara, T. Oura, H. Yamamoto, Y. Hase, H. Aoki, G. Isshiki and T. Tada, in Recent Developments in Mass Spectrometry in Biochemistry and Medicine, ed. by A. Frigerio, p. 203. Plenum, New York (1978)
4. T. Kuhara and I. Matsumoto, Biomed. Mass Spectrom., 7, 424 (1980)

DETERMINATION OF POLYOLS IN BIOLOGICAL FLUIDS AND TISSUES BY SELECTED ION MONITORING.

John Roboz, Elisabeth Barfod, and Robert Suzuki

Department of Neoplastic Diseases
The Mount Sinai School of Medicine of the City University of New York
New York, N.Y. 10029

Serum arabinitol levels were found to be of importance in diagnosing invasive candidiasis in immunosuppressed patients (Roboz, Suzuki, and Holland, J. Clin. Microbiol., 12, 594, 1980). To investigate the possible importance of other polyols, a technique was developed for the quantitation of 7 additional polyols: erythritol, threitol, adonitol, xylitol, mannitol, galactitol, and sorbitol. Polyols were analyzed as acetate derivatives to provide optimal chromatographic separation (3% SP-2340, Supelco, Inc.); trimethylsilyl derivatives are not adequate for the pentitols. In serum, proteins were removed with methanol, lipids extracted with hexane-chloroform, and the aqueous layer was evaporated. Urine was desalted with methanol and the supernatant evaporated. Organ tissues (kidney, liver, spleen, heart, and lung) were ground in ice-cold methanol, hydrolyzed in acidic methanol, and evaporated. Acetate derivatives were made by heating with acetic anhydride and pyridine. For quantitation the M-59 ions (loss of CH_3COO) obtained in chemical ionization (methane) were monitored. Normal values were obtained for all 8 polyols in the matrices studied. Abnormal serum polyols were found in several patients suspected of invasive candidiasis and aspergillosis. Elevated polyol patterns were also found in culture media in which fungi were grown. Unlike in serum, no significant differences were as yet found in polyol patterns between normal and pathological samples. Significant increases were found in tissue arabinitol and some other polyol concentrations in experimental animals infected with candida in the neutropenic state.

This work was partially supported by Grant CA-15936 from the National Cancer Institute and by the T.G. Martell Memorial Foundation for Leukemia Research.

PROFILING OF ORGANIC ACIDS IN HUMAN AMNIOTIC FLUID AND THE DYSMATURE FETUS

K. Mitsutake, T. Shinka, I. Matsumoto, °K. Kabashima and °T. Kato

Res. Inst. of Medical Mass Spectrom. and °Dept. of Obstet. and Gynec.
Kurume Univ. Sch. of Med., Kurume, Fukuoka 830, Japan

We have studied the profiles of organic acids in amniotic fluid for four years. In this report, we discuss the organic acid profiles of amniotic fluid from dysmature infants born after placental transfer dysfunction. These infants have some similar characteristics. Usually they are of normal length for this gestational age. We also notice an abnormal lack of subcutaneus tissue and distended abdomen. These characteristics lead us to guess that she experienced starvation in the uterus. As these infants are very sensitive to hypoglycemia and infection, they have high perinatal mortality and mobidity rates. In order to make it possible to diagnose this condition before birth, we have studied the organic acid profiles of amniotic fluid from such fetuses.

Thirty one specimens of amniotic fluid at 35 to 41 weeks gestation were obtained at delivery or Ceasarean section avoiding contamination by blood. The material was classified into two groups. One group consisted of infants which were found to have an appropriate size for gestational age. The other group consisted of infants which were found to have a birth weight below the tenth percentile according to the Japanese standard growth curve. Sample preparation was performed as follows: Three ml of amniotic fluid was used for the analysis of organic acids. Fifty μg of heptadecanoate was added to the amniotic fluid before deproteinization with cold ethanol. Organic acids were extracted three times with a mixture of diethyl ether and ethyl acetate under acidic conditions. The combined extracts were evaporated to dryness under a nitrogen stream and a residue was derivatized with bis-(trimethylsilyl)trifluoroacetamide(BSTFA). For the GC/MS analysis, JEOL D-100 combined with a JMA-2000 data acquisition and processing system was used. A 2 m glass column packed with 3% OV-17 was used for the separation of organic acids. Column temperature was kept at 80°C for 2 min and then programmed from 80 to 290°C at 6°C/min.

Figure 1 shows the gas chromatogram of organic acids from amniotic fluid. Of more than 46 peaks detected, 23 peaks were identified by comparison of their mass spectra and methylene unit values with reference data. Lactate, glycolate, 3-hydroxybutyrate, phosphate, lactate dimer, citrate, palmitate and stearate were detected in relatively large peaks.

Figures 2-5 indicate the concentration of typical compounds in normal amniotic fluid comparing with those of dysmature infants. The values were expressed as the relative peaks ratios to the internal standard. In Fig. 2, lactate concentration in amniotic fluid are shown. As stated in a previous report (1), normal amniotic fluid has a large amount of lactate compared to the other body fluid such as urine or serum, and it decreases with gestation. The mean concentration of lactate in amniotic fluid was lower in dysmature infants than in the normal infants especially from 35 to 38 weeks gestation. Peak No.18 on gas chromatogram was identified as 3-deoxy-2-C-hydroxymethyl-pentono-1,4-lactone, using deuteriotrimethylsilyl derivative. Although the origin of this compound is not known yet, this metabolite in dysmature infants was significantly lower than that of normal amniotic fluid (Fig. 3). We also found that amniotic fluid 3-hydroxybutyrate in dysmature infants was significantly higher than that of normal infants shown in Fig. 4. Other organic acids in amniotic fluid such as palmitate and palmitoleate (Fig. 5) were not significantly different in both groups.

Placental transfer dysfunction may lead to an inadequate supply of glucose and other nutrients for the fetus and a failure to synthesize substrates necessary for fetal growth. A decreasing supply of glucose leads to the increased oxidation of free fatty acids and ketone bodies, sparing the non-obligatory oxidation of glucose. A large amount of acetyl-CoA produced by β-oxidation of fatty acids causes hyperketonemia. So we guess that ketone bodies such as 3-hydroxybutyrate increase in fetal blood and perhaps in amniotic fluid (2) and fetal lung alveolus are filled with amniotic fluid. Thus analysis of organic acid in amniotic fluid by GC/MS may lead to an accurate and rapid diagnosis in prenatal diagnosis of dysmature infants.

(1) K. Mitsutake, T. Shinka, T. Kuhara, I. Matsumoto, K. Kabashima and T. Kato, 28th Annual Conference on Mass Spectrometry and Allied Topics, 288(1980).
(2) D. R. Abramovich, Obstet. Gynecol., 54, 15(1979).

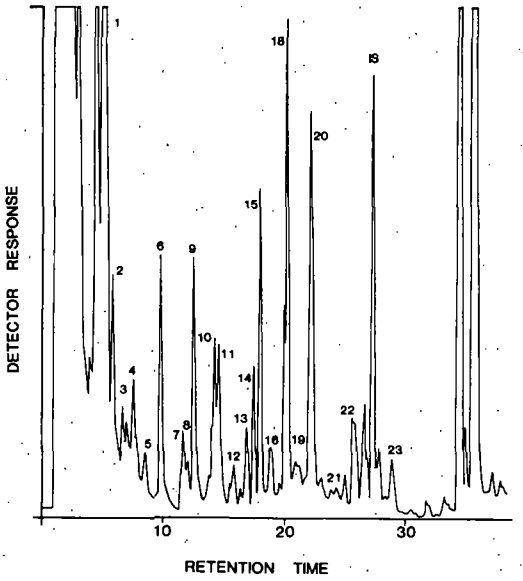

Fig.1; Gas chromatogram of organic acids in amniotic fluid
1: lactate, 2: glycolate, 3: 2-OH butyrate, 4: 3-OH butyrate, 3-OH propionate 5: oxalate, 7: urea, phosphate, 8: glycerate, 9: succinate, fumarate, 10: lactate dimer, 12: malate, 16: laurate, 18: 3-deoxy-2-C-hydroxymethyl-pentono-1,4-lactone 19: β-glycerophosphate, 20: citrate, myristate, 22: palmitate & palmitoleate, 23: stearate, oleate & linoleate.

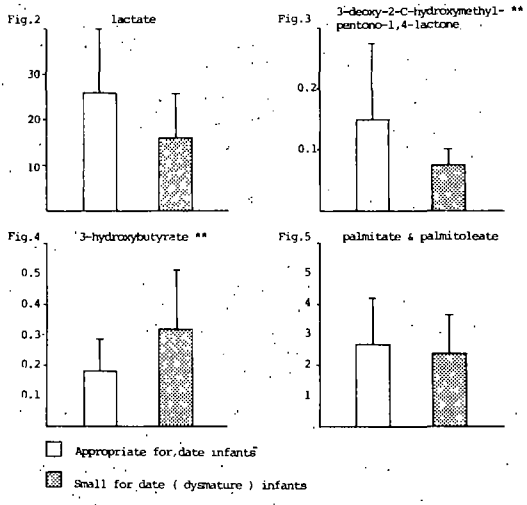

Fig.2-5; Concentrations of lactate, 3-deoxy-2-C-hydroxymethyl-pentono-1,4-lactone, 3-hydroxybutyrate, palmitateand palmitoleate in amniotic fluid of patients with appropriate-for-date infants and small-for date (dysmature) infants.

SIMPLIFIED LC-MS SYSTEMS USING THE THERMOSPRAY TECHNIQUE; C. R. BLAKLEY and M. L. Vestal; Dept. of Chem., University of Houston, Houston, TX 77004.

Recently a new electrically heated vaporizer has been developed as a replacement for the flame and laser vaporizers used in our earlier work. Performance of the LC-MS systems obtained with the new vaporizer is comparable to, or better than, the best performance obtained with the flame or laser vaporizers. Furthermore, the electrically heated system gives better stability and reproducibility and it is much less expensive than the earlier approaches. Our present system appears somewhat more efficient and less expensive than the jet separators commonly employed for GC-MS. This version of the vaporizer has recently been installed on all of our operating LC-MS systems including the second-generation prototype instrument at the University of Utah, a Biospect quadrupole, and a CH-5 magnetic instrument. The latter two installations involve minor modifications to the standard commercial instruments. Details of the modifications are presented and data on the performance of these LC-MS systems are given. These data were obtained using reversed-phase LC conditions on nonvolatile biomolecules such as amino acids, small peptides, nucleosides, and nucleotides.

USE OF NON-VOLATILE BUFFER SOLUTIONS WITH LC/MS

Paul E. Kelley
Finnigan-MAT Corp.

INTRODUCTION

Spectinomycin is an antibacterial isolated from the fermentation broth of Streptomyces spectabilis.[1,2] Its hydrolysis with hydrochloric acid produces actinamine. Gas chromatography (GC) analysis of silylated spectinomycin can produce several peaks, depending upon the reagent and conditions used.[3]
Myers and Rindler[4] have described a rapid and relatively simple method of separation for these compounds, using paired ion HPLC (high-performance liquid chromatography). Because spectinomycin and actinamine lack UV (ultraviolet) adsorbing chromaphores. conventional LC detection is difficult without post-column derivatization. On the other hand, the mass spectrometer coupled to the HPLC via a moving-belt LC/MS interface provides rapid separation and positive identification of spectinomycin in the presence of actinamine without any post-column treatment.

EXPERIMENTAL

The mass spectrometer used for these experiments was a Finnigan Model 4000 equipped with the Incos data system, the Finnigan LC/MS interface, and an Altex gradient-elution HPLC Model #332.

MS Conditions (chemical ionization)

electron energy	70 eV
emission	0.35 mA
source temperature	250°C
mass range	185 - 650 AMU
scan time	3 s
CI reagent gas	methane
ion source	0.33 torr (44 Pa)

LC/MS Interface Conditions

belt	Kapton
sample split	0.1 cm^3/min to mass spectrometer
infrared heater	100%
vaporizer heater	270°C
clean-up heater	280°C
belt scrubbing solution	65% methanol/25% H_2O/10% Snoop

HPLC Conditions

column	150 mm x 4.6 mm Ultrasphere-ODS
flow	1 cm^3/min
mobile phases	A = 0.2 M sodium sulfate, 0.02 M sodium heptanesulfonate and 0.1% acetic acid in water. B = acetonitrile
gradient	linear 95% A to 70% A in 10 min.
injector loop	20 uL

Standards of spectinomycin and actinamine (Upjohn Company, Kalamazoo, MI) were made to 0.5 mg/ml and 1.0 mg/ml respectively.
The presence of the buffer salts necessitated use of a wiping mechanism to prevent build-up of salt deposits on the LC/MS belt. This wiper was in the LC/MS interface under the infrared heater on the return section of the belt. (See Figure 1.) The salt deposits were washed from the belt by continuous extraction with a solution of water/methanol/Snoop at a flow rate of 0.1 cm^3/min. The residual Snoop also acted as a wetting agent, which aids the non-polar Kapton belt surface in accepting and evenly distributing the polar mobile phase from the HPLC.

RESULTS AND DISCUSSION

Figure 2 shows the CI methane positive ion current plot (time vs. intensity) of the M + H ions m/z 333 and m/z 207 for spectinomycin and actinamine. The Ultrasphere-ODS column provided baseline resolution of the two components. The CI methane positive ion mass spectrum for actinamine gives the protonated molecular ion (M + H) at m/z 207 and the M + C_2H_5 and M + C_3H_5 adducts at m/z 235 and m/z 247. The mass spectrum of spectinomycin, which was eluted approximately 11 minutes into the analysis, produces a strong protonated molecular ion at m/z 333 and, like actinamine, gives the M + C_2H_5 and

$M + C_3H_5$ confirmation.
Although much attention has in the past been focused toward non-polar mobile phases, these data demonstrate that the belt-transport LC/MS interface can operate satisfactorily with polar solvents (such as water) and non-volatile buffer salts. The belt extraction or wiping process is also a useful tool for analyses involving ion-paired liquid chromatography. It should also be noted that the presence of non-volatile salts does not modify the CI reagent gases.

CONCLUSION

Coupled to the mass spectrometer via the moving belt LC/MS interface, the HPLC provides rapid analysis and positive identification. The moving belt interface also offers capabilities for non-polar and polar mobile phases, volatile and non-volatile buffers, and chemical and electron impact modes of ionization.

REFERENCES

(1) Wiley, P.F., Argondelis, A.D. and Hoeksema, H., J. Amer. Chem, Soc. 85 (1963) 2652.
(2) Mason, D.J., Dietz, A. and Smith, R.M., Antibiot, Chemother., 11 (1961) 118.
(3) Brown, L.W. and Bowman, P.B., J. Chromatog. Sci., 12 (1974) 373.
(4) Myers H.N. and Rindler, J.V., J. Chromatogr. 176 (1979) 103.

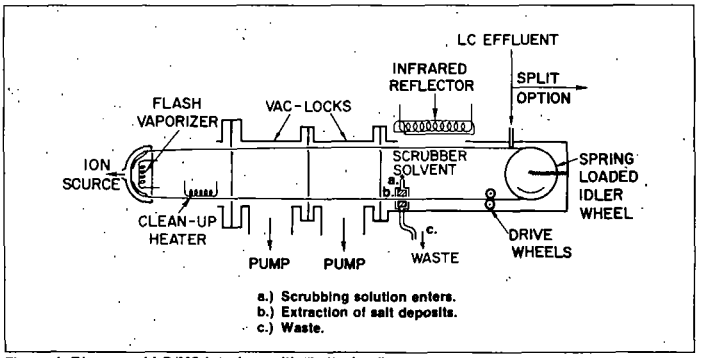

Figure 1. Diagram of LC/MS interface with "belt wiper".

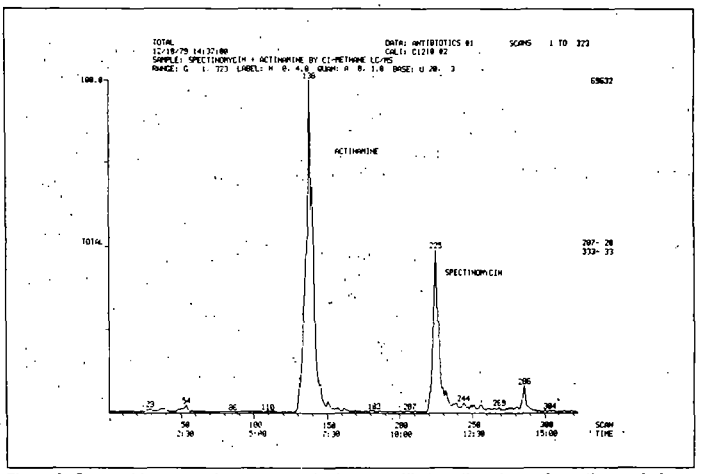

Figure 2. Summed ion mass chromatogram for ions specific to actinamine and spectinomycin from PICI mass spectra.

LC/MS of Lipophilic Compounds Using Nonaqueous Reversed-Phase Chromatography

Patricia C. Tway and Walton B. Caldwell; Merck Sharp & Dohme Research Laboratories, P.O. Box 2000, Rahway, NJ 07065.

Most liquid chromatography work on lipophilic low polarity samples is done using a reversed-phase column with an aqueous mobile phase. Some of these compounds have little UV absorbance above 230 nm so that detection is generally by infrared or refractive index which are relatively insensitive detection systems. LC/MS would be an ideal way not only to detect these compounds at low levels, but also to obtain structural information about unknown peaks in the chromatogram. The belt LC/MS interface system, however, can only handle small amounts of water so that it is generally necessary to split the mobile phase onto the belt which limits the sensitivity of the system. Many of these lipophilic compounds have very limited solubility in an aqueous mobile phase so large sample quantities cannot be injected onto the column to make up for the lost sensitivity from the split.

The avermectins, a group of natural products, are potent, broad spectrum anti-parasitic agents which are isolated from the mycelia of streptomyces avermitilis.

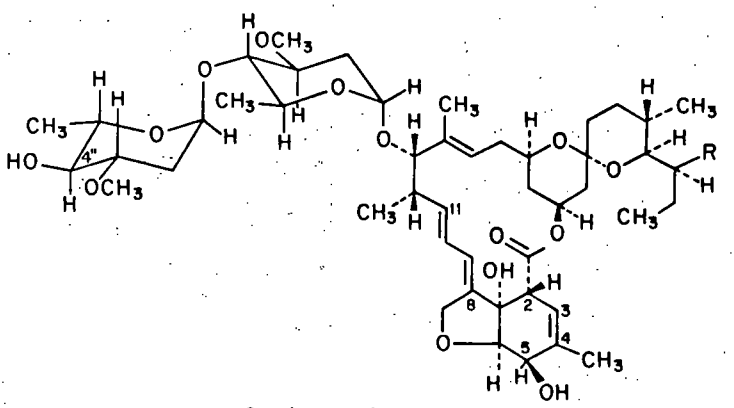

B_{1a} Avermectin

Information about the other components present in the avermectin broth samples would allow the microbiologist to better understand the fermentation process and to develop higher yielding fermentation conditions. The main objective of this work was to develop a liquid chromatographic system which could separate a mixture of avermectin-type compounds and which could be readily used with LC/MS to characterize and identify the different components in the avermectin broth samples. All of the previous liquid chromatography on these samples had been done on reversed-phase systems using buffered aqueous eluents.

Nonaqueous reversed-phase liquid chromatography (NARP) is generally applicable to low polarity lipophilic compounds and was found to give good separation of the avermectin broth samples. The use of organic eluents enables larger than normally expected quantities of sample to be injected onto the column and also allows a higher portion of the sample to be put into the mass spectrometer via the belt interface.

A NARP LC/MS system was developed to monitor four components in broth sample which had previously been identified. These compounds have no UV above 220 nm, so the LC system was developed using the LC/MS. In addition, by changing the mobile phase, other components in the broth samples were separated and characterized. Fingerprint patterns from various sample batches were compared, although no new major components were found.

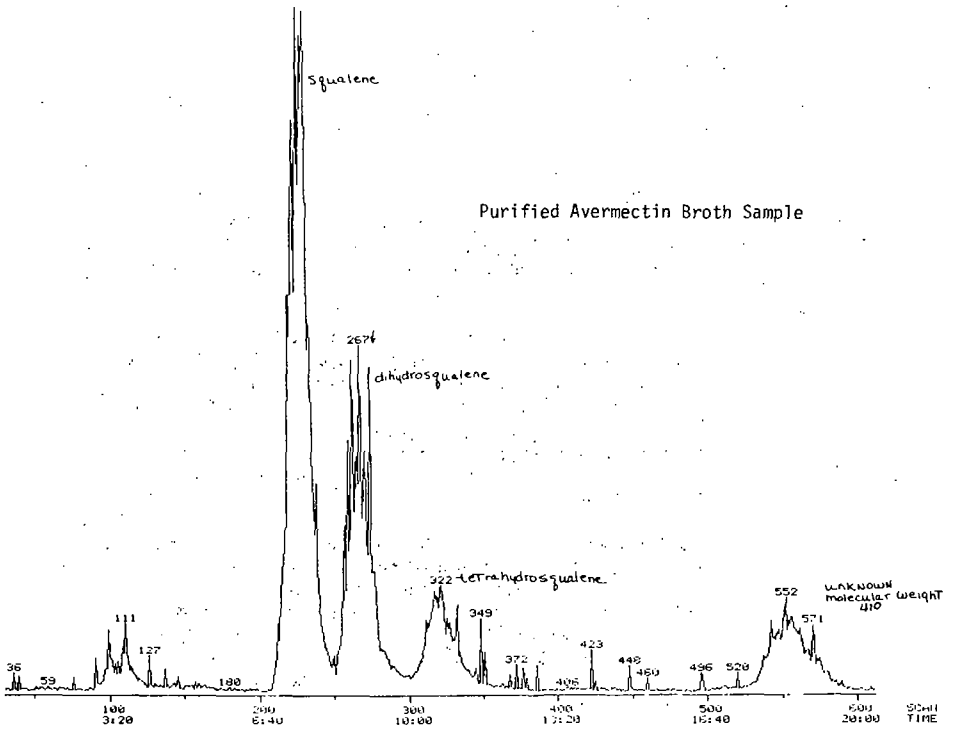

NARP LC/MS was also found to be applicable to other compounds of pharmaceutical interest and has been used to study these samples.

LC/MS INTERFACE FOR EI AND DCI TECHNIQUE; C. BRUNNEE, L. DELGMANN, G. DIELMANN, W. MEYER, P. THORENZ; Varian MAT GmbH, 2800 Bremen, Barkhausenstrasse 2, Germany

The system is based on the moving belt principle. Technical features: The belt carries the sample directly into the ionization chamber through two differentially pumped vacuum stages. The heated part of the belt in the source has a length of a few millimeters only. Therefore very rapid heating is achieved, allowing the ionization of labile compounds. The whole transport system of the belt can be assembled outside the vacuum and put into place in less than a minute.

Performance data: Maximum flow for eluents from LC containing up to 50 % water is 1 ml/min. Usable spectra can be obtained from samples in the ng range. Typical examples of LC/MS analyses will be presented. For adenosine using H_2O as reactant gas the only significant peak in the mass region between 100 and 300 is the quasi-molecular peak M + 1. The labile adenosine monophosphate shows a quasi-molecular peak of 5 % height, the base peak being at mass 251 (M - H_2PO_3).

UNIMOLECULAR DECOMPOSITION OF ETHOXYTRIMETHYLSILANE. David A. Herold, Department of Pathology, University of Virginia, Charlottesville, VA 22908, Jean H. Futrell, Department of Chemistry, University of Utah, Salt Lake City, UT 84112.

The spectrum of ethoxytrimethylsilane is well documented and the peaks identified by accurate mass measurements; however, the mechanisms of decompositions have not been explored. The multiplicity of decomposition pathways and the commerical availability of the deuterium labeled ethanols made the investigation of the labeled ethoxytrimethylsilane most attractive.

The mass spectra and metastable transitions are shown for the ethoxytrimethylsilane and the deuterated analogues. Discussion is based on the unlabeled ethoxytrimethylsilane. The DADI (Direct Analysis of Daughter Ions) analysis of the molecular ion (m/z 118) gave the following 2 daughter ions: 1) 118 $\xrightarrow{-CH_3}$ 103

This represents an alpha cleavage of the Si-CH_3 bond. 2) 118 $\xrightarrow{-C_2H_4O}$ 74

This loss was not observed in the mass spectra of the 1,1-d_2-TMS-d_9 (spectrum 6) or the 1,1,2,2,2-d_5-TMS-d_9 (spectrum 8), where it would be seen free from interferences. Based on the mechanism presented in Scheme I, it was thought that this ion should appear at m/z 84, 2 amu above the $^{+}Si(CD_3)_3$ peak. The small peak at m/z 84 resulted only from isotopic contributions from $^{+}Si(CD_3)_3$. One explanation for this is that the resultant $^{+}Si(CD_3)_3$ species had sufficient internal energy to decompose rapidly when formed in the source.

DADI analysis of the M-15 ion (m/z 103) gave transitions for 3 daughter ions.

1) 103 $\xrightarrow{-C_2H_4}$ 75 This loss of ethylene had several potential sources. DADI analysis showed that the loss occurred exclusively by the mechanism shown in Scheme II. This was confirmed by the mass spectrum of ethoxy-1,1-d_2-TMS (spectrum 2). Had the loss occurred as shown in Scheme IV, there would have been a peak at m/z 77 due to the CH_3-CD_2-O-$Si^{+}H_2$ species; however, the peak at m/z 77 was due solely to the isotopic contributions from m/z 75.

2) 103 $\xrightarrow{-CH_2O}$ 73 The loss of CH_2O occurred as shown in scheme III. Examination of the spectra of ethoxy TMS (spectrum 1), ethoxy-2,2,2-d_3-TMS (spectrum 3), and ethoxy-TMSd_9 (spectrum 5) demonstrated that m/z 73 had two origins: (A) the alpha cleavage from the molecular ion, which accounted for approximately 2/3 of the ion current and (B) the rearrangement presented in Scheme III, which accounted for the remaining 1/3.

3) 103 $\xrightarrow{-C_2H_4O}$ 59 The loss of C_2H_4O can be explained as a variant of Scheme I. Transfer of the proton (deuterium) from the 1 position of the ethoxy-TMS was established from the 1 amu shift up in those species labeled in the 1 position in reference to the unlabeled species.

DADI analysis of m/z 75 and m/z 73 revealed one transition each. 1) 75 $\xrightarrow{-C_2H_4}$ 47 2) 73 $\xrightarrow{-C_2H_4}$ 45. The elimination of ethylene can be explained by the mechanism in scheme IV.

The DADI analysis of m/z 59 gave two metastable transitions. 1) 59 $\xrightarrow{-CH_4}$ 43

This would be the loss of CH_4 in a variation of Scheme IV (not shown in diagram).

2) 59 $\xrightarrow{-C_2H_4}$ 31.

A loss of ethylene by Scheme IV would explain this final transition.

The decomposition of ethoxytrimethylsilane occurred with numerous rearrangement processes which have been elucidated by the mass spectra and DADI analysis of the deuterated analogs.

We thank Ellen Jenkins for technical assistance.

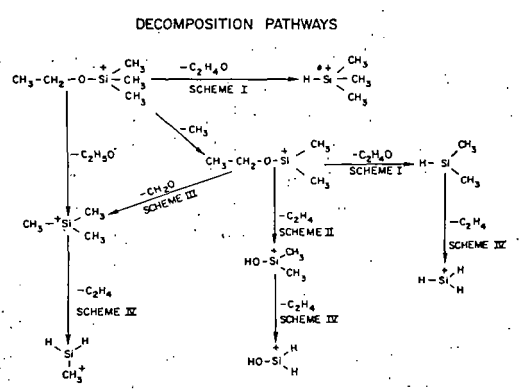

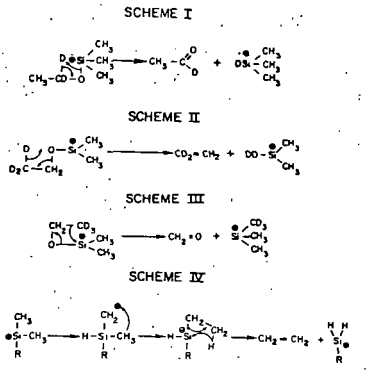

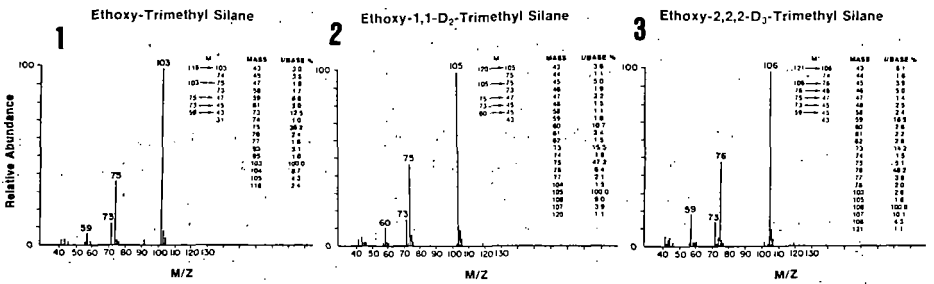

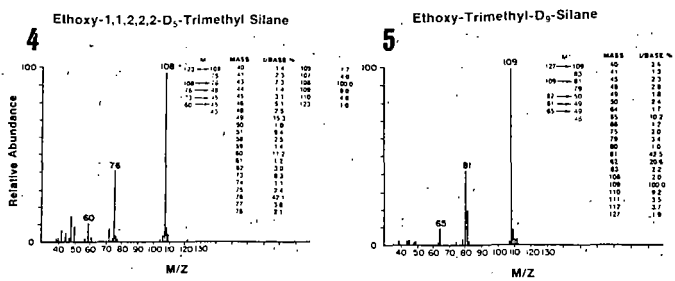

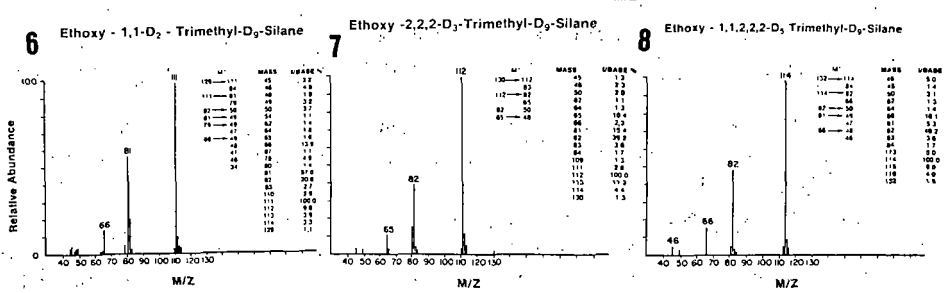

STEREOCHEMISTRY OF WATER AND ACETIC ACID LOSS FROM TETRALIN RADICAL CATIONS

G. Groenewold and M.L. Gross
Department of Chemistry
University of Nebraska
Lincoln, Nebraska 68588

The mechanism of expulsion of water and acetic acid from tetralin radical cations has been under investigation since 1976.[1,2,3] The purpose of the present study is to investigate the stereochemistry of the water and acetic acid losses and to examine the hydrogen scrambling processes occurring in the system. The strategy chosen for this work involved synthesis of specifically deuterium labeled compounds to be studied using ultra high resoultion and metastable techniques.

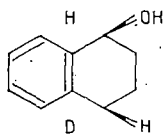

I

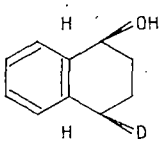

II

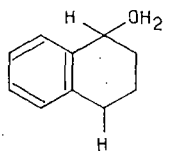

III

A stereospecific epoxide cleavage gave trans-4-d_1-1-tetralol (I). The cis-4-d_1-1-tetralol (II) was obtained by epimerizing the trans- compound. Mass spectral analysis showed that the (M-HOH/M-HOD) ratio for I was 4.5/1.0 and was 1.2/1.0 for II. These experiments were done at R > 80,000 to separate the M-HOD from a M-HOH,H interference. Unimolecular MIKES spectra were obtained using beams of R = 50,000 to minimize ^{13}C and incomplete labeling interferences. These experiments showed that the (M-HOH/M-HOD) ratio was 6.0/1.0 for I and 3.1/1.0 for II. In addition, similar examinations of the cycloreversion reaction occurring in I, II, 1-tetralol-OD and 4,4-d_2-1-tetralol revealed that the hydroxyl and 4C hydrogens exchange prior to cycloreversion.

These results are interpreted in terms of an ionic epimerization and a slower hydroxyl - 4C hydrogen exchange which is subject to an isotope effect and becomes competitive with the epimerization in the metastable time window. Structure III is proposed as a probable intermediate in the elimination of water and in the exchange of hydrogen.

The 1,4 elimination of acetic acid from cis- and trans-4-d_1-1-acetoxytetralin was also examined and was observed to exhibit some stereospecificity via ultra high resolution. However, the (M-HOAc/M-DOAc) ratio obtained from the MIKES spectra is 2.8/1.0 for both compounds, demonstrating that the stereochemical integrity of the elimination has disappeared within 1 to 10 microseconds. The results of this study will be submitted to Organic Mass Spectrometry for publication.

1. M.L. Gross and F.L. DeRoos, J. Amer. Chem. Soc., 98, 7128-7132 (1976).

2. M.L. Gross, E. Chiu, D. Pokorny and F.L. DeRoos, Org. Mass Spectrom., 12, 55-62 (1977).

3. S.F. Wojinski and M.L. Gross, Org. Mass Spectrom., 14, 135-139 (1979).

DIRECT DETERMINATION OF DEUTERIUM IN WATER USING METASTABLE IONS.

J.P. Schmit and G. Boulay

Dept. of Chemistry, Univ. of Sherbrooke, Sherbrooke, CANADA. J1K 2R1

Deuterium determination in water is usualy obtained in two steps: first by reducing water into hydrogen with uranium furnace, and second by measuring the ratio H_2/DH with a mass spectrometer especially designed for the isotopic measurements.

Taking advantage of the capability of double focusing mass spectrometer to retrace parent ions, it is possible to quantify deuterium in water with good occuracy at ppm level.

The method is based on the isotopic exchange properties of the hydroxylic hydrogen of n-propanol with water.

$$C_3H_7OH + DOH \rightleftharpoons C_3H_7OD + HOH$$

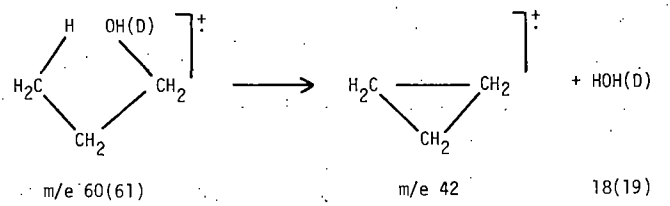

m/e 60(61) m/e 42 18(19)

Assuming that the deuterium content of the terminal methyl group of n-propanol is a constant, the exchanged deuterium is measured by comparison of the intensity ratio between $61^{+\cdot} \longrightarrow 42^{+\cdot}$ and $60^{+\cdot} \longrightarrow 42^{+\cdot}$ transitions for the unknowns and the standards, when scanning up the accelerating voltage the magnetic and electrostatic sectors being set on the $42^{+\cdot}$ ion properties.

The calibration curve with standards from natural level to 100% deuterated water yields a second degree polynomial curve with R-Square of 0.9994. From 0 to 1% of deuterium in water the curve can be assimilated to a straight line (degree 1) with R-Square of 0.9993

and Y intercept equal to 0.061 ± 0.001 (n = 4).

D_2O/H_2O CALIBRATION (0.025 % to 98.2 % D_2O)

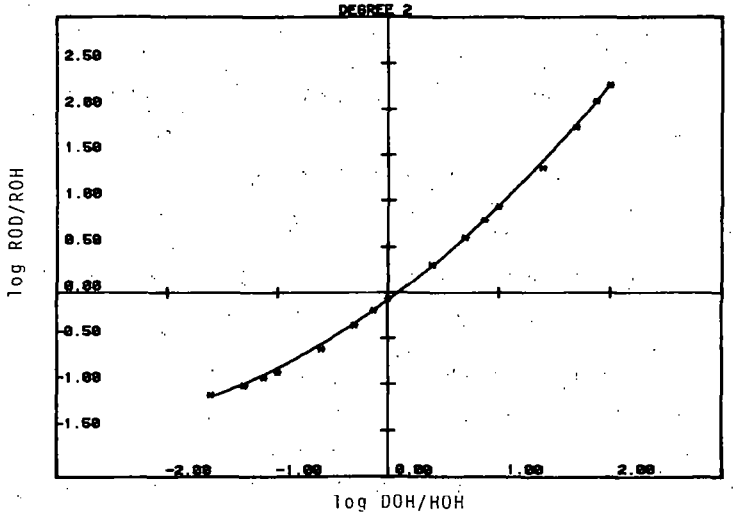

D_2O/H_2O CALIBRATION (0 % to 1 % D_2O)

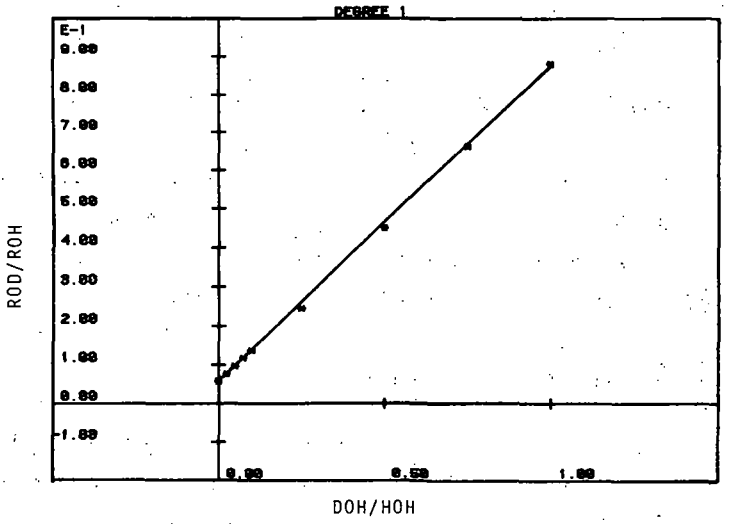

THE DETERMINATION OF STRUCTURES OF ION-MOLECULE REACTION INTERMEDIATES USING A TRIPLE ANALYZER MASS SPECTROMETER

Jackson O. Lay, Edward K. Chess, and Michael L. Gross
Department of Chemistry, University of Nebraska
Lincoln, Nebraska 68588

The investigation of the mechanistic details of ion-molecule reactions would be greatly aided if the structure of the collision complex could be determined. This is difficult because the complex is often too short-lived under the single collision conditions in an Ion Cyclotron Resonance (ICR) cell, for example. Thus, it can only be investigated by studying its fragments, using both normal and isotopically-labelled reagents, and by establishing mechanistic pathways using double resonance experiments. Recent investigations, using a high pressure (1 torr) chemical ionization (CI) source to provide stabilizing collisions, have led to the observation of collision complexes whose structures can be probed using their unimolecular and collision-induced decomposition (CID) reactions. The experiments have been conducted using the MS50-TA, a high resolution triple analyzer mass spectrometer (1). The high mass resolution available with this instrument allows unambiguous selection of the ion to be investigated, here, the collision complex. These techniques have been applied to several systems previously studied by ICR and Fourier-transform mass spectrometry (FT-MS).

The structure of the ion-molecule adduct formed in the reaction of the allyl ion and C_6H_5R (R=H,OH) has been investigated by comparison of the CID spectrum of the adduct with that of several model compounds. The adduct shows a large loss of ethene and very small methane loss with benzene as the neutral, consistent with a structure resembling protonated allylbenzene or β-methylstyrene (Table 1). The CID spectrum is substantially different than those of protonated indane, α-, o-, m-, and p-methylstyrene. The adduct formed in the reaction with neutral phenol gave a CID spectrum which was consistent with protonated allylphenol rather than protonated allyl phenyl ether as the ion-molecule product (Table 2).

Table 1

NATURE OF THE COLLISION COMPLEX: 50% CID OF PROTONATED NEUTRALS GIVING POSSIBLE COLLISION COMPLEXES

M/Z	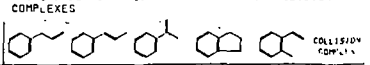 COLLISION COMPLEX					
103	3	3	8	3	8	4
91*	44	45	27	26	13	53
77	4	4	8	4	2	4
41	6	3	4	1	1	4

±1% ABSOLUTE
* INCLUDES A SMALL METASTABLE CONTRIBUTION

Table 2

$C_3H_5^+$ AND PHENOL+ RING OR OXYGEN ATTACK 50% CID OF PROTONATED NEUTRALS GIVING POSSIBLE COLLISION COMPLEXES

M/Z	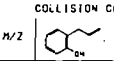	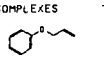	COLLISION COMPLEX
115	7	2	5
107	30	16	26
77	9	14	9
41	13	24	15

±2% ABSOLUTE

The structure of various $C_3H_5^+$ isomers have also been determined by investigating the adduct formed with benzene as the neutral reactant (Table 3). The premise is that each structurally distinct isomer should give a unique collision complex, or perhaps a different and distinguishable set of isomeric collision complexes. Thus, 1-propenyl, 2-propenyl, and allyl cations should be distinguished easily based on the CID spectra of their pressure-stabilized adducts with benzene. This was found to be true. The 2-propenyl cation and benzene give an adduct with relatively more methyl and less ethene loss than allyl cation and benzene. This is

consistent with the CID spectrum of the model compound, protonated α-methylstyrene. On the other hand, 1-propenyl cation gives a unique ion-molecule product whose CID spectrum is intermediate between that for either allyl or 2-propenyl cation.

The o-quinodimethane (2) and styrene (3) radical cations react with neutral styrene in an ICR spectrometer to yield product ions suggestive of different activated collision complexes. By using a 4:1 mixture of NO:He as the low energy charge-exchange ionizing gas, the collision complexes from both of these reactions have been generated in good yield in a CI source. Subsequent investigations of these complexes have revealed that their structures are, indeed, very different. We have shown that the o-quinodimethane ion (I) reacts with styrene through a Diels-Alder type cycloaddition to yield 2-phenyltetralin (II) by comparing the unimolecular and CID spectra of the complexes with those of model compounds, and through the use of deuterium labelling.

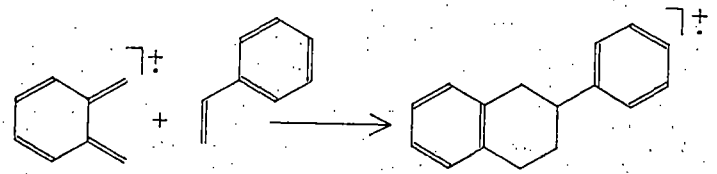

I II

Similar experiments have shown that the collision complex from the styrene + styrene ion-molecule reaction is definitely not 1- or 2-phenyltetralin, [2.2]paracyclophane, or any other reasonable acyclic structure, such as 2,3-diphenyl-2-butene, 2,4-diphenyl-2-butene, or 1,4-diphenyl-1-butene. The diphenylcyclobutanes were ruled out in a previous study (3). This complex shows a high tendency to return to starting materials without H/D scrambling, unlike any of the model systems. Thus, we propose structure III or IV as the complex for this reaction, and have initiated further studies to synthesize appropriate precursors which will decompose to form these structures.

Table 3.

NATURE OF THE REACTING $C_3H_5^+$ ION: 50% CID OF THE COMPLEX FROM VARIOUS $C_3H_5^+$ IONS REACTING WITH BENZENE

M/Z	△			
103	3.9±0.1	4.0±0.7	5.8±0.4	7.3±0.6
91*	42.9±1.6	53.1±1.7	42.7±1.5	40.6±6.6
77	4.6±0.3	4.4±0.8	6.1±0.2	6.9±0.6
41	3.6±0.5	4.1±0.5	3.7±0.3	4.4±0.3

* INCLUDES A SMALL METASTABLE CONTRIBUTION

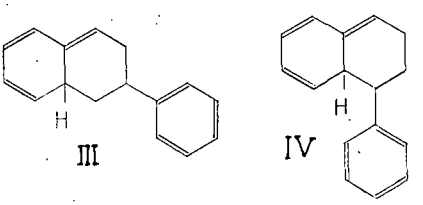

III IV

1) M. L. Gross, P. A. Lyon, F. W. Crow, and S. Evans, presented at the 28th Annual Conference on Mass Spectrometry and Allied Topics, New York, N.Y., May 25-30, 1980.
2) Unpublished results.
3) C. L. Wilkins, M. L. Gross, J. Am. Chem. Soc., 93, 895(1971).

KINETIC ENERGY RELEASE - A SENSITIVE PROBE FOR THE GAS PHASE UNIMOLECULARE ISOMERISATIONS OF IONIZED STEROID ALCOHOLS; ZE'EV V.I. ZARETSKII and PNINA DAN; Isotope Dept., The Weizmann Institute of Science, 76 100 Rehovot, Israel.

It has been found recently that kinetic energy release (KER) measured for the transitions occurring in the MIKE spectra are very sensitive to the stereochemical differences in steroid hydrocarbons and ketones[1]. This paper reports a study of the mechanism of the CH_3 and H_2O losses occurring from the ionized androstane alcohols (eleven stereoisomers differing in both configuration of the OH groups and the mode of the rings A/B junction), vitamins D_2 and D_3, ergosterol (provitamin D_2) and cholesterol, using KER which accompanies dissociation. The critical energy values [$E_c \simeq A(X)^+ - I(M)$] and metastable/daughter ions

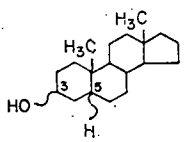

1 5α,3β
2 5α,3α
3 5β,3β
4 5β,3α

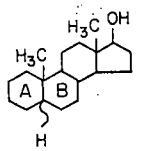

5 5α
6 5β

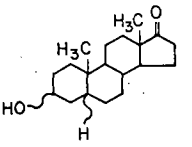

7 5α,3β
8 5α,3α
9 5β,3β
10 5β,3α

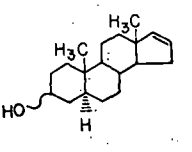

11 3α
12 3β

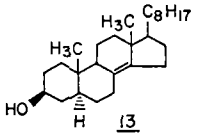

13

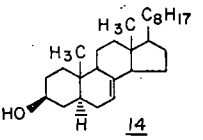

14

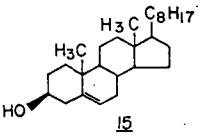

15

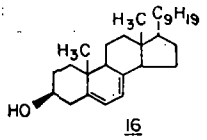

16

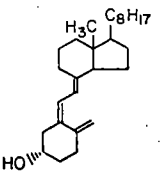

17

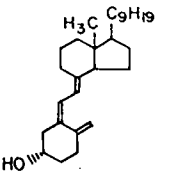

18

ratios (m^*/D^+) were also determined for the reactions studied. The KER values have been measured with Varian MAT-731 double focusing mass spectrometer, of Mattauch-Herzog geometry[2], for the $M^{\cdot+} \rightarrow (M-CH_3)^+$, $M^{\cdot+} \rightarrow (M-H_2O)^{\cdot+}$, $(M-H_2O)^{\cdot+} \rightarrow (M-H_2O-CH_3)^+$ and $(M-CH_3)^+ \rightarrow (M-CH_3-H_2O)^+$ metastable transitions occurring in the 1st FFR, by scanning the accelerating voltage with fixed electric sector voltage and fixed magnetic field. It was demonstrated that while the H_2O elimination reactions give rise to narrow metastable peaks, thus indicating little KER, the losses of the angulare CH_3 from both $M^{\cdot+}$ and $(M-H_2O)^{\cdot+}$ ions produce, in many cases, broad metastable peaks. This suggests that a rate determining isomerisation, prior to decomposition, occurs and a large quantity of kinetic energy releases upon subsequent CH_3 loss, especially from the $(M-H_2O)^{\cdot+}$ ions. The isomerisation mechanisms, preceding the decompositions, will be discussed.

Table: KER Data (T_{50}, meV; mean error ± 5%) for Steroids 1-18.

Compound	$M^{+\cdot}$-CH_3	$M^{+\cdot}$-H_2O	$(M\text{-}H_2O)^{+\cdot}$-CH_3	$(M\text{-}CH_3)^{+}$-H_2O
1	45	33	95	27
2	43	27	86	28
3	-	23	81	28
4	-	26	67	29
5	62	25	85	31
6	42	25	54	30
7	99	45	176	35
8	92	46	186	36
9	72	39	76	41
10	116	35	105	42
11	67	-	-	28
12	71	-	-	31
13	133	-	-	-
14	122	-	-	-
15	94	58	161	34
16	154	-	282	55
17	169	87	213	49
18	168	88	355	69

REFERENCES

[1]Z.V.I. Zaretskii, E. Larka, I. Howe and J.H. Beynon, 28th Annual Conf. on Mass Spectrometry and Allied Topics, N.Y. (1980).
[2]U. Herzig and P. Krenmayr, Org. Mass Spectrom., 14, 75 (1979); Z.V.I. Zaretskii and P. Dan, submitted to Org. Mass Spectrom.

MIKE SPECTROMETRY OF SOME NITRAMINE EXPLOSIVES

J. Yinon*, D.J. Harvan and J.R. Hass

NIEHS, Research Triangle Park, N.C. 27709

The mass spectrometry of nitramines has always been of great interest because of their use as explosives. The EI mass spectra of nitramines have been characterized by abundant fragment ions and very scarce molecular ions (1,2). Moreover, large differences in the relative abundances of the major ions have been reported by various groups (3), which were attributed to the formation of thermal decomposition fragments prior to ionization. CI mass spectra of nitramines, although producing in some compounds abundant $(M + X)^+$ ions, have also been characterized by abundant fragment ions (2,4,5,6).

In order to learn more about the fragmentation processes of nitramines, Mass-Analyzed Ion Kinetic Energy (MIKE) Spectrometry (with and without collision-induced decomposition) has been used to study the fragmentation pathways in both EI and methane-positive CI of some nitramine explosives, including *RDX*, *HMX* and *tetryl*. *MIKE* spectra were obtained on a VG Micromass ZAB-2F reversed geometry mass spectrometer with a combined EI/CI source and connected to a modified Finnigan Incos data system (7). Collision-induced MIKE spectra were obtained with helium in the collision cell. Accurate mass measurements of the nitramine mass spectra were done on a VG Micromass 70-70F double focusing mass spectrometer with a 22-50 data system.

The data obtained was used to determine fragmentation maps for the studied compounds in both EI and CI modes. The figure shows the fragmentation map of RDX in the EI mode. Results showed that the fragmentation pathways of RDX and HMX are very similar but differ from the fragmentation pathway of tetryl which is both a nitramine and a nitroaromatic compound. Ions which appeared in the mass spectrum but did not have an apparent precursor (according to the MIKE measurements) could be formed by thermal decomposition (in the solid probe or the ion source) followed by ionization. In compounds where no molecular ions were observed in their mass spectrum, fragment ions appearing in the mass spectrum but without an apparent precursor ion, could be formed by either fragmentation or thermal decomposition or both (these pathways are shown in the figure by broken lines). Nevertheless, ions which have a precursor and seem therefore to be formed by fragmentation, could be in part due to thermal decomposition.

References

1. S. Bulusu, T. Axenrod and G.W.A. Milne, Org. Mass Spectr. 3, 13 (1970).
2. S. Zitrin and J. Yinon, Advances in Mass Spectr. in Biochem. and Medicine, 1, 369 (1976).
3. J. Yinon and S.Zitrin, "The Analysis of Explosives", Pergamon Press, Oxford, 1981.
4. J. Yinon, Biom. Mass Spectr. 1, 393 (1974).
5. P. Vouros, B.A. Petersen, L. Colwell, B.L. Karger and H. Harris, Anal. Chem. 49, 1039 (1977).
6. J. Yinon, Org. Mass Spectr. 15, 637 (1980).
7. M. Weiss, J. Karnofsky, J.R. Hass and D.J. Harvan, Proc. of 27th Annual Conference on Mass Spectrometry and Allied Topics, Seattle, Washington, 1979. p. 270.

---

* On sabbatical leave from the Weizmann Institute of Science, Rehovot, Israel.

RDX - EI

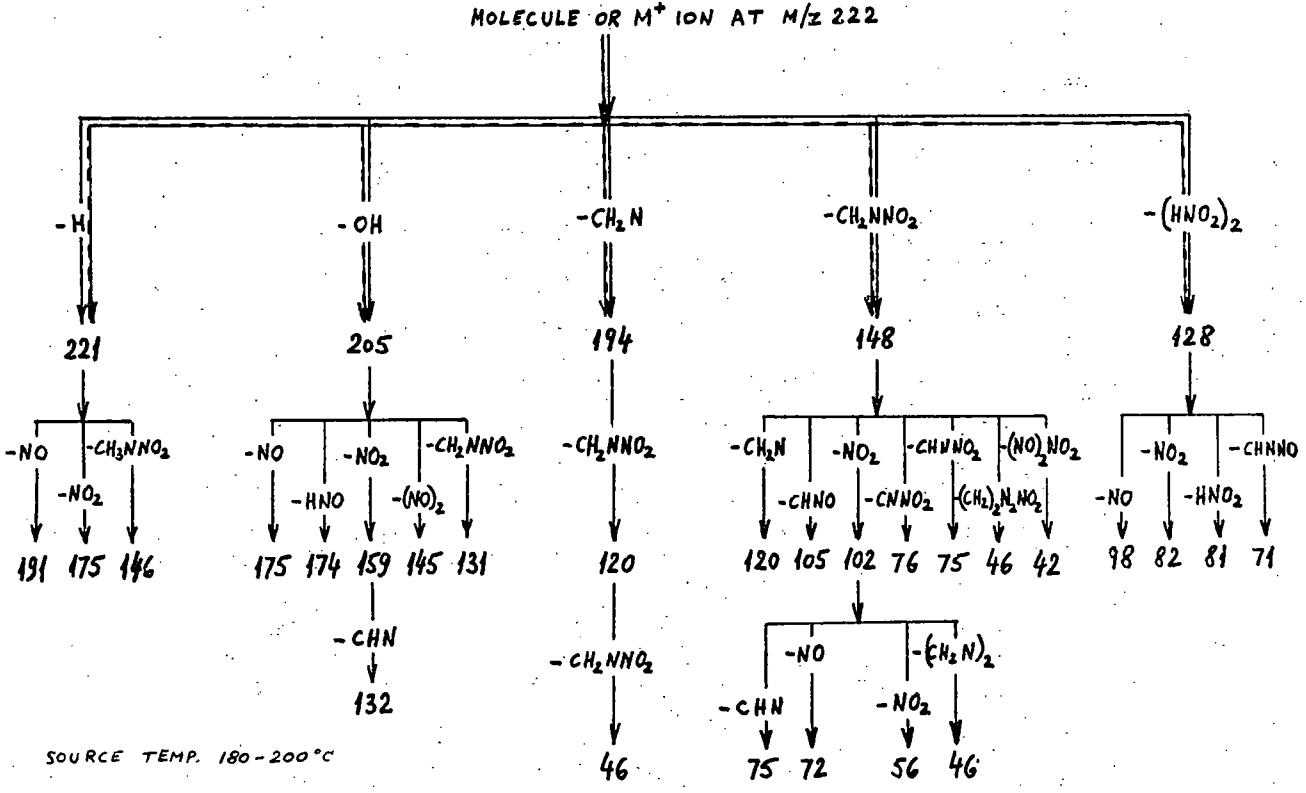
MOLECULE OR M+ ION AT M/Z 222
-H
-OH
-CH2N
-CH2NNO2
-(HNO2)2
221
205
194
148
128
-NO
-CH3NNO2
-NO2
191 175 146
-NO
-NO2
-HNO
-(NO)2
-CH2NNO2
175 174 159 145 131
-CHN
132
-CH2NNO2
120
-CH2NNO2
46
-CH2N
-NO2
-CHNO2
-CNNO2
-(CH2)2N2O2
-(NO)2NO2
120 105 102 76 75 46 42
-CHN
-NO
-(CH2N)2
-NO2
75 72 56 46
-NO
-NO2
-CHNNO
-HNO2
98 82 81 71
SOURCE TEMP. 180-200°C

GC/MS ANALYSIS OF SUBSTITUTED 1,3-OXAZOLIDINES, TETRAHYDRO-1,3-OXAZINES AND 1-OXA-4-AZASPIRO[4.5]DECANES

K. J. WELCH AND T. A. LAJINESS

Corporate Research, S. C. Johnson & Son, Inc., Racine, WI 53403

In order to study the relationship between structure and biological activity, a series of biologically-active compounds are being investigated.(1) This collection of compounds has provided an opportunity to study the mass spectra of some structurally-related heterocycles.

The mass spectra of the oxaza compounds were taken with a Finnigan 4000 GC/MS (electron impact and methane chemical ionization). High resolution mass spectra (electron impact) of selected compounds were obtained at the Midwest Center for Mass Spectrometry, University of Nebraska, Lincoln, Nebraska 68588.(3)

Mass Spectra of the Alkyl-Substituted Oxazolidines and Tetrahydrooxazines

The electron-impact spectra for the alkyl oxazolidines (Scheme I n=1), and the alkyl tetrahydrooxazines (Scheme I n=2) were characterized by the facile loss of the alkyl substituent (R_1) to form the species A. Loss of ketene from A produced the stable ion C. There was evidence for a secondary route to C via the species B. The origin of the ions D and E appears to be the result of CO loss from A and C respectively.

Ions common to the EI spectra were found in the CI spectra. In some cases the masses of the ions were shifted due to different decompositions of even-electron species (CI) versus odd-electron species (EI). An ion scarcely observed in the EI spectra was found which corresponded to the rearrangement and rupture of the MH^+ ion at the dashed line a.

Mass Spectra of the Phenyl-Substituted Oxazolidines

The EI fragmentation of the phenyl-substituted oxazolidines (Scheme II) produced ions corresponding to the loss of the phenyl group (C) and loss of the acetyl radical (B). The phenyl oxazolidines also produced the species A which appeared to be formed from the rearrangement and rupture of the heterocyclic ring (dashed line a). The most probable precursor of the intense benzoylium ion D is A. However, a portion of the benzoylium abundance may be due to the rupture of B and E as shown (dashed line b). This would be the converse of CO elimination noted in the other compounds.

Mass Spectra of the Oxaazaspirodecanes

The EI fragmentation of the spiro compounds (Scheme III) had ions (cir. 1% RA) corresponding to the loss of the acetyl radical or an alkyl (R_1 or R_2) radical. The major ions appeared to be from decompositions involving the alicyclic ring. Rupture of the alicyclic ring combined with hydrogen migration (dashed line a) formed the species A. Further fragmentation of A to B, E and F is consistent with the other compounds studied. There appears to be evidence for an alternate decomposition of M through rupture (dashed line b) and loss of an even-electron molecule to form C. Chou(2) reported an odd-electron species for a similar molecule. Since the loss of ketene from C could occur at two locations, the structure for D is not attempted. The CI mass spectra, as expected contained no ions corresponding to C or D.

1. T.A. Lajiness, E.S. Oonnithan and A.G. Hageman, "Abstracts of Papers", 181st National Meeting of the American Chemical Society, Atlanta, GA, March 1981; American Chemical Society: Washington, D.C., MEDI 43.

2. S. Chou, J.A. Nelson and T.A. Spencer, J. Org. Chem. 1974, 39, 2359.

3. Mass spectral data presented at the meeting will be made available upon request.

SCHEME I

FRAGMENTATION OF ALKYL-SUBSTITUTED OXAZOLIDINES AND ALKYL-SUBSTITUTED TETROHYDROOXAZINES

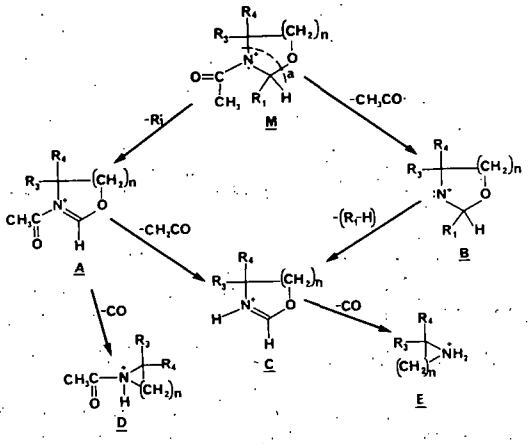

SCHEME II

EI FRAGMENTATION OF PHENYL-SUBSTITUTED OXAZOLIDINES

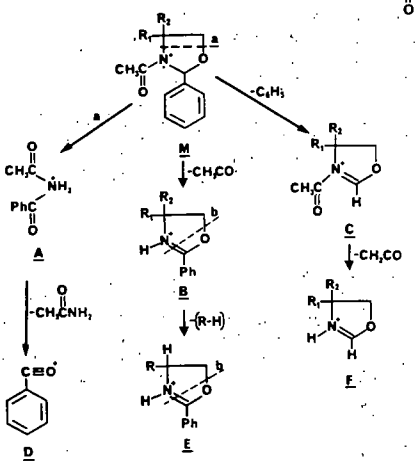

SCHEME III

EI FRAGMENTATION OF SUBSTITUTED OXAAZASPIRODECANES

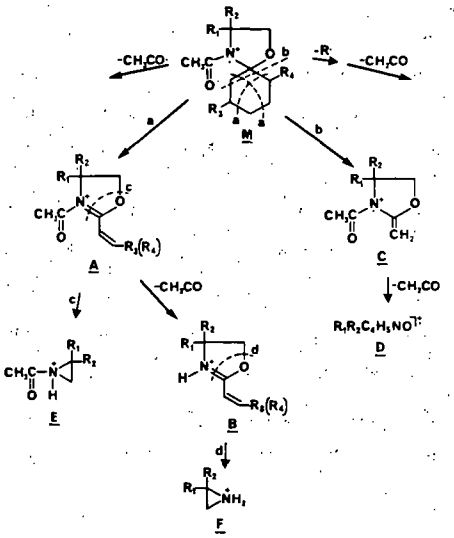

UNIQUE HYDROGEN REARRANGEMENT DURING THE REDUCTION OF MALEIMIDE WITH LITHIUM ALUMINUM DEUTERIDE; M.S.B.NAYAR, L.A.GEELHAAR and P.S.CALLERY; Dept. of Medicinal Chemistry, University of Maryland, 636 W.Lombard St.,Baltimore, MD 21201.

Attempted preparation of pyrrolidine-2,2,3,4,5,5-$^2H_6$ by the reduction of maleimide with lithium aluminum deuteride surprisingly resulted in the formation of pyrrolidine containing only 5 deuterium atoms, as indicated by the mass spectrum of the N-trifluroacetyl derivative. The labeled pyrrolidine was oxidized to 1-pyrroline with sodium persulfate and reacted with HCN to obtain 2-cyanopyrrolidine. The mass spectrum of its trifluroacetyl derivative indicated the presence of four deuterium atoms. 1-Pyrroline was further oxidized with rabbit liver homogenate to obtain 4-aminobutanoic acid. The mass spectrum obtained after derivatization with dimethyl acetal of dimethylformamide indicated that the oxidation product is a mixture of 2,4,4-$^2H_3$ and 3,4,4-$^2H_3$ analogues of 4-aminobutanoic acid.

A mechanism is proposed for the reaction based on the structure of pyrrolidinone-$^2H_3$ (5) isolated from the reaction mixture(Scheme 1).[1] 3-Pyrrolinone, which is a postulated intermediate, on reduction with lithium aluminum deuteride yielded pyrrolidine-$^2H_3$ (Scheme 2).

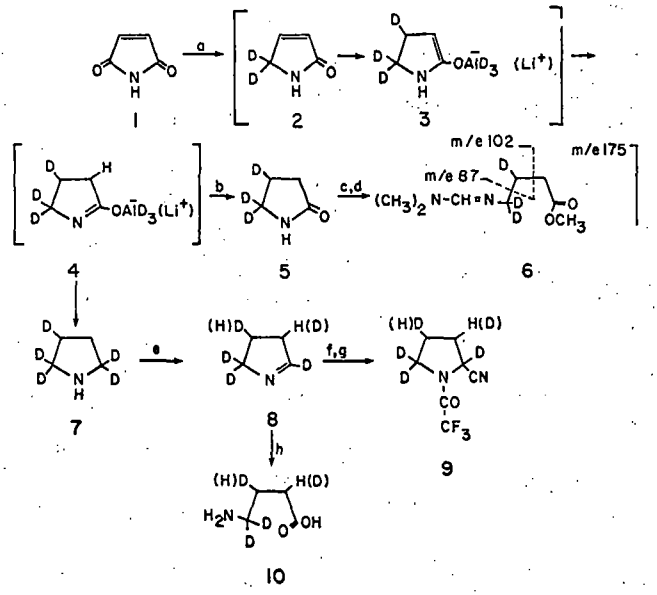

(a) $LiAlD_4$; (b) H_2O; (c) 5 N HCl; (d) dimethylformamide dimethyl acetal; (e) $Na_2S_2O_8$, NaOH; (f) HCN; (g) $(CF_3CO)_2O$; (h) rabbit liver homogenate

Scheme 1

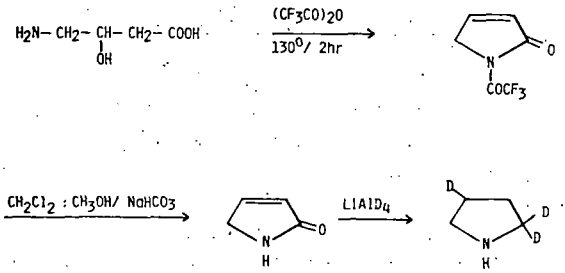

Scheme 2

Irrespective of the mechanism, it is obvious that a migration of hydrogen from N to C has taken place, since reduction of maleimide-^{2}H with lithium aluminum hydride led to the formation of pyrrolidine-3-^{2}H. Although it is generally accepted that metal hydrides abstract active hydrogen atoms with the liberation of H_2,[2] our findings indicate that the reaction of maleimide with lithium aluminum hydride does not take this course.

(*1*) M.S.B.Nayar and P.S.Callery, *J.Org.Chem. 46*, 1044 (1981).

(*2*) W.G.Brown, *Org. React. 6*, 469 (1951).

LC - MS - NCI OF EXPLOSIVES

R.D. Voyksner[1,2], Y. Tondeur[1], C.E. Parker[1], J.D. Henion[3], and J. Yinon[1,4]

1. NIEHS. Research Triangle Park, N.C. 27709
2. Department of Chemistry, U.N.C.-C.H., Chapel Hill, N.C. 27514
3. N.Y. State College of Veterinary Medicine, Cornell University, Ithaca, N.Y. 14853
4. On sabbatical leave from the Weizmann Institute of Science, Rehovot, Israel

The analysis of explosives mixtures is of major importance in several analytical fields such as forensic identification of post-explosion residues and environmental analysis of water contaminated by explosives.

A variety of methods and techniques have been used for the analysis of explosives (1) with various degrees of success.

We have used a direct LC-MS combination (2,3) for the analysis of explosives in order to combine the separation capability of the HPLC with the specificity and sensitivity of the mass spectrometer.

The mass spectrometer used in this research was a Finnigan 3300 CI mass spectrometer (previously modified for negative ion CI operation) connected to a Finnigan/Incos 2300 data system.

The HPLC consisted of two Waters Associates 600 A pumps, a Waters Associates 660 Solvent Programmer and a Perkin-Elmer LC-55 Variable Wavelength UV detector.

The LC-MS interface was an unmodified Hewlett-Packard Direct Liquid Insertion Probe LC-MS Interface, a variable split-type interface.

The probe inlet system of the MS was modified to accept the 1/2" OD LC probe, and a sliding fit "desolvation chamber" was threaded into a modified source input adaptor plate on the Finnigan source. No modifications of the pumping system were necessary.

The investigated explosives were pure standards (obtained from the Israel Police Headquarters, Jerusalem, Israel) and military mixtures (obtained from the N.C. State Bureau of Investigation, Raleigh, N.C.)

The investigated mixtures were octol (consisting of TNT and HMX) and tetrytol (consisting of tetryl and TNT). A standard mixture was made up of pure compounds and consisted of RDX and tetryl.

Best LC separation results were obtained under the following conditions: RP-18 reversed-phase column, 4.6 mm X 10 cm length (Brownlee Labs, Inc.). Solvents were acetonitrile: water (50:50) and methanol: water (50:50). Flow rate was 1 ml/min. UV detector wavelength was 254 nm.

Negative - ion chemical ionization was found to be the most sensitive MS mode of operation. The LC solvents function as electron energy moderators, and the mode of ionization is by electron capture. The figure shows the LC-MS-NCI spectra of Octol.

Sensitivity measurements were done by injecting various amounts of TNT (in acetonitrile/water solution) into the LC-MS system, and scanning the mass spectrometer over a 100-400 amu range at 4 sec/scan. The smallest detectable amount of TNT was 100 ng, injected on column (or approximately 1 ng to the MS source).

A TNT-acetonitrile/water solution, continuously flowing through the LC and into the mass spectrometer was used to investigate the temperature effects in the ion source under NCI conditions. Experiments were done in the temperature range of 160-260°C. It was found that relative ion abundances (relative to m/z 197) of high mass ions (m/z 227, 210) were decreasing with increasing temperature, while abundances of lower mass ion fragments (m/z 152, 167, 181) were increasing, m/z 226 ion abundance was constant throughout the investigated temperature range.

Although more research has to be done in the use of LC-MS of explosives, it seems to be a powerful technique for the analysis of explosives mixtures in both forensic and environmental applications.

References

1. J. Yinon and S. Zitrin, "The Analysis of Explosives", Pergamon Press, Oxford, 1981.

2. J.D. Henion, Anal. Chem., 50, 1687 (1978).

3. A. Melera, Advances in Mass Spectr., 88, 1597 (1980).

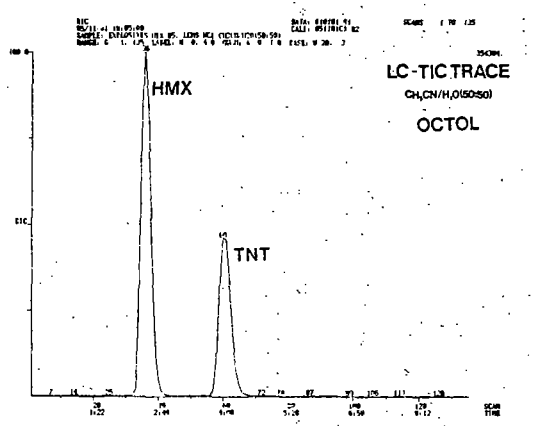
HMX
TNT
LC-TIC TRACE
CH3CN/H2O(50:50)
OCTOL

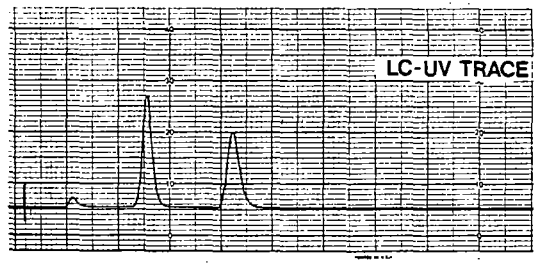
LC-UV TRACE

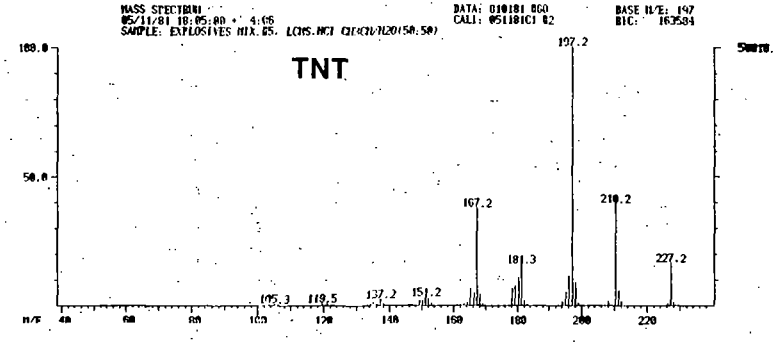
TNT
197.2
107.2
210.2
181.3
227.2
105.3
119.5
137.2
151.2

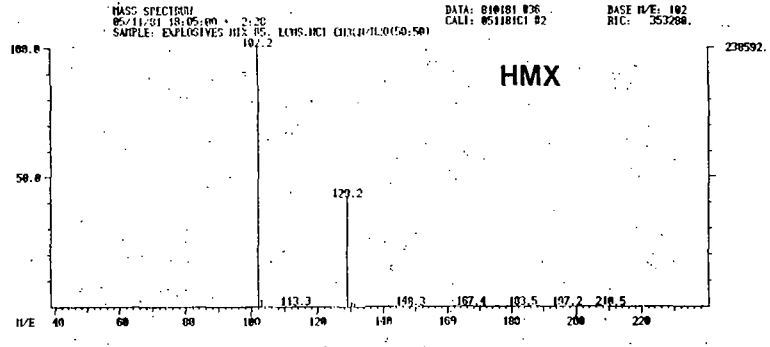
HMX
102.2
129.2
113.2
149.2
167.4
183.5
197.2
210.5

CAPILLARY COLUMN GC/MS CHARACTERIZATION OF DIESEL EXHAUST PARTICULATE EXTRACTS

T. J. Prater, T. Riley and D. Schuetzle
Analytical Sciences Department
Scientific Research Laboratory
Dearborn, Michigan 48121

INTRODUCTION

Previous studies have shown that most of the direct-acting Salmonella typhimurium mutagenic activity (>50%) in diesel exhaust particulate extracts is concentrated in chemical fractions which contain compounds of moderate polarity (1). Analytical-scale normal phase high performance liquid chromatography(NP-HPLC) (2), packed-column GC/MS and high resolution MS analysis were used in that work to determine that these moderately-polar fractions consisted primarily of polynuclear aromatic hydrocarbon (PAH) derivatives. The objective of this study was to extend the previous work by developing preparative scale NP-HPLC fractionation followed by fused silica capillary GC/MS analysis in order to improve component resolution.

EXPERIMENTAL

Light duty diesel exhaust particulate samples were collected on T60A20 Pallaflex filters using a dilution tube and a chassis dynomometer test facility. Filter samples were soxhlet extracted with dichloromethane (DCM).

HPLC analysis was performed on a Varian Model 5600 LC equipped with a 7.8 mm i.d. x 30 cm long Microporasil 10 column. The solvent program consisted of 100% hexane for 5 min, then 1% DCM/min for 5 min, followed by a linear gradient to 100% DCM in the next 25 min, 100% DCM for 10 min, then 10% acetonitrile/min for 10 min, and a final 10 min flush with 100% acetonitrile. The chromatographic separation was monitored by UV at 254 nm and by fluorescence at 254/320 nm. Further details of this technique are presented elsewhere (3).

GC/MS analyses were performed on a VGMM ZAB-2F mass spectrometer equipped with a 30 m long x 0.25 mm i.d. SE54 fused silica capillary column interfaced directly to the mass spectrometer source. Sample injections were directly on-column and temperature programming was 80° to 270° at 4°/min. Electron impact ionization techniques were used.

RESULTS AND DISCUSSION

This investigation emphasized the analysis of HPLC fractions containing nonpolar and moderately polar PAH derivatives. Nonpolar aliphatic and highly polar HPLC fractions were not characterized by GC/MS. The nonpolar and moderately polar PAH derivatives which were identified are listed respectively in Tables I and II. Many of the compounds identified have a large number of isomers as indicated by the parentheses in the tables. This is illustrated by the mass chromatograms in Fig. 1 which show the increasing complexity of the isomer series as methyl substituents are added to anthracene and phenanthrene. There are probably more isomers for the methylated anthracene and phenanthrenes than we were able to resolve even with the high-resolution fused-silica capillary column. It would be difficult and of limited utility to identify every specific isomer present in these fractions. For this reason, synthesis of standards and identification of isomers are only being undertaken on those groups of PAH and PAH-derivatives which yield a relatively high level of direct- or indirect-acting Ames activity. This has been found to be the case for the nitrated-PAH derivatives which tend to show high levels of direct-acting mutagenicity compared to other PAH and PAH derivatives in these samples. In summary, the combination of normal phase HPLC fractionation followed by capillary GC/MS analysis proved to be a very useful approach to the characterizaiton of diesel exhaust particulate extract.

1. Schuetzle, D., Lee, F.S.-C., Prater,T. J. and Tejada, S. B., Intern. J. Env. Anal. Chem., 9, 93, 1981.

2. Schuetzle, D. and Perez, J. M., Proceedings of the 74th Annual Meeting of the Air Pollution Control Association, Paper #81-56.4, Philadelphia, PA (June 21-26, 1981).

3. Levine, S. and Skewes, L., J. Chromatogr., In preparation (1981).

Table I. Nonpolar PAH Identified in Diesel Exhaust Particulate Extract

dibenzothiophene
methyl dibenzothiophene isomers(3)
dimethyl dibenzothiophene isomers(7)
fluoranthene and pyrene
BaP, BeP, perylene,and isomers(3)
tetramethyl dibenzothiophene isomers(12)
benzo(g,h,i) fluoranthene
methyl benz(a)anthracene isomers(4)
pentamethyl dibenzothiophene isomers(4)
methyl (fluoranthene and pyrene)isomers(7)
anthracene and phenanthrene
methyl (phenanthrene and anthracene) isomers(4)
dimethyl (phenanthrene and anthracene) isomers(13)
trimethyl dibenzothiophene isomers(9)
trimethyl (phenanthrene and anthracene) isomers(15)
tetramethyl (phenanthrene and anthracene) isomers(16)
benz(a)anthracene, chrysene, benzo(c)phenanthrene, triphenylene isomers(2)
dimethyl benz(a)anthracene isomers(2)

Table II. Moderately Polar PAH Derivatives Identified in Diesel Exhaust Particulate Extract

benz(a)anthracene dione
thioxanthone isomer
pyrenone
methyl thioxanthone
benz(d,e)anthrone and isomers(3)
1,1' biphenyl-ol
(pyrene or fluoranthene) carboxaldehyde
phenanthrone
xanthone
(anthracene or phenanthrene) dione
methyl (anthracene or phenanthrene)dione
anthracene carboxaldehyde
dimethyl (anthracene and phenanthrene) carboxaldehyde isomers(8)
methyl (anthrone and phenanthrone) isomers
dimethyl (anthrone and phenanthrone) isomers
trimethyl (anthrone and phenanthrone) isomers
dimethyl thioxanthone
1-nitropyrene
fluorenone
dibenzofuran carboxaldehyde
anthrone isomer
xanthene carboxaldehyde
dibenzothiophene carboxaldehyde
phenanthrene carboxaldehyde
methyl (anthracene and phenanthrene) carboxaldehyde isomers(9)

Figure 1. Mass chromatograms of phenanthrene(P) and anthracene(A) (178), methyl-A and -P (192), dimethyl-A and -P(206), and trimethyl-A and -P(220)

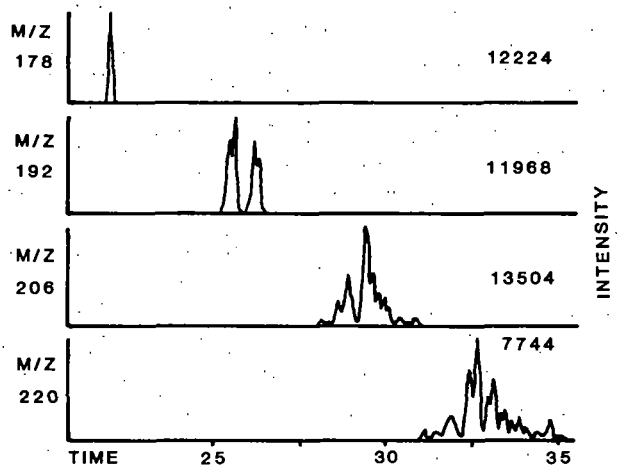

GC/MS ANALYSIS OF PRIORITY POLLUTANTS: A COMPARISON OF PACKED COLUMN AND FUSED SILICA CAPILLARY GC/MS ANALYSES; J.E. WILKINSON, B.N. COLBY, and T.R. SMITH; Systems, Science and Software, La Jolla, CA 92038 and A.D. SAUTER, US-EPA, Environmental Monitoring and Support Laboratory, Box 15027, Las Vegas, NV 89114

The accepted standard for the analysis of extractable priority pollutants is a packed column GC/MS, Method 625.[1] Excellent precision and accuracy, however, has been reported[2] for selected priority pollutants using a fused silica capillary column directly coupled with the GC/MS ion source (FSCC/MS). This enables compositing of acid and base/neutral fractions for simultaneous analysis at low nanogram levels in one forty minute acquisition. A SE-54 fused silica capillary column is temperature programmed from 30° (3 min) to 285° at 10°/minute after splitless injection. Carrier gas (He) flow is maximized at 48 cm/second. Data obtained by both separate and composited fraction analyses are comparable to Method 625 data.[3]

There are several other advantages of the FSCC/MS technique. Interferences are minimized due to increased chromatographic resolution. Accuracy is improved by eliminating the problem of compound crossover during sample extraction. Analyses of acid and base/neutral fractions of an extremely complex sample indicates that up to 20% of some base/neutral compounds can crossover into the acid fraction. Compositing the fractions just prior to GC/MS analysis eliminates this potential problem, thus increasing analytical accuracy. Since total GC/MS analysis time is decreased by a factor of two, analytical costs are considerably decreased.

1 Federal Register, Vol. 44, No. 233, pp. 69540, 69552, December 3, 1979.

2 A.D. Sauter, et al., 28th Annual Conference on Mass Spectrometry and Allied Topics, 1980, NY, NY.

3 Data provided by Dr. R.G. Beimer of TRW, Inc.

Capillary Column GLC-EIMS Assay For Xylonidine in Chicken Eggs

R.W. Walker, J.E. Taylor, A.A. Van Iderstine
R.M. Weppelman, H.E. Mertel and W.J.A. VandenHeuvel

Merck Sharp & Dohme Research Laboratories
Rahway, New Jersey 07065

INTRODUCTION

Various aryl iminoimidazoline derivatives including the antihypertensive drug clonidine have marked anovulatory and antigonadal activities in laying hens.[1] Among the most active of these is xylonidine [2-(2,6-xylylimino)-imidazoline], the structure of which is shown. Because of its avian antifertility action, xylonidine was of interest as a forced molting agent. Forced molting refers to the practice of forcing hens to stop laying eggs for a period of several weeks.[2,3] One result of this lull in reproductive activity is a molt which gives the practice its name. There are several economic advantages to forced molting. When molted hens resume production, they generally lay more eggs and produce eggs with more durable shells and at smaller cost in feed than untreated hens. Unfortunately, the only procedure currently available for forced molting hens is starvation, usually for a period of about 10 days. This drastic treatment almost certainly is detrimental to health and viability. In contrast, xylonidine appeared quite safe for laying hens and thus offered a desirable alternative to starvation.

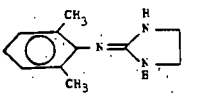

For xylonidine to become a viable candidate as a forced molting agent, the xylonidine concentration in eggs from treated hens had to be determined. This, in turn, required the development of a very sensitive, selective assay procedure. Toward this end a capillary column gas-liquid chromatographic (GLC) with electron impact ionization mass spectrometric (MS) procedure was developed, xylonidine-d_4 serving as the internal standard. Although the structure of xylonidine would suggest the need for derivatization of this drug prior to analysis, the GLC-MS detection limit of the assay for underivatized drug (0.3 ppb) was sufficient to permit quantification of xylonidine in yolk and albumen from eggs produced by chickens on-drug and for up to two weeks post-medication.

Isolation

Yolk and albumen samples to which internal standard (200 ng) had been added were deproteinated with perchloric acid. Supernatants were first washed with chloroform to remove lipids, and then extracted with toluene after pH adjustment to >9. The toluene residue was equilibrated with 0.1N acetic acid/petroleum ether and the aqueous phase recovered and reduced to dryness. The resulting residue was dissolved in methanol and charged to a 10 m SE-30 capillary column using a dropping needle injector.[4]

GLC-MS Instrumentation

A Finnigan 3200-6110 GC-MS-COM instrument operated in the electron impact mode and utilizing selected ion monitoring was used. Chromatographic conditions were as follows:

10 m x 0.33 mm I.D. glass capillary column coated with SE-30
Oven temperature = 190°C
Injection port temperature = 220°C
Carrier gas (helium)
Flow rate ca. 2 ml/min
Retention time of xylonidine = 0.8 min

The mass spectrometer was operated using the following conditions:

Ionizing potential = 70 ev
Emission current = 0.8 mA
Electron multiplier = 1800 V

The M-15 ions for xylonidine (m/e 174) and xylonidine-d_4 (m/e 178) were monitored and the peak height intensities obtained via computer printout.

Calibration Standards

Calibration mixtures each containing 200 ng of xylonidine-d_4 and xylonidine levels up to 2000 ng were prepared. The m/e 174 to m/e 178 peak height intensity ratios from a series of isolates obtained from control egg yolk and albumen (to which the standard mixtures had been added) were measured and linear calibration plots constructed.

Regression equations and correlation coefficients, calculated with the R 5/1 Computer System (Bolt, Beranek and Neuman, Inc., Cambridge, MA), are shown in the following table:

Regression of I_{174}/I_{178} vs. ng Xylonidine for Standards and Spiked Extracts

Samples	No. of Points	Regression Slope + SD[a]	Equation Intercept + SD	r^2
Standards	22	.005182 ± .00007	.0579 ± .0542	.9996
Yolk Isolates	6	.004428 ± .00004	.1524 ± .0375*	.9997
Albumen Isolates	6	.004589 ± .00004	.1395 ± 0429*	.9996

[a]All slopes are significantly different ($p < .05$).

*Significantly different from zero.

CONCLUSIONS

When hens were medicated with 75 ppm xylonidine in the feed for two weeks, the concentration of drug in the yolks of eggs laid prior to cessation of egg production reached a maximum of ~75 ppb. The drug residues in the albumen of these eggs was highly correlated with the yolk residue and was ~1/4 as great. Following the removal of xylonidine from their diet the hens resumed laying. No albumen samples from any post-treatment eggs contained detectable (0.3 ppb) xylonidine. Drug concentrations of up to 11 ppb were found in the yolks of eggs from those chickens which resumed production within a few days post dose.

REFERENCES

1. R. M. Weppelman, R. L. Tolman, A. VanIderstine, L. Peterson and G. Olson, Experientia (in press).
2. H. H. M. Zeelen, World's Poultry Science Journal 31, 57 (1975).
3. D. E. Wakeling, World's Poultry Science Journal 33, 12 (1977).
4. P. M. J. van den Bergh and P. H. Cox, Chromatographia 5, 301 (1972).

Trace Analysis of Organic Diamines in Urine. R. L. Settine, F. Fish and R. E. Hurst. The UAB GC/MS Center and Department of Public Health, University of Alabama in Birmingham.

Dyes and pigments derived from benzidine and benzidine congeners are used extensively in the leather, textile, and paper industries by a multitude of workers who are routinely exposed to these chemicals. Benzidine and 3,3'-dichlorobenzidine common precursors for the manufacture of dyes and pigments of this type are either officially classified as bladder carcinogens or are strongly suspected of being carcinogenic. Without a knowledge of the metabolism in humans of each dye or pigment and with the knowledge of precursor activity, demonstration of risk to workers is dependent on the identification of carcinogenic compounds or metabolites in body fluids. The method used to identify such substances in body fluids must be: 1) sensitive at low concentrations; 2) have a high degree of structural specificity; and 3) be free from interference by other body fluid contaminants.

A number of methods have been reported in the literature for the determination of organic diamines in complex aqueous matrices. While these methods are adequate in one or more of the above areas, they fall short of an unequivocal sensitive methodology.

We are reporting herein a method based upon fused silica capillary gas chromatography (GC) and single ion monitoring mass spectrometry (SIM) that allows one to measure these levels of potentially carcinogenic amines and their metabolites in body fluids such as urine.

Urine specimens (100 ml) were extracted at pH 6-7 with chloroform, and the extracts were evaporated to dryness after adding p-chlorobiphenyl as an internal standard. The residue was dissolved in 100 µl benzene containing 1% butylamine and 1 µl aliquots were used for GC/MS analysis. The analysis of underivatized diamines was made possible by introducing the fused silica capillary column directly into the ion source of the Hewlett-Packard 5985-A GC/MS system.

The marked effect of removing the glass-lined transfer tubing is graphically illustractd in Fig. 1 which shows the elution profiles of DCB before and after modification. Both peaks are displayed against a common time interval of 30 sec., and the peak heights have been normalized to the same absolute scale. With the unmodified instrument 700 pg of DCB afforded a broad peak with extensive tailing, but after removal of the transfer tubing 200 pg of DCB afforded a sharp, almost symmetrical peak with a tailing factor of less than 1.3. The dynamic ranges of response curves with various substituted benzidines were linear from 50 pg to 20 ng. (See Fig. 2.) Quantitation was unreliable below 50 pg because of statistical scanning errors and the column was overleaded above 20 ng. In analysis of urine, the amines could be quantified at 100 parts per trillion of urine, and detected at 50 parts per trillion.

In conclusion, we have described a convenient method for detecting quantifying aromatic diamines in urine with a sensitivity of at least 200 parts per trillion. Major contributing factors to this sensitivity are the lack of interferences from other urinary constituents and the very low baseline signal at the selected ions. When this sensitivity is coupled with the requirement that a positive response be simultaneously observed for several characteristic ions, the possibilities of false positive or false negative results are minimized. The sensitivity is not limited by the volume of urine extracted since only 1 µl is actually injected.

The procedure was applied to 16 urine samples not expected to contain any aromatic diamines or their metabolites and three samples spiked with DCB as a check for potential interferences. The entire procedure was found to be convenient for analyzing multiple samples and the analyses of the spiked samples were in close agreement with the amounts added. Most importantly, there was no indication that other constituents

would either mask or falsely indicate the presence of any of the four amines examined. Thus the procedure seems to be eminently well-suited to use in industrial toxicology settings as well as in research laboratories investigating the metabolism of the benzine-based dyes and pigments.

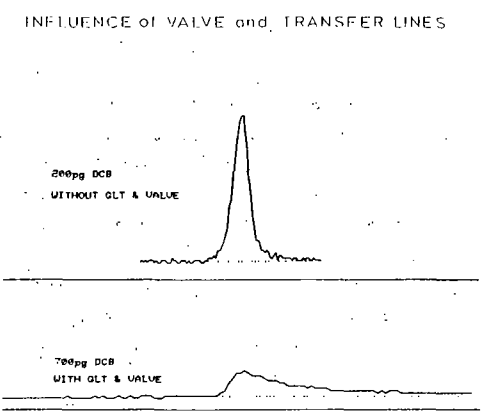

Figure 1

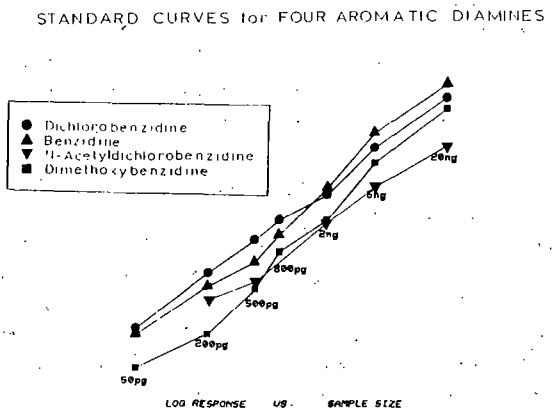

Figure 2

HIGHLY SELECTIVE PROCEDURES FOR THE MASS SPECTROMETRIC DETERMINATION OF STEROIDS AT THE PICOGRAMME LEVEL

Simon J. Gaskell, Tenovus Institute for Cancer Research, Welsh National School of Medicine, Heath, Cardiff, CF4 4XX, U.K.
Paul W. Brooks, VG Analytical Ltd., Tudor Road, Altrincham, Cheshire, WA14 5RZ, U.K.

The selectivity of detection during gas chromatographic-mass spectrometric (GC-MS) analyses of biological extracts frequently determines the degree of confidence in the identification and quantification of trace components. Established techniques of selected ion monitoring (SIM) at enhanced MS resolution[1] and of metastable peak monitoring[2] are of proven value in the analysis of steroids at the picogramme level in biological samples. Thus, for example, both techniques have been applied to the characterisation and quantification of dehydroepiandrosterone and testosterone in male saliva, where concentrations of 70-300 pg/ml have been observed[3]. Recent studies of negative chemical ionisation (CI) MS suggest the value of this technique for highly sensitive and selective analyses, particularly when ionisation takes place by electron capture. Here we report an exploratory study of the utility of GC-negative CIMS in the detection of steroids at the picogramme level, exemplified by the analysis of testosterone in saliva.

Male saliva (3-15 ml) was extracted with 4 volumes of diethyl ether. After preparation of the oxime derivative, a steroid 3-oxime fraction was obtained by chromatography on a micro-column of sulphoethyl-Sephadex LH-20[4]. Aliquots of the fraction were converted to methyl oxime (MO) or pentafluorobenzyl oxime (PFBO) derivatives by oxime exchange[5]. Conversion of the MO fraction to tert-butyldimethylsilyl (TBDMS) ethers gave a suitable derivative for detection of testosterone by high resolution selected ion monitoring or metastable peak monitoring. The PFBO fraction was trimethylsilylated. GC-MS analyses were performed using VG 7000 series double-focusing mass spectrometers. Separations were achieved on glass capillary columns (20 m) coated with OV-1 liquid phase.

The electron impact mass spectrum of testosterone PFBO, TMS ether included an intense molecular ion (m/z 555). GC-high resolution MS with SIM of $M^{+\cdot}$ indicated a detection limit of ca. 10 pg. Analysis of a derivatised saliva extract confirmed the presence of testosterone; the detection of two peaks of characteristic relative abundance, corresponding to the syn and anti isomers of the oxime, further substantiated the identification.

The negative CI (isobutane) spectrum of testosterone PFBO, TMS ether showed a base peak of m/z 181 ($C_6F_5CH_2^-$) and an ion of m/z 535 ($|M-H-F|^-$) of moderate intensity; no molecular ion was observed. GC-MS with SIM of m/z 535 (at a resolution of 1000) gave a detection limit of 30 pg whereas 3 pg was detectable by monitoring m/z 181. Testosterone was detected in male saliva by monitoring either m/z 181 or 535.

The Table summarises the selective procedures currently available for high sensitivity GC-MS analyses of testosterone in biological samples. While individual procedures may be preferable for certain applications, the value of complementary evidence obtained by several procedures is important when unequivocal identification and reliable quantification are required.

References

1. Millington DS. J Steroid Biochem 1975; 6 : 239.
2. Gaskell SJ, Millington DS. Biomed Mass Spectrom 1978; 5 : 557.
3. Gaskell SJ, Pike AW, Griffiths K. Steroids 1980; 36 : 219.
4. Axelson M, Sjovall J. J Chromatog 1976; 126 : 705.
5. Axelson M. Anal Biochem 1978; 86 : 133.
6. Gaskell SJ, Finney RW, Harper ME. Biomed Mass Spectrom 1979; 6 : 113.

Table. Procedures for the selective GC-MS detection of testosterone

Derivative*	Technique†	Approximate Detection Limit	References
TBDMS ether	EI, high resolution SIM: $\lvert M-C_4H_9\rvert^+$	20 pg	3
MO, TBDMS ether	EI, high resolution SIM: $\lvert M-C_4H_9\rvert^+$	30 pg	3
	EI, metastable peak monitoring: $M^{+\cdot} \rightarrow \lvert M-C_4H_9\rvert^+$	20 pg	6
TBDMS oxime, TBDMS ether	EI, high resolution SIM: $\lvert M-C_4H_9\rvert^+$	10 pg	7
PFBO, TMS ether	EI, high resolution SIM: $M^{+\cdot}$	10 pg	This work
	-ve CI, SIM: $\lvert M-H-F\rvert^-$	30 pg	This work
	$\lvert C_6F_5CH_2\rvert^-$	3 pg	This work

* TBDMS : tert-butyldimethylsilyl; MO : methyl oxime; PFBO : pentafluorobenzyl oxime; TMS : trimethylsilyl.

† EI : electron impact; CI : chemical ionisation; SIM : selected ion monitoring

Acknowledgement

SJG gratefully acknowledges the support of the Tenovus Organisation.

QUANTITATION OF THE LOCAL ANESTHETIC DIBUCAINE WITH GAS CHROMATOGRAPHY / MASS SPECTROMETRY

DAVID ALKALAY AND STEPHEN CARLSEN

RESEARCH DEPARTMENT, PHARMACEUTICALS DIVISION,

CIBA-GEIGY CORPORATION, ARDSLEY, NY 10502

DIBUCAINE, NUPERCAINAL^{R}, 2-BUTOXY-N-[2-(DIETHYLAMINO)-ETHYL]-4-QUINOLINECARBOXAMIDE, IS A POTENT LOCAL ANESTHETIC USED FOR RELIEVING A NUMBER OF PAINFUL SKIN CONDITIONS. IT IS ALSO BEING USED AS AN INJECTABLE PREPARATION FOR SPINAL ANESTHESIA.

A CHEMICAL IONIZATION AND AN ELECTRON IMPACT GC/MS ASSAYING APPROACHES ARE PRESENTED FOR DETERMINING CONCENTRATIONS OF UNCHANGED DRUG IN BIOLOGICAL FLUIDS. BOTH USE DEUTERIUM-LABELED DIBUCAINE AS THE INTERNAL STANDARD AND RELY ON THE SAME SAMPLE EXTRACTION AND PREPARATION PROCEDURE. DIBUCAINE IS STABLE IN HUMAN SERUM AT LEAST FOR ONE MONTH WHEN STORED AT -20°C. OVERALL DRUG EXTRACTION AND PROCESSING RECOVERIES AVERAGE 54%, AS DETERMINED ON THE BASIS OF SAMPLES SPIKED WITH RADIOACTIVE DRUG.

UNDER CHEMICAL IONIZATION CONDITIONS (CH_4), THE ASSAYING LIMITS ARE IN THE RANGE OF 1-80 NG/ML OF SERUM. UNDER ELECTRON IMPACT CONDITIONS, THE ANALYTICAL RANGE IS 20-800 NG/ML.

BOTH PROCEDURES ARE SPECIFIC AND ACCURATE. FOR CONCENTRATIONS EXCEEDING 2 NG/ML, THE LONG-TERM PRECISION IS ASSOCIATED WITH AN OVERALL STANDARD DEVIATION OF 8%. LOWER CONCENTRATIONS TEND TO BE SOMEWHAT OVERESTIMATED AND LESS PRECISE. THE CHEMICAL IONIZATION PROCEDURE HAS BEEN FOUND SUITABLE FOR MONITORING THERAPEUTIC LEVELS IN MAN.

Metabolic Studies Using GC/CI/MS and Stable Isotope Tracers*

T.D. Paul, J.H. McReynolds, M. Anbar and M.D. Scanlon
Department of Biophysical Sciences, SUNY at Buffalo
Buffalo, NY 14214

Stable isotope labelled compounds ($^{13}C_2$, ^{15}N alanine and uniformly labelled ^{13}C glucose) and GC/CI/MS have been utilized in human and animal experiments to examine substrate utilization and availability in energy producing metabolism.

Multiple system organ failure (MSOF) is a physiological response of patients which is usually triggered by an infectious agent. This syndrome is the major cause of late mortality following trauma. The clinical course following injury and medical intervention is temporary recovery followed by pulmonary failure associated with abnormal metabolism for energy production which eventually results in aberrant substrate flow between organs. The derangement in substrate utilization and availability leads to autocannibalism of peripheral muscle and breakdown of metabolism in the heart and liver and eventually the sequential organ failure results in death. We are studying human patients using stable isotope tracer techniques and GC/CI/MS to elucidate the biochemical mechanism of the syndrome.

In the MSOF patients blood was drawn before, during and after a 2 hr perfusion experiment (1 mg/kg + 0.02 mg/kg/min $^{13}C_2$, ^{15}N ALA) from three locations (radial artery, femoral vein and right atrium). Plasma was deprotienized and separated by cation exchange chromatography. Methyl lactate, ethoxime-methyl pyruvate, and N-acetyl-n-propyl-Ala were analyzed by GC/MS and isobutane chemical ionization. A separate deprotienized plasma sample was separated by anion exchange chromatography for glucose and urea. These components were analyzed by direct probe GC/CI/MS; NH_3 was used as the reagent gas for glucose.

The significant arterial venous differences in the alanine pool and in the lactate pool suggest that there is muscle cannibalism to generate amino acids and that the muscle is synthesizing lactate for energy production. The alanine pool and lactate-pyruvate pool enrichments suggest that alanine is being converted to lactate-pyruvate directly and that these two pools are trying to supply substrate to the heart for energy metabolism. The relatively small glucose enrichment suggests that very little of the lactate pool that comes from alanine is produced by glycolysis. This metabolic shunt may serve to conserve glucose for the brain by substituting lactate as the major energy source for the heart.

Chemical evidence has accumulated suggesting that hypothermic, hyperkalemic cardiac arrest during surgery has a preserving effect on the heart, facilitating clinical post-operative recovery. It has been suggested that additional improvement in myocardial preservation could be achieved by supplying appropriate nutrients during hypothermic and hyperkalemic conditions. Consequently a better understanding of the biochemistry of nutrient utilization is called for. Myocardial metabolism has been investigated in a surgical preparation which allows complete control of arterial inflow and coronary venous outflow in a segment of the intact working canine heart.

In the canine heart perfusion experiment; heart tissue was homogenized in the cold with ethoxyamine and $HClO_4$. The precipitate was processed by basic digestion, EtOH precipitation and acid hydrolysis to isolate the glucose incorporated into glycogen. The glucose was analyzed by direct probe

NH_3-CI-MS. Methyl and ethoxime-methyl esters of the Keto acids and Krebs cycle acids found in the supernatant were analyzed by GC/isobutane CI/MS.

The lack of significant ^{13}C incorporation into the unperfused heart tissue and thigh muscle indicated that the pedicle perfusion technique can be a powerful tool to study selective substrate utilization in a representative part of the heart while leaving the rest of the organism virtually intact. The results from the ^{13}C labelling studies indicate that various metabolic processes were acting over the one hour perfusion period. Since the lactate and pyruvate ^{13}C incorporation were equal and the citric acid cycle incorporation was approximately one-third the lactate and pyruvate incorporation, the data suggest that whereas glucose was used as an energy source during the perfusion period, it was not the sole energy source. To account for the ^{13}C dilution in the Krebs cycle intermediates other sources such as endogenous fatty acids or muscle branch chain amino acids must also be metabolized.

These studies indicate that stable isotope labelled compounds and GC/CI/MS provide a specific and sensitive technique to study metabolic mechanisms of substrate utilization and distribution in MSOF and energy conversion metabolism in perfused heart tissue. The ultimate goal in both studies is to develop rational treatment strategies which result in increased surivival in MSOF and decreased post-surgical complications and increased survival during prolonged periods of cardiac bypass and myocardial preservation.

*These studies were supported by Grant HL 15676 from the National Heart, Lung and Blood Institute and Grant GM 15768 from The National Institutes of General Medical Sciences.

AUTOMATED QUALITATIVE AND QUANTITATIVE ANALYSIS OF URINARY STEROIDS WITH A GAS CHROMATOGRAPHY MASS SPECTROMETRY-COMPUTER SYSTEM. JAMES VRBANAC AND CHARLES SWEELEY, Department of Biochemistry, Michigan State University, East Lansing, Michigan

Introduction: Urine contains a complex mixture of organic compounds that represent the end products of metabolism of proteins, fats, carbohydrates, steroid hormones, drugs and other substances of endogenous and exogenous origin. Urine is a useful physiological fluid for "metabolic profiling" studies since it does not require an invasive technique to obtain the samples and the levels of metabolites are much higher than in other physiological fluids. Previous work (1) in this laboratory has involved a system, called MSSMET, which uses methylene unit retention indices in performing an off-line reverse library search of selected mass chromatograms from repetitive scanning gas chromatography/mass spectrometry data. This system has provided automated qualitative and quantitative analyses of organic acids in urine The research described here is a parallel effort to develop a reproducible procedure for the isolation and derivatization of urinary steroids and to apply the MSSMET system for the automated qualitative and quantitative analysis of this important class of metabolites.

Methods: Various procedures for the isolation and derivatization of urinary steroids were investigated for the reproducibility. The method of Leunissen and Thijssen (2) was found to give the desired reproducibility. Reproducibility of the method was determined by capillary column GC using a Hewlett-Packard 5840A GC equipped with flame ionization detection. Samples were analyzed by GC/MS with an LKB-2091 with dual processor foreground/background data system equipped with both packed and capillary column capabilities. Samples were ionized by electron impact at 70 eV using a 4 second scan cycle time for packed column (m/s 50-750) and a 2 second scan cycle time for the capillary column (m/s 50-550). Columns were temperature programmed from 180-280 deg C at 2 deg/min.

Results: Following establishment of a quantitative procedure for the isolation and derivatization of urinary steroids, attention was turned to development of optimum qualitative and quantitative conditions for GC/MS analysis of urinary steroids. A 3M OV-101 packed column was evaluated first. Although it was known that many of the steroids do not separate satisfactorily by packed column chromatography, mass chromatography was examined for its potential in quantitating poorly resolved GC peaks. The results of these studies demonstrated that many steroids can be quantitated by mass chromatography, and that certain poorly resolved steroids on packed columns have almost identical mass spectra and thus cannot be adequately analysed by mass chromatography: ie., androsterone and etiocholanolone; THF and αTHF, etc. An alternative approach, using capillary columns for the automated GC/MS/Computer analysis of urinary steroids, was then investigated. To accurately quantitate the sharper capillary column peaks the scan cycle time was shortened to 2 seconds. The data in Figure 1 were obtained with a 50M OV-101 WCOT capillary column. The total ion intensity is plotted on the ordinate and scan number is plotted on the abscissa. Some of the major steroid peaks have been labelled.

For each compound searched for by the MSSMET program (within a "window" defined by the retention times of the co-injected hydrocarbons), one ion that is both characteristic and intense is used for quantitative purposes (the designate ion) and a few other ions produced during fragmentation are used to confirm the identity of the compound in question. Table I shows the integrated areas of the designate ion determined by MSSMET expressed as a percent of the sum of the areas for these 5 urinary steroids. The data are from 4 separate GC/MS analyses of the same sample and demonstrate the overall good reproducibility of the computer-assisted automated metabolic profiling of urinary steroids using capillary column GC/MS.

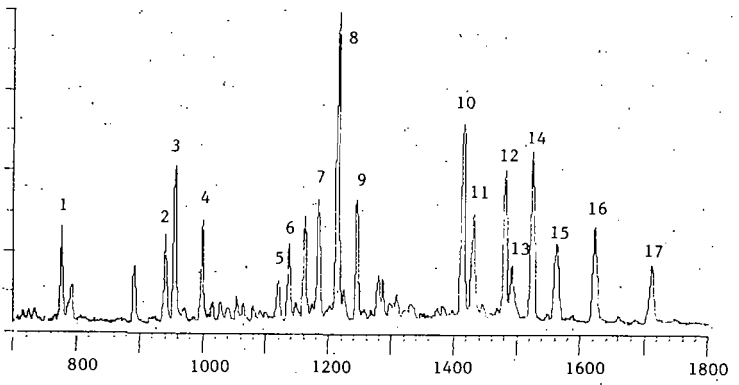

Figure 1. GC/MS analysis of urinary steroids using a 50M WCOT OV-101 capillary column. The total ion intensity is plotted on the ordinate and scan number is plotted on the abscissa (2 second scan cycle time). Identity of peaks: 1) C-24 hydrocarbon, 2) androsterone, 3) etiocholanolone, 4) C-26 hydrocarbon, 5) 11β-hydroxy-androsterone, 6) 11β-hydroxy-etiocholanolone, 7) 16α-hydroxy-dehydroepiandrosterone, 8) pregnanediol and C-28 hydrocarbon, 9) pregnanetriol, 10) THE, 11) C-30 hydrocarbon, 12) THF, 13) αTHF, 14) α-cortolone, 15) β-cortolone and β-cortol, 16) α-cortol, 17) C-32 hydrocarbon.

TABLE I

Precision: Capillary Column GC/MS Profiling of Urinary Steroids[1]

Steroid	Run Number 1	2	3	4	Mean ±S.D.[3]
Androsterone	9.45	8.59	10.1	10.1	9.56 ±0.72
Etiocholanolone	11.6	11.5	12.9	12.7	12.2 ±0.7
Pregnanediol	59.1	58.6	56.6	56.3	57.7 ±1.4
Pregnanetriol	14.4	15.6	14.6	15.1	14.9 ±0.5
THE	5.44	5.77	5.80	5.86	5.72 ±0.19
Etio./Andro.[2]	1.22	1.33	1.28	1.26	1.27 ±0.05

[1]Values are the integrated peak areas determined by MSSMET of a characteristic ion for each steroid expressed as a percent of the sum of the areas for these 5 urinary steroids. Data are from 4 separate GC/MS analyses of the same sample.

[2]Ratio of etiocholanolone to androsterone.

[3]Overall precision was ±4.4 percent.

References

1. Gates, S.C., Smisko, M.J., Ashendel, C.L., Holland, J.F., and Sweeley, C.C.: Automated Simultaneous Qualitative and Quantitative Analysis of Comples Organic Mixtures with a Gas Chromatography-Mass Spectrometry Computer System. Anal. Chem. 50:365-380, 1978.

2. Leunissen, W.J.J. and Thijssen, J.H.H.: Quantitative Analysis of Steroid Profiles From Urine by Capillary Gas Chromatography. Accuracy and Reproducibility of the Sample Preparation. J. Chromatogr. 146:365-380, 1978.

METABOLIC PROFILES OF ORGANIC ACIDS FROM HUMAN PLASMA. David Issachar and Charles C. Sweeley. Department of Biochemistry Michigan State University, East Lansing, Michigan 48824

The comprehensive metabolic profiles of plasma organic acids from Normal, Polyserositis and diabetic patients has been studied. For this purpose a new method, called ORUF, has been developed. The ORUF is based on the addition of oleic acid to a plasma sample before the ultrafiltration step. The oleic acid, which effectively competes for binding sites on the protein, results in the release of other organic acids which are then recovered in the ultrafiltrate. Use of ORUF, followed by anion exchange, gives a plasma organic acids fraction in high and reproducible yields.

The derivatized samples (oxime-TMS) were analyzed with an LKB-2091 gas chromatograph/mass spectrometer which is connected to a computer. The identification and quantitative determination was done by the Mass Spectral Metabolic Program (MSSMET), using a reverse library search.

Figure 1 represents a typical chromatogram of plasma organic acids from normal, polyserositis and diabetic patients. Table 1 represents the normalized concentration factors of selected organic acids found in plasma samples of those patients. The data in Table 1 shows high levels of several acids such as: 2-Hydroxybutyric; 3-Hydroxybutyric and Glucose. For polyserositis patients it seems that the high level of pyruvic and the relatively low level of citric might be significant and characteristic for this metabolic disease.

Using the capillary GC/MS system, better resolution was obtained. Figure 2 represents a chromatogram of plasma organic acids obtained with a scan cycle of 2 seconds. The 16 second width of a typical peak in this chromatogram allows automated metabolic profiling using capillary GC/MS with a 2 second scan cycle.

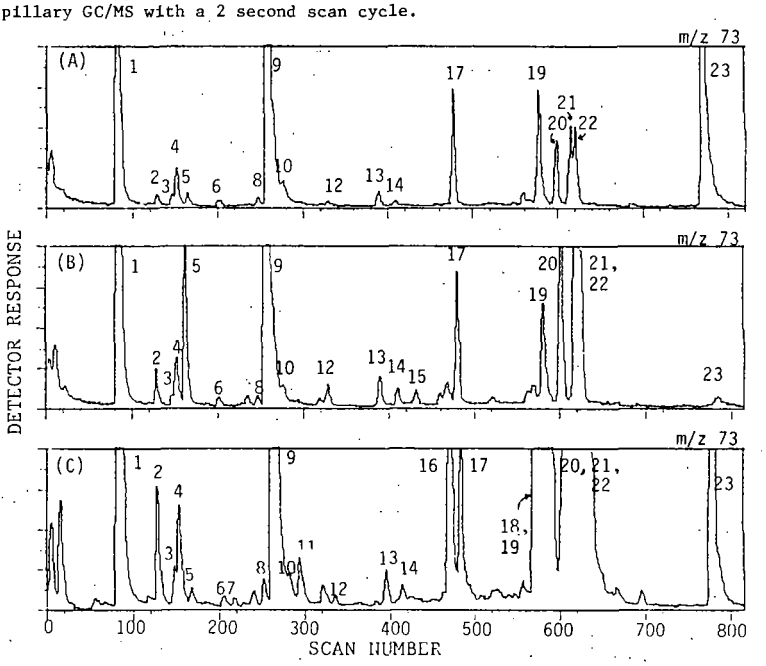

Figure 1 Chromatograms of plasma organic acids (presented by m/z 73) extracted from: (A) Normal; (B) Polyserositis (Familial Mediterranean Fever); (C) Diabetes. The peaks are: (1) Lactic, Background; (2) 2-Hydroxybutyric; (3) 2-Hydroxyisovaleric; (4) 3-Hydroxybutyric; (5) Pyruvic oxime; (6) UNK-DI-6; (7) Ketoisocaproic; (8) 2-Ketoisocaproic oxime; (9) Phosphoric (10) 4-Deoxytetronic; (11) UNK-DI-30; (12) 2-Deoxytetronic; (13) Erythronic; (14) Threonic; (15) O-Hydroxybenzoic; (16) UNK-DI-35; (17) Tropic I.S.; (18) Glucose; (19) Citric, U-59; (20) UNK-17; (21) Glucose oxime; (22) Hexuronic; (23) Uric.

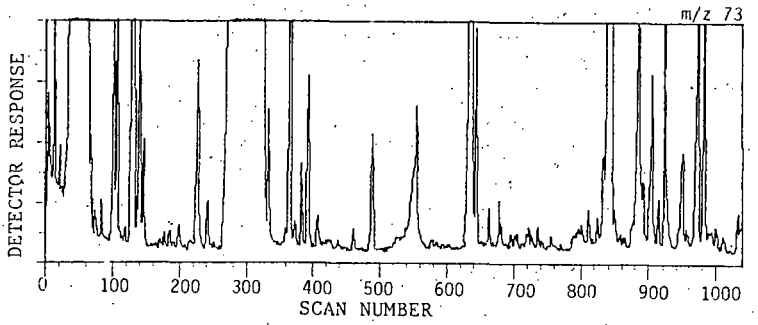

Figure 2 Capillary GC/MS chromatogram of organic acids from normal human plasma.

Table I

Normalized concentration factors of selected plasma organic acids

R.I.	Acid	(n=3) Normal	(n=3) Diabetic	(n=3) Polyserositis
1085	2-Hydroxyisobutyric	16	24	18
1102	Lactic	Overload	Overload	Overload
1131	Caproic	--	4	9
1132	Phenol	93	49	234
1166	2-Hydroxybutyric	17	72	19
1200	3-Hydroxybutyric	133	754	140
1219	Pyruvic oxime	114	79	300
1274	Glycerol	37	44	46
1293	2-Keto-isocaproic	10	13	8
1320	Acetoacetic	30	23	41
1362	4-Deoxyerythronic	22	53	45
1382	4-Deoxythreonic	35	23	18
1404	Fumaric	--	3	--
1433	Phenylacetic	1	1	2
1433	O-Methylbenzoic	1	1	1
1445	3-Deoxytetronic (UN-20)	4	5	21
1464	2-Deoxytetronic (UN-22)	16	15	31
1497	Glutaric	--	4	--
1560	Erthronic (UN-28)	66	68	103
1586	Threonic (UN-30)	31	41	54
1600	Adipic	--	--	1
1625	O-Hydroxybenzoic	3	11	2770
1678	5-Hydroxymethyl-2-Furoic (UN-38)	1	--	48
1698	2-Phenyllactic	5	1	7
1690	O-Hydroxyphenylacetic	--	1	1
1796	Suberic	1	6	3
1883	Citric	227	590	102
1899	Myristic Tetradecanoic	11	5	14
1892	Azelaic Nonanedioic	14	28	13
1952	Glucose oxime (UN-57)	48	853	174
1958	O-Hydroxycinnamic	7	7	32
1962	Galacturonic-(1)	87	52	268
1963	Gluconic	14	9	39
1994	Pentadecanoic	3	--	3
2194	3-Indoleacetic	23	24	20
1342	2-Keto-isocaproic/ 2-Keto-3-methyl-valeric	24	49	14

DEHYDRATION AND N-ACYLATION OF PRIMARY AMIDES AS DERIVATIZATION METHODS FOR GAS CHROMATOGRAPHY-MASS SPECTROMETRY, MARTIN STOGNIEW AND PATRICK S. CALLERY; DEPT. of MED. CHEM. U. of MARYLAND, BALTIMORE, MD. 21201

Rapid and reproducible methods for the preparation of stable derivatives are important for quantitative mass spectral analyses. There are few suitable derivatization methods for primary amides. Here we present studies on the derivatization of primary amides using phenylacetamide as a model compound. Treatment with trifluoroacetic anhydride (TFAA) followed by GC/MS analysis revealed multiple compounds including phenylacetonitrile and N-trifluoroacetylated phenylacetamide. This nitrile was formed in the injector port since and infrared spectrum recorded prior to injection showed no absorption in the nitrile region. A TFAA-pyridine system produced phenylacetonitrile nearly quantitatively in solution thus removing the need for thermal degradation in the injector port. The results are consistent with nitrile formation proceeding through O-trifluoroacylation followed by thermal or base catalyzed elimination of trifluoroacetic acid.

Reaction of phenylacetamide with N-methyl-bis-(trifluoroacetamide) (MBTFA) yielded exclusively N-trifluoroacetylphenylacetamide (1), which was stable and has better GC/MS characteristics when compared to the parent amide. The assignment of N-acylation, rather than O-acylation, was based on infrared spectroscopy, electron impact fragmentation, and deuterium labeling studies. The IR spectrum of 1 showed a strong absorption of 3380 cm^{-1} indicating an N-H stretch. This removed the possibility of a carbinolimine (-$\overset{OH}{C}$=N-) tautomer. The mass spectrum showed a base peak at m/z 118 which can be accounted for by loss of trifluoroacetamide from N-acylated phenylacetamide or loss of trifluoroacetate from the O-acylated phenylacetamide. When 1-N-D (1 exchanged in D_2O) was analyzed by mass spectrometry, a base peak at m/z 118 indicated that the fragment did not contain the label. This indicated that the compound was the N-acylated amide and not O-acylated amide, since the deuterated O-acylated amide would have displayed a base peak at m/z 119. This mass spectral analysis must be considered tentative, sine the exact structure of the ion m/z 118 was not determined. The possibility remained that m/z 118 arose from O-acylated amide through the loss of trifluoroacetamide. Indirect evidence was obtained by reducing 1 with lithium aluminum hydride. O-Acylated material would be expected to reduce to phenethylamine, while N-acylated material would reduce to N-(2,2,2-trifluoroethyl)-2-phenethylamine (2). GC/MS analysis of the reduction mixture gave a major component with a mass spectrum consistent with 2. Neither phenethylamine nor phenethanol was detected in the mixture. Authentic 2 was synthesized by the reduction of N-trifluoroacetylphenethylamine and found to have the same mass spectrum as the reduction product of 1.

Two methods for the quantitative derivatization of primary amides are presented. Nitrile formation with TFAA employing pyridine as catalyst for pre-column dehydration increases the yield and the precision of the procedure. N-Trifluoroacetylation with MBTFA has the advantage of increasing the molecular weight and adding fluorine atoms which could be useful for negative chemical ionization analysis.

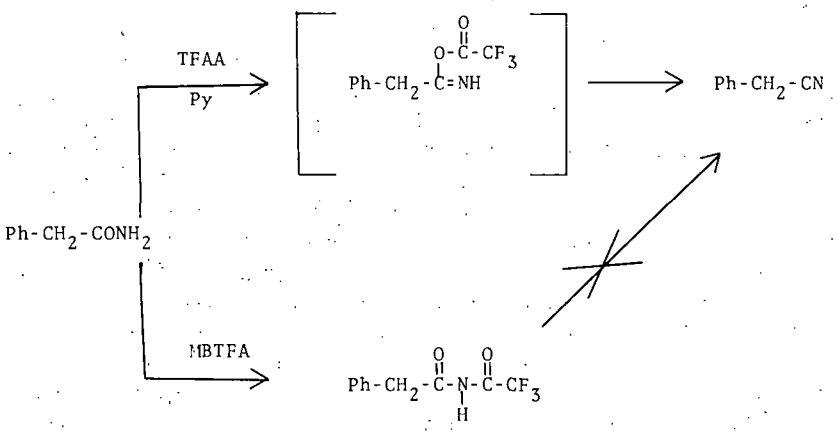

Routine Automated GC-MS for Biochemical Analysis

Graham S. King and Brian R. Pettit
Bernhard Baron Memorial Research Laboratories
Queen Charlotte's Maternity Hospital
London W6 0XG. U.K.

Michael J. Wallington
V.G.Analytical Ltd.
Altrincham
Cheshire U.K.

Due to the routine nature of a lot of the analyses performed at Queen Charlotte's Hospital when considering the purchase of new high-performance mass spectrometry equipment it was decided to install an automatic liquid injector to reduce the amount of time spent by skilled staff on mundane operations. It was also hoped that such a facility would increase the sample throughput. In due course the equipment was installed and this comprised a VG70-70F mass spectrometer and 2250 data system with a Hewlett-Packard 5700-series gas chromatograph, combined packed-capillary inlet system and 7672A auto-sampler. The control system for automatic operation is described in the following figure:

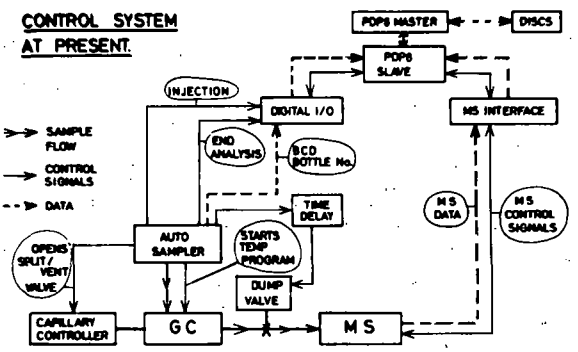

It has been found that for handling small samples it is essential to use the alternate wash option on the 99 sample injector and so this effectively reduces the sampler's capacity to 49. Because this option is used it has been important to make the BCD bottle code available to the data system, on infrequent occassions it has been known for the belt to get out of phase.

There are two ways in which we have used the machine for unattended operation: for repetitive scanning of temperature programmed runs and for selected ion monitoring. We have as yet not attempted high resolution runs unattended. Typical instrumental conditions are as follows:

1. Repetitive scanning at 3 seconds/decade for 20 to 30 samples at 30 minutes per analysis, plus 10 minutes to recycle the oven. Total run time may be about 20 hours.

2. Selected ion monitoring of two to four ions in about 40 samples, including six standards and two blanks. This can vary from 5 to 30 minutes per analysis, when the total run time is from 3 hours to 20 hours. We prefer to use isothermal operation when possible.

The main use to which we have applied automatic injection for repetitive scanning of gas chromatograms is in organic acid profile analysis. Organic acids are analysed as their TMS-ester-ethers on a temperature programmed run using 3% OV1. The procedure is applied to pediatric urine samples looking for metabolic problems and also to animal urines in drug metabolism studies. It is quite feasible with 5MBytes of disc storage to analyse 20-25 samples on a overnight run.

Two examples are given of the types of assays performed using selected ion monitoring assays. Phenylacetic acid is being studied in our unit as part of an investigation of the biological significance of phenylethylamine[1,2]. A high sensitivity and high throughput assay was required for the compound in CSF and plasma. An electron capture procedure using pentafluorobenzyl esters has been adapted for selected ion monitoring. The molecular ion at m/z 316 is compared with the molecular ion of the phenyl penta-deuterium analogue at m/z 321. The lock mass is column bleed from the 3% OV1 column at m/z 281. Peaks corresponding to the range 10pg to 4ng are commonly detected. Each single analysis takes about 4 minutes.

Galactosemia is an inherited disease of galactose metabolism. To date the method of diagnosis (prenatal and postnatal) involves cell culture and enzyme studies; this can be a long and expensive procedure. We have developed a rapid and specific method for diagnosis based upon measurement of the galactose reduction product galactitol[3]. Significantly increased levels of galactitol (8 micromol/l) occur in amniotic fluid from affected pregnancies, the normal level is 0.5±0.2 micromol/l. We have also studied the distribution of hexitols in a variety of body materials with various pathologies.

The assay uses the epimer iditol as an internal standard and all of the mamallian epimeric hexitols (mannitol, sorbitol, galactitol and myo-inositol) are analysed as their hexa-acetates on a Silar10C column. The raw sample is acetylated with acetic anhydide and 1-methylimidazole, the product partitioned between water and ethyl acetate and an aliquot injected on column. The coefficient of variance is usually well below 5%.

The analyses shown here use the ion at m/z 259 ($C_{11}H_{15}O_{10}$) for SIM of the alditols and m/z 210 ($C_{10}H_{10}O_5$) for inositol; in this case m/z 207 of column bleed is used as a lock mass. Recent experiments have shown that m/z 361 ($C_{15}H_{21}O_{10}$) for the alditols and m/z 373 ($C_{16}H_{21}O_{10}$) for inositol, with m/z 355 as a lock is superior for the analysis. Interference from minor ions in glucose pentaacetate is thereby eliminated. In spite of the small proportion of the total ion current carried by these ions, the low isolation losses and high instrument sensitivity give an excellent assay. Each single analysis takes about 25 minutes.

Conclusions

Unattended operation of selected ion monitoring has emphasised the following points:-

1. A lock-mass or anti-drift arrangement is essential.
2. Temperature programming reduces sample throughput.
3. Automatic methods for processing the large volume of data in a multi-sample run are essential.
4. Failsafe operation is imporant to avoid loss of valuable samples
5. Data must be consolidated on the disc after each injection to allow for unforseen halts in an overnight run.
6. Considerable savings in operator time can be made for selected ion monitoring. Overnight runs can be routine on packed columns.

References

1. L.E.Fellows, G.S.King, B.R.Pettit, B.L.Goodwin, C.R.J.Ruthven, M.Sandler; Biomed. Mass Spectrom. 5, 508-511(1978).
2. M.Sandler, C.R.J.Ruthven, B.L.Goodwin, G.S.King, B.R.Pettit, G.P.Reynolds, S.P.Tyrer, M.P.Weller, S.R.Hirsch; Commun. Psychopharm., 2, 199-201(1978).
3. B.R.Pettit, G.S.King, K.Blau; Biomed. Mass Spectrom., 7, 309-313(1980).

Quantitative HRGC-HRMS: Study on the use of a non-isotopically labelled internal standard in the analysis of 2,3,7,8-TCDD in environmental samples.

Yves Tondeur; J.Ronald Hass, Phillip W. Albro, and Kun Chae; National Institue of Environmental Health Sciences, Research Triangle Park, N.C. 27709

A high resolution glass capillary column gas chromatograph coupled to a high resolution mass spectrometer has proven itself useful as an analytical tool in meeting the requirements to positively identify, confirm and quantitate trace-levels of TCDD. During the past few years, specific qualitative criteria (retention time, chlorine isotope ratio, $^{S}/N \geq 2.5$ ...) have been developed although debate continues.

Quantitative analysis usually involves the use of internal standards which are typically an isotopic variant of TCDD added to compensate for sample handling losses. Potential problems associated with their use are discussed. By conducting a set of experiments at low levels (ppt) using selected ion monitoring techniques, the extent and the limitations of the use of a non-isotopically labelled internal standard yielding a different ion than the toxic material of interest in the GC-MS determination step are evaluated and discussed.

A Multifunctional GC-TOFMS Interface, By A. Kornel and R. A. Day, University of Cincinnati, Department of Chemistry, Cincinnati, Ohio 45221

The modified TOFMS in our laboratories showed a high degree of sensitivity and has been further modified to incorporate use of a capillary GC system (Ref. 1). The GC interface previously used was for packed columns and employed either a membrane separator or an open splitter, thus, diverting only a fraction of the sample to the ion source. It was decided to change this interface to one compatible with all types of GC columns available (i.e. packed, microbore, SCOT, WCOT, or wide bore WCOT of glass, stainless, or fused silica) with emphasis for use with capillary columns.

The entire GC gas inlet system up to and including the injection port were redesigned. These changes include: 1) use of oxygen and H_2O removal traps prior to 2) incorporation of a precise helium flow control unit with provisions for make up gas for a separator (Chromalytic PL) and 3) a modified injection port utilizing Grob style splitless injection (Chromalytic PL).

The multifunctional GCMS interface centers around an all glass jet separator (SGE). This separator can be used with any of the columns desired including WCOT or other capillary columns. (Separator requires make up gas with use of capillary columns.) The separator vacuum side is monitored by a thermocouple gauge tube, thus, allowing reproducible make up-gas flow settings. A plug-in divert valve (Analtech Ass.) is used to initially calibrate the make up gas flow. (Range of 20 to 35 atm ml min^{-1} for capillary columns.) The separator connecting lines (glass lined tubing, SGE) and valves (SGE) are situated in an oven between the GC oven and the ion source oven of our modified TOFMS. The valving permits one to use the interface as a direct inlet, or a splitter, or through the separator as mass spectrometer pumping rates dictate. The interface also lends itself to use of the sub-atmospheric pressure capillary GC method (Ref. 2).

As was stated, the separator unit lies between the GC and ion source and, thus, heated connecting lines must be used. For WCOT fused silica columns, the column end may be directly brought up to the separator interface, or if desired, the column may be run through the oven directly into the ion source for use at sub-atmospheric pressures. For the use with packed or glass columns, a stainless steel or nickel 200 (Analtech Ass.) transfer line may be employed. In order to maintain even heating and ease of installation of these lines (or columns), a simple heated transfer pipe was devised. This consists of clamping the desired length and wattage of cromalux heat pipe parallel to alcoa 5052-0 aluminum tubing 1/4 inch O.D. with stainless hose clamps. The tube/heat pipe is then bent to the desired shape and the transfer line or fused silica column can be easily slipped through. Thermo couples were used at several intervals to check for temperature stability. The heat pipes' temperatures were regulated using inexpensive lamp dimmers (Triac), (auto transformers, etc. could also be used).

Further, the TOFMS at our disposal required some modification of the pumping system. The analyser diffusion pump was changed from mercury to use polyphenyl ether (Santovac 5, Monsanto). This required changing the heater to 1500 W from 750 W. Also, the source housing had a 2 inch diffusion pump added directly beneath with no trap or baffle. This pump also uses Santovac 5. Finally, all roughing lines were shortened.

The interface described is relatively easy to construct, using readily obtainable materials, and is very competitive with respect to cost when considering prefab units. It is multifunctional, thus, not limiting the type of columns which can be used. The design is readily adaptable to other configurations as GC and MS systems dictate.

Ref. 1 A. Kornel, E. Younginger, R.A. Day, ASMS presentation, 1981 Nat'l Meeting

Ref. 2 C.A. Cramers, G.J. Scherpenzeel and P.A. Leclercq, J. of Chromatog. 203 (1981) 207-216.

GC/MS ANALYSIS OF VOLATILE ORGANIC COMPOUNDS BY FUSED SILICA CAPILLARY COLUMN, A. E. Rosecrance, N. W. Flynn, J. E. Nemmers, Science Applications, Inc., P. O. Box 2351, La Jolla, California 92038.

Fused silica capillary columns can provide significant advantages over packed columns for GC/MS analysis by improving chromatographic resolution and increasing instrumental sensitivity. The resolution, inertness, flexibility and stability of fused silica capillary columns make them well suited for GC/MS analysis of low level organic pollutants and complex mixtures that are often encountered in environmental samples. The analysis of volatile organic compounds in environmental samples is routinely accomplished in our laboratory using the same fused silica (SE-54) wall coated open tubular column that we employ for the analysis of acid, base and neutral extractable compounds. Volatile organic analysis by fused silica capillary columns proceeds as analysis by packed columns with the additional use of cryogenic focusing during the desorption phase of the analysis. Desorption of volatile organic compounds is accomplished co-incident with cryogenic focusing at the initial loop of the capillary column. The focal area is intrinsic to the column instead of in a trap preceeding the column which was generally the method employed when using Boro-silicate columns. We have found that instrumental sensitivity is greatly increased when comparing capillary columns with packed columns for volatile organic analysis and data reliability is excellent even when analyzing complex environmental samples. Precision and accuracy data will be presented for volatile organic analyses of a variety of environmental samples. Comparison of the effectiveness of several adsorbant materials for volatile organic compounds will also be discussed.

COMPOUND IDENTIFICATION CRITERIA FOR AUTOMATED GC/MS DATA REDUCTION; B.N. COLBY and T.R. SMITH; Systems, Science and Software, La Jolla, CA 92038

In recent years, user oriented software has become available from data system manufacturers. One consequence of this has been an increase in data reduction automation for both qualitative and quantitative analyses. With this increase in automation, the analyst has had to transfer more and more of his decision making to the data system in some form of computer program which can mimic the analyst and produce the desired data in a convenienc and economical form. In order to achieve this goal, the analyst must provide the program with criteria identifying such things as what constitutes a peak in the chromatogram, whether or not to perform background subtraction, what is acceptable agreement for a data base library search, and so on. In this presentation the criteria which can be used to locate and identify target compounds, specifically some of the EPA Consent Decree Priority Pollutants, will be discussed. Specifics which will be covered include retention time and relative retention time plus a collection of forward, reverse and comparative data base spectral matching parameters. Several novel approaches to spectral comparison will be included among the comparative data base spectral matching routines and parameters tested. Test parameters have been addressed using triplicate standard analyses in order to identify short-term, long-term and concentration dependent variations.

Alternate Approaches to Quantitative Data Reduction from Capillary Column GC/MS

J. M. McGuire, W. M. Shackelford, John S. Craig, A. W. Garrison, and J. D. Pope
Environmental Research Laboratory
U.S. Environmental Protection Agency
College Station Road, Athens, GA 30613

Three different approaches for quantitative processing of capillary column GC/MS data acquired in scanning mode were evaluated. The first approach utilized the Finnigan-MAT SS200 program ACLEAN to recognize each GC peak and extract the best spectrum for each. This program provides as an output the sum of the absolute intensities for all ions within the extracted spectrum. It was this summation that was chosen as the first response. The second approach was a minor modification of the first: the most intense peak height within the extracted spectrum was used as the response. The third approach utilized a system of programs that we had obtained from Stanford and optimized in-house for processing packed column GC/MS runs. The output used as a response from these programs was the background-corrected, integrated area of the most intense ion in those spectra selected as comprising a GC peak.

Relative molar response factors (RMR) for each of the above outputs for 35 compounds were calculated relative to the corresponding response of 4-fluoro-2-iodo toluene. Single operator precision and accuracy were determined and are summarized in the table.

Table
RMR Statistics

Approach	Min.	Max.	Min CV	Max CV	Av CV
1	.32	4.48	1	64	26
2	.33	9.17	2	71	43
3	.38	7.16	2	67	41

Utilizing the determined RMR's for Approach 1 where available, and a weighted average RMR where not, a spiked complex environmental sample was analyzed. Recoveries found were reasonable.

Qualitatively, the spectra extracted by Approaches 1 and 3 were put through both PBM and a modified Biemann search. Both gave excellent results. Consequently, we conclude that it is possible to obtain both qualitative and quantitative information about an unknown sample from a single GC/MS run.

References

1. Research Triangle Institute
Master Scheme for the Analysis of Organic Compounds in Water: Interim Protocols, Environmental Protection Agency, Contract 68-03-2704, October, 1980

2. J. M. McGuire and R. G. Webb
Organic Water Pollutant Analysis by Gas Chromatography-Mass Spectrometry in "Water Quality Measurement: The Modern Analytical Techniques" (H. Mark and J. Mattson, Ed.) pp 1-32, Marcel Dekker, Inc., New York (in press)

3. D. Henneberg, H. Damen and B. Weimann
Computer-Aided Automatic Extraction of Relevant Data from Mass Spectra Series in "Advance in Mass Spectrometry" 7B (N. R. Daly, Ed.) pp 975-984, Heyden, London (1978)

4. H. S. Hertz, R. A. Hites, and K. Biemann
Identification of Mass Spectra by Computer-Searching a File of Known Spectra, Anal. Chem. 40, 681-691 (1971)

PAPER TPB - 17

AN AUTOMATIC ANALYSIS PROGRAM FOR GC/MS DATA, D. Thomas Terwilliger, Department of Chemistry, University of Pennsylvania, Philadelphia, Pa. 19104, and Walter C. Davidson, Halcon Research and Development Corporation, Montvale, N.J. 07645

This paper presents a description of an algorithm for identifying components in GC/MS runs of mixtures. It is designed to identify components automatically, providing background-free spectra which are corrected for changes in concentration during the course of the scan, the latter being most important for capillary runs. These spectra are passed to an in-house library search system (1) for identification. This program has been incorporated into both the Varian SS/100 and the Kratos DS-50-S data systems.

The work of Dromey et.al. (2) demonstrated the utility and general principles of a computerized analysis of GC/MS data from the viewpoint of enhancing chromatographic information. They developed an elaborate procedure which identifies peaks by coincidence of individual mass chromatogram peaks, and predicts the shape of mass chromatograms within an area of multiple incompletely resolved eluants, based on a model calculated from components which are completely resolved in the same analysis.

These two determinations allow closely eluting components to be discerned and further permit calculation of a "resolved" mass spectrum for unresolved analytes, including estimation of ion abundance for those ions common to the unresolved components. This work is extremely complex and not readily adaptable to other systems, as it is partially programmed in language unique to the D.E.C. computer family. Dromey's algorithm is the most sophisticated published to date. Others have used electronic data processing to reduce, somewhat, manual inspection of data (3), or for routine qualitative analysis of complex samples (4).

The primary goal of our algorithm was not to design a program that would be foolproof in the worst possible test case, but to develop a good working system which could be used routinely on all GC/MS data taken in the laboratory. It has been designed to be run by the chemist who is not necessarily a computer expert, and to provide a quick indication of the composition of an unknown mixture. Thus our program is substantially less complicated than other programs which have attempted similar tasks, requiring only a minimum number of options and parameters to be specified. It is written entirely in fortran, and is readily adaptable to other data systems.

Our algorithm, like that of Dromey (2), relies on the coincidence of mass chromatogram peaks, but tests for them only within a peak defined by the summed ion current. The summed ion current chromatogram is computed by summing the abundance of many, but generally not all, of the ions in each scan, and thus is different from the T.I.C. or R.I.C. values. In this way the contribution to the baseline "noise" of large background ions may be eliminated by excluding them from the sum. This approach is, perhaps still less sensitive than Dromey's, but the positive identifications are very reliable. The slope threshold for detection of a peak may be set very low, as all peak occurrences are "cross checked" with mass chromatogram data. Integration of peak areas and determination of peak start and end times is simplified by this approach. Ions which are unique to, or predominant in the spectrum of each (unresolved) component within a chromatographic peak are thus found and listed, but no attempt is made to estimate a corrected intensity for ions common to the spectra of more than one unresolved component. These spectra of "unique ions" are stored and may be plotted out at the conclusion of the run.

Our analysis does correct data for the change of eluant concentration during a scan, and allow subtraction of any two such corrected spectra. The results are then available for manual interpretation or library searching (1). Reverse search techniques are employed, thus the disadvantage of not producing a completely resolved spectrum is reduced. This technique avoids the problem which might be caused by an inappropriate model (such as might be produced from non-ideal chromatography) which could cause very poor searching results and complicate manual interpretation if ions present in a component were subtracted out.

The algorithm described here uses the above approach to provide the benefits of:

1.) Definition of chromatographic peaks from the summed ion current chromatograms

2.) Enhanced use of chromatographic resolution by close inspection of mass spectral data to discern overlapping components within a chromatographic peak.

Our experience with this system to date has been very encouraging. Typically the program locates and quantifies all significant GC peaks, usually picking out several that are not noticeable to the analyst; these trace components often being the ones of greatest interest to us. Unresolved GC components are separated correctly in most cases where the overlap is not too severe.

The T.I.C. trace of a GC/MS run of the products from the pyrolysis of di-thiomethyl-benzoate is shown in Fig. 1. In this analysis, 33 separate components were

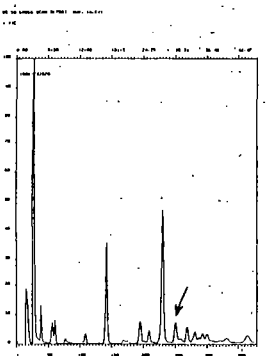

Fig. 1 TIC

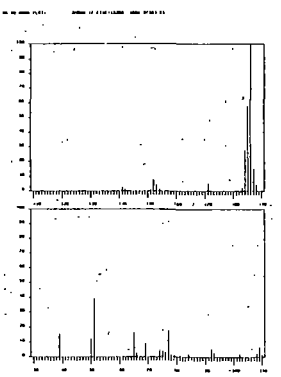

Fig. 2 OUTPUT

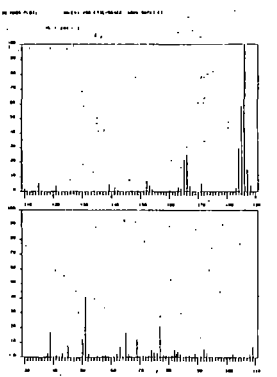

Fig. 3 Scan 250

located by the program and spectra such as the one shown in Fig. 2 were generated. This spectrum, identified as di-phenyl sulfide, is considerably different from the simple plot of scan number 250, shown in Fig. 3. The region from m/e 160 to m/e 170 shows the presence of impurities most clearly. In all, four components were identified by the program as eluting at this time. Most of the observable GC peaks in Fig. 1 actually consist of two or more components which can be easily discerned from the program output, but which are not at all obvious from the T.I.C. trace.

In conclusion, this system is able to provide useful identifying information to the chemist who is able to use his own interpretive skills to supplement output from the program. It is simple and quick enough to be run routinely, but sophisticated enough to provide reliable information which can reduce interpretation time substantially.

REFERENCES

1 a.) W.C. Davidson, M.J. Smith, and D. Shaefer, Anal. Lett. 10, 309 (1977).

b.) D.T. Terwilliger and W.C. Davidson, A.S.M.S. 28'th Annual Conference (New York), paper MPMP-18 (1980).

2.) R.G. Dromey, M.J. Stefik, T.C. Rindfleisch, and A.M. Duffield, Anal. Chem. 48, 1368 (1976).

3.) R.A. Hites and K. Biemann, Anal. Chem. 42, 855 (1970).

4.) S.C. Gates, M.J. Smisko, C.L. Ashendel, N.D. Young, J.F. Holland, and C.C. Sweeley, Anal. Chem. 50, 1433 (1978).

QUANTIFICATION OF DIETHYLSTILBESTROL PRODUCED FROM STILPHOSTROL USING CAPILLARY GC/MS/SIM TECHNIQUES.

FRED P. ABRAMSON[1] AND HARRY C. MILLER, JR.[2]
DEPARTMENTS OF PHARMACOLOGY[1] AND UROLOGY[2]
GEORGE WASHINGTON UNIVERSITY
WASHINGTON, DC 20037

Stilphostrol, diethylstilbestrol diphosphate, is a prodrug form of diethylstilbestrol (DES). Several clinical investigators have noted that one or two weeks of 1000 mg/day infusions of stilphostrol produced subjective and objective improvement in patients with advanced prostatic carcinoma in whom oral doses of DES (1-5 mg) were no longer effective. There are two possible explanations for this increased therapeutic effect. The high levels of acid phosphatase in the prostate gland could selectively dephosphorylate stilphostrol and lead to a selective concentration of DES. Alternatively, the use of a 1000-fold higher dose might explain these observations, although the bioavailability of DES from either intravenous or oral stilphostrol had not been established. To answer these questions, A GC/MS assay for DES was developed and applied to the production of DES from stilphostrol in experimental animals as well as patients with prostatic carcinoma.

Originally, a packed column interfaced to the mass spectrometer with a jet separator was used. To adequately study the pharmacokinetics of small oral doses of DES, which produced plasma concentrations averaging less than 3 ng/ml, the original assay (Abramson and Miller, Proc. ASMS, 1977) was modified by directly coupling a polymethoxysiloxane fused silica capillary to the Dupont 21-491 mass spectrometer while using a 4-channel multiple ion detector. Dimethylstilbestrol now serves as an internal standard.

One ml of plasma is adjusted to pH 5.8 with one ml of a phosphate-citrate buffer and extracted with 3 ml of methylene chloride. The CH_2Cl_2 is evaporated and the residue is derivatized with TFAA (25% in CH_2Cl_2) for 20 minutes at room temperature, then evaporated again and reconstituted in 50 microliters of CH_2Cl_2. 1.5 µl of this solution are fronted by ½ µl of n-dodecane and injected over a 30 second period using a splitless technique. Thirty seconds later the splitter is opened and the column is programmed at 15°/min to 225° from its initial temperature of 150°. The molecular ion of DES-di-TFA is monitored at M/z 460, the molecular ion of the internal standard-di-TFA appears at M/z 432, and the $(M-29)^+$ ion from DES is also monitored at M/z 431. When tissue samples are analyzed, 200 mg samples are initially homogenized in 3 ml of the pH 5.8 buffer and then extracted and processed as were plasma samples.

Blank plasma, prostate, liver, and muscle tissues show little interference. Analyses of spiked samples show that the limit of quantitation is less than 0.5 ng/ml of plasma or ng/gm of tissue. The system is linear up to 10,000 ng/ml.

Initial experiments demonstrated that intravenous stilphostrol infusions produced approximately 1000 times the plasma concentrations of DES which were found in other patients receiving conventional oral DES therapy (3600 ng/ml vs 2.4 ng/ml).

The tissue distribution of DES was compared for intravenous DES and stilphostrol in male rats. Using comparable doses (1.2 mg/kg or 2.0 mg/kg respectively), the amount of DES in prostate, liver and muscle at 5 hours after the dose compared to the plasma concentration at that time showed no selective advantage for stilphostrol over DES itself. Thus, the higher plasma concentrations of DES produced by stilphostrol infusions must explain the improved efficacy of stilphostrol over DES.

The bioavailability of DES from oral stilphostrol was also unknown. Using dogs, the plasma concentrations of DES were compared for a single 50 mg tablet of stilphostrol and a 31.3 mg dose of DES (50 mg of diethylstilbestrol diphosphate contains 31.3 mg of DES). These studies showed that the bioavailability of stilphostrol was 29% higher than for DES itself. Thus, oral stilphostrol can be used as an alternative source of DES.

Finally, several metabolites of DES have been detected in plasma and various tissues of rats. Dienestrol was the most abundant metabolite in all tissues examined, as well as the most abundant in the plasma of the one patient examined for metabolites following a stilphostrol infusion.

Other metabolites detected were O-methyl DES, methoxy-DES and hydroxy-DES.

Suppported by NIH Grant No. CA 20753

QUALITATIVE ANALYSIS OF TRIMETHYLSILYLATED DAUNOSAMINE AND N-ALKYLATED ANALOGUES BY ISOBUTANE CHEMICAL IONIZATION GC/MS. P.A. ANDREWS, F.E. CHOU, and N.R. BACHUR, Department of Medicinal Chemistry, University of Maryland, Laboratory of Clinical Biochemistry, BCRP, DCT, NCI, Baltimore, Maryland 21201

The search for anticancer anthracycline antibiotics with diminished toxic side effects has led to the development of compounds with alterations on the glycosidic portion of the molecule. The N,N-dialkylated analogues have proven particularly promising in reducing the dose-limiting cardiotoxicity of the anthracyclines (1). Metabolism and disposition studies in rodents on some of these analogues have shown that N-dealkylation of the daunosamine moiety is an important metabolic pathway for these drugs (2,3). Previously, examination of the metabolic alterations on the glycosidic portion of these anthracycline antibiotics could have employed field desorption mass spectrometry of the intact metabolite, insensitive and imprecise TLC methods applied to the hydrolytically removed sugar, or electron impact analysis of the peracetylated sugar (4). In order to elucidate the structural changes on the sugar residue of metabolites of the N,N-dialkylated anthracycline analogues, we have devised an isobutane chemical ionization (CI) GC/MS analysis of the trimethylsilylated sugar residues.

Parent drugs or purified isolated metabolites are hydrolyzed with 0.2 N HCl for 30 min at 100°C. The generated aglycones are removed by ethyl acetate extraction. The remaining aqueous extract is dried with a nitrogen jet. The residue is dissolved in 25-100 μl of trimethylsilylimidazole/pyridine (1:4), heated 10 min at 65°C, and an aliquot injected onto a 1.8 m x 2.6 mm I.D. glass column packed with 3% OV-17 on 100/120 Gas Chrom Q. The carrier gas is helium at a flow rate of 40 ml/min and the column temperature is programmed, after a 5 min hold, from 120° to 250°C at 10°/min. The column is coupled via a jet separator maintained at 200-250°C to the source of a VG 30F mass spectrometer operated under VG Datasystems 2040 computer control. The source conditions for CI analysis are 150°C, 52 eV, 4 kV, and 170 μA emission current.

Electron impact analysis of the derivatized sugars gave spectra displaying extensive fragmentation and no parent ions. Isobutane CI provided spectra with strong quasi-molecular ions $(MH)^+$ and limited fragmentation. GC analysis indicated the presence of the α-anomer in all analogues studies. The natural β-anomer which was presumed to be the major peak eluted first. In all cases, the later eluting α-anomer gave identical although more intense fragments than the β-anomer. The following sugars have been analyzed:

Sugar	Retention Time (min) β (α-Anomer)	Lowest Amount Detected* (nmol)
Daunosamine	9.1 (9.5)	5.7
Dimethyldaunosamine	9.0 (9.5)	7.6
Monobenzyldaunosamine	17.1 (17.8)	8.6
Dibenzyldaunosamine	(23.8) 25.7 (27.2)	73.5
Rabbit Metabolite	17.1 (17.8)	—

* Defined as detectable $[MH]^+$ peak

Daunosamine and the N-mono or di-alkylated analogues follow common and predictable fragmentation pathways when subjected to isobutane CI. The following schemes are proposed:

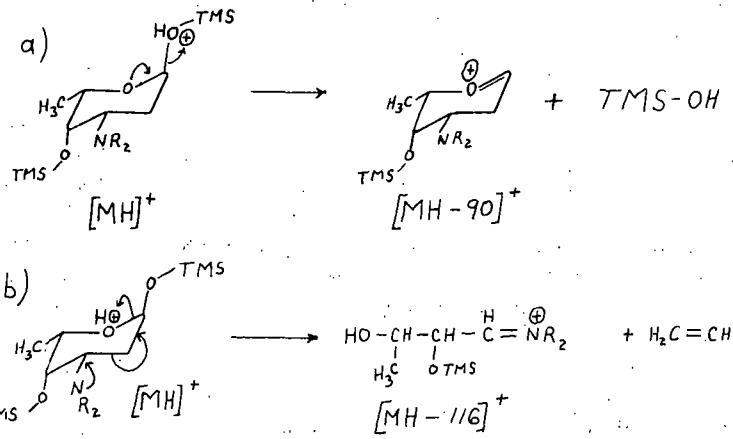

Following dosing with 3.0 mg/kg N,N-dibenzyldaunorubicin, the bile from a 2-3 kg rabbit was collected 0-8 hr through a surgically cannulated bile duct. Parent drug and bile metabolites were extracted into ethyl acetate and the major metabolite isolated by TLC. The metabolite was purified by passing through a C_{18} Sep-Pak cartridge, then hydrolyzed, extracted, and derivatized as above. Isobutane CI GC/MS analysis of this sugar gave an identical retention time and mass spectra as N-monobenzyldaunosamine.

In conclusion we have utilized an alternative, highly sensitive and precise isobutane chemical ionization GC/MS method for conclusive chemical identification of N-mono and di-alkylated daunosamine analogues. We identified a major biliary metabolite of N,N-dibenzyldaunorubicin in rabbits as N-monobenzyldaunorubicinol. We are investigating the application of this method to epimeric, N-acetylated, and other N-alkylated analogues.

ACKNOWLEDGMENTS:

We thank Dr. Merrill J. Egorin and Mr. Steven Engle for providing the rabbit biliary metabolite and Dr. Edward M. Acton of Stanford Research Institute for providing N-monobenzyldaunorubicin.

REFERENCES:

1. G.L. Tong, H.Y. Wu, T.H. Smith and D.W. Henry, J. Med. Chem. 22(8), 912 (1979).
2. M.J. Egorin, R.E. Clawson, L.A. Ross, F.E. Chou, P.A. Andrews and N.R. Bachur, Drug Metab. Disp., 8(5), 353 (1980).
3. J.H. Peters, D. Kashiwase, G.R. Gordon, C.A. Hunt and E.M. Acton, Proc. Am. Assoc. Cancer Res., 22, 256 (1981).
4. A. Vigevani, B. Gioia and G. Cassinelli, Carbohydr. Res., 32, 321 (1974).

QUANTITATIVE ANALYSIS OF Δ^9 - TETRAHYDROCANNABINOL AND METABOLITES USING NEGATIVE ION CHEMICAL IONIZATION

Rodger L. Foltz and Dennis M. Chinn
Center for Human Toxicology, University of Utah
Salt Lake City, Utah 84112

OBJECTIVE: Development of a rapid GC/MS assay for Δ^9 -tetrahydrocannabinol (THC) and two of it's metabolites, 11-hydroxy- Δ^9 -THC and 9-carboxy-Δ^9 -THC, which has sufficient sensitivity and specificity to permit accurate quantitation of these compounds in body fluids at concentrations as low as 100 pg/ml.

BACKGROUND: The sensitivity of previously published GC/MS and immunological assays has not permitted reliable measurement of THC at body fluid concentrations below 1 ng/ml(1). However, the plasma concentration of THC falls below that level within a few hours after smoking a marijuana cigarette (2), so a more sensitive assay is needed for medicolegal examinations and for pharmacokinetic studies. Electron impact (EI) and positive ion chemical ionization (CI) offer similar sensitivities for THC, although CI using ammonia as reagent gas is more selective than EI ionization (3,4). After extraction from the body fluid, cannabinoids are normally converted to less polar derivatives to improve their chromatographic behavior. Trimethylsilylation has been most widely used for this purpose.

METHOD: After addition of deuterium-labeled analogs of each of the cannabinoids to the body fluid specimen, the cannabinoids are extracted by means of the scheme shown in FIGURE 1. For each body fluid sample, two extracts are generated, one containing THC and 11-hydroxy-THC, and the other containing 9-carboxy-THC. The THC and hydroxylated metabolite are converted to their trifluoroacetate (TFA) derivatives by briefly heating an ethyl acetate solution of the extract with trifluoroacetic anhydride. The carboxy metabolite is first converted to its methyl ester by reaction with diazomethane and then treated with trifluoroacetic anhydride. For the GC/MS analysis we have used either packed columns (OV-17, SP-2250, SE-30) or capillary columns (SE-52, OV-101). With a packed column methane serves as the carrier gas; for capillary columns hydrogen is used as the carrier gas and methane is added to the ion source through a make-up gas inlet. Ionization of the derivatized cannabinoids is achieved by means of electron-capture formation of negative ions at an ion chamber pressure of 0.3 to 0.4 torr and a temperature of approximately 150°C. The ion currents are monitored at m/z 410 and 413 (corresponding to the molecular anions for THC-TFA and THC-d_3-TFA), m/z 408 and 411 (corresponding to loss of trifluoracetic acid from the molecular anion of the bis-TFA derivative of 11-hydroxy-THC and its trideuterated analog), and m/z 454 and 457 (corresponding to the molecular anion of the TFA derivative of 9-carbomethoxy-THC and its trideuterated analog).

DISCUSSION: Previously in our laboratory, THC was extracted from blood or plasma with hexane (4). However, the extraction efficiency varied widely from sample to sample and was particularly poor in the case of decomposed blood. The new procedure involves the addition of acetonitrile to the body fluid to separate the cannabinoids from blood proteins in a manner similar to a procedure reported by Rosenthal and Brine (5). After removal of the precipitated protein by decantation and the acetonitrile by evaporation, the cannabinoid can be efficiently extracted from the aqueous residue. At a concentration of 10 ng/ml, the overall recovery of THC by this procedure varies from 40-70%, in contrast to recoveries of THC of 0 to 60% following a simple hexane extraction of the body fluid. An even more significant improvement is the use of negative ion chemical ionization of the TFA derivatives of the cannabinoids, rather than either ammonia positive ion chemical ionization or electron impact ionization of their trimethylsilyl derivatives. In the case of THC, a direct comparison of sensitivities has shown that at least a ten-fold improvement in sensitivity can be achieved by the new method. Furthermore, there is less interference from endogenous components of body fluid under the conditions of negative ion CI. The negative ion CI mass spectra of the TFA derivatives of THC and 9-carbomethoxy-THC each show only one prominent peak, and it corresponds to the derivative's molecular anion, a circumstance ideally suited for quantitative analysis by selected ion monitoring. The negative ion CI mass spectrum of the 11-hydroxy-THC is not as well suited for selected ion monitoring because its base peak corresponds to the trifluoroacetate anion. Nevertheless, a peak at m/z 408 with a relative abundance of 12% can be monitored for quantitative measurements. FIGURE 2 shows the ion current profiles resulting from analysis of plasma containing 100 pg/ml of THC and 5 ng/ml of the internal standard, THC-d_3. The assay was performed on a Finnigan Model 4000 GC/MS using a 25 meter capillary column coated with OV-101. Two microliters of extract

was injected without splitting at a column temperature of 150° C. After 1 minute the GC oven temperature was increased to 250° C at 15° per minute. The amount of THC-TFA introduced into the capillary column was approximately 5 pg. Because of the extremely high ionization efficiency of negative ion chemical ionization of this THC derivative, the assay's sensitivity is limited primarily by the biological background. If necessary the background contribution could be reduced by a chromatographic clean-up of the biological extract, or by use of a MS/MS technique as recently reported by Harvey, et al. (6).

Negative ion chemical ionization of the pentafluorobenzyl (PFB) ether of THC has also been explored. Under CI conditions the PFB derivative of THC undergoes dissociative electron capture to give an intense peak at m/z 313. Preliminary data indicate that the negative ion current generated from the PFB derivative is approximately 10 times the negative ion current generated from an equal amount of the TFA derivative of THC. However, the relative freedom from interferences in analysis of biological extracts remains to be evaluated.

REFERENCES:

1. J.A. Vinson, Cannabinoid Analysis in Physiological Fluids, ACS Symposium Series, no. 98, American Chemical Society, Washington, D.C., 1979.
2. A. Ohlsson, J-E. Lindgren, A. Wahlen, S. Agurell, L.E. Hollister, and H.K. Gillespie, Clin. Pharmacol. Ther., 28, 409 (1980)
3. D. Rosenthal, T.M. Harvey, J.T. Bursey, D.R. Brine, and M.E. Wall, Biomedical Mass Spectr., 5 , 312 (1978).
4. R.L. Foltz, A.F. Fentiman, Jr., and R.B. Foltz, GC/MS Assays for Abused Drugs in Body Fluids, NIDA Research Monograph Series, No. 32, Suprt. of Docs., U.S. Govt. Print. Off., Washington, D.C. (August 1980)
5. D. Rosenthal and D. Brine, J. Forensic Sci., 24, 282 (1979)
6. D.J. Harvey, J.T.A. Leuschner and W.D. M. Paton, J. Chromatogr., 202, 83 (1980)

ACKNOWLEDGEMENTS: This research was supported by the Insurance Institute for Highway Safety and the National Institute on Drug Abuse, Contract # 271-80-3719.

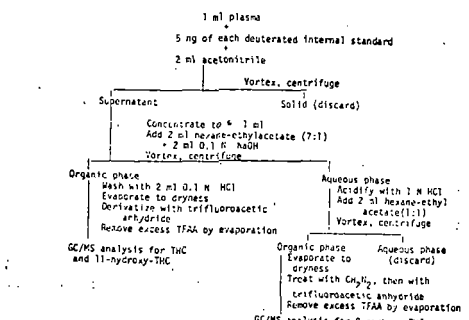

FIGURE 1. Scheme for extraction of THC, 11-hydroxy-THC, and 9-carboxy-TCH from plasma and other body fluids

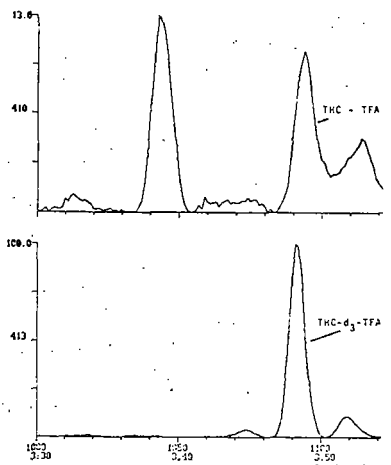

FIGURE 2. Ion current profiles from an analysis of plasma containing 100 pg/ml of THC (top) and 5 ng/ml THC-d_3 (bottom)

EVALUATION OF GLUCOSE CARBON RECYCLING AND TRUE GLUCOSE TURNOVER IN HUMANS USING ul[^{13}C]GLUCOSE TRACER ALONE WITH CHEMICAL IONIZATION GC/MS AND RATIO MASS SPECTROMETRY.

KOU-YI TSERNG and SATISH C. KALHAN. Div. of Ped. Metab., Case Western Reserve Univ. at Cleveland Metropolitan General Hospital, Cleveland, OH, 44109

In order to quantify "true" glucose production rates, as well as glucose carbon recycling in humans without the use of multiple isotopic tracers, a method using ul[^{13}C]glucose alone has been developed. This method is based on the following rationale: During metabolism, glucose uniformly labelled with ^{13}C (m + 6) will split into three carbon intermediates. As a result of dilution with unlabelled intermediates, the chances of two labelled intermediates joining together to form a uniformly labelled glucose (m + 6) are negligible. Thus, measurement of the uniformly labelled molecule (m + 6) will have only a negligible contribution by recycled glucose carbon and the "true" rate of glucose production can be estimated. The glucose production rate, including the recycling, can be quantified by measuring the ^{13}C enrichment of glucose carbon by converting the plasma glucose to CO_2, by enzymatic decarboxylation, and measuring the $^{13}C/^{12}C$ ratio of the CO_2 using an isotope ratio mass spectrometer.

The plasma glucose enrichment of (m + 6) ion was measured by chemical ionization GC/MS. The plasma sample was deproteinized and the glucose converted to the aldonitrile penta acetate derivative. A six feet 3% OV-17 column at 200C was used. Methane at 10 ml/min was used as a carrier and a reagent gas. The CI spectrum of this derivative showed only quasimolecular ion (m/e 328), with no background at m/e 334, resulting in marked sensitivity. Enrichments as low as 0.01% could be easily detected. Glucose turnover and recycling were estimated in six normal subjects. The tracer was administered as prime-constant rate infusion. The mean rate of glucose production was 2.1 mg/kg.min which is similar to the published reports using non-recycling tracers. Glucose carbon recycling was 3 to 26% in the postabsorptive state.

Serum vs. Plasma Levels of Tricyclic Antidepressants

by
Joseph J. Saady[1] and
N. Narasimhachari[2]
Departments of Pathology[1] and Psychiatry[2], Medical College of Virginia, Box 597
Richmond, Virginia 23298

OBJECTIVE

Since the late 1960's to early 1970's, the idea of therapeutic drug monitoring has expanded from the monitoring of anticonvulsant drugs by GLC, to present day monitoring of tricyclic antidepressant drugs (TCA) by GC/MS. There has been a great deal of interest in recent years of monitoring TCA levels and correlating them to clinical response. Unfortunately, many blood collecting tubes (1), methodologies and instrumentation lend themselves to interferences and cause erroneous results. One of the areas that we felt needed investigation was serum vs. plasma levels of TCA. Most of the work which correlates TCA blood levels and therapeutic response report plasma levels, while a few reports use serum values, and others use the two terms interchangeably. This study was performed to demonstrate the difference, if any, between serum and plasma levels of TCA.

PROCEDURE

Two 7 ml Venoject (Kimble-Terumo, Inc.) blood collection tubes were simultaneously collected from each patient, one red top tube (serum) and the other a sodium heparin green top tube (plasma). Three of the patients were taking desipramine (DMI); eight, imipramine (IMI); and one, nortriptyline (NTR). After allowing time for clotting, cells were spun down and the serum and plasma were transferred to appropriately labeled tubes, then frozen until analysis by GC/MS.

The analysis was performed in accordance with the method of Narasimhachari (2), which makes use of deuterated IMI and DMI as internal standards. 2000 ng each of D4 IMI and D4 DMI were added to 2 ml patient plasma and serum as internal standard. 1 ml of 1N NaOH was added along with 10 ml of hexane-isopropanol (90:10), and extracted for 5 min. on a Rotorack. The solvent was evaporated to dryness and the residue derivatized with N-methyl-bistrifluoroacetamide at 80°C for 15 min. Samples were injected into a Hewlett Packard 5985 A GC/MS, and quantitation performed using standard curves.

RESULTS

The electron impact mode was used for monitoring IMI and DMI selected ion monitor of m/z 234 and 208 respectively (Fig. 1 and 2). For NTR, the same extraction and derivization method was used except the methane chemical ionization mode was used monitoring m/z 360, and m/z 367 for the D4 DMI (Fig. 3). The results have been tabulated in Table 1. An intraclass correlation between serum and plasma was performed for IMI, DMI, and the sum of IMI and DMA. The correlation values were 0.97, 0.96, and 0.965 respectively.

CONCLUSION

It can be seen from Table 1 and the statistical analysis that plasma and serum levels for IMI and DMI are clinically and statistically the same for patients taking IMI. Further, the studies suggest that the same is true for patients taking DMI or NTR. These data show that venoject red top tubes can be substituted for venoject sodium heparin green top blood collection tubes without affecting results significantly. Although one must be cautious about the various methodologies used in research, these data suggest that clinicians can equate the serum and plasma level data found in the literature with a higher degree of confidence.

REFERENCES

1. Veith, RC, Raisys, VA, Perera, C, The clinical impact of blood collection methods on tricyclic antidepressants as measured by GC/MS-SIM, Psychopharmacol Comm. 2:491-494 (1978).

2. Narasimhachari, N, Friedel, RO, and Saady, JJ, Improved tricyclic antidepressant assay by GC/MS, Reserach Comm. in Psychol, Psychiatr, and Behavior 4, No 4:477-490 (1979).

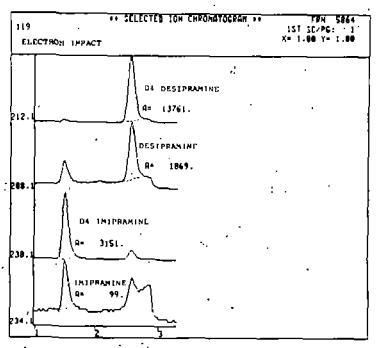

Figure 1
GC/MS SIM of Patient Taking Imipramine

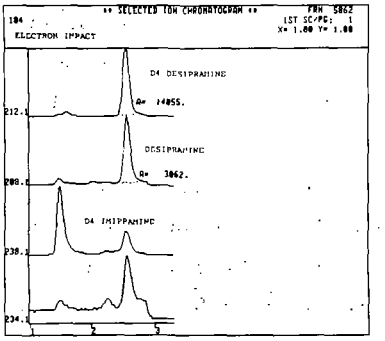

Figure 2
GC/MS SIM of Patient Taking Desipramine

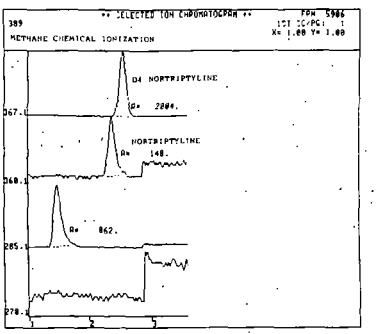

Figure 3
GC/MS SIM of Patient Taking Nortriptyline

PATIENTS TAKING IMIPRAMINE

PLASMA LEVELS			SERUM LEVELS		
IMI	DMI	IMI + DMI	IMI	DMI	IMI + DMI
98	105	203	97	130	227
152	52	204	150	58	208
106	90	196	90	85	175
121	100	221	132	205	209
49	50	99	77	62	77
68	60	128	68	65	103
57	46	83	58	63	75
35	71	106	37	69	106

CORRELATIONAL VALUES OF SERUM VS PLASMA

IMI	.97
DMI	.96
IMI + DMI	.97

PATIENTS TAKING DESIPRAMINE

PLASMA LEVELS	SERUM LEVELS
96	40
155	155
350	360

PATIENT TAKING NORTRIPTYLINE

PLASMA LEVELS	SERUM LEVELS
14	13

Table 1
Comparison of Plasma and Serum Levels of Patients on Imipramine, Desipramine, and Nortriptyline

A GC/MS, STABLE-ISOTOPE DILUTION ASSAY FOR 4-HEPTANONE

4-Heptanone Formation in Diabetes Mellitus

Wm. F. Bryant, J. R. Althaus, and J. P. Freeman

National Center for Toxicological Research

Jefferson, Arkansas 72079

During the past decade GC/MS techniques have provided sensitive methods for identification of biochemical markers associated with specific disease states in humans. One such marker associated with diabetes mellitus is 4-heptanone. However, the clinical significance of 4-heptanone elimination remains obscure. Little information is available concerning the mechanism of formation, distribution, or metabolism. We therefore undertook the development of an assay method employing 3,3,5,5-[$^2H_4$]-4-heptanone as the internal standard. This assay method has been used in studies of the effect of hypoglycemia on 4-heptanone elimination.

The general theory of stable-isotope dilution mass spectrometry developed by Pickup and McPherson gave the following predictions for the form of the calibration graph to be expected for 4-heptanone when the indicated internal standard is used: (1) the function for this system is a special case where the general calibration function (Eq. 1) reduces to a linear form; and (2) the function passes through the origin.

$$Y_{114/118} = \frac{N P_{114} + M Q_{114}}{N P_{118} + M Q_{118}} \qquad \text{(Eq. 1)}$$

The prediction of linearity arises because there is no overlap in the mass spectra between the two forms of 4-heptanone; hence, Q_{114} and P_{118} are both zero. Thus, Eq. 1, which is non-linear, reduces to Eq. 2.

$$Y_{114/118} = \frac{N}{M} \times \frac{P_{114}}{Q_{118}} \qquad \text{(Eq. 2)}$$

Eq. 2 is a linear function where P_{114}/Q_{118} is the slope and the intercept is obviously zero.

Mixtures containing varying amounts of 4-heptanone (10^{-2}, 10^{-3}, 10^{-4}, 10^{-5}, 10^{-6}, 10^{-7} m-moles/ml) and 10^{-4} m-moles/ml of the internal standard were used to obtain experimental estimates of the calibration parameters. Linear regression analysis gave an intercept of $3.26 \times 10^{-5} \pm 3.3 \times 10^{-5}$ CI (95%), a slope of 0.9930, and a correlation coefficient of 0.999. Thus, both predictions based on Eq. 1 were confirmed. Precision for the method was assessed using five measurements of response ratio for each of the calibration standards. Relative standard deviations ranged from 0.6/100 at a molar ratio of 100 to 2/100 at a molar ratio of 0.01. At the limit of detection the relative standard deviation was about 14/100 and corresponded to a concentration of 4-heptanone in urine of 1.2 ng/ml.

The internal standard was checked for stability against back-exchange in aqueous solutions buffered at pH 7. The mole per cent deuterium distribution of the ketone isolated after 24 hr was unchanged from that used in preparing the mixture: 96.6 mole % of $^{2}H_{4}$ and 3.4 mole % $^{2}H_{3}$.

Preliminary studies of 24 hr urine elimination by diabetics and controls confirmed that 4-heptanone elimination by the diabetics was considerably greater. The mean values for diabetic subjects (N = 6) was found to be 2.9 mg/24 hr, whereas that for controls (n = 3) was 0.18 mg/24 hr.

BIOCHEMICAL INVESTIGATIONS OF DICARBOXYLIC ACIDURIA BY GAS CHROMATOGRAPHY-MASS SPECTROMETRY

Toshihiro Shinka, Tomiko Kuhara and Isamu Matsumoto

Research Institute of Medical Mass Spectrometry, Kurume University School of Medicine, Kurume Fukuoka 830, Japan

Medium-chain dicarboxylic acids are usually found in small amounts in normal urine. Unusually high amounts of dicarboxylic acids are excreted by dicarboxylic aciduria patients, however. In order to investigate long-chain fatty acid metabolism in dicarboxylic aciduria, urine samples from patients with ketotic and non-ketotic dicarboxylic aciduria were analyzed using GCMS.

Urine was frozen to -20°C immediately after collection and stored at this temperature until analysis. Urinary organic acids were extracted with two volumes of diethyl ether and trimethylsilylated with BSTFA (bis-trimethylsilyl trifluoroacetamide). Organic acids were separated by gas chromatography on a 2 m glass column packed with 3% OV-17 on Gas Chrom Q. Oven temperature was maintained at 80°C for 2 min, then programmed from 80°C to 290°C at 6°C/min. A JEOL JMS-D 100 gas chromatography-mass spectrometer on line with a JMA-2000 data acquisition and processing system was used.

Large amounts of adipate, suberate, and 3-hydroxydecanedioate, were found in the urine of both ketotic and non-ketotic patients. No medium-chain monocarboxylic acids or their 3-hydroxyderivatives were detected in either group, however. Futhermore, large amounts of sebaciate were found in the non-ketotic patients, but only small amounts were found in the ketotic patients. The increase of ketone bodies in ketotic patients was not proportional with their excretion of medium-chain dicarboxylic acids.

Long-chain fatty acids are usually transported into the mitochondria and then oxidized by the mitochondrial β-oxidation system. Medium-chain fatty acyl-CoA, an intermediate in the catabolism of long-chain fatty acids, can not pass through the mitochondrial membrane. However, free medium-chain fatty acids can easily pass through the membrane. Medium-chain fatty acids are oxidized by the microsomal ω-oxidation system and converted to corresponding medium-chain dicarboxylic acids. There are three possible causes of dicarboxylic acid formation: (1) an enzyme dificiency in the mitochondrial β-oxidation cycle, (2) enzyme inhibition, as in hypoglycine A treatment[1], and (3) transport defects, such as the decrease in flow into the mitochondria observed in carnitine deficiency. Several researchers have suggested that a possible enzyme defect in mitochondrial -oxidation is one of three

kinds of acyl-CoA dehydrogenase found in mitochondria[2,3] and that this enzyme defect causes accumulation of mono-carboxylic acids, which are then converted to corresponding dicarboxylic acids in the microsome. The existance of a β-oxidation system in the outer mitochondria has been previously reported. Peroxisomal fatty acyl-CoA oxidase in human liver has maximal activity for fatty acids with C_{12}-C_{18}. Activity with C_6, however, is less than 10% of that for C_{16}[4]. Peroxisomal β-oxidation in rats was reported to be enhanced to the mitochondrial level by some drugs[5]. We found large amounts of 3-hydroxydecanedioate in both types of patients. It seems, therefore, that enzyme inhibition occurs below the C_{10} level. We also found that adipate is the predominant compound in dicarboxylic aciduria, and that the increase in ketone bodies was only indirectly related to the excretion of medium-chain dicarboxylic acids. These factors lead us to assume that most of fatty acid β-oxidation occurs in the peroxisome in dicarboxylic aciduria and that the accumulation of dicarboxylic acids is caused by the substrate specificity of peroxisomal β-oxidase.

1. Tanaka, K., Kean, E. A. and Johnson, B. (1976) New Eng. J. Med. 295, 461-467
2. Tanaka, K., Mantagos, S., Genel, M., Seashore, M. R., Billings, B. A. and Baretz, B. H. (1977) Lancet ii, 986-987
3. Gregersen, N., Rosleff, F., Kolvraa, S., Hobolth, N., Rasmussen, K., and Laurizen, R. (1980) Clin. Chim. Acta 102, 179-189
4. Bronfman, M., Inestrosa, N. C., Leighton, F. (1979) Biochem. Biophys. Res. Commun. 88, 1030-1036
5. Shindo, Y. and Hashimoto, T. (1978) J. Biol. Chem. 84, 1177-1181

URINARY EXCRETION OF C_4-C_{10}-DICARBOXYLIC ACIDS*

	3-OH-Butyric acid	Acetoacetic acid	Succinic acid	Adipic acid	Suberic acid	Sebacic acid	3-OH-Decane dioic acid
K.S.	333.2	53.4	0.7	4.1	1.8	N.D.	2.6
T.O.	243.8	95.6	0.5	6.6	3.0	N.D.	2.7
T.K.	147.7	62.4	0.5	10.4	2.5	N.D.	3.1
E.K.	105.2	46.4	0.6	1.2	2.2	N.D.	1.2
K.M.	27.4	20.8	0.8	7.4	3.2	0.1	4.4
N.F.	0.9	N.D.	2.5	11.5	14.2	3.9	4.9
Normal	0.2±0.1	N.D.	1.0±0.9	0.1±0.1	0.2±0.1	N.D.	0.4±0.3

* Relative peak area

ANALYSIS OF DEOXYALDONIC ACIDS IN ISCHEMIC AND INFARCTED HEART MUSCLE BY GC/MS

Shin-Ichi Haraguchi, Hironori Toshima,
°Isamu Matsumoto, °Tomiko Kuhara and °Toshihiro Shinka

The 3rd Department of Internal Medicine and °Research Institute of
Medical Mass Spectrometry, Kurume University School of Medicine,
Kurume, Fukuoka 830, Japan

The profile of organic acids in the normal rat heart muscle has been studied. For the purpose of examining change of the organic acid in pathological conditions, the organic acids in the rat heart muscle disturbed by reducing a blood supply, were investigated.

In order to examine the variation of the organic acids by the time elapsed after decapitation, rat hearts were obtained with the following time interval; 2 min, 4 min, 6 min, 10 min, 15 min and 30 minutes. They were immediately frozen in dry ice-acetone. The tissues were rinsed with a saline solution to remove the blood in the heart, and then minced with scissors. After 20 ug of heptadecanoic acid per mg of protein was added as an internal standard, they were homogenized and deproteinized with cold ethanol. The protein concentration was determined by a BIO-RAD Protein Assay Method. Organic acids were extracted at pH 1 with diethyl ether and ethyl acetate. After trimethylsilylation, the samples were analyzed by GC/MS with a 3% OV-17 column on Gas Chrom Q (80-100 mesh). Oven temperature was programmed at a rate of 6°C/min from 80°C up to 290°C. The temperature of a molecular separator was kept at 280°C and the electron energy was 75 eV. The date were processed with a Chromatopac 4-B for GC and a JMA-2000 data acquisition and processing system for GC/MS.

Over 40 peaks were detected on the gas chromatogram and the identified compounds were demonstrated, as shown in Fig. 1. The identification was performed by comparison of their retention time and mass spectra with those in references (1). And a profile of organic acid of the healthy rat heart muscle was established.

The variation of these organic acids in rat heart muscle by the time elapsed after decapitation was examined. It is presumed that supply of oxygen and coronary blood flow is extremely reduced at 4 minutes after decapitation, and it is observed that the heart stopped beating and coronary flow was at a standstill in 6 minutes after decapitation. At 4 minutes time elapsed, almost all peaks increased as compared with that of control, especially, peak No.2, No.26, No.28, No.36 and peak No.40. At 10 minutes after decapitation, the peaks which increased at 4 minutes decreased, but two peaks of peak No.16 and No.20 newly increased and unknown peaks appeared at position of peak No.24, No.28, No.32, No.36 and so on.

A variation of these organic acids by the time elapsed after decapitation is tabulated, as shown in Fig. 2. The diagram shows that lactate, glycolate, 3-deoxy-2-C-(hydroxymethyl)-tetronate, 3-deoxyerythropentonate, 3-deoxy-2-C-(hydroxymethyl)erythropentonate and fatty acids of palmitate and stearate were increased by time elapsed until 4 minutes, but they were decreased from 6 minutes, when the rat heart stopped beating. On the contrary, 2-deoxytetronate and dideoxypentonate increased from 6 minutes.

As an increase in fatty acid and lactate has already been reported in ischemic heart muscle (2), it is reasonably understood that the fatty acids and lactate were accumulated in rat heart muscle which was obtained by 4 minutes time elapsed and in which coronary blood flow might be reduced. It is presumed that a temporal decrease in fatty acids at 2 minutes might be related to decrease in uptake of fatty acids by ischemic myocardium (3). As it is not clearly known on metabolism of deoxyaldonic acids, it is hard to discuss the variation of these deoxyaldonic acids, biochemically. Lawson (4) reported that urinary excretion of 2-deoxytetronic acid changed more than that of the other deoxytetronic acids in an experiment in which a high glucose diet was given. And it is known that oxidation of pentose and deoxypentose may yield pentonic acid and 2-deoxypentonic acid, and that ascorbic acid is metabolized via threonic acid and pentonic acid. It is, therefore, strongly suggested that the deoxyaldonic acids in the heart muscle might be related to glucose metabolism, and their variation might be also concerned with disturbance of carbohydrate metabolism, especially, pentose phosphate shunt, by reducing the coronary blood flow.

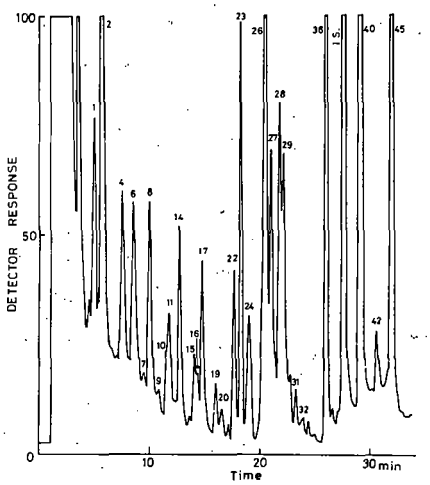

Fig. 1

The gas chromatogram of organic acid in rat heart muscle. The peaks were identified as follows ; 1) lactic acid, 2) glycolic acid, 4) 3-hydroxypropionic acid, 7) glycerol, 9) 2-methylglyceric acid, 10) phosphoric acid, 11) glyceric acid, 14) succinic acid + fumaric acid, 15) 3-deoxytetronic acid, 16) 2-deoxytetronic acid, 17) 3-deoxy-2-C-(hydroxymethyl)tetrono-1,4-lactone, 19) malic acid, 20) dideoxypentonic acid, 22) 3-deoxy-2-C-(hydroxymethyl)tetronic acid, 23) 3-deoxypentono-1,4-lactone, 24) 3-deoxyerythropentonic acid, 26) 3-deoxy2-C-(hydroxymethyl)pentono-1,4-lactone, 27) β-glycerophosphoric acid, 28) α-glycerophosphoric acid + 3-deoxy2-C-(hydroxymethyl)-erythropentonic acid, 36) palmitic acid, 40) stearic acid.

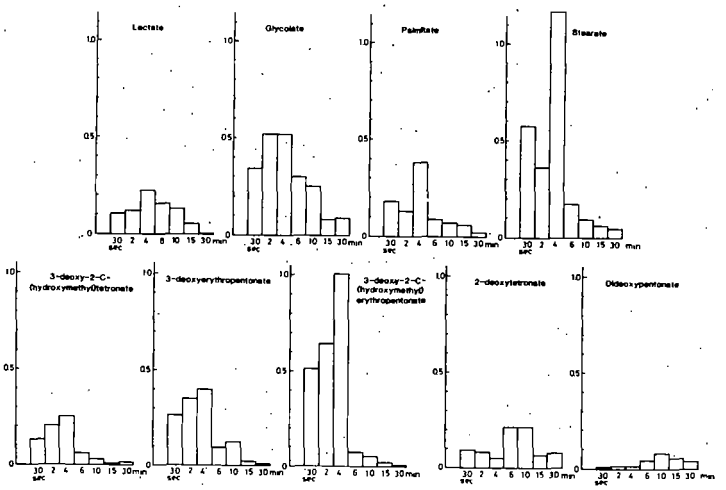

Fig. 2

(1) S. Haraguchi, H. Toshima, T. Kuhara, T. Shinka and I. Matsumoto, 28th Annual Conference on Mass Spectrometry and Allied Topics, 279 (1980).
(2) J. T. Whitmer, J. A. Idell-Wenger, M. J. Rovetto and J. R. Neely, J. Biol. Chem., 253, 4305 (1978).
(3) L. H. Opie, Jpn. Circul. J., 42, 1223 (1978).
(4) A. M. Lawson, R. A. Chalmers and R. W. Watts, Clin. Chem., 22(8), 1283 (1976).

THE CERTIFICATION OF ORGANIC ANALYTES IN A HUMAN SERUM STANDARD REFERENCE MATERIAL BY ID/MS

M. J. Welch, E. White V, L. T. Sniegoski, R. Schaffer, H. S. Hertz, and A. Cohen

Center for Analytical Chemistry
National Bureau of Standards
Washington, DC 20234

Introduction. A serum matrix containing accurately known concentrations of analytes is needed as a clinical chemistry accuracy base for routine and reference methods. To help meet this need, the National Bureau of Standards has issued a freeze-dried human serum Standard Reference Material in which five inorganic and three organic analytes have been certified by isotope dilution mass spectrometric (ID/MS) techniques. This paper describes the methods used and the results obtained for cholesterol, glucose, and uric acid in this material. These methods have been previously tested on frozen serum pools and found to provide results of high precision and accuracy [1, 2].

Methods

Serum Preparation. Vials of the freeze-dried serum from each of the machines used for vial filling were randomly chosen. The contents of each vial were weighed and dissolved in a weighed quantity (10.00 ± 0.02 mL) of diluent water supplied with the serum.

Addition of Labeled Material. For each analyte a known weight of the liquid serum was added to an aqueous solution containing a known weight of a stable isotope labeled analogue of the analyte. The labeled materials used were cholesterol-d_7, glucose-U-^{13}C, and uric acid-$^{15}N_2$. For cholesterol and glucose the quantity of labeled material used for each sample was such that the unlabeled/labeled ratio measured by mass spectrometry would be in the range of 0.9 to 1.1. For uric acid the labeled material was added in excess to facilitate the isolation steps, resulting in unlabeled/labeled ratios of 0.11 to 0.14. The spiked serum was allowed to equilibrate before isolation of the analyte was begun.

Isolation and Derivatization. For cholesterol, the serum was treated with KOH to hydrolyze esters. The cholesterol was extracted with hexane, dried, and treated with bis(trimethylsilyl)acetamide to form the TMS ether. For glucose, the serum was treated with a large volume of ethanol to precipitate protein. The resulting solution was deionized and then freeze-dried. To the residue was added 1-butylboronic acid in dry pyridine and the mixture was heated. Next, acetic anhydride was added to complete the derivative, α-D-glucofuranose cyclic 1,2:3,5-bis(butylboronate)-6-acetate or glucose BBA. For uric acid, the serum was freeze-dried. The residue was then dissolved in an aqueous lithium carbonate solution and treated with triethylanilinium carbonate to form a mixture of several tetraethyl uric acid isomers. These were sublimed and then separated by thin-layer chromatography. The most abundant isomer (3,7-dihydro-8-ethoxy-1,3,7-triethyl-1H-purine-2,6-dione), designated as the A isomer, was utilized for the measurements.

Calibration Standards. For each analyte, a series of standards were prepared to cover the unlabeled/labeled range described above. Each standard consisted of known weights of pure unlabeled analyte (SRM) and the labeled analogue and was derivatized as described for the serum samples.

GC/MS. Isotope ratio measurements were made with a low resolution magnetic sector instrument operated in the electron impact mode at 70 eV. Magnetic switching was employed to alternately measure labeled and unlabeled ions for one second intervals. Measurements were made on the following masses: cholesterol, 458, 465; glucose, 297, 302; uric acid, 280, 282. Samples were introduced to the mass spectrometer via a gas chromatograph. For cholesterol, the packed column was 1.5 m long with a 3 percent coating of a nonpolar silicone phase. At a column temperature of 250-255 °C cholesterol-TMS eluted in six minutes. For glucose the column was a 100 m SCOT column with a nonpolar silicone phase. The glucose BBA eluted in 45 minutes at a column temperature of 210 °C. For uric acid a 6 m portion of the glucose column was used. The tetraethyluric acid A isomer eluted in 10 minutes at a column temperature of 162 °C.

Measurement Protocol. Each sample was measured between measurements of the two standards whose ratios most closely bracketed the sample. Cholesterol and uric acid measurements followed the protocol previously described in detail [1]. For glucose BBA, with its long retention time, the protocol utilized was similar to that described for urea [3]. Linear interpolation of the measured ratio of the sample between the measured ratios of the bracketing standards was used to find the original analyte concentration. The measurement order was reversed on a second day and the mean of the two days' measurements was the reported result.

Results. The following tables show the results for the three analytes.

Table 1. Cholesterol Content of the Human Serum SRM

Set	# of Vials	mg Cholesterol / g Dry Serum	% CV
1	6	17.955	0.15
2	7	17.853	0.07
3	10	17.886	0.10
Mean		17.898	0.29

Table 2. Glucose Content of the Human Serum SRM

Set	# of Vials	mg Glucose / g Dry Serum	% CV
1	6	15.013	0.16
2	6	15.002	0.40
Mean		15.008	0.29

Table 3. Uric Acid Content of the Human Serum SRM

Set	# of Vials	mg Uric Acid / g Dry Serum	% CV
1	6	1.0185	0.10
2	5	1.0187	0.17
Mean		1.0186	0.13

Discussion. The results demonstrate that the serum is homogeneous with respect to these three analytes. The coefficients of variation are generally in the ranges expected for multiple samplings of one serum pool using these ID/MS methods. Measurements of different masses (329 and 336) made on a few of the cholesterol samples confirmed the results reported in Table 1. Measurements of another tetraethyl isomer made on the uric acid samples confirmed the results shown in Table 3. The most significant variations found were in the fill weights of the vials. Therefore, it is necessary to weigh the contents of each vial for the most accurate results.

Conclusion. Our results demonstrate that this material can provide an accuracy base for clinical chemistry.

References

[1] A. Cohen, H. S. Hertz, J. Mandel, R. C. Paule, R. Schaffer, L. T. Sniegoski, T. Sun, M. J. Welch, and E. White V, Clin. Chem., 26, 854-860 (1980).

[2] A. Cohen, H. S. Hertz, R. Schaffer, L. T. Sniegoski, M. J. Welch, and E. White V, presented at the 27th Annual Conference of Mass Spectrometry and Allied Topics, Seattle, WA, June 3-8, 1979.

[3] M. J. Welch, E. White V, L. T. Sniegoski, R. Schaffer, H. S. Hertz, and A. Cohen, presented at the 28th Annual Conference of Mass Spectrometry and Allied Topics, New York, NY, May 25-30, 1980.

THE CHARACTERIZATION OF CORTISOL AND RELATED STEROID DERIVATIVES BY ELECTRON IMPACT AND NEGATIVE ION CHEMICAL IONIZATION MASS SPECTROMETRY

J. S. Holler, D. G. Patterson, and L. W. Yert
Department of Health and Human Services, Public Health Service, Centers for Disease Control, Center for Environmental Health, Clinical Chemistry Division, Atlanta, Georgia 30333

A knowledge of the decomposition products and metabolic products of cortisol is a prerequisite to the development of biologically based reference materials. The development of a validated, quantitative GC/MS method for serum cortisol requires an examination for possible interferences. A number of possible decomposition products have been analyzed to establish chromatographic behavior, reference mass spectra, and non-interference in the mass spectral method. With few exceptions, the electron impact mass spectra of the methoxime-trimethyl silylethers (MO-TMS) exhibit molecular ions. Major fragmentation pathways involve reactions of the protecting groups. Ions at M-15 (loss of CH_3) and M-31 (loss of OCH_3) can be attributed to the methoxime group. The ions characteristic of the TMS derivatives are observed: $^{m}/_{z}$=73 and 75 and neutral losses of 15 μ and 90 μ. Significant stereochemical effects are observed for one pair of stereoisomers studied.

A key component in the use of mass spectrometry in quantitation is the high specificity generally observed in multiple ion monitoring techniques. Additional specificity may be obtained by using an alternate ionization technique such as negative ion chemical ionization (NCI). Negative chemical ionization has been shown to be very sensitive for certain compounds, and may be the method of choice for the accurate, precise quantitation of trace compounds below the 1 ppb level. Under conditions of methane chemical ionization, the negative ion mass spectrum of the cortisol derivative is characterized by a base peak at $^{m}/_{z}$=459. This ion does retain the label portion of the analysis of the d-3 cortisol derivative, and hence could be used in quantitative studies. An examination of the NCI spectra of the decomposition products studied indicates gas chromatographic separation of those compounds exhibiting a significant ion at $^{m}/_{z}$=459.

The NCI spectra of these steroid derivatives exhibit the $(M-H)^-$ ion in all cases. The major fragmentation of the TMS derivatives are the loss of 73 μ and the formation of the ion at $^{m}/_{z}$=89. Most derivatives exhibit only small peaks due to loss of CH_3 and OCH_3. The observed NCI spectra were less intense than the spectra obtained in electron impact ionization. Exact comparisons are difficult because of different injection volumes and a loss of source tuning and sensitivity in chemical ionization conditions. Reconstructed Ion Chromatograms are 50 to 400 times less intense in negative chemical ionization. There are fewer fragment ions in negative chemical ionization, hence a greater number of ion counts per fragment ion. The base peaks in negative chemical ionization were 20 to 200 times less sensitive than the base peaks in electron impact.

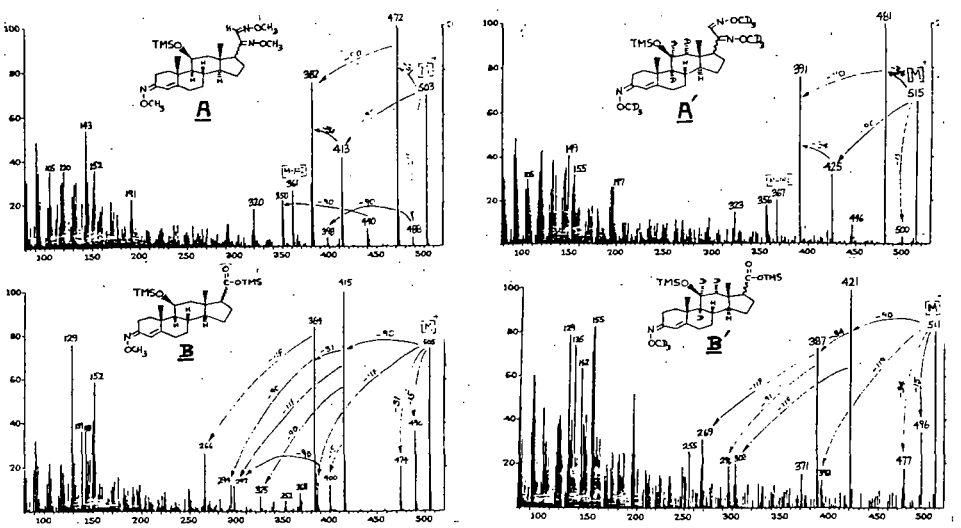

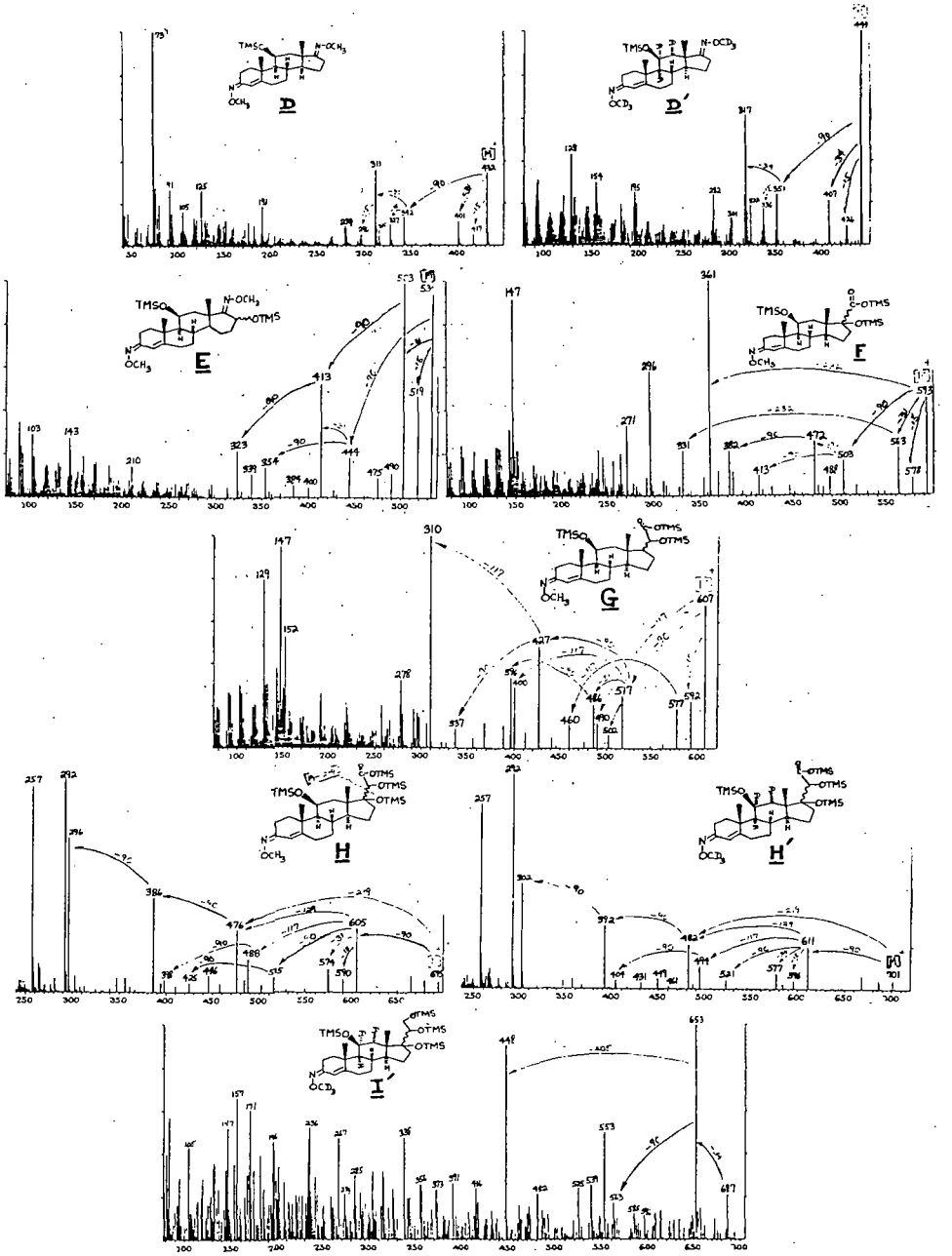
D
D'
E
F
G
H
H'
I'

THE ORIGIN OF THE $(M-1)^-$ ION IN THE NEGATIVE CHEMICAL IONIZATION (NCI) MASS SPECTRA OF THE 1,4-BENZODIAZEPIN-2-ONES W.A. GARLAND and B.J. MIWA, Department of Biochemistry and Drug Metabolism, Hoffmann-LaRoche Inc., Nutley, New Jersey 07110.

NCI is an excellent ionization technique for the mass spectral analyses of trace amounts of the medically important 1,4-benzodiazepin-2-ones in complex biological matrices (1-3). The low temperature, i.e., an ion source temperature less than 125° C, NCI mass spectra of this class of compounds consist principally of $M^{\pm}$ and $(M-1)^-$ ions. The generation of $(M-1)^-$ ions is favored by the presence of trace amounts of air in the ion source. The NCI mass spectra of analogs of diazepam ($R=CH_3$) either trideuterated at the methyl position, pentadeuterated at 2', 3', 4', 5', and 6' or trideuterated at 6, 8 and 9 show $M^{\pm}$ and $(M-1)^-$ ions, but no $(M-2)^-$ ions. The NCI mass spectrum of an analog of diazepam dideuterated at position 3, however, shows both $M^{\pm}$ and $(M-2)^-$ ions indicating that this position is the origin of hydrogen atom lost to generate the $(M-1)^-$ ion. The NCI mass spectrum of 3, 3-dideuterated desmethyl diazepam (R=H), on the other hand, shows only $M^{\pm}$ and $(M-1)^-$ ions as does the mass spectra of 2', 3', 4', 5', 6' pentadeuterated desmethyl diazepam and 6, 8, 9 - trideuterated desmethyl diazepam. By elimination, we suggest that for desmethyl diazepam the hydrogen atom lost to generate the $(M-1)^-$ ion is that located on the amide nitrogen. The spectrum of desmethyl diazepam deuterated at the amide nitrogen, although complicated by exchange of the deuterium in the CI ion source, supports our suggestion.

1. W.A. Garland, B.H. Min, J. Chromatogr., 172, 279 (1979)

2. W.A. Garland, B.J. Miwa, Env. Health Persp., 36, 69 (1980)

3. B.J. Miwa, W.A. Garland, Anal. Chem., in press, April or May, 1981

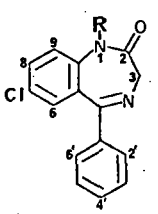

NEGATIVE ION MASS SPECTRA OF ALCOHOLS

J. M. Knox and A. B. Denison, Dept. of Physics and Astronomy
University of Wyoming, Laramie, WY 82071.*

Negative ion fragments from alcohols have been observed for both high energy (70eV) and low energy (2-20eV) impact electrons. In the lower energy range, several resonant dissociative attachment (DA) processes have been observed. Isopropanol and five isomers of n-nonanol were examined. The spectrometer used was a Bendix Model 14 Time-of-Flight which had been modified for increased negative ion sensitivity by adjusting the high voltage on the various plates of the detector (1). A digital data acquisition system was developed using a linear gate and stretcher as described by Seyse, et al. (2). For the electron impact energy calibration, the known (3) DA resonance of O^- from background oxygen was used. The data were treated with a 1-2-1 smoothing before the instrument function was removed using a deconvolution procedure similar to that of Christophorou, et al. (3).

Isopropanol

For isopropanol the mass spectra obtained at 70eV were in good general agreement with the previous published work (4). The ionization efficiency curves for O^- and OH^- were also in good agreement with the previous work. After deconvolution, resonant dissociative attachment processes were observed with maximum intensity at 8.65 ± .3 eV in OH^- and at 6.6 (calibration standard), 9.5 ± .2, and 11.3 ± .3 eV in O^-. As shown in Figure 1, there is an indication that the 11.3eV resonance may itself be split into two or three peaks with maxima at 10.8, 11.6, and 12.6eV.

The 6.6eV DA intensity was found to be essentially pressure independent, Figure 2 and was observable in the background gas. We have therefore assumed throughout this work that this peak always arises from background oxygen and have used it as the energy calibrant. This assumption was regularly checked by pressure studies. The other isopropanol resonance peaks were found to be linearly dependent on the sample pressure.

n-Nonanol

Negative ion mass spectra were obtained at 70eV for each of the five n-nonanol isomers. (See the table.) Several relatively intense peaks are seen to be common to all of the isomers studied: 16, 17, 20, 24-27, 35, 37, 41, 43, 141, and 143. Peaks that are less intense, but common to all the isomers, include 12-15, 18.5, and 32. Fragments in the mass range of 49-137 amu are not observed in all isomers and may be a useful tool in the identification of particular isomers.

Several fragments were observed to have DA resonances. Fragments at m/e = 1, 16, 17, and 141 are resonant in all isomers. The energy of the peak maxima are indicated in figures 3-6. These energies were not found to vary with OH position for the accuracy of our equipment. Other DA processes observed for particular isomers are given in the table below.

Additional Fragments

Molecule	Fragment (m/e)	DA Resonance Peak (eV)
3-nonanol	57	7.8 ± .4
4-nonanol	71	8.3 ± .1
	99	8.0 ± .1, 9.8 ± .2
5-nonanol	85	8.2 ± .4, 10.7 ± .5
	99	7.8 ± .9, 11.1 ± .8

(1) W. W. Hunt, et al., Rev. Sci. Inst., 36, 10 (1965).
(2) R. J. Seyse, et al., ibid., 44, 1673 (1973).
(3) L. G. Christophorou, et al., J. Phys. B4, 1163 (1971).
(4) S. Tsuda, et al., Bul. Chem. Soc. Japan, 42, 2514 (1969) and references therein.

*Work supported in part by Laramie ETC (DOE), Laramie, WY 82071

TABLE 1. Observed negative ion mass spectra for the five nonanol isomers. All intensities are given relative to the most intense peak at M/e = 16.

Molecule \ M/e	1	12	13	14	15	16	17	18	18.5	19	20	24	25	26	27.2	32	35	37	41
1-Nonanol	6.1	1.86	1.38	1.39	1.14	91.79	11.78	-	1.79	1.64	1.89	3.06	10.94	5.41	2.43	1.50	24.85	7.04	1.86
2-Nonanol	2.36	2.69	2.20	2.55	2.73	98.37	15.42	-	4.19	-	2.44	4.05	19.58	10.16	13.89	1.56	3.14	2.52	3.13
3-Nonanol	-	2.48	2.23	1.99	1.55	95.46	14.36	3.21	3.24	-	3.37	4.24	20.74	11.30	12.66	1.46	5.96	3.45	2.90
4-Nonanol	1.5	2.25	1.61	1.75	1.50	96.58	5.49	1.60	1.54	-	1.88	2.42	11.31	5.06	3.94	1.22	2.07	1.72	3.19
5-Nonanol	3.1	2.53	1.60	1.68	1.30	99.68	5.40	1.67	1.77	-	3.52	2.70	7.64	3.13	3.55	1.24	2.31	1.59	4.63

Molecule \ M/e	43	46	49	51.2	55	57	59	70	71	72	83	85	99	113	127	132	137	141	143
1-Nonanol	1.65	3.07	-	-	1.13	1.21	-	1.93	-	1.58	-	-	-	-	-	1.51	1.57	-	6.36
2-Nonanol	3.76	1.39	1.19	-	-	1.62	1.20	-	-	-	-	-	-	-	2.07	-	1.21	2.87	6.20
3-Nonanol	2.01	2.20	1.41	1.21	1.13	1.75	-	-	1.87	-	1.17	1.14	-	1.55	-	-	-	5.40	6.09
4-Nonanol	1.92	-	-	1.24	-	-	-	-	1.62	-	-	1.43	1.75	1.57	-	-	1.15	3.12	3.93
5-Nonanol	1.60	1.26	1.20	-	-	-	-	-	-	-	1.17	2.53	1.57	1.26	-	-	-	3.30	3.86

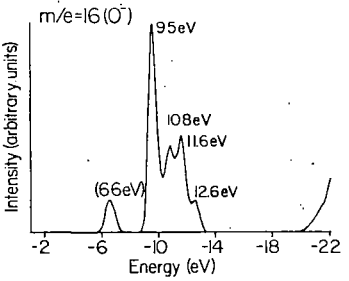

FIGURE 1

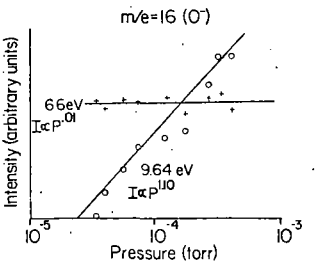

FIGURE 2

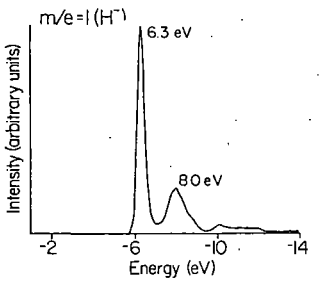

FIGURE 3

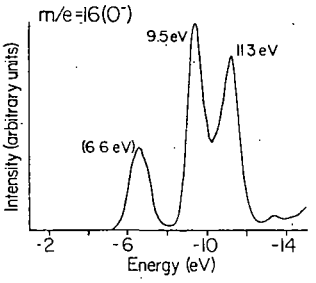

FIGURE 4

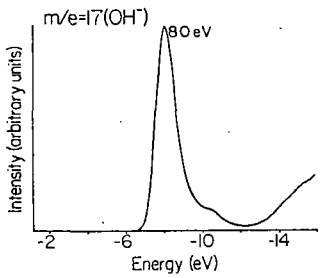

FIGURE 5

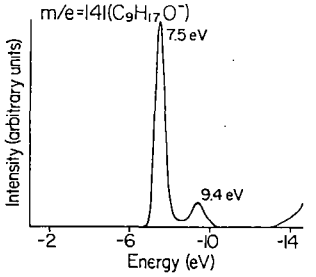

FIGURE 6

Evaluation of SEP-PAK C_{18} Cartridges for Biological Sample Clean-Up for Tricyclic Antidepressant Assays

N. Narasimhachari
Department of Psychiatry, Medical College of Virginia, Richmond VA 23298

Introduction

The extraction method is the most commonly used method for biological sample clean-up for the assay of tricyclic antidepressants and their metabolites. We have recently reported an extraction procedure for the quantitation of tricyclic antidepressants and metabolites using deuterated compounds as internal standards (1, 2). SEP-PAK cartridges (Waters Associates, Milford, Mass.) have recently been used for the clean-up of serum or plasma samples for nucleoside and warfarin analysis. We have now examined the use of C_{18} SEP-PAK cartridges for separating tricyclic antidepressants, their desmethyl metabolites and hydroxy metabolites from plasma, urine and saliva samples. We have evaluated the advantages specifically sample cleanliness, specificity, efficiency, reproducibility over the conventional extraction method.

Materials and Methods

All solvents are pesticide grade. Tricyclic antidepressant drugs were all obtained from pharmaceutical research laboratories as mentioned in a previous report [2]. d_4-Imipramine and desipramine were used as internal standards for all tricyclic drugs [2]. In addition dideuteromethyl amitriptyline and dideuteromethyl doxepin were prepared by reduction of N-formyl derivatives of nortriptyline and desmethyl doxepin using Li aluminum deuteride. C_{18} cartridges were purchased from Waters Associates.

Carbonate-bicarbonate buffer: A mixture of 5 g each of sodium carbonate and sodium bicarbonate were dissolved in 100 ml of water and stored in a refrigerator.

C_{18} SEP-PAK Clean Up Procedure: The cartridge is activated by passing 2 ml of methanol by pressurizing through a plastic or glass syringe followed by 2 ml of distilled water.

0.5 ml of sodium carbonate-bicarbonate buffer was added to the aqueous solution, or plasma solution, the mixture thoroughly mixed on a vortex mixer, and passed through the cartridge via the syringe at a flow rate not greater than 5 ml/min. followed by one milliliter of washings from the sample tube. The cartridge was then washed by passing 2 x 2 ml of distilled water.

Ten milliliters of solvent mixture, hexane and isopropanol (9:1) were passed through the cartridge and the eluate collected in a 15 ml glass stoppered centrifuge tube. The eluate consisted of 0.4 ml of aqueous layer from the void volume of the cartridge, and was drawn off and discarded. The organic layer was evaporated under a current of nitrogen, the residue derivatized to trifluoroacetyl derivative using N-methyl-trifluoroacetamide according to the method described in an earlier report [2].

Gas chromatographic-mass spectrometry: The GC and GC-MS-SIM conditions for quantitation of all tricyclic antidepressant drugs were described in detail [2]. All quantitations were carried out using the EI mode with ionization potential 70 ev, source temperature 260°, separator temperature 250°C. In all cases in these initial evaluation studies, the complete mass spectra of the drug peaks were obtained from plasma and urine samples in order to ascertain the sample cleanliness.

Results

Column efficiency: The extraction efficiency of added standards was over 90% and more consistent than extraction method. The calibration curves were linear and similar to those reported by extraction method [2].

Final Sample Cleanliness: As illustrative examples, a few of the mass spectra obtained from patient plasma and urine samples processed through the SEP-PAK cartridges are given in Fig. 1 and 2. In over 20 samples that we have so far processed by this method under the GC-MS conditions we have used, the spectra indicated that the sample peaks were clean and contained only the drug or the drug and internal standard. The samples were at least as clean as those obtained by the conventional extraction method we have been using in our laboratories. The SIM recording for desipramine assay is shown in Fig. 3. Parellel determinations of clinical

samples (20) were carried out for all tricyclic drugs by the two methods, one using the SEP-PAK and the second by extraction method. The results are in good agreement.

Conclusions

The saving in time for the analysis using SEP-PAK cartridges is the most important favourable factor for this method. The three step extraction method involves shaking, centrifuging, withdrawal of solvent or aqueous layers, in all the three steps. In parallel experiments we found that 8 samples and two standards could be readied for GC-MS analysis in 40 minutes, while the conventional extraction methods took 150 minutes. Another advantage in the SEP-PAK cartridge is that the organic layer is quantitatively recoverable, while in extraction method, only a fraction is recoverable, and sometimes losses are high due to emulsification.

References

1. N. Narasimhachari and R. O. Friedel, Res. Comm. Psych. Psych. Beh., 4, 477 (1979).

2. N. Narasimhachari and R. O. Friedel, Federation Proceedings 30, 209 (1980).

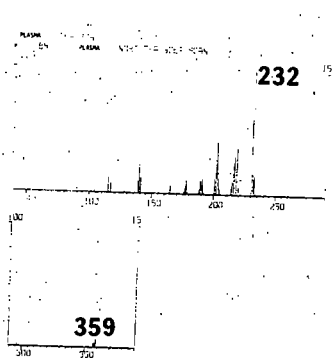

Fig. 1

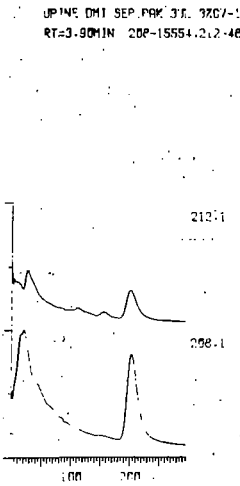

Fig. 3

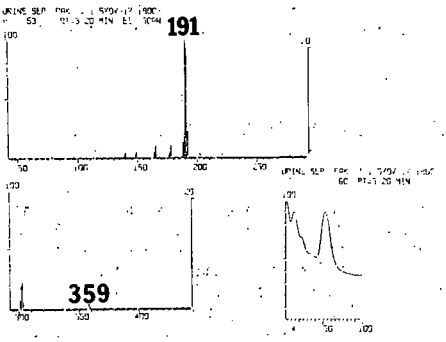

Fig. 2

Fast Atom Bombardment Mass Spectrometry

by

M. Barber, R.S. Bordoli, R.D. Sedgwick and A.N. Tyler,

U.M.I.S.T. Chemistry Department, Sackville St. Manchester. M60 1QD

England.

The technique of fast atom bombardment, as a means of inducing sputtering of large organic molecules from the solid, has been developed at U.M.I.S.T. over the last four years.[1,2] The use of neutral species as the sputtering medium has two major advantages; ease of introduction of the beam into the high voltage region of large magnetic instruments, and a diminution in the charging effect associated with ion bombardment of insulators.

The techniques of producing beams of fast neutral particles (1-10 KeV and typically rare gases) are well known. Indeed, any high pressure discharge ion source will produce a considerable yield of fast rare gas atoms. This occurs by resonant charge exchange to produce atoms with essentially the same kinetic energy as the original ions. In the original work the ion source of an MS902 was modified to accept the fast atom beam and samples mounted on a stage which was inserted to intercept the beam th rough an axially mounted vacuum lock. We have recently modified, in a similar way, the ion source of the V.G. ZAB for this purpose. The characteristics of this ion source are,

(i) production of high intensity pseudomolecular ions of the form $(M+X)^+$ or $(M-X)^-$ where X is either a proton or some suitable cation,

(ii) structurally significant fragmentation and metastable information,

(iii) sufficient sensitivity to deal with sub nanomole quantities of materials.

Originally the sample lifetime was low. However, we have developed methods of prolonging the lifetime (tens of minutes to hours) by the use of suitable viscous, low vapour pressure sample substrates, e.g. dissolution of the sample in glycerol, and by heating the stage, to provide surface mobility and "healing" properties. The quality of the results obtained is demonstrated by the accompanying mass spectrum of the co-enzyme of Vit. B_{12} shown in the figure. We have applied this technique to many classes of compounds, and the versatility of the method is shown by the following brief list of materials successfully analysed:

oligosaccharides, peptide antibiotics, glycopeptides, penicillins and cephalosporins (both free and as their salts) glycoside antibiotics (both free and as salts), oligo peptides (maximum so far 26 amino acids) glycolipids, oligo nucleotides, neurotoxins, metal bearing compounds of biological importance, e.g. VIT B_{12}, siderophores, etc., and a range of organo metallic salts.
We now intend to extend the application of this ion source to encompass on-line L.C.M.S.

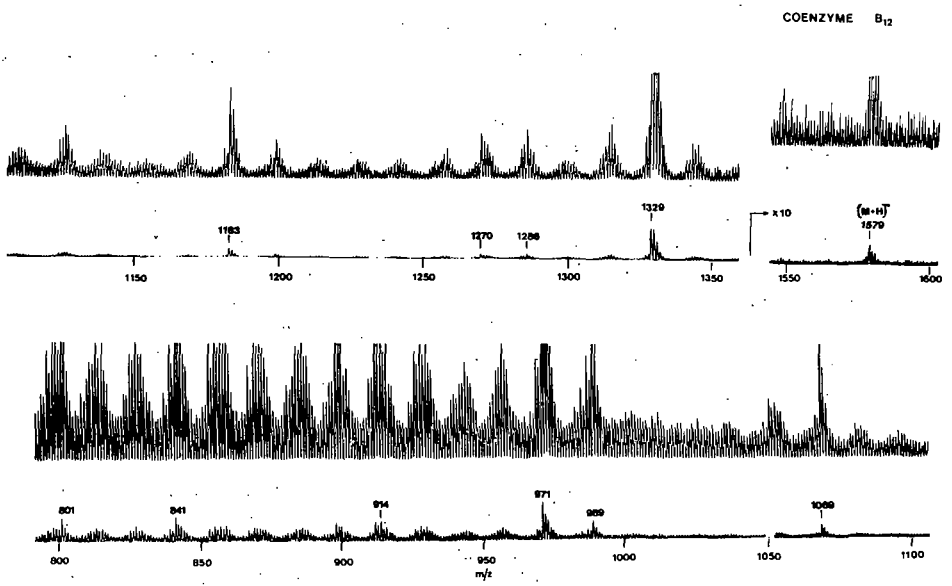

1. M. Barber, R.S. Bordoli, R.D. Sedgwick and A.N. Tyler, J.C.S. Chem. Comm., 325, 1981.
2. D. Surman and J.C. Vickerman, J.C.S. Chem. Comm., 324, 1981.

DEVELOPMENT OF THE FAST ATOM BOMBARDMENT SOURCE, L.C.E. Taylor, S. Evans, H.J.M. Fitches, K.R. Compson, Kratos Limited, Manchester, England.

The fast atom bombardment source pioneered by Barber et al has its origins in secondary ion mass spectrometry. The advantages of a fast atom beam as opposed to a charged particle beam are obvious when used in conjunction with a high voltage double focussing mass spectrometer. The problems associated with steering a charged primary beam are eliminated when a neutral beam is employed to bombard the target sample. Consequently no special problems are encountered when operating the mass spectrometer in negative ion mode.

As with SIMS techniques the sample material is supported on a target stage, conveniently this may be of copper although other metals may be used e.g. silver, gold.

Sample preparation is an essential requirement for SIMS and FAB spectrometry, both of which are subject to sample "fading" effects. However, the use of a suitable liquid support medium of low vapour pressure has been found to prevent the sample fading phenomenon. The use of glycerol has been very effective for many sample materials although this is by no means general and liquids such as tetragol and poly glycol ethers have been used successfully in cases where glycerol is unsuitable.

In conjunction with the MS50 high resolution mass spectrometer the FAB source has proven very effective in obtaining mass spectral information on many compounds previously not emenable to conventional ionization techniques. This includes not only high molecular weight involatile thermally labile compounds such as peptides but in addition low molecular weight organic sulphate and sugar containing samples. The spectra observed generally produce an extensive amount of structurally significant fragments including second field free region metastables. The use of FAB is not restricted to high voltage instruments and can be used very effectively on lower voltage instruments such as the MS80.

The properties of the source may best be described by reference to one particular compound, in this case cyanocobalamin (vitamin B_{12}). This material runs easily by FAB, and is typical of the average sensitivity that can be obtained. Many samples give better intensity (up to 10^2) depending upon the polarity of functional groups within a particular molecule. Generally compounds which are good proton donors or acceptors will give the most intense spectra.

The samples of B_{12} were loaded into a matrix of glycerol acidified with dil HCl. Typical sample quantity was 10-20µg of B_{12}.

The use of an acid medium was found to enhance the intensity of the $(M + H)^+$ ion. The general appearance of the low resolution positive and negative ion spectra is shown in Figs 1 and 2 respectively. It can be seen that the observation of a peak at every nominal mass value is characteristic of FAB mass spectra in both detection modes. In both these spectra the most intense peak corresponds to the loss of CN viz: 1329 is $(M + H - CN)^+$ and 1328 is $(M-CN)^-$. In both cases the spectra contain significant fragment ion peaks, for example, the m/z 1270 peak due to the loss of acetamide from the $(M + H - CN)^+$ species. This has been reported in the FD spectrum by B_{12} by Schulten. The 1183 peak corresponds to the loss of the 5,6-Dimethylbenzimidazolyl group attached to the central Co ion. The positive LRP spectrum has a metastable at 1053 due to this process. The loss of the 5,6-Dimethylbenzimidazolyl and the attached sugar group is indicated at m/z 1069.

Mass measurement at LRP by peak matching of the 1329 peak using Ultramark 1621 as a reference gave a 2.6 ppm error for the $(M + H - CN)^+$ species, however, at high resolution the $(M + H)^+$ was measured to 0.3 ppm.

The quality of spectra and ion intensity allows low resolution data acquisition using pre-calibration from the usual fluorocarbon reference materials. Examples are shown in Figs 1 and 2 for a scan rate of 30 sec/decade although faster scans are possible, but not necessary due to prolonged sample lifetime.

One feature of the B_{12} spectrum is the fast decay of the $(M + H)^+$ adduct ion compared to the duration of the rest of the spectrum peaks, which are detected for periods in excess of 30 minutes. This would appear due to reduction of the B_{12} to an oxidation state of +2 with the loss of the cyanide group. Collision induced decomposition has been used to obtain a B/E spectrum from m/z 1329, indicating the fragment ions arising from the $(M + H - CN)^+$ ion.

The maximum usable resolution is limited only by sensitivity. In the case of B_{12}, we have been able to obtain acceptable signal to noise at about 40,000 resolution, whereas for the major peaks of triazine, in excess of 80,000 has been obtained.

The ability to operate at high resolution is valuable as this permits more accurate mass measurements to be obtained.

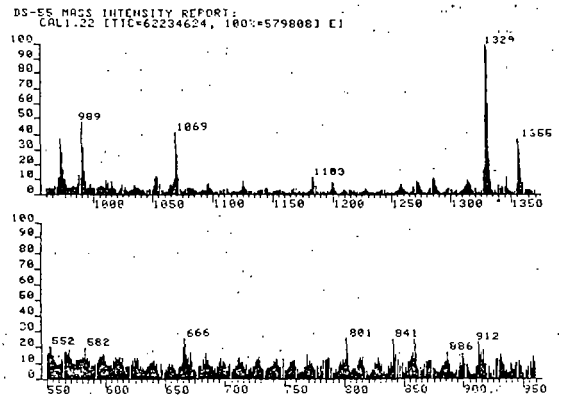

Figure (1) MS50/DS55: FAB SPECTRUM OF B_{12} (POSITIVE IONS)

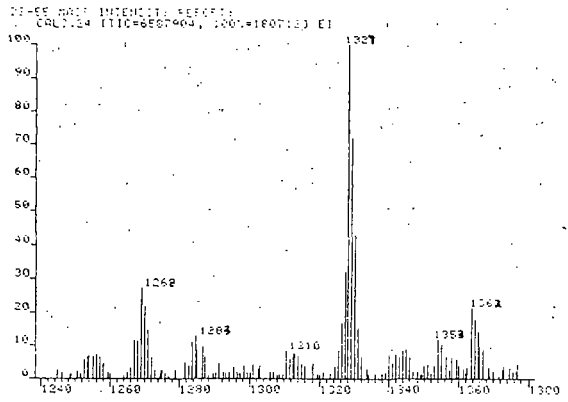

Figure (2) MS50/DS55: FAB SPECTRUM OF B_{12} (NEGATIVE IONS)

CONVERSION TO FAST ATOM BOMBARDMENT AND ITS APPLICATION

R.A. McDowell, A. Dell and H.R. Morris
Department of Biochemistry, Imperial College, London , U.K.
T. Redfern
M-Scan Ltd, 5 The Ridgeway, Iver, Bucks, U.K.

Following the announcement of Fast Atom Bombardment by Barber, Sedgwick, Bordoli and Tyler (1) we have developed a number of FAB systems for use on ZAB, MS 50 and MS 902 mass spectrometers. We investigated the performance characteristics of a number of ion producing sources and chose to assess the Townsend discharge and the saddle-field guns for our mass spectrometric purposes.

The saddle-field gun was originally used by Barber and co-workers and is currently fitted to commercial systems being marketed by Kratos and VG Analytical. This gun (2) is a cold cathode device and has a unique electrostatic saddle-field configuration. The basic source has been modified by the manufacturers and is marketed as a fast atom source. The performance specification of this type of source has been reported (3) and it should be noted that the supply current is much higher than the output beam i.e. there is low electrical efficiency in beam production and considerable heat generation.

The alternative type of ion source assessed in our FAB studies is a commercially available Townsend discharge source which is marketed (4) as an ion source with a small percentage of inherent neutrals in the output beam. The beam obtained from the Townsend discharge source increases with increased throughput of gas and/or increased applied voltage. This is accompanied by an increase in the gas utilisation efficiency. For a fixed operating voltage - and thus beam energy - the transmitted beam can therefore be controlled by the gas flow. Electrical efficiency is around 98% i.e. supply current is approximately equal to the beam current and no noticeable heat is produced.

A convenient power supply arrangement to make use of the above features of the Townsend gun includes a fixed high voltage power supply to operate the gun efficiently and another supply which sets the chosen beam energy.

The Townsend discharge gun is physically small and lends itself to installation inside the source housing. This maximises the beam flux bombarding the sample and, combined with minimal heat generation, allows the utilisation of a variety of mountings. For these reasons we have concentrated our efforts on the design of FAB systems incorporating the Townsend discharge source rather than the saddle-field source.

The gun has been mounted on a probe suitable for direct insertion into the mass spectrometer source and we have also studied methods of introducing the gun via the variety of inlet ports on our mass spectrometers.

On the ZAB mass spectrometer we have used the standard FD source with minor modifications to the source optics. On the MS 902 and MS 50 instruments we have used a simple two plate focussing system. The sample target is of ribbon form and can be heated if required.

We conclude from our investigation of guns and power supplies that it is possible to modify the existing commercial systems to produce sources which are better suited to mass spectrometric requirements. In particular we have built several discharge sources of various lengths and diameters for different applications.

We are using our new FAB systems in our continuing investigations of important biological substances and have examined a variety of compounds including peptides, antibiotics and high mass underivatised oligosaccharides. We now report some of our data on the bleomycin family of antibiotics, molecules which are particularly intractable to structural analysis because of their complexity and polarity. In an earlier publication (5) we have reported that excellent FD data can be obtained on these substances provided appropriate emitters and sample handling procedures are used. However, considerable skill is required if good spectra are to be reproducibly obtained in the FD mode. In contrast, FAB mass spectrometry yields data on these molecules with comparative ease. We have examined various bleomycins and their derivatives and have selected two examples

to illustrate key points.

Figure 1 shows the molecular ion region of demethylbleomycin A_2 run using two FAB systems (a) the Townsend discharge source mounted on the VG ZAB mass spectrometer and (b) the commercial Kratos FAB source on the MS 50 instrument. Note that the spectra are identical (the slight difference in appearance is due to different scan speeds; the spectra were traced directly from the oscillograph paper), the major species being the pseudomolecular ion at m/z 1400 and a fragment ion at m/z 1298.

(a) (b)

Fig.(1) FAB MS of demethylbleomycin A_2 obtained using (a) the M-Scan FAB system mounted on the VG ZAB and (b) the Kratos MS 50 FAB system

Figure 2 shows comparative FD/FAB data on copper-Blenoxane. We note two points of interest; firstly FAB yields both $M^{+\cdot}$ and $(M+H)^+$ ions while FD gives only $M^{+\cdot}$, and secondly the major fragment ions observed in FD are not found in FAB spectra.

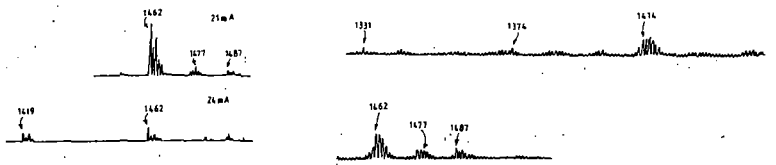

(a) (b)

Fig.(2) (a) FD spectrum of Cu-Blenoxane obtained on the Kratos MS 50
(b) FAB spectrum of Cu-Blenoxane obtained on the M-Scan FAB system

In conclusion, the FAB systems which we have developed are suitable for all types of mass spectrometers and the design allows coupling with alternative sample introduction devices such as a moving belt interface. In addition the MS 50 and MS 902 FD sources can be used for FAB without major conversion, by incorporating the gun and sample target on the same insertion probe.

(1) Barber M., Bordoli R.S., Sedgwick R.D. and Tyler A.N. (1981) Chem. Commun., 325-327.
(2) Ion-Tech Ltd, 2 Park St., Teddington, Middlesex U.K.
(3) Franks J. and Ghander A.M. (1974) Vacuum, 24, 489-491.
(4) Oxford Applied Research Ltd., Crawley Mill, Witney, Oxfordshire. U.K.
(5) Dell A., Morris H.R. Hecht S. and Levin M.D. (1980) Biochem.Biophys.Res.Commun., 97, 987-994.

FAST ATOM BOMBARDMENT/SECONDARY ION QUADRUPOLE MASS SPECTROMETRY

Donald F. Hunt and William M. Bone
Department of Chemistry
University of Virginia
Charlottesville, Virginia 22901

Fast Atom Bombardment/Secondary Ion Mass Spectrometry, FAB/SIMS, is carried out on nonvolatile and/or thermally labile organic molecules such as salts, polypeptides and nucleotides to yield intense $(M+H)^+$ or $(M-H)^-$ ions. The sample is prepared by dissolving the solid in glycerol and applying the matrix to a copper tipped solids probe. Bombardment of this matrix by Argon or Xenon ions or neutrals of >3KV energy affords a mass spectrum with fragments characteristic of the sample structure in addition to abundant ions characteristic of sample molecular weight. Addition of oxalic acid to the sample matrix produces up to a 10-fold increase in $(M+H)^+$ ion current depending on the sample. Table 1 illustrates the effect of adding oxalic acid to the sample matrix as well as using argon or xenon ions or neutrals as the primary beam. The addition of oxalic acid to the matrix has a greater effect on the $(M+H)^+$ ion current when an ion beam rather than a neutral beam is employed.

Xenon, being a heavier gas, has a greater sputter yield than argon at a given energy. Neutral beams produce little or no charging of the matrix.

Table 2 illustrates how the $(M+H)^+$ ion current varies with temperature. The experiments are explained in terms of the viscosity of glycerol as a function of temperature. At low temperatures, <20°C, the glycerol flows very slowly and cannot "renew" the surface presented to the primary atom beam and the $(M+H)^+$ ion current is minimal. As the probe is slowly heated and the viscosity of the glycerol decreases it begins to flow and can continuously rejuvenate the surface presented to the primary beam. At temperatures >40°C the vapor pressure of the glycerol increases enough to produce an increase in the analyzer pressure. The glycerol quickly evaporates from the probe tip and the sample surface cannot be "renewed" as shown by a dramatic decrease and then disappearance of the $(M+H)^+$ ion current. The optimum viscosity for the glycerol to efficiently renew the sample surface occurs at about room temperature. At room temperature the vapor pressure is low enough to allow the sample to be continuously monitored for longer than 30 min. in most cases.

The detection limit for our FAB/SIMS system appears to be in the low monogram range. To date full spectra have been obtained on 10ng of sample.

FAB/SIMS/MS on a Finnigan Triple State Quadrupole, TSQ, mass spectrometer were performed on an oligopeptide sample. The $(M+H)^+$ ions undergo CAD in Q2 to yield unambiguous sequence information on each peptides present in a mixture. In addition the CAD process can be used to generate useful structural information on relatively pure samples.

At the 28th ASMS conference in New York, May, 1980 we described how the Finnigan moving belt LC-Interface had been modified to pass through the ion source of a Finnigan 4000 for Laser Desorption studies. We have now used this system to continuously introduce samples into the ion source for FAB/SIMS analysis. Spectra of AMP-Na^+ salt and angiotensin heptapeptide were obtained and are representative of FAB spectra from samples off the LC-interface moving belt.

Negative Ion FAB spectra have been obtained from the trinucleotide Guanylyl (3'-5') Cytidylyl (3'-5') Uridine and the dinucleotide shown in Figure 1. Both examples yield intense $(M-H)^-$ and $(M-2H+Na)^-$ ions in addition to useful fragment ions.

In summary, Fast Atom Bombardment Quadrupole Mass Spectrometry is extremely useful for the analysis of fragile organic compounds and can easily be accommodated for TSQ CAD studies in addition to the FAB desorption of samples off a modified LC-interface.

Ar vs Xe as PRIMARY BEAM GAS

RIC for (M+1) ION	Ar^+	Xe^+	Ar^o	Xe^o
NO ACID	1	3	12	36
WITH ACID	6	30	24	60
SAMPLE: MET-ARG-PHE-ALA acetate				

Table 1.

FAB Se EFFECT of HEATING SAMPLE

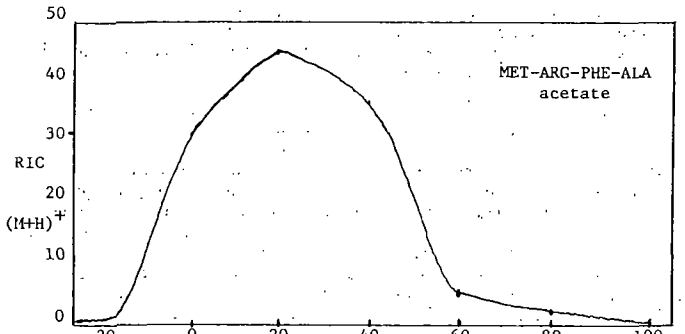

Table 2.

NI-FAB SPECTRUM- MW. 976

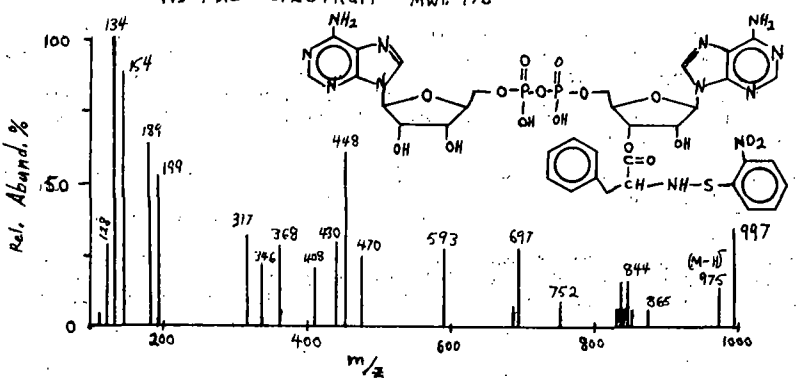

Fig. 1

Fast Atom Bombardment (FAB); A New Method of Studying Intractable Antibiotics.

by

M. Barber, R.S. Bordoli, R.D. Sedgwick and A.N. Tyler,
Chemistry Department, U.M.I.S.T., Manchester. M60 1QD
England

Development of the fast atom bombardment (FAB) ion source began at UMIST in 1974, and reached fruition in 1979. We initiated the techniques of using liquid sample supports, or heating to melt the sample in vacuo, to prolong the lifetime of the spectra, facilitate the use of metastable scanning techniques and increase the sensitivity. For the past two years we have routinely used the source to obtain mass spectra from a wide variety of previously intractable molecules (1).

Among the more intractable species we have studied are the glycopeptide antibiotics. In this communication results are presented for vancomycin and the bleomycins. These complex antibiotics are produced by various streptomyces and have received considerable attention as therapeutic agents. It is known that the bleomycins differ from one another only in the structure of the terminal amine unit, however with the absence of accurate molecular weight data the structural elucidation of the glycopeptide skeleton was complicated.

What is now accepted to be the correct structure was finally deduced following PDMS studies on bleomycin B_1, and subsequently confirmed by NMR and XRD data from other bleomycins and related compounds. Recently FD has been applied to bleomycin B_2 and the related phleomycins D_1 and E. (2)

Bleomycin A_2 and the clinical mixture comprising mainly A_2 and B_2 were obtained from Lundbeck. 1μg of sample was deposited on to the sample stage with 10μL of glycerol as a liquid support medium and analysed by a Vacuum Generator ZAB reverse geometry mass spectrometer fitted with a prototype FAB source. All analyses were carried out at ambient temperature.

For the clinical mixture a protonated molecular species $(M+H)^+$ is observed at m/z 1425 and the sulphonium cation of A_2 at m/z 1414 in accord with the proposed structures of the components. Additionally an ion is observed at m/z 1512 corresponding to an $(M+H)^+$ for the A_2 sulphate. A significant ion at m/z 1400 was initially thought to be the $(M+H)^+$ for demethyl A_2 since it is known that A_2 in common with other sulphonium ions of this type will readily demethylate.

Chromotographic data obtained from the A_2/B_2 mixture and pure

A_2 indicate that m/z 1400 is too large to be an $(M+H)^+$ for demethyl A_2 and the origin of this ion is thought therefore to be a fragment, probably from a sulphate containing ion.

The spectrum from pure A_2 contains structurally significant fragment ions in addition to the ions at m/z 1414 and 1512. It appears that the fragmentation originates from m/z 1400 from which the terminal sugar and amino acid residue are lost.

The bleomycins complex with various metal ions and in this form has been suggested as the active cytotoxin. It is thought that the ferrous complex is an oxygen carrier which effects oxidative degradation of DNA. The FAB spectrum of the ferrous complex of bleomycin A_2 conforms with the proposed structure.

The broad spectrum antibiotic Vancomycin (3) has also been studied by FAB and the high mass region of the positive ion spectrum is shown in the figure. An intense psuedomolecular ion $(M+H)^+$ is observed at m/z 1448 which shows the dichloro isotopic pattern. The peaks marked X are thought to be indicative of the presence of a previously unknown dechloro species of which m/z 1414 is the psuedomolecular ion $(M+H)^+$.

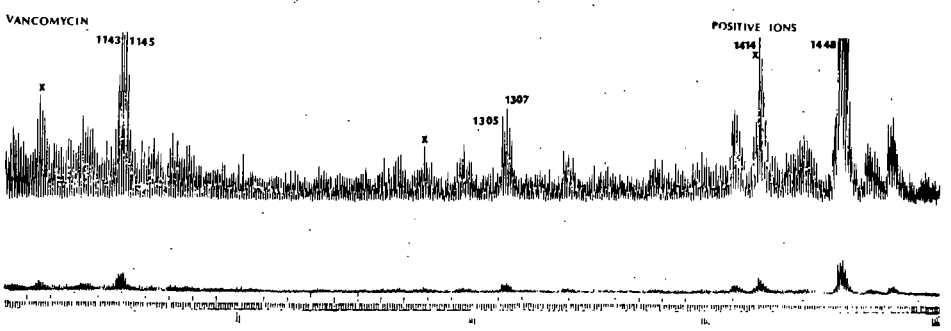

1. M. Barber, R.S. Bordoli, R.D. Sedgwick and A.N. Tyler, J.C.S. Chem. Comm., 325 (1981).
2. A.Dell, H.R. Morris, S.M. Height and M.D. Levin, Biochem. Biophys. Res. Comm., 97, 987 (1980).
3. G.M. Sheldrick, P.G. Jones, O. Kennard, D.H. Williams and G.A. Smith, Nature, 271, (1978).

PEPTAIBOPHOL ANTIBIOTICS STUDIED BY FAST ATOM BOMBARDMENT MASS SPECTROMETRY

K. L. Rinehart, Jr., L. A. Gaudioso, M. L. Moore, J. C. Cook, Jr.
School of Chemical Sciences, University of Illinois, Urbana, IL 61801

M. Barber, R. S. Bordoli, R. D. Sedgwick, A. N. Tyler
University of Manchester, Institute of Science and Technology, U.K.

B. N. Green
VG Analytical, Ltd., Altrincham, U.K.

We have previously studied the peptaibophol antibiotics (which are characterized by their membrane pore-forming activity) by a combination of HRFDMS, HREIMS, and GC/HRMS.[1] The zervamicins, which belong to this class, contain tryptophan and threonine and are not amenable to some of the above techniques. We have now investigated the peptaibophols by fast atom bombardment mass spectrometry (FABMS),[2] employing a prototype FAB source on a VG FAB 2F mass spectrometer. FAB mass spectra provide three types of information for the zervamicins which assign much of their structural detail even in the absence of other information: a) molecular weights assigned by M + H and M - H peaks in the positive and negative ion modes; b) peaks characteristic of the amino acids at low masses (e.g., m/z 58, 70, 72, 86, and 130 for Aib, Pro, Val or Iva, Leu or Ile or Hyp, and Trp), and c) very clear sequence peaks for CO-N peptide cleavages (*Scheme I*).

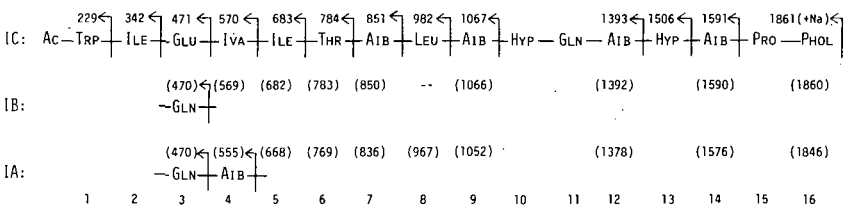

SCHEME I. FABMS FRAGMENT IONS OBSERVED FOR ZERVAMICIN IC, WITH AMINO ACID REPLACEMENTS AND KEY FRAGMENT IONS FOR ZERVAMICINS IIA AND IIB.

FABMS spectra are quite characteristic of the structures of the previously assigned peptaibophols such as antiamoebin I and alamethicin, and FABMS (together with FDMS and GC/MS information) has now been used to assign sequences to the peptaibophol antibiotics zervamicins IA, IB, IB', IC (all acidic), IIA, IIB, II-1, II-2, II-3, II-4, and II-5 (all neutral) and to establish the identity of emerimicins IIA and IIB with zervamicins IIA and IIB.

ZIA: Ac-Trp-Ile-Glu-Iva-Val-Thr-Aib-Leu-Aib-Hyp-Gln-Aib-Hyp-Aib-Pro-Phol

ZIB: Ac-Trp-Val-Glu-Iva-Ile-Thr-Aib-Leu-Aib-Hyp-Gln-Aib-Hyp-Aib-Pro-Phol

ZIB': Ac-Trp-Ile-Glu-Aib-Ile-Thr-Aib-Leu-Aib-Hyp-Gln-Aib-Hyp-Aib-Pro-Phol

ZIC: Ac-Trp-Ile-Glu-Iva-Ile-Thr-Aib-Leu-Aib-Hyp-Gln-Aib-Hyp-Aib-Pro-Phol

ZIIA: Ac-Trp-Ile-Gln-Aib-Ile-Thr-Aib-Leu-Aib-Hyp-Gln-Aib-Hyp-Aib-Pro-Phol

ZIIB: Ac-Trp-Ile-Gln-Iva-Ile-Thr-Aib-Leu-Aib-Hyp-Gln-Aib-Hyp-Aib-Pro-Phol

ZII-1: Ac-Trp-Ile-Gln-Aib-Val-Thr-Aib-Leu-Aib-Hyp-Gln-Aib-Hyp-Aib-Pro-Phol

ZII-2: Ac-Trp-Ile-Gln-Aib-Ile-Thr-Aib-Val-Aib-Hyp-Gln-Aib-Hyp-Aib-Pro-Phol

ZII-3: Ac-Trp-Val-Gln-Aib-Ile-Thr-Aib-Leu-Aib-Hyp-Gln-Aib-Hyp-Aib-Pro-Phol

ZII-4: Ac-Trp-Ile-Gln-Iva-Val-Thr-Aib-Leu-Aib-Hyp-Gln-Aib-Hyp-Aib-Pro-Phol

ZII-5: Ac-Trp-Ile-Gln-Iva-Ile-Thr-Aib-Val-Aib-Hyp-Gln-Aib-Hyp-Aib-Pro-Phol

Aib, α-aminoisobutyric acid; Phol, phenylalinol; Ac, acetate

(1) K. L. Rinehart, Jr., R. C. Pandey, M. L. Moore, S. R. Tarbox, C. R. Snelling, J. C. Cook, Jr., and R. H. Milberg, "Peptides. Structure and Biological Function," Proc. 6th American Peptide Symposium, E. Gross and J. Meienhofer, Eds., Pierce Chemical Co., Rockford, IL, 1979; pp 59-71.

(2) M. Barber, R. S. Bordoli, R. D. Sedgwick, and A. N. Tyler, J. Chem. Soc., Chem. Commun., 235-236 (1981).

Fast Atom Bombardment (FAB) MS of Glycoalkaloids

L.C.E. Taylor and S. Evans, Kratos Ltd., Manchester, UK., and R. Self and D.T. Coxon, Food Research Institute, Colney Lane, Norwich, UK.

Glycoalkaloids are naturally occurring compounds found in many plants in the family Solanaceae. The compounds, which are highly polar and involatile, contain an oligosaccharide unit linked to a steroidal alkaloid via a glycosidic bond. Only D-glucose, D-galactose, D-xylose and L-rhamnose commonly occur in the sugar moeity but mono-, di-, tri- and tetra-saccharides in both linear and branched units are all found, and a variety of aglycones occur in different plant species. Hence a great many different glycoalkaloid structures are possible. Classical identification of glycoalkaloids has depended on determining the aglycone and oligosaccharide structures separately after hydrolysis. Permethylation of intact glycoalkaoids enables molecular weights to be determined from EI spectra but the fragmentation is mainly associated with the aglycone.

FAB mass spectrometry, which is a new technique for obtaining spectra on polar and involatile compounds has been evaluated as a method for the structure elucidation of underivatised glycoalkaloids. FAB mass spectra are now reported on a series of five glycoalkaloids including di-, tri-, and tetra-saccharides representing three aglycone types. The compounds studied were α-solanine (glucosyl-(rhamnosyl)-galactosyl-solanidine), α-chaconine (rhamnosyl-(rhamnosyl)-glucosyl-solanidine), β-chaconine (rhamnosyl-glucosyl-solanidine), β-solamarine (rhamnosyl-(rhamnosyl)-glucosyl-tomatidenol) and α-tomatine (xylosyl-(glucosyl)-glucosyl-galactosyl-tomatidine). All the spectra gave intense $(M+H)^+$ ions and all showed a consistent pattern of fragmentation which allowed identification of the respective sugar residues (as hexose, rhamnose or xylose) and the aglycones. Fragment ions with masses which could correspond to a cleavage on either side of each glycosidic bond were observed. Each ion (R^+) corresponding to apparent glycosidic cleavage on the side nearest the aglycone has associated with it an ion which was 46 mass units heavier. This may be a J type ion[1] $R\text{-}\overset{+}{O}\text{=CH-OH}$ which would be a likely precursor of the ion R^+.

Thus for example the major ions occurring in the spectrum of α-tomatine can be rationalised as follows m/z 1034 (M+H), 1016 (M+H-18), 930 (884+46, J ion derived from xylose), 900 (M-Xyl and/or J ion derived from glucose, 854+46), 884 (M-XylO), 870 (M-Glu), 854 (M-Glu-O), 706 (M-XylO-GluO+H), 704 (M-XylO-GluO-H), 606 (560+46, J ion derived from glucose), 576 (M-XylO-GluO-Glu), 560 (M-XylO-GluO-GluO), 444 (398+46, J ion derived from galactose), 414 (M-XylO-GluO-GluO-Gal), 398 (M-XylO-GluO-GluO-GalO).

The M+1 ion and the aglycone derived ion at m/z 398 are major peaks in the spectrum and apart from the ions listed above which often have corresponding ions at 2 mass units higher or lower there are very few others present in the spectrum. The application of FAB mass spectrometry to glycoalkaloids provides spectra, with intense M+1 ions, and a simple fragmentation pattern which can be readily interpreted to provide detailed structural information without the need for derivatisation.

Reference

1. N.K. Kochetkov and O.S. Chizhov, Adv. Carbohydrate Chem. (1966) 21, 39-93.

STRUCTURAL STUDIES OF CEPHALOSPRINS USING A FAST ATOM BOMBARDMENT SOURCE:

V. C. PARR, B. N. Green, R. H. Bateman, J. C. Bill.
V. G. Analytical Limited, Tudor Road, Altrincham, Cheshire WA14 5RZ England.

The Fast Atom Bombardment (FAB) source[1] has provided a method of ionization for samples which were previously inaccessible to mass spectrometry, and the spectra thus produced yield valuable information both on molecular weights and in structural studies. In order to evaluate the study of ions produced by FAB in the MIKES (Mass analysed Ion Kinetic Energy Spectrometry) experiment, a Micromass ZAB2F mass spectrometer was used to examine two structurally related cephalosporins (cephalexin and cephaloglycin).

Fig. 1 is an example of a FAB spectrum of one of the cephalosporins, cephaloglycin, and typifies the positive ion spectra produced from both samples. This spectrum contains a protonated molecular ion and a protonated dimeric species, as well as structurally significant ions at m/z106 and m/z158. The acetylated sample, cephaloglycin, shows similar fragmentation plus the loss of a molecule of acetic acid from the protonated molecular ion; this is absent from the spectrum of cephalexin.

The negative ion mass spectra show ions arising from decarboxylation, and significant structural ions due to cleavage across the ring system. There is a marked increase in fragmentation in the negative ion mode. As with the positive ion spectra, the difference between the two negative ion spectra is a result of the acetylated portion of the cephaloglycin molecule, the base peak of the negative ion spectrum of cephaloglycin being m/z 59.

Fig. 2 outlines the postulated structures of ions resulting from the major fragmentation processes for the cephalexin molecule in both positive and negative ion modes. Accurate mass determinations by peak matching at a resolution of 10,000 confirmed the elemental compositions of some of the structurally significant ions.

The stable ion currents resulting from FAB are of sufficient intensity to enable MIKES scans to be carried out on the (M+H)+ and (M-H)- ions of the two cephalosporins in both positive and negative ion detection modes, and fragmentation pathways from the pseudo-molecular ion spectra may be determined from the results. In the case of the cephalexin molecule, major transitions occur from m/z 348 to give m/z 191, m/z158, m/z 174 and m/z 106 (Fig. 3). This is in marked contrast to the normal spectrum, which does not exhibit a significant ion at m/z 191. The MIKES spectrum of the pseudo-molecular ion of cephaloglycin results in only one major peak, that due to the loss of the acetic acid molecule; however, the MIKES spectrum of this ion, m/z346, is almost identical with that of the pseudo-molecular ion of cephalexin.

The use of MIKES, therefore, on ions produced from a Fast Atom Bombardment source has proved to be of considerable assistance in the confirmation of fragmentation pathways, and is applicable to both positive and negative ions; the technique has obvious use in structure elucidation.

1. Barber M., Bordoli R.S., Sedgwick R. D. and Tyler, A. N., JCS Chem. Comms. 325 (1981)

Fig.1

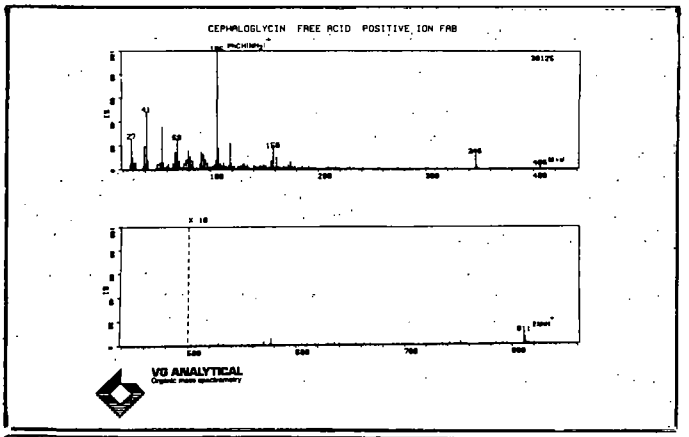

Fig. 2

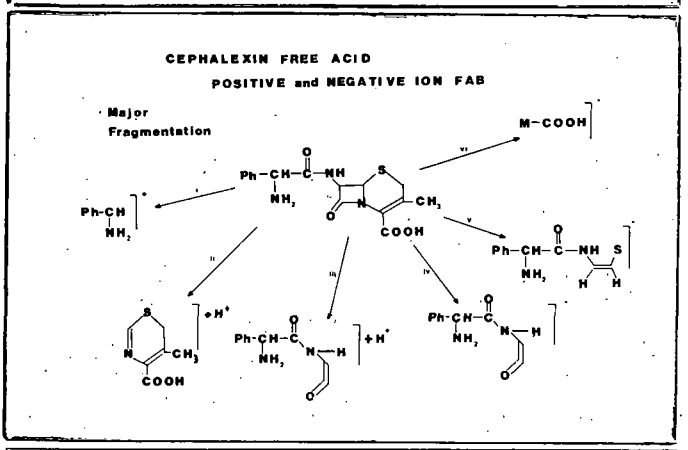

Fig.3

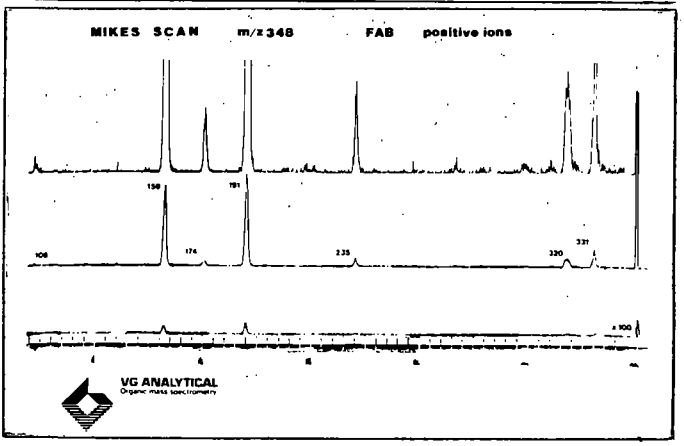

The Fast Atom Bombardment (FAB) Mass Spectra of Glucosinolates

L.C.E. Taylor and S. Evans, Kratos Ltd., Manchester, UK; and R. Self and G.R. Fenwick, Food Research Institute, Norwich, UK.

Glucosinolates, a unique group of sulphur containing anionic glycosides, occur widely in certain plant families, most notably in the Cruciferae.[1] At the present time almost 100 of these compounds have been isolated and identified and all contain the same general structure, (I), and differ only in the nature of the side chain, R.

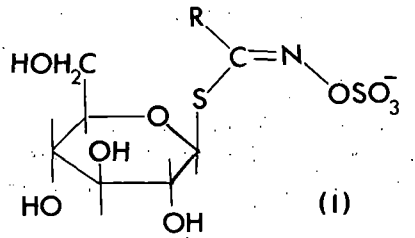

(I)

Ia, R= $CH_2=CH-CH_2-$

Ib, R= $CH_3-SO-C_3H_6-$

Ic. R= $CH_3-SO_2-C_3H_6-$

Id, R= $Ph-CH_2-$

Ie, R= $p-HO-C_6H_4-CH_2-$

Although of interest to the natural product chemist and chemotaxonomist these compounds are of more general importance since they are the precursors of the pungent compounds in mustard, radish and related salad crops and vegetables.

Compounds I a) - e) were examined as the potassium salts and their FAB-MS were characterised by abundant cationized and protonated ions of the type $(M+H+K)^+$ and $(M+2K)^+$. Limited fragmentation occurred from the former ion, involving loss of SO_3. Both Ib) and Ic) also possess fragment ions corresponding to loss of the sugar fragment ($C_6H_{11}O_5$ and $C_6H_{11}O_5S$) from the $(M+H+K)^+$ ion.

When glucosinolates Id) and Ie) were analysed as the tetramethylammonium (TMA) salts, ions of the type $(M+H+TMA)^+$ and $(M+2TMA)^+$ were observed. Loss of $C_6H_{11}O_5$ from the former afforded m/z 393 (Id) and 409 (Ie) respectively. The FAB-MS of both these aromatic glucosinolates exhibited ions corresponding to the protonated molecular ions of the desulphoglucosinolates (II).

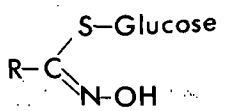

(II)

The FAB-MS of the purified desulpho analogue of Id) contained the protonated molecular ion (MH^+ m/z 330). Loss of the glucose and thioglucose fragments from this ion were confirmed by the presence of the appropriate metastable ions.

In the natural state, glucosinolate Ie) often occurs as the sinapinium ion (III). The FAB-MS of this sinapinium salt of Ie) showed ions corresponding to this cation alone, M = 310; $\overline{\quad}M\text{-}N(CH_3)_3\overline{\quad}^+$ at m/z 251: $\overline{\quad}M\text{-}C_2H_4O\text{-}N(CH_3)_3\overline{\quad}^+$ at m/z 207 and $HOCH_3CH_2\overset{+}{N}(CH_3)_3$ at m/z 104.

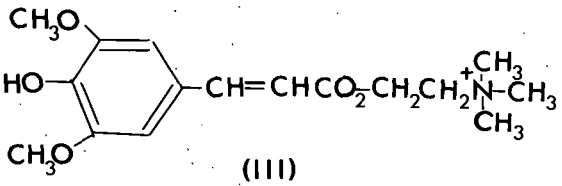

(III)

The analysis of an extract of a mixture of white mustard, containing Ie) as the TMA salt and brown mustard, containing Ia) as the potassium salt enabled both glucosinolates to be determined. Compound Ia) showed a series of adduct ions, m/z 398$(M+K+H)^+$; 436 $(M+2K)^+$; 471 $(M+K+TMA)^+$ and 506 $(M+2TMA)^+$ whilst the other glucosinolate enhibited ions at m/z 537 $(M+K+TMA)^+$ and 572 $(M+2TMA)^+$.

Preliminary investigation of the negative ion FAB-MS of Ia) - e) showed abundant molecular ions occurring at m/z 358, 422, 438, 408 and 424 respectively.

Most glucosinolates, being metabolised from amino acids, possess side chains having a unique mass. Thus the analysis of complex mixtures of glucosinolates might be possible using FAB-MS and in particular, negative ion FAB-MS techniques. In cases where further information is needed about the structure of the side chain, this can often be obtained by direct analysis of the glucosinolate or desulphoglucosinolate by EIMS[2] or ammonia CIMS[3]. Complex mixtures of glucosinolates may also be separated and analysed by GC/MS as their volatile aglycone products following enzyme treatment[4] or by GC/MS of the volatilised per-trimethylsilyl desulphoglucosinolates[5]. With the exception of the FAB-MS discussed here, none of these techniques allows the direct determination of the molecular ion. The presence of molecular ions and cationized molecular ions in the spectra of anionic compounds such as the glucosinolates clearly demonstrates the potential of this technique.

References

1. Kjaer, A. Food Chemistry 6, 223 (1981).
2. Fenwick, G.R., Eagles, J., Gmelin, R. and Rakow, D., Biomed. Mass Spectrom. 7, 410 (1980).
3. Eagles, J., Fenwick, G.R., Gmelin, R and Rakow, D., Biomed. Mass Spectrom (in the press)
4. Spencer, G.R. and Daxenbichler, M.E., J. Sci. Fd. Agric., 31, 359 (1980).
5. Eagles, J., Fenwick, G.R. and Heaney, R.K., Biomed. Mass Spectrom. (in the press).

POLYENE ANTIBIOTICS STUDIED BY FAST ATOM BOMBARDMENT MASS SPECTROMETRY

K. L. Rinehart, Jr., J. C. Cook, Jr., R. C. Pandey, M. D. Lee
School of Chemical Sciences, University of Illinois, Urbana, IL 61801

C. P. Schaffner
Rutgers University, New Brunswick, NJ 08903

M. Barber, R. S. Bordoli, R. D. Sedgwick, A. N. Tyler
University of Manchester, Institute of Science and Technology, U.K.

B. N. Green
VG Analytical, Ltd., Altrincham, U.K.

Polyene antibiotics comprise an important class which includes amphotericin B, the drug of choice for treatment of systemic mycoses, topical antifungal agents such as nystatin, and candicidin, a polyene reported to be of use in treatment of benign prostatic hyperplasia and in reduction of blood cholesterol. Tetraenes and heptaenes, which contain both an amino sugar and a carboxyl group, are zwitterionic and have proved intractable or difficult by nearly all mass spectrometric techniques, including FDMS and, sometimes, PDMS. We have now studied a number of zwitterionic polyene antibiotics by the new technique of fast atom bombardment mass spectrometry (FABMS),[1] employing a prototype FAB source on a VG ZAB 2F mass spectrometer. Amphotericin B, an aliphatic heptaene, and the related nystatin give intense positive ions in both the molecular ion region and the M-mycosamine region; negative ions are also intense in both regions. The tetraene antibiotics pimaricin and lucensomycin, as well as rimocidin sulfate, behave similarly. The larger, more refractory aromatic heptaenes such as candicidin, partricins A and B, hamycin A, and aureofungins A and B are far more difficult. However, for the most part the antibiotics do give interpretable spectra similar to the others (Tables) and spectra of their derivatives confirm the conclusions where necessary.

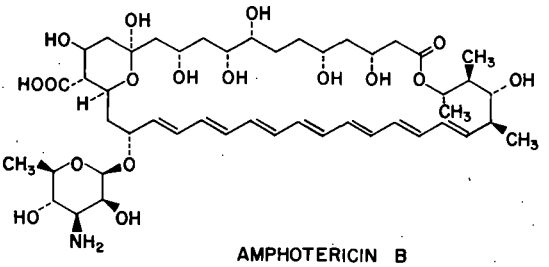

AMPHOTERICIN B

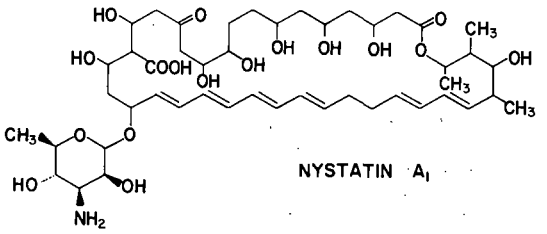

NYSTATIN A_1

The use of FABMS in solving structural problems dealing with polyene antibiotics can be illustrated by three examples relating to heptaenes. In the first, the molecular weight of amphotericin A has been shown to be the same as that of nystatin, agreeing with HPLC results indicating their identity. In the second, the molecular weights of hamycin A and aureofungins A and B have been shown to be 16 amu less than those expected from earlier structural investigations;[2,3] thus, the antibiotics contain one hydroxyl less than anticipated. In the third example, three components of a commercial sample of the investigational drug AME have been shown to be the expected amphotericin B methyl ester and analogs of the latter containing dimethylated and tetramethylated sugars.

Ions in FAB Mass Spectra of Tetraenes

		Positive Ions										Negative Ions		
						M + H - S - nH_2O								
Tetraene	M, Expd.	M + Na	M + H	M	M + H - H_2O	n = 0	n = 1	n = 2	n = 3	n = 4	Mycos-aminyl	M - H	M - H - H_2O	M - S
Pimaricin	665		666		648	503	485	467			146	664		502
Lucenso-mycin	707		708		690	545	527	509			146	706		544
Tetrin A	681	704		681	664	519	501	483	465	447	146	680		
Tetrin B	697	720	698	697	680	535	517	499	481	463	146	696	678	
Rimocidin sulfate	767		768		750	605	587	569	551	533				

Ions in FAB Mass Spectra of Heptaenes

		Positive Ions								Negative Ions			
Heptaene	M, Expd.	M + K	M + Na	M + H	M + H - H_2O	M + Na - S	M + H - S	M + H - S - H_2O	M + Na - H_2	M - H	M - H - H_2O	M - S
Amphotericin B	923		946	924	906		761	743		922		760
Nystatin[a]	925		948	926	908			745		924	906	762
Candicidin	1108	1147	1131	1109		968				1107		945
Partricin A	1126			1127						1125		963
Partricin B	1112			1113						1111		949
Hamycin A	1114			1099 (1097)						1097 (1095)		
Tetradecahydro-hamycin A	1128			1113 (1127)					1133 (1147)	1111		
Hamycin B				1113 (1111)						1109 (1111)		
Aureofungin A	1126			1111 (1113)	1093							
Aureofungin B	1087									1070		

References

(1) M. Barber, R. S. Bordoli, R. D. Sedgwick, and A. N. Tyler, J. Chem. Soc., Chem. Commun., 235-236 (1981).

(2) M. D. Lee and K. L. Rinehart, Jr., 16th Interscience Conference on Antimicrobial Agents and Chemotherapy, Chicago, IL, Oct. 27-29, 1976; Abstract 40.

(3) R. C. Pandey and K. L. Rinehart, Jr., ibid.; Abstract 41.

FAST ATOM BOMBARDMENT MASS SPECTROMETRY : APPLICATION TO LEUKOTRIENES AND SLOW-REACTING SUBSTANCES

H.R. Morris, P.M. Clinton and G.W. Taylor
Department of Biochemistry, Imperial College, London, U.K.
M. Barber, R.S. Bordoli, R.D. Sedgwick and A. Tyler
Department of Chemistry, UMIST, Manchester, U.K.
B.N. Green
VG Analytical, Altrincham, U.K.

The structure of slow-reacting substance of anaphylaxis (SRS-A) from lung was determined as the novel peptidolipid 5-hydroxy-6-cysteinylglycinyl-7,9,11,14-eicosatetraenoic acid by a combined mass spectrometric-protein chemistry approach (1) ; the full stereochemistry was later determined by HPLC comparison with synthetic material (2).

SRS-A is biosynthesised by glutathione conjugation with lipoxygenase-produced arachidonate metabolites, forming glutathionyl, cysteinylglycinyl (SRS-A) and cysteinyl slow-reacting substances ; these are now termed Leukotriene C, D and E (LT- C, D, E) respectively.

The original structure elucidation of SRS-A (LT-D) was hampered by manifest difficulties in producing an EI mass spectrum on the minute quantities (<5 µg) of the natural material available. Although the full structure could be built up from the observed fragment ions, definitive molecular weight data was only obtained by N-terminal isotope labelling (1:1 $CH_3CO:CD_3CO$) coupled with a knowledge of radical losses from the molecular ion of the methyl ester derivative used (i.e. loss of $^{\bullet}CH_3$ and $^{\bullet}OCH_3$). Inconclusive results were obtained from FDMS at the µg level - only a weak $(M+Na)^+$ ion could be observed.

In contrast to these difficulties, molecular species were readily obtained at the one µg level for SRS-A (LT-D) and its γ-glutamyl homologue (LT-C) by Fast Atom Bombardment (FAB) - MS. In the positive mode quasimolecular ions were observed at m/z 497 $(M+H)^+$, 519 $(M+Na)^+$ and 535 $(M+K)^+$ for LT-D, and, similarly, at m/z 626, 648 and 664 for LT-C (molecular weights of 496 and 625 m.u. respectively). In the negative spectra strong $(M-H)^-$ ions were observed at m/z 494 (LT-D) and 626 (LT-C), with weaker signals 22 mass units higher arising from the carboxylic acid sodium salt (COO^-Na^+) of the $(M-H)^-$ molecular species.

At the low microgramme level no fragmentation occurred in either positive or negative modes - similarly, glutathione itself appears not to fragment ($(M+H)^+$: m/z 308). Weak ions were however present 16 mass units above the major molecular species (<10% intensity) and probably correspond to oxidation to the sulphoxide during handling.

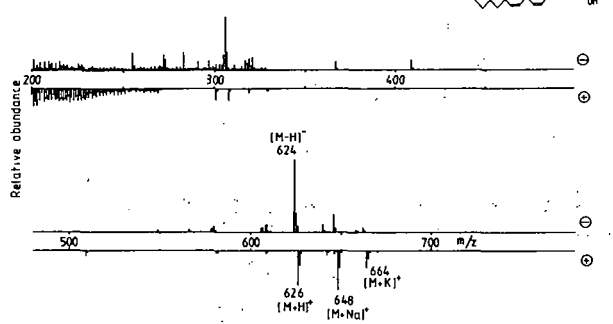

Positive and negative FAB MS of Leukotriene C (approx. 1 µg)

The N-acetyl (1:1 CH_3CO:CD_3CO) derivatives of LT-C and LT-D were prepared by reaction with methanol : acetic anhydride (3:1 v/v) for 15 min. This reaction does not affect the leukotriene chromophore and was used as the first derivatisation step prior to mass spectrometric analysis during the structure determination of SRS-A (LT-D) (1).

In both positive and negative FAB spectra intense 1:1 doublet ions were observed, 3 mass units apart (arising from one isotopically labelled NH_2 group); however these ions did not correspond to the calculated molecular species ($(M+H)^+$ 668, 539; $(M-H)^-$ 666, 537) for the leukotrienes. In the negative mode there were signals at m/z 648 (LT-C) and 519 (LT-D), with accompanying carboxylic acid sodium salt (COO^-Na^+) signals 22 mass units higher. The major positive ion species were at m/z 672 (LT-C) and 543 (LT-D). We interpret these signals as arising from the elimination of water on the formation of a lactone during acetylation (probably the δ lactone at C-5 of the lipid chain); there is virtually no lactone in the free leukotrienes. The observed signals may be rationalised as follows :

Ac. LT-C lactone $(M-H)^-$: 648 m.u. ; $(M+Na)^+$: 672 m.u.
Ac. LT-D lactone $(M-H)^-$: 519 m.u. ; $(M+Na)^+$: 543 m.u.

It is interesting that no $(M+H)^+$ ion was observed in the positive FAB spectra.

The lactone is readily opened (e.g. by methanol/HCl) as the full EI spectrum of the TMS ether, N-acetyl methyl ester derivative shows (1).

In conclusion, intense FAB spectra in both positive and negative modes have been obtained from leukotrienes C and D at the one µg level. At this level little fragmentation occurs with the ion current being carried mainly by the molecular species. We are currently exploiting this in quantitative studies on the leukotrienes and their metabolites.

References

(1) Morris H.R., Taylor G.W., Piper P.J. and Tippins J.R. (1980) Nature , 285, 104-106.
(2) Morris H.R., Taylor G.W., Rokach J., Girard Y., Piper P.J., Tippins J.R. and Samhoun M.N. (1980) Prostaglandins , 20, 601-607.

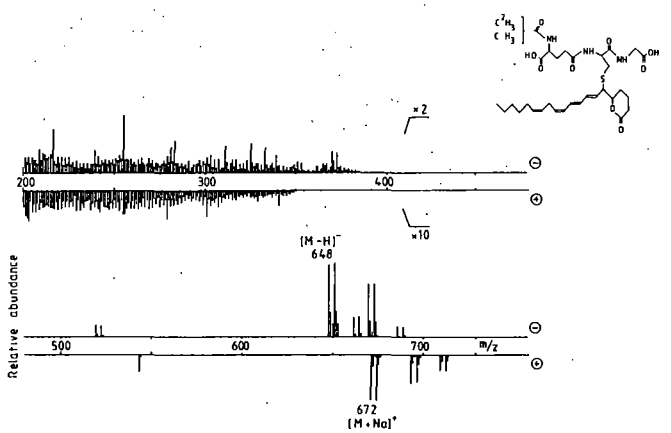

Positive and negative FAB MS of the N-acetyl (1:1 CH_3CO:CD_3CO) derivative of Leukotriene C showing formation of a lactone.

Structural Studies on Peptides by Mass Spectrometry: Application of Fast Atom Bombardment

D.H. Williams, C. Bradley, S. Santikarn and G. Bojesen
(University Chemical Laboratory, Lensfield Road, Cambridge, CB2 1EW, U.K.

L.C.E. Taylor and S. Evans
(Kratos Ltd., Urmston, Manchester, England).

The potential of fast atom bombardment (FAB) mass spectrometry has been evaluated by the study of a wide range of organic compounds, and particularly peptides.

The FAB mass spectra was obtained by bombarding the sample with argon atoms of kinetic energy ca 4 keV. The sample is normally dissolved in glycerol or, less frequently, trigol (1) or tetragol (2), which adhers to a copper probe tip; the probe is introduced into the source through a conventional vacuum lock.[1]

$HO(CH_2CH_2O)_nH$

1, n = 3

2, n = 4.

$(C_6H_5)_3\overset{+}{P}CH_2COOEt\ Br^-$

3

Molecular weight information is usually obtained from $(MH)^+$ ions in positive ion spectra, and from $(M-H)^-$ ions in negative ion spectra. These spectra are in general produced with comparable sensitivities; possible exceptions are discussed subsequently. The technique is particularly suited to the study of organic salts, and relatively polar molecules up to high molecular weights (e.g. compounds in the range 1000-2000 Daltons have been studied routinely). The method is less well suited to the study of non-polar molecules which possess neither charged nor relatively acidic or basic centres (e.g. cholesterol).

Thus, the positive ion FAB was spectrum of the phosphonium salt 3 contains a very abundant ion due to the cationic portion (m/z 349); and the negative ion spectrum shows Br^-. Similarly, the quaternary salt of thiamine gives an abundant ion m/z 265 corresponding to the cation 4; and the potassium salt of penicillin G gives in its negative ion spectrum an intense peak due to the carboxylate anion 5.

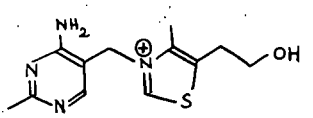

4

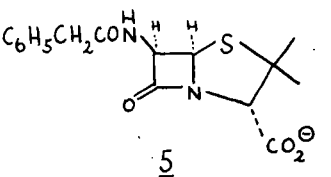

5

A wide range of underivatized peptides has been studied. Molecular weights can generally be determined from either $(M-H)^-$ or MH^+ ions on ca 1 nmol. However, it often appears advantageous to run peptides with a net positive charge at pH 6.5 in the positive ion mode; and those with a net negative charge at this pH in the negative ion mode. If necessary, spectra can be directly counted up to ca m/z 2000 to give precise determination of integral molecular weights.

Sequence ions, which are normally less abundant than $(M-H)^-$ or $(MH)^+$ ions, and therefore conveniently observed using 10-50 nmol of peptide, corresponding to the following fragmentations (6-8) have been widely observed.

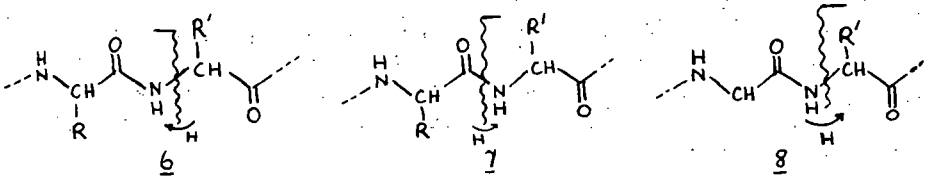

6 7 8

In 6, the charge is retained by the N-terminal portion, either with a net negative or positive charge. In 7 and 8, the charge is retained by the C-terminal portion, again with a net negative or positive charge. The fragments due to 7 and 8 are characteristically separated by 15 m.u.

The principles of peptide analysis will be illustrated by numerous examples, and the sequence determination[2] of some "difficult peptides" from a Paracoccus cytochrome c-550 discussed.

References

1. L.C.E. Taylor, S. Evans, H.J.M. Fitches, and K.R. Compson, 29th Annual Conference on Mass Spectrometry and Allied Topics, Minneapolis, 1981.

2. D.H. Williams, G. Bojesen, A.D. Auffret and L.C.E. Taylor, FEBS Letters, in press.

FAST ATOM BOMBARDMENT : PEPTIDE STRUCTURE DETERMINATION AND MIXTURE ANALYSIS

H.R. Morris, M. Panico, M. Judkins, A. Dell and R. McDowell
Department of Biochemistry, Imperial College, London, U.K.

Over the past ten years this laboratory has developed and applied different mass spectrometric methods for the sequence analysis of proteins and biologically important peptides. This work has included the structure elucidation of proteins of M.W. 18,000-30,000 (one of which - DHFR - was analysed completely independently of classical methodology), the identification of the enkephalins, adipokinetic hormone and slow-reacting substance of anaphylaxis, and countless other peptide sequences (1). This work has been carried out mainly by E.I. and C.I. M.S., by the mixture analysis method, giving both molecular weight and sequence information, and also by F.D.M.S. (molecular weight data only).

We have now extended our studies into the nascent area of Fast Atom Bombardment (FAB) M.S.. A series of free and derivatised peptides (containing all of the normal protein derived amino acids) have been studied in positive and negative ionisation modes, and we report a simple and rapid method which allows the unambiguous structure determination of unknown peptide sequences.

In each of the peptides studied we have observed quasimolecular ions ($(M-H)^-$, $(M+H)^+$, $(M+Na)^+$ etc.) together with partial or full sequence information. For example, in the positive mode, the tetrapeptide Phe-Gly-Gly-Phe gives an intense quasimolecular ion at m/z 427, and major sequence ions which may readily be assigned to fragments of known structure.

FAB-MS fragmentation is similar to that observed for CIMS, except the FAB spectra are, if anything, more "pure", e.g. the 'N-C' cleavage (McLafferty rearrangement) ions are absent in the positive mode. N-terminal (N_t) sequence ions are formed by cleavage at the peptide bond; C-terminal ions (C_t) are similarly formed, but are accompanied by hydrogen rearrangement. In negative ion spectra C_t ions again arise by cleavage at the peptide bond (no H-rearrangement), but N_t ions are formed by cleavage of N-C bonds in the peptide backbone. As a result, the positive and negative sequence ions differ by 15 mass units for N_t ions, and by 2 mass units for C_t ions.

To rationalise the spectra and differentiate between C_t and N_t ions we recommend the use of a simple isotopic labelling experiment : N-acetylation with a 1:1 mixture of $(CH_3CO)_2O$ and $(CD_3CO)_2O$ in methanol. The N_t ions of the acetylated peptide appear as 1:1 doublets three mass units apart, while C_t ions remain as singlets ; if two amino groups are acetylated (e.g. an additional ϵ-NH_2 of lysine) a 1:2:1 triplet pattern is observed further aiding interpretation. The value of this approach is clearly seen in the case of the natural opioid peptides - the enkephalins. Their structures were determined in this laboratory by EI mass spectrometry of the N-acetyl-N,O-permethyl derivative, but interpretation of the spectrum took several days due to the absence of a molecular ion together with a complex fragmentation pattern. In contrast, the FAB spectra of a few µg of the 1:1 labelled N-acetyl derivative could be readily interpreted from the quasimolecular ion and the accompanying sequence ions.

We have applied this method to assist colleagues at Cambridge (MRC Molecular Biology) to complete the sequence of a bovine ATP-ase derived peptide. By using the isotope labelling technique in both positive and negative FAB modes, a partial structure could be readily assigned. The positive FAB spectrum is shown in Figure 1. Note the high mass 1:1 doublets assigned to either quasimolecular ions or N_t ions. The lower mass end of the spectrum is dominated by C_t signals (singlets) and the partial structure H.....Asp-Ala-Thr-Thr-Val-.....OH is assigned via signals at m/z 360, 459, 560, 661, 732, 847. We note that this data is in conflict with the partial sequence already determined classically. However, in contrast to the classical data, the FAB-derived sequence is homologous with an ATPase peptide from an E. coli enzyme which strongly suggests that the classical sequence is incorrect.

Peptide mixtures (both as free materials and 1:1 labelled N-acetyl derivatives) have been analysed by FAB-MS. We now report one example to illustrate the problems encountered when mixtures are examined using FAB ionisation. Mixture B is a peptide pool obtained from tryptic digestion of pepsin. It contains the three peptides : Val-Gly-Leu-Ala-Pro-Val-Ala, Ala-Asn-Asn-Lys

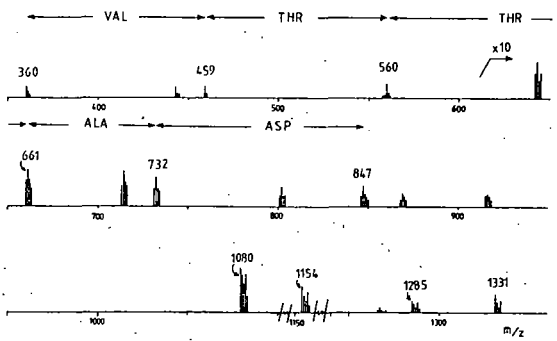

Fig. 1 FAB MS of Acetyl (1:1) ATPase peptide

and Gln-Tyr-Tyr-Thr-Val-Phe-Asp-Arg. The positive FAB spectra of both free and acetyl Mixture B contained quasimolecular ions for the valine peptide and for the glutamine peptide. The latter appeared as a mixture of the Gln and PCA (cyclic) residues at the N-terminus. Only Val-Gly-Leu-Ala-Pro-Val-Ala yielded sequence ions (the full sequence could be obtained from the N_t and C_t ions). Neither Gln-Tyr-Tyr-Thr-Val-Phe-Asp-Arg nor PCA-Tyr-Tyr-Thr-Val-Phe-Asp-Arg fragmented to produce sequence ions. The third component in the original mixture, Ala-Asn-Asn-Lys, was not observed as the free peptide. We interpret this behaviour as arising from preferential binding of one or more components to the glycerol matrix thus reducing their ionisation efficiency. Indeed under drastic conditions, by allowing the glycerol to evaporate, a weak spectrum of the "bound" component was obtained for acetyl-Mixture B.

In conclusion, we have studied both known and unknown peptides at the µg level by FAB-MS, and have defined general fragmentation pathways. Strong quasimolecular ions were observed for all peptides with complete sequence information available for many. Interpretation of these spectra was simplified by a simple N-terminal isotope labelling step. Although peptide mixtures may readily be studied, full sequence information is not always obtained for each component and some components may not ionise.

Mass spectrometry of peptides has already assisted in the solution of many problems of biological interest - FAB, especially with the high field magnet facility, will greatly extend our horizons.

(1) Morris H.R. (1980) Nature , 286, 447-452

γ -Glu-Cys-Gly
Ac.Ala-Ser-Phe
Phe-Gly-Gly-Phe
Pro-Phe-Gly-Lys
Ala-Asn-Asn-Lys
Trp-Met-Asp-$PheNH_2$

Tyr-Leu-Pro-Glu-Phe
Tyr-Leu-Gly-Glu-Phe
Tyr-Gly-Gly-Phe-Met
Lys-Phe-Ile-Gly-Leu-$MetNH_2$

Val-Gly-Leu-Ala-Pro-Val-Ala
Gln-Tyr-Tyr-Thr-Val-Phe-Asp-Arg
Arg-Pro-Pro-Gly-Phe-Ser-Pro-Phe-Arg
Val-Val-Tyr-Pro-Trp-Thr-Gln-Arg-Phe
Ac. Ser-Tyr-Ser-Met-Glu-His-Phe-Arg-Trp-Gly-Lys-Pro-$ValNH_2$
Tyr-Gly-Gly-Phe-Met-Thr-Ser-Glu-Lys-Ser-Gln-Thr-Pro-Leu-Val-Thr

PEPTIDES EXAMINED BY FAB MASS SPECTROMETRY

Mass Spectra of Free Polypeptides by Fast Atom Bombardment (FAB)

by

M. Barber, R. D. Sedgwick, R. S. Bordoli and A. N. Tyler
Chemistry Department, U.M.I.S.T., Manchester M60 1QD, England.

The technique of fast atom bombardment ionisation is the basis of a new ion source which has been developed at U.M.I.S.T. FAB has been used by us, routinely, for two years to obtain high quality mass spectra from a wide range of thermally labile and previouslyintractable molecules (1).

Additional to the practical advantages which are inherent in a neutral bombardment system, we have developed methods of prolonging the lifetimes of the sputter mass spectra. This requires that the sample be presented in a viscous fluid support medium which causes a constantly renewed source of the sample to be exposed to the atom beam. The most successful of these systems, for peptides and many other compounds, involves dissolution in glycerol. A typical sample preparation involves the deposition of 5 μl of glycerol onto the metallic sample stage, to which is added 500 pmol of peptide dissolved in 1 μl of methanol. Such a sample will produce intense spectra of either polarity, which are stable for the lifetime of the glycerol, say 20 min., after which the sample can be rejuvenated by the addition of more glycerol.

Using a Vacuum Generators ZAB mass spectrometer with a prototype FAB ion source, we can produce good quality mass spectra with almost complete reliability from any free peptide with a molecular weight below 1800. Above this mass limit it becomes necessary to reduce the ion energy with an attendant loss in sensitivity and/or resolving power.

Studies on synthetic tripeptides (2), enkephalins (3), bradykinins (4), angiotensins and fibrinopeptides have revealed six series of fragment ions from which sequence information may be deduced. Three of these produce fragments containing the terminal -COOH group and involving cleavage of the CO-NH peptide bond in two cases, without and with hydrogen transfer, and cleavage of the CH-NH bond in one case. Additionally we have identified three ion series in which the terminal $-NH_2$ group is retained. These involve cleavage of the CH-CO, CO-NH and CH-NH bonds respectively with the first being the most significant. Cyclic amino acid units such as proline are unable to give either of the CH-NH bond cleavages.

Peptides with two basic (arginine) units, such as the bradykinins, show doubly charged ions of the form $(M + H_2)^{++}$ and also show good intensities of both C- and N-terminal fragment ions.

Peptides with excess acid groups, e.g. fibrinopeptide A which contains glutamic acid, show a dominance of C-terminal fragments.

The reliability of the FAB method has allowed us to monitor the quality of commercially available peptides used as standards in biological tests in the department of Pharmacology. We have only encountered problems eith the human fibrinopeptides. Only one in three suppliers of human fibrinopeptide A have proved satisfactory and to date we have been unable to obtain a good sample of human fibrinopeptide B.

In addition to the sequence information in the normal FAB mass spectrum, it is possible to make use of the reversed geometry of the VG-ZAB instrument to record the MIKES spectra (5). The figure shows such a scan for isoleucine-angiotensin-1 in which the daughter ions of the psuedo-molecular ion at m/z 1296^+ have been traced. Eight of the ten possible cleavages of the CH-CO bonds are visible, giving fragments retaining the terminal $-NH_2$ sequence.

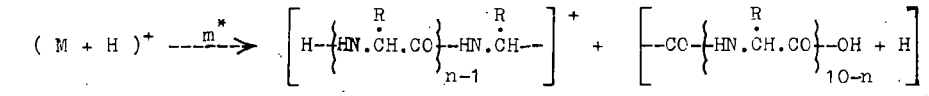

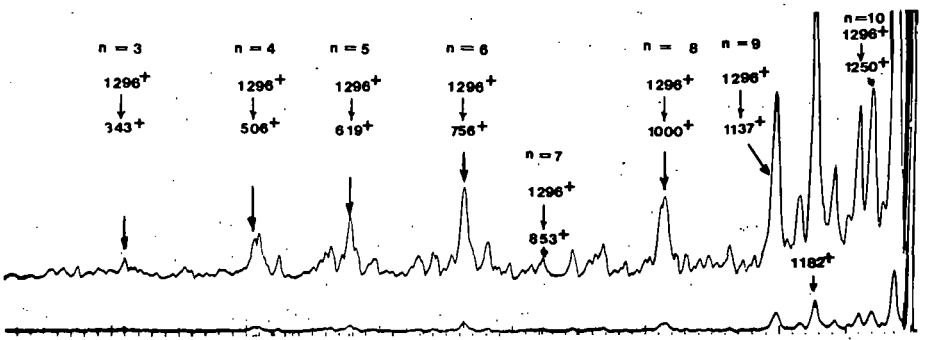

(1) M.Barber,R.S.Bordoli,R.D.Sedgwick and A.N.Tyler,J.C.S.Chem.Comm.,325, (1981).

(2) M.Barber,R.S.Bordoli,R.D.Sedgwick and L.W.Tetler,Org.Mass Spectrom., in press, (1981).

(3) M.Barber,R.S.Bordoli,R.D.Sedgwick,A.N.Tyler,G.V.Garner,D.B.Gordon and L.W.Tetler, Biochem. J., in press, (1981).

(4) M.Barber,R.S.Bordoli,R.D.Sedgwick,A.N.Tyler and E.T.Whalley, Biomed. Mass Spectrom.,in press, (1981).

(5) R.P.Morgan,J.H.Beynon,R.H.Bateman and B.N.Green,Int. J. Mass Spectrom. Ion Phys., 28 , 171 (1978).

FAST ATOM BOMBARDMENT MASS SPECTROMETRY : APPLICATION TO PEPTIDE SEQUENCING AND THE IDENTIFICATION OF NOVEL PITUITARY PEPTIDES

H.R. Morris, A.Dell, A.T. Etienne and M. Panico
Department of Biochemistry, Imperial College, London U.K.
M.Barber, R.S. Bordoli, R.D. Sedgwick and A Tyler
Department of Chemistry, UMIST, Manchester, U.K.
G.P. Vinson
St Bartholomew's Medical College, London , U.K.
B.J. Whitehouse
Queen Elizabeth College, London U.K.
B.N. Green
VG Analytical, Altrincham, U.K.

The explosion of interest into neuroactive and related peptides has arisen from a realisation not only of their fundamental role in the control of major bodily processes, but also from a growing belief in their implication in the expression of both mental and physical illnesses (e.g. schizophrenia, senile dementia, Parkinsonism etc.). Our understanding of the functions and interrelationships of neuropeptides is still severely limited by a lack of hard data on their identity, quantity and location throughout the body. The search for this data poses a fundamental challenge for the structural chemist.

The determination of peptide structure is a rewarding but difficult task, not least when applied in the neurochemistry area; here the new DNA technology is of little value in the identification of small quantities of biologically active peptides such as the enkephalins. Neuropeptides are both structurally complex, with problems such as blocked N-termini greatly complicating classical analysis, and, to make analysis more difficult, are only present in low quantities (often picomolar levels) in crude biological extracts such as plasma. Characterisation is often only by chromatographic comparison with standards, coupled with biological or radioimmunoassay. Our confidence in this data increases concomitantly with the degree of purification (and is very high when reverse-phase HPLC is used (1)), but only becomes absolute upon full structure elucidation i.e. mass spectrometric analysis.

Present MS methodology has relied on the generation of small fragments from the unknown (by enzymic or hydrolytic approaches) followed by derivatisation and EI or CI analysis. Variable yields in derivatisation and lack of molecular ion data only compound analytical difficulties. Although FDMS is capable of giving molecular weight data, the sequence of an unknown peptide could not be deduced from its FD fragmentation pattern.

These problems may now be solved following the advent of Fast Atom Bombardment (FAB)-MS. Both molecular weight and sequence data may be obtained from many (although not all) peptides at the nanomole and sub-nanomole level. We have demonstrated that full or partial sequence data may be obtained from both known and unknown peptides (see accompanying paper, Morris et al, WAMOA13) and report here sensitivity studies on neuropeptides and the application of FAB to the solution of a biochemical problem.

The sensitivity of this technique was readily demonstrated with the antidiuretic hormone - lysine vasopressin. Intense molecular species at m/z 1056 $(M+H)^+$, 1078 $(M+Na)^+$ and 1094 $(M+K)^+$ were observed with only 2 nanomoles of material. Further, only 300 picomoles of the opioid peptide α-endorphin were required to give a reasonable $(M+H)^+$ signal at m/z 1745. At this level, however, no sequence information could be obtained, whereas at higher loadings, C-terminal ions were observed for α-endorphin. Both a strong quasimolecular ion at m/z 1664 and fragment ions were observed in the positive FAB spectrum of 300 picomoles of α-MSH. However sequence ions were not present, and it would have been difficult, if not impossible, to derive the structure of α-MSH if unknown from the fragmentation pattern. To overcome this problem we investigated whether collision induced fragmentation could be employed in these cases to obtain sequence information. Our preliminary data was not encouraging, and it appeared that collisional activation would not in general prove valuable for solving unknowns.

We recently isolated a peptide from a pituitary extract with potent aldosterone-stimulating

activity when tested on adrenal zona glomerulosa. Following mass spectrometric and protein chemical analysis the substance was identified as α-MSH (2). Two other peaks of biological activity, "B" and "C", eluting after α-MSH were observed following reverse phase HPLC. The earlier of these peaks had the same amino acid composition as α-MSH and could not be distinguished from it by EIMS of the N-acetyl N,O-permethyl derivative; further, mild base hydrolysis of peak B resulted in the formation of α-MSH. Clearly, peak B is a derivative of α-MSH - but how do these two compounds differ? To answer this question we analysed peak B by FAB MS. An intense quasi-molecular positive ion at m/z 1706 was observed, 42 mass units higher than the $(M+H)^+$ ion of α-MSH (m/z 1664) strongly suggesting that peak B is an acetyl derivative of α-MSH. The base lability of peak B indicates that it is an O-acetyl rather than an N-acetyl derivative, and explains why the two substances give identical EI spectra for the acetyl permethyl derivative.

Investigation of the third minor component - peak C - indicated the presence of a small peptide moiety. FAB signals were observed at m/z 1193 (negative) and m/z 1195 (positive); on short acetylation in methanol/acetic anhydride these shifted to m/z 1235 and 1237 respectively (i.e. plus 42 mass units) consistent with the formation of an N-acetyl derivative from a free N-terminus. EIMS of the N-acetyl N,O-permethyl derivative gave the following partial sequence : Val-Val-Tyr-Pro- (Trp, Glx, Phe present). From our earlier studies on the isolation and structure elucidation of peptides found in the brain we recognised this sequence as being part of the β-chain of haemoglobin. From these data, together with the molecular weight of the peptide obtained from FAB we deduced that peak C contains the peptide : Val-Val-Tyr-Pro-Trp-Thr-Gln-Arg-Phe (although not necessarily as the biologically active species). Investigations into the biological role (if any) of this peptide are now underway in this laboratory.

The subnanomole sensitivity of FAB MS, especially when used in conjunction with the high field magnet, offers great advantages for the structural analysis of neuropeptides. Because structural information may be obtained from free underivatised peptides we suggest that HPLC MS will now find wider use in the neuropeptide field e.g. by using the moving belt system to both deliver samples into the source and also act as the FAB target.

We have shown that FAB MS can be used successfully in the solution of biological problems. With anticipated future developments in both sensitivity and quantitation we feel that FAB MS will offer a viable and more specific alternative to the biological or radioimmunoassay analysis of neuropeptides, and should open the way for a more rational understanding of the complex area of human neurochemistry.

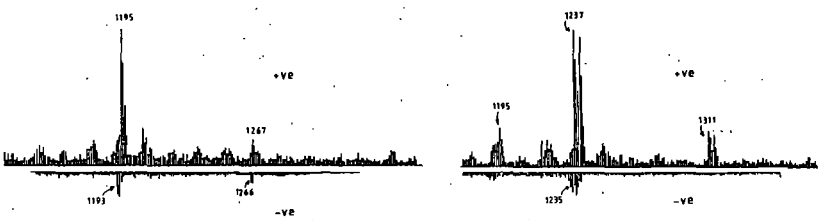

(a) (b)

Figure : (a) Positive and negative FAB spectra of peak C
(b) Positive and negative FAB spectra of acetyl (1:1 labelled) derivative of peak C

References

(1) Morris H.R., Etienne A.T., Dell A. and Albuquerque R. (1980) J. Neurochem., 34, 574-582.
(2) Vinson G.P., Whitehouse B.J., Dell A., Etienne A.T. and Morris H.R. (1980) Nature, 284, 464-467.

CAN THE PRIORITY POLLUTANTS BE MEASURED WITHOUT GC/MS?

Ronald A. Hites
School of Public and Environmental Affairs
and Department of Chemistry
400 East Seventh Street
Indiana University
Bloomington, Indiana 47405

The priority pollutant story begins with the passage of the Federal Water Pollution Control Act in 1972. Section 101a of that act stated that its objective was "to restore and maintain the chemical, physical, and biological integrity of the Nation's waters," and that "it is the national policy that the discharge of toxic pollutants in toxic amounts be prohibited." The definition of what was, in fact, a toxic pollutant was left to the EPA administrator. Section 307a of that act stated: "The administrator shall publish a list which includes any toxic pollutant for which an effluent standard will be established. The administrator shall take into account toxicity, persistence, degradability, and the effect of the toxic pollutant."

Establishing this list of toxic pollutants proved to be a difficult task for the EPA, and eventually the EPA was taken to court by a combination of public interest groups. The suit was settled out of court on June 7, 1976, and the now famous consent decree established for the first time a list of toxic pollutants. This list had 65 entries, several of which were classes of compounds needing further definition. This was accomplished, after some negotiation with the plaintiffs, and a list of 129 specific substances was established. These are now known as the priority pollutants.

The ultimate goal of the priority pollutants program is to regulate the emission of these compounds into the water supply of the nation. Before these regulations could be put in place, however, it was necessary to obtain information on the prevalence of the individual compounds so that regulatory activity could be focused on those compounds which present the greatest problem. Therefore, the first phase of the priority pollutant program has been the so called "screening" phase which lasted from 1976 to 1979. An ancillary goal of this phase was to determine waste treatment capabilities for the priority pollutants. False positives (analytical measurements which were too high) were acceptable in the screening phase (Neptune, 1980). The methods used for these studies were based on gas chromatographic mass spectrometry, methylene chloride extraction of the semivolatile compounds at various pH's, and purge and trap techniques for the volatile compounds. Some results of the screening phase have been published (Keith and Telliard, 1979). Those compounds which occurred in more than 5% of the samples were: alkyl and chlorobenzenes, C_1 and C_2 chlorinated solvents, polycyclic aromatic hydrocarbons, and phenols. There were only six compounds which occurred in more than 20% of the samples: benzene, toluene, methylene chloride, chloroform, bis(2-ethylhexyl)phthalate, and phenol. These results are not very surprising, but they do provide a guide to the groups of compounds which should be regulated first.

The Clean Water Act of 1977 (Public Law 95-217) incorporated the priority pollutant list in its revised section 307a. Furthermore, this act required the EPA administrator to "promulgate" test procedures for the analysis of the priority pollutants (section 304h). To meet this legislative requirement, the EPA has established the so called "600 level" methods. Some of these methods are based on gas chromatography only (with selective detectors) and some are based on gas chromatographic mass spectrometry. Figure 1 shows block diagrams summarizing six of these "600 level" methods. The methods for the volatiles are based on either an electrolytic conductivity detector, a photo-ionization detector, or a gas chromatographic mass spectrometer. The phenol method is based on gas chromatography with either a flame ionization detector or (after derivatizing with a pentafluorobenzyl group) an electron capture detector. Polycyclic aromatic hydrocarbons are analyzed either with a gas chromatograph equipped with flame ionization detection or with a high pressure liquid chromatograph equipped with ultraviolet and fluorescence detection. The "625" method is very similar to the screening method and is based on extraction with methylene chloride at two pH's followed by GC/MS. These methods were released for public comment in late 1979, and they are soon to be released in their final form.

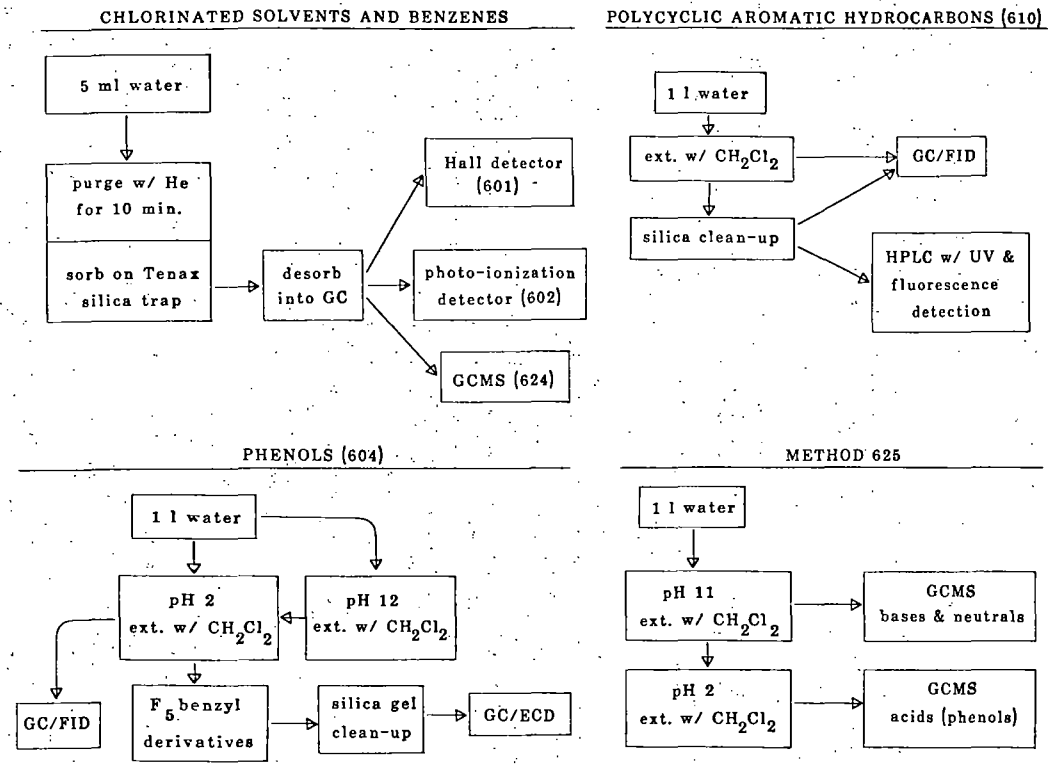

Figure 1. Block diagrams summarizing six "600 level" methods for the analysis of priority pollutants (Federal Register, 1979).

There have been two main issues of controversy surrounding these "600 level" methods. The first complains that the methods have not been completely validated by the EPA, and the second berates the use of the GC only methods (as opposed to GC/MS). Both of these problems stem from two important facts: (a) Most industrial waste streams change qualitatively from plant to plant, from stream to stream, and even from day to day. Thus, the matrix in which the priority pollutants will be measured is highly complex and varies both with time and location. (b) Secondly, unlike the screening phase, false positives are a disaster. Clearly, if a company is faced with a penalty for exceeding an effluent limitation, they (and presumably the EPA) want to be very certain that the measurement, which shows them to be in violation, is qualitatively and quantitatively accurate.

With these two facts in mind, we can now address the two problems of validation and GC only methods. Discussion of the validation question is beyond the scope of this paper. Let it be said, however, that given the high degree of variability of the matrix in which the priority pollutants will be measured, any validation by a systematic set of model samples will be virtually impossible, and that validation of individual data sets will be achieved only by the implementation of vigorous quality assurance programs. The GC only question centers on the argument that any method based on GC without mass spectrometry cannot provide the necessary specificity of analysis. It is really a simple question: Can the priority pollutants be measured without GC/MS? This question is of great interest to many people, not the least of whom are manufacturers of gas chromatographs and mass spectrometers. Let us see if we can't summarize the pro's and con's of GC only methods and of GC/MS methods and then see if we can't reach a conclusion about the above question.

The advantages of GC only methods derive from the use of simple and inexpensive equipment which can be operated routinely by high school drop-outs. Furthermore, GC methods can, in special circumstances, produce reliable identifications. This may sound like heresy, but I should point out that in many sets of samples the pattern of peaks is reproducible. Thus, if one always sees the same fingerprint, but its quantity goes up and down, one can be fairly confident that the identification of the components has not changed.

The disadvantage of GC only methods stem from their lack of specificity. Even those GC only methods outlined in Figure 1, which use selective GC detection, are not fully specific, and compounds which are not priority pollutants can respond. In some cases, it is even impossible to distinguish among the priority pollutants by the GC only methods. All of this means that the probability of false positives with GC only methods is high. Furthermore, the GC only methods require a great deal of clean-up and sample preparation before analysis. The formation of chemical derivatives and the use of silica chromatography (see Figure 1) are not simple steps; they add a degree of complexity which is probably not compatible with the simplicity of the GC instrumentation.

There are several advantages of GC/MS methods. Clearly these methods are capable of reasonably specific compound identifications. Thus, these methods will require less preliminary sample clean-up and are less subject to matrix variations. A new compound which is not a priority pollutant, but which suddenly appears in a sample, can be identified by GC/MS. In addition, isotopically labelled internal standards can be used with GC/MS methods, but not with GC only methods. On the other hand, GC/MS is a complex and expensive instrument. Furthermore, GC/MS cannot distinguish between some isomers. This problem includes some of the polycyclic aromatic hydrocarbon isomers and isomers with various ring substitutions.

Considering all of these factors, the main issue in the debate between GC only and GC/MS boils down to cost. What are the facts? There have been several cost estimates of the "600 level" GC only and GC/MS methods. The Federal Register (1979) suggests that all of the organic compounds can be measured by the GC only methods for about $2,100. Finnigan et al. (1979) suggests that they can be measured by GC only for $557. The truth must be somewhere in between. GC/MS analysis of all the organic priority pollutants is estimated to cost either $1,500 (Federal Register), $328 (Finnigan et al., 1979), or $600 (Eastern Analytical Symposium, 1980). While the range of the cost estimates for both GC and GC/MS is high, it is clear that GC/MS methods are no more expensive than GC only methods.

The question of false positives is critically important. For the reason explained above, industry cannot tolerate data in which a false positive appears. Therefore, whenever a measurement (by any technique) indicates that an effluent stream is in violation, the

most sophisticated, specific, and accurate technique will be used to verify that measurement. Thus, it seems to me that the GC methods will be used only if the sample is negative or if the pattern of GC peaks is very clear. Otherwise, if anything is present, the more specific GC/MS methods will certainly be preferred. In fact, since the cost differential between the GC only and GC/MS methods is not great, there seems to be little reason to use the less specific GC only methods at all. Finally, in answer to the question posed by the title of this paper: no.

Acknowledgement

The preparation of this paper was supported by the U.S. Environmental Protection Agency's Environmental Monitoring and Support Laboratory through cooperative agreement number R808865.

References

Eastern Analytical Symposium (1980) "Aqueous Environmental Analysis by GC/MS," November 20, 1980.

Federal Register (1979) "Guidelines Establishing Test Procedures for the Analysis of Pollutants," 44, 69464-69575 (December 3, 1979).

Finnigan, R. E., Hoyt, D. W., and Smith, D. E. (1979) "Priority Pollutants, II, Cost Effective Analysis," *Environ. Sci. Tech.*, 13, 534-541.

Keith, L. H. and Telliard, W. A. (1979) "Priority Pollutants, I, A Perspective View," Environ. Sci. Tech., 13, 416-423.

Neptune, D. (1980) "Verification Procedures - Results to Date," in Proceedings of the Seminar for Analytical Methods for Priority Pollutants, Norfolk, VA, January 17-18, 1980.

INCREASED SPECIFICITY IN OPTICAL DETECTION FOR LIQUID CHROMATOGRAPHY; J. L. DiCesare and L. S. Ettre; The Perkin-Elmer Corporation, Norwalk, CT 06856

The purpose of this paper is to discuss new applications of optical instrumental methods for selective detection in liquid chromatography.

Infrared Spectrophotometry. The use of IR for detection is compatible with some forms of nonaqueous normal-phase and reversed-phase chromatography or GPC using typically THF, chloroform, acetonitrile-THF or hexane-chlorocarbon, each in relatively narrow wavelength ranges. It has special advantages in specific functional group monitoring which can be highly selective. The fact that in this way interfering compounds can be minimized is particularly important in quantitative analysis: examples are the analysis of polystyrenes and phthalates (aromatic stretch at 1604 cm^{-1}), cholesterol (OH stretch and 3401 cm^{-1}) and phospholipids (OH stretch plus C-H stretch at 1741 cm^{-1}).

Fluorescence Spectrophotometry. Usually, fluorescence is considered only as a detection method for trace analysis where high sensitivity is required. However, in addition, one of the most powerful fingerprinting techniques is the use of synchronously excited fluorescence emission spectra where excitation and emission are scanned together at an appropriate wavelength offset. The resulting spectrum generally contains one fairly sharp peak the maximum of which is fairly unique to the particular substance. For example the maximum for phenylanalyne is at 260/280 nm (ex./em.) Examples for the use of this type of selective detection with aromatic amino acids and polynuclear aromatic hydrocarbons will be presented.

Polarimetry. Many times, the combination of a mass detector (e.g. refractive index) with measurement of optical activity provides additional possibilities in both qualitative and quantitative analysis. In this way errors by interfering components can be avoided and quantitation of the (D) and (L) forms in a peak can be performed. An example for the former is the analysis of fruit juices for carbohydrates where the interference of co-eluting compounds is eliminated while examples for the latter is the analysis of penicillamine where the total amount is measured by R.I. and the amount of the two optical forms by a polarimeter in series to the refractometric detector.

LIQUID CHROMATOGRAPHY WITH ELECTROCHEMICAL DETECTION: A SENSITIVE ALTERNATIVE TO GCMS IN SELECTED APPLICATIONS. RONALD E. SHOUP, Research Laboratories, Bioanalytical Systems, 1205 Kent Ave., W. Lafayette, IN 47906

Since the initial development of thin-layer amperometric detectors for liquid chromatography in 1972, they have grown in popularity to the point where they now rival fluorescence as the second most popular LC detector for trace determinations. The electrochemical detection of oxidizable substances eluted from reverse phase columns is widely used for a variety of industrial, environmental, and biological applications. In optimum cases, as little as 10 picograms injected into the system may be detected. LCEC has also been used for reducible substances, but progress in this area has been developing more slowly until very recently. In addition, the use of multielectrode detectors can afford considerable advantage in improving the identification of detected peaks.

Although relatively few types of functional groups are electrochemically reactive, those that do exhibit redox activity are sufficiently important from either a biochemical or industrial standpoint to establish LCEC as a useful analytical procedure. Phenols aromatic amines, sulfhydryls, nitro compounds, quinones, and nitroso compounds all possess redox activity. Examples from these groups will be discussed in terms of advantages LCEC offers over more conventional schemes such as LCUV, LCF, or GCMS.

Recent Development in Catecholamine Analysis by HPLC: A Review

Paul S. Satoh, Ph.D. and Rose Mary Kupiecki
Upjohn Diagnostics, The Upjohn Company, Kalamazoo, Michigan 49001

INTRODUCTION

Analysis of catecholamines, especially Epinephrine (E), Norepinephrine (NE), and Dopamine (DA) in plasma and urine was considered important for monitoring patients with hypertension, neurocrest tumors, melanoma and some autonomic nervous system disorders. Methods for quantitative measurements for these catecholamines have wide ranges of sensitivity which limits the application of particular methodology. A spectrophotometric method for Epinephrine and Norepinephrine gives a sensitivity range of 1 ng to 1 microgram. However, a fluorometric method combined with high performance liquid chromatography (HPLC) provides sensitivity applicable for determination of plasma catecholamines in as low as from 100 microliters of specimens as described by Yui and his coworkers (1). Gas Chromatography (GC) and GC-Mass Spectroscopy (GC-MS) provide high sensitivity applicable for any biological fluid. However, the latter method requires high cost instrumentation, extraction and derivatization of the samples prior to injection into GC or GC-MS.

Fluorometric method, namely Trihydroxyindol method (THI), shows extremely high sensitivity when combined with HPLC and post-column derivatization. Yet, the limitation of this method is that it is not applicable for determination of Dopamine.

Finally, electro-chemical detector combined with HPLC separation, though it requires extraction and sample preparation, also provides relatively high sensitivity 1f10 pg to 1 ng. The method is applicable for determination of plasma catecholamines if specimen size is adequately large, e.g., 1 to 5 ml. When assaying catecholamines at low concentration using an electrochemical detector, the electrode must be carefully maintained as it becomes part of the reactant.

RADIOENZYMATIC ASSAY OF CATECHOLAMINES:

In 1977, Peuler and Johnson (2) developed a radioenzymatic method for quantitative determination of catecholamines. This method, though requiring extraction, provides the sensitivity high enough to assess the plasma catecholamine levels of 50 µl of subjects.

The radioenzymatic method uses an enzyme reaction catalized by catechol-o-methlyl transferase. A radioactive methyl group is transferred from S-Adnosyl-Methionine (SAM). The major products of this enzyme reaction are 3-Methanephrine (3MN), 3-Normetanephrine (3NMN), and 3-Methoxy-Tyramine (3MT). These products are extracted with toluene/isoamyl alcohol in the presence of large excess of carrier methylated catecholamines. The organic layer is acidified to transfer the methyl catecholamines to the acetic acid layer. The compounds are then mixed with ethanol to be applied on a Thin Layer Chromatography plate (TLC). Since the reagent to stop the catecholo-transferase (COMT) contains standard compounds as carrier, these products can easily be visualized on the TLC plates under UV light. While the reaction products of the COMT contain radio-labeled methyl group, it is possible to collect radioactive fractions corresponding to the standard compounds, and the unknown specimens are assayed as compared with the standard. The sensitivity of the assay at twice the blank level is 5 picograms for NE, 3 picograms for E, and 20 picograms for DA per 50 µl plasma sample. Intra-assay precision (CV) between 0 to 3000 picograms is 4.2% for NE, 3.6% for E and 4.6% for DA. Inter-assay CV is 9.6% for NE, 8% for E and 30.4% for DA. This radioenzymatic assay is available as CAT-A-KIT™ from Upjohn Diagnostics. Tassaron, et al evaluated the performance of the assay kit (3).

HPLC ANALYSIS OF CATECHOLAMINE:

There are several HPLC methods for determination of catecholamines: Mell and Gustafson (4) by reverse phase HPLC and THI, Kissinger by reverse phase and EDC (5), Yui by ionexchange column and THI (1) and Scratchley, et al (6) to compare various methods.

More recently the products of COMT reactions are separated by HPLC to facilitate the automated radioenzymatic analysis of catecholamines. Klaniecki, et al (7), Endert (8) and Muller (9) made successful separation of COMT products.

We reproduced Mullers HPLC system, which showed four peaks out of six COMT products (3 NMN, 3-MN + 4 NMN, 3 MT + 4 MN, and 4 MN). We developed a new HPLC system using radial compression C-18 column (Waters Associates) with mobile phase of 0.6 part phosphonic acid, 1 part pentane sulfuric acid and 0.5 part acetonitrile per 1000 parts of distilled water. This system separated all 6 COMT products, in 6 minutes. Using this HPLC system, we were able to determine plasma catecholamine levels semi-automatically. The plasma catecholamine levels obtained by HPLC separation were comparable to those obtained by TLC separation.

REFERENCES:

(1) Yui, Y., Fujita, T., Yamamoto, T., Itokawa, Y., and Kawai, C. Liquid Chromatographic Determination of Norepinephrin and Epinephrine in Human Plasma, Clin. Chem., 26 (2) 194-196 (1980).

(2) Peuler, J.D., and Johnson, G.A. Simultaneous Single Isotope Radioenzymatic Assay of Plasma Norephinephrine, Epinephrine and Dopamine, Life Science, 20, 625-636 (1977).

(3) Tassaron, S.J.A., Tiolet, J.W.T., and Lillbrands, A.F. Evaluation of Radioenzymatic Assay for Catecholamines, Clin. Chem., 26 (1), 120-122 (1980).

(4) Mell, L.D. and Gustafson, A.B. Urinary Free Norepinephrine and Dopamine Determined to Reverse Phase HPLC, Clin. Chem., 23 (3), 473-476 (1977).

(5) Kissinger, P.T., Craig, S., Brunetlett, S., Davis, G.C., et al. Recent Development in Clinical Assessment of Aromatic Catecholamines by HPLC, Clin. Chem., 23 (8), 1449-1455 (1977).

(6) Scratchley, G.A., Masoud, A.N., Stohs, S.J. and Wingard, D.W. HPLC Separation and Detection of Catecholamines, J. Chromatography, 169, 313 (1979).

(7) Klaniecki, T.S., Corder, C.N., McDonald, R.H. and Feldman, J.A. J. Lab. Clin. Med., 90, 604-612 (1977).

(8) Endert, E. Determination of Noradrenaline and Adrenaline in Plasma by Radioenzymatic Assay Using High Pressure Liquid Chromatography for the Separation of the Radiochemical Products, Clinica Chim. Acta., 96, 233-239 (1979).

(9) Muller, T.H., Hofschuster, E., Kuss, H.J. and Welter, D. A Highly Sensitive and Precise Radioenzymatic Assay for Plasma Epinephrine and Norepinephrine, J. Neural Transmission, 45, 219-225 (1979).

PRINCIPLES OF RADIOIMMUNOASSAY APPLIED TO LOW MOLECULAR WEIGHT COMPOUNDS; F. A. FITZPATRICK, Drug Metabolism Research, The Upjohn Company, Kalamazoo, MI 49008

Immunoassay saturation binding methods, typified by radioimmunoassay, are powerful analytical methods. Conventional radioimmunoassays exist for scores of macromolecules (insulin, albumins, polypeptide hormones...) and for small molecules, designated haptens (steroids, prostaglandins, cyclic nucleotides, pharmaceuticals, enkephalins...). Provisionally, radioimmunoassay (RIA) is a sensitive, selective, reliable, and productive method. In this context we will examine complementary and competitive features of RIA versus mass spectroscopy by, first, defining the principles of the radioimmunoassay, its practical requirements, and its known limitations. Second, we will present some concrete examples of RIA as a quantitative method for measuring low molecular weight lipids (prostaglandins), juxtaposed with similar measurements by GC/MS.

THE USE OF GC/MS AND GC/FTIR TO SOLVE INDUSTRIAL PROBLEMS

David M. Hindenlang and Danne E. Smith

Allied Corporation, P.O. Box 1021R, Morristown, NJ 07960

The combination of gas chromatography with mass spectrometry (GC/MS) has been recognized for some time as one of the most powerful techniques available to the analytical chemist. However, analysis by GC/MS alone does not always provide sufficient information to make possible unambiguous identification of unknown components. While the analyst may obtain a molecular weight and empirical formula for each component in a mixture from GC/MS, he still may not be able to determine the substitution pattern in the molecule. The combination of gas chromatography with Fourier transform infrared spectroscopy (GC/FTIR) can provide such structural information for each individual component even in complex organic mixtures. Hence, the data obtained from GC/MS and GC/FTIR are complementary, and the combination often aids the analytical chemist in his problem-solving.

Two examples of the combined application of GC/MS and GC/FTIR to industrial analytical problems serve to illustrate. In a commercial mixture of cis and trans isomers of 1,4-dicyano-1-butene, a third component was observed by GC. Methane chemical ionization mass spectrometry (CIMS) indicated this component to have the same molecular weight as the knowns. GC/FTIR was used to identify which GC peaks corresponded to the cis and trans isomers as well as to identify the third component as trans-1,4-dicyano-2-butene.

Methane CIMS revealed that each of two unknown components in a sample of tar acids had a molecular weight of 144. Application of GC/FTIR resulted in the identification of these components as 1-naphthol and 2-naphthol using digital subtraction to clean up the spectra and a computer search of a vapor phase spectral library to verify the identifications.

IMPROVED ORGANIC IDENTIFICATION USING COMBINED CAPILLARY GAS CHROMATOGRAPHY/MASS SPECTROMETRY/FOURIER TRANSFORM INFRARED (GC/MS/FTIR)

R. W. Crawford, T. B. Hirschfeld, R. H. Sanborn, C. M Wong, and H. R. Brand

Lawrence Livermore National Laboratory
P. O. Box 808, L-325
Livermore, CA 94550

Although GC/MS is a very powerful tool, it is weak in two areas: (1) Ability to distinguish between isomers and (2) Ability to rapidly identify unknowns not contained in libraries of reference spectra. We have interfaced a FTIR to our GC/MS to help alleviate these problem.

A simple splitter is connected to the end of a SCOT column and 90% of the effluent is sent to the FTIR with the remainder going to the MS. Makeup gas is added to the FTIR stream to maintain resolution in the light pipe. Separate computers on each spectrometer control the instruments and acquire and store data. Library searching is done on each separate computer system.

Applications of this new technique to a variety of sample types will be described. Significant speed and lack of ambiguity have been realized by combining the instruments, especially in complex mixes.

Progress will be reported on increasing FTIR sensitivity using smaller light pipes and detectors. Also, progress on a computer network using a third computer as a "mother" for both instruments will be described.

Work performed under the auspices of the U. S. Department of Energy at the Lawrence Livermore National Laboratory under Contract W-7405-Eng-48.

ON THE POPULATION OF BENZYL AND TROPYLIUM IONS ORIGINATING FROM $C_7H_8^+$; P. AUSLOOS and S. G. Lias; National Bureau of Standards, Washington, D. C. 20234

Benzyl and tropylium ions were prepared by ionization of toluene and toluene-α-d_3 through electron impact and charge transfer from Xe^+, Kr^+, and Ar^+ in an ion cyclotron resonance spectrometer.
The fraction of the $C_7H_7^+$ ions which react with toluene as benzyl ions was found to increase with the energy content of the molecular ion from 57% at 2.9 eV (Xe^+ precursor), to 76% at 4.7 eV (Kr^+ precursor), and 83% at 6.4 eV (Ar^+ precursor). (About 2.1 eV is required for the process: $c\text{-}C_6H_5CH_3^+ \rightarrow C_6H_5CH_2^+ + H.$) Also, an increase in electron energy from 12 to 70 eV results in a continuous rise of the benzyl ion population from 20% to 63%. These findings are in apparent conflict with recent collisional activation[a] studies which show a gradual increase of the percent benzyl ions from threshold to 15 eV, followed by a sharp decline to reach a benzyl ion fraction of 30% at 70 eV. The fall-off at high energies has been attributed to a fast equilibration [$cyclo\text{-}C_7H_7^+ \rightleftarrows C_6H_5CH_2^+$], favoring the tropylium structure. The discrepancy between the CA and ICR results would then be explainable by assuming a displacement of the equilibrium by ion-molecule collisions. In order to assess this hypothesis, the degree of H/D scrambling in benzyl-d_2 ions from $C_6H_5CD_3$ was measured as a function of energy. It was found that unscrambled $C_6H_5CD_2^+$ ions account for 19%, 32%, and 46% of the benzyl-d_2 population produced in charge transfer from Xe^+, Kr^+, and Ar^+, respectively.

a. F. W. McLafferty and F. M. Bockhoff, J. Am. Chem. Soc. 101, 1783 (1979).

THE BENZYL AND TROPYLIUM CATIONS, TWO DISTINCT AND STABLE SPECIES IN THE GAS PHASE. D. K. SEN SHARMA and P. KEBARLE, Chemistry Department, University of Alberta, Edmonton, Canada T6G 2G2.

Evidence that the tropylium cation is a major constituent of the $C_7H_7^+$ ions produced by electron and photon impact from toluene and alkyl-benzenes has existed in the literature for some years. The rearrangement benzyl$^+ \rightleftarrows$ tropylium$^+$ is one possible route by which the tropylium cation may be formed. Ion molecule reaction studies involving $C_7H_7^+$ species produced by hydride abstraction from toluene or chloride abstraction from benzyl chloride show that these ions engage in a number of characteristic reactions. The $C_7H_7^+$ ions produced by hydride abstraction from 1,3,5-cycloheptatriene do not participate in any of the above reactions. These ions are very stable and so far were not observed to engage in any reactions. On basis of this distinction, it is concluded that the reactive $C_7H_7^+$ species produced from toluene and benzyl chloride are benzyl cations, while the $C_7H_7^+$ from 1,3,5-cycloheptatriene is tropylium$^+$. The rearrangement benzyl$^+ \rightleftarrows$ tropylium$^+$, does not occur in the gas phase even at temperatures as high as 300°C. It does not occur even if the benzyl$^+$ resp. tropylium$^+$ are highly vibrationally excited.

A complete account of the above investigations will appear in the Canadian Journal of Chemistry, summer 1981.

THE $C_7H_7O^+$ ION: BENZYL VS TROPYLIUM ION STRUCTURES; D. H. RUSSELL; Dept. of Chem., Texas A&M Univ., College Station, TX. 77843; E. H. MCBAY and D. C. CANADA, Anal. Chem. Div., Oak Ridge Nat'l Lab., Oak Ridge, TN. 37830

The $C_7H_7O^+$ ion (m/z 107) is an important secondary ion in the mass spectra of many alkyl phenols, substituted benzyl alcohols, and substituted alkyl phenyl ethers, and with respect to the question of benzyl vs tropylium ion structures. In an earlier study on the unimolecular dissociation reactions of various $C_7H_7O^+$ ions the experimental results were interpretated as the ions generated by fragmentation of the methyl phenols not isomerizing to a tropylium ion structure, i.e, the hydroxytropylium ion. However, more recent investigations using collision-induced dissociation (CID) have revealed that the methyl phenol and hydroxytropylium $C_7H_7O^+$ ions are indistinguishable by this technique. The results of the CID experiments and the apparent ambiguities of the unimolecular/CID results will be discussed. In addition, the CID spectra of a number of other $C_7H_7O^+$ ion will be discussed. A detailed discussion of the thermochemistry of the $C_7H_7O^+$ ion will be presented.

KINETIC EVIDENCE FOR TWO DISTINCT STRUCTURES OF $C_3H_3^+$; S. G. LIAS and P. Ausloos; National Bureau of Standards, Washington, D. C. 20234

It has recently been suggested[a] that $C_3H_3^+$ is the main precursor ion leading to the nucleation processes resulting in soot formation in acetylene and benzene flames. Until now, however, there have been no systematic investigations of the bimolecular reactions of $C_3H_3^+$ with organic molecules, and in fact, this species is generally believed to be chemically unreactive. Results obtained in a pulsed ICR indicate that while $C_3H_3^+$ ions formed at energies close to threshold for formation of the ion from the parent molecule ion have the cyclic structure, the $C_3H_3^+$ ions formed in allene, propyne, and propargyl halides with 1-2 eV excess energy have two distinct structures, one of which is reactive towards the parent molecule and one of which is not. The reactive $C_3H_3^+$ ions, which can be identified with the linear propargyl structure, react rapidly with acetylene to form condensation products; this reaction has been proposed as the first step in the process leading to soot formation. The cyclic $C_3H_3^+$, although unreactive towards alkanes and lower molecular weight aromatic molecules, is found to react with a variety of high molecular weight saturated molecules by hydride transfer, while condensation-type reactions occur with highly unsaturated hydrocarbons.

PROPYL IONS AND PROTONATED CYCLOPROPANE AS INTERMEDIATES IN THE REACTION OF METHYL CATIONS WITH ETHYLENE

R. N. Abernathy and F. W. Lampe
Department of Chemistry, The Pennsylvania State University
University Park, Pennsylvania 16802

Despite the large amount of published work on ion-molecule reactions in hydrocarbon systems, only one report describing the reaction of CH_3^+ with C_2H_4 has appeared in the literature. Fiaux, Smith and Futrell[1] showed that at low collision energies the reaction proceeds via a short-lived $C_3H_7^{+*}$ intermediate in which complete randomization of H-atoms occurs before decomposition takes place to the observed products $C_2H_3^+$, $C_3H_3^+$ and $C_3H_5^+$. This is a quite different behavior than that reported[2-4] for the formally similar reaction of SiH_3^+ with C_2H_4. The latter reaction has been shown to proceed via an intermediate $SiC_2H_7^{+*}$ (thought to be $CH_3CH_2SiH_2^+$) that is sufficiently long-lived to be observable at collision energies below 1 eV. It is of interest to examine the questions of (1) the structure of the $C_3H_7^+$ intermediate and (2) why the intermediates in these analogous reactions should be so different.

The reaction was studied in an ion-beam-scattering-gas apparatus that has been described in the literature.[5] $^{12}CH_3^+$, and $^{13}CH_3^+$ ions obtained from the decomposition of $^{12}CH_4$ and $^{13}CH_4$ in an arc discharge and having 2.6 eV of kinetic energy were injected into C_2H_4 or C_2D_4 at 0.25-2.5x10^{-3} torr and the product ion spectrum recorded. The fractional abundances of ionic products were extrapolated to zero pressure in order to eliminate secondary reactions. The results are shown in Table 1.

Table 1

Ton($\frac{m}{q}$)	$^{13}CH_3^+/C_2H_4$	$^{12}CH_3^+/C_2D_4$	$^{12}CH_3^+/C_2D_4$ (Statistical)	$^{13}CH_3^+/C_2H_4$
16		0.01		
17		0.01		
18		0.01		
27	0.81	0.03	0.022	0.34
28	0.02	0.25	0.267	0.50
29	0.01	0.33	0.401	
30		0.17	0.039	
39	0.04			
40		0.01	0.015	0.05
41	0.12	0.02	0.022	
42		0.01	0.005	0.10
43		0.03	0.036	
44		0.08	0.073	
45		0.02	0.018	

The data in the second column show that $C_2H_3^+$ is by far the major product for 2.6 eV CH_3^+ ions; $C_2H_3^+$ is the major ionic product for 0.1 eV CH_3^+ ions also, but the ion fraction at this lower energy is 0.53.[1] The reaction forming this ion, namely (1), is formally a hydride-ion transfer which, at low energies[1], proceeds

$$CH_3^+ + C_2H_4 \rightarrow C_2H_3^+ + CH_4 \qquad (1)$$

by decomposition of a $C_3H_7^{+*}$ intermediate. The data in the third and fourth columns of Table 1, relative to the reaction of $^{12}CH_3^+$ with C_2D_4 show that at 2.6 eV also the reaction proceeds via a $C_3H_7^{+*}$ intermediate in which H and D atoms undergo complete scrambling before decomposition.

The data in the fifth column of Table 1 are the fractional ion intensities observed when $^{13}CH_3^+$ ions are injected into C_2H_4. The distribution of the vinyl ion ($^{12}C^{12}CH_3^+$ and $^{12}C^{13}CH_3^+$) intensities at m/q=27 and 28 amu indicates that, like the hydrogen atoms, the carbon atoms also become nearly indistinguishable in the intermediate $C_3H_7^+$. If the intermediate complex had the normal propyl ion structure ($^{13}CH_3CH_2CH_2^+$), the predicted intensity ratio of m/q=28 to m/q=27 is 1. If, however, protonated cyclopropane were the intermediate complex, the predicted intensity ratio of m/q=28 to m/q=27 is 2. Since the observed ratio of 1.5 is intermediate to those predicted by the models, we conclude that protonated cyclopropane and secondary propyl ion play equally important roles as intermediates in the major reaction of CH_3^+ with C_2H_4.

In contrast to the SiH_3^+/C_2H_4 reaction, in which over 90% of the decomposition of the intermediate $SiC_2H_7^+$ is back to reactants, decomposition of the $C_3H_7^+$ intermediate back to reactants is negligible. This suggests that in the CH_3^+/C_2H_4 system, the activation energy back to reactants, E_{ob}, is greater than that in the forward direction to products, namely E_{of}, while the reverse is true in the SiH_3^+/C_2H_4 system. Because $E_{of} < E_{ob}$ the collision complex $C_3H_7^{+*}$ must contain an excitation energy higher than the lowest barrier to decomposition (i.e. E_{of}) of at least E_{ob}~E_{of}. Having always a significantly high excitation energy above the lowest decomposition barrier, the collision complexes are predicted by unimolecular rate theory to be short-lived. On the other hand, in the SiH_3^+/C_2H_4 system $E_{of} > E_{ob}$ so that most of the complexes decompose in the backward direction. In this case, the excitation energy in the $SiC_2H_7^{+*}$ above the lowest barrier to decomposition approaches zero as the kinetic energy approaches zero. Hence, for the latter case, the complexes are long-lived for reactant ions of low kinetic energy.

---

1. A Fiaux, D. L. Smith and J. H. Futrell, Int. J. Mass Spectrom. Ion Phys. 25, 281 (1977).

2. T. M. Mayer and F. W. Lampe, J. Phys. Chem. 78, 2433 (1974).

3. W. N. Allen and F. W. Lampe, J. Am. Chem. Soc. 99, 6816 (1977).

4. R. N. Abernathy and F. W. Lampe, J. Am. Chem. Soc. 103, xxxx (1981) IN PRESS.

5. G. W. Goodloe and F. W. Lampe, J. Am. Chem. Soc. 101, 6028 (1979).

GAS-PHASE ION CHEMISTRY WITH AND WITHOUT SOLVENT. Diethard K. Bohme* and Gervase I. Mackay. Department of Chemistry, York University, Downsview, Ontario M3J 1P3.

Room-temperature measurements with a flowing plasma mass-spectrometer (flowing afterglow) system are reported which explore the transition in the kinetics and energetics of ion-molecule reactions from their solvent-free behaviour to that observed in solution. Results are reported for proton-transfer reactions of the type:

$$B^-.S_n + AH = A^-.S_m + (n-m)S + BH$$

and nucleophilic displacement reactions of the type:

$$B^-.S_n + CH_3Br = Br^-.S_m + (n-m)S + CH_3B$$

The kinetics of these reactions are followed as a function of the step-wise solvation of B^- up to $n = 3$. The results provide a vivid confirmation of our qualitative concepts of solvent effects and an indication of the absolute influence of solvent on such reactions.

TANDEM MASS SPECTROMETRIC STUDIES OF THE REACTIONS OF SOLVATED ANIONS

P. M. Hierl,* M. J. Henchman,# and J. F. Paulson
Air Force Geophysics Laboratory, Hanscom AFB, MA 01731

Summary

A tandem mass spectrometer has been used to measure cross sections for the reactions of the solvated ion $OH^-(H_2O)_n$ (where n = 0, 1, 2 or 3) with the neutral molecules CO_2, SO_2, CH_3Cl, and CH_3Br over the range of reactant translational energy 0.15 - 25 eV (LAB). With CO_2 and SO_2 the major reaction channels are solvent switching (with the neutral reactant replacing one or more of the water molecules) and collision-induced dissociation. With the methyl halides the major reaction channels are nucleophilic substitution, proton transfer and collision-induced dissociation.

Experimental

The measurements reported here were made with the AFGL tandem mass spectrometer.[1] Reactant negative ions were formed indirectly by ion-neutral reactions in a high-pressure, electron-bombardment ion source. These ions were mass analyzed by a 2.54 cm, 90° magnetic sector mass spectrometer and then decelerated to the desired kinetic energy before entering the neutral gas collision chamber. Since the target gas pressure (measured by a capacitance manometer) was typically 2-3 mtorr and the collision path length was 0.2 cm, single collision conditions obtained. Reactant and product ions emerging from this chamber were accelerated by a series of grids and mass analyzed in a 46 cm quadrupole mass filter before being counted with a particle multiplier and conventional nuclear pulse counting equipment.

Results

CO_2, SO_2: At collision energies less than about 1 eV (CM) the solvated anions $OH^-(H_2O)_n$ (n = 1 - 3) react very rapidly with CO_2 and SO_2. In all cases but one, the major products are HCO_3^- and HSO_3^-, respectively. (The exception is the system $OH^-(H_2O)_3 + CO_2$, for which the major product is $HCO_3^-\cdot H_2O$.) Apparently the excess energy released in these exothermic solvent switching reactions causes H_2O "boil off" from the products.[2] The cross sections for these reactions are very large, approaching several hundred square Ångstroms at low collision energies. These cross sections generally decrease with collision energy as $E^{-1/2}$ up to about 1 eV; at higher collision energies, the cross sections generally decrease much more rapidly with energy. This is most noticeable in the reactions leading to hydrated ionic products (e.g., $HCO_3^-\cdot H_2O$), where the increased collision energy facilitates the boil off of the water of hydration.

CH_3Cl, CH_3Br: Nucleophilic substitution is the dominant reaction channel at collision energies less than about 1 eV. The major products are the unsolvated ions Cl^- and Br^-, although the singly hydrated products $Cl^-\cdot H_2O$ and $Br^-\cdot H_2O$ are also observed. It is found that increasing the solvation of the reactant nucleophile substantially decreases the rate constant for nucleophilic substitution. This could be a consequence of steric hindrance as the nucleophile approaches the substrate, or of charge delocalization in the attacking nucleophile, or both.

With the unsolvated OH^- reactant proton transfer yielding CH_2Cl^- or CH_2Br^- competes effectively with nucleophilic substitution at collision energies above 1 eV. With the solvated reactant anions, collision-induced dissociation becomes the dominant reaction channel at collision energies about 1 eV.

A more complete description of this work is being prepared for publication.

* Permanent Address: Department of Chemistry, University of Kansas, Lawrence, KS 66045

‡ Permanent Address: Department of Chemistry, Brandeis University, Waltham, MA 02154

References

1. J. F. Paulson, J. Chem. Phys. 52, 963 (1970).
2. F. C. Fehsenfeld and E. E. Ferguson, J. Chem. Phys. 61, 3181 (1974).

THE TEMPERATURE DEPENDENCE OF ION-MOLECULE REACTIONS AND ION DIFFUSION IN N_2, CO AND A CO/CO_2 MIXTURE.

J.V.Headley, R.S.Mason & K.R.Jennings

Department of Chemistry and Molecular Sciences,
University of Warwick, Coventry, CV4 7AL. U.K.

As part of a study of ion-molecule reactions believed to be of importance in controlling graphite corrosion in gas-cooled nuclear reactors, three body association reactions of the type $A^+ + 2A_2 \rightarrow A_2^+ + A$ have been studied as a function of temperature and pressure in a pulsed electron beam high pressure source fitted to an MS50 mass spectrometer (Kratos Scientific Instruments Ltd.). Literature values on the temperature dependence of these reactions show considerable discrepancies so that extrapolation of the data to 600-750 K, the operating temperature of the reactors, is subject to considerable error.

Ions are produced by a 1-10 μs pulse of 400 eV electrons in the pressure range 0.5-3.2 Torr over the temperature range 324-550K. After leaving the ion exit slit, ions are accelerated towards a high transmission grid at a potential of -50V with respect to the source before being subjected to the full accelerating voltage of 8000V. The open construction in this region minimises the occurrence of collision-induced decompositions. In order to avoid problems arising from the formation of oxide layers in the presence of oxygen-containing molecules, all surfaces in the ion source were gold-plated on nickel. Immediately after the pulse of electrons, charged species are lost by ambipolar diffusion until their density is sufficiently low for there to be a sharp change to loss of positive ions by free diffusion. All observations were carried out in this second region of diffusive loss, when reactant ions are lost both by chemical reaction and by diffusion. It has been customary to allow for diffusive loss of ions by normalising ion currents but in the presnt work, data have been analysed to allow explicitly for loss by both chemical reaction and diffusion.

At constant pressure and temperature, both processes give rise to a pseudo-first order decay of A^+ ions if the back reaction can be neglected:

$$A^+ + 2A \xrightarrow{k_1} A_2^+ + A \qquad (1)$$

$$A^+ \xrightarrow{a'} \text{Lost on walls} \qquad (a)$$

where k_1 and a' are the pseudo-first order rate constants.

Therefore $\frac{-d[A^+]}{dt} = k_1[A^+][A]^2 + a'[A^+]$

so that $\frac{-d[A^+]}{[A^+]} = k_1[A]^2 + a' = (k_1' + a')dt \qquad [1]$

where $k_1' = k_1[A]^2$

Putting $I(A^+) \propto [A^+]$ and integrating,

$$I(A^+)_t = I(A^+)_{t=o}\ e^{-(k'_1 + a')t}$$

A plot of $\ln I(A^+)_t$ against t at constant pressure therefore gives a straight line of slope $S = (k' + a')$. The pseudo-first order rate constant $k'\alpha\ [A]^2$ and $a'\alpha\ [A]^{-1}$ so that

$$S = k_1[A]^2 + a/[A] \quad \text{or} \quad S[A] = k_1[A]^3 + a$$

Hence a plot of $S[A]$ against $[A]^3$ gives a straight line of slope k_1 and intercept a. By working at different temperatures, the temperature dependences of these two rate constants can be obtained.

Results

(a) Values of k_1 for various association reactions at 300K are given in the following Table together with values of n where $k_1 = CT^{-n}$. Literature values are included for comparison.

Reaction	$k_{300}/10^{-29}$ cm^6 molecule^{-2}s^{-1}	n	Ref.
$N_2^+ + 2N_2 \rightarrow N_4^+ + N_2$	4.5	3.8 ± 0.3	This work
	10	1.7	1
	8.0	4	2
$CO^+ + 2CO \rightarrow (CO)_2^+ + CO$	13	3.3 ± 0.2	This work
	11.4	1.5	1
$CO_2^+ + CO_2 + M \rightarrow (CO_2)_2^+ + M$ (M = CO, CO_2)	26	4.5 ± 0.2	This work
$CO_2^+ + CO + M \rightarrow (CO_2.CO)^+ + M$	29.3	3.8 ± 0.4	This work
$HCO^+ + 2CO \rightarrow H(CO)_2^+ + CO$	0.10	6.9 ± 0.4	This work
		3.2	1
		6.4	3

(b) Diffusion coefficient temperature dependences x, where $Dn/\lambda^2 = \alpha T^x$, were determined as follows:

Ion/Gas	N_2^+/N_2	N_4^+/N_2	CO^+/CO	$(CO)_2^+/CO$
x	0.62 ± 0.4	0.80 ± 0.3	0.10 ± 0.6	0.32 ± 0.1

Discussion

Literature values of n tend to fall into low or high values and where comparison is possible, the results of the present work favour the higher temperature dependence. The values are qualitatively in agreement with predictions of RRK theory but a detailed interpretation must await a more thorough treatment in terms of RRKM theory. If the experimental data are analysed using the usual normalised ion current method, k_{300} increases by about 20% but the value of n does not change significantly. The Chapman Enskog theory predicts $D\ \alpha T^{0.67}$ for an r^{-12} potential and $D\ \alpha T$ for an r^{-4} potential. The values of x obtained for the four ions show unexpectedly that the dimer ions diffuse more rapidly than the monomeric ions. This is ascribed to the effects of resonance charge transfer and to ion or solvent molecule switching reactions.

A full account of this work has been submitted to J. Chem. Soc. Faraday Transactions I.

References

1. M. Meot-Ner & F. H. Field, J. Chem Phys. (1974), 61, 3472.
2. A. Good D. A-Durden & P. Kebarle, J. Chem. Phys. (1970), 52, 212.
3. K. Hiraoka, Int. J. Mass Spectrom. Ion Phys. (1980), 33, 73.

GAS-PHASE NUCLEOPHILIC REACTIONS AT SATURATED AND CARBONYL CARBON. Richard N. McDonald* and A. Kasem Chowdhury, Department of Chemistry, Kansas State University, Manhattan, Kansas 66506.

Our gas phase studies of ion-molecule reactions are carried out in a flowing afterglow apparatus with helium as the buffer gas (conditions: P_{He} = 0.5 torr, $\bar{v}$ = 80 m s^{-1}, and 298K). Phenylnitrene anion radical ($PhN^{\cdot-}$) ($PhN_3 + e^- \rightarrow PhN^{\cdot-} + N_2$) is kinetically a poor nucleophile in S_N2 displacement reactions (with CH_3Br, k = 1.8 x 10^{-11} cm^3 $molecule^{-1}$ s^{-1}). However, we have shown that $PhN^{\cdot-}$ is a good nucleophile toward addition to carbonyl groups.[1] Since the addition adduct 1 is a free radical as well as an anion, radical β-fragmentation yields the observed acyl-anilide anion products. In support of this mechan-

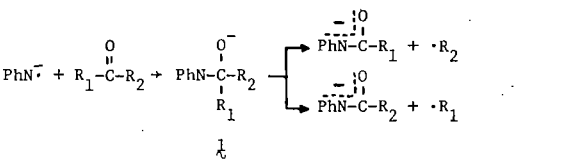

(1)

(2)

ism, we have found that the reactions of $PhN^{\cdot-}$ with $CF_3CO_2CH_3$, $CF_3CO_2C_2H_5$, and $CF_3CO(SC_2H_5)$ (i) occur with the same rate constant ((8±1) x 10^{-10} cm^3 $molecule^{-1}$ s^{-1}), (ii) are independent of the overall exothermicity (-16, -13, and -44 kcal $mole^{-1}$, respectively), and (iii) exclusively yield the same product ion $PhN{=}C(O^-)CF_3$ (eq 1; $R_1 = CF_3$, $R_2 = OCH_3$, OC_2H_5, or SC_2H_5). The absence of rate constant dependency on reaction exoergicity is consistent with the intermediacy of tetrahedral adduct 1 in the slow step followed by an equivalent, fast fragmentation step from the three adducts. Formation of 1 then effectively "insulates" the rate constant from ΔH_{rx}.

$S^{\cdot-}$ is known to be a better S_N2 nucleophile than $PhN^{\cdot-}$.[2] The fast reaction of $S^{\cdot-}$ with $CF_3CO_2CH_3$ yields 35% CF_3COS^- and 65% $CF_3CO_2^-$ while the equally fast reaction with $CF_3CO_2C_2H_5$ gives 96% CF_3COS^- and 4% $CF_3CO_2^-$; CF_3COS^- formed by addition/fragmentation and $CF_3CO_2^-$ from S_N2 displacement (or E2 elimination from the ethyl ester). These results are consistent with similar rate constants for C=O addition and an S_N2 rate ratio of $k_{CH_3}/k_{C_2H_5}$ = 16, the latter value in good agreement with various solution data. A three-minimum potential surface is used to describe these addition/fragmentation processes by hypovalent anion radicals.

It was found that reactions of CF_3CO_2R with various closed shell nucleophiles (e.g. allyl anion) produce $^-CF_3$ as the major, first formed product ion, rather than $CF_3CO_2^-$ if the reaction channel leading to $CF_3CO_2^-$ is highly exothermic ($CF_3CO_2^- \rightarrow {}^-CF_3 + CO_2$; ΔH = +38.8 kcal $mole^{-1}$), along with lesser amounts of carbonyl addition products. The observation (or absence) of $^-CF_3$ has been used to determine whether the S_N2 displacement or the E2 elimination mechanism is the major process involved in certain reactions. F_3C^- was shown to undergo fast and efficient (≥ 0.5) reactions with the starting ester, CF_3CO_2R, yielding variable amounts of $CF_3CO_2^-$ and the addition adducts depending on the nature of R.

The reaction of allyl anion with $(CF_3)_2C{=}O$ yields two product ions, $(CF_3)_2CO^{\cdot-}$ and $H_2C{=}CHCH{=}C(O^-)CF_3$. The channels leading to both products are considered to proceed via a common loose, charge-transfer collision complex. This has important implications in a

number of condensed-phase "nucleophilic" mechanisms considered to involve single electron transfer as the first step.

(1) (a) McDonald, R. N.; Chowdhury, A. K., J. Am. Chem. Soc., 1980, 102, 6146. (b) Ibid., 1981, 103, 674.

(2) Tanaka, K.; Mackay, G. I.; Payzant, J. D.; Bohme, D. K., Can. J. Chem., 1976, 54, 1643.

GAS PHASE HYDROGEN-DEUTERIUM EXCHANGE REACTIONS IN CARBANIONS: EXCHANGE OF VINYL AND ARYL PROTONS BY D_2O. Robert R. Squires, C.H. DePuy and Veronica M. Bierbaum, Department of Chemistry, University of Colorado, Boulder, Colorado 80309

The mechanism and practical applications of gas phase hydrogen-deuterium exchange by D_2O of vinyl and aryl protons in carbanions are reported. Using the flowing afterglow method, we find that under the proper conditions D_2O is capable of exchanging hydrogens which are up to 10-20 kcal/mol less acidic than those in water. Thus, in the 2-phenylallyl anion up to 8 of the possible 9 hydrogens can be observed to exchange in the presence of D_2O:

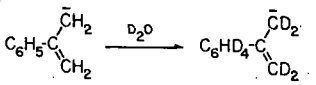

We ascribe this behavior to the presence of the ion-dipole energy in the D_2O-carbanion complex which allows multiple endothermic proton transfers to occur. The key here is that the relative acidity of the allylic and aryl hydrogens must not exceed the ion-dipole energy of the initially formed complex. A simple symmetrical reaction profile for this process is shown below:

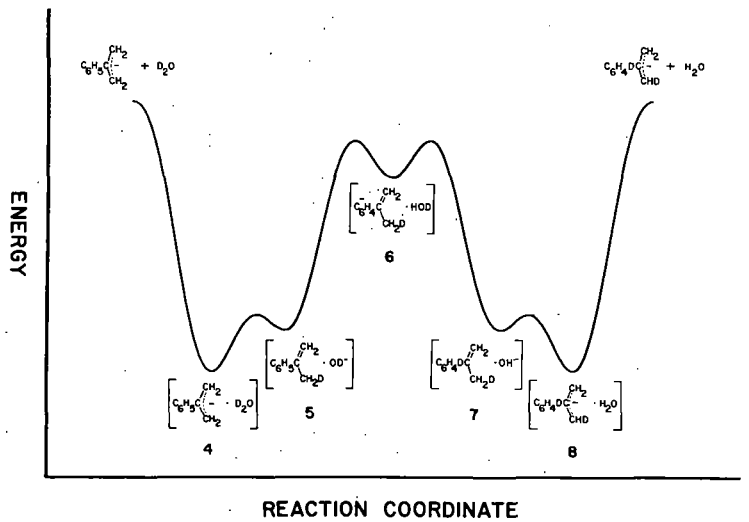

The initially formed ion-molecule complex 4 has up to 20 kcal/mol of excess energy. Some of this energy (say 3 kcal/mol) is used in an endothermic deuteron transfer to form 5. An endothermic proton transfer to OD^- of up to 17 kcal/mol is still possible to form 6. Separation of the complex is only possible when all of the necessary internal energy is regained via intermediates 7 and 8. It is apparent that this mechanism requires an exchange agent possessing at least two deuteriums in order for exchange at the less acidic sites to be observable.

We have observed multiple exchanges of this type in many other anions and a few of these are listed in the Table. These results obviously present a complication with regard to the specificity of H-D exchange. At the same time they offer useful new applications of the technique since in many cases protons of different types in a carbanion can be distinguished by their relative rates of exchange. For example, in the isoprene anion, the four allylic hydrogens exchange most rapidly ($k = 9 \times 10^{-10}$ cc/molec·sec). A fifth proton, which we formulate as that in the 3-position exchanges more

slowly but at a rate which is similar enough to that of the first four to prevent a reliable dissection of its intrinsic exchange rate constant. The final two hydrogens exchange more slowly still with an estimated rate constant of 1 x 10^{-11}cc/molec·sec. Thus, by determining not only the maximum number of exchangeable hydrogens but also their relative ease of exchange, we can gain important information about the structure of the carbanion. Further, in bracketing hydrocarbon acidities the presence or absence of multiple exchanges may serve to fix an upper or lower limit for certain types of hydrogens in the molecule. For instance, we have found that in the 2-t-butylallyl anion only the four allylic hydrogens exchange with D_2O.

Table I. Extent of Hydrogen-Deuterium Exchange of Carbanions with D_2O

Neutral (HA) Producing Anion (A^-)	No. of H Atoms in A^-	Maximum No. of H-D Exchanges Observed
$CH_2=C(CH_3)CH=CH_2$	7	7
$C_6H_5C(CH_3)=CH_2$	9	8
$C_6H_5CH=CH_2$	7	7
2-METHYLENE-5-NORBORNENE 	9	7
C_6H_5F	4	4
$C_6H_5CF_3$	4	4
$CH_2=CHCN$	2	2
$(CH_3)_3CC(CH_3)=CH_2$	13	4

REFERENCES

Stewart, J.H., Shapiro, R.H., DePuy, C.H., Bierbaum, V.M, Jour. Amer. Chem. Soc. 1977, 99, 7650-7653

DePuy, C.H., Bierbaum, V.M., King, G.K., Shapiro, R.H., Jour. Amer. Chem. Soc. 1978, 100, 2921-2922

Hunt, D.F., Sethi, S.K. Jour. Amer. Chem. Soc. 1980, 102, 6953-6963

ISOMERIZATION OF BENZYL CHLORIDE RADICAL CATION DETERMINED BY ICR PHOTODISSOCIATION SPECTROSCOPY;
J. P. Honovich and R. C. Dunbar, Chemistry Department, Case Western Reserve University, Cleveland, OH 44106

The structure of benzyl chloride radical cation produced by electron impact has come into dispute in the literature. Results ranging from zero to seventy percent rearrangement have appeared. Employing ICR photodissociation techniques the authors will present evidence that benzyl chloride radical cations undergo a bimolecular isomerization reaction to yield a rearranged product.
The experiments utilize the fact that different ionic structures have unique photodissociation spectra. A gated laser source in the 458-615 nm region is used to probe the ion population as a function of ion residence time in the ICR cell. Results indicate that electron impact ionization produces a homogeneous population of red absorbing ions of benzyl structure. These ions upon collisions with neutral benzyl chloride react to give an isomeric mixture of red and blue absorbing ions. The blue absorbing ions are presumably chlorotoluene structure. This result will be discussed in the light of previous investigations.

Metastable CH_4^+ and Some of Its Isotopic Analogs: Tunneling through the Centrifugal Barrier

A. J. Illies, M. F. Jarrold and M. T. Bowers; Dept. of Chem., Univ. of California, Santa Barbara, CA 93106.

The metastable (MS) reaction from CH_4^+ (and its isotopic analogs CD_4^+ and CD_3H^+...)

$$CH_4^+ \rightarrow CH_3^+ + H \qquad (1)$$

have been the subject of many experimental and theoretical studies. The long lifetimes involved indicate statistical theory cannot be invoked to explain the rates of reactions. However, the long lifetimes may be explained by either a curve crossing mechanism or by tunneling through the centrifugal barrier.

Solka, Beynon, and Cooks [1] studied this reaction as a function of ion source temperature (~400-525 K) and found that the kinetic energy (KE) release (determined from the MS peak at half height) increases with temperature. This increase was ascribed to tunneling through the centrifugal barrier. Subsequent appearance potential (AP) measurements for the MS process by Flamme, Momigny and Wankenne [2] indicated that the AP for the MS ion was ~1.7 eV above threshold. This result was interpreted in terms of tunneling, however it is more consistant with the curve crossing mechanism.

We have reinvestigated the MS arising from CD_3H^+, CD_4^+ and CH_4^+ over the temperature range $125 \leq T \leq 575$ K on a high resolution reverse geometry mass spectrometer fitted with a temperature variable ion source built from oxygen free high conductivity copper. Both ion intensities were obtained from the peak areas using analog detection, while the KE release distributions were determined from MS peaks obtained at high energy resolution (~0.25 eV FWHM) using a pulse counting detection system.

Figure 1 gives a plot of the average KE release (determined from the KE release distribution points) versus T and Figure 2 a plot of the MS intensities (points) versus T for reaction 2;

$$CD_3H^+ \rightarrow CD_3^+ + H \qquad (2)$$

the data show that both the KE release and intensity increase with temperature. Our own AP measurements indicate that the MS process and the direct process have the same threshold energy. This result is in agreement with an earlier study by Dibeler and Rosenstock [3] but is in contrast to that reported by Flamme et al.

We have modelled the MS in terms of a tunneling mechanism. Statistical theory is used to determine the frequency for encounter with the centrifugal barrier and the WKB approximation is used for the tunneling probability. Figures 3 and 4 show the experimental (points) and calculated (histogram) KE release distributions for reaction (2) at two temperatures (143 and 425 K). The curves in Figure 1 and 2 represent the calculated average KE (absolute) and the calculated intensities (normalized) obtained from our model.

The agreement between all our experimental and calculate results leads us to conclude that the MS, reaction (2), occurs by tunneling through the centrifugal barrier. Studies on CD_4^+ and CH_4^+ indicates similar conclusions can be drawn for these systems.

The support of the National Science Foundation is greatly acknowledged.

(1) B. H. Solka, J. H. Beynon and R. G. Cooks, J. Amer. Chem. Soc. 79 859(1975).
(2) J. P. Flamme, J. Momigny and H. Wankenne, J. Amer. Chem. Soc. 98 1045(1976).
(3) V. H. Dibeler and H. M. Rosenstock, J. Chem. Phys. 39 1326(1963).

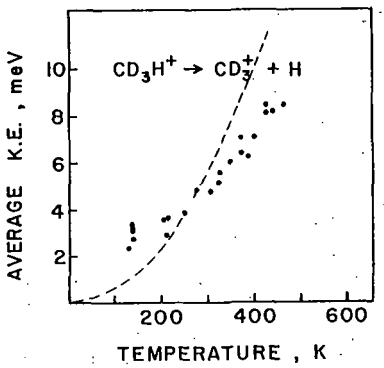

Normalized metastable ion intensities as a function of ion source temperature for reaction (2).

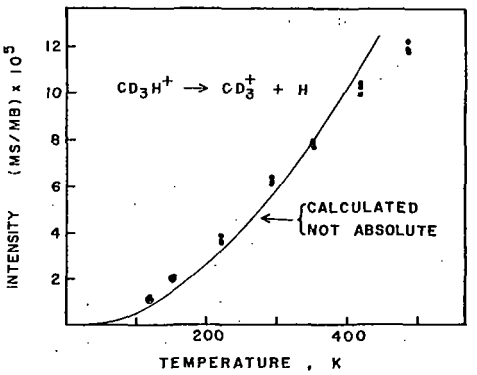

Average kinetic energy release as a function of ion source temperature for reaction (2).

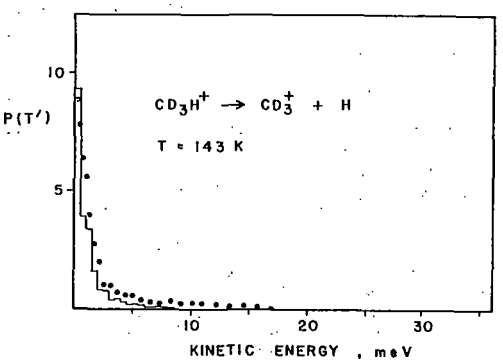

Experimental (points) and calculated (histogram) kinetic energy release distribution at 143 K for reaction (2).

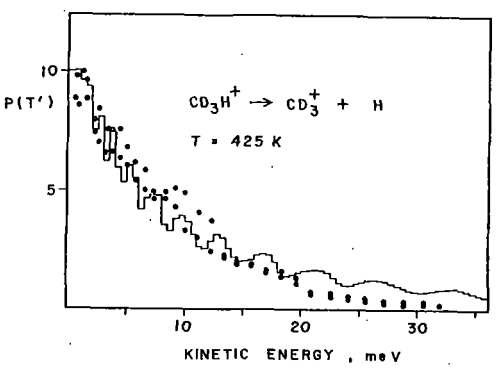

Experimental (points) and calculated (histogram) kinetic energy release distribution at 425 K for reaction (2).

GAS PHASE REACTIONS OF EXCITED Cr^+

R. B. Freas, D. P. Ridge, University of Delaware, Newark, De. 19711

There has long been an interest in the activation of the relatively inert chemical bonds of saturated hydrocarbons with simple molecular substrates. Recent developments include the oxidative addition of transition metal atoms[1], clusters[2] and ions[3,4] to insert into or cleave the carbon-carbon or carbon-hydrogen bonds in simple alkanes. The reactions of first row transition metal ions with small hydrocarbons have been studied in our laboratory using the technique of ion cyclotron resonance spectrometry (ICR). The metal ions have been produced in the source by electron impact on the corresponding metal carbonyl. The group VIII metal atoms, Fe^+, Co^+ and Ni^+, have been observed to insert into the C-C and C-H bonds of butane according to the following scheme:

$$M^+ + n\text{-}C_4H_{10} \longrightarrow \begin{cases} MC_2H_4^+ + C_2H_6 \\ MC_3H_6^+ + CH_4 \\ MC_4H_8^+ + H_2 \end{cases} \qquad [1]$$

The predominant product in all cases observed corresponds to cleavage of the weakest bond. Thus, in the case of n-butane, the major product ion is $MC_2H_4^+$. The collision-induced decomposition (CID) spectra[5] of the $MC_4H_{10}^+$ ions formed by the ligand substitution reaction of MCO^+ and neutral butanes evidence a number of species, all quite similar either to product ions observed in the ICR, or to proposed intermediate species[4].

Electron impact on the binuclear metal carbonyls produces a significant amount of the metal dimer ion, M_2^+. Mn_2^+ and Co_2^+, as well as Mn^+ were found to be unreactive towards the alkanes.

Cr^+, formed by electron impact on $Cr(CO)_6$, was found to react with alkanes to almost exclusively eliminate H_2 from the molecule. The sole case of C-C bond cleavage observed was the rupture of the weakest bond in all of the alkanes observed, the 2,3 C-C bond in n-butane. Cr^+ was also seen to react with methane to eliminate H_2 as indicated in scheme [2]:

$$Cr^+ + CH_4 \longrightarrow CrCH_2^+ + H_2 \qquad [2]$$

$$CrCO^+ + CH_4 \longrightarrow CrCH_4^+ + CO \qquad [3]$$

The CID spectrum of $CrCH_4^+$, produced by the carbonyl displacement reaction shown in [3], is vastly different from the spectra obtained from the Fe^+-butane ions described earlier[4]. The only decomposition product observed is Cr^+, indicating that the $CrCH_4^+$ species is a loosely bound complex.

Results from ion beam studies by Beauchamp et al.[6] yield a chromium carbene bond strength, $D^o(Cr^+-CH_2) = 65 \pm 7$ kcal/mole. This leads to the reaction of Cr^+ and CH_4 being endothermic by 45 kcal/mol.

$$Cr^+ + Cr(CO)_6 \longrightarrow \begin{cases} Cr(CO)_5^+ + CrCO \\ Cr_2(CO)_{6-n}^+ + n\ CO \end{cases} \qquad [4]$$

Studies were done in the ICR to determine the kinetics of the reactions in scheme [4]. The kinetic evidence obtained indicates that Cr^+ formed by 70 eV electron impact on $Cr(CO)_6$, is present in two states which react with $Cr(CO)_6$. The more rapidly reacting state has an approximate rate constant of 1.0×10^{-9} molec./cm^3 sec. and comprises about 28% of the Cr^+ intensity. The other state reacts with a rate constant of 2.0×10^{-9} molec./cm^3 sec. It is thus likely that the loosely bound complex corresponds to the ground state of Cr^+, and only the excited state is responsible for the formation of $CrCH_2^+$.

In conclusion, Fe^+, Co^+ and Ni^+ react to oxidatively cleave C-C and C-H bonds in alkanes whereas Mn^+, Mn_2^+ and Co_2^+ do not. Cr^+ reacts to cleave C-H bonds in alkanes, and kinetic and thermochemical evidence exists for the possibility that these reactions correspond to an excited state of Cr^+.

[1] R.J.Remick, T.A.Asunta, P.S.Skell; J. Am. Chem. Soc., 101, 1321 (1979).
[2] P.H.Barrett, M.Pasternak, R.G.Pearson; J. Am. Chem. Soc. 101, 222 (1979); S.C.Davis, K.J.Klabunde; J. Am. Chem. Soc., 100, 5973 (1978).
[3] J.A.Allison, R.B.Freas, D.P.Ridge; J. Am. Chem. Soc., 101, 1332 (1979).
[4] R.B.Freas, D.P.Ridge; J. Am. Chem. Soc., 102, 7129 (1980).

[5] CID spectra were taken on a VG Micromass ZAB Spectrometer; Grateful acknowledgement is made to the duPont Co., Dr. C. E. McEwen and Dr M. A. Rudat for its use and their assistance.

[6] L.F.Halle, P.B.Armentrout, J.L.Beauchamp, unpublished results.

GAS PHASE ION CHEMISTRY AND PHOTOCHEMISTRY OF $C_7H_7O^+$

C.J. Cassady and B.S. Freiser

Department of Chemistry
Purdue University
West Lafayette, Indiana 47907

D. Russell

Department of Chemistry
Texas A & M
College Station, Texas 77843

As part of our continuing interest in the area of the gas phase chemistry of isomeric ions, we report an ion cyclotron resonance (ICR) study on $C_7H_7O^+$. Photodissociation (PDS) was used to study $C_7H_7O^+$ generated from benzaldehyde, tropone, o-cresol, p-cresol, and 2 -chloro-5-methylphenol. Proposed structures for these $C_7H_7O^+$ ions are:

The PDS spectra of the cresols and tropone gave one peak with a maximum of 300 nm. The PDS products were m/e = 79 and m/e = 91, with the proposed reactions being:

$$C_7H_7O^+ + h\nu \rightarrow C_6H_7^+ + CO \quad (m/e = 79)$$

$$C_7H_7O^+ + h\nu \rightarrow C_6H_3O^+ + CH_4 \quad (m/e = 91)$$

The PDS spectra of benzaldehyde showed an intense short wavelength peak at 300 nm and a weak long wavelength peak at 370 nm. The only PDS product observed for benzaldehyde was m/e = 79 ($C_6H_7^+$). Figures 1 and 2 show PDS spectra of benzaldehyde and tropone taken with a

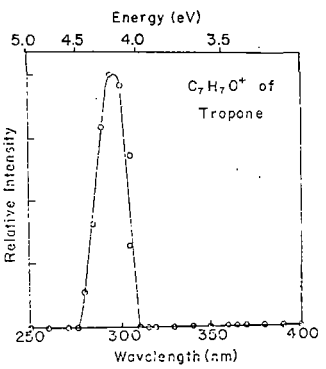

Figure 1

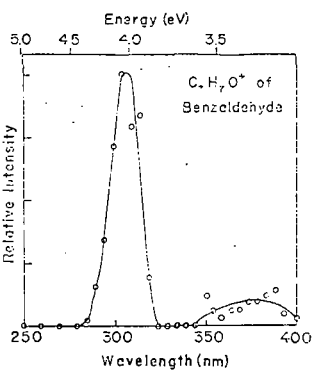

Figure 2

conventional ICR and a 3.5 kW Hg-Xe arc lamp. A summary of our PDS results obtained using this experimental set-up is given in Table 1.

Table 1.

Compound	λ_{max}, nm	% PDS at λ_{max}	% Products, masses: 79	91
Benzaldehyde	300-305 370	60	100	0
p-Cresol	300-310	100	90	10
o-Cresol	305	60	80	20
2-Chloro-5-methyl-phenol	295	60	40	60
Tropone	295-300	60	90	10

Figure 3.

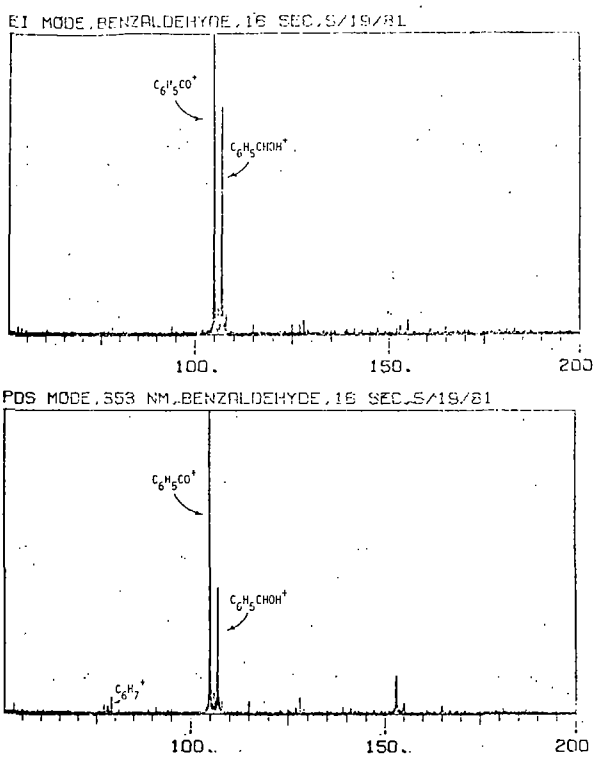

It was confirmed that benzaldehyde did have the long wavelength band by using a Nd:YAG laser set at 353 nm in conjunction with a Nicolet FT-MS. These spectra are shown in Figure 3. This same experiment was also run on tropone, with no photodissociation being observed.

As seen in Figure 4, our results compare favorably with PDS studies of $C_8H_9^+$.

From our preliminary studies we have concluded that the dissociating structure for the $C_7H_7O^+$ ion from benzaldehyde is structure I, while the dissociating structure of the cresol and tropone ions is structure III. In both cases the non-dissociating structure is believed to be the hydroxytropylium ion, structure II. Further studies in this area are currently being undertaken in our laboratory.

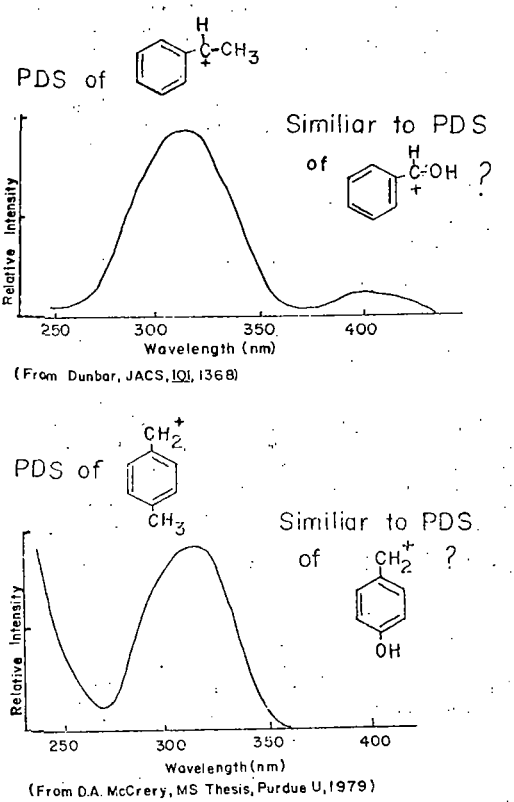

Figure 4

Systematic Error in Isotopic Analysis of Noble Gas Mixtures

Robert E. Ellefson, Monsanto Research Corporation, Mound Facility, Miamisburg, Ohio 45342

Noble gas mixtures of helium-neon, helium-argon, and helium-xenon, with one or both gas components enriched, are frequently prepared at Mound. Ultimate uses of these mixtures include gas lasers, atmospheric tracers, and reactor fuel element tags.

Mixtures are analyzed using a modified DuPont 21-620A mass spectrometer operated in the Dempster mode for helium measurements and the cycloidal mode for higher masses. The resolution for cycloidal operation is 200. High vacuum is provided by an Edwards EO-2 diffusion pump using polyphenyl ether pumping fluid. Sensitivity for argon, xenon, neon, and helium are 18, 12, 6, and 1 x 10^{-9} A/torr, respectively.

Analyses of known standard mixtures in Fig. 1 show significant biases in measured ratio which change with sample (inlet) pressure. Also, analyses of 25% and 50% ^{3}He in xenon standards, each analyzed at 200μm sample pressure, show biases of 0.4% relative and 3.8% relative, respectively; thus, bias magnitude appears dependent on component partial pressure and not total sample pressure.

Quantitative gas analysis assumes a linear relationship between measured ion current, I_i, and partial pressure, PP_i, of a corresponding component in the inlet system: $PP_i = I_i/S_i$ where S_i is the sensitivity parameter (assumed constant). Figure 2 shows that for this mass spectrometer, sensitivity is not constant but varies with pressure and is different for each gas. Gas flow through the mass spectrometer is described in Fig. 3. Ion current from a mole fraction, X_i, is related to source pressure, P_S, and ion production factor, K_i, by

$$I_i = K_i X_i P_S = K_i \frac{F_I}{F_S}\left(1 + \frac{F_S}{F_H}\right) X_i P_I.$$

Identifying $X_i P_I$ as PP_i, sensitivity is given by

$$S_i = K_i \frac{F_I}{F_S}\left(1 + \frac{F_S}{F_H}\right).$$

Nonlinear operation can arise from three factors determining sensitivity. Factor K_i, if it varies at all, should depend on total pressure, not partial pressure. Conductance effects of the molecular leak (F_I) and source exit ports (F_S) should have positive slopes for all gases if deviations from molecular flow were significant.[1] Changes in diffusion pumping speed (F_H) by varying the power produce sensitivity changes as shown in Fig.4. Reciprocal of sensitivity changes reflect change in F_H; magnitude and profile of Fig. 4 is similar to the effect of decrease in heat input to the diffusion pump.[2] The variation shown in Fig. 2 is attributed to changes in F_H from a "cooling" effect on pumping fluid with increased gas load.

Independent flow of gas components implies that the use of a sensitivity, S_i, appropriate for the partial pressure of the component should minimize systematic errors in ratios:

$$S_i = S_{o_i}[1 + \Delta S_i (X_i \cdot P_I)].$$

Applying this model to the data in Fig. 1 reduces the systematic error as shown in Fig. 5, confirming the usefulness of the model. Hardware changes that could also minimize the effect would be higher pumping speed, F_H, and/or decreasing source conductance, F_S.

Acknowledgments

The author thanks Mrs. M. J. Garrod and Ms. L. A. Afanador for performing analyses and other measurements. This work was performed at Mound Facility for the U. S. Department of Energy under Contract No. DE-AC04-76-DPO0053.

References

1. S. Dushman, **Scientific Foundations of Vacuum Technique,** Wiley (1962), pp. 87, 110.

2. M. H. Hablanian and A. A. Landfors, **Ind. Res & Dev.,** September 1980, p. 132.

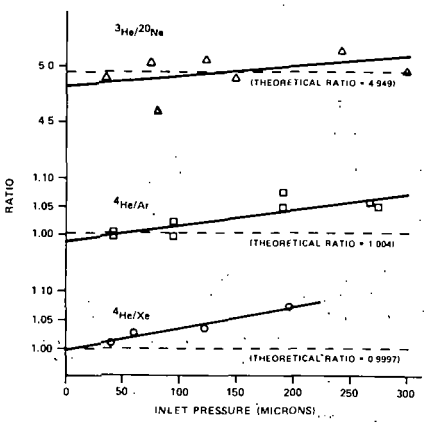

Fig. 1 Bias in measured ratio for a given mixture depends on inlet pressure.

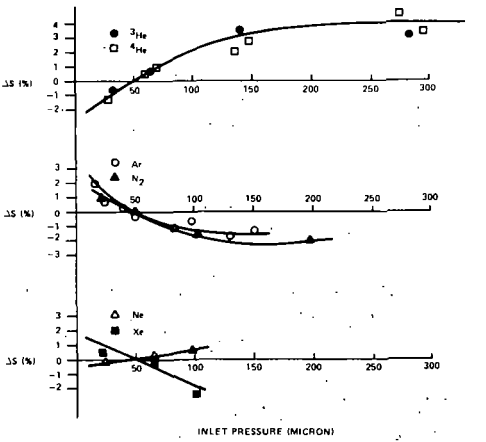

Fig. 2 Variation of sensitivity with pressure is dramatically different for helium compared with other gases for this cycloid mass spectrometer.

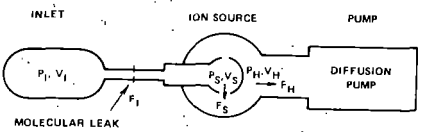

Fig. 3 Sample gas flows from inlet through ion source to diffusion pump providing target gas in the source.

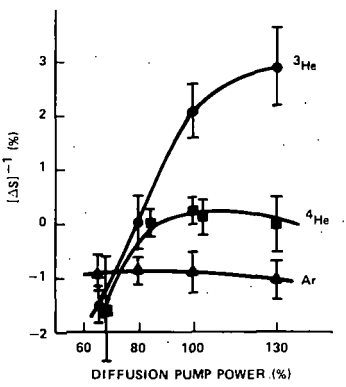

Fig. 4 Sensitivity is also dependent on pumping speed of the diffusion pump.

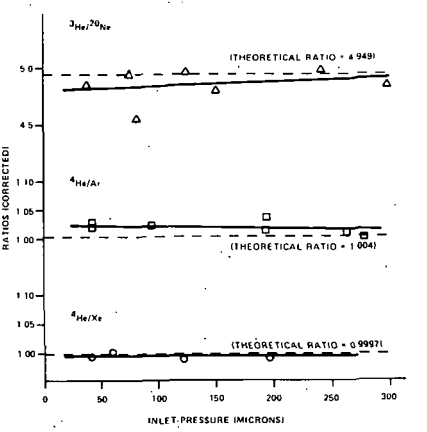

Fig. 5 Corrected ratios using model in text.

IMPROVED PRECISION OF DIFFERENTIAL HYDROGEN ISOTOPE RATIO ANALYSIS THROUGH THE USE OF TWO ISOTOPIC STANDARDS

D.A. Schoeller, D.W. Peterson, and J.M. Hayes

Department of Medicine, The University of Chicago, Chicago, Ill. 60637, and Department of Chemistry, Indiana University, Bloomington, Ind. 47401.

Deuterium/hydrogen differential isotope ratio analysis employs the same general methodology that was developed by Nier (1), and McKinney et al. (2) for $^{13}C/^{12}C$ and $^{18}O/^{16}O$ isotope ratio analyses. While the analytical considerations for each of the three techniques are quite similar, hydrogen isotope ratio analysis is uniquely subject to interference from an $(M+1)^+$ ion. The H_3^+ ion has the same nominal mass as the minor isotopic species DH^+ and generally comprises 15 to 30% of the total ion current at m/z 3. In order to obtain accurate results, the observed isotopic abundances must be corrected for the H_3^+ contribution. The correction can be performed either after data collection using a mathematical technique based on the second power relationship between the major ion intensity and the H_3^+ ion intensity, or during data collection using an electrical compensation circuit that is adjusted to null the H_3^+ signal. However, because both correction techniques require an independent calibration process to determine the H_3^+ correction factor, they are both subject to error due to uncertainty in the calibration and small variations in the efficiency of H_3^+ formation.

A third approach which might eliminate the uncertainty in the H_3^+ correction was proposed by Terwilliger (3). This approach involves the use of the two standard H_2 samples which are introduced into the ion source in succession with the unknown sample. The relative isotopic abundance of the unknown is calculated by linear interpolation between the observed m/z 3 to m/z 2 ion current ratios of the unknown (R_u) and the standards (R_a and R_b), and the known D/H ratios of the standards (A and B).

$$U = \frac{A(R_a-R_b) + B(R_u-R_b)}{R_a-R_b}$$

Based on the mathematical model, Terwilliger predicted that the use of two standards and linear interpolation would provide superior precision compared to the typical H_3^+ correction using a single standard. The double-comparison method, however, has never been evaluated in practice. We have, therefore, compared the precision of the double-comparison technique with the one-standard techniques using either mathematical

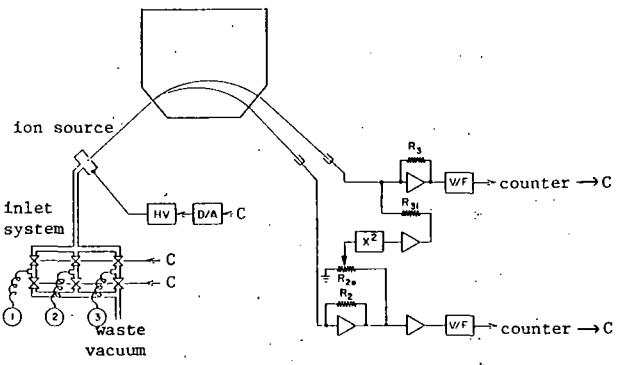

Figure 1. Mass spectrometer system employing a Nuclide 3-60 RMS, a triple viscous leak inlet, and optional electrical H_3^+ compensation. The inlet valves, accelerating voltage, and detectors are interfaced to a TI 980B minicomputer (C).

Table 1. Comparison of the precisions of the D/H analyses.

	Standard deviations of δD measurements, ‰		
	linear calculation	mathematical correction	electrical compensation
one-standard		1.44[c]	0.72[c]
double-comparison	6.71[a];1.68[b]	1.49[c]	0.41[c]

Coefficient of variation of m/e 2 ion-current matching; a, 0.6%; b. 0.05%; c, either. Integration time = 100 s.

or electrical H_3^+ correction. In addition, the double-comparison method was combined with mathematical or electrical H_3^+ correction and the results were compared with those obtained without an independent H_3^+ correction.

Single aliquots of six hydrogen gas samples with ^2H relative abundances between -183 and 193‰ vs. SMOW were prepared and stored in glass bulbs sealed with high vacuum teflon stopcocks. Two of the gases (-148.1 and 54.4‰) were arbitrarily designated as standards, while the remaining four gases were used as "unknowns". The isotopic abundance measurements were performed using a Nuclide 3-60 ratio mass spectrometer (State College, Pa.) that had been modified by the addition of a third inlet reservior and viscous leak. The inlet and mass spectrometer were interfaced to a TI-980 B minicomputer for automated isotope ratio analysis (Fig. 1). The analyses were performed at a major-isotope ion beam current of 1.5×10^{-9} amp and a total integration time for each gas of 100 sec for electrical compensation and 300 sec for mathematical correction. The H_3^+ correction factor was determined on each of the nine occasions on which the techniques were compared during the six-week study period. The H_3^+ correction factor averaged 6.9×10^4 amp^{-1}, or about 30% of the minor beam current. The coefficient of variation was slightly less than 2%.

The precisions (1 SD) of each of the techniques are shown in Table 1. The double-comparison technique had a precision of 0.4‰ when combined with electrical H_3^+ compensation. This was superior to that obtained using the one-standard technique with either mathematical or electrical H_3^+ correction. In the absence of an independent H_3^+ correction, however, the precision of the double-comparison technique was poor and varied as a function of the accuracy of the matching of the major ion currents of the unknown and standard gases. When the ion currents were matched manually with a relative precision of 0.6%, the precision of the double-comparison linear calculation technique was 6.7‰. The precision of the double-comparison, linear calculation technique was improved (1.7‰) when the ion beams were matched under computer control with a relative precision of 0.05%.

The poor precision of the double-comparison technique using only the linear calculation to correct for H_3^+ was due to the slight differences in the sample fluxes of the standards and unknowns. The ion current mismatching produced a small difference in the relative H_3^+ contributions to each of the observed ion current ratios and, thus, violated the basic assumption of the technique. It was determined by an analysis of the propagation of error that the major ion currents of the three gases would have to be matched with a relative precision of 0.01% in order to obtain a 0.4‰ precision for the double-comparison, linear-calculation technique. A combination of electrical H_3^+ compensation with the double-comparison technique reduces the requirement for intensity matching to 1%. Under these conditions, the double-comparison technique compensates for the small (< 3%) inaccuracies and variations in the H_3^+ correction factor that limit the precision of the one-standard technique, and therefore provides superior precision for the determination of deuterium/hydrogen isotope abundances.

This work was supported by NIH grants GM18947 and AM26678.

1. Nier, A.O. Rev. Sci. Instrum. 18:398, 1947.

2. McKinney, C.R., J.M. McCrea, S. Epstein, H.A. Allen, and H.C. Urey. Rev. Sci. Instrum. 21:724, 1950.

3. Terwilliger, D.T. Int. J. Mass Spectrom. Ion Phys. 25:393, 1977.

ISOTOPIC ANALYSIS VIA ATOMIC EMISSION SPECTROSCOPY - AN OLD TECHNIQUE WITH NEW PROMISE FOR THE 'EIGHTIES.

Martin C. Edelson and Velmer A. Fassel
Ames Laboratory, USDOE, Iowa State University, Ames, Iowa 50011

This paper describes the application of a new atomic emission excitation source, the inductively coupled plasma (ICP), to the isotopic analysis of atomic species in solution by atomic emission spectroscopy (ICP-AES).

ICP-AES is rapidly becoming an important analytical tool for the simultaneous multielemental analysis of solutions[1]. For these analyses, the ICP offers many advantages over classical excitation sources such as arc and spark discharges, flames, and hollow cathode lamps[1]. The many merits of ICP-AES prompted the investigation of its potential use for isotopic analysis. Unanswered questions regarding the new source at the beginning of this research were, "Do the normal operating conditions of the ICP (i.e., T=5000-8000 K, atmospheric pressure) produce lines that are too broad to allow isotopic resolution?" and, "Can the isotopic components of an element with a rich spectrum (e.g., uranium) be isolated and measured to provide the basis of an isotopic assay by ICP-AES?" We have determined in this study that, *i*) isotopic components of the ICP-AES lines of heavy elements, such as Pb and U, can be resolved with a high resolution spectrometer, *ii*) a good estimate of the usefulness of an ICP-AES line for isotopic analysis can be simply obtained by comparing its Doppler width with its isotope shift, and *iii*) the uranium line at 4244Å can provide a useful means for the isotopic assay of U-235/U-238 mixtures. These findings are illustrated in the figures accompanying this extended abstract.

The Doppler width of spectral lines constitutes a serious impediment to the application of ICP-AES to the isotopic analysis of those elements whose emission lines suffer only small isotope shifts. We expect that the use of a single-frequency tunable dye laser to excite the fluorescence of ICP atomized material, coupled with novel spectroscopic techniques, such as Doppler-free two-photon spectroscopy or quasi-collimated "atomic beams", will permit the extension of ICP-AES to the isotopic analysis of a number of elements possessing small isotope shifts.

We expect to see a rekindling of interest in the AES method of isotopic analysis in the coming decade. The ease of such analyses, the ability to perform them simultaneously on several elements along with elemental concentration determinations, will make this analytical technique an attractive one in the years ahead. Because the isotopic analysis of solution species by ICP-AES may become a useful analytical tool in the near future, and no analytical technique should exist without an appropriate acronym, we propose Inductively Coupled Plasma - Atomic Multielement Emission Spectroscopy - Isotope Analysis or ICP-AMES-IA!

References:

1. V. A. Fassel, Science 202 (1978) 183-191.

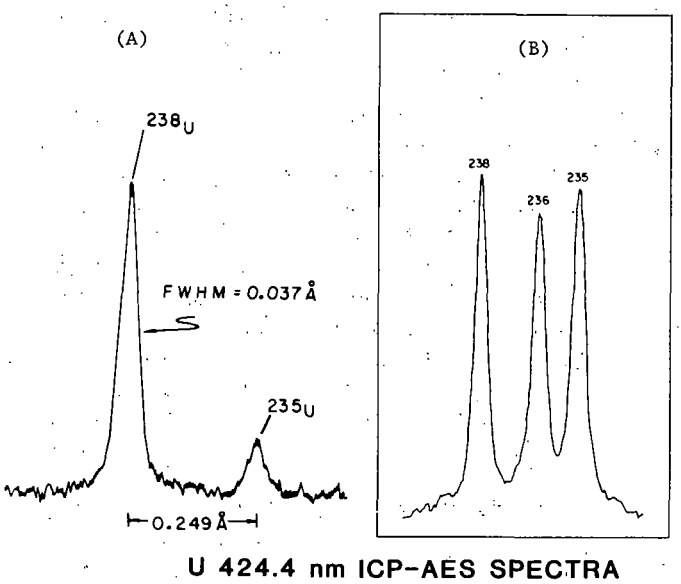

Fig. 1. (A) 1:5 U-235:U-238 mixture (U-235 concentration = 25 ppm);
(B) A 1: 0.9 : 1 U-235:U236:U-238 mixture (U-235 = 100 ppm)

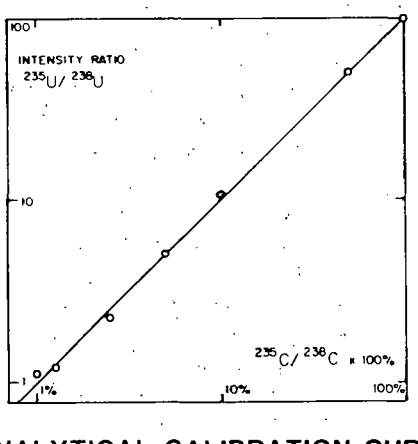

Fig. 2. UII 424.4 nm ICP-AES line used for U-235/U-238 isotopic measurements.

ELECTRODEPOSITION AS A SAMPLE MOUNTING TECHNIQUE FOR U AND Pu ISOTOPIC ANALYSIS

R. E. Perrin, D. J. Rokop, J. H. Cappis, and W. R. Shields
Los Alamos National Laboratory

GROUP CNC-7 AT LOS ALAMOS NATIONAL LABORATORY UTILIZES TWO SINGLE STAGE 12 INCH, 90° SECTOR MASS SPECTROMETERS EQUIPPED WITH PULSE COUNTING DETECTOR SYSTEMS FOR ISOTOPIC ANALYSIS OF NANOGRAM QUANTITIES OF U AND Pu. THE USE OF SINGLE STAGE INSTRUMENTS WITH HIGHLY SENSITIVE DETECTORS PRESENTS UNIQUE PROBLEMS. SCATTERED IONS FROM INTENSE ION BEAMS CAN CAUSE SIGNIFICANT BACKGROUNDS EVEN WHEN THE MASS OF THE INTENSE ION BEAM IS FAR REMOVED FROM THE MASS REGION BEING MEASURED. ADDITIONALLY, VERY SMALL AMOUNTS OF HYDROCARBONS CAN CONTRIBUTE A SIGNIFICANT BACKGROUND OVER THE ENTIRE MASS RANGE OF INTEREST. ANALYSIS OF NANOGRAM QUANTITIES OF U AND Pu SEPARATED FROM 1 TO 10 GRAMS OF MATRIX MATERIAL PRESENT A DIFFICULT CHALLENGE TO THE SEPARATIONS CHEMIST. SMALL AMOUNTS OF ALKALI METALS (PARTICULARLY Na, K AND Ca) ARE ESPECIALLY DIFFICULT TO REMOVE. HYDROCARBONS IN THE FORM OF PARTIALLY DECOMPOSED ION EXCHANGE RESIN ARE AN ADDITIONAL PROBLEM. SODIUM AND POTASSIUM ION BEAMS IN THE RANGE OF 6.5×10^8 to 9.6×10^8 CPS ARE COMMON WHEN SAMPLES ARE LOADED BY DIRECT EVAPORATION OF THE SEPARATED SAMPLE ON TO A Re FILAMENT. ION BEAMS OF THIS INTENSITY WILL CAUSE A GENERAL SCATTERED ION BACKGROUND OF 200 TO 300 CPS FROM MASS 230 TO MASS 250. UNDESTROYED HYDROCARBONS CONTRIBUTE AN ADDITIONAL BACKGROUND OF 300 TO 3000 CPS IN SAMPLES LOADED BY DIRECT EVAPORATION. TO ACHIEVE THE NEEDED ACCURACY FOR MEASUREMENT OF THE MINOR ISOTOPES IT IS NECESSARY TO REDUCE THE BACKGROUND INTERFERENCES FROM ALL OF THE ABOVE SOURCES TO LESS THAN 0.05 CPS.

RESOLUTION OF THE PROBLEM BY IMPROVEMENTS IN THE CHEMICAL SEPARATIONS WAS CONSIDERED UNLIKELY BECAUSE OF THE DIFFICULTY OF REMOVING TRACE QUANTITIES OF THE INTERFERENCES FROM BOTH REAGENTS AND GLASSWARE. REMOVAL OF THE INTERFERENCES JUST PRIOR TO ANALYSIS WAS CONSIDERED TO BE THE MOST ATTRACTIVE APPROACH. DIRECT ELECTRODEPOSITION OF THE U AND/OR Pu ONTO THE MASS SPECTROMETER FILAMENT OFFERED THE GREATEST POTENTIAL FOR THE NEEDED SEPARATION WITH THE LEAST PROBABILITY OF RECONTAMINATION. ELIMINATION OF THE EFFECTS OF ALKALIES RELEASED FROM THE FILAMENT SUPPORT PINS CAN BE ACCOMPLISHED EITHER BY CHANGING THE FILAMENT SUPPORTS OR BY LOWERING THE OPERATING TEMPERATURE OF THE FILAMENT. REC AND CO-WORKERS HAVE REPORTED ON A TECHNIQUE FOR IMPROVING SINGLE FILAMENT IONIZATION OF U AND Pu BY SPUTTERING A COATING OF Re OVER THE SAMPLE SUPPORTED BY A Re FILAMENT. THIS PERMITS IONIZATION OF U AND Pu BELOW 1700°C. AT THIS TEMPERATURE THE HEATING OF INSULATOR GLASS IS REDUCED TO AN ACCEPTABLE LEVEL. ELECTRODEPOSITION OF THE RHENIUM AFTER ELECTRODEPOSITION OF THE U AND/OR Pu APPEARS TO HOLD PROMISE AS A SATISFACTORY SOLUTION FOR THE PROBLEMS DISCUSSED.

APPARATUS WAS DESIGNED TO PROVIDE A SIMPLE, RELIABLE TECHNIQUE FOR DIRECT ELECTRODEPOSITION OF U, Pu, AND Re. A STRIP OF TEFLON TAPE .250" WIDE PASSES OVER A PAIR OF SUPPORT RODS AND UNDER THE RHENIUM FILAMENT. TWO SMALL ALLIGATOR CLIPS PROVIDE SUFFICIENT TENSION TO SEAL THE TAPE AGAINST THE LOWER SURFACE OF THE FILAMENT AND THUS ASSURE DEPOSITION ONLY ON THE UPPER SURFACE. A PLATINUM ANODE IS PLACED ABOVE THE SURFACE OF THE FILAMENT. THIS CONFIGURATION CAN SUPPORT UP TO 150 μℓ OF ELECTROLYTE. A SIMILAR SYSTEM CAN BE USED FOR DEPOSITION ONTO SIDE FILAMENTS FOR TRIPLE FILAMENT ANALYSES.

THREE CONCENTRATIONS OF HCl (1M, 1.5M AND 2M) WERE PREPARED IN TEFLON CONTAINERS. PORTIONS OF EACH WERE ADJUSTED TO pH VALUES OF 1.7, 2.7 AND 3.7 RESPECTIVELY. PLATING EFFICIENCY CURVES FOR EACH OF THE NINE ELECTROLYTES WERE DETERMINED BY PLATING 1 ng PORTIONS OF

Pu-239 OR 10 ng PORTIONS OF U-233 (DISSOLVED IN 10 µℓ OF 0.1 M HCl) FROM 100 µℓ PORTIONS OF THE ELECTROLYTE AT A VOLTAGE OF 3.5 V. RECOVERY WAS MEASURED AS TOTAL ALPHA ACTIVITY IN A 2π GAS PROPORTIONAL COUNTER. ALL ELECTROLYTES PROVIDE 95 TO 100% RECOVERY OF U AND Pu AFTER 20 MINUTES OF PLATING AT 3.5V. THE 1.5M HCl AT A pH OF 2.7 WAS CHOSEN FOR FURTHER TESTING BECAUSE IT REPRESENTS A "MIDDLE OFF THE PLATEAU" WITH A RELATIVELY LARGE MARGIN OF SATISFACTORY PERFORMANCE.

THE EFFECT OF VOLTAGE ON RECOVERY AFTER 20 MINUTES PLATING TIME WAS TESTED USING THE 1.5 M HCl AT A pH OF 2.7 FOR 1 µg Pu, 10 ng U-233 AND 10 ug U-500 SPIKED WITH 10 ng U-233. THE ELECTRODEPOSITION OF U AND Pu MUST BE CARRIED OUT AT A VOLTAGE OF AT LEAST 3.5 VOLTS IF SATISFACTORY RECOVERY IS TO BE ACHIEVED IN 20 MIN.

RHENIUM SOLUTIONS WERE PREPARED IN 0.1 M AND 1.5 M HCl. AMMONIUM PERRHENATE WAS DISSOLVED IN THESE ACIDS AT VARIOUS CONCENTRATIONS AND ADJUSTED OVER A pH RANGE OF 1.7 TO 2.7. RHENIUM CONCENTRATIONS WERE VARIED FROM 1 TO 200 mg/mℓ. Re OVERPLATING COULD BE ACHIEVED OVER THE ENTIRE RANGE OF CONCENTRATIONS AND pH. PLATINGS CAN BE ACCOMPLISHED FROM 2V TO 4V. HOWEVER, AT VOLTAGES ABOVE 3.2 THE Re OVERPLATE BECOMES POROUS, ADHERES POORLY TO THE SUBSTRATE, AND TENDS TO ENTRAP IMPURITIES.

DIRECT ELECTRODEPOSITION OF U AND Pu REDUCED THE SODIUM AND POTASSIUM BEAM INTENSITIES TO LESS THAN 1.3×10^{6} CPS WHEN THE IONIZING FILAMENT TEMPERATURES WERE REDUCED TO $<1700^{o}C$. THIS REDUCED THE INTENSITY OF SCATTERED IONS TO 0.05 CPS IN THE MASS REGION FROM 230 TO 250. UP TO 5 mg OF SODIUM AND POTASSIUM CHLORIDE WERE ADDED TO ALIQUOTS WHICH WERE THEN ELECTRODEPOSITED. NO INCREASE IN Na AND K ION BEAMS WAS OBSERVED. THE Pu BLANK FROM THE ELECTRODEPOSITION PROCEDURE IS LESS THAN 1.00×1^{-15} GRAMS. THE U BLANK FROM THE ELECTRODEPOSITION IS LESS THAN 4×10^{-13} GRAMS. HYDROCARBON PEAKS WERE ALSO REDUCED TO 0.05 CPS IN THE MASS REGION FROM 230 TO 250. THIS IS EQUAL TO THE DARK CURRENT OF THE DETECTION SYSTEM.

SPECIFIC PROCEDURES HAVE BEEN DEVELOPED FOR THE ISOTOPIC ANALYSES OF 1 ng OF Pu, 10 ng OF U, AND 10 µg OF U USING ELECTRODEPOSITRON AND Re OVERPLATE AS THE SAMPLE MOUNTING PROCEDURE. DURING THE DEVELOPMENT OF EACH PROCEDURE VARIABLES SUCH AS PLATING CONDITIONS, OVERPLATING CONDITIONS, SAMPLE DRYING CONDITIONS, SAMPLE SIZE AND HEATING PATTERN WERE TESTED. LIMITS WERE ESTABLISHED FOR EACH OF THESE PARAMETERS. FRACTIONATION CORRECTIONS WERE DETERMINED BY REPLICATE ANALYSIS OF THE NBS STANDARDS. THE PULSE COUNTING DATA ARE ALSO CORRECTED FOR COUNTING DEAD TIME.

THE MEASURED VALUES FOR ALL ISOTOPES OF ALL STANDARDS SHOW NO BIAS OUTSIDE THE UNCERTAINTIES OF THE CERTIFIED VALUES. ALL MEASURED VALUES FOR ISOTOPIC RATIOS GREATER THAN 10 TO 1 ARE ACCURATE TO BETTER THAN 0.1 RELATIVE % AT THE 95% CONFIDENCE INTERNAL. RATIO FRACTION WITH TIME IS LINEAR WITH TIME AND IS LESS THAN 0.2 RELATIVE % IN 50 MINUTES.

DIRECT ELECTRODEPOSITION PROVIDES AN EFFECTIVE METHOD OF ELIMINATING THE LAST TRACES OF ALKALI METALS AND HYDROCARBONS FROM SAMPLES OF U AND Pu PRIOR TO ISOTOPIC ANALYSIS. ELECTRODEPOSITION OF RHENIUM OVER THE ELECTRODEPOSITED U AND Pu IS AN EFFECTIVE MEANS OF INCREASING ION BEAM STABILITY AND CONTROLLING FRACTIONATION OF THE MEASURED RATIOS. THE LOWER FILAMENT TEMPERATURES PERMITTED BY THE SINGLE FILAMENT TECHNIQUE PERMIT REDUCTION OF THE SCATTERED ION BACKGROUND TO 0.05 CPS. UTILIZATION OF THE PROCEDURES DESCRIBED WILL PERMIT MEASUREMENT OF THE ISOTOPIC COMPOSITION OF U AND Pu WITH ACCURACIES OF 0.1 RELATIVE % OR BETTER FOR THE MAJOR ISOTOPES.

ISOTOPIC RATIO MASS SPECTROMETERS FOR THE ANALYSIS OF URANIUM HEXAFLUORIDE*

C. Sulfridge and H. C. Jones

Oak Ridge Gaseous Diffusion Plant
Union Carbide Corportion, Nuclear Division
Oak Ridge, Tennessee 37830

Two isotopic ratio mass spectrometers have been developed at the Oak Ridge Gaseous Diffusion Plant (ORGDP) for the analysis of uranium hexafluoride (UF_6). One of the instruments, a 40-centimeter radius, 90°-deflection mass spectrometer, was developed to meet the sensitivity and precision requirements of development and improvement programs at ORGDP and at the Paducah Gaseous Diffusion Plant (PGDP). The other instrument, a 20-centimeter radius, 90°-deflection, isotopic mass spectrometer, was developed for the universal application to on-stream monitoring of UF_6 in enrichment facilities.

40-CENTIMETER INSTRUMENT

The long radius was chosen to provide the necessary resolving power to enable precise isotopic ratio measurements to be made on UF_6 samples in the laboratory. Second-order focusing is accomplished by machining the magnet pole faces to provide a normal-circle magnetic field. The analyzer tube geometry is designed to compensate for the effects of the magnet fringe field. The fact that the magnetic field extends beyond the pole piece boundaries has always been a problem in the design of sector-type mass spectrometers. Nier[1] and others have conveniently machined the real pole boundaries one gap width less than the effective boundary. This procedure, which was used for the 20-centimeter instrument described in this paper, does compensate for the finge field to a great extent. In the case of a normal circle boundary configuration, however, the Nier method cannot be used. Instead, the finge field correction must be made by repositioning the ion source and the collector from their ideal positions, assuming no fringe field effect. Information obtained from a discussion of ion optics theory by Kerwin[2] was used extensively in determining the ion trajectory, angle of entry into the uniform magnetic field, and the necessary ion source and collector offset to compensate for the fringe field. Figure 1 shows the dimensions arrived at for the ORGDP instrument.

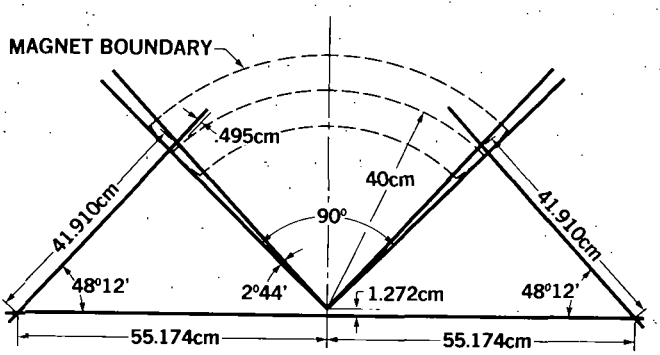

Figure 1
40-Centimeter Geometry

The ion source and collector are securely anchored to a surface plate with flange saddles for long-term mechanical stability.

A Nier-type ion source was modified for up to 10-kilovolt operation by replacing metal studs with tapped alumina studs. The ion source is also a simplified molecular beam type similar to the one described by Smith and Langdon.[3] The UF_4 monitor technique is used for automatic beam positioning.

*Based on work performed at the Oak Ridge Gaseous Diffusion Plant, operated by Union Carbide Corporation, Nuclear Division, for the U. S. Department of Energy.

Ion source region isolation valves permit quick recovery of vacuum after a source change. The instrument can be operated within two hours after a source change; however, more precise analyses can be made after the ultimate vacuum is approached in six to eight hours.

20-CENTIMETER INSTRUMENT

The on-stream monitoring mass spectrometer uses Nier-type geometry with a 20-centimeter radius and 90° deflection. A compact permanent magnet assembly is used, and the analyzer hardware is mounted on a surface plate similar to the long radius instrument. The ion source and most of the electronic components are interchangeable with the long-radius instrument.

Provision is made for UF_6 to flow around the orifice in the variable leak for fast response to changes in stream isotopic composition. The instrument operates automatically with or without a programmable calculator, and the weight percent U-235 is displayed on a strip chart recorder or by the calculator printer.

RESULTS

The standard deviation of a single isotopic ratio-of-ratios type measurement is ±0.00007 on the long radius instrument. The measurement time is 12 minutes. Four long-radius instruments are operating successfully, two at ORGDP and two at PGDP.

Two of the 20-centimeter, on-stream instruments have been completed; one is being used successfully at PGDP, and one is being installed at ORGDP. A precision of ±0.03% relative standard deviation for naturally occurring isotopic abundance of U-235 is achieved within 10 minutes. Up to 4,000 hours source life has been demonstrated with the 20-centimeter instrument.

REFERENCES

1. Nier, A.O.C., Rev. Sci. Instr., 11, 212, (1940).

2. Kerwin, L., *Mass Spectrometry*, (McDowell, Charles A., ed.), P 104, McGraw-Hill, New York, (1963).

3. Smith, L. A. and Langdon, A., *Recent Developments In Mass Spectroscopy*, (K. Ogata and T. Hayakawa, eds.), p 450, University Park Press, Baltimore, MD (1970).

THE DETERMINATION OF SUBNANOGRAM QUANTITIES OF URANIUM BY ISOTOPE DILUTION MASS SPECTROMETRY.

W. R. KELLY and J. D. FASSETT; Center for Analytical Chemistry, National Measurement Laboratory, National Bureau of Standards, Washington, DC 20234

A technique has been investigated for the determination of subnanogram quantities of U by IDMS in natural matrices using ^{233}U (SRM 955) as a spike. This technique involves sample dissolution and chemical separation of U in high yields under clean room conditions and measurement using a pulse counting single stage thermal ionization mass spectrometer. The chemically purified U is loaded onto a single anion resin bead and placed into a Re "V" filament. The bead serves an efficient point source emitter of U ions with ionization efficiencies of 0.2% routinely achieved. Freeze-dried bovine livers containing 700 pg U/g have been analyzed. Typically 0.5 g of dried liver is decomposed using nitric and perchloric acids. An aliquot containing 0.1-0.2 g equivalent of dried liver or about 100 pg U is chemically processed on a 1 mL anion column in the nitrate form and further purified on a 0.06 mL anion column in the chloride form. The chemically separated U is concentrated in a minimum of 8N HNO_3, equilibrated with the resin bead, dried onto the bead, and loaded into the mass spectrometer. A Chesapeake Bay water sample has also been analyzed by the same procedure without the necessity for sample dissolution and found to have 2 ng U/g. Both chemical and mass spectrometric blanks have been measured and chemical yields determined on every sample. The mass spectrometric blanks were determined by loading 25-100 pg of ^{233}U spike directly onto resin beads and ranged from 15-50 fg (10^{-15} g). The dissolution and column blanks are 5 pg which result in a blank correction of a few percent for the liver samples. Presently the relative large chemical blank correction is the dominating source of error for bovine liver. On the other hand, the U content in 1 g of a Chesapeake Bay water sample has been determined to 0.5% with negligible blank correction.

EXPERIMENTAL STRATEGIES FOR FULLY AUTOMATED HIGH PRECISION ISOTOPE RATIO DETERMINATIONS.

K. HABFAST and D. TUTTAS, Varian MAT GmbH, Bremen

We will present isotope ratio measurements for the following elements

- Strontium (σ < 0.002%)
- Uranium, including minor isotopes (σ < 0.01%)
- Lead (σ < 0.02%)
- Calcium (σ < 0.05%)
- Neodymium (σ < 0.002%)

All results have been obtained by application of fully automated measuring procedures, including automatic sample heating, data collection and data evaluation.

All relevant parameters for getting such results without manual operator intervention will be discussed.

A COMBINED MASS SPECTROMETRIC ATOMIC ABSORPTION TECHNIQUE FOR EVALUATION OF VAPORIZATION MECHANISMS*

D. L. Styris and J. H. Kaye
Pacific Northwest Laboratory,+ Richland, Washington 99352

Mass spectrometric and atomic absorption techniques are used in this work to investigate mechanisms which control vaporization processes important to furnace atomic absorption spectrometric (AAS) analysis. These mechanisms are largely responsible for AAS performance and have therefore received considerable attention. Numerous models of vaporization from AAS type furnaces have resulted primarily from evaluations of AAS data and thermodynamic equilibrium calculations involving analyte, matrix and furnace material interactions (1-6). Ambiguities in these models suggest, however, that additional experimental methods need to be applied. The philosophy of the work presented here is to apply MS techniques simultaneously with AAS methods in order to identify the vaporized atoms and molecules that appear as precursory and concomitant signals with the AAS signal for a particular atomic species. These correlated data are then used with chemical thermodynamic evaluations to help formulate the vaporization mechanisms for a given system.

The ultra high vacuum, combined MS/AAS apparatus used for this work is illustrated schematically in Figure 1. The furnace which is heated resistively is shown in contracted and extended positions which are controlled by the linear translator. Two stage differential pumping using 1200 L/s cryopumps and a 3.2mm diameter conductance limiter orifice allows two orders of magnitude pressure differential between stages. The quadrupole mass analyzer (QMA) system is an Extranuclear ELF quadrupole with axial electron impact ionizer.

Both vitreous carbon and tantalum furnaces were used in these experiments. Three analytes were studied: Rb (as RbOH and RbCl), Ag (as $AgNO_3$) and V (as V_2O_5). The QMA signal for a given mass and the atomic absorption and temperature signals were monitored simultaneously with a three beam oscilloscope. Composites of results for different masses (excluding background signals) for the RbCl in Ta and V_2O_5 in vitreous carbon experiments are shown in Figures 2 and 3, respectively. Results from the RbOH and $AgNO_3$ in vitreous carbon did not exhibit precursors that could be identified as containing the analyte. This is indicative of either (i) reduction to the liquid or gaseous phase of the analyte, or (ii) congruent vaporization to the gaseous phase of the analyte. Volatile carbides were not observed in any of these experiments.

The data from the RbCl in Ta studies are explained by the reaction

$$10(RbCl)_s + 6(Ta_2O_5)_s = 2(TaCl_5)_s + 10(RbO_2)_g + 10(Ta)_s + 5O_2.$$

Free rubidium atoms appear when the $(RbO_2)_g$ dissociates at a higher temperature.

The data from the V_2O_5 studies imply reduction and congruent vaporization at 1200K and 1800K, respectively. At the lower temperature the appearance of $(VO_2)_g$ and $(VO)_g$ can be explained by the V_2O_5 reduction reaction

$$2(V_2O_5)_s + 3(C)_s = (VO_2)_g + (VO)_g + (V_2O_4)_s + 3(CO)_g.$$

At 1800K the $(V_2O_4)_s$ from the above reaction melts and decomposes to $(VO_2)_g$ which is then reduced to the liquid phase of vanadium by the reaction

$$(VO_2)_g + (C)_s = (V)_\ell + (CO_2).$$

Equilibrium calculations show these reactions to be favored at the temperatures stated.

* This research is sponsored by the Division of Chemical Sciences of the Department of Energy and performed under DOE Contract Number DE-AC06-76RLO-1830.
+ Operated by the Battelle Memorial Institute for the Department of Energy.

[1] B. V. L'vov, D. A. Katskov, L. P. Kraglikova and L. K. Polizik, Spectrochim. Acta 31B, 49 (1976).
[2] W. C. Campbell and J. M. Ottaway, Talanta 21, 837 (1974).
[3] J. Aggett and A. J. Sprott, Anal. Chim. Acta 72, 49 (1974).
[4] R. H. Eklund and J. A. Holcombe, Talanta 26, 1055 (1979).
[5] R. F. Sturgeon, C. L. Chakrabarti and C. H. Langford, Anal. Chem. 48, 1972 (1976).
[6] D. C. Johnson, B. L. Sharp, T. S. West and R. M. Dugnal, Anal. Chem. 47, 1234 (1975).

SCHEMATIC OF COMBINED MS-AAS APPARATUS

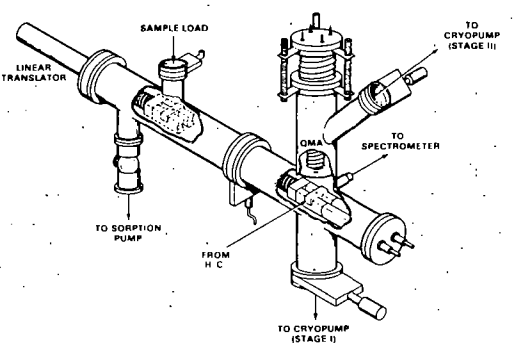

FIGURE 1.

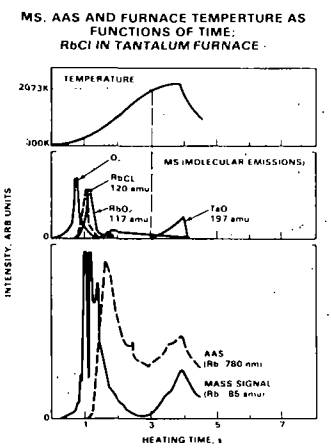

FIGURE 2.

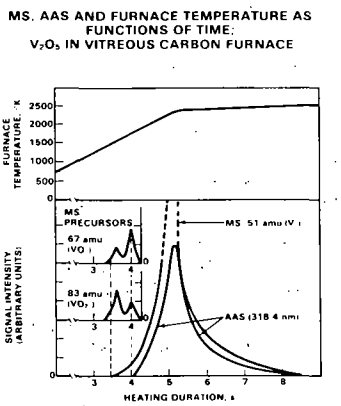

FIGURE 3.

RECENT DEVELOPMENTS IN NUCLIDE GAS-SOURCE ISOTOPE RATIO MASS SPECTROMETERS

M.M. Michlik, D.A. Smith, T.J. Eskew, and L.F. Herzog

NUCLIDE CORP., State College, PA 16801

Nuclide has been building high-precision mass spectrometers for both "flow" and "static" isotope abundance measurements of gaseous samples commercially since 1954. Some recently introduced configurations, options, and accessories are described, including:

THE AUTOMATED 6-60-RMS/TA — the latest in a sequence of 6" 60 analyzer multicollector isotope ratio instruments that commenced in 1954, it features an externally-switchable triple collector for m/e 44-5-6, 28-9-30, etc., a high accuracy triple (interpolative) inlet, a second "mass 2" analyzer arm for HH/HD, HP85 or other programmable-calculator automation with automatic peak-centering, and numerous other advanced features.

THE LOW VOLUME, HI-T BAKEABLE, FULLY AUTOMATED 12-90-SGA FLOW/STATIC GAS ANALYZER is optimized for ultra-small sample analysis (e.g., 10^4-10^5 atoms). Externally-variable object and image slits can be set for high resolution and abundance sensitivity or high transmission efficiency as needed, while in operation. Zr(Al) or Ti static-mode getter pumps and an oil-free-turbopumped-inlet are offered. A small size, low noise ceramic multiplier is used for ion detection by ion-counting; it or an externally interchangeable F-cup can be used for simultaneous detection of ^3He and ^4He, with excellent resolution of HD^+ from ^3He and minimal crosstalk. This instrument extends the range of tritium measurements to smaller samples than can be measured by other techniques; it also has ideal characteristics for ^3He earthquake prediction studies.

A 3-60-RMS/HD SPECIALLY CONFIGURED FOR "CO_2 ISOTOPE BREATH TESTS" in clinical medicine — with automated, multiplexed sample purification, inletting and pumpaway, and flow control. The 3-60-RMS still offers X10 better carbon-13/12 ratio measurement precision than is achievable with the most modern ultra-high resolution tunable-diode laser, low pressure, infrared absorption instruments — at a lower cost.

AUTOMATED GAS-OF-INTEREST EXTRACTION/PURIFICATION SYSTEMS, for example, for:

- Extracting CO_2 from breath, or other gaseous samples
- Extracting H_2 from H_2O — via U-furnace and U-pumping
- CO_2/O_2 Equilibration system for extracting oxygen from water samples
- Extracting N_2 from agricultural and biological, etc., samples by automated reactions
- Extracting noble gases from rocks, meteorites, lunar samples, etc. — by electron bombardment or R-f heating at T up to 2000 C
- Extracting gases from small areas in rocks, etc., by Laser or E-Beam flash vaporization/ionization.

STATE-OF-THE-ART COMPONENTS TO UPDATE Nuclide and other isotope ratio-difference measurement instruments; complete modernization can be performed at plant or site.

MULTIPLEX, AUTOMATED INLET SYSTEMS capable of controlling sample flow, opening and closing valves, etc.

AUTOMATIC SAMPLE/STANDARD FLOW EQUALIZATION SYSTEMS for GLASS-reservoir inlet systems as well as METAL (see below)

Automation of Variable-Volume Glass/Mercury Sample Reservoirs

For analyzing small samples, glass reservoirs, in which changing the mercury level is used to vary the reservoir volume, have certain advantages over multi-convolution-bellows variable-volume metal reservoirs: (1) the minimum volume achievable is considerably smaller, (2) they are much less expensive, (3) they can be readily modified, and (4) leaks can be located more easily, and (5) repaired by glass-blowing. Therefore, glass/Hg reservoirs have been used extensively in MS for over 30 years — especially in dual-inlet isotope ratio difference measurement systems.

To achieve high precision in ratio-difference analyses it is very important to keep flow rates of sample and standard(s) into the MS closely identical; hence, if the sample is small relative to the standard(s), one has to adjust the volume of one reservoir or the other (or the conductance of the leak) quite often, as gas flows out into the MS, to keep flow rates equal.

A system that does this automatically has now been developed by Nuclide. The mercury level, and hence, reservoir volume, is changed by changing the air pressure on the "other" (air) side of the mercury column.

The intensity of the major isotopic ion's current in (usually) the standard gas (i.e., mass 44, for CO_2), is used as a reference. The system automatically, periodically, compares to it the intensity of the same isotope's ion current in the unknown, when it is in the MS, and if it detects a difference, either raises or lowers the mercury level until they are again equal.

The first such system is now in routine operation, as a part of a Nuclide CO_2 Isotope Breath Test system at a hospital in Tokyo.

It includes, as photographs exhibited show, a small vacuum pump, a supply of air, and an "absolute pressure regulator" (APR) with its servomotor — as well as the same PRC-1A and PAC-1 pressure-difference-sensing and APR-initializing and stopping electronic control units used on Nuclide's variable-metal-reservoir system; however, in the glass-Hg variable reservoir system, the APR, pump and air inlet take the place of the motor-drive of the bellows volume in the metal system.

RECENT DEVELOPMENTS IN NUCLIDE THERMIONIC-SOURCE ISOTOPE RATIO MASS SPECTROMETERS

L.F. Herzog, J.H. Szybist and T.J. Eskew, Nuclide Corp.
State College, PA 16801

Nuclide has added to its "thermionic" (surface ionization) source mass spectrometer family new instrument configurations, options and accessories, and improvements of earlier designs, including the following — most of which can also be added to existing Nuclide instruments:

"CAROUSEL" SAMPLE-CHANGER, with a capacity of up to 16 single, double or triple filaments — which can be interchanged in any order without breaking vacuum.

DESKTOP CALCULATOR AND COMPUTER KEYBOARD-REPROGRAMMABLE CONTROLS FOR CAROUSEL AND OTHER SOURCES, e.g., for filament position and temperature, ion lens voltages, etc., as well as data-taking via peak stepping, and data processing

DOUBLE DISPERSION GEOMETRY 12"-90° ANALYZER, with an effective radius of 61 cm and with inherent Z-focusing

MULTIPLE (2-5) F-CUP COLLECTOR ARRAYS for simultaneously measuring all the isotope ratios of certain elements, e.g., strontium, neodynmium, lead, uranium, plutonium — to increase sensitivity while at the same time decreasing time per analysis by large factors (X2-4)

AUXILIARY RATIOMETER ("Nth NUMERATOR") MODULES for simultaneously measuring "N" isotope ratios using the IR3A integrating digital ratiometer

NEW SINGLE-ION DETECTOR SYSTEMS, e.g.,
An ultra-low-background CERAMIC MULTIPLIER
A high efficiency ION TO ENERGETIC-ELECTRON TO PHOTON DETECTOR FOR NEGATIVE IONS as well as positive ions — for pulse counting

FAST, FULL-RANGE (10^{-20} to 10^{-8} A), HIGH-PRECISION INTENSITY MEASUREMENT SYSTEMS — using ion counting and F-cup with V-to-F digitizer

HIGH SPEED TURBOMOLECULAR AND HYBRID (e.g., turbo-ion-cryo) pumping systems

DIGITAL MAGNET SUPPLY as well as other new digital MS controls

A COMPLETELY REDESIGNED 15 CM RADIUS SINGLE-FILAMENT TIMS (model 6-60-S) — optimized for labs for which moderate-throughput-rate analysis for precise isotope ratios of Sr and other light elements, is sufficient

ALTERNATE RAPID SAMPLE CHANGERS, e.g.,
An END-ON, VALVED VACUUM LOCK SAMPLE-CHANGER, (discussed below) — also readily adaptable to many already-operating TIMS analyzers
An IMPROVED, GASKETED, MOTOR-OPERATED, VALVELESS VACUUM LOCK sample-changer

SOLID-STATE ELECTRONICS TO REPLACE OBSOLETE EQUIVALENTS, as well as COMPLETE UPDATING/UPGRADING KITS AND SERVICING for Nuclide 12-60-SU, CEC 21-702/3 and other older TIMSs — electronics, data system, detectors, pumping system, vacuum lock, etc.

ELECTRON MULTIPLIER AND/OR FARADAY CUP ION DETECTORS FOR 2 AND 3 STAGE MASS SPECS — which can be switched in or out after the first magnetic ion analyzer

A SMALL-RADIUS POST-DETECTOR-SLIT ENERGY FILTER — retrofits 12-90-SUs and some 6-60s in field, to increase abundance sensitivity

FOR THERMIONIC ANALYSIS USING THE GRAF IIIS SPECTROGRAPH — new high-efficiency ion lens and ion detection systems and a high speed pumping system

AN INEXPENSIVE BELL-JAR FILAMENT PRECONDITIONING SYSTEM — low cost, ion pumped

A NEW THERMIONIC "SOFT IONIZATION" SOURCE FOR PRODUCING COPIOUS BEAMS OF NEGATIVE IONS — of SF_6, UF_6, etc.

These and other recent developments in Nuclide's thermionic-MS program are described. Additional details on certain items are given below; publications on all are available on request.

New End-On (Valved) Vacuum Lock Sample-Changer

This means of rapidly changing sample-loaded filaments for analysis can be added to most earlier-delivered Nuclide (and other) TI-MSs in the field, with a minimum of rework. Usually, only the "J1" plate which carries the filament assembly need be replaced or modified, since, in this system, it has to include a "docking" mechanism which mates with another on the filament-mount assembly, which now enters via the lock; these each have 6 contactors, for 3 filaments.

This inexpensive changer eliminates the need to bring source up to 1 atmo. to interchange samples — thereby increasing the maximum analysis rate achievable significantly. It accomodates either single, dual or triple filament arrays, and both glass-button and metal filament-support mounts can be used. (An adapter that fits on J1 is provided for button mounts to insure that filaments are properly positioned). The VL-shaft is hollow, so that a window can be installed on its end for measuring ionizing filament temperature by optical pyrometer. The piston, which carries the filament mount carriage in and out, is differentially pumped — the inner stage by a diffusion pump, if desired.

FPS/VP-1 Filament Preconditioning System

A need was recognized for an inexpensive preconditioning system for thermionic-source filaments, hence, we designed one using a standard 8" glass bell-jar as the vacuum chamber. Nevertheless, it has 12 leadthroughs, for heating up to 6 filaments, all in series or in series-parallel groups. The entire unit is mounted on a wheeled lab cart, with bell jar (with protective wire mesh cover) and electronic controls on the top shelf, and pumps mounted on the lower shelf. High vacuum can be obtained by ion (standard), turbomolecular, or diffusion (either oil or Hg) pumping, and forevac by rotary or cryosorb pumping. With getter-ion pumping, a special valving system is provided to "bleed" bell-jar gas into the ion pump until its pressure is low enough to open the main valve without stalling the pump.

Multiple F-cup Collectors

Simultaneous collection of several isotopes by "N" F-cups, long used to achieve high precision in gas-sample isotopic analysis, can be applied to good advantage also in thermionic analysis, to increase the efficiency of sample utilization and decrease the time required for an analysis.

In the triple collector (shown) — for example there is provision to vary the center-to-center spacings between the 3 slits and also the slit widths, while the MS is in operation, so that it can be shifted from the analysis of one element to another without breaking vacuum. (The same collector can of course also be used for ions from gas samples such as CO_2).

A five-slit/cup collector for Nd is offered for the 12-90-EG "extended geometry" analyzer, which has the dispersion of a conventional magnetic analyzer of 61 cm radius.

RECENT ADVANCES IN FULLY AUTOMATIC COMPUTER CONTROLLED STABLE ISOTOPE RATIO ANALYSIS; J.E.Cantle, R.M. Elliott; V.G.Isotopes Ltd., Winsford, Cheshire, UK.

This poster paper will describe recent developments in computer controlled automatic operation of the Micromass range of stable isotope ratio mass spectrometers. The flow diagram can best illustrate the comprehensive interlocking and interfacing that is required when full automation is contemplated. Manual toggle levers on the inlet are replaced by pneumatic actuators which in turn are driven by compressed air. All valves are fail-safe with respect to power failure, i.e. they close, thus preventing sample loss. Provision is made to bake the manifold and for elevated temperature operation (as for SO_2 analysis).

Both variable volumes are stepper motor driven and can cover the whole range 10-70cm^3. Microswitches are mounted to detect the volume limits. The standard balancing mode is set to reference volume to give a major beam ion current of $4x10^{-9}$ amps and then to alter the sample volume to give the same sample major beam ion current. If this cannot be achieved then the reference volume can be altered to allow balancing to take place. The normal sample volume that can be measured automatically is 2-4atm cm^3.

The signal from the Faraday collectors is amplified by a chopper amplifier and then using VFC's and counters converted to a digital value with six figures DVM readout. Timing from the control system sets the changeover valve timing, wait time, and measure time.

THE APPLICATION OF PYROLYSIS-GAS CHROMATOGRAPHY-MASS SPECTROMETRY TO THE STRUCTURAL CHARACTERIZATION OF AUSTRALIAN COALS; R.P.PHILP and T.D.GILBERT, CSIRO Division of Fossil Fuels, P.O.Box 136 North Ryde NSW 2113 Australia

The structural characterization of coal is particularly relevant at this time in view of their importance as alternative sources of liquid hydrocarbons. This paper will describe results obtained from the characterization of Australian coals by microscale pyrolysis combined directly with gas chromatography-mass spectrometry. These studies are important for obtaining structural information on the coals and also information on the nature of the products produced by large scale liquefaction of the coals.

Low rank brown coals from the Yallourn deposits in Victoria produce pyrolysis products dominated by various alkyl-substituted methoxyphenols. These pyrolysis products can be related directly to the lignin structures of the woods initially responsible for the formation of the coals. Higher rank coals from the Sydney Basin produce far more complex pyrograms and are generally dominated by alkyl substituted naphthalenes, anthracenes and phenanthrenes and contain few, if any, phenolic components.

A UNIVERSAL MAGNETIC TAPE FORMAT FOR GC/MS DATA

L.E. Slivon
Battelle Columbus Laboratories
Columbus, Ohio 43201

and

W.L. Budde
U.S. Environmental Protection Agency
Cincinnati, Ohio 45268

The lack of a universal standard format for the storage of raw GC/MS has resulted in numerous difficulties among analysts having dissimilar instruments and data systems. Various versions of the EPA format are incompatible among different GC/MS data systems resulting in the fact that archived raw data is readily accessible only by the same data system as that used originally.

It is the intent of this study to introduce a preliminary design ("Strawman") for a universal archival magnetic tape format. The development and implementation of such a format will allow various GC/MS facilities the capability of exchanging computer readable low resolution data independent of the instrument and data system used to acquire that data. Furthermore, a universal format will facilitate the development of large scale multi-laboratory analytical programs and inter-laboratory quality assurance efforts related to such programs. Although no existing format is universally applicable to all data systems, certain aspects of various EPA formats which have been used to archive mass spectral data provide a useful template for the development of a universal format.

The format consists of three fixed file header records, a variable number of optional method-parameter-history records followed by the successive raw mass spectra. All descriptive and mass-intensity information is ASCII coded into 80 character records. Many features of existing EPA formats have been retained in order to allow the possibility that many existing EPA formatting programs can be modified rather than completely re-written. Significant features of the Strawman format include:

1) Flexibility for future expansion. Additional method-parameter-history records may be added without requiring extensive software modifications.

2) Integer (wide range) or moderate accuracy mass assignments available within the same format.

3) Unique four digit floating representation of ion intensities provides three significant figures of information over a dynamic range of 10^{11}.

Details of the above strawman format are available from the authors.

IMPROVED SYSTEMS FOR COMPUTER RETRIEVAL AND INTERPRETATION OF MASS SPECTRA. I. K. MUN, D. B. STAUFFER, R. G. DROMEY,* S. O. RUSSO, AND F. W. MCLAFFERTY; Dept. of Chem., Cornell Univ., Ithaca, NY 14853 (*University of Wollongong, NSW 2500, Australia)

The Cornell data base has been expanded to include approximately 55,000 different spectra of 43,000 different compounds, with correction of numerous errors in the previous data base. This has improved the performance of our Probability Based Matching (PBM) system, which is designed for matching an unknown mass spectrum against a large reference collection of electron ionization spectra collected under a wide variety of experimental conditions. Despite the enlarged data base, ordering this for the PBM search has greatly improved the time requirement; the search is limited to those reference spectra whose most important peak is among the most important peaks in the unknown spectrum. This importance is determined by the sum of the PBM "uniqueness" and "abundance" values. In a test of 431 unknown spectra of pure compounds run against 41,000 reference spectra no correct answers were missed while searching only 7.5% of the file. With reduced restrictions, 99.2% of the reference spectra were retrieved by searching only 3.8% of the file, and 97.5% were retrieved by searching only 1.6% of the file.

A further improvement to PBM has been provided by an optimum scaling of the unknown spectrum which compensates for mass discrimination and changing concentration effects. This matches the abundances of the unknown spectrum to those of the reference with a quadratic function. This has been particularly valuable in improving the reliability of results at high recall.

If a reference spectrum of the compound is not in the data base, our Self-Training Interpretive and Retrieval System (STIRS) is designed to provide information on the molecular weight and substructures present in the unknown. Recent publications listed below describe improvements to this system, which with PBM can be accessed directly on the Cornell computer by both U.S. and international customers over the TYMNET and TELENET computer networks.

References:

I. K. Mun, R. Venkataraghavan, and F. W. McLafferty, Computer Prediction of Molecular Weights from Mass Spectra, Anal. Chem., 53, 179-182 (1981).

K. S. Haraki, R. Venkataraghavan, and F. W. McLafferty, Prediction of Substructures from Unknown Mass Spectra by the Self-Training Interpretive and Retrieval System, Anal. Chem., 53, 386-392 (1981).

I. K. Mun, R. Venkataraghavan, and F. W. McLafferty, Molecular Weight Parity Predicted from the Parity Values of Mass Spectral Peaks, Org. Mass Spectrom., 16, 82-84 (1981).

QUANTITATION OF MASS SPECTRAL DATA WITH A MICROCOMPUTER SYSTEM*

Michael A. Grayson
McDonnell Douglas Research Laboratories

Charles H. Brennenstuhl
McDonnell Douglas Automation Company

McDonnell Douglas Corporation
St. Louis, MO 63166

A variety of data systems for the acquisition and processing of mass spectral data for quantitative analysis has been described in the literature. Most of these systems rely on the use of a minicomputer and require specially designed hardware to interface the mass spectrometer output to the data system.[1] We describe a data system capable of quantitating the information from up to nine channels of mass spectral data from an instrument operating in the continuous ion-monitoring mode. Further, this system uses a general-purpose microcomputer (Digital Equipment Corporation MINC 11) equipped with standard interface modules.

Hardware – A block diagram of the hardware used for the acquisition of data is given in Fig. 1. Most of the data from the experiment are in the range of 0–5 V dc, and these analog data lines are wired directly to the MINC input plugs. All of the data from the MARK V chassis is outside the range of the analog-to-digital converter (ADC) and is conditioned by voltage divider networks, with the exception of the trap current, which is conditioned with an operational amplifier configured in an emitter-follower circuit. Because of the large number of analog channels which must be digitized, two multiplex modules are required to feed the analog-to-digital converter. The only digital data acquired by the system are from an ionization gauge controller (Veeco RG 1002).

Software – The software system that performs the acquisition and processing of data from these experiments consists of the following programs: MASGET, MASCAL, POST, PAMPLT, and MASTUN. The relation of the various programs and their input/output files is illustrated in Fig. 2.

The complete data acquisition process is software controlled by the program MASGET. Thus, the data acquisition rate and the data channels to be digitized are selected by an interactive routine in the beginning of MASGET. This mode of operation was selected because the experimental conditions and nature of the sample can vary over a large range. For example, in some cases, the only compound evolved from the sample may be water, which can be recorded with one gate. In other instances, five or six compounds are evolved from the sample upon abrasion, and all must be recorded. Thus, MASGET was designed to acquire data from the most demanding experiment that could be performed with the mass spectrometer as it is configured, yet also to be efficient for simpler experiments.

The data from MASGET are stored in a GET file which contains the raw data in binary form from the data acquisition process. Every effort has been made to make MASGET an efficient, fast data acquisition program; consequently the acquired data are written directly to disk storage without any data processing. During the experiment, MASGET permits the user to observe the ion current collected at one mass in real time by displaying the change in ion current on the cathode ray tube (CRT) as the data are sampled.

MASCAL is an interactive program to obtain sensitivity factors for the compounds of interest. The program permits multiple determination of the sensitivity factor at different mass flow rates of gas into the instrument. Thus, an average sensitivity factor based on data over a range of mass flow rates is obtained.

POST is a batch program which permits conversion of the raw data from GET files into weight percent data using the sensitivity factors from MASCAL.

PAMPLT is a plotting program which permits the display of any two measured variables in terms of a third. Typically, the indigenous volatile content in weight percent is plotted for two volatile compounds as a function of the position of the tool in the sample. However, the program is flexible enough that it can plot any of the measured variables weighted by a scaling factor entered at the terminal. In addition, there are routines for filtering the data, performing deconvolution analyses of the data, or integrating the area under the distribution profile to obtain total indigenous volatile content of the sample.

MASTUN is an interactive utility used to display the digitized data from any channel in a strip-chart mode on the CRT. This program is used to tune the mass spectrometer and position gates in the spectrum.

The use of a general-purpose, microprocessor-based computer with standard interface modules as a means of acquiring and processing mass spectral has been demonstrated. The data system has been successfully applied to the quantitation of indigenous volatile compounds desorbed from the abrasion of various polymeric materials.[2]

This research was conducted in part under the McDonnell Douglas Independent Research and Development Program.

References

1. *A. L. Burlingame, T. A. Baillie, P. J. Derrick, and O. S. Chizhoz, Anal. Chem. 52, 214R (1980).*
2. *M. A. Grayson, Resins for Aerospace (Clayton May, Ed.) (American Chemical Society, Washington, D. C., 1980) p. 449.*

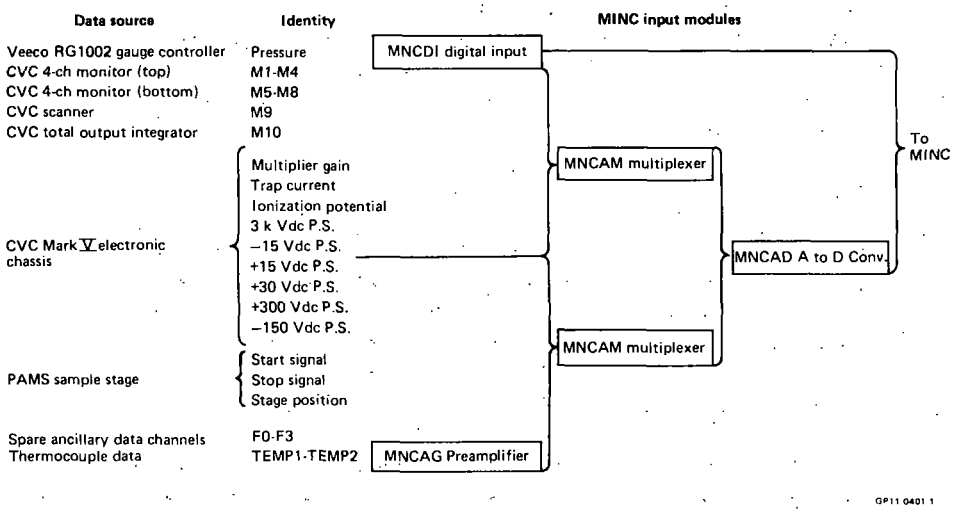

Fig. 1 Hardware used to acquire mass spectral and ancillary data for PAMS experiments.

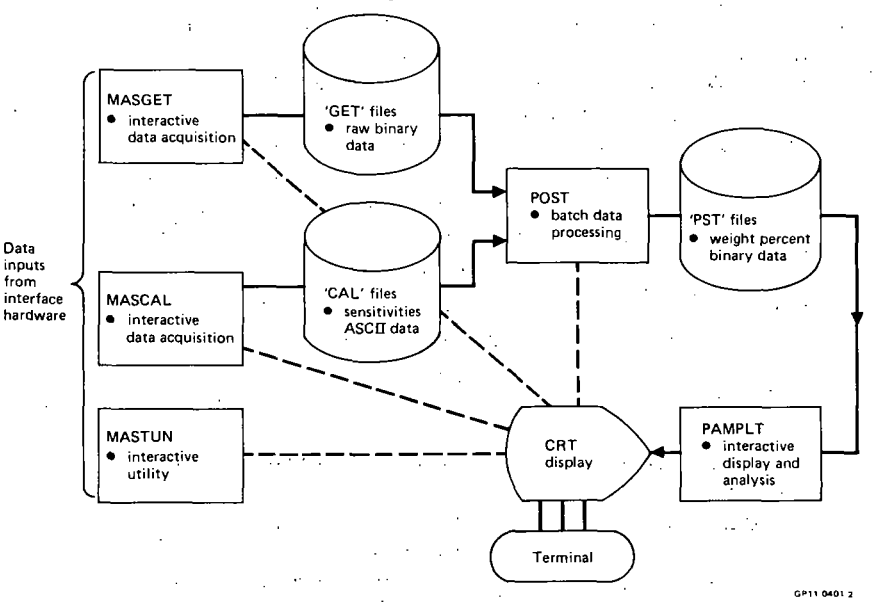

Fig. 2 Program relationship and data flow diagram for microcomputer-based quantitative data system.

DESIGN AND TESTING OF A NEW MULTICHANNEL ANALYSER

by P.BOULANGER, R. BISSON, M BARIL, départ. Physique et C.R.A.M., Université Laval, Ste Foy, Québec, Canada G1K 7P4; R. PAQUIN, Ministère de l'agriculture, de l'alimentation et des Pêcheries du Québec, 2700 Einstein, Ste Foy, Quebec, Canada G1P 3W8.

GENERAL DESCRIPTION

This new multichannel analyser has been designed to meet the requirements of special purpose mass spectrometers such as a multipassage magnetic mass spectrometer, the analyser is built around readely available texas instruments industrial boards (TM990/101 16 bits microprocessor) and one custom designed board.

The apparutus contains two independent processors: The first processor is programmed in assembly language and is assigned to multiscaling,pulse height analysis and graphic display; The second is programmed in T.I.'S POWER BASIC and performs the various high level tasks such as data treatment, communication with a mainframe computer, A X-Y recorder and a high speed printer, both processors share access to an intelligent floppy disk system.
This mode of operation enables the user to configure the system with high level language programming. One typical application of this system is the time study of a phenomena: Data is acquired for a 20 minutes period and transferred to Disk, memory is reset and process restarts.

The BASIC program required to perform this task follows:

```
10 GOSUB 4000 20 MIN.DELAY DURING ACQUISITION
20 PRINT "<OB>AA<OD>" STOP ACQUISITION
30 GOSUB 2000         ACQUISITION STOP DELAY
40 REM
50 REM INITIATE TRANSFER OF GROUP 0  TO FLOPPY DISK
60 REM
70 PRINT "<13><OB>CS  0<OD>"
80 GOSUB 3000         TRANSFER DELAY
90 PRINT "<OB>CL 0"   CLEAR ALL DATA OF GROUP 0
100 PRINT "<OB>AD<OD>"RESTART ACQUISITION
110 GOTO 10
```

The system may monitor other signals during acquisition
- vacuum system
- parameters of an experiment

It allows data treatment such as:
- Peak Finding
- Spectrum analysis

And other features facilitating the user's work:
- Programmed change of the parameters of experiment
- Communication with a host computer
- Automatic optimisation of operating parameters of the mass spectrometer.

GENERAL CHARACTERISTICS:

(1) MODULAR SYSTEM
(2) MULTIPROCESSOR MODE
(3) ACQUISITION TYPE:

NAME	TYPE	TIME CHARACTERISTICS
MCA*	Standard	1ms/channel---900s/channel
MCA*	Lock-in	1ms/channel---900s/channel
MCA	Ultra fast	1µs/channel--- 10s/Channel
A/D	Standard RTI board from ANALOG DEVICES	100µs/channel
PHA	Standard PHA from Canberra or Ortec	

(4) All acquisition points are written into memory in 32 bits words.
(5) Numerical treatment in BASIC of full APL language.
(6) Interactive system setup
(7) Text editing through sykes disk system
(8) Use of standard boards from Texas Instruments
(9) Graphic display with low cost X-Y-Z CRT.
(10) Memory:
In acquisition processor:
ROM 12K control programs
RAM 12K for control register and data storage.
BASIC processor (Available)
ROM 16K BASIC interpreter
RAM 16K user programs
APL processor (Coming)
RAM 256K
(11) Low cost (~9,000.00 U.S.) with BASIC interpreter
* The maximum frequency of the counter is 100MHz

THE DIGITAL LOCK-IN

In the design of the multipassage mass spectrometer, the ions are pulsed into the mass spectrometer to meet the requirements of its operation. We used this characteristic to discriminate the real information from the noise background.
To do so we use an UP/DOWN counter that is synchronised with the pulse generator of the ion source. This circut acts as an analog lock-in.

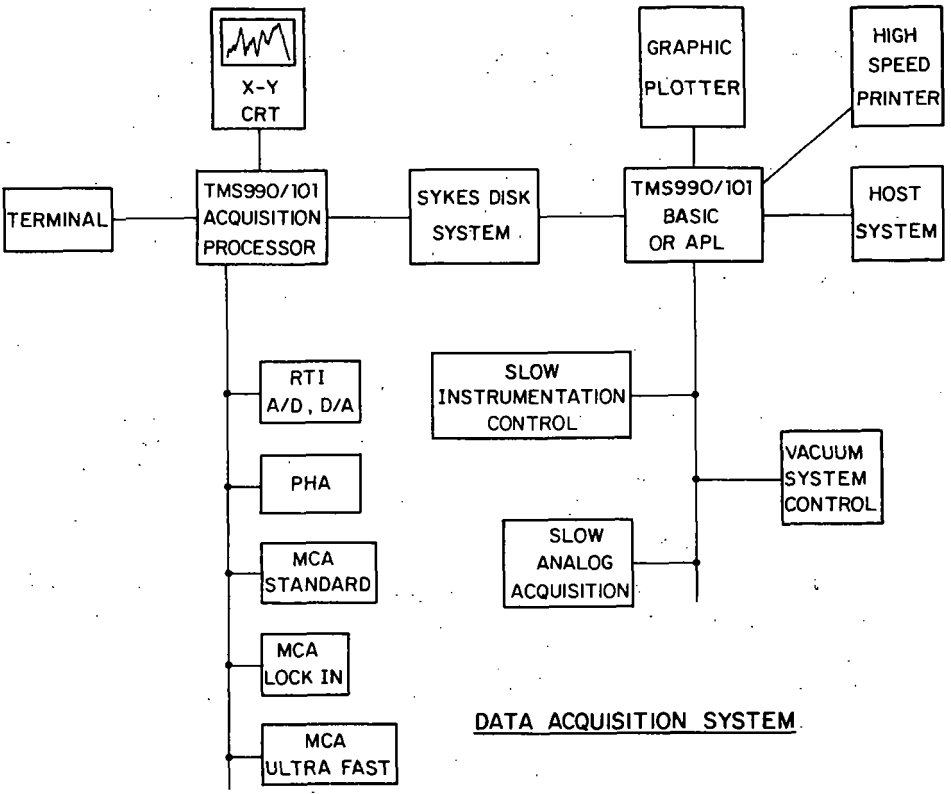

DATA ACQUISITION SYSTEM

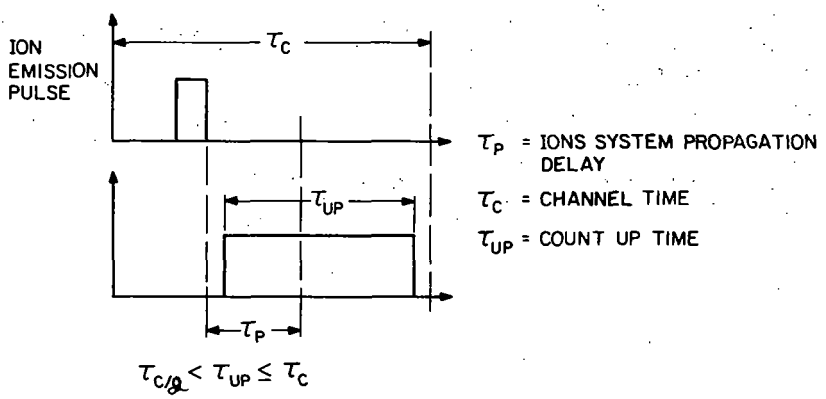

$\tau_{c/g} < \tau_{UP} \leq \tau_C$

COMPUTER ASSISTED MS/MS FOR MIXTURE ANALYSIS

A. E. Schoen, D. Zakett, and R. W. Korzeniowski,
Department of Chemistry, Purdue University
West Lafayette, Indiana 47907

Automation of the MIKE [1] spectrometer was undertaken to provide access to system configurations which were not available using analog circuitry. The motivation behind this research project was to allow creative utilization of all mass spectrometric parameters in experimental design, and to present the possibility of combining those parameters to access new fundamentals of ion chemistry.

The Purdue Mass Spec Data System is based on HP's RTE II disc operating system for a 2100a minicomputer. This system uses custom drivers and modified system software to control the accelerating voltage, magnetic field, and electrostatic analyzer voltage of a reversed geometry mass spectrometer. Hardware and software interfacing is optimized for simple, versatile programming via a high level language (FORTRAN IV). Utility subroutines in FORTRAN and HP assembly language handle most of the necessary machine oriented control which allows the spectroscopist to design programs in terms of relevant and familiar parameters such as kinetic energy or magnetic field. All software is modular, which allows new applications to build on the formats and conventions of previously developed programs. This design permits experiments such as neutral loss or B/E linked scans to be easily programmed. In addition to the ability to execute unique experiments, routine MS/MS work is greatly enhanced by the speed of automation. A complete software package provides for ESA scan control; data accumulation and ensembling in both pulse counting and analog detection modes; data file creation, manipulation, and display; and a library indexing and search system. A programmed executive leads the spectroscopist through the available options from finding the mass-analyzed ion beam of interest to plotting the final, publication-ready spectrum. Table I illustrates the time savings which have been realized by this project.

TABLE I : Typical Times Required for Various MIKES Operations

		Before Computerization	After Computerization
1.	MS/MS spectrum data acquisition	300-600 sec.	10-50 sec. (one scan)
2.	MS/MS data reduction	1-2 hours	2 min.
3.	MS/MS spectrum plot (publication quality)	2-4 hours	5 min.
4.	Neutral loss scan	not possible	2 min.
5.	Selected fragment scan	not possible	2 min.
6.	Multiple fragment monitoring	not possible	0.1 sec./ion
7.	Ensemble Averaged MS/MS	not possible	as long as needed
8.	Laser Synchronized MS/MS with ensemble averaging	not possible	possible

Hardware is also modular and may be added to easily without major modification of the operating system. This is accomplished through extensive use of the IEEE-488 interfacing standard. All I/O ports are standard HP parts except for a 32 bit parallel input for the eight digit BCD counter. All input/output operations and program swapping is under standard operating system control. This requires substantial system overhead to service data acquisition interrupts, which adds approximately seven seconds to every computer driven ESA scan. All ESA scans are totally asynchronous however, so the inconvenience is minimal and more than compensated for by the versatility available.

In the context of a research oriented environment, this design approach has proven to be essentially adequate. Figure I shows a block diagram of the instrument and the associated interfacing. Examples of current system application are: routine mixture analysis, ion structure determinations via consecutive collision reactions, mixture analysis via neutral loss and selected fragment scans, charge inversion studies, laser desorption and time profiling. The ability of this system to grow and service the needs of a large and innovative research group demonstrates the practicability of this system design.

FIGURE I

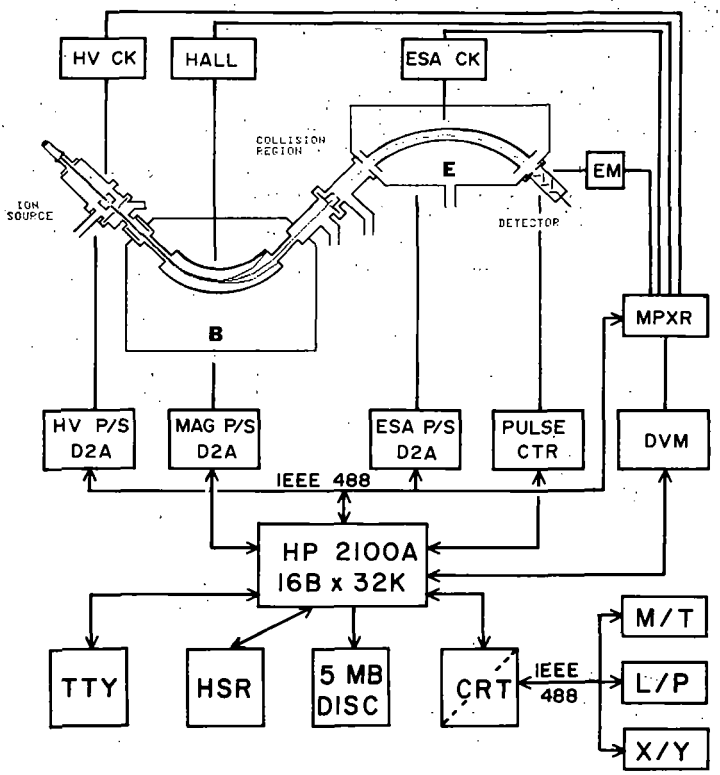

1. J. H. Beynon, R. G. Cooks, J. W. Amy, W. E. Baitinger and T. Ridley, Anal. Chem., 45 (1973) 1023a.

AN AUTOMATED TRIPLE QUADRUPOLE MASS SPECTROMETER

H.R. Gregg, J.W. Chai, J.A. Chakel, P.A. Hoffman,
R.K. Latven, R.S. Matthews, C.A. Myerholtz, B.H. Newcome, C.G. Enke
Department of Chemistry
Michigan State University, East Lansing, MI 48824

In the two years since the introduction of the triple quadrupole mass spectrometer, 1,2. our instrument has evolved into a much more flexible system. We have automated a number of parameters and are on the way to a completely automated instrument. Below are described the enhancements made in the past two years.

Ion Sources

Two ion sources are presently employed: an electron impact type of our own design, and a Finnigan model 3000 for chemical ionization.

The EI source is a cross-axial type with a magnetically confined electron beam, and an elongated ionization region for electron energy homogeneity and minimum interactions between newly formed ions. The source is highly sensitive, and has fine structure definition to about 0.25 eV.

The CI source is a Finnigan 3000, modified to mate with the Extranuclear quadrupole. The source temperature is programmable between ambient and 280°C.

Ion Path and Detector

The electrostatic lens and quadrupole offset potentials are controlled by a series of digitally programmed power supplies, designed and built in-house. The present system can regulate up to 64 devices of this sort through a range of ±200 volts, with 0.1 volt resolution.

Quadrupoles 1 and 3 are standard Extranuclear Labs 0.95 cm diameter x 20 cm long rods (1-1000) amu) while quad 2 was constructed in-house with 0.954 cm x 21.6 cm rods. Each quadrupole is controlled by an Extranuclear Labs quadrupole power supply (QPS). Mass selection is accomplished by programming the QPS with a 0-1 mA current proportional to the mass.

The detection system consists of a Galileo channel electron multiplier followed by a Keithley picoammeter and an analog to digital converter. The picoammeter's amplification is controlled by a microprocessor providing a useful dynamic range of 10^5.

Mechanical Construction and Vacuum System

Enhancements in mechanical construction and vacuum system have greatly increased reliability and performance on the TQMS.

The 40 liter vacuum chamber consists of three differentially pumped chambers housing the source, the pressurized second quadrupole, and the detector. The turbomolecular pumps provide a good (low 10^{-8} torr), clean vacuum with little chance of backstreaming oil. These turbo pumps have made instrument modifications (changing sources) routine; vacuum-to-vacuum time is less than 45 minutes.

Absolute pressure measurements are made with an MKS capacitance manometer, while ion gauges monitor the pressure of each chamber and of the target gas. A Granville-Phillips pressure controller maintains a constant collision gas pressure throughout an experiment.

The "ion gun" consists of the three quadrupoles, interquad lenses, detector and housing, and the quad 2 gas inlet and pressure measurement tubes all mounted off the rear flange. This arrangement facilitates removal, assembly, and possible modification.

Microprocessor Control System

In the near future a new control system will be implemented to allow more rapid scanning and a friendly human interface.

A multiple microprocessor system has been developed to allow for the distribution of tasks among the several processors for simultaneous and non-interfering execution. This allows higher speed operation and flexibility due to the inherently modular nature of both hardware and software. The eventual system will involve five microprocessors operating in parallel with a PDP-11/23 for data processing and graphics display.

Hardware for our microprocessor based system was developed in-house and is modular, reliable, and adaptable. Small cards, each encompassing a separate function, are soldered "piggy-back" onto a "motherboard", effectively making a 4 layer board. These motherboards are then connected via a backplane/bus arrangement on which all I/O connections are made.

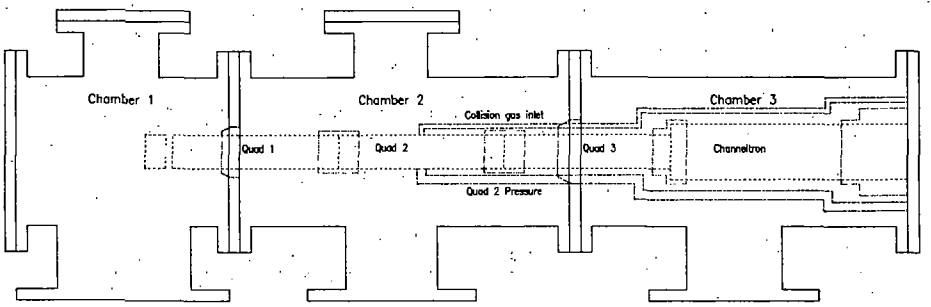

Figure 1.

References

1. Yost, R.A., Enke, C.G., McGilvery, D.C., Smith, D. and Morrison, J.D. Int. J. of Mass Spec. and Ion Physics, 30, 127 (1979).

2. Yost, R.A., and Enke, C.G., Anal. Chem., 51, 1251A (1979).

This work was supported in part by grants from The Office of Naval Research and the National Institutes of Health.

A USER-ORIENTED DATA SYSTEM FOR A TRIPLE QUADRUPOLE MS/MS SYSTEM; S.W. QUIGLEY, M.R.A. SMITH, W.R. DAVIDSON, AND J.A. BUCKLEY; SCIEX INC., 55 Glencameron Rd., Thornhill, Ontario, Canada.

Triple quadrupole MS/MS systems can be sophisticated instruments which provide users with vast quantities of data. To simplify operation, yet provide more meaningful data, the TAGA™ 6000 MS/MS system employs a powerful data system, which through operator interaction, controls the complete MS/MS hardware, provides several data acquisition modes, manages the acquired data efficiently and displays the output data in a variety of formats for ease of interpretation by the operator. The data system revolves around the PDP-11/23 processor with an RSX-11M Multitasking and Multiuser Operating System. All mass spectrometer functions, focussing lens voltages, and specialized features of a triple quadrupole MS/MS system are under direct computer control. Data may be acquired in several modes at the discretion of the operator. These modes include: Scan-Scan, in which the first quadrupole, Q1, and the third quadupole, Q3, are both scanned; Daughter Ion Scan, in which Q1 operates in a multiple ion mode and Q3 is scanned; Parent Ion Scan, in which Q3 operates in a multiple ion mode and Q1 is scanned; Multiple Reaction Monitoring, where Q1 and Q3 are operated in multiple ion modes; Sychronous Scan, where Q1 and Q3 are scanned simultaneously with a constant amu difference between them to show constant neutral loss or gain; and Conventional Scan, where either Q1 or Q3 is in an RF-only mode while the other mass analyzer is scanned. The methods in which data may be displayed for interpretation are numerous since the data has four dimensions: parent ion mass, daughter ion mass, daughter ion intensity and time. The software is extremely flexible in that the data may be plotted in several three dimensional or two dimensional formats. Up to four separate plots may be output on one terminal screen page. Details of the above features of the TAGA™ 6000 MS/MS Data System will be presented.

COMPUTER ASSISTED HIGH RESOLUTION MS/MS

F.W. CROW and R.L. LAPP;
Midwest Ctr. for Mass Spec.,
Univ. of Neb.,
Lincoln, NE 68588

The Kratos MS-50 triple analyzer mass spectrometer has been interfaced to a Data General Nova 4X computer for data acquisition of metastable and collision-induced spectra. This is the first step in developing an automated high resolution MS/MS for the purpose of sequential multicomponent analysis of complex mixtures.

Software has been developed to facilitate signal averaging of MIKES data. The number of scans averaged and the number of data points per scan are determined by the operator. The computer initiates each individual scan, sums the spectra, displays the data and transfers the data to disk. The data displayed and saved on disk may be either individual scans or the sum of a preselected number of scans. The system includes two 10 Megabyte disk drives (DG Model 6045) and a high speed dual-density tape drive (Kennedy Model 9300) for data storage.

The first stage of data processing includes assigning the mass and intensity scales followed by displaying the spectra on an interactive graphics terminal (Tektronix 4025). The second stage includes: 1. data smoothing, 2. baseline subtraction, 3. spectral magnification and multiplication, 4. curve fitting and 5. spectrum labeling. All processing is entirely under operator control and is designed with maximum flexibility. Each option is described briefly as follows.

Three data smoothing algorithms have been incorporated: moving average, Savitsky-Golay and a modified three-point smooth as described by Trott and Beynon (1). The user may select the width of the smoothing window with the first two algorithms,and for all three, the user specifies the number of iterations to be performed.

For baseline subtraction, the user may either define a single value to be subtracted from the entire spectrum or define several points through which a straight line will be fitted using least-squares methods.

The user can easily define a window to enclose a selected region of the displayed spectrum. The data within that window may then be multiplied or divided by a user specified factor or it may be expanded to fill the entire plotting area. In addition to multiplying a selected region the user has the option of magnifying the entire spectrum to locate small peaks or to scale the data appropriately for observation.

As an aid in documentation the user may place the run title, experimental parameters, a structural drawing and/or any other informative text at any specified location on the plot. After composing the plot on the VDU screen the contents of the screen can be duplicated on a hardcopy device (Calcomp 1012 plotter).

All of the commands used for processing consist of single keystrokes which are easily learned by the user. This software and hardware arrangement allows the experimenter to proceed from raw data to publication quality plots within a few minutes.

Reference:
1) G.W. Trott and J.H. Beynon, Int. J. Mass Spectrom. Ion Phys., 31(1979)37-49.

AUTOMATION OF A HIGH-RESOLUTION MS/MS INSTRUMENT. I. K. MUN, M. P. BARBALAS, D. C. MCGILVERY, T. A. MCCARRICK, P. J. TODD, I. J. AMSTER, A. S. BISHOP, AND F. W. MCLAFFERTY: Dept. of Chem., Cornell Univ., Ithaca, NY 14853.

The on-line computer has been applied advantageously to high-resolution mass spectrometers (MS) and both the reversed-geometry and tandem quadrupole MS/MS instruments. Our high-resolution MS/MS utilizing tandem double-focusing mass spectrometers has now been interfaced to PDP-11/45 and -11/10 computers with a graphics display control system. It is necessary to operate MS-II as much as 20 keV off ground; the MS-I, MS-II, and β'-detectors are coupled to the multiplexer and computer through fiber-optics datalinks. The ion lens after the collision region and the electrostatic analyzer and magnet of MS-II are operated in a "linked scan" mode under computer control in order to scan the MS-II spectrum.

A data base containing more than 700 CA spectra of ions of average mass greater than 100 have been collected; the data base is available from the authors. CA spectra measured by MS-II are matched against this data base in real-time using an algorithm patterned after that for "Probability Based Matching" for normal mass spectra. The resulting substructural information is displayed on a graphics terminal, as are the elemental composition data from MS-I. A variety of menu functions are available for operator manipulation of the data to construct molecules consistent with these data.

For routine quantitative analysis of complex mixtures, MS-II can be used in a "multiple ion monitoring" mode under computer control; the low impedance magnet allows switching to and measurement of an individual peak in ~0.1 sec.

COMPUTER-CONTROLLED ICR MASS SPECTROMETER FOR ANALYSIS OF ION-MOLECULE RATE CONSTANTS; V. G. Anicich and W. T. Huntress; California Institute of Technology, Jet Propulsion Laboratory, Pasadena, California 91109.

The ICR at the Jet Propulsion Laboratory has been interfaced to a TI 990/10 minicomputer. When operating in the trapped ion mode, the computer controls the reaction time and digitizes the peak heights. After the computer accumulates several sets of data it then analyzes the data and outputs the measured rate constant with a graphical representation of the computer fit to the experimental measurements including error bars. This innovation reduces both measurement bias and the time it takes to measure a rate constant.

THE DEVELOPMENT OF A FULLY COMPUTER CONTROLLED DOUBLE FOCUSSING MAGNETIC SECTOR MASS SPECTROMETER:

J.C. Bill, T.R. Kemp, J.C. Sadler, M.J. Wallington;
VG Analytical Ltd, Tudor Road, Altrincham, Cheshire WA14 5RZ, England.

Previous work on the computer control of mass spectrometers has generally been applied to quadrupole instruments. Magnetic sector instruments have proved to be problematical because of the eddy currents and hysteresis effects of the magnet. A new laminated magnet[1] and a sophisticated digitally controlled scan function generator[2] have been combined, and provide the basic elements for complete computer control of a double focussing mass spectrometer. The magnet, plus an appropriate power supply, is capable of scan rates faster than 0.1 sec/decade, and cycle times of less than 0.3 secs are easily obtainable. More significantly, because of the drastic reduction in both eddy currents and hysteresis, wide range magnetically selected ion recording (M.S.I.R.) has become practicable.

With the availability of this increased flexibility and performance in the magnetic sector, the incorporation of comprehensive computer controlled scan facilities was made possible. In order to provide full digital control of both magnetic and electrostatic sectors, without encroaching upon the processing capability of existing mass spectrometry data systems, the digital scan generator is based on the use of a dedicated microprocessor.

With reference to Figure 1, the development has placed special emphasis in the following areas:

A) The use of Direct Memory Access facilities between the Control and Acquisition Interface, and the main system Data Processing and Storage computer. Similar DMA interfacing is used to drive the high speed interpretive graphics terminal. This ensures that all data transfer operations are fully optimised.

B) The implementation of a colour raster graphic display with integral bit-slice image processor, and complete with a rate-type joystick cursor control. This combination provides much faster image display and faster more accurate cursor positioning than is available with conventional serial line driven displays.

C) Provision of a dedicated micro-processor for control of all scan and signal functions, including: normal B and E scans; linked B/E, B^2/E and $B/E(1-E)^{\frac{1}{2}}$; peak switching; auto-ranging of variable gain instrumentation amplifier.

D) Real time status information and keyboard control of the mass spectrometer by means of a dynamic graphics VDU terminal. The result of applying the above consideration to the proven ion-optical assembly of the Micromass 7070 mass spectrometer, has been an instrument embodying a greater degree of computer control than has previously been possible in medium resolution high performance magnetic sector instruments.

1. P. Burns et al. Paper TPMP16 28th ASMS New York NY.
2. J.C. Bill et al. Paper MPMP23 28th ASMS New York NY.

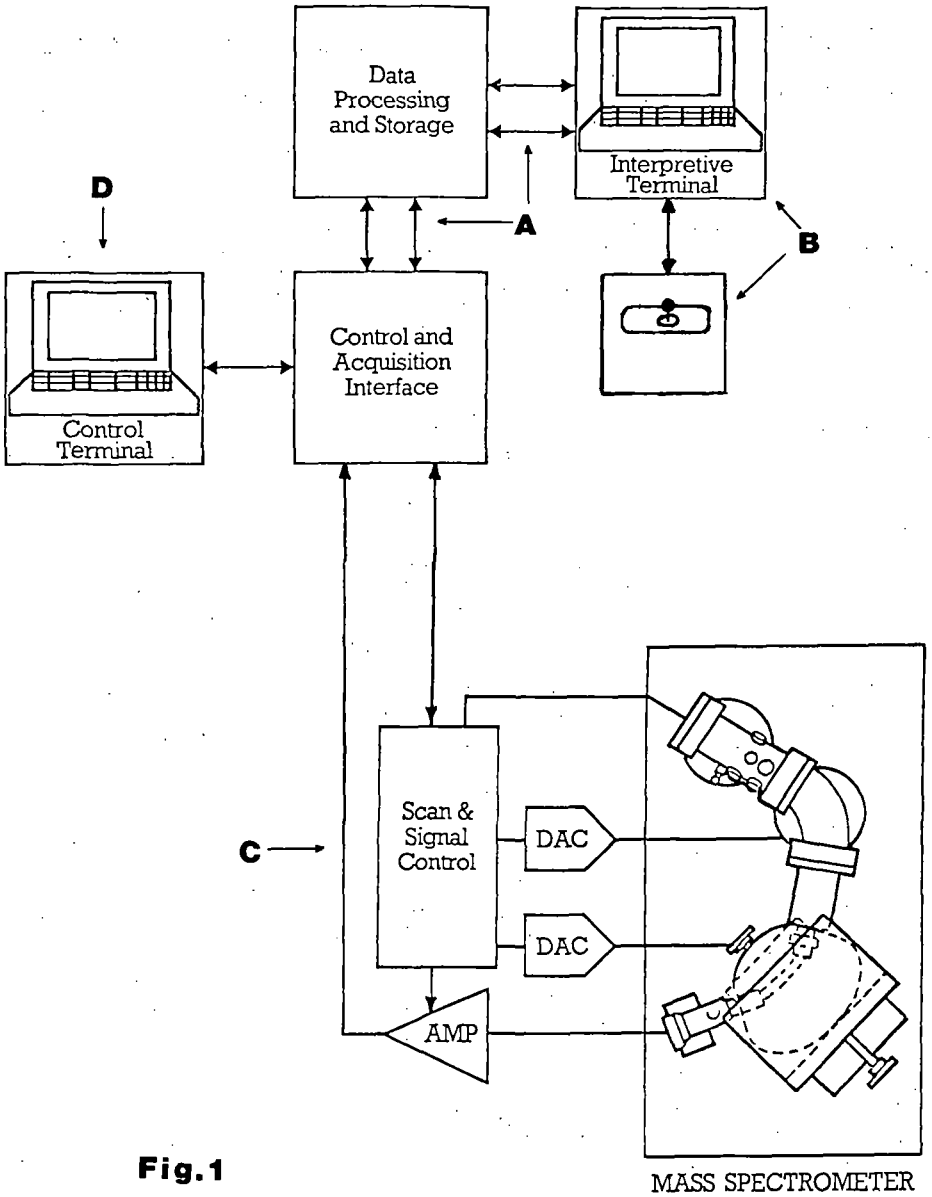
Data
Processing
and Storage
Interpretive
Terminal
D
A
B
Control and
Acquisition
Interface
Control
Terminal
C
Scan &
Signal
Control
DAC
DAC
AMP
MASS SPECTROMETER

Fig.1

OPTIMIZED FAST SCANNING WITH A HIGH PERFORMANCE SECTOR FIELD GC^2/MS/DS SYSTEM;

H. KAUFMANN, U. RAPP, K. WEISSENBERG AND M. SCHMIDT, Varian MAT GmbH, Barkhausenstr. 2, D-2800 Bremen 14, W. Germany.

Since the introduction of high performance glass capillary columns (GC^2) to mass spectrometry one has tried to optimize magnetic type mass spectrometers to the requirement of handling small GC peak widths in an optimal way. In this connection the scanning speed of the mass spectrometer seems to be one crucial point, one other being the processing speed of the data system coupled to the GC/MS system.
The key question in dealing with this type of analysis is the ratio of measuring time to cycle time of the complete system. In this respect the speed and preparation time required by the data system needs optimally designed software and hardware.

The concept of a data system featuring an acquisition processor based on a fast microprocessor together with a new scanning technique is optimally suited for the above described measuring problems. An approach will be presented achieving cycle times of 0.5 s/decade with a MAT 212/SS 200 configuration. The measuring time within the 0,5 s cycle time is about 0.4 s, meaning that 80 % of the total time is used for measuring. Details of the technical solution will be explained together with application measurements of samples where the need for fast scanning instructively is shown by comparing with "standard parameter acquisitions".

UPACS II - Mass Spectrometry System; L. Baczynskyj, D.J. Duchamp, L.C. Jones, M.D. Kenny, D. Marks, J.F. Zieserl, and J.B. Aldrich; The Upjohn Company, Kalamazoo, MI 49001.

The Upjohn Physical and Analytical Chemistry System (UPACS) is a computer system for laboratory automation of analytical instruments. The interfacing of three mass spectrometers and other instruments to an IBM 1800 computer has been described previously and summarized recently.* This system was called UPACS I.

In the last two years, Physical and Analytical Chemistry Research has moved to a new location, and a new computer system - the Harris S200 - has been acquired. This system is composed of two CPU's with shared memory and shared disks. At present, there are two 300 MByte disks for data storage and application programs and two 80 MByte disks for systems programs. One of the CPU's is used for real-time data acquisition and data processing, whereas the other one supports interactive programs such as interactive graphics, library searches, new program development, etc. This new system is called UPACS II.

At present, the following instruments are interfaced to this new system: two single crystal X-Ray diffractometers, three C, H, and N elemental analyzers with two analytical balances, a CD/ORD spectropolarimeter, and four mass spectrometers. All instruments acquire and process data simultaneously and store the results on disk.

The four mass spectrometers (CEC 21-110B, MAT CH5 DF, MAT CH7A, and LKB 9000) are connected to the computer via separate hardware interfaces, one at each instrument. The role of these interfaces is to digitize the output of the electron multiplier at the instrument and to send it in digital form to the computer. The hardware interfaces also provide mass markers for the CEC, CH5, and CH7 mass spectrometers. The Harris computer controls the start and stop of scans and data rate from each of the mass spectrometers. Digital data are entered into the computer via a Computer Products Inc. parallel DMA interface. Only data (electron multiplier signals) that are over an operator-selected threshold are sent to the computer for data reduction. Total ion current, probe temperature, ion source temperature, and GC oven temperature are sent in analog fashion to the computer.

The data acquisition program is resident in the memory of the computer. It processes the incoming data in three ways. For low resolution mass spectra it picks two high points of the incoming spectral peaks and writes these into a table of raw data. For high resolution mass spectra, it passes the peak profiles to the processing programs for further manipulations. A data averaging scheme of several points (digital smoothing) is also available for use in conjunction with selected ion recordings (SIR), metastable ion scans, etc.

The processing programs take the raw data and extract the desired information according to modes. Thus in low resolution mode, each ion is assigned the proper mass value and the ion intensities are normalized, whereas in the high resolution mode, the data can be smoothed, the peak centers determined and the intensities normalized. The results of these operations are written on disk into temporary files, one for each instrument. The mass spectra stored in these temporary files can be further processed. Thus averaging, background subtraction, printing, plotting, and storing of the spectra can be performed in the mass spectrometry laboratory. The input commands to the computer are transmitted via T.I. Silent 700 terminals. Hard copy outputs are generated on a Versatec electrostatic printer plotter. Tektronix 4014 CRT's are used to display mass spectra, chromatograms, etc.

Two libraries are available for identity searching. The first is the NIH/EPA collection of spectra leased from NBS, the second is our own library (ca. 12,000 mass spectra). Either library can be searched on either CPU. It takes ca. 2 min. 15 sec. to perform an identity search of our library and ca. 6 min. to search through the NBS library.

Other programs for structure entry and aids to interpretation of mass spectra are under development.

*L. Baczynskyj in "Biochemical Application of Mass Spectrometry", 1st Suppl. Vol., G.R. Waller and O.C. Dermer, Ed.; p. 77, Wiley Interscience, New York, 1980.

SOFTWARE FOR AUTOSAMPLING ON A FINNIGAN/INCOS GC/MS/DS.

SCOTT CAMPBELL

Shell Development Company
Biological Sciences Research Center
Box 4248, Modesto, California, 95352

Addition of an autosampler to a GC/MS/DS is an excellent method of increasing sample throughput. Several programs have been written for the Finnigan/Incos Data System that facilitate operation of an autosampler system. One routine enables prior input of accounting information for each sample in an autosampler run, and allows subsequent transfer of this information to the proper data file. Other routines allow foreground/background sample injection and acquisition/data processing.

The Finnigan supplied autosampling system using a Varian 8000 autosampler, installed on a Finnigan 4023 GC/MS/DS, works well. However, the capability to input accouting information, for example, sample, conditions, and analyst, which in manual operation is input in response to the "A" command in ACQU, is not provided. An MSDS compatible Fortran program, AASK, has been written to perform this task. The program AASK allows the user to input, store, and retrieve accounting data for a series of samples to be injected by an autosampler. AASK is compatible with MSDS procedure language; thus accounting data can be written to each of the data files using a procedure and will appear on output generated by manual or automatic processing of the GC/MS data.

AASK performs the following functions:

1. Read the file names contained in the current name list.
2. Read the contents of the file AASK.99 which contains entries previously created by AASK.
3. Read the contents of BXSCANINST.99 where X = job number and INST = instrument name.
4. Input data: If no entries are present, defaults to the responses contained in BXSCANINST.99.
5. Write data: The accounting data is written to a file named AASK.99.
6. Transfer data: The accounting data for the current name list entry is retrieved from AASK.99 and is then written to BXSCANINST.99.
7. Other manipulations of accounting data as detailed in the AASK command list.

```
AASK accepts the following commands:
D (J,K) ;Display current list (from entries J to K)
H (J,K) ;Hardcopy current list (from entries J to K)
A (J)   ;Ask for input (beginning entry J)
C  J    ;Change entry J
-       ;Delete all entries
-  J    ;Detete entry J
-  J,K  ;Delete entries J through K
W       ;Write current list
T (J)   ;Transfer data for current name list entry to ACQU
        ;(Entry J)
I       ;Initialize
E (Z)   ;Exit to MSDS
Q       ;Hardcopy this page
```

AASK is used in conjunction with an autosampler. AASK creates a file of accounting data (sample, conditions, etc.) for each entry in the current name list. AASK then transfers the data for a particular name list entry to ACQU (B_SCAN_____.99). A procedure using AASK (after creating the name list and entering the data for each sample) might contain:

```
GETN;RUN AASK (T;E);RUN AUTOS;ACQU...;LOOP
```

INCOS procedure language is a powerful tool for creating routines to automatically acquire and process mass spectrometry data. The use of MSDS user variables, including file names, the name list, scan list, quantification list, and integer variables, is essential in writing procedures to perform automatic data reduction. In the composition of complex procedures, however, it would be advantageous to have access to a larger number of variables. Examination of INCOS software reveals that the STAT list of variables is stored in a disk file name BXMSDSMSDS.99 where X = job number. This file is written in response to the KEEP command in MSDS and is read by the INCOS program MSDS. To expand on this process, two MSDS compatible Fortran programs were written, STORE and RECALL. These programs also write and read sets of MSDS variables to as many as ten different disk files. The files are name BXMSDSMSOY.99 where X = job number and Y = 0 to 9. The value Y is passed to each program in MSDS variable !1. For example:

```
>SET1 #5; RUN STORE   or: >STORE #5 (STORE.PR=RUN STORE)
```

The programs STORE and RECALL could be used, for example, in procedures employing AASK and AUTOS programs for unattended data acquisition with concurrent processing (e.g. plotting, quantification, library search, etc.) of the data files. The status of the acquisition is periodically polled, and if complete, another sample injection and acquisition is initiated, and data processing is continued. Two procedures are to accomplish this: One to inject and acquire and the othe other to process data, each procedure having its own set of variables. For example, the position in the name list might be different for the set of files being acquired and the set of files being processed. STORE and RECALL could be used to swap the two sets of variables.

AUTOMATED ACQUISITION AND PROCESSING OF PHOTOPLATE HIGH RESOLUTION MASS SPECTRAL DATA BY AN 'INCOS' - 'VARIAN' SYSTEM*

W. D. JAMIESON, F. G. MASON and D. E. WEBBER
Atlantic Research Laboratory, National Research Council of Canada
1411 Oxford Street, Halifax, N.S., Canada, B3H 3Z1

The system developed is based on earlier photoplate data acquisition systems developed and used in our laboratory (1-3). A VARIAN 620/L-100 computer controls the operation of a GAERTNER M1205PC comparator-densitometer to acquire data recorded on IONOMET photoplates by a CEC 21-110B mass spectrometer. The hardware-software approach to acquiring spectral line optical density-distance profiles allows sampling intervals of 0.25, 0.50 or 1.00 micrometers as described before (1,2). The software (VARIAN Assembler) was extended for convenient operator interaction to set parameters controlling sensitivity, noise rejection, automatic line detection, and automatic background correction. The software was also extended to control operation of the comparator-densitometer and allow sequenced multiple scans.

Computer control of the comparator-densitometer was effected without changing the original DC shunt motor drive system. The interface developed is controlled by a VARIAN relay output module (DM-177, 16 bits) and uses 6 relays to provide programmable scan rates, forward, reverse and stop functions, and an end-of-scan signal. Manual operation of the comparator remains possible.

Data from photoplate scans at rates to 0.83 mm/sec are accommodated in VARIAN core buffer ($\leq$ 12 K), then formatted as an INCOS "profile" file and emptied to INCOS disk storage as a background job as permitted by other INCOS activity, or written to VARIAN peripheral cassette tape if the INCOS system is not available.

Data is transferred to INCOS at 9600 baud using a 60 m dedicated line as described before (3). Our earlier INCOS-resident software for this required alteration of the IDOS system. Current software, written in FORTRAN and Assembler, does not alter IDOS and should be usable with any Level 3.1 MSDS system.

The INCOS MSDS programs CALI/HCAL, COMP, COPY, ENHA, PARA, PROF, SAVE, STAB and SYST were extended to handle photoplate-derived data more effectively. The use of a quadratic scan function with $(m/z)^{\frac{1}{2}}$ proportional to distance along the photoplate led to acceptably accurate calibrations and mass assignments, and required minimal changes in the MSDS programs.

Mass assignment accuracies within 3 ppm are usual for a single acquisition (8kv, 12 kg; C.E.C. 21-110B at >5000 resolution; IONOMET photoplates). Accuracy is improved by merging the results from multiple acquisitions, since the offset error for repeated scans is random and usually less than 1 ppm.

Program listings and other information are available.

We acknowledge gratefully the assistance of E. W. Dyer, D. J. Embree and P. D. Mack.

REFERENCES

Papers presented at Annual Conferences on Mass Spectrometry and Allied Topics:

1. W. D. Jamieson and F. G. Mason. 23rd, Houston, May, 1975. Proc, pp. 222-4.
2. W. D. Jamieson and F. G. Mason. 25th, Washington, May, 1977. Proc., pp. 668-670.
3. W. D. Jamieson, E. W. Dyer, F. G. Mason and M. Weiss. 27th, Seattle, June, 1979. Proc., pp. 258-9.

*NRCC No. 19061

PROFILE DATA
DATE: 12/05/81 TIME: 0
SAMPLE: HUTZINGER HCBP-3 + PFK
BASELINE SUBTRACTED: 0

SAMPLE RUN: PPHCBP3 SCAN 4
CALIB. RUN: ALIHS4HCBP3 SCAN 5

DATA: PLATE 115 BAND 6

INDEX	MASS	INTEN	% FS	HEIGHT	WIDTH: (UM	SI	mmU)	RESOL
1	374.3888	1522.	4.08	167	10.000	20	22	20568.
2	373.9815	5898.	13.50	553	12.500	25	27	18471.
3	373.8817	1549.	3.38	135	11.000	22	24	19373.
4	373.8384	21835.	31.99	1310	21.000	42	46	13539.

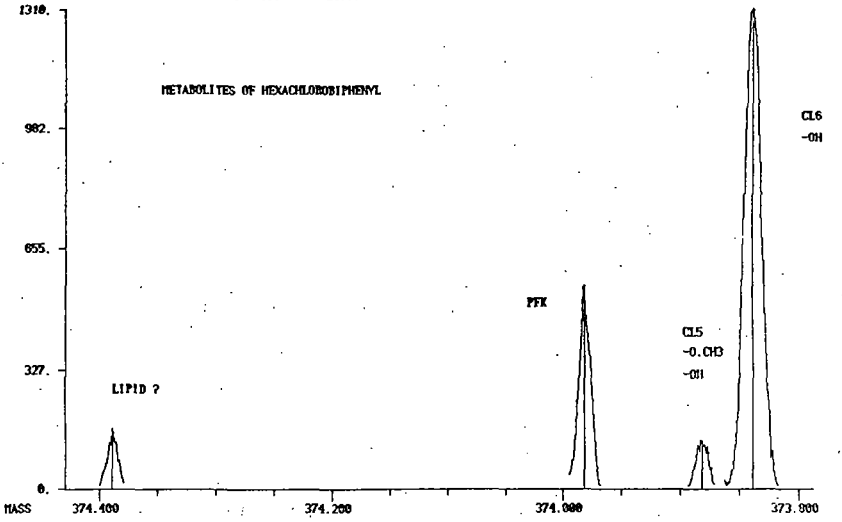

DIAGNOSTICS/STABILITY
12/05/81 PLATE: 115 B: 6
SAMPLE: HUTZINGER HCBP-3 + PFK
I.E. (EV): 8000 MAG. (KG): 10 RESOL.: 1500.. SI/PEAK: 40. UM/SI: 0.50

DATA: ALIHPPHCBP3.HI SCANS 1 TO 4

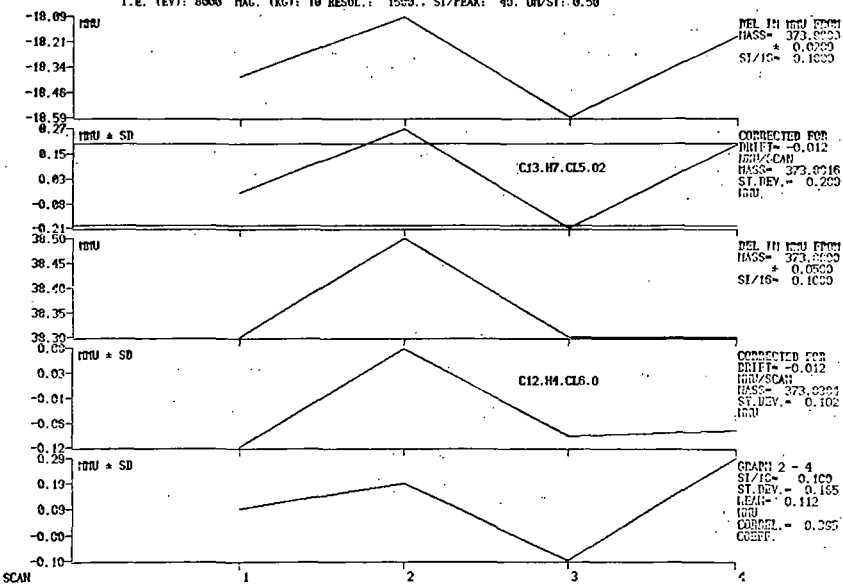

The NIH/EPA Mass Spectral Search System. A Status Report

D. P. Martinsen, Fein-Marquart Associates,
7215 York Road, Baltimore, MD 21212
S. R. Heller, U.S. Environmental Protection Agency,
401 M Street, S.W., Washington, DC 20460
G. W. A. Milne, National Institutes of Health,
Bethesda, MD 20205
W. L. Budde, U.S. Environmental Protection Agency,
26 W. St. Clair Street, Cincinnati, OH 45628

The NIH/EPA Mass Spectral Search System (MSSS) is one of the components of the NIH/EPA Chemical Information System (CIS). The CIS is a collection of various types of chemical data which may be searched and retrieved using the commands of the system. In addition to mass spectral data, both EI and CI, the CIS contains C-13 NMR, IR, powder diffraction, and crystallographic data. There are also a number of data bases in the CIS which contain toxicity values, spill response information, Federal Register citations, and chemical structure and nomenclature. The CIS, including MSSS, is available on a commercial computer which may be accessed via local telephone calls from most major cities in the U.S. and Western Europe.

MSSS consists of a set of programs to search data bases of EI spectra, CI spectra, and proton affinity/gas-phase basicity values. The EI data base contains spectra of nearly 34,000 compounds. Spectra are received from laboratories around the world and are used to update the data base approximately once a year. The EPA, through its Cincinnati office and with the assistance of Radian Corporation, is attempting to add to the data base spectra for 2,500 compounds from the Toxic Substances Control Act (TSCA) Inventory List and from the list of chemicals for priority testing for which mass spectral data are not available. These spectra will be added to the data base over the next two years. The EI data base, on magnetic tape, may be leased from the National Bureau of Standards, and is also available as a four volume set plus one supplementary volume from the Government Printing Office.

The CI data base contains approximately 1500 spectra, most of which were obtained using methane as the reagent gas. The NBS file of proton affinity and gas-phase basicity values contains approximately 650 measurements for 420 compounds. Citations to the literature describing the measurements are also included.

The MSSS programs allow one to search the data base in a number of ways to retrieve information. Compounds may be retrieved on the basis of molecular weight, molecular formula, and partial formula. Because of the capabilities of other components in the CIS, compounds may also be retrieved on the basis of chemical names, trade names, CAS Registry Number and structure. The mass spectrum may be used as the basis for an interactive peak search, in which compounds containing specific peaks with specific intensity ranges are retrieved. The KB and PBM searches retrieve spectra similar to an unknown spectrum based on an algorithm comparing abbreviated forms of the spectra.

Although the data base of EI spectra contains many compounds, it is by no means complete. Therefore, a number of pattern recognition programs have been developed to provide certain information about a compound even when the library searches fail to provide any good matches. The MOLION program, written by Dromey and co-workers at Stanford University, determines likely molecular weights for a compound based on the spectrum.[1] The MSTREE program, developed by Technology Services Corporation, determines the presence or absence of specific functional groups and assigns a probability to each determination. The program currently checks for chlorine and bromine, and work is under way to implement tests for nitrogen and phenyl groups.[2]

1. R. G. Dromey, B. G. Buchanan, D. H. Smith, J. Lederberg and C. Djerassi, J. Org. Chem. 40, 770 (1975).
2. W. S. Meisel, M. Jolley, S. R. Heller, and G. W. A. Milne, Anal. Chim. Acta 112, 407 (1979).

AN IMPROVED MULTIPLE ION DETECTION SYSTEM

D. E. Giblin and F. W. Crow
Department of Chemistry, University of Nebraska
Lincoln, Nebraska 68588

A multiple ion detection system (MID) has been developed to facilitate the rapid selection of the primary ion beams at high resolution in MS/MS and GC/MS experiments. This device will serve an integral part in the development of an automatic multicomponent analysis system employing the Kratos MS-50 triple analyzer mass spectrometer. Design goals for the MID system included the capability of front panel or computer programming, data acquisition by simple signal averager or by the MS computer system, and the flexible manipulation of the scan and signal parameters from the front panel for maximum use of signal information.

Our design features up to eight sequentially-switched channels in stand-alone operation or an unlimited number under computer control. Preview and manipulation of parameters and insertion/deletion of channels can be effected by pushbutton control from the front panel in stand-alone operation. The MID system incorporates the following channel-independent programmable features: (1) variable scan width (0,1ppm to 100%) which permits full spectrum scanning, peak profile or peak top monitoring, (2) accelerating potential from 1 to 8 kV in 7 steps, (3) a trigger pulse from any channel, (4) sweep reset time from 0.01 to 1.00 sec., and (5) the assignment of the special function mass ratios "Hold" and "Start" to any channel. The channel-dependent programmable features are (1) scan times of 0.01 to 1000 sec., (2) 1-100 repetitions of a channel, (3) mass ratio, (4) signal amplification of 1 to 1000, (5) filter cutoff frequency of 0.1 Hz to 10 kHz, (6) the use of the Kelvin-Varley voltage divider for calibration, and (7) the modulation and/or displacement of the scope trace (Y-axis).

The accelerating voltage and the first ESA can by coupled in the normal mode or in one of three metastable modes corresponding to E, V, or $E/V^{1/2}$ scans. The second ESA can be coupled to the first ESA or held constant. Furthermore, ESA#2 may be scanned to obtain a full MIKES spectrum or used in a selected-reaction monitoring mode while the accelerating voltage and first ESA are held constant.

Among the more significant electronic features are crystal-controlled scan and reset times, full isolation between the analog and digital sections of the MID and between the digital sections of the MID and the MS-50 by separate power supplies, opto-couplers and relays, and six-BCD-digit multiplying DAC's for normal and "Hold" mass selection.

The evaluation of the performance of the MID system was performed using standard compounds and known reactions. The level of reproducibility of multi-peak scanning was indicated by the fact that there was no broadening of spectral profiles for data collection over a time span of 6 min. and 50 sec. at a resolution of 30,000. A deviation of mass ratio of 2ppm was found over a peak switch range of 1:0.644 at a resolution of 30,000 by comparing the output with that obtained using the standard Kelvin-Varley voltage divider. The accuracy of scan width was measured using the molecular ions of the $C_5{}^{13}CH_6$ isotope of benzene and the normal isotope of pyridine and was found to deviate by less than 0.1 per cent. A dynamic range of over 30,000 was indicated by measuring the intensities of the normal and first three ^{13}C isotopes of the benzene molecular ion. The relative accuracy of signal gain was measured using standard voltages and found to deviate by 0.5 per cent or less.

As an indication of some of the capabilities of the MID system,

we show a selected-ion monitoring experiment of the unimolecular breakdown of the nitrobenzene molecular ion in $E/V^{1/2}$ space illustrated in Fig. 1. The full CID MIKES spectrum of nitrobenzene molecular ion in shown in Fig. 2.

Fig. 1

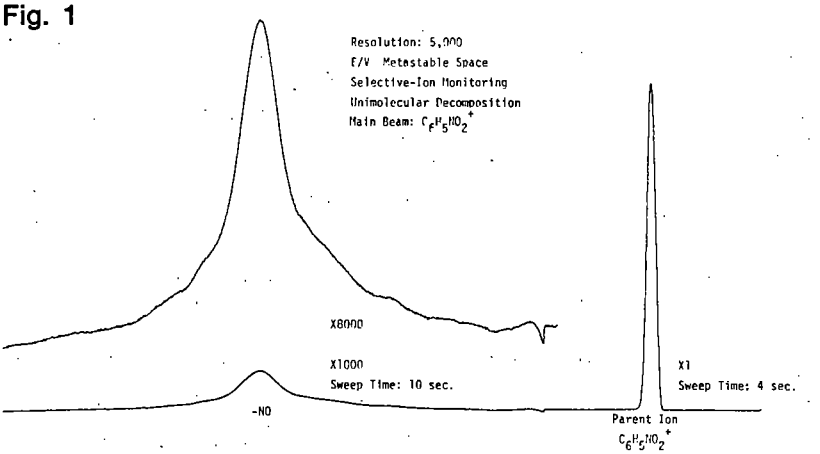

Fig. 2

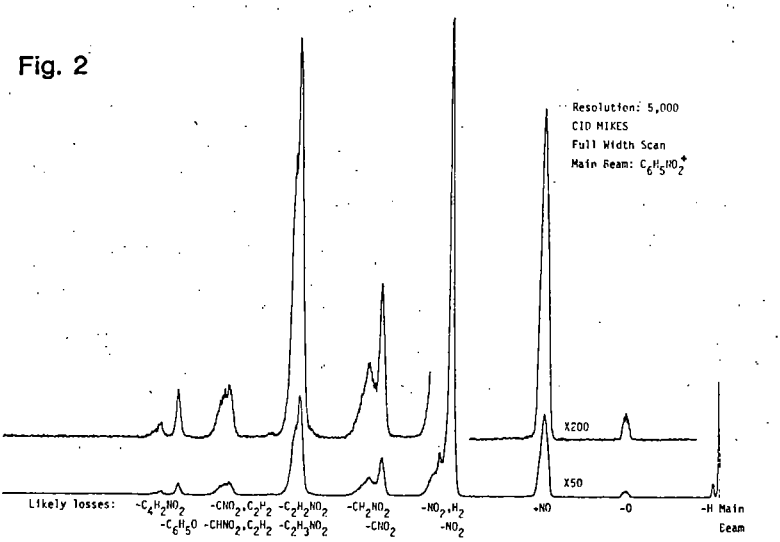

COMPUTER CONTROL FOR SSMS ELECTRICAL DETECTION

P. Marushia and J. Delmore

Exxon Nuclear Idaho Company, Inc.
Idaho National Engineering Laboratory
Idaho Falls, Idaho 83401

To enhance the usefulness of the Spark Source Mass Spectrometer (SSMS) in the electrical detection mode, a 32K word Data General computer has been interfaced to drive the instrument and collect and reduce data.

The interface has 15 bits of control for the magnet and high voltage. There are nine sets of rotary switches, two sets of push-buttons, a programmable clock interrupt, manual interrupt, and three control relays.

The analog-to-digital converter used to read data from the instrument has 12 bits of conversion, 4 channels, with X15 gain and maximum multiplication of 1000.

The peripherals used are a Hewlett-Packard 1310A display, a Tektronix 4010 terminal with cursor capability, a 10 megabyte disk, and a Data General Dasher hardcopy unit.

Software was written with the Real-time Disk Operating System supplied by Data General in FORTRAN IV and assembly language. The program uses the multitasking, overlays, clock, file storage, and user-interrupt capabilities of that system. All operations are initiated from the keyboard of the Tektronix 4010 terminal with only the optimum high voltage setting and high voltage scan limits being input via the interface. Peak stepping with the magnet is the method used to read isotopes.

The operator centers known peaks with standards. The computer stores these magnet locations on disk and calculates a least-squares fit from this mass versus location data.[1] This least-squares calculation is then used to predict magnet locations for any mass. Mass-versus-location data and least-squares fit line may be plotted, or a hard copy of masses and magnet locations made.

To locate the magnet position of a mass, the operator can initiate a magnet scan beginning with a magnet location input via the interface, or more usually, a location calculated from a mass entered on the terminal. As the magnet scans, the ratio of the electrometer to the total ion monitor is displayed on the Tektronix 4010 CRT showing the isotope peaks as their magnet location is passed. The magnet location of the desired mass is selected by the operator via the cursor of the Tektronix 4010, and input through the terminal.

When taking data, the high voltage parameter will be held at some optimum voltage and the magnet stepped from sample isotope magnet location to standard isotope magnet location. The computer fine centers these magnet locations by manipulating the high voltage and magnet so that the magnet location is centered at the optimum high-voltage setting. To find the exact magnet location of a mass peak, an approximate magnet location is entered from (1) the cursor of the Tektronix 4010 set in the scan routine, (2) a computed location from the least-squares fit of a mass, or (3) the location file for updating. The high voltage,

---

[1] P. Paulsen, National Bureau of Standards, personal communication, November 1978.

which has a much finer resolution than the magnet, is scanned about its optimum point. Reading the analog divider gives a profile of the isotope peak. On the first pass, the magnet is either incremented or decremented by a number derived from the difference in high-voltage location of the highest point on the peak and the optimum high voltage divided by the resolution ratio of high voltage to magnet. Then the magnet is moved, one location at a time, reading the peak each time the magnet is moved, to bring the location of the average of the half-peak-height locations to the optimum high voltage.

The measurements of the isotope peaks are done in two different ways. If there is more than one isotope of the standard or of the sample, all measurements on a given isotope are made before moving to the next isotope. The operator inputs the number of sample isotopes to be read before the standard isotopes are read again. This allows the operator to somewhat tailor the running of the sample.

If only one isotope of standard and one isotope of sample are involved, they are read alternately. One reading is taken on the standard isotope, and magnet is moved and one reading is taken on the sample isotope. This tends to maximize settling times on the electrometers and minimize heterogenity affects.

Concentration calculations from the internal standard require the operator to input the concentration of the internal standard and the isotopes to be read. Unless isomers are involved, abundance and molecular weight data are retrieved from the disk and verified by the operator. Of course the magnet location for the isotopes should have already been determined and stored so these are retrieved.

Isotope dilution calculations require the operator to input the isotopes involved, the concentration of the spike, and the altered abundances of the isotopes in the spike. Again, natural abundances and locations for the isotopes are retrieved from the disk.

A running, relative standard deviation for the data is output while data are taken. Grubbs T Test at the 10% confidence level is used for outlier rejection.[2] Final output of data, statistics and concentration in atomic and weight units is output on the Data General Dasher hardcopy unit.

Computer assistance for the JEOL SSMS electrical detection allows experimentation, development, and instrument tuneup not easily done with the analog equipment. Data taking procedure can be customized to individual samples and statistical tests can be made immediately to prove their worth. The time involved to run a sample, especially if isotopes not previously read are involved, is significantly reduced. The possibility of operator error is reduced in several ways. The determination of the locations of the isotopes must fit the least-squares calculation and isotopes nearby can be seen easily on the scan, making isotopic comparison simple. Isotope data retrieved by the computer from disk reduce entry errors as do programmed calculations and statistics.

---

[2] Report No. 1705, Material Science Center, Dept. of Chemistry, Cornell Univ., Ithaca, N.Y. (Dec. 1971).

MINIMUM-NOISE DATA COLLECTION WITH VARIABLE SCAN RATE: A DIGITAL FILTERING METHOD

T.J. Eskew, Nuclide Corporation, State College, PA 16801

We have tested several schemes for noise reduction by digital filtering during data collection by scanning. In a magnetic mass spectrometer with given slit sizes, the peak shape is known in advance, and the peak width can be calculated for a specified scan rate. One can take advantage of this knowledge to improve the signal-to-noise ratio and to reduce the detection limit for small peaks.

For a rectangular peak, the optimum filter is simply a running mean,

$$y_i = \frac{1}{n}\sum x_i \ ,$$

where the x's are the raw readings of a digital voltmeter or ion counter and n, the number of terms included in the sum, is set equal to the number of readings made in crossing the peak. This filter is particularly simple to implement in the case of an exponential scan, since n is constant. For a scan half-period T (specified by the operator),

$$n = aT \ ,$$

Where the constant a depends on the slit widths and on the geometry of the instrument; it is determined experimentally. In this case, the filter becomes simply a running sum, which can be updated at high speed by a desktop computer or a programmable calculator.

We performed a set of experiments to show that this method (the theoretical optimum for rectangular peaks with only random noise) also gives good results for trapezoidal or Gaussian peaks. The experiments made use of an ion-counting system, since in that case the theoretical minimum noise can be calculated. A small peak was scanned ten times, and the relative standard deviation (r.s.d.) of the ten peak-height readings was calculated. This r.s.d. was minimized when n (the number of readings included in the running sum) was equal to the number of readings between the 60% points on each side of the peak (although the standard deviation increases only slightly if n is made twice as large). We estimated the theoretical minimum r.s.d. as $\sqrt{c}/c$, where c is the number of ion counts in the running sum at its maximum. For various scan rates from 4000 seconds/octave to 40 seconds/octave, the ratio of measured r.s.d. to theoretical minimum r.s.d. ranged from 1.2 to 1.8. Thus, we conclude that this simple filter is a good approximation to an ideal filter, at least for the case of purely random (statistical) noise.

The kind of non-random noise most likely to be encountered in mass spectrometry is a modulation of the ion-beam intensity with line-frequency harmonics. This noise can be almost completely eliminated if the digital-voltmeter integration time (or the ion-counting time) is an integral multiple of the line frequency (i.e., 16 2/3 ms in this country).

MIAQ: INCOS MULTIPLE-ION AUTOMATIC QUANTITATION - THE CORRECT WAY TO QUANTITATE; PAUL P. DYMERSKI, Arthur G. Palmer, and James R. Dahlgran; O. H. Materials Co., Findlay, Ohio 45840

The single ion quantitation methods offered on the Incos data system provide insufficient information about the precision and accuracy of the compounds identified and quantitated. To improve both the accuracy and precision of GC/MS/DS quantitation, a set of FORTRAN programs have been written and integrated into the Incos procedures to quantitate up to four ions for M entries in a MSDS reduced library. These programs:

1. Create a response factor table for N masses/M standards ($x \leq 4$).
2. Eliminate noise peaks.
3. Check area ratios of the quantitation ions vs. the standard ion ratios.
4. Remove ions with "interference".
5. Quantitate on the remaining ion areas.
6. Report quantities, averages, standard deviation, and flag the "suspect" ion areas (excluded from quantitation).
7. Final tabulation is printed in a report-ready format.

MIAQ programs utilize the capabilities of CHRO to locate and quantitate mass ion areas from a standard MSDS "reduced" library. The quantitation report is read by a FORTRAN program and tested.

Settable parameters include:

A Minimum absolute area threshold.
S Scan and relative retention time window.
R Mass ion area ratio error limit.

A reference response factor table is automatically constructed for a standard sample mixture. This is done on the daily standard run so that the table contains the empirical mass ion ratios, reducing the errors due to instrumental parameters.

For a sample peak MIAQ checks the area ratios against the standard table. A ratio less than the standard ratio indicates a spurious peak and the compound is removed from the quantitation list.

A mass ion ratio greater than the standard ratio indicates an "interference" at that mass. Since the remaining ions may be pure, the suspect ion is removed and the remaining ratios recalculated. If N-1 ratios are incorrect the base peak ion may be interfered with. It is removed and the process repeated. If less than two mass ions are found pure, the compound identification is discarded.

The final report generates a short form (Fig.1) which reports: Compound name, quantitated amount as an average of all confirmed mass ion areas, the number of masses found versus the number of masses in the reduced library, and the standard deviation of the averaged amounts.

The long form (Fig.2) reports all the statistical information necessary for the mass spectrometer operator to properly evaluate the data. This includes the data on the short form plus, for each mass ion, the scan number, area, calculated amount, and mass ion ratio; the ratios for the standard are also reported.

Useful commands include:

Ai,j Set minimum and maximum amounts to report.
U For duplicate entries eliminate all but entry with largest amount.
M Merge duplicate entries.
F Short form/long form.
H Hard copy.

SHORT FORM

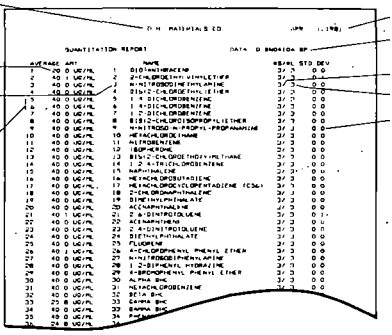

1. Laboratory Name
2. Date
3. Data File
4. Amount (Average)
5. Library Name
6. Number of Masses Found
7. Masses in Library
8. Standard Deviation
9. Reporting Options:
   M = Merge Duplicates.
   U = Largest Only.
   A i, j = Amount Limits.
   i = lower limit
   j = upper limit

LONG FORM
(STATISTICS)

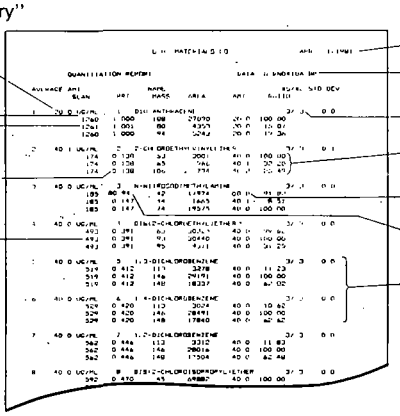

From MSDS "Quantitation Library"
a. Std. Amount
b. Units
c. In. Std. Rt.

2
3
6,7
10. Sample Area Ratios
11. Ratio Error (Not included in average).
12. Correct Ratio
13. Duplicates Reported (Remove with A,U,M commands)

Relative Retention Times

Exact Scans

CHARACTERIZATION OF NATURAL MIXTURES OF STEROL PEROXIDES BY LC/MS USING DIRECT LIQUID INLET (DLI) INTERFACE (1)

François R. SUGNAUX*, A.A. Leslie GUNATILAKA** and Carl DJERASSI

Department of Chemistry
Stanford University
Stanford, California 94305

Sterol peroxides (SP) constitute a significant portion of the sterol fraction in many marine species. Unlike regular sterols, these compounds are polar and heat sensitive. Therefore they cannot be analyzed by GC/MS. Furthermore, in the solid probe EI mode they yield highly fragmented spectra with very weak molecular ions. Consequently these peroxides were good candidates for low temperature LC/MS.

HPLC separation of fifteen SP (1-15) from four different marine sources

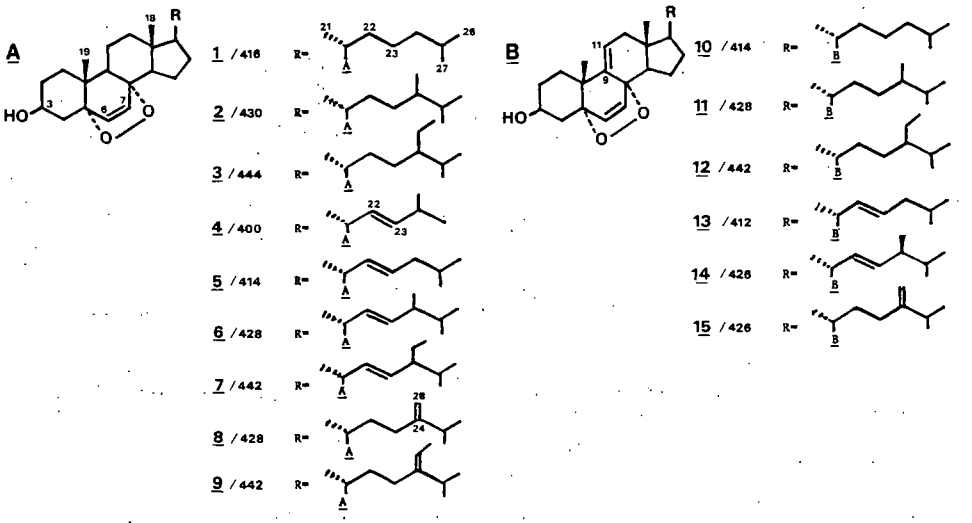

was performed on a 4.6 mm ID X 150 mm, 5 µm, RP-18 column (Ultrasphere-ODS, Altex, Berkeley, CA). The complete LC/MS system comprised a Beckman (Fullerton, CA) HPLC pump model 100A, a Rheodyne (Berkeley, CA) loop injector, a Ribermag (Nermag, Rueil-Malmaison, France) model 10-10-B quadrupole mass spectrometer equipped with a DLI interface (2,3) and a SADR data acquisition system.
The solvent for HPLC and chemical ionization MS was methanol adjusted to a flow of 1 mL/min through the HPLC column and a flow of about 10 µL/min into the MS, by means of a splitter. The MS source pressure was 0.14 atm and the source heater block temperature was 100 to 112 °C. The mass range 150-500 was continuously scanned at an average speed of 30 msec/mass decade.

(1) A more detailed account of this work will be published in Org.Mass Spec. (1981)
(2) P.J. Arpino, B.G. Dawkins and F.W. McLafferty, J.Chrom. Sci. 12(1974) 574
(3) P.J. Arpino, P. Krien, S. Vajta and G. Devant, J.Chrom., 203(1981) 117

* Visiting research associate on sabbatical leave from University of Geneva, Switzerland
** Visiting research associate on sabbatical leave from University of Peradeniya, Sri Lanka

The careful selection of the source temperature permitted to operate the interface continuously without an active cooling.
The reconstructed ion chromatograms, of which an example is given in figure 1, have shown that the interface does not affect the HPLC peak symmetry or show a memory effect.

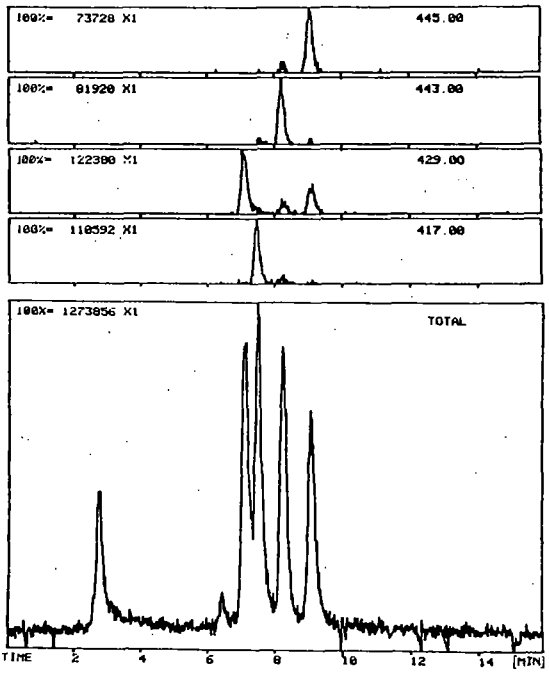

Figure 1. LC/MS analysis of the sterol peroxides fraction of Ascidia nigra, a tunicate.

HPLC and MS conditions indicated in the text; temperature: 108 °C.

Top traces: extracted ion current profiles for the ions corresponding to $M + H^+$.

Bottom trace: total ion current.

The CI mass spectra of the sterol peroxides separated have shown intense (50 to 100% relative intensity) $M + H^+$ (Figure 2). The other peaks arise due to a $(M+H^+ - H_2O)$, $(M+H^+ - O_2)$ and $(M+H^+ - H_2O_2)$ fragmentation process.

These results demonstrate that the samples are efficiently nebulized in the source at a low temperature.

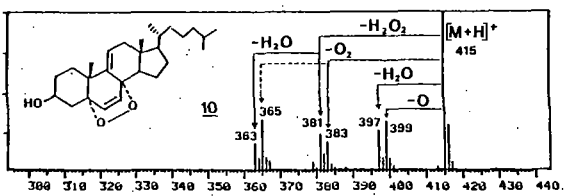

Figure 2. Example of a mass spectrum taken at maximal peak height on the chromatogram of Aplysia dactylomela mixture, for compound 10.

Acknowledgements

This work was supported by the National Institutes of Health under Grant GM 28352.
F.R. Sugnaux was recipient of a postdoctoral fellowship from the Swiss National Funds for Scientific Research (79-GE-34).

CHARACTERIZATION OF TWO NEW MODIFIED URACIL DERIVATIVES FROM HUMAN URINE BY COMBINED LIQUID CHROMATOGRAPHY-MASS SPECTROMETRY; C. G. Edmonds, E. E. Jenkins and James A. McCloskey: Department of Medicinal Chemistry, University of Utah, Salt Lake City, Utah 84112 and C. R. Blakley and M. L. Vestal: Department of Chemistry, University of Houston, Texas 77004 and N. C. De, A. Farber, S. P. Dutta and G. B. Chheda: Department of Biophysics, Roswell Park Memorial Institute, Buffalo, New York 14263.

Two new modified 6-aminouracil derivatives from human urine, 6-amino-3-methyl-5-(N-formylamino)uracil (1) and 6-amino-1-methyl-5-(N-formylmethylamino)uracil (2), are isolated and characterized by a number of chromatographic and spectroscopic methods including LRMS, HRMS and LC/MS.

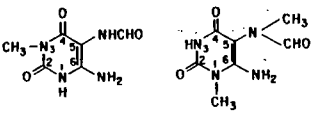

1 2

Conventional mass spectrometric techniques are of limited value due to the unexpected similarity of EI spectra of candidate model compounds and extensive dehydration occurring during chemical derivitizations procedures. The particle beam LC/MS is uniquely useful in the characterization of (1) and (2) and the several possible monomethyl and dimethyl reference compounds synthesized for comparison. Full scan spectra obtained by injection of samples in solution are in all cases structurally specific and LC retention data are likewise indicative as exemplified by the LC/MS experiments summarized in Figure 1.

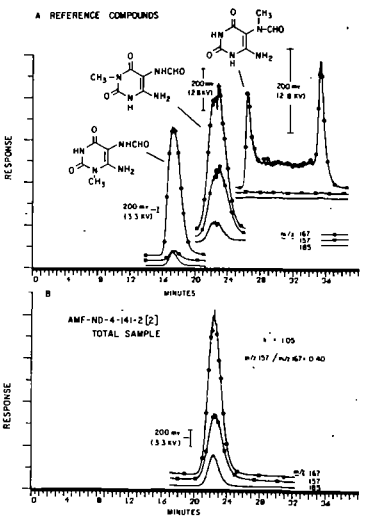

Fig. 1. On-line LC/MS MID experiments on the monomethyl reference compounds and compound (1).

In the upper panel (A.) a composite of three on-line LC/MS MID experiments is represented: (left to right) 6-amino-1-methyl-5-(N-formylamino)uracil, 6-amino-3-methyl-5-(N-formylamino)uracil and 6-amino-5-(N-formylmethylamino)uracil are chromatographed on a 25 cm x 4.6 mm i.d. Ultrasphere C_{18} column with 0.01 M aqueous ammonium formate (pH5.5)(2.5% MeOH as organic modifier) as mobile phase and introduction into the LC/MS instrument at 0.2 ml/min. The latter of these reference compounds in common with all 5-N-methlated materials in this study shows a prominent bifrucate peak possibly arising in the equilibrium of open form with closing of the 6-amine with the adjacent 5-N-formyl carbonyl group to yield the closed 2-hydroxydihydroimidazole structure. The botton panel (B.) shows the LC/MS experiment

for the total biological sample and confirms the 3-methyl structure by relative abundances of protonated molecular ion (m/z 185) and fragment ions ((MH-18)$^+$, m/z 167 and (MH-28)$^+$, m/z 157) and by chromatographic retention. Similar experiments unambigously characterize compound (2).

Of further data presented to illustrate the suitability of the LC/MS instrument in nucleoside analysis notable is the measurement of instrument sensitivity as 5.4×10^{-10} coulombs/µg of adenosine injected as determined by response at m/z 136, the adenine base fragment plus two protons. This affords an analytically useful signal at the protonated molecular ion (m/z 268) linear over four orders of magnitude with a limit of detection of the order of few tenths of a nanogram.

Suitability for on-line LC/MS analysis of nucleic acid constituents is further demonstrated by the analysis of several derivatives of 5-fluorouracil (5-FU) shown in Figure 2. Excellent chromatographic fidility is shown among the MID negative CI ion profiles and the simultaneously obtained UV absorbance chromatogram.

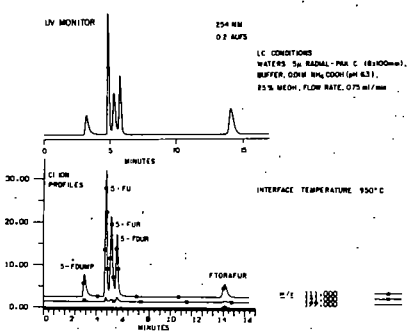

Fig. 2. On-line LC/MS analysis of a mixture of compounds related to 5-fluorouracil (5-FU). "Filament off" mass spectra of several nucleotides are also shown and discussed.

THE CURRENT STATUS OF PARTICULATE IMPACT MASS SPECTROMETRY

Frank T. Greene
Midwest Research Institute
Kansas City, Missouri 64110

Particulate Impact Mass Spectrometry was proposed as a technique for mass spectrometry of nonvolatile substances and LCMS at this meeting in 1975 (1). In this technique the substance to be studied is dissolved in a volatile solvent and converted to a high velocity aerosol beam, which impacts a hot plate above the electron beam in the ion source of a mass spectrometer. Evidence for the quantitative vaporization of the nonvolatile solute with the solvent has been previously presented (1-3).

Current research has been directed principally toward improvements in the apparatus and in the sensitivity of the technique. A multistage, differentially pumped aerosol beam system, which utilizes a two-stage expansion, has been developed for use in electron impact mass spectrometry. This system provides high aerosol beam densities with reduced vacuum pumping and virtually eliminates the superimposed molecular beam from the initial expansion. A "continuum" which degrades the S/N ratio at large values of m/e has been found to correlate with the presence of solvent clusters, and appears to result from metastable cluster ions. This interference, which has been observed for several important solvents, is substantially reduced with the attenuated molecular beam so that ppb sensitivities should be generally obtainable.

This work was supported in part by The Environmental Protection Agency, Grant No. R807636010.

---

1. Greene, F. T., "Particulate Impact Mass Spectrometry," Presented at the 23rd Annual Meeting of ASMS, Houston, TX, May 25-30, 1975.

2. Greene, F. T., "Mass Spectrometry of Nonvolatile Materials and Solutions by the Particulate Impact Technique," Presented at the 24th Annual Meeting of ASMS, San Diego, CA, May 9-13, 1976.

3. Greene, F. T., "Further Development of Particulate Impact Mass Spectrometry," Paper Presented at the 28th Annual Meeting of ASMS, New York, N.Y., May 25-30, 1980.

LIQUID IONIZATION MASS SPECTROMETRY ---- THE EFFECT OF SOLVENTS

M.Tsuchiya, Y.Sugano, T.Taira and Y.Saito, Faculty of Engineering
University of Tokyo, Bunkyo-ku, Tokyo, Japan 113

Recently we reported a new method (Liquid ionization) for ionizing organic compounds in solution at atmospheric pressure[1]. The effects of solvents and temperature on mass spectra were investigated in order to find how to desorb less- or involatile compounds quickly from a sample probe.

The instrument used is a modified quadrupole mass spectrometer[1] (ANELVA TE 600) equipped with a Extranuclear Laboratories' quadrupole power supply (#011 -15) and Shimadzu's micro-computerized data processing system (GCMSPAC 90).

Samples used were mostly amino acids in aqueous solution (0.1 - 0.5 %). One μl of sample was deposited on a sample holder[1] which is similar to a direct probe used in in-beam technique[2].

By testing acids (CH_3COOH, HCl, HNO_3, etc), bases (NaOH and NH_4OH) and organic solvents (CH_3OH, acetone, etc) as an additive to aqueous solution of amino acids, HCl (pH = 1) and/or NaOH (pH = 13) were found to be the best for increasing the abundance of molecular ions (MH^+).

As an example, the time (temperature) dependences of major ions for lysine in aqueous solutions are shown in Fig.1 (a ; neutral, b ; basic, c ; acidic). A mass spectrum between m/z 10 and m/z 400 was measured in 6 sec and the scan was repeated every 15 sec. Most of water was evaporated before introducing a sample into the ion source to avoid too many water ions. A heater inside the sample probe was turned on 30 sec after the sample introduction. Final probe temperature is estimated to be about 200°C at a heater current of 3.0 A. The coordinate indicates the ion abundances and the figures shown in Fig.1 mean the full scale count for each ion. The ions at m/z 293, 147 and 84 are M_2H^+, MH^+ and $MH^+ - HCOOH - NH_3$, respectively. The M_2H^+ and MH^+ ions were most abundant in basic solution and their maximum abundances were attained at relatively low temperature as seen in Fig.1, b. A mass spectrum of lysine at optimum condition (basic) shown in Fig.2 indicates usefullness of the method.

In general, basic amino acids such as lysine and arginine appear to give more MH^+ ions from basic (NaOH) solution and neutral amino acids (alanine, leucine, glycine, methionine, etc) appear to give more MH^+ ions from basic and/or acidic (HCl) solution. Addition of NaCl increased the abundance of MH^+ ions a little. Function of these additives may be similar to that reported in FD[3], although the effect was not very significant in our case.

A mixture of succinic acid and leucine (0.1 % each) in aqueous solution was measured. The time (temperature) dependences of major ions are shown in Fig. 3 and the mass spectra at optimum condition for each compound are shown in Fig.4. The heater current was increased from 0 A, 0.5 A/min stepwise, to 4.0 A. The ion source block was heated at about 100°C. The mass spectra show peaks at m/z 119, 132, 136, 237, 250 and 263, corresponding to MH^+ (succinic acid ; M_S), MH^+ (leucine ; M_b), $(M_S+NH_4)^+$, $(2M_S+H)^+$, $M_SHM_b^+$ and $(2M_b+H)^+$, respectively. The temperature dependence of ions at m/z 119, 136 and 237 are similar, indicating the ion at m/z 136 is $(M_S+NH_4)^+$. It is interesting that the ion at m/z 136 was more abundant for acidic solution and proton bound dimer ions (including $M_SHM_b^+$) were often observed for this type of compounds.

The MH^+ and M_2H^+ ions for leucine were observed at higher temperature than those for succinic acid. Thus a mass spectrum of each component can be measured separately (at 2.0 A and 4.0 A) as shown in Fig.4. By increasing the pinhole potential[1], fragment ions are obtained easily at each optimum condition. Namely this instrument can be used as a sort of MS/MS. It is necessary however, for LC/MS system to attain flash desorption of solutes by rapid heating, or to find good additives to desorb all components at low temperature. A solute of 1 μg used is too much for quantitative analysis, because it gives the MH^+ ion for 7 min or more (for leucine, more than 20 min). In this case, the ion abundance should be accumulated by a computer system. Or a smaller size of sample should be used, because the detection limit of this method is thought to be in the range of $10^{-8} - 10^{-12}$g.

Application to reaction product. This method is useful for determining what the reaction product is, because the sensitivity is high and sample preparation is simple. A dimer produced from an oxazoline derivative was hydrolyzed with conc. HCl for determining the structure of the dimer. The product of hydrolysis was diluted with water and mass analysed without any separation. The mass spectra showed intense peak at m/z 119, 132 and 136 indicating the existence of succinic acid and leucine, but no other compound. This is consistent with the reaction process and other observations using GPC, ^{1}H-NMR, and IR. The abundance of mass 136 ions, however, was very abundant in the product and appears to be increased with HCl and time after the reaction.

Addition of NaOH and/or HCl increased the abundance of MH^+ ions. It is important to find good additives for quick desorption of solutes. The method provides useful information about them. The advantages of the method are ; 1) easiness of sample handling, 2) good mass spectrum (MS/MS), 3) few contamination in vacuum, 4) wide application.

Reference

1) M.Tsuchiya and T.Taira, Int. J. Mass Spectrom. Ion Phys., 34, 351 (1980)
M.Tsuchiya, K.Seita and T.Taira, Mass Spectroscopy (Japan), 28, 235 (1980)
2) G.Hansen and B.Munson, Anal. Chem., 52, 245 (1980)
3) T.Keough and A.J.DeStefano, Anal. Chem., 53, 25 (1981)

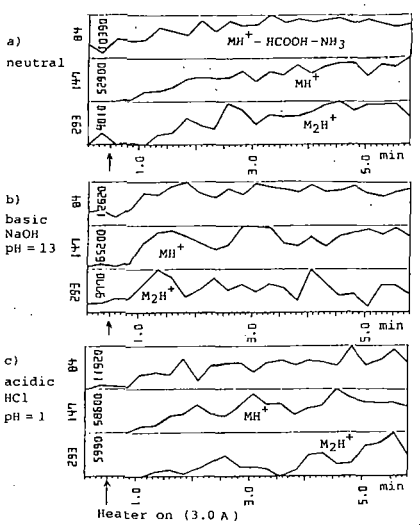

Time (temperature) dependence of major ions for lysine in different solutions

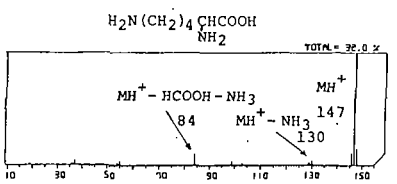

Fig.2 Mass spectrum of lysine at pH = 13

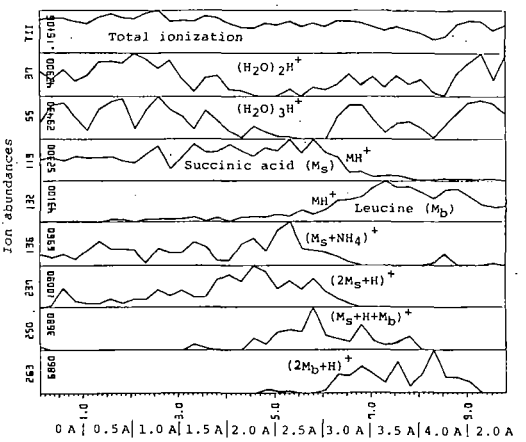

Time (temperature) dependences of a mixture of succinic acid and leucine in aqueous solution (0.1 % wt each)

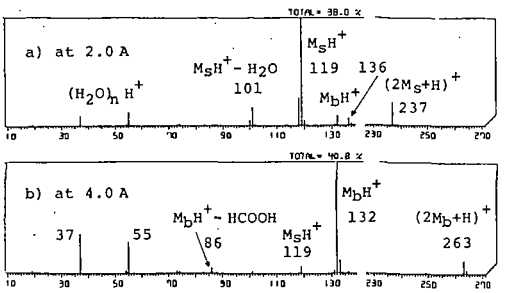

Fig.4 Mass spectra of the mixture a) at 2.0 A b) at 4.0 A

THE CONSTRUCTION AND USE OF A NEW DLI MICRO LC/MS DIAPHRAM INTERFACE,
Jack Henion, Diagnostic Laboratory, NYS College of Veterinary Medicine, Cornell University, Ithaca, NY 14853

We report the construction and preliminary results of a modified DLI micro LC/MS interface patterned after the unit recently introduced by Hewlett Packard Co. (1). This device offers several advantages over existing commercial units which include: (a) increased routine sensitivity approaching that afforded by modern (GC/MS), (b) reduced construction and LC solvent costs, and (c) practical add-on to existing GC/MS instruments equipped with a chemical ionization (CI) source. While micro LC/MS has been proposed (2) and reported (3, 4), the present apparatus is the first to combine the simplicity of unchanged, commercially available LC pumps and hardware with total effluent introduction into the mass spectrometer (MS).

EXPERIMENTAL

In this DLI micro LC/MS probe interface (Figure 1), a central, small bore (0.004 in id) stainless steel tube transfers total micro LC effluent to the water-cooled probe tip housing a thin, stainless steel diaphram. The diaphram has a precisely centered "one-shot" laser generated pinhole (5 micron diameter) which is held firmly against the exit end of the small bore tubing at the probe tip. The threaded end-cap accomplishes this by pressing the diaphram against the O-ring and the probe tip pedestal. The metal-to-metal diaphram seal affords zero dead volume at the probe tip while permitting total transfer of the micro LC effluent through the 5 micron pinhole into the CI ion source. The rounded end-cap butts against the ion source probe inlet affording the necessary "tightness" for CI.

Construction of the probe tip is facilitated by a two-part process. The entire cooling chamber (Figure 1) and diaphram support pedestal is fabricated separately from the main probe shaft. This allows machining the cooling chamber, soldering the three 1/16 inch tubes comprising the throughput and coolant tubing, and smoothing the pedestal surface. A teflon gasket provides a vacuum and coolant seal when the diaphram support pedestal is tightened onto the main probe shaft.

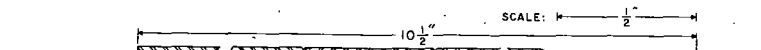

Figure 1. Diagram of new micro LC/MS probe.

The central small bore throughput tubing (0.004 in id x 0.009 in od is soldered carefully inside a 0.010 in id x 1/16 in od stainless tube to afford strength and ease of coupling to the micro LC column exit. The overall length of this throughput tube is kept to a minimum to reduce extra column effects. Both ends are machined smooth and flat for efficient transfer of total micro LC effluent. The micro LC column exit is attached directly to the micro LC/MS probe throughput tube with a symmetrical in-line Valco low dead volume filter union.

The UV detector is eliminated from the system to exclude its large extra column effects. The micro LC column used in this work was a 1.0 mm id x 1.58 mm od x 15 cm 10 micron HRSM C_{18} column (C-M Laboratories, Nutley, NJ). It had a plate count of 9000 plates/meter and was attached directly to a U6K injector (Waters Assoc., Milford, MA). The injector was connected by 0.010 in id tubing through a 0.4 micron in-line filter to a Waters Model 6000 pump driven by an M-660 solvent progammer. Micro LC flow can be accomplished with this equipment by setting the pump at zero mL/min eluant flow while the M-660 solvent programmer is set at 0.1 mL/min B with the percent B set at 50%. This combination of settings on the unchanged hardware yields a nominal eluant flow rate of 50 µL/min but a measured flow rate of 35 µL/min. This system provided reliable micro flow under these conditions.

When the above conditions had been established, the micro LC/MS probe produced the steady, one-inch long "jet" of total micro LC effluent (CH_3CN/H_2O) necessary for optimum micro LC/MS performance as determined by previous experiments. When the "jetting" micro LC/MS probe was inserted into the standard solid probe inlet of a Hewlett-Packard 5985B MS, a stable ion current baseline from m/z 100-500 was maintained over four hour time periods. The ion source temperature was maintained at 250°C and the liquid nitrogen cryropump on the MS was operated in the normal manner.

The MS was operated in either the NCI or PCI mode in these experiments using the micro LC eluant as the CI reactant gas (6). The compounds studied in this work display comparable micro LC/MS sensitivity response for both NCI and PCI modes, although certain molecules containing more electronegative heteroatoms can reveal enhanced sensitivity.

CONCLUSIONS

The new DLI micro LC/MS probe described here offers access to higher chromatographic efficiency afforded by the new micro LC columns, and elimination of the LC effluent split required by the conventional DLI LC/MS methods. These factors contribute to increased LC/MS capabilities including sensitivity. Results from further work in this work will be reported subsequently.

LITERATURE CITED

1. A. Melera, Paper No. 085, 30th Pittsburg Conference on Analytical Chemistry and Applied Spectroscopy, Cleveland, OH, March 5-9, 1979.

2. F.W. McLafferty and M.A. Baldwin, US Patent #3,997,298 (1976).

3. S.Tsuge, Y. Hirata and T. Takeuchi, Anal. Chem., (1979) 51, 166-169.

4. J.D. Henion, J. Chromatogr. Sci., (1981) 19, 57-64.

5. M.S. Baldwin and F.W. McLafferty, Org. Mass Spectrom., (1973) 7, 1353-54.

6. P.J. Arpino and G. Guiochon, Anal. Chem., (1979) 51, 682A-701A.

MICRO-COLUMN LC/MS

David E. Games, Michael S. Lant, and Steven A. Westwood; Department of Chemistry, University College, P.O. Box 78, Cardiff CF1 1XL, Wales and Brian J. Woodhall, I.C.I. Pharmaceutical Division, Hurdsfield Industrial Estate, Macclesfield, Cheshire, SK10 2NA, England.

The use of capillary[1] or microbore columns[2] provide a number of advantages for high-performance liquid chromatography (LC). Because less packing material and solvent are required, running costs are considerably reduced, higher efficiency and mass sensitivity can be achieved and since low solvent flow rates are used, combination of the LC with a mass spectrometer (MS) is much easier. From published data it appears that packed microbore columns (0.5 - 1 mm i.d.) offer the most effective current system. This approach to LC has, however, many difficulties which include the availability of low dead volume injection systems, the techniques required for packing high efficiency columns, the availability of a low dead volume, low time constant detectors and the relatively small amounts of sample which can be handled before column overload occurs with subsequent loss of efficiency.

Jasco have developed a commercial microbore LC system, which has been used by a number of groups for LC-MS studies. The approach has been utilized mainly with the direct liquid introduction LC-MS coupling[3-6], since it enables all of the effluent from the column to be introduced into the mass spectrometer resulting in considerable improvements in sensitivity. Enrichment LC-MS systems of the jet[7] or nebulizing[8] type have also utilized microbore LC. Although initial studies[9] with a moving belt interface utilized this approach it has seen little subsequent usage. Most of the studies reported to date have paid little attention to the efficiency of the LC system, but in one case the microbore LC column was incorporated directly into the direct liquid introduction system to reduce dead volumes.[5]

Our studies have utilized a JASCO microbore LC system with a LC-MS interface of the moving belt type (Finnigan). We have been concerned with four aspects of its performance. Improving the efficiency of the system, examining its ability to improve the LC-MS handling of solvent systems containing a high proportion of water, the development of techniques to overcome the problems associated with column overload and finally to see if better LC-MS sensitivity could be achieved.

Our initial studies were disappointing in that column efficiencies only of the order of 1000 theoretical plates could be achieved.[10] Whilst it might be argued that this is not particularly important in that unresolved peaks could be resolved using the data system. The sample we were studying, a crude extract of timbo powder, consisted predominantly of two pairs of isomeric rotenoids and the CI spectra of the first two components (MW 410) were virtually identical, as were the spectra of the latter pair of isomers (MW 394) and hence the data system could not be used to resolve them.[11] Modification of the technique for packing the microbore PTFE columns, by use of a Waters 6000 pump fitted with a constant pressure device which enabled a packing pressure of 1000 p.s.i. to be maintained has enabled us to obtain efficiencies of the order of 10,000 theoretical plates using packed 350 x 0.5 mm columns at acceptable flow rates. One advantage of the moving belt interface over other types of LC-MS interface is that the microbore LC column can be directly connected to the LC interface hence ensuring a very low dead volume. Using this technique we were able to obtain similar efficiencies for a naphthalene, biphenyl mixture by LC-MS to that which we obtained using a modified low dead volume cell for the JASCO UV detector. We feel that it will be difficult to improve efficiencies of the PTFE columns further and for the full advantage of microbore LC to be available for LC-MS systems of the type described by Scott[12,13], will have to be utilized.

We have achieved considerable improvements in the reduction of background peaks in the mass spectrometer using microbore LC, this is largely due to the much lower solvent volumes being handled (10µl min^{-1} as compared with 1 ml min^{-1} for conventional columns). This results in improved sensitivity and further improvements accrue with aqueous solvent systems since the necessity of splitting off a portion of eluant is avoided.

A major problem with LC-MS systems of the moving belt type has been the difficulties encountered in handling eluting systems which have a high proportion of water. Microbore LC offers an extremely effective solution to this problem. We have obtained excellent

data from solvent systems consisting of acetonitrile: water (20:80) by feeding a flow of 0.2 ml min^{-1} of ethanol onto the interface behind the microbore LC column.

When studying samples of biological origin or searching for minor components in a mixture it is often necessary to inject a large amount of sample onto the LC column. We have found with our JASCO system that column overload occurs when samples in excess of 5 µg are injected on-column. This results in dramatic loss of efficiency and merger of previously resolved peaks. In irder to overcome this difficulty we have developed a manual column switching technique which we have found to be effective in the LC-MS mode.

Microbore LC offers considerable advantages for LC-MS studies particularly with regard to easier handling of more difficult solvent systems and improved sensitivity. Systems of the JASCO type whilst easy to operate do not enable the full advantage of microbore LC to be exploited and the use of higher efficiency systems of the type developed by Scott[12,13] should lead to further improvements in LC-MS.

References

1. M. Novotny, J. Chromatogr. Sci., 1980, 18, 473.
2. R.P.W. Scott, J. Chromatogr. Sci., 1980, 18, 49.
3. P.J. Arpino and G. Guiochon, Anal. Chem., 1979, 51, 682 A.
4. J.D. Henion and G.A. Maylin, Biomed. Mass Spectrom., 1980, 7, 115.
5. J.J. Brophy, D. Nelson, and M.K. Withers, Int. J. Mass Spectrom. Ion Phys., 1980, 36, 205.
6. K.H. Schafer and K. Levsen, J. Chromatogr., 1981, 206, 245.
7. T. Takeuchi, Y. Hirata and Y. Okumura, Anal. Chem., 1978, 50, 659.
8. S. Gauge, Y. Hirata, and T. Takeuchi, Anal. Chem., 1979, 51, 166; Y. Yoshida, H. Yoshida, S. Tsuge, T. Takeuchi, and K. Mochizuki, J. High.Res.Chromatography and Chromatography Communications, 1980, 3, 16.
9. W.H. McFadden, H.L. Schwartz, and S. Evans, J. Chromatogr., 1976, 122, 389.
10. D.E. Games, P. Hirter, W. Kuhnz, E. Lewis, N.C.A. Weerasinghe, and S.A. Westwood, J. Chromatogr., 1981, 203, 131.
11. S.A. Westwood, D.E. Games, and L. Sheen, J. Chromatogr., 1981, 204, 103.
12. R.P.W. Scott, and P. Kucera, J. Chromatogr., 1979, 169, 51.
13. R.P.W. Scott, P. Kucera, and M. Munroe, J. Chromatogr., 1979, 186, 475.

ROUTINE DIRECT LIQUID INTRODUCTION LC/MS

Jack Henion, Diagnostic Laboratory, NYS College of Veterinary Medicine, Cornell University, Ithaca, NY 14853

INTRODUCTION

As we near completion of the first ten years since the earlier reports of continuously monitored LC/MS, publications on the subject are increasing at an exponential rate. This appears to be due in part to researchers' eagerness to develop a viable technique for accomplishing LC/MS and also to the commercial availability of LC/MS equipment from at least four manufacturers.

In spite of increasing sales of commercial LC/MS interfaces, however, LC/MS experiments are not considered routine by many who in fact have the necessary equipment. An even greater number of people seem to have purchased an LC/MS interface but have never used it. This paper highlights the important factors necessary to routinely conduct satisfactory LC/MS experiments using one popular technique eg. the direct liquid introduction (DLI) method (1).

We have conducted LC/MS experiments on quadrupole mass spectrometers (MS) for six years since the first DLI report was made from a high acceleration voltage magnetic MS (2). To date we have successfully carried out these experiments on five different quadrupole MS instruments and five different high pressure liquid chromatographs. Although the earlier work was not considered routine, refinements and knowledge in the technique now provide routine LC/MS capabilities with no unusual operational constraints.

These experiments may be conducted daily without adverse effects on any of the equipment. Ion source cleaning becomes necessary after awhile, but has been required only once per month with sixteen days of LC/MS during the month. On the average we clean the ion source every three months which includes routine GC/MS, LC/MS and solid probe sample introduction.

EXPERIMENTAL

Successful DLI LC/MS requires particular attention to certain important experimental details. It is preferable to optimize all HPLC separations off line. This frees the MS for other work and reduces exposure of the ion source to excess solvent and sample. HPLC separations should provide relatively short analysis time and narrow component peaks as is also important in GC/MS. LC peaks are often wider than, for example, capillary GC peaks so it is beneficial to utilize slower MS scan rates during LC/MS. This allows the MS to sample a larger fraction of the LC peak and thus provides increased sensitivity.

The removable stainless steel diaphram containing a five micron orifice in the LC/MS interface probe tip (3) provides a convenient means of accomplishing DLI LC/MS. This probe offers water cooling of the tip and removal of the diaphram should the pinhole orifice become plugged. The absence of both features in the glass capillary probe (2, 4) made the latter much less routine.

To minimize constriction or plugging of the diaphram all LC eluants and injected samples should be pre-filtered through 0.4 micron filters. In addition, all connecting stainless steel tubing should be pre-cleaned with cleaning solution followed by exhaustive rinsing with filtered solvents. All solvent/solution containers should be covered to exclude airborn particulate matter. Finally, an in-line 0.4 micron filter should be installed both after the LC pumps and immediately before column effluent enters the LC/MS probe. These seemingly redundant steps virtually guarantee trouble-free transfer of LC effluent through the diaphram.

Satisfactory DLI LC/MS results demand that a fine "jet" of LC effluent spray out from the diaphram pinhole into the ion chamber of the MS. This jet must be relatively short (1 inch) and very straight. If the jet of liquid is deflected off center it may impact the "desolvation region" (3) walls prematurely and fail to carry the solute to the ionization region. Finally, the LC/MS probe tip must be cool and the ion source hot. With some exceptions the source temperature should be maintained above 225°C to assure a stable vacuum and ion current.

Initial LC/MS experiments should utilize continuous flow of a 10-20 ppm solution of a representative solute into the MS to allow optimization of tuning and pressure variables. This procedure is analogous to tuning procedures routinely used prior to EI or CI GC/MS experiments which may utilize perfluorotributyl amine as the standard tuning compound. When tuning parameters have been optimized, the solution may be removed from the system, and LC/MS experiments may commence. These preliminary tuning procedures are required only when an unfamiliar LC eluant is being used.

CONCLUSION

In summary, the DLI LC/MS technique can be a routine laboratory experiment comparable to CI GC/MS. Useful information can be obtained from molecules not amenable to GC/MS techniques. Attention to the above mentioned details can provide gratifying success and we urge interested persons to come on in; the water, or eluant, is fine!

References

1. P.J. Arpino and G. Guiochon, Anal. Chem. (1979) 51, 682A-701A.

2. M.A. Baldwin and F.W. McLafferty, Org. Mass Spectrom., (1973) 7, 1353-54.

3. A. Melera, Paper No. 085, 30th Pittsburg Conference on Analytical Chemistry and Applied Spectroscopy, Cleveland, OH, March 5-9, 1979.

4. J.D. Henion, Anal. Chem., (1978) 50, 1687-1693.

LC-MS Method for the Separation and Quantitation of the Cis Trans Isomers of Thiothixene

by
N. Narasimhachari, S. Goldin, M. Mumtaz and R. O. Friedel
Department of Psychiatry, Medical College of Virginia, Richmond VA 23298

Introduction

Thiothixene (Navane, Roerig) exists in two isomeric forms, cis and trans (Fig. 1). The cis form of thiothixene is the active antipsychotic drug used in antipsychotic therapy, while the trans thiothixene is relatively inactive. Bombardt and Friedel (1) reported a gas chromatographic separation of cis-trans isomers using SP-2250 column and quantitated plasma levels of thiothixene using GC-CIMS and d_3 thiothixene as internal standard. We experienced difficulties in obtaining consistent results with this column both in regard to separation of cis and trans forms as well as column stability at the high temperatures used for analysis. We have therefore investigated high performance liquid chromatography (HPLC) for the separation of the cis and trans forms of thiothixene and their quantitation in biological samples in combination with mass spectrometry. To our knowledge only one HPLC method is reported for the determination of thiothixene in pharmaceutical formulations and no separation of cis and trans forms is reported (2).

Materials and Methods

Pure cis and trans forms of thiothixene samples, d_3-thiothixene (cis form) were generous gifts from Pfizer Research Laboratories. Solvents were all HPLC grade from Burdick and Jackson Laboratories Inc.

Methods:	Instrument:	Waters 440 Liquid Chromatograph
	Column:	Radial Compression Module (Waters Associates) RCM-100 silica cartridge (B 10) 10 microns
	Solvent Systems:	(1) Acetonitrile methanol 2:1; (2) Acetonitrile menthanol 1:1; (3) Hexane methanol 3:5; (4) Hexane isopropanol 9:1
	To all solvent mixtures was added NH_4OH (0.1% by vol.)	
	Detector:	254 nm UV fixed, Variable UV detector 220, 230, 254 nm
	Solvent Flow:	1.0 ml 1.2 ml 1.5 ml

Standards: Standard solutions of cis and trans thiothixene and d_3-cis thiothixene were separately prepared in HPLC grade methanol to contain 1 mg/ml. Serial dilutions were prepared from the stock solution to contain 2 ng/ml, 10 ng/ml and 100 ng/ml. A standard mixture of cis and trans thiothixene containing 10 ng of cis and 20 mg of trans/ul was also prepared.

Extraction of biological samples: To 2 ml of plasma sample, 100 ng of d_3-cis thiothixene was added and the sample extracted with hexane isopropanol (9:1) using the two step extraction procedure. Final extract was evaporated to dryness under nitrogen, redissolved in hexane-isopropanol and used for HPLC, gc and gc-ms analysis.

Results

With all the solvent systems used, we could separate the cis and trans isomers effectively, the separation being better than the gc method: Fig. 2 and 3. In recovery studies with plasma samples, blank plasma did not show any interfering peaks. Using variable UV detector, settings at 220 or 230 nm, gave higher detector response and therefore higher sensitivity than 254 nm. Standard calibration curves for both cis and trans isomers were linear in the tested ranges of 10 ng-100 ng and 100 ng-1000 ng. HPLC fractions when tested by gc or gc-ms were found to be homogeneous and did not contain any contaminants. The results of HPLC and gc-ms-sim in samples tested by both methods were within experimental error. The SIM of HPLC fraction is shown in Fig. 4.

In a few plasma samples that we tested we did not find any evidence of trans thiothixene by HPLC. However, irradiation of solutions using samples of cis-thiothixene under ultra violet lamp (TLC scanner, 15W), for 15 minutes caused 50% isomerization of the cis form to transform. Similarly, solutions of pure standards of cis thiothixene showed contamination by trans after a few days. So one has to be cautious about methods of collection, storage etc. in interpreting data from biological samples.

Conclusions

We have shown that cis and trans forms of thiothixene can be separated by HPLC. This

method can be used to monitor plasma levels of thiothixene. UV detector at 230 or 220 nm increases sensitivity two fold compared to 254 nm. Exposure to UV light causes rapid isomerization of the active cis form to inactive trans form. LC-MS can be used for quantitation of cis and trans thiothixene, with d_3-internal standard, using EI or CI modes.

References

1. P. A. Bombardt and R. O. Friedel; Comm. Psychopharm. (1977) 1, 49.
2. C. K. Wong, D. M. Cohen, and K. P. Munnelly; J. Pharm Sci. (1976) 7, 1090

THIOTHIXENE

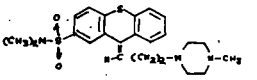

CIS

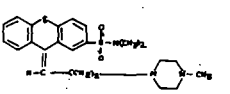

TRANS

Fig. 1

GC SEPARATION OF CIS-TRANS THIOTHIXENE

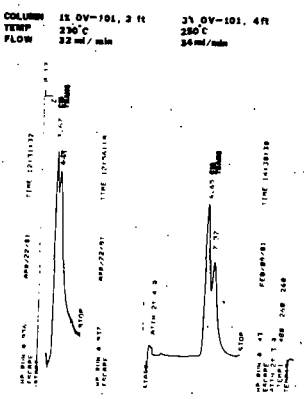

Fig. 2

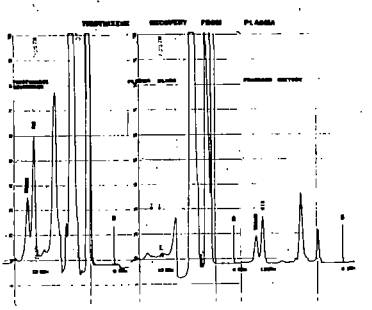

Fig. 3

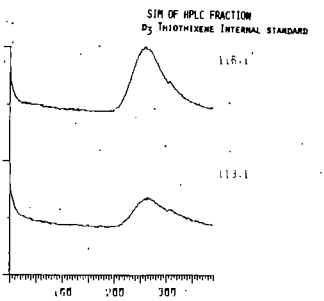

Fig. 4

ANALYSIS OF BIOMASSS SAMPLES USING AN LC-MS INCORPORATING SIMS, RIBBON STORAGE TECHNIQUES, AND A TRIPLE QUADRUPOLE MASS SPECTROMETER

Richard D. Smith and A. L. Johnson
Physical Sciences Department, Pacific Northwest Laboratory
Richland, Washington 99352

A LC-MS interface, described elsewhere at this meeting, has been applied to the analysis of complex biomass materials. The LC-MS is of the moving ribbon design with several new features. One feature results from use of a 320 cm ribbon length for storage of chromatographically separated material on the ribbon for re-analysis using other techniques or conditions[1-3]. The instrument includes a dual ionization capability allowing both thermal desorption/electron impact ionization (TD/EI) and ionization by the impact of high energy ions on the surface--Secondary Ion Mass Spectrometry (SIMS). In order to evaluate these techniques we have attempted the analysis of both simple mixtures and an extremely complex biomass "bottom product" (wood liquefaction residue).

The initial analysis of biomass bottom products utilized ternary gradient elution normal phase (amino 5 μm column) separation using a Spectra Physics Model 8700 HPLC. As expected the level of separation was insufficient due to the extreme complexity of the samples. Subsequent semi-prep scale separations were made of methylene chloride and methanol extracts using a similar ternary gradient elution program; seventeen fractions were collected in sufficient quantity for multiple analyses. These fractions were then analyzed individually by reverse phase (C-18, 5 μm column) HPLC using a methanol-water gradient program. The normal phase separation results in a rough division of compounds by chemical class and polarity while reverse phase separations are most effective for analysis within compound classes. This combination of analytical techniques, coupled with LC-MS using TD/EI and SIMS, for the ionization of nonvolatile or thermally labile compounds, should be particularly effective for analysis of these and similar complex samples. The triple quadrupole mass spectrometer, with collision induced dissociation (CID) capability, should also be effective for separations of coeluting compounds with interferring spectra and for assisting in identification.[3]

Figure 1 illustrates the application of ribbon storage techniques in the TD/EI mode of operation for a biomass sample. The figure gives the reconstructed total ion chromatogram for a single separation using normal phase tertiary gradient elution (hexane, methylene chloride, and 2-propanol) at three passes of the ribbon at temperatures of 150, 254 and 350°C, respectively. The ribbon speed was 10 cm/min and the mass spectrometer required approximately 10 sec/scan. These results for a hexane extract of the wood liquefaction distillation residue illustrate the effect of the flash heater temperature for the analysis of complex mixtures. The reconstructed ion chromatograms for 150, 254 and 350°C ribbon passes show significant variations in relative intensity. These variations are reflected in the mass spectra as illustrated by the eight single ion chromatograms illustrated in Figure 2. It should be noted that, depending upon desorption temperatures and compound volatility, the same compound can sometimes be observed at more than one temperature. As demonstrated, compounds are selectively observed at certain flash heater temperatures and discriminated against at higher or lower temperatures. This technique can assist in interpreting complex chromatograms since it provides differential information related to compound volatility. For experiments where mass spectrometer scan requirements are more demanding the LC effluent can be deposited on the moving ribbon and the mass spectrometer analysis performed at a different ribbon speed after completion of the liquid deposition thereby totally decoupling mass spectrometer and HPLC operation.

The use of SIMS ionization in conjunction with the moving ribbon LC-MS interface adds a unique potential to "on-line" mass spectrometric analysis by allowing the analysis of nonvolatile and thermally labile compounds. Our results indicate that the most useful information is present in the low energy secondary ion spectra. The removal of the high energy ions by the energy filter not only limits loss of mass spectrometer resolution but also reduces contributions to the mass spectra from high energy processes which contain little useful information. Our results indicate that for primary ion currents of $\sim 10^{-6}$ Amp/cm^2, a typical ribbon speed of 10 cm/min, a primary ion beam 1 cm in diameter, the exposure time for a sample is 6 sec, and consumption of approximately 6% of a monolayer occurs on each pass. It appears that the restriction to low primary ion beam currents used for "static-SIMS" is minimized under our conditions where the exposure time for a sample is on the order of a few seconds. We suggest that under the present conditions the larger primary ion currents provide a rapid means for obtaining useful spectra on an essentially real time basis. An example of a LC-MS analysis using the SIMS mode is illustrated in Figure 3 which

gives four reconstructed ion chromatograms for a biomass fraction obtained by semi-prep scale normal phase HPLC and analyzed by reverse phase. Figure 3 gives the reconstructed single ion chromatograms for several ions observed in the mass spectra. The characterization of these materials will require more extensive analysis using the triple quadrupole CID capability in conjunction with comparison with the more conventional TD/EI spectra.

References:

1. R. D. Smith and A. L. Johnson, Anal. Chem. 53, 739 (1981).
2. R. D. Smith and A. L. Johnson, Anal. Chem., in press.
3. R. D. Smith, J. E. Burger, and A. L. Johnson, Anal. Chem., to be published.

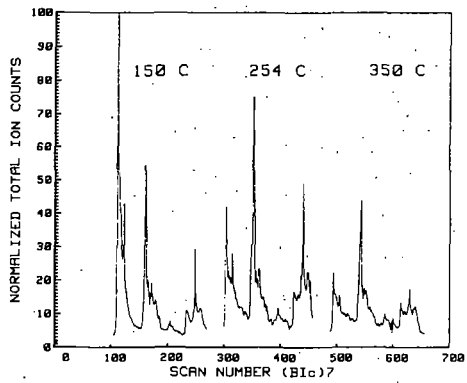

FIGURE 1. Normalized total ion counts as a function of scan number for an LC-MS analysis of a hexane extract of a wood liquefaction distillation residue. The reconstructed ion chromatograms were obtained in the TD/EI mode (15 eV electrons) and represent three passes of the separated material through the analysis region at the indicated temperatures.

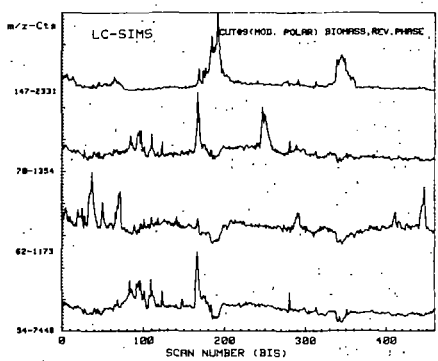

FIGURE 3. Reconstructed ion chromatograms for four typical ions in the reverse phase LC-SIMS analysis of a normal phase HLPC semi-prep fraction.

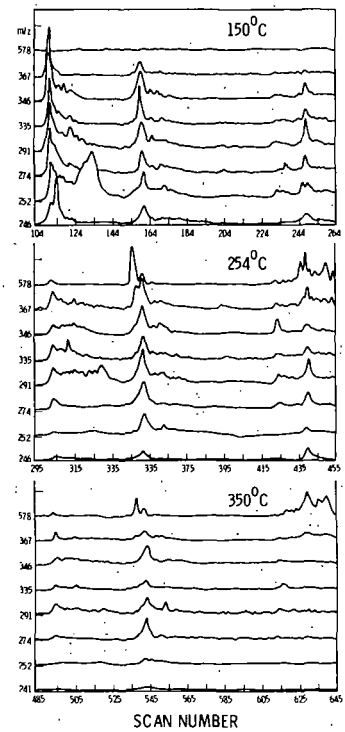

FIGURE 2. Reconstructed ion chromatograms of eight typical ions, for the analysis given in Figure 1, at three different ribbon passes through the "flash heater." Ribbon speed was 10 cm/min and each mass spectrometer scan required 10 sec.

Prepared for the U.S. Department of Energy under Contract DE-AC06-76RLO 1830.

STUDIES OF ERGOT ALKALOIDS USING LC/MS AND MS/MS

David E.Games, Christine Eckers, Department of Chemistry, University College, P.O.Box 78, Cardiff, Wales, Brian P.Swann and David N.B.Mallen, Lilly Research Centre Ltd., Windlesham, Surrey, England.

Crude extracts of ergot fermentation broths are being investigated in our laboratories in a search for new structural types. The extracts examined to date contain only alkaloids of the clavine type. Our methodology consists of initially establishing suitable high performance liquid chromatographic conditions for examination of the extract. This is followed by combined high performance liquid chromatographic - mass spectrometric study, using both electron ionization (EI) and chemical ionization (CI). Amine bonded, C18 reversed phase, and silica columns were used in these studies. Best data was obtained with a Spherisorb 5 column (250 x 5mm) using a mixture of methylene chloride, methanol and ammonium hydroxide (95:5:0.1) as eluant. Combined high-performance liquid chromatography/ mass spectrometry (LC/MS) using a Finnigan moving belt system enabled seventeen alkaloids to be located, twelve were the known alkaloids, agroclavine, setoclavine, festuclavine, palliclavine, noragroclavine, elymoclavine, penniclavine, isochanoclavine I, norchanoclavines I and II and chanoclavines I and II. The remainder being probably new alkaloids. In general EI was much more informative than CI however problems were encountered with palliclavine which was present as a minor component and appeared to decompose on LC/MS in the EI mode, whereas in CI it gave an excellent spectrum. Field desorption (FD) spectra were run on the crude extract to provide a molecular weight profile which served as a check for sample loss or decomposition during LC/MS.

Alkaloids of interest were subsequently isolated by preparative or semipreparative LC. High-performance liquid chromatographic/mass spectrometric study of fractions obtained in this way revealed the presence of additional alkaloids. When obtained chromatographically pure structural assignments were made for the new alkaloids on the basis of nuclear magnetic resonance, ultraviolet, infrared and mass spectral data and in some cases comparison with synthetic material.

Recently there has been considerable interest in mass spectrometry/mass spectrometry as a method for examination of crude mixtures.[1-3] Some authors[1,2] offer it as an alternative to combined chromatographic/mass spectrometric methods whilst others[3] suggest the techniques are complimentary and may be most effective when used in combination. We have undertaken a comparative study of LC/MS and MS/MS on our ergot extract to evaluate the relative merits of the two approaches. MS/MS studies were performed on a VG70-70H mass spectrometer using B/E linked scans of the $(M+1)^+$ ions obtained under CI conditions (methane, isobutane and ammonia). Collisional activation spectra were also obtained from ions of interest using B/E scans. The samples were introduced using the direct insertion probe and examination of the mass chromatograms of the $(M+1)^+$ ions of interest (m/z 271, 259, 257, 255, 243, 241, 239 and 225) showed that they vaporized into the ion source at a similar temperature, thus ensuring that no components were lost or required higher probe temperatures for distillation. FD and desorption CI spectral studies confirmed this finding. The data obtained from the mixture was compared with that obtained from authentic samples of known alkaloids.

Ammonia was found to be the reagent gas of choice, since there was less deterioration in source conditions and no complications due to the formation of addition ions. Chanoclavines I (1) and II (2) and isochanoclavine I (3) are not readily distinguished on the basis of their EI spectra. CI enables (3) to be distinguished from (1) and (2) but does not enable (1) and (2) to be readily differentiated. Spectra obtained by B/E scans of the $(M+1)^+$ ions of (m/z 257) of the three isomers enables them to be differentiated and similar results are obtained with collisional activation. However when m/z 257 was examined in the mixture, whilst we were able to positively identify (3) it was not possible to say if (1) and (2) were both present. From our LC/MS studies we know that all three isomers were present. Isomer differentiation was not possible when alcohol functionality was absent. This presents problems e.g. with m/z 241, we were able to identify norisosetoclavine (4) and the second component could be festuclavine (5) or its isomer pyroclavine (6) which have identical B/E spectra. LC/MS showed festuclavine only to be present. Difficulties were also encountered with m/z 239 the $(M+1)^+$ ion of agroclavine a major component of the mixture. Whilst ions were present in the B/E spectrum corresponding to agroclavine, additional ions were present and the peak at m/z 183 was of much higher abundance than in the standard spectrum of agroclavine. Further studies dhowed m/z 239 to be a fragment ion from the chanoclavines and comparison of the B/E scan of this ion in the chanoclavines showed that it accounted for the additional

ions present in the spectrum and the high abundance of m/z 183. Other ions examined presented fewer problems and enabled alkaloids known to be present in the mixture to be identified.

In conclusion we found that LC/MS is preferable to MS/MS for studies aimed at the location of new compounds in complex mixtures, because it enables isomers to be readily differentiated and provides ready made conditions for the isolation of compounds of interest which is necessary if they are to be fully characterized. MS/MS we feel is a useful additional technique for studies of this type and should be particularly useful when used in combination with GC/MS or LC/MS. Its major utility is for the rapid examination of mixtures for new major components (if they are not isomers) and for known compounds. Apart from our difficulties and differentiation of isomeric species other problems encountered with the MS/MS technique we used were, rapid source contamination with some reagent gases, the presence of artefact peaks in some spectra and lack of resolution of ions present in the mixture. Other types of MS/MS overcome the latter problem, but many of the other difficulties remain.

REFERENCES

1. R.W.Kondrat and R.G.Cooks, Anal.Chem., 1978, 50, 81A.

2. D.F.Hunt, J.Shabanowitz and A.B.Giordani, Anal.Chem., 1980, 52, 386.

3. F.W.McLafferty, Acc.Chem.Res., 1980, 13, 33.

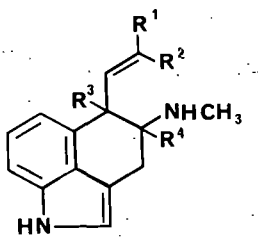

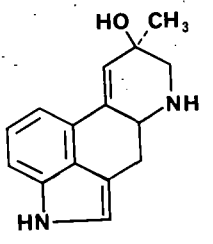

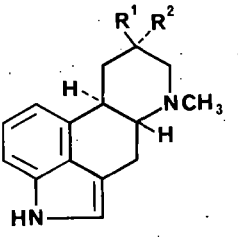

1. $R^1 = CH_2OH$, $R^2 = CH_3$
   $R^3 = R^4 = H$(trans)
2. $R^1 = CH_2OH$, $R^2 = CH_3$
   $R^3 = R^4 = H$(cis)
3. $R^1 = CH_3$, $R^2 = CH_2OH$
   $R^3 = R^4 = H$(trans)

4

5. $R^1 = CH_3$, $R^2 = H$
6. $R^1 = H$, $R^2 = CH_3$

Amino Acid Analysis by Electron Capture Negative Ion Chemical Ionization Mass Spectrometry

Donald F. Hunt and Mary Sisak

Department of Chemistry
University of Virginia
Charlottesville, Virginia 22901

We have developed a methodology for the determination of the amino acid composition of peptides. The unique aspects of this procedure is that it does not require the use of deuterated amino acids as standards and the analysis is done by electron capture negative ion chemical ionization mass spectrometry.

After the acid hydrolysis of the peptide in constant boiling hydrochloric acid, the liberated amino acids plus an internal standard are acetylated by treatment with a sodium bicarbonate solution (pH 8.5) for one minute at room temperature followed by a 1/3 mixture of D_6-acetic anhydride/methanol. A standard equal molar mixture of all the amino acids plus an equal amount of the internal standard is similarly acetylated with the exception that nondeuterated acetic anhdride replaces the deuterated acetic anhydride. This reaction goes to 95% completion after two minutes at room temperature at which time the reaction mixtures are combined by transferring both to a new tube and taken to drieness under a stream of nitrogen. The entire mixture is then benzylated with pentafluorobenzyl bromide in acetonitrile with diisopropylethylamine as a catylyst. The derivatized amino acids must be evacuated on a mechanical pump for approximately one hour prior to the analysis to remove the excess reagent pentafluorobenzyl bromide and the HBr formed in the reaction to prevent them from interfering with the analysis. The analysis is performed by taking the derivatives up in ethyl acetate and applying them to the end of a solids probe for introduction into the chemical ionization source. For all the amino acids that did not occur in the peptide, one observes a singlet, for the amino acids that did occur in the peptide, one observes a doublet separated by three mass units, the ratio of these peaks determines the number of amino acid residues.

All amino acids not containing additional functional groups fragment to yield the carboxylic acid anion as the only peak in the negative ion spectrum. The amino acids containing hydroxyl groups show an additional peak 18 mass units lower corresponding to the loss of water. This dehydration is a functional not only of source temperature but also the matrix of the sample. The dicarboxylic amino acids form two derivatives during the derivatization which are the benzylation of both carboxyl groups and the methylation of one of the carboxyl groups with benzylation of the other. In the positive ion spectrum, both of these derivatives yield the M + 1, 29, and 41 but in the negative ion mode, one only observes the peak corresponding to the carboxylic acid anion of the methylated species and a peak 32 mass units lower which is the result of the loss of methanol from the methylated species and the loss of pentafluorobenzyl alcohol from the dibenzylated species. The derivatization of histidine gives rise to three products all of which fragment to yield the carboxylic acid anion. The major product is the expected derivatization with additional benzylation of one of the nitrogens of the imidazole ring. Minor products are the acetylation of the nitrogen of the ring and no derivatization of the ring. Care must be taken not to benzylate both nitrogens of the imidazole ring since this would cause the formation of the quaternary salt of the derivative making it involatile. Our experience has been that if the excess reagent is not greater than 10 - 50 fold , histidine will be observed. The derivatization of lysine results in only one product which is diacetylated to that the peaks used to determine the number of lysines are separated by three mass units.

The difference for analyzing the derivative in the negative versus the positive mode was demonstrated by injecting decreasing amounts onto a capillary column while scanning the instrument from 60-760, first in the positive mode and then in the negative mode. We found that the negative to positive ratio of the base peaks was 395 indicating that if this derivative was analyzed in the negative ion mode, one would require 400 times less material.

This analysis is presently being done on 1 nanomole of peptide material. Standard curves were run for all the amino acids in the range of 1 to 20 nanomoles and the results indicate that the response is linear throughout. Coefficients of variation for 10 determination of a glucagon hydrolysate range from 0.25% for glutamic acid to 8.1% for serine. Serine poses the greatest problem during the analysis and observations indicate that rapid work up is necessary to prevent the loss of serine in both the sample and the standard.

QUANTIFICATION OF PICOMOLE AMOUNTS OF LEU-ENKEPHALIN IN CANINE BRAIN CAUDATE NUCLEI WITH FD-MS; D.M. DESIDERIO AND S. YAMADA, Department of Neurology and Stout Neuroscience Mass Spectrometry Laboratory, University Tennessee, 800 Madison Avenue, Memphis, TN 38163.

A combination of chromatographic separation and mass spectrometric techniques has been developed for a novel method for measurement of picomole amounts of endogenous oligopeptides in biologic tissue. High performance (pressure) liquid chromatography is utilized for rapid high resolution separation of peptides.(1) A new buffer system using dilute (0.04M) triethylamine-formic acid is utilized. The buffer system possesses excellent UV transparent properties enabling femtomole sensitivity for measurement of standard solutions of somatostatin(2) Use of porous polystyrene-divinylbenzene copolymer and octadecylsilyl columns facilitate retention of a peptide fraction from biologic extracts. Advantage was taken of field desorption-mass spectrometric methods to eliminate chemical derivatization of peptides and to produce protonated molecular ions which retain total molecular information of the peptide. Use of appropriate internal standards and selected ion monitoring methods enabled nanogram sensitivity and, more importantly, optimized structural specificity of the compound being quantified.(3) Results are compatible with radioimmunossay data. Data obtained with FDMS provide, for the first time, measurement of intact, chemically underivatized oligopeptides extracted from biologic matrices and, significantly, provide an analytic method to calibrate RIA data. This novel combination of methods is being applied to measurement of peptides (leu-enkephalin, met-enkephalin, somatostatin, etc.) in canine brain regions and dental pulp tissue.

A Varian-Finnigan MAT 731 Mass Spectrometer outfitted with a f.d.-f.i.-e.i. combination source was used in the f.d. mode. An overall recovery of tritiated leu-enkephalin of 26% was obtained during extraction. HPLC and FDMS measurements employed both an internal standard (^{2}ala-LE) and spiked (200 ng LE) samples. HPLC measurement yielded 272 ng/g canine caudate nucleus. RIA data reported values of 520, 200, 64, and 14 ng LE/g caudate nucleus based on 10% protein per gram wet tissue.

Supported by NIH-GM-NS-26666

REFERENCES

1) D.M. Desiderio, S. Yamada, F. S. Tanzer, J. Horton, and J. Trimble, J. Chromatogr., in press.

2) D. M. Desiderio and M. D. Cunningham, J. Liq. Chromatogr., in press.

3) D. M. Desiderio, S. Yamada, J.Z. Sabbatini, and F.S. Tanzer, Biomed. Mass Spectrom. 8, 10 (1981).

IN BEAM CHEMICAL IONIZATION OF PEPTIDES AND PEPTIDOLIPIDS

W. Rodney Mathews, Keith L. Clay, and Robert C. Murphy
University of Colorado Medical School
Department of Pharmacology
Denver, Colorado 80262

Desorption chemical ionization (DCI) is a relatively new in-beam chemical ionization technique (1) that allows one to produce spectra of relatively non-volatile molecules that are otherwise difficult to obtain. Placing the sample on the DCI probe has been done either by direct loading of crystalline samples or application of a dissolved sample with a microliter syringe followed by evaporation of the solvent. As neither of these methods are entirely satisfactory in many cases, we have developed an electrospray loading technique to deposit samples onto the DCI wire. The method follows the technique of McNeal and McFarlane (2). In contrast to direct sample application, evaporation of the solvent is exceedingly rapid, typically occurring during the spraying itself. If the water content of the solvent is low, comparatively large volumes can be easily loaded. A simple apparatus (Fig. 1) was constructed to electrospray the DCI probe. A positive voltage (4KV) is applied to a microliter syringe containing the sample. It has been found that a rounded needle-point greatly improves the spray characteristics. The probe tip, which is at ground potential, focuses the spray (Fig. 2) due to the high electrical fields.

Experiments with ^{35}S-cysteine dissolved in methanol have indicated that the distance between the needle and probe tip as well as the applied potential are critical (Table 1). The best results were obtained with a 2 mm separation and 4 KV which yielded 99% of the ^{35}S-cysteine deposited on the emitter wire.

TABLE 1: Effect of Voltage and Distance on Electrospray Loading.

Voltage (KV)	Distance (mm)	Recovery % (S.E.)	Comments
4	2	99(1.4)	Excellent
4	5	95(14)	Excellent
4	10	70(3.3)	Wide spray
4	15	56	
3	5	30(15)	Very poor
5	5	93(6.8)	Excellent
6	5	83(0.9)	Wide cone

TABLE 2: Effect of Solvent on Electrospray[1]

Solvent % water	Rate ul/sec	Spray[2]	Comments
0	13	++	
10	18	++	
20	30	++	
30	35	+	Some sputtering
40	38	0	Drops on DCIprobe
50	44	0	Spray only at 1cm
iPrOH/MeOH	20	++	

1) 4 KV, 5 mm
2) ++, Excellent; +, good; 0, poor

The effects of various solvents on the electrospray have been examined (Table 2). In general the rate of electrospray is dependent on the water content in methanol solutions. However above 30% water, problems of sputtering and collection of drops on the DCI wire begin. The methanol/isopropanol/water (1/1/1) solvent system described previously (2) results in an excellent spray as well.

The DCI mass spectra of glutathione (GSH, a tripeptide) using NH_3 as the reagent gas loaded by electrospray was compared to that loaded directly by microliter syringe. Qualitatively the spectra were identical. Measurement of the abundance of the MH^+ ion at m/z 308 from both techniques were not statistically different when 0.33 to 1.33 ug were loaded. Due to the rapid heating technique, elution of the sample from the DCI probe required the use of a multi-channel analyzer to collect the data.

The DCI mass spectrum of a leukotriene E derivative, the dimethyl ester of 6-(N-acetylcyseinyl)-5-hydroxyeicosatetraenoic acid, using NH_3 as reagent gas, is shown in Fig. 3A. Direct solid probe CI(NH_3) did not reveal any ions above 200 amu. (Fig. 3B). In contrast the MH^+ species was clearly evident along with structurally diagnostic ions at m/z 144, 161, 333, 478, and 492, using the electrospray technique and DCI. The mass spectra of the important neuropeptides Met-enkephalin (Tyr-Gly-Gly-Phe-Met) and the synthetic analog 2-D-Ala-Met-enkephalinamide have been obtained with these techniques. Quasi-molecular ions (MH^+) were easily measured down to 100 ng.

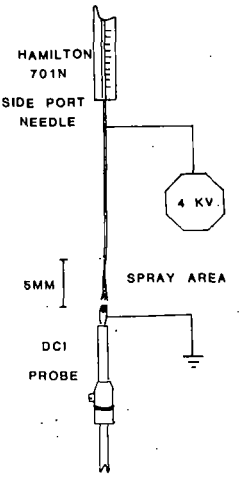

Figure 1: Diagram of the electrospray apparatus using a rounded side-port needle of a microliter syringe.

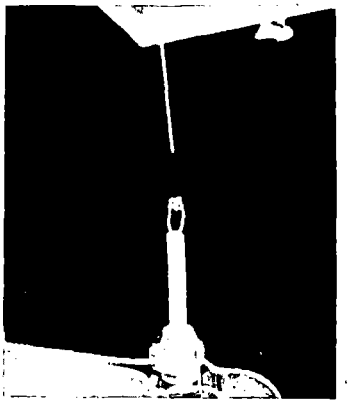

Figure 2: Electrospray at 4KV with 5 mm separation. Spray is focused onto the DCI probe.

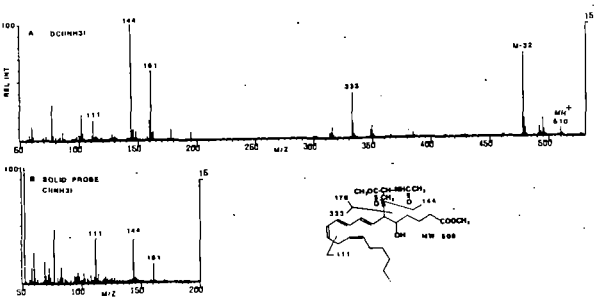

Figure 3: A. Mass spectrum of Leukotriene E_4 derivative obtained by DCI(NH_3) and loaded by electrospray. B. Identical amount of Leukotriene E_4 analyzed by direct solid probe CI(NH_3).

ACKNOWLEDGEMENT

This work was supported by a grant from the National Institutes of Health HL 25785.

REFERENCES

1. R.J. Cotter, Anal. Chem. 52, 1589A (1980).
2. C.J. McNeal and R. McFarlane, Anal. Chem. 51, 2036 (1979).

THE ROLE OF PEPTIDE SEQUENCING BY GCMS IN THE DETERMINATION OF THE STRUCTURE OF LARGE PROTEINS

N.J. Royal, W.C. Herlihy, Steven A. Carr, R.J. Anderegg, and K. Biemann

Department of Chemistry
Massachusetts Institute of Technology
Cambridge, MA 02139

The determination of the primary structure of proteins is presently carried out in general either by the Edman degradation (1) in which one amino acid after the other is cleaved off from the N-terminus of the protein itself or of a polypeptide derived from the protein by specific cleavage or, more recently, by the determination on the sequence of nucleic acid bases (2) in the DNA molecule coded for the biosynthesis of the protein, followed by a translation of the genetic code into the corresponding amino acids. Mass spectrometric methods have been devised for the sequencing of peptides which then can be reassembled to the original protein structure (3). All three approaches have certain advantages and disadvantages. The Edman degradation is very reliable for the beginning of the sequential degradation, namely the N-terminal region of the polypeptide but becomes less reliable as the experiment continues and rarely reaches the C-terminus. The DNA method is very fast but one has to determine three times as many units (bases) of the DNA structure then there are amino acids in the corresponding protein. However, the possibility of an error is finite and such an error shifts the triplets of the genetic code and thus leads to a completely incorrect amino acid sequence from that point on. The mass spectrometric method requires the unambiguous identification of a sufficient number of small peptides to align them to one unique protein structure. All three techniques can give a large portion of the structure of a protein relatively quickly but the remaining ambiguities are all difficult to resolve and this process may require a long period of time and a rather large amount of material. It is therefore most economical to combine data from an Edman degradation or from the DNA sequence with mass spectrometric peptide information in such a way that they complement and reinforce each other. Since these techniques are so different, it is highly unlikely that they will encounter the same difficulties. A few examples shall outline this approach.

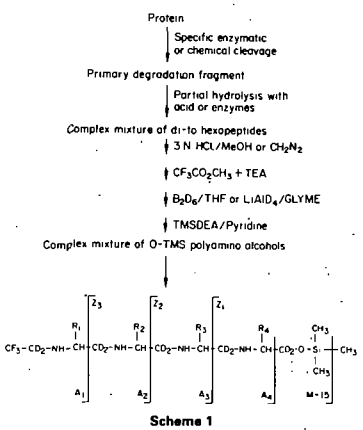

Scheme 1

INFORMATION REQUIRED WHEN USING CYANOGEN BROMIDE FOR SPECIFIC CLEAVAGE OF PROTEIN:

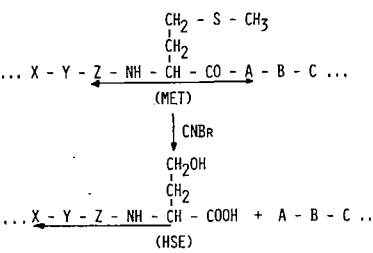

Scheme 2

In our mass spectrometric peptide sequencing scheme, a complex mixture of N-trifluoroethyl polyamino alcohol O-trimethylsilylethers are produced (Scheme 1) which are then injected into a gas chromatograph-mass spectrometer where the derivatives are separated and mass spectra of each fraction are obtained in the continuous scanning mode. The mass spectra exhibit a very straight forward fragmentation at the N-C-C-N bond, leading to a series of ions indicative of the sequence as read from the N-terminus (A_1-A_n) and another series which reads from the C-terminus (Z_1-Z_n) (4). Since the gas chromatographic behavior of these derivatives is well understood, the retention index of each of them can be calculated and one can therefore use mass chromatograms of specific sequence ions to search for the presence or absence of certain sequences.

When using the Edman degradation for the determination of the structure of the protein, one often cleavaes the protein with cyanogen bromide at the amino acid methionine which in the process is converted to homoserine. Thus, this reaction produces a set of peptides of

varying size, all ending in Hse (Sch. 2). These are then separated by chromatography and each one subjected to the Edman degradation. As outlined earlier, this sequence information rarely reaches the C-terminus, namely homoserine. Our mass spectrometric method makes it quite easy to search in a partial hydrolyzate (using aqueous acid or enzymes) for any small peptide that terminates in homoserine by plotting the mass chromatogram of the Z_1 fragment of homoserine (m/z 266) which will show a maximum at the point where the C-terminal peptide derivatives elute. Inspection of the mass spectra recorded at those maxima will reveal the sequence of these peptides and thus identify the C-terminal region. If this is, for example, the peptide Leu-Thr-Hse one then can search in the same manner for peptide derivatives ending in leucine and thus extend the sequence from the C-terminus towards the N-terminus until one reaches unambiguous overlap with the N-terminal sequence derived from the Edman degradation. Needless to say, in the course of the analysis of this mixture a large number of other peptide derivatives will have been identified which then corroborate the Edman data or point out any errors therein.

Once one has determined the sequence of all oligopeptides derived from the protein by cleavage at methionine, one has to determine the sequence of these peptides within the protein. This requires the identification of the amino acids surrounding each methionine in the protein molecule. This is accomplished by generating a partial hydrolyzate from the entire protein or large fragments thereof prepared by enzymatic cleavage and searching the mixture of derivatives for those containing the Z-Met-A sequence where Z is the amino acid preceeding Hse in one of the cyanogen bromide peptides and A is the N-terminal amino acid of that one which follows. Plotting the mass chromatogram of the A_2 ion of the sequence Z-Met one will find not only this dipeptide but also the derivative of the tripeptide Z-Met-A and possibly larger ones such as Z-Met-A-B-..., etc. In this way all methionine overlaps can be identified in a single experiment. This approach was used in the determination of the sequence of bacteriorhodopsin, a protein 248 amino acids long (5).

The corroboration of the protein sequence derived from the sequence of the DNA coded for its synthesis requires a completely different approach. Since a base sequence of a DNA molecule can be read in three different ways depending on which base turns out to be the first of the triplet denoting the first amino acid any DNA sequence can be translated into three entirely different amino acid sequences. It is therefore necessary to provide some protein sequence information to establish the proper "reading frame"(Sch. 3). While this can be accomplished by merely determining the N-terminal and C-terminal sequence of the protein which of course must fit the same reading frame, any misidentification, deletion or addition of a base along the DNA sequence will cause a completely false amino acid sequence. It is therefore important to have peptide information scattered all along to make sure that all amino acid sequences identified fall in the same reading frame. If they do not, an error must have occurred in the base sequence between the last amino acid that fits correctly and the first that appears in the wrong reading frame. From the shift one can tell whether a base was omitted or incorrectly inserted and it is then quite easy to check the base sequence in this narrow region and discover the error. For this approach to work unambiguously it is necessary to use only peptide sequences that are unique, that is, occur only once in the entire protein. Inspection of known sequences of large proteins (500 to 1000 amino acids long) revealed that tetra and pentapeptides are very unique, tripeptides much less so and dipeptides repeat very frequently. We have therefore developed a strategy that allows the identification of a relatively large number of tetra and pentapeptides in the partial hydrolyzate of the entire protein or a large segment thereof and to match these with the amino acid sequence derived by the translation of segments of the DNA as they are being sequenced.

We have developed and tested this approach with alanine tRNA synthetase (ARS) from *E. coli*, a protein of molecular weight about 95,000. The DNA sequence of the region of the gene coded for the synthesis of this enzyme was determined by Professor P. Schimmel and Dr. S. Putney of the Department of Biology, M.I.T., while we determined portions of the amino acid sequence of the enzyme randomly scattered throughout the protein (6). For this purpose we subjected a segment (T_1) containing about 400 amino acids to partial hydrolysis with various enzymes, derivatized the mixture and identified as many tetra and pentapeptides as possible by computer-aided interpretation of the mass spectral data (7) and matched them with the amino acid sequence in the three reading frames derived from the base sequence of the various segments of the gene produced by specific enzymatic cleavage of the DNA. Both the translation and the matching of the peptides is done with appropriate computer programs. If any of the peptides identified in the partial hydrolyzate of the protein fit one of the three reading frames, it establishes this one as the correct one. If some fit one reading frame and others another, an error in the DNA sequence is obvious. The same approach was used with the remaining part of ARS which led to the determination of the sequence of this protein which turned out to contain 875 amino acids which corresponds to a segment of DNA in which 2625 nucleic acid bases had to be correctly assigned. At this point one can inspect the

```
    DNA SEQUENCE    GAGATCCGTCAGGCGTTTCTCGAC
READING FRAME 1     GAG ATC CGT CAG GCG TTT CTC GAC
                    GLU ILE ARG GLN ALA PHE LEU ASP
READING FRAME 2   G AGA TCC GTC AGG CGT TTC TCG AC
                    ARG SER VAL ARG ARG PHE SER
READING FRAME 3  GA GAT CCG TCA GGC GTT TCT CGA C
                    ASP PRO SER GLY VAL SER ARG

                       DELETION OF A BASE
                  GAG ATC CGT AGG CGT TTC TCG
                  GLU ILE ARG ARG ARG PHE SER

                      INSERTION OF A BASE
                  GAG ATC CGT TCA GGC GTT TCT CGA
                  GLU ILE ARG SER GLY VAL SER ARG

                   MISIDENTIFICATION OF A BASE
                  GAG ATC CGT CAG GGG TTT CTC GAC
                  GLU ILE ARG GLN GLY PHE LEU ASP
```

Scheme 3. Translation of base sequence into the three possible amino acid sequences (reading frames) and effects of a single error in the DNA sequence.

resulting amino acid sequence for unique tripeptides and match those with the pool of tripeptides found in the course of the identification of tetra and pentapeptides (Fig. 1). All in all about 25% or all amino acid linkages in the proteins were identified by mass spectrometry, thus greatly increasing the confidence we can place in the correctness of the structure of alanine tRNA synthetase. It is clear that without such corroboration, the chances of establishing the DNA sequence correctly would be remote or would require a large number of redundant DNA sequencing experiments to achieve a reasonable level of confidence. On the other hand, to determine the amino acid sequence of a protein 875 amino acids in length would be extremely time and material consuming. The combination of two entirely different methods operating on the two components of the system, namely the gene and the protein, greatly enhances the reliability of the result while keeping the time and effort required to accomplish the task at a minimum.

Acknowledgements. This work was supported by Grant GM 05472 from the National Institutes of Health (K. Biemann, Principal Investigator).

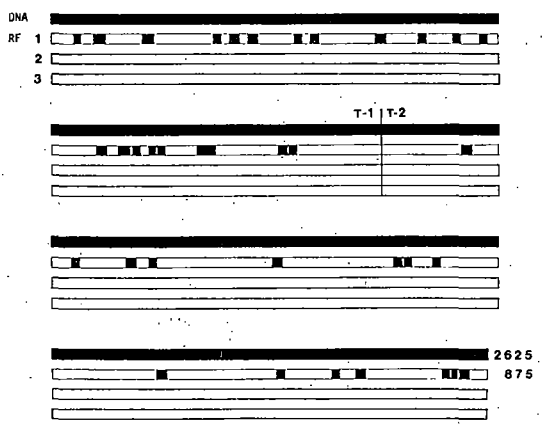

Figure 1. Schematic representation of the DNA sequence (black bar, 2625 bases) and the segments of amino acid sequences determined by GCMS (black rectangles)*from partial degradation of alanine tRNA synthetase. They clearly fit only reading frame 1 which thus is the correct structure (for actual sequence see Ref.8).

*Only segments representing tetra and pentapeptides are shown.

(1) For a review see, H.D. Niall, Methods Enzymol. 27, 942 (1973).
(2) A.M. Maxam and W. Gilbert, Proc. Natl. Acad. Sci. USA 74, 560-564 (1977).
(3) K. Biemann in Biochemical Applications of Mass Spectrometry, First Supplementary Volume, ed. by G.R. Waller and O.C. Dermer, p. 469. Wiley-Interscience, New York (1980).
(4) S.A. Carr, W.C. Herlihy and K. Biemann, Biomed. Mass Spectrom. 8, 51 (1981).
(5) W.C. Herlihy, R.J. Anderegg and K. Biemann, Biomed. Mass Spectrom 8, 62 (1981).
(6) W.C. Herlihy, N.J. Royal, K. Biemann, S.D. Putney and P.R. Schimmel, Proc. Natl. Acad. Sci. USA 77, 6531 (1980).
(7) W.C. Herlihy and K. Biemann, Biomed. Mass Spectrom. 8, 70 (1981).
(8) S.D. Putney, N.J. Royal, H. Neuman de Vegvar, W.C. Herlihy, K. Biemann and P.R. Schimmel, to be published.

PROTEIN SEQUENCING BY LIQUID FLOW MASS SPECTROMETRY; E. DVORIN, P. TAO, J. CARMODY, C.R. BLAKLEY, D. DYCKES, AND M. L. VESTAL; Dept. of Chem., Univ. of Houston, Houston, TX 77004.

A new technique for protein sequencing has been developed which may prove to be both faster and more sensitive than presently available methods. The approach employs a new mass spectrometer inlet system recently developed in our laboratory as a liquid-chromatograph-mass spectrometer system applicable to relatively involatile biological molecules. The significant feature of the liquid-flow mass spectrometer is that a flowing liquid stream can be totally vaporized, ionized, and mass analyzed, allowing continuous, rapid analysis of a flowing liquid of changing composition. This instrument provides a new and powerful tool for continuous monitoring of fast reactions in solution. In the new protein sequencing technique, enzymatic hydrolysis of terminal amino acids is carried out in a small reaction chamber terminated by a membrane which transmits the amino acids released by the reaction but which retains both the protein substrate and the enzyme. A continuous flow of buffer is pumped through the reaction chamber and into the mass spectrometer which continuously monitors the amino acid composition as a function of time. These data are acquired and analyzed by an on-line data system to yield the sequence of amino acids in the protein. The major limitation on speed and sensitivity of the new technique is imposed by the variability in enzymatic rates which depend on the nature of the amino acids adjacent to the bond being cleaved. Results on preliminary studies aimed at optimizing the reaction kinetics are presented together with the results of performance tests on known peptides.

STUDIES ON MOLECULAR SPECIES OF GLYCEROPHOSPHOLIPIDS BY A GC-MS SYSTEM

Kunihiko Saito, Minoru Kino and Masami Gamo, Department of Medical Chemistry, Kansai Medical School, Osaka, Japan 570

The most common glycerophospholipids in nature are choline and ethanolamine glycerophospholipids. They have many molecular species by combination of the constituent fatty acids and fatty alcohols including vinylalcohols. The species are usually divided into 4 types, i.e., (A) 1,2-diacyl, (B) 1-alk-1'-enyl-2-acyl- (plasmalogens), (C) 1-alkyl-2-acyl- and (D) 1,2-dialkyl glycerophosphoryl bases.

The molecular species of ethanolamine glycerophospholipids are more complicated and less elucidated than those of choline glycerophospholipids by GC-MS system. Because ethanolamine glycerophospholipids consist of 1,2-diacyl and 1-alk-1'-enyl (or alkyl)-2-acyl types and the constituent fatty acids are longer and more unsaturated than those of choline glycerophospholipids.

To overcome these two points we prepared the ter-butyldimethylsilyl derivatives, instead of trimethylsilyl ones, and analyzed in a GC-EI-MS system by selected ion monitoring technique (1). The derivatives were prepared as follows: glycerophospholipids were hydrolyzed with B. cereus phospholipase C and resulting 1-acyl (or alk-1'-enyl)-2-acyl glycerols were converted to ter-butyldimethylsilyl derivatives. To separate 1-alk-1'-enyl (or alkyl)-2-acyl and 1,2-diacyl derivatives, preparative thin layer chromatography was used.

For the polyunsaturated species which contained, for example, $C_{20:4}$ $C_{22:6}$, FD-MS seemed to be better than EI-MS. Therefore, FD-MS and GC-EI-MS were compared. The apparatus used for GC-EI-MS was Shimadzu GC-MS PAC 300. The column was OV-1 and electron energy was 22.5 eV. For FD-MS, Hitachi M-80 with carbon emitter was used. An individual molecular species was calculated from $[M-57]^+$ in EI-MS and from $[M]^+$ in FD-MS. The samples analyzed were ter-butyldimethylsilyl derivatives of 1-alk-1'-enyl-2-acyl and 1,2-diacylglycerols of ethanolamine glycerophospholipids obtained from rat uterus.

As shown in Fig. 1, the molecular species composition of 1-alk-1'-enyl-2-acyl derivatives obtained by both methods is quite similar, where abscissa indicates the number of double bonds and the total carbon number of vinylalcohol and fatty acid residues in the molecule. On 1,2-diacyl derivatives, similar results were obtained. Wood et al (2) directly analyzed the authentic phospholipids, without converting to the derivatives, by FD-MS. We have also obtained the same results but for a mixture of natural phospholipids derivatives would be better.

The changes in molecular species of ethanolamine glycerophospholipids with biomedical phenomina have been studied by GC-EI-MS. Fig. 2 shows the influence of estradiol on molecular species of ethanolamine glycerophospholipids obtained from oophorectomized rat uteri. Remarkable changes in some molecular species were found, indicating that the physicochemical properties and biological function of biomembranes were regurated by hormon.

(1) K. Saito, H. Ogino and K. Satouchi in "MEMBRANE FLUIDITY: Biophisical Techniques and Cellular Regulation", ed. by M. Kates & A. Kuksis: THE HUMANA PRESS, INC., Clifton, New Jersey ; p 33 (1980)
(2) G. W. Wood, P. Y. Lau, G. Morrow, G. N. S. Rao, D. E. Schmidt Jr., and J. Teubner, Chem. Phys. Lipids 18, 316 (1977)

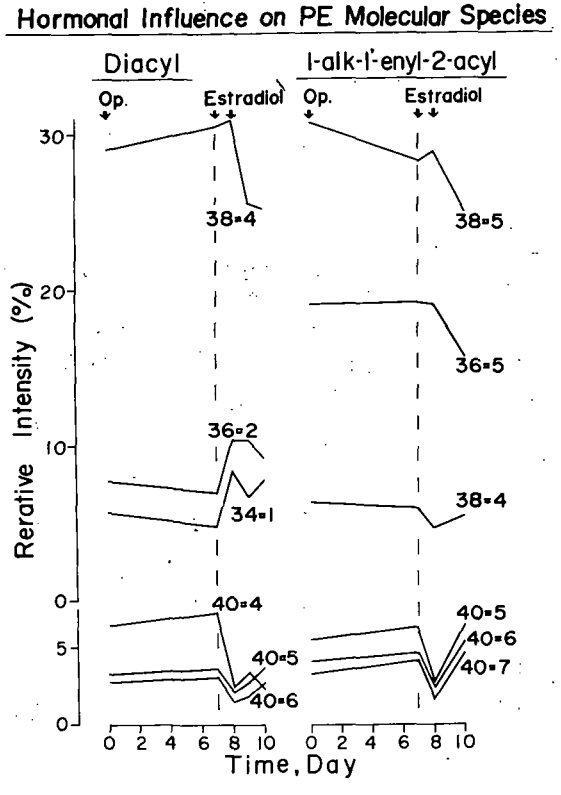
Hormonal Influence on PE Molecular Species
Diacyl
1-alk-1'-enyl-2-acyl
Op.
Estradiol
Op.
Estradiol
38:4
38:5
36:5
36:2
34:1
38:4
40:4
40:5
40:6
40:5
40:6
40:7
Rerative Intensity (%)
30
20
10
0
5
0
0 2 4 6 8 10
0 2 4 6 8 10
Time, Day

Fig. 2

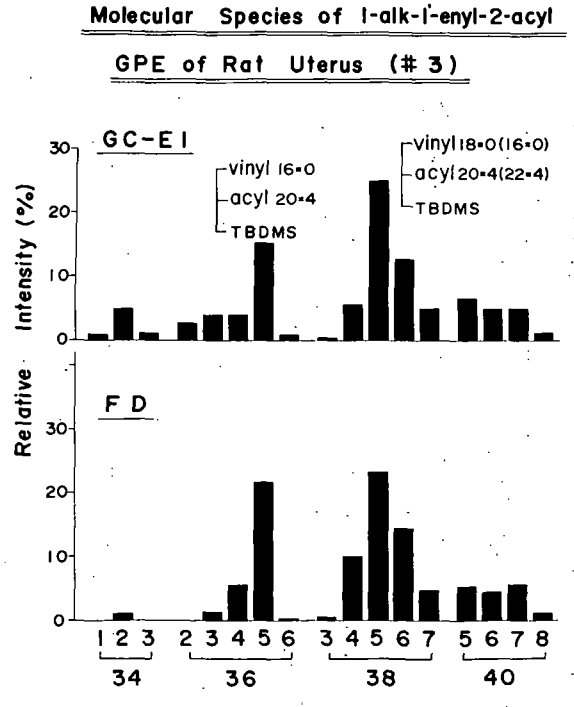
Molecular Species of 1-alk-1'-enyl-2-acyl
GPE of Rat Uterus (# 3)
GC-EI
vinyl 16:0
acyl 20:4
TBDMS
vinyl 18:0(16:0)
acyl 20:4(22:4)
TBDMS
FD
Relative Intensity (%)
30
20
10
0
1 2 3 2 3 4 5 6 3 4 5 6 7 5 6 7 8
34
36
38
40

Fig. 1

APPLICATION OF CHEMICAL IONIZATION MASS SPECTROMETRY TO THE STRUCTURAL CHARACTERIZATION OF COMPLEX MACROLIDE ANTIBIOTICS

Makoto SUZUKI, Ken-ichi HARADA, Naohito TAKEDA and Akira TATEMATSU
Faculty of Pharmacy, Meijo University, Tempaku, Nagoya 468 JAPAN

Electron ionization mass spectrometry (EIMS) has been successfully used in the structure elucidation of a number of macrolide antibiotics, particularly when the shifting technique between peracetyl and perdeuteroacetyl derivatives is employed[1].

Recently, in addition to the earlier works in the application of chemical ionization mass spectrometry (CIMS)[2], we have accomplished the basic approach to the structural characterization of 16-membered ring macrolides containing one aminosugar moiety, M-4365 A_2 and G_2, with their intact molecules[3].

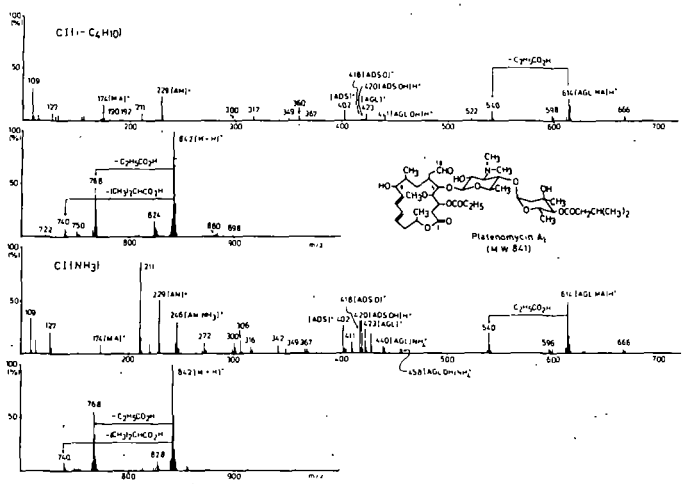

Fig. 1

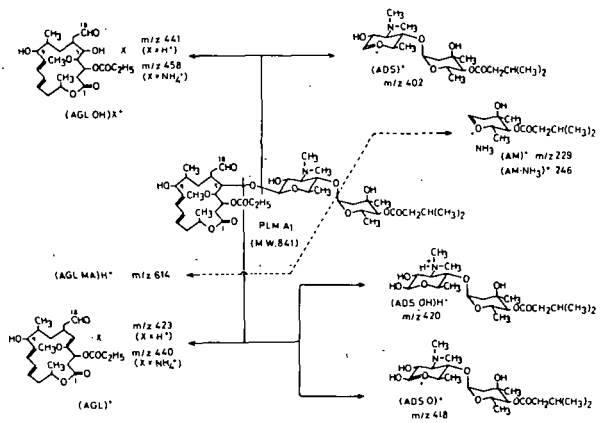

Fig. 2

We wish to present the results of CIMS of more complex macrolide antibiotics, Platenomycin A, B, Tylosin and Angolamycin, which contain two or more sugar moieties, using both isobutane and ammonia as the reagent gases.

All CI mass spectra show abundant protonated molecular ions (MH^+) and the aglycone and sugar derived ions srisen from cleavage of the glycosidic linkages.

As a typical instance, the CI mass spectra and major fragmentation pathways of Platenomycin A_1 are shown in Fig. 1 and Fig. 2, respectively. The structures of these ion species were determined by the shifting technique using ammonia-d_3 as a reagent gas and high resolution CI (isobutane) mass spectrum[4].

As a extensive application of such investigations, we attempted to characterize the structures of a new family of macrolide antibiotic, Mycinamicins (Fig. 3), which contain a novel 16-membered skeleton with neutral and aminosugar moieties.

Diagnostic ions of Mycinamicin I - V under CI condition were summarized in Table I, and these informations were quite useful for the structure elucidation of Mycinamicin series.

Under the investigation, we found out a specific fragment ion (m/z 424) in the spectra of Mycinamicin I and II. This ion was considered to be produced through fragmentation mechanism involving carbon-carbon bond cleavage of the conjugated epoxide group.

Fig. 3

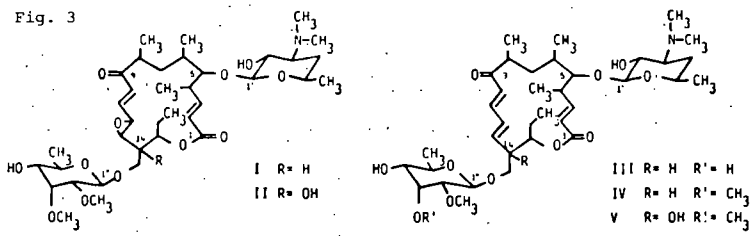

Table I. Diagnostic Ions of Mycinamicin Series under CI Condition

	MH^+	AGL-Des$^+$	$(AGL\text{-}OH)H^+$	AGL^+	Amino sugar	Neutral sugar
I	712	538	381	363	176, 174, 158	175(192)
II	728	554	397	379	176, 174, 158	175(192)
III	682	522	365	347	176, 174, 158	161(178)
IV	696	522	365	347	176, 174, 158	175(192)
V	712	538	381	363	176, 174, 158	175(192)

( )···NH_3 as reagent gas

References

1) M.Suzuki; J. Synth. Org. Chem. Japan, 30, 784 (1972)

2) L.A.Mitscher, H.D.Showalter; J. Antibiotics, 26, 55 (1973)

3) M.Suzuki, K.I.Harada, N.Tateda, A.Tatematsu; Heterocycles, 8, 199 (1977)
Biomed. Mass Spectrom., 8, in press (1981)

4) M.Suzuki, K.I.Harada, N.Takeda, A.Tatematsu; Heterocycles, 15, 1123 (1981)

IDENTIFICATION BY HIGH RESOLUTION MASS SPECTROMETRY OF 5-CARBOMETHOXYVALERAMIDINE, A HYDROLYSIS PRODUCT OF THE ANTISICKLING AGENT DIMETHYL ADIPIMIDATE

S. Lewis,[1] R. Pennathur-Das,[2] R. Halpin,[3] K. Cerrone,[4] B. Lubin,[2] G.L. Kenyon[3] and W.C. Mentzer[4]

[1]Biomedical Mass Spectrometry Resource, University of California, Berkeley, CA 94720; [2]Bruce Lyon Memorial Laboratory, Children's Hospital Medical Center of East Bay, Oakland, CA 94609; [3]Dept. of Pharmaceutical Chemistry, University of California, San Francisco CA 94143; [4]Northern California Comprehensive Sickle Cell Center, San Francisco General Hospital, San Francisco, CA 94110

Imidoesters have been used in biological studies to measure interresidue distances of proteins and macromolecular complexes, and in hematology as antisickling agents (1). Treatment of human red blood cells with ^{14}C-labeled dimethyl adipimidate (DMA), a bifunctional imidoester with antisickling properties, was followed by gradual loss of radioactivity from the treated cells. It became important to identify this released product so that its potential toxicity could be defined prior to experimental reinfusion in human volunteers of sickle cells treated in vitro with the drug. Preliminary studies indicated that the radioactive released product had identical TLC properties to the major product of DMA hydrolysis in vitro at physiological pH in phosphate buffer. The DMA hydrolysate was identified by high resolution mass spectrometry (HRMS) as 5-carbomethoxyvaleramidine. Fig. A is the mass spectrum obtained by direct probe insertion on a modified Kratos/AEI MS-902 mass spectrometer. Table 1 is the accurate mass data used for structural elucidation. In addition, the structure is supported by evidence determined by carbon-13 NMR, ultraviolet and infrared spectroscopy. The hydrolysate was also shown to be the radioactive product released from the red cells. The mass spectrum obtained from analysis of concentrated supernatant fluid in which the cells were stored contained all of the accurate masses of the hydrolysate.

A proposed mechanism which describes formation of 5-carbomethoxyvaleramidine predicts the existence of a 7-membered cyclic intermediate of MW 140 (Fig. B). UV studies support this hypothesis and indicate the presence of a short-lived chromophore (Fig. C). This mechanism has been previously hypothesized for the formation of 3-carbomethoxypropionamidine from dimethyl succinimidate through the formation of a 5-member cyclic intermediate (2).

HRMS evidence for the existence of the intermediate was obtained by analyzing both a solution of DMA in phosphate buffer and a control solution of DMA in methanol (pH 7.4) by using direct probe insertion within 10 min of preparation. The results show the presence of a compound other than DMA in buffer which has mass spectral properties that can be attributed to the proposed cyclic intermediate. Fig. D is the spectrum of the intermediate. In addition, studies with $^{15}NH_4Cl$ show a lack of ^{15}N in the hydrolysis product formed in the presence of excess $^{15}NH_3$ indicates that the second nitrogen in the amidine function arises from an intramolecular rearrangement of the DMA molecule, as is postulated to occur when the cyclic intermediate forms, and not from an intermolecular process involving free NH_3.

It is worth noting that the proposed intermediate could be reactive as a cross-linking agent. If the ring were to persist after formation of a cross-link, the distance between the reactive amino groups would be less than 5 Å rather than the 9 Å expected for the fully extended DMA molecule. This would complicate interpretation of nearest neighbor analyses which employ DMA to estimate the distance between adjacent molecules in membranes or other biological structures.

With regard to the use of DMA in humans as an antisickling agent, it is reassuring to know that the major hydrolysis product of this compound is 5-carbomethoxyvaleramidine since such compounds are known to be quite unreactive and thus have little or no potential toxicity.

Acknowledgements. This work was supported by NIH Division of Research Resources Grant RR00719, USPHS Grants AM 17323 and HL 20985, and National Foundation Grant 6-49.

References

1. B.H. Lubin, V. Pena, W.C. Mentzer et al., "Dimethyl Adipimidate, A New Antisickling Agent," Proc. Natl. Acad. Sci. USA 72, 43-46 (1975).
2. S.M. McElvain and J.P. Schroeder, "Orthoesters and Related Compounds from Malono- and Succinonitriles," J. Amer. Chem. Soc. 71, 40 (1949).

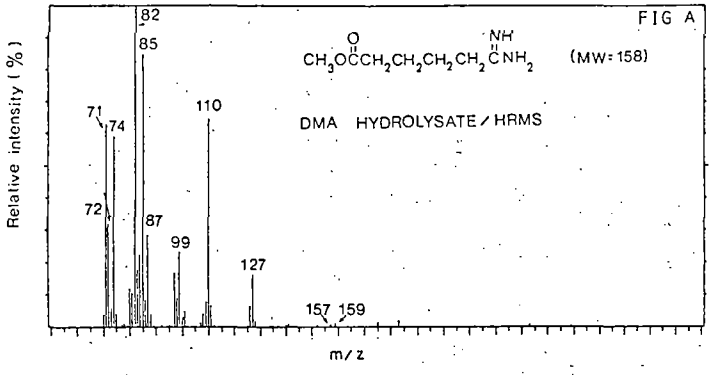

Table 1. Accurate Mass Data Used to Identify DMA Hydrolysate

m/z	Composition	Proposed Fragment
159.1142	$C_7H_{15}O_2N_2$	$M^{+\cdot}$ + H
[158	$C_7H_{14}O_2N_2$	$M^{+\cdot}$]^a
157.0965	$C_7H_{13}O_2N_2$	$M^{+\cdot}$ - H
127.0856	$C_6H_{11}ON_2$	$M^{+\cdot}$ - OCH_3
110.0591	C_6H_8ON	$M^{+\cdot}$ - $HOCH_3$,NH_3
99.0909	$C_5H_{11}N_2$	$M^{+\cdot}$ - $COOCH_3$
87.0445	$C_4H_8O_2$	$M^{+\cdot}$ - $C_3H_7N_2$
85.0758	$C_4H_9N_2$	$M^{+\cdot}$ - CH_2COOCH_3
82.0661	C_5H_8N	$M^{+\cdot}$ - $COOCH_3$,NH_3
74.0360	$C_3H_6O_2$	$M^{+\cdot}$ - $C_4H_8N_2$
71.0608	$C_3H_7N_2$	$M^{+\cdot}$ - $C_4H_7O_2$

a Inferred

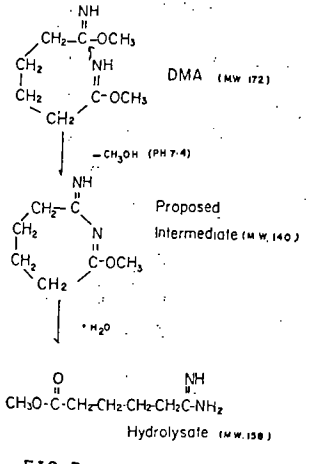

FIG B

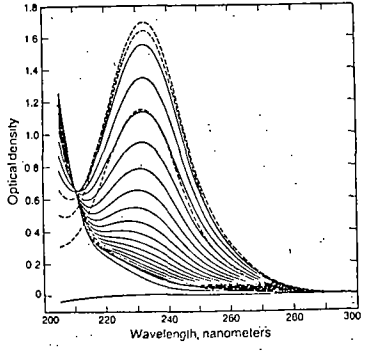

FIG C

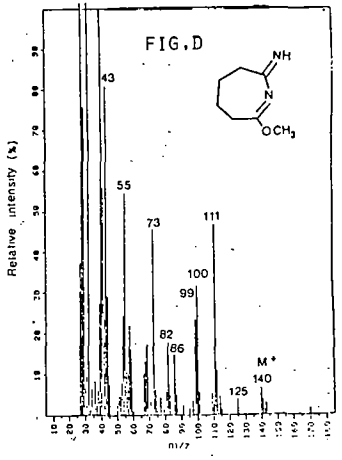

THE DETERMINATION OF STEROID CONJUGATES IN SALIVA

Simon J. Gaskell, Elizabeth M.H. Finlay and Michael S. Morton, Tenovus Institute for Cancer Research, Welsh National School of Medicine, Heath, Cardiff, CF4 4XX, U.K.

Salivary analyses of steroids are of interest because of the ease of serial sampling of saliva and the apparent correspondence between salivary concentrations and the concentrations of non-protein bound steroids in blood plasma. A number of unconjugated steroids have been determined in saliva using radioimmunoassay (see, for example, references 1-3) and gas chromatography-mass spectrometry (GC-MS)[4,5]. The low concentrations observed pose a particular challenge to the analytical methodology. Thus, the specificity of all stages of the analytical procedure must be maximised to ensure correct identification and quantification of the steroids of interest.

Little attention has hitherto been paid to analyses of steroid conjugates in saliva. Here we report the identification and quantification of dehydroepiandrosterone sulphate (DHAS) in saliva using high resolution GC-high resolution MS. Saliva (2 ml) was extracted with diethyl ether/ethanol (3/1) and a monosulphate fraction was obtained by chromatography on a micro-column of triethylaminohydroxypropyl-Sephadex LH-20[6]. Following enzymic hydrolysis, the tert-butyldimethylsilyl (TBDMS) ether or methyl oxime (MO), TBDMS ether was formed prior to high resolution GC-high resolution MS with selected ion monitoring (SIM) of $|M-C_4H_9|^+$ ions. GC-MS analyses employed a Varian MAT 731 instrument at a resolution of 8000 (10% valley). Separations were performed on a 20 m glass capillary column coated with OV-1 liquid phase.

The identification of DHAS was based on the following criteria: (a) the mobility of the compound during ion exchange gel chromatography, indicating a monosulphate; (b) the effectiveness of enzymic hydrolysis, consistent with a 3β-sulphate moiety; (c) the GC retention times of the TBDMS ether and MO, TBDMS ether derivatives of the unconjugated steroid; (d) the detection of ions of appropriate exact mass during SIM of the same derivatives.

Quantitative analyses of DHAS employed a deuterium-labelled analogue as internal standard. $|7,7\text{-}^2H_2|$DHA was synthesised from 5-androstene-3β,17β-diol, according to the procedure of Blair et al.[7] and the sulphate conjugate prepared. After addition of internal standard to the saliva sample, the analytical procedure described above was followed. Prior to GC-MS, androsterone TBDMS ether was added as chromatography standard to enable the determination of the relative responses to DHA TBDMS and $|^2H_2|$DHA TBDMS by a two-stage single ion monitoring procedure[8]. Validation experiments indicated satisfactory precision and accuracy in the determination of DHAS in saliva supplemented with the steroid. Endogenous DHAS concentrations have been observed in the range 0.3-23 ng/ml.

References

1. Walker RF, Riad-Fahmy D, Read GF. Clin Chem 1978; 24 : 1460.
2. Walker RF, Read GF, Riad-Fahmy D. Clin Chem 1979; 25 : 2030.
3. Smith RG, Besch PK, Dill B, Buttram VC. Fertil Steril 1979; 31 : 513.
4. Gaskell SJ, Pike AW, Griffiths K. Steroids 1980; 36 : 219.
5. Gaskell SJ, Finlay EMH, Pike AW. Biomed Mass Spectrom 1980; 7 : 500.
6. Setchell KDR, Almé B, Axelson M, Sjovall J. J Steroid Biochem 1976; 7 : 615.
7. Blair IA, Phillipou G, Seaborn C. J Label Compds Radiopharm 1978; 15 : 645.
8. Finlay EMH, Gaskell SJ. Clin Chem 1981; in press.

Acknowledgement

This work was generously supported by the Tenovus Organisation.

METABOLISM OF NEPETALACTONE AND RELATED COMPOUNDS IN NEPETA CATARIA L. AND COMPONENTS OF ITS BOUND ESSENTIAL OIL; GEORGE R. WALLER and RONALD D. JOHNSON, Dept. of Biochem. Okla. State Univ., Stillwater, OK 74078

Metabolism of nepetalactone-G-^{14}C by Nepeta cataria plants yielded significant amounts of dihydronepetalactone-^{14}C which was bound to plant components. Isomeric forms of dihydronepetalactone-G-^{14}C and nepetadiol-G-^{14}C were synthesized from nepetalactone-G-^{14}C. Upon administration of synthetic α-and β-dihydronepetalactone-G-^{14}C to N. cataria plants, label was incorporated into 7aα,7aβ,7aγ- nepetalactone, 4aβ,7aβ,7aβ-nepetalactone, a new nepetalactol and 10-dimethylnepetalactone . Nepetadiol-G-^{14}C did cause incorporation of significant amounts of label into 4aβ,7aβ,4aβ-nepetalactone and into new dehydrated derivatives of nepetadiol. The structures of the new compounds were determined by mass spectrometry. Analysis by GC and GC/MS also showed that treatment of the plant residues with 2N HCl liberates four times as much steam-volatile material containing diastereoisomeric dihydronepetalactones as does steam distillation of neutral residues. A metabolic scheme is proposed, and possible biological significance of the results is discussed. (Supported in part by Research Grants GM-08624 from the National Institutes of Health and GB-20,926 from the National Science Foundation).

GAS PHASE CHEMISTRY OF METAL- AND METAL-CONTAINING IONS WITH AMINES; John Allison, S.K. Huang, M. Lombarski, B. Radecki, Department of Chemistry, Michigan State University, East Lansing, MI 48824

There are many reasons for studying the chemistry of metal- and metal-containing ions with organic molecules in the gas phase. Our goals are to identify the basic mechanisms through which metal centers and molecules interact, and the reasons for changes in these basic mechanisms when the metal and/or the organic molecule changes. Metal containing compounds may have use as chemical ionization reagents; this aspect also merits investigation. Finally, we hope that our basic investigations may be of use to synthetic chemists.

The current areas of research in metal-ion bimolecular reactions can be divided into the following areas:

1. Metal Ion Reaction Energetics
2. Determination of Bondstrengths and Rate Constants
3. Mechanistic Studies
   a. clustering reactions
   b. formation of polynuclear clusters
   c. ligand substitution reactions
   d. rearrangements of organic molecules on metal centers

Areas 1 and 2 (above) are vital for a proper interpretation of the mechanistic studies, 3. The work done to date in the area of Mechanistic Studies will be briefly discussed below.

Clustering reactions involve the addition of small ligands to a metal center, e.g.

$$Cu^+ + NH_3 \rightarrow CuNH_3^+ \rightarrow Cu(NH_3)_2^+ \qquad (1)$$

see, e.g., ref. 1 and RAMOC3.

Polynuclear cluster formation reactions occur in systems of metal carbonyls, when ionic fragments react with the neutral metal carbonyl to form a product ion containing two metal atoms. Successive reactions can produce 3,4,5-metal atom clusters. See, for example, ref. 2; the typical reaction of this type being

$$Ni^+ + Ni(CO)_4 \rightarrow Ni_2(CO)_2^+ + 2CO. \qquad (2)$$

Ligand substitution reactions provide useful information on the relative binding energies of molecules to metal centers. Ref. 3 is typical in this area. Reaction (3) shows, for example, that PH_3 is a "better" ligand than CO for $Co(CO)_2NO^+$.

$$Co(CO)_3NO^+ + PH_3 \rightarrow Co(CO)_2NO(PH_3)^+ + CO \qquad (3)$$

The fourth area of Mechanistic Studies is that of rearrangements of organic molecules on metal centers. A reaction typical of this area is the decarbonylation of aldehydes induced by a nickel metal center, rxn. (4) (ref. 4).

$$C_5H_5Ni^+ + CH_3CHO \rightarrow C_5H_5NiCO^+ + CH_4 \qquad (4)$$

Historically, the area of Organometallic Chemistry in the Gas Phase began with studies of metal ions with alkyl halides and alcohols, in which alkali ions and transition metal ions react with RX to eliminate HX, resulting in a metal-olefin complex.

The alkali ions react through an internal charge-transfer mechanism, e.g.

$$Li^+ + iC_3H_7Cl \rightarrow Li^+\text{-}ClC_3H_7 \rightarrow LiCl\text{-}C_3H_7^+ \rightarrow (HCl)Li^+(C_3H_6) \rightarrow LiHCl^+, LiC_3H_6^+$$

Transition metal ions form the same products through a metal-insertion, β-H atom shift mechanism, e.g.

$$Fe^+ + C_3H_7Cl \rightarrow C_3H_7\overset{+}{F}eCl \rightarrow C_3H_6\overset{+}{F}eClH \rightarrow C_3H_6Fe^+, \overset{+}{F}eHCl$$

It was somewhat unexpected to learn that alkanes, with no functional group, are also reactive with transition metal ions. Reactions which are observed appear to proceed by insertions into C-C and C-H bonds by the transition metal, see, e.g. refs. 5 and 6. Alkane reactions typically involve alkane and/or molecular hydrogen elimination, e.g.

$$TiCl^+ + n\text{-}C_6H_{14} \longrightarrow ClTiC_4H_6^+ + C_2H_6 + H_2 \qquad (5)$$

$$\hookrightarrow ClTiC_6H_{10}^+ + 2H_2 \qquad (6)$$

Basic mechanistic studies of "small" molecules with metal ions, in addition to thermodynamic bondstrength determinations have been vital in understanding the chemistry of larger molecules which exhibit rich chemistries with metals. The chemistry of olefins, ketones and esters (refs. 7,8 and 9) with metals show a common sequence of steps. First, the metal interacts strongly with an electron rich group in the molecule (O-atom, double bond). Then, an empty orbital of the metal interacts with an atom or group of atoms elsewhere in the molecule, usually via a 5- or 6-membered ring. The metal assists the movement of this species to another part of the molecule, and subsequent fragmentation occurs. The usual result is the elimination of a stable neutral such as H_2, an olefin, an alcohol, etc. For example,

$$TiCl_3^+ + \text{2-pentanone} \rightarrow TiCl_3(C_2H_4O)^+ + C_3H_6$$

We are currently investigating the chemistry of ionic-metal centers with amines. It is surprising to find that the chemistry of RNH_2 with metal ions resembles not that observed for ROH and RCl, but rather that of RH. In most cases, the chemistry of butylamines with Co^+ does not appear to occur by metal insertion into the C-N bond, except in the case of t-butyl amine, in which elimination of C_4H_8 is observed.

$$Co^+ + t\text{-}C_4H_9NH_2 \longrightarrow CoNH_3^+ + C_4H_8 \qquad (7)$$

$$\hookrightarrow C_3H_7N^+ + CH_4 \qquad (8)$$

Many reactions can be explained as occurring through a 5-membered ring intermediate. For example, iso- and sec-butyl amines react with Co^+ to form $CH_3CoNH_2^+$, which may be formed through an intermediate such as is shown in reaction (9).

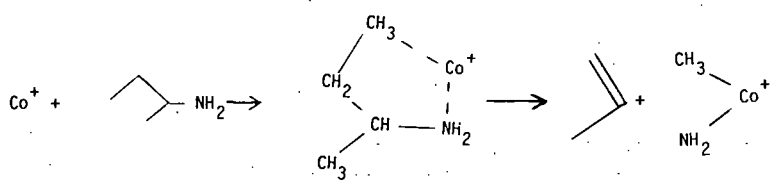

The same scheme applied to n-$C_4H_9NH_2$ accurately predicts the formation of $C_2H_5CoNH_2^+$. Many reactions observed indicate the preference of transition metals to insert into C-C bonds instead of C-N bonds, e.g.

$$Co^+ + n\text{-}C_4H_9NH_2 \longrightarrow \begin{cases} CoCH_2NH_2^+ + C_3H_7 \\ CoC_2H_5^+ + C_2H_4NH_2 \end{cases}$$

$$Fe^+ + sec\text{-}C_4H_9NH_2 \longrightarrow \begin{cases} FeC_2H_4NH_2^+ + C_2H_5 \\ FeC_3H_6NH_2^+ + CH_3 \end{cases}$$

When $W(CO)_6$ was used to generate metal ions, the ions WC^+ and WO^+ reacted more readily than W^+. Typical reactions again resemble alkane reactions, e.g.

$$WC^+ + t\text{-}C_4H_9NH_2 \longrightarrow \begin{cases} WC(C_3H_7N)^+ + CH_4 \\ WC(C_3H_5N)^+ + CH_4 + H_2 \end{cases}$$

We are currently investigating the chemistry of amines with a number of transition metals in an effort to determine what thermodynamic and structural effects control the observed reactions.

References

1. R.C. Burnier, T.J. Carlin, W.D. Reents, J.B. Cody, R.K. Lengel, B.S. Freiser, J. Amer. Chem. Soc., 101, 7127 (1979).
2. J. Allison, D.P. Ridge, J. Amer. Chem. Soc., 101, 4998 (1979).
3. G.H. Weddle, J. Allison, D.P. Ridge, J. Amer. Chem. Soc., 99, 105 (1977).
4. R.R. Corderman, J.L. Beauchamp, J. Amer. Chem. Soc., 98, 5700 (1976).
5. J. Allison, R.B. Freas, D.P. Ridge, J. Amer. Chem. Soc., 101, 1332 (1979).
6. P.B. Armentrout, J.L. Beauchamp, 103, 784 (1981).
7. J. Allison, D.P.Ridge, J. Amer. Chem. Soc., 99, 35 (1977).
8. J. Allison, D.P. Ridge, J. Amer. Chem. Soc., 100, 163 (1978).
9. R.C. Burnier, G.D. Byrd, B.S. Freiser, Anal. Chem., 52, 1641 (1980).

STUDIES OF CLUSTERS ABOUT METALLIC IONS

A.W. Castleman, Jr., P.M. Holland, D.M. Lindsay*, T.D. Märk†, K.I. Peterson, F.J. Schelling, R.J. Stanley, and B.L. Upschulte, Department of Chemistry and Chemical Physics Lab., CIRES††, University of Colorado, Boulder, Colorado 80309, USA

The bonding of polar molecules to a wide assortment of monovalent metallic cations of different electronic configurations has been the subject of an ongoing systematic investigation in our laboratory in recent years. Thermodynamic parameters derived from high-pressure mass spectrometric studies provide unique information on the strength of bonding and structure of these complexes, information which is relevant to a number of current research areas. Structural computations using quantum-mechanical and electrostatic theories provide further insight into the nature of bonding and arrangement of ligands about the central ion. Details of the solvation process, evidence to support proposed identifications of cluster species in the atmosphere, and extended understanding of transition-metal complexes serve as examples of the range of applicability of these results. An interpretation of the formation mechanism of similar cluster species observed in surface analysis studies may rely on such gas-phase thermodynamic stability data.

More recently, we have initiated a study of changes in the electronic character of neutral metallic clusters. Using multiphoton and electron-impact techniques, quadrupole mass spectrometry is then utilized for the determination of the properties of species in the molecular beam. The influence of surface-related effects and the approach to the conductive state of bulk metal can thereby be ascertained. Preliminary appearance potential measurements demonstrate the possibility of determining electronic properties of metallic aggregates in the presence or absence of adsorbed molecules. Results of this work are expected to enhance understanding of the catalytic properties of small metallic particles.

Details of the high-pressure mass spectrometer employed for studies of ion-molecule clustering have been published previously [1]. Under the influence of a low electric field gradient, ions emitted thermionically are directed into an essentially field-free reaction chamber containing up to 20 torr of a gas mixture [Fig. 1]. The slowly flowing reactant gas mixture is generally composed of an inert carrier gas which serves to introduce the clustering molecules and to ensure thermalization of the ions. Sampling of the population distribution of ionic species effusing through a small orifice into a quadrupole mass spectrometer allows a determination of ion ratios. After ensuring the attainment of thermodynamic equilibrium and minimizing mass-discrimination effects, these ratios, combined with a knowledge of temperature and reactant partial pressures, yield a measurement of the equilibrium constants for a series of clustering reactions. Correlating the data obtained over a wide temperature range in the form of a van't Hoff plot (ln K vs. 1/T) provides values of the enthalpic and entropic contributions to the Gibbs free energy changes involved in the formation of clusters. Comparison of the results between different ion-ligand entities and in relation to various theoretical models provides the clues from which conclusions may be drawn regarding the structure and stability of such clusters.

In comparing strengths of first ligand-ion bonds, for example, a strong radial dependence is observed for alkali metal ions, as would be expected from a purely electrostatic model [2]. However, the first ligand binds to cations of the transition metals much more strongly. As is borne out by extended Hückel calculations, this is evident for the presence of partial covalent hybrid bonding [3]. Differences in bonding strengths between an ion and different ligands have also been resolved. The larger enthalpies of ammoniation relative to hydration for alkali metals, for example, have been traced to the greater polarizability of the ammonia molecule, despite the larger dipole moment of the water molecule [4].

A number of conclusions may be derived as well from a consideration of multiple-ligand clusters. The observation of solvation breaks in plots of successive enthalpy changes as a function of the number of ligands illustrates the formation of coordination shells [4]. Of possibly greater significance are similar studies of mixed-ligand clusters. The preferential binding of ammonia over water to copper and silver ions reverses after the addition of the first two ligands, a crossover phenomena explaining the observed solution complexes of these ions [4]. Mixed-ligand studies are also valuable in constructing Born-Haber cycles for checking the consistency of experimental results and for investigating such ligand-switching reactions. As part of this work, data regarding several charge-transfer reactions have also been obtained, particularly for the silver-pyridine and sodium-water systems [5,6].

In the future, our continuing study of ion-molecule clustering, in addition to our new investigation of neutral clusters, will continue to extend our knowledge of the properties of small particles.

References:

(1) A.W. Castleman, Jr., P.M. Holland, D.M. Lindsay, and K.I. Peterson, J. Am. Chem. Soc., 100, 6039 (1978)

(2) A.W. Castleman, Jr., "Nucleation and Molecular Clustering About Ions" in: Advances in Colloid & Interface Science "Nucleation," A. Zettlemoyer, Ed. (Elsevier Press, Oxford, England, 1979) pp. 73-128

(3) A.W. Castleman, Jr., Chem. Phys. Lett., 53, 560 (1978)

(4) A.W. Castleman, Jr., "Studies of Ion Clusters: Relationship to Understanding Nucleation and Solvation Phenomena" in: Kinetics of Ion Molecule Reactions, P. Ausloos, Ed. (Plenum Press, N.Y., 1979) pp. 295-321

(5) T.D. Märk, K.I. Peterson, and A.W. Castleman, Jr., Nature, 285, 392 (1980)

(6) P.M. Holland, "Structure in Cluster Ions: Gas Phase Clustering about the Ag^+, Cu^+ and H^+ Ions," Thesis, University of Colorado, Boulder, 1980

*Present address: Dept. of Chemistry, City College of New York, Convent Ave. at 138th St., New York, NY 10031

†Present address: Institut f. Experimentalphysik, Leopold-Franzens-Universität, A-6020 Innsbruck, Austria

††The Cooperative Institute for Research in Environmental Sciences is jointly sponsored by the University of Colorado and the National Oceanic and Atmospheric Administration.

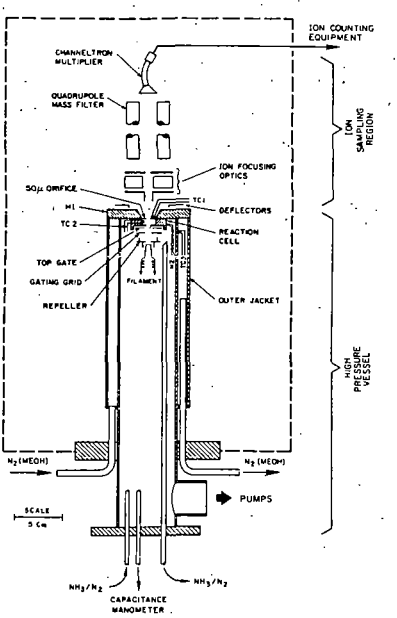

FIGURE 1

ATMOSPHERIC CHEMISTRY OF METEOR DERIVED IONS; ELDON FERGUSON; Aeronomy Laboratory, NOAA, Boulder, CO 80303

Atomic ions including Fe^+, Mg^+, Si^+, Na^+, K^+, Ca^+, Al^+, Cr^+, Ni^+, Mn^+ and Ti^+ have been observed in the upper atmosphere as a consequence of meteor ablation of neutral atoms subsequently ionized by charge-transfer with ambient NO^+ and O_2^+ ions. These meteoritic atomic ions are often concentrated into intense thin layers by electrodynamic forces. The ions are lost by association with O_2 and subsequent neutralization by electrons and negative ions. New laboratory ion-molecule reaction measurements will be presented which yield an explanation for the observed depletion of Si^+ ions with respect to the comparably produced Fe^+ and Mg^+ ions below $\sim$100km altitude. Si^+ ions react rapidly ($k=2.3(\pm 10)cm^3 s^{-1}$) with H_2O to form $HOSi^+$ ions. The reactions of Mg^+ and Fe^+ with water are both endothermic. Si^+ ions associate with O_2 to form stable SiO_2^+ ions with a very large three-body rate constant. A mechanism to explain this anomaly will be presented with supporting measurements of the energy dependence of the endothermic $Si^+ + O_2 \rightarrow SiO^+ + O$ reaction carried out in the NOAA Flow Drift Tube. Because of the low ionization potentials of the metals they may form oxides and hydroxides with large proton affinities. Recent laboratory studies of sodium ion reactions lead to the conclusion that any gas phase sodium compound (NaOH, NaCl or $NaNO_3$) in the stratosphere would react with the ambient $H^+(H_2O)_n$ proton hydrates and the ambient stratospheric water to produce hydrated Na^+ ions. These measurements will be presented. Recent balloon borne mass spectrometer studies of the stratosphere show that hydrated Na^+ ions are not present. It is therefore concluded that the metallic meteor ablation products are converted into particulates before reaching the stratosphere, i. e. at all altitudes below $\sim$60km.

GAS PHASE STUDIES OF LASER GENERATED TRANSITION METAL IONS

R.C.Burnier, G.D.Byrd, T.J.Carlin, M.B.Wise,
R.B.Cody, and B.S.Freiser

Department of Chemistry
Purdue University
West Lafayette, IN 47907

The development of a combined pulsed laser source-ion cyclotron resonance spectrometer in our laboratory has proven to be a convenient and powerful method for generating metal ionsand for studying their subsequent chemistry in the gas phase. In particular our main emphasis this past year has been on the applications of metal ions as selective chemical ionization reagents and our progress in this area will dominate this discussion. In addition we report the first results combining laser ionization with a NICOLET FTMS-1000 prototype spectrometer recently put into operation in our laboratory and discuss some of the advantages of this approach.

The goal of this research is to identify trends in reactivity i.e. reaction mechanisms useful in interpreting the chemical ionization spectra of unknown compounds and to test for for the the functional group selectivity of various metal ions. Our first detailed study was on Cu^+ which was observed to display definite patterns of reactivity for different classes of oxygenated compounds. Dissociative attachment reactions of Cu^+ with esters,for example, occur in which the ester is cleaved either to alcohols and ketenes or to carboxylic acids and alkenes. The reaction pathway was shown to be strongly influenced by the thermodynamics of the dissociation channels of the free ester. The products react further with the substrate ester by ligand displacement. The reactions of Cu^+ with methyl acetate and ethyl formate are typical. These reactions are illustrated in Figures 1a and 1b which show schematically ion intensity at three arbitrary trapping times for Cu^+ in the presence of methyl acetate and ethyl formate, respectively. The variation in the spectra demonstrates clearly the "tunability" afforded by varying the trapping times in the ICR, as well as the type of information available by Cu^+ chemical ionization. The spectra are simple, with the pseudo molecular ions for the isomers(both at M/z 137) dominating at long times. These isomers are readily distinguished and identified by the characteristic dissociative

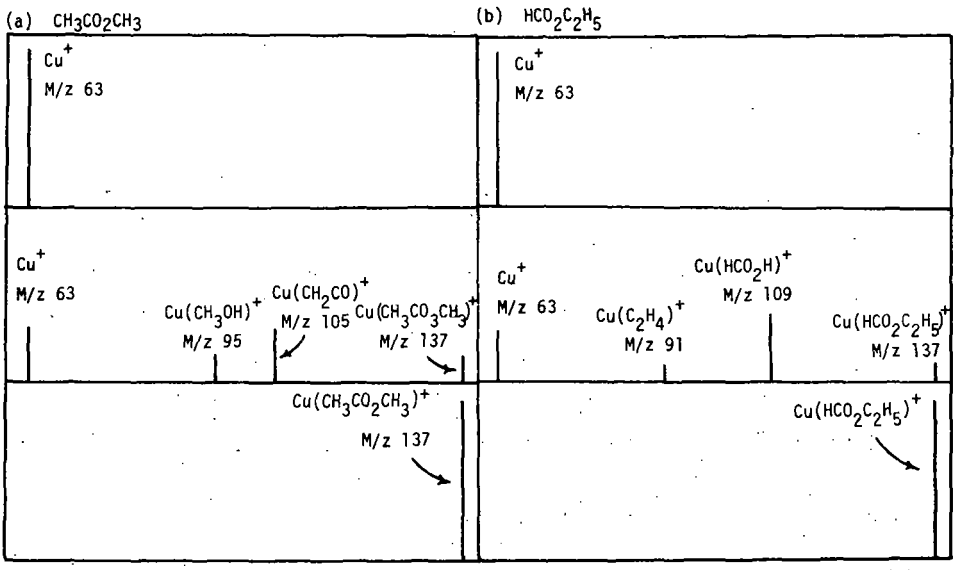

Figure 1. Ion intensity at three arbitrary trapping times for Cu^+ in the presence of (a) methyl acetate and (b) ethyl formate. Time increases from top to bottom.

attachment products at intermediate times.

If a particular metal ion is not sufficient for sample identification, one can readily take advantage of a series of different metal ion chemical ionization spectra. Table I illustrates this point by showing what we have termed a periodic reactivity plot for 2-butanone. The periodic reactivity plot is a "fingerprint" or "computer punch card" for a particular species which, if matched, identifies its presence in the spectrometer. The widely differing reactivities shown in Table I are striking. Al^+ does not undergo any dissociative reactions with the 2-butanone. The strength of the Ti-O bond is evident in that TiO^+ is the only reaction product observed when Ti^+ reacts with the butanone. Interestingly, the reactivity of TiO^+ is observed to be completely different than that of Ti^+ and suggests that these reagent ions may be further tailored for specific needs. The V^+ reacts similarly to Ti^+, forming VO^+ exclusively and again VO^+ is observed to react differently than V^+, and so forth.

Table I. Periodic Reactivity Plot for 2-Butanone

for the process:

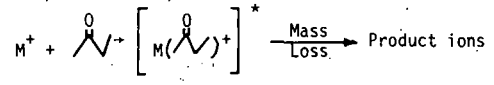

M^+ =	Al^+	Ti^+	TiO^+	V^+	VO^+	Co^+	Fe^+	Cu^+
Mass Loss								
2					x		x	
16						x	x	
18					x			x
28			x		x	x	x	
44					x	x	x	
54			x					
56		x		x				

These studies are greatly facilitated by our new NICOLET Fourier transform instrument. Fourier transform ion cyclotron resonance (FT-ICR) spectroscopy, also called Fourier transform mass spectrometry or FTMS, is a new method for conducting ICR experiments which was first demonstrated by Comisarow in 1974. The method involves the simultaneous excitation of the entire frequency domain ICR spectrum, sampling the resultant transient response of the system, and numerical Fourier transformation to obtain the ICR frequency or mass spectrum. This holds several key advantages for the laser ionization experiment. A complete mass spectrum may be obtained rapidly from one laser pulse as demonstrated by Figure 2. Several thousand laser shots would normally be required to obtain a similar spectrum using a conventional ICR. Thus, a smaller sample may be studied or,alternatively, less laser damage is sustained by the sample or target. In addition, because the entire mass spectrum is obtained from each laser shot, the FT experiment is far less susceptible to problems arising from pulse to pulse variations of the laser signal and signal averaging may readily beaccomplished. Two other major advantages of the FT instrument are the increased mass range and resolution. To date using a magnetic field of 9kG, for example, we have been able to identify ion-molecule product peaks as high as M/z 1100 and have achieved a resolution of about 200,000 at M/z 100.

As a final demonstration of the laser ionization-FTMS technique, some results are presented from a study we have initiated on the cluster chemistry of the transition metal carbonyls. Beauchamp et.al. have shown that the primary ions from $FeCO_5$ undergo sequential clustering reactions to produce multi-metal species with various numbers of carbonyls attached. In particular Fe^+ is observed to react with $FeCO_5$ to produce $Fe_2CO_4^+$ which

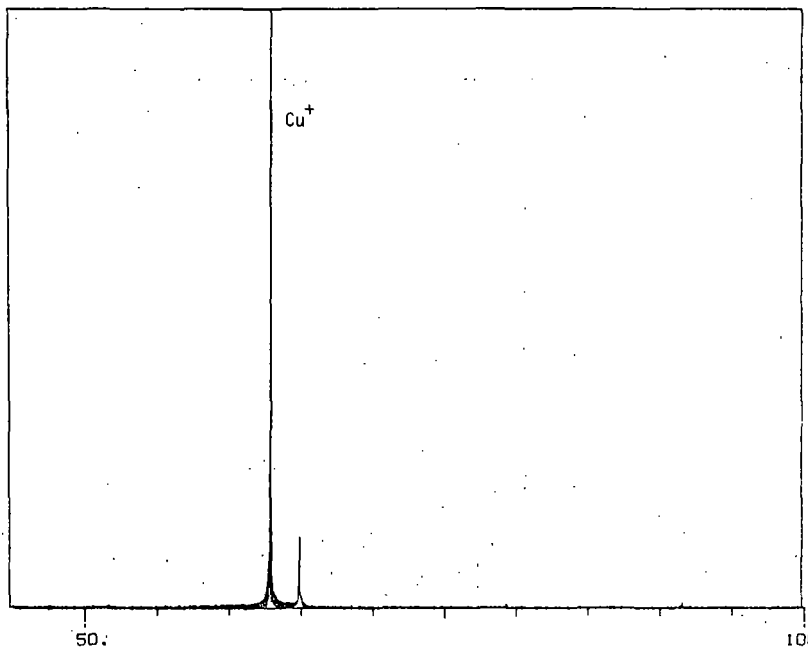

Figure 2. LASER IONIZATION MODE,COPPER TARGET,4 NANOTORR,ONE SHOT,5/6/81

subsequently produces $Fe_3CO_7^+$, $Fe_3CO_8^+$, and eventually $Fe_4CO_{10}^+$. What effect would, for example, Cu^+ have on this cluster chemistry? The data in Figure 3 answer this question. Figure 3a shows the trapped ion spectrum arising from electron impact on $FeCO_5$. Fe^+ and the cluster ions which arise from its subsequent reactions are labeled. Figure 3b shows the Cu^+ chemical ionization spectrum of $FeCO_5$ under otherwise similar conditions. With the exception of $CuFeCO_3^+$, whose analog $Fe_2CO_3^+$ was not reported by the Beauchamp group, the cluster chemistry of the mixed Cu-Fe species looks remarkably similar to the pure Fe analogs. Further work is underway in this area varying both the metal ion reagent as well as the metal carbonyl. Of particular interest will be the effect of mixed metal clusters on ligand exchange reactions.

1. R.B.Cody, R.C.Burnier, W.D.Reents, Jr., T.J.Carlin, D.A.Mcrery, R.K.Lengel, and B.S. Freiser, Int. J. Mass Spec. Ion Phys., 33, 37 (1980).

2. R.C.Burnier, G.D.Byrd, and B.S.Freiser, Anal. Chem., 52, 1641 (1980).

3. M.B.Comisarow in "Transform Techniques in Chemistry"; P.R.Griffiths, Ed.; Plenum Press, New York, 1978; p.282.

4. M.S.Foster and J.L.Beauchamp, J. Am. Chem. Soc.,97, 4808 (1975).

(a)

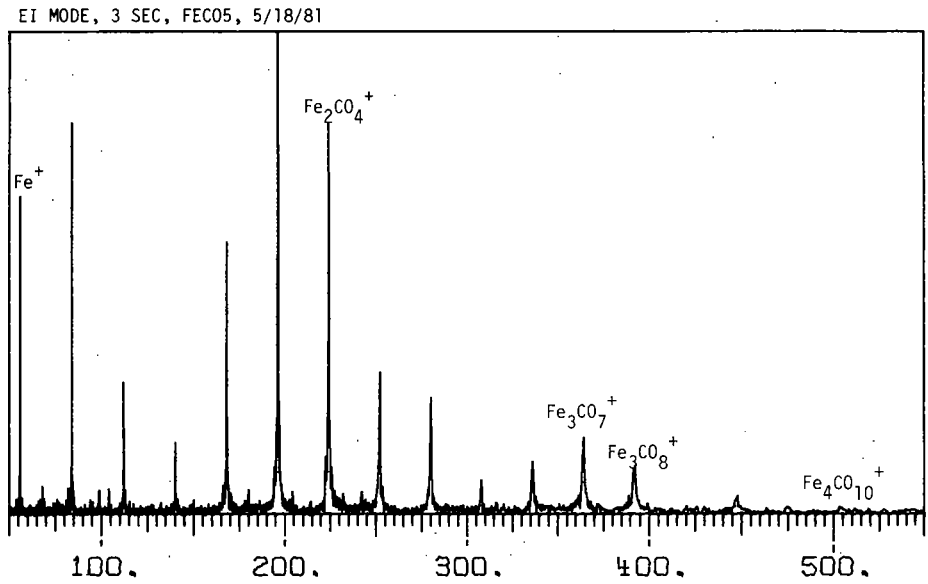
EI MODE, 3 SEC, FECO5, 5/18/81
Fe^+
$Fe_2CO_4^+$
$Fe_3CO_7^+$
$Fe_3CO_8^+$
$Fe_4CO_{10}^+$
100.
200.
300.
400.
500.

(b)

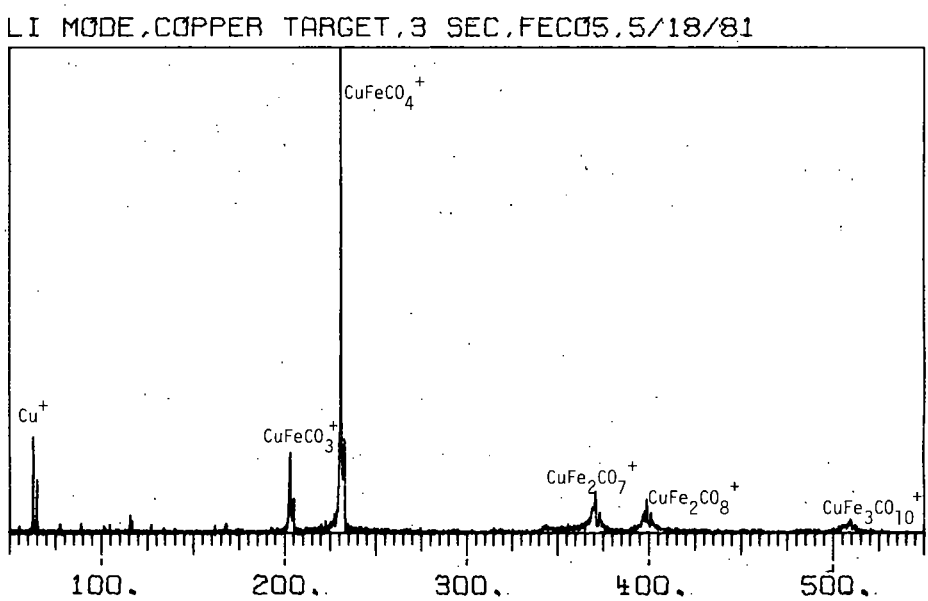
LI MODE,COPPER TARGET,3 SEC,FECO5,5/18/81
$CuFeCO_4^+$
Cu^+
$CuFeCO_3^+$
$CuFe_2CO_7^+$
$CuFe_2CO_8^+$
$CuFe_3CO_{10}^+$
100.
200.
300.
400.
500.

Figure 3

SECONDARY ION MASS SPECTRA OF SOME PROTECTED OLIGONUCLEOTIDES. W. ENS and K.G. Standing, Physics Department, University of Manitoba; J.B. WESTMORE, Chemistry Department, University of Manitoba, Winnipeg, Canada R3T 2N2, and K.K. OGILVIE, Chemistry Department, McGill University, Montreal, Canada H3A 2K6.

Fully protected oligonucleotides synthesized at McGill by the phosphite triester method (1) have been examined in the Manitoba time-of-flight mass spectrometer (2). We have studied in some detail protected ribo-dinucleotides with uracil and adenine bases; mass spectra of ten such compounds, with various permutations of bases and protecting groups, have been obtained. In addition we have made preliminary measurements on one trinucleotide and one tetranucleotide.

Samples were electrosprayed from a methanol solution onto aluminized polyester film. The target was bombarded by a pulsed beam of Cs^+ ions of energy 5 keV to 30 keV. Secondary ions emitted from the target were accelerated across 10 kV and detected by a chevron microchannel electron multiplier at the end of a 1.6 m flight tube.

Some of the compounds studied have also been examined by fission fragment bombardment (3-5), yielding mass spectra very similar to ours. This is consistent with results obtained by direct comparison of the two techniques for various biomolecules (6,7).

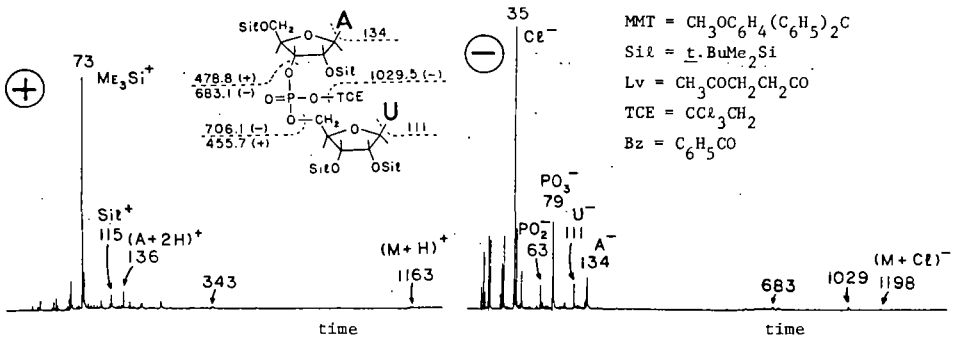

Fig. 1 - Positive and negative ion time-of-flight spectra of a protected ribonucleotide (mol. wt. = 1161.9).

The positive ion and negative ion mass spectra of one of the protected dinucleotides are shown in Fig. 1 and 2. These spectra contain several useful features:

1. Ions characteristic of the intact molecule, from which the molecular weight can be deduced (i.e. $[M + H]^+$, together with $[M + Na]^+$ in some spectra, M^- and/or $[M - H]^-$, and $[M + Cl]^-$.
2. Ions characteristic of protecting groups present (i.e. $[Sil]^+$ and $[M - TCE]^-$).
3. Ions characteristic of the bases present (i.e. $[A + 2H]^+$, U^-, A^-).
4. Ions characteristic of the base sequence, which result from fission of internucleotide bonds between C and O and which yield positive carbonium ions and/or negative phosphate ions.

Ions which decompose after acceleration yield fragments which continue on to the detector with velocities unchanged except for a small contribution arising from the kinetic energy release in the decomposition. Such decompositions can be detected by recording the arrival of neutral products at the detector, when all charged ions are removed by deflecting electrodes located approximately one-third of the distance along the flight tube. Such time-of-flight spectra of "metastable ions" (lifetimes ~ 0.1 - 10 μs) are also shown in Fig. 2.

The data collected in Table 1 illustrate the good agreement between observed ion masses and calculated masses (chemical atomic weights) for a few representative ions of four of the dinucleotides studied. The spectra of the trinucleotide and the tetranucleotide show similar properties; quasi-molecular ions are clearly visible at mass ~ 2100 u.

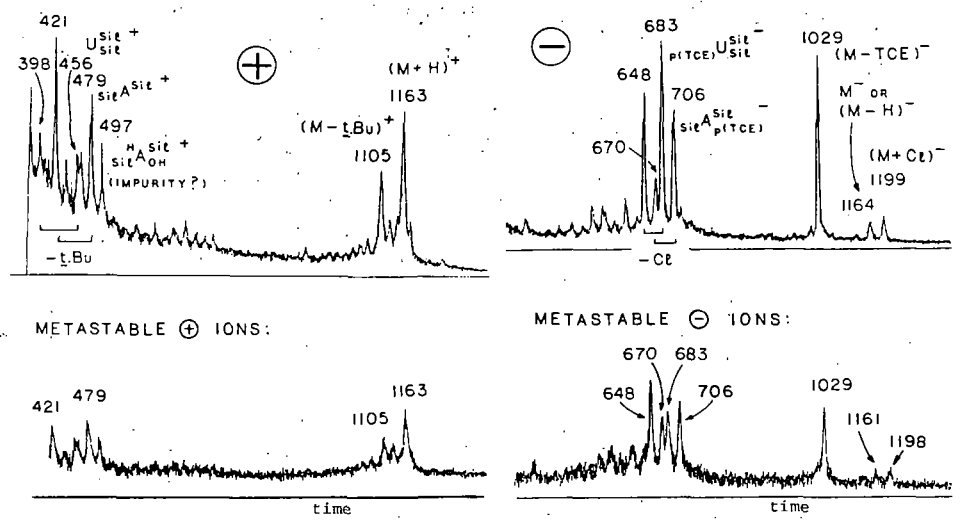

Fig. 2 - Top: Expansion of the high mass regions of the spectra shown in Fig. 1. Bottom: Time-of-flight spectra of neutral fragments from decomposition of ions in the first ~50 cm of flight path.

TABLE 1.

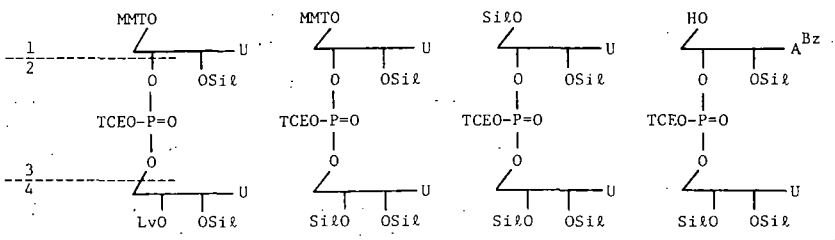

	obs (calc)	obs (calc)	obs (calc)	obs (calc)
$(M + Na)^+$	1304 (1303.7)	1320 (1319.9)	1162 (1161.8)	1175 (1174.7)
$(M + H)^+$	1281 (1281.7)	1297 (1297.7)	1140 (1139.8)	1152 (1152.7)
$(M - t.Bu)^+$	1224 (1223.6)	1240 (1239.8)	1082 (1081.7)	1094 (1094.6)
1 (+)	614 (613.8)	456 (455.7)	456 (455.7)	456 (455.7)
4 (+)	440 (439.6)	456 (455.7)	456 (455.7)	456 (455.7)
$(M + Cl)^-$	1317 (1316.2)	1333 (1332.4)	1174 (1174.3)	1188 (1187.2)
$(M - H)^-$	1280 (1279.7)	1297 (1295.9)	1138 (1137.8)	1151 (1150.7)
$(M - TCE)^-$	1149 (1148.3)	1164 (1164.5)	1006 (1006.4)	1020 (1019.3)
2 (-)	667 (666.9)	683 (683.1)	683 (683.1)	683 (683.1)
3 (-)	841 (841.2)	841 (841.2)	683 (683.1)	(696.0)

REFERENCES

1. R.L. Letsinger and W.B. Lunsford, J. Am. Chem. Soc. 98, 3655 (1976).
2. B.T. Chait and K.G. Standing, Int. J. Mass Spectrom, Ion Phys. 1981 (in press).
3. C.J. McNeal, S.A. Narang, R.D. Macfarlane, H.H. Hsiung and R. Brousseau, Proc. Natl. Acad. Sci. USA 77, 735 (1980).
4. C.J. McNeal, Ph.D. Dissertation, Texas A and M University, 1980.
5. C.J. McNeal and R.D. Macfarlane, personal communication.
6. W. Ens, K.G. Standing, B.T. Chait and F.H. Field, Anal. Chem. 1981 (in press).
7. K.G. Standing, W. Ens, B.T. Chait and F.H. Field, in "Ion Formation from Organic Solids", Springer 1981 (in press.)

IDENTIFICATION OF MODIFIED BASES AND NUCLEOSIDES FROM ALKYLATED NUCLEIC ACIDS BY CHROMATOGRAPHY/SECONDARY ION MASS SPECTROMETRY AND MASS SPECTROMETRY/MASS SPECTROMETRY

S.E. UNGER, D.V. DAVIS, AND R.G. COOKS, CHEMISTRY DEPARTMENT, PURDUE UNIVERSITY, WEST LAFAYETTE, IN 47907 AND C.-J. CHANG, J. GOMES, AND D. ASHWORTH, DEPARTMENT OF MEDICINAL CHEMISTRY AND PHARMACOGNOSY, PURDUE UNIVERSITY, WEST LAFAYETTE, IN 47907

Modified nucleosides of both DNA and RNA are identified with high sensitivity and without thermal decomposition by secondary ion mass spectrometry (SIMS) and laser desorption (LD) mass spectrometry. Desorption ionization methods such as SIMS or LDMS which sample directly from the solid phase obviate ambiguities inherient in direct probe pyrolysis experiments. In conjunction with prior chromatographic separation (1) or two stages of analysis, ms/ms (2), these ionization methods are particularly useful in characterizing modified nucleosides from mixtures.

SIMS AND LD/MIKE spectra of alkylated nucleosides generated by reaction of methyl methanesulfonate with various nucleosides are presented. The intact cation, as well as intense signals due to the modified base, are seen in the SIMS spectra of 7-methylguanosine (Figure 1), 1-methyl-2'-deoxyadenosine, 7-methyl-2'-deoxyguanosine, 3-methylcytidine (Figure 2), and 3-methyl-2'-deoxycytidine. Enhanced sensitivity for alkylated nucleosides is observed when the analyte exists as a preformed ion (salt).

Analyses of enzymatically degraded, methylated polycytidylic acid using an internal standard (see $126^+/129^+$ ratio in Figure 3) has determined the extent of modification with both precision and accuracy, as confirmed by nmr and HPLC measurements (3). Quantitation may also be performed with a compound similar to the analyte, such as the use of 50 ng of [$^2H_3$-methyl]-7-methyl-2'-deoxyguanosine to quantitate 400 ng of 7-methylguanosine. Detection limits approach 1 ng, while quantitation is accurate with as little as 10-50 ng of the alkylated nucleoside.

LD/MIKE spectra of the methylated base fragment ion from 7-methylguanosine (166^+), 1-methyladenosine (150^+), and 3-methylcytidine (126^+) provide structural information which distinguishes isomeric forms. The LD/MIKE spectrum of the 150^+ ion generated from 1-methyladenosine by laser desorption (Figure 4) matches that obtained by pyrolysis (4), while the dissociation spectrum of the 166^+ ion from 7-methylguanosine obtained by laser desorption (Figure 5) shows characteristic fragment ions expected from the 7-methyl-guanine cation (5).

1. Benninghoven, A., Eicke, A., Junack, M., Sichtermann, W., Crizek, J., Peters, H., Org. Mass Spectrom. 1980, 15, 459.
2. Zakett, D., Schoen, A.E., Cooks, R.G., Hemberger, P.H., J. Am. Chem. Soc. 1981, 103, 1295.
3. Ashworth, D.J., Chang, C.-J., Unger, S.E., Cooks, R.G., J. Org. Chem., submitted.
4. Schoen, A.E., Cooks, R.G., Wiebers, J.C., Science 1979, 203, 1249.
5. Unger, S.E., Schoen, A.E., Cooks, R.G., Ashworth, D.J., Gomes, J.D., Chang, C.-J., J. Org. Chem., submitted.

Figure 1

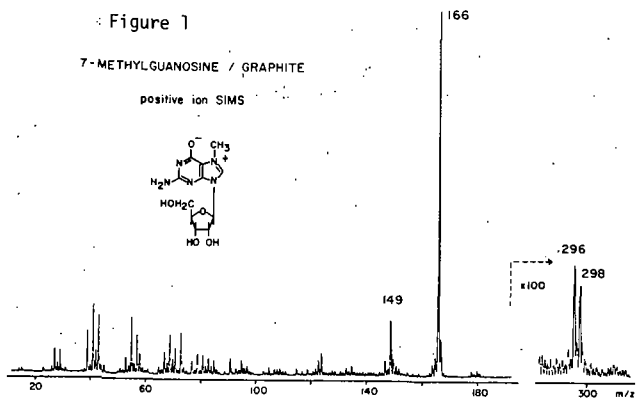

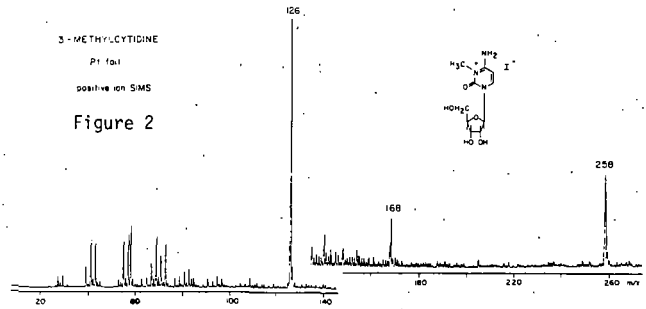

Figure 2

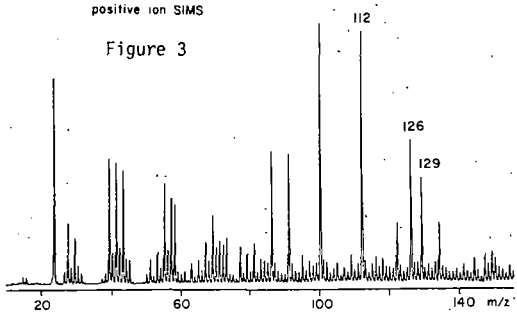

Figure 3

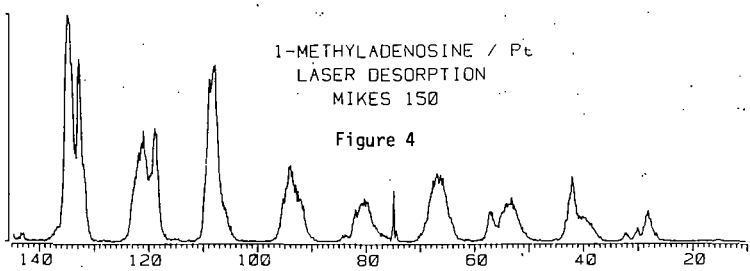

Figure 4

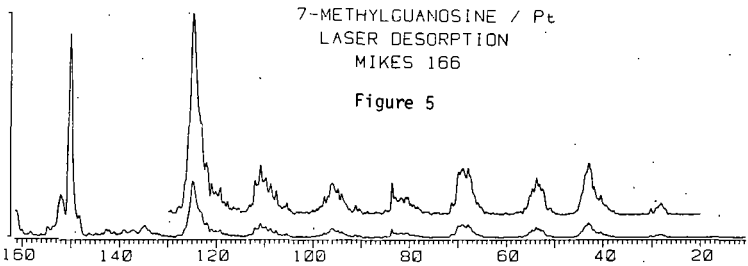

Figure 5

APPLICATION OF THE ION-DRIFT SPECTROMETER TO MACROMASS SPECTROMETRY. III. FINAL REPORT AND CONCLUSIONS

K. Nakamae, Vijay Kumar and Malcolm Dole
Department of Chemistry, Baylor University
Waco, Texas 76798

Some years ago (1) we invented an electrospray process for producing intact gas phase ions of macromolecules. We were unable to measure accurately their mass to charge, M/z, ratio in a time of light mass spectrometer because of the failure of the magnetic electron multiplier to respond to the heavy macroions. We then transferred our efforts to the Plasma Chromatograph (PC), or ion-drift spectrometer (3). Our results with this instrument (2,4,5) were similarly disappointing in that the peaks of the ion current versus drift time curves of polystyrene (PS) ions of 51,000 amu overlapped with those of 200,000 amu. We attributed this to cluster formation. Plasmagrams of the pure solvent used in this work, a 9/1/0.4 (ACB) mixture of acetone, cyclohexane and benzene, also showed the presence of clusters of about 90 msec drift time, Fig. 1, but not in the case of a 20/1 mixture of ethanol and water. Fig. 2 illustrates a plasmagram of 97,200 amu PS on electrospraying a 0.002 wt % solution in ACB. No peaks at longer drift times than about 120 msec were observed.

To reduce the difficulties due to aggregation and/or adsorption of solvent ions by the macroions we modified our drift cell so that it could be heated to 175° or operated down to 360 Torr pressure. The effect of temperature on the drift times of 51,000 and 200,000 amu PS is shown in Fig. 3. Note that at higher temperatures the drift time of the solvent ions at about 15-20 msec decreases, but that the drift times of the macroions increase markedly with temperature. We attribute the latter to a decrease of the amount of adsorbed solvent ions, that is, a decrease of z, with rise of temperature. The curves of Fig. 3 also demonstrate the inability to distinquish clearly between the peaks due to the 51,000 and 200,000 amu PS. Finally in Fig. 4 we illustrate the effect of reduction in drift tube pressure on the shift of the 51,000 amu peak with pressure. Unfortunately, no data were taken on 200,000 amu PS because of difficulties with the equipment.

We conclude that accurate molecular weights of macromolecules cannot be measured with the PC.

Acknowledgement. This research was supported at first by the National Science Foundation and more recently by income from the Chair in Chemistry established at Baylor University by a gift of The Robert A. Welch Foundation.

References

1. Dole, M.: Mack, L.L.; Hines, R. L.; Mobley, R.C.; Ferguson, L.D.; Alice, M.B. J. Chem. Phys. 1968, 49, 2240
2. Dole, M.; Gupta, C.V.; Mack, L.L.; Nakamae, K.; Polymer Preprints, 1977, 18, 188
3. Plasma Chromatograph is a registered trademark of PCP, Inc.
4. Gieniec, J.; Cox, H.L.; Teer, D.; Dole, M.; Proc. 20th Conference on Mass Spectrometry and Allied Topics, Dallas, 1972, 276
5. Dole, M.; Gieniec, J.; Proc. 23rd Conference on Mass Spectrometry, Houston, 1975, 84.

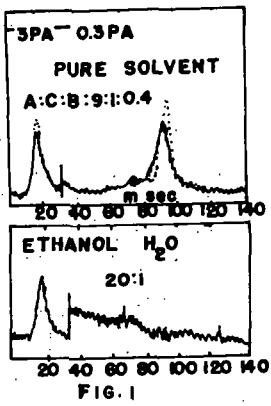

FIG. 1

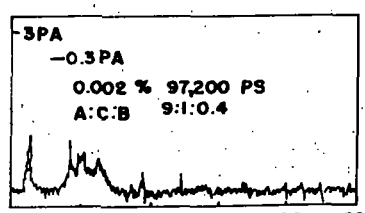

FIG. 2

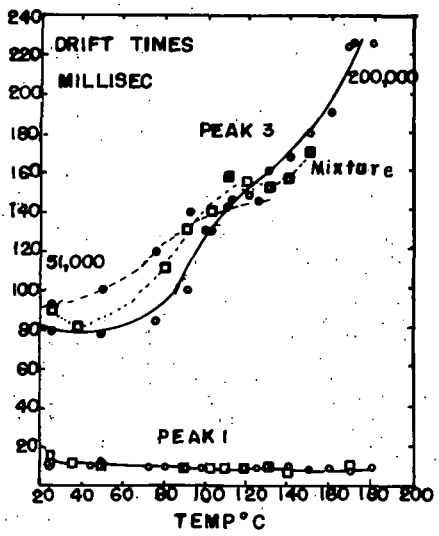

FIG. 3

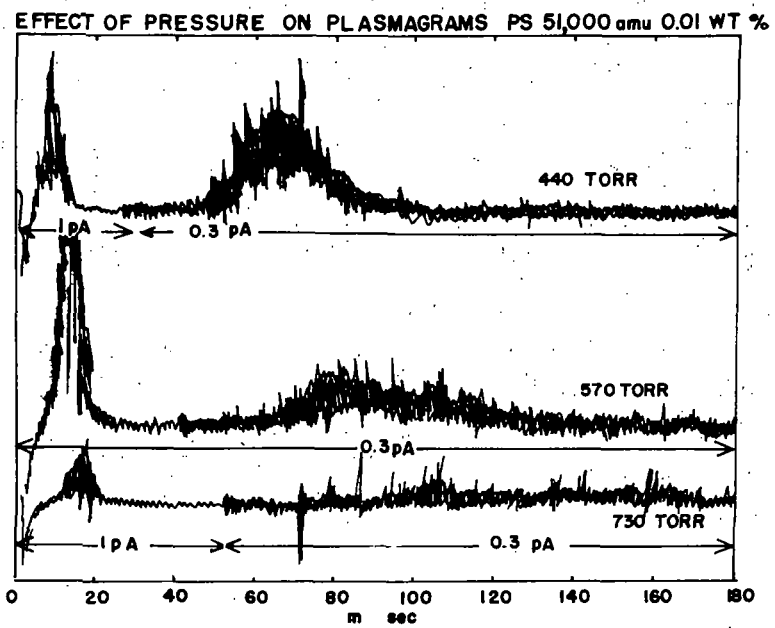

FIG. 4

INTENSE MOLECULAR IONS FROM LABILE AND POLAR COMPOUNDS BY ION EVAPORATION; J.V. Iribarne and P.J. Dziedzic, Dept. of Physics, University of Toronto, Toronto, Ontario; and B.A. Thomson; SCIEX INC., 55 Glencameron Rd., Thornhill, Ontario, Canada. L3T 1P2

Introduction and Experimental

A variety of approaches to the analysis of labile and polar compounds by mass spectrometry have been reported in the literature in the past few years. The presence of a molecular ion in the spectrum is necessary to provide molecular weight information, while some fragments are required in order to provide structural information and aid in compound identification. Most ionization techniques provide too much of one and not enough of the other for satisfactory performance as an analytical technique. The recent advent of tandem mass spectrometry (MS/MS), however, seems to provide the potential for the desirable combination of a "soft" ionization technique which produces only molecular or quasi-molecular ions, with electronically controllable fragmentation of the molecular ion independent of the ionization process. In addition, MS/MS combined with a "soft" ionization process provides in many cases the ability to analyze mixtures directly without chromatographic preseparation of the components.

This paper reports on recent results obtained with the technique of ion evaporation (1,2). An ion evaporation source has been coupled with a TAGA™ 6000 triple quadrupole system, and several types of labile and polar species examined. In ion evaporation, charged aqueous droplets containing the dissolved material to be analyzed (generally in a dissociated or ionized form in the liquid) is sprayed into the air at atmospheric pressure. As the droplets evaporate, single ions clustered with a few solvent molecules are emitted into the air from the surface of each drop. The ions are drawn by an electric field from the region of evaporating spray, and are sampled into the mass spectrometer system through the vacuum orifice of the TAGA™. The system operates by continuous liquid feed from a pump into the sprayer. Sample changeover is easily accomplished by changing the reservoir from which the liquid is withdrawn. The system appears to have the potential of being linked to a liquid chromatograph to provide continuous LC/MS analysis of ions, simply by feeding the column effluent directly into the sprayer.

As the ions pass into the vacuum chamber, the clustered solvent molecules are collisionally stripped from the ion of interest. This declustering can be controlled to provide some fragmentation of the ion if desired. The mass spectra which are observed, however, suggest that the ion evaporation process produces exclusively molecular ions which are the same ions present in the liquid solution. Compounds which have basic functions are generally observed in the positive ion mode as the protonated molecule. Compounds which have acidic hydrogens are observed as the deprotonated ion which is present in the liquid. Optimum conditions are generally achieved by adjusting the pH of the liquid to provide the maximum degree of ionization in the solution. Compounds which have both acidic and basic functions (amino acids, for example) can be detected as either positive or negative ions by changing the pH. In addition, certain compounds (sugars, for example) can be detected as neutrals clustered to sodium, by adding NaI into the liquid before it is sprayed. Inorganic monovalent ions are also readily detected if present in the solution.

Results

The analytic potential of the technique is still being explored. A wide variety of compounds have so far been detected: alkaloids, amino acids, sugars, inorganic ions, nucleosides, nucleotides, catecholamines, sulfonic acids, organic acids and quaternary ammonium salts. Although the sensitivity observed has varied from compound to compound, a detectability in the low parts-per-billion (w/w) has been achieved for some. The following spectra show examples of the mass spectra of ions from the ion evaporation source, as well as CID (collision induced dissociation) spectra of selected parent ions. In most cases, only the molecular ion is observed in the mass spectrum (other peaks present are usually due to impurities in the water or in the formulation analyzed); some spectra, however, show small fragments generated in the declustering region.

Conclusion

Ion evaporation appears to provide a simple and sensitive means of analyzing a variety of labile and polar species with a mass spectrometer. In combination with an MS/MS system, it provides an attractive combination of molecular weight and structural information.

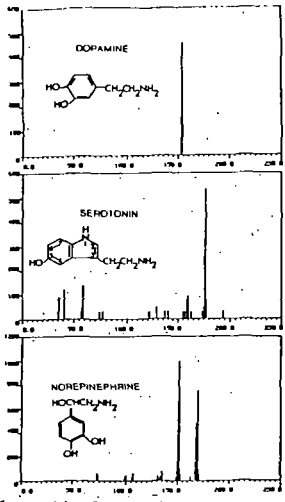

Figure 1. Single quadrupole positive ion mass spectrum of solutions of dopamine, serotonin and norepinephrine. In each case the protonated molecular ion is the dominant or in the latter case, a major) ion in the spectrum.

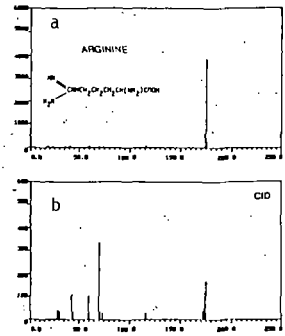

Figure 3. a) Positive ion mass spectrum of arginine hydrochloride solution; b) daughter on spectrum of the protonated parent ion at m/z=175.

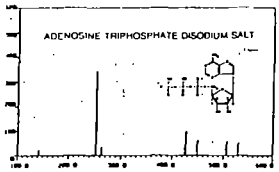

Figure 2. Negative ion mass spectrum of ions from a solution of adenosine triphosphate disodium salt. The peak at apparent mass 252.5 is the doubly charged ion of mass 505 while the peak at m/z=528 is the singly dissociated species, and the peak at m/z=506 is the singly charged species with one proton substituted in place of a sodium. Other peaks are related contaminants.

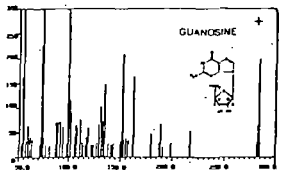

Figure 4. Single quadrupole positive ion spectrum ofguanosine solution at pH=3. The ion at m/z=284 is the protonated guanosine molecule. The other mass peaks are contaminants in the solution.

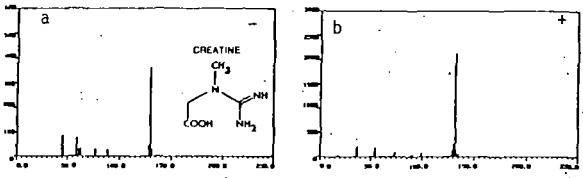

Figure 5. a) Negative ion mass spectrum of creatine, showing the parent anion $(M-H)^-$ at m/z=130; b) Positive ion mass spectrum of creatine, showing the parent cation MH^+ at m/z=132.

ELECTRON IONIZATION-FLASH DESORPTION MASS SPECTROMETRY USING ELECTRO-OPTICAL ION DETECTION

T.D. Lee, W.R. Anderson, Jr., and G.D. Daves, Jr.
Department of Chemistry and Biochemical Sciences
Oregon Graduate Center, Beaverton, Oregon 97006

H.G. Boettger and C.E. Giffin
Jet Propulsion Laboratories
Pasadena, California 91103

The utilization of electro-optical ion detection[1] in electron ionization-flash desorption mass spectrometry[2,3] is advantageous in at least two respects. The greater sensitivity of this ion detection system as compared with photoplate detection ($\sim 10^3$) permits a corresponding reduction in the amounts of material required to record a spectrum. Also, the increased sensitivity of ion detection has permitted the recording of EI-flash desorption mass spectra of many molecules for which earlier attempts using photoplate detection were unsuccessful. For example, using photoplate detection we succeeded in recording EI-flash desorption mass spectra of disaccharides[4] and of one trisaccharide. Using the more sensitive electro-optical ion detector, spectra of the tetrasaccharide stachyose and of α-cyclodextran (Figure 1) were recorded readily. Similarly, EI-flash desorption of a series of nickel(II)-amino acid complexes yielded spectra containing cluster ions at m/z values in excess of 1000 (e.g. Ni^{2+}-valine, Fig. 2) in contrast to earlier experiences using photoplate detection which exhibited only low mass ions.

A second advantage of the electro-optical detection system is its computer compatibility which permits more convenient operation and increased numbers of analyses.

References

1. H.G. Boettger, C.E. Giffin, D.D. Norris, W.J. Dreyer and K. Kuppermann, Adv. Mass Spectron. Biochem. Med., 2513 (1977).

2. T.D. Lee, W.R. Anderson, Jr., and G.D. Daves, Jr., Anal. Chem, 53, 304 (1981).

3. G.D. Daves, Jr., T.D. Lee, W.R. Anderson, Jr., D.F. Barofsky, G.A. Massey, J.C. Johnson and P.A. Pincus, Adv. Mass Spectrom., 8, 1012 (1980).

4. W.R. Anderson, Jr., W. Frick and G.D. Daves, Jr., J. Am. Chem. Soc., 100, 1974 (1978).

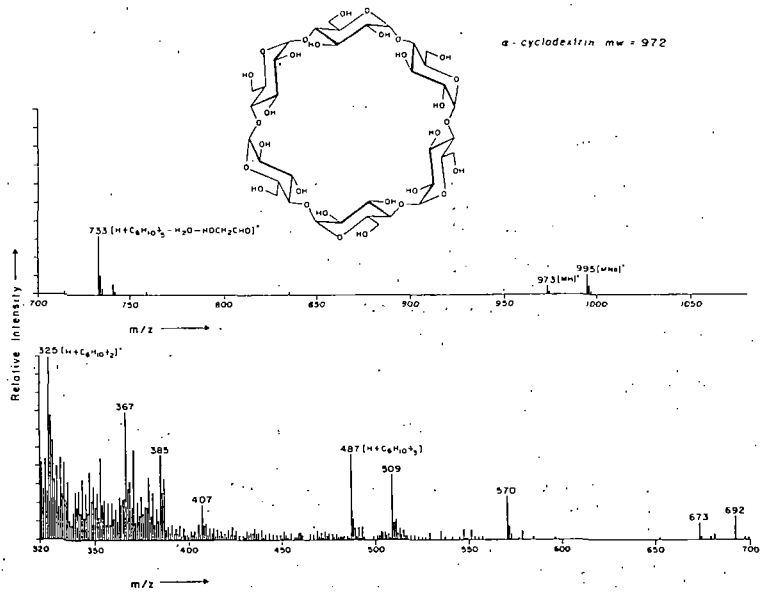

Fig. 1. EI-Flash desorption mass spectrum of α-cyclodextran.

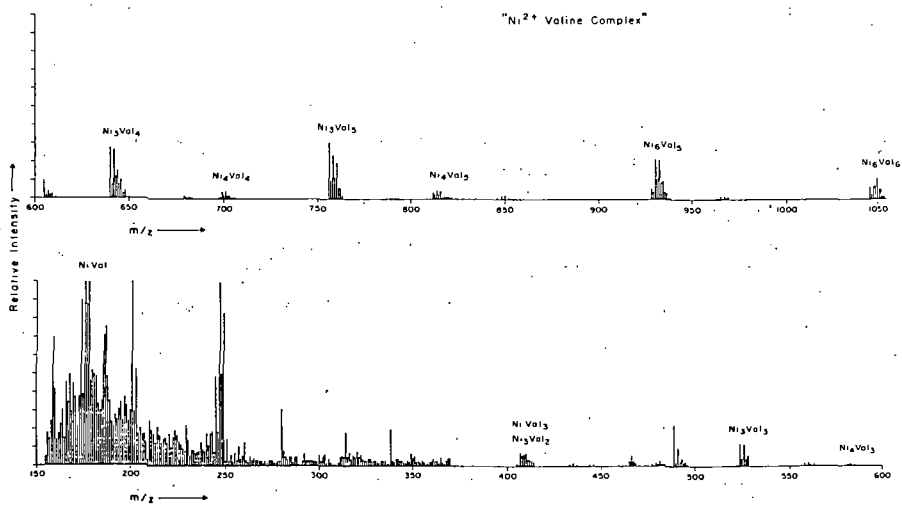

Fig. 2. EI-Flash desorption mass spectrum of a "Ni^{2+}-valine complex."

IONIZATION PROCESSES IN LASER DESORPTION

R. J. Day and D. M. Hercules
Department of Chemistry
University of Pittsburgh
Pittsburgh, PA 15260

The application of laser desorption to mass spectrometry is rapidly expanding. Although the technique can be used with virtually any mass analyzer, an instrument with a time of flight spectrometer is commercially available. It focuses the output of a Q-switched, frequency quadrupled Nd-YAG laser onto the sample, the TOF timing circuitry being triggered by the laser pulse. Thus, a mass spectrum is obtained for each firing of the laser.

Because LD mass spectra appear to be invariant for different wavelengths and laser pulse widths, the process is thought to be thermal. The emission of cationized molecules is consistent with this hypothesis.[1,2] The fact that other mechanisms are operative is supported by the observation of $(M-HCl)^{-\cdot}$ ions for safranin O, a quaternary ammonium salt (Figure 1). The results are best explained by dissociative electron attachment to desorbed salt molecules with HCl loss. Radical anion emission dominates the negative ion LD mass spectrum of bianthrone, as well (Figure 2). The base peak corresponds to $(M-H_2)^{-\cdot}$.

LD mass spectra have been obtained for a series of conjugated and unconjugated bile acids. Both positive and negative ion mass spectra are characterized by the presence of quasi-molecular ions and the absence of fragment species. The observation of $C_nH_m^{+/-}$ ions at low mass suggests that some pyrolysis of the sample also occurs as a result of pulsed laser irradiation.

In several cases, $(M+H)^+$ has been observed in LD mass spectra of acids. This is unusual in that LD normally generates cationized species. For example, a protonated molecule was detected for glycocholic acid (Figure 3), whereas Cotter[1] reported only $(M+Na)^+$ for LD of this compound. It is interesting that $(M+H)^+$ was only apparent in spectra obtained from crystals of the solid. When a thin film of glycocholic acid was evaporated from solution onto the sample support, only cationized species were detected. These results suggest that under some conditions of sample morphology, a region of local high pressure is generated in the laser focus and that proton transfer processes take place in this zone.

Detection of molecular clusters gives added support to this hypothesis. For example, nicotinamide gave abundant cationic and anionic dimers and trimers upon laser irradiation (Figure 4).

1. Cotter, R. J. Anal. Chem. 1981, 53, 719-720.
2. Stoll, R.; Röllgen, F. W. Org. Mass Spectrom. 1981, 16, 72-75.

FIGURE 1

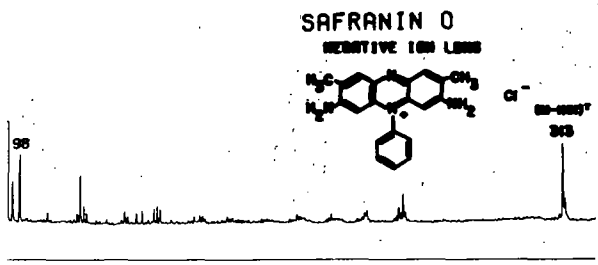

FIGURE 2

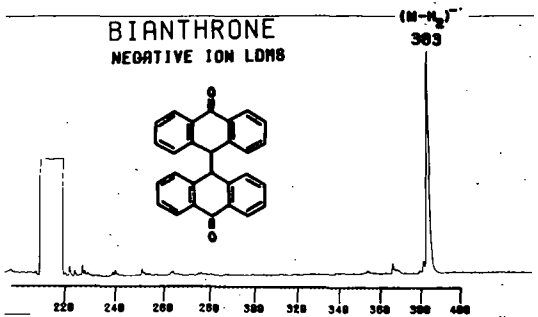

FIGURE 3

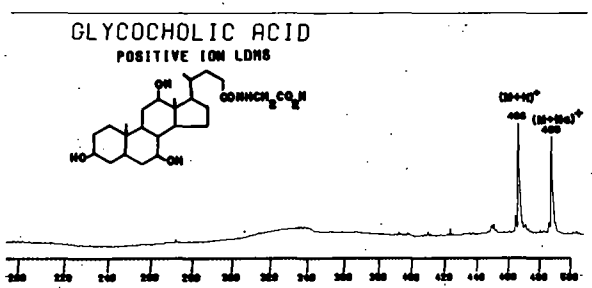

FIGURE 4

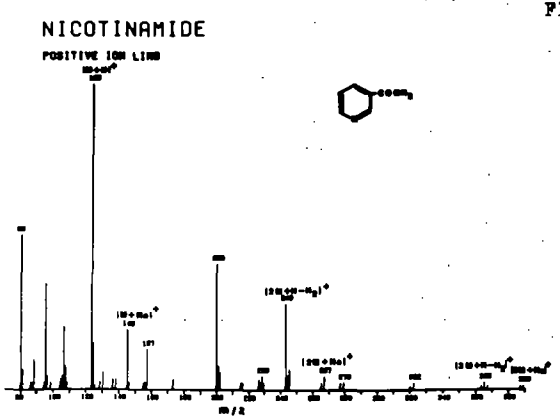

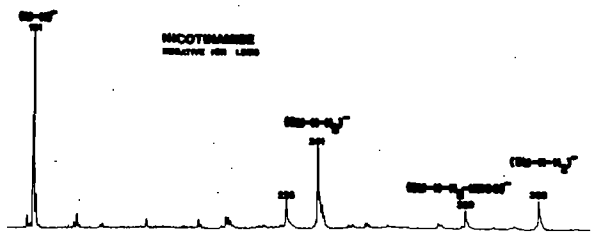

The Determination of Molecular Weight Distributions of Polyglycol Oligomers by Field Desorption Mass Spectrometry

Robert P. Lattimer
The BFGoodrich Research & Development Center
9921 Brecksville Rd, Brecksville, Ohio 44141

and

Gordon E. Hansen
Middle Atlantic Mass Spectrometry Laboratory
The Johns Hopkins University School of Medicine
725 North Wolfe Street, Baltimore, Maryland 21205

Field desorption mass spectrometry (FDMS) has been shown to be a method of choice for determining molecular weights of nonvolatile and higher molecular weight chemicals. Numerous reports from several laboratories have shown that FDMS can be used to obtain good qualitative distributions of oligomers for low molecular weight polymers. We have reported the use of FDMS to determine accurate molecular weight averages ($\bar{M}_n$ and $\bar{M}_w$) for a series of low molecular weight polystyrene standards.[1] It was found that FDMS derived molecular weight parameters compared favorably to values obtained by conventional techniques (vapor pressure osmometry, intrinsic viscosity, kinetic data and gel permeation chromatography).

Polystyrene is a relatively stable polymer in mass spectral analysis and has been used in a number of higher mass studies. More polar, less volatile polymers are generally more troublesome to analyze by mass spectrometry. One general class of polar polymers of commercial importance is the hydroxy-terminated polyglycols. In order to assess the applicability of FDMS to direct analysis and molecular weight characterization of this general class of polymers, we have studied several commercially available glycol polymers. These include poly(propylene glycol) (PPG, manufactured by Waters Associates), poly(ethylene glycol) (PEG, J. T. Baker), and poly(tetrahydrofuran) (PTHF, Polymer Laboratories).

FD mass spectra of PPG have recently been studied in detail.[2] Several low molecular weight PPG batches yielded major peaks corresponding to MH^+ ions (or MNa^+ ions if sodium iodide were added to the sample). Strong ions corresponding to fragmentation of the polymer chains were also observed; the mechanisms of fragment ion formation were considered.[2] FD mass spectra of several PPG and PEG samples (including copolymers) have been reported in another recent article.[3] Both MH^+ and MNa^+ ions were observed along with numerous fragment ions. PEG has recently been analyzed by electrohydrodynamic ionization mass spectrometry (EHMS).[4] The PEG polymers were dissolved in glycerol with NaI added to the solution. Sodium attachment ions (MNa^+) were observed by EHMS, and these ions were used to determine $\bar{M}_n$ and $\bar{M}_w$. $\bar{M}_n$ values agreed well with values obtained by end group titration.[4]

In this report we describe the FDMS analysis of three types of polyglycol oligomers - PPG, PEG, and PTHF:

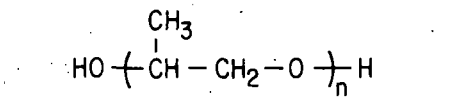

PPG
mol. wt. = 58n + 18

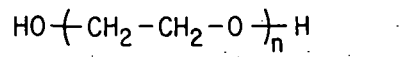

PEG
mol. wt. = 44n + 18

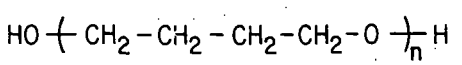

PTHF
mol. wt. = 72n + 18

Using either protonated (MH^+) or cation attachment (MNa^+) ions, we have determined average molecular weight parameters ($\bar{M}_n$ and $\bar{M}_w$) for several low molecular weight batches of these polymers (Table I). The methods of calculation are essentially identical to those described previously for polystyrene. Despite the fact that these polymers are thermally and structurally fragile, good agreement was found between the FDMS derived parameters and those determined by classical methods. It thus appears that FDMS has considerable potential for making average molecular weight determinations for a large number of oligomeric systems.

1. R.P. Lattimer, D.J. Harmon, and G.E. Hansen, Anal. Chem., 52, 1808 (1980).
2. G.M. Neumann, P.G. Cullis, and P.J. Derrick, Z. Naturforsch., 35A, 1090 (1980).
3. J. Saito, S. Toda, and S. Tanaka, Shitsuryo Bunseki, 28, 175 (1980).
4. S.-T. F. Lai, K. W. Chan, and K. D. Cook, Macromolecules, 13, 953 (1980).

Table I

FDMS Molecular Weight Averages for Polyglycols.

Polymer	Data Source	$\bar{M}_n$	$\bar{M}_w$	$\bar{M}_w/\bar{M}_n$
PEG 400	Titration[a]	406	-	-
(Baker)	EHMS[a]	406	428	1.05
	FDMS[b]	444	464	1.05
PEG 600	Titration[a]	605	-	-
(Baker)	EHMS[a]	572	607	1.06
	FDMS[b]	601	632	1.05
PEG 1000	Titration[a]	1041	-	-
(Baker)	EHMS[a]	962	1007	1.05
	FDMS[b]	1010	1040	1.03
PEG 1540	Titration[a]	1396	-	-
(Baker)	EHMS[a]	1365	1397	1.02
	FDMS[b]	1360	1400	1.03
PPG 41993	Waters[c]	790	-	≈1.05
(Waters)	FDMS[b]	805	835	1.04
	FDMS[d]	819	855	1.04
PPG 41994	Waters[c]	1220	-	≈1.03
(Waters)	FDMS[b]	1240	1280	1.03
	FDMS[d]	1190	1220	1.03
PPG 41985	Waters[c]	2020	-	≈1.02
(Waters)	FDMS[e]	1930	1980	1.03
PTHF 1000	PL[f]	1050	1208	1.15
(PL)	FDMS[b]	1110	1220	1.10

[a] End-group titration and electrohydrodynamic ionization mass spectrometry data from Reference 4.

[b] Data from MNa^+ ion intensities (FD/NaCl/MeOH); Varian MAT 311A (The BFGoodrich Co.).

[c] Data from Waters Associates data sheet.

[d] Data from MH^+ ion intensities (FD/THF); Varian MAT 311A (The BFGoodrich Co.).

[e] Data from MNa^+ ion intensities (FD/NaCl/MeOH); Kratos MS-50 (The Johns Hopkins University).

[f] Data from Polymer Laboratories data sheet.

ENHANCEMENT OF FIELD DESORPTION MASS SPECTRA OF ALKALI METAL SALTS BY POLYHYDROXYL ADDITIVES;

GORDON W. WOOD and WING FUNG SUN; Dept. of Chem., Univ. of Windsor, Windsor, Ontario, Canada N9B 3P4.

FDMS of alkali metal salts are characterized by fluctuating ion current, high anode temperature, abundant metal ions, and low abundance of structurally significant organic ions. For example, sodium acetate has been found to yield Na^+ as base peak, along with lesser amounts of clusters $Na^+ \cdot x(NaOAc)$. As part of a continuing study of matrix effects on the FD process, we have now found that pentaerythritol (1) and *cis*-inositol (2) cause a marked improvement in a variety of such spectra. Results will be presented for sodium acetate; sodium propionate; anthraquinone-2-sulfonic acid, sodium salt; anthraquinone-2,6-sulfonic acid, disodium salt; and fluorescein, sodium salt; among others.

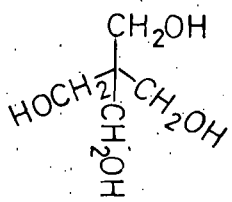

(1)

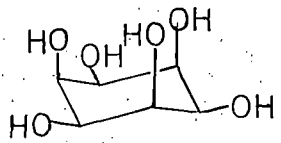

(2)

FIELD DESORPTION MASS SPECTROMETRY AND FAST ATOM BOMBARDMENT MASS SPECTROMETRY IN STRUCTURAL STUDIES OF HIGH MASS OLIGOSACCHARIDES (~4000 DALTONS)

A.L. Burlingame,[1] C.E. Ballou,[2] and A. Dell[3]
[1]Biomedical Mass Spectrometry Resource, University of California, Berkeley and San Francisco, CA 94720; [2]Dept. of Biochemistry, University of California, Berkeley; [3] Dept. of Biochemistry, Imperial College, London, England SW7 2AZ

Field desorption techniques have been developed in our laboratories in order to obtain mass spectral information directly on underivatized, labile (chemically and/or thermally) biological substances. We have recently demonstrated the feasibility and considerable merits of these techniques for molecular weight determination and structural characterization of a series of mycobacterial methylmannose polysaccharides in the mass range up to 2500 daltons (1,2). In this paper, we explore the potential of FDMS for the examination of larger polysaccharides and we describe FD data which have resulted in the structure correction of a glycolipid of molecular weight ~ 3500 daltons. Further, we present preliminary results using fast atom bombardment mass spectrometry (FAB MS) (3) which indicate that this new ionization technique shows promise for the examination of intermediate sized high mannose oligosaccharides of the type found in immunoglobulins.

The FDMS of an unfractionated sample of methylmannose polysaccharides, a mixture of several homologues, is shown in Fig. 1. Fig 1b shows major signals at m/z 1978, 2154 and 2330 corresponding to the M + Na quasimolecular ions of oligosaccharides containing 11, 12 and 13 sugar units, respectively. At higher wire currents (Fig. 1a), the next homologue is observed at m/z 2506 (14 sugar units); note the tenfold increase in gain in Fig. 1a.

Using a high-field magnet we have obtained molecular weight data on a lipopolysaccharide (code MGP) from mycobacteria (4) which has led to the structure revision of this molecule from an 18 sugar unit polymer of molecular weight 3176 to a 20 sugar unit polymer of molecular weight 3514. FDMS at 5.5 kV on the permethyl derivative of MGP yielded β of the type shown in Fig. 2. Signals are obtained between m/z 4200-4250. The complexity of the spectrum is due to multiple undermethylation and cationization.

We have obtained excellent FD data on high mannose oligosaccharides of the type $Man_xGlcNAcH_2$ where x = 8, 10 and 11, and FAB spectra on $Man_8GlcNAcH_2$. Intense quasimolecular ions (M + Na) are observed in the FD spectra of all these molecules. Fragmentation occurs sequentially from the nonreducing end of the molecules and is therefore structurally uninformative. It is recommended that EIMS of permethyl derivatives be used to define the branch points of this type of molecule. The molecular ion regions of $Man_8GlcNAcH_2$ are shown in Figs. 3 and 4. The FD M + H ion is present at 1521 daltons and the M + Na at 1543 -- the latter also showing loss of water at 1525 daltons. Note the signal at 1585 daltons, possibly indicating an additional component containing a GlcNAc moiety instead of a Man moiety (+ 42 amu). Both M + H and M + Na species are observed in the FAB spectrum. The mass assignment was obtained by counting the spectrum and this leads to the one mass unit difference in nominal mass compared with FD (FD calibrated with respect to a fluorinated reference compound).

Acknowledgments. This work was supported by NIH Division of Research Resources Grant RR00719 and by the British Science and Medical Research Councils.

References

1. J. D'Angona, M. Linscheid, A.L. Burlingame, H. Hamada, C.E. Ballou and A. Dell, 28th Annual Conference on Mass Spectrometry & Allied Topics, New York, NY, 1980, pp. 495-496.

2. M. Linscheid, J. D'Angona, A.L. Burlingame, A. Dell and C.E. Ballou, Proc. Natl. Acad. Sci. USA 78, 1471-1475 (1981).

3. M. Barber, R.S. Bordoli, R.D. Sedgwick and A.N. Tylor, J. Chem. Soc. Chem. Comm. 325-327 (1981).

4. C.E. Ballou, Accts. of Chem. Research 1, 366-373 (1968).

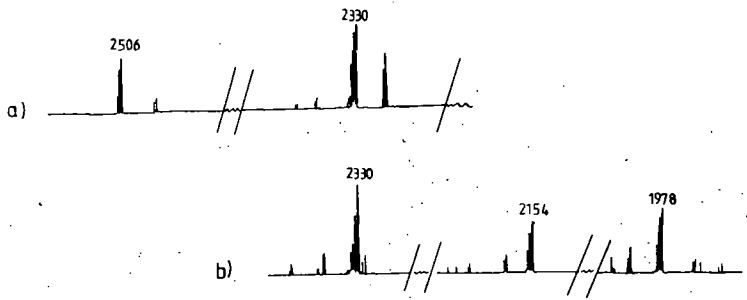

Fig.1

FD SPECTRA OF MMP_C ; (a) is at 10 times the gain of (b) and was obtained at a higher emitter current

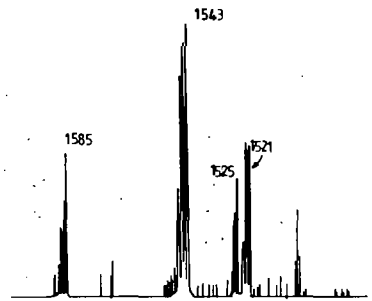

Fig.3 FD SPECTRUM OF $Man_8GlcNAcH_2$ (Molecular ion region)

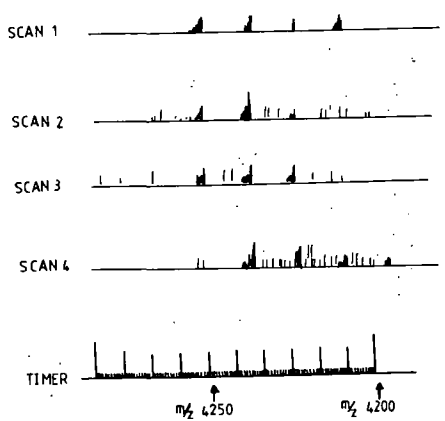

Fig.2 MGP (PERMETHYL DERIVATIVE) FD (5.5 kV; HIGH-FIELD MS 50)

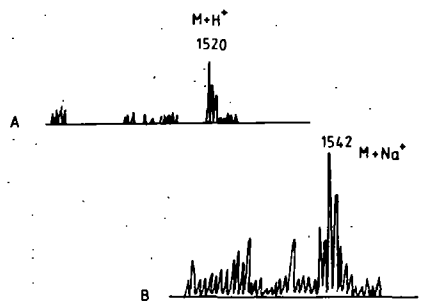

Fig.4

FAB (M-SCAN/ZAB) of Man_8GNAcH_2 (B taken after reloading)

HIGH RESOLUTION-HIGH MASS BY FT-MS; SAHBA GHADERI, VERN BURGER, ROBERT SPENCER, JOHN MARRA, RICHARD HEIN, TERRY PETERSON; Nicolet Instrument Corporation, Madison, WI 53711

In the Fourier transform mass spectrometer, (FT-MS), mass resolution is determined by the length of signal detection (observation time), unlike in a conventional mass spectrometer in which mass resolution is dependant upon the width of the ion exit slits. Because in the FT-MS instrument ion formation and detection takes place in a trapping source, it is possible to detect all the ions present in the mass spectrometer source for a longer period of time. Furthermore, FT-MS is an ion frequency measurement device and ion cyclotron resonance frequency is dependant upon the magnetic field strength, so it is also possible to increase mass resolution using a higher magnetic field. These factors result in ultra high resolution spectra achieved by the FT-MS instrument (higher than a good double focussing mass spectrometer).

In order to obtain high resolution in conventional sector magnet spectrometers, it is necessary to reduce the slit width which results in lower sensitivity, and that puts a limit on high resolution experiments especially for high mass molecules which fragment easily under EI conditions. In FT-MS, however, all ions are detected and high resolution is obtained by increasing detection time which also results in higher sensitivity.

These features of the FT-MS instrument plus others such as rapid data acquisition, signal averaging, use of a high field super conductive magnet, and also the chemical ionizing technique make it an attractive tool for high resolution analysis of high molecular weight compounds.

The ease of chemical ionization by FT-MS, especially the possibility of self-CI (reagentless CI), is also important for identification of the molecules of high mass and for obtaining molecular weight information. In this presentation we demonstrate the capabilities of the first commercial FT-MS instrument for high resolution analysis of high mass molecules.

THE INTERACTION OF HEAVY WATER CLUSTER IONS WITH NEUTRAL GASES

H. Udseth, H. Zmora,* R. J. Beuhler and L. Friedman
Chemistry Department, Brookhaven National Laboratory, Upton, New York 11973

A 2-m length time-of-flight mass spectrometer capable of analyzing dc ion signals was built and incorporated in interaction studies of water clusters with neutral gases.

Water clusters ranging in size from m/e ∿ 100 to 15,000 were produced by expansion into vacuum of a water-saturated He or Ar beam through a 150 μm nozzle. The carrier gas was skimmed off from the beam by a skimmer, placed about 5 mm from the nozzle.[1]

A three-grid system and a high-power, fast rise-time pulser were used to chop the ion beam for a time-of-flight analysis. The grid nearest to the drift tube (the "stopper") is biased at a positive potential, sufficient to prevent any ions from passing through it when the high voltage is off. A pair of grids in front of it are driven by a high power pulser. The grid next to the stopper is pulsed positively to a voltage sufficient to drive the ions which have accumulated in the space between it and the stopper into the drift tube. At the same time, this pulse prevents any ions on the source side of the pulsed grid from entering the drift tube. The third grid served as a return path for the pulsed current. The mass resolution obtained with a surface ionization source was 150. Due to the initial higher ion energy and energy spread, the best mass resolution achieved with the water cluster source was about 50.

The purpose of the experiment was to examine the cluster ion beam attenuation upon passage through a neutral scattering gas. For these experiments a collision cell and two pairs of xy deflection plates were added to the apparatus, between the ion source and the grid assembly. Two types of experiments were carried out: (1) the mass spectrum of the fraction of the beam passing through the chamber was recorded as a function of pressure, and (2) the total intensity of the transmitted beam (mass integrated) was recorded as a function of pressure. He, Ar, C_3F_8 and C_6F_6 were used as target gases in the scattering chamber. The laboratory energy of the water clusters was varied from 10 to 2000 eV.

The average cluster size of the beam emerging from the scattering chamber was found to vary linearly with the gas pressure in the cell. An average mass degradation figure of about 45 $\pm$ 15 amu/mtorr was found, independent of cluster size and energy, or the type of gas used. The results of the mass integrated attenuation measurements are summarized in Fig. 1. Plotted are the reduced attenuation cross sections (measured values divided by the cross-sectional area, assuming a spherical shape) as a function of center-of-mass energy. The measured cross sections show a transition from low values below a threshold center-of-mass energy of 2-3 eV, to a higher value above that energy.

These results can be explained in terms of energy transfer from the target gas to the clusters, causing the latter to lose water molecules. It was found that, on the average, two water molecules are lost per collision.

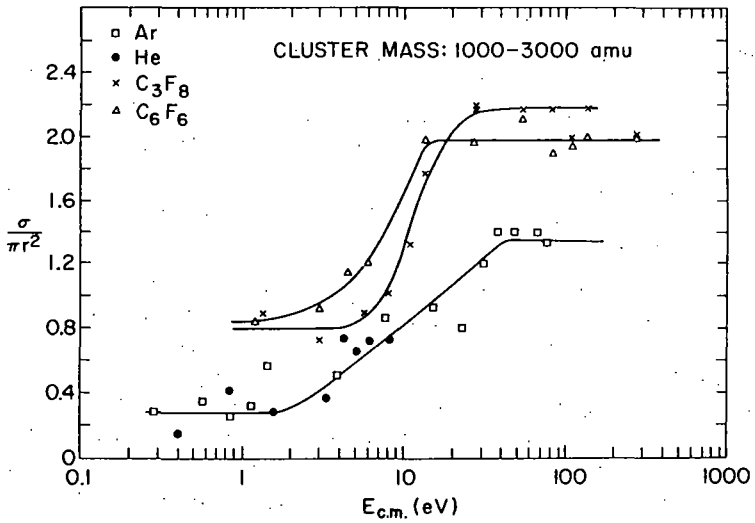

Fig. 1. Summary of cross section measurements.

This research was carried out at Brookhaven National Laboratory under contract with the U. S. Department of Energy and supported by its Division of Basic Energy Sciences.

*On leave from Soreq Nuclear Research Center, Yavneh, Israel.

[1]R. J. Beuhler and L. Friedman, Nucl. Instr. Methods 170, 309 (1980).

A SENSITIVE AND SPECIFIC STABLE ISOTOPE ASSAY FOR WARFARIN AND ITS METABOLITES

E. D. Bush, L. K. Low and W. F. Trager
Department of Medicinal Chemistry, BG-20
University of Washington
Seattle, Washington 98195

Although several assays for warfarin and its metabolites have been reported, none offered the sensitivity and specificity necessary for our metabolic studies of warfarin in man and rat. In particular, resolution and quantitation (in the range of 10-500 ng/ml) of warfarin, its diastereomeric reduced alcoholic metabolites and its hydroxylated (6-,7-,8- or 4'-OH) metabolites were required. In addition since both deuterium and ^{13}C are used as stable isotope markers on the parent compound, an MS assay was required to differentiate between labeled and unlabeled drug or metabolites. Therefore, a capillary GC-MS method was developed in our laboratories that provided excellent resolution of the parent anticoagulant drug and all the metabolites listed above. Quantitation of warfarin and metabolites from plasma or microsomal incubations was achieved through the use of the corresponding d_5 labeled internal standards (for all compounds except 4'-OH warfarin in which case a d_4 labeled standard was utilized).

Since warfarin is commonly present in a large excess (100 to 1000 fold) in comparison to its metabolites in human plasma and rat liver microsomal incubates, an extraction scheme was employed which preferentially removed the parent drug. In addition to selectively (ca. 80%) removing warfarin, the extraction scheme also eliminated other lipophilic impurities thus alleviating possible overloading of the capillary column. The extraction scheme for 1 ml of plasma or microsomal incubations was as follows:

1. 600 µl acetone-centrifuge and remove protein precipitate
2. 200 µl 0.5M NaH_2PO_4; to pH $\sim$ 5.8-6.0
3. 3 x 2 ml extractions with cyclohexane to remove warfarin
4. 2 x 2 ml extractions with ethyl ether-ethyl acetate (1:1) to recover the metabolites and the rest of the warfarin

Treatment of the dried ethyl ether-ethyl acetate extracts with diazomethane provided the methyl ether derivatives (at the enolic C-4 OH and phenolic OHs). After removal of excess diazomethane, N,O-bis (trimethyl silyl)-trifluoroacetamide (BSTFA, Pierce Chem. Co., Rockford, IL) was added to derivatize the warfarin alcohols and to serve as the injection solvent. Analysis of the derivatized samples was performed in the SIM mode on a HP 5985 or a VG Micromass 7070H GC-MS fitted with a fused silica capillary GC solumn running directly into the source.

Although several types of columns from different manufacturers were utilized in the assay, the best results were obtained using a chemically bonded DB-5 (equiv. to SE-52) phase from J & W Scientific Co., Rancho Cordova, CA [30 meter x 0.4 mm i.d. (wide bore); 0.25 µ film thickness] GC-MS conditions were as follows: MS:EI mode, 70 ev, filament + 50-100 µA, source temp 200°C. GC:He carrier gas, injection port temp. 250°C; column temp. 160°C isothermal for 1-2 min, then increased at a rate of 30°C/min to 250°C; GC-MS interface temp. 240-250°C. All injections were made in splitless mode with a vent delay of 30 sec. Standard curves were determined as functions of the base ion chromatographic peak height and/or area ratios vs. ratio of ng sample compound/ng d_4 or d_5 internal standard. In our microsomal studies, the standard curves covered a 100 fold change in the ratio of metabolite to internal standard which is in the range of values expected for <u>in vitro</u> metabolism of warfarin. Typical standard curves for hydroxylated warfarin metabolites are represented by a family of linear regression lines having the slope, intercepts and correlation coefficients shown in Table I.

TABLE I

	4'-OH	6-OH	7-OH	8-OH
slope ± S.D.	0.990 ± .006	0.996 ± .007	1.089 ± .003	0.921 ± .007
y-intercept ± S.D.	-0.019 ± .022	-0.014 ± .021	-0.008 ± .013	-0.016 ± .023
r^2	>0.999	0.996	>0.999	>0.999

The GC-MS assay has a cycle time of less than 15 minutes, is reproducible and is capable of detecting levels as low as 1 ng/ml of warfarin metabolites in plasma.

The GC-MS method described above has been extensively employed in our studies to investigate the mechanistic details of aromatic hydroxylation of warfarin in rat liver microsomes and to evaluate changes in the stereoselective metabolism of the two enantiomers of warfarin induced by the concurrent use of other drugs in man. A comparison of results using the present capillary GC-MS assay to results using a previous TLC assay in warfarin metabolism by rat liver microsomes is shown in Figure 1.

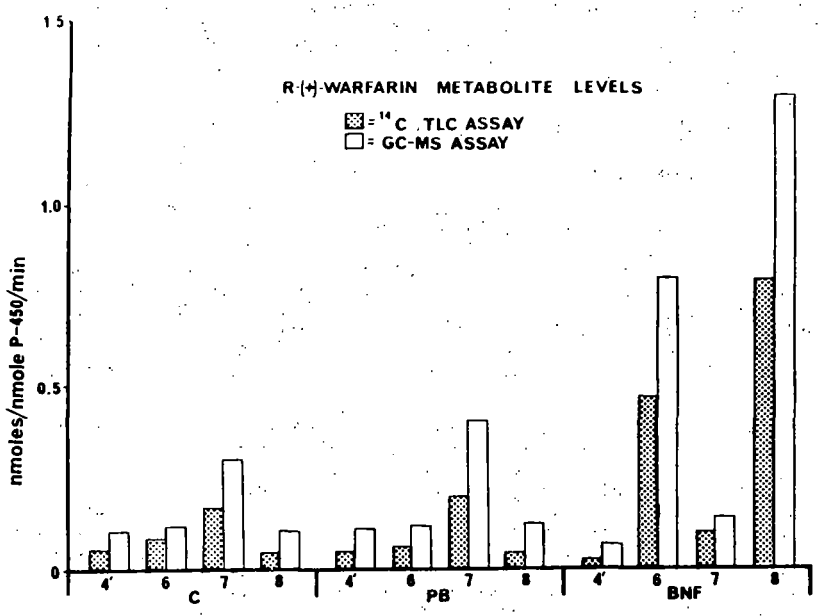

Figure 1. Comparison of metabolite levels obtained using a previous TLC assay vs. the GC-MS assay. Results are in nmoles product/nmole P-450/min. from rat liver microsomes of uninduced animals (C), phenobarbitol induced animals (PB) and β-napthoflavone induced animals (BNF).

METASTABLE ION MONITORING FOR THE MEASUREMENT OF Δ^9-TETRAHYDROCANNABINOL IN PLASMA TO THE LOW PICOGRAM LEVEL

D.J. HARVEY, J.T.A. LEUSCHNER, W.D.M. PATON

University Department of Pharmacology,
South Parks Road,
Oxford, OX1 3QT, U.K.

The plasma levels of Δ^9-tetrahydrocannabinol (Δ^9-THC, I), the major psychoactive principle of marihuana, are typically in the middle to low nanogram/ml range during intoxication by the drug and rapidly fall to the picogram/ml range. Detection and quantitation of the drug in plasma is therefore difficult and even the most sensitive and selective methods, usually based on GC/MS or radioimmunoassay, only allow the drug to be monitored for a few hours after administration[1-3]. Typical detection limits are in the range 0.1-1 ng/ml from plasma compared with a limit of about 1 pg which can be achieved by GC/MS with the pure compound as its trimethylsilyl (TMS) derivative. The difference is attributable to co-extracted lipid material which, together with limiting sensitivity, usually necessitates a purification stage between the extraction of the drug from plasma and its measurement by GC/MS.

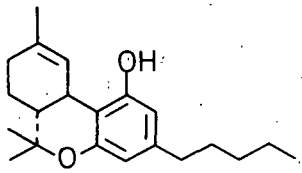

Δ^9-THC, I

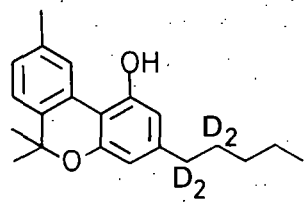

[1",1",2",2"-$^2H_4$]CBN, II

Two methods based on mass spectrometry, high resolution selected ion monitoring and metastable ion monitoring[4], have recently been investigated to improve sensitivity in cases where contamination from similar compounds occurs. The metastable ion technique involves increasing the accelerating voltage of a double focussing mass spectrometer to a value which gives the daughter ion from a metastable transition occurring in the first field free region sufficient energy to be transmitted through the system which is tuned to the daughter ion mass. Ions of the same mass formed in other transitions will have different energies and will not be transmitted through the electrostatic analyser. As these ions are largely responsible for the interference causing poor detection limits, the sensitivity of the system is considerably improved. This method was investigated for monitoring plasma levels of Δ^9-THC.

Measurements were made with a VG Micromass 7070F mass spectrometer interfaced via a glass jet separator to a Varian 2400 gas chromatograph containing a 2 m x 2 mm (ID) glass column packed with 3% SE-30 on 100-120 mesh Gas Chrom Q. Operating conditions were: helium flow rate, 30 ml/min; column temperature, 220°; injector, separator and ion source temperatures, 300°C, 280°C and 260°C respectively; trap current, 1 mA; electron energy, 70 eV. The instrument was tuned to m/z 371, the mass of the $[M\text{-}CH_3]^+$ ion from the TMS derivative of Δ^9-THC, with the accelerating voltage at 4 kV and the resolution set to about 700 to give flat top peaks. The accelerating voltage was then raised to 4.16 kV to bring the metastable ion into focus and the ion-source controls were optimised for maximum sensitivity. Repeated injections of Δ^9-THC TMS ether into this system established a linear response with a detection limit of 500 fg (2:1 S/N ratio).

The internal standard adopted for the assay was cannabinol labelled with four

deuterium atoms (II) to bring its mass up to that of THC. Its spectrum also contained a prominent metastable ion corresponding to $M^+ \rightarrow [M-CH_3]^+$ and it was sufficiently well separated from Δ^9-THC on the SE-30 column to enable both compounds to be monitored on a single channel. Lee and Millard[5] have demonstrated higher precision with this type of assay than with multiple ion monitoring.

Extraction of Δ^9-THC and the standard was achieved with hexane[6]. This gave a 70% recovery and reduced contamination by co-extracted lipids compared with the more commonly used 1.5% isoamyl alcohol:hexane. The solvent was doubly distilled and all glass-ware was silanized with dimethyldichlorosilane before use. Extracts were sufficiently clean to be examined by GC/MS without further purification although some residual contamination was still present. As the compounds producing the extra peaks appeared to be fatty acids, the sample was methylated with diazomethane prior to TMS ether formation with the result that the peaks disappeared leaving a clean background against which Δ^9-THC could be measured to 5 pg/ml. Δ^9-THC did not react with diazomethane under these conditions. The calibration curve was linear over the range tested (1 µg/ml - 5 pg/ml), and a complete assay could be performed in 1 hour.

The assay was used to examine the pharmacokinetics of Δ^9-THC in the female New Zealand white rabbit. Animals (2.5 kg) were treated intravenously (marginal ear vein) with the drug in Tween 80 and isotonic saline either once, or daily for 8 days at doses of 1 and 0.1 mg/kg. Serial blood samples were collected from the other ear into heperinized tubes starting immediately after the final dose. These were centrifuged, and the plasma was stored at -30°C until required for analysis. The internal standard in 1-2 µl of ethanol was added and the extractions and derivatization were performed in batches of 48 samples. Following a single injection of 1 mg/ml, the drug could be monitored for 7 days. Multiple dosing caused accumulation of the drug in tissues and under the conditions used, the drug could still be measured 3 weeks after the last dose.

This method is 10-100 times more sensitive than existing methods for Δ^9-THC measurements in plasma and has the advantage that no purification step is required between the extraction and measurement. We hope to extend it to human studies where at present accurate pharmacokinetic data are lacking. Part of this work has been published in J. Chromatogr., 202, 83 (1980).

Acknowledgements

We thank the Medical Research Council for support under a Programme Research Grant and the Wellcome Trust for additional financial support. We are also grateful to the British Mass Spectrometry Society for a generous contribution to travel costs and to Mr. D. Perrin and Miss J. Hughes for expert technical assistance.

References

1. R. E. Willette (Editor) Cannabinoid Assays in Humans, Res. Monogr. Ser. No. 7, NIDA, Rockville, MD, 1976.

2. J. A. Vinson (Editor) Cannabinoid Assays in Physiological Fluids, ACS Symposium Ser. No. 98, American Chemical Society, New York, 1979.

3. P. L. Williams, A. C. Moffat and L. J. King, J. Chromatogr., 155, 273 (1978).

4. S. J. Gaskell and D. S. Millington, Biomed. Mass Spectrom., 5, 557 (1978).

5. M. G. Lee and B. J. Millard, Biomed. Mass Spectrom., 2, 78 (1975).

6. D. Rosenthal, T. M. Harvey, J. T. Bursey, D. R. Brine and M. E. Wall, Biomed. Mass Spectrom., 5, 312 (1978).

IDENTIFICATION AND SIMULTANEOUS QUANTITATION OF CODORPHONE AND FIVE OF ITS METABOLITES IN HUMAN URINE AS THEIR TMS OXIME, N-TMS, O-TMS DERIVATIVES VIA GC/MS

James V. Evans, Richard J. Helms and Jerry L. Leeling

Miles Laboratories, Inc., Elkhart, IN 46515

During the development of the methodology for the analysis of codorphone (IIa) (an analgesic-narcotic antagonist drug under development) and its metabolites (IIb-h), certain structural features were present which created problems in the analysis that had not been addressed in previous investigations of morphine-like compounds. One such problem concerned the derivatization of the metabolites in conjunction with the drug. Although the drug did not require derivatization for analysis by gas chromatography and mass spectrometry, a number of the metabolites did require such treatment. Specifically, the N-dealkylated metabolites (IId-f) required blockage of the secondary nitrogen since the underivatized secondary amine behaved very poorly gas chromatographically. Moreover, a derivatization procedure was necessary which would accurately reflect the identity of the metabolites present in a biological mixture by enhancing the chromatographic and mass spectrometric properties.

Under normal conditions, one would not expect codorphone to derivatize since there are no labile hydrogens present. When BSTFA in the presence of 1% TMCS and pyridine were introduced to the drug, however, two prominent peaks were produced. The identity of the two peaks was confirmed by mass spectrometry. The second peak to elute was the unchanged compound. The first peak to elute from the GC was identified as the TMS derivative of the enol form of the drug. Numerous attempts were made to obtain all as the enol form or all as the underivatized form. All of these attempts failed.

To avoid this difficulty, a procedure reported by Sternowsky et al. some years ago in connection with the GC/MS analysis of α-keto acids was applied (1). They reported a procedure whereby the trimethylsilyloxime derivative was formed by a two step procedure. More importantly, they reported that an aliquot of the reaction mixture was injected directly into the GC with no adverse effects.

This is essentially the approach that we took in connection with the derivatization of codorphone and its metabolites. We modified the TMS oxime derivatization, however, to a one step procedure. In order to do this, we selectively silylated hydroxylamine with trimethylsilylimidazole (to form trimethylsilyloxyamine) by combining TSIM, $HONH_2$ and pyridine prior to introducing them to the compound to be derivatized. Introduction of this reagent combination formed the oxime at the 6-position. Due to the excess TSIM present, hydroxyl groups were also derivatized, but not the secondary nitrogen. To complete derivatization of the nitrogen, therefore, an aliquot of BSTFA was added.

Oxime formation by this method occurred very rapidly with the majority of the compound derivatized in 15 to 20 minutes of moderate heating. Once combined, the reagent mixture was effective for derivatization for several months when stored in the cold. Most importantly, an aliquot of the reaction mixture was injected directly into the GC for analysis without the prior extraction necessary in methyloxime formation of these compounds.

The gas chromatographic trace of codorphone derivatized in this manner showed a single peak with a small amount of underivatized compound amounting to about 1% of the major peak. The mass spectrum of the TMS oxime derivative of codorphone showed an intense molecular ion at m/z 454. Numerous diagnostic fragment ions were also observed. All of the synthetic metabolite derivatives were characterized mass spectrometrically after derivatization in this manner for comparison with authentic metabolite derivatives found in the biological samples.

During the course of phase I clinical trials, human volunteers were given various doses of codorphone either intramuscularly or orally. In the group that received the oral doses a portion of the subjects receiving higher doses of the drug complained of some side-effects such as nausea. One of the questions which subsequently arose was: is there any connection between the amounts of metabolites and drug produced versus the side-effects observed? To answer this question, the above procedure was employed for quantitation using selected ion monitoring. We monitored simultaneously derivatives of five metabolites (IIb-f) and the

drug (IIa) in urine samples from human volunteers. A seventh peak, the internal standard (IIi), was also monitored.

There were several observations from the quantitation study for levels of codorphone and its metabolites in humans. First, the average recovery of metabolites and drug versus the amount of drug administered was about 50% in each group. Secondly, there was a correlation between the levels of the "nor" metabolites (IId-f) produced and the routes of administration. The quantity of the "nor" metabolites was only about 40% of the total recovery in the group receiving intramuscular doses; however, the subjects receiving oral doses almost doubled the production of "nor" metabolites. This observation was attributed to a first pass effect where the drug was largely metabolized to N-dealkylated compounds in the liver of subjects receiving oral doses. The metabolism of the drug of subjects receiving intramuscular injections, however, probably occurred extrahepatically, thus the reduced incidence of N-dealkylation. Moreover, the major metabolite observed in the subjects receiving intramuscular doses was compound IIb where the only permutation of the drug was reduction of the 6-keto group to the 6-hydroxy group. (Of the metabolites where a 6-hydroxy function appeared, only the β-isomer was observed. These were readily distinguishable from their corresponding α-isomer by gas chromatography.)

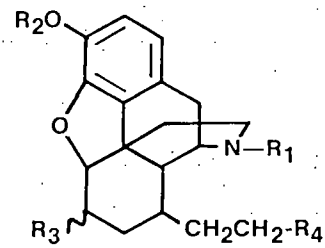

II

	R_1	R_2	R_3	R_4
IIa	CH_2-cyclopropyl	CH_3	=O	H
IIb	CH_2-cyclopropyl	CH_3	H, OH(β)	H
IIc	CH_2-cyclopropyl	H	H, OH(β)	H
IId	H	CH_3	=O	H
IIe	H	H	=O	H
IIf	H	H	H, OH(β)	H
IIg	CH_2-cyclopropyl	CH_3	=O	OH
IIh	CH_2-cyclopropyl	H	=O	H
IIi	CH_2-cyclopropyl	CH_3	=O	CH_3

1) H.J. Sternowsky, J. Roboz, F. Hutterer and G. Gaull, Clinica Chimica Acta,47,371 (1973).

Improvements in a GC/MS Assay for l-α-Acetylmethadol (LAAM) and Its Metabolites:

Dennis M. Chinn and Rodger L. Foltz; Center for Human Toxicology, The University of Utah, Salt Lake City, UT 84112.

l-α-Acetylmethadol (LAAM) is a narcotic analgesic which is being investigated as a replacement for methadone in the treatment of heroin dependence. Several years ago a gas chromatography--chemical ionization--mass spectrometry assay was developed to measure plasma concentrations of LAAM and its two major metabolites, nor-LAAM and dinor-LAAM (1). Recently the assay was modified and the new method shown to have more sensitivity, better reproducibility, to require less time to perform. The major procedural changes include conversion of the metabolites to their N-trifluoroacetyl derivatives and measurement of the ion currents corresponding to the protonated molecule ion (MH^+) of LAAM and the ammonium attachment ions (MNH_4^+) of the derivatized metabolites. Use of both packed and capillary GC columns will be discussed.

This research was supported by the Insurance Institute for Highway Safety and the National Institute on Drug Abuse, contract 271-80-3719.

1. T. A. Jennison, B. S. Finkle, D. M. Chinn, and D. J. Crouch, J. Chromatogr. Sci., 17, 64 (1979).

QUANTITATION OF METHADONE AND METABOLITES IN HUMAN FECES BY DIRECT PROBE CHEMICAL IONIZATION MASS SPECTROMETRY. M.J. KREEK, F.A. BENCSATH, A.M. FANIZZA, and F.H. FIELD, The Rockefeller University, New York, N.Y. 10021.

Balance study techniques are essential to determine some of the effects of chronic diseases (e.g. liver disease) on drug disposition. Previously we have developed techniques for simultaneous quantitation of the long-acting narcotic methadone and its metabolites in urine of maintenance patients using direct probe chemical ionization mass spectrometry (CIMS) [1]. Now we have developed a method using CIMS for the simultaneous measurement of methadone (m/z 310) and 4 of its metabolites (m/z 264, 278, 312 and 326) in fecal homogenates from patients maintained on methadone. Direct probe introduction of these compounds can be used when appropriate sample preparation procedures and ethylenediamine-modified isobutane chemical ionization are used. Pentadeuteromethadone was used as the internal standard [2]. Fecal samples from 13 unmedicated subjects were analyzed. Amounts of interfering materials at masses of interest were very low (expressed as ng equivalent of pentadeuteromethadone per ml of fecal homogenate: $\bar{m} \pm$ SEM values are 0.35 ± 0.26, 5.32 ± 2.18, 2.75 ± 2.65, 0.0, 0.34 ± 0.23, and 0.16 ± 0.16 at m/z 264, 278, 310, 312, 315 and 326 respectively. The amounts of these interferences were < 1 to 5% of the lowest concentrations of metabolites at the corresponding masses in feces of medicated patients. Analyses of feces from collections in maintained patients, including 4 otherwise healthy subjects and 9 patients with chronic liver disease, have been made. The predominant compound excreted in feces is the pyrrolidine metabolite (m/z 278). The ratio of pyrrolidine to unchanged methadone is around 9:1. Concentrations of metabolites down to 2 to 10 ng/ml of homogenate can be detected using this method.

1. M.J. Kreek, F.A. Bencsath and F.H. Field, Biomed. Mass Spectrom. 1980, 7:385.
2. D.L. Hachey, M.J. Kreek and D.H. Mattson, J. Pharm. Sci. 1977, 66:1579.

METABOLISM AND DISPOSITION OF INHALED 2-BUTANONE IN RATS DETERMINED BY GAS CHROMATOGRAPHY-MASS SPECTROMETRY. E. L. WHITE AND D.E. RICKERT, Chemical Industry Institute of Toxicology (CIIT), P. O. Box 12137, Research Triangle Park, NC 27709

A widely used industrial solvent, 2-butanone (methyl ethyl ketone, MEK) potentiates the neuropathy caused by n-hexane and several of its major metabolites, e.g. 2-hexanone and 2,5-hexanedione. To understand the disposition of MEK after inhalation exposure in rats, a gas chromatographic-mass spectrometric (GCMS) method using stable isotope dilution was developed to detect MEK and its metabolites, 2-butanol (2-BOH), 3-hydroxy-2-butanone (3H2B) and 2,3-butanediol (2,3-Bdiol) in tissues.

Male Fischer-344 rats were exposed by inhalation to 500, 1500 and 5000 ppm MEK for 6 hr and then sacrificed by decapitation. Samples of blood, brain, liver, lung, kidney and sciatic nerve were weighed and frozen. Prior to analysis, the samples were thawed and 1 ml of acetone/ml of blood or /g wet weight of tissue containing $[^2H_5]$-MEK and 2-$[^2H_{10}]$ BOH (4 $\mu g\ ml^{-1}$) was added. Tissues were homogenized at 0^oC and centrifuged. A 2 μl aliquot of the supernatant was subjected to GCMS analysis. Separation was accomplished using a 6 ft x 2 mm i.d. glass column packed with 10% FFAP on 80/100 Chromosorb W AW. The column oven was held at 80^oC for 0.5 min, then programmed to 200^oC at $20^oC\ min^{-1}$.

Maximum concentrations of MEK in blood (86.3, 331.1 and 739.3 $\mu g\ ml^{-1}$) were observed immediately after the end of exposure to 500 and 1500 ppm, and at 0.5 hr after exposure to 5000 ppm respectively. Maximum concentrations of 2-BOH were 3.4, 13.1 and 33.5 $\mu g\ ml^{-1}$, and maximum 3H2B concentrations were 2.7, 10.7 and 52.3 $\mu g\ ml^{-1}$. Maximum concentration of 2,3-Bdiol in blood (42.9, 101.4 and 195.7 $\mu g\ ml^{-1}$ at 500, 1500 and 5000 ppm, respectively) were observed 4-6 hr after the end of exposure. Maximum concentrations observed for other tissues were comparable to those found in blood. There were no dose-dependent changes in the pharmacokinetics of MEK at the three exposure concentrations used.

Application of Chemical Ionization Mass Spectrometry to the Identification and Characterization of Trialkylphosphate Flame Retardants and their Metabolites; J. M. Kennish, Chemistry Department, University of Alaska, Anchorage, Anchorage, AK 99504; K. Wong, C. Garvie-Gould and R. K. Lynn, Pharmacology Department, University of Oregon Health Sciences Center, Portland, OR 97201

Tris(2,3-dibromopropyl)phosphate (TDBP) and tris(1,3-dichloro-2-propyl)-phosphate (TDCP) are flame retardant chemicals formerly used in the apparel industry to confer flame-resistant properties to polyester fabric. TDBP and TDCP were used in childrens sleepwear which is required by law to meet flame resistance standards. In 1977 TDBP was banned for use in sleepwear due to its charcinogenicity in rats and mice (1,2). TDCP was used temporarily as a substitute for TDBP in sleepwear and is currently used as a flame retardant in flexible polyurethane foam. It was recently demonstrated that TDCP was present in concentrations of 5-50 ppb in the seminal fluid of 34 out of 123 subjects (3).

Studies were undertaken to determine quantitatively the metabolism, distribution and excretion of TDBP and TDCP in the rat. Using radiotracer techniques and GCMS analysis we have demonstrated that TDBP is metabolized at least in part to bis(2,3-dibromopropyl)phosphate (BDBP) and 2,3-dibromopropanol. TDCP, similarly, is metabolized to bis(1,3-dichloro-2-propyl)phosphate (BDCP), 1,3-dichloro-2-propylphosphate and 1,3-dichloro-2-propanol. For metabolite identification urine,feces or bile were obtained from Sprage Dawley rats following intraperitoneal administration of ^{14}C-TDBP (25mg;sp.ac. 65.2 µCi/100mg) and ^{14}C-TDCP (80mg;sp.ac. 10µCi/100mg) dissolved in emulphor 620. The animals were housed in a glass metabolism cage which permitted the separate collection of urine and feces. Urine was cooled in an ice bath during the collection period and stored at -20°C prior to the analysis. Two ml of the first 24 hr urine sample was adjusted to pH 8.5 with phosphate buffer (0.5 ml pH 8.5; 0.5M) and extracted with diethyl ether (10ml x 2). The ether layers were discarded and the lower layer titrated to pH 1 with 12N HCl. The aqueous layer was extracted with diethyl ether (10ml) and 2ml evaporated to dryness under nitrogen. The residue was treated either by dissolution in pyridine (50µl) followed by addition of BSTFA (30µl) containing 1% TMCS or by dissolution in methanol and treatment with etherial diazomethane. Samples obtained from a control animal were treated in the same manner. Bile samples were evaporated under nitrogen and derivatized as above.

The derivatized urine extracts were analyzed on a Hewlett Packard model 5830 gas chromatograph equipped with a flame ionization detector and a 1.5m x 2mm i.d. glass column packed with 1.5% OV-101 on Gas-Chrom Q (100-120 mesh). The column temperature was maintained at 100°C for 1 min then programmed to 320°C at 10°C per min. Hydrogen, air and nitrogen flows were 30, 250 and 30ml/min respectively. Mass spectra were obtained in a Finnigan Model 4021 GCMS equipped

with a jet separator and a dual electton impact-chemical ionization source. Electron impact (EI) spectra were obtained at 250°C with an ionization potential of 70eV. Chemical ionization (CI) spectra were obtained with methane, isobutane or ammonia as the reagent gas. The EI and CI spectra of the metabolites were identical to the chemically synthesized material.

The CI spectr of the methyl derivatives of BDCP and 1,3-dichloro-2-propyl-phosphate displayed ion clusters corresponding to $[M+H]^+$, $[M+C_2H_5]^+$ and $[M+C_3H_5]^+$. The relative intensities of the isotopic peaks within these clusters were consistent with the assigned structure. Neither metabolite displayed a molecular ion in its EI spectrum. The ions of highest m/e represent loss of Cl and CH_2Cl from the parent molecule in each case. Loss of a dichloroisopropyl group accompanied by double hydrogen rearrangement produced the cluster at m/e 223 (BDCP) and m/e 127 (1,3-dichloro-2-propylphosphate). The EI and CI spectra of the TMS derivatives were consistent with the assigned structure of the metabolites.

The mass spectra of the methyl derivatives of bis(2,3-dibromopropyl)-phosphate contained ions produced by loss of Br and/or HBr from the halo-alkyl substituents. Other ions produced by loss of the halo-alkyl group(s) accompanied by single and double hydrogen atom rearrangements were also observed in the EI spectrum.

The absence of molecular ions in the EI spectra of TDBP and TDCP and their derivatized metabolites is consistent with previous reports (4) that trialkyl posphates display weak or non-existent molecular ions. Therefore, chemical ionization mass spectrometry was necessary for determination of the molecular ions. Double hydrogen rearrangements are commonly observed in mass spectra of carboxylic esters (5) and have been previously observed in the spectra of alkyl phosphates (4,6).

Research supported by NIEHS NO1-ES-7-2126.

1. National Cancer Institute (1978). Bioassay of tris(2,3-dibromopropyl)-phosphate for possible carcinogenicity. National Cancer Institute Carcinogenesis technical report series No. 76

2. Van Duuren, B.L., Loewengart, G., Seidman, I. Smith, A.C. and Melchionne, S. (1978). Mouse skin carcinogenicity tests of the flame retardants tris(2,3-dibromopropyl)phosphate, tetrakis(hydroxymethyl)phosphonium chloride, and polyvinyl bromide. Cancer Res. 38, 3236-40.

3. Hudec, T., Thean, J., Kuehl, D., and Dougherty, R.C., Science 211, 951 (1981).

4. Quayle, A., in Adv in Mass Spec (J Waldrom, Ed,), pp 365-383, Pergamon, London, 1956.

5. Beynon, J. H., Saunders, R. A. and Williams, A.E., Anal Chem, 33, 221 (1961)

6. McLafferty, F. W., Anal Chem, 28, 306 (1956).

Studies on the Metabolism of Procarbazine by Mass Spectrometry

Simon H. Kuttab[a], S. Tanglertpaibul[a] and Paul Vouros[b]
College of Pharmacy, Section of Medicinal Chemistry[a]
and
Institute of Chemical Analysis and Department of Chemistry[b]
Northeastern University
Boston, Mass. 02115

Procarbazine, N-isopropyl-α-(2-methylhydrazino)-p-toluamide 1, displays antitumor effects in a spectrum of animal neoplasms and is used clinically in the treatment of Hodgkin's disease, brain tumors, and other cases involving malignant tumors. Like many other cytotoxic agents, procarbazine has a variety of biological effects including leukopenia, thrombopenia, immunosuppression, carcinogenesis, teratogenesis, and depression of spermatogenesis. Its mode of cytotoxic action is believed to be mediated by inhibition of protein, RNA and DNA synthesis. The N-methyl group has been found to be essential for its cytotoxic action. Hydrogen peroxide formed during procarbazine oxidation has also been implicated in its cytotoxic action.

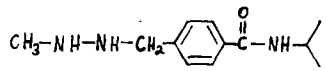

1

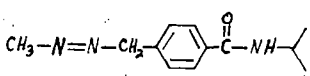

2

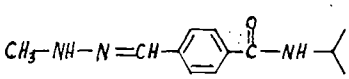

3

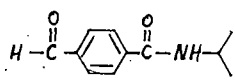

4

It has been proposed that procarbazine is metabolically converted into a number of compounds, among them the azo and hydrazone derivatives, 2 and 3. In a recent report it was suggested, based on HPLC analysis, that the azo compound, 2, was the major *in vivo* metabolite of procarbazine. Other investigators, using GC/MS have reported the aldehyde, 4, as the primary metabolite. In either case, the techniques used are likely to cause decomposition of the compounds under the conditions of the analysis. In view

of these considerations we examined the metabolism of procarbazine using electron impact MS and minimum sample manipulation. Our approach consisted of the use of a simple ether extraction of a plasma sample, evaporation of the solvent under N_2, reconstitution into methyl alcohol and analysis of an aliquot by MS using the direct insertion probe.

The mass spectra of the parent drug and the compounds previously reported as *in vivo* metabolites of procarbazine were first examined in detail using isotopic labeling. Significant and readily explainable differences in their mass spectra were observed. A fragmentation process involving an intramolecular methyl group transfer in the spectrum of the azo derivative, 2, provided the key to distinguishing mass spectrometrically between that and its isomeric hydrazone counterpart, 3.

Results from *in vivo* experiments using plasma samples of rats administered 23.2 mg of procarbazine showed that the azo compound, 2, is the principal circulating metabolite of procarbazine. No evidence was found for the presence of procarbazine, the hydrazone, or the aldehyde.

METABOLISM OF TWO TETRACHLOROBIPHENYL ISOMERS IN RHESUS MONKEYS

H.T. CORY, G.D. DAVES (1) and W.P. McNULTY (2)
(1) Oregon Graduate Center, Beaverton, Or 97006
(2) Oregon Regional Primate Research Center, Beaverton, Or 97006

In an earlier study (1), we compared the metabolism and fat storage of two tetrachlorobiphenyl (TCB) isomers of contrasting toxicity towards rhesus monkeys. 3,3',4,4'-TCB (34TCB) induces severe gastric, thymic and skin lesions when fed chronically at 1 - 10 ppm in the diet, whereas 2,2',5,5'-TCB (25TCB) appears to be completely inocuous at this dose level (2). The present study forms part of a larger investigation of the pathology, toxicology, metabolism and liver enzyme induction in rhesus monkeys exposed to a range of PCB isomers of differing chlorine substitutions by chronic dietary contamination or administration of a single large dose of compound. In this study, 2 animals received 1 mg/kg 34TCB, 3 animals received 25 mg/kg 25TCB and there were 2 controls. The following samples were collected at intervals over a 32-day period:

a) Blood and adipose tissue biopsies, for measurement of parent TCB.
b) Excreta - urine and feces - for measurement of parent TCB and metabolites.

Blood samples (2ml) were freeze-dried then shaken with chloroform, filtered, dried and concentrated. Fat samples (10 - 200 mg tissue wt. range) were ground in a mortar with sodium sulfate, extracted with chloroform: methanol 2:1 and the extract dried and weighed. The residue was dissolved in hexane, washed with conc. sulfuric acid then water, concentrated and dried. A known amount of internal standard (2,2',4,4',6,6'-HCB) for GCMS analysis was added to the blood and fat samples at the start of the extraction. Urine and feces samples were extracted with chloroform as previously described (1). Conjugated metabolites present in the urine were hydrolyzed either with HCl or glucuronidase; samples were derivatized with diazomethane or silanizing reagent prior to analysis.

The samples were examined by selected ion monitoring GCMS for specific compounds of known molecular weight containing four chlorine atoms. The first two masses in the molecular ion cluster were monitored.

GC conditions: Varian Aerograph 2700; GC column: 2m x 2mm i.d. glass column packed with 1% OV 17 on 100/120 mesh Supelcoport; Injector and Detector temperatures: 250°; Carrier Gas Flow: 40 ml Helium /min; Oven Temp: 220° isothermal, or temperature program 190° to 270° at 8°/min.

Mass Spectrometer: Dupont 21-491B Mass Spectrometer equipped with 4-channel Dupont SMID accessory and Gould Brush 6-channel recorder. Ionizing voltage: 70 eV; Filter: 1 Hz; Sampling frequency: 40 peaks/sec; Limit of Detection: 10 pg of 25TCB.

Blood and Fat: Levels of 34TCB and 25TCB in the blood reached a peak at 1/3 to 1 day after administration of the TCB: in the case of the fat this occurred at 1-2 days. The maximal levels of TCB reached in the two tissues was correlated with the dose of the TCB. Thereafter levels in both fat and blood declined at an exponential rate with a half life of 7-10 days for both tissues. Surprisingly, no difference in half life was found between the animals receiving 34TCB and 25TCB.

Urine and Feces: Parent TCB was found to be present in the urine and feces from both groups of animals. Excreted levels of TCB also correlated with dosage. In contrast, no TCB had been detected in the urine of the animals given chronic smaller doses of the TCBs in our previous study.
Metabolites: Both 34TCB and 25TCB gave rise primarily to hydroxylated metabolites, as was found in the earlier, chronic study. 34TCB formed one monohydroxy metabolite (as yet not structurally identified) and 25TCB formed equal amounts of 3- and 4-hydroxy-25TCB. Animals fed 25TCB also formed three dihydroxylated metabolites, two minor and one major isomer, not structurally identified, but no dihydroxy compounds were formed from 34TCB, as before. A dihydrodiol metabolite however was detected in enzyme-hydrolyzed urine extracts of animals given 25TCB; this metabolite has been reported previously in rhesus monkeys (3) but we had been unable to detect it in our extracts of urine of rhesus monkeys chronically fed with 25TCB at 1 ppm.

The above data can be correlated with other data on enzyme induction in liver (4) , to throw light on the interrelationship between the persistence of TCB in the body and its metabolism on the one hand, and the duration of inductive effects of TCB in primates on the other.

1) Cory, H.T., Isabelle, L.M., Smith, R.G., McNulty, W.P. and Daves, G.D. (1981) Submitted for publication

2) McNulty, W.P., Becker, G.M. & Cory, H.T. (1980) Toxicol. Appl. Pharmacol. 56, 182.

3) Hsu, I.C., Van Miller, J.P. & Allen, J.R. (1975) Bull. Environ. Contam. Toxicol. 14, 223.

4) K. Nielsen-Smith M.S. Thesis, 1980.

HPLC AND FD MASS SPECTRAL IDENTIFICATION OF THIOLYTIC CONJUGATION AND DEGRADATION METABOLITES OF THE ANTICANCER DRUG m-AMSA. M.PRZYBYLSKI[+], I.DIETRICH[+], D. SHOEMAKER[++] and R.L.CYSYK[++], Institut f.Org.Chemie, Universität Mainz, D-6500 Mainz, W.-Germany[+] and Lab.Chem. Pharmacology, Nat'l Cancer Institute, NIH, Bethesda, MD 20205[++].

4'(9-Acridinylamino)methanesulfone-m-anisidide (m-AMSA) is a new antitumor agent that has shown high activity in animal experimental tumors and has been introduced into phase I and II clinical trials. Studies on its pharmacologic disposition in rats had shown that the drug is extensively metabolized in the liver to conjugates that are primarily excreted in the bile. Since the metabolic pathway of m-AMSA has been related to its susceptibility to nucleophilic attack at the acridinyl moiety, the conjugation with endogenous thiols was studied by using chiefly HPLC in combination with FD mass spectrometry. After administration of m-AMSA-hydrochloride (NSC-141549) to rats, a major biliary metabolite was isolated and identified as the 9-acridinyl thioether of glutathione (GSH)[1].The corresponding 9-acridinyl conjugates were formed spontaneously in vitro (phosphate buffer pH 7.3) after incubation of m-AMSA with GSH, cys and N-acetyl-cys, as established by HPLC and FD mass spectra. The thiolytic pathway results in the release of 4-amino-3-methoxymethanesulfonanilide and of several acridinyl degradation products identified by high resolution EI and by FD mass spectrometry. Recent results show microsomal oxidation of m-AMSA as an other important metabolic pathway, leading to the formation of an AMSA-GSH conjugate as the major bile product after administration of m-AMSA-free base (NSC-249992)[2]. The oxidative vs. thiolytic metabolism of m-AMSA is probably significant for the formation of cytotoxic and of excretion products; it may depend highly on the quarternization of the acridine ring, and is currently under investigation. (supported by grant PTB 8207 from the Bundesministerium für Forschung u. Technologie, Bonn,W.-Germany).

1)M.Przybylski, et al.,Proc.Am.Ass.Cancer Res.20,1165(1979)
2)L.Malspeis, et al.,Proc.Am.Ass.Cancer Res.21,594 (1980)

SECONDARY ION MASS SPECTROMETRY FOR IDENTIFICATION OF NEUROACTIVE CHOLINEAZIRIDINIUM ANALOGS, Adam Vincze*, R. Graham Cooks, Dept. of Chem., Purdue University, West Lafayette, IN 47907 and Israel Hannin, Abraham Fisher, Univ. of Pittsburgh, School of Med., Pittsburgh, PA 15261.

Secondary ion mass spectrometry (SIMS) is an established technique for studying involatile organic compounds[1,2]. It is particularly sensitive for charged compounds including onium salts such as choline and muscarine which can be determined even in biological tissues[3,4]. This paper describes the application of the method to study the centrally active cholinergic ethylaziridiniumcholine (EtAzCh)[5,6] and other analogs. EtAzCh is capable of binding to nerve terminals thereby inducing cholinergic hypofunction in rodents, a pathological state needed in order to study the effect of certain drugs developed to remedy the same in humans suffering from debilitating neuromuscular distrophies. The SIMS of EtAzCh (Figure 1) shows the intact cation at m/z 116 and elaborate fragmentation (Figure 2); a sensitivity of 30 picomoles was achieved even without ensemble averaging (Figure 3). The feasibility of detecting EtAzCh in mouse brain tissue was explored. While there is no problem of detecting it in spiked brain homogenates (Figure 4), it has not so far been detected in vivo. The reason for this is as yet unclear; it can be due to fast and strong binding of this alkylating agent. Much bulkier choline analogs gave information by SIMS (Figure 5). SIMS quantitation was shown to be feasible with choline and other quaternaries (Figure 6)[7]. In view of these results, molecular SIMS seems to be the mass spectral method of choice for quaternaries related to choline.

(1) R.J. Day, S.E. Unger and R.G. Cooks, Anal. Chem. (1980) 52, 557A.
(2) A. Benninghoven and W. Sichtermann, Anal. Chem. (1978) 50, 1180.
(3) S.E. Unger, T.M. Ryan and R.G. Cooks, Surf. and Int. Anal. (1981) 3(1), 12.
(4) S.E. Unger, A. Vincze, R.G. Cooks, R. Chrisman and L.D. Rothman, Anal. Chem. (in press).
(5) B.J. Rylett and E.H. Colhun, J. Neurochem. (1980)34, 713-719.
(6) A. Fisher, et. al. (1981), Amer. Soc. Neurochem., 12th annual meeting.
(7) A. Vincze, K.L. Busch, R.G. Cooks and B. Lindström (to be published).

*On leave from the Israel Institute for Biological Research, P.O. Box 19, Ness Ziona 70450 ISRAEL.

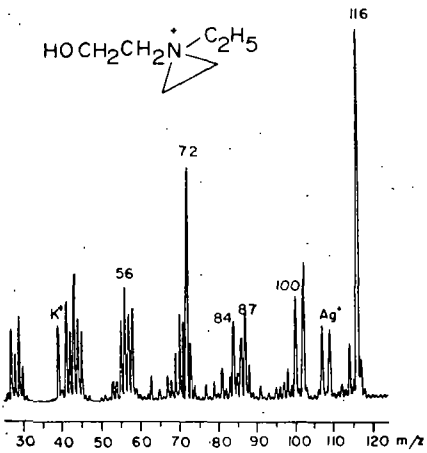

Figure 1

Aziridiniumethylcholine

tentative structure assignments

m/z	structure	m/z	structure
29	$C_2H_5^+$	84	
43		86	
44		87	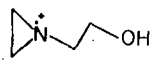
45		88	
56		100	
72			

Figure 2

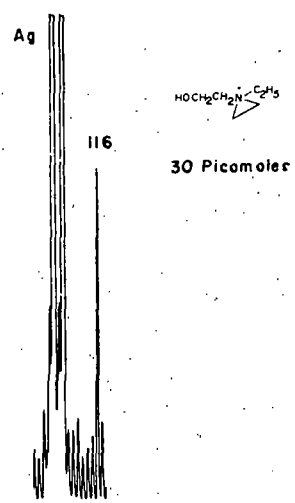

Figure 3

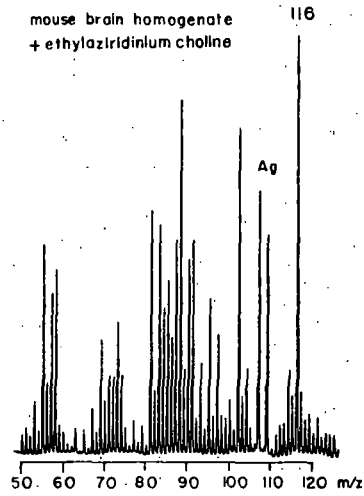

Figure 4

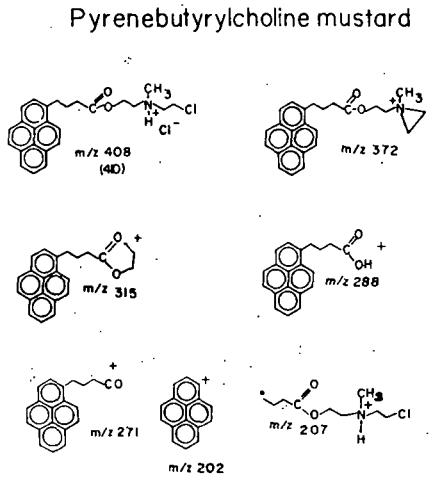

Figure 5

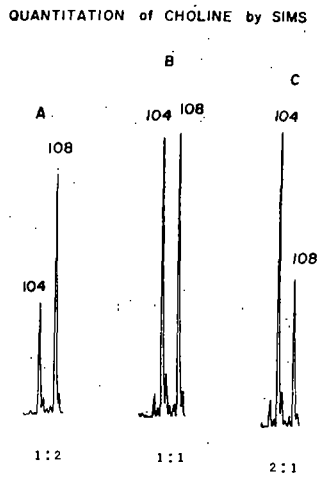

Figure 6

ACCURATE MASS CHROMATOGRAPHY AS A HIGHLY SPECIFIC TECHNIQUE FOR THE DETECTION OF DRUG METABOLITES IN COMPLEX MIXTURES OF BIOLOGICAL ORIGIN; THOMAS A. BAILLIE, Dept. Pharm. Chem., Univ. of Calif., San Francisco, CA 94143

The computer-based technique of "mass chromatography", in which the variation with time in intensity of the ion current at a given m/z value is reconstructed from a series of repetitively scanned mass spectra, has found widespread application in "screening" complex biological extracts by GC-MS analysis for known or suspected drug metabolites. When the GC-MS analysis is performed under conditions of low mass resolution, however, difficulties may arise in the detection of those drug-related components present at low concentration due to the extent of nonspecific interference from endogenous metabolites, even when highly efficient capillary GC columns are used. One solution to the problem is to simplify the initial extract by means of chromatographic procedures (e.g., HPLC) prior to GC-MS analysis; this approach suffers from the disadvantage that some arbitrary decision usually has to be made concerning the optimum procedure to be adopted and risks the possibility that metabolites of unknown structure and physicochemical properties are lost inadvertently from the sample. An alternative solution being explored in our laboratory is to analyze the crude extract directly by computerized GC-MS under conditions of high mass spectrometric resolution, where advantage may be taken of the high specificity of the mass spectrometer for the detection of metabolites which yield ions of a given exact mass, corresponding to a unique elemental composition. This presentation will deal with preliminary work on the application of such an approach to studies of drug metabolism, where the potential of accurate mass chromatography for the detection of specific products of biotransformation in complex mixtures will be illustrated with examples taken from studies on the metabolism of ketamine, an anesthetic agent, and clonidine, an anti-hypertensive drug.

Supported by NIH Div. of Research Resources Grant RR00719.

GAS-PHASE ATOMIC METAL CATIONS. LIGAND BINDING ENERGIES, OXIDATION CHEMISTRY AND CATALYSIS; RALPH H. STALEY; Department of Chemistry, Massachusetts Institute of Technology, Cambridge, Massachusetts 02139

Pulsed laser volatilization/ionization of metal targets has been utilized as a source of atomic metal cations for studies of their chemistry with a variety of molecules. Elimination-displacement and direct condensation pathways lead to the formation of metal-ligand cation complexes with one or two ligand molecules. Equilibrium constants for the ligand exchange reactions of these complexes when two types of ligands are present have been determined. Combining the corresponding free energies for an interlocking series yields a scale of relative ligand binding energies. Such scales have been obtained for Al^+ and Mn^+ with one ligand and Co^+, Ni^+, and Cu^+ with two ligands. These data provide a measure of the relative basicity of the ligand molecules with respect to each of the reference acids (metal cations) studied. Comparisons are made of these data sets with one another and with similar data sets such as that for H^+ which have been previously obtained.

Comparison of the ligand binding energy results for Mn^+ with available results for other reference acids reveals some interesting points about the nature of the metal-ligand bonding interaction. Figure 1 shows a plot of the relative ligand binding energies to Al^+, $\delta D(Al^+\text{-}L)$, versus the results for Mn^+, $\delta D(Mn^+\text{-}L)$. The 15 oxygen basis show a good linear correlation. A least squares fit to this data gives: $\delta D(Al^+\text{-}L) = 1.22\delta D(Mn^+\text{-}L) - 6.1$ kcal/mol (correlation coefficient $r = 0.97$). The slope of this line, 1.22, shows that as basicity increases the strength of the bond to Al^+ increases slightly faster than that to Mn^+. This suggests that the ligand-metal bond distance for $Al(ligand)^+$ complexes is slightly shorter than for $Mn(ligand)^+$ complexes. With a shorter bond distance the effect of a larger alkyl substituent may be expected to be greater since it is closer to the charge center which remains on the metal atom.

Two data points for nitriles in Figure 1 fall on a line given by $\delta D(Al^+\text{-}L) = 1.13\delta D(Mn^+\text{-}L) - 9.4$ kcal/mole. This has the same slope as the line for oxygen bases but is offset by 3.4 kcal/mol on the $\delta D(Mn^+\text{-}L)$ axis. The offset can be attributed to π-backbonding by 3d-electrons on Mn^+ into empty π^* CN orbitals on the nitriles. Offsets of 6 kcal/mol for nitriles compared to oxygen bases have been observed in plots of binding energies to $CpNi^+$ versus binding energies to H^+ [1] and to Al^+. The smaller effect by about a half which is observed for Mn^+ compared to $CpNi^+$ is reasonable for π-backbonding since the 3d orbitals on Mn^+ have only one electron each whereas for $CpNi^+$ they are nearly full.

Comparison of the results for Mn^+ with data for Li^+ [2], Figure 2, also shows a good linear correlation for oxygen bases. Remarkably the two nitriles in this data set are on the line with the oxygen bases. A least squares fit to the seven oxygen bases and two nitriles gives $\delta D(Li^+\text{-}L) = 0.93\delta D(Mn^+\text{-}L) + 35.3$ kcal/mol ($r = 0.98$). Here the slope shows slightly stronger binding to Mn^+ compared to Li^+ with increasing basicity suggesting that the metal-ligand bond distance for Mn^+ is slightly shorter than for Li^+.

Several bases fall off the linear correlation in Figure 2: Me_2S (7.0), benzene (3.6), NH_3 (2.7), and Me_3N (5.0) where the offset on the $\delta D(Mn^+\text{-}L)$ axis from the linear correlation is given for each molecule in parentheses in kcal/mol. The offsets toward stronger bonding to Mn^+ for Me_2S and benzene could be explained in terms of π-backbonding which certainly does not occur for Li^+ but could be of some importance for Mn^+ as suggested by the preceding discussion of the Al^+ versus Mn^+ comparison in Figure 1. However, the lack of offset for the nitriles in Figure 2 must then be regarded as bizarre since an offset is seen for the nitriles in the Al^+ versus Mn^+ comparison of Figure 1.

It is therefore reasonable to conclude that other factors in addition to π-backbonding and of comparable magnitude contribute to determining the offsets for functional group correlation lines. Such factors might include the strength of the ionic bond, bond distance, and covalent σ-bonding.

In a given correlation plot of binding energies of molecules to one metal versus those to another, it is thus to be expected that the molecules for each functional group may in general fall on different lines. Some of these

lines may happen to be approximately the same such as alcohols and esters in Figure 1 and nitriles and the oxygen bases in Figure 2. Some evidence for this view has been previously noted. In the comparison of $D(B-H^+)$ to $\delta D(Al^+-L)$ it was seen that esters fall on a line somewhat apart from the general correlation line for all bases. [3] Correlations for $CpNi^+$ versus Mn^+ and for H^+ [3] versus Mn^+ lend further support to this idea.

The variation of slopes of the linear correlations in the comparisons studied to date follow a systematic pattern. The slopes of the lines for oxygen bases for H^+, Al^+, Li^+, and $CpNi^+$ versus Mn^+ are 2.08, 1.22, 0.93, and 0.87 respectively. For nitriles these slopes are 1.63, 1,30, 0.93, and 0.79 in the same order. Slopes for all the linear correlations obtained to date are given in Table I. The results all follow the same order $H^+ < Al^+ < Mn^+ < Li^+ < CpNi^+$.

As discussed above, this order may reflect the ligand-metal bonding distance for the atomic metal cations: H^+ having the shortest effective bonding distance and Li^+ the longest. Where there is significant delocalization of charge away from the metal, as with H^+, the distance to the charge center ra-

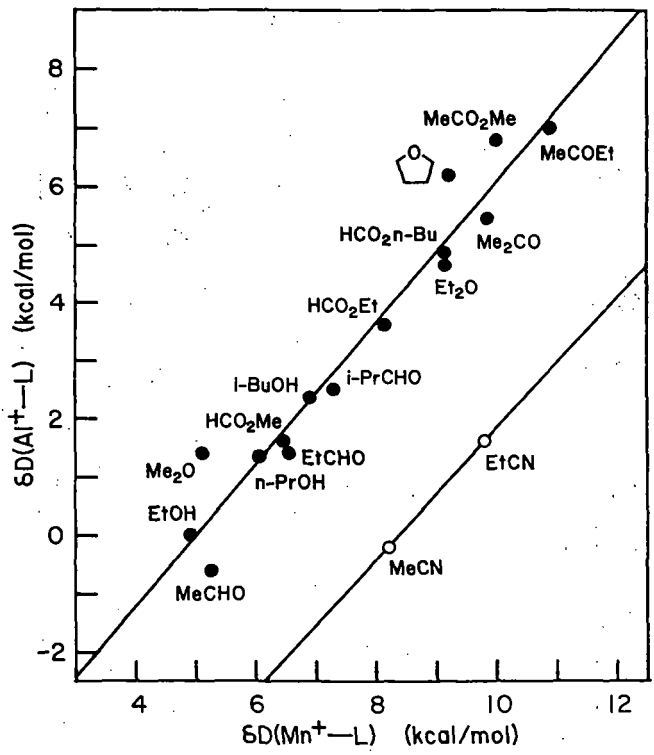

Figure 1. Comparison of relative binding energies of molecules to Al^+ and Mn^+. The upper solid line is a least squares fit to the data for the oxygen bases: $\delta D(Al^+-L) = 1.22\delta D(Mn^+-L) - 6.1$ kcal/mol (correlation coefficient $r = 0.97$). The line through the two data points for nitriles is given by $\delta D(Al^+-L) = 1.13\delta D(Mn^+-L) - 9.4$ kcal/mol. This corresponds to an offset on the $\delta D(Mn^+-L)$ axis of 3.4 kcal/mol.

ther than the bond distance to the center of the metal atom may be the controlling parameter. For $CpNi^+$ it seems likely that the slope of the correlation plot is due to another factor, the presence of a second ligand. Polarization of the $CpNi^+$ group produces an internal dipole moment which opposes the dipole moment induced in the ligand in the $CpNi(ligand)^+$ complex. This tends to cancel the favorable interaction of $CpNi^+$ charge with the induced ligand dipole. No such cancellation occurs for the atomic metal cation complexes with ligands since the atomic metal cations do not have internal dipole moments.

Two-ligand complexes of Co, Ni, and Cu cations show an interesting synergistic effect in the mixed-ligand species. In equilibrium measurements of metal-ligand bond energies, it is observed that mixed σ-base/π-base complexes are stabilized with respect to the σ/σ and π/π species. The stabilization energy is about 0.8, 1.2, and 0.9 kcal/mol for Co^+, Ni^+, and Cu^+ complexes respectively. The σ-bases include alkyl halides, alcohols, ethers, aldehydes, ketones, esters, isocyanates, and nitro compounds. The π-bases include olefins and aromatics. Similar but smaller effects are seen for sulfur bases (alkyl mercaptans and sulfides) and nitrogen bases (alkyl amines and cyanides) with both the σ-bases and the π-bases. The observation of this synergistic bonding effect constitutes a direct measurement of thermodynamic trans-influence in the relatively simple case of gas-phase two-ligand complexes.

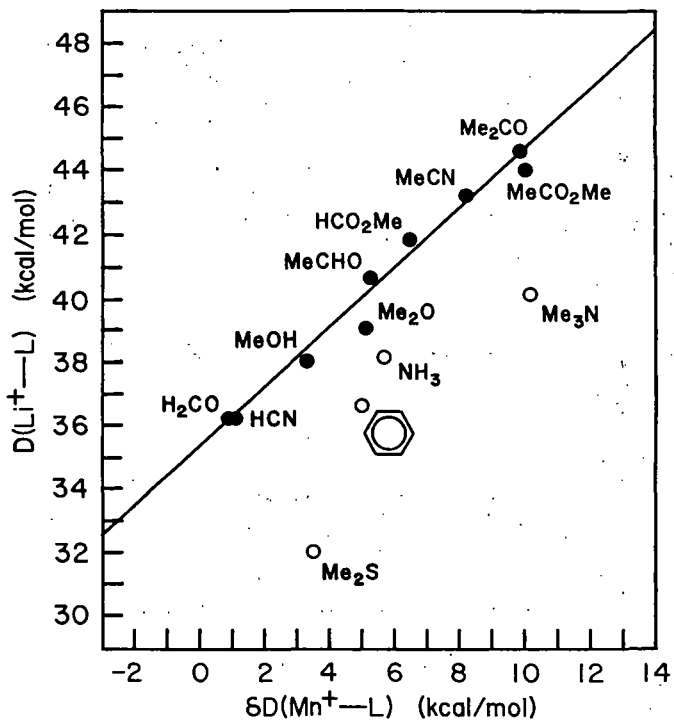

Figure 2. Comparison of relative binding energies of molecules to Li^+ and Mn^+. The solid line is a least squares fit to the data for the seven oxygen bases and two nitriles (solid circles): $D(Li^+-L) = 0.93\delta D(Mn^+-L) + 35.3$ kcal/mol ($r = 0.98$).

Table I. Slopes for Linear Correlations in Plots of Ligand Binding Energies to One Metal versus Another for Oxygen Bases.[a]

Metal Cation	Versus H^+	Al^+	Mn^+	Li^+	$CpNi^+$
H^+	1.00	1.53	2.08	2.71	3.38
Al^+	0.65	1.00	1.22	--	1.68
Mn^+	0.48	0.82	1.00	1.08	1.15
Li^+	0.37	--	0.93	1.00	--
$CpNi^+$	0.30	0.60	0.87	--	1.00

[a]Data from references 1-3 and the present work.

A number of interesting mechanistic studies have also been carried out: selected hydrocarbon-metal-cation complexes will exchange D for H when reacted with D_2. Oxidation of metal cations to metal oxide cations can be carried out by reaction with appropriate simple oxidants, e.g., N_2O or O_3. Observation of oxygen atom transfer from various oxidants to transition metal cations is used to establish upper and lower limits for metal-oxide-cation bond dissociation energies, $D(M^+-O)$. For MgO , AlO^+, MnO^+, CoO^+, NiO^+, CuO^+ and ZnO^+ the results bracket $D(M^+-O)$ between $D(O_2-O)$ = 25.5 kcal/mol and $D(N_2-O)$ = 40.0 kcal/mol. For V^+ and Fe^+ the results also bracket the bond energy in relatively narrow ranges: $D(V^+-O)$ = 135 $\pm$16 kcal/mol and $D(Fe^+-O)$ = 101 $\pm$18 kcal/mol. The VO^+ produced by reaction of V^+ with N_2O reacts with H_2 or CH_4 to give VOH^+. However, when VO^+ is produced by reaction of V^+ with O_2, D(O-O) = 119.2 kcal/mol, reaction to give VOH^+ does not occur. These results suggest that the VO^+ product of the reaction of V^+ with N_2O is an excited state species with a lifetime at least as long as the reaction time, about 150 ms in these experiments. Other mechanistic studies have been carried out, especially with the Fe^+ and FeO^+ systems. Of particular interest is the observation of catalytic reaction cycles. In nearly all of the cases observed, the overall result of the catalytic process is to transfer an oxygen atom from a neutral donor, usually N_2O, to an acceptor molecule. For example, Fe^+ reacts with N_2O to give FeO^+. FeO^+ then reacts with CO to produce CO_2, regenerating Fe^+. Similar two-step catalytic cycles involving the ions Fe^+ and FeO^+ are observed with other oxygen acceptors such as ethylene and propylene. An interesting three-step cycle occurs when acetylene reacts with FeO^+. $FeCH_2^+$ is found as a second intermediate. Both CO and CH_2O are formed in the overall process. Five other transition metal systems examined, Ti, V, Cr, Zr, and Nb, all show two-step cycles with MO^+ and MO_2^+ intermediates but not with M^+ and MO^+.

(1) Corderman, R.R.; Beauchamp, J.L. J. Am. Chem. Soc. 1976, 98, 3998.

(2) Staley, R.H.; Beauchamp, J.L. J. Am. Chem. Soc. 1975, 97, 5920.

(3) Wolf, J.F.; Staley, R.H.; Koppel, I.; Taagepera, M.; McIver, R.T. Jr.; Beauchamp, J.L.; Taft, R.W. J. Am. Chem. Soc. 1977, 99, 5417.

ION BEAM STUDIES OF REACTIVE INTERMEDIATES IN ORGANOMETALLIC CHEMISTRY; J. L. BEAUCHAMP, L. F. HALLE and P. B. ARMENTROUT; Dept. of Chem., Calif. Inst. of Tech., Pasadena, CA 91125

An ion beam apparatus has been used to examine the reactions of atomic transition metal ions and clusters with small organic molecules. Thresholds for endothermic reactions yield bond dissociation energies. Reaction mechanisms are inferred by examining product distributions as a function of relative kinetic energy in conjunction with isotopic labelling experiments and thermochemical arguments. The use of surface ionization to generate atomic transition metal ions yields mainly ground state reactants. Electron impact fragmentation of organometallic compounds and collisional excitation processes yield excited state species with remarkably different reactivity. These results will be reviewed with an emphasis on periodic trends in thermochemical properties and reactivity.

SIMS of Alkali Halides: Stability of High Mass Clusters, T. M. Barlak, J. E. Campana, R. J. Colton, J. J. DeCorpo, and J. R. Wyatt, Naval Research Laboratory, Chemistry Division, Washington, DC 20375.

A high-performance secondary ion mass spectrometry (SIMS) instrument described elsewhere[1,2] was used to examine the alkali iodides (MI). The high ion transmission and high-mass capabilities of this instrument permitted recording of alkali iodide cluster ion intensities of the form $[M(MX)_n]^+$ from Ar^+ bombardment to n=22 for NaI and KI; n=19 for CsI; n=16 for RbI; and n=2 for LiI. Using Xe^+ primary ions permitted extension of these measurements to n=36 for NaI and n=70 for CsI.

The recorded mass spectra generally decreased with increasing n except for obvious anomalies as seen in the figure. Various instrumental properties such as spectrometer transmission and the ion-to-electron conversion efficiency of the particle multiplier were eliminated as possible causes of the anomalies. Similarly, ion formation and emission processes such as beam-surface interactions and target composition and structures were also eliminated. The anomalies were finally explained by cluster stability. The cubic structure consisting of three atoms per edge (i.e., 3x3x3) corresponds to the intense n=13 cluster. Similarly the (3x3x5) structure correlates with the n=22 intensity. The enhanced intensity expected for the n=4 (3x3x1) cluster was not observed for the alkali iodides. This condition is attributed to effects of ion radii on the atomic lattice spacing and cluster stability.

Less pronounced cluster ion peaks were observed at n=6, 9, and 12. The n=6 peak was associated with a hexagonal structure postulated by Martin.[3] The n=9 and n=12 clusters are thought to be formed by addition of hexagonal rings to the n=6 structure.

The bulk structure of cesuum iodide is body centered cubic (bcc), but cubic-like structure account for the observed cluster intensity distribution. In particular, the anticipated n=7 bcc structure was not observed to be intense.[4] These results favor initial CsI crystal growth in other than bcc form.

The unimolecular decomposition of metastable ion clusters formed during SIMS were observed for the first time. Voltage scanning permitted determination of the parent ion.

The large number of atoms in the alkali iodide clusters supports a direct emission mechanism of sputtering for alkali iodides.

1. R. J. Colton, J. E. Campana, T. M. Barlak, J. J. DeCorpo, and J. R. Wyatt, Rev. Sci. Instrum., 1980, 51, 1685-1689.
2. T. M. Barlak, J. R. Wyatt, R. J. Colton, J. J. DeCorpo, and J. E. Campana, submitted for publication.
3. T. P. Martin, J. Chem. Phys., 1980, 72, 3506-3510.
4. T. P. Martin, J. Chem. Phys., 1978, 69, 2036-2042.

$[Cs\ (CsI)_n]^+$
4.7 KeV Xe^+ PRIMARY BEAM
0.3 KeV SECONDARY IONS

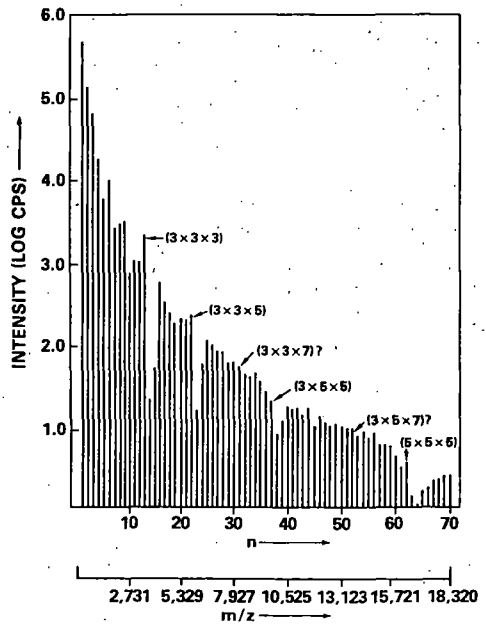

$[M\ (MX)_n]^+$ STRUCTURES

CUBIC

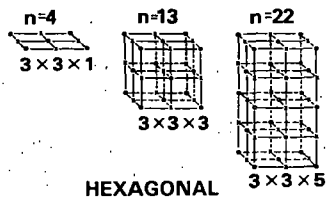

HEXAGONAL

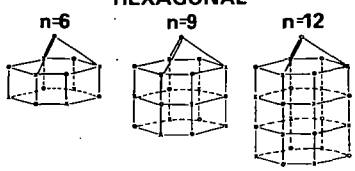

SECONDARY ION MASS SPECTROMETRY OF SMALL-MOLECULE SOLIDS AT 15K: CLUSTER FORMATION

Robert G. Orth and Josef Michl

Department of Chemistry
University of Utah
Salt Lake City, Utah 84112

The first results on secondary ion mass spectrometry (SIMS) of cryogenic solids, such as solid N_2 and solid CO, have appeared recently.[1] We now report the SIMS of a series of additional molecular solids: rare gases, nitrogen oxides, oxygen, CO_2, COS, and CS_2. With the heavier primary ions, extensive positive and negative cluster ion formation is observed up to the mass limit of the instrument (1000 amu), particularly at higher primary ion energies. An example is shown in Fig. 1. The repeating unit in the clusters does not always reflect the stoichiometry of the molecular solid. Thus, for nitrogen oxides, even for N_2O and NO, the prevalent clusters are $NO^+(N_2O_3)_x(N_2O_4)_y$. A hypothesis for the origin of such clusters will be presented.

The effect of dilution of H_2O and CO_2 by an inert gas solid have also been investigated. At matrix-isolation ratios of about 500:1 or higher, clusters of the solute are no longer observed and a simple mass spectrum of the matrix-isolated species is obtained, along with clusters of ion originating from the solute with the matrix gas (argon).

---

[1] H.T. Jonkman and J. Michl, J. Am. Chem. Soc., 103, 733 (1981); R.G. Orth, H.T. Jonkman, and J. Michl, J. Am. Chem. Soc., 103, 1564 (1981). See also, H.T. Jonkman, J. Michl, R.N. King, and J.D. Andrade, Anal. Chem., 50, 2078 (1978).

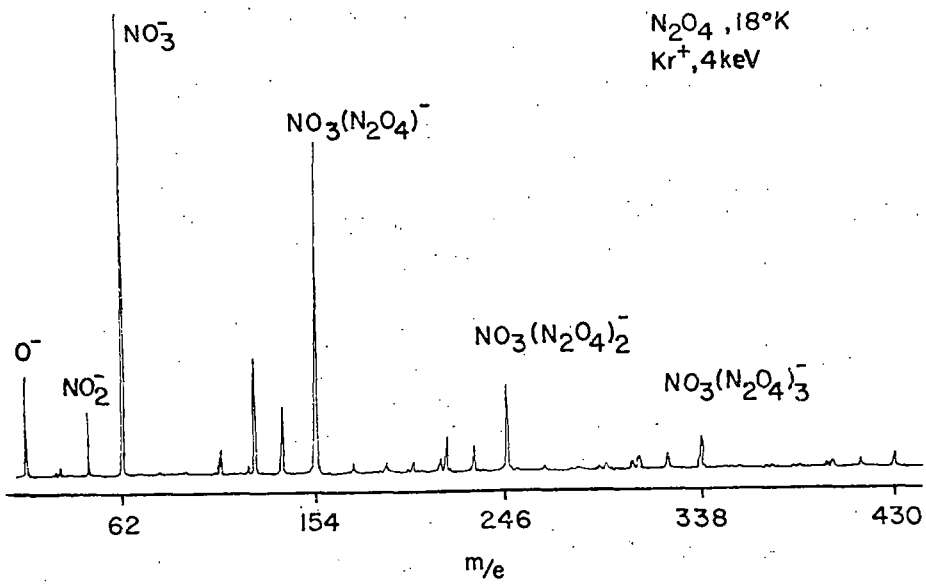

Figure 1.

SECONDARY ION MASS SPECTROMETRY OF FROZEN AQUEOUS SOLUTIONS

Robert G. Orth and Josef Michl

Department of Chemistry
University of Utah
Salt Lake City, Utah 84112

The characterization of nonvolatile organic and inorganic species by mass spectrometry has become a major area of interest due to the large number of important compounds which fall into this category and cannot be examined easily by standard mass spectrometry. Several methods, such as field desorption, plasma desorption, or secondary ion mass spectrometry (SIMS), have been developed for ionizing these compounds. They generally require removal of any solvent from the sample to be analyzed.

Recently, the feasibility of SIMS matrix isolated species has been demonstrated.[1] The spectra contain peaks due to the matrix and peaks due the solute. For sufficiently large matrix isolation ratios, the spectra of the solute do not contain ions originating in more than one solute molecule. So far, the matrix materials were the solid inert gases. We now wish to report the SIMS of solutes in other matrices such as ice. In these cases, the SIMS of the matrix by itself is more complex but can still be interpreted without much trouble. Thus the SIMS of a frozen 0.01M aqueous solution of $Ca(OH)_2$ contains the readily identified matrix cluster ions $H^+(H_2O)n$ and also peaks for Ca^+ and $[Ca(OH)(H_2O)n]^+$, $n \geq 0$ (Fig. 1). Similarly, a frozen 10^{-3}M aqueous solution of CsCl yields the $Cs^+(H_2O)n$, $n \geq 0$ ions. At very high concentrations (1M), cluster ions containing two cesium atoms are also observed. The ions H_3O^+ and, depending on experimental conditions, $H^+(H_2O)n$, which are present as well, are due to the ice matrix (Fig. 2).

Positive and negative SIMS results on frozen solutions of a series of nonvolatile inorganic salts will be presented and their analytical implications will be discussed.

---

[1] H.T. Jonkman and J. Michl, J. Chem. Soc., Chem. Commun., 751-2 (1978); R.G. Orth, H.T. Jonkman, D.H. Powell, and J. Michl, J. Am. Chem. Soc., in press.

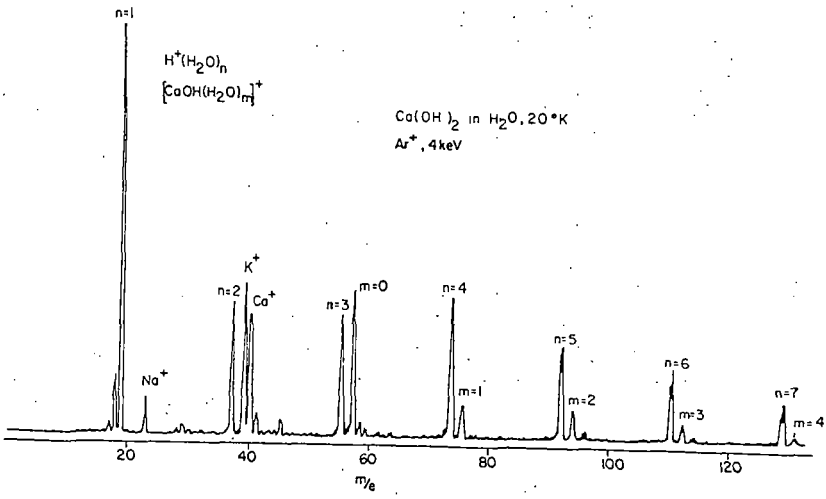

Figure 1.

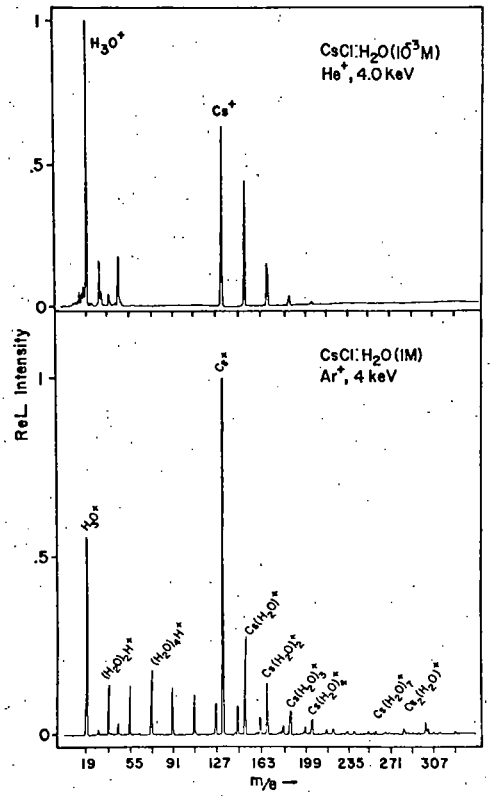
CsCl:H2O(10^-3M)
He+, 4.0 KeV
H3O+
Cs+
CsCl:H2O(1M)
Ar+, 4 keV
Rel. Intensity
m/e
19
55
91
127
163
199
235
271
307

Fig. 2

Intensity Calibration Standards for Molecular SIMS, J. E. Campana, J. J. DeCorpo, J. R. Wyatt, and R. J. Colton, Naval Research Laboratory, Chemistry Division, Washington, DC 20375.

Mass reference compounds and ion intensity calibration standards have been the subject of considerable interest in mass spectrometry for a number of years. Recently this interest has been directed toward a search for high-mass reference compounds and ion intensity calibration standards for quadrupole mass spectrometers. This paper addresses both of these types of calibrants with respect to secondary ion mass spectrometry (SIMS) and fast atom bombardment (FAB) or more precisely neutral atom bombardment.

The quadrupole mass analyzer is currently the most widely used analyzer for low-mass resolution applications in mass spectrometry and SIMS. While it has many advantages, it suffers from two disadvantages related to ion transmission; that is, ions of different mass and energy do not necessarily have the same transmission through the quadrupole field and this gives rise to so called mass and energy discrimination which leads to incorrect ion abundance measurements.

The ion abundance calibration problem has been neglected in SIMS. The advent of the new beam excitation techniques of molecular SIMS and FAB has produced a requirement for mass reference compounds and ion abundance calibrants. Recently we have described a high-performance SIMS instrument based on a double-focusing mass analyzer.[1] This instrument is relatively free from discrimination effects. We propose that data generated with this instrument be used as ion abundance calibrants in quadrupole SIMS and as high-mass references in SIMS and FAB.

Ion bombardment of alkali iodides (MI) produces clusters of the type $[M(MI)_n]^+$ and $[I(MI)_n]^-$, where n=1-70 for certain alkali iodides. We propose the use of Na_nI as an ion abundance calibrant for quadrupole SIMS instruments. Statistically significant data on NaI cluster intensities to m/z 1073 is presented in Table 1 for one of the many sets of data we have analyzed. The instrumentation and data reduction techniques were tested by measuring the isotope ratios of the silver monomer and trimer. We have used this data to calibrate a quadrupole SIMS instrument for ion abundance measurements. Table 2 lists intensity values 1-7 of three peak ratios which were obtained at seven different ion optic and quadrupole controller settings. The variation of the peak ratios of m/z 46/323 varies by a factor of more than 25. This illustrates the discrimination problem. Experiment 4 shows that the quadrupole can be tuned to give ion abundances close to those obtained with the double-focusing instrument. The quadrupole was tuned by monitoring the m/z 46, 173, and 323 peak heights while tuning the electronics. The ratio of m/z 323/150 was then measured as an unknown and its value fell within the confidence limits of the double-focusing value.

NaI can produce clusters spaced nominally 150 mass units and CsI gives clusters spaced 260 mass units. NaI data has been obtained to m/z > 5000 and CsI data is shown in Figure 1 to m/z > 18,000. These can serve as mass references in both high-performance SIMS and the related technique of FAB.

1. R. J. Colton, J. E. Campana, T. M. Barlak, J. J. Decorpo, J. R. Wyatt, Rev. Sci. Instrum. 1980, 51, 1685-1689.

Table 1.

Peak Ratio	Value	Peak Ratio	Value	Peak Ratio	Value
173[a]/46[b]	7.01 ± 0.20	323/473	8.33 ± 0.61	773/923	1.25 ± 0.22
46/323	1.56 ± 0.08	473/623	2.64 ± 0.29	923/1073	1.44 ± 0.31
173/323	11.2 ± 0.2	623/773	3.06 ± 0.54	373/150[c]	15.6 ± 1.5

a. m/z_+ correspond to $[Na(NaI)_n]^+$ where n=1-7
b. Na_2^+
c. $[NaI]^+$

Table 2. Calibration of Quadrupole SIMS Instrument for Ion Abundance Measurements.

Peak Ratio	Double-Focusing	1	2	3	4	5	6	7
$\frac{46}{323}$	1.58 ± 0.07	0.50	0.88	0.98	1.43	1.64	9.64	13.2
$\frac{173}{46}$	7.23 ± 0.27	21.0	6.66	2.74	7.73	17.4	1.69	1.79
$\frac{173}{323}$	11.2 ± 0.2	10.5	5.84	2.67	11.0	28.5	16.3	23.6
$\frac{323}{150}$	19.7 ± 2.3	-	-	-	21.0	-	-	-

1-3 Low-mass adverse discrimination
5-7 High-mass adverse discrimination
4 Acceptable calibration
$\frac{373}{150}$ Ratio was determined after calibration

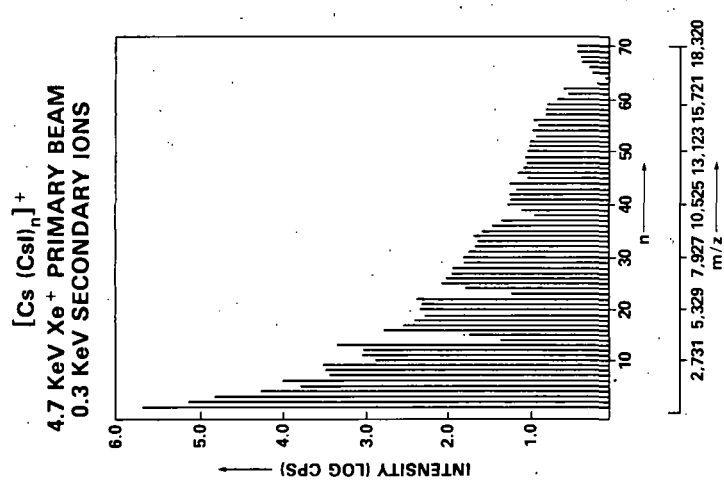

Figure 1.

QUADRUPOLE SIMS: FUNDAMENTAL PRINCIPLES, PREFILTER TRANSMISSION CHARACTERISTICS AND PERFORMANCE CHARACTERISTICS; GENE R. SPARROW; *Advanced R&D, Inc.*, 245 East Sixth Street, Suite 807, St. Paul, MN 55101; JOHNIE BROWN; Kratos Scientific Instruments, 24 Booker Street, Westwood, NJ 07675

The development of SIMS instrumentation requires an understanding of the effect of certain parameters on the secondary emission of ions from surfaces. These parameters originate either from sample effects or from instrumental effects. Sample effects include ion yields, sputtering yields, damage cross sections, induced reactions, matrix effects, ion energy distribution, morphology and surface chemistry. These can be varied to some extent using reference materials, but they are more often very complex interactive unknown parameters. Instrumental parameters affecting results include the characteristics of the ion beam, vacuum system, optics geometry and especially the geometry of the ion prefilter.

As the probe beam size is decreased, not only do ion yield statistics become more prominent, but the effects of surface morphology and chemistry become very critical. Spectral variations are also affected by whether "static" SIMS or conventional SIMS techniques are employed. Both differentially pumped ion guns and back-filled systems were employed in these studies. This paper discusses SIMS studies utilizing low energy ion beams of 30 μm diameter to approximately 1 mm. Measurements of Secondary Ion Energy Distributions and Ion Prefilter Transmission characteristics will also be presented.

ANALYSIS OF POLYMERS BY PYROLYSIS MASS SPECTROMETRY

D.C. CONWAY and ROMAN MARAK

Dept. of Chem., Texas A&M Univ., College Station, Texas 77843

A time-of-flight mass spectrometer has been constructed in which the mass spectrum is collected in a multichannel analyzer. Ion flight times are converted to pulse heights with a time-to-amplitude converter. The spectrum is processed by a microcomputer--dual floppy disk data system to obtain the integrated peak intensities. This type of instrument has the advantage that one ion in the mass range (typically 20-740 amu) can be detected every 80 microsec, whereas only one peak can be measured at a time in magnet or quadrupole mass spectrometers. This property is particularly advantageous where the mass spectrum is changing rapidly, such as in rapid pyrolysis.

Several synthetic polymers were analyzed by pyrolysis mass spectrometry using chemical ionization with 0.5 torr Ar and a trace of isopentane. When this gas mixture is ionized, the original Ar^+ ions rapidly react with the isopentane to produce mostly $C_5H_{11}^+$. The $C_5H_{11}^+$ ions usually ionize molecules with very little fragmentation by proton transfer. The pyrolysis of addition type polymers (polystyrene and polypropylene) yielded rather simple spectra. The main peaks were HM_n^+ peaks (M=monomer), but there were other peaks corresponding to different ruptures along the carbon chain backbone. The pyrolysis of simple condensation type polymers (Mylar and Nylon-66) were also easy to interpret, since there were many peaks at ±1 or -3 mass units from fragments of the polymer chain. The pyrolysis of polyurethanes yielded more complex spectra, which were difficult to interpret.

The results obtained for polystyrene will be described in more detail. The main peaks were HS_n^+ ($S \equiv C_8H_8$) where n=1-3 for a pyrolysis temperature of 406°C. There were several less intense peaks due to charge transfer (S_n^+, n=1-3) and an unresolved peak ($S_4^+ + HS_4^+$). Among the other ions produced were CH_3S^+ and $CH_3S_2^+$, which contain an odd number of C atoms from the backbone, and $C_2H_3S^+$ and $C_2H_3S_2^+$, which have an even number of backbone C atoms, but have each lost a $C_6H_5\cdot$ radical. The carbonium ions are expected to have rearranged to their most stable structures, e.g.

CH_3S^+ is $CH_3\text{-}\overset{+}{\underset{\phi}{C}}\text{-}CH_3$ and $C_2H_3S^+$ is $CH_2{=}CH\text{-}\overset{+}{\underset{\phi}{C}}\text{-}CH_3$, etc.

A TECHNIQUE OF FOCUSED CRYOGENIC TRAPPING FOR HEADSPACE AND PYROLYTIC ANALYSIS OF POLYMERS ON A FUSED SILICA CAPILLARY COLUMN

James G. Moncur, Terry E. Sharp, Leroy M. Law, Lockheed Missiles & Space Company, Inc., Palo Alto, CA 94304

INTRODUCTION

In the analysis of high molecular weight organic polymers, thermal degradation has been used to produce low molecular weight products. The complex mixture of degradation products has traditionally been analyzed by gas chromatography or mass spectrometry. Using packed column GC and flame ionization detection, Hu[1] has shown that useful simplification results when the thermal degradation is conducted in two steps, 1) a low temperature thermolysis to drive off volatiles for analysis, followed by 2) a high temperature pyrolysis to degrade the polymer backbone into low molecular weight compounds for analysis. In the present work, this two-stage thermal degradation is combined with the improved resolving power of a fused silica capillary column (FSCC) and the identification capability of a computerized, fast scanning quadrupole mass spectrometer. Thermolysis is conducted for an extended period to insure complete stripping of volatiles from the sample; these volatiles are trapped directly inside the fused silica capillary column. This focused cryogenic trapping procedure permits clean injection of the sample and enhanced resolution and sensitivity as shown by Trussell, Moncur, et al[2,3] for analysis of priority pollutants. (These papers demonstrated separation of a mixture compounds ranging from methyl chloride (BP -25°C) to polynuclear aromatics (MW 278), and proved the inertness of FSCC's toward acidic and basic, polar and nonpolar organic compounds at picogram levels). The mechanical properties of the FSCC allow a loop to be formed in the column for immersion in liquid nitrogen for focused cryogenic trapping and also allow the capillary column to be coupled directly to the mass spectrometer (see Fig. 1). The full capabilities of the capillary GC/quadrupole MS/data system have proved to be highly useful in troubleshooting applications of complex industrial polymer products.

RESULTS

Chromatographic comparisons of focused cryogenic trapping versus no trapping were performed on a readily available room temperature cure epoxy, (see Fig. 2). Figure 3 illustrates the ability of liquid nitrogen to trap and optimize chromatographic resolution on volatiles generated from heating at 250°C for 15 minutes. The compounds seen in this headspace analysis may arise from a number of sources: unreacted and age-created monomers, processing solvents and contaminants, plasticizers, and antioxidants. Figure 4 illustrates the high degree of chromatographic resolution and sensitivity available when pyrolyzing into FSCC's with focused cryogenic trapping. The identifications of compounds 53 and 56 exemplify the power of the pyrolysis technique for polymer structure identification using a 600°C temperature. An absence of focused cryogenic trapping during the pyrolysis step results in some coelution of very early eluters but is not shown here.

EXPERIMENTAL

A pyrolyzer (Chemical Data Systems Pyroprobe, Model 100) is attached to the injector assembly of a gas chromatograph/mass spectrometer (Finnigan, Model 4021). The inlet of a polymide coated, fused silica capillary column (J&W Scientific, Model SE54-30N) is directly coupled to the capillary injector. This open tubular column, 30m long X 0.25mm ID, is coated with SE-54 stationary phase. The outlet of the column is threaded into the ion source region of the mass spectrometer. At a pressure of 7.5 psi, helium carrier gas sweeps the pyrolyzer and enters the injector, where the flow is split and enters the column for analysis. Split ratio and column heating conditions are adjusted to optimize experimental results. The mass spectrometer is run in electron impact mode, emission current 0.5mA, electron energy 70eV, with scanning from mass 33 to 533 in 0.95 seconds and a 0.05 second hold at the bottom.

REFERENCES

1. Hu, John Chih-An, Anal. Chem., 49, 4, April 1977, 537.
2. Trussell, Albert R.; Moncur, James G.; and Lieu, Fong-Yi, "Parts-Per-Trillion Analysis of Volatile, Base/Neutral, and Acidic Water Contaminants on a Single Fused Silica Capillary Column", Identification and Analysis of Organic Pollutants in Water, Vol. II, L. Kieth, Ed., (Ann Arbor Science), 1981.
3. Trussell, Albert R.; Moncur, James G.; Lieu, Fong-Yi; Leong, Lawrence Y. C., "Simultaneous Analysis of All Five Organic Priority Pollutant Fractions", Journal of High Resolution Chromatography & Chromatographic Communications, April 1981.

FIG 1

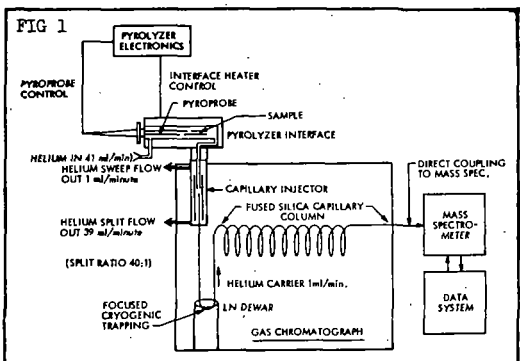

FIG 2

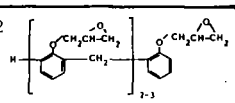

POLYGLYCIDYL ETHER OF A PHENOLFORMALDEHYDE NOVOLAC

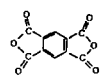

PYROMELLITIC DIANHYDRIDE

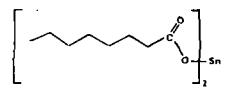

STANNOUS OCTANOATE

FIG 3

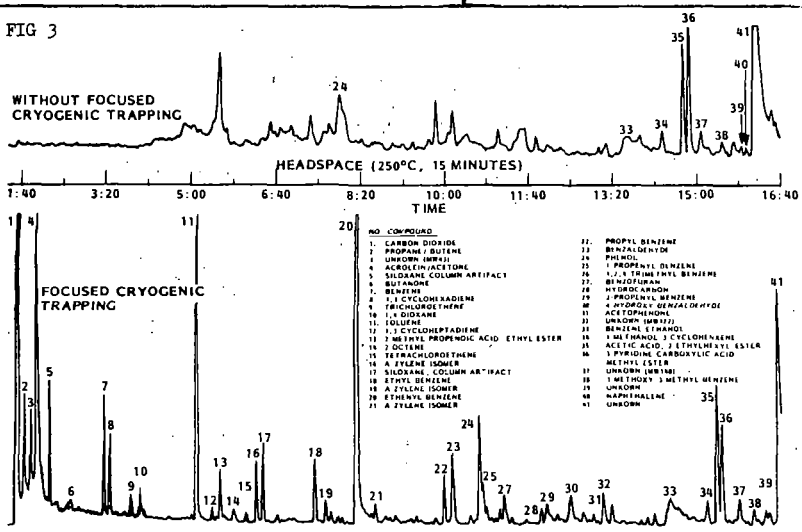

FIG 4

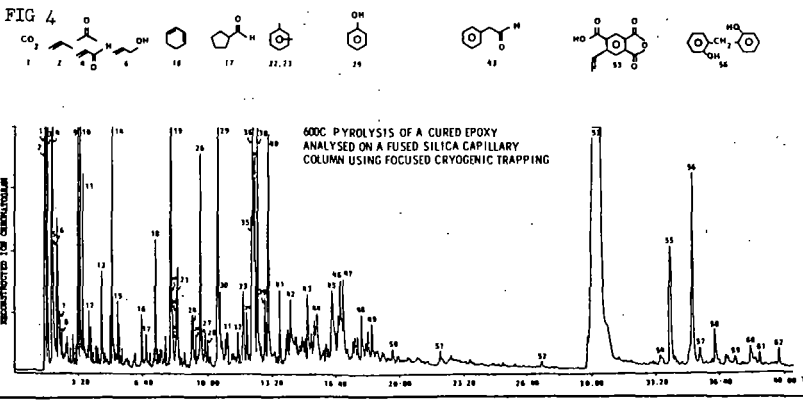

THIS PAGE LEFT
INTENTIONALLY BLANK

THERMAL ANALYTICAL CHARACTERIZATION OF POLYMER COATED PAPER

by

J. A. Nikora, C. M. Yavornitzky & R. A. Yount

THE BFGOODRICH CHEMICAL GROUP
Avon Lake Technical Center
P. O. Box 122
Avon Lake, Ohio 44012

As part of a recent program to develop an ovenable polymer coating for paper board food containers, it became necessary to characterize the thermal off-gases from several paper boards, a styrene-ethyl acrylate copolymer, polyester terephthalate (PET), and the polymer coated papers. The emphasis of the study was directed at determining the thermal stability of the coated paper boards which were being designed for frozen and baked goods and for microwave as well as conventional oven heating to temperatures of 260°C. Thermal stability was examined in terms of off-gas identification and semi-quantitation, weight loss as a function of time and temperature, smoke generation under smoldering and combusting conditions, and product self- and flash ignition temperatures. The temperature ranges selected for study were to simulate normal and extreme cooking conditions as well as severe partial combustion conditions.

Weight loss - temperature or time profiles of the uncoated and coated paper boards were determined by TGA with programmed and isothermal heating. Standard headspace- and pyrolysis - GC/MS with a calibrated CDS 120 Pyro-probe interfaced to a gas chromatograph and a DuPont 21-490 mass spectrometer and data system were utilized to identify the off-gases at temperatures up to 550°C. Small pieces (15g) of the coated paper boards were heated in a Potts furnace in the NBS smoke chamber to provide quantitative data for aliphatic and aromatic hydrocarbons, CO, CO_2, HCl, and SO_2. Smoke density measurements in optical density units were made at 90s, 4m and at the maximum attained smoke density under smoldering and combusting conditions. ASTM test D1929-B was used to determine the self and flash ignition temperatures of the samples. In this test, 2.5 g samples are heated with hot air flowing at the rate of 1.5m/min. as measured at a 25mm orifice. The flash ignition tests use a small pilot light downstream of the sample to ignite the thermally released off-gases.

TGA measurements were made in 20% O_2-helium mixtures at 220° and 260°C for 1-2h and at a programmed heating rate of 10C°/min to 525°. In the programmed heating mode, rapid thermal degradation (weight loss) for the two polymer systems occurs between 400 and 420°C with a leveling off at 450°C. Rapid thermal degradation of the uncoated paper boards commenced at 360°C and was complete by 390°C. The TGA profiles obtained from the polymer coated boards were identical to the uncoated boards with the major sample degradation occurring between 360 and 390°C. Above 400°C, only minor differences attributed to polymer degradation were observed. Isothermally at 260°C, 5-6% weight losses were observed for 2h heating periods with only slight discoloration of the coated paper boards being observed.

Qualitative GC/MS measurements of the off-gases were made on a 4.9m SS Porapak QS gc-column. The major thermal off-gas materials were correlated with the TGA weight loss values at the specified temperatures. Headspace - GC/MS analyses of the copolymer and coating compound indicated the following organic materials: at 95°C - ethanol, acetone, t-butanol, ethyl propanoate and ethyl benzene; at 315°C - same plus SO_2, acetaldehyde, ethyl chloride and styrene. Ethanol, ethyl propanoate and ethyl benzene are monomer impurities. The major off-gases obtained from the paper boards at 315°C are: CO_2, H_2O, acetaldehyde, furan, furfural and methyl furfural. At 315°C, the only off-gases observed

from the PET polymer are CO_2 and H_2O. At higher temperatures, the major off-gas was acetaldehyde. PET coated paper board produces only the paper degradation products at 315°C. Analyses of the polymer coated paper boards correlated well with the TGA results, i.e., for temperatures below about 375°C, the only identifiable off-gas materials result from the paper degradation and not from the polymer coatings.

The following tables summarize the analytical results obtained from the NBS smoke chamber measurements and the ignition temperature studies.

SMOKE CHAMBER OFF-GAS QUANTITATION

Smoldering, PPM	CO	CO_2	ARO	ALI	HCL	SO_2
Paper Boards	4800	10100	325	80	32	28
Copolymer-Board	4600	10000	380	100	30	28
PET-Board	4800	11200	280	75	40	30
Combusting, PPM						
Paper Boards	1600	19900	295	45	40	<10
Copolymer-Board	1550	24600	365	55	45	<10
PET-Board	1600	25700	340	50	60	<10

CHAMBER SMOKE DENSITY MEASUREMENTS

Smoldering, O.U.	Ds (90s)	Ds (4m)	D max	Time to Max.
Paper Boards	24	25	390	18 m
Copolymer Boards	24	25	420	19 m
PET-Board	27	30	380	27 m

Combusting, O.U.	Ds (90s)	Ds (4m)	D max	Ignition time
Paper Boards	21	26	123	34s
Copolymer Board	28	30	154	50s
PET-Board	21	23	34	18s

ASTM TEST D1929-B IGNITION TEMPERATURES

	Flash Ignition, °C	Self Ignition, °C
Paper Boards	355	395
Copolymer Boards	370	405
PET-Board	370	400

The combined analytical techniques of TGA and GC/MS along with the results obtained from NBS smoke chamber measurements and ignition tests have established the upper temperature limit for polymer coated papers at about 350°C. Above 350°C, the papers rapidly degrade prior to the onset of polymer degradation. No unusual organic off-gases were observed in the designed temperature range of usage.

Some Examples of Californium-252 Time of Flight Mass Spectrometry

C. J. McNeal, R. D. Macfarlane and H. M. Fales
Dept. of Chemistry, Texas A&M University, College Station, Texas 77843

and National Heart, Lung, and Blood Institute, Bethesda, MD 20205

A second generation ^{252}Cf time of flight mass spectrometer has been constructed embodying improvements in pumping and sample handling, and using a new faster and more accurate digitizer. Some applications to samples originating at NIH are described below:

1. A sample of digitonin (1) was dissolved in hot, deuterated dimethylsulfoxide for nmr purposes. After recovery from the solvent, the sample was found to be much more soluble in water than the original digitonin. No change in the nmr spectrum was visible. ^{252}Cf-mass spectrometry showed the sample to be identical in mass (M+Na 1252.35, calc. 1252.31) and fragmentation (M-sugar A=1090; M-sugar B=1188) with the original. Traces of cholesterol, etc., have an enormous effect on the solubility of digitonin and it is considered likely that such an impurity was removed by the dimethylsulfoxide treatment.

- H. Yeh (NIAMDD) and N. Cornell (NIAA)

2. A complex of aminorhodomine and dexamethazone bridged by a thioethylthiourea link was prepared for use as a fluorescent tag for steroid receptor sites in vivo. The usual methods of characterization (nmr, etc.) were not effective. Nevertheless, ^{252}Cf spectrometry revealed the compound to be substantially one material (MH^+ 895.54, Calc. 895.35) with fragmentation at the aminorhodamine-thiocarbonyl bond (m/z 402). A trace impurity of desmethyl aminorhodamine (m/z 388) may also be present.

- S. Sims (NIAMDD)

3. A series of synthetic encephalin analogues have been prepared and identified using ^{252}Cf. Their general structures are:

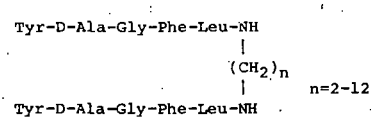

The peptides (both free and t-BuOCO-blocked) all show intense M+Na ions (e.g. n=8, 1270.07, Calc 1270.54) as well as smaller peaks for cleavage on both sides of every alpha carbon, amino, and carbonyl group, revealing the sequence.

Y. Shimohigashi (NICHHD)

FAST HEAVY IONS INDUCED DESORPTION MASS SPECTROMETRY OF NUCLEOSIDES MODIFIED BY CARCINOGENIC POLYCYCLIC HYDROCARBONS

S. Della Negra*, Y.M. Ginot**, Y. Le Beyec*, M. Spiro**, and P. Vigny**

*Institut de Physique Nucléaire, B.P. 1, 91406 Orsay, France
**Institut Curie and Université Paris VI, 75231 Paris Cedex 05, France

The heavy ions desorption mass spectrometry (1) is currently used in our laboratories to investigate molecular structures and masses (2). The method has been applied to the fundamental problem of DNA chemical modifications induced by carcinogenic polycyclic hydrocarbons. Such compounds are known to be activated *in vivo* into ultimate carcinogens which are able to react as electrophiles at various nucleophilic sites on DNA. Attention has been focused recently on these modifications since they constitute the primary step in the induction of a mutation and thus trigger a series of events leading to a transformed cell. Numerous studies have brought the evidence that the main pathway in the *in vivo* metabolic activation of polycyclic hydrocarbons is the conversion of the molecules into specific diol-epoxides. These species give rise to a carbocation that reacts further with DNA. Physico-chemical techniques have been looked for to investigate this problem at the molecular level. Among them, photon-counting fluorimetry has assisted in identifying the metabolites involved in the reaction with DNA (See for example references (3) and (4)). Attempts have been made to identify the major adducts of *in vitro* reactions of the ultimate carcinogens with DNA, after enzymic degradation to nucleosides. Nuclear magnetic resonance has thus allowed to solve the structure of the major guanosine adducts after the chemical attack of DNA by Benzo(a)pyrene-7,8-diol 9,10 oxide. This was confirmed by mass spectrometry studies obtained after derivatization of the adducts (5). We wish to report preliminary results obtained with underivatized adducts by using ^{252}Cf Plasma Desorption Mass Spectrometry.

Samples were prepared in collaboration with the group of Prof. P. Sims and Dr. P.L. Grover (Chester Beatty Research Institute, London). Benzo(a)pyrene-7,8-diol 9,10 oxide (BPDE) and Benz(a)anthracene-8,9-diol 10,11 oxide (BADE) were prepared from the corresponding diols and reacted with DNA (Salmon sperm, type III) obtained from Sigma Chemical Co. and deproteinized before use. DNA was then enzymically hydrolysed to nucleosides and chromatographed on Sephadex LH20 columns that were eluted with water-methanol gradients under gravity. Eluent fractions containing nucleoside-hydrocarbon adducts that were to be analysed further were pooled and then further purified by high pressure liquid chromatography (HPLC) using a Dupont Model 848 and a Zorbax ODS column. The fluorescence of the eluted fractions was monitored.

A few µg of the products are deposited by electrospray onto a thin metallic foil and bombarded in the mass spectrometer by the fission fragments of a ^{252}Cf source (2). The ionized and desorbed molecules are accelerated by a 10 KV acceleration voltage and time of flight spectra are measured by means of standard nuclear electronics. It includes two timing discriminators, time amplitude converter, analogic digital converter and multichannel analyser (4000 or 8000 channels). For some spectra the time amplitude converter was replaced by a new one start-multistop module (6). The spectrometer is connected to an IBM computer so that the spectra can be stored on disk for subsequent analysis.

In a first step we modified DNA by Benzo(a)pyrene-7,8-diol 9,10 oxide (BPDE). We isolated and purified the major adduct which is known to be a guanine adduct involving a binding between BPDE and the exocyclic amino group of the purine. Its mass spectrum can be observed with ^{252}Cf Plasma Desorption Mass Spectrometry. Fragmentation occurs giving rise to peaks around $M \sim 200$ to 250 corresponding to the hydrocarbon skeleton. This is confirmed by the fact that a similar pattern is observed with the tetrol of Benz(a)pyrene. However the main feature of the BPDE-guanine adduct is that molecular ions are observed (Figure 1) at M = 592 and 615 corresponding to Na ions attachments.

In a second step we have undertaken a detailed study concerning the binding reaction of Benz(a)anthracene-8,9-diol 10,11 oxide to DNA. This intermediate species (BADE) is of importance since it has been shown recently to bind covalently *in vivo* to DNA (3) and since it is not a bay-region diol-epoxide. Such a behaviour might be related to the

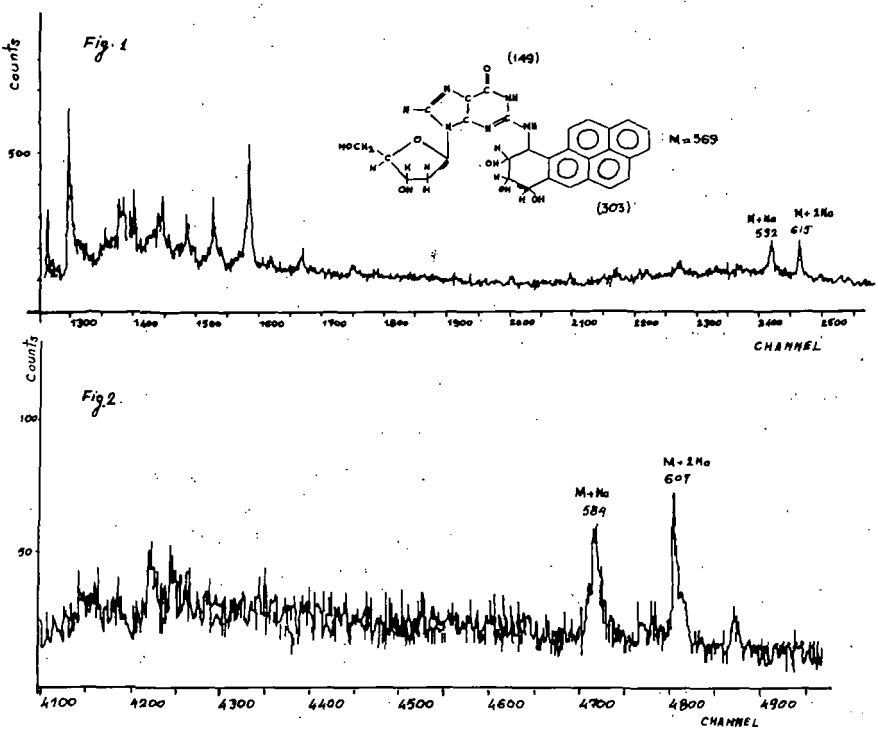

fact that Benz(a)anthracene is only a poor carcinogenic hydrocarbon. It is therefore of interest to know more about the binding properties of BADE. We have thus prepared guanine-BADE and adenine-BADE adducts to check if underivatized products from Benz(a) anthracene could be studied by ^{252}Cf Plasma Desorption Mass Spectrometry. As an example, Figure 2 shows that guanine-BADE also gives molecular ions. Work is now in progress to investigate the complete reaction of the non-bay region diol epoxide of Benz(a)anthracene with DNA.

This work shows that heavy ions desorption mass spectrometry allows polycyclic hydrocarbon nucleoside adducts to be readily handled and studied without derivatization. It is our opinion that PDMS should be an important tool in this field.

REFERENCES

(1) TORGERSON, D.F., R.P. SKOWRONSKI and R.D. MACFARLANE, Biochem. Biophys. Res. Commun. *60* (1974) 616-621.
(2) LE BEYEC, Y., S. DELLA NEGRA, C. DEPRUN, P. VIGNY and Y.M. GINOT, Rev. Phys. Appl. *15* (1980) 1631-1637.
(3) VIGNY, P., M. KINDTS, M. DUQUESNE, C.S. COOPER, P.L. GROVER and P. SIMS, Carcinogenesis, *1* (1980) 33-36.
(4) VIGNY, P., Y.M. GINOT, M. KINDTS, C.S. COOPER, P.L. GROVER and P. SIMS, Carcinogenesis, *1* (1980) 945-950.
(5) STRAUB, K., T. MEEHAN, A.L. BURLINGAME and M. CALVIN, Proc. Natl. Acad. Sci. USA, *74* (1977) 5285-5289.
(6) FESTA, E., et al., Nucl. Instr. and Method (to be published).

FAST ATOM BOMBARDMENT MASS SPECTROMETRY OF MOLECULAR CATIONS, ANIONS, AND ZWITTERIONS

G.HANSEN, C.FENSELAU, T.CHEN, D.HELLER, and R. COTTER

Middle Atlantic Mass Spectrometry Facility
The Johns Hopkins University School of Medicine
Baltimore, MD 21205

Fast Atom Bombardment (FAB) mass spectrometry has been shown to be useful for the analysis of thermally labile and involatile compounds.[1] the technique consists of depositing the sample in a fluid matrix onto a copper probe surface. The sample is then irradiated with 4KV argon atoms at a beam current of approximately .2 mA. Both positve and negative spectra may be obtained.

A FAB source has recently been installed on the Kratos MS-50 at the Middle Atlantic Mass Spectrometry facility. The goal of the work presented here carried out at the MAMS facility has been to study the FAB mass spectrometry of highly polar molecules such as organic cations and anions, compounds containing acidic functional groups such as phosphate and carboxyl groups in both free acid and salt forms, and zwitterions such as 7-methyl guanosine monophosphate which contain quaternary nitrogen as well as a phosphate group.

1. ORGANIC SALTS: Quaternary ammonium salts such as 7-methyl guanosine and 2,3,5 triphenyl tetrazolium chloride give strong positive ion FAB spectra. The spectra are dominated by the intact cation and little fragmentation is generally observed. Ion clusters of the form $(C_n^+ X_{n-1}^-)^+$ where C is the cation and X is the inorganic anion may also be observed. Negative ion spectra have not been observed for the organic cation salts. Organic anion salts such as sodium tetraphenyl borate give strong negative ion spectra with little fragmentation. Positive ion spectra have not been obtained for the anion salts.

2. ZWITTERIONS: Compounds such as 7-methyl guanosine monophosphate, which contain a quaternary nitrogen and a phosphate group give both positive and negative FAB spectra. The positive FAB spectrum of 7-methyl GMP contains the intact cation as well as ions showing the exchange of one and two protons with sodium. These ions were observed for both the free acid and sodium salt form of 7-methyl GMP. The negative FAB spectrum of 7-methyl GMP contains an M-2 ion (M defined as the fully protonated form). This ion may contain a mixture of charge centers, one positive charge on the quaternary nitrogen and two negative charges on the phosphate group resulting in a net -1 charge on the molecule.

3.PHOSPHATES, CARBOXYLATES, and SULFATES: Compounds containing acidic groups such as phosphate, carboxylate, or sulfate give strong positive and negative FAB spectra for both free acid and salt forms. Positive ion spectra show both proton and cation attachment as well as proton-cation exchange. Negative ion spectra exhibit cation or proton removal to give the negatively charged species.

1. M. Barber, R.S. Bordoli, R.D. Sedgwick, and A. Tyler, 325, J.C.S. Chem. Comm. (1981)

FAB SPECTRUM OF BOVINE BRAIN SPINGOMYELIN

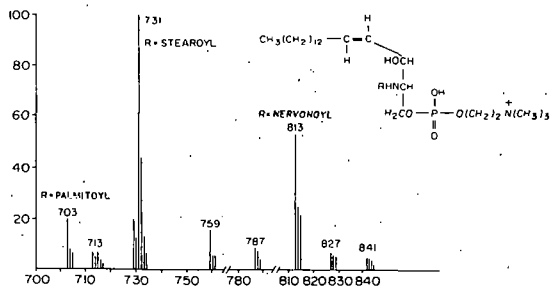

NEGATIVE ION FAB β-ESTRADIOL-3-SULFATE-17-GLUCURONIDE (K SALT)

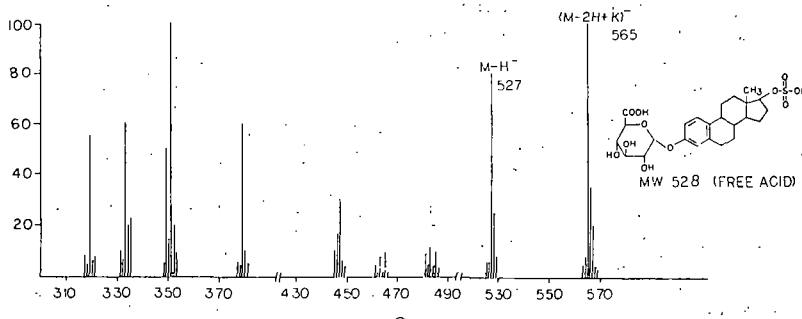

NEGATIVE FAB OF NADPH
$C_{21}H_{30}O_{17}N_7P_3$ (free acid)
MW 745

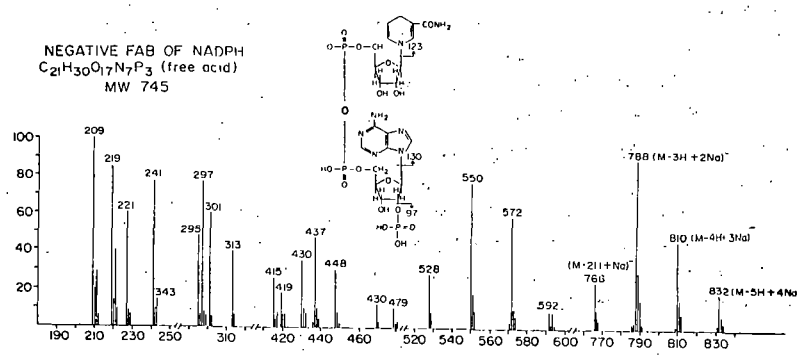

Negative Ion Mass Spectrometry of Middle Molecules: Chemical Ionization and Fast Atom Bombardment; Heller, D. N., Chen, T. S., Hansen, G., Fenselau, C.; Middle Atlantic Mass Spectrometry Facility, Johns Hopkins University, Baltimore, MD 21205

Much of the work to date on analyses of negative ions has been carried out on quadrupole mass spectrometers, which are currently limited in their performance above 1000 amu. The extension of these studies into the mass range well beyond 1000 is now possible with magnetic sector instruments, taking advantage of their higher resolving power and better ion transmission in the middle molecule range (1000 - 10,000). Studies in the MAMS Facility have been carried out on the Kratos MS-50 equipped with high field magnet.

The goal of the present work has been to lay a foundation for use of **two** types of negative ion techniques to obtain molecular weight and structural information:

- Chemical Ionization with CH_4 which acts as a moderator gas for resonance electron capture
- Fast Atom Bombardment, in which fast moving argon atoms are delivered to the sample on a solid probe

A variety of compounds were studied and compared in these techniques according to the following criteria:

- Detection of molecular ion species
- Quality of fragmentation for structure elucidation
- Utility as calibration compounds for manual counting, peak matching, or computer calibration

NEGATIVE ION FAB

Negative ion FAB has been shown to yield molecular ion species and useful fragmentation patterns for oligosaccharides, oligopeptides and compounds containing phosphate groups.

FOMBLIN OIL Poly (Perfluoropropylene oxide)

In electron capture NCI with methane, Fomblin Oil yields oligomeric ions up to and beyond m/e 3500. This spectrum can be used with the DS-55 data system programs for computer calibration. Calibration to m/e 1900 is carried out readily with the MS-50 at the MAMS Facility.

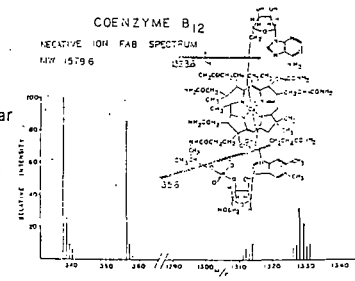

DOLICHOL MONOPHOSPHATE
NEGATIVE ION FAB SPECTRUM OF 20 ng SAMPLE
15 SCANS RECORDED ON VARIAN 1024 CAT

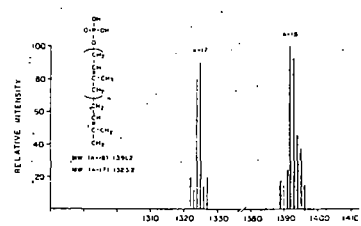

PHOSPHAZENE 2828 AND 3628
NEGATIVE ION FAB SPECTRA
RECORDED SEQUENTIALLY ON VARIAN 1024 CAT

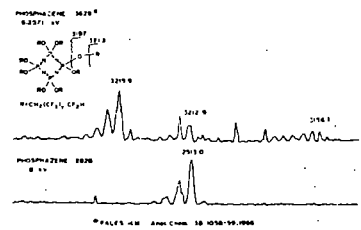

PHOSPHAZENE AND TRIAZINE DERIVATIVES

Perfluoroalkyl phosphonitrilates ("phosphazenes") and *perfluoroalkyl triazines yield very intense ions at regular intervals* in the high mass range.

CONCLUSION

Negative ions can be formed and analyzed from molecules in the middle mass range.

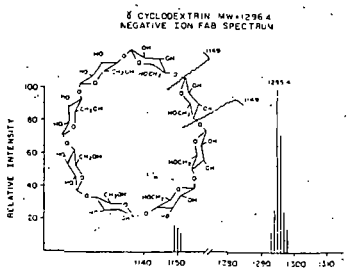

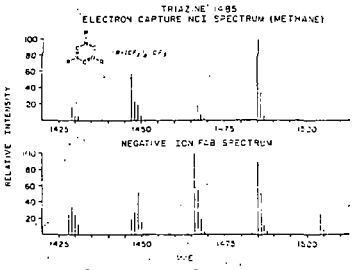

The electron capture NCI spectrum of triazine 1485 shows ions at (M - nF)⁻ when n is even and at (M - nF - H)⁻ when n is odd. Although the mechanism for this is not clear it may indicate transfer of a hydrogen from the reagent gas (methane). The spectrum is different from the negative ion FAB spectrum which shows ions at (M - nF)⁻ when n = 1, 2, 3,

PHOSPHAZENE 2121 / 2828

Negative ion FAB and electron capture NCI spectra of this mixture of phosphazenes are quite similar.

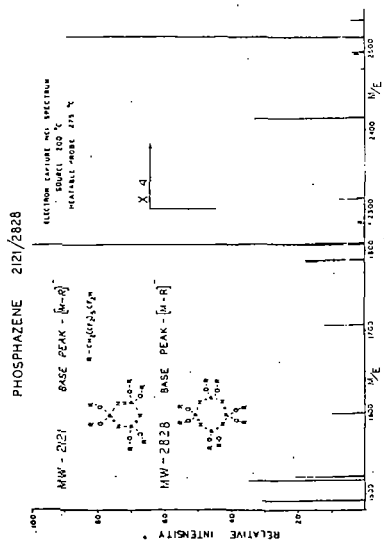

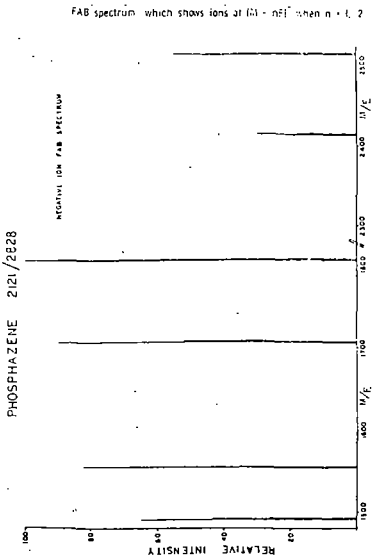

QUANTITATIVE ANALYSIS IN BIOLOGICAL FLUIDS OF THE QUATERNARY AMMONIUM SALTS, PANCURONIUM AND NORCURON (ORG NC 45), BY DIRECT INSERTION CIMS.

T-L. NGUYEN, L. D. GRUENKE, R. A. UPTON, N. CASTAGNOLI, Jr., and R. D. MILLER
Depts. of Anesthesia, Pharmaceutics and Pharmaceutical Chemistry,
Univ. of Calif., San Francisco, CA 94143.

The bisquaternary ammonium salt pancuronium bromide 1 has been widely used as a non-depolarizing muscle relaxant since its introduction into anesthetic practice.[1] Its mono-quaternary analog, Org NC 45, 2 is currently undergoing clinical evaluation.

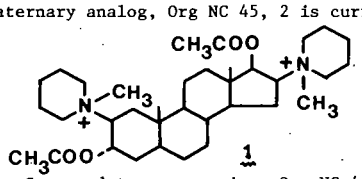

1

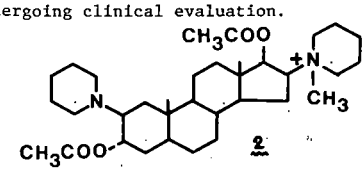

2

Compared to pancuronium, Org NC 45 is more potent, has a shorter duration of action and has none of the cardiovascular side effects.[2]

Pharmacokinetic studies have been limited by the lack of a sufficiently specific and sensitive method of detection. Chromatographic assays such as GLC and HPLC are largely precluded because of the low volatility of these drugs and their lack of a strong UV chromophore. Current methods of analysis for pancuronium rely on forming complexes of the drug with organic dyes which can be determined by spectrofluorimetry[3] or by spectrodensitometry.[4] The reported sensitivity of these methods is 20 ng/ml plasma. In order to obtain good pharmacokinetic data at realistic doses (50 µg/kg or less), an assay with at least an order of magnitude greater sensitivity and the ability to distinguish the drugs from their metabolites is required. The CIMS assay described here meets these requirements.

The CIMS of both drugs is nearly identical showing a quasimolecular ion at m/e 543, $MH^+ - 2CH_3Br$ for pancuronium and $MH^+ - CH_3Br$ for Org NC 45. Stable isotope analogs (bis-acetoxy-D_3) of each drug were synthesized for use as internal standards by hydrolysis of the parent drug followed by reacetylation with acetyl chloride-D_3.

The simple extraction scheme shown below was found to isolate the drugs from the biological fluids studied (serum, urine and bile) in 80-95% yield and sufficiently free from impurities to allow analysis by direct insertion CIMS without interference at the monitored masses.

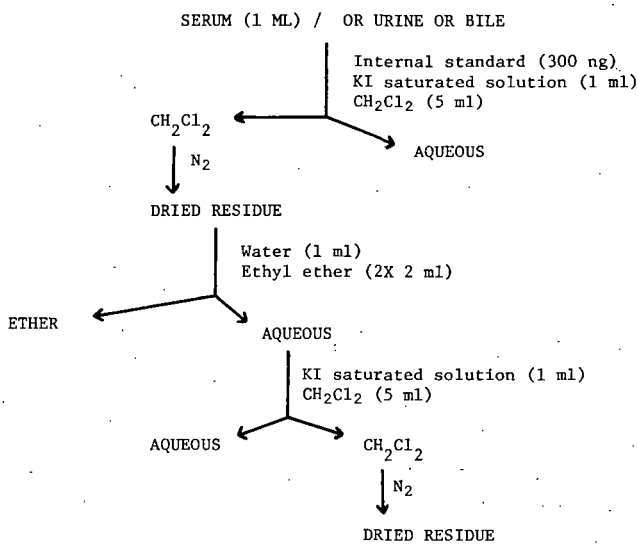

All measurements were obtained on an AEI MS 902 mass spectrometer which had been modified for CIMS. Isobutane was used as the reagent gas. Two methods for obtaining ion current ratios were evaluated: repetitive narrow scans from m/e 553 to m/e 540 at a scanning rate of 38 min per decade and selected ion recording[5] (SIR) at m/e 549 and at m/e 543. The results for 1 ml human serum samples spiked with pancuronium bromide are shown in table 1. Similar results were obtained from urine or from bile or when Org NC 45 was assayed.

Table 1

Analytical Results From Human Serum Spiked With Pancuronium Bromide

Amount Added (ng)	Amount Found by[a] Narrow Scan (ng) ± Standard Deviation	Amount Found by[b] SIR (ng) ± Standard Deviation	n
0	0.3 ± 0.6	0.0 ± 0.14	8
20	17.6 ± 1.6	18.9 ± 0.7	4
200	207 ± 6	208 ± 2.2	4
2000	1993 ± 28	1940 ± 38	4

a. Standard curve $y = mx + b$: $m = 0.00300$, $b = 0.0117$; $r^2 = 0.9993$
b. Standard curve $y = mx + b$: $m = 0.00311$, $b = 0.0079$, $r^2 = 0.9986$

The data from both methods shows acceptable accuracy and linearity in the range studied. Based on the standard deviations at the lowest levels, the minimum detectable sample (Students t test, P = 0.95) is about 2 ng for the narrow scan method and about 0.5 ng for the SIR method. The sensitivity of the SIR method is probably limited by sample impurities rather than by ion statistics.

The success of this direct insertion CIMS analysis in the low nanogram range without extensive sample purification is due to three factors:

1. The salt like character of these drugs allows purification by simple extraction techniques.
2. The masses being monitored are high.
3. The pyrolysis of these drugs occurs in a narrow range at a relatively high temperature, thus allowing impurities to be driven off by heating the probe to intermediate temperatures.

Pharmacokinetec studies in humans and in experimental animals are currently underway.[6]

REFERENCES

1. J. L. Neigh, Surgical Clinics of North America, 55, 837 (1975).
2. R. D. Miller, Brit. J. Anaesth., 52, Suppl. 1, 71S (1980).
3. U. W. Kersten, D. K. F. Meijer and S. Agoston, Clin. Chim. Acta, 44, 59 (1973).
4. K. Tanaka, M. Hioki and H. Shindo, Chem. Pharm. Bull., 22, 2599 (1974).
5. L. D. Gruenke, J. C. Craig and D. M. Bier, Biomed. Mass Spectrom., 7, 381 (1980).
6. R. A. Upton, T-L. Nguyen, R. D. Miller and N. Castagnoli, Jr., Anaesth. In Press.

IN-BEAM ELECTRON IMPACT AND MASS ANALYSED ION KINETIC ENERGY STUDIES OF QUATERNARY AMMONIUM SALTS.

M. Ohashi, R. Barron, and W. Benson
FDA, Division of Drug Chemistry
Washington, D. C. 20204

Until recently, quaternary ammonium salts were believed to only undergo thermal degradation prior to ionization in a mass spectrometer. Consequently report documenting the fragmentation of intact quaternary ammonium ions by electron impact were not found. However, in 1980 Röllgen and Stoll have shown that tetraalkylammonium salts are evaporated and dissociated to yield the corresponding quaternary ammonium cation by only heating (1), whereas Daves et al. proposed that electron impact is necessary to cause dissociation of gaseous quaternary salts to give the corresponding ammonium cation(2). Cotter and Yergey also reported the observation of the thermal degradation spectra of intact quaternary ammonium cations(3). We now report our recent studies on in-beam EI mass spectrometry(4) of these compounds. The series; tetraethyl, tetrapropyl, tetrabutyl, and tetrapentyl ammonium bromide were selected as typical examples and examined by the techniques of in-beam EI mass spectrometry and mass analysed ion kinetic energy spectrometry as well as high voltage scanning ion kinetic energy spectrometry. Our results are summarized as follows:

(i) When the compound was loaded on a metal tip and inserted into the hot ion source (ca. 280°C) and heated to 350°C by the sample heater or the compound was deposited on an unactivated FD wire of 10 μM dia. tungsten and quickly heated, only the corresponding tetraalkylammonium cation was recorded. Without an electron beam, no fragment ions were detected under these conditions.

(ii) When the electron beam (filament) was turned on and the in-beam EI spectra were recorded, significant increase in the abundance of the quaternary ammonium cation was observed.

(iii) The in-beam EI spectra of tetrapropyl and tetrabutylammonium bromide are shown in Figure 1 as typical examples. In addition to these peaks, weak but remarkable cluster ions, $((R_4N)_2Br)^+$ and $(R_4N\ Br - H)^+$ were observed.

(iv) MIKES confirmed the direct formation of several fragment ions from the R_4N^+ cation. The results are shown in Table 1. Five transitions were commonly observed. In the case of tetraethyl derivative, three metastable transitions producing R_3NH^+, $R_3N^{+\cdot}$, and $R_2N^+{=}CHR'$ from R_4N^+ were clearly observed. In the other three cases the transitions leading to $R_3N^{+\cdot}$ from R_4N^+ were not clear because of three overlapping transitions for $R_3N^{+\cdot}$, R_3NH^+, and $R_2N^+{=}CHR'$ from R_4N^+.

(v) In order to clarify the ambiguous processes in MIKES due to overlapping peak, particularly for the process: $R_4N^+ \rightarrow R_3N^{+\cdot}$ ion kinetic energy spectra were obtained by acceleration voltage scanning to attempt to determine the parent ions of certain daughter ions. The results are summarized in Table 1. The parent ions of $R_3N^{+\cdot}$ corresponding to the molecular ions of trialkylamine (a possible thermal degradation product), were clearly shown to be derived by electron impact induced fragmentation from the tetralkylammonium cation, R_4N^+.

Of course from these data we cannot exclude contribution of thermal decomposition products to the in-beam spectra. However, we can conclude safely that the following reactions take place commonly in the first and second field free regions in the reversed Nier Johnson geometry.

(1) Stoll, R.; Röllgen, F. W, J. Chem. Soc. Chem. Commun. 1980, 789.
(2) Lee, T. D.; Anderson, W. R.; Daves, G. D., Jr. Anal. Chem. 1981, 53, 304.
(3) Cotter, R. J.; Yergey, A. L., J. Am. Chem. Soc. 1981, 103, 1596.
(4) Ohashi, M.; Tsujimot, K.; Yasuda, A., Chem. Lett. 1976, 439; Cotter, R. J., Anal. Chem. 1980, 52, 1589A.

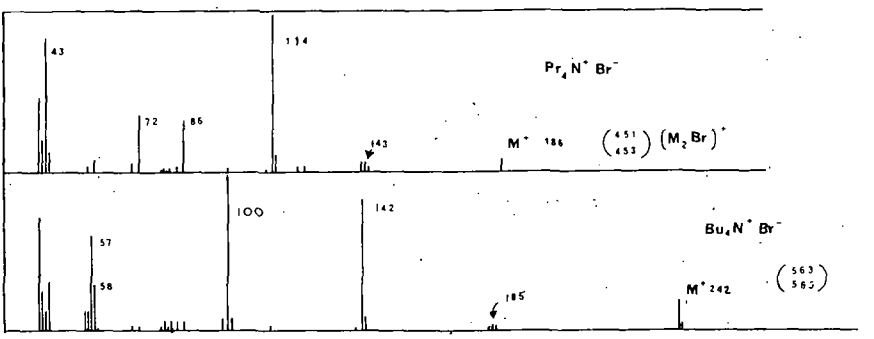

Fig. 1. In-beam EI spectra (80 eV) of tetrapropyl- and tetrabutylammonium bromide.

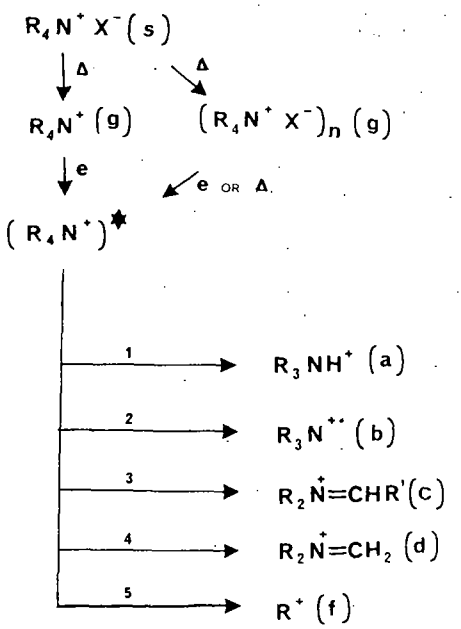

Scheme Fragmentation processes of tetraalkyl ammonium cations upon electron impact

Table I. MIKES and IKES of Tetraalkylammonium Cations

R	transitions[a]	fragment (m/z)	E/E_0[b]	V/V_0[c]
Et	1	102(a)	0.781	1.275
	2	101(b)	0.776	1.288
	3	100(c)	0.766	1.301
	4	86(d)	0.659	e
Pr	1	144(a)	0.774	1.290
	2	143(b)	d	1.300
	3	142(c)	0.762	1.309
	4	114(d)	0.611	1.633
	5	43(f)	0.229	e
Bu	1	186(a)	0.768	1.302
	2	185(b)	d	1.306
	3	184(c)	0.761	1.314
	4	142(d)	0.588	1.703
	5	57(f)	0.233	e

a See Scheme
b MIKES of tetraalkylammonium cation
c IKES obtained by acceleration voltage scanning
d Overlapping peaks
e No data obtained

Mass Spectral Analysis of Long Chain Quaternary Amine Mixtures

Robert J. Cotter and Gordon Hansen, Middle Atlantic Mass Spectrometry Facility
Johns Hopkins University, Baltimore, MD 21205, and

Thomas R. Jones, Southern Clay Products, Gonzales, TX 78629

Objectives:

The objectives of this research are to examine and evaluate the analytical utility of several ionization techniques for the determination of the composition of quaternary ammonium salt mixtures manufactured industrially from hydrogenated tallow. The ionization techniques employed include: direct exposure chemical ionization, field desorption, and fast atom bombardment. The analytical questions include: the relative abundances of C-14, C-16 and C-18 alkyl chains, the amount of mono- and tri-alkyl impurities present in the di-alkyl mixtures, and the abundance of amide impurities which are introduced in the manufacturing process.

Introduction:

Quaternary ammonium salts, in which one or two long-chain hydrocarbon groups are directly attached to the nitrogen atom, are an important group of industrial chemicals, whose uses include flocculation, soil stabilization, and the manufacture of organophilic colloids. The total U.S. market is approximately 10^8 Kg per year. They are non-toxic, biodegradeable, cationic surface active agents, and in the household they appear in fabric softeners, hair conditioners, germicides, and as organophilic colloids in cosmetics, lubricating greases and paints.

The long chain amines are manufactured via the fatty acids, derived from natural fats and oils such as tallow, coconut or palm, which are each mixtures of acids of different chain lengths. Conversion of the fatty acids to the nitrile, followed by catalytic hydrogenation, produces primary and secondary amines. The quaternary amine is then completed by the addition of methyl or benzyl groups. The mixture of stearic, oleic, linoleic, palmitic and myristic acids found in beef tallow, upon hydrogenation, produces a corresponding mixture of C-18, C-16 and C-14 alkyl groups with relative abundances of 65% ±6%, 28% ±4%, and 4.5% ±1.5% respectively.

Direct Exposure Chemical Ionization

Direct Exposure CI provides a means for determining the mixture of chain lengths. Molecular ions are observed (Figure 1), but more reliable results are obtained from peaks corresponding to the protonated amines, produced after the loss of methyl or alkyl groups. In the example shown, the five peaks corresponding to loss of methyl produce a composition of 66.8%, 29.9%, and 3.1%. The three low mass peaks corresponding to the loss of one of the alkyl chains produced a composition of 63.8%, 33.9%, and 3.3% for C-18, C-16, and C14. In addition, high resolution/direct exposure CI revealed that peaks at 536, 508, etc. included a small amount of amide impurity.

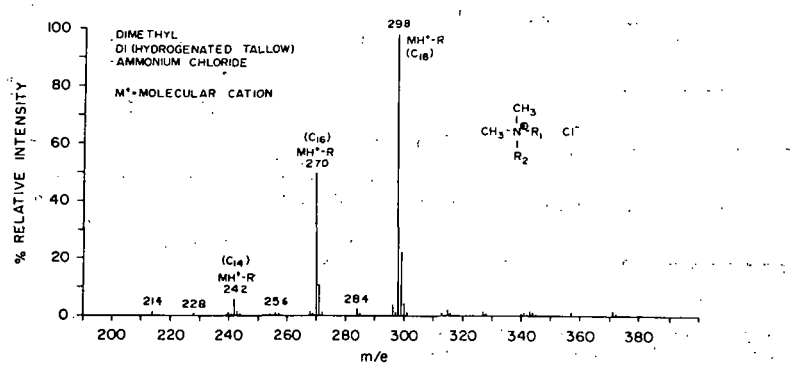

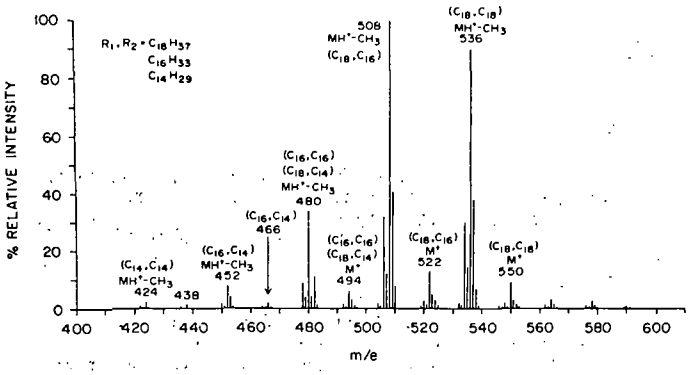

Field Desorption

While this technique produced more abundant molecular ions, spectra were somewhat irreproducible, since decomposition was dependent upon emmitter temperature, and relative abundances varied with time as the sample was desorped from the surface.

Fast Atom Bombardment

This technique made possible the observation of mono-alkyl and tri-alkyl impurities. The spectrum is shown in Figure 2. The abundances of the tri-alkyl impurities, relative to the total di-alkyl species were compared for two amines with results obtained from HPLC. FAB/MS results were 10.3% and 10.1% for the two amines, while the HPLC determination gave 7.4% and 7.1% respectively.

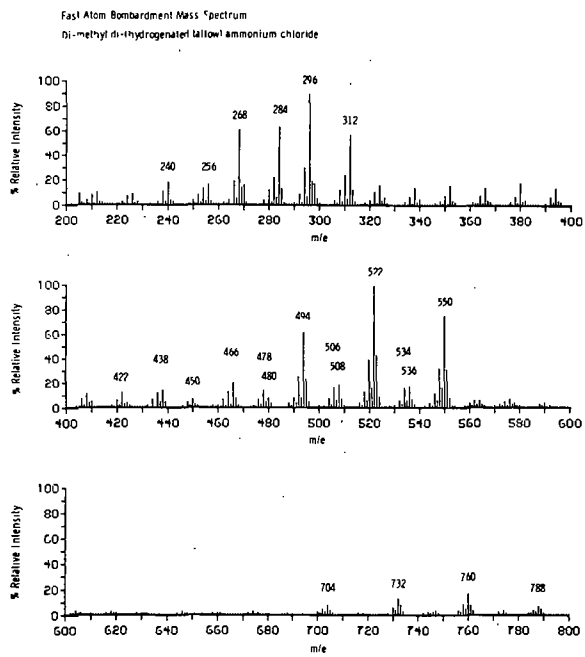

CHEMICAL IONIZATION MASS SPECTROMETRY OF THERMOLABILE ORGANIC COMPOUNDS. ADDUCT ION FORMATION WITH AMMONIA, TRIETHYLAMINE OR PYRIDINE. D. I. CARROLL, J. G. NOWLIN, R. N. STILLWELL and E. C. HORNING; Inst. for Lipid Research, Baylor College of Medicine, Houston, Texas 77030

Thermally induced dehydration is a common reaction for most organic compounds with hydroxyl groups, and for direct chemical ionization spectra obtained under protonating conditions, it is not possible to determine if the initial ion in a sequence with ions 18 amu apart corresponds to MH^+, $(MH-18)^+$ or $(MH-36)^+$. A way of recognizing ions containing sample molecules in their entirety, for many compounds, is to generate adduct ions which contain an easily recognized isotope label using direct chemical ionization techniques. The results obtained under these conditions are described in this paper for a wide range of representative thermally labile ketons, esters, acids, phenols, alcohols and conjugates. In most cases the isotope labeled adduct ion is either the base peak or easily recognized.

THE THERMAL DESORPTION CHEMICAL IONIZATION MASS SPECTROMETRY OF 1,3,5,7-TETRANITRO-1,3,5,7-TETRAAZACYCLOOCTANE (HMX); RUSSELL C. SPREEN and BURNABY MUNSON; Department of Chemistry, University of Delaware, Newark, Delaware 19711

Contrasting literature reports and experiments in our laboratory indicate that the chemical ionization mass spectra of 1,3,5,7-tetranitro-1,3,5,7-tetraazacyclooctane (HMX) are extremely sensitive to experimental parameters. Methane CI spectra differing greatly in ionic abundances and with no $(M+H)^+$ ions or significant amounts of $(M+H)^+$ ions have been reported (1,2). Vastly different iso-butane CI spectra have also been reported (1,3). Source temperature (2) and reagent gas pressure (3) were blamed for these. In order to examine this phenomenon in detail temperature dependent CI mass spectra have been obtained using butane, iso-butane, 99.5% propane/0.5% dimethyl ether and ammonia as reagent gases.

These experiments consist of depositing 3 micrograms of HMX from an acetone solution (3 μg/μl) into the bottom of the sample well of a conventional probe. The probe is home-made and a thermocouple simulates the sample temperature to within ±5°C. The probe is slowly heated to 75°C to remove the acetone and then cooled to room temperature before introduction into the mass spectrometer. Once in position inside the instrument the probe is heated at 15°C/min while spectra are acquired every 6 seconds by computer. Reproducible and well shaped ion intensity profiles are obtained.

Our experience indicates that sample size, sample location in the probe well, reagent gas pressure and heating rate are important parameters for the collection of reproducible data. Samples significantly larger than 3 micrograms and samples not located in the base of the probe well do not desorb smoothly. Heating rate and reagent gas pressure are important parameters in regulating the partial pressure of HMX in the ion source. If the gas phase concentration of HMX is high, sample ion/sample molecule reactions will occur rapidly to yield $(M+H)^+$, $(M+NO_2)^+$, and $(M+CH_3N_2O_2)^+$. At present the effect of source temperature has not been examined, but these experiments are planned for the future.

Once it was possible to obtain reproducible desorption profiles for HMX we felt it important to determine the proton affinity. A bracketting technique was used and the criteria for reaction was based on the following sequence.

$$RH^+ + (CH_2N_2O_2)_4 \longrightarrow ((CH_2N_2O_2)_4 + RH)^{+*} \longrightarrow ((CH_2N_2O_2)_n + RH)^+ \qquad n = 1\text{-}4$$

$$((CH_2N_2O_2)_4 + RH)^{+*} \xrightarrow{A} ((CH_2N_2O_2)_n + H)^+ \qquad n = 1\text{-}4$$

Proton transfer was indicated by a significant increase in the sum of selected protonated fragments and protonated HMX, accompanied by a corresponding decrease in the intensity of the reagent ion. Addition reactions were indicated in a similar fashion. Table 1 shows our results for the three reagent gases used. The spectra obtained are shown in Figures 1, 2 and 3. Since in this and in previous work we have observed dissociative proton transfer to be the dominant process in proton transfer reactions with HMX, it was necessary to show that HMX is a stable gas phase species. An experiment was carried out in which HMX was desorbed from the probe to the source block at 80°C. The source block was then heated slowly and spectra were acquired repetitively under ammonia CI conditions. A single peak was observed in the total sample ion profile at 175°C. The spectrum showed a base peak at M/Z = 314 corresponding to $(HMX+NH_4)^+$, a prominent ion at M/Z = 331 due to $(HMX+(NH_3)_2H)^+$ and essentially no higher mass ions. Spectra obtained with the reagent gases listed in Table 1 show the proton affinity of HMX to be between 181 and 190 kcal/mol. Thus proton transfer (with or without dissociation) was not expected to occur with ammonia as the reagent gas and none was observed.

Table 1.

Reagent Gas	R	P.A. (kcal/mole)	Rxn. A
n-butane		181	fast
i-butane		194	slow
dimethyl ether	—O—	190	slow

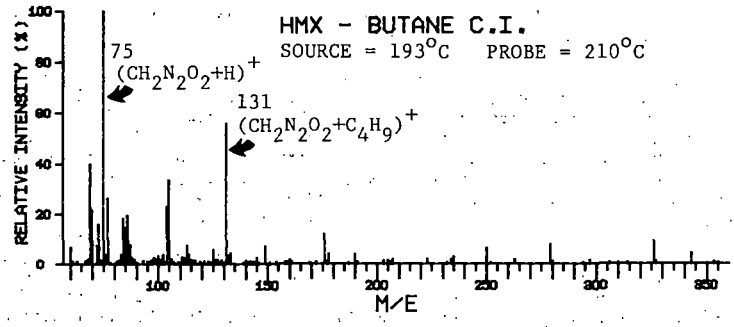

Figure 1. Reagent Ion Ratio M/Z 57:71 = 100:15

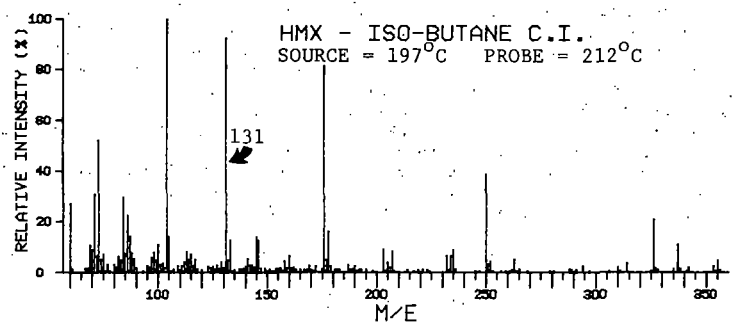

Figure 2. Reagent Ion Ratio M/Z 57=100% all others < 3%

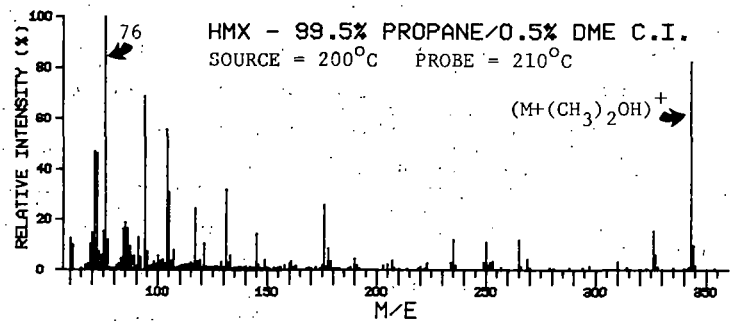

Figure 3. Reagent Ion Ratio M/Z 43:47:93 = 34:100:35

1. J. Yinon, Biomed. Mass Spectrom., 1, 393 (1974).
2. P. Vouros, B. A. Peterson, L. Colwell, B. L. Karger and H. Harris, Anal. Chem., 49, 1039 (1978).
3. R. Saferstein, J. M. Chao and J. Manura, J. Assoc. Off. Anal. Chem., 58, 734 (1975).

High-Performance Molecular SIMS, J. E. Campana, T. M. Barlak, J. R. Wyatt, J. J. DeCorpo, and R. J. Colton, Naval Research Laboratory, Chemistry Division, Washington, DC 20375.

A high-performance secondary ion mass spectrometer has been designed in our laboratory,[1] especially for the study of the secondary ion emission process and for analytical applications of molecular SIMS. This instrument has several notable attributes among which are dynamic (>10^{-5} A/cm^2), static (<10^{-9} A/cm^2), and neutral beam excitations, ultra-high mass capability (>m/z 18,000), high ion transmission (>1:10^4), adequate resolving power (>350), and the absence of detrimental mass and energy discrimination effects. This system has allowed us to propose ion abundance calibration standards for conventional SIMS instruments (see paper RPMOC6). The instrument also has a large viewing area (1 cm^2) which allows a "milliprobe" imaging capability with possibilities for molecular imaging (see paper MPB10). Two of these features, the high-mass capability and static SIMS applied to the characterization of polymeric thin films, are discussed.

Recent studies in our laboratory on the alkali iodides (MI) have shown that a series of cluster species $[M(MI)_n]^+$ (CsI, n=1-19) are produced by argon ion bombardment (see paper RPMOC3). Ultra-high mass spectral data (>m/z 18,000 and n=1-70) induced by xenon ion bombardment of CsI (see Figure 1). The intensity distributions are discussed elsewhere (see paper RPMOC3). These 300 eV m/z 18,000 ions move through the mass spectrometer at Mach 5.4 compared to m/z 100 ions which move through organic mass spectrometers with 8000 eV of energy or speeds of Mach 375. The decreased extraction efficiency of the optics at low accelerating voltage is offset because the ion source is so bright (i.e., secondary ion yield is very high for CsI).

Static SIMS also termed low-damage and molecular SIMS can be used as an "apparent" non-destructive analytical technique for the characterization of polymeric thin films. This method has been applied to a series of poly (alkyl) methacrylates shown in Table 1. The ions used to distinguish the homologs are characteristic of the substituent group and are shown in Table 2. These ions are also significantly intense relative to the other backbone (hydrocarbon) type ions in the mass spectrum. The most intense ions in the spectra are ions characteristic of the silver substrate or polymer impurities, i.e., Na^+, K^+, Ar^+, Ag^+, and Cs^+. The observation of these species indicate an incomplete coverage (submonolayer perhaps) of the silver substrate (Figure 2). This low-damage method offers a means of direct and "apparent" non-destructive analysis of polymeric thin films whereas the various pyrolysis techniques and LAMMA are indirect and destructive.

1. R. J. Colton, J. E. Campana, T. M. Barlak, J. J. DeCorpo, and J. R. Wyatt, Rev. Sci. Instrum., 1980, 51, 1685-1689.

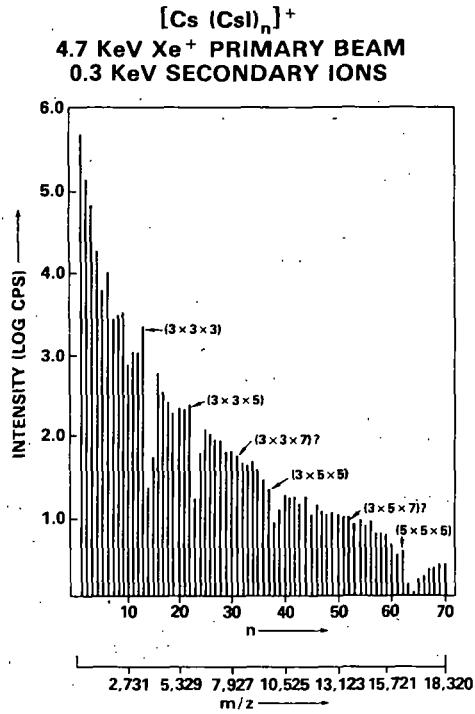

Figure 1.

POLYMER CHARACTERIZATION
POLYALKYLMETHACRYLATES

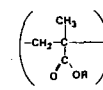

NAME	ACRONYM	R
POLYMETHYLMETHACRYLATE	PMM	$-CH_3$
POLYETHYLMETHACRYLATE	PEM	$-CH_2CH_3$
POLYISOBUTYLMETHACRYLATE	PIM	$-CH_2CH(CH_3)_2$
POLY(n-BUTYL)METHACRYLATE	PNB	$-(CH_2)_3CH_3$
POLYLAURYLMETHACRYLATE	PLM	$-(CH_2)_{11}CH_3$

Table 1.

POLY(ALKYL)METHACRYLATE
CHARACTERIZATIONS

m/z	SPECIES
15	$(CH_3)^+$
29	$(C_2H_5)^+$
43	$(C_3H_7)^+$
55	$(C_4H_7)^+$

PMM	m/z 15 > 55 > 29 > 43
PEM	m/z 29 > 43 > 15 ≈ 55
PIB	m/z 29 > 43 ≈ 55 > 15
PNB	m/z 43 > 29 ≈ 55 > 15
PLM	m/z 55 > 43 > 29 > 15

Table 2.

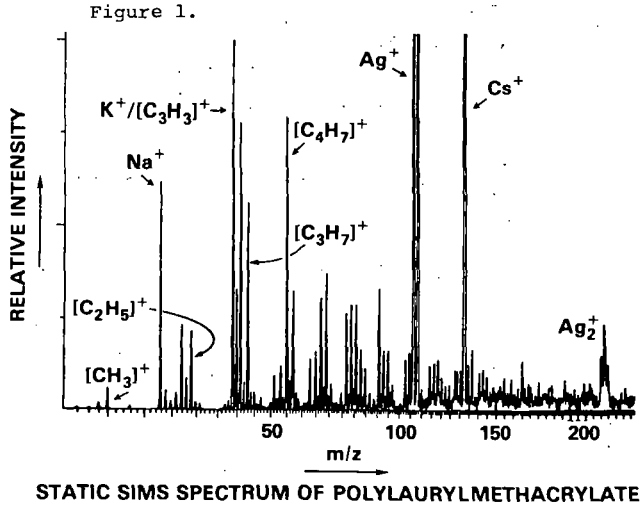

Figure 2.

A CERAMIC DIRECT INSERTION TIP FOR DESORPTION CHEMICAL IONIZATION. F.A. BENCSATH and F.H. FIELD, The Rockefeller University, New York, N.Y. 10021

We describe a ceramic probe tip for desorption chemical ionization (DCI) which shows some advantages over the commonly used metal coil [1] or Vespel-tip [2]. A ceramic tube (MV20 Mullite single bore insulator, McDaniel) was melted closed at one end, and a chromel wire coil was placed inside to provide heating. The tip thus constructed was fitted to a DuPont 21-492 sample probe. The tip was deactivated by coating with "Dexsil" and subsequent mild burning with a CH_4-O_2 flame (to orange-red heat), and it remained inert for months. The porosity of the ceramic facilitates sample loading from solutions, and the hardness of the ceramic facilitates the loading of powdered samples. The tip can be easily cleaned by flame in a few seconds, which makes the repeated sampling often necessary in DCI work very time efficient.
This probe has been used extensively for biomedical service work in the last two years. Among the samples run successfully were synthetic nucleoside derivatives, corticosteroid derivatives and steroid glucuronides containing 4 to 5 hydroxyl groups, synthetic oligopeptide intermediate preparations, a complex sulfonic acid, heteroaromatic sulfonic acid, thermosensitive alkylacrylamides, tetraselenium compounds, and high molecular weight opiates. Satisfactory spectra can be obtained with sub-microgram amounts of sample. Spectra illustrating the utility of the tip will be given.

1. J.R. Chapman, S. Evans, C.J. Wakefield, K.R. Compson and D. Haselby, paper presented at the 28th Annual Conference on MS and Allied Topics, New York 1980; and A.P. Bruins, ibid.
2. R.F. Cotter, C. Fenselau, Biomed. Mass Spectrom. 1979, 6, 287.

FIELD DESORPTION AND DESORPTIVE CHEMICAL IONIZATION MASS SPECTRAL STUDIES OF PHORBOL ESTERS; C.E. COSTELLO, A. SCHKUTA, and K. BIEMANN; Dept. of Chem., M.I.T., Cambridge, MA 02139 and V.N. REINHOLD, Dept. of Biol. Chem., Harvard Medical School, Boston, MA 02115.

Since some of the phorbol esters were shown to be the active principles of croton oil, the classical tumor promotor, there has been much interest in the synthesis, isolation and characterization of these compounds. It is hoped that the use of structural variants will provide some clues to the mechanism of carcinogenesis. Likewise, the isolation of metabolites of phorbol esters from exposed tissues may give information about the biochemical pathways involved. These compounds, however, have provided an analytical challenge because of the lability of the functional groups and the difficulty of distinguishing among isomers which differ only in the locations of the acyl substituents. The limited sample size available for metabolite studies has also been a problem.

The electron impact mass spectral fragmentation pattern provides some useful structural information but it is rarely possible to obtain a molecular ion or any ions at high mass. Isobutane chemical ionization of the 4aα-series has been shown to provide protonated molecular ions of very low abundance and more diagnostic fragments at high mass than does EI. Samples of 5-10 μg were required for low resolution spectra.[1]

In this study, the field desorption (FD) and desorptive or direct chemical ionization (DCI) mass spectra of 4aα- and 4aβ -phorbol (MW 364) and 25 variously substituted esters having molecular weights from 482 to 982 were obtained. In all cases, it was possible to determine the molecular weight and to distinguish among isomers.

FDMS were obtained using a MAT 731 double focussing instrument fitted with a combined EI/FI/FD source and benzonitrile-activated tungsten wire emitters. The molecular ion and/or protonated molecular ion was the base peak in the spectrum of all the compounds (Fig. 1) except in the case where R_3 = trityl, for which the ion at m/z 243 $(C_3)^+$ was the most abundant. Ions which corresponded to loss of the R_1 group as an acyl moiety from M^+ or loss of the acid from MH^+ were the only fragments with significant intensity in many of these spectra. It is thus possible to deduce which acyl group is located at postion R_1. Low resolution FD spectra were recorded oscillographically at M/ΔM = 1000. Exact mass measurements were made by recording the spectra on Ionomet photoplates at a resolution of M/ΔM = 5000, using an overlaid EI spectrum of Fomblin^R oil at M/ΔM. Mass accuracy was within 10 ppm. Sample size was 1-2 μg or less.

DCI mass spectra were obtained with a MAT 312 instrument having a combined EI/CI source, operated at a resolution of M/ΔM = 1000. An SS200 data system was used for data acquisition and processing. The probe (emitter) tip furnished by the manufacturer is a bare nichrome wire. Improved results were obtained when this wire was replaced with one which had been coated with a polyimide polymer.[2] Figs. 2 and 3 compare the results on the two surfaces when ammonia was used as the reagent gas. Using ammonia and the coated emitter, the base peak of the phorbol spectra was usually the $(M + NH_4)^+$ species. Unsaturation in the substituents resulted in a lower relative abundance of this ion. The high sensitivity of the method permitted scanning complete spectra at the 100 ng level. With no special adjustments, samples as small as 3 ng could be detected by monitoring the $(M + NH_4)^+$ peak.

Compounds used in the study were purchased or were furnished by P. Blumberg, Harvard Medical School and M. Neeman, Roswell Park Memorial Institute. This work is supported by grants numbered DRR 00317 and 5 P01 GM 26625 from the National Institutes of Health.

[1] J.J. Solomon, B.L. VanDuuren and S.-S. Tseng, Biomedical Mass Spectrom. 5(2) 164-9 (1978).

[2] V.N. Reinhold and S.A. Carr, (1981) Twenty-ninth Annual Conference on Mass Spectrometry and Allied Topics, Minneapolis, Minnesota. Paper number RPA12.

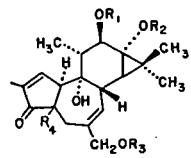

PHORBOL, PHORBOL ESTERS

R_1 = H, ACYL

R_2 = H, ACYL

R_3 = H, ACYL, ALKYL

R_4 = αOH, βOH

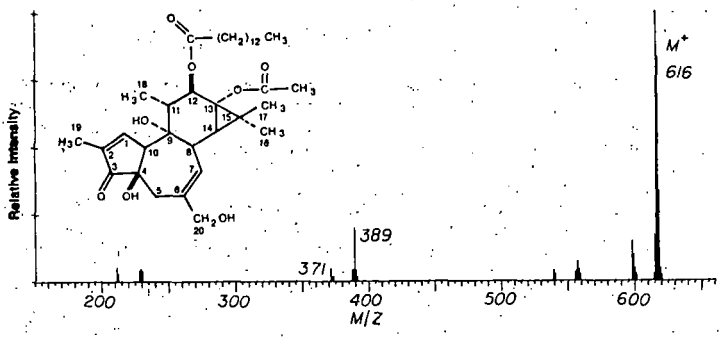

Figure 1. Field Desorption mass spectrum of Phorbol 12-Myristate-13-Acetate, recorded at 22 mA emitter current.

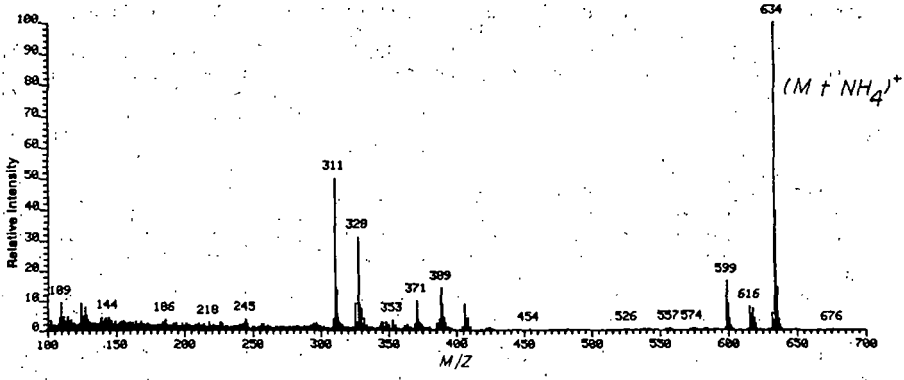

Figure 2. Desorptive Chemical Ionization mass spectrum of Phorbol 12-Myristate-13-Acetate. Reagent gas: Ammonia. Sample on Polyimide-coated emitter.

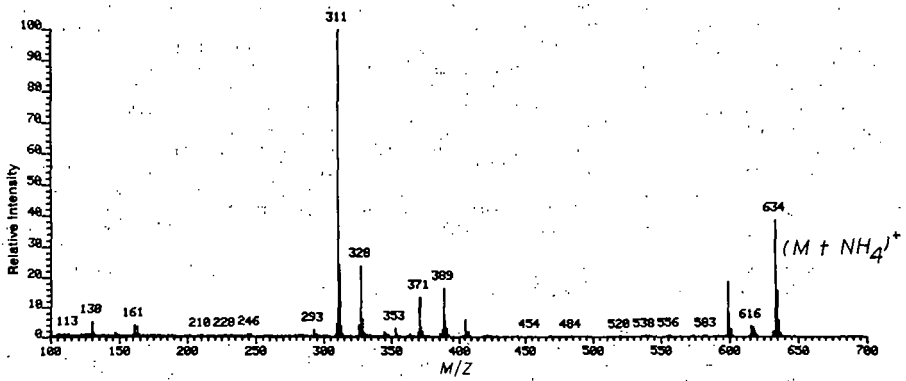

Figure 3. Desorptive Chemical Ionization mass spectrum of Phorbol 12-Myristate 13-Acetate. Reagent gas: Ammonia. Sample coated on bare wire emitter.

DESORPTIVE CHEMICAL IONIZATION OF POLYPEPTIDES AND POLYPEPTIDE DERIVATIVES, STEVEN A. CARR V.N. REINHOLD; Dept. Biol. Chem. & Lab. Human Reprod. & Reprod. Biol., Harvard Med. Sch., Boston, MA 02115 and K. BIEMANN, Dept. Chem., M.I.T., Cambridge, MA 02139.

We have explored the applicability of desorptive or direct chemical ionization mass spectrometry (DCI)[1,2] to the problem of oligopeptide sequence analysis at the subnanomole level. The DCI spectra of a series of synthetic underivatized and simply derivatized peptides up to ten amino acids in length have been obtained using from 0.1 to 1 µg of material. Ions characteristic of the molecular weight and abundant, easily interpretable sequence ions were produced when ammonia was used as the reagent gas.

The most abundant sequence ions in the NH_3-DCI mass spectra of peptides and their derivatives (Scheme 1) are the N-terminal amide ions = $X\text{-}NH\text{-}CHR_n\text{-}CO\text{-}NH_3^+ + (NH_3)_m$, and C-terminal ammonium ions = $^+NH_3\text{-}CHR_n\text{-}CO\text{-}Y + (NH_3)_m$. These structures are indicated on the mass spectra as $(A_n'+2H)^+$ and $(Z_n'+2H)^+$ for m = 0, and $[(A_n'+H) +NH_4]^+$ and $[(Z_n'+H) +NH_4]^+$ for M = 1; the X and Y groups denote the remainder of the peptide chain. The N-terminal cationized amide ions (A'series) produced in the NH_3-DCI mass spectra are probably formed via reaction of the reagent gas with the carbonyl groups of the peptide chain.[3] These ions are not observed by conventional CI using methane or isobutane as the reagent gas[4], or tandem mass spectrometry using NH_4^+ as the ionizing species.[5] For these latter techniques, the major N-terminal fragments are acylium ions of the type $(H_2N\text{-}CHR\text{-}CO^+)$ from which other abundant fragments are produced by neutral losses of CO, H_2O or NH_3. Acylium ions are usually of low abundance in the NH_3-DCI mass spectra.

The NH_3-DCI mass spectrum of the underivatized peptide Phe-Asp-Ala-Ser-Val is typical of those obtained for a wide range of polar and non-polar side chain-containing linear peptides (Fig. 1). In general, the ions of highest mass correspond to $(M)^+$, $(M+H)^+$ or a combination of these. The molecular ion, together with the abundant A' and Z' series sequence ions are usually sufficient to establish the sequences. While not essential, the amino acid composition of the peptide is usually available and provides confirmatory evidence for the proposed structure.

Polar peptides, particularly those with carboxylate side chain-containing amino acids (Glu and Asp) undergo a minor side reaction in which $R'\text{-}CO_2R$ (R = H or CH_3) groups are converted to $R'\text{-}CONH_2$ by reaction of ammonia with these groups. Cyclic peptides such as gramicidin S, a cyclic decapaptide, yield abundant cationized molecular ions but no readily interpretable sequence ions.

Simple derivatization of peptides to the corresponding acetyl or perfluoroacyl methyl esters affects both molecular ion abundance and relative intensities of sequence ions. Acylation of the amino terminus has the general effect of increasing the amount of ion current carried by the $(NH_4)^+$ cationized molecular ions and their fragment ions. Introduction of an acetyl group does not cause significant change in the relative intensities of sequence ions, whereas perfluoroacyl groups cause a marked increase in the intensity of the A_1' series ions.

The effects of modifying the desorption surface have also been examined. We have found that peptides (and many other compound classes)[6] desorbed from DCI emitters coated with a thermally stabilized polyimide exhibit enhanced relative abundance and overall yield of molecular ions, and a decrease in the abundance of fragments that lack sequence information. The total ion current (TIC) profiles for 0.3 µg of dipentafluoropropionyl-Phe-Asp-Ser-Val-$(OCH_3)_2$ desorbed from a bare wire and a coated wire are compared in Fig. 2. The intensity of the $(M+NH_4)$ ion (m/z 875) is approximately five times greater, and the number of spectra in which $(M+NH_4)^+$ is present are more than doubled for the sample desorbed from the coated wire. In addition, the spectrum of the sample desorbed from bare wire exhibits several new ions which correspond to loss of CF_3CF_2CO and $CF_3CF_2CONH_2$ from sequence ions.

The NH_3-DCI approach lends itself best for the determination of the structure of individual oligopeptides, such as the many important physiologically active peptides or peptide antibiotics. It is not well suited for the complex mixtures of peptides encountered in protein sequencing because it would require extensive separation of these mixtures prior to mass spectrometric analysis.

This work is supported by grant No. 5 P01 GM 26625 from the National Institute of General Medical Sciences, National Institutes of Health.

1. Baldwin, M.A. and McLafferty, F.W. (1973) Org. Mass Spectrom. 7, 1353-56.
2. Hunt, D.F., Shabanowitz, J., Botz, F.K. and Brent, D.A. (1977) Anal. Chem. 49, 1160-63.
3. Haegele, K.D. and Desiderio, D.M. Jr. (1974) J. Org. Chem. 39, 1078-82.
4. Mudgett, M., Bowen, D.V., Field, F.H. and Kindt, T.J. (1976) Biomed. Mass Spectrom. 4, 159-71.

5. Beuhler, R.J., Flanigan, E., Greene, L.J. and Friedman, L. (1974) Biochem. 13, 5060-68.
6. Reinhold, V.R. and Carr, S.A. (1981) 29th Ann. Conf. on Mass Spectrom. and Allied Topics, Minn., Mn. Paper No. RPA 17.

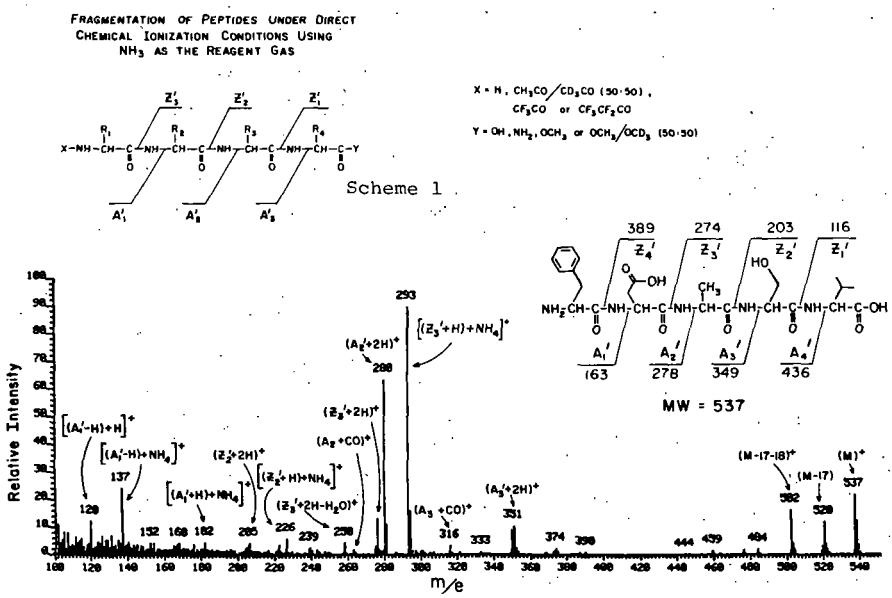

1. Ammonia-DCI mass spectrum of H_2N-Phe-Asp-Ala-Ser-Val-OH.

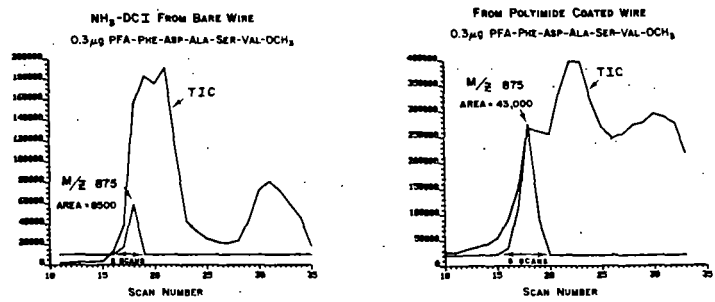

2. Total ion current profiles and mass chromatograms of m/z 875, $(M+NH_4)^+$, for desorption of 0.3 ug of $(PFA)_2$-Phe-Asp-Ala-Ser-Val-$(OCH_3)_2$ from a) bare wire, and b) polyimide coated wire.

Desorptive Chemical Ionization (DCI) Studies of Carbohydrates and Glycoconjugate Materials

V. N. Reinhold and S. A. Carr
Department of Biological Chemistry and
Laboratory of Human Reproduction and Reproductive Biology
Harvard Medical School
Boston, Massachusetts 02115

Direct mass measurement of polar, thermally labile molecules has received much attention in recent years. This has been stimulated in large part by techniques that provide molecular weight information directly while avoiding derivatization. In this study numerous carbohydrate oligomers have been investigated to assess sequence information and several glycolipids to determine structural moieties.

In general, with adequate sample size, desorption of polar materials from bare rhenium wires by programmed heating provides structurally informative ions only during the first few mass spectral scans of the total-ion profile. Latter scans are dominated by fragments arising via thermal degradation which totally consumes the major part of the sample. Much of this loss has been decreased by electrically coating the wires with a polyimide surface which increased considerably the concentration of structurally significant ions.† This coating (thermally stable well beyond the sample desorptive profile) enhanced the over-all sensitivity as well as molecular ion related intensities.

Methane, isobutane and ammonia have been used as reagent gases and, comparable to earlier chemical ionization studies of oligosaccharides (1), ammonia provided mass fragments of the greatest structural interest. The spectra (Figure 1) are dominated by a series of even-mass ions derived from ammonia attachment of primary cleavages on either side of the interceding glycosidic oxygen. This attachment of ammonia, as shown earlier by metastable studies (1), was confirmed in this work using a deuterated reagent gas. The reduced glycosidic moiety provided a 2 amu shift which allowed sequence reading from the terminal (Z) or the reducing (A) end (Figure 2). The simplicity of the fragmentation and the intensity of the high mass fragments suggests that the size of the oligomer suitable for sequencing can be extended markedly by this DCI method and with much greater sensitivity.

The DCI mass spectra of several glycocerebrosides have also shown considerable ion stability and simplicity with pronounced intensity in the molecular ion region as well as abundant ions at conjugate points to ascertain structural moieties.

This work was supported by grant number 5 P01 GM 26625 from the National Institute of General Medical Sciences, National Institutes of Health.

†Preparation of polyimide coated nichrome wires suitable for use in a Finnigan-MAT 312 mass spectrometer equipped with a DCI probe.
Nichrome wire (7 cm x 0.0125 in.) is oxidized with an AC voltage dipped into polyimide "Primer" and polymerized with an AC voltage. This latter step is repeated four times with polyimide "Topcoat". "Primer" and "Topcoat" are Pyre-ML Dupont products available from American Durafilm Company, Newton Lower Falls, Massachusetts.

(1) R. C. Dougherty, J. D. Roberts, W. W. Binkley, O. S. Chizhov, V. I. Kadentsey and A. A. Solor'yov, Journal of Organic Chemistry, 39, 451 (1974).

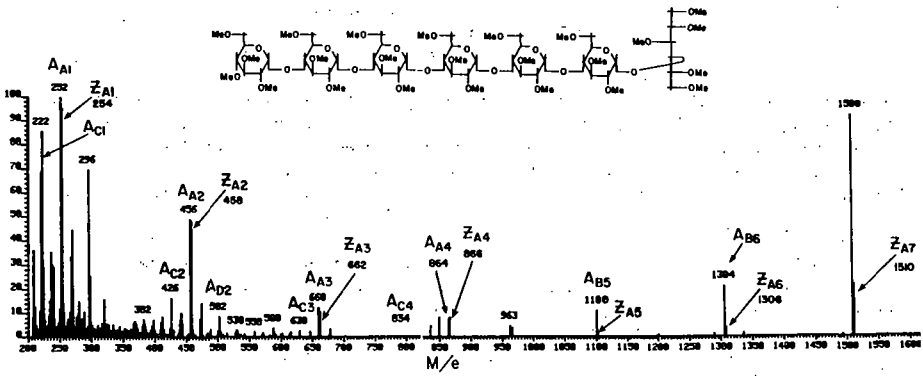

Reduced Permethylated Heptasaccharide

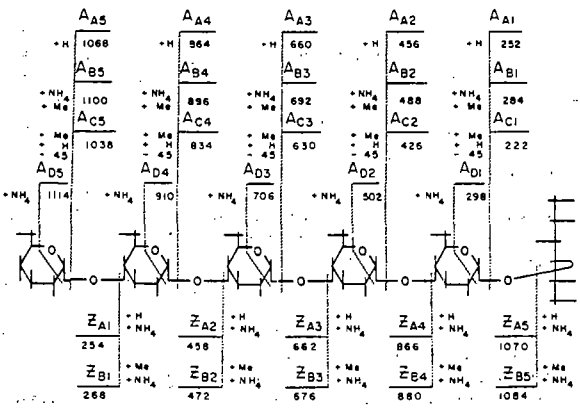

Reduced Permethylated Hexasaccharide M.W. 1286

PULSED FIELD DESORPTION TIME-OF-FLIGHT MASS SPECTROMETER

S. E. Buttrill, Jr., R. H. Fleming, M. Rossi,
W. Gohl and L. N. Goeller
Mass Spectrometry Development Program
SRI International, Menlo Park, CA 94025

We recently described a novel pulsed field desorption time-of-flight mass spectrometer.[1] The advantage of this configuration is that all ions formed by the field ionization or field desorption process are collected and mass analyzed. This paper describes improvements which we have made in the instrument, the factors which limit its resolution, and some very recent experiments using laser desorption as a source of ions.

Instrument Improvements

The channeltron multiplier previously used as the ion detector was replaced by a 40 mm diameter multichannel plate detector. This detector is capable of giving improved resolution in the time-of-flight measurement because its flat surface may be aligned perpendicular to the ion flight path. In contrast, the Channeltron multiplier has an effective depth of 3-4 mm, which limits the time resolution achievable, especially for higher mass ions.

A heated desorption probe was built and installed. The probe is equipped with a thermocouple in direct contact with the FD emitter, thus allowing direct measurement of the emitter temperature.

A facility was constructed to produce silicon activated emitters following the procedure of Matsuo et al.[2] Emitters were constructed from 0.5 inch lengths of 0.063 inch diameter tungsten rod. One end of these rods was polished to a flat surface, and the silicon activation was deposited on this end. The resulting large flat emitting surface is well suited to the geometry of the time-of-flight mass spectrometer.

The silicon activated emitters generally gave poor sensitivities in the pulsed field desorption mode for compounds such as arginine, adenosine, and sucrose. Very large signals could be observed for Li^+, Na^+, K^+ at high temperatures (200°C). In view of previous good results with silicon activated emitters in the normal DC FD configuration, these results suggest that the high electric field plays a role in the transport of molecules to the active sites of the emitter.

The instrument was also tested in the FI mode of operation, in which methyl salicylate vapor was introduced into the mass spectrometer vacuum system. As would be expected, the field ionization signal went down as emitter temperature was increased. Nonetheless, the field ionization signal was much stronger than could be obtained for field desorption of organic compounds.

The time-of-flight mass spectrometer is equipped with an electrostatic reflector which provides second order focusing with respect to ion energy.[3] In other words, when the voltages on the reflector are properly adjusted, the first and second derivatives of the ion arrival time with respect to energy are zero. This design is capable of compensating for a wide spread in ion energy. However, by placing a high voltage on the first region of this reflector, it is possible to reflect the ions back to the detector with very little energy focusing. When operated in this mode, the mass spectrometer gives a time-of-flight spectrum which reflects the ion energy distribution. Experiments of this type showed that ions produced by pulsed field desorption or pulsed field ionization had an energy spread of over 300 volts at a nominal ion energy of 1500 volts. Although the electrostatic reflector successfully compensated for much of this very wide energy spread, the limiting time-of-flight resolution at m/e 152 was about 400.

The high energy spread arises from the interaction of the packet of field desorbed or field ionized ions with the high voltage pulse. The interaction of the ion packet with this pulse is unavoidable because the ions travel such a short distance during the 80-150 nanoseconds duration of the pulse.

Pulsed Laser Desorption

Since high voltage pulses were incapable of providing very short pulses of ions of uniform energy, we took advantage of an opportunity to evaluate the use of a pulsed laser to produce narrow packets of ions for time-of-flight mass analysis. The laser was a Quanta-Ray DCR1 Nd:YAG laser which has a 10 ns pulse width. The main beam of this laser is at 1064 nm and was partially doubled to 532 nm in the green. The presence of the visible component in the beam greatly increased the conveneince and safety of the experiment. No significant wavelength dependence of the pulsed laser desorption was found when these two wavelengths were compared.

In the pulsed laser mode of operation, the emitter was maintained at a constant potential of 1700 volts. A grounded grid was positioned approximately 0.005 inches away from the emitter. The laser beam was directed onto the emitter through the grid in near normal incidence. Ions formed as a result of the laser pulse were rapidly accelerated to the grounded grid, focused by an einzel lens, and deflected by two perpendicular pairs of electrostatic reflector located approximately one meter away. The multichannel plate detector was located directly above the ion source. A large number of emitter materials were tried including silicon whisker activated tungsten rods, polished tungsten rods, broken tungsten rods, gold coated tungsten rods, gold coated silicon whisker activated rods, silver alloy brazing rod, and silver coated rods. All emitters were found to give similar results.

There were two modes of ion formation which could be obtained using the pulsed laser irradiation. At low laser powers, measured to be less than 20 Mwatt/cm^2, a phenomenon which can be described as photo desorption of ionic species occurred. Substances which normally exist in ionic form such as salts of lithium, sodium, cesium, potasium, and tetralkylammonium compounds are desorbed from the emitter during the laser pulse. Hundreds to thousands of ions of these species were desorbed and detected for each laser pulse. Saturation of the multichannel plate detector was frequently observed when monitoring these ions at relatively low laser power.

Operation of the time-of-flight mass spectrometer with pulsed laser desorption of ionic species allowed us to demonstrate the high resolution expected from the electrostatic reflector configuration. The tetraethylammonium ion at m/z 242 could be recorded on a 100 MHz storage oscilloscope with a full width at half height of only 50 nanoseconds. The arrival time of this peak was 72.67 microseconds which gives us a time resolution of 1450. Because the mass resolution of the time-of-flight mass spectrometer increases as the square root of the ion mass, these results indicate the potential for unit mass resolution at masses over 2000. The desirability of utilizing the ion reflector principle with other methods of pulsed ion information, such as plasma desorption, are apparent.

At low powers no ions could be obtained from compounds which are normally present on the surface as neutral species. Compounds tested include sucrose, argenine, and adenosine. At higher powers (greater than 20 Mwatt/cm^2) a new phenomenon was observed. At these powers, electrical breakdown of the emitter surface occurs and a surface plasma forms. The plasma is opaque to the laser radiation and absorbs essentially all of the incident energy. The result is a very hot surface plasma which persists for over 100 microseconds. During this time extremely large ion currents are produced, which threaten to overload the multichannel plate detector. Because of the very long duration of this ion formation process, the time-of-flight mass spectrometer was totally unsuited to mass analysis of these ions.

1. R. W. Odom and S. E. Buttrill, Jr., Presented at the 27th Annual Conference on Mass Spectrometry and Allied Topics, Seattle, WA, June 3-8, 1979.
2. T. Matsuo, et al., Anal. Chem., 1979, 51, 69.
3. B. A. Mamyrin, et al., Sor. Phys.-JETP, 1973, 37, 45.

A METHOD FOR THE MASS CALIBRATION OF PHOTOPLATES IN FIELD DESORPTION AND ITS APPLICATION TO SOME PEPTIDES

R. Espinosa-Leniz and J. E. Girard, Department of Chemistry, The American University, Washington, D.C. 20016

E. White V, Center for Analytical Chemistry, National Bureau of Standards, Washington, D.C. 20234

A method, applicable to field desorption, has been developed for establishing a high resolution mass scale on a photoplate by a double exposure in which sample and calibrating material are separately desorbed onto the same line of the photoplate. Mass calibration is achieved by field desorption of a mixture of silver methanesulfonate and trifluoromethanesulfonate which gives cluster ions of the general formula $[Ag_{m+n+1}(O_3SCH_3)_m(O_3SCF_3)_n]^+$. These ions provide calibration masses about every 50 mass units to about 1400 (1).

Experimental: Tungsten emitter wires (10 μm diameter), activated at high temperature with benzonitrile were loaded with the calibration mixture by dipping into an aqueous 0.5 M silver methanesulfonate/0.5 M silver trifluoromethanesulfonate solution. Desorption was accomplished by slowly heating the loaded emitter to about 30 mA. Polypeptides were loaded by either dipping the emitter in a 30 percent aqueous formic acid solution of the peptide or by syringe loading and desorbed at about 20 mA. Polypeptides and calibrating material were desorbed from the same emitter in either order. The emitter was thoroughly washed in between to avoid contamination of the peptide from the calibrating material or vice versa.

Spectra of calibrating material and peptide were recorded on the same exposure of an evaporated silver bromide photoplate with exposure times ranging from a few seconds to several minutes as required.

Results: The precision and accuracy of the calibration were tested using polypeptides of known mass.

The precision was evaluated using two pentapeptides, Methionine enkephalin, and Leucine enkephalin, known to give good low resolution spectra. Table I presents 19 measurements on $[M+H]^+$ ion obtained on five photoplates over a 20 week period. Each represents an individual exposure.

The accuracy of the method was evaluated by using five polypeptides of known mass. The masses obtained for $[M+H]^+$ and for other ions are compared to the theoretical masses in Table II.

Conclusions: A mixture of silver methanesulfonate and silver trifluoromethanesulfonate is a good calibrating material for high resolution field desorption mass spectra using photoplate detection. Calibration by this method shows satisfactory precision and accuracy.

Some advantages of the method are: calibration is done in the FD mode with no switching between EI and FD required; the calibration material leaves the activated emitter wire undamaged so that sample and calibration material can be desorbed one at a time in either order from an emitter; the components of the calibration material are commercially available; the calibration masses are spaced at reasonable intervals over a large mass range; the mass defect of the calibration material makes sample ions easily distinguishable from calibration ions; and the existence of two silver isotopes at a ratio close to 1:1 leads to clusters from which lines of appropriate intensity can be chosen.

(1) G. D. Robert and E. White V, unpublished results.

TABLE I

Methionine-Enkephalin Tyr-Gly-Gly-Phe-Met
Theoretical Mass of $[M+H]^+$ Ion: 574.2335

Measured Mass (Mass Units)	Difference Measured-Theoretical (Millimass Units)
574.2367	+ 3.2
574.2332	- 0.3
574.2278	- 5.7
574.2268	- 6.7
574.2254	- 8.1
574.2394	+ 5.9
574.2311	- 2.4
574.2265	- 7.0
574.2309	- 2.6
574.2437	+10.2
574.2233	-10.2
MEAN 574.2314	
S.D. 0.0063	

Leucine-Enkephalin Tyr-Gly-Gly-Phe-Leu
Theoretical Mass of $[M+H]^+$ Ion: 556.2771

Measured Mass (Mass Units)	Difference Measured-Theoretical (Millimass Units)
556.2740	-3.1
556.2804	+3.3
556.2740	-3.1
556.2679	-9.2
556.2835	+6.4
556.2805	+3.4
556.2778	+0.7
556.2806	+3.7
MEAN 556.2773	
S.D. 0.0051	

TABLE II

Peptide	Theoretical Mass (Mass Units)	Measured Mass (Mass Units)	Measured-Theoretical (Millimass Units)
Trp-Met-Asp-Phe-Amide Gastrin Related Tetrapeptide	$[M+H]^+$: 597.2495	597.2501	0.6
Tyr-Ile-His-Pro-Phe Angiotensin II Pentapeptide	$[M+H]^+$: 676.3459	676.3471	1.2
Lys-Phe-Ile-Gly-Leu-Met-Amide Eledoisin Related Peptide	$[M+H]^+$: 707.4278	707.4187	-9.1
Tyr-Gly-Gly-Phe-Met	$[M+H]^+$: 574.2335	574.2311	-2.4
Met-Enkephalin	$[M+Na]^+$: 596.2155	596.2247	9.2
	$[M+^{107}Ag]^+$: 680.1308	680.1287	-2.1
	$[M+^{109}Ag]^+$: 682.1304	682.1301	-0.3
	Gly-Phe-Met: 354.1487	354.1483	-0.4
Tyr-Gly-Gly-Phe-Leu	$[M+H]^+$: 556.2771	556.2778	0.7
Leu-Enkephalin	$[M+Na]^+$: 578.2591	578.2559	-3.2
	Gly-Phe-Leu: 336.1922	336.2070	4.8

Negative Ion Field Desorption Mass Spectra of Complex Anions Containing Technetium

S. A. Carr, C. E. Costello, C. Orvig, A. Davison and K. Biemann
Department of Chemistry
Massachusetts Institute of Technology
Cambridge, Massachusetts 02139

We have previously shown that positive ion field desorption mass spectrometry (FDMS) is a useful method for the characterization of anionic coordination complexes containing technetium and rhenium (1-3). These compounds are important because of their extensive use as radioimaging agents in clinical chemistry. The positive ion spectra consisted almost entirely of ions corresponding to the cationic portion of the complex, $(C)^+$, $(M)^+$ and $(M+C)^+$. Ions derived exclusively from the Tc-containing anionic portion of the molecule were only observed in the spectra of complexes containing an aromatic anionic ligand. Although quite good sensitivity was obtained for these species, these spectra were still dominated by ions arising from the counter-cation.

We have now obtained the negative ion FD mass spectra of a series of Tc anionic coordination complexes. In sharp contrast to the positive ion spectra, these spectra consist exclusively of $(anion)^-$ and $(M+anion)^-$, thus deriving all the ion current from the portion of the molecule which is of greatest interest. A typical negative FD spectrum is shown in Figure 1.

Sensitivity is high, sufficient for analysis of Tc complexes at therapeutic levels. This has been demonstrated by administering a carrier-added preparation of n-tetrabutylammonium oxobis(N,N'-ethylenebismercaptoacetamido)technetate, TBA^+ $[TcO(ema)]^-$, to three rats [^{99}Tc) = 10^{-3}M and (^{99m}Tc) = 10^{-13}M]. The bladders were removed and the components in the urine were separated by reversed phase ion$^-$ pair HPLC. Ninety per cent of the radioactivity eluted in one peak, which was collected and desalted using a Sep-Pak^R C_{18} cartridge. Radioactive fractions were pooled, evaporated to dryness and redissolved in chloroform. This solution was applied to the FD emitter by dipping. The $(anion)^-$ region of the resulting spectrum is shown in Figure 2. Other experiments have indicated that 10^{-4}M solutions are adequate for analysis. The $(anion)^-$ peak may still be detected at the 10^{-5}M level.

This technique is therefore suitable for the characterization of new synthetic compounds and the materials present in clinical kits and should be useful for the structure determination of metabolites.

The assistance of Eric Kleeman (MAT-Bremen) in converting the MAT-731 instrument to negative ion operation and the aid of James Brodack (Massachusetts Institute of Technology) in the animal studies are greatly appreciated. This work is supported by grants from the National Institutes of Health (RR00317 and GM 23270) and the National Science and Engineering Research Council of Canada (to C. Orvig).

1. Wilson, B. W., Costello, C. E., Carr, S. A., Biemann, K., Orvig, C., Davison, A. and Jones, A. G. (1979). Analytical Letters 12, 303-311.

2. Carr, S. A., Costello, C. E., Wilson, B. W., Orvig, C., Davison, A. and Biemann, K. (1979). Twenty-seventh Annual Conference on Mass Spectrometry and Allied Topics, Seattle, Washington, pp. 48-49.

3. Costello, C. E., Carr, S. A., Mancuso, N. R. and Biemann, K. (1979). Twenty-seventh Annual Conference on Mass Spectrometry and Allied Topics, Seattle, Washington, pp. 51-52.

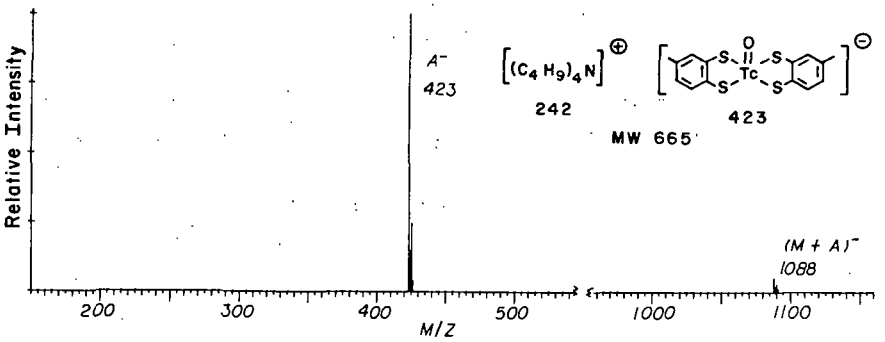

1. Negative ion FDMS of tetrabutylammonium oxobis(3,4 toluenedithiolato)technetate ($TBA^{+}TDT^{-}$), 19 mA.

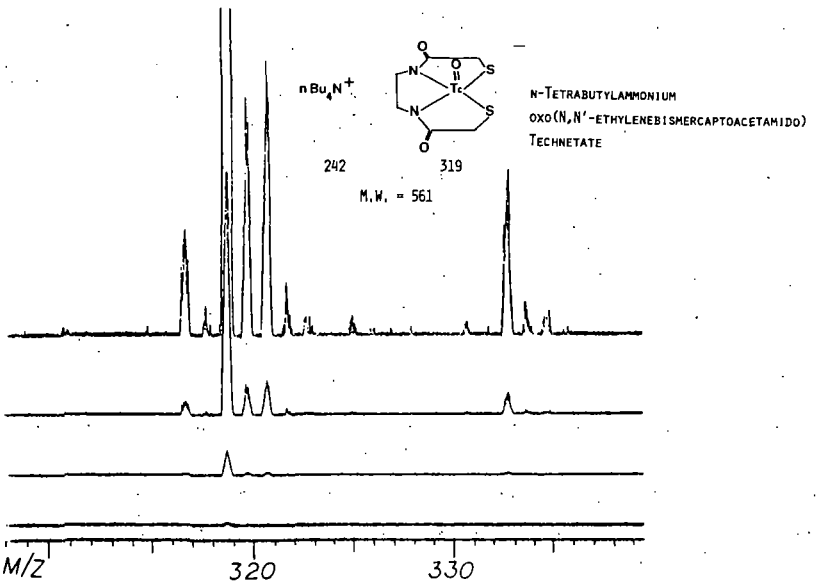

2. Oscillograph trace of $(anion)^{-}$ region of negative ion FDMS of recovered $TBA^{+}(TcO(ema))^{-}$, 22 mA. Emitter loaded by dipping into a final volume of 30 ul of approximately 10^{-3}M.

A FIELD IONIZATION MASS SPECTROMETER SYSTEM FOR DETECTION OF ORGANIC VAPORS IN AIR

Ronald H. Fleming and S. E. Buttrill, Jr.
SRI International, Menlo Park, CA 94025

A field ionization mass spectrometer system capable of detecting organic vapors in air has been assembled.[1] The system is based on an Extranuclear Laboratories model 324-9 (3/4" rods) quadrupole mass filter. The field ionization source is of the volcano style. Ion optics include a re-entrant focus lens near the ionizer followed by a double plate extractor lens and an Extranuclear ELFS ferrite tube entrance lens. In the field free region between the two extractor plates is a quadrupole beam steering assembly.

Sample is introduced into the vacuum system by drawing air through an inlet and across a section of dimethyl silicone membrane (46 mm^2 x .025 mm). The permeability of the membrane to organic substances is typically 15 to 500 times the permeability to air. The membrane thus serves to concentrate organic molecules relative to air at the same time it provides a barrier between the atmosphere and the high vacuum of the mass spectrometer.

The mass analyzed ions are detected in the ion counting mode using a continuous dynode electron multiplier. A computer collects data and controls the mass analyzer. The software permits scanning of a complete spectrum or numerous small regions of a spectrum. Several masses can be followed as a function of time.

Figure 1 shows the spectrum of diisopropyl methylphosphonate (DIMP) in air. The sample was introduced by holding an open bottle near the air inlet. Using the same instrument settings with the mass tuned to m/z 181 ($DIMP\text{-}H^+$), the data in Figure 2 were obtained. The sample was injected into an exponential dilution flask to make an initial concentration of 1 ppm. The output of the dilution flask was then led to the air inlet of the mass spectrometer. The sensitivity demonstrated in Figure 2 is about 4 ppb.

Operation of the volcano under conditions which produce high sensitivity tend to reduce its useful lifetime. Presumably this effect is due to the action of residual oxygen which is present during air sampling. Future work will include evaluation of new volcano construction materials in order to improve the trade-off between sensitivity and source lifetime.

[1]S. E. Young and S. E. Buttrill, Jr., 28th Annual Conference on Mass Spectrometry and Allied Topics, New York, NY, May 25-30, 1980, page 334.

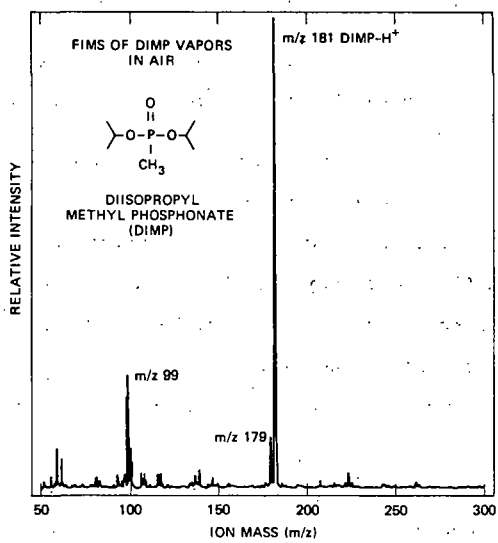

FIGURE 1 FIELD IONIZATION MASS SPECTRUM OF DIMP VAPORS IN LABORATORY AIR

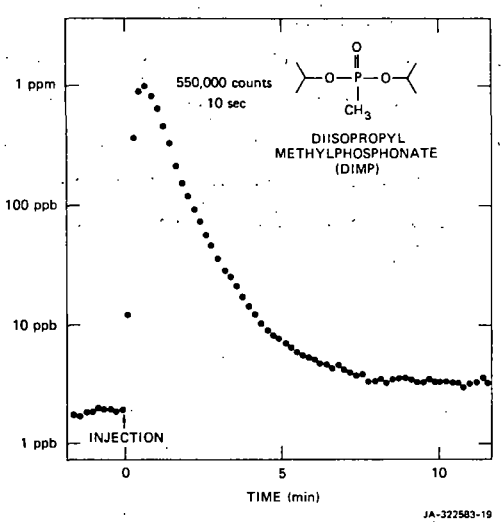

FIGURE 2 FIELD IONIZATION OF DIMP USING THE EXPONENTIAL DILUTION FLASK

MINICOMPUTER-BASED MULTICHANNEL ANALYZER FOR ACQUISITION OF LOW INTENSITY MASS SPECTRA

Charles R. Snelling, Jr., J. Carter Cook, Jr.,
Richard M. Milberg, and Kenneth L. Rinehart, Jr.

School of Chemical Sciences, University of Illinois, Urbana, IL 61801

Several problems in mass spectrometry are amenable to solution by the use of a computer to acquire and sum multiple scans. One of these involves obtaining useful data from the low-intensity spectra inherent in both low and high resolution field desorption (FD) and in high resolution electron impact (EI) mass spectrometry. Another problem solved by multiple scans involves spectra that change with time or are only present for a short period of time such as those frequently encountered in GC/HRCI and GC/EI isotope ratio studies.

To deal with these problems, we have developed a hardware/software multichannel signal averager (MSA) system using ion counting techniques. The MSA system is based on the pulse analyzer system of Ligon[1] but is more versatile since all data handling is performed by software. The system permits real-time acquisition and observation of multiple scans for averaging and is designed for both low resolution and high resolution determinations.

Figure 1 contains a general block diagram of the system and Figure 2 is a list of the major hardware and software features. The MSA system currently employs a DEC PDP-8a minicomputer which is part of a VG-Micromass M-82 Multispec Mass Spectrometer Data System. However, the design requires minimal hardware and is transferable to any data system that supports FORTRAN.

---

(1) W. V. Ligon, Jr., 28th Ann. Conf. Mass Spectrom. Allied Topics, New York, NY, May 25-30, 1980; Paper No. RAMOB5.

BLOCK DIAGRAM OF "SOFTWARE"
MULTI CHANNEL ANALYZER

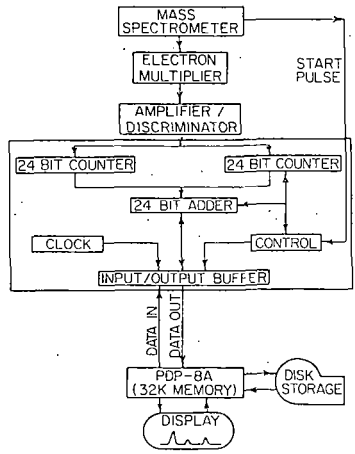

Figure 1

SYSTEM FEATURES

- COMPUTER - PDP-8A (32K MEMORY)
- DISCRIMINATOR-AMPLIFIER - PACIFIC PRECISION INSTRUMENTS (AD6)
- SCAN FUNCTION - LINEAR
- SCAN SPEED - 0.3 TO 10 SEC (LONGER IF NEEDED)
- SCAN WIDTH - LESS THAN 1 AMU TO +/- 10% OF NOMINAL MAGNET SETTING
- MAXIMUM COUNT RATE - 35 MHz (AMPLIFIER SATURATES AT 32 MHz)
- DWELL TIME/CHANNEL - 3 MSEC TO SCAN TIME
- DEAD TIME - 400 NSEC
- NUMBER OF CHANNELS - 100 TO 2000 (MORE IF NEEDED)
- MAXIMUM ION COUNT/CHANNEL - 2^{24}
- MINIMAL HARDWARE - INTERFACE IS ESSENTIALLY A 24-BIT ADDER, A CLOCK AND TWO 24-BIT COUNTERS
- SOFTWARE WINDOW FILTERS OUT ABNORMALLY HIGH COUNTS ASSOCIATED WITH ARC-OVERS.
- AUTORANGING
- AUTO AND MANUAL CENTROID CALCULATIONS
- HORIZONTAL AND VERICAL PEAK EXPANSION
- SAVITZKY-GOLAY SMOOTHING
- SAMPLE AND REFERENCE DATA CAN BE STORED SEPARATELY
- ANALOG RATE METER

Figure 2

THE ANALYSIS OF PARAQUAT RESIDUES IN WHEAT USING GAS CHROMATOGRAPHY - CHEMICAL IONIZATION MASS SPECTROMETRY

PERRY S. WILKES AND GERALDINE D. SANDERS
Food and Drug Administration, Atlanta Regional Laboratory, Atlanta, GA. 30309

The herbicide Paraquat (1, 1' - dimethyl-4, 4'-bipyridylium dichloride) is used for defoliation and desiccation of certain trees, crops and grasses. Recently, an accidental spraying of paraquat on an unharvested wheat field resulted in non-permitted residues of this herbicide. Paraquat was found in the wheat at a level of 0.5 ppm using an ion-exchange cleanup and colorimetric detection method (1). Due to low levels of paraquat and interfering co-extractives, a problem arose when attempts were made to confirm paraquat by TLC and HPLC. Derivative formation and detection of paraquat by GLC using a specific detector and identity confirmation using GC/MS was successful.

The GLC method of Kahn (2) for determining diquat and paraquat residues in soil was used as a guide and was adapted to wheat. This method utilizes an acid digestion procedure for extraction of paraquat from soil. The extract is hydrogenated using platinum oxide as a catalyst. Hydrogenated paraquat is readily soluble in organic solvents and can be separated from extraneous materials by GLC.

For the determination of retention time and detector response, a TRACOR 560 gas chromatograph equipped with a nitrogen-phosphorus (N-P) detector was used. The operating parameters were:

Column:	6' X 2 mm i.d. glass packed with 5% carbowax 20M + 2.5% KOH on 80/100 mesh Chromosorb W (HP)
Column Temperature:	160°C
Injector Temperature:	225°C
Detector Temperature:	250°C

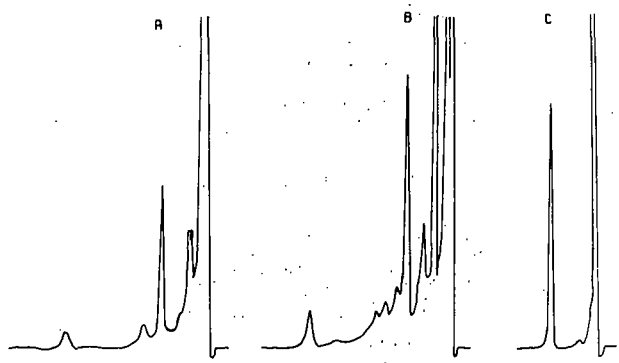

Figure 1. Typical gas chromatograms from the nitrogen-phosphorus detector for (a) a wheat sample spiked with paraquat, (b) a wheat sample found to contain paraquat and (c) paraquat

Samples, standard and spike samples exhibited identical retention times of 6.25 mins. Typical chromatograms are shown in Figure 1. A recovery of 75% was obtained from a wheat sample spiked with 1.17 ppm of paraquat.

The GC/MS analysis of the derivatized paraquat confirmed the GLC-NP findings. Identity confirmation of the hydrogenated paraquat was accomplished by the comparison of retention time and mass spectral data of the sample extract to that of a hydrogenated paraquat standard analyzed under identical GC/MS conditions. The instrument used was a Finnigan 3300 GC/MS System with a 6000 Data System. The chemical ionization mode was used with methane as the reagent gas. The operating parameters were:

Column:	6' X 2 mm i.d. glass packed with 5% carbowax 20M + 2.5% KOH on 80/100 mesh Chromosorb W (HP)
Column Temperature:	140°C
Carrier gas:	Methane, flow adjusted to give 1 torr of pressure in the CI source
Injector and transfer line temperature:	250°C
Electron Energy:	150 ev
Emission Current:	1.5 mamp.

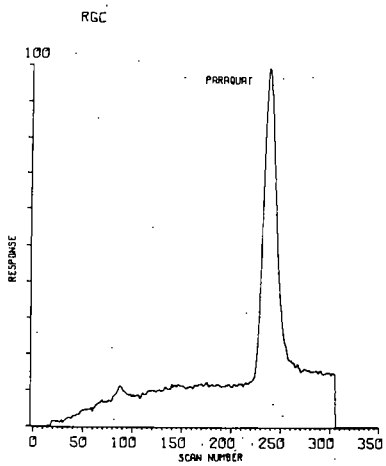

Figure 2. Reconstructed gas chromatogram of hydrogenated paraquat

Figure 2 shows a total ion chromatogram of hydrogenated paraquat from wheat, and Figure 3 shows the chemical ionization mass spectrum of hydrogenated paraquat. Ions are observed for the $M^+ + 1$ (m/8 197), $M^+ + 29$ (m/z 225) and $M^+ + 41$ (m/8 237) and an abundant $M^+ - 1$ ion at m/z of 195.

The reaction diagramed below shows the hydrogenation of paraquat to produce a bipiperidine. The presence of the $M^+ - 1$ ion, under chemical ionization conditions, can be attributed to hydrogen-ion abstraction which is observed for hydrocarbons.

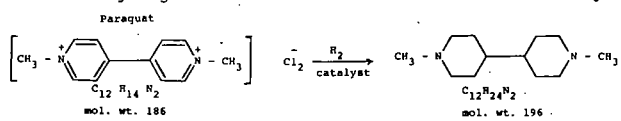

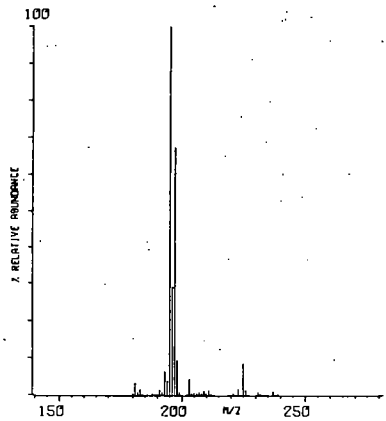

Figure 3. CI mass spectrum (methane) of hydrogenated paraquat

References

1. Food and Drug Admin., Pesticide Analytical Manual, Vol. II, Sec. 180.205

2. Kahn, Shamat U., J. Agr. Food Chem., 22, 863-867 (1974)

Falcarinol in Carrots by GC-MS

R. D. Plattner, Roger E. England, Kathleen L. Payne-Wahl and Shelly G. Yates; Northern Regional Research Center, Science and Education Administration, Agricultural Research, U.S. Department of Agriculture, Peoria, IL 61604

Naturally occurring toxicants have been identified in many plants that are used for food or feed. Although no immediate health hazards are apparent, research is in progress to quantitate the contents of such toxicants in commercial vegetable cultivars, to develop baseline information for use by plant breeders, and to evaluate toxicity levels and effects in test animals and humans. Falcarinol (cis-heptadeca-1,3-diene-4,6-diyne-3-ol) is a naturally occurring toxic substance found in carrots. Extracts of carrot root were reported toxic to an indicator organism (Daphnia magna Straus) by Crosby and Aharonson (1). The purified toxin they isolated produced "neurotoxic symptoms upon injection into mice;" LD_{50} was estimated to be 100 mg/kg. Since carrot root contributes about 14% of our national intake of vitamin A, 0.6% of our national intake of vitamin B_6, and 0.6% of our national intake of magnesium (2), it is worthy of close attention. Wolf et al. (3) reported a HPLC procedure to quantitate falcarinol in steam distillate of carrot roots. The analytical GC-MS procedure reported here for the analysis of carrot roots uses a methylene chloride extract of chopped root.

Carrot roots, Daucus carota, were bought in commercial markets, grown and harvested at NRRC, or grown and harvested at various field locations as directed by the Department of Horticulture, University of Wisconsin, Madison. The methylene chloride extraction procedure used was as follows: 50 g of carrot pieces (~1 X 1 X 0.2 cm) was added to a blender cup with 100 ml of methylene chloride. The mixture was blended at moderate speed for 12 min. Alternate cycles of blending and cooling (4 min each) reduced evaporation of methylene chloride. Methylene chloride lost by evaporation was replaced, and the entire sample was transferred to a 250-ml centrifuge bottle and centrifuged for 15 min at 2500 rpm. A 2.0 ml aliquot of the clear extract was then evaporated to dryness under a stream of N_2. Methyl palmitate (10-50 µg) was added as an internal standard and the TBDMS derivative was formed by adding 50 µl of 1.0 millimolar t-butyl dimethylchlorosilane and 2.5 millimolar imidazole in DMF. After 1 hr at room temperature, derivative formation was complete. The sample was then analyzed by GC-MS on a MS 30 mass spectrometer. A 1 m X 2 mm column packed with 3% OV-1 on gaschrom Q was temperature programmed from 150°C to 250°C at 4°C per minute. The TBDMS derivative of falcarinol eluted in about 9 min. Quantitation was made using the areas of the peaks from the MPM chromatograms of M/z 270, the molecular ion of the internal standard, and M/z 301 and M/z 245 from M-57 and M-113 of the falcarinol TBDMS derivative. Standard mixtures of the internal standard and falcarinol over the range of 1/10 to 5/1 gave a linear response for the area ratio vs. weight ratio over the entire range. With linear regression, correlation coefficients of better than 0.99 were obtained with five known mixtures across the range. To minimize variability of instrumental tuning parameters, two standards were run with each day's analysis and the area/weight ratios of the standards were used for calculation of the falcarinol concentration in the unknowns. The concentration of falcarinol found in five carrot varieties is shown in Table 1. The falcarinol content for the varieties grown in Florida tended to be higher than the same carrot variety grown in California.

References

1. Crosby, D. G., Aharonson, N., Tetrahedron 23, 465 (1967).
2. Senti, F. R., Rizek, R. L., Crop Science Society of America, Special Publication #5, 7 (1974).
3. Wolf, L. W., Nagel, C. W., Branen, A. L., J. Agric. Food Chem. 26, 1390 (1978).

Table 1

Analysis of Carrot Samples for Falcarinol

Variety	Falcarinol (ppm)	SD (number of samples)
Bel Ridge	15.8	0.66(8)
Imperator (Fla.)	49.6	0.62(8)
Imperator (Ca.)	25.5	3.0(8)
Danvers 126 (Ca.)	22.1	1.9(8)
Danvers 126 (Fla.)	49.8	0.95(6)
Spartan Bonus	31.2	3.0(6)
High Color 9	17.2	0.84(8)

GC/MS ANALYSIS OF ANIMAL TISSUE SAMPLES FOR TRACE LEVELS OF DIETHYLSTILBESTROL

M. K. Hoffman and P. C. Hsu, U. S. Dept. of Agriculture, Food Safety and Quality Service, Science, CDLB, Beltsville, Maryland 20705

It is well documented that the use of Diethylstilbestrol (DES) as a feed supplement or implant in cattle leads to increased weight gains compared to control groups.[1,2,3] In 1954, the Food and Drug Administration approved the use of DES as a feed additive for beef cattle following extensive hearings which documented the estrongenic effects of DES. The carcinogenic effects of DES are also well documented.[4,5,6] Recent animal feeding studies of DES (.1 ug/1Kg body weight) produce elevated FSH and LH levels in infant rhesus monkeys.[7] A "no effect level" has not been established for DES.

Following extensive hearings, FDA revoked the approved use of DES as a feed supplement and an implant in cattle was revoked on November 1, 1979.[8] In the Spring of 1980, numerous violations were reported throughout the Midwest. Prior to the ban on the use of DES, the USDA - FSQS action level was 0.5 ppb. Subsequent to that ban, detection of DES at any level was indicative of illegal contamination. Previous confirmatory methodology utilized derivation of DES with dichloroacetyl chloride (DCAC) followed by multiple ion monitoring of the molecular ion cluster at m/z, 488, 490 and 492. To enhance specificity by supplying more information than that provided by the molecular ion cluster and to enhance sensitivity by use of a mono-isotopic derivative, the bis heptafluorobutyrl ester of DES was synthesized.[9] Earlier GC studies had indicated an approximately 10-fold increase in response of an electron capture detector for the bis HFB-DES derivative compared to that for the BIS-DCA derivative. A study of a variety of gas chromatographic phases indicated that a 3 % OV-101 packed column provided the greatest response and less interfering column bleed than OV-17, or than mixed phase columns with OV-202/17, OV-210/17. Although use of a capillary column (dimethylsilicone) provided better gas chromatographic separation, absolute mass spectral sensitivity was not enhanced. Mass spectra were obtained under electron impact conditions. Positive and negative ion chemical ionization spectra were obtained using methane as the reagent gas. Comparative mass spectra are shown in Figure 1. Rapid relative sensitivity studies indicated that although negative ion chemical ionization was slightly more sensittive than electron impact, the electron impact fragmentation pathways provided ions which were more useful structurally for confirming the presence of DES from tissue matrices at low levels (ppt). Sphon[10] has discussed the issue of using mass spectrometry to the presence of a substance and has recommended that at least three ions be monitored. For the DES study, the ion current profile of five or six ions were monitored. The existence of both cis-and trans-isomers of DES provide further confirmatory criteria. Selected ion current profiles from spiked and incurred kidney samples permitted confirmation at the 0.02 ppb level. Confirmation required injection of sample aliquots which contained approximately 100-200 pg of DES. That DES can be confirmed in spite of the presence of large amounts of extraneous materials present after workup indicates both the sensitivity and specificity of low resolution GC/low resolution mass spectrometry for regulatory work.

1. R. R. Oltjen and R. E. Davis, J. Anim. Sci., 23, 887 (1964).
2. R. R. Oltjen and R. E. Davis, J. Anim. Sci., 24, 198 (1965).
3. P. A. Putnam, R. R. Oltjen, and J. Bond, J. Anim. Sci., 28, 256 (1969)
4. G. H. Gross, D. Coates, and N. Graham, J. Natl. CAncer Inst., 33, 971 (1964).
5. J. A. McLachlan, J. Toxicol. Environ, Health 2, 527 (1977).
6. M. Bibbo, W. B. Gill, F. Azizi, R. Blough, V. S. Fang, R. L. Rosenfield G. F. B. Schumacher, K. Sleeper, M. G. Sonek and G. L. Wied, J. Obstet. Gynecol. 49, 1 (1977).
7. W. C. Hobson, personal communication.
8. 44 FR 24852, Sept. 21, 1979 and 44 FR 17070, March 20, 1979.
9. C. F. Poole and A. Zlatkis, Anal. Chem., 52, 1002A (1980).
10. J. Sphon, J. Assoc. Off. Anal. Chem., 61, 1247 (1978).

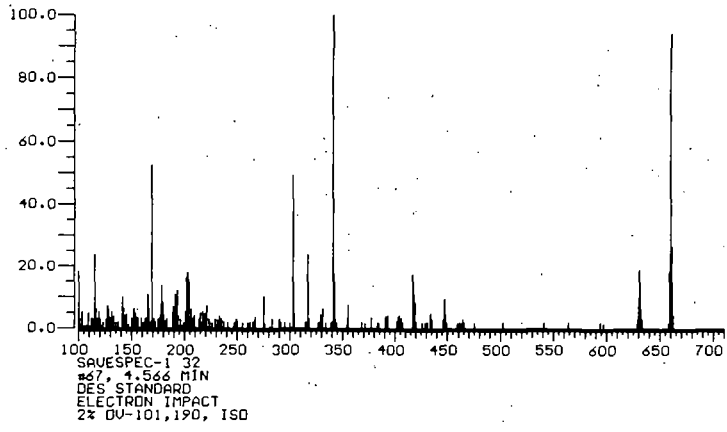
100.0
80.0
60.0
40.0
20.0
0.0
100 150 200 250 300 350 400 450 500 550 600 650 700
SAVESPEC-1 32
#67, 4.566 MIN
DES STANDARD
ELECTRON IMPACT
2% OV-101,190, ISO

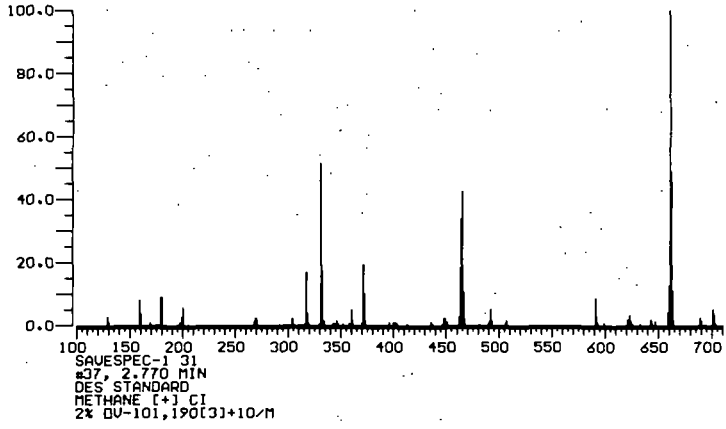
100.0
80.0
60.0
40.0
20.0
0.0
100 150 200 250 300 350 400 450 500 550 600 650 700
SAVESPEC-1 31
#37, 2.770 MIN
DES STANDARD
METHANE [+] CI
2% OV-101,190[3]+10/M

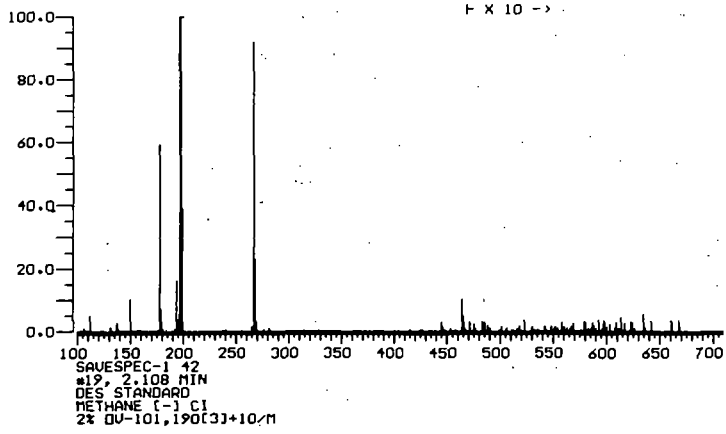
⊢ X 10 →
100.0
80.0
60.0
40.0
20.0
0.0
100 150 200 250 300 350 400 450 500 550 600 650 700
SAVESPEC-1 42
#19, 2.108 MIN
DES STANDARD
METHANE [-] CI
2% OV-101,190[3]+10/M

A CONFIRMATORY METHOD FOR FOSTHIETAN RESIDUES IN CORN TISSUE BY GAS CHROMATOGRAPHY-NEGATIVE ION CHEMICAL IONIZATION MASS SPECTROMETRY

S. J. Stout, M. O. Poeppel, J. W. Higham

American Cyanamid Company, Agricultural Research Division, P. O. Box 400, Princeton, New Jersey 08540

Introduction

Fosthietan is the active ingredient of NEM-A-TAK® Nematicide-Insecticide. The recommended procedure for determining fosthietan residues in corn tissue involves injection of the cleaned up extract into a gas chromatograph equipped with a flame photometric detector (GC-FPD). In the event of an apparent residue exceeding 0.05 ppm, a confirmatory method of analysis is required.

Objective

Develop a GC-CIMS method to confirm the identity of apparent residues of fosthietan in corn tissues at levels of 0.05 ppm or greater.

Experimental

Analyses of fosthietan residues in corn tissue using multiple ion detection (MID) employed the following analytical conditions:

1. GC-MS instrumentation	Finnigan 4000
2. Data System	INCOS 2300
3. Column	10% OV-101 on 100/120 Gas Chrom Q (6' x 2 mm ID)
4. Carrier-reagent gas	CH_4
5. Column oven temperature	220°C
6. Injection port temperature	250°C
7. Interface temperature	200°C
8. Source temperature	250°C
9. Methane flow rate	15 ml/min
10. Source pressure	400 microns
11. Conversion Dynodes	+ 3.0 Kv
12. Electron multiplier	900 volts
13. Preamplifier range	10^{-7} amp/volt
14. Ions monitored	m/z 241^-, 166^-, 58^-

Summary

A confirmatory method of analysis for residue levels (0.05 ppm) of fosthietan in corn silage, fodder and grain has been developed using gas chromatography-negative ion chemical ionization mass spectrometry (GC-NICIMS). Using methane as the GC carrier gas-CI reagent gas, NICI generated principal ions at m/z 241^- ($M^{\bullet}$), 166^- ($M^{\bullet} - C_2H_5^{\bullet}$, $CH_2{=}S$) and 58^- ($[N{=}C{=}S]^-$). Positive ion (PI) CI was also investigated, but was not further pursued when it showed a response to fosthietan which was 50-fold less than the NICI response. By applying multiple ion detection (MID) techniques to the ions characteristic of fosthietan, GC-NICIMS demonstrated a linear response range of 0.5 ng to 5.0 ng injected on column. Based on the injection aliquot corresponding to 25 mg of corn tissue, this response range is equivalent to 0.02 ppm to 0.20 ppm fosthietan in the corn tissue.

Several control and fortified corn tissue samples previously analyzed by GC-FPD were analyzed by GC-NICIMS. No interferences were detected for the ions monitored at the retention time of fosthietan. There was close agreement between recoveries calculated from the GC-NICIMS data and those calculated from the GC-FPD data.

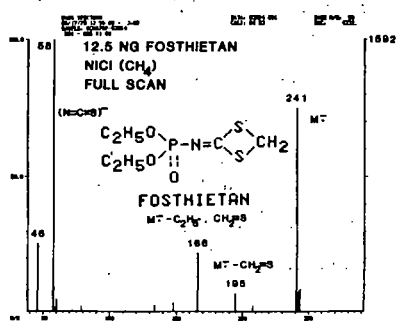
12.5 NG FOSTHIETAN
NICI (CH_4)
FULL SCAN
241
M⁻
(N=C=S)⁻
C_2H_5O
C_2H_5O
P-N=C
S
S
CH_2
O
FOSTHIETAN
M⁻-C_2H_5, CH_2S
M⁻-CH_2S
58
46
1592

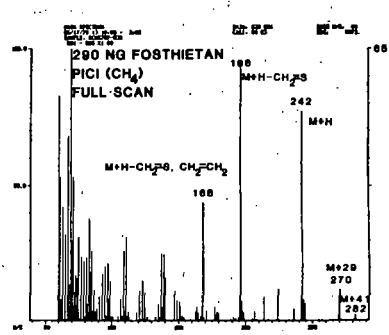
290 NG FOSTHIETAN
PICI (CH_4)
FULL SCAN
M+H-CH_2S
M+H
M+H-CH_2S, CH_2=CH_2
M+29
270
M+41
282
651

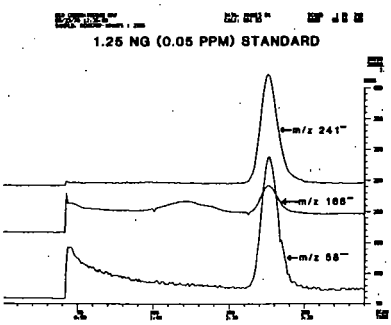
1.25 NG (0.05 PPM) STANDARD
m/z 241⁻
m/z 166⁻
m/z 58⁻

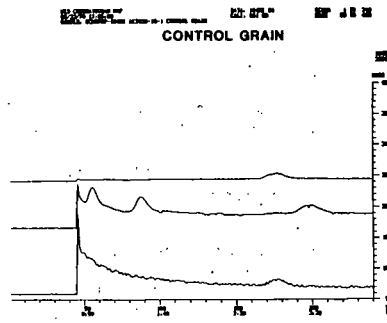
CONTROL GRAIN

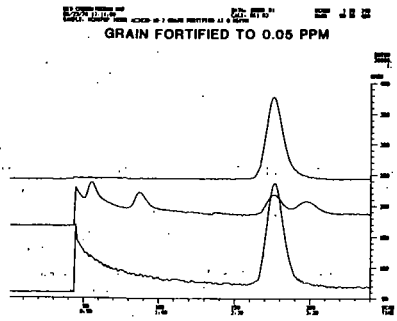
GRAIN FORTIFIED TO 0.05 PPM

MASS SPECTROMETRIC STUDY OF ETHOPROP (O-ETHYL-S, S-DIPROPYL PHOSPHORODITHIOATE). W. T. LEWIS AND A. K. BHATTACHARYA, MOBIL CHEMICAL COMPANY, RESEARCH & DEVELOPMENT DEPARTMENT, EDISON, NJ 08817

A GC/MS STUDY OF O-ETHYL-S,S-DIPROPYL PHOSPHORODITHIOATE (ETHOPROP) SHOWED THIS COMPOUND TO HAVE A STRONG TENDENCY TO CHEMICAL IONIZATION (SELF-INDUCED) EVEN AT LOW SAMPLE PRESSURES. FURTHER STUDIES SHOWED THAT THE DEGREE OF CHEMICAL IONIZATION VARIED THROUGHOUT THE GAS CHROMATOGRAPHIC PEAK (RIC) SUGGESTING THE ELIMINATION OF A NEUTRAL MOLECULE WHICH COULD SUBSEQUENTLY BEHAVE AS A CI GAS.

EXAMINATION OF THE EI SPECTRUM OF ETHOPROP SHOWS TWO MAJOR STABLE FRAGMENTS AT m/z 200 AND m/z 158. THIS SUGGESTS THE ELIMINATION OF PROPENE (2 MOLES). THE CI(CH_4) AND CI(ISOBUTANE) SPECTRA ARE PRESENTED FOR COMPARISON.

THE NEGATIVE ION SPECTRUM AND THE NEGATIVE ION CI(CH_4) SPECTRUM BOTH SHOW ONLY A STRONG m/z 199 PEAK AGAIN SUGGESTING THE ELIMINATION OF PROPENE. THE UNIQUENESS OF THE NEGATIVE ION DATA HAS BEEN USED TO IDENTIFY RELATED COMPOUNDS.

UNUSUAL POLYCHLORINATED XENOBIOTIC CHEMICALS FOUND IN FISH FROM MAJOR WATERSHEDS IN THE GREAT LAKES

Brian C. Butterworth and Kenneth L. Johnson
Center for Lake Superior Studies
University of Wisconsin-Superior
Superior, Wisconsin 54880

and

Douglas W. Kuehl and Edward N. Leonard
Environmental Research Laboratory-Duluth
U.S. Environmental Protection Agency
Duluth, Minnesota 55804

The chemical residue biomonitoring program at the Environmental Research Laboratory-Duluth, is a part of the U.S. EPA's hazard assessment program for the regulation of industrial activity to ensure environmental protection. Basic research aimed at the isolation, identification and quantification of trace levels of hazardous xenobiotic chemicals in fish can provide an accurate description of actual chemical residues existing in our environment. This information can be used to establish priorities in regulatory and health related research activities, as well as providing validation of predictions made from laboratory experiments.

Three primary tasks of our biomonitoring program have been: 1) The yearly collection of fish from 50-100 major watersheds in Great Lakes States, including fish from all five Great Lakes, 2) The development of methods for the isolation, identification and quantification of unknown trace polychlorinated chemicals in fish tissue, and 3) The chemical characterization of residues in at least 25 new watersheds per year.

This study involves the collection of fish from 48 watersheds within U.S. EPA Region V, which includes the states of Minnesota, Wisconsin, Illinois, Indiana, Michigan and Ohio. Samples were prepared for analysis by gel permeation chromatography[1,2] and screened by a pattern recognition electron capture gas chromatographic technique[3]. Analyses for polychlorinated xenobiotic were by gas chromatography mass spectrometry.

Polychlorinated biphenyl (Arochlor 1242, 1248 and 1254), p,p'-DDE, hexachlorobenzene and four major components of tech-chlordane (cis-chlordane, trans-chlordane, cis-nonachlor and trans-nonachlor) have been observed as the most frequently occurring contaminants in previous studies[4,5] as well as this study, and therefore, have been quantified by electron capture GC and MID GC/MS.

The next most frequently occurring chemical has been tentatively identified by electron impact and chemical ionization mass spectrometry as pentachloropyrrolidine, however, no standards are currently available to confirm this observation. Other unusual polychlorinated chemicals observed include isomers of pentachloro- through octachlorostyrene, dichloro- through pentachloroterphenyl, dichloro- through hexachloronaphthalenes, trichloro- through heptachlorodibenzofurans, trichloro- through pentachloroanilines, trichloro- through pentachloroanisoles, dichloro- through pentachlorobenzenes and trichloro- through pentachlorophenols. Individual compounds found include mirex, photomirex, hexachlorocyclohexane, hexachlorocyclopentadiene, hexachloronorbornadiene, chlorobenzocinnoline, 3-(tetrachlorophenyl)-propyl alcohol and 3-(pentachlorophenyl)-propyl alcohol. In all, over 55 different types of polychlorinated chemicals were found in fish from 25 watersheds.

1. Kuehl, D.W., and Leonard, E.N., Anal. Chem. 50(1): 182-185 (1977).
2. Veith, G.D., and Kuehl, D.W., Anal Chem. 1981 in press.
3. Weininger, D.W., and Burkhart, L., PCB Analysis by Pattern Recognition of High Resolution Capillary Column Electron Capture Gas Chromatography. 1981, in preparation, U.S. Environmental Protection Agency.
4. Veith, G.D., Kuehl, D.W., Leonard, E.N., Puglisi, F.A., and Lemke, A.E., Pest. Monit. J., 13(1): 1-11 (1979).
5. Veith, G.D., Kuehl, D.W., Leonard, E.N., Welch, K.J., and Pratt, G., Pest. Monit. J., 1981 in press.

Mass Spectral Identification of Chlorinated Organic Compounds from Sediments Collected Near an Industrial Area:

Douglas G. Burrows, William D. MacLeod, Jr., L. Scott Ramos, Donald W. Brown; National Analytical Facility, Environmental Conservation Division, Northwest and Alaska Fisheries Center, 2725 Montlake Boulevard East, Seattle, Washington 98112.

Hundreds of unusual halogenated compounds were present in the extracts of marine sediment samples collected from Commencement Bay, Puget Sound near an industrial area of Tacoma, Washington. The concentrations of 36 isomeric groups of halogenated compounds identified in these sediment extracts and some mass spectral information (molecular weight and major ion) are listed in the table. Mass spectra that are representative of some of the classes of compounds are shown below. Although the toxicity of most of these xenobiotics is presently unknown, some may have environmental significance. The concentrations of the more commonly reported pollutants, such as aromatic hydrocarbons, chlorinated pesticides and polychlorinated biphenyls, found in these environmental samples were reported by Malins et al. (1).

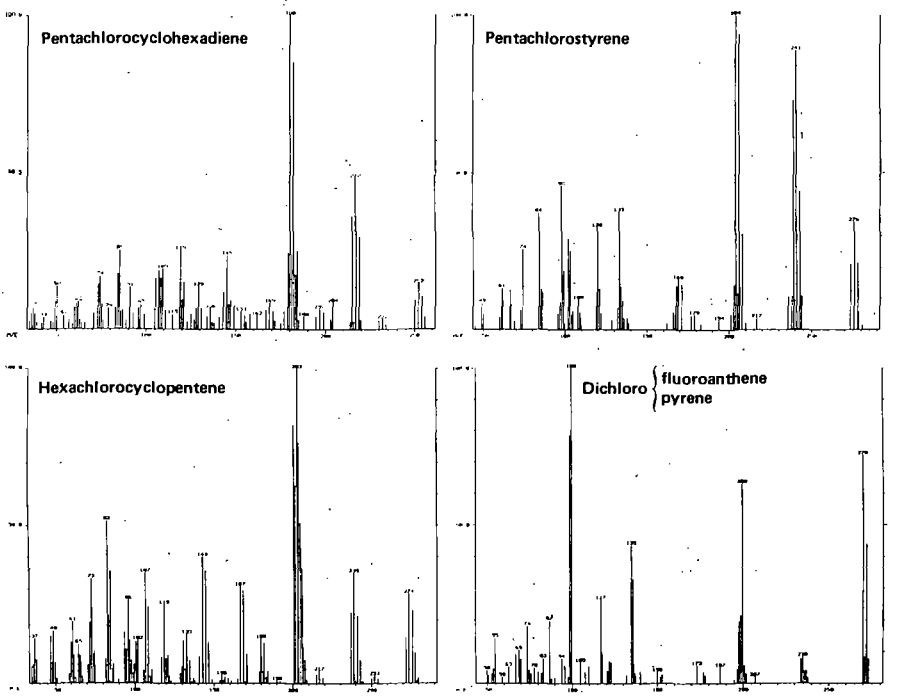

Mass spectra which are representative of some of the main classes of compounds presented in this paper.

The sediment extracts were separated into fractions using silica gel chromatography and Sephadex LH-20 column chromatography (1). The fraction containing the aromatic and chlorinated hydrocarbons was rechromatographed on silica gel into 5 fractions. The concentrated extract fractions were analyzed on a Hewlett Packard 5840A gas chromatograph equipped with a 30 m X 0.25 mm, SE-54 coated, fused silica capillary column interfaced to a Finnigan 3200 quadrupole mass spectrometer. Two uL of extract was injected splitless at 50°C and the GC column was programed from 50° to 280°C at 4° C/min. Compounds were identified by using the NIH/EPA mass spectral library, by comparison to published spectra and by analysis of mass spectra.

This study was supported by the Pacific Office of the Office of Marine Pollution Assessment of the National Oceanic and Atmospheric Administration

(1) Malins, D.C., McCain, B.B., Brown, D.W., Sparks, A.K., and Hodgins, H.O. (1980) Chemical Contaminants and Biological Abnormalities in Central and Southern Puget Sound. NOAA Tech. Memo. OMPA-2, 295p.

GROUPS OF ISOMERS DETERMINED BY GAS CHROMATOGRAPHY/MASS SPECTROSCOPY

COMPOUNDS	MW	MAJOR ION	CONCENTRATIONS (ng/gm dry wt.) SEDIMENT Hylebos	SEDIMENT Old Tacoma
Dichlorobutadiene	122	87	10	6
Trichlorobutadiene	156	121	4000	90
Tetrachlorobutadiene	190	155	3000	300
Pentachlorobutadiene	224	191	1000	90
Hexachlorobutadiene	258	225	1000	90
Dichlorocyclohexadiene*	148	77	0.03	
Trichlorocyclohexadiene*	182	111	10	
Tetrachlorocyclohexadiene*	216	145	20	
Pentachlorocyclohexadiene*	250	180	40	
Hexachlorocyclohexadiene*	284	216	50	3
Heptachlorocyclohexadiene*	318	250	6	
Octachlorocyclohexadiene*	352	250	30	
Trichlorostyrene	206	136	1	
Tetrachlorostyrene*	240	170	10	
Pentachlorostyrene*	274	204	50	
Hexachlorostyrene*	308	240	40	
Heptachlorostyrene*	342	274	10	
Octachlorostyrene	376	217	20	
Trichlorocyclopentene*	170	99	0.04	
Tetrachlorocyclopentene*	204	133	100	60
Pentachlorocyclopentene*	238	167	20	
Hexachlorocyclopentene*	272	203	60	20
Heptachlorocyclopentene*	306	237	10	
Chlorofluoranthene/pyrene†	236	100	0.8	80
Dichlorofluoranthene/pyrene*	270	100	0.7	50
Trichlorofluoranthene/pyrene*	304	117		6
Tetrachlorofluoranthene/pyrene*	338	340	0.2	30
Pentachlorofluoranthene/pyrene*	372	116		30
Bromochlorofluoranthene/pyrene*	314	100	1	20
Bromofluoranthene/pyrene*	280	100	60	50
Dibromofluoranthene/pyrene*	358	100	30	200
Chlorophenanthrene/anthracene	212	212	0.4	30
Dichlorophenanthrene/anthracene	246	246	0.3	40
Trichlorophenanthrene/anthracene	280	280		10
Tetrachlorophenanthrene/anthracene*	314	316		2
Bromophenanthrene/anthracene*	256	88		0.6

*Not confirmed by standards

†Slash(/)means either chlorofluoranthene or chloropyrene

QUANTITATIVE ANALYSIS OF POLYCHLORINATED STYRENES, BENZENES, AND HEXACHLOROBUTADIENE IN GREAT LAKES FISH

Kenneth L. Johnson and Brian C. Butterworth,
Center for Lake Superior Environmental Studies
University of Wisconsin-Superior
Superior, Wisconsin 54880

and

Douglas W. Kuehl and Edward N. Leonard
Environmental Research Laboratory-Duluth
U.S. Environmental Protection Agency
Duluth, Minnesota 55804

Since 1969 residues of octachlorostyrene (OCS) have been observed as major components in fish and birds from the Rhine River in the Netherlands[1]; fish and birds from the Great Lakes of North America[2,3]; and fish from coastal waters of Norway. OCS has also been found in the blood of the human population living near an industrial area where OCS is being discharged[4]. In addition to our original findings of OCS in the Great Lakes, we have also found high levels of OCS in fish from the Ashtabula River/Fields Brook area near Ashtabula, Ohio[5]. In every case where OCS has been found, lower chlorinated styrenes, chlorinated benzenes and hexachlorobutadiene has also been found.

As a part of a hazardous chemical assessment program for the regulation of industrial activity to insure environmental protection, and as a result of our interest in OCS as an unusual environmental contaminant, we initiated a quantitative investigation of OCS and related chemicals in Great Lakes fish collected between 1974 and 1980.

Our data basically showed that levels of OCS were less than 1 ppb in the two upper Lakes, Superior and Michigan. OCS was found as high as 280 ppb in lake trout caught in Lake Ontario in 1979. A 1980 catfish/carp composite from Saginaw Bay of Lake Huron contained 111 ppb OCS. Carp caught during 1980 in Lake St. Clair contained 227 ppb. A northern pike caught in the Ashtabula River during 1979 contained 405 ppb.

Although samples containing high levels of OCS also contained elevated levels of hexachlorobenzene (HCB) and hexachlorobutadiene (HCBO), no specific relationship was observed between any of these compounds. This may be due to a variety of industrial processes producing these products.

1. Koeman, J.H., Ten Noever de Brauw, M.C., and de Vos, R.H., Nature (London) 221: 1126-1128 (1969).
2. Kuehl, D.W., Kopperman, H.L., Veith, G.D., and Glass, G.E., Bull. Environ. Contam. Toxicol. 16: 127-132 (1976).
3. Reichel, W.L., Pronty, R.M., and Gay, M.L., J. Assoc. Off. Anal. Chem. 60: 60-62 (1977).
4. Lunde, G., and Bjorseth, A., Sci. Total Environ. 8: 241-246 (1977).
5. Kuehl, D.W., Leonard, E.N., Welch, K.J., and Veith, G.D., J. Assoc. Off. Anal. Chem. 63: 1238-1244 (1980)

QUANTITATION OF HALOGENATED ORGANIC COMPOUNDS
II. DIOXINS AND FURANS

C.E. Parker, P.W. Albro, and M.J. Bobenrieth

NIEHS, P.O. Box 12233, Research Triangle Park, NC 27709

There are 75 isomers of polychlorinated dibenzo-p-dioxins, and 135 isomers of polychlorodibenzofurans. This paper examines the errors introduced when one isomer of a given compound class is used as a standard for another isomer. Also done was a comparison of relative areas by gas chromatography with a Hydrogen Flame Ionization Detector (HFID), with areas obtained from reconstructed gas chromatograms of M^+ and $(M + Z)^+$ Ions, and from the total ion current peaks.

The mass spectrometry was done on a VG micromass 7070/F Mass Spectrometer, operated at 70 eV . The mass range scanned was 670 to 20 amu, at 1 second per decade. Sample introduction was done with a Hewlett-Packard HP-5710 gas chromatograph, fitted with OV 1, Dexsil 410, and SE 30 capillary columns. Data acquisition, and RGC and TIC peak area determinations were done with a VG 2250 F/B Data System. The HFID results were obtained on a Varian 1200 gas chromatograph.

Six mixtures were studied, with a minimum of three analyses of each mixture. For these known mixtures of dioxins and furans, good correlations were obtained between the HFID peak areas and the TIC, M^+, and $(M + 2)^+$ peak areas.

For dioxins: $TIC\% = 1.022\ (HFID\%) - 0.4896,\ r = 0.9801$

$M^+\% = 0.8945\ (HFID\%) + 2.490,\ r = 0.9494$

$(M + 2)^+\% = 0.9987\ (HFID\%) + 0.0555,\ r = 0.9783$

For furans: $TIC\% = 1.0260\ (HFID\%) - 0.5750,\ r = 0.9894$

$M^+\% = 1.0110\ (HFID\%) - 0.2517,\ r = 0.9963$

$(M + 2)^+\% = 1.0280\ (HFID\%) - 0.6196,\ r = 0.9870$

A set of 16 polychorinated dibenzo-p-dioxins, and a set of 8 polychlorinated dibenzofurans were studied (see Tables 1 and 2). The proportion of the TIC carried by the molecular ion cluster was fairly constant over all of the dioxin and furan isomers studied. No significant correlation between the %TIC in the molecular ion cluster and the number of chlorines in the molecule was obtained. The average value for the %TIC carried by the molecular ion cluster was $47.4 \pm 4.89\%$ for dioxins and $52.0 \pm 5.33\%$ for furans. This gives an indication of the error introduced by using M^+ or $(M+2)^+$ peak areas from one isomer for quantitation of another.

Table 1.

DIOXINS

COMPOUND	% TIC CARRIED BY MOLECULAR ION CLUSTER
1 - Cl_1	47.6 ± 2.46
2 - Cl_1	46.9 ± 6.53
2,3 - Cl_2	55.0 ± 7.02
2,7 - Cl_2	38.8 ± 8.8
2,8 - Cl_2	36.0 ± 1.04
1,2,4 - Cl_3	45.3 ± 0.12
2,3,7 - Cl_3	47.5 ± 9.3
2,6,8 - Cl_3	48.4 ± 5.86
1,2,3,4 - Cl_4	51.8 ± 3.46
2,3,7,8 - Cl_4	49.9 ± 6.9
1,2,3,7,8 - Cl_5	48.4 ± 4.26
1,2,4,7,8 - Cl_5	49.9 ± 1.9
1,2,3,6,7,8 - Cl_6 & 1,2,3,7,8,9 - Cl_6	46.1 ± 3.6
1,2,3,4,6,7,8 - Cl_7	51.4 ± 2.4
1,2,3,4,6,7,8,9 - Cl_8	53.1 ± 6.5
MEAN	47.4 ± 4.89

Table 2.

FURANS

COMPOUND	% TIC CARRIED BY MOLECULAR ION CLUSTER
2,8 - Cl_2	46.1 ± 4.82
2,4,6 - Cl_3	52.5 ± 4.75
2,3,8 - Cl_3	56.8 ± 3.03
2,4,6,8 - Cl_4	51.5 ± 4.76
2,3,6,8 - Cl_4	54.8 ± 3.09
1,3,4,7,8 - Cl_5	51.7 ± 3.96
2,3,4,6,7,8 - Cl_6	49.4 ± 7.15
1,2,3,4,6,7,8,9 - Cl_8	52.0 +10.4
MEAN	52.0 ± 5.33

COMPARISON OF GC/MS WITH MS/MS IN THE ANALYSIS OF PCBs IN COMPLEX MIXTURES

R. D. Voyksner[1,2], G. W. Sovocool[3], M. M. Bursey[2], J. R. Hass[1]

1. National Institute of Environmental Health Sciences, P. O. Box 12233, Research Triangle Park, NC 27709
2. Department of Chemistry, University of North Carolina, Chapel Hill, NC 27514
3. U.S. Environmental Protection Agency, Environmental Toxicology Division, Research Triangle Park, NC 27711

GC/MS is the method of choice to perform analysis on volatiles in complex mixtures, but because of chromatographic drawbacks and long analysis time interest in MS/MS has developed. MS/MS presumably can perform an analysis in a fraction of the time without GC drawbacks. To compare the techniques we present the results from an analysis of PCBs as a function of speed, qualitative, and quantitative information.

The comparison was made on the VG Micromass ZAB-2F equipped with a Finnigan/INCOS data system. Standards were made from Monsanto Aroclor 1254 with dilutions made with pesticide grade hexane. Samples studied were human blood extracted with hexane, human fat extracted with ether from florisil; and monkey fat extracted with benzene.

The GC/MS analysis was performed with a fused silica OV-1 20 m column with an initial temperature of 150°C to a final temperature of 250°C at 8°/min. The mass spectrometer was operated at 70 eV ionization energy, 8 KeV accelerating potential at a 5K resolving power.

Multiple Ion Detection (MID) was used to observe the $[M]^+$ and $[M+2]^+$ ions for tetra, penta, and hexachlorobiphenyls to give a good combination of sensitivity and specificity. Each window was 300 ppm wide and was observed for 0.2 seconds. The lock mass was 281 of PFK. Typical response to an Aroclor 1254 standard (Fig. 1) showed the total ion current for each channel. If one looks at the profile data obtained from MID, one can see the various windows as well as the response for a hexachlorobiphenyl. We observed no interferences in these windows except interferences of fragment ions from higher mass PCBs in lower mass windows: the ratios of $[M+2]^+$ to $[M]^+$ for hexachlorobiphenyls were confirmed to agree reasonably with the expected ratio for an ion containing six chlorines. Thus, neither channel had any detectable interference.

MS/MS experiments were done by direct probe for selecting $[M]^+$ for hexachlorobiphenyl (m/z 358) with 600 Resolving Power. CID of the main beam was done using Helium and the mass range of 270-360 was scanned in 2.4 sec, to observe losses to produce $[M-Cl]^+$ and $[M-2Cl]^+$ fragments. The standards show no other significant peaks in this mass range but if one looks at the blood sample (Fig. 2) one can observe a number of interferences in the primary ion beam. Some of these interferences could be in the $[M-Cl]^+$ and $[M-2Cl]^+$ area.

The analysis time of about 6 min. is much less than the 45 min. for GC/MS but no isomer information, nor information about tetra- and pentachlorobiphenyls, is obtained.

Quantitation of PCBs presents a challenge due to the large number of isomers, different responses for different isomers and the lack of similarity between Aroclor 1254 and the samples. Calibration curves showed linearity for MS/MS from 100 Ng to 1 Ng with detection limits of about 500 PG. GC/MS showed linearity from 100 NG to 100 PG with detection limit of 5 PG.

Results are given in Table 1. The MS/MS results are 2 to 9 times higher than the GC/MS results. A possible explanation is interferences, especially interferences from the primary ion beam and interferences by fragments from hepta- and octachlorobiphenyls. Since there is no correct answer, one has no basis to say which method is more accurate because true levels in these samples are not known a priori.

The conclusions of various aspects of GC/MS and MS/MS analysis are shown in Table 2. In this instance GC/MS seems to be the favored techniques. Because of its higher resolution capability it can remove interferences either by GC or MS means.

TABLE 1

Sample	µg/g GC/MS	µg/g MS/MS
Monkey Fat #1	16.5	40.5
Monkey Fat #2	14.5	35.9
Monkey Fat #3	14.9	58.6
Monkey Fat #5	1.7	15.6
Human Fat	0.10	0.53
Blood 013	0.006	0.05
Blood 015	0.003	0.02

TABLE 2

Function	MS/MS	GC/MS
Speed	6 min	45 min
Isomer Resolution	No	Yes
Detection Limit	500 Pg	5 Pg
Quantitation	MS/MS values average 5X GC/MS values	
Detectable Interferences Present	Yes	No

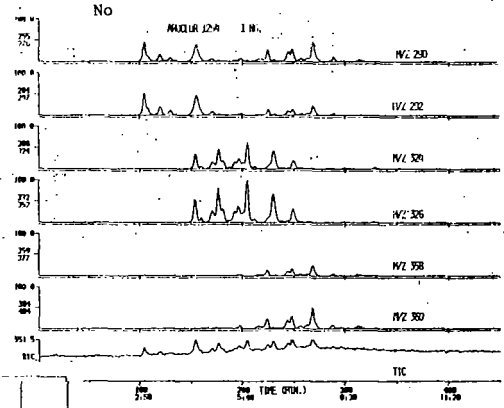

Fig. 1

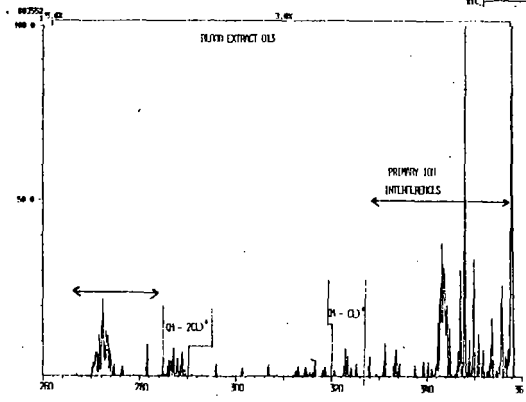

Fig. 2

A QUALITY ASSURANCE PROGRAM FOR A GC/MS/COMPUTER SYSTEM ENGAGED IN ANALYSIS OF VOLATILE ORGANIC COMPOUNDS; D. J. SMITH, E. D. PELLIZZARI, N. CASTILLO, M. D. ERICKSON, C. S. SPARACINO; Research Triangle Institute, Research Triangle Park, NC 27709.

Techniques have been developed in this laboratory for the sampling and analysis of organic compounds in various environmental media, including air, water, breath, sediment, and sludge, for example. A program of quality assurance has also been developed to guarantee the consistency and accuracy of qualitative and quantitative data obtained by use of the thermal desorption inlet. The mass spectrometer is tuned and calibrated daily using perfluorokerosene. The intensity and relative ion abundances of selected masses in the perfluorokerosene spectrum are monitored and must fall within specific tolerances before beginning any analysis. Perfluorotoluene is dosed onto each control and sample cartridge analyzed and a compilation of the intensity and relative ion abundance at selected masses is a measure of instrument stability under GC conditions (a variation of a certain percentage is tolerated at each selected mass). The quality of chromatography is most important since the accuracy and precision of the analysis are directly affected. Chromatography on glass capillary columns is evaluated by running a column performance mixture and determining factors such as percent peak asymmetry factor, separation number, resolution, acidity and basicity. These values provide a continuous check on system performance and can provide early warning of developing problems, as well as alerting the user to deterioration of the chromatographic column before irreplaceable samples are lost.

TRACE DETECTION IN REAL TIME OF CHLORINE AND SULFUR-CONTAINING COMPOUNDS OF ENVIRONMENTAL CONCERN; S.D. Tanner and B.A. Thomson; SCIEX INC., 55 Glencameron Rd., Thornhill, Ontario, Canada, and G.B. DeBrou and N.H. Hijazi, Ontario Ministry of the Environment, Toronto, Ontario, Canada.

The range of compounds for which the TAGA™ mass spectrometer system is a sensitive detector and quantifier has been expanded to include the simple aliphatic halocarbons and sulfides. Equipped with the Atmospheric Pressure Chemical Ionization (APCI) source, the TAGA™ has already been shown to be sensitive (sub-ppt) to a wide range of compounds of environmental and industrial concern. The reagent ions in this source are $H_3O^+ \cdot (H_2O)_n$, $O^- \cdot (H_2O)_n$ and $O_2^- \cdot (H_2O)_n$ ($n \geq 0$). The thermodynamics of these ions defines the range of sensitivity: compounds having relatively high proton affinities (positive mode) or high electron/low proton affinities (negative mode), as well as specific compounds which react via substitution, elimination or association. The kinetics and energetics of the ion chemistry of the simple aliphatic halocarbons and sulfides often make their detection under ambient air APCI conditions unfavorable. We present here two approaches to a solution of this problem.

The more general of the two approaches involved the development of a Reduced Pressure Chemical Ionization (RPCI) source for the TAGA™ system. A modified Townsend discharge source has been designed specifically for direct sampling of room or outdoor air. Energetic electrons are injected into a variable-pressure chemical ionization region where electron impact on the ambient gas (air) generates the reagent ions. Ionization of the trace species occurs and the ions are extracted for analysis under the influence of a variable drift potential. A final variable field region provides for controlled ion fragmentation which aids in sample identification. The source gives the operator a great deal of flexibility. The reagent ion itself may be changed simply by varying the source pressure and/or the drift potential (time). When ambient air is sampled directly into the ion source, the more "energy-rich" (compared to APCI) reagent ions O_2^+ and H_3O^+ (unsolvated) are formed. The energetics of these ions are appropriate for the ionization by charge transfer and proton transfer of halocarbons and sulfides. Experimental results are given for the detection in real time of trace amounts of trichloroethylene (see Figure 1), vinyl chloride, methyl mercaptan and bis(2-chloroethyl) ether in room air. In addition, it was found that the thiols form resilient clusters with NO^+ and NO_2^+ even at reduced pressures; this may prove useful as a class-separator. The ion chemistry proceeding in the source has been modelled; the evolution is presented as a function of both time and pressure over the domains accessible to the operator. The model may be consulted to select the optimum conditions to generate the appropriate CI reagent ion.

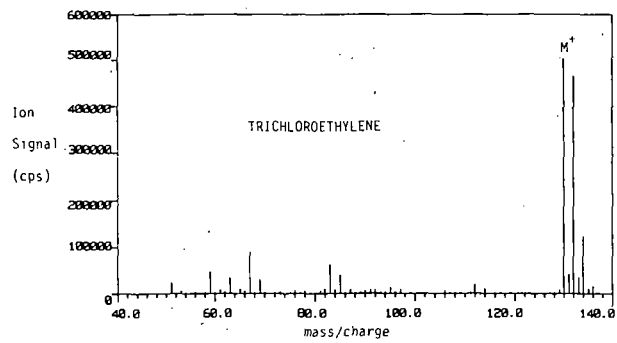

Figure 1. Detection of Trichloroethylene at the level of 5 ppm in ambient room air. (The background spectrum, in the absence of Trichloroethylene, has been subtracted.) The RPCI source was used under conditions emphasizing O_2^+ charge transfer.

The alternate approach is directed at specific compounds or classes of compounds. It involves the development and addition of reagent gases which are effective under ambient air APCI conditions. This includes reagents which convert the trace to a more-easily

ionizable form via neutral gas-phase reactions prior to APCI ionization as well as the more conventional gases which directly generate a more appropriate CI reagent ion. We have found that the addition of benzene into the intake air stream, which generates $C_6H_6^+$ as the dominant reagent ion, facilitates the detection of chloroethyl ethyl sulfide. As well, the power of the MS/MS technique is demonstrated by fragmenting the parent sulfide ion in the CID region of the TAGA™ 6000 and scanning the resultant daughter ion spectrum: the structual information obtained thereby permits the definite identification of the trace. A novel technique which is, apparently, specific for the highlighting of thiols involves the addition of ozone into the air stream. Preliminary evidence suggests that thiols are oxidized in the gas-phase by (neutral) ozone yielding the thiol acids and other thiol oxides. Upon proton abstraction by $O^-\bullet(H_2O)_n$ and $O_2^-\bullet(H_2O)_n$, the characteristic ions RSO_n^- (n=0 to 3) are observed. Since ozone is readily generated by UV irradiation of the directly sampled air, the thiols in a mixture may be highlighted simply by subtracting the background spectrum obtained with the UV source off from the spectrum recorded during the irradiation. An example is given in Figure 2, wherein benzenethiol has been highlighted from the background of ambient room air.

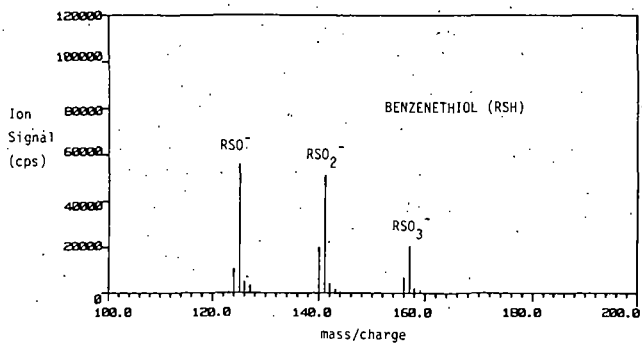

Figure 2. Benzenethiol is highlighted in ambient room air. The spectrum shown is the result of subtracting the background spectrum in the absence of ozone from the spectrum obtained during UV irradiation.

PULSED POSITIVE ION NEGATIVE ION CHEMICAL IONIZATION MASS SPECTROMETRIC APPLICATIONS TO ENVIRONMENTAL AND HAZARDOUS WASTE ANALYSIS

by

L. D. Betowski, H. M. Webb and A. D. Sauter
Environmental Monitoring Systems Laboratory
U.S. Environmental Protection Agency
Las Vegas, Nevada 89114

The simultaneous acquisition of both positive ion and negative ion data under chemical ionization mass spectrometric conditions can aid in the confirmation of assignments made by electron impact GC/MS or electron capture GC. Pulsed positive ion negative ion chemical ionization (PPINICI) mass spectrometry coupled with fused-silica capillary column gas chromatographic methods can provide ancillary information on compound identity in environmental and hazardous waste samples. The enhanced sensitivity of negative ion chemical ionization for certain classes of compounds, for example, halogenated pesticides, can be employed to identify these analytes at sensitivities that approach electron capture gas chromatography. The lower detection limits (as compared to electron impact or positive ion chemical ionization) for negative ion chemical ionization for compounds that capture electrons are shown to aid in the characterization of complex environmental extracts for target compounds (i.e., priority pollutants) and non-target compounds analysis.

Negative ion/positive ion ratios had been measured for the priority pollutants at three different methane reagent gas pressures to investigate the level at which negative ion chemical ionization can be useful for confirmation purposes. The conditions that give a molecular ion under negative ion chemical ionization are maximized at the highest pressure of methane in the ion source (0.4 Torr indicated). Methane proved to be the best reagent gas tested as far as sensitivity and information content delivered. However, the other moderator gases used, argon and nitrogen, have the practical advantage of maintaining a cleaner ion source for long periods of time.

The priority pollutant pesticides were detected using full scan (m/z 30 to m/z 435 in one second) under negative ion chemical ionization at less than 50 pg. Most of the total ionization is due to Cl^-. The total mass spectrometric response for the pesticides is linear from 50 pg to (1-10) ng. Above these levels a state of chemical saturation results wherein the population of thermal electrons in the ion source is depleted. The decrease of the ion current due to m/z 146 from trace amounts of SF_6 in the background was observed at the onset of saturation (see Figure 1). This observation suggests that monitoring of unique background ions which capture electrons can serve as a probe for saturation.

With methane as the reagent gas and the ion source temperature at 120°C (the ion source temperature was usually 240°C) the spectra of several of the pesticides, e.g., endosulfan, show a marked increase in the parent ion (or pseudo-molecular ion) cluster.

In certain cases the loss of a small group will be predominant in the chemical ionization spectrum in one of several structural isomers to form a stable ion. This results in isomer differentiation, as in the case of 2- and 4-nitrophenol.

Response factors generated for many of the priority pollutants under PPINICI conditions showed precision equivalent to electron impact GC/MS experiments. The mean relative standard deviation for 31 priority pollutants under positive ion (methane) chemical ionization was 8.5% for four consecutive injections. The mean relative standard deviation for 27 priority pollutants under negative ion (methane) chemical ionization was 11.3% for four consecutive injections. Response factors were also generated at multiple level concentrations under PPINICI conditions to demonstrate the potential for quantitation.

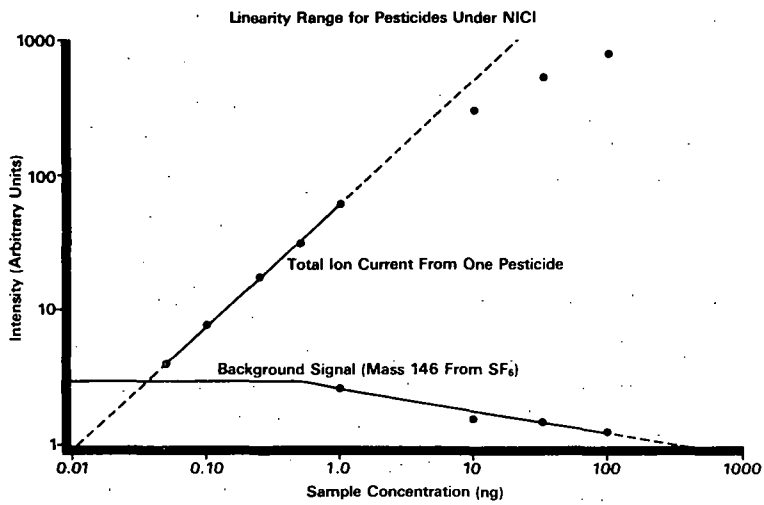

Figure 1

GC-MS TECHNIQUES FOR COMPREHENSIVE ASSESSMENT OF CHLORINATED DIBENZO-p-DIOXINS AND DIBENZOFURANS IN COMBUSTION PARTICULATES

G.F. VanNess, M.L. Taylor, J.H. Garrett, J.G. Solch and T.O. Tiernan
Brehm Laboratory and Depts. of Chemistry and Pharmacology/Toxicology
Wright State University, Dayton, Ohio 45435

An analytical scheme has been developed for comprehensive analyses of particulates resulting from various combustion processes for the content of chlorodibenzo-p-dioxins (CDDs) and chlorodibenzofurans (CDFs), (Cl_1 through Cl_8). The procedures entail Soxhlet extraction of the solids, followed by a sequence of base and acid washes of the extracts, liquid chromatographic separation using silica and alumina columns, high performance reverse-phase liquid chromatographic fractionation, and GC-MS analysis of the final extract. The efficiency of various solvents in removing CDDs and CDFs from these particulates was briefly assessed, as indicated by the results shown in Table 1. In general, benzene appeared to be superior for this purpose.

TABLE 1. COMPARISON OF TCDD LEVELS IN VARIOUS COMBUSTION PARTICULATES AS INDICATED BY ANALYSES IN WHICH VARIOUS EXTRACTION SOLVENTS WERE USED

Sample Type	Extraction Solvent Used	Quantity TCDD Found (ng/g)	% Recovery $^{37}Cl_4$-2,3,7,8-TCDD	Minimum Detectable Concentration (ng/g)
Coal Fly Ash	Benzene	N.D.	40	0.30
Coal Fly Ash	Toluene	N.D.	57	0.30
Fireplace Ash	Hexane/Acetone	0.65	69	0.15
Fireplace Ash	Benzene	0.55	80	0.15
Particulate Filter	Benzene	16.0	110	1.00
Diesel Muffler	Hexane/Acetone	N.D.	93	0.08
Diesel Muffler	Benzene	N.D.	95	0.08
PCP Composite Ash	Benzene	0.8	85	0.20
Electrostatic Precipitator	Benzene	8.4	65	0.5
Electrostatic Precipitator	Hexane/Acetone	--	<10	--
Electrostatic Precipitator	Carbon Dioxide	--	<10	--

GC-MS Analyses were accomplished using OV-101, Silar-10C and Silov-82 (a new mixed phase) capillary columns. The instrumentation employed included a coupled Perking Elmer Sigma III GC-Kratos MS-25 MS (DS-50S Data System), and a Varian 3700 GC-AEI MS-30MS. The latter provides both high resolution GC and high resolution MS capability. A selected-ion monitoring scheme was developed to permit determination of the entire group of monochlorinated through octachlorinated CDDs and CDFs from only two injections of a given sample extract. Table 2 shows the ion masses monitored for each CDD and CDF species.

In Table 3 are shown the results of analyses of Cl_4 through Cl_8 CDDs and CDFs in extracts of an air filter particulate and ash produced by combustion of wastes containing pentachlorophenol (PCP). The use of capillary GC columns permits resolution of many of the CDD and CDF isomers of a given chlorinated group, but not all of these can be identified, since authentic standards are unavailable in many cases. At least one CDD or CDF isomer of each class was available and was used for instrument calibration. Similar results for other combustion products are described, along with the details of the analytical procedures.

Table 2. LIST OF ION PASSES MONITORED USING GC-SELECTED-ION MONITORING MASS SPECTROMETRY FOR SIMULTANEOUS DETERMINATION OF MONO-, DI-, TRI-, TETRA-, PENTA-, HEXA-, HEPTA-, AND OCTA-CHLORINATED DIBENZO-P-DIOXINS AND DIBENZOFURANS

Class of Chlorinated Dibenzodioxin or Dibenzofuran	Monitored m/z for Dibenzofurans $C_{12}H_{8-n}OCl_n$	Monitored m/z for Dibenzo-p-dioxins $C_{12}H_{8-n}O_2Cl_n$	Approximate Theoretical Ratio Expected on Basis of Isotopic Abundance
Mono-	202.019[A]	218.013[A]	1.00
	204.016	220.011	0.35
Di-	235.980[A]	251.974[A]	1.00
	237.977	253.972	0.69
Tri-	269.941[A]	285.940[A]	0.99
	271.938	287.937	1.00
Tetra-	303.902[A]	319.897[A]	0.74
	305.899	321.894	1.00
		327.885[B]	--
		256.933 [C]	0.21
		258.930 [C]	0.20
Penta-	337.863[A]	353.858[A]	0.57
	339.860	355.855	1.00
Hexa-	373.821	389.816	1.00
	375.818	391.813	0.87
Hepta-	407.782	423.777	1.00
	409.779	425.774	1.00
		431.765[B]	--
Octa-	441.743	457.738	0.86
	443.740	459.735	1.00

A. Molecular ion peak.

B. $^{37}Cl_4$-labelled CDD standard peak.

C. Ions which can be monitored in TCDD analyses for confirmation purposes.

TABLE 3. RESULTS OF HIGH RESOLUTION GAS CHROMATOGRAPHIC-MASS SPECTROMETRIC ANALYSES OF PARTICULATE SAMPLES

Dibenzofurans	No. of Apparent Isomers	Total Detected (ng)	No. of Apparent Isomers	Total Detected (ng/g)
Tetra-	17	90	7	7
Penta-	13	200	5	8
Hexa-	7	1305	5	5
Hepta-	4	1806	2	6
Octa-	1	325	1	2
Dibenzo-p-Dioxins				
Penta-	12	107	5	32
Hexa-	5	1000	5	81
Hepta-	2	8050	2	117
Octa-	1	710,000	1	198

ANALYSIS OF GREAT LAKES FISH SAMPLES FOR 2,3,7,8-TCDD

D. R. Hilker, P. W. O'Keefe and Carol Meyer
Toxicology Institute, New York State Department of Health, Albany, N.Y.

We have developed an isomer specific analysis for 2,3,7,8-tetrachlorodibenzo-p-dioxin (I) in biological samples. The analysis has been applied to fish samples taken from various bodies of water in and around New York State. Varying

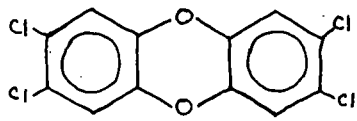

(I.)

numbers of samples were taken from each of the Great Lakes, the Niagara River, the Delaware River, Cayuga Creek (Niagara Falls, N.Y.), an Adirondack Lake and the Atlantic Ocean. The analysis is sensitive to as little as 1 part-per-trillion of 2,3,7,8-TCDD as is required by the extreme toxicity of this compound. The method employs HPLC, high resolution gas chromatography and high resolution mass spectrometry for maximum specificity. The procedure is also capable of isolating octachlorodibenzo-p-dioxin.

The sample extraction and clean-up procedure involves several steps to insure the specificity of the analysis. Basically the extraction involves two columns one of MgO/Celite and alumina and a second of florisil (4cm) and alumina (10cm). The first of two HPLC steps is a reverse phase step on a dual Zorbax-ODS (DuPont) column using methanol as the solvent. A second normal phase HPLC step is carried out on a dual DuPont silica gel column with a mixed solvent of .4% toluene and 99.6% hexane. An indepth description of the extraction and high pressure liquid chromatography employed will be forthcoming in a major publication.

A Kratos Carlo-Erba/MS-50/DS-55 GC/MS system is used for the mass spectrometric analysis. This system provides for chromatographic as well as mass specificity. An acquisition system under control of recently written DS-55 software controls the mass spectrometer and collects and stores data so as to preserve the high resolution of the chromatographic and mass data. The sensitivity of the MS-50 allows detection limits as low as 1 part-per-trillion even if recoveries are low due to an extensive clean-up. The mass spectrometer is tuned to 10,000 RP (10% valley). Perfluorokerosene is used as a mass standard to calibrate the mass scale during an electric sector scan. The calibration data is used to locate the mass regions of interest during the experiment.

For this work the mass spectrometer was scanned over 300 ppm mass regions centering around m/e-319.8965, 321.8936 and 328.8881. Injections are made onto an OV-275 glass capillary column using an on-column injection technique. The chromatograph is interfaced to the source of the mass spectrometer through a jet separator. In real-time a summed mass chromatogram is displayed on the VDU while the mass ions making up the chromatogram are visible on the MS-50 console oscilloscope as the compounds of interest elute. 2,3,7,8-tetrachlorodibenzo-p-dioxin is quantitated using the peak areas of the native and internal standard.

The following results are from spiked fish samples. The spiked concentration was added to the samples before the extraction procedure and the quantitated concentration is obtained from the MS-50 peak areas.

Sample	Spiked Conc. (ppt.)	Quantitated Conc. (ppt.)	Limit of Detection	% Recovery
347B	2.5	3.1	0.5	22
O	5	5.4	1.4	53
N	5	6.1	1.5	43
Q	5	5.2	0.5	52
M	5	4.9	0.8	18
U	40	43	1.3	34
S	40	38	0.9	28
T	40	38	1.1	38
PO339	40	36	1.4	26
W	100	115	3.1	20

The average per cent deviation from the spiked concentration is 10.3. The average detection limit is 1.25 ppt. An additional indication of the reproducibility of the method is the results of analysis of split samples. In these cases the fish samples were analyzed twice. Five samples were subjected to this dual analysis and the average per cent deviation between the two determinations is 7.

The computer output illustrates a typical signal for a 5 ppt. spiked fish.

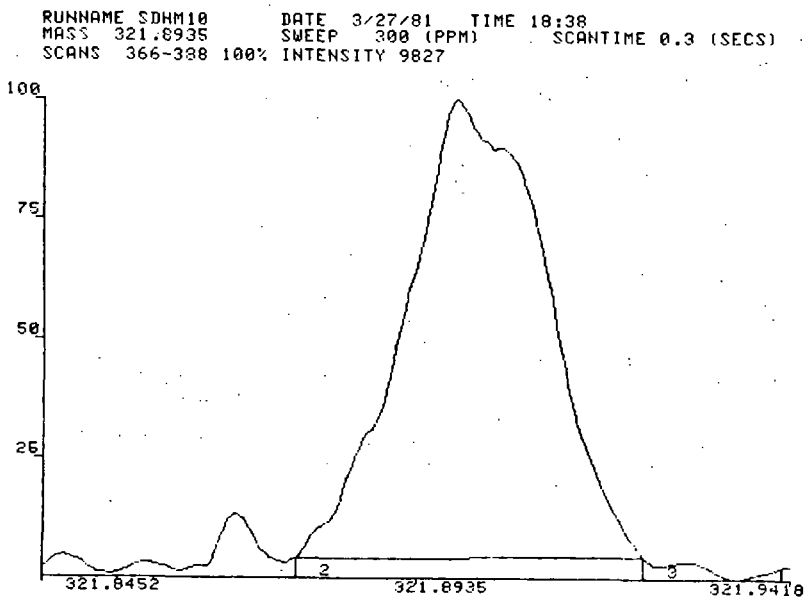

RAPID SCREENING OF ENVIRONMENTAL SAMPLES FOR LOW TO SUB-PPT LEVELS OF POLYCHLORINATED DIBENZO-p-DIOXINS USING TRIPLE QUADRUPOLE MASS SPECTROMETRY. G.A.V. Rees and H. Tosine, Pesticide Section, Ministry of the Environment, Box 213, Rexdale, Ontario, Canada. M9W 5L1. and T. Sakuma, W.R. Davidson, B.A. Thomson, L.M. Danylewych, B. Shushan, J.E. Fulford and N.M. Reid, SCIEX INC., 55 Glencameron Road, Thornhill, Ontario, Canada. L3T 1P2.

Introduction

Because of the toxicity of some of the dioxins, notably 2,3,7,8-tetrachlorodibenzo-p-dioxin, and the growing indication of its ubiquity in the environment and the biosphere, it is desirable to develop rapid analysis techniques which can detect the compound with high sensitivity and high specificity. The TAGA™ 6000 MS/MS system has been used to detect TCDD in organic solvents, 2,4-D extracts, Aroclor matrices and fish extracts, without significant interference from PCBs, DDE or other matrix components.

Experimental

A schematic representation of the TAGA™ 6000 MS/MS is shown in Figure 1. As indicated, it is a triple quadrupole system utilizing an ultra high capacity cryopump. The first and third quadrupoles (Q1 and Q3) are used for mass filtering while the second quadrupole (Q2), acting in an R.F. only or total ion mode, functions as a dynamic focussing region for the parent and fragment ions which are present together in the CID (collisionally induced dissociation) gas target region. The gas ion mixture from the ion source is admitted at one end of the vacuum chamber and expands in a free jet. The gas molecules follow their expansion trajectories, until they are collected by the first set of cryoarrays, while the ions are collimated by the ion lenses and then injected into the first mass filter for separation. Ions selected by Q1 enter the region of the second quadrupole and the CID gas target where they undergo collisionally induced dissociation (if a CID gas is used). A second set of cryoarrays, connected to the same cryopump, pumps the CID gas target region. Q3 is then used to analyze the mass of the ions leaving Q2. An electron multiplier operated in a pulse counting mode detects the ions selected by Q3. The pulses leaving the multiplier are processed by signal handling electronics and then sent on to the computer for counting.

Crude mixtures or organic extracts, after a brief sample clean-up are introduced into the TAGA™ 6000 atmospheric pressure ionization (APCI) region with a direct insertion probe which is designed for rapid and easy sample introduction. The sample is deposited in solution and, after a few seconds allowance for solvent evaporation, the direct insertion probe is rapidly heated to desorb the material into a laminar carrier gas stream for transport to the ion source. After charge transfer from the benzene CI reagent, the parent ions of interest are subjected to CID for quantitation and identification.

Results

Quantitation of TCDD in complex matrices is achieved by monitoring the $[M-COCl]^+$ (m/z 259), $[M-2(COCl)]^+$ (m/z 196), and/or $[M-2(COCl)^{37}Cl]^+$ (m/z 159) daughter of the parent ion (m/z 322). The daughters are free from some interferences commonly encountered in environmental samples as demonstrated in Figure 2 and work is continuing to further characterize potential interferences.

Figure 3 shows a calibration curve obtained from measuring the areas under the desorption curve of the two daughter ions. Response is linear from the detection limit of 400 fg (S/N = 3) up to at least 800 pg of TCDD.

The fish extract analysis shown in Figure 4 corresponds to 0.5 ppt in the 10g fish sample and the ratio of the fragment ions (background subtracted) is within 12% of the value observed with the TCDD standard, providing confirmation of the identity of TCDD in the fish extract. The workup of the fish extract involved the removal of lipids, pesticides and PCBs and this procedure was tested by quantitation of a ^{13}C - labelled TCDD internal standard.

Herbicide formulations have been rapidly analyzed for TCDD using a single alumina cleanup as in the 2,4-D formulation shown in Figure 5. This 2,4-D extract contains a 1 ppm spike of TCDD and the daughter ion branching ratios are virtually identical to those obtained from the m/z 324 parent in the pure TCDD standard.

Conclusions

Triple quadrupole mass spectrometry coupled with atmospheric pressure chemical ionization has a demonstrated capability for rapid screening of environmental samples for TCDD. Following a chemical workup, extracts have been analyzed for TCDD without inferences or memory effects, at a rate of about one sample per minute.

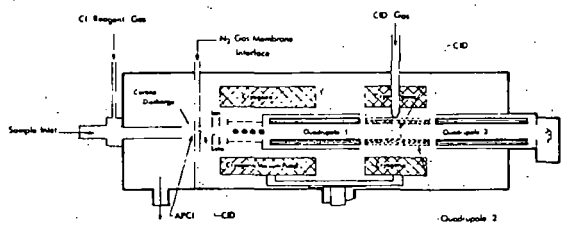

Figure 1. Schematic of TAGA™ 6000 MS/MS.

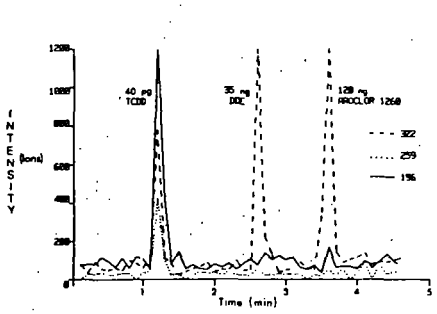

Figure 2. Large excesses of PCBs and DDE do not exhibit m/z 259, and 196 daughters.

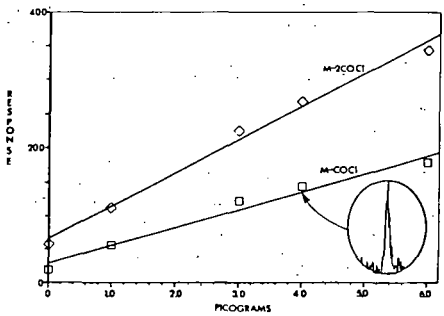

Figure 3. Calibration curve for 2,3,7,8-TCDD.

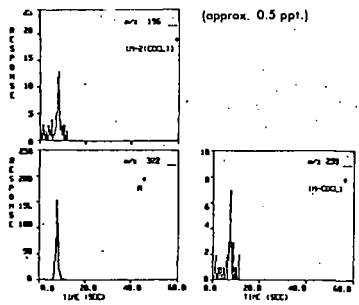

Figure 4. Fish extract injection containing 0.5 ppt TCDD.

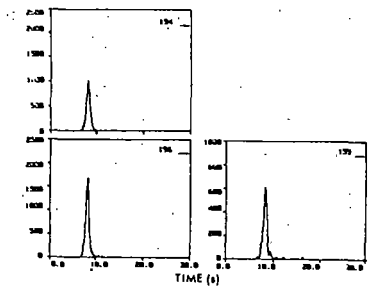

Figure 5. Herbicide (2,4-D) extract containing 1 ppm TCDD spike (m/z 324 parent).

ANALYSIS OF PCB COMPONENTS HAVING NO ORTHO SUBSTITUTED CHLORINES IN ENVIRONMENTAL SAMPLES, G.R. DUBAY, L.M. SMITH, D.L. STALLING, J.D. PETTY. Columbia National Fishery Research Lab., RR 1, Columbia, MO 65201

The use and disposal of approximately 5×10^8 lbs of PCB has resulted in extensive environmental contamination. PCBs were found to be toxic to fish and mammals. A significant portion of the toxicity was attributed to components of the mixture which have no ortho substituted chlorines. Using activated carbon chromatography developed in our laboratory, the non-o-Cl substituted PCBs were separated from o- or o,o'-Cl substituted PCBs. No other separation technique has demonstrated the specificity necessary to efficiently separate non-o-Cl substituted PCBs. One of the non-o-Cl substituted PCB separated with carbon was found to be highly toxic to fish. This component 3,4,3',4'-tetrachlorobiphenyl (TCB) and two other non-o-Cl substituted PCBs were identified and quantitated in fish tissue extracts using high resolution (HR) GC/MS with multiple ion detection.

Analysis of fish tissue samples found the combined concentration of the 3 non-o-PCBs was between 0.1 and 2 ppb. This can be compared to TCDD levels of from 0 to 14 ppt in the fish. Thus, toxic non-o-Cl substituted PCB components are approximately 100 times more prevalent in fish. As a result, non-o-PCB components may also be important contaminants which should be investigated.

A quadruple GC/MS system with a 30M fused silica WCOT column connected directly to the source with changes of the ions monitored during a run achieved a sensitivity of 3 ppt for 100g of fish tissue. The sensitivity provided by this technique demonstrated the existence of non-o-PCBs in fish from different watersheds. Certain watersheds have very high levels of these contaminants.

STRUCTURAL AND ANALYTICAL APPLICATIONS OF HIGH RESOLUTION MS/MS. M. P. BARBALAS, M. T. CHENG, C. WESDEMIOTIS, I. J. AMSTER, C. J. SACK, AND F. W. MCLAFFERTY; Dept. of Chem., Cornell Univ., Ithaca, NY 14853.

Our tandem double-focusing MS/MS instrument makes possible high-resolution separation of ions of a specific mass in MS-I. These undergo metastable or collisionally-activated (CA) decompositions in a special interface region, with separation of the ionic products in the double-focusing MS-II. The added energy focusing of MS-II produces a dramatic improvement in resolution over that using the electrostatic analyzer alone, which often cannot resolve even low mass CA peaks. A valuable advantage of this peak narrowing is an impressive improvement in the signal-to-noise ratio of measurements. Secondly, unit mass resolution of CA spectra of higher mass ions shows interesting details which were obscured on those spectra obtained from reverse-geometry instruments. For example, isotopic peaks show relative abundances determined statistically from the isotopic ratio in the precursor ion, not the natural isotopic abundance, as shown in the Figure.

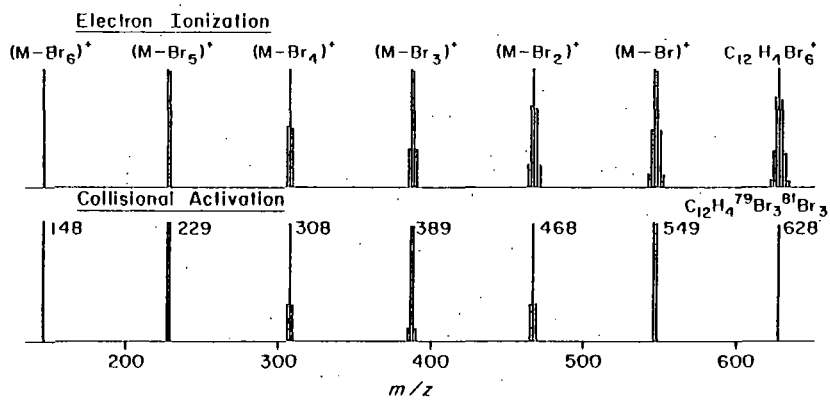

The CA spectrum of a fragment ion is characteristic of its structure, providing valuable additional information concerning unknown molecules introduced into MS-I. This instrument is of particular value for such studies of high mass ions because of its much higher mass range and higher collision energies as well as higher resolution. For example, in a series of 3-hydroxypregnanes, the m/z 166 peaks gave nearly identical CA spectra, indicative of the A/B ring substructure but without definitive stereochemical information. The CA spectra of m/z 148, formed by loss of water from m/z 166 similarly was characteristic of the A/B ring substructures without stereochemical information. However, the m/z 234 peak, which corresponds to the complete A, B, and C rings, gave four different spectra for the four isomers 3α,5α-, 3α,5β-, 3β,5α-, 3β,5β. Structural consistencies can be noted in these spectra; for example the largest loss of water is found for the isomer in which abstraction of the tertiary-9-hydrogen atom is sterically most favorable. The utility of such spectra in structure determination is shown by the CA spectrum of the m/z 234 peak from 3α-hydroxy-5α-cholestane, which is the same as the CA spectrum from the corresponding pregnane. Similarly, the m/z 374 peak from digitoxin, which is presumably formed by loss of the glycosidic units from the 3-oxo position with rearrangement of a hydrogen back to the oxygen, gives the same CA spectrum as the molecular ion m/z 374 peak from digitoxigenin of that structure.

CA spectra can also supply structural information on fentanyl-type compounds of high narcotic activity; one such compound "China-White" attracted a great deal of publicity recently when it was discovered as a street drug of unknown structure.

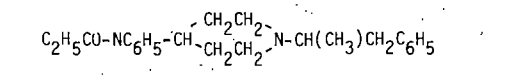

A prominent $C_3H_5O^+$ peak was readily identified from its CA spectrum as having the propionyl structure $C_2H_5\text{-}CO^+$. Prominent m/z 146 peaks in different derivatives were shown to be due to several isomeric ions. For example, all of the $C_6H_5\text{-}NH^+{=}C_4H_6$ isomers gave large m/z 77 peaks in their CA spectra, while a $C_6H_5CH_2\text{-}NC_3H_5^+$ ion gave a very large m/z 91 peak.

The improved resolution and sensitivity of this instrument is also of value for routine analyses with high specificity for trace constituents in complex mixtures with a minimum of sample workup. Tetrachlorodibenzodioxin can be determined in the presence of PCBs and DDE.

The Analysis of Nitrated Polynuclear Aromatic Hydrocarbons in Diesel Exhaust Particulates by Mass Spectrometry/Mass Spectrometry Techniques

T. Riley, T. Prater and D. Schuetzle,
Ford Motor Co, Scientific Research Lab., Dearborn, Mi 48121;
T. M. Harvey and D. Hunt
Dept. of Chem., Univ. of Virginia, Charlottesville, VA 22901

Introduction

Recent investigations have indicated that organic solvent extracts of light-duty diesel exhaust particulates exhibit direct-acting mutagenicity when tested using the Ames assay. Preliminary estimates indicate that a significant portion of this direct-acting mutagenicity may be due to the presence of nitrated polynuclear aromatic hydrocarbons (nitro-PAH).[1] Mass analyzed ion kinetic energy spectrometry (MIKES) and triple stage quadrupole (TSQ) analytical techniques used to characterize these compounds in diesel exhaust are described.

Experimental

Light duty diesel exhaust particulate samples were collected on T60A20 Pallaflex filters using a dilution tube and a chassis dynamometer test facility. Filter samples were extracted with dichloromethane.

MIKES analyses were performed on a Vacuum Generators ZAB-2F mass spectrometer using both electron impact (EI) and negative ion methane chemical ionization (NICI) procedures. All experiments were conducted using a magnetic sector resolution of approximately 2000 and helium as a collision gas (1×10^{-7} torr).

A Finnigan TSQ mass spectrometer was used to perform collisionally activated dissociation (TSQ-CAD) and constant neutral loss studies. All experiments were conducted using positive ion methane chemical ionization (PICI) procedures. In the TSQ-CAD studies the first quadrupole was set to transmit a parent ion of interest into the second quadrupole which functioned as a collision cell (N_2, 5×10^{-3} torr). The third quadrupole was scanned repetitively to collect daughter ion spectra. In the constant neutral loss studies, the first and third quadrupoles were scanned in parallel with a 17 amu mass deficit. Under these conditions, only ions which experience the loss of a 17 amu neutral fragment when collisionally dissociated in the second quadruple are detected. This ion reaction was found to be characteristic of nitro-PAH compounds.

Results and Discussion

The TSQ constant neutral loss analysis was found to be a very useful screening procedure for nitro-PAH compounds. Table I lists 20 different nitro-PAH derivatives which were tentatively identified in diesel particulate extract using this procedure. It must be emphasized that this technique only monitors a reaction characteristic of nitro-PAH compounds and does not confirm their presence.

Table II illustrates the concentration of 1-NP in the exhaust particulate extract from four different diesel engines as determined by MIKES and TSQ-CAD analysis. These quantitation studies indicated that both MS/MS techniques lacked sufficient resolution on the first mass filter to eliminate positive interferences in the daughter ion spectra completely. The M-16 daughter ion fragment (M+1 - OH) was found to be specific for 1-NP and was used for quantitation by TSQ-CAD, but the electrostatic sector of the MIKES instrument did not resolve this daughter ion adequately. It was necessary to prefractionate the OP-1 and PG-1 samples by preparative scale high performance liquid chromatography and to use NICI techniques to accomplish an interference-free MIKES analysis of 1-NP.

Neither MS/MS technique distinguished between nitro-PAH isomers. This information was obtained by capillary GC-MS.

1 Schuetzle, D., Prater, T., Riley, T., Durisin, A., and Salmeen, I., "Analysis of Nitrated Derivatives of PAH and Determination of their Contribution to Ames Assay Mutagenicity for Diesel Particulate Extracts," Fifth International Symposium on Polynuclear Aromatic Hydrocarbons, Columbus, OH, 10/28-30/80.

Table I. Nitro-PAH Derivatives Tentatively Identified in Diesel Particulate Extracts by TSQ Constant Neutral Loss Analysis

Nitroacenaphthylenes
Nitro(acenaphthlenes, biphenyls)
Nitronaphthaquinones
Nitrodihydroxynaphthalenes
Nitrofluorenes
Nitro(methylacenaphthalenes, methylbiphenyls)
Nitro(trimethylnaphthalenes)
Nitro(naphthalic acid)
Nitro(anthracenes and phenanthrenes)
Nitro(fluorenones and methylfluorenes)
Nitro(methylanthracenes and methylphenanthrenes)
Nitro(anthrones and phenanthrones)
Nitro(pyrenes and fluoranthenes)
Nitro(dimethylanthracenes and dimethylphenanthrenes)
Nitro(methylpyrenes and methylfluoranthenes)
Nitro(pyrones and fluoranthones)
Nitro(pyrene and fluoranthene)quinones
Nitro(dimethylphenanthrene and dimethylanthracene) carboxaldehydes
Nitro(methylbenzo(a)anthracenes, methylchrysenes and methyltriphenylenes)
Nitro(benzo(a)pyrenes, benzo(e)pyrenes and perylenes)

Table II. Quantitation of 1-NP in Diesel Exhaust Particulate Extract using MS/MS Techniques

Engine Sample	Instrument	Ionization	Concentration (ppm)
N1-1	TSQ	PICI	2285±230
	MIKES	EI	2080±220
OL-1	TSQ	PICI	204±30
OP-1	TSQ	PICI	77±15
	MIKES	EI	<105
	MIKES	NICI	55±11
PG-1	MIKES	NICI	150±30

IDENTIFICATION OF ACID FRACTION COMPONENTS OF PRIORITY POLLUTANT MIXTURES BY TRIPLE QUADRUPOLE MASS SPECTROMETRY

J.A. Chakel, C.A. Myerholtz, C.G. Enke
Department of Chemistry
Michigan State University, East Lansing, MI 48824

A Triple Quadrupole Mass Spectrometer (TQMS) was utilized for the analysis of the acid extractable priority pollutants. Included in this fraction are: phenol, 2,4-dimethylphenol, 2-chlorophenol, 2-nitrophenol, 4-nitrophenol, 4-chloro-m-cresol, 2,4-dichlorophenol, 2,4-dinitrophenol, 2,4,5-trichlorophenol, 4,6-dinitro-o-cresol, and pentachlorophenol.

Mass-selected ions pass Quad 1 and can undergo low energy collision activated decomposition (CAD) after an interaction with neutral species (Ar) in the positive focusing, RF-only field of Quad 2. Ionic collision products are mass-analyzed by Quad 3 and detected.

The CAD spectra obtained from pure samples of each component were unique. A mixture was prepared from pure samples. CAD spectra were obtained from mass-selected characteristic ions of each component. The correlation between pure sample reference CAD spectra and mixture mass-selected parent ion CAD spectra provides positive identification. The results of low energy electron impact (EI) and negative-ion chemical ionization (NCI) sample ionization techniques were compared. Sample introduction was via a direct insertion probe.

The source parameters for the EI study were 20 eV electron energy and 0.5 mA emission current. The Quad 2 collision chamber was pressurized to 2 x 10^{-4} Torr argon and had an ion axial energy of -15V. Results obtained with low energy EI for 4-chloro-m-cresol, 2,4-dinitrophenol and 2,4,6-trichlorophenol are shown on the following page where the CAD spectra of ions selected from the mixture and pure reference CAD spectra are compared.

The source parameters for the NCI study were 150 eV electron energy, 1.0 mA emission current and a CH_4/N_2O CI gas in a 1.6:1 ratio maintained at 1 Torr. The Quad 2 collision chamber was pressurized to 1 x 10^{-3} Torr argon and had an ion axial energy of +10 V. Negative ions were detected using a conversion dynode. The OH^- reagent ion generated in the source reacts with the sample to produce abundant $(M-1)^-$ ions. Results obtained with NCI for 2-nitrophenol, 4-nitrophenol, and 2,4-dinitrophenol are shown. The two isomeric nitrophenols can be differentiated since the reference CAD spectrum for 2-nitrophenol shows a $(M-1-16)^-$ ion, not present for the other isomer, and the nitrophenols come off of the probe at different temperatures.

Positive ion CI was examined using both methane and isobutane as the reagent gas. The degree of interfering fragments and addition products rendered this method unsuitable for this type of analysis.

In general, EI allows most of the compounds to be separated with the mass selection function of Quad 1. However EI suffers from the potential interferences of other fragment ions from the source. With NCI predominately $(M-1)^-$ ions are produced in the source which simplifies the separation process since no interfering fragments are generated. The CAD spectra of negative parent ions exhibit less fragmentation than their EI counterparts.

This work was supported in part by grants from NASA and the MSU Agricultural Experiment Station.

SELECTED ION SPECTRA

REFERENCE SPECTRA

EI (20eV)

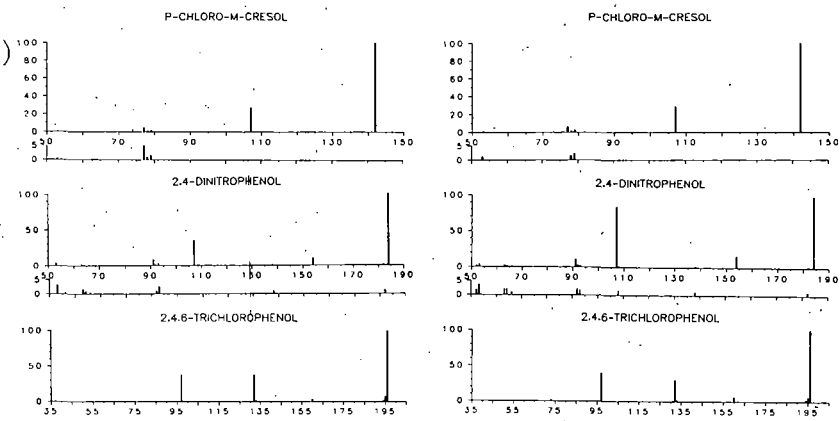

NCI

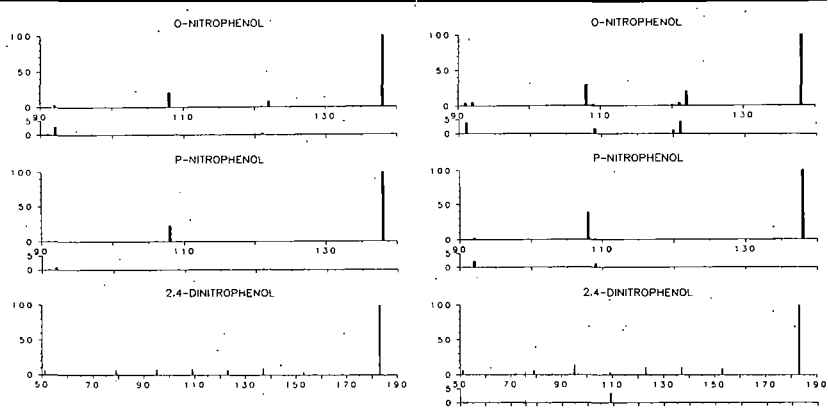

FUNDAMENTAL FACTORS WHICH INFLUENCE CID (MS/MS) SPECTRA IN TRIPLE QUADRUPOLES; P.H. DAWSON, Physics Division, National Research Council, Ottawa, Canada K1A 0R6, J.B. FRENCH, University of Toronto, Institute of Aerospace Studies, Downsview, Ontario, Canada, J.A. BUCKLEY, D. SIMMONS and D.J. DOUGLAS, Sciex Inc., 55 Glen Cameron Road, Thornhill, Ontario, Canada L3T 1P2.

Triple quadrupoles are already finding widespread application in analytical studies utilising sequential mass spectrometry. It is important that the influence of the instrument parameters on the observed CID spectra be well understood, so that standard operating conditions for the accumulation of spectral libraries can be established. The parent ions are separated in the first quadrupole, undergo collision, preferably with a well-defined gas target, in the second quadrupole and product ions are mass analysed in the third quadrupole (Fig. 1). Each of the quadrupoles has its own transmission characteristics which depend upon the choice of rf/dc ratios, the dc offsets of each quadrupole from ground and the chosen mode of operation such as constant parent, constant daughter or linked scan (Fig. 2). The discussion of the optimisation of these parameters is illustrated by a comprehensive experimental study of the dissociation of the protonated parent ion of a phosphorous ester, DMMPA, at mass 196. The instrument was a triple quadrupole (TAGA 6000) of high ion transmission efficiency. Both the

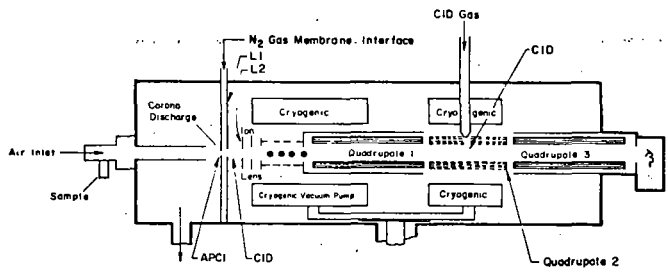

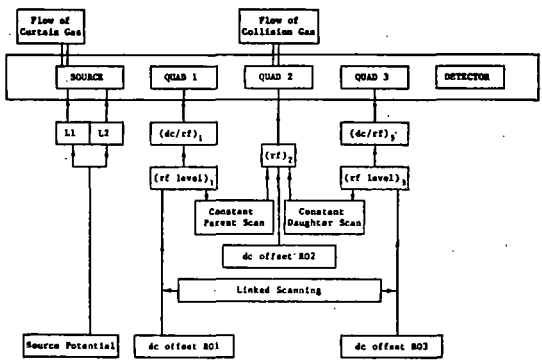

cross-sections for dissociation as a function of collision energy and the associated changes in fragmentation pattern were measured (Fig. 3). By increasing target thickness, the sequential dissociation of daughter ions into granddaughters etc. was observed (Fig. 4). Velocity distributions of daughter ions were measured. The decomposition of the daughter ions could be individually studied by producing them independently by CID in the source region. In this way a complete dissociation sequence (or "genealogical tree") could be established (Fig. 5). With no target gas present in the central quadrupole, decomposition of metastable ions of the parent could also be observed. The optimisation of the instrument parameters for analytical purposes is discussed on the basis of the observations described above.

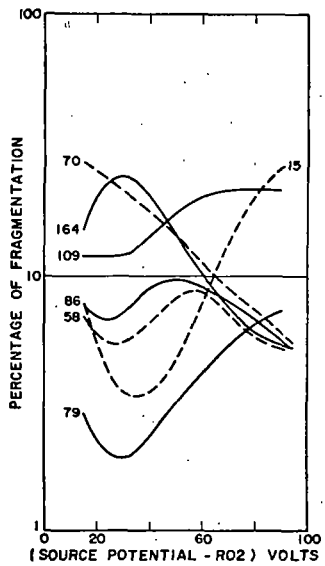

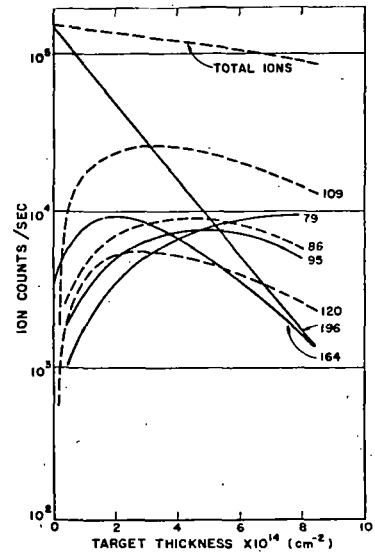

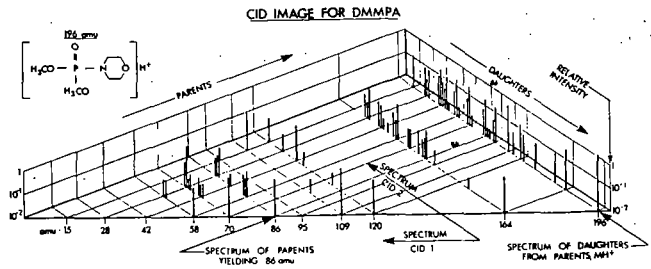

MS/MS CHARACTERIZATION OF DIESEL EMISSIONS

Thomas R. Henderson, Robert E. Royer and Charles R. Clark
Lovelace Inhalation Toxicology Research Institute
P. O. Box 5890
Albuquerque, New Mexico 87185

Increased use of diesel engines in light-duty vehicles is expected in the near future because of increased fuel efficiency and the ability of diesel engines to utilize a wide range of fuels. Correlations between direct-acting mutagens in diesel exhaust particulate extracts and the activity of synthetic nitro-PAHs with Salmonella tester strains TA98 and TA100 have been noted, but detection of nitro-PAHs in diesel emissions extracts has proven difficult.

In the studies reported here, MS/MS (triple-stage quadrupole mass spectrometry) was used to detect masses of nitro-PAHs in diesel soot extracts and in fractions of the extracts. Comparison by MS/MS of an aromatic fraction from diesel fuel reacted with NO_2 vs. extracts of particulate emissions from an engine running on the same fuel showed the range of nitro-PAH masses was similar. Therefore, one mechanism for the formation of nitro-PAHs in diesel exhaust may be the reaction of unburned fuel components with NO_x.

METHODS

Diesel exhaust samples were collected from a light-duty diesel engine. The displacement was 1.5 liters and the engine was operated on the EPA Federal Test Procedure. The samples were collected on Pallflex T60-A20 filters after dilution in a dilution tunnel. CH_2Cl_2 extraction was carried out as described previously (Royer, Sturm and Walter, 1980). A standard #2 diesel fuel was used in the engine and as a source of aromatic hydrocarbons for preparation of nitro-PAHs. The fuel aromatics were prepared as described previously (Henderson et al., 1981).

MS/MS analyses were carried out with a modified Finnigan 3200 MS at the University of Virginia (Hunt, Shabanowitz, and Giordani, 1980). Samples of 10 to 50 µg in capillaries were volatilized into the ion source by heating of the solid probe from 50 to 350°C. Tuning and standardization was accomplished using 1-nitropyrene (synthesized by Dr. R. E. Royer) and the m/e 231 ion. The ionizer was operated under isobutane CI conditions with 0.4 torr isobutane pressure. The first quadrupole was scanned with 1.3 sec scan time over a mass range of 80 to 450 amu. The second quadrupole was operated in RF only, with N_2 collision gas adjusted for maximal 231 ion signal with nitropyrene standard. The third quadrupole was linked to scan 17 amu behind quadrupole #1. The reaction monitored was:

$$R\text{-}NO_2 \longrightarrow R\text{-}NO_2\text{-}H^+ \xrightarrow{-OH} R\text{-}N^+O$$

Thus, the only ions detected were those which lost 17 amu in passing from quadrupole #1 to quadrupole #3, this loss being relatively specific for nitro-compounds.

The aromatic fraction derived from fuel was analyzed by GC/MS, using a Finnigan 4023 MS. The instrument was equipped with a 20-m SP-2100 fused silica column inserted directly into the ion source of the MS. The transfer ovens were maintained at 250°C. The GC was temperature programmed from a 2 min hold at 50°C, to 250°C at 2°C/min. The INCOS data system used standard 3.1C software and NBS mass spectral libraries. Fourteen standard PAHs were run to verify the library entries and the column performance.

The nitro-fuel PAH fraction was prepared as described previously by treating fuel PAHs with NO_2 (Henderson et al., 1981). This preparation had a direct mutagenic activity (no S-9) of 172 revertants/µg in the Ames bioassay with Salmonella TA98. The fuel PAH fraction was inactive with TA98 in the presence or absence of S-9.

RESULTS AND DISCUSSION

GC/MS analyses of the standard diesel fuel aromatic fraction showed that the fuel PAHs were principally 2 ring PAHs and methylated derivatives thereof. The relative concentrations were calculated from the RIC peak height, assuming equal response factors and were

normalized relative to dimethylphenanthrene (=1). The relative concentrations of major components which were present at greater than 10 times the concentration of dimethylphenanthrene were: methylnaphthalenes, 97; dimethylnaphthalenes, 130; methylbiphenyls, 20; and trimethylnaphthalenes, 78. No four or five-ring PAHs, such as pyrenes or fluoranthenes were detectible in aromatic extracts from diesel fuels.

MS/MS analysis of the fuel aromatic fraction reacted with NO_2 showed that the ions corresponding to mono-nitro derivatives of fuel PAHs were present along with some dinitro-derivatives. The major ions (greater than 50% relative abundance) and possible identifications were: 171, nitro-methylnaphthalenes; 183, nitro-biphenyls; 185, nitro-dimethylnaphthalenes; 197, nitro-methylbiphenyls; 211, nitro-dimethylbiphenyls; 221, nitro-methylphenanthrenes. Although pyrene was not detectible in fuel PAH fractions by GC/MS, MS/MS detected a 231 amu peak corresponding to nitropyrenes in nitro-fuel PAHs. This was quantitated by standard additions of nitropyrene to replicate samples for analysis. The nitropyrene concentration was calculated to be 1000 ppm. This extrapolates to a contribution of nitropyrene to the total mutagenicity of less than 5%.

An extract of a diesel fuel particulate sample from an engine running on the standard diesel fuel showed the same range of nitro-PAH masses as the fuel nitro-PAHs. No significant masses higher than 231 (four-ring nitro-PAHs) were observed on MS/MS spectra, and the predominant ions were m/e 171, 183, 185, 197, 207, 211, 221 and 231, which correspond to 2, 3 and 4-ring nitro-PAHs and methylated derivatives thereof.

MS/MS analyses were also used to compare an unfractionated diesel exhaust particle extract, a DMSO/aromatic fraction thereof, and a Sephadex LH-20 fraction of the starting material. The DMSO fractionation concentrations the direct-acting mutagens ca 10 fold; the Sephadex chromatography ca 5 fold (Henderson et al., 1980). The range of nitro-PAH masses were very similar to the nitro fuel PAHs reported above, and the nitro-PAHs observed in the concentrated fractions were very similar to the unfractionated starting material.

These results are in agreement with the hypothesis that nitro-PAHs may be responsible for at least part of the direct-mutagenicity of diesel emissions extracts. Also, these results suggest that unburned fuel PAHs may contribute to exhaust mutagenicity by reacting with NO_x formed in the combustion process.

REFERENCES

Henderson, T. R., Clark, C. R., Hanson, R. L., and Royer, R. E. Proceedings 28th Annual Conference ASMS (1980) p. 243-244.

Henderson, T. R., Li, A. P., Royer, R. E., and Clark, C. R. (1981) Environ. Mutagenesis (in press).

Royer, R. E., Sturm, J. C., and Walter, R. A. (1980) Inhalation Toxicology Research Institute Annual Report, 1978-1979, p. 207-210.

Hunt, D. F., Shabanowitz, J., and Giordani, A. B. (1980) Anal. Chem. 52:386-390.

ACKNOWLEDGEMENTS

Research performed under U. S. Department of Energy Contract DE-AC04-76EV01013. We are grateful to Drs. T. M. Harvey and D. F. Hunt of the University of Virginia for MS/MS instrumentation and operation.

Analysis of Phenolic and Polynuclear Aromatic Hydrocarbon Species in Alternate Fuels and Effluents

L. R. Hilpert and K. L. Richie, Center for Analytical Chemistry, National Bureau of Standards, Washington, D.C. 20234

Energy demand in the U.S. has intensified efforts to develop alternate energy sources such as coal, oil shale, and tar sands. The large amounts of water used in the mining and refining operations for some of these processes result in a significant environmental threat. It is, therefore, important that the aqueous effluents be monitored for their toxic organic compound content. A simple organic extraction has been used to isolate phenolic and polynuclear aromatic hydrocarbon species from several coal gasification, oil shale refinery, and oil refinery aqueous effluents. Quantitative determinations were made by selected ion monitoring GC/MS using internal standards.

Samples

The aqueous effluents were obtained from the Gulf South Research Institute, New Orleans, Louisiana. They were stored in amber glass bottles at 4 °C until analyzed. Prior to analysis, each sample was equilibrated at room temperature, homogenized by mixing vigorously for 1 minute, and filtered through Whatman #41 paper to remove any suspended particulate matter and/or insoluble oil. The samples were analyzed as described below:

Polynuclear Aromatic Hydrocarbons

The effluent (100 mL) was placed in a separatory funnel. One to 10 μg of pyrene-d_{10} in methanol was added as an internal standard and the sample was extracted with 50 mL CH_2Cl_2. The organic extract was dried by filtering through a cone of anhydrous Na_2SO_4 and the volume reduced to ∿100 μL under a stream of dry nitrogen. One to two μL of the concentrated extract was chromatographed on a 30 m x 0.25 mm I.D. fused silica SE-30 wall coated open tubular column, which was interfaced directly into the ion source of a quadrupole mass spectrometer. The molecular ions for the analytes [fluoranthene, pyrene, benzo(e)pyrene, benzo(a)pyrene, and perylene] and the pyrene-d_{10} internal standard were monitored with a mass spectrometer dwell time of 100 ms per ion.

Phenols

One hundred (100) mL of the effluent was spiked with an appropriate amount of 2-chlorophenol as an internal standard. The pH of the sample was adjusted to 1-2 with H_2SO_4 and the sample was extracted with 50 mL CH_2Cl_2. The organic extract was dried by filtering through a cone of anhydrous Na_2SO_4, and the volume reduced to ∿100 μL under a stream of dry nitrogen. One to two μL aliquots of the extract were analyzed by GC/MS with selected ion monitoring. Chromatographic separations were carried out on a 20 m x 0.25 mm I.D. Pluronics PL-64 WCOT column. The column was connected through an open split interface to a quadrupole mass spectrometer. The molecular ions for the analytes [phenol, o-cresol, m-cresol, p-cresol, 2,4- and 2,5-dimethylphenol (DMP), and 2,6-dimethylphenol] and the 2-chlorophenol internal standard were monitored with a 100 ms dwell time in order to insure at least 20 data points across each chromatographic peak.

Response factors for the analytes relative to the internal standards were determined from gravimetrically prepared solutions of the pure compounds. The response factors must be determined under identical chromatographic and mass spectrometric conditions as the samples. Individual analyte concentrations were determined from the analyte and internal standard peak areas and the experimentally determined relative response factors. The results of these determinations are shown in Table 1 for the PAH and in Table 2 for the phenols.

Table 1
Polynuclear Aromatic Hydrocarbons in Energy Effluents

Sample	Analyte Concentration (ppb)				
	Fluoranthene	Pyrene	Benzo(e)pyrene	Benzo(a)pyrene	Perylene
CG-04	11.6	11.0	0.92	1.6	0.5
CG-06	303	281	30	58	18
OR-21	<1.0	<1.0	<1.0	<1.0	<1.0
OS-43	<1.0	<1.0	<1.0	<1.0	<1.0

Notes: Values represent an average of 2 determinations
CG = coal gasification effluent
OR = oil refinery effluent
OS = oil shale effluent

Table 2
Phenols in Energy Effluents

Sample	Analyte Concentration (ppb)					
	Phenol	2,6-DMP	2,4- and 2,5-DMP	o-Cresol	m-Cresol	p-Cresol
CG-04	1040	27	190	300	16	27
CG-06	730	290	890	490	330	250
OS-42	<10	<10	<10	<10	<10	<10
OS-43	<10	<10	ND	<10	ND	ND
OR-21	<10	<10	<10	<10	<10	<10
OR-23	<10	<10	ND	<10	ND	ND
OR-25	<10	<10	<10	<10	ND	ND

Notes: Values represent an average of 2 determinations
CG = coal gasification effluent
OR = oil refinery effluent
OS = oil shale effluent
ND = not detected

Results and Discussion

The use of high resolution wall coated open tubular columns with a polar phase such as the Pluronics PL-64 and a non-polar methylsilicone phase such as SE-30 allows facile separation of toxic priority pollutants from complex mixtures. Especially noteworthy is the resolution of all of the C_1 and C_2 alkylated phenols with the Pluronics phase except for the 2,4- and 2,5-dimethylphenol which are not completely resolved, and are reported as the sum of the concentrations of the two isomers. The 30 m fused silica SE-30 column provides baseline resolution of the benzo(e)pyrene and benzo(a)pyrene isomers, allowing each to be quantified independently. These columns coupled with the use of internal standards and selected ion monitoring detection, allow compound concentrations in the part per billion range to be determined precisely. The relative standard deviation of replicate analyses was less than 10 percent.

EXTENDED USE OF THE PURGE AND TRAP TECHNIQUE ON LOW VOLATILITY ORGANICS IN WATER

Albert R. Trussell, JMM Environmental Research Laboratory, Pasadena, California 91101

James G. Moncur, Lockheed Missiles and Space Company, Palo Alto, California 94304

INTRODUCTION:

The purge and trap technique introduced by Bellar about seven years ago has proven to be a very useful and popular technique for the analysis of certain volatile organic components in water.[1] This dynamic headspace isolation technique recovered purgeable organic compounds in the boiling point range from -25°C (methylchloride) to 150°C (bromobenzene). The authors adapted this technique by adding the use of a fused silica capillary column and focused cryogenic trapping to lower the detection limits an order of magnitude and extend the boiling point range to -25°C to 275°C (acenaphthene).[2] This adaptation allowed the further development of a simultaneous chromatographic technique for volatile, base/neutral, acid extractable and pesticide fraction organic priority pollutants.[3] Further modifications involving the use of an elevated purge temperature (50°C), a larger 500 ml sample size and salting out with sodium sulfate extend the range of the technique to compounds with boiling points around 300°C (fluorene) with only an 8 minute purge time and without sacrificing sensitivity for extremely volatile components. If recovery of the most volatile components is unnecessary, the purge time can be lengthened to 80 minutes which extends the boiling point range of the technique to 350°C (anthracene) or a Closed Loop Stripping Analysis (CLSA) method can be used to recover compounds whose boiling points are as high as 400°C (pyrene).

EXPERIMENTAL:

Purge and Trap

Purge and trap analyses were conducted on a Finnigan 4021 GC/MS (Finnigan Corporation, Sunnyvale, California) interfaced with a Tekmar LSC-2 Liquid Sample Concentrator (Tekmar Inc., Cincinnati, Ohio). The sample size utilized in this study was 500 mls, 15 grams of sodium sulfate were added to the sample to improve purging efficiency of less volatile organic compounds. The water samples were heated to 50°C and purged for 8 or 80 minutes with a flow of 40 ml/minute into a Tenax/silica gel trap at 25°C. The compounds were desorbed at 200°C for 2.5 minutes with a 15 ml/min flow rate. During the desorption step the volatile organics were trapped on a loop at the front of the capillary column by the application of liquid nitrogen. The column utilized was a fused silica open tubular capillary column 0.25 mm X 30 M, coated with the liquid phase SE-54 (J&W Scientific, Rancho Cordova, California). A split ratio of 10:1 was used during the desorption step. The gas chromatograph was held isothermal at 30°C for 2.5 minutes, then the oven was programmed to 250°C at 8°C per minute where the temperature was held for the duration of the run. The mass spectrometer was run in the electron impact, direct mode, with an emission current of 0.5 ma, an electron energy of 70 eV, the electron multiplier at 1600 volts and the ion source at 250°C. The data system was programmed to scan from m/e 33 to 383 in 0.75 seconds with a 0.05 second hold at the bottom.

Closed Loop Stripping Analysis

The closed loop stripping technique utilized was adapted from the work conducted by Grob in 1974.[4] The only major modification which has been made is the incorporation of all glass and teflon parts. The 500 ml water sample maintained at 50°C was stripped by the recirculating air flow for 80 minutes at a flow rate of approximately 100 ml/min. The activated carbon filter was extracted sequentially with three 10 microliter portions of carbon disulfide and 2 microliters of this extract were injected in the splitless mode on the same fused silica capillary column and under the same chromatographic conditions as described above.

RESULTS:

The table below shows the comparative recoveries of the base/neutral fraction organic priority pollutants by three different techniques: an eight minute purge, and 80 minute purge and closed loop stripping. Water samples were spiked with 10 ug/l of the 47 base/neutral and 11 acid fraction organic priority pollutants. Under the neutral pH conditions, at which these experiments were conducted, none of the acid fraction compounds were recovered. 19 of the base/neutral fraction components were recovered by the 8 minute purge, 24 were recovered by the 80 minute purge and 27 base neutrals were recovered by CLSA. The CLSA technique showed generally higher recoveries and was superior for higher molecular weight, higher boiling point compounds, especially polynuclear aromatics. The 80 minute purge technique was comparable or superior for many of the compounds with boiling points less than 250°C. The 80 minute purge did not recover the more polar compounds N-nitrosodipropylamine, isophorone and bis(2-chloroethoxy)methane. The 8 minute purge technique showed uniformly lower sensitivity with the

exception of N-nitrosodiphenylamine. The authors have not determined at this time why the trend for this compound is reversed with CLSA showing the poorest recovery. The authors have previously demonstrated[2] that focused cryogenic trapping in conjuction with capillary chromatography can extend the range of the purge and trap technique when utilizing a 25 ml sample at ambient temperature to include such compounds as dichlorobenzenes, 4-chlorophenyl-phenylether, bis(2-chloroisopropyl)ether, hexachloroethane, trichlorobenzenes, naphthalene, hexachlorobutadiene, 2-chloronaphthalene, acenaphthylene, and acenaphthalene. The work presented here demonstrates that certain modifications to the more typical technique (larger sample volumes, addition of salt, heating to 50°C, and longer purge times) can further extend the range and sensitivity of the purge and trap method. Closed loop stripping analysis may be more sensitive and and recover compounds in higher boiling point ranges such a chyrsene (boiling point 448°C) *when the stripping time is increased.*[5] *However, at the other end of the boiling point* range the purge and trap technique is superior and the analytical trace organic chemist will have to choose which technique to apply depending upon the compounds of interest.

COMPARATIVE RECOVERIES OF 8 MINUTE PURGE, 80 MINUTE PURGE, AND CLOSED LOOP STRIPPING ANALYSIS (CLSA) AT THE 10 ug/L LEVEL IN WATER

				Ion Areas		
No.	Compound	Retention Time	Quantitation Ion	8 Min. Purge & Trap	80 Min. Purge & Trap	CLSA 80 Min.
1	Bis(2-Chloroethyl) Ether	8:50	93	13908	262515	331462
2	1,3-Dichlorobenzene	9:17	146	763129	1620780	1041050
3	1,4-Dichlorobenzene	9:26	146	760091	1806440	1034020
4	1,2-Dichlorobenzene	9:54	146	617222	1694640	1038960
5	Bis(2-Chloroisopropyl) Ether	10:16	45	45370	590651	534554
6	Hexachloroethane	10:44	117	584801	975090	552052
7	N-Nitrosodipropylamine	10:37	70	—	—	99200
8	Nitrobenzene	10:58	77	—	218204	221186
9	Isophorone	11:39	82	—	—	18682
10	Bis(2-Chloroethoxy)Methane	12:25	93	—	—	70935
11	1,2,4-Trichlorobenzene	12:53	180	383478	1553890	947997
12	Naphthalene	13:02	128	409378	1902600	1661890
13	Hexachlorobutadiene	13:39	225	356893	654510	350164
14	Hexachlorocyclopentadiene	15:57	237	414	45260	67408
15	2-Chloronaphthalene	16:44	162	54726	1036570	1260120
16	Acenaphthylene	18:04	152	27533	440801	815708
17	Acenaphthene	18:42	154	29429	317745	955650
18	N-Nitrosodiphenylamine	18:52	169	26869	3220	830
19	Fluorene	20:20	166	8415	165208	510941
20	4-Chlorophenylphenyl Ether	20:26	204	1581	26608	218662
21	Diphenylhydrazine	20:56	77	1996	81227	405893
22	4-Bromophenylphenyl Ether	22:02	248	767	32367	333463
23	Phenanthrene	23:27	178	251	9605	82458
24	Anthracene	23:35	178	—	9623	43273
25	Dibutyl Phthalate	25:48	149	—	3131	886892
26	Fluoranthene	27:25	202	—	77	3322
27	Pyrene	28:12	202	—	108	2042

REFERENCES:

1. Bellar, T.A.; Lichtenberg, J.J.; "The Determination of Volatile Organic Compounds at Microgram per Liter Levels in Water by Gas Chromatography," Journal AWWA, 66:12:739 (December 1974)
2. Trussell, A.R.; Moncur, J.G.; Lieu, F.Y.; "Parts Per Trillion Analysis of Volatile Base/Neutral and Acidic Water Contaminants on a Single Fused Silica Capillary Column, Advances in the Identification and Analysis of Organic Pollutants in Water. Editor - L. Keith, Ann Arbor Science, (August, 1980)
3. Trussell, A.R.; Moncur, J.G.; Lieu, F.Y.; Leong, L.Y.C.; "Simultaneous Analysis of all Five Organic Priority Pollutant Fractions," Journal of High Resolution Chromatography, 4:81 (April, 1981)
4. Grob, K.; "Organic Substances in Potable Water and in its Precursor, Part I, Methods for Their Determination by Gas-Liquid Chromatography," Journal of Chromatography, 84:255-273 (1973)
5. Melton, R.G. et al "Comparison of Grob Closed Loop Stripping Analysis (CLSA) to Other Trace Organic Methods. Advances in the Identification and Analysis of Organic Pollutants in Water. Editor - L. Keith, Ann Arbor Science, (August, 1980)

CHEMICAL CHARACTERIZATION OF MUTAGENIC EXTRACTS OF BAG FILTER ASH FROM AN EXPERIMENTAL FLUIDIZED BED COAL COMBUSTOR

Ray L. Hanson, C. R. Clark, C. H. Hobbs;
Lovelace Inhalation Toxicology Research Institute,
P. O. Box 5890, Albuquerque, New Mexico 87185

Fluidized bed combustion of coal is being developed as an alternative to pulverized coal combustion. Lower emissions of SO_2 and NO_x result from the addition of limestone to the bed as a sulfur dioxide sorbent and the lower combustion temperature in the fluidized bed. The Inhalation Toxicology Research Institute and the Morgantown Energy Technology Center have a collaborative research program to characterize effluents from an experimental fluidized bed combustor. This research has involved sampling and analysis of the process stream and fly ash collected in the cleanup devices (1,2,3,4). This work describes characterization of samples of bag filter ash from the combustion of a bituminous coal, a subbituminous coal, a lignite and a washed lignite.

The ash samples were extracted with dichloromethane in an ultrasonic bath. The extractable mass was determined after solvent removal by rotary evaporation and evaporation of the solvent under nitrogen. The extracted residues were divided into two portions; one for chemical analysis using GC/MS and one for use in the Salmonella mutagenicity assay. A description of the Salmonella mutagenicity assay and results from a variety of samples from fluidized bed combustion of coal have been published (5). The extracts were analyzed using a Finnigan Model 4023 GC/MS with a 30 m WCOT SP-2100 glass capillary column with splitless injection of 1µl. The temperature program was 50°C for 2 minutes, 4°C/minute to 270°C, hold at 270°C for 15 minutes. Electron impact spectra at 70 ev were recorded every 1.6 seconds with scans from 50 to 650 daltons. Tentative identifications were based upon retention times and the fits obtained from the library search routine of the INCOS data system and the NBS-EPA-NIH library provided by Finnigan.

The results of the extraction and the mutagenicity assay in which the extractable organic matter from up to 2 g of ash was tested are given in Table 1. Washing the lignite before combustion resulted in bag ash that was not mutagenic. Several combustion tests were conducted with the subbituminous coal. The ashes with the greatest concentration of extractable organic material were mutagenic. There was no general relationship between fuels for quantity extractable and mutagenicity. The bituminous coal bag filter ash extract was not mutagenic, although this ash had a higher concentration of extractable material than the mutagenic extract of lignite bag filter ash. The analysis of the mutagenic extracts by GC/MS indicated the presence of several

polycyclic aromatic hydrocarbons that are known mutagens. These compounds require enzymatic activation to give a mutagenic response, while the mutagenic extracts of bag filter ash did not require enzymatic activation.

Nitroarenes are potent bacterial mutagens in the Salmonella assay presumably because of the high nitroreductase activity in the bacteria. The mutagenicity of a number of fly ash extracts was reduced when evaluated in Salmonella strains that give a reduced respose to nitroarenes. One of these extracts was analyzed by capillary gas chromatography using a nitrogen specific thermionic detector and a flame ionization detector. Several compounds were present that gave an enhanced response with the nitrogen specific detector when compared to the flame ionization detector. These compounds appear to be present in low concentrations. If nitroarenes are present, they may have been formed by reactions between the polycyclic aromatic hydrocarbons and the nitrogen oxides in the combustion effluents. (Research performed under U.S. Department of Energy, Contract Number DE-AC04-76EV01013.)

TABLE 1

Coal Type	Mutagenicity Revertants/μg Extract*	Extractable Concentration (μg/g)
Bituminous	0 (100 μg)	51
Washed Lignite	0 (100 μg)	58
Lignite	20	30
Subbituminous	1	13
Subbituminous	2	22
Subbituminous	30	47
Subbituminous	35	61
Subbituminous	50	78
Subbituminous	110	92

*Highest amount tested in parentheses for negative extracts.

REFERENCES

1. Newton, G. J., R. L. Carpenter, H. C. Yeh and E. R. Peele, Environ. Sci. Technol. 14: 849-853, 1980.
2. Carpenter, R. L., G. J. Newton, S. J. Rothenberg and P. B. DeNee, Environ. Sci. Technol. 14: 854-859, 1980.
3. Hanson, R. L., R. L. Carpenter, G. J. Newton, S. J. Rothenberg, J. Environ. Sci. Health A14: 223-250, 1979.
4. Hanson, R. L. Carpenter, R. L. Newton, G. J., in Polynuclear Aromatic Hydrocarbons: Chemistry and Biological Effects, (A. Bjorseth and A. J. Dennis, ed.), Batelle Press, Columbus, Ohio, 1980, 599-616.
5. Clark, C. R. and C. H. Hobbs, Environ. Mutagen. 2: 101-109, 1980.

A SOPHISTICATED AUTOMATIC PROCEDURE FOR THE QUANTITATIVE DETERMINATION OF PRIORITY POLLUTANTS. P.A. Ryan, C.J. Wakefield, H.J.M. Fitches, K.R. Compson, Kratos Limited, Barton Dock Road, Urmston, Manchester.

Many GC/MS analyses require a large number of repetitive experiments run under identical experimental conditions. As machines have proved to be more reliable than humans at routine operations of this nature a computer-controlled method has been implemented.

Although this technique has many applications, its first application has been in the analysis of the "Priority Pollutants" in water.

The basic technique for identification and quantification is as follows:

The sample was prepared with a known concentration of an internal standard. In our example the internal standard used was Anthracene -d_{10}. The sample was a mixture of 30ng of six pesticides (see fig 1). The sample was analysed using GC/MS with a 25 Metre SE54 column and an MS25 scanning at 1 sec/decade. The data was acquired and processed using a DS55 Data System.

The first phase of the data processing operation is the identification of the internal standard. The program searches for the internal standard by looking within a time-window of its expected retention time. The search procedure has two stages. The first stage is a search for the four "characteristic ions" of the internal standard maximising in intensity in the same or adjacent scans. The scan selected is then verified against the spectrum of the internal standard by reverse library search.

Once the standard has been positively identified the quantity present is used to calculate response factors for use later in the procedure.

The target compounds in the library are now searched for in turn. The first stage of this search is based on the retention index of each compound. The program contains a retention index file which has been obtained under the same GC conditions as the sample now being analysed. This file relates retention indices to actual retention times, and in fact, many such files may be stored for various different GC conditions. Each target compound in the library has two associated retention indices, one for non-polar and one for polar columns. Each target compound has its expected retention time calculated from the relevant retention index and the data stored in the retention index file. A search is now made within a time window in an identical fashion to that described for the internal standard.

If a positive match is found, the quantity is determined using the response factors of the characteristic ions of the compound with respect to the characteristic ions of the internal standard and a continually updated concentration curve for each compound with respect to each internal standard.

The positive matches are printed out together with a mean concentration and a standard deviation (see fig 2). Positive matches may also be flagged on the report if the concentration exceeds a user - specified maximum so that high concentrations are immediately apparent on inspection of the results.

The program also prints a total ion current chromatogram of the experiment with all the positive matches marked (fig 3).

This search and quantitation method has been automated by the use of an autosampler controlled from the data system.

Each injection is identified by its rack and vial identity and also the injection number from that particular vial. The solvent vent valve is also controlled by the computer to avoid waste of storage space on disk and contamination of the mass spectrometer source. The computer controls the time of the injection, the length of time of the analysis and also monitors the GC temperature so that the next sample is not injected until the experimental conditions are correct. Certain samples may be designated as wash samples in which case no acquisition is performed.

This system provides the user with completely automatic data collection and analysis procedures. Because of the high degree of computer control, exact reproduction of experimental conditions for each injection is possible and multiple analyses can be performed reliably without any operator intervention.

COMPOUNDS SEARCHED FOR

ENTRY #	MOL. WT.	RETENTION INDEX NON-POLAR	RETENTION INDEX POLAR	FORMULA	NAME
2	288	1760	-	C6.H6.CL6	LINDANE (22545)
3	316	2200	-	C14.H8.CL4	D.D.E. (24677)
4	352	2369	-	C14.H9.CL5	D.D.T. (26973)
5	362	1985	-	C12.H8.CL6	ALDRIN (27529)
6	378	2210	-	C12.H8.CL6.O	DIELDRIN (28298)
7	378	2250	-	C12.H8.CL6.O	ENDRIN (28299)
8	188	1805	-	C14.H10	ANTHRACENE D-10

Figure (1)

POSITIVE MATCHES

SCAN #	ACTUAL R.T.	EXPECTED R.T.	LIB ENTRY #	MATCH SCORE	CONCENTRATION(PPB) MEAN	S.D.	IONS USED	FLGS
387	14:34	14:34	2	81	27.19	0.68	4	
577	21:44	21:58	3	91	30.04	1.11	4	
646	24:21	24:33	4	90	22.94	0.97	4	***
488	18:23	18:27	5	77	27.49	1.69	4	
579	21:49	22: 3	6	85	28.20	2.16	4	
599	22:34	22:48	7	83	30.54	1.81	4	
401	15: 6	15: 6	8	82	28.92	1.39	4	

KEY TO FLAGS

- ^ SATURATED SAMPLE IN PEAK
- * NON-PEAK MASS IN PEAK
- # INSUFFICIENT CALIBRATION DATA FOR QUANTIFICATION
- ? OUTSTART FAILURE ON PEAK
- *** CONCENTRATION EXCEEDS STATED LIMIT

Figure (2)

DS-55 LIBRARY SEARCH - TIC REPORT

RUNNAME POL131 100% INTENSITY 2917696

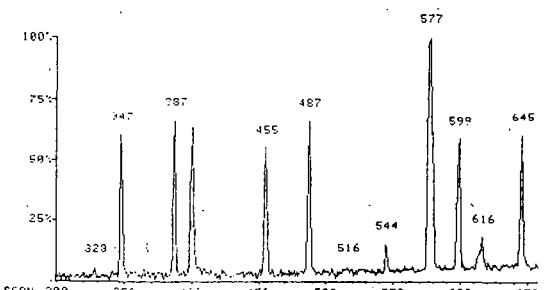

Figure (3)

COAL STRUCTURE: GC-MS STUDIES OF THE OXIDATIVE DEGRADATION PRODUCTS OF COAL AND "OXYCOAL," R. Minard, N. Deno, J. Stroh, C. Koch, T. Reed, S. Soboczenski, D. Jones; Department of Chemistry, Penn State Univ., University Park, PA 16802.

Pertrifluoroacetic acid (H_2O_2-CF_3COOH-H_2SO_4) oxidative degradation of coal converts a major portion of the aromatic carbon of coal to CO_2 while the aliphatic part remains unoxidized and is isolatable as alkonic acids. Almost 50 of these organic acids have been identified by EI and CI gc-ms methods. (See references).
The discovery that the product compositions from these oxidations changes as the coal sample ages confirms that coal structure is dramatically altered on exposure to air and it appears that many laboratory studies may have been conducted on this altered form of coal called "oxycoal."

BRIEF DESCRIPTION OF WORK

Insight into coal structure has been garnered from the examination of products from oxidative degradation of coals and coal models with per TFA reagent (CF_3COOH-H_2O_2-H_2SO_4) wherein much of the aromatic structure is oxidized to CO_2 while the aliphatic structure remains largely intact:

Examples:

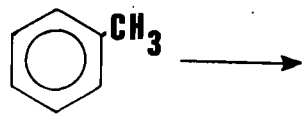

Carboxyl groups deactivate ring to further oxidation

In the process of applying this method to numerous coals, we found large variations in certain products from the same coal oxidized at various times over the period of a year or more.

There is considerable evidence that the air oxidation of coal leads to changes in coal characteristics and properties (reflectance, Giesler plasticity, coking quality) and that these changes are associated with increased aromaticity in this "oxycoal." We find that this idea appears substantiated by our examination of the per TFA oxidation products from a lignite coal and its corresponding "oxycoal" derived by heating it in air at 100°C for 1 week. At present, the "coal model" compound that gives a per TFA oxidation product distribution closest to coal is 9,10-dihydronapthacene:

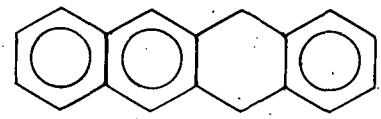

We believe lignite coal contains dihydroaromatic structures which are air oxidized to fully aromatic structures in the "oxycoal." In particular, we see a large increase in phthalic acid, a major product from polynuclear aromatics but not dihydroaromatics.

EXPERIMENTAL

GC*/F.I.D. on a Perkin Elme- Sigma 3B
G.C.*-MS on a Finnigan 3200 EI/CI System
*0.3 MM X 25 meter OV101 fused silica column
Oxidation products (carboxylic acids) are converted to methyl esters with BF_3/methanol before chromatography. Identification of esters is by retention time and mass spectral comparison with known standards.

RESULTS

Many coals, oxycoals and model compounds have been studied by the per TFA oxidative method and the data presented here is representative of all of this work. The product distributions for 11 predominant carboxylic acids from the lignite, the oxidized lignite and our best coal model to date, 9,10-dihydronophacene, are shown in table I. At least 40 other products make up the remaining 50-60% of the total gc-fid area. The major product changes between coal and the oxycoal are increases in oxalic, malonic, propanetricarboxylic and phtholic acid and decreases in the ethane and oxirane tricarboxylic acids.

We feel these changes can be rationalized in terms of the increasing aromaticity of oxycoal and we are doing work with other model systems to substantiate this idea. The fact that the coal model appears to be similar to oxycoal with respect to ethane- and propanetri carboxylic acids and phthalic acid but closer to coal with respect to oxirane and benzene tricarboxylic and benzene tetracarboxylic acids shows that it is not a perfect model. However, our ultimate conclusion is that structural studies of coal are subject to inconsistencies stemming from the continuous modification of coal structure by exposure to air.

REFERENCES

F. Goodarzi and D. G. Murchison. "Petrography and Anisotropy of Carbonized Preoxidized Coals" Fuel, 1976, 55, 141.

N. C. Deno, B. A. Greigger and S. G. Stroud. "A New Method for Determining the Chemical Structure of Coal" Fuel, 1979, 57, 455.

N. C. Deno, K. W. Curry, B. A. Greigger, A. D. Jones, W. Rakitsky, K. Smith, K. Wagner, R. Minard. "Dihydroaromatic Structure of Illinois No. 6 Monterey Coal" Fuel, 1980, 59, 694.

TABLE 1: RELATIVE AMOUNTS OF SELECTED CARBOXYLIC ACIDS FROM PER TFA OXIDATION OF A COAL, ITS OXYCOAL AND A COAL MODEL.* (X = CARBOXYL GROUP).

COAL OXIDATION PRODUCT ACIDS	COAL			OXYCOAL			COAL MODEL		
	% AREA A	% AREA B	RET TIME	% AREA A	% AREA B	RET TIME	% AREA A	% AREA B	RET TIME
OXALATE	1.8	3.3	3.63	5.3	12.5	3.64	0	---	---
MALONATE	17.3	31.5	5.63	20.2	47.8	5.67	0.2	0.5	5.62
SUCCINATE	6.3	11.5	8.20	5.8	13.7	8.24	0.3	0.7	8.23
ETHANE TRIX	2.3	4.2	15.29	0.1	0.2	15.30	0.2	0.5	15.31
OXIRANE TRIX	14.5	26.4	17.78	0.4	0.9	17.74	4.1	9.3	17.74
PROPANE-1,2,3-TRIX	0.3?	0.5?	---	1.2	2.8	17.84	2.0	4.5	17.83
BENZENE-1,2-DIX	0.5	0.9	18.69	1.5	3.5	18.72	22.3	50.7	18.73
OXIRANETETRAX	6.3	11.5	22.91	5.9	13.9	22.97	0	---	---
BENZENE-1,2,4-TRIX	3.1	5.6	26.56	0.4	0.9	26.56	10.3	23.4	26.57
BENZENE-1,2,4,5-TETRAX	2.2	4.0	31.91	0.5	1.2	31.92	4.6	10.5	31.91
BENZENEPENTAX	0.4	0.7	36.07	1.0	2.4	36.08	0	---	---
TOTAL %	55	100	---	42.3	100	---	44	100	---

*RETENTION TIME IN MINUTES. AREA % IN COLUMN A IS RELATIVE TO TOTAL AREA FROM ALL PRODUCTS IN THE GC-FID CHROMATOGRAM. AREA % IN COLUMN B IS % OF TOTAL AREA FOR COMPOUNDS SHOWN IN TABLE ONLY.

ANALYSIS OF ORGANO SULFUR COMPOUNDS IN CRUDE OIL AND COAL LIQUEFICATION SAMPLES

Donald F. Hunt and Jeffrey Shabanowitz
Department of Chemistry
University of Virginia
Charlottesville, Virginia 22901

Crude oil and coal from different geographic regions vary greatly in sulfur content. Organo sulfur compounds are important to the energy industry because they poison the catalysts employed in the "cracking process". The availablility of a satisfactory method for the analysis of sulfur compounds by functional group would allow industry to choose the most appropriate scheme for the economical and efficient handling of feed stocks rich in sulfur containing components.

Presently the method of choice for organo sulfur analysis involves low voltage electron ionization on double focusing mass spectrometers having a resolving power in excess of 50,000 (1). Resolution of this magnitude is required to separate compounds containing C_3 and SH_4 doublets ($C_9H_{20}S$ and $C_{12}H_{16}$) at m/z 160. Disadvantages of the above approach include the high cost of the instrumentation, the failure of the method to resolve doublets at higher m/z values, and an inability to provide information concerning the nature of the sulfur compounds detected (RSH, R_2S, RSOR, etc.).

Below we outline an alternate approach based on a combination of chemical derivatization and collision activated dissociation mass spectrometry on a triple quadrupole instrument (2).

Aliphatic sulfides are analyzed by converting them to sulfoxides and sulfones on treatment of the crude sample with m-chloroperbenzoic acid. Under chemical ionization conditions with NO^+ as the reactant ion (3) aliphatic sulfoxides and sulfones attach NO^+ to form $M+30^+$ ions. These in turn suffer dissociation to NO^+ in the collision cell. Polynuclear aromatic hydrocarbons containing thiophene ring systems are also oxidized to sulfoxides and sulfones but these compounds undergo charge exchange with NO^+ in the ion source or add NO^+ but then dissociate to M^+ plus neutral NO in the collision chamber. Thus, by setting Q3 on mass 30 and scanning Q1 (parent scan), it is possible to analyze for all aliphatic sulfides in the petroleum matrix.

Analysis of compounds containing the thiophene ring system is accomplished under positive ion chemical ionization conditions with Q1 and Q3 set to scan at a fixed mass separation of 33 amu (neutral loss scan). All $M+1^+$ ions from aromatic thiols, thiophenes, benzthiophenes, dibenzthiophenes, etc., suffer loss of $SH^\cdot$ (MW 33) on collision with molecular nitrogen in the collision chamber and tnerefore pass through Q3 to the detector. No other components lose 33 amu in the collision cell, so the above approach is specific for molecules containing thiophene rings and aromatic thiols.

The technique thus allows for rapid screening of petroleum samples for organo sulfur content.

References:

1. Aczel, T.; Williams, R.B.; Brown, R.A.; Pancirov, R.J., "Analytical Methods for Coal and Coal Products", Karr, Clarence, Ed., Academic Press, New York, 1978, Ch. 17.

2. For recent reviews see: (a) McLafferty, F.W., Acc. Chem. Res., 1980, 13, 33-39; (b) Kondrat, W.R.; Cooks, R.G., Anal. Chem., 1980, 52, 81A-92A.

3. Hunt, D.F.; Harvey, T.M., Anal. Chem., 47, 1975, 2136-2141.

DITHIENYL mw 166

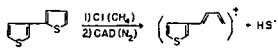

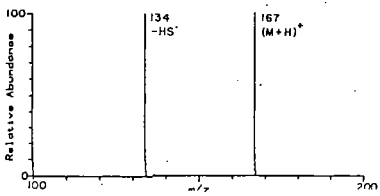

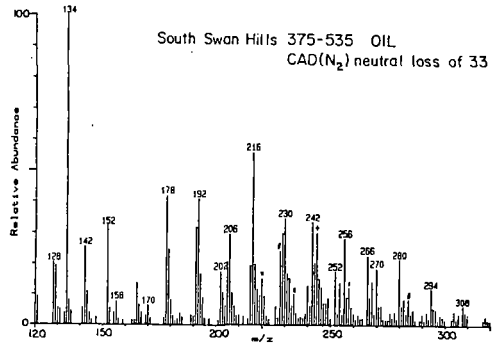

NAPHTHALENETHIOL mw 160

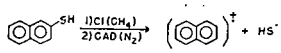

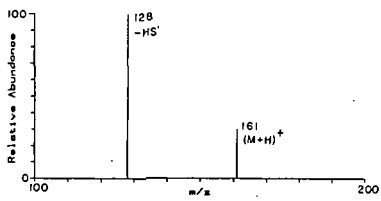

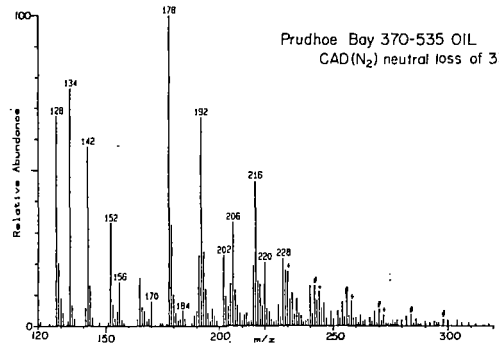

n-DODECYL SULFIDE mw 370

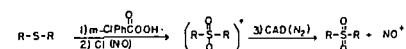

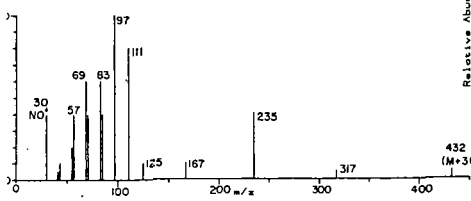

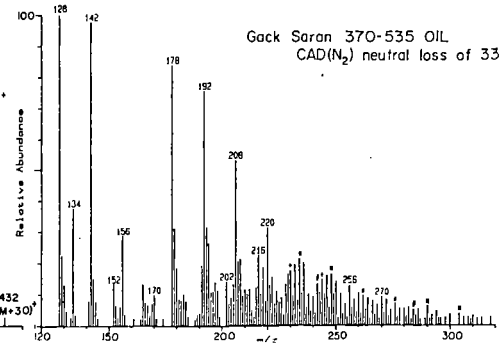

MASS SPECTROMETRIC ANALYSIS OF BIOMARKERS IN CHINESE YANGSANMU CRUDE OIL

WANG XIEQING, LANG RENCHI and SU HUANHUA
Research Institute of Petroleum Processing, Beijing, China

Triterpanes, steranes and porphyrins in crude oil and its sedimentary rock extracts are the well known biological marker compounds. The characteristic of such compounds is that they are quite stable during the diagenetic process and therefore permits differentiation between individual source beds and oils. Analytical results are important to the knowledge of migration, accumulation and maturation of petroleum[3,4].

By means of liquid chromatography, chemical treatment, UV-Vis spectrophotometry, atomic absorption spectrometry, mass spectrometry and GC/MS/C techniques, steranes, triterpanes and nickel porphyrins have been studied in Chinese Yangsanmu crude oil.

EXPERIMENTAL

Sample characteristics

Basin: North China, 1220-1430 m depth, U. Eocene

Physical properties: d_4^{20} 0.9492, pour point -2° C, viscosity (50°C) 637.9 cst, sulphur 0.33%, nitrogen 0.31%, asphaltene none

Instrumentation

Varian Aerograph 2740 gas chromatography/Varian MAT 311 mass spectrometry/ SS 100 MS data system, Biemann-Watson molecular separator, SCOT capillary column (OV 101, 50 m x 0.5mm i.d.) 70 eV, 300 μA, 5 sec/dec scan, LVMS 15 eV 300 μA, Hitachi 340 UV-Vis spetrophotometry 300-700 nm scanning.

RESULTS AND DISCUSSION

1. Hydrocarbon group analysis by MS and GC (wt %)

Boiling point °C	IBP-200	200-250	250-300	300-350	350-400	400-450	450-500
Alkanes	15.4	9.3	12.0	13.1	2.9	0.8	-
n-paraffins	-	-	-	-	-	-	-
i-paraffins	15.4	9.3	12.0	13.1	2.9	0.8	-
Naphthenes	78.8	76.6	60.5	50.1	47.5	51.9	53.4
1 ring	45.1	30.4	15.9	9.4	6.7	1.6	-
2 ring	33.7	37.3	31.3	26.8	12.2	10.9	8.3
3 ring	-	8.9	13.3	13.9	11.3	17.1	23.2
4 ring	-	-	-	-	13.1	18.7	18.7
5 ring	-	-	-	-	4.2	3.3	3.2
6 ring	-	-	-	-	-	0.3	-
Aromatics	5.8	14.1	27.5	36.8	44.2	42.2	40.0
mono-	5.7	12.8	19.0	18.5	16.6	14.6	10.0
di-	0.1	1.2	8.2	16.1	17.5	12.1	11.4
tri-	-	0.1	0.3	2.2	6.1	6.5	6.5
tetra-	-	-	-	-	2.0	4.8	4.9
penta-	-	-	-	-	0.5	0.7	1.4
unidentified	-	-	-	-	1.5	3.5	5.8
Thiophenes	-	-	-	-	1.1	1.0	0.9
Resin	-	-	-	-	4.3	4.1	5.7

2. Assignment of steranes and triterpanes by mass chromatogram and mass spectra

Total ionization current (TIC) can be obtained by GC/MS/C, from which about 60 peaks may be characterized by m/e 191 and 217 representing triterpanes and steranes base peaks respectively (Fig. 1) For further confirmation, 29 chromatographic peaks have been identified by mass spectra. Regular and rearranged steranes and triterpanes were found in 450-500°C fraction (Fig. 2).

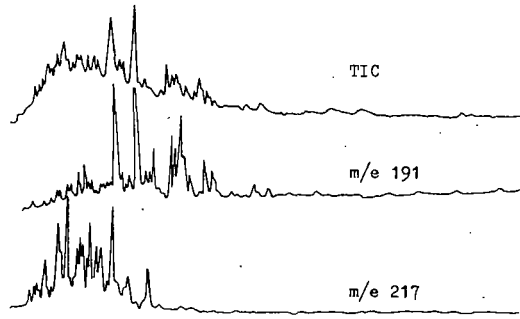

Fig. 1. TIC and mass chromatograms

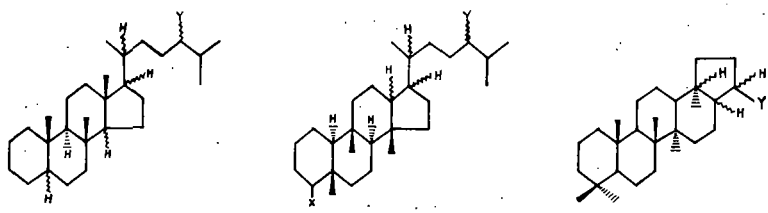

Regular Steranes

a. 5α, 14α, 17α, 20R
b. 5β, 14α, 17α, 20R
c. 5α, 14α, 17α, 20S
d. 5α, 14β, 17β, 20S or 20R
Y= H, CH_3, C_2H_5

Rearranged Steranes

a. 13β, 17α, 20S
b. 13β, 17α, 20R
c. 13α, 17β, 20S or 20R
X= H, CH_3
Y= H, CH_3, C_2H_5

Triterpanes

a. 18α(H)-22,29,30-Trisnorhopane
b. 17α(H)-22,29,30-Trisnorhopane
c. 17α(H), 21β(H) and 17β(H), 21α(H) 22S or 22R
Y= H, CH_3, C_2H_5.....C_8H_{17}

Fig. 2. Stereochemistry

3. Identification of nickel porphyrins

The crude oil contains 25.8 ppm. Ni and 0.9 ppm. V. After demetallization by methylsulfonic acid, porphyrin series of ETIO C_{28}-C_{36}, DPEP C_{28}-C_{36} and DiDPEP C_{34}-C_{37} has been identified by LVMS.

SUMMARY AND CONCLUSIONS

Group analysis of Yangsanmu crude oil was made by mass spectrometry and the steranes and triterpanes have been found in 450-500°C fraction by GC/MS/C. None of n-paraffins was discovered in crude oil. More than 20 regular and 16 rearranged steranes of C_{27}-C_{31} range and 18 triterpanes of C_{27}-C_{35} range have been identified. Due to the low vanadium content, only nickel porphyrins of DPEP, ETIO and DiDPEP series have been detected. Conclusion can be made that Yangsanmu crude oil is a less maturated, high degraded naphthenic oil with low sulfur content.

LITERATURE

1. Gallegos, E.J., GC/MS/C Analysis of Yangsanmu crude oil, (unpublished)
2. Mulheirn, L.J. and Ryback, G., Nature, 256, 301 (1975)
3. Seifert, W.K. and Moldowan, J.M., Geochim. Cosmochim. Acta, 42, 77 and 473 (1978), 43, 111 (1979)
4. Seifert, W.K. and Moldowan, J.M., 10th World Petroleum Congress, Vol. 2, 425 (1979) etc.

THE EFFECT OF MULTIPLE COLLISIONS ON THE COLLISIONALLY ACTIVATED DECOMPOSITIONS OF GASEOUS IONS. P. J. TODD AND F. W. MCLAFFERTY; Dept. of Chem., Cornell Univ., Ithaca, NY 14853.

Multiple collisions can provide a simple and predictable way to vary the energy transferred by collision to an ion of high kinetic energy. For CH_4^+ precursor ions of 10 keV energy a high collision-gas pressure (8.5% transmittance of CH_4^+) produces a CA spectrum indicating a collisional energy transfer equivalent to that from 64 keV CH_4^+ ions under single collision conditions, reflecting the 3.6 (weighted average) collisions at the high pressure. Equations are derived to explain the effect of collision gas pressure on CA product ion yield. Doubling the ion kinetic energy decreases the collisional loss cross-section by ~30% while increasing the collisional activation cross-section by ~5%. Multiple collisions should be particularly important for obtaining characteristic CA spectra of high-mass ions.

The full paper is scheduled for publication in Int. J. Mass Spectrom. Ion Phys., 38, 371-378 (1981).

DETERMINATION OF RADICAL ISOMERIZATION RATES USING MS/MS

C. N. McEwen and M. A. Rudat
E. I. Du Pont de Nemours & Co.
Central Research & Development Department
Wilmington, DE 19898

Intramolecular radical isomerization by H atom transfer has been known for some time[1], has found synthetic utility[2], and has been proposed as a mechanism for branching in certain polymers.[3] The rates for 1-4 and 1-5 secondary to primary intramolecular H atom migration (hereafter referred to as 5sp and 6sp isomerization, respectively) have been reported for gas phase pentyl[4] and hexyl[5] radicals. The reported rates are several orders of magnitude faster for these same H atom migrations in vibrationally excited alkyl radicals.[6]

The absolute rate of the 5sp isomerization in gas phase pentyl radicals can be estimated from the mass analyzed collisional activation spectrum of the tetracyanoquinodimethane (TCNQ) radical anions in which ·CN groups have been replaced by pentyl radicals[7], and from the calculated rate of capture of the pentyl radicals by TCNQ (i.e., ca. $10^2 s^{-1}$). The relative rates of the 6pp (H atom migration from a primary to a primary site through a 6-membered ring), 7pp, and 6sp isomerizations can be determined from primary radicals deuterated in the C-1 position and compared to the 5sp isomerization rate[8]. Propyl radicals do not isomerize under the conditions employed, ca. 14% of the primary butyl radicals isomerize through a 5pp process in 10^{-2}s, ca. 86% of primary pentyl radicals isomerize through 5sp and 6pp processes in a 0.4 to 1.0 ratio, and ca. 97% of primary hexyl radicals isomerize through 5sp, 6sp, and 7pp processes in a 0.05:1.0:0.3 ratio, respectively.

From the above data, the calculated absolute rates for the 5sp and 6sp processes at a 450° source temp. are $1 \times 10^2 s^{-1}$ and $2 \times 10^3 s^{-1}$ as compared to the literature values of $0.8 \times 10^2 s^{-1}$ [4] and $1.9 \times 10^3 s^{-1}$ [5], respectively at 450°. These values are ca. 1000X slower than the rates of H atom migration in vibrationally excited radicals[6], and suggests that the TCNQ trapped pentyl radicals have thermal energies. This is true only because the radicals, which are produced by alpha cleavage of ketone molecular ions deuterated on the alpha carbon atoms, generally have sufficient internal energy to fragment and are trapped by TCNQ as smaller radicals and mass rejected in the instrument. Of the primary pentyl radicals produced in the mass spectrometer ion source, greater than 90% undergo fragmentation before a stabilizing collision. Thus, high energy radicals are selectively removed by fragmentation and only those radicals with insufficient energy to fragment are analyzed using the mass selective CA technique.

The TCNQ trapped radical mass spectrum of C-1 deuterated pentyl radicals shows that over half of the pentyl radicals that fragment isomerize before fragmentation. If it is assumed that fragmentation must precede a stabilizing collision, then the rate of isomerization of the fragmenting radicals is in the range reported for vibrationally excited radicals.[6]

1) A. Kossiakoff and F. O. Rice, J. Am. Chem. Soc., 65, 590 (1943).
2) D. H. R. Barton and L. R. Morgan, J. Chem. Soc., 622 (1962).
3) V. B. Sefton and D. J. LeRoy, Can. J. Chem., 34, 41 (1956).
4) L. Endrenyi and D. J. LeRoy, J. Phys. Chem., 70, 4081 (1966).
5) K. W. Watkins and L. A. Ostreko, ibid., 73, 2080 (1969).
6) E. A. Hardwidge, C. W. Larson, and B. S. Rabinowitch, J. Am. Chem. Soc., 92, 3278 (1970).
7) C. N. McEwen and M. A. Rudat, ibid., 101, 6470 (1979).
8) The CID spectra of the deuterium labeled radicals were obtained on a triple quadrupole mass spectrometer. Courtesy of Prof. D. F. Hunt.

ION ENERGETICS OF CO^+ BY TRIPLE QUADRUPOLE MASS SPECTROMETRY

R.K. Latven and C.G. Enke
Department of Chemistry
Michigan State University
East Lansing, MI 48824

It has been well established that ions can be induced to fragment upon collision with neutral gas molecules if the ions have translational energies on the order of tens of volts. The triple quadrupole mass spectrometer is ideally suited for studying not only the analytical applications of this phenomenon, but also its fundamental processes.

In this paper, data are presented which explore the relationships among electron energy, axial energy, and target gas pressure, and their effect on the collisionally activated decomposition of CO^+ as it is formed from the molecules CO, CO_2, methanol, acetaldehyde, and formic acid.

Figure 1 presents ion intensity vs. EI source electron energy for CO. The ionization probability curve for CO^+ from CO is seen on the left, and its MS/MS analog, the formation of C^+ through Ar CAD on CO^+, on the right. The curves are nearly identical. The collision cross-section parameter, σ, which is of the form $\sigma = -\ln[1 - I_f/(I_f+I_p)]$ is a function of the relative intensities I_p and I_f of the parent and fragment ions. The cross-section for the fragmentation of CO^+ from CO is seen to be nearly constant throughout the range of usable electron energies.

However, Figure 2 shows a similar experiment with CO_2 as the source of the CO^+ parent ion. In this case CO^+ at m/z = 28^+ is selected by the first mass filtering quadrupole. The cross-section is seen to be constant from -70eV to ca. -40eV; at electron energies less than -40eV a sharp attenuation in cross-section is observed. Since all other operating parameters remain constant, including the composition and structure of the selected ion, the only remaining factor which can influence the collision efficiency is the internal energy of the selected ion. Figure 3 shows cross-section results from CO and CO_2 as well as the other sources of CO^+ studied. It must be concluded that similar ions from unlike molecules possess differing amounts of internal energy, and this results in disparate collisional cross-sections.

Another parameter which affects the energetics of collision is the axial energy, i.e., the offset voltage between the ion source and the quadrupole rods of the collision cell. This effect has been studied for various parent ions, collision gas species, collision gas pressures and daughter fragments. If the CO^+ collision process is monitored by observing the fragment intensity versus axial energy, (V_{ax}), there exists a particular V_{ax} at which the ion intensity is a maximum. It is seen that this point, V^o_{ax}, is constant for a given CAD transition (for example $28^+ \rightarrow 16$) regardless of parent ion (Figures 6,7), CAD pressure, and target gas species (cf. V_{cm}, figures 4,5).

These data suggest that while the nature of the precursor molecule at a particular electron energy dictates the internal energy of the selected ion, the axial energy for maximum fragmentation is independent of source electron energy, and, in addition, is independent of the nature and pressure of the target gas.

The differences in the fragmentation cross-sections of the CO - CO_2 system has been used to mask CO_2 interference in the detection of CO in air when monitoring the $28^+ \rightarrow 12^+$ transition. In addition, these results have implications as to an additional mode of molecular characterization in quadrupole MS/MS, i.e., based on a process' electron energy cross-sectional signature, it may be possible to predict the structure of the molecule from which the selected ion arose.

This work was supported in part by grants from The Office of Naval Research and the National Institutes of Health.

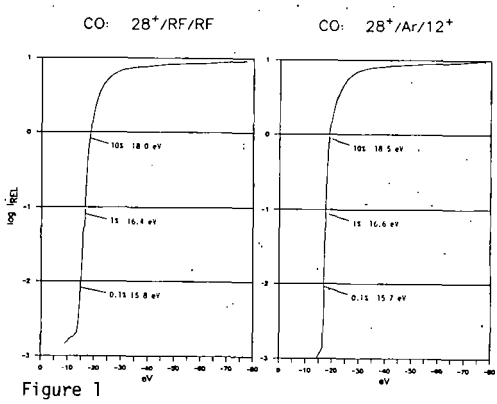

Figure 1

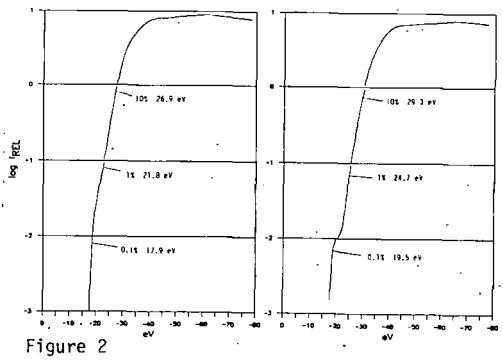

Figure 2

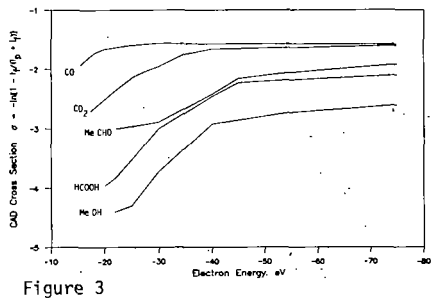

Figure 3

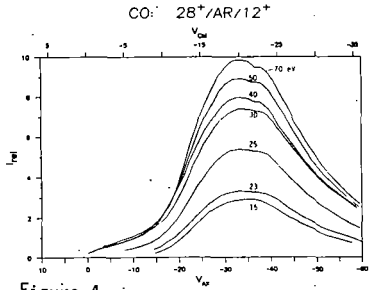

Figure 4

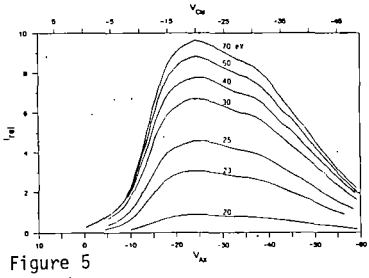

Figure 5

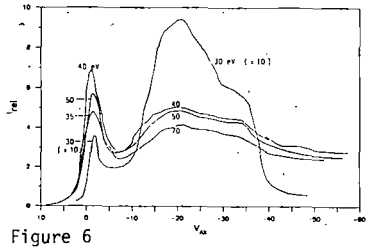

Figure 6

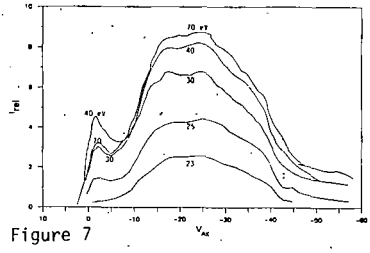

Figure 7

MULTIPLE DISSOCIATION REACTIONS IN A TRIPLE SECTOR MASS SPECTROMETER

D.J. BURINSKY and R.G. COOKS
DEPARTMENT OF CHEMISTRY
PURDUE UNIVERSITY
WEST LAFAYETTE, IN 47907

E.K. CHESS and M.L. GROSS
DEPARTMENT OF CHEMISTRY
UNIVERSITY OF NEBRASKA
LINCOLN, NE 68588

A triple analyzer mass spectrometer has the unique capability of unambiguously specifying the products of sequential gas-phase dissociation reactions. The resulting spectra are of high quality and compare extremely well with conventional ms/ms spectra. The utility of such a technique as applicable to the determination of complex mixtures was demonstrated through the analysis of model systems.

The experiments were performed on a triple sector mass spectrometer (Kratos MS50-T.A.) of the EBE configuration. The reaction sequence utilized for these experiments is illustrated in Figure 1, which also indicates the sequence of the analyzers and the three reaction regions of the instrument. In this study, ions emerging from the source were collisionally dissociated in the first reaction region. A specific fragment ion was then transmitted to the third reaction region by setting both the first electrostatic analyzer and the magnetic sector to the appropriate values. This ion was then itself collisionally dissociated with mass analysis of the resulting fragment ions being accomplished by scanning the second electric sector.

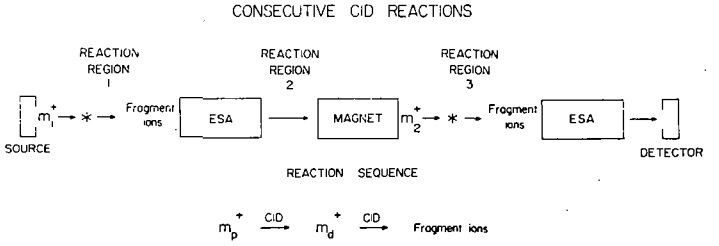

FIGURE 1. Schematic Representation of the Reaction Sequence Used for the Described Experiments

The general method was tested with several compounds including n-hexane, n-decane, 2-pentanone, and 3-methyl-2-butanone. In all cases the ions of interest gave very favorable agreement in their fragment ion spectra regardless of the location of the formation of the parent ion (ion source vs. first reaction region). This point is illustrated in Figure 2 which shows the collision-induced dissociation spectra of $C_5H_{11}^+$ ions (m/z 71) originating in each of the two previously mentioned regions.

The existence of structural isomers is a particularly difficult problem in the analysis of complex mixtures by ms/ms. However, it is possible through the use of consecutive dissociations to differentiate, for example, between the molecular ion of one mixture constituent and an isomeric fragment of another. Consider a mixture of o-cresol and benzyl acetate with the cresol present in a 30-fold excess. Since both compounds exhibit ions in their respective mass spectra at m/z 108 ($C_7H_8O^{+\cdot}$) a conventional ms/ms spectrum with ion m/z 108 as the parent would yield the sum of what under normal circumstances would be two quite distinct spectra. As illustrated in Figure 3, a quite reasonable daughter ion spectrum of even a very minor isomeric constituent (benzyl acetate in the present case) can be obtained by utilizing the consecutive collision capability.

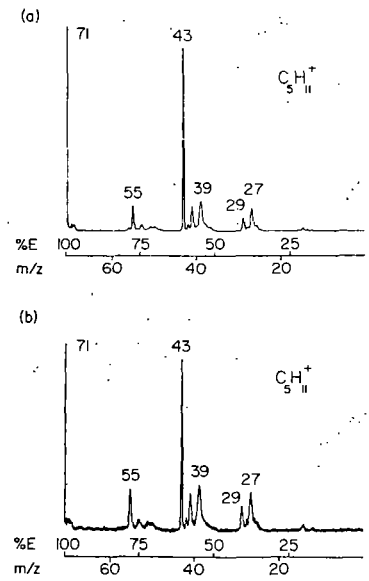

FIGURE 2. CID Spectra of (a) the 71+ Ion of n-Hexane Formed in the Source, and (b) the 71+ Ion of n-Hexane Formed in a Prior High Energy Collision.

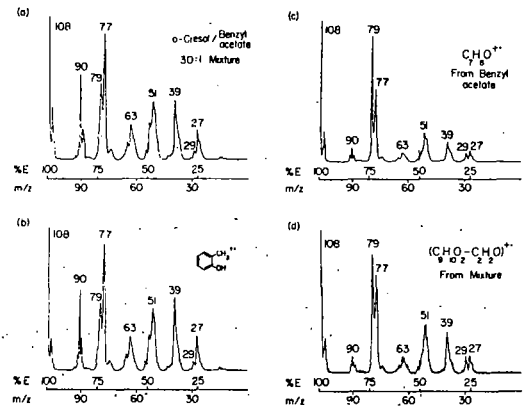

FIGURE 3. CID Spectra of (a) the 108+· Ion Formed in the Source From a 30:1 o-Cresol/Benzyl acetate Mixture, (b) the Molecular Ion of o-Cresol, m/z 108, (c) the 108+· Ion Formed in the Source From Benzyl acetate, and (d) the 108+· Ion Produced by Prior Collision of the Molecular Ion of Benzyl acetate.

The ms/ms technique evolved from conventional mass spectrometry in response to demands of such problems as ion structure determination and complex mixture analysis. The present study appears to demonstrate a useful role for increasing the complexity of mass spectral analysis, viz from ms to ms/ms to consecutive collision-induced dissociation reactions (ms/ms/ms).

STUDIES USING TANDEM QUADRUPOLE MASS SPECTROMETRY; Donald F. Hunt, Anne B. Giordani, Jeffrey Shabanowitz, and Gerald Rhodes; Dept. of Chem, Univ. of Virginia, Charlottesville, VA. 22901

We have completed a variety of studies, including both mixture analysis and ion structure analysis applications of the MS/MS technique, using Tandem Quadrupole Mass Spectrometry. The versatility of our quadrupole instrumentation has been thoroughly exploited. Operational modes which enable selective detection of collisionally activated decomposition (CAD) fragment ions, selective detection of all precursors to a particular CAD fragment ion, or selective detection of all ions which lose a particular neutral in their CAD spectrum, have been used to solve the different problems of analysis encountered in this work.

It was previously demonstrated that neutral loss (eg. 44 amu--loss of CO_2) scanning provides a MS/MS method for the selective detection of carboxylic acid components in a complex mixture such as urine.[1] Our data suggests that metabolic profiling of urinary carboxylic acid compounds using Tandem Quadrupole Mass Spectrometry compares favourably to GC/MS methodology in numbers of peaks which can be quantitated, and in median relative standard deviation values. Quantitation of individual carboxylic acid components using our Tandem Quadrupole Mass Spectrometric methodology agrees well with literature values determined using GC/MS methodology. Reasonably, exceptions are carboxylic acid compounds which are of the same molecular weight as other common urinary carboxylic acids, or compounds whose CAD mass spectra show unusual intensity for the CAD fragment ion which has undergone the neutral loss empolyed to detect these compounds.

In contrast to GC/MS, the MS/MS methodology does not require separation of the organic acid fraction from the urine, derivativization, or GC separation of the mixture components. Elimination of these steps results in a considerable time savings. Derivativization often introduces artifacts into the analysis and procedures used to separate the organic acid fraction from the urine matrix are either very time consuming, or limit the quantitative potential of the analysis. In all, the Tandem Quadrupole Mass Spec methodology investigated here meets the need for a semi-quantitative metabolic profiling technique which is rapid enough to handle large numbers of samples.

A syndrome suggestive of toxicity due to the absorption of polyethylene glycol was observed in certain patients treated at the UVa Burn Center.[2] These patients were all treated with a topical antimicrobial cream containing nitrofurazone in a polyethylene glycol base (Furacin Soluble Dressing, Norwich-Eaton Pharmaceuticals, Norwich, NY 13815). Polyglycols (I) and products of the oxidative metabolism of polyglycols (II and III) were selectively detected in both urine and deproteinated serum of a patient exhibiting this syndrome using Tandem Quadrupole Mass Spectrometry. Fifteen microlitres of urine or serum was acidified with dilute H_2SO_4, and pumped to dryness in a melting point capillary tube. The tip of the tube, containing the sample residue, was inserted directly into the ion source of the mass spectrometer by means of the solids probe. While the sample was heated, and ionized by OH^- CI reactant ions, polyglycols were detected as precursor ions of m/z 61$^-$ (IV) and polyglycolic acids were detected as precursors of m/z 75$^-$(V) in the N_2 CAD mass spectrum. The mixed alcohol/acids appeared as precursors of both fragment ions. CAD mass spectra of reference compounds suggests that neutral loss scanning will provide another method to selectively detect these compounds in urine and serum.

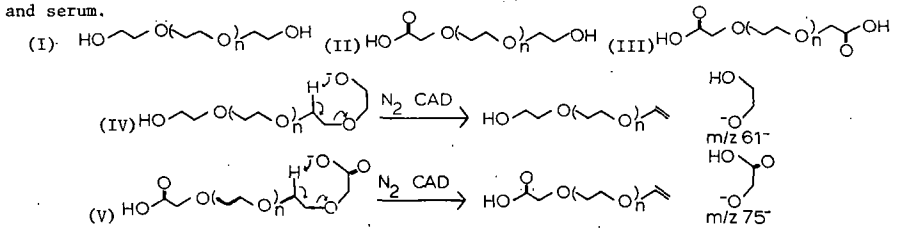

[1] D. F. Hunt, J. Shabanowitz and A. B. Giordani, paper RAMOA8, 28th Annual Conference on Mass Spectrometry and Allied Topics, New York, N. Y., May 25-30, 1980.

[2] D. A. Herold, D. E. Bruns, D. Spyker, G. T. Rodeheaver, and R. F. Edlich, 13th Annual Meeting of the American Burn Association, Washington, D. C., April 2-4, 1981.

In the course of developing MS/MS methodology for selective detection of carboxylic acids in complex mixtures, CAD mass spectra of the $(M-1)^-$ ions have been obtained for 90 different carboxylic acid compounds. Loss of stable neutral molecules is the chief fragmentation pathway observed for both aliphatic and aromatic carboxylic acids. The most common neutral losses observed are: 44 amu (loss of CO_2; observed in reference CAD mass spectra of 68 of the compounds studied), 18 amu (loss of H_2O; 25 carboxylic acids), 46 amu (loss of HCO_2H; 13 carboxylic acids); 28 amu (loss of CO; 8 carboxylic acids), 90 amu (loss of CO_2 and HCO_2H; 6 carboxylic acids), 72 amu (loss of CO and CO_2; 6 carboxylic acids), 80 amu (loss of CO_2 and $2H_2O$; 3 carboxylic acids.

Certain carboxylic acid anions fragment, under CAD conditions, only to a very small extent--the selected ion carries more than 95% of the total ion current in the CAD spectrum. These include monofunctional aliphatic carboxylic acids (eg. pentanoic, heptanoic), low molecular weight α-keto carboxylic acids, and structures which, other than the carboxylic acid moiety, do not contain a site able to stabilize a negative charge, or structures in which such a site is remote from the acid anion (eg. hydrocinnamic acid). With few exceptions, carbon dioxide loss is the major fragmentation pathway for aromatic carboxylic acids.[3] Aliphatic carboxylic acids also show the loss of 44 amu, but the losses of 62 amu, or 80 amu are more important for many of the hydroxy acids, or diacids longer than five carbons. Lower molecular weight α-keto carboxylic acids lose CO, although only weakly. Phenyl pyruvic acids favour the loss of 72 amu. The loss of 46 amu is observed for aliphatic-type hydroxy carboxylic acids, eg. 2-hydroxy-4-methylpentanoic acid. Loss of 90 amu is observed for diacids containing seven or more carbons, and small, polyhydroxy dicarboxylic acids.

Collisionally activated ion-molecule isotope exchange reactions are observed when D_2O or MeOD is used as collision gas in the quadrupole collision chamber of the Tandem Quadrupole Mass Spectrometer. In a complex mixture, chemical ionization deuterium exchange methods have limited utility for determining the structure of an ion because background ions may interfere, or obscure the ions having deuterium incorporation.

The proposed mechanism for deuterium exchange in the collision chamber is the same as for the CI methodology,[4] with qualifications: protons on polyfunctional molecules which are involved in intramolecular hydrogen bonds undergo exchange only slowly. Exchange is not observed for protons on sites far removed from the anionic site. Examples are illustrated below:

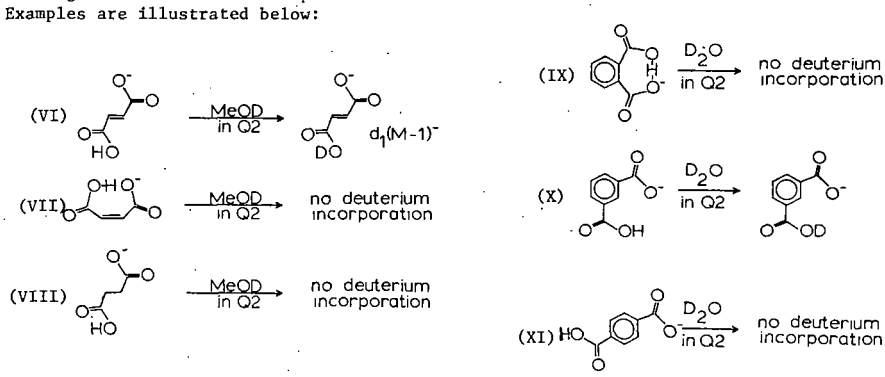

The trans configuration of the fumaric acid anion (VI) prevents formation of an intramolecular hydrogen bond, so deuterium exchange in Q2 is observed, unlike for maleic (VII) or succinic (VIII) acids. Exchange is not observed for phthalic acid anion (IX), again probably due to intramolecular hydrogen bonding. Exchange is not observed for the para positional isomer, terephthalic acid (XI), due to the distance between the anionic site and the remaining proton. Thus exchange is only observed for isophthalic acid (X).

The studies discussed here provide further illustration of the usefulness of the MS/MS technique, in particular Tandem Quadrupole Mass Spectrometry, for mixture analysis and ion structure analysis problems.

[3] G. A. McClusky, R. W. Kondrat, and R. G. Cooks, J. Am. Chem. Soc., 100, 6045-51 (1978).

[4] D. F. Hunt and S. K. Sethi, J. Am. Chem. Soc., 102, 6953-63 (1980).

THIS PAGE LEFT
INTENTIONALLY BLANK

DESCRIPTION AND APPLICATIONS OF A HYBRID MS/MS INSTRUMENT OF BQQ DESIGN

G. L. GLISH
Oak Ridge National Laboratory
Box Y, Building 9735
Oak Ridge, Tennessee 37830

S. A. McLUCKEY and R. G. COOKS
Department of Chemistry
Purdue University
West Lafayette, Indiana 47907

A hybrid instrument for MS/MS applications has been built. It consists of a magnetic sector (B) and two quadrupole mass analyzers (Q). In its basic configuration it is run as a BQQ (shown in Figure 1) with the first quadrupole being used in the rf only mode as a collision chamber. Some advantages of this design are moderate precursor ion resolution (up to ∿5000), unit mass resolution of the daughter ions and the ability to vary the collision energy.

The typical operating scheme is as follows: ion formation (EI or CI), extraction, acceleration to 10,000 eV, momentum analysis (B), deceleration (variable, but typically to between 10 - 100 eV), collision in rf quadrupole, mass analysis in the second quadrupole and then detection. Using argon as the sample and electron impact ionization, a 11 nanoamp beam was measured for 40^+ following momentum analysis at 10,000 eV and deceleration to 20 eV. With both quadrupoles in the rf only mode a final beam current of 10 nanoamps was measured and with the second quadrupole in the mass analysis mode, a current of 1.5 nanoamps was measured at the detector.

The variability of the precursor ion axial energy and its effect upon collision spectra has proven to be quite useful. In fact, variation of the precursor ion energy provides, in essence, another resolution element, internal energy selection in the collision process. This is analogous to the high energy angle-resolved technique[1] and while variation of the ion axial energy at kilovolt energies has some effect on the resulting spectra, it is no where near as drastic as the changes seen in the low energy (1 - 100 eV) collisions in the BQQ.

One application of the variation of ion axial energy is the differentiation of isomers. Figure 2 shows plots of the relative abundance of $C_3H_4^+$ from allene and propyne, vs. axial energy. As can be seen, they are quite different, indicating different ion structure. Figure 3 shows similar plots for the $C_3H_3^+$ ions obtained from the same compounds. Here the plots are almost identical, indicating that the fragmentation is occuring from a common structure.

One of the design criteria of the instrument was modularity so that changes in configuration could be easily achieved. One such change is the switching of the source and detector. Preliminary data has been obtained in the QB configuration.

[1]J. A. Laramee, P. H. Hemberger, and R. G. Cooks, J. Am. Chem. Soc., 101, 6460 (1979).

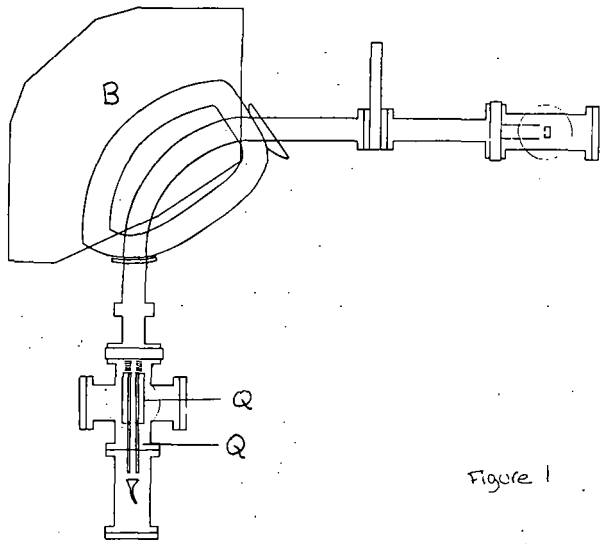

Figure 1

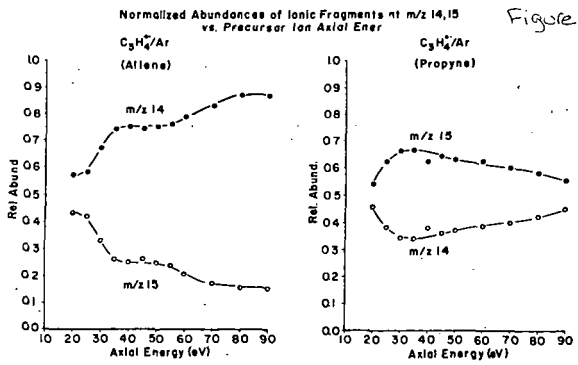

Figure 2

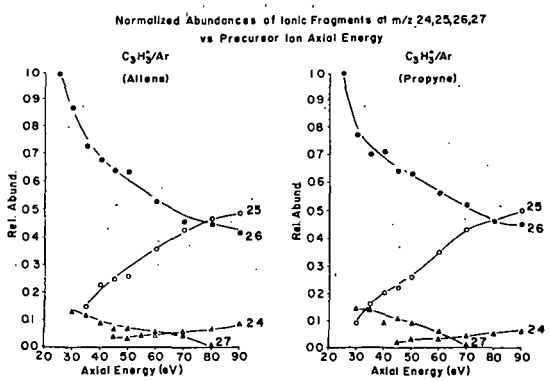

Figure 3

An Atmospheric Pressure Ionization MS/MS and Its Applications

V. Caldecourt, D. Zakett, J. Tou
Analytical Laboratories
Michigan Division
Dow Chemical Company
Midland, MI 48640

Continuing development in atmospheric pressure ionization mass spectrometry (API MS) has focussed on improved ion efficiency so as to reach even lower detection limits and on methods such as MS/MS (1) to identify the constituents detected. The present paper discusses the performance and applications of an API MS/MS (Fig. 1) system designed with the above two goals in mind.

A diagram of the API source is shown in Figure 2. Ionization is produced by a corona discharge formed at the tip of a 7 mil diameter Ir wire. The wire is not ground to a point, but operates with the rounded tip produced by sputtering. The current is limited to about 3 μA by a 1000 megohm resistor in series with 5 KV D.C. With the 4 mil entrance aperture, several months of operation are attained before cleaning. The ion source incorporates a declustering chamber of the type described by H. Kambara et al. (2) with about a factor of five greater ion output. V_A-V_B is normally 15v unless fragmentation is desired. The entire source is insulated from ground with the 13 mil exit aperture at +75v to ground.

The current delivered by the ion source is measured by using quadrupole, Q1, as a Faraday cup. At V_A-V_B of 15v the ion current (5×10^{-10}A) to Q1 is approximately 10% of the ion current entering the 4 mil aperture. As the voltage V_B-V_{Q1} is reduced the current collected by Q1 decreases becoming nearly zero (Fig. 3) at -0.4v. This shows the multiple collisions have reduced the energy spread of the ions and the 13 mil exit aperture potential, 75v, can serve as a reference point in measuring the energy of the ions.

When an ion m/e 153 selected by Q1 is fragmented in Q2 at 10^{-3} Torr and then the fragment ion at m/e 94 is selected by Q3, the maximum ion intensity occurs at an ion energy of 10 ev. The lower curve in Figure 4 illustrates the ion intensity vs. ion energy without RF applied to Q2. The upper curve shows the plot of the ion intensity vs. ion energy with RF applied. Thus, the utility of the instrument to investigate higher energy collisions is significantly reduced.

The ion transmission of Q2 was found to be a complex function of the applied RF voltage, particularly if the ion energy is such the ion is subject to less than 10 cycles of RF voltage in traveling through the quadrupole. Possibly the performance with more energetic ions could be improved by using a longer quadrupole at Q2, but the maxima may be caused by the particular geometry used.

Two applications of the API MS/MS system to analyze odors are presented.
First is the odor observed in the headspace above some organophosphorothioate crystals. The second is the odor emitted from the waxy material produced upon oxidative pyrolysis of polyethylene. In both cases a complex spectrum results in which collision activated decomposition, CAD, in Q2 aid in the identifications.

The spectrum of the vapor above the organophosphorothioate crystals is given at the top of Figure 5. Groups of peaks are observed from mass 129 to over 215 which could be divided into two sequences with 14 amu intervals, suggesting two series of homologous compounds yielding quasi-molecular ions at m/e 185, 199, etc. and 155, 169, etc. The CAD spectrum of the ion at m/e 185 from the sample is in the lower left hand side of Figure 5.

The consecutive losses of 28 amu indicate the presence of two ethyl groups. Based on this information and the chemistry involved, the structure was proposed to be O-methyl O,O-diethyl phosphorothioate and this assignment was further confirmed by the odor and the CAD spectrum of a standard of this compound. The concentration in the headspace was determined to be 0.5 ppm. The homologous series are proposed to be methylated and ethylated phosphorothioates and phosphates from additional CAD spectra.

The spectrum of the vapor from the waxy material formed by oxidative pyrolysis of polyethylene was more complex and appeared to contain many isomers. Additional details will be forthcoming in a future publication.

References

1. R. A. Yost, C. G. Enke, D. C. McGilvery, D. Smith, J. D. Morrison, Int. J. Mass Spectrom. don Physics, 30, 127-136 (1979).

2. H. Kambara and I. Kanomata, Anal. Chem., 49, 270 (1977).

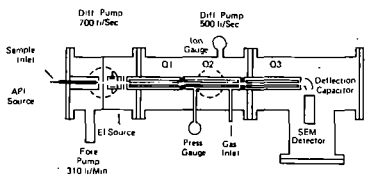

Fig. 1

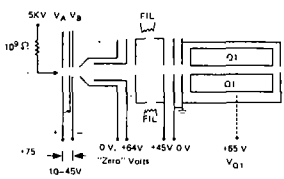

Fig. 2

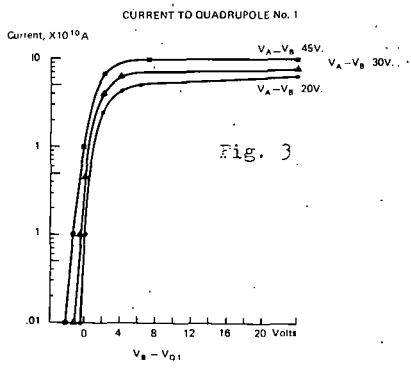

Fig. 3

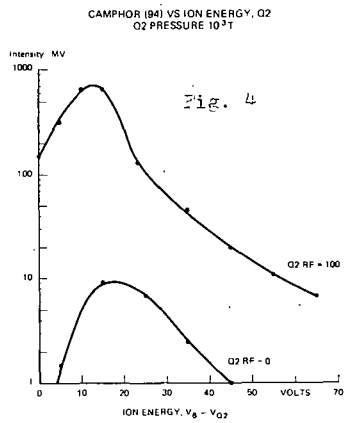

Fig. 4

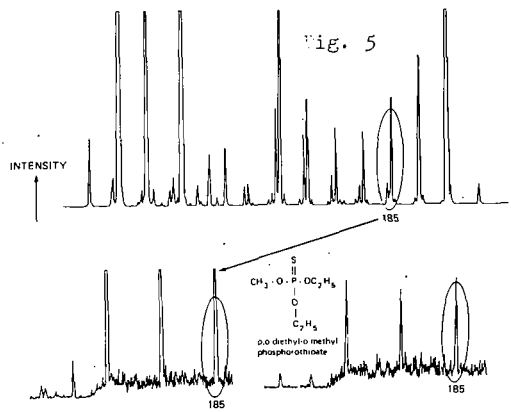

Fig. 5

AN INTEGRATED APPROACH TO THE RAPID SCREENING OF TRACE COMPONENTS IN COMPLEX MIXTURES BY MS/MS; W.R. Davidson, J. Fulford, N.M. Reid, T. Sakuma, B. Shushan and B.A. Thomson. SCIEX INC., 55 Glencameron Rd., Thornhill, Ontario, Canada. L3T 1P2.

Introduction

One of the advantages of MS/MS lies in the ability to reduce analysis time while retaining high specificity by rapidly screening complex mixtures for the presence of targeted compounds or compound classes. Although the potential of the technique has probably not yet been fully explored, it is apparent that large gains in efficiency can be expected if the system is designed to allow rapid and easy introduction of different types of samples in a semi-routine or routine manner. The samples may be solids, liquids or gases, with the compounds of interest contained in matrices of varying complexity. Inlets must either be designed with some flexibility, to be able to be adapted to the situation at hand, or a variety of specialized inlets must be available. An analytical routine might require, for example, that a batch of samples be first screened by direct probe (in the case of solids or involatile liquids) or by direct purge (in the case of volatiles in liquids), followed by a rapid cleanup or extraction of a small subset of these, with further analysis either by direct probe again, or by GC/MS/MS or LC/MS/MS.

Instrumentally, this requires an ion source into which samples can easily be introduced, and which exhibits little or no memory effect or contamination problems (particularly important because of the crude or raw samples which may now be introduced directly). In addition, exchange of the inlet systems must be fast and easy, allowing the operator to move from the direct probe to the GC to direct air sampling to purge and trap to pyrolisis probe, etc. This feature will also be of help to those laboratories which desire to use the instrument for a variety of applications in order to justify acquisition of such a sophisticated system.

The number of analysis modes which are possible with an MS/MS system make it important in addition to have all instrumental and data collection parameters under software control. Analytical protocols may require a sample to be analyzed by rapidly performing various combinations of single MS scans (for sample characterization), daughter ion scans, multiple ion monitoring of parents and daughters, constant neutral loss scans or constant daughter ion scans. Each mode requires different hardware and data collection parameters which must be able to be set automatically. The large volume of data which can be generated calls for a variety of specialized data collection, display and manipulation routines. Thus, to make the MS/MS a useful laboratory analytical tool, and to provide maximum utilization of its sensitivity, selectivity and speed, a complete instrumental approach is required, extending from inlets to ion sources to mass spectrometers to detectors to data systems.

Experimental

The TAGA™ 6000 is a triple quadrupole mass spectrometer system which is described in more detail in Paper RPB18. The ion source of most general applicability is an Atmospheric Pressure Chemical Ionization source which combines the sensitivity of atmospheric pressure chemical ionization with an ion source design which allows crude or dirty liquids (e.g., water, urine, organic extracts), solids (e.g., soil) or gases (e.g., air, breath, stack gas) to be introduced directly, with minimal contamination problems. The APCI source couples to a variety of inlet systems which are rapidly demountable, including a direct insertion probe, a gas chromatograph, a direct air inlet system, a short-term adsorber system and a breath analysis system. In addition, development of a liquid ion evaporation source for gentle ionization of labile compounds is underway (Paper RPM0A4), and a low pressure chemical ionization source for direct air analysis is being explored (Paper RPB13).

The system is operated under complete digital control by a PDP 11/23 minicomputer. Special data collection and display routines allow keyboard control and switching among seven possible operation modes.

Results

The examples presented are chosen to represent the variety of sample types, inlets and operational modes.

Figure 1 shows a sample (an extract of a bacterial culture) which was essentially unknown, and which was first characterized by placing a small aliquot on the direct insertion probe and heating it while scanning Q1 with Q3 in the RF-only mode. This produces a mass spectrum showing all components of the sample which react by charge transfer with the $C_6H_6^+$ reagent ions. From this spectrum, peaks of interest were chosen and the parent ions fragmented to produce characteristic daughter ion spectra. The example shown in Figure 1b is the CID spectrum of the ion at m/z=290 (a small peak in the single MS spectrum of Figure 1a). The successive loss of chlorine atoms (m/z=35) shown by the spectrum allowed the compound to be identified as tetrachlorobiphenyl, apparently a metabolite of 3,4-dichloroaniline which was added to the original bacterial culture.

Figures 2a and 2b show respectively the CID spectrum of the parent ion of m/z=178 from a crude extract of Athabasca Tar Sands oil introduced directly on the solid probe (again with $C_6H_6^+$ CI), and a reference spectrum of anthracene. Agreement is good, but the differentiation of anthracene from phenanthrene (which has the same molecular weight) has not been explored, and may in fact require the use of GC/MS or GC/MS/MS to resolve.

An example of targeted compound analysis performed by multiple ion monitoring is shown in Figure 3. A fast one step extraction of peanuts was carried out, and the extract placed on the probe and thermally desorbed in a pulse of several seconds duration. By transmitting the parent ion of aflatoxin with Q1, and rapidly monitoring the characteristic daughter ions with Q3, the compound was detected and compared with a standard spiked in the same matrix. Daughter ion intensity ratios compared very well with the standard, providing, along with the daughter ion masses, positive identification of aflatoxin B_1.

Conclusion

Performance of the MS/MS as a useful analytical tool is closely linked with the performance of the data system and sample introduction systems. Atmosphere pressure chemical ionization allows rapid sample introduction and analysis by direct probe (screening of samples at rate of more than one per minute), easy changeover from one inlet system to another, and minimal source contamination problems. Large or small amounts of crude samples can be introduced directly. Complete digital control of all instrumental and hardware parameters is necessary to allow accuracy and precision in the variety of operational modes which are possible, and to allow efficient collection and manipulation of the data which is collected. A fully integrated system will provide qualitative and quantitative analysis at trace levels in applications ranging from rapid screening to full identification of isomeric compounds by GC/MS or GC/MS/MS.

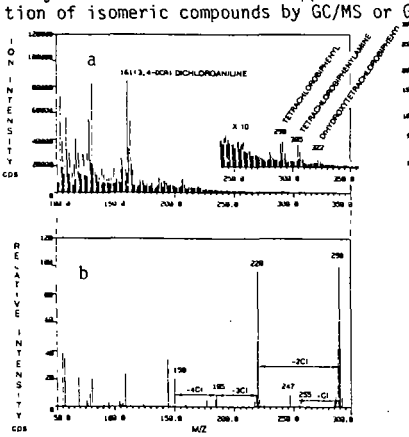

Figure 1. a) Benzene CI mass spectrum of an extract of E. Coli after metabolism of 3,4-dichloroaniline; b) CID spectrum of the parent ion of m/z=290, identified by the successive losses of chlorine as tetrachlorobiphenyl.

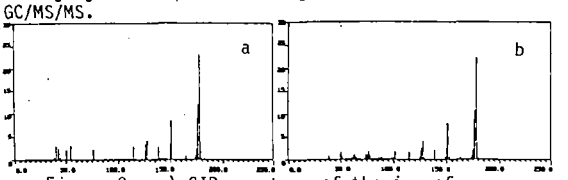

Figure 2. a) CID spectrum of the ion of mass 178 from an extract of Athabasca Tar Sands oil; b) Reference CID spectrum of anthracene.

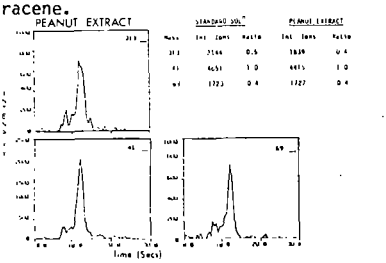

Figure 3. Multiple ion monitoring of the parent MH^+ (m/z=313) and two daughter ions (m/z=41 and 69) from aflatoxin B_1 in a peanut extract.

DIRECT ANALYSIS OF COMPLEX ENVIRONMENTAL MATRICES FOR PRIORITY POLLUTANTS BY TRIPLE QUADRUPOLE MASS SPECTROMETRY; T. MICHAEL HARVEY, DONALD F. HUNT, JEFFREY SHABANOWITZ; HARVEY LABORATORIES INC., P.O. Box 5323, Charlottesville, VA 22905

We describe here a systematic approach for direct analysis of complex environmental matrices for priority pollutants by triple quadrupole mass spectrometry. The method involves both chemical derivatization and functional group analysis using collision activated dissociation techniques.

When applied to industrial sludge, the protocol first requires the sample to be freeze dried, producing a fibrous residue. A portion of this sample is then treated with reagents to convert phenols to their carbamates. Polynuclear aromatic hydrocarbons are subsequently converted to mono and/or dinitro derivatives. The sample is then thermally desorbed directly into the ion source of the triple quadrupole which in turn is operating in a three scan sequence. Positive ion chemical ionization using isobutane as the reagent gas produces $M+H^+$ ions for phthalates, carbamates, and nitroaromatics. Collision activated dissociation of these $M+H^+$ ions in Q2 produces abundant fragment ions at M+H-17 for nitroaromatics, M+H-57 for carbamates, and m/z 149 for phthalates. A three scan sequence including a linked scan for loss of 17, a linked scan for loss of 57, and a precursor ion scan for m/z 149 (2 second cycle time) is performed during the thermal desorption. This allows all three classes to be determined from the same sample at the 100 ppb level with a high degree of specificity. Totalanalysis time, excluding the freeze drying step, is 15 min. In addition, this approach allows other members of each class not present on the Priority Pollutant list to be identified and their concentrations estimated.

Additional preliminary results suggest these techniques can be applied to an even larger fraction of the Priority Pollutants.

A CURIE-POINT MS/MS SYSTEM FOR ANALYSIS OF BIOMATERIALS AND FOSSIL FUELS

Henk L. C. Meuzelaar, William H. McClennen, Gary S. Metcalf and George R. Hill; Biomaterials Profiling Center, University of Utah, Salt Lake City, Utah 84108.

When subjected to analytical or industrial pyrolysis procedures, complex organic materials, such as found in biopolymers, body fluids, cells, tissues, coals or shales, usually produce extremely complex mixtures of pyrolysis products. Detailed analysis of such mixtures, containing compounds which vary widely in molecular size, polarity and stability presents a major challenge. This is especially true when total sample amounts are in the microgram range or when reaction products are only available for a few seconds such as in most pyrolysis mass spectrometry (Py-MS) experiments. An Extranuclear 1-5000-1 Curie-point Py-MS system was converted into a Py-MS/MS system by simply exchanging the quadrupole head for a double head with collision cell and vacuum envelope extension and installing a second quadrupole hf power supply, a scan control unit and a collision cell voltage control unit. The special MS/MS quadrupole head was similar to that described by Siegel (*Anal. Chem. 52*, 1790, 1980). No additional vacuum pumping was required as ion source pressures in the 10^{-5} Torr range were maintained by the single 400 ℓ/s oil diffusion pump when optimum collision chamber pressures of approx. 10^{-2} Torr were reached using HE as collision gas. Typical collision energies were between 15 and 30 eV with the lower value representing initial ion energy and the upper value the maximum ion energy obtained with additional 15 eV acceleration in the ferrite collision chamber. Satisfactory CID spectra were obtained from submicrogram quantities of compounds produced by Curie-point pyrolysis of nonvolatile materials or Curie-point desorption of relatively volatile samples.

Usually all or most peaks in the CID spectra of molecular ions can be found back in the 70 eV EI library spectra of the corresponding compound. However, the reverse is not necessarily true since the CID spectra are relatively simple. In fact, as shown in Figure 1, the CID spectra obtained under our conditions resemble low voltage EI spectra rather than 70 eV spectra.

Specific applications investigated thus far include detection of white blood cell nucleic acid components in .5 µl of whole blood, determination of drugs and metabolites in single drops of urine, identification of biological compounds in synthetic polymer implants after prolonged *in vivo* exposure, and characterization of minor oxygen compound series in coal hydroliquefaction fraction, as shown in Figure 2.

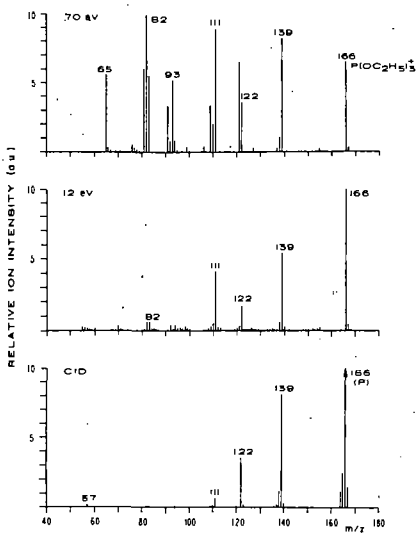

Figure 1. Comparison of 70 eV and 12 eV EI spectra of triethylphosphite with the CID spectrum of the molecular ion. The 12 eV spectrum represents a sample taken by head space sampling using a 510°C Curie-point filament coated with activated carbon, whereas the other two spectra were obtained in a direct probe mode. Estimated sample size is several micrograms. Note that the CID spectrum resembles the low voltage EI spectrum much more closely than the regular 70 eV spectrum. For CID conditions see text.

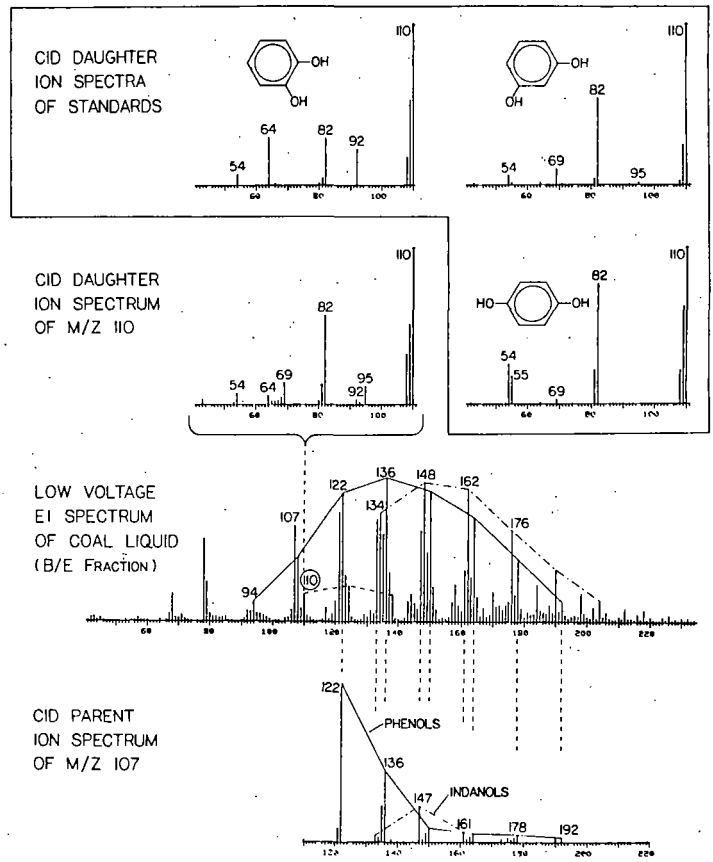

Figure 2. Use of CID techniques for identification of individual compounds as well as compound series in a complex coal liquid (benzene ether fraction of EDS Raw Solvent). The Low Voltage (12 eV) EI spectrum is dominated by two homologous series of molecular ions known to represent alkylphenols and alkylindanols respectively (for a more detailed account see: Meuzelaar *et al. Fuel*, in press). Note that the CID spectrum of m/z 110 indicates the presence of metadihydroxybenzene (m/z 64!) whereas no obvious contribution of paradihydroxybenzene is observed, as judged by the intensity of the ion signal at m/z 55. The single daughter ion scan at m/z 107 highlights the alkylphenol molecular ion series (especially with regard to the contribution of n-alkylphenols) although a contribution of alkylindanol fragment ions is also found. The Low Voltage EI spectrum was obtained by flash vaporization of the coal liquid sample from a 510°C Curie-point filament, whereas the CID spectra were obtained in a direct probe mode. For CID conditions: see Text.

SIMS + MS/MS = SIMS/MS*

G. L. GLISH and P. J. TODD
Analytical Chemistry Division
Oak Ridge National Laboratory
Oak Ridge, Tennessee 37830

Secondary ion mass spectrometry (SIMS) has proven to be a very useful method for generating ions from involatile organic compounds. Mass spectrometry/mass spectrometry (MS/MS) has shown itself to be a technique of particular value for the determination of gas phase ion structures. We report here our initial investigation into the combination of these two techniques.

A SIMS ion source, designed and constructed at ORNL, has been attached to a three sector (EBE) mass spectrometer. Secondary ions are formed by primary ion bombardment of a solid organic sample on a metal substrate. Typically, 1-5 keV argon ions are used. The ions formed are then extracted out of the source and accelerated to 10 keV. The desired precursor ion is then selected by the first two sectors. A collision gas is introduced between the second and third sectors by a hypodermic needle that is directed towards the throat of a 1500 l/sec pump. Collisions of the precursor ions here lead to daughter ions. Daughter ions thus formed are then mass analyzed by the second electric sector.

Figure 1 shows the SIMS/MS spectrum of tetramethylammonium ion, obtained from tetramethylammonium chloride. The two major fragments, loss of 28 and 30, correspond to the protonated dimethylamine ion and the methyl immonium ion. Figure 2 shows the SIMS/MS spectrum of the m/z 60 ion found in the tetramethylammonium chloride SIMS spectrum. The major daughter ions m/z 44 and 45 (loss of methane and methyl), as well as the rest of the spectrum, are exactly those which would be expected from protonated trimethylamine.

In Figure 3 the spectra of the dimethyl immonium ion formed via electron impact ionization (top) and SIMS (bottom) are shown. The only difference in these two spectra is the relative abundance of the fragment at m/z 30. This difference is due to the fact that m/z 30 in the top spectrum is predominately a metastable fragment, while only a collision induced fragment is observed from the SIMS generated ion.

MS/MS of SIMS generated ions is not limited to organics. Figure 4 shows an example of inorganic SIMS/MS spectrum. This spectrum of FeOH (from the stainless steel source), shows the two expected peaks, loss of H and loss of OH.

*Research sponsored by the U. S. Department of Energy, Division of Basic Energy Sciences, under Contract W-7405-eng-26 with the Union Carbide Corporation.

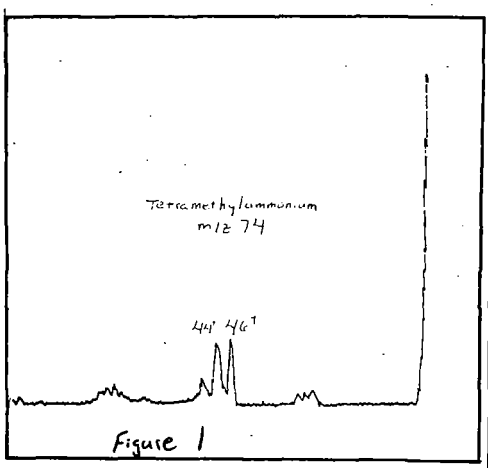

Figure 1

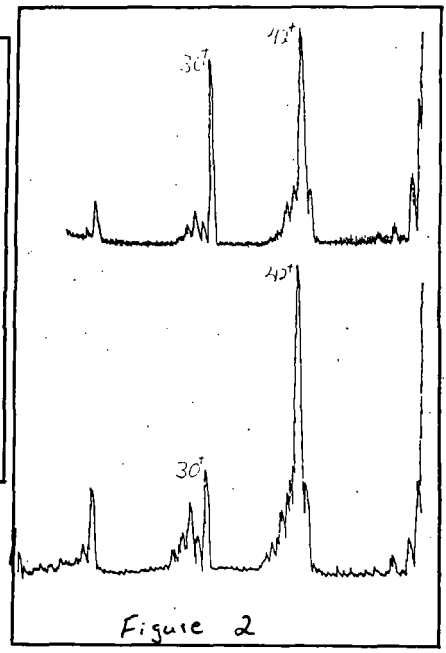

Figure 2

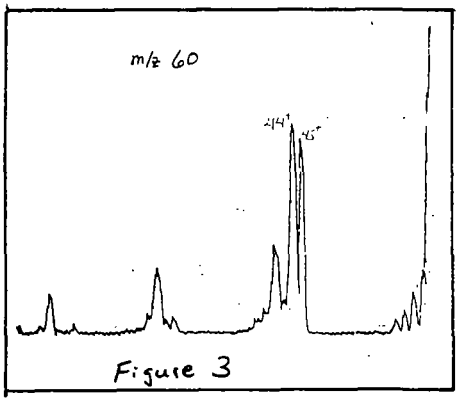

Figure 3

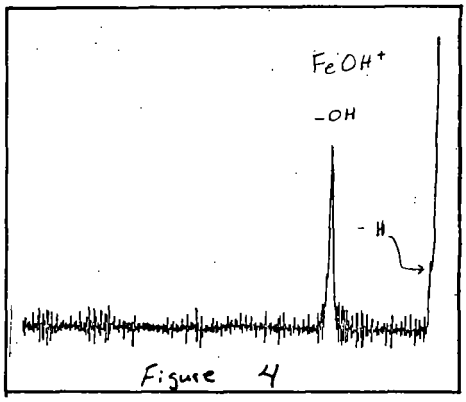

Figure 4

ATMOSPHERIC PRESSURE ION CLUSTERS

IDENTIFIED BY

COLLISION INDUCED DISSOCIATION

M.W. Siegel and H.H. Lo

Extranuclear Laboratories, Inc.
Pittsburgh, PA 15238

In atmospheric pressure ionization mass spectrometry[1] a carrier gas is ionized by high energy electrons, and a chain of ion-molecule reactions leads to a terminal distribution of reagent ions characteristic of the carrier gas. Ion-molecule and electron-capture reactions between this plasma and imbedded sample molecules results in preferential transfer of charge to appropriately vulnerable sample molecules; the preference often favors species of environmental and biological interest. Furthermore the atmospheric pressure plasma is itself an interesting object of study, the observations therein often being applicable to ion processes in the natural atmosphere.

The particular device we have employed is a 0.1-cm^3 ionization chamber with 1 mCi of ^{63}Ni on its cylindrical wall and a 40 μm sampling aperture at the end connecting it to the mass spectrometer vacuum. The vacuum system is divided by a differential pumping wall into a high pressure ($\approx 3 \times 10^{-4}$ torr) ion focusing region and a low pressure ($\approx 1 \times 10^{-6}$ torr) mass analysis region containing a quadrupole mass filter and a particle multiplier detector. This has recently been extended to include a second quadrupole, the two being joined by a collision cell made of a ferrite-ceramic material which shields the interior from the DC (resolving) quadrupole field while transmitting the RF (confining) quadrupole field.[2] When loaded with collision gas to an internal cell pressure of $\approx 10^{-2}$ torr, the analysis chamber pressure is raised to $\approx 1 \times 10^{-5}$torr. This apparatus is schematically depicted in Figure 1.

The reagent ion spectrum for a clean, nearly dry N_2 carrier gas consists of N_3^+, N_4^+, O_2^+ and NO^+ (due to reactions with trace oxygen), H_2O^+, H_3O^+, and their clusters with N_2 and H_2O; when appropriate cleaning steps are taken, the negative charge resides in a thermal electron cloud, although traces of O_2^- and halogen negative ions are difficult to eliminate entirely. The cluster ions extend to 200 amu or more, depending on the source temperature, and while plausible mass assignments in terms of the above named cluster ions were made several years ago, there has always been a measure of prudent caution associated with the identification of the highly clustered ions, e.g., $H_3O^+ \cdot (H_2O)_2 \cdot (N_2)_4$ at 167 amu. The addition of the collision cell and second mass filter makes it possible to demonstrate by collision induced dissociation (CID) that these ions have been correctly identified. Qualitatively similar CID spectra are obtained with N_2, Ar, and He gas targets.

The matrix (Figure 2) indicates the 48 major ions observed in the primary spectrum to 200 amu, and their collision fragments observed to 60 amu. The sloping lines identify families of cluster ions, e.g., $NO^+ \cdot N_2$, $O_2^+ \cdot N_2$, $H_3O^+ \cdot H_2O \cdot N_2$, $N_3^+ \cdot N_2$ on the same line, all represent primary or pseudo-primary ions clustered with one nitrogen molecule. The information contained in Figure 2 leads directly to the simple clustering scheme of Figure 3, which accounts for all 48 major ions.

As has been previously described, the β-ray ionization yields N^+ and N_2^+; these rapidly cluster to give pseudo-primary ions N_3^+ and N_4^+. Ion-molecule

reactions with trace concentrations of O_2 and H_2O lead to NO^+, O_2^+, and H_2O^+. The routes depicted correspond to generally accepted reaction mechanisms,[3] e.g., N_3^+ leads to NO^+ and O_2^+, but not H_2O^+, while N_4^+ leads to O_2^+ and H_2O^+ but not NO^+. While the literature also identify N_3^+ as leading to NO_2^+,[4] collison induced dissociation indicates that under our operating conditions most if not all the mass 46 ions are $H_2O^+ \cdot N_2$. This observation is in agreement with our previous statement,[1] based on the increase of the mass 46 signal with H_2O concentration, but its decrease in favor of mass 50 ($O_2^+ \cdot H_2O$) with O_2 concentration, that this ion is $H_2O^+ \cdot N_2$ rather than NO_2^+. Also, H_2O^+ rapidly reacts with H_2O to give H_3O^+, which at typical operating temperature ($\approx$ 200C), rapidly clusters to $H_3O^+ \cdot H_2O$ at mass 37, frequently the dominant species in positive ion spectrum. Subsequent clustering reactions lead to the five series $N_3^+ \cdot (N_2)_n$, $NO^+ \cdot (H_2O)_m \cdot (N_2)_n$, $O_2^+ \cdot (H_2O)_m \cdot (N_2)_n$, $H_3O^+ \cdot (H_2O)_m \cdot (N_2)_n$, and $N_4^+ \cdot (N_2)_n$, accounting for 41 of the 48 major ions to 200 amu. The remaining seven ions N_3^+, N_4^+, NO^+, O_2^+, H_2O^+, H_3O^+, and $H_2O^+ \cdot N_2$ have been accounted for above.

References

[1] M.W. Siegel and W.L. Fite, J. Phys. Chem. 80 (1976) 2871-81.

[2] M.W. Siegel, Anal. Chem. 52, (1980) 1790-2.

[3] D.L. Albritton, Atomic Data and Nuclear Data Tables 22, (1978) 1-101.

[4] D.B. Dunkin, F.C. Fehsenfeld, A.L. Schmeltekopf and E.E. Ferguson, J.Chem. Phys. 54 (1971) 3817-22; W. Lindinger, J. Chem. Phys. 64 (1976) 3720-3; D. Smith, N.G. Adams, and T.M. Miller, J. Chem. Phys. (1978).

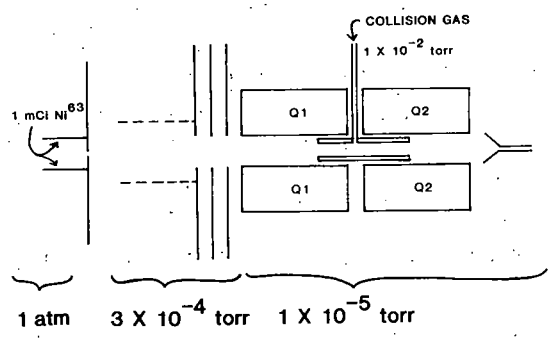

Figure 1 Schematic diagram of API/MS/MS apparatus.

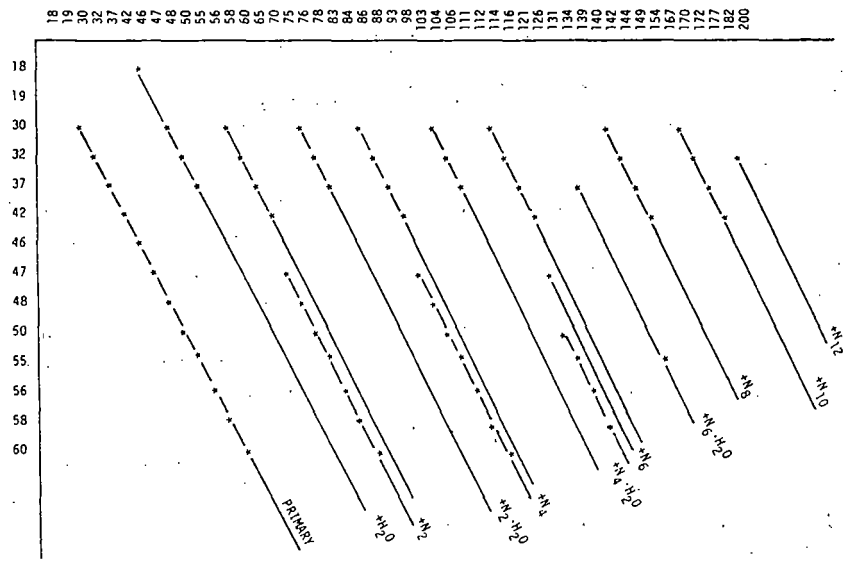

Figure 2 Matrix of daughter ions (vertical) from parent ions (horizontal).

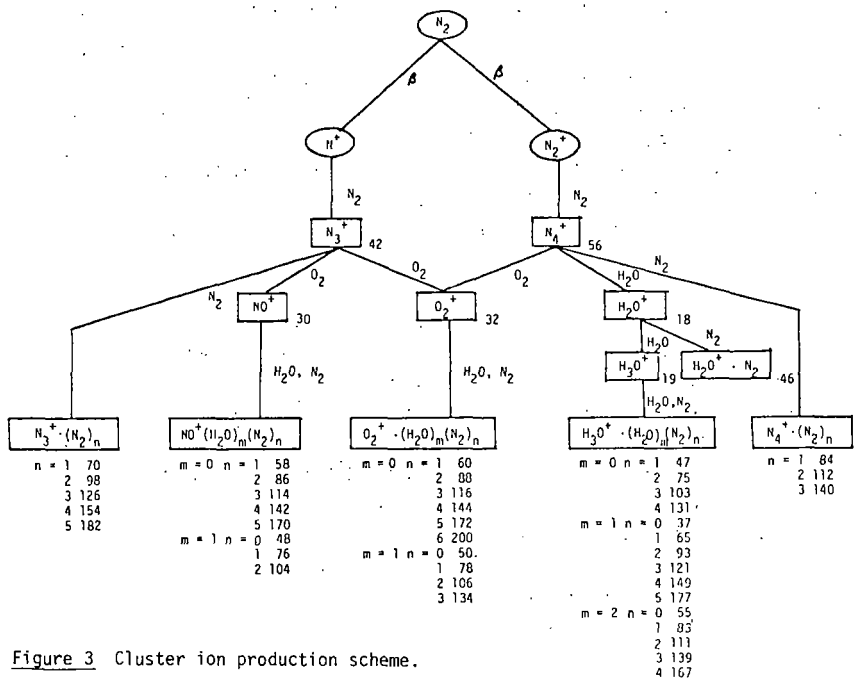

Figure 3 Cluster ion production scheme.

NCI SPECTRA OF SOME TRANSITION METAL CHELATES

I.K. Gregor & K.R.Jennings, Dept. of Chemistry
& Mol. Sci. University of Warwick, Coventry CV4 7AL.UK.
and G.A.Warburton, Kratos Scientific Instruments Ltd.,
Urmstone, Manchester, UK.

Negative chemical ionisation mass spectra of a number of metal chelates have been investigated with a view both to correlate features of the spectra with the chemistry of the metals and to develop a method of detecting organometallic compounds present in trace quantities in hydrocarbon mixtures. Spectra were obtained using an MS80 mass spectrometer/DS55 data system (Kratos Scientific Instruments Ltd.), samples being introduced using a solids probe. An equimolar mixture of methane and nitrous oxide was used to generate OH^- ions which constituted 70% of the total reagent ion current.

Five compounds of nickel of the type ML_2 (L = Acetylacetonate, Dipivaloylmethane, tBu-Sac-Sac-tBu, Dimethylgl yoxime and Dimethyldithiophosphate) and manganese dihexafluoroacetylacetonate were investigated, using CH_4/N_2O as reagent gas. Nickel(dimethylglyoxime)$_2$ gives no negative ions but all others give as the main reaction

$$ML_2 + OH^- \longrightarrow MLOH + L^- \qquad (1)$$

Only $Ni(Me_2DTP)_2$ gives a negative molecular ion from which other fragment ions are formed. None of these compounds gives any addition products of the type ML_2OH^- and it was concluded that a slightly softer base than OH^- may be a more useful reagent ion.

Attention was therefore concentrated on obtaining chloride ion attachment spectra of a series of metal acetylacetonates. Various reagent gases were used in an attempt to generate high yields of Cl^- ions in the absence of cluster ions or other interfering ions, and CH_3Cl, CF_3Cl, CF_2Cl_2, $CHCl_3$ and CCl_4 all gave useful spectra with $Zn(AcAc)_2$. Most spectra were obtained using CF_2Cl_2 as reagent gas which in addition to Cl^- ions gives low yields of F^- and $CFCl_2^-$ ions. CH_3Cl gives a cleaner reagent gas spectrum but it also gives a higher yield of electrons thereby enhancing the yields of ions derived from electron attachment.

A wide variety of behaviour was observed with ions being observed which arise from Cl^- and electron attachment. $Zn(AcAc)_2$ is an example of a compound which gives no ions arising from electron attachment. A group of ions giving peaks at m/z = 297-303 is due to $Zn(AcAc)_2Cl^-$ ions; the intensities of these peaks are usually somewhat lower than those at m/z = 233-241 which are due to $Zn(AcAc)Cl_2^-$ ions. Peaks at m/z = 169-179 are due to $ZnCl_3^-$ ions and these, together with a low intensity peak at m/z = 99 due to $(AcAc)^-$ ions are the only ions of significance seen at low gain. They are believed to be formed in a sequence of reactions such as:

$$Zn(AcAc)_2 + Cl^- \longrightarrow Zn(AcAc)_2Cl^- \qquad m/z = 297\text{-}303 \qquad (2)$$

$$Zn(AcAc)_2Cl^- \longrightarrow Zn(AcAc)Cl + (AcAc)^- \quad m/z = 99 \qquad (3)$$

$$Zn(AcAc)Cl + Cl^- \longrightarrow Zn(AcAc)Cl_2^- \qquad m/z = 233\text{-}241 \qquad (4)$$

$Zn(AcAc)Cl_2^-$ ⟶ $ZnCl_2 + (AcAc)^-$ m/z = 99 (5)

$ZnCl_2 + Cl^-$ ⟶ $ZnCl_3^-$ m/z = 169-179 (6)

At higher gain, at higher pressures of reagent gas, a similar series of peaks at lower intensities was observed arising from $Zn(AcAc)(Cl\text{-}AcAc)Cl^-$ m/z = 331-337.

Compounds which give prominent groups of peaks arising from Cl^- attachment to the molecule include $Mg(AcAc)_2$, $Co(AcAc)_2$ $Th(AcAc)_4$ and $Cu(AcAc)_2$. When $Co(AcAc)_3$ was introduced, a spectrum very similar to that given by $Co(AcAc)_2$ was obtained, indicating that Co^{III} is readily reduced to Co^{II}. Low intensity peaks due to Cl^- attachment were given by $Cr(AcAc)_3$ and $Fe(AcAc)_3$ indicating the formation of 7-coordinate species but in the case of $Cr(AcAc)_3$, the base peak was $(AcAc)^-$ whereas $Fe(AcAc)_3$ gives $Fe(AcAc)_2Cl_2^-$ as the major group of ions giving peaks at m/z = 324-328 which are often observed as impurity peaks.

The compounds of the inert metals ruthenium and platinum, $Ru(AcAc)_3$ and $Pt(AcAc)_2$, give no Cl^- attachment ions and electron attachment is the major mode of ion formation. Whereas $Ru(AcAc)_3$ gives only $(AcAc)^-$ in addition to the Cl^- attachment ion, $Pt(AcAc)_2$ was unique among the complexes studied in that peaks are observed arising from the loss of groups derived from the ligand, e.g. $(M\text{-}CH_3)^-$ and $(M\text{-}CH_3COCH_2)^-$ ions. Although palladium is more labile than platinum, $Pd(AcAc)_2$ largely yields M^- and loss or replacement of the ligands occurs only to a very small extent. Other compounds which gave few or no Cl^- attachment ions are $Cr(AcAc)_3$, $Rh(AcAc)_3$ and $Be(AcAc)_2$ resemble each other in giving $(M\text{-}H)^-$ ions.

In summary, Cl^- attachment appears to be a useful technique for producing ions from metal acetylacetonates although some features of the solution chemistry of the various metals are reflected in the behaviour of the systems in the gas-phase.

QUALITATIVE AND QUANTITATIVE APPLICATIONS OF NEGATIVE CHEMICAL IONIZATION MASS SPECTROMETRY: ANALYSIS OF CATECHOLAMINE METABOLITES AND INDOLEAMINE-ALDEHYDE CONDENSATION PRODUCTS;

KYM F. FAULL, MANISHA SAHNI and JACK D. BARCHAS; Dept. of Psychiatry, Stanford Univ., Stanford, CA 94305

For specific compounds, in particular halogenated species, negative chemical ionization (NCI) mass spectrometry offers the advantage of increased sensitivity over both electron impact (EI) and positive chemical ionization (PCI) mass spectrometry. We have been able to take advantage of this in developing quantitative assays for the catecholamine metabolites metanephrine and normetanephrine in human lumbar CSF samples, and in developing quantitative analyses for indoleamine-aldehyde condensation products in rat brain homogenates.

Recent reports suggesting altered epinephrine and norepinephrine turnover in affective disorders underscores the need for a sensitive and reliable quantitative method for metanephrine and normetanephrine in small samples of human lumbar CSF. These compounds, which are the O-methylated metabolites of epinephrine and norepinephrine respectively, are recovered from CSF using solvent extraction and ion exchange chromatography. Conversion to volatile, thermally stable derivatives is achieved by treatment with methanolic-HCl followed by heptafluorobutyric anhydride. The derivatives, which separate on packed column GC, fragment under both EI and NCI conditions to yield ions suitable for quantitative SIM analysis.

Renewed interest in the biochemistry and pharmacology of indoleamine-aldehyde condensation products has stemmed from recent reports of the natural occurrence of these compounds and their ability to displace ^{3}H-diazepam from benzodiazepine receptors in rat brain membrane preparations. We have investigated NCI GC/MS of perfluorenated acyl derivatives of these compounds to establish a sensitive assay for them in brain homogenates. Results of our work on both of these topics will be presented.

NEGATIVE MASS SPECTRA OF THE DINITROTOLUENE ISOMERS;

MICHEL J.F. ASSELIN AND JOCELYN J.R. PARE;
DEFENCE RESEARCH ESTABLISHMENT VALCARTIER
P.O. BOX 8800, COURCELETTE, P.Q., G0A 1R0 CANADA

In this work we studied the influence of the isomeric chemical configuration of dinitrotoluene (DNT) on the atmospheric chemical ionisation product ions by comparing the behaviour of the six DNT isomers.

A TAGA 3000 mass spectrometer (Sciex Inc., Toronto) was used with a point-to-plane corona discharge source to initiate and sustain the atmospheric pressure chemical ionisation. An electric field selects the polarity of the ions and draws them to the atmospheric pressure/vacuum interface. A dry inert gas (nitrogen) flows between the two main plates of this interface. This gas blows out any particulate and vapor that might enter the ionization source region, thus preventing any clogging of the atmospheric pressure/vacuum orifice; it also reduces the clustering encountered in the free-jet expansion of the ion-air mixture into the vacuum[1].

EXPERIMENTAL

Each isomer was dissolved in methanol and injected continuously in a flow (39 L/min) of ambient air, 40 cm ahead of the corona discharge, with a 10-mL syringe pump (Sage Instrument, Model 355). The wall of the 22 mm glass tube leading to the ionisation source was heated outside the source assembly at 425 K. To eliminate the formation of drops at the end of the needle, its tip was made to touch a small piece of ground glass placed in the middle of the 22 mm tube. The injection rate of 16.8 µL/min produced a stable concentration of about 50 ppb.

Furthermore, 2,4-DNT was also studied in pure nitrogen. One gram of purified 2,4-DNT was placed in a clean tube above which nitrogen was circulated at 2 L/min. This tube was thermostated at 325 K. The ambient source housing was also purged with another flow of 1 L/min of the same nitrogen.

RESULTS AND DISCUSSION

The recorded intensitites of the most significant anions peaks are listed in Table I for the six DNT isomers and for a typical background of the laboratory ambient air recorded under the same conditions.

TABLE I

Intensities of the Most Significant Peaks in Ions/s							
M/z	2,3-DNT	2,4-DNT	2,5-DNT	2,6-DNT	3,4-DNT	3,5-DNT	Lab. Air
46	212384	24220	29788	35624	49525	43208	30956
152	894	410	3163	1503	1620	2818	185
168	2863	79	184	136	10257	677	76
181	56	54587	0	0	183	51	103
182	14535	7848	58572	65280	17992	42280	56
197	124	429	15	316	1280	1580	51
198	43	204	1009	76	162	652	39
212	2439	44	52	108	708	82	20
228	976	58	13	54	369	840	17

It must be noted that these experiments were not set up to determinate the ultimate sensitivity of the TAGA 3000 to DNT. There was considerable loss of sample on the surface of the inlet and ionisation source which had to be cleaned between samples; furthermore the instrument was not adjusted for high sensitivity, but rather for good resolution.

The mass spectra of 2,4-DNT, was run in pure dry nitrogen, directly from the vapor above the solid. Because of the mode of sample injection the 2,4-DNT concentration was weaker then when recorded in air. The following intensities (ions/s) were observed: 46 amu (3611), 152 amu (114), 181 amu (0), 182 amu (19856), 198 amu (35).

a) The 2,5-, the 2,6- and the 3,5-DNT Isomers

The molecular ion, $[DNT]^-$ at 182 amu is the principal product ion, with intensities between 42 000 and 65 000 ions/s and little fragmentation (Table I). The ionisation of these DNT isomers in air is mainly caused by electron transfer form the superoxide anion $[O_2]^-$ to DNT. The high EA of nitro derivatives of benzene favours this transfer[2].

b) The 2,3- and 3,4-DNT Isomers

Again the molecular ion at 182 is evidence of the electron transfer from the superoxide anion, $[O_2]^-$, but its intensity is much lower than for the 2,5-, 2,6- and 3,5-DNT being only 14 000 and 18 000 ions/s. On the other hand Table I shows that the fragmentation is much higher. Particularly for 2,3-D[illegible], where the most intense product ions is $[NO_2]^-$ at 46 amu. For 3,4-DNT the intensity of the product ion at 168 amu is 57% of the molecular ion and represents the lost of a nitrogen atom, possibly by capture of a $[O_2]^-$ follow by elimination of $[NO_2]^-$.

Important for the stability of aromatic molecules is the resonance energy gained by the delocalisation of the π electron system. In the 2,3- and 3,4-DNT there is a strong steric inhibition to resonance because of the large tilt angle of the nitro groups due to their steric interactions. For 2,3- and 3,4-DNT the first electronic transitions are respectively at 210.0 nm and 219.0 nm similarly to the case of benzene itself. On the other hand, the four other DNT isomers absorb between 240.0 and 265.5 nm indicating that for 2,3- and 3,4-DNT both nitro groups are significantly out-of-plane with the benzene ring[3]. A lost of resonance energy by steric inhibition in the 2,3- and 3,4-DNT molecules and additional tension arising form the ortho NO_2 - NO_2 repulsion are responsible for the lower stability of the molecular anion $[DNT]^-$. The enthalpy of formation of the isomers is also a good indication of the importance of the resonance energy for the stability of the molecules: 2,3-DNT, -87.4 kJ/mole; 3,4-DNT, -80.3 mJ/mole; 2,5-DNT, -188.3 kJ/mole; 3,5-DNT, -238 kJ/mole; 2,6-DNT, -241 kJ/mole and the most stable 2,4-DNT, -374.5 kJ/mole.

c) The 2,4-DNT Isomer

This isomer produces $[DNT-H]^-$ at 181 amu and its contribution to the molecular ion (182 amu) is less than 5%. The lack of subsequent fragmentation observed indicates a high stability for this quasimolecular anion. This behaviour results from the concerted effort of the two nitro groups to withdraw electrons from the benzene ring and induce a positive charge on the methyl group. The acidity of this methyl permits a proton transfer between this group and the superoxide anion $[O_2]^-$.

A situation allowing a positive concerted effort of both the resonance and induction effect of both nitro groups is, at first sight, possible for the 2,4- and 2,6-DNT. But a large steric effect exists in the case of 2,6-DNT which rules out the contribution of the resonance effect of one of the nitro group. This is well illustrated by the ultra-violet absorption spectra: the 2,4-DNT absorbs at 252.0 nm and the 2,6-DNT at 241.0 nm[3]. Thus only for the 2,4-DNT will we have the concerted action of both nitro groups sufficiently strong to permit the abstraction of a proton.

To confirm the proton acidity of 2,4-DNT and its reaction with $[O_2]^-$, the mass spectra of 2,4-DNT in the gas phase were run in pure nitrogen. The absence of proton abstraction is made evident by the low intensity of mass 181 and the strong molecular ion peak at mass 182. The formation of this anion is due to non-dissociative thermal electron capture. The acidity of the methyl was previously observed by mass spectrometry in the case of 2, 4, 6-trinitrotoluene[4] and of the 2,4-DNT[5].

Finally, we noted that the DNT isomers all formed ion clusters of low intensities. The following is a tentative attribution: 197 amu $[DNT-H + O]^-$, 198 amu $[DNT + O]^-$, 212 amu $[DNT + NO]^-$ and 228 amu $[DNT + NO_2]^-$.

1. F. Karasek, Ind. Res./Dev., Dec 1978, p. 86
2. M. Batley and L.E. Lyons, Nature 196, 573, 1962
3. C.P. Conduit, J. Chem. Soc., 3273, 1959
4. I. Dzidic, D.I. Carroll, R.N. Stillwell and E.C. Horning, J. Am. Chem., 96, 5258, 1974
5. G.E. Spangler and P.A. Lawless, Anal. Chem., 50, 884, 1978

LIMITATIONS OF NICI-GCMS FOR ANALYSIS OF BIOGENIC AMINES

C. M. Williams, J. R. Crowley and M. W. Couch
VA Hospital and Department of Radiology, University of Florida, Gainesville, Florida

m-Synephrine, a strong pressor agent, has recently been identified in adrenal gland (1). This suggested a possible role for m-synephrine in blood pressure regulation and prompted the search for an analytical method for its determination. Attempts to measure m-synephrine in blood and urine by an EI-GCMS method capable of detecting 1-10 ng ml^{-1} were unsuccessful. For this reason we have turned to electron capture NICI-GCMS because of its reported 10-100 fold increase in sensitivity over EI-GCMS and PICI-GCMS methods (2).

NICI-GCMS was performed with a Hewlett-Packard 5985B. Source pressure 1.0 torr; emission current, 300 μA; electron energy, 240 eV. GC condition: glass column (2 mm x 1.8 m) with 5% OV-101 on 100/120 mesh Chromosorb GHP: carrier methane; column 180°C; injection, 250°C; GC-MS interface, 250°C; NICI ion source, 100°C.

The pentafluoropropionyl (PFP) derivative of m-synephrine was found to be a stable electron-capturing compound with relatively high yields of the structure specific anions M and M-HF. Major fragment ions of PFP derivatives of 8 closely related biogenic amines are listed in Table I. The PFP derivative of m-synephrine is separated from its positional isomers o-synephrine and p-synephrine. p-Octopamine-PFP and norepinephrine-PFP have retention times which overlap with m-synephrine-PFP. There are no ions in the norepinephrine-PFP or p-octopamine-PFP spectra which would interfere with the ions for detection and quantitative

TABLE I. ELECTRON CAPTURE NEGATIVE ION CHEMICAL IONIZATION MASS SPECTRA

PFP Derivative	Kovats' Index	% Total Negative Sample Ion Current MW	M^-	$(M-HF)^-$	Other m/z
o-Octopamine	1335	591	22	18	163(8)[a]
m-Octopamine	1410	591	18	5.0	163(17)[a]
o-Synephrine	1430	605	3.0	4.0	163(32)[a]
p-Octopamine	1450	591	38	2.7	163(9)[a]
Norepinephrine	1450	753	33	6.0	589(9)[c]
m-Synephrine	1455	605	6.0	10	163(27)[a]
Epinephrine	1490	767	23	1.0	620(16)[d]
p-Synephrine	1500	605	10	7.0	163(40)[a]

[a] $C_2F_5CO_2$. [b] M-$C_2F_5CO_2H$. [c] M-C_2F_5CO.

analysis of m-synephrine-PFP. Trideuterated m-synephrine was synthesized and a linear calibration curve was obtained over the range 0-20 pg. With two-ion monitoring and electron multiplier voltage 3000 the minimum detectable amount of m-synephrine was about 500 fg.

We have confirmed Hunt's report (2) that measurement of electron capture agents must be carried out on small quantities of sample to avoid saturation of the negative ion signal. The increase in negative ion current as a function of sample concentration became nonlinear when the sample size exceeded 10 ng and saturation occurred above 20 ng. This effect is of major importance in the quantitative analysis of compounds extracted from a biological matrix, since other electron-capturing compounds may be found at the same retention time as the unknown. p-Octopamine-PFP elutes slightly before m-synephrine-PFP. The absolute abundances of the M and M-HF ions of m-synephrine-PFP were reduced when 100 pg and 1 ng of p-octopamine-PFP was coinjected, but the ratio of the two ions was constant. However with coinjection of 10 ng and 100 ng of p-octopamine-PFP the character and relationship of M and M-HF ions of m-synephrine-PFP was markedly distorted, with assymmetry of peak shape and significant discrepancy between the retention times of the two ions. From these results it was anticipated that electron-capturing co-eluting peaks in amounts above 10 ng would significantly reduce the detection of ions from the desired compound. This anticipation was borne out by experiment. Table 2 shows the effect on the absolute abundance of the M and M-HF ions of 100 pg of m-synephrine-d_0-PFP when coinjected with varying amounts of a mixture of o-, m- and p-octopamine-d_3 and o- and m-synephrine-d_3-PFP. The three octopamine and o-synephrine derivatives elute from the GC column during the 1 minute immediately preceeding the appearance of m-synephrine-d_0-PFP. Amounts above about 5 ng of electron capturing compounds eluting immediately before or simultaneously with m-synephrine were found to significantly reduce sensitivity and alter ion ratios.

TABLE II. SATURATION EFFECT ON DETECTION OF M-SYNEPHRINE-D_0

m-Synephrine-d_0	100 pg	100 pg	100 pg	100 pg
Amine-d_3 mixture*	0	15 ng	150 ng	1,500 ng
Absolute abundance m/z 605	48,742	30,972 (63%)	1,469 (3%)	240 (0.5%)
Absolute abundance m/z 585	61,958	40,532	3,389	503
Ratio of 605/585	0.79	0.76	0.43	0.48

*3 ng each of o-, m-, p-octopamine-d_3-PFP and o-, m-synephrine-d_3-PFP

We attempted to clean up urine by a procedure (3) using two consecutive ion-exchange chromatographic steps: (1) AG-50X-2 (100-200 mesh, 5 g, H^+) and (2) BioRex 70 (200-400 mesh, 5 g, NH_4^+). The 70-120 ml fraction was desalted, reduced to dryness and reacted with PFP anhydride (100 µl, 30 min, 60°C). The PFPA was evaporated under N_2, and the residue taken up in 500 µl of ethyl acetate which was washed with (1) 100 µl H_2O and (2) 100 µl saturated $NaHCO_3$ (4). Washing the derivative was necessary to remove electron-capturing background (residual PFPA) which sharply reduced sensitivity for periods of time up to 1 hr.

An internal standard containing 100 ng each of o-, m-, and p-synephrine-d_3 was added to urine containing 10 mg creatinine and acid hydrolyzed. After clean up, the dried derivatized residue was taken up in 500 µl of ethyl acetate. Figure 1a shows the ion response to 100 pg m-synephrine-PFP. Figure 1b shows the response to 1 µl of the urine extract. Figure 1c shows that coinjection of 1a and 1b reduces the response to 100 pg m-synephrine-d_0 to 1% of response to 100 pg m-synephrine injected alone (1a). This is attributed to other electron-capturing (PFP) derivatives in the urine. The majority of urine specimens examined were

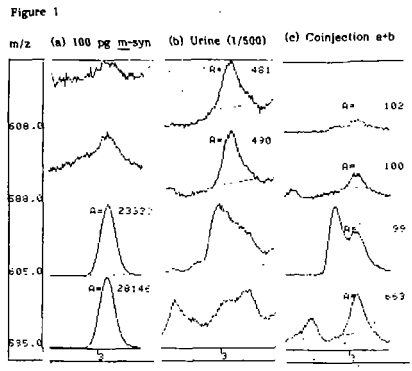

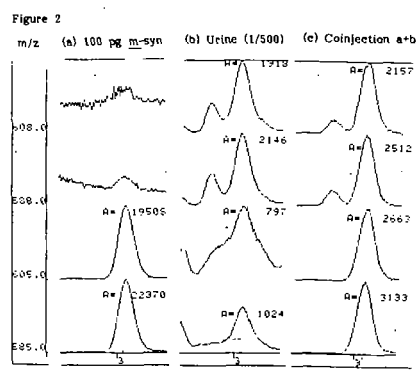

similar to Figure 1. In one urine specimen less electron-capturing impurities allowed a higher (15%) response to coinjected m-synephrine-d_0 (Figure 2a and 2c) and 6 ng m-synephrine-d_0 mg^{-1} creatinine was found to be present in the urine (Figure 2b).

Tissue (rat adrenal) and serum (human) also contained, upon derivatization, large amounts of other electron-capturing compounds which reduced the sensitivity of coinjected m-synephrine. This reduction in sensitivity is due to depletion of electrons in the ion source available for sample ionization by other derivatized (PFP) compounds in the biological matrix eluting just before or simultaneously with the compound of interest. It was concluded that NICI-GCMS using a two-stage clean-up procedure and packed column GC could not be used for the quantitative determination of picogram levels of biogenic amines in biological tissues or fluids (serum, urine). It is possible that the use of capillary column GC or a more elaborate clean-up procedure may render practical the use of NICI-GCMS for this analytical application.

References

1. Midgley, J. M., Couch, M. W., Crowley, J. R. and Williams, C. M. J. Neurochem. 34, 1225 (1980)
2. Hunt, D. F. and Crow, F. W. Anal. Chem. 50, 1781 (1978)
3. Kakimoto, Y. and Armstrong, M. D. J. Biol. Chem. 237, 422 (1962)
4. Lewy, A. J. and Markey, S. P. Science 201, 741 (1978)

NEGATIVE ION CHEMICAL IONIZATION (OH^-) MASS SPECTRA OF TRICHOTHECENES

W.C. Brumley, D. Andrzejewski, P.A. Dreifuss, J.A.G. Roach, J.A. Sphon
Div. of Chemistry and Physics, Food and Drug Administration, Washington, DC 20204

Trichothecenes are a group of related sesquiterpenoids derived from the 12,13-epoxytrichothec-9-ene ring system (Fig. 1). They are naturally occurring mycotoxins produced by several species of fungi and are divided into four structural classes. This report emphasizes the behavior of compounds of classes A and B under negative ion chemical ionization conditions using OH^- as the reagent ion.

Figure 1 gives the OH^- spectrum (Finnigan 3300F) of verrucarol (class A). A relatively abundant $(M-H)^-$ ion is produced at m/z 265. An $(M-H-30)^-$ ion at m/z 235 is correlated with the presence of a $-CH_2OH$ group in the neutral molecule. This ion is postulated to form from a six-membered transition state in which the -OH hydrogen is transferred to the ether oxygen (position 1) with ring opening and elimination of CH_2O. Ions corresponding to $(M-H-18)^-$ and $(M-H-30-18)^-$ at m/z 247 and 217 are also observed. A structurally significant fragment ion occurs at m/z 143 which we designate $(R_A+H)^-$. We postulate cleavage across the bonds indicated on the structure with a hydrogen transfer to produce an ion indicative of the right (epoxide-containing) side of the molecule. High resolution (HR) mass measurements (ZAB-2F) indicate that the elemental composition of at least part of the ion current at m/z 143 is consistent with this hypothesis. The m/z 125 ion corresponds to loss of water from m/z 143 as supported by HR mass measurement of m/z 125 and the MIKE spectrum (ZAB-2F) of m/z 143.

In OH^- spectra of eight class A trichothecenes, the $(M-H)^-$ ion ranges from 1.5 to 100% relative abundance (RA). The $(R_A+H)^-$ ion ranges from 0.5 to 79.0% RA. In compounds where CH_3COO- replaces -OH, a nucleophilic displacement results in an abundant m/z 59 ion in the spectrum. When $(CH_3)_2CHCH_2COO-$ is substituted in position 8, then m/z 101 is observed as the base peak in the spectrum.

Figure 2 gives the OH^- spectrum (Finnigan 3300F) of diacetylnivalenol (class B). The spectrum exhibits a relatively abundant $(M-H)^-$ ion indicative of molecular weight. In class B compounds, a structurally significant fragment now represents the left (carbonyl-containing) side of the molecule (Fig. 2) which has lost a proton. We represent this fragment as $(L_B-H)^-$ which occurs at m/z 195. HR mass measurements of a related compound (deoxynivalenol) from class B reveals an elemental composition consistent with this hypothesized fragmentation. Presumably, the m/z 195 ion loses acetic acid by rearrangement to produce m/z 135 in this spectrum. Nucleophilic displacement is also a major process and results in m/z 59.

In OH^- spectra of seven class B trichothecenes, the $(M-H)^-$ ion ranges from 3.4 to 100% RA. The $(L_B-H)^-$ ion ranges from 1.7 to 100% RA. Nucleophilic displacement

is an important process as well when CH_3COO- or other organic acid derivatives are present. The presence of the $-CH_2OH$ group is associated with observance of an $(M-H-30)^-$ ion. Observance of relatively abundant even mass ions in the spectra of many class B compounds reflects the stabilizing effect of the conjugated carbonyl group during negative ion formation.

The OH^- spectra of trichothecenes exhibit relatively abundant ions indicative of molecular weight and fewer fragment ions than do EI spectra. The occurrence of fragment ions that may be correlated with structure suggests that the OH^- spectra of trichothecenes may be useful for structure determinations and for confirmation of these compounds when present in foods and feed. As an additional note, we mention that chloride attachment affords spectra with base peak $(M+Cl)^-$, which is indicative of molecular weight, and essentially no fragmentation, provided at least one free -OH group is present in the neutral trichothecene.

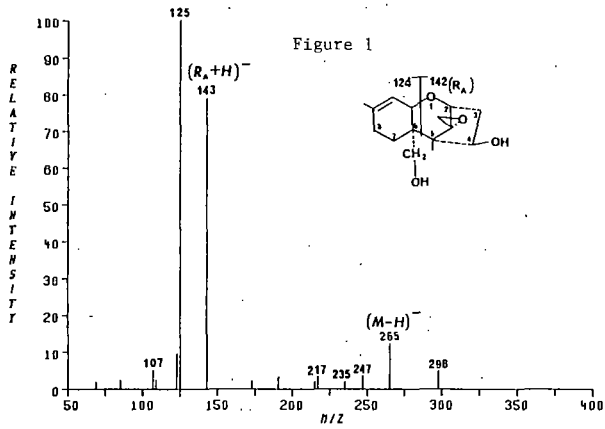

Figure 1

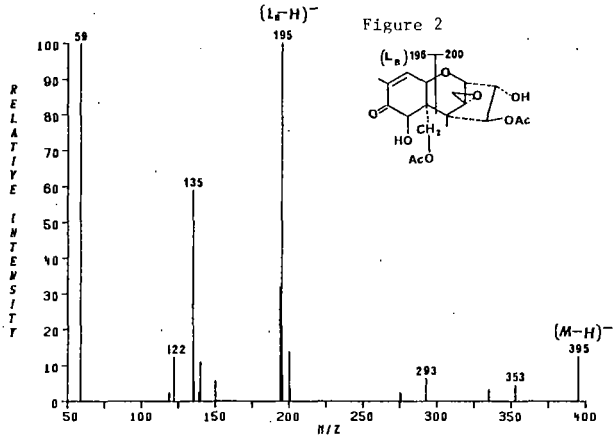

Figure 2

POSITIVE AND NEGATIVE CHEMICAL IONIZATION MASS SPECTROMETRY OF N-PROTECTED AMINO ACIDS.

GEORGE BARANY and MARK A. STEINE. Dept. of Chemistry, University of Minnesota, 207 Pleasant Street, S.E., Minneapolis, Minnesota 55455.

A major research interest of this laboratory is the development of new N^{α}-amino protecting groups for peptide synthesis. Chemical ionization mass spectrometry has proven to be an exceptionally valuable technique for the characterization of the new derivatives that we have synthesized. Furthermore, we needed to prepare a host of standard amino acid derivatives in order to pin down details of the fragmentation patterns. The amino acid residue selected was the simplest one, glycine. This choice was made so as not to complicate spectra with side-chain fragmentation ions. The C^{α}-carboxyl group of glycine was left free, or it was bound as the salt with dicyclohexylamine, or it was protected as a methyl, ethyl, or tert-butyl ester. We thus have a "library" of over sixty glycine derivatives, all purified to satisfactory analytical criteria, and representing over two dozen amino protecting groups. Anticipating the mass spectral work to come, a conscious effort was made to prepare appropriate homologous series, in a way that would highlight trends with a given fragmentation ion, and also resolve ambiguities of mass coincidences.

A starting point for these investigations was the observation that in positive ion chemical ionization, certain urethanes of the general structure (I) produced a so-called protonated carbamic acid ion (II) derived by loss of the appropriate alkene from the molecular $(M + 1)^+$ ion of the parent (I). The detection of (II) was particularly surprising because in the condensed phase at room temperature, protonated carbamic acids are known to lose carbon dioxide essentially instantaneously.

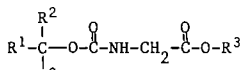

(I)

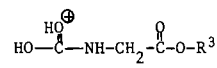

(II) $(Carb)^+$

Table I gives the structures of some amino protecting groups, listed in order of decreasing lability to acid, and the amounts of each of the $(M + 1)^+$ and the $(Carb)^+$ ions formed upon isobutane chemical ionization at a source temperature of 130 °C.

TABLE I.

NAME	Stability order	R^1	R^2	Ion (% base) M + 1	Carb
Bpoc			CH_3	2	77
Ppoc			CH_3	3	100
Boc		CH_3	CH_3	25	100
Tcboc		CCl_3	CH_3	75	82
iProc		H	CH_3	100	13
Eoc		CH_3	H	100	0
Msc		$CH_3SO_2CH_2$	H	100	0

The lability of these protecting groups to acid in solution correlates well with the ease of formation of a carbonium ion upon scission of an alkyl-oxygen bond in the urethane. This correlation apparently can be extended to a discussion of the gas phase chemistry demonstrated in Table I. Formation of the protonated carbamic acid ion (II) was negligible or non-existent for all acid-stable protecting groups examined.

Since formation of (II) seems to involve elimination of an alkene from (I), it was natural to enquire whether this fragmentation could be arrested if the alkyl group of the starting urethane was one which could not be induced to form a double bond. The adamantyloxycarbonyl derivative (III) and the tert-butyldimethylsilyloxycarbonyl derivative (IV) were synthesized in order to address this question. Both (III) and (IV) are at least as labile to acid in solution as is the tert-butyloxycarbonyl (Boc) group (Table I, line 3). (III) cannot form a carbonium ion or a double bond at the bridgehead, and (IV) may be predicted to be unlikely to form a siliconium ion or a silicon-carbon double bond. Gratifyingly, both (III) and (IV) gave appreciable $(M + 1)^+$ ions (20% and 100% of base, respectively), but none of the carbamic acid ion (II).

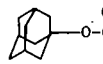

(III) Adoc-Gly-OH

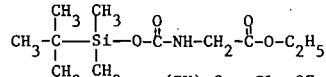

(IV) Soc-Gly-OEt

We also looked for a protonated thiocarbamic acid ion (V) in the mass spectra of appropriate thiourethanes (VI) and thionourethanes (VII). In solution, compounds (VI) are substantially more stable than the corresponding alkoxycarbonyl derivatives (I), whereas the isomeric (VII) are substantially more labile. This pattern was entirely reflected in the mass spectra. All compounds examined gave an $(M + 1)^+$ ion as the base (100%). Protonated thiocarbamic acid ions (V) were observed, at ~15%, in just two cases. These were the tBumc group (VIa) and the iPrtc group (VIIa), both at the extreme in acid-lability of the respective structural classes. Incidentally, the hypothetical tButc derivative was synthetically inaccessible, presumably because of its great lability to acid.

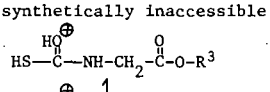

(V) $(Thiocarb)^+$

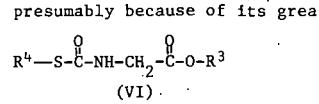

(VI)

R^4 = tert-butyl (VIa) tBumc
= ethyl (VIb) Emc

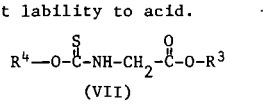

(VII)

R^4 = isopropyl (VIIa) iPrtc
ethyl (VIIb) Etc
methyl (VIIc) Mtc

The specificity in the formation of the protonated carbamic acid ion (II) was studied by examining the chemical ionization mass spectrum of d_9-tert-butyloxycarbonylglycine. The base peak occurred at m/e 121, indicating the incorporation of exactly one deuteron derived from the original tert-butyl group. An intramolecular fragmentation pattern appears to be involved, without any pickup of a proton from an external source. We also synthesized and examined d_6-tert-butyloxycarbonylglycine, containing one CH_3 and two CD_3 radicals. A 67:33 distribution of m/e 121 : m/e 120 would be expected on purely statistical grounds; the found ratio of 60:40 reflects a slight bias in favor of transfer of a proton from CH_3 rather than a deuteron from CD_3.

Finally, the effects of variations in chemical ionization reagent gas and source temperature were investigated. The ratio of $(M + 1)^+/(Carb)^+$ decreased with increasing source temperature (two-fold in going from 100 to 200 °C), and with more acidic reagent gas (three-fold in going from isobutane to methane). When ammonia was used for chemical ionization, the amount of molecular ion formed was relatively the highest, but it was predominantly in the form of $(M + NH_4)^+$, with much less of both $(M + 1)^+$ and $(M + N_2H_7)^+$.

We also report, for the first time, results of negative ion chemical ionization of N-protected amino acids. Most compounds examined gave large $(M - 1)^-$ ions, although several gave appreciable $M^{-\cdot}$ molecular anions. Other than readily identifiable cluster ions, a small number of characteristic fragmentation ions were detected. Most interesting among these were the carbamate or thiocarbamate anions (VIII), at two mass units lower than the protonated ions (II) and (V) already extensively discussed for the positive spectra.

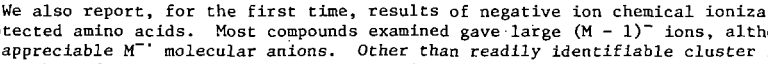

(VIII) X,Y = O, S $(Carb)^-$ or $(Thiocarb)^-$ ions

An attempt was made to correlate the appearance and quantitative extent of (VIII) with the known lability of the parent protecting groups in basic solution. The $(Carb)^-$ ion was not observed for Boc-glycine, consistent with the known resistance of this tertiary alkoxycarbonyl protecting group to nucleophiles. However, the $(Carb)^-$ ion was prominent in the spectra of Bpoc and Ppoc derivatives (Table I, lines 1 and 2), calling to question this interpretation. A modestly successful application of the idea that negative ion gas phase chemistry parallels base-promoted removal of a protecting group in solution is shown below:

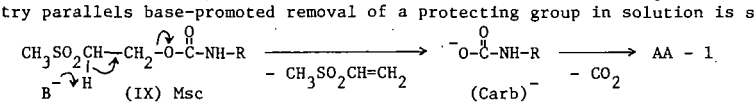

(IX) Msc

The isobutane negative chemical ionization spectrum of Msc-Gly-OEt, measured at source temperature 130°C, showed (M - 1) at 38%, $(Carb)^-$ at 100%, and AA - 1 at 8%. The corresponding numbers for Mteoc-Gly-OEt = $CH_3SCH_2CH_2$-O-CO-NH-$CH_2CO_2C_2H_5$ were 100%, 24%, and 5%. The Mteoc group, with a β-sulfide, is not nearly as activated for the diagrammed β-elimination reaction as is the Msc group with the electron-withdrawing β-sulfone.

Acknowledgments. Supported by NIH, Research Corporation, and U of M Graduate School.

CHEMICAL IONIZATION WITH CF_4

M. A. Rudat
E. I. Du Pont de Nemours & Co., Inc.
Central Research and Development Dept.
Wilmington, DE

Use of CF_4 as the reagent gas under positive and negative ion chemical ionization conditions has not been thoroughly studied previously, so a survey study of a wide variety of compounds was undertaken. In the course of this work, a number of interesting reactions in the CF_4 plasma were found.

The positive ion reagent spectrum consists mostly of CF_3^+ and some CF_2^+; the negative ion spectrum is primarily F^-. CF_3^+ appears to react relatively slowly with most compounds, as judged by the relatively low sensitivity obtained and the nature of the spectra observed. Charge-exchange and ion-molecule addition of CF_3^+ are the principle modes of reaction; for many compounds ionization is apparently followed by a rapid reaction with the first sample molecule encountered to yield the $[M+1]^+$ ion, even at the lowest sample pressures used (<1% of the total pressure). Some compounds, particularly aromatics, produce ions from reaction with CF_3^+ which are sufficiently stable to be observed. Table I summarizes the general observations made in the positive ion mode.

In the negative ion mode, ionization was primarily by electron capture, with some instances of F^- ion-molecule reactions, particularly with alcohols. Therefore, in general the negative ion spectra are similar to those generated using other reagent gases. The results are summarized in Table II.

Two types of unusual reactions were found in these studies: ion-molecule reactions followed by the loss of specific identifiable neutral entities, and radical reactions followed by ionization. Toluene and xylene react with CF_3^+ to produce the adduct, followed by elimination of H_2, HF, CH_3F, and CH_2F_2. Methyl-group labeling shows these to be losses from an unrearranged ion.

Polycyclic aromatics (such as tetracene and pentacene) apparently react with $\cdot F$ and $\cdot CF_3$ radicals to produce a series of ions in both the positive and negative ion modes corresponding to the replacement of several H with F and/or CF_3. The reaction behavior parallels that observed for the radical reactions of TCNQ with alkyl radicals (1).

(1) C. N. McEwen and M. A. Rudat, J. Am. Chem. Soc., in press.

TABLE I

CF_4 C.I. POSITIVE ION MODE

$[M-1]^+$	$M^{+\cdot}$	$[M+1]^+$	$[M+CF_3]^+$	UNUSUAL
AMINES	AROMATICS	KETONES	AROMATICS	ALCOHOLS $[M-17]^+$
CYCLIC ALCOHOLS	SOME CYCLICS	AMINES		ALCOHOLS $[M+F]^+$
ALDEHYDES (?)		ACIDS		SUBST. BENZENES $[M+49]^+$
		ETHERS		BENZYL CMPDS. 159^+
		ALDEHYDES		
		AMINO ACIDS		
		ESTERS		

UNRESPONSIVE TO C.I.

THIOPHENE
OCTANE
CITRIC ACID
ADIPAMIDE

TABLE II

CF_4 C.I. NEGATIVE ION MODE

$[M-1]^-$	$[M+F]^-$	UNUSUAL	UNRESPONSIVE
ALDEHYDES	ALCOHOLS	ALCOHOLS $[M-3]^-$	AMINES
ALCOHOLS	ACIDS		ADIPAMIDE
ACIDS			DL-MENTHOL
ESTERS			GLYCINE

REDUCTION OF TRINITROAROMATIC COMPOUNDS IN WATER BY CHEMICAL IONIZATION MASS SPECTROMETRY

Jehuda Yinon and Miriam Laschever

Department of Isotope Research, The Weizmann Institute of Science, Rehovot, Israel

During our work on the analysis of explosives in water by direct injection CI mass spectrometry (1), we observed in the mass spectra of the trinitroaromatic compounds, highly abundant peaks at m/z corresponding to loss of 30 mass units from the MH^+ ion. Such ions had been observed previously at lower abundances in the CI spectra of various nitroaromatic compounds and were assumed to be due to $(MH - NO)^+$. As previous workers (2,3,4) had claimed that the $(MH - 30)^+$ ions might be due to their initial reduction to corresponding amines, we recorded the CI spectra of a series of trinitroaromatic compounds with H_2O and D_2O as reagents in order to determine more definitively the origin of the $(MH - 30)^+$ ions. Mass spectra were recorded with a Varian MAT CH7 mass spectrometer previously modified for CI. The investigated compounds included 1,3,5-trinitrobenzene (TNB), 2,4,6-trinitrotoluene (TNT), 2,4,6-trinitro-m-cresol (TNC), 2,4,6-trinitroaniline (picramide) and 2,4,6-trinitrophenol (picric acid). Samples, dissolved in H_2O and D_2O, were introduced through a special quartz probe (1) made to fit the entrance port of the solid probe. The quartz probe was heated and had a septum seal through which samples were injected into the source. It was found that the $(MH - 30)^+$ ion in most of these compounds was due to a reduction process:

$$R - NO_2 \xrightarrow{H_3O^+} [RNH_3]^+$$

rather than to loss of NO from the MH^+ ion. This was proved by using D_2O as reagent, where the reduction process forms:

$$R - NO_2 \xrightarrow{D_3O^+} [RND_3]^+ \Longrightarrow (MD - 28)^+ \text{ ions}$$

while loss of NO will form

$$[MD - NO]^+ \Longrightarrow (MD - 30)^+ \text{ ions.}$$

Results indicate clearly the occurence of a strong reduction process in TNB, TNT, TNC and picric acid. In these compounds low abundance ions were observed at m/z corresponding to the loss of NO from the protonated molecular ion, indicating that this process is also occurring. In picramide no reduced ions were observed and therefore loss of NO is the only process involved in the formation of the $(MH - 30)^+$ ion in this compound.
Figures 1 and 2 show the CI spectra of TNB in H_2O and D_2O respectively, illustrating the reduction process.

Acknowledgement

The research reported herein has been sponsored in part by the U.S. Army through its Research and standardization Group (Europe).

References

1. J. Yinon and M. Laschever - To be published.

2. J.J. Brophy, V. Diakiw, R.J. Goldsack, D. Nelson and J.S. Shannon, Org. Mass Spectr. 14, 201 (1979).

3. A. Maquestiau, Y. Van Haverbeke, R. Flammang, H. Mispreuve and J. Elguero, Org. Mass Spectr. 14, 117 (1979).

4. A.G. Harrison and R.K. Mohan Roao Kallury, Org. Mass Spectr. 15, 284 (1980).

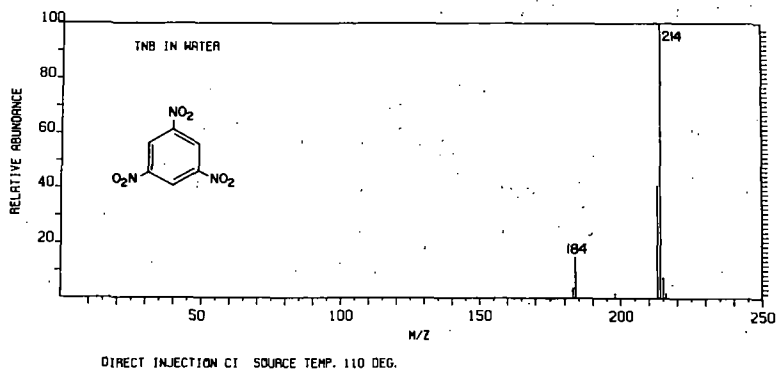
TNB IN WATER
214
184
RELATIVE ABUNDANCE
100
80
60
40
20
50
100
150
200
250
M/Z
DIRECT INJECTION CI SOURCE TEMP. 110 DEG.

FIG 1

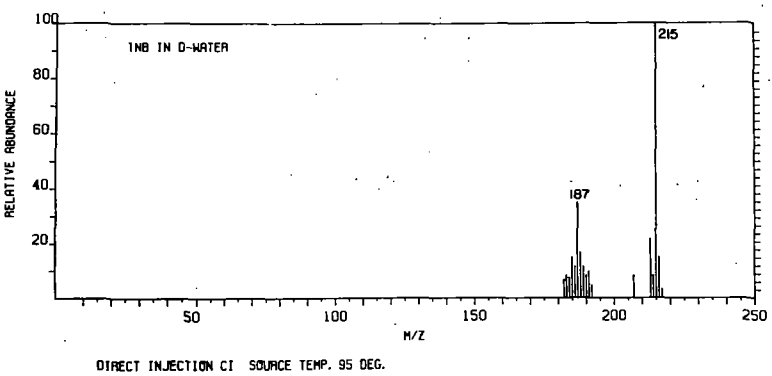
TNB IN D-WATER
215
187
RELATIVE ABUNDANCE
100
80
60
40
20
50
100
150
200
250
M/Z
DIRECT INJECTION CI SOURCE TEMP. 95 DEG.

FIG 2

THE ASSESSMENT OF MATRIX EFFECTS ON IDENTIFICATION AND QUANTITATION BY CHEMICAL IONIZATION MASS SPECTROMETRY

G. J. Kallos, V. Caldecourt and J. C. Tou
Analytical Laboratories, Michigan Division
Dow Chemical U.S.A.
Midland, Michigan 48640

During the past decade chemical ionization mass spectrometry (CIMS) has gained increasing importance in structure identification and quantitation. Although it is realized that the formation of the quasi-molecular ion and its fragment ions are mainly governed by the nature of the reactant ions, simultaneous monitoring of these two types of ions are generally lacking, because of the overwhelming difference in their intensities. A Finnigan model 4021 quadrupole mass spectrometer has been modified to rapidly switch the electron multiplier voltages during a scan in order to monitor both reactant and product ions. The circuit diagram is shown in Figure 1.

Through this technique, several model CI reactions were studied under the influence of a controllable amount of the selected matrix components being introduced into the ion source. The methane reagent gas was introduced into the source (250°C) through an exponential dilution flask at a rate of 125 μg/sec (0.2 torr). Known amounts of a selected matrix component and a sample component were then introduced into the ion source through the exponential dilution flask from the GC oven and through a batch inlet system containing a molecular leak, respectively. In the case of a mixture, individual components were separated by GC. The model matrix components were still introduced through the batch inlet system.

The effect of methanol on reactant ion CH_5^+ and quasi-molecular ion of n-butyl benzoate (m/e 179) is shown in Figure 2. Even in typical CI conditions where the concentration of the reagent gas is one-thousandfold excess, the effect of solvent on the product ion is obvious even when 5% of CH_5^+ is depleted.

The effect of methanol on CH_5^+ and quasi-molecular ions of various components is GC analysis of mixture are shown in Figures 3 and 4. The reconstructed total ion chromatogram has not changed when 125 ngs/sec of methanol was added to the CI system. Similarly, the depletion of the reactant ion CH_5^+ due to the GC separated components are very comparable before and after the introduction of methanol, which is a technique reported by Munson and coworkers (1) for quantitation of GC separated components. As expected, the total reactant ion intensity was decreased when methanol was introduced. However, the intensities of the individual quasi-molecular ions have changed noticeably.

The effect of residual water and methanol desorbed from the solids probe on the reactant and product ions is demonstrated in Figure 5. Although no significant changes were observed in the reactant ion CH_5^+ when introduced n-butyl benzoate through the exponential dilution flask, drastic changes were noted when inserted a blank solids probe into the CI source. Water and other polar components are particularly very difficult to eliminate in the solids probe inlet.

In summary, 1) The degree of the matrix effect on fragmentation pattern and quantitation was found to be dependent on the types of the matrix components. 2) Extreme care has to be paid to the quantitation of a minor component in a complex mixture especially by the solids probe technique. 3) Simultaneous monitoring of the reactant and product ions as the method developed can be utilized in the assessment of the effect.

References

1. a). F. Hatch and B. Munson, Anal. Chem., 49, 169-174 (1977)
b). C. W. Polley, Jr. and B. Munson, Anal. Chem. 53, 308-312 (1981).

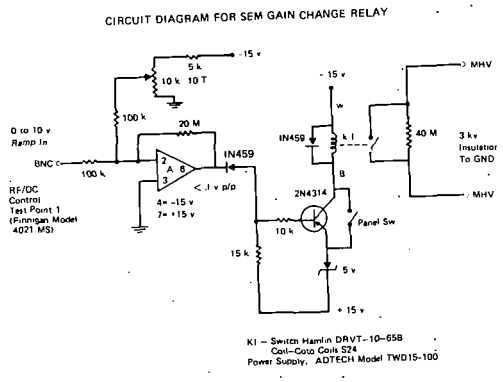

Fig. 1

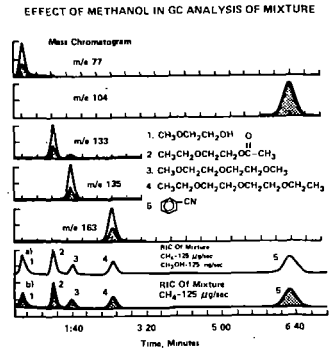

Fig. 3

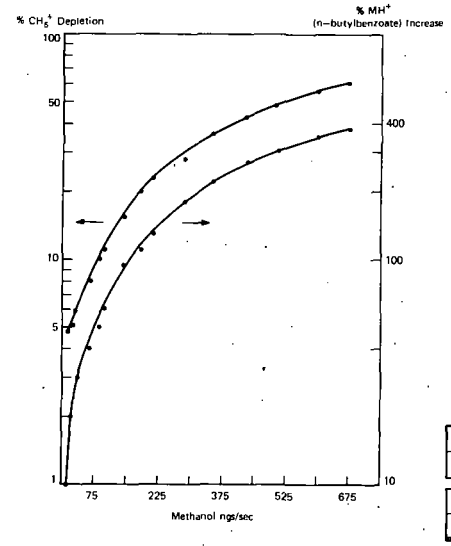

Fig. 2

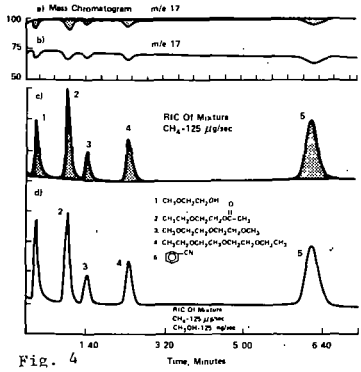

Fig. 4

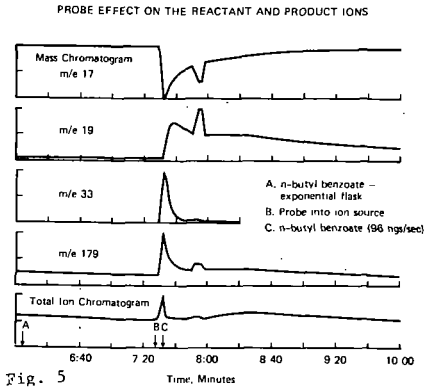

Fig. 5

RING AND SUBSTITUENT PROTONATION OF SUBSTITUTED ANILINES AND HYDRATION OF THE RESULTING IONS. Y. K. LAU, K. NISHIZAWA AND P. KEBARLE, Chemistry Department, University of Alberta, Edmonton, Canada T6G 2G2

The proton affinities of a number of substituted anilines were determined by measurement of proton transfer equilibria. Comparison of the proton affinities with measured core 1s nitrogen photoionization energies shows that, m-CN, m-CF_3, m-F, M-Cl, m-Br, M-I, o-NH_2, p-NH_2 and m-H are protonated on the amino group. m-SCH_3, m-OCH_3 and m-NH_3 are ring protonated. The proton affinities for N-protonation or ring protonation of m-CH_3, m-C_2H_5 and m-OH are close. The hydration equilibria $BH^+ + OH_2 = BHOH_2^+$ were measured for most of the protonated species discussed above. As expected, much more stable hydrates are observed for the N protonated species, since in these systems hydrogen bonding to H_2O is possible. Hydration of ring protonated species, whose proton affinities are only slightly lower, leads to a proton rearrangement so that the hydrate is protonated on the amino group. Isomers like m-NH_2 and p-NH_2 aniline which are ring and nitrogen protonated respectively, can be distinguished by their chemical ionization spectra in H_2O or NH_3. At a suitable temperature the NH_3 or H_2O adduct to the M + 1 ion will not be observed for the ring protonated species.

A complete account of the above investigations will appear under the same title in the Journal of the American Chemical Society towards the end of 1981.

DESORPTION CHEMICAL IONIZATION (DCI) WITH THE RIBERMAG R10-10 QUADRUPOLE MASS SPECTROMETER: APPLICATION TO THE DETERMINATION OF STEREOISOMERS OF 3-HYDROXY STEROIDS AND DERIVATIVES.

Pierre Tecon, Yutaka Hirano and Carl Djerassi
Dept. of Chemistry, Stanford University, Stanford CA 94305

INTRODUCTION

The Desorption Chemical Ionization (DCI) [1] is a rapidly growing technique which has shown its capability to bring towards mass spectral analysis thermally labile or non-volatile samples. Because the desorption rate from the filament is competitive with the fragmentation [1b], non-fragmented species (protonated molecular ions or adduct ions) are present in the DCI spectra of samples which would only display fragment ions under conventional introduction and ionization techniques. This fact may be of interest when the stereochemistry of the eliminated substituent has to be determined. As an example, the EI spectra of 3α- and 3β-acetate-Δ^5-cholesterol are identical [2], while their DCI spectra clearly show differences.

RESULTS

The following Table shows the results obtained for several pairs of epimers of 3-hydroxy steroids and derivatives under NH_3 DCI conditions.

TABLE

COMPOUND	A^+	P^+	$M^{+\cdot}$	S^+	E_1^+	$E_2^{+\cdot}$
Δ^5-3α-acetate cholesterol (EI)	0	0	0	0	0	100
Δ^5-3α-acetate cholesterol	100	8	0	4	20	25
Δ^5-3β-acetate cholesterol	100	0	0	13	30	27
5 H-3α-benzoate cholestanol	100	20	1	1	27	20
5 H-3β-benzoate cholestanol	100	38	2	1	22	24
Δ^5-3α-benzoate cholesterol	100	13	0	39	61	42
Δ^5-3β-benzoate cholesterol	100	0	0	22	60	35
Δ^4-3α-benzoate cholesterol	7	9	3	40	100	21
Δ^4-3β-benzoate cholesterol	1	0	3	18	100	9
19-nor-Δ^5-3α-benzoate cholesterol	99	100	1	12	15	47
19-nor-Δ^5-3β-benzoate cholesterol	100	1	0	14	23	26
Δ^5-3α-benzoate androsten-17-one	100	37	0	13	3	27
Δ^5-3β-benzoate androsten-17-one	100	0	0	12	12	14
Δ^4-3α-hydroxy cholesterol	6	1	16		100	1
Δ^4-3β-hydroxy cholesterol	2	2	22		100	3

A^+ : adduct ion $(M+NH_4)^+$
P^+ : protonated molecular ion $(MH)^+$
$M^{+\cdot}$: molecular ion
S^+ : substitution ion $(M-OR+NH_3)^+$
E_1^+ : elimination ion $(MH-HOR)^+$
$E_2^{+\cdot}$: elimination ion $(M-HOR)^{+\cdot}$

DISCUSSION

The first obvious characteristic of these results is that the spectra of the C-3 epimers are different when there is a double bond at C-4 or C-5. Indeed, the intensity of P^+ is higher for the 3α-compounds. This may be rationalized by a stabilizing interaction of the protonated substituent with the neighboring double bond. Such an interaction is not possible for a 3β-substituent, located farther from the double bond. Thus, providing the protonation is well controlled, and if there is no immediate elimination of the substituent, a priori determination of the configuration is possible.

Another important feature is the formation of the substitution ion S^+ by NH_3, and this only occurs when there is a double bond in the vicinity of the substitution center. This is in agreement with previous observations [3], even though the present results suggest a two step rather than a S_{N2} mechanism. Deuterated reagent gases, or high resolution MS is necessary to distinguish S^+ species from $M^{+\cdot}$ species if the substituent is hydroxy.

Finally, the $E_2^{+\cdot}$ elimination ion seems to be peculiar to our experimental conditions, as it is generally not observed in CI studies reported on similar samples.

EXPERIMENTAL

The spectra were measured with a Ribermag R10-10 quadrupole mass spectrometer using the SADR data system. Source pressure was typically 10^{-1} torr and the temperature was kept below 100C. The desorption filament was heated from 20 to 400 mA at 8 mA/s.

A more thorough account of this work will appear in Org. Mass Spectrom.

Financial support by NIH (Grant GM-28352) and by the "Fonds National Suisse pour la Recherche Scientifique) is gratefully acknowledged.

REFERENCES

1) a P.J. Arpino and G. Devant, Analusis, 7, 348 (1979)
b R.J. Cotter, Anal. Chem., 52, 1589A (1980)
2) L.G. Partridge and C. Djerassi, J. Org. Chem., 42, 2799 (1977)
3) J. Bastard, D. Do Khac, M. Fetizon and J. C. Tabet, submitted to J. Chem. Soc.

Factors Affecting Reactivity in Ammonia Chemical Ionization Mass Spectrometry, T. Keough and A. J. DeStefano, The Procter & Gamble Co., Miami Valley Laboratories, P.O. Box 39175, Cincinnati, OH 45247.

Ammonia chemical ionization (NH_3CI) mass spectrometry has recently emerged as a useful technique for the qualitative analysis of a wide variety of acid-labile compounds. Given the analytical utility of this ionization method, we decided to investigate some of the molecular factors that affect reactivity in NH_3CI. Factors selected for study include sample proton affinity, site of NH_4^+ attachment, site of protonation, and substituent effects.

To judge the extent to which proton affinity influences the formation of $M \cdot NH_4^+$ adduct ions, we measured the absolute intensities of the adduct ions formed from equimolar quantities of several compounds with proton affinities less than that of NH_3. The results, Fig. 1, indicate an increase in sensitivity by a factor of ~400 as the proton affinity increases from 182 kcal/mole (MeOH) to 197 kcal/mole (Et_2O).

The site of NH_4^+ attachment may override the influence of sample proton affinity as shown by the data in Table 1. All of the compounds listed have been previously studied by ICR[1], high-pressure mass spectrometry[2] or D_2O CI[3]. The series is reasonably well characterized as to the site of protonation (R=ring, S=substituent) with an acidic gas-phase reagent ion. We observe no NH_4^+ attachment to benzene, toluene, or 1,2,3-trimethyl benzene, compounds in which the ring is the most basic site, even though the proton affinities increase from 184 kcal/mole to ~198 kcal/mole. Benzonitrile, benzaldehyde, and acetophenone, all of which protonate on the substituent, exhibit intense $M \cdot NH_4^+$ adduct ions in NH_3CI. Interestingly, we observe no adduct ion formation for either phenol or anisole. We conclude, as did Kebarle[2], that the ring is the most basic site in these gaseous molecules.

Results obtained for a series of substituted anilines are summarized in Table 2. The previously determined sites of protonation[4] (R=ring, N=nitrogen) are also listed. The p-isomers of toluidine, anisidine, and phenylenediamine, all of which N protonate, exhibit reproducibly greater quantities of $M \cdot NH_4^+$ (relative to MH^+) than the m-isomers which are believed to ring protonate. Based on Kebarle's work[2], we expect that the hydrogen bond between NH_3 and the ring-protonated anilines would be much weaker than the hydrogen bond between NH_3 and the N-protonated anilines. However, this correlation is not perfect since m-and p-chloroaniline, both of which N protonate, do not yield detectable quantities of the $M \cdot NH_4^+$ adduct ion. Thus, kinetic factors may also be important.

The spectra of many compounds containing a good leaving group (X=halide, hydroxyl, alkoxy, etc) often exhibit intense $(M \cdot NH_4 - HX)^+$ ions, formed by a direct substitution reaction, in addition to the $M \cdot NH_4^+$ ions. For aromatic compounds, the extent of the substitution reaction depends not only upon the presence of a good leaving group but also upon substituent effects. This is illustrated by the data in Fig. 2 for a series of substituted benzyl alcohols. The compounds possessing an electron-donating substituent (p-Me, p-MeO, and p-OH) exhibit increased amounts of $(M \cdot NH_4 - H_2O)^+$ ions at the expense of $M \cdot NH_4^+$.

Differences in reactivity in NH_3CI may often be used to differentiate isomers. Isomers may be differentiated because of differences in proton affinities, differences in sites of NH_4^+ attachment or protonation, or because of differences in the electron donating/withdrawing properties of substituents in the m- vs. the o- and p-positions.

1. B. S. Freiser, et al., J. Am. Chem. Soc., 97, 6893 (1975).
2. Y. K. Lau and P. Kebarle, J. Am. Chem. Soc., 98, 7452 (1976).
3. D. P. Martinsen and S. E. Buttrill, Jr., Org. Mass Spectrom., 11, 762 (1976).
4. K. Summerhays, et al., J. Am. Chem. Soc., 99, 4585 (1977).
5. Y. Lau, et al., submitted to J. Am. Chem. Soc.

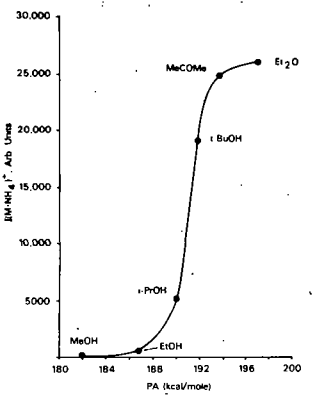

Figure 1: The variation in intensity of the $M \cdot NH_4^+$ adduct ion with sample proton affinity.

Table 1: The correlation between site of NH_4^+ attachment and site of protonation in aromatic compounds.

Compound	Proton Affinity (kcal/mole)	Site of Protonation	NH_4^+ Attachment
Benzene	183.7	R	No
Toluene	190.0	R	No
1,2,3 Trimethyl-benzene	198.0	R	No
Phenol	194.6	R,S	No
Anisole	199.4	R,S	No
Benzonitrile	194.7	S	Yes
Benzaldehyde	198.7	S	Yes
Acetophenone	203.1	S	Yes

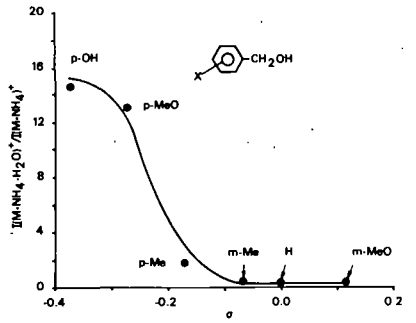

Figure 2: The effect of electron donating ability (σ) on the formation of $(M \cdot NH_4 - H_2O)^+$ in the NH_3 CI spectra of benzyl alcohols.

Table 2: Correlation between the site of protonation and adduct ion formation for substituted anilines.

Compound	Proton Affinity (kcal/mole)	Site of Protonation	$\frac{(M \cdot NH_4)^+}{MH^+}$
Aniline	208.9	N	0.22
m-Toluidine	211.6	R	0.15
p-Toluidine	211.6	N	0.60
m-Anisidine	214.0	R	0.00
p-Anisidine	212.3	N	0.51
m-Phenylenediamine	221.1	R	0.00
p-Phenylenediamine	-	N	0.31
m-chloroaniline	205.9	N	0.00
p-chloroaniline	206.9	N	0.00

FINGERPRINTING OF NATURAL FAT SAMPLES (TRIGLYCERIDES) BY THE DCI TECHNIQUE; M. HOEHN AND U. RAPP, Varian MAT GmbH, Barkhausenstr. 2, D-2800 Bremen 14, W. Germany.
E. SCHULTE, Institut für Lebensmittelchemie der Westfälischen Wilhelms-Universität, Piusallee 7, D-4400 Münster/Westf., W. Germany.

To identify and characterize a fat sample or to determine unaccustomed additions, the fatty acid pattern was hitherto used for analysis. However, the more reliable way obviously is to analyze the triglyceride pattern itself.
The analytical separation of triglycerides has been performed moreover by GC, TLC and HPLC. All the methods mentioned comprise significant draw backs such as insufficient separation or low sensitivity or unadequate and indefinitive attribution of components.

The DCI technique enables one to deduce triglyceride pattern of fat samples without prior separation. According to the C number and the number of double bonds the separation is achieved. The samples are introduced into the ion source of the mass spectrometer by means of a special DCI sample rod, permitting a fast and reproducible total evaporation. The spectra acquired during the evaproation process are summed up to yield one spectrum representative of the fat sample.
The total sample-spectrum can be used for fingerprinting of different varieties of fat.
Examples will be presented where natural cocoabutter is compared with commercial products containing besides the natural also substitute fats.
Furthermore the easy differentiation e.g. of lard and beef-suet will be explained.

Some Applications of Ammonia Chemical Ionization Mass Spectrometry, A. J. DeStefano and T. Keough, The Procter & Gamble Co., Miami Valley Laboratories, P.O. Box 39175, Cincinnati, Ohio 45247

Isobutane chemical ionization ($i\text{-}C_4H_{10}CI$) has proven to be a very useful technique for the analysis of oxygen-containing compounds. However, we have encountered a number of acid-labile oxygen-containing compounds for which ammonia chemical ionization (NH_3CI) provided complementary or additional structural information. We present several examples below.

Figure 1 compares the $i\text{-}C_4H_{10}$ and NH_3CI spectra of the t-butyl perester of octanoic acid. The perester is protonated by $C_4H_9^+$, but the resulting product is unstable and we observe only the $OC(CH_3)_3^+$ ion. In contrast, the ammonia CI spectrum shows the $(M+NH_4)^+$ ion as the base peak and allows the molecular weight of the perester to be determined.

The same result is observed in Figure 2, which compares the $i\text{-}C_4H_{10}$ and NH_3CI spectra of an endoperoxide. The isobutane spectrum is dominated by fragments corresponding to the loss of water and HOOH from the MH^+ ion. On the other hand, NH_4^+ does not protonate the endoperoxide and the $(M+NH_4)^+$ adduct ion dominates the NH_3CI spectrum.

The insertion of a double bond in the ring of the above endoperoxide results in an increased proton affinity and a markedly different NH_3CI spectrum (Figure 3). A small MH^+ ion is observed in addition to a large $(M+NH_4)^+$ ion. The spectrum shows substantial fragmentation, and the fragmentation pattern is similar to that observed in the $i\text{-}C_4H_{10}CI$ spectrum.

Figure 4 shows the CI spectra obtained for the acetate derivative of a compound resulting from autoxidation of a methyl linoleate photooxidation product. The NH_3CI spectrum shows some MH^+ ion, but is dominated by the $(M+NH_4)^+$ ion. In contrast, the $i\text{-}C_4H_{10}CI$ spectrum contains large fragment ions corresponding to losses of acetic acid, acidic acid plus water, and acetic acid plus methanol from the MH^+ ion.

We have studied a number of other methyl linoleate oxidation products by NH_3CI, including secondary alcohols and hydroperoxides. In general, when compared to the i-butane CI spectra, the NH_3CI spectra show more intense ions in the molecular ion region and reduced fragmentation. However, all these compounds are quite thermally labile and the spectra can change rapidly as a function of time. In most cases we find that the ions in the molecular ion region are enhanced very early in the analysis and when the direct insertion probe is rapidly heated.

Finally, Figure 5 shows the NH_3CI and $(CH_3)_2NH$ CI spectra of a polyol containing two $C(C_6H_5)_3$ blocking groups. The NH_3CI (and the i-butane CI) spectrum shows only the $C(C_6H_5)_3^+$ ion at m/z=243. Using dimethyl amine, which is considerably more basic, as the reagent gas leads to an ion at $(M+(CH_3)_2NH_2)^+$ and molecular weight information can be obtained.

We conclude that the $(M+NH_4)^+$ adduct ion can provide useful molecular weight information for many acid-labile compounds whose proton affinities are less than that of NH_3 ($PA(M)<PA(NH_3)$). If $PA(M)>PA(NH_3)$, NH_4^+ addition can still compete favorably with protonation and provide molecular weight information in some cases. If no $(M+NH_4)^+$ ion is observed, a more basic reagent gas might provide the required molecular weight information.

Acknowledgements

We gratefully acknowledge the assistance of E. D. Mihelich, D. W. Bjorkquist and J. P. Brown in providing us with the purified synthesized compounds used in this study.

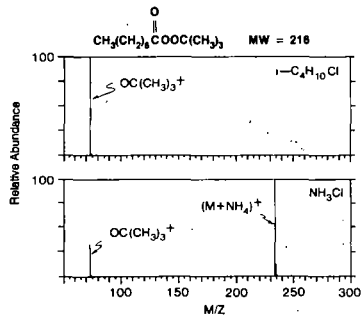

Fig. 1

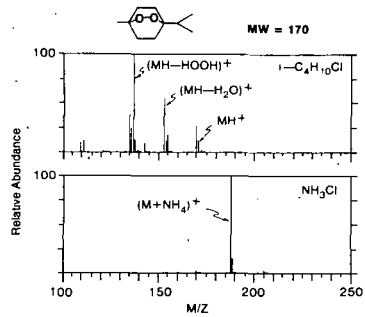

Fig. 2

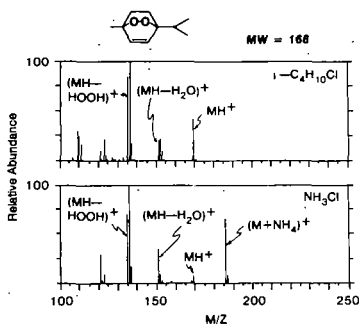

Fig. 3

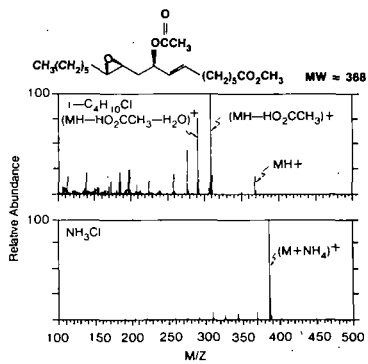

Fig. 4

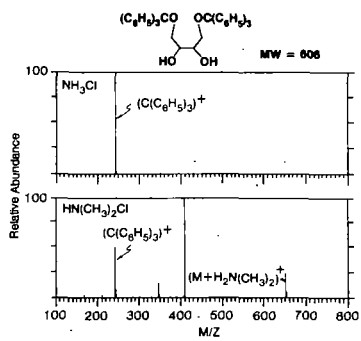

Fig. 5

METHYL CATION TRANSFER REACTIONS

Karl Blom and Burnaby Munson
University of Delaware
Newark, Delaware 19711

The cyclic halonium ions are well established species in electron ionization mass spectrometry and the di-alkylhalonium ions have been prepared by ion/molecule studies, although little work has been reported on the reactions of these ions themselves.[1] Our work shows that the dimethylhalonium ions, $(CH_3)_2Cl^+$ and $(CH_3)_2Br^+$, react with many organic compounds by what appears to be a methyl cation transfer reaction to give $(M + CH_3)^+$ ions.

The known reactions in methyl chloride are sufficiently rapid that $(CH_3)_2Cl^+$ is the dominant species in the source of our mass spectrometer at pressures greater than about 0.3 torr:

$$CH_3Cl^+ + CH_3Cl \longrightarrow CH_3ClH^+ + CH_2Cl \qquad (1)$$

$$CH_3ClH^+ + CH_3Cl \longrightarrow (CH_3)_2Cl^+ + HCl \qquad (2)$$

The reactions of the primary ions of CH_3Br with CH_3Br are relatively slow. However, $(CH_3)_2Br^+$ can be obtained as the major ion at high pressures of a CH_4/20% CH_3Br mixture.

$$CH_5^+ + CH_3Br \longrightarrow CH_3BrH^+ + CH_4 \qquad (3)$$

$$CH_3BrH^+ + CH_3Br \longrightarrow (CH_3)_2Br^+ + HBr \qquad (4)$$

Reactions have been observed to give $(M + CH_3)^+$ ions with alcohols, ethers, aldehydes, ketones, acids, esters, nitriles, and nitro-compounds from both $(CH_3)_2Cl^+$ and $(CH_3)_2Br^+$. Some apparently exothermic methyl cation transfer reactions, however, seem to occur very slowly, if at all: $(M + CH_3)^+$ ions were not observed with benzene, 1-decene, bromobenzene, and butyl bromide. Endothermic methyl cation transfer reactions are not observed under our experimental conditions.

The methyl cation affinity is defined in the usual way as the negative enthalpy of the reaction:

$$M + CH_3^+ \longrightarrow MCH_3^+$$

For a few compounds, heats of formation data are available for the $(MCH_3)^+$ species from ionization or appearance potential measurements and methyl cation affinities can be readily calculated for M:

$$MCA(M) = \Delta H_f(M) + \Delta H_f(CH_3^+) - \Delta H_f(MCH_3^+) \qquad (5)$$

In other cases, water and alcohols, amonia and primary and secondary amines, and acids, the methyl cation affinity can be obtained from the proton affinity of the next homolog in the series. That is, the methyl cation affinity of water can be obtained from the proton affinity of methanol, since both involve the species, $CH_3OH_2^+$. Similarly, the methyl cation affinity of methanol can be obtained from the proton affinity of dimethyl ether, since they both involve the species, $(CH_3)_2OH^+$.

$$MCA(HX) = PA(CH_3X) + \Delta H_f(HX) - \Delta H_f(CH_3X) + \Delta H_f(CH_3^+) - \Delta H_f(H^+)$$

The proton affinities of other species (ethers, ketones, alkyl halides) can only be obtained from ion/molecule reactions -- either from reaction kinetics or from equilibrium measurements.

The methyl cation affinity of CH_3Br has been estimated by the bracketing technique: 82 kcal/mole $\lesssim$ MCA(CH_3Br) $\lesssim$ 86 kcal/mole. Preliminary experiments place MCA(CH_3Cl) between 67 and 78 kcal/mole. The order of methyl cation affinities can be readily established for many compounds from the observed methyl cation transfer reactions. Some caution must be exercised in the interpretation of these data since some exothermic methyl cation transfer reactions apparently occur very slowly for reasons that are yet obscure.

Many of the methyl cation transfer reactions are obviously rapid, but we have no data yet on the absolute rate constants for any of these reactions. A few experiments have been done to determine relative rate constants from the technique of Reactant Ion Monitoring[2] and some preliminary data are reported in Table I. Additional experiments are planned.

Table I. Relative Rate Constants

Compound	$k/k_{acetone}$
Benzonitrile	1.6
Acetone	1.0
Cyclohexanol	0.8
n-Butylbromide	0.1
Cyclohexane	0.0

Mixtures of CH_4 with alkyl halides may prove useful in obtaining molecular weight information for alcohols and ethers in CIMS. Methyl cation affinity data can give heats of formation of ions which could not be obtained previously.

---

[1]Beauchamp, J.; Holtz, D.; Woodgate, S.; Patt, S. J. Am. Chem. Soc., 1972, 94, 2798-2807.

[2]Hatch, F.; Munson, B. J. Phys. Chem., 1978, 82, 2362-2369.

INFRARED TWO-LASER PHOTODISSOCIATION SPECTROSCOPY OF VAN DER WAALS CLUSTERS USING MASS SPECTROMETRIC DETECTION

Mark Hoffbauer, Kopin Liu, W.R. Gentry, and C.F. Giese
Chemical Dynamics Laboratory
Department of Chemistry and Physics
University of Minnesota
Minneapolis, Minnesota 55455

The infrared photodissociation dynamics of van der Waals clusters present simple systems for studying intramolecular energy transfer [1]. Typical van der Waals bonds are so weak that the absorption of a single CO_2 laser photon will provide enough energy to dissociate the cluster. The unimolecular decomposition process then occurs from a relatively well defined initial state in contrast to studies involving either chemical activation or infrared multiphoton dissociation. The rate of unimolecular dissociation is determined by the rate of intramolecular energy transfer from the excited monomer mode to the much lower frequency van der Waals bond vibration.

We have used a pulsed, line-tunable CO_2 TEA laser to study the photodissociation dynamics of the van der Waals clusters $(C_2H_4)_2$, $(C_2D_4)_2$, $(C_2H_4)\cdot(C_2D_4)$, $(OCS)_2$, $(OCS)_3$, $Ar\cdot OCS$ $(CH_3OH)_2$, and $(CH_3OH)_3$ using a unique pulsed molecular beam apparatus which is described in detail elsewhere [2,3]. Briefly, a pulsed molecular beam source (~20 μ sec fwhm) is operated with several atmospheres pressure of He or Ar seeded with a small amount (typically 0.1%-10%) of the desired monomer species. The source conditions are adjusted so as to maximize the concentration of the desired clusters while keeping the concentration of interfering clusters low. The molecular beam pulse is collimated and crossed with the unfocused output of the CO_2 laser. Photodissociation is detected as the laser induced change in the mass spectrum of the appropriate van der Waals cluster. Measurements of attenuation as a function of laser pulse energy at fixed frequency suggest that the dynamics are that of a single-photon absorption followed by rapid dissociation of the clusters into monomer fragments.

Attenuation of the molecular beam as a function of laser frequency at fixed laser energy yields the photodissociation spectra of the complexes. This is shown in Fig. 1 for $(C_2H_4)_2$ and $(C_2D_4)_2$. The peak absorption frequencies are close to those of the gas-phase monomers, with small shifts similar to those observed in liquids and solids of the same species. However, the observed linewidths are much wider than can be accounted for by either power broadening or rotational structure of the dimer. By using two lasers, one at a fixed frequency near the center of the absorption peak and the other scanning over the absorption peak at fixed laser energy, it is possible to determine that the entire linewidth of the dissociation spectra must be due to homogeneous broadening. This is

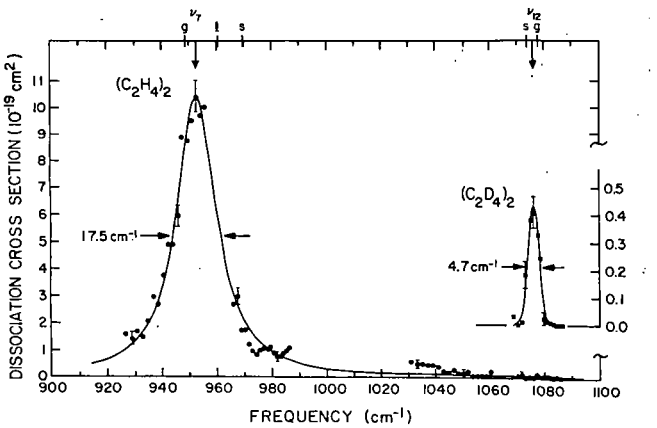

Fig. 1 Infrared photodissociation spectra of $(C_2H_4)_2$ and $(C_2D_4)_2$.

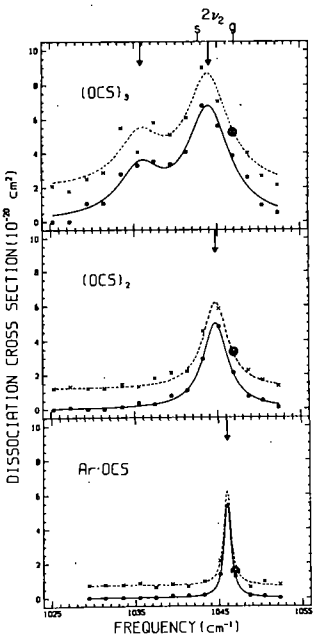

Fig. 2 Dissociation spectra of OCS clusters. The solid line is the best Lorentzian fit to the single laser data (o). The dashed line is the solid line scaled to fit the two laser data (x). The fixed laser frequency is indicated by ▣. The laser energies were both ∿0.4 J/cm^2.

illustrated in Fig. 2 for clusters of OCS. Similar results have been obtained for $(C_2H_4)_2$, $(C_2D_4)_2$, $(C_2H_4)\cdot(C_2D_4)$ and $(CH_3OH)_2$. Such broad, Lorentzian bandshapes are characteristic of lifetime-broadened transitions, implying, for example, that the lifetime of the state excited in $(C_2H_4)_2$ is about 3×10^{-13} seconds.

Additional information on the dissociation process is provided by our measurements of the speed and angle distribution of the monomer products, as shown in Fig. 3 for the photodissociation of $(C_2H_4)_2$. From these data it is found that the average product translational energy is small, leaving most of the energy available to the products in internal excitation. The angular distribution is isotropic in center of mass coordinates implying a dissociation lifetime longer than one rotational period of the excited cluster (∿10^{-11} seconds for $(C_2H_4)_2$).

In order to reconcile the two apparent lifetimes we conclude that the decay rate of the state prepared by the laser with respect to anharmonic intramolecular energy transfer and/or dephasing occurs on a picosecond (.3-5×10^{-12} second) timescale as the dissociation spectra indicate. However, the actual dissociation lifetime is probably several orders of magnitude longer (10^{-11}-10^{-10} seconds) as the angular distribution measurements suggest.

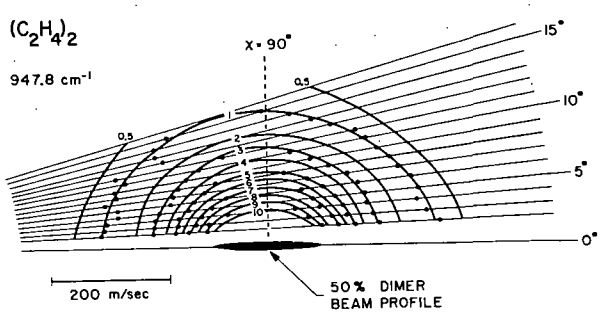

Fig. 3 Center of mass contour map representing the speed and angular distribution of C_2H_4 from the photodissociation of $(C_2H_4)_2$

References

1. T.E. Gough, R.E. Miller and G. Scoles, J. Chem. Phys. 69, 1588(1978); J. Opt. Soc. Am. 68, 694(1978)
2. W.R. Gentry and C.F. Giese, J. Chem. Phys. 67, 5389(1977); Phys. Rev. Lett. 39, 1259(1977); Rev. Sci. Instrum. 49, 595(1978)
3. Mark A. Hoffbauer, Kopin Liu, W.R. Gentry, and C.F. Giese, J. Chem. Phys. (to be published)

THE MAGNITUDE OF COLLISIONAL EXCITATION OF IONS MEASURED AS A FUNCTION OF ION ENERGY, TYPE OF COLLISION GAS AND GAS PRESSURE. I.W.Griffiths, E.S.Mukhtar, R.E.March,* F.M.Harris and J.H.Beynon. Royal Society Research Unit, University College of Swansea, Singleton Park, Swansea SA2 8PP, U.K.

This investigation was undertaken to obtain accurate values for the average increase in internal energy of ions as the result of excitation in collisions with neutral gas molecules. Calibration data were used from photodissociation studies in which ions are photoexcited using photons of known energy. When the molecular ion of n-butylbenzene is photoexcited,[1] for example, two competing reactions take place :-

$$C_{10}H_{14}^{+\cdot} \rightarrow C_7H_7^{+} + C_3H_7^{\cdot}$$
m/z 134 m/z 91

and

$$C_{10}H_{14}^{+\cdot} \rightarrow C_7H_8^{+\cdot} + C_3H_6$$
m/z 134 m/z 92

which have critical energies[2] of 2.6 eV and 1.4 eV respectively. The relative magnitudes of the peaks due to 91^+ and 92^+ ions are very sensitive to the photoexcitation energy and thus provide an accurate and sensitive measure of the effect of changing the ions' internal energy. These results, and similar results for n-pentylbenzene molecular ions, have been used in the present study to provide calibration data for ions excited in collisions with gas molecules. The ratios of peak heights resulting from the above competing reactions for collisionally excited ions are measured and compared with the data from photoexcitation studies.

The experiments were performed on a ZAB-2F spectrometer using a collision cell situated just after the intermediate slit in the second field-free region. Gas pressures in the cell were not measured directly but a constant fraction ($\sim 10^{-3}$) of their values obtained by measuring the pressure above a diffusion pump situated below the field-free region. Since unimolecular dissociation can contribute strongly to the 92^+ fragment-ion currents, spectra acquired without collision gas were subtracted from those obtained with gas in the cell. The gain of the electron multiplier was adjusted to allow for any reduction of the main beam of ions due to scattering.

Helium and nitrogen collision gases were used. The dependence of collisional excitation on the translational energy of the ions was first studied using low gas pressures. A stronger dependence on ion energy was found for N_2 than He. For n-butylbenzene ions, for example, the collisional excitation increased from 2.2 to 2.5 eV for a change in ion energy from 2 to 8 keV. For helium, it remained at about 2.4 eV over the same translational energy range.

A study of the effect of gas pressure was made by working at one translational energy of 5 keV. Below about 5×10^{-6} torr gauge reading, the collisional excitation was found to be independent of pressure and the same for N_2 and He collision gas. The constant values were 2.3 ± 0.1 eV for n-butylbenzene ions and 2.6 ± 0.1 eV for n-pentylbenzene. Above 10^{-5} torr, however, the collisional excitation increases rapidly with increase in pressure. This effect may be due to either an increased probability of closer and thus more energetic ion-neutral particle interactions or to ions on average undergoing more than one collision with neutral particles in traversing the collision region. The results also show that, at any pressure between 10^{-5} and 10^{-4} torr, collisions involving nitrogen molecules result in larger inputs of excitation energy than collisions with helium atoms.

References.

1. E.S.Mukhtar, I.W.Griffiths, F.M.Harris and J.H.Beynon, Int.J.Mass Spectrom. Ion Phys. 37, 159, 1981.

2. P.Brown, Org.Mass Spectrom. 3, 1175, 1970.

* Permanent address : Department of Chemistry, Trent University, Peterborough, Ontario, Canada.

A STUDY OF THE FRAGMENTATION OF METASTABLE H_2S^+ IONS.

M.F. Jarrold, A.J. Illies, and M.T. Bowers
Department of Chemistry, University of California
Santa Barbara, California 93106

Hydrogen sulphide molecular ions undergo unimolecular fragmentation via reaction 1

$$H_2S^+ \rightarrow S^+ + H_2 \quad (1)$$

In addition to an abundent fragment ion in the mass spectrum there is also an intense metastable arising from the slow unimolecular reaction of H_2S^+ ions with internal energy close to the thermochemical threshold. The existence of this metastable cannot be explained by statistical theories since the theoretically predicted lifetime is too short. Experimental evidence suggests the S^+ ion arises from the predissociation of H_2S^+ in the first excited $^2A_1$ electronic state [1] to produce ground state S^+ and H_2. In the fragmentation of metastable H_2S^+ the available energy is insufficient to rotationally excite the product H_2 [2]. Thus this energy must be partitioned between the relative kinetic energy of the products and the rotational energy of the H_2. Since the rotational constant for H_2 is large the number of available rotational levels is also severly limited and H_2 can carry away relatively large amounts of rotational energy for low angular momentum.

We report here the results of a study of the metastable reaction using mass analyzed ion kinetic energy spectrometry (MIKES). Kinetic energy release distributions have been derived from the MIKES peaks. Resolved structure is evident in the release distributions. When the metastable reaction is assigned to the specific H_2S^+ ($^2A_1$) vibronic levels (known from fluorescence lifetime measurements to lie in the metastable lifetime range), good correlation is found between the position of the structure in the distributions and predicted transition energies for products in which the H_2 molecule occupies specific rotational quantum states. An example is shown in Fig. 1. The data indicate that substantial rotational excitation of the product is occuring. The average kinetic energy release in the metastable reaction was found to increase with ion source temperature. This is ascribed to the release of the increased rotational energy of the H_2S^+ as relative kinetic energy of the products.

A comparison between our data for the metastable reaction and the PIPECO data [1] shows that the percentage of the available energy partitioned into rotational energy decreases as the available energy increases. We suggest that the most likely mechanism for rotational excitation of the H_2 is due to the partitioning of the thermal angular momentum for rotation about the symmetry axis predominently into H_2 rotational angular momentum. The fact that a larger proportion of the available energy is partitioned into kinetic energy as the energy is raised is because only the thermal angular momentum is available for rotational excitation of the products.

There is at present no convincing explanation for why the reaction is slow near threshold. We propose that the metastable reaction occurs on a different set of potential surfaces than the fast reaction at energies significantly above threshold. Instead of undergoing predissociation from the $^2A_1$ state (which is not possible for energetic reasons close to threshold) the ion undergoes a slow transition to the $^2B_1$ ground state induced by Renner-Teller coupling and then rapidly predissociates.

References

1. J.H.D. Eland, Int. J. Mass Spectrum Ion Phys. 31 (1979) 161.
2. E.G. Jones, J.H. Beynon, and R.G. Cooks, J. Chem. Phys. 57 (1972) 3207.

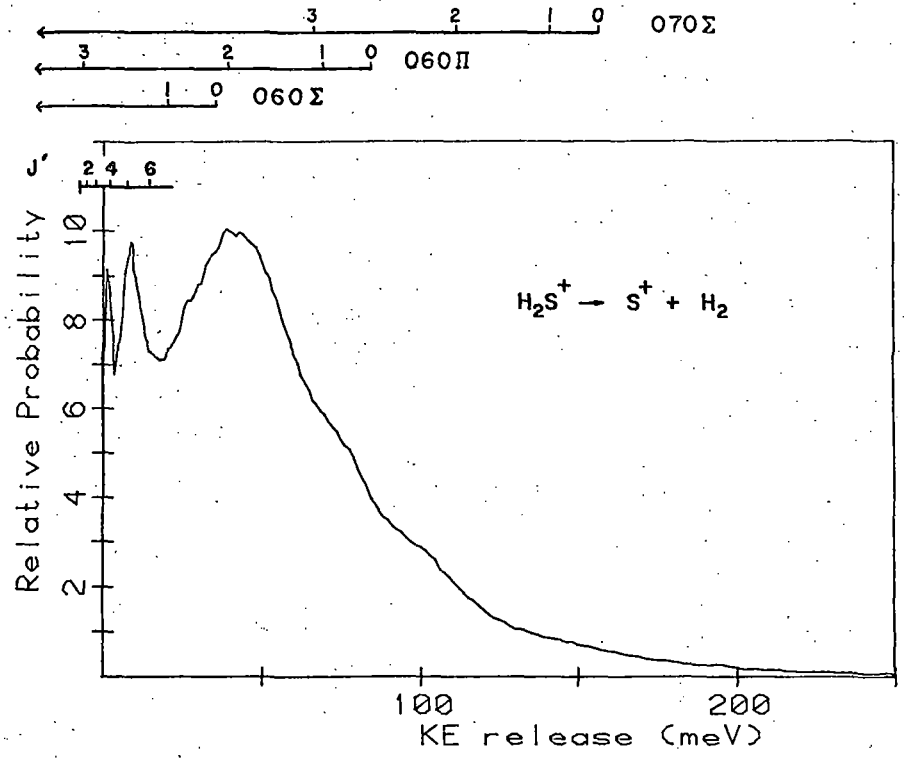
3
2
1
0
070Σ
3
2
1
0
060Π
1
0
060Σ
J'
2 4 6
Relative Probability
2
4
6
8
10
$H_2S^+ \rightarrow S^+ + H_2$
100
200
KE release (meV)

FIGURE I

THE UNIMOLECULAR DECOMPOSITION RATES OF ENERGY SELECTED METHYLNITRITE IONS

J.P. Gilman, T. Hsieh and G.G. Meisels, Department of Chemistry, University of Nebraska, Lincoln, Nebraska 68588

It has been recently shown that the fragmentation of the methylnitrite ion to NO^+ (m/e 30) and CH_3O^+ (m/e 31) occurs from non-interconverting electronic states (1) and is thus an exception to a common assumption made when the widely accepted statistical theory of mass spectra is applied to larger organic ions. We report here measurements of the fragmentation rate constant yielding the NO^+ and CH_3O^+ ions as a function of internal energy based on time-of-flight (TOF) spectra produced in our threshold photoelectron-coincident photoion mass spectrometer (TPE-CPI MS).

The TPE-CPI apparatus has been described previously (2); metastable and collision-induced dissociation (CID) processes were investigated using a triple sector (EBE) mass spectrometer (Kratos MS50-TA). Both methylnitrite and deuterated methylnitrite were synthesized by dripping stoichiometric amounts of dilute sulfuric acid into a cold solution of sodium nitrite and methanol (CD_3OD was used for CD_3ONO). The escaping gas was passed through a concentrated solution of NaOH to remove NO_2 and through a $CaCl_2$ drying tube; it was collected at -77°C. Bulb to bulb distillation was repeated several times before the product was stored in a dry ice-acetone bath in the dark. Mass spectral, IR, and NMR analysis were performed to insure purity of these products.

Decay lifetimes were obtained by fitting calculated TOF curves based on a single unimolecular dissociation rate constant for each product ion to the experimental curves, adjusting the rate constant until the best fit was obtained. An ion TOF curve for methylnitrite at 10.836 eV (Fig. 1) clearly shows asymmetric peak broadening for CH_3O^+ ion. Symmetric peak broadening also occurs corresponding to a kinetic energy release (KER) of 53 meV; it does not contribute significantly to asymmetric peak broadening observed for CH_3O^+. Decay lifetimes from the calculated TOF curves at this energy were at least five times faster for NO^+ formation than for CH_3O^+ formation. Verification that mass 31 was CH_3O^+ and not HNO^+ was obtained using CD_3ONO in which DNO^+ intensities were not seen at energies up to 1 eV above the threshold of CD_3O^+ (m/e 34) ion formation indicating that HNO^+ has no significant intensity in the same energy region examined. The breakdown graph of CH_3ONO, and the HeI PES are shown in Fig. 2. It can be seen that at energies where there is a significant CH_3O^+ relative abundance there is also overlap of the electronic states in the PES indicating that two electronic states are being populated in that energy region. The onset of CH_3O^+ is at 10.69 eV, 0.31 eV higher than the parent ion threshold, and the relative abundance of CH_3O^+ reaches about 60% at 10.87 eV.

The ion TOF curves for CD_3ONO (Fig. 3) are very similar to those of methylnitrite. Asymmetric broadening is observed for CD_3O^+ (m/e 34) fragment and again the KER was small (70 meV). The rate constants for NO^+ formation were found to be at least 10 times larger than those for CD_3O^+ formation between 10.83 and 11.78 eV. The breakdown graph of CD_3ONO^+ (Fig. 4) shows that the relative intensity of CD_3O^+ at its maximum is 5% (at 11.00 eV). Although the breakdown graph of CD_3ONO has not been corrected for the transmission of energetic electrons through the TPE detector (see MAMOB7) this correction would not affect the relative abundance of CD_3O^+ by more than a few percent and does not account for the difference observed between the CD_3O^+ and CH_3O^+ breakdown curves.

Theoretical and experimental evidence on most molecules indicates that near the threshold the rate constant of a given decomposition process rises rapidly with increasing internal energy and levels off at higher energies. This phenomenon is observed with the rate consant for NO^+ formation from both CH_3ONO and CD_3ONO (Fig. 5) where the rate constant changes from 0.0 to $\geq 1.0 \times 10^7$ sec^{-1} within a few meV. However, the rate constant for formation of CH_3O^+ formation has a value of 1×10^6 sec^{-1} over an energy range of 0.13 eV and starts to rise only slowly with internal energy ($k = 2.5 \times 10^6$ sec^{-1} at 0.65 eV). In CD_3ONO this rate constant is 1.0×10^6 sec^{-1} and remains at this value over an energy range of 0.95 eV. Relative population changes in the syn and anti rotational isomers in CH_3ONO and CD_3ONO which rapidly interconvert at room temperature cannot be responsible for the large differences observed in the behavior of the rate constants because preliminary studies have indicated that there is no significant relative population change in these isomers on deuteration. We are currently continuing our investigation on methyl and deuterated methylnitrite to gain a better understanding of these systems.

This investigation was supported in part by the Department of Energy under contract #DE-AS02-76ER0257 and the National Science Foundation through the regional facility at the University of Nebraska. The authors also wish to express their thanks to Mr. Pradip R. Das for his assistance in preparing the manuscript.

REFERENCES:

1. G.G. Meisels, T. Hsieh and J.P. Gilman, J. Chem. Phys., **73**, 4126 (1980). 2. (a) C.F. Batten, J.A. Taylor and G.G. Meisels, J. Chem. Phys., **65**, 3316 (1976); (b) C.F. Batten, J.A. Taylor, B.P. Tsai and G.G. Meisels, J. Chem. Phys., **69**, 2417 (1978).

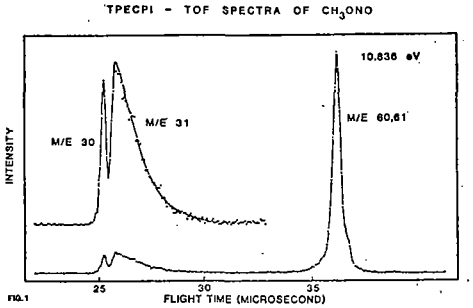

FIG.1

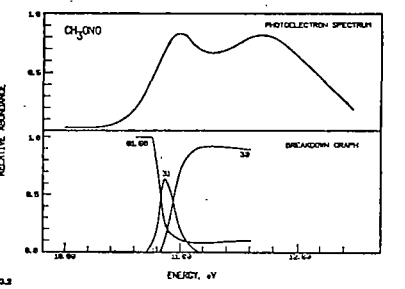

FIG.2

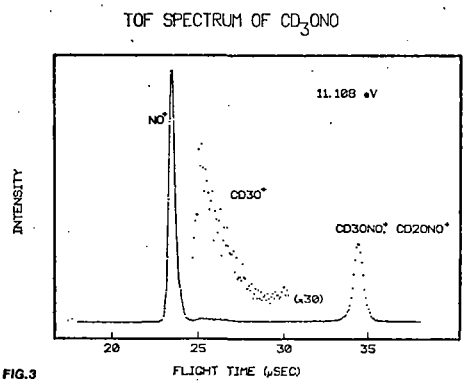

FIG.3

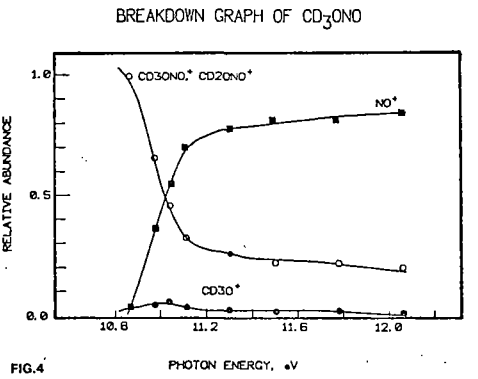

FIG.4

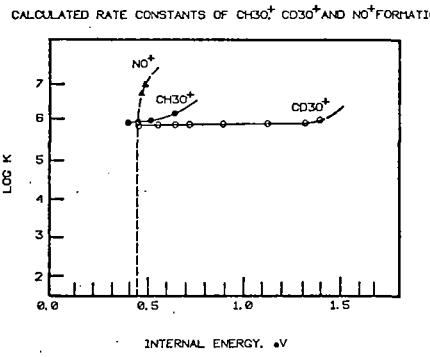

FIG.5

Resonance Effects in the Angular Distributions and Branching Ratios of the Photoelectrons in C_2H_2 and C_2N_2

Albert C. Parr[†] and D. L. Ederer
SURF-II, National Bureau of Standards
Washington, D.C. 20234

John B. West*
Daresbury Laboratory
Science Research Council
United Kingdom

J. L. Dehmer**
Argonne National Laboratory
Argonne, Illinois 60439

The angular distributions of the vibrationally resolved photoelectron spectra of acetylene and cyanogen have been measured over the photon energy range of 15 eV to 26 eV. The asymmetry parameters for the vibrationally resolved electronic states and the unresolved electronic bands show structure which is interpretable as shape resonance effects. This work will be compared to other recent work on angle resolved photoelectron spectra. The completed study will be published in the literature.

[†]Work supported in part by the Office of Naval Research, Washington, D.C.
*Work supported in part by a NATO grant.
[†]**Work supported in part by the Department of Energy, Washington, D.C.

THE DYNAMICS OF $C_3H_6O^{+\cdot}$ DISSOCIATION

C. Lifshitz and E. Tzidony
Department of Physical Chemistry
The Hebrew University of Jerusalem, Jerusalem 91904, Israel

Kinetic energy release distributions (KERDs) were determined from metastable peak shapes for the reaction,

$$C_3H_6O^{+\cdot} \longrightarrow C_2H_3O^{+} + CH_3\cdot \qquad (1)$$

of the enol ion of acetone and some of its deuterium and carbon-13 labelled analogues. Two methyl losses are possible — one involves the original methyl of the enol ion and the other is made up of the original methylene and the enolic hydrogen. The KERDs were observed to be bimodal for both cleavages and of different shapes for the losses of the two methyl groups [1]. The kinetic energy release for the methyl cleavage involving the enolic hydrogen is invariably higher than for the other methyl group. Thus, for the ^{13}C-labelled ions [2] $T_{\frac{1}{2}}$ values are (in meV),

	$^{13}CH_3$	$^{12}CH_3$
$H_2C = C(OH)^{+\cdot}{}^{13}CH_3$	59.4	71.5
$H_2{}^{13}C = C(OH)^{+\cdot}CH_3$	74	62.2

Kinetic energy releases for reaction (1) of the enol ion were observed to be different from those obtained for acetone ions with the same amount of total energy, as obtained [3] by PIPECO.

Kinetic energy release distributions have been calculated for reaction (1) using Klots' reformulated Quasiequilibrium Theory [4] and were employed as prior expectations for surprisal calculations [5]. A surprisal plot is shown in Figure 1; two different slopes are clearly observable.

The non-statistical behavior of the enol ion system is ascribed to the formation of a short-lived (5×10^{-13} sec) acetone ion intermediate, in which internal energy is not randomized. The study of the possible formation of $C_2H_3O^{+}$ ions other than acetyl ions via reaction (1) is being pursued [6].

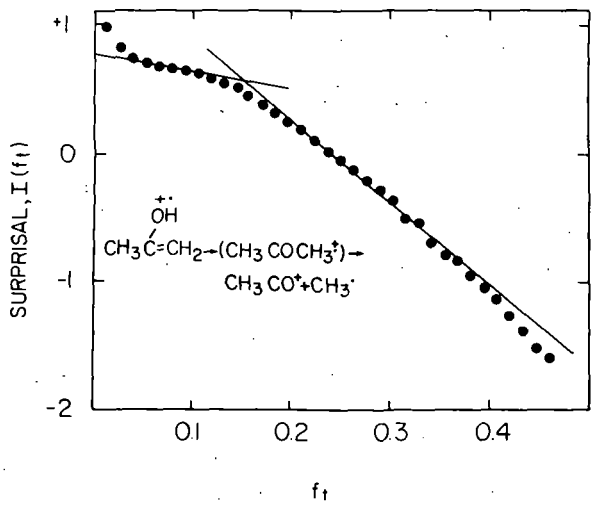

Figure 1

Kinetic energy distribution surprisals
(f_T is the fraction of the total available energy
in the products which appears as translational motion)

REFERENCES

1. C. Lifshitz and E. Tsidony, Int. J. of Mass Spectrom. & Ion Phys., in press; C. Lifshitz, E. Tsidony, D.T. Terwilliger and C.E. Hudson, Adv. Mass Spectrom., 8A, 859 (1980).
2. G. Depke, C. Lifshitz, H. Schwarz and E. Tzidony, Angew. Chemie, in press.
3. D.M. Mintz and T. Baer, Int. J. Mass Spectrom. Ion Phys., 25, 39 (1977).
4. C.E. Klots, J. Phys. Chem., 75, 1526 (1971); Z. Naturforsch. A27, 553 (1972); J. Chem. Phys., 58, 5364 (1973); J. Chem. Phys., 64, 4269 (1976).
5. R.D. Levine and R.B. Bernstein, Accounts Chem. Res., 7, 393 (1974).
6. J.L. Holmes, C. Lifshitz et al., to be published.

FOURIER TRANSFORM MASS SPECTROMETRY STUDIES OF GAS PHASE CARBANION CHEMISTRY

ROBERT L. WHITE, ALLISON HOWARD, S. W. STALEY AND C. L. WILKINS, Department of Chemistry, University of Nebraska, Lincoln, NE 68588

Solution methods of deuterium exchange with organic compounds and subsequent mass spectrometric analysis have been widely used for structure analysis of molecules. More recently, techniques have been developed in which deuterium is exchanged within the mass spectrometer via chemical ionization. Using Fourier Transform Mass Spectroscopy (FTMS), it is possible to observe ion-molecule reactions such as deuterium exchange in the absence of solvent and counterion effects since the reaction chamber pressure is maintained in the 10^{-5} to 10^{-7} torr range. Ion molecule reactions can be studied by varying the time that the ions are allowed to react and observing changes in the time resolved mass spectra of product ions.

The results of positive and negative ion deuterium exchange reactions with D_2O using FTMS for three unsaturated hydrocarbons with similar pi-systems are given in table 1. Both cycloheptatriene and benzocyclopropene were found to undergo positive ion exchanges with the exchange of two deuteriums preferred (Figures 1-2). The preferred exchanges probably occur at the carbon atoms not involved in the pi-systems. No exchange was observed for bicyclo [6.1.0] nonatriene. This would indicate that the proton affinity of bicyclo [6.1.0] nonatriene is less than that of D_2O.

Table 1 Deuterium Exchange Results

	COMPOUND		
	CYCLOHEPTATRIENE	BICYCLO [6.1.0] NONATRIENE	BENZOCYCLOPROPENE
			
POSITIVE ION D-EXCHANGE	d_2 PREFERRED d_1-d_6 OBSERVED	NO EXCHANGE	d_2 PREFERRED d_1-d_4 OBSERVED
NEGATIVE ION D-EXCHANGE	NO EXCHANGE	d_1-d_4 OBSERVED	ANION NOT FORMED WITH CH_3ONO

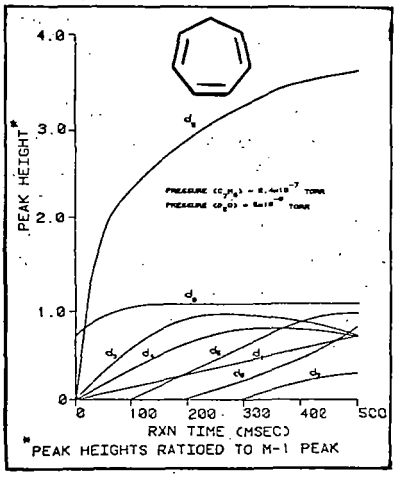

Figure 1

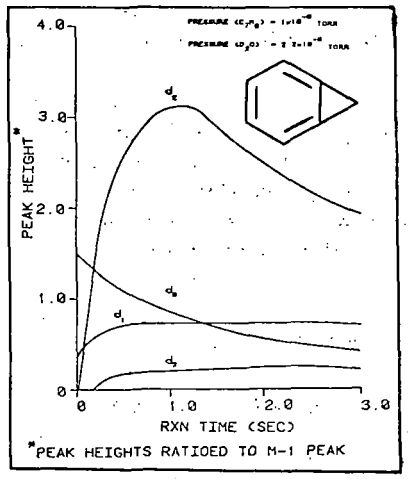

Figure 2

Negative ions were formed from the sample compounds by proton abstraction from the neutral using methoxide anion as a reagent. The methoxide anion was formed from CH_3ONO via capture of 0.2 eV electrons and subsequent decomposition into CH_3O^- and NO. The partial pressure of CH_3ONO was kept at $1x10^{-7}$ torr and electron ejection was used.[1] M-1 anions were formed for both cycloheptatriene and bicyclo [6.1.0] nonatriene. No exchange was observed for cycloheptatriene whereas four deuterium exchanges could be seen for bicyclo [6.1.0] nonatriene. This is consistent with solution studies of bicyclo [6.1.0] nonatriene which indicate that the negative charge on the anion is distributed among four sites on the molecule after ring opening (reaction 1).[2]

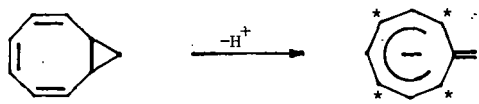

(1)

[1]John E. Bartmess, Judith A. Scott, and Robert T. McIver, Jr., JACS, 101, pp 6046-6055(1979)

[2]Stuart W. Staley, Gerard E. Linkowski, and Marye Anne Fox, JACS, 100, pp 4818-4821(1978)

FORMATION OF ETHYL AND PROPYL IONS FROM C_2H_5I $1\text{-}C_3H_7I$, and $2\text{-}C_3H_7I$; R. BUFF*, H.M. ROSENSTOCK, M.A. ALMOSTER FERREIRA**, A.C. PARR, R. STOCKBAUER, National Bureau of Standards, Washington, D.C. 20234, and J.L. HOLMES, Dept. of Chemistry, University of Ottawa, Ottawa, Canada.

The primary fragmentation process of the ethyl, 1-propyl and 2-propyl iodide ions was studied by means of photoelectron-photoion coincidence mass spectrometry. Breakdown curves were measured and analyzed using the independently determined apparatus function and the appropriate thermal rotational and vibrational population distributions. The form of the breakdown curves for iodoethane and 1-iodopropane was explained quantitatively, and zero kelvin threshold values were obtained. The breakdown curve for 2-iodopropane showed a small but definite dependence on the ion source residence time, and also showed a broadening. Both of these must be explained by slow fragmentation at threshold. The difference in fragmentation behavior was also examined by study of the unimolecular meta table transitions. The thermochemical and structural implications of the fragmentation threshold behavior is discussed and compared to previous work.

The partial support of this work by the U.S. Department of Energy, Office of Environment, Contract No. 80EV10373.000, is gratefully acknowledged.

*Intergovernmental Personnel Act Appointee at NBS. Permanent address: Dept. of Physics and Astronomy, University of Alabama, University, AL 35486.

**Guest Worker, University of Lisbon, Lisbon, Portugal.

THE FRAGMENTATION BEHAVIOR OF FORMALDEHYDE MOLECULAR CATIONS*;

R. BOMBACH, J. DANNACHER**, J.-P. STADELMANN, AND J. VOGT
Physikalisch-Chemisches Institut der Universität Basel Klingelbergstrasse 80, CH-4056 Basel (Switzerland)

Dedicated to Professor Edgar Heilbronner on the occasion of his sixtieth birthday.

Outstanding experimental [1] and theoretical [2] work instigated the present photoelectron-photoion coincidence study on formaldehyde and it's dideutero derivative. Considering the unusually detailed knowledge available about the thermochemistry and the properties of the reactants as well as the dissociation products, coincidence experiments appeared to be the method of choice to answer some of the raised questions. Using our (He-Iα) photoelectron photoion coincidence spectrometer we determined the breakdown diagrams, the kinetic energies released on fragmentation and, moreover, in time-resolved measurements, the average life-times of the excited CD_2O^+ ($\tilde{A}^2B_1$;v) molecular cations. These experiments are characterized by an adequate mass resolution, a high ion transmission coefficient, an achieved photoelectron energy band width of significantly less than .1 eV, and the absence of autoionization phenomena.

Photoionization measurements [1] gave evidence that the thermoneutral reaction $X_2CO^+(\tilde{A}^2B_1) \rightarrow CO^+(^2\Sigma^+) + X_2(^1\Sigma_g^+)$(X = H,D) involves no activation energy. Employing the concept of conical intersections it was possible to account theorectically for this observation [2]. However, the coincidence experiments yielded a substantially higher appearance energy [3] for this reaction which indicated that the detected activation energy free pathway is practically inaccessible in the absence of autoionization. This conclusion was further supported by the measured kinetic energies released on fragmentation. Consequently it has been demonstrated that the dissociation behavior of isoenergetic cations may well depend on their origin in direct ionization or autoionization of superexcited Rydberg states. This example shows that conventional PI appearance energy (AE) data do not unambiguously prove that molecular cations formed by direct ionization in an electronically excited state located above this AE do dissociate into the corresponding reaction channel.

Statistical theories of mass spectrometry generally assume that any electronic excess energy is rapidly converted into vibrational energy of the electronic ground state. The energetically accessible fragmentation reactions then take place competitively on a single electronic surface and the corresponding unimolecular rate constants can be calculated by means of transition state theory. According to these models the unimolecular rate constant for a particular dissociation process increases smoothly with increasing excitation energy. The slowest dissociations detectable in conventional mass spectrometers, which are called metastable transitions,

normally originate in molecular ions with relatively long life-times (several μs) and thus are believed to possess only little excess energy. In striking contrast to these expectations, the onset for the metastable transition $CD_2O^+ \rightarrow CDO^+ + D$ is about two eV higher than the experimental (and thermochemical) threshold energy for this reaction [1]. Since the onset of this metastable coincides with the adiabatic ionization energy of the first excited electronic state $\tilde{A}^2B_1$, this behavior was tentatively assigned [1] to an extraordinarily slow radiationless transition $(\tilde{A} \rightarrow \tilde{X})$, preceding the actual fragmentation.

We determined the average life-times of the $CD_2O^+(\tilde{A}^2B_1;v)$ molecular cations as a function of their vibrational energy, using a time resolved version of the coincidence experiment [4]. Our results revealed quantitatively that this constitutes a rare example where the internal conversion is unambiguously the rate determining step of a fragmentation process. Note, that ion fluorescence $\tilde{A} \rightarrow \tilde{X}$ does not occur $(\Phi < 10^{-3})$ [5] in agreement with the dipole forbidden nature of such a transition.

To complete our knowledge about the fragmentation behavior of excited CX_2O^+ molecular cations we measured the corresponding breakdown diagrams up to an ionization energy of 18 eV. This diagram consists of the breakdown curves for the parent and the four fragment ions XCO^+, CO^+, X_2^+, and X^+. Furthermore, in many cases the kinetic energies released were also measured [6].

---

*Research sponsored by the Swiss Nationalfonds, Ciba-Geigy SA, Sandoz SA and F. Hoffmann-LaRoche & Co. Sa. One of us (J.D.) would like to thank the Schweizerischer Nationalfonds for a fellowship. This work is part C20 of Project No. 2.212-0.79 of the Schweizerischer Nationalfonds zur Förderung der wissenschaftlichen Forschung.

**On leave, present address: Radiation Physics Division, National Bureau of Standards, Washington, D.C. 20234, USA.

[1] P.M. Guyon, W.A. Chupka, and J. Berkowitz, J. Chem. Phys. 64 (1976) 1419.

[2] M. VazPirez, C. Galloy, and J. C. Lorquet, J. Chem. Phys. 69 (1978) 3242.

[3] R. Bombach, J. Dannacher, J.-P. Stadelmann, and J. Vogt, Chem. Phys. Lett. 76 (1980) 429.

[4] R. Bombach, J. Dannacher, J.-P. Stadelmann, and J. Vogt, Chem. Phys. Lett. 77 (1981) 399.

[5] J. P. Maier, private communication.

[6] R. Bombach, J. Dannacher, J.-P. Stadelmann, and J. Vogt, Int. J. Mass Spectrom. Ion Phys., 1981, in press.

TIME RESOLVED PHOTOIONIZATION AND ELECTRON IMPACT MASS SPECTROMETRY IN THE MILLISECOND RANGE; THE KINETIC SHIFT IN PYRIDINE

Chava Lifshitz
Department of Physical Chemistry
The Hebrew University of Jerusalem, Jerusalem 91904, Israel

Time resolved appearance energies (appearance potentials) have been measured for the reaction,

$$C_5H_5N^+ \longrightarrow C_4H_4^+ + HCN \qquad (1)$$

in pyridine by electron impact trapped ion mass spectrometry (TIMS). Ions were trapped in an electron space charge for up to 3 milliseconds, following a short (1-2 μsec) ionizing pulse. At the end of a variable delay time they were removed for mass analysis by a positive pulse applied to a repeller electrode. A kinetic shift of 0.8 Volts was obtained for a delay time change from 5 μsec to 1000 μsec. Figure 1 represents the dependence of $AP(C_4H_4^+) - IP(C_5H_5N)$ on delay time.

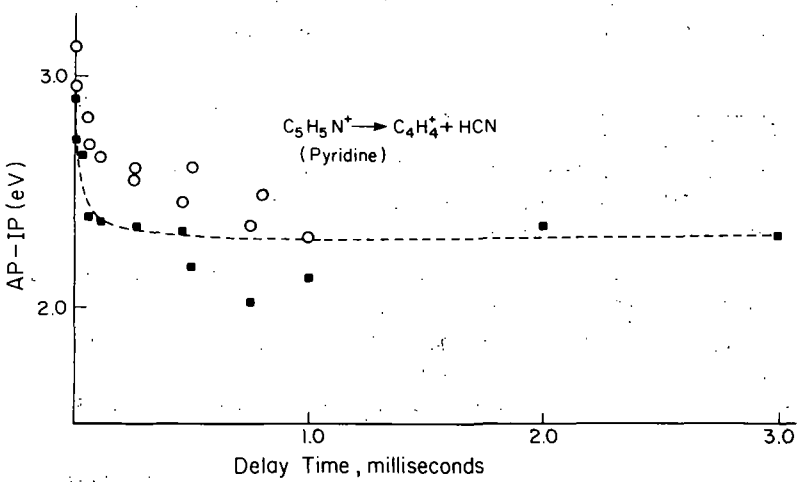

Figure 1

Dependence of AP-IP (the difference between the appearance potential of $C_4H_4^+$ and the ionization potential of pyridine) on the delay time between ionization and repelling pulses

The appearance potentials are observed to level off at long delay times, the values obtained from $I/I_{30V} = 10^{-3}$ (filled squares) doing so more rapidly than the ones based on $I/I_{30V} = 10^{-2}$ (open circles) do. The long-time limit is,

$$AP(C_4H_4^+) - IP(C_5H_5N) = 2.3 \pm 0.1 \text{ Volts} \qquad \text{I}$$

Independent experiments were carried out, in which the ionization energy (ionization potential) of pyridine was measured relative to ethane, aniline and methyl iodide. The resulting value, irrespective of trapping time, is

$$IP(\text{pyridine}) = 9.65 \pm .10 \text{ eV} \qquad \text{II}$$

By combining I and II, one obtains the long-time limit for the appearance potential of $C_4H_4^+$ from pyridine,

$$AP(C_4H_4^+) = 11.95 \pm 0.2 \text{ eV} \qquad \text{III}$$

Eland et al. [1] have set limits of 11.8-12.0 eV on the true threshold for $C_4H_4^+$ formation, on the basis of their photoionization and PIPECO study of pyridine. Rosenstock et al. [2] prefer, on the basis of variable time PIPECO, a 0°K fragmentation threshold of 12.15 ± 0.02 eV. Our result, obtained at 423°K (eqn III), is in agreement with both sets of data, yet the error limits are still quite large.

Time resolved breakdown curves were obtained experimentally and calculated by the QET. Good agreement was obtained between the calculated and experimental crossover shifts.

A trapped photoion mass spectrometry (TPIMS) experiment is now under construction. This includes VUV photoionization, a quadrupole mass spectrometer and a cylindrical ion trap (CIT) [3]. It combines the excellent energy resolution of photoionization with the wide time range available to TIMS and will allow a more accurate measurement of the kinetic shift in pyridine.

REFERENCES

1. J.H.D. Eland, J. Berkowitz, H. Schulte and R. Frey, Int. J. Mass Spectrom. Ion Phys., 28, 297 (1978).
2. H.M. Rosenstock, R. Stockbauer and A.C. Parr, in press.
3. J.E. Fulford, R.E. March, R.E. Mather, J.F.J. Todd and R.M. Waldren, Can. J. of Spectroscopy, 25, 85 (1980).

AUTOMATED TIME-RESOLVED ION-MOLECULE REACTION STUDIES BY FOURIER TRANSFORM MASS SPECTROMETRY; ROBERT B. SPENCER, VERN BURGER, SAHBA GHADERI, JOHN MARRA, RICHARD HEIN, TERRY PETERSON; Nicolet Instrument Corporation, Madison, WI 53711

Fourier Transform Mass Spectrometry (FT-MS) is a technique well-suited to the study of ion-molecule reactions at low pressures. Reaction and analysis are performed in a trapped-ion cell, which can retain ions for a significant length of time. Ion populations may be measured as a function of time after reaction for periods up to ca. one minute. Each experiment in a time-resolved study consists of a sequence of events in the order of: ion formation - reaction time period - ion population measurement, in which the ion population measurement is done by FT-MS. In cases where the ion signals are weak for a single series of events, ensemble averaging is used to achieve a suitable signal-to-noise ratio. Time resolution is achieved by performing a series of experiments with different reaction-time periods.

As described, the study is a series of repeated, similar experiments. As such, it may be made a highly automatic procedure, provided software of the requisite power is available. Data presentation, in the form of relative ion population vs. time plots may also be automated. For this, either mass-spectrum peak heights or peak areas may be used, with peak areas the usual preference.

THE THERMOCHEMISTRY AND DISSOCIATION DYNAMICS OF STATE SELECTED $C_4H_8O_2^+$ IONS: ETHYL ACETATE, p-DIOXANE, AND n-BUTYRIC ACID, Maria L. Fraser Monteiro, Luis Fraser Monteiro, JAMES J. BUTLER, Tomas Baer, Department of Chemistry, University of North Carolina, Chapel Hill, NC 27514 and J. Ronald Hass, NIEHS, Research Triangle Park, NC 27709.

The thermochemistry and dissociation dynamics of state selected ethyl acetate, p-dioxane, and n-butyric acid ions were studied in the 8 to 14 eV photon energy region using photoion-photoelectron coincidence (PIPECO). The three $C_4H_8O_2^+$ isomeric ions were found to have very different fragmentation patterns, and all the evidence indicates that the $C_4H_8O_2^+$ ions do not isomerize to a common structure prior to dissociation. This is seen in Table I, a compilation of heats of formation at 0K and 298K of fragment ions from the three isomeric precursor molecules obtained in our laboratory.

Dissociation rates for the metastable dissociation of ethyl acetate ion to $C_4H_6O^+ + H_2O$ were measured in the 10.4 to 10.8 eV photon energy range and were fit by RRKM theory. The results of the statistical theory predicted that ethyl acetate ion must first isomerize to a lower energy structure prior to dissociation to $C_4H_6O^+$ and H_2O. The lower energy structure may be the enol form of the molecular ion lying 0.66 eV lower in energy than the keto form. Likewise the dissociation rates of metastable p-dioxane ions to $C_3H_6O^+ + H_2CO$, $C_2H_5O^+ + C_2H_3O$, and $C_2H_4O^+ + C_2H_4O$ were measured between the photon energies of 10.7 and 11.0 eV and were fit by RRKM theory. A good fit to the rate data for the dissociation to $C_3H_6O^+$ was obtained using the vibrational frequencies of p-dioxane for both the molecular ion and the transition state and an appearance energy of 10.65 eV at 0K. Kinetic energy release distributions (KERDS) extracted from the symmetrically broadened Gaussian TOF peaks for $C_3H_6O^+$ at energies above 11.0 eV in combination with the results of a mass-analyzed ion kinetic energy study of $C_3H_6O^+$ from p-dioxane metastables produced small values for the average kinetic energy released near the onset for $C_3H_6O^+$. From the results of the kinetic energy release data, the dissociation of p-dioxane to $C_3H_6O^+$ has a negligible reverse activation barrier and occurs at an energy of 10.60 eV at 0K, in good agreement with the predictions of the RRKM fit of the rate data. Furthermore, our calculated heat of formation of 827 kJ/mol for $C_3H_6O^+$ is in good agreement with a theoretical calculation by Bouma *et al.*[1] of 833 kJ/mole for the CH_2-CH_2-O-CH_2^+ structure of $C_3H_6O^+$. This is certainly not an unreasonable structure for the $C_3H_6O^+$ ion from p-dioxane.

Contrary to the results of previous mass spectrometric investigations[2,3] including studies that we performed on the ZAB MIKES spectrometer, n-butyric acid was not seen to dissociate to $C_2H_4O_2^+$ at m/e 60 and $C_3H_5O_2^+$ at m/e 73 in the microsecond time scale using PIPECO. Asymmetric peaks characteristic of the metastable dissociation of parent ion were not seen in the TOF distributions for m/e 60 or m/e 73 at several energies at and above their appearance energies. A slight amount of asymmetry in the tail of the m/e 60 TOF peak was found to be independent of the ion internal energy and collision induced, disappearing with a lowering of the sample pressure. Breakdown curves for the major fragment ions from n-butyric acid were measured in the 10.3 to 14.0 eV photon energy region. Breakdown curves were calculated using the statistical theory with the measured appearance energies for fragment ions at m/e 60 and m/e 73. This indicates that the dissociation of n-butyric acid to m/e 60 and m/e 73 is consistent with a single precursor state of the molecular ion and therefore contradicts the previous evidence of an isolated state in the dissociation to m/e 60 and m/e 73.[3] Finally, we note that the activation energy for dissociation (AE-IE) in n-butyric acid is only 0.2 eV, far too small to give a metastable ion consistent with the statistical RRKM theory. The discrepancy between the mass spectrometric MIKES experiments and our PIPECO data is dramatic and as yet unexplained.

REFERENCES

1. William J. Bouma, John K. MacLeod, and Leo Radom, J. Am. Chem. Soc., 102, 2246 (1980).

2. John L. Holmes and F. P. Lossing, J. Am. Chem. Soc., 102, 3732 (1980).

3. D. J. McAdoo, D. N. Witiak, F. W. McLafferty, and J. D. Dill, J. Am. Chem. Soc., 100, 6639 (1978).

TABLE I

m/e	ion/neutral	precursor	ΔH_{f298K}(kcal/mole) ion/neutral	ΔH_{f0K}(kcal/mole) ion/neutral
88	$C_4H_8O_2^+$	$CH_3COOC_2H_5$	125 ± 1	131 ± 1
	$C_4H_8O_2^+$	dioxane	136 ± 1	144 ± 1
	$C_4H_8O_2^+$	C_3H_7COOH	121 ± 1	128 ± 1
73	$C_3H_5O_2^+/CH_3$	$CH_3COOC_2H_5$	105 ± 2/34.0	109 ± 2/34.8
	$C_3H_5O_2^+/CH_3$	C_3H_7COOH	98 ± 1/34.0	103 ± 1/34.8
71	$C_4H_7O^+/OH$	C_3H_7COOH	154 ± 2/—	159 ± 2/9.25
70	$C_4H_6O^+/H_2O$	$CH_3COOC_2H_5$	194 ± 2/-57.796	198 ± 2/-57.102
61	$C_2H_5O_2^+/C_2H_3$	$CH_3COOC_2H_5$	76 ± 2/69 ± 2	80 ± 2/70 ± 2
60	$C_2H_4O_2^+/C_2H_4$	C_3H_7COOH	118 ± 1/12.5 ± .3	122 ± 1/14.5 ± 3
58	$C_3H_6O^+/CH_2O$	dioxane	198 ± 2/026.0 ± .2	202 ± 2/-25.1 ± .2
57	$C_3H_5O^+/CH_3O$	dioxane	184 ± 2/3.5	187 ± 2/5.1
45	$C_2H_5O^+/C_2H_3O$	$CH_3COOC_2H_5$	— /-5.4	145 /-4 ± 2
	$C_2H_5O^+/C_2H_3O$	dioxane	176 ± 2/-5.4	180 ± 2/-4
44	$C_2H_4O^+/C_2H_4O$	dioxane	211 ± 2/-39.6 ± .1	213 ± 2/-37.1 ± .1
43	$C_2H_3O^+/C_2H_5O$	$CH_3COOC_2H_5$	151 /-4	153 ± 2/-0.5
	$C_2H_3O^+/C_2H_5O$	dioxane	⩽209 /-4	⩽210 /-0.5
	$C_3H_7^+$ /COOH	C_3H_7COOH	191 ± 1/-50 ± 1	195 ± 1/-49 ± 1
42	$C_3H_6^+$ $/CH_2O_2$	C_3H_7COOH	239 /-90.5 ± 0.1	243 /-88.9
29	$C_2H_5^+$ $/C_2H_3O_2$	$CH_3COOC_2H_5$	219 /-60 ± 1	222 /-58 ± 1
	$C_2H_5^+$ $/C_2H_3O_2$	C_3H_7COOH	215.3 ± 1.0/-57.7 ± 1.0	218.2 ±1.0/55.2±1.0
28	$C_2H_4^+$ $/C_2H_4O_2$	C_3H_7COOH	— /-103.3 ± 0.1	257/-99.9 ± 0.1

THE STRUCTURES OF BROMO-CARBONIUM IONS

John L. Holmes, F.P. Lossing and R. McFarlane, Chemistry Department, University of Ottawa, Ottawa, Ontario K1N 9B4 and Johan K. Terlouw, Analytical Chemistry Laboratory, University of Utrecht, Utrecht, The Netherlands.

The energetics, dissociation characteristics and collisional activation (CA) mass spectra of a series of bromo-carbonium ions $[C_nH_{2n}Br]^+$ have been studied with the aim of establishing their structures. The ions were generated by the dissociative ionisation of appropriate dibromides and bromoalkanes. The chief conclusions from this preliminary survey are given below.

1. The most stable isomeric form of $(C_nH_{2n})Br^+$ ions (i.e. that having the lowest heat of formation (ΔH_f)) is an ion having the bromine atom attached to charge-bearing carbon (e.g. the bromo-sec-butyl carbonium ion $CH_3\overset{+}{C}BrCH_2CH_3$, ΔH_f = 173 kcal mol^{-1}). Such ions have characteristic CA mass spectra, displaying significant losses of $H^\bullet$ and $Br^\bullet$, unlike all other isomeric $C_nH_{2n}Br^+$ ions prepared in this study. Only upper limits for ΔH_f could be obtained for these particular bromo-carbonium ions when derived from the appropriate dibromides because their AE values were equal to the IE for the compound. However, they could also be generated from 1-bromoalkanes.

2. The $[C_2H_4Br]^+$ ions generated from CH_3CHBr_2 and CH_2BrCH_2Br had closely similar ΔH_f values (207 and 209 kcal mol^{-1} respectively, see also ref 1), but their CA mass spectra were markedly different. The $[C_2H_4Br]^+$ ions from the former showed significant peaks at m/z 92 and 28 (losses $CH_3^\bullet$ and $Br^\bullet$) while the latter had a dominant m/z 93 peak (loss CH_2). Although these observations are compatible with the structures[1] $CH_2\overset{Br^+}{\diagdown\diagup}CH_2$ and $CH_3\overset{+}{C}HBr$ respectively, the cyclic bromonium ion structure is not easily compatible with observations on the $[C_3H_6Br]^+$ analogues.

3. The ions derived by $Br^\bullet$ loss from $CH_3CHBrCH_2Br$ (i) and $BrCH_2CH_2CH_2Br$ (ii) had closely similar CA mass spectra, each dominated by HBr loss, and clearly different from those produced from $CH_3CBr_2CH_3$ (iii) and $CH_3CH_2CHBr_2$ (iv). The observed heats of formation were ΔH_f(i) $\leq$ 195 kcal mol^{-1}, ΔH_f(ii) = 201 kcal mol^{-1}, ΔH_f(iii) $\leq$ 183 kcal mol^{-1} and ΔH_f(iv) = 201 kcal mol^{-1} respectively, certainly indicating no special stability for the putative cyclic ion $CH_2\overset{Br^+}{\diagdown\diagup}CH_2{-}CH_2$.

4. The $[C_4H_8Br]^+$ ion derived from $CH_3CBr_2CH_2CH_3$(v) had the lowest $\Delta H_f \leq 181$ kcal mol^{-1}. The CA mass spectra of the ions derived from $BrCH_2CH_2CH_2CH_2Br$ and $CH_3CHBrCH_2CH_2Br$ were closely similar as were their ΔH_f values, ≤ 185 and 186 kcal mol^{-1}, again raising questions as to the existence of a stable 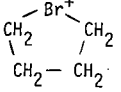 ion.

5. The ions generated by loss of an alkyl radical from $CH_3(CH_2)_n Br$ ions, n = 5,6 and 7, had heats of formation of 173 ± 1 kcal mol^{-1} and CA mass spectra closely similar to that of (v). The formation of the bromo-sec-butyl cation $CH_3\overset{+}{C}BrCH_2CH_3$ from the 1-bromo alkanes requires appreciable rearrangement and further experiments to investigate this are in progress. The low ΔH_f for the $[C_4H_8Br]^+$ daughter ion certainly shows why these ions are so prominent[2] in the mass spectra of the alkyl bromides and are able to compete with the fragmentation [1-alkyl bromide] → [sec-alkyl cation] + $Br^{\bullet}$.

References 1. R.H. Staley, R.D. Wieting and J.L. Beauchamp, J. Amer. Chem. Soc., 99, 5964 (1977).

2. F.W. McLafferty, Anal. Chem., 34, 2 (1962).

QUANTITATIVE AND QUALITATIVE ANALYSIS OF INTACT CONJUGATED BILE SALTS IN HUMAN BILE USING RADIAL COMPRESSION HPLC, FIELD DESORPTION AND FAST ATOM BOMBARDMENT MASS SPECTROMETRY

J.O. Whitney,[1,2] S. Lewis,[3] K.M. Straub,[2,3,4] F.C. Walls,[4]
A.L. Burlingame[2,3,4] and M.M. Thaler[1,2]

[1]Dept. of Pediatrics, [2]Liver Center, [3]Dept. of Pharmaceutical Chemistry, University of California, San Francisco, CA 94143 and [4]Biomedical Mass Spectrometry Resource, University of California, Berkeley 94720 and San Francisco, CA 94143

Bile acids occur in biological fluids in the form of highly polar taurine and glycine conjugates. Conventional methodology for the identification and quantitation of conjugated bile salts includes lengthy and incomplete extraction procedures, poor chromatographic resolution of taurine and glycine conjugates, and destruction of the taurine or glycine bond since hydrolysis, solvolysis, re-extraction and derivatization are necessary for analysis by GC/MS. Alternately, electron impact spectra of conjugated bile salts are difficult to obtain because of their high polarity and low volatility with molecular ions generally less than 3% of the base peak. We have developed a simple and rapid extraction procedure and an efficient HPLC system which, combined with field desorption (FD) and fast atom bombardment (FAB) mass spectrometry, permits the direct identification and quantitation of intact conjugated bile salts in clinically relevant samples.

Standard bile salts and duodenal bile from children with cystic fibrosis, celiac disease and "failure to thrive" were extracted on Sep-pak C_{18} cartridges (1 x 1 cm) and quantitated at the 1-1000 µg level on an HPLC Radial Compression Separation System using a C_{18} reversed phase cartridge (10 x 0.8 cm). Figure 1A demonstrates that the eight commonly occurring bile salts can be completely resolved in 12 min. Chromatographic separation of duodenal bile (50 µl) from a child with cystic fibrosis (2, taurocholate, 3, glycocholate, 4, taurochenodeoxycholate and 5, glycochenodeoxycholate), illustrating the characteristically large concentration of Na glycocholate associated with this disease, is shown in Figure 1B. Individual bile salt peaks from both standard solutions and from human specimens were collected, re-extracted on Sep-pak C_{18} cartridges (to remove contaminating salts) and analyzed by FD and FAB/MS on a modified Kratos/AEI MS-902 mass spectrometer, interfaced to a LOGOS II data system. FD spectra were obtained with a combined FE/EI ion source, using conventional benzonitrile activated emitters. FAB spectra were obtained with a prototype (Kratos) FAB ion source, utilizing a neutral argon atom beam (intensity 40-60 µA, energy range 6-8 kV). Major ions of FD and FAB spectra of standard bile salts are given in the table. FD spectra of standards contain a major ion representing the molecular ion plus Na $(M^+ + Na)^+$ and a doubly charged ion representing the molecular ion plus 2 Na $(M^+ + 2Na)^{2+}$. FAB spectra contain the molecular ion of the Na or K salts and the molecular ion plus Na. MS analysis by FAB was found to have the following advantages: greatly increased ion current (10-1000 times that observed for FD/MS), enhanced ion beam stability, and simplicity of operation. In addition, it is possible to recover unused sample from the insertion probe target. The FD and FAB spectra obtained from the glycocholate RC-HPLC peak of a child with cystic fibrosis are shown in Figure 2. Characteristic fragments in both spectra are the molecular ion (m/z 488) and the molecular ion plus Na (m/z 510). A doubly charged ion (m/z 267) is present in the FD spectrum. The ion at m/z 544 indicates that the column fraction was contaminated with Na taurochenodeoxycholate. In addition, FD and FAB/MS can be used to directly identify bile salts in unchromatographed mixtures. Figure 3 illustrates FD and FAB spectra of Sep-pak C_{18} extracted human duodenal bile from a patient with "failure to thrive". Ions resulting from Na taurocholate, glycocholate, taurochenodeoxycholate and glycochenodeoxycholate are present.

Conclusion: FD and particularly FAB/MS can be used in the identification of intact conjugated bile salts isolated in column fractions, to determine the purity of column fractions and to identify the major bile salts present in human bile without the necessity of chromatographic fractionation. These procedures, therefore, should help clarify alterations in bile salt metabolism associated with hepatobiliary and intestinal disorders.

Acknowledgement: This work was supported in part by NIH Grant HD-03148 and in part by NIH Division of Research Resources Grant RR00719.

Fig. 1A

RC-HPLC OF STANDARD BILE SALTS EXTRACTED FROM SALINE WITH SEP-PAK C^{18} CARTRIDGES

(SOLUTION SYSTEM: pH 5 , MeOH : H_2O : HAc (75:25:4) FLOW RATE = 2.5 ml/min , COLUMN , 10 cm C^{18} CARTRIDGE)

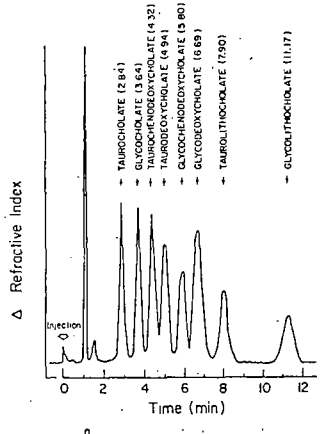

Fig. 1B

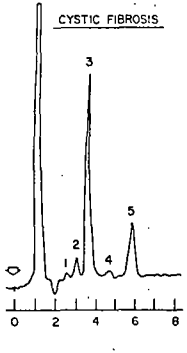

MAJOR IONS IN FD AND FAB SPECTRA OF COMMON BILE SALTS

	FD		FAB		
	M^+ Na salt + Na	M^{2+} Na salt + 2 Na	M^+ Na salt	M^+ K salt	M^+ Na salt + Na
Taurocholic Acid	560	291.5	537	553	560
Glycocholic Acid	510	267.5	488	504	510
Taurochenodeoxy-cholic Acid	544	283.5	522	538	544
Glycochenodeoxy-cholic Acid	494	258.5	472	488	494
Taurodeoxy-cholic Acid	544	283.5	522	538	544
Glycodeoxy-cholic Acid	494	258.5	472	488	494
Taurolitho-cholic Acid	528	275.5	506	523	528
Glycolitho-cholic Acid	478	250.5	456	472	478

Fig. 2

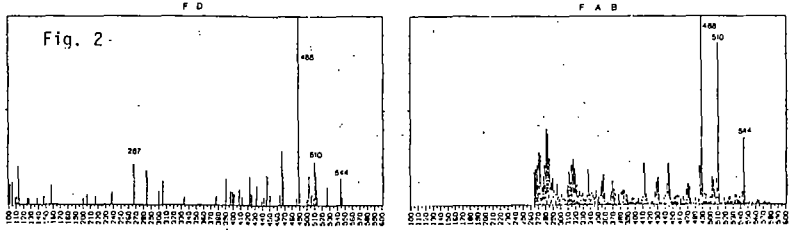

Fig. 3

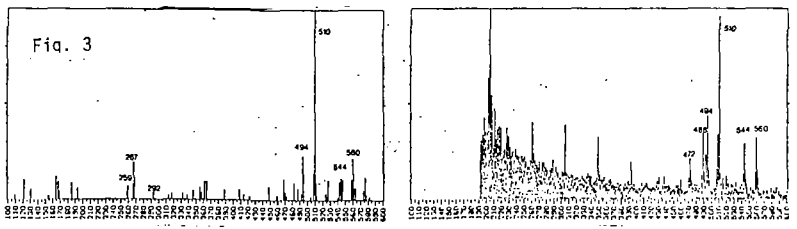

Use of GC/MS in the Identification of Abnormalities in Steroid Biosynthesis: P.V. Fennessey and E.R. Orr, Departments of Pediatrics and Pharmacology, School of Medicine, University of Colorado Health Sciences Center, Denver, Colorado 80262

SUMMARY:

The urinary steroid metabolic profile of patients with suspected problems of steroid biosynthesis (i.e., enzyme blocks, tumors, unusual compounds) will be presented. The samples have been analyzed by both classical laboratory methods and by gas chromatography/mass spectrometry. The results of each analysis will be reviewed in light of the suspected problem and the clinical results.

INTRODUCTION:

The application of gas chromatography/mass spectrometry as a practical clinical tool has been developing over the past few years. There are many reasons for the slow extension of this powerful technique from the chemical laboratory into actual clinical application. Two of the more important of these include the low natural abundance of the physiologically active steroid hormones and their similar chemical structures. The former leads to the need for large quantities of fluids for the quantative extraction and isolation of these compounds, while the latter has made their separation and identification a challenging chemical problem. Over the past few years tremendous progress has been made in the quantative isolation of steroids from physiological sources. These advances combined with the commercial development of capillary gas chromatography/mass spectrometry has made possible the practical extension of these techniques to the study of unusual diseases of steroid biosynthesis.

After appropriate consideration for rapid turn around time and developing workable clinical protocols, our laboratory has actively participated in the following cases:

PATIENT - A

A 47 year old female who had had no known hormone problems prior to this admission. At the time she experienced menapause she noticed an increased amount of hair growth on her face, shoulders, breasts and extremities. In addition, she developed a receding temporal hairline and a filling out of her face (moon). These external developments were accompanied by a mild hypertension (B.P. 182/18).

Laboratory analysis showed high normal steroid levels for ketosteroids, 17-hydroxy steroids, ketogenic steroids and cortisol, but elevated levels of testosterone, androstenedion and dihydroepiandrosterone. CAT scan showed a strange mass in one lobe of the liver.

A steroid profile revealed no unusual steroids but an increase in the concentration of many of the normal steroids. These data were in concert with an adrenal tumor. Figure 1 presents the steroid pattern before surgery and during follow-up (one month post-op). Additional follow-up studies (6 & 9 months) have shown a gradual increase of the steroid pattern which may parallel an regrowth of the tumor material.

PATIENT - B

An 18 year old female who presented in the Endocrine Clinic with a complaint of slow development of secondary sexual characteristics and primary amenorrhea. All laboratory tests on steroids showed normal levels and revealed no detectable problem.

The steroid profile showed an abnormal pattern in the ratio of 5α to 5β isomers. This refers to the stereochemistry of the junction at the A-B ring. A review of our own data on normals and of literature values reveals a problem with this patient (see Figure 2). We are presently looking into a possible reduction in the enzyme 5-α reductase and into a more detailed study of diurnal and long-term variation in the 5α/5β ratio.

CONCLUSION:

In addition to the usual requirement of precision and accuracy placed on a quantative scheme, a clinical program must have rapid turn around and a high level of cooperation and trust between the clinical and laboratory staffs. We have tried to show using just two examples how this cooperation can lead to a direct benefit to each patient. We have also applied these techniques to other adrenal tumor patients and to patients with inborn errors of steroid metabolism.

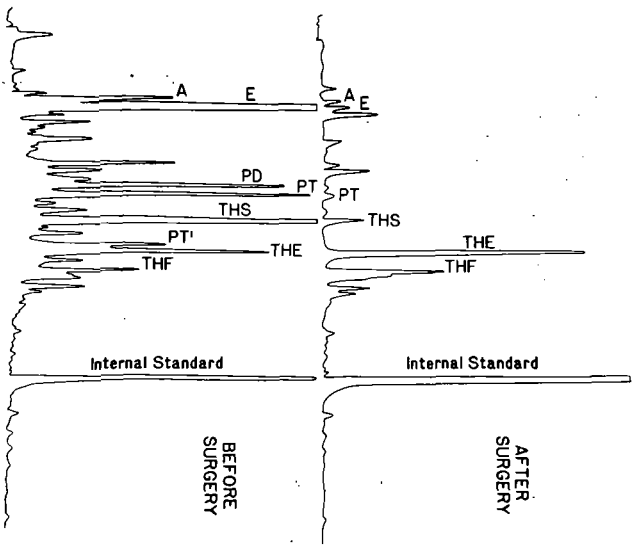

Figure 1

	ETIOCHOLANOLONE / ANDROSTERONE	(RANGE)	TETRAHYDROCORTISOL / allo-TETRAHYDROCORTISOL
EXPERIMENTAL			
SEVEN NORMAL MALES	0.72 ± 0.25 (0.97 → 0.33)		1.41 ± 0.47 (2.11 → 0.81)
PATIENT B	3.33		2.52
LITERATURE*			
TWENTY-ONE NORMAL MALES	(0.89 → 0.31)		(1.99 → 0.91)

*PFAFFENBERGER AND HORNING, ANALYTICAL BIOCHEMISTRY 88, 689 (78)

Figure 2

QUANTITATIVE STEROL ANALYSIS BY SELECTIVE ION MONITORING USING A DIRECT INSERTION PROBE

T. A. Wittstruck* and E. Caspi

Worcester Foundation for Experimental Biology
Shrewsbury, MA 01545

A method was needed for the determination of cholesterol and desmosterol in the nonsaponifiable fraction (NSF) of the brains of rats. Because of the number of brains to be analyzed, it was desirable that the method be both rapid and accurate. Analysis by gc/ms required derivatization and elution times were longer than 30 minutes per injected sample. In contrast, direct insertion probe (DIP) evaporation does not require derivatization of the sterols, and the amounts of cholesterol and desmosterol present in a typical brain NSF totally evaporate from the DIP within ca. 5 minutes.

Selective Ion Monitoring (SIM) was used to follow the evaporation profiles. A different ion was chosen to characterize each compound. The intensities were measured over the duration of evaporation and the peak areas obtained by integration. For example, m/e 386.4 was used to characterize cholesterol.

Desmosterol also exhibits a peak at m/e 386.4. Hence, in any mixture of these two sterols, the contribution arising from desmosterol to the measured intensity of the peak at m/e 386.4 must be subtracted, in order to obtain the peak area representing cholesterol. In order to make the corrections, the relative peak areas of each of the monitored ions were first determined for each sterol, by examining the SIM profiles of the pure compounds. Cholestane was then used as internal reference, and calibrations were determined for peak area ratio (RA) vs compound weight ratio (RW) for various mixtures of cholesterol:cholestane and desmosterol:cholestane.

A known amount of cholestane was added to each NSF, and its SIM profile obtained. Data (peak areas) were corrected, as described above, and the RA's determined for cholesterol:cholestane and desmosterol:cholestane. Using the calibration curves, RW's were determined for each pair, and since the amount of added cholestane was known, the weight of each sterol in the NSF was determined.

Obviously, components other than cholesterol and desmosterol present in the NSF might contribute to the monitored peaks. Examination of the gc of a typical rat brain NSF showed that cholesterol and desmosterol together comprise ca. 95-98% of the total. Hence, even if the other components contribute to the monitored peaks (which is not necessarily the case), neglecting their contribution will only lead to a small error.

This work was supported by NIH Grant AM 12156. A Nuclide Mass Spectrometer, Model 12-90-G, equipped with a DACSI.2 data acquisition system, was used.

---

*Present address: Nuclide Corporation, Box 135, Acton, MA 01720.

THE SPECTRA OF POLYPEPTIDES OBTAINED WITH CF-252 FISSION FRAGMENT MASS SPECTROMETRY; B.T. CHAIT, J. SHPUNGIN, B.F. GISIN, and F.H. FIELD, The Rockefeller Univ., New York, N.Y. 10021

The positive and negative ion spectra of several polypeptides obtained using Cf-252 fission fragment mass spectrometry are presented. The compounds included in this study contained between three and thirty amino acid residues. The main features of the spectra including the major fragmentation pathways are discussed.
A portion of the fragmentation produces the types of ions observed previously in this laboratory[1] with i-butane chemical ionization. Thus the fragmentation pattern was found to contain substantial sequencing information data.
We give examples of the utility of the method, e.g., we were asked to establish whether a synthetically produced polypeptide antibiotic (with 20 amino acid residues) was identical to the natural product. We have shown that both compounds have the same molecular mass (M=1963) and there is a close identity of the meaningful and extensive fragmentation patterns.

1. Mudgett, M.; Bowen, D.V.; Field, F.H.; Kindt, T.J. Biomed. Mass Spectrom. 1977, 4, 159.

FRAGMENTATION OF TRIMETHYLSILYLATED MONOGLUCURONIDES OF DIHYDRODIOLS FROM NAPHTHALENE; J. BAKKE, C. STRUBLE and V. J. Feil, Metabolism and Radiation Research Lab and NDSU Animal Science Dept., State Univ. Station, Fargo, ND 58105

Mass spectra from per-trimethylsilyl (per-TMS) derivatives of glucuronides in which the aglycones were dihydrodiols of naphthalene were obtained during metabolism studies on naphthalene and 1-naphthyl-N-methylcarbamate. The fragmentation patterns were different enough from other types of perTMS glucuronides that we considered they may be characteristic for structures related to those shown for I, II and III (Gl = glucuronic acid). Glucuronide I was isolated from the bile from rats dosed with 1-naphthyl-N-methylcarbamate. Glucuronide II was isolated from the urine from rats dosed with naphthalene.

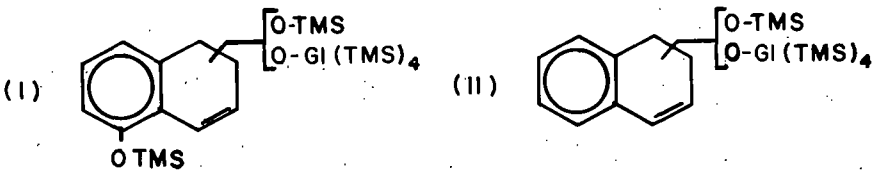

Glucuronide III was isolated from the urine from rats dosed (injected into the cecum) with N-acetyl-S-(1,2-dihydro-1-hydroxy-2-naphthyl)-L-cysteine (mercapturate). The mercapturate used for dosing was isolated from the urine of rats dosed with naphthalene. The glucuronide was characterized to have the general structure shown.

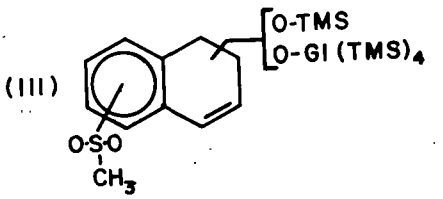

The mass spectra from the perTMS derivatives of these three glucuronides were unusual when compared to mass spectra reported for other perTMS glucuronides in three respects. First, an intense set of ions (most intense ions above m/z 100) appeared at M^+ - 481 and M^+ -482 that result from the fragmentations shown:

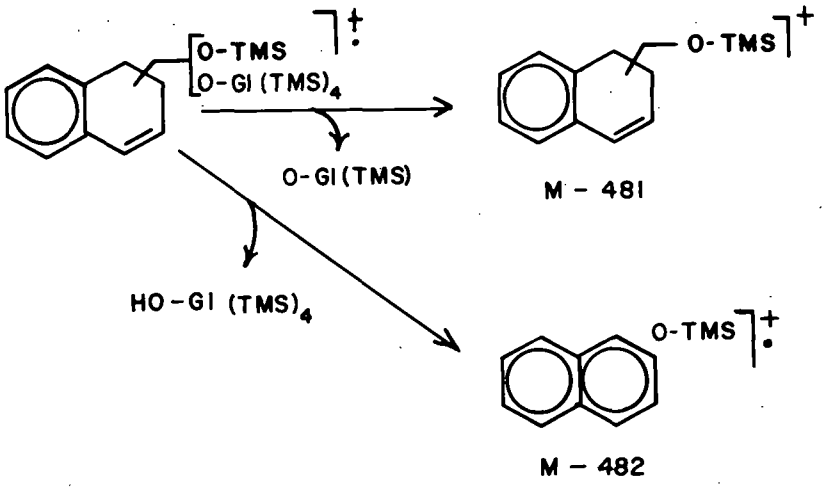

Second was the presence in the mass spectra of an ion at m/z 553 that had an exact mass compatible with the structure shown:

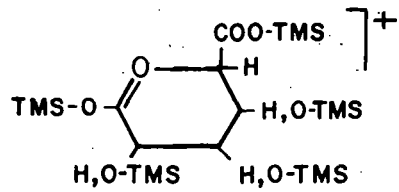

m/z 553

The hydrogen lost from the TMS glucuronic acid moiety was shown to be from the sugar and not the TMS groups because the m/z 553 ion shifted to m/z 598 for the derivative formed with deuterated TMS reagent.

The third characteristic of these spectra was the paucity of fragment ions above m/z 553. Only perTMS III gave an M - 15 ion at m/z 761. PerTMS I and II gave no ions above m/z 553.

The mass spectra from perTMS derivatives of the glucuronides II and III that were methylated with diazomethane (CH_3TMS) had the same characteristics except that CH_3TMS I had M^+ and $M^+ - CH_3$ ions, and CH_3TMS II had a $M^+ - CH_3$ ion. These ions were of very low intensity.

As a comparison, glucuronide I was hydrogenated. The two perTMS glucuronides shown below were separated after derivatization and gas liquid chromatography.

(IV)

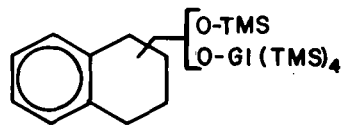

(V)

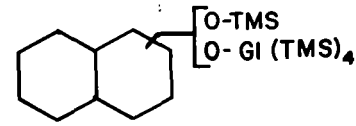

M^+ - 481 and 482 ions were present in the mass spectra but they were not as intense as for perTMS I, and there was no ion at m/z 553. There was an ion at m/z 539 that had an exact mass corresponding to the M - CH_3 ion from penta-TMS glucuronic acid. This ion has not been reported before in perTMS glucuronide spectra and is the highest mass ion observed in the mass spectra from perTMS glucuronic acid.

MASS SPECTROMETRY OF GLUTATHIONE, CYSTEINE, AND MERCAPTURIC ACID CONJUGATES OF STYRENE OXIDE; D.J. Harvan, B. Yagen, O. Hernandez, J.R. Hass; NIEHS, P.O. Box 12233, Research Triangle Park, N.C., 27709

Conjugation of toxic chemicals and their metabolites with sulfhydryl- containing amino acids is important in the removal of these chemicals from the body. The investigation of the mass spectral properties of these conjugates with model compounds is necessary for an understanding of these processes. Figure 1 shows the structure of the compounds studied.

A comparison of the mass spectra of styrene oxide conjugated with either glutathione, cysteine or mercapturic acid and ionized by different methods has been undertaken. The ionization techniques were; electron impact (EI) iso-butane positive ion chemical ionization (PCI), methane enhanced negative ion chemical ionization (MNCI), and field desorption (FD). The styrene oxide conjugates with mercapturic acid were separated by HPLC into the benzylic hydroxyl and benzylic thioether isomers. The other conjugates were run as mixtures.

Several general conclusions are:

1) The EI spectra were useless for molecular weight information and of limited values for structural information, being dominated by small mass fragments.
2) The PCI spectra gave protonated molecular ions for the less polar samples, but not for styrene oxide-glutathione. Methylated and N-acetylated glutathione conjugates gave low intensity protonated molecular ions. There was some useful structural information, because the fragment ions were higher mass than in the EI spectra. Ions were generally observed for the loss of water from the protonated molecular ion. Fragments were observed for cleavages on either side of the C-S-C bonds.
3) The MNCI spectra were useful in distinguishing the benzyl -OH from benzyl-S- conjugates of mercapturic acid. The ability to generate benzyl radicals is a dominant force governing the fragmentations observed in these spectra.
4) The FD spectra gave molecular ions and protonated molecular ions in all cases. There were fragmentations similar to the PCI spectra. The reproducibility of the FD spectra was not very good. The intensity of the protonated molecular ion and the extent of fragmentation was variable from run - to - run. Incorporation of an emitter current programmer into our system may help solve this problem.

Figure 1

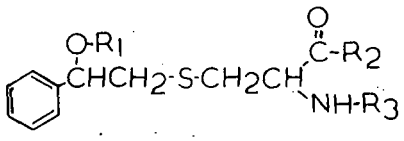

COMPOUNDS	R_1	R_2	R_3
Styrene oxide cysteine	-H	-OH	-H
S.O.- mercapturic acid	-H	-OH	$-COCH_3$
S.O.- methyl mercapturate	-H	$-OCH_3$	$-COCH_3$
S.O.- glutathione	-H	$-NHCH_2CO_2H$	$-COCH_2CH_2\underset{NH_2}{CO_2H}$
S.O.- glutathione OMe, di Me ester	$-CH_3$	$-NHCH_2CO_2CH_3$	$-COCH_2CH_2\underset{NH_2}{CO_2CH_3}$
S.O. - glutathione, N-Ac OMe, di Me ester	$-CH_3$	$-NHCH_2CO_2CH_3$	$-COCH_2CH_2\underset{NHCOCH_3}{CO_2CH_3}$

Interchange the positions of OR_1 and -S for the benzylic thioethers.

QUEUINE. STRUCTURAL STUDIES AND DISTRIBUTION IN NATURE

P. F. Crain, S. K. Sethi, B. P. Basile, C. S. Cheng, T. Kinoshita and J. A. McCloskey, Dept. of Medicinal Chemistry, Univ. of Utah, Salt Lake City, UT 84112; and J. R. Katze, Dept. of Microbiology, Univ. of Tenn. Center for Health Sciences, Memphis, TN 38163.

A compound which is present in bovine amniotic fluid in relatively large amounts (~2 mg/liter), and which is a substrate for tRNA:guanine transglycosylase,[1] has been characterized as queuine, 1, a hypermodified base which also occurs in transfer RNA.[2]

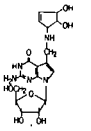

1

During the course of mass spectrometric structural studies, trimethylsilylation using BSTFA + 1% TMCS and DMF (90:10) gave the expected hexasilyl product; and, in addition, substantial amounts of a second component (Fig. 1) of MW 760.

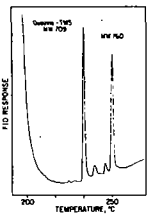

Fig. 1. Products of silylation of tRNA:guanine transglycosylase substrate using BSTFA/DMF (4' 1% OV-17, temperature programmed from 200 deg. at 10 deg./min.).

High resolution mass measurements indicated that the second component had structural similarities to the queuine moiety[2] (Fig. 2, LKB 9000S, 70 eV).

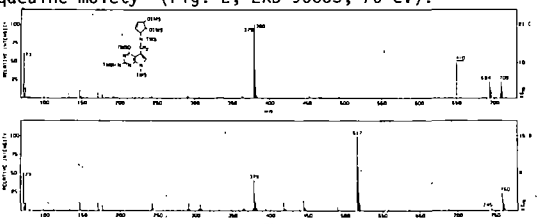

Fig. 2. Mass spectra of the principal GC peaks shown in Fig. 1.

The ion at m/z 379 ($C_{16}H_{31}N_4OSi_3$) is characteristic of queuine, and the composition of the fragment lost in the m/z 760 ⟶ 517 transition was consistent with the elements of cyclopentenediol-TMS_2. However, a molecular ion composition could not readily be derived from the exact mass data, using biochemically-reasonable heteroatoms. When additional derivatization studies showed that appearance of the MW 760 component specifically required both BSTFA and DMF, further examination of HRMS data yielded an F_3-containing composition ($C_{30}H_{55}N_6O_4Si_5F_3$, 760.3079 fd., 760.3083 calc.). Mass spectra of derivatives prepared with DMF-d_7 or dimethyl-(formamide-^{13}C) (one deuterium or one ^{13}C incorporated), as well as ^{13}C- and ^{19}F-NMR data led

to the structure shown in Fig. 3 for the MW 760 component.

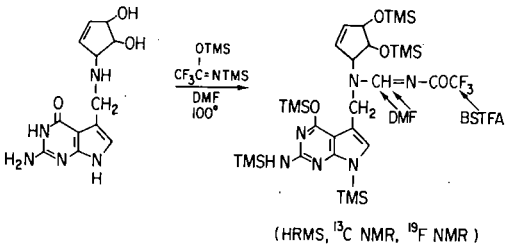

(HRMS, ^{13}C NMR, ^{19}F NMR)

Fig. 3. Structure of the product formed by reaction of queuine with BSTFA/DMF.

Preliminary GC/MS studies using selected ion monitoring have indicated occurrence of queuine in a variety of biological sources, including Drosophila melanogaster and human amniotic fluid (Fig. 4., LKB 9000S, 1% OV-17). Further studies are underway which involve

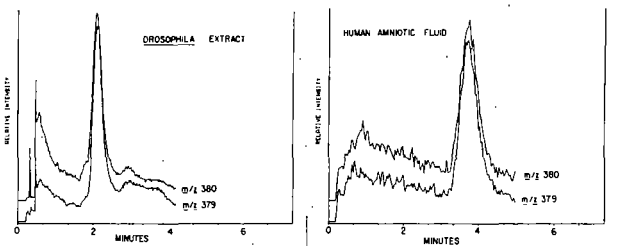

Fig. 4. Selected ion recordings of the TMS_6 derivative showing presence of queuine in Drosophila (29 ng/gm flies; 15 ng injected) and human amniotic fluid (119 ng/ml; 5 ng injected).

quantitative measurements of queuine in natural sources, using a labeled internal standard, prepared by the route shown in Fig. 5.

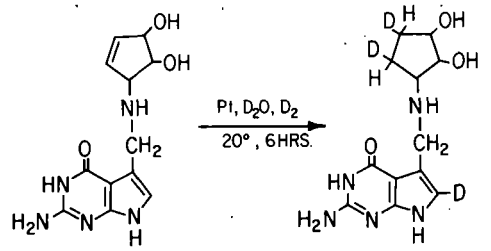

Fig. 5. Synthesis of a deuterium-labeled internal standard for quantitative measurement of queuine by selected ion monitoring.

References

1. Katze, J. R. and Farkas, W. R. (1979) Proc. Natl. Acad. Sci. U.S.A. 76, 3271-3275.

2. Crain, P. F., Sethi, S. K., Katze, J. R. and McCloskey, J. A. (1980) J. Biol. Chem. 255, 8405-8407.

THE STRUCTURAL DETERMINATION OF 3-(2-CARBOXYETHYL)CYTOSINE FOLLOWING IN VITRO REACTION OF BETA-PROPIOLACTONE WITH CALF-THYMUS DNA: JEROME J. SOLOMON, ALVIN SEGAL, JOHN MIGNANO and JOHN DINO: Department of Environmental Medicine, New York University Medical Center, 550 First Avenue, New York, N.Y. 10016

Beta-propiolactone (BPL) is a direct-acting alkylating agent which has been shown to be both mutagenic and carcinogenic. It produces squamous cell carcinomas in mice by skin painting, and subcutaneous fibrosarcomas by injection in rats. BPL has been shown to cause G·C→A·T transitions and base-pair substitutions in eukaryotic and prokaryotic test systems, respectively. BPL has been used in the workplace as an intermediate in synthetic fiber production, and as a sterilant for surgical equipment. Previous work performed in this laboratory has noted the production of 1-(2-carboxyethyl)adenine (1-CEA) and 3-(2-carboxyethyl)thymine (3-CET) following reaction of BPL with calf thymus DNA, in addition to the formation of 7-(2-carboxyethyl)guanine (7-CEG). This work represents the first report of the formation of 3-(2-carboxyethyl)cytosine (3-CEC) and 3,N^4-bis(2-carboxyethyl)-cytosine (3,N^4-BCEC) following reaction of BPL with 2'-deoxycytidine or calf thymus DNA.

Mass spectrometry of underivatized 3-CEC yielded ions only when direct-probe temperatures exceeded 400°C. The resulting spectrum was simply that of the pyrolysis products, free cytosine and acrylic acid. A methyl ester of the carboxylic acid function gave the first volatile derivative of 3-CEC. It yielded an M^+ consistent with the hypothesized structure of 3-CEC. Further support was afforded by production and mass spectral analysis of trimethylsilyl (TMS) derivatives of 3-CEC and 3,N^4-BCEC. 3-CEC, trimethylsilylated with N,O-Bis(trimethylsilyl)-trifluoroacetamide, exhibited an M^+ indicating the presence of 3 TMS groups. A preparation of 3-CEC-[TMS(d_9)]$_3$ yielded an M^+ indicating the presence of 3 TMS groups and distinguishing between TMS and carboxyethyl groups. Similarly, trimethylsilylated 3,N^4-BCEC yielded a molecular ion with the characteristic fragmentation of two silyated carboxyethyl side chains.

SYNTHESIS AND GC/MS OF O'-METHYLATED NUCLEOSIDES AND DEUTERATED ANALOGS

R.G. TEECE and K.H. SCHRAM, Department of Pharmaceutical Sciences, University of Arizona, Tucson, AZ 85721

In this study 2'-O-methylated nucleosides and their 2'-O-deuteromethyl analogs were synthesized to be subsequently used as standards in a qualitative and quantitative GC/MS study of these compounds isolated from normal and pathological urine. Reaction of adenosine and cytidine with dimethyl sulfate - $(CH_3)_2SO_4$ or $(CD_3)_2SO_4$ - in alkaline medium affords a mixture of primarily ribose-O-methylated products.[1] After the mixture was neutralized on

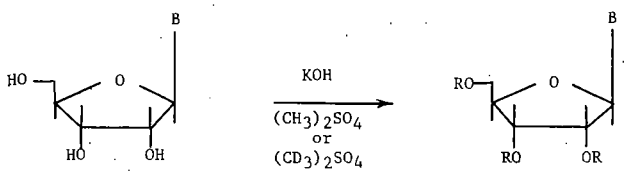

R = H, CH_3 or CD_3

a Dowex 50W (H form) column the first step in separation was accomplished using a Dowex 1-X2 anion exchange resin. Gradient elution was performed with a two reservoir solvent system (A and B) where B contained a 60:40 v/v of CH_3OH/H_2O and A contained H_2O. The reservoirs were interfaced at their base and the solvent was directed to the Dowex column from reservoir A by gravity feed. The O'-methylated derivatives that eluted from the column were collected in fractions, monitored by UV at 280 nm and their absorbance recorded on chart paper. Fractions under each peak were combined and rotoevaporated to dryness. The final separation and hence isolation of compounds was accomplished using Analtech silica gel GF, 2000 micron, preparative TLC plates or a Whatman Magnum 9 semi-preparative silica gel HPLC column. The solvent system for both methods was $CHCl_3/CH_3OH$, 85:15 v/v for the former and a gradient elution of 0% to 15% at 1%/min. for the latter. Column pressure was 1800 psi and the flow rate was maintained at 6.0 ml/min. The combination of the above techniques has afforded a good yield of 2'-O-methyladenosine 1 and 2'-O-methylcytidine 2 and their deuterated analogs 3 and 4. Reaction of 2 with bisulfate anion[2] produced the uridine analog 5 in good yield.

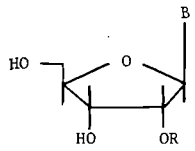

1; B=adenine; R=CH_3
2; B=cytosine; R=CH_3
3; B=adenine; R=CD_3
4; B=cytosine; R=CD_3
5; B=uracil; R=CH_3

Gas chromatography/mass spectrometry was used to confirm the identity and purity of the 2'-O-methyl derivatives as well as to determine isotopic incorporation of the labeled compounds. Trimethylsilyl derivatives of the 2'-O-methylated products and their deuterated analogs were formed using BSTFA in order to enhance their volatility for gas phase analysis. Gas chromatography was accomplished using a Varian 3700 series instrument equipped with a 6' x ¼" x 2 mm all glass coiled column packed with 3% SE-30 on Chromosorb W (HP). Injection port and detector temperatures were held isothermally at 280°C and the column temperature was programmed from 170° to 260°C at 4°/min. The GC was interfaced to a Varian Mat 311A mass spectrometer via an all glass jet separator. Low resolution mass spectra were acquired under the following instrumental conditions: accelerating voltage; 3 KV; ionizing potential, 70 eV; ionization current, 500 ma; interface temperature, 280°C; and source temperature, 250°C. Resolution was adjusted to 1000. Mass spectra of underivatized samples taken via the direct probe were temperature programmed from 50° to 400°C at 500°/min.

The identity of the 2'-O-methylated nucleoside derivatives was confirmed by matching

their mass spectra against standards and/or mass spectra of the same reported in the literature.[3]

Figures 1 & 2 - TMS derivative of 2'-O-methyladenosine and its deuterated analog.

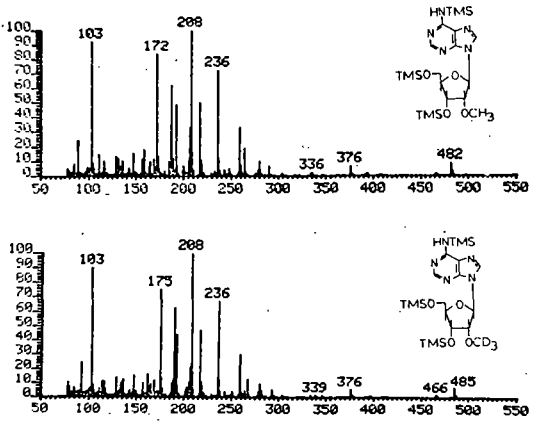

Figures 3, 4 & 5 - Probe samples of labeled and unlabeled 2'-O-methylcytidine and 2'-O-methyluridine

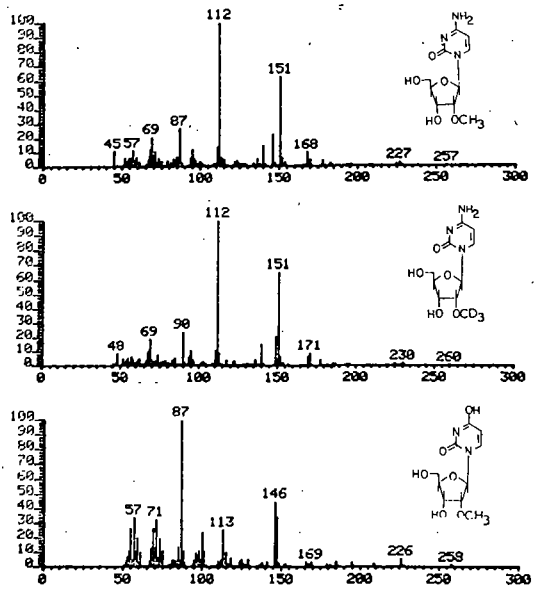

1. Z. Kazimierczuk, E. Darzynkiewicz and D. Shugar, Biochem., 15, 2735 (1976).
2. R. Shapiro, JACS., 92, 422 (1970).
3. J.A. McCloskey in "Basic Principles in Nucleic Acid Chemistry", Vol. 1, P.O.P.TsO, Ed., Academic Press, Inc., New York, 1974.

THE INCORPORATION OF ^{13}C AND ^{15}N LABELED PRECURSORS INTO THE URIDINE NUCLEOTIDE POOL IN VITRO AND IN VIVO

Lawrence Anderson, Anne Monks, Christine Chisena, Richard Cysyk, and John Strong, NCI, NIH, Bethesda, MD

Antitumor agents have been developed which inhibit de novo pyrimidine synthesis. In theory, these antimetabolites should reduce the formation of nucleotides and eventually "starve" rapidly dividing cancer cells. To date, the efficacy of these drugs has been varied and as a result has prompted numerous investigators to examine more closely the de novo pathway leading to formation of pyrimidine nucleotides. The most commonly used method for studying this pathway in vitro involves the use of radiolabeled precursors such as ^{14}C-bicarbonate. At a particular point, the products are isolated and their specific activity determined as a measure of the flux through this pathway. The use of this method in vivo is limited due to gross dilution of the tracer bicarbonate pools in the intact animal. We have developed a method to quantitate the incorporation of stable precursors, such as ^{13}C-bicarbonate which can be synthesized to contain 100% ^{13}C thus offsetting the dilution effects encountered in vivo. This study presents a comparison of bicarbonate incorporation into the uracil derivatives of L1210 cells in vitro as determined using both ^{13}C-bicarbonate and ^{14}C-bicarbonate. Additionally we present results from initial studies of the incorporation of administered $^{13}CO_2$, 5-^{15}N-L-glutamine, and $^{15}NH_4Cl$ into the pyrimidine nucleotide pool of mouse tumors growing in situ. Incorporation of the labeled precursors into either uridine or uracil was measured after isolating the nucleotide pool and reducing the uracil derivatives to their respective nucleoside or base.

To test the applicability of the method, the incorporation of ^{13}C and ^{14}C was compared in L1210 cells in vitro. Total uridine was quantitated in an aliquot of each sample by an HPLC analysis, and the uridine peak was collected and counted to determine the ^{14}C enrichment. The remainder of the sample was used to measure the ^{13}C enrichment of the uridine by the technique of selected ion monitoring (SIM). Uridine was analyzed by GC-MS as its permethylated derivative, formed by addition of DMSO, t-butoxide, and CH_3I.

The ion fragments $(C_7H_9N_2O_3)^+$ and $(^{13}CC_6H_9N_2O_3)^+$ containing the base moity at m/z 169 and m/z 170, respectively, were used to determine the ^{13}C incorporation into the molecule. Figure 1 shows the incorporation of ^{13}C derived from bicarbonate into uridine and compares the results obtained by both the radiolabeled and stable labeled techniques.

Incorporation of $^{13}CO_2$, $^{15}NH_4Cl$, and 5-^{15}N-L-glutamine into the uracil moity of the nucleotide pool was determined by SIM after administration of these labeled precursors to mice. Uracil was analyzed as it di-heptyl derivative formed by addition of n-$C_7H_{15}I$, $(CH_3)_4NOH$, and acetone. Ion fragments at m/z 291 and m/z 292 were chosen to quantitate the ^{13}C and ^{15}N enrichment in the uracil molecule. These ions represent loss of (OH) from the molecular ion as confirmed by synthesizing uracil containing an ^{18}O atom in the 4 position of the ring. Table 1 shows the reproducibility of this analysis and table 2 gives the results of preliminary studies where labeled precursors of the de novo pyrimidine pathway were administered to mice in vivo.

The results of these studies have demonstrated the applicability of stable lableled precursors in combination with electron impact mass spectrometry and technique of SIM for monitoring their incorporation into the pyrimidine nucleotide pool in vitro and in vivo. The methods described have the required sensitivity and reliability to measure the enrichment of uracil by ^{13}C and ^{15}N precursors at biologically significant levels.

INCORPORATION OF 4-AMINO-5-HYDROXYMETHYLPYRIMIDINE INTO THIAMINE BY MICROORGANISMS

Robert H. White
Department of Biochemistry and Nutrition
Virginia Polytechnic Institute and State University
Blacksburg, Virginia 24061

The pathway for the biosynthesis of the pyrimidine moiety of thiamine (4-amino-5-hydroxymethyl-2-methylpyrimidine) has yet to be established. Early studies on the incorporation of radioactive precursors into the pyrimidine moiety of thiamine clearly showed that this pyrimidine was formed by a pathway different from those by which other pyrimidines are made. Further work has shown, that 5-aminoimidazole ribonucleotide, an intermediate in purine metabolism, is also an intermediate in the biosynthesis of this pyrimidine[1,2]. The problem of 4-amino-5-hydroxymethyl-2-methylpyrimidine biosynthesis then is one of understanding how the methyl group is formed at C-2 of the pyrimidine and how the 2-carbon unit is inserted into the imidazole ring. One possible pathway would be to ring-expand the imidazole to a pyrimidine and have the methyl group introduced as a last step. If this pathway were correct then 4-amino-5-hydroxymethylpyrimidine could possibly function as a precursor. This relationship was easily tested by growing organisms with 4-amino-5-hydroxydideuteromethylpyrimidine and testing for its conversion into the pyrimidine of thiamine by gas chromatographic-mass spectrometric analysis of deuterium incorporation into 4-amino-5-ethylthiomethyl-2-methylpyrimidine, a product of the cleavage of thiamine with ethanethiol[2]. When this was done for the thiamine produced by the organisms shown in Table 1, no indication of thiamine containing a deuterated 4-amino-2-methyl-5-pyrimidylmethyl moiety was found. However, 4-amino-5-ethylthiomethylpyrimidine was clearly present indicating that the demethylated pyrimidine was being incorporated directly into the thiamine.

TABLE 1

Incorporation of deuterated 4-amino-5-hydroxymethylpyrimidine into thiamine by microorganisms

organism/strain	adenine fed (μg/ml)	4-amino-5-hydroxymethyl-pyrimidine fed (ng/ml)	ratio demethylthiamine / thiamine	total thiamine μg/g wet wt
1. *E. coli* K12 pur I	0.1	50	> 55.0	4.7
2. *E. coli* K12 wt	0.2	50	0.88	2.8
3. *E. coli* B	0.0	50	0.14	1.1
4. *E. coli* B	0.1	50	0.50	-
5. *E. coli* B	0.2	50	0.93	-
6. *E. coli* B	0.4	50	1.42	0.69
7. *B. subtilis*	0.0	50	2.20	0.80
8. *B. subtilis*	0.3	50	4.80	0.53
9. *S. cerevisiae*	0.0	50	1.71	0.60
10. *S. cerevisiae*	0.3	50	1.49	1.31

In order to prove conclusively that this pyrimidine had been incorporated into the thiamine, the thiamine was isolated, dephosphorylated, and oxidized to the thiochrome. The resulting thiochrome and demethylthiochrome were then separated by tlc and quantified by their fluorescence and deuterium content. The results of these determinations clearly showed that the demethylated pyrimidine was readily incorporated into thiamine without the methyl group.

That this demethylated thiamine was in fact functioning as a thiamine coenzyme in the cells was confirmed by work on the E. coli K12 purI mutant. This mutant requires both the pyrimidine moiety of thiamine and a purine for growth due to its lack of phosphoribosylaminoimidazole synthetase. As can be seen in Table 1, only the demethylated thiamine was found in these cells when they were grown with 4-amino-5-hydroxymethylpyrimidine. Addition of this compound at levels of 0.5 ug to 100 ug/ml gave log phase growth rates the same as those for wild-type E. coli K12 or for the mutant when grown with thiamine.

The data in Table 1 also establish that, at least in E. coli and in B. subtilis, a connection exists between purine metabolism and the biosynthesis of the pyrimidine moiety of thiamine. Increasing the amount of adenine added to the medium results in an increased amount of the 4-amino-5-hydroxymethylpyrimidine incorporated into the thiamine. Adenine, a feedback inhibitor, inhibits the production of 5-aminoimidazole ribonucleotide which occurs at the branch point for the pyrimidine biosynthesis. The cell simply makes up for the loss in the production of the methylated pyrimidine by using the demethylated pyrimidine. This argument is in agreement with the well-established inhibition of purine biosynthesis in these organisms by adenine.

Purine biosynthesis in yeasts is also inhibited by adenine, however, the data in Table 1 shows no increased incorporation of 4-amino-5-hydroxymethylpyrimidine into thiamine on the addition of adenine to the growth medium. This is consistent with the biosynthesis of the pyrimidine moiety of thiamine in yeast not originating from aminoimidazole ribonucleotide and supports the idea that yeasts biosynthesize the pyrimidine in a different manner. This is also consistent with incorporation studies which showed formate to be incorporated into the C-4 of the pyrimidine in yeasts, whereas it is incorporated at C-2 in E. coli.

REFERENCES

1. I. G. Leder, in "Metabolic Pathways: Metabolism of Sulfur Compounds," 3d ed, (D. M. Greenberg, ed), Vol. VII, pp. 57-85. Academic Press, New York, 1975.

2. R. H. White and F. B. Rudolph, Biochemistry 12, 2632-2636 (1979).

ALKYLATION REACTIONS OF GUANOSINE 5'-MONOPHOSPHATE BY PHOSPHORAMIDE MUSTARD

V. T. Vu, C. C. Fenselau and O. M. Colvin
The Johns Hopkins University School of Medicine
Baltimore, Maryland 21205

Cyclophosphamide is one of the most important drugs in cancer chemotherapy. Its therapeutic effect requires biotransformation to the active metabolite, phosphoramide mustard. It is believed that the interaction of phosphoramide mustard with cellular nucleic acids is responsible for the cytotoxic effect of cyclophosphamide. Thus, it is important to elucidate the primary molecular modification involved in this interaction. While cross-linking of DNA has been reported, no attempts were made to identify the sites of alkylation and the nature of the substituents(1). Recently, guanosine/ deoxyguanosine-phosphoramide mustard adducts at the 7 position were identified by FD mass spectrometry(2). These findings prompted us to report our studies of the alkylation reactions o phosphoramide mustard at the nucleotide level.

Guanosine 5'-monophosphate was reacted with phosphoramide mustard in aqueous solution at pH 4.5 and at 37°. Three products, two monomers and a cross-linked dimer, were isolated and purified by reverse phase HPLC. The structures of these alkylated nucleotide adducts were characterized by FAB mass spectrometry as N-[2-(N-7 guanosine 5'-monophosphate) ethyl] phosphorodiamidic acid (Figures 1 and 2), 2-chloro,2'-(N-7 guanosine 5'-monophosphate)diethylamine (Figure 3), and N,N-bis[2-(N-7 guanosine 5'-monophosphate) ethyl] phosphorodiamidic acid (Figure 4). The positions of alkylation on the nucleotide of all three compounds were confirmed by UV spectrophotometry to be 7-substituted guanosine 5'-monophosphate.

We conclude that phosphoramide mustard can modify nucleic acids by monofunctional attachment and by forming cross-links through guanine moieties at the 7 position. These reactions could be responsible for its cytotoxicity in vivo.

1. Y. A. Surya, J. M. Rosenfeld, and B. L. Hillcoat, Cancer Treat. Rep. 62, 23(1968).
2. J. R. Mehta, M. Przybylski, and D. B. Ludlum, Cancer Res. 40, 4183(1980).

Fig.1 POSITIVE ION FAB ADDUCT I GMP-PM

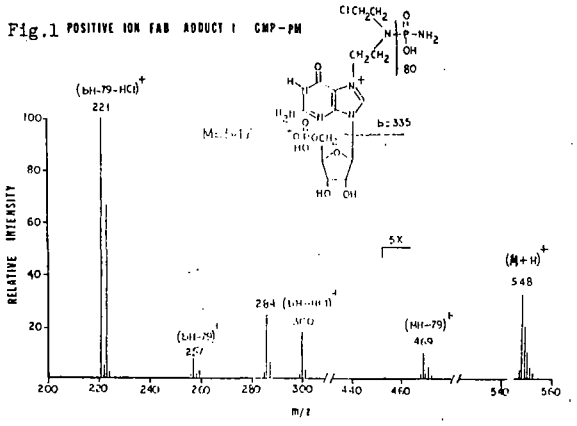

Fig. 2 NEGATIVE ION FAB ADDUCT I GMP-PM

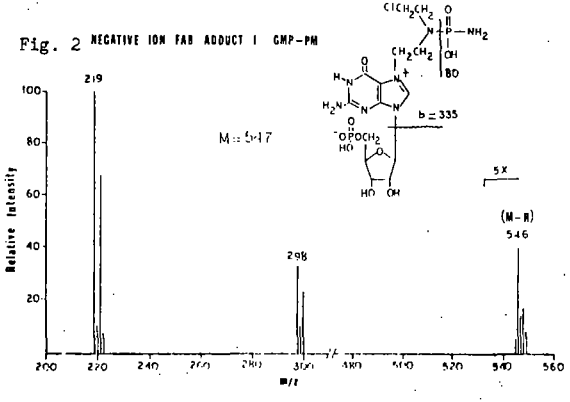

Fig. 3 POSITIVE ION FAB ADDUCT II GMP-NORNITROGEN MUSTARD

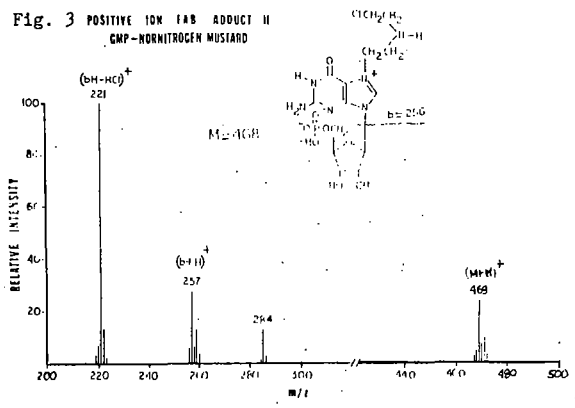

Fig. 4 POSITIVE ION FAB ADDUCT III diGMP-PM

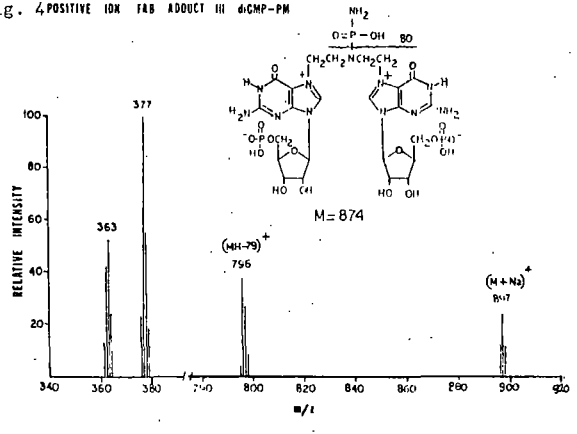

A NOVEL NUCLEOPHILIC AROMATIC SUBSTITUTION OF AN ACYLOXY GROUP AT O^6 OF DEOXYGUANOSINE: JEROME J. SOLOMON, ALVIN SEGAL, BENJAMIN L. VAN DUUREN AND URSZULA MATE; Lab. Org. Chem. and Carcinogenesis, Inst. of Env. Med., New York Univ. Med. Center, New York, N.Y. 10016.

Dimethylcarbamyl chloride (DMCC) is a potent carcinogen in the mouse via skin painting and subcutaneous injection and in the rat following inhalation. We have examined the reaction of this direct-acting acylating agent with 2'-deoxyguanosine (dGuO) prior to in vitro reaction with calf thymus DNA. DMCC reacts with dGuO at 37°C and pH 7.0-7.5 to produce a blue fluorescent O^6-acyl derivative, 2-amino-6-dimethylcarbamyloxy-9-(2-deoxy-β-D-erythro-pentafuranosyl)purine (DMCC-dGuO). This adduct was characterized by its UV, NMR and EI and isobutane CI mass spectra. DMCC-dGuO undergoes a novel nucleophilic aromatic substitution with dimethylamine to form a C-6 dimethylamino derivative, 2-amino-6-dimethylamino-9-(2-deoxy-β-D-erythro-pentofuranosyl)purine. Source insertion isobutane chemical ionization mass spectrometry was required to prevent the thermal decarboxylation of the O^6-acyl derivative to the C-6 adduct and confirm this novel displacement reaction. The importance of O^6-acylation of guanosine in light of the correlation between O^6-alkylation of guanosine in DNA and mutagenesis and carcinogenesis will be discussed.

PRODUCTS OF THE REACTION OF BLEOMYCIN WITH DNA

L. Giloni, C. R. Iden and A. P. Grollman

Department of Pharmacological Sciences
SUNY at Stony Brook
Stony Brook, N.Y. 11794

The bleomycins are a family of glycopeptides with antineoplastic activity that bind to DNA causing strand scission. In a reaction requiring oxygen and Fe(II), single and double stranded breaks occur preferentially at guanine-pyrimidine base sequences.[1,2] The products of the reaction include free bases, oligonucleotides modified at the 3'-termini, and several compounds that form chromophores with thiobarbituric acid (TBA).

Discussion

A standard reaction mixture contained 50mM potassium phosphate buffer, pH 7.2, 230μM calf thymus or HeLa cell DNA, 230μM bleomycin, and 230μM $Fe(NH_4)_2(SO_4)_2$. The reaction was initiated by the addition of the ferrous salt, and the mixture was incubated in an ice bath for 30 minutes.

Eight low molecular weight compounds were isolated from the bleomycin-DNA digest by thin layer chromatography on silica gel (Fig. 1). Each compound absorbed in the UV region, and four formed chromophores with TBA, having maximum absorption at 532 nm. Four of the compounds were identified as thymine, adenine, guanine, and cytosine based on migration relative to standard compounds in three thin layer chromatographic systems.

The four unidentified compounds labelled 1,3,4, and 5 were hydrolyzed with 88% formic acid under conditions that produce minimal destruction of bases. After evaporating to dryness, trimethylsilyl (TMS) derivatives were prepared, and products were analyzed by GC/MS. Again the bases, thymine, adenine, guanine, and cytosine were identified; one base being the hydrolysis product of each of the unknown compounds. The molar ratioes of base:unknown were determined for compounds 1 and 3 and found to be 1.01 and 1.04 respectively.

Compounds 1 and 3 were reduced with sodium borohydride and the TMS derivatives were prepared. High resolution accurate mass measurement showed that compound 3 was $C_{14}H_{25}N_5OSi_2$. Analysis of the high resolution mass spectrum (Fig. 2), ^1H NMR spectrum, and synthesis of a standard by an unambiguous route[3] have served to identify the original reaction product as 3-(adenin-9'-yl)propenal. In an identical manner compound 1 was identified as 3-(thymin-1'-yl)propenal (Fig. 3). We conclude that the four unknown reaction products have the common structure: Base-CH=CH-CHO.

Residual oligonucleotides have a free phosphate ester at the 5'-termini and a modified 3'-termini. The chemical nature of the 3'-end was determined by post-treating oligonucleotides from the standard reaction mix with (a) venom 5'-exonuclease followed by alkaline phosphatase, (b) alkaline phosphatase followed by spleen 3'-exonuclease, or (c) 6 N HCl for 2 hr at 100°C followed by alkaline phosphatase. Products of these reactions were resolved by thin layer chromatography and paper electrophoresis. After elution from paper, the TMS derivatives were made and analysed by GC/MS. Glycolic acid was identified as a product of each of the reactions (Fig. 4). Glycolic acid was not found when bleomycin was omitted from the original reaction mixture. An additional product from step (c) was identified as levulinic acid; however, this is a secondary product of the hydrolysis and was found when bleomycin was omitted from the reaction mixture.

Conclusions

Four new products of the reaction of bleomycin with DNA have been isolated, two of which have been identified. The products have a common structure: Base-CH=CH-CHO. Oligonucleotides, produced by bleomycin induced strand scission, were found to contain glycolic acid residues esterified through the hydroxyl group to the 3' phosphate termini. These observations are consistent with a reaction initiated by free radical abstraction of the C4' proton of deoxyribose, leading to oxidative cleavage of the C3'-C4' bond.[4]

Acknowledgement

This work was supported, in part, by Grant CA 17395 from the National Cancer Institute, Department of Health and Human Services.

References

1. A.D. D'Andrea and W.A. Haseltine, Proc. Natl. Acad. Sci. 75, 3608 (1978).
2. M. Takeshita, A.P. Grollman, E. Ohtsubo, and H. Ohtsubo, Proc. Natl. Acad. Sci. 75, 5983 (1978).
3. D.T. Brown, J. Eisinger, and N.J. Leonard, J. Am. Chem. Soc. 90, 7302 (1968).
4. L. Giloni, M. Takeshita, F. Johnson, C. Iden and A.P. Grollman, J. Biol. Chem. (in press).

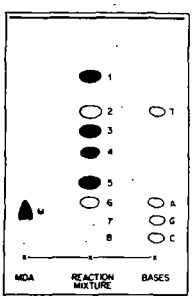

Fig. 1

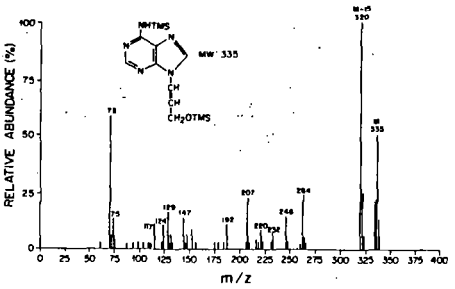

Fig. 2

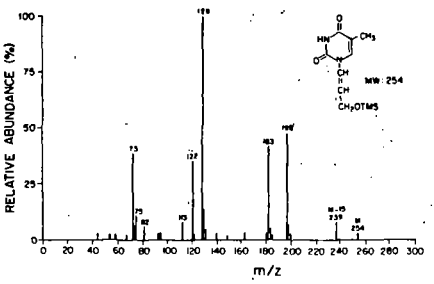

Fig. 3

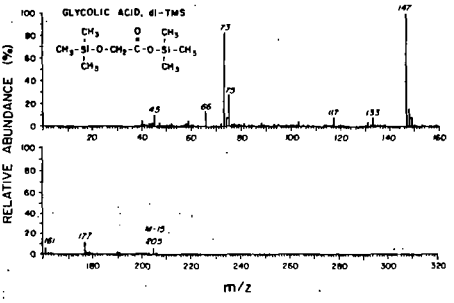

Fig. 4

MICRO STRUCTURE DETERMINATION OF LEPIDOPTERAN SEX PHEROMONES USING GC-MS

Ryohei Yamaoka(Lab. of Biochemistry, Kyoto Technical Univ.), Tamio Ueno and Hiroshi Fukami (Pesticide Research Inst. Kyoto Univ.), 606 Kyoto Japan

Sex pheromones secreted by virgine females of moths are highly potent volatile chemicals which attract males of the same species in extremely dilute concentration. But in isolation and structure determination of the compounds we are confronted with sevaral difficulties owing to their extremely scant presence in natural sources. However their specific bilogical activity has attracted organic chemists to determine their chemical structures. At present, the structures are known in many lepidopteran species and in most cases the structures are composed of carbon chain (C_{10}-C_{21}) containing several (1-3) C=C bonds in addition to hydroxy, ester, epoxide, ketone or aldehyde as the functional group.

The cruxes in the structure elucidations are regarded to be (1):determination of the C=C bond positions and (2):determination of geometries of the C=C bonds by micro analysis in submicrogram order. Previously employed techniques for other sex pheromones were of limitted value, because geometries of the C=C bonds could not be determined in submicrogram order and the arrangements of the geometries were demonstrated after total syntheses of every possible isomers. We have developed a generally applicable strategy using GC-MS and high resolution GLC to resolve these cruxes including the geometries.

Three sex pheromones (A, B and C) were isolated from adult females of potato tuberworm moth (*Phthorimaea operculella*, A:7μg from 400,000 virgine females), a pest insect of potato production, and webbing clothes moth (*Tineola bisselliela*, B:6μg and C:12μg from 40,000 virgine females), a pest insect of woolen clothes. EI mass spectra of these compounds indicate that they are composed of the following structural features; A: m/z 236($M^{+\cdot}$; $C_{15}H_{24}O_2$), m/z 176 ($M^{+\cdot}$- CH_3COOH suggests the presence of acetoxy group) and m/z 147, 133, 119, 105 and 91($C_nH^+_{2n-7}$ show a straight carbon chain containing three C=C bonds), B: m/z 266($M^{+\cdot}$; $C_{18}H_{34}O$), m/z 284($M^{+\cdot}$- H_2O), m/z 237($M^{+\cdot}$- 29) and m/z 111, 97 and 83($C_nH^+_{2n-1}$) suggest a *n*-octadecenal and C: m/z 264($M^{+\cdot}$; $C_{18}H_{32}O$), m/z 246($M^{+\cdot}$- H_2O), m/z($M^{+\cdot}$- 29) and m/z 109, 95 and 81($C_nH^+_{2n-3}$) suggest a *n*-octdecadienal. Functional group analyses using Kovats retention indices also indicate the presence of three isolated C=C bonds and a primary acetoxy group in A, an α,β-unsaturated aldehyde in B and C and an isolated C=C bond in C. Consequently, these sex pheromones A, B and C are concluded to be tridecatrienyl acetate, 2-octadecenal and octadecadienal.

Determination of the positions and the geometries of the C=C bonds were performed by the following micro analytical techniques combined with micro chemical reactions (See Fig. 1). Geometry of 2-position in B was confirmed to be *E* by total syntheses of both *E* and *Z* isomer. C was converted to the corresponding octadecadienyl acetate (C') by $LiAlH_4$ reduction followed by acetylation. In order to determine the positions and the geometries of the C=C bonds, A and C were partially hydrogenated by micro diimide reduction modified in the course these studies[1] and then each half amount of the reaction mixtures was subjected to micro ozonolysis to determine the C=C bond positions in the molecules of A and C'. The mass chromatographic (A) and GLC analysis (C') indicated the presence of the following compounds as the major products; from A: OHC-$(CH_2)_9$-OAc, OHC-$(CH_2)_6$-OAc and OHC-$(CH_2)_3$-OAc and from C': $C_{15}H_{31}CHO$ and OHC-$(CH_2)_{12}$-OAc. These results clearly demonstrate that the C=C bonds locate on 4, 7 and 10-position of tridecatrienyl acetate in A and 2 and 13-position of octadecadienyl

acetate in C'. The remaining half amount of the partially hydrogenated reaction mixtures were used to determine the geometries of CH=CH bonds. The produced monoenyl acetates were analyzed by mass fragmentography or GLC using a capillary SCOT column and their retention indices were compared with those of synthesized authentic specimens; from A, 4*E*, 7Z and 10Z-tridecenyl acetate were identified and from C', 2*E* and 13Z-octadecenyl acetate were identified respectively. As the results, the structures of these sex pheromones were unequivocally concluded to be as follows; A: 4*E*,7Z, 10Z-tridecatrienyl acetate, B: 2*E*-octadecenal and C: 2*E*,13Z-octadecadienal (See Fig. 2).[2-4] The results of the total syntheses followed by bioassay of A and B indicate that the validity of these proposed structures. Roelofs *et al.* reported 4*E*,7Z-tritridecadienyl acetate as a sex pheromone instead of A.[5] This discrepancy was solved by Persoons *et al.*, that is, the natural sex pheromone is a 4 : 1 mixture of both compounds.[6]

1) F. Alyward and Sawistwska, *Chem. & Ind.*, 484(1962)
2) R. Yamaoka, T. Ueno, H. Fukami and S. Ishii, *11th Symposium on Mass Spectrometry of Organic Compounds in Japan, Abstract* p79-82(1976, Chiba)
3) R. Yamaoka, H. Fukami and S. Ishii, *Agric. Biol. Chem.*, 40, 1971(1976)
4) R. Yamaoka, Y. Shiraishi, T. Ueno and H. Fukami, *14th Symposium on Mass Spectrometry of Organic Compounds in Japan, Abstract* p44-46(1979, Osaka)
5) W. L. Roelofs, J. P. Kochansky, G. G. Kennedy, C. A. Henrick, V. L. Cobin and J. N. Laboritz, *Life Sciences*, 17, 699(1975)
6) C. J. Persoons, S. Voerman, P. E. J. Verwiel, F. J. Ritter, W. J. Nooyen and A. K. Minks, *Ent. Exp. & Appli.*, 20, 289(1976)

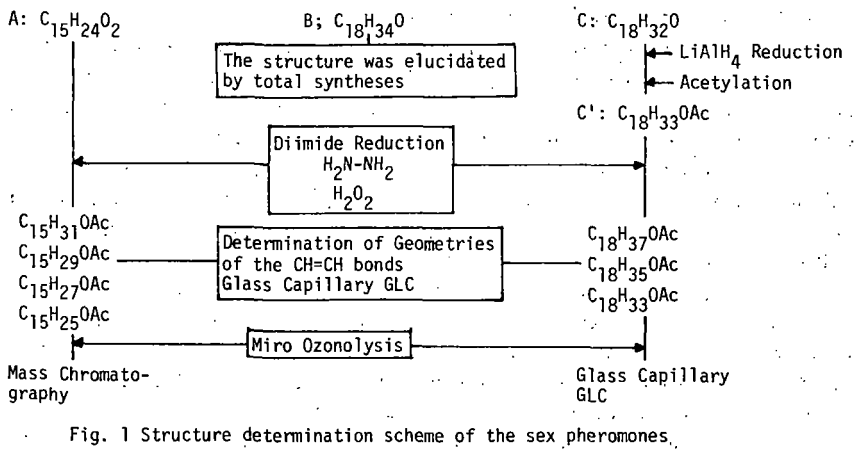

Fig. 1 Structure determination scheme of the sex pheromones

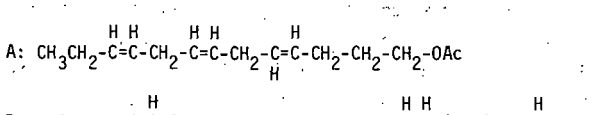

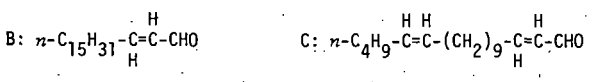

Fig. 2 Structures of the sex pheromones A, B and C

Application of Mass Spectrometry to Microanalysis of Chinese Herbs

Chen Yao-zu, Ma Xu-yi and Zhang Hue-die
(Laboratory of Organic Analysis, Institute of Organic Chemistry, Lanzhou University, Lanzhou, China)

Abstract

Mass spectrometry is one of powerful tools for micro organic analysis. A research project on study of application of mass spectrometry to micro identification of chemical ingredients of Chinese medicinal herbs is being carried on in our laboratory. In present paper, a brief abstract of analysis of chemical ingredients of Angelica Sinensis (oliv.) Diels (China name " Dang-gui ") is reported.

Angelica Sinensis (oliv.) Diels is a Chinese medicinal herb. Due to its sedative and analgesic effects and the effect on improving circulation and relieving stasis, it has been used as gynaecological medicine for hundreds years in China. Its predominant effects on cure of thromboangiitis obliterons and acute cerebral embolism have been deserved attention recently.

For analysis of chemical ingredients of A. S. Diels, we used micro scale procedure of steam distillation and water extraction of the powdered root of this herb. The essential oil obtained from steam distillation was analyzed via capillary column chromatography in conjunction with mass spectrometry. Two kinds of chromatograph column might be used, column I: SE-30 coated glass column (18M X ϕ3mm) or column II: liquid crystal M-103 coated glass column (30M X ϕ3mm). Sixteen chemical ingredients have been identified. They are: myrcene, β-phellandrene, α-pinene, camphene, p-cymene, carvacrol, azebaic acid, sebacic acid, anisic acid, myristic acid, camphoric acid, phthalic anhydride, n-butrlphythalide, n-butylidene phthalide andligustilide. The MS data of the last three compounds are: n-butylphthalide m/e (%): 190 (M^+) (2), 148(3.0), 133(100), 105(29), 77(9); n-butylidenephthalide: 188(M^+) (17.0), 159(100), 146(30), 131(20), 77(17); Ligustilide: 190(M^+) (52.5), 161(100), 148(72.5), 133 (15), 105(45), 77(37).

UV, IR and NMR of these compounds were also obtained. But the mass spectrometry was found to be the most satisfactory method for identification of phthalides and showed a definite systematic fragmentation starting from the cleavages at the allylic position or through McLafferty rearrangement.

After concentration of the hot water extraction, a syrup was obtained, from which four compounds were identified as ferulic acid, stigmasterol, β-sitosterol and D-glacoside of β-sitosterol by liquid chromatography

and mass spectrometry. A mixture of stigmasterol and β-sitosterol may be even identified directly through mass spectra. These identification were also confirmed by UV, IR and NMR data.

References

1. Lin Mao, Zhu Chaode, Sun Qingmin and Fang Qicheng, Acta Pharmaceutica Sinica, 14, 534(1979)

2. S. Takahshi, H. Hikino and Y. Sasaki, J. Pharm. Soc. Japan, 78, 1156(1958)

3. T. Yamagishi and H. Kaneshima, J. Pharm. Soc. Japan, 97, 237(1977)

4. F. W. McLafferty, Interpretation of Mass Spectra, 3rd. Ed. (University Science Books, 1980)

Paper No.	Page No.	Author
WAM0A2	353	COMPSON, K. R.
RPC13	650	COMPSON, K. R.
MPC8	157	CONNOLLY, J.
RPM0C8	565	CONWAY, D. C.
WAM0A6	361	COOK, J. C.
WAM0A10	369	COOK, J. C.
RPA20	602	COOK, J. CARTER
TPM0C4	260	COOK, KELSEY D.
MAM0B4	27	COOKS, R. GRAHAM
MAM0B6	30	COOKS, R. G.
MPM0B7	72	COOKS, R. G.
RPM0A2	515	COOKS, R. G.
RPM0B11	549	COOKS, R. GRAHAM
FAM0A4	663	COOKS, R. G.
FAM0A6	666	COOKS, R. G.
RPM0B9	546	CORY, H. T.
RPA12	588	COSTELLO, C. E.
RPA17	598	COSTELLO, C. E.
RPA3	572	COTTER, R.
MAM0B2	23	COTTER, ROBERT J.
MPC6	155	COTTER, ROBERT J.
RPA7	580	COTTER, ROBERT J.
FAM0B4	685	COUCH, M. W.
WAM0A7	363	COXON, D. T.
TPB16	323	CRAIG, JOHN S.
FPA8	739	CRAIN, P. F.
MPM0A3	51	CRAMERS, C. A.
MPB9	137	CRAWFORD, C. K.
TPM0B5	238	CRAWFORD, D. W.
MPC13	167	CRAWFORD, RICHARD W.
WAM0B8	391	CRAWFORD, R. W.
TAM0B3	184	CREWS, T.
TAM0B3	184	CROUTHAMEL, W. G.
WPB8	448	CROW, F. W.
WPB17	460	CROW, F. W.
TPM0C8	265	CROW, FRANK W.
FAM0B4	685	CROWLEY, J. R.
RPM0B10	548	CYSYK, R. L.
FPA12	744	CYSYK, RICHARD
WPB20	465	DAHLGRAN, JAMES R.
TPA9	289	DAN, PNINA
FAM0C9	720	DANNACHER, J.
RPB18	631	DANYLEWYCH, L. M.
MPB7	134	DAVES, G. D.
RPM0A5	521	DAVES, G. D.
RPM0B9	546	DAVES, G. D.
TAM0B8	192	DAVIDSON, WILLIAM R.
TPB17	325	DAVIDSON, W. C.
TPM0A4	218	DAVIDSON, W.
WPB7	447	DAVIDSON, W. R.
RPB18	631	DAVIDSON, W. R.
FAM0A8	670	DAVIDSON, W. R.
RPM0A2	515	DAVIS, D. V.
RPA17	598	DAVISON, A.
MPA12	116	DAWSON, P. H.
RPC6	640	DAWSON, P. H.
MPC15	170	DAY, R. A.
TPB13	320	DAY, R. A.
RPM0A6	523	DAY, R. J.
TPM0B6	240	DE BIEVRE, P.

Paper No.	Page No.	Author
TAM0B6	188	DE LEENHEER, A. P.
RAM0A2	469	DE, C. N.
MPB10	139	DECORPO, J. J.
RPA10	585	DECORPO, J. J.
RPM0C3	557	DECORPO, J. J.
RPM0C6	562	DECORPO, J. J.
FAM0C5	714	DEHMER, J. L.
TPA4	280	DELGMANN, L.
WAM0A3	355	DELL, A.
WAM0A13	375	DELL, A.
WAM0A15	379	DELL, A.
RPM0A10	528	DELL, A.
TPM0B4	236	DELMORE, J. E.
WPB18	462	DELMORE, J.
TPC12	347	DENISON, A. B.
MPC16	171	DENNE, D. P.
RPC14	652	DENO, N.
TPM0C9	267	DENTON, M. D.
WAM0C10	406	DEPUY, C. H.
RAM0B2	487	DESIDERIO, D. M.
FAM0B12	700	DESTEFANO, A. J.
FAM0B14	703	DESTEFANO, ANTHONY J.
WAM0B2	385	DICESARE, J. L.
TPA4	280	DIELMANN, G.
RPM0B10	548	DIETRICH, T.
FPA9	741	DINO, JOHN
RAM0A1	467	DJERASSI, CARL
FAM0B11	698	DJERASSI, C.
MPC3	150	DJURIC, N.
RPM0A3	517	DOLE, MALCOLM
MPA12	116	DOUGLAS, D.
TAM0C4	202	DOUGLAS, D. J.
FAM0B5	687	DREIFUSS, P. A.
WPB2	437	DROMEY, R. G.
MAM0C2	43	DROWART, J.
TPM0A10	230	DUBAY, G. R.
RPC1	633	DUBAY, G. R.
WPB13	454	DUCHAMP, D. J.
TPM0C2	256	DUGGER, DONALD L.
MPA16	118	DUNBAR, R. C.
WAM0C11	408	DUNBAR, R. C.
MPB2	127	DURDEN, DAVID A.
RAM0A2	469	DUTTA, S. P.
RAM0B5	493	DVORIN, E.
RAM0B5	493	DYCKES, D.
MPM0C8	91	DYKE, J. M.
WPB20	465	DYMERSKI, PAUL P.
RPM0A4	519	DZEIDZIC, P.
TPM0B7	242	EBY, R. E.
TPM0B8	244	EBY, R. E.
TPM0B10	248	ECHO, M. W.
RAM0A10	484	ECKERS, CHRISTINE
WPA3	420	EDELSON, MARTIN C.
FAM0C5	714	EDERER, D. L.
RAM0A2	469	EDMONDS, C. G.
MPM0C11	97	EIGENDORF, G. K.
WPA1	416	ELLEFSON, ROBERT E.
WPA11	434	ELLIOTT, R. M.
MPB13	144	ELLIS, H. W.
RPB2	607	ENGLAND, ROGER E.
WPB6	445	ENKE, C. G.
RPC5	638	ENKE, C. G.

Business Meeting of the American Society for Mass Spectrometry
Wednesday, May 27, 1981, 6 P.M.

President Munson introduced Judith Watson (PAM) to the approximately 200 assembled members of the Society and briefly explained her activites on our behalf. The Secretary asked for corrections for the minutes of the previous year which were then approved as read. He exhibited the election results, noting the very close contests and introduced the successful candidates.

VP Programs	Keith Compson	247
	Michael McKeown	237
Secretary	Terry Ashe	255
	Charles Wilkins	227
Director-at-large	Fred Lampe	277
	Steve Heller	215

A slide was presented showing near linear growth of the Society at 100 members/year since 1969. The present membership is 1736. Makeup of the Society by type of member and nationality was also presented. The Secretary then introduced the winners of the travel scholarships who were applauded by the meeting. Brief mention was made of the untimely death of ASMS member Peter Brown, an excellent and widely liked organic mass spectrometrist from Arizona State University. The Secretary asked those assembled to inform him of any other losses of which it was aware; the Society is so large now that such matters can easily escape notice.

Treasurer Frisch then presented slides showing the financial condition of the Society. The balance on hand as of May 21, 1981, is $88,254.80. The Treasurer's report was approved as read.

Fenselau then presented a review of the Minneapolis program: 462 abstracts were reviewed and 452 accepted, composed of 223 oral sessions, 197 posters, 28 symposia, 2 educational and 2 plenary. She then thanked the abstract review committee composed of T. Aczel, D. Ridge, W. Fite, R. Cotter, and L. Powell, and invited the membership to submit ideas for session topics next year.

Munson then discussed the Hawaii Conference in detail, noting that the Hilton Hawaiian Village required ASMS to work through a travel coordinator. We have chosen GTU (Group Travel Unlimited) who will arrange all flight and hotel booking. Members who preregister will save $10; and GTU will mail a brochure to the membership early in June explaining details and costs. Conference rates will apply the week before and after the meeting. Rooms will be approximately $50/single.

V.P. for Arrangements Wolstenholme continued discussion of future meetings after thanking the Society for the opportunity to serve as an officer The schedule is as follows: 1982, Honolulu, HI; 1983 Boston, MA; 1984, San Antonio, TX; 1985 San Diego, CA; 1986, East Coast. An earnest effort will be made to find alternative hotel accommodations in all future meetings to assist those on limited budgets.

Past President McCloskey then read a letter from a mass spectrometry society currently forming in the People's Republic of China. They hope to have at least one representative in Honolulu. Japan currently estimates that approximately 130 members of their two societies will attend the Conference in Honolulu.

Fite also thanked the Society for the opportunity to serve on the Board of Directors and then briefly discussed the Conference Abstracts, emphasizing the title "Abstracts" that will henceforth be used exclusively in describing this publication. Once again, he intends to produce the volume in timely fashion with the aid of Judith Watson (ASMS Staff) and ASTM's publishing facilities. He especially thanked the committee chairmen for submitting their reports promptly. In turn, Munson expressed the Society's profound appreciation to Fite for organizing the Abstracts into a truly viable operation.

Member at large Jack Watson then presented a brief summary of the salary survey and answered questions on its rationale. An extended discussion was planned for the next day and a more complete summary will be published in the 1981 Abstracts.

Munson expressed the Society's thanks for jobs well done to each of the outgoing Board members who were roundly applauded by those assembled. T. Aczel moved adjournment at 6:40 P.M.

H. Fales

ASMS COMMITTEES

Fundamentals	M. T. Bowers, Department of Chemistry, University of California, Santa Barbara, CA 93106
Computer Applications	Roger Upham, Department of Chemistry, University of Minnesota, MN 55455
Biomedical Applications	W. R. Sherman, Psychiatry Department, Washington University, St. Louis, MO 63110
Quantitative Organic Analysis	Marjorie Horning, Institute for Lipid Research, Baylor College of Medicine, Houston, TX 77030
Solid and Surface Analysis	Peter Williams, Materials Research Laboratory, University of Illinois, Urbana, IL 61801
Education	Harry S. Hertz, National Bureau of Standards, A113 Chemistry, Washington, DC 20234
Qualitative Organic Techniques	Maurice Bursey, Department of Chemistry, University of North Carolina, Chapel Hill, NC 27709
Isotope Ratio Measurements	Lura J. Powell, National Bureau of Standards, Building 221, Room A21, Washington, DC 20234
Environmental Applications	Ralph Dougherty, Department of Chemistry, Florida State University, Tallahassee, FL 32306
Forensic Applications	Richard Saferstein, New Jersey State Police Laboratory, PO Box 7068, West Trenton, NJ 08625
Nomenclature	John Beynon, Department of Chemistry, University College, Swansea, SA2 8PP, Wales
Nominating	Rodger Foltz, Center for Human Toxicology, University of Utah, Salt Lake City, UT 84112
High Temperature & Inorganic	Donald L. Hildenbrand, SRI International, Menlo Park, CA 94025
Good Laboratory Practices	A. J. Destefano, Proctor & Gamble, PO Box 39175, Cincinnati, OH 45247

ASMS Committee on Fundamentals

Technical Activities:

In 1981 Committee II sponsored one symposium (Gas Phase Metal Ion Chemistry from Catalysis to the Ionisphere), one workshop (MS/MS: Fundamental Aspects and New Techniques) and was responsible for suggesting one of the plenary lecturers (Dr. Richard Zare - Laser Multiphoton Ionization: Writing an Optical Signature on Mass Spectrometry). The symposium was well organized by Dr. Douglas Ridge whose choice of speakers spanned the experimental state of the art of the field. The symposium was very well attended. The workshop, organized and lead by Graham Cooks, was very stimulating. A panel of representatives of five of the leading manufacturers of MS/MS equipment were asked eleven questions covering the entire range of technical and chemical state of the art. Comments were also solicited from the audience of several hundred. Feedback on the format was mixed but generally favorable, particularly concerning the manufacturers view of where MS/MS is and is going. Finally, the plenary lecture of Dr. Zare was a rousing success and served to excite everyone about the prospects for application of multiphoton ionization to mass spectrometry.

Business Meeting:

The committee has a few general comments to make about this years meeting and about next years meeting in Hawaii. Concerning this years meeting, many attending the committee meeting voiced dissatisfaction with the distribution of oral sessions of interest to fundamentalists. While acknowledging scheduling the program is a difficult proposition at best the feeling was unanimous that the Society's interest would be best served if the preliminary program could be reviewed by a member of the fundamentals committee before being finally approved and sent to the printer. It was felt the potential for avoiding scheduling conflicts outweighed the problems caused by a delay of several days in final approval of the program. On the positive side, those attending the committee meeting unanimously and enthusiastically endorsed the concept of Introductory Lectures and strongly encouraged their continuation.

Turning to next years meeting in Hawaii, two main issures were raised. First, those attending the meeting voted unanimously for maintaining our traditional meeting format rather than the proposed format of long mornings for regular sessions and afternoons for workshops. They also supported evening workshops similar to those held this year. They reasoned that this meeting provided their primary opportunity for sharing scientific progress of the past year and felt that fact should override any worries about sparsley attended sessions. Further they strongly endorsed the idea of bunching the bulk of the fundamentals papers into 2-3 days rather than spreading them randomly throughout the week. There were mixed feelings in the committee regarding the elimination of plenary lecturers and the usual symposium format with a majority favoring their retention. Most members were sympathetic with the scheduling problems that could arise if they were included, however. Finally, the committee enthusiastically endorsed the lead lecture concept of symposium organization and felt that the Hawaii meeting would provide an excellent opportunity for experimenting with this format. A letter outlining specific suggestions will be sent to the board for consideration.

Respectfully submitted,

Michael T. Bowers, Chairman
Committee II Fundamentals

MTB:mrk

Business Meeting.

The Committee on Computer Applications business meeting was attended by about 25 ASMS members.

The interest expressed last year in communications between different computers is still present. Several members volunteered to form a sub-committee to review the topic including the status of any computer industry standards.

There was some discussion about formats for presenting spectra for the data base files. It was suggested that an attempt be made to have manufacturers provide a program which would enable a user to place a spectrum in a file in a format suitable to the large data bases. It was noted that one problem existing in the commercial systems was the different interpretations of the EPA suggested format.

There was agreement again that an inventory of data systems users should be compiled. The E-14 committee is doing a limited survey with which we might cooperate, but it was felt a survey of the full ASMS membership was also necessary.

The members felt that the new introductory lectures provided this year were very useful and suggested that one be held on computer techniques.

Topics suggested for next year's sessions were:

1. Custom Enhancements to Commercial Data Systems

2. Symposium on Software and Hardware for Inter-Computer Communications

Committee Members:

I. K. Mun

David Martinen

COMMITTEE REPORT
QUANTITATIVE ORGANIC ANALYSIS

The major committee activities for 1981 were the symposium "Are their alternative methodologies to GCMS?" and the joint sponsorship of a workshop on standards and methods validation. The former was moderately well attended, considering its position on the program opposite to the hottest meeting topic, fast atom bombardment. Those attending found the topics and views presented of considerable interest, and perhaps a welcome hiatus in the mass spectrometry program. The workshop on standards and methods validation was very well attended, although several members of the audience suggested that future workshops be more highly focussed on one particular aspect of quantitative methodology.

The business meeting was directed toward topics of interest for next year's program. Of greatest interest was a symposium on non-chromatographic methods of mass spectrometric quantitation-pros and cons. Probe (DCI, pyrolysis, FD, FAB, 252-Cf, etc.), tamdem MS, (neutral loss, daughter ion, etc.), and batch inlet techniques for quantitative analysis could be reviewed and critically evaluated by authors with experience with several alternative techniques.

Attendees at the business meeting included:

J. Paulson	S. Hattox
G.P. Sturm, Jr.	Q. Grindstaff
T. Marriott	G. Fallos
R.C. Murphy	J. Holler
D.Schoeller	D. Patterson
C. Judson	R.P. Barron

Submitted by: S.P. Markey for
M.G. Horning, Chairman

ASMS EDUCATION COMMITTEE REPORT

The Education Committee sponsored two short courses on the weekend preceding the Annual Conference on Mass Spectrometry and Allied Topics. The courses were held at the Radisson Downtown Hotel in Minneapolis, Minnesota. Each of the courses, one on Interpretation of Mass Spectra and the other on Quantitative Mass Spectrometry, had an enrollment of greater than 20 students. The instructional staff consisted of:

Dr. Fred P. Abramson, George Washington University Medical Center, Washington, DC
Mr. Mike Carter, Environmental Protection Agency, Washington, DC
Dr. Henry M. Fales, National Institutes of Health, Bethesda, MD
Dr. Stephen R. Heller, Environmental Protection Agency, Washington, DC
Dr. Harry S. Hertz, National Bureau of Standards, Washington, DC
Dr. James A. Kelley, National Institutes of Health, Bethesda, MD
Dr. Edward White V, National Bureau of Standards, Washington, DC
Dr. Alfred L. Yergey, National Institutes of Health, Bethesda, MD

Based on comments by the students, both courses were well received. In a meeting of the Education Committee following the short courses several suggestions were made about future educational activities for the ASMS. The Education Committee proposed a workshop on aspects of teaching mass spectrometry at next year's annual meeting. It was also proposed that a third short course be added in future years. This short course would be on a current topic in mass spectrometric research. The course would be aimed at practicing mass spectrometrists and would be taught by people expert in the particular topic. The topic for this short course would change from year to year. We hope to offer the first course in this series at the Honolulu ASMS meeting.

Respectfully submitted,

Harry S. Hertz
Education Chairman

ASMS Committee IV. Isotope Ratio Measurements

At the Minneapolis meeting of the ASMS, the Committee on Isotope Ratio Measurements sponsored a symposium, a poster session, and two workshops. All activities were exceptionally well attended; with many new participants as well as strong support from the isotope ratio core group.

The symposium, Advances in Isotope Ratio Measurements, held in honor of Albert O. Nier, was highly successful. Both the program and Nier's 70th birthday celebration were very well received. The poster session, Isotope Ratios, drew an encouraging number of papers due, in part, to the diligence of its organizer, Jack Fassett. The workshops, Computer Software for Automated Isotope Ratio Mass Spectrometers and Gravimetric Procedures for Isotope Dilution, provided an opportunity for lively discussions and a free exchange of ideas and information. The gravimetric workshop offered a "hands-on" opportunity for its attendees. This marks the second time the "hands-on" approach has been used successfully in a Committee IV Workshop, dictating continued use in the future.

During the past four years, this committee has gradually accumulated a rather broad support group, largely due to the efforts of the charter organizers Ernest Garner and Don Rokop. During the next few years, we hope to broaden this base of support by expanding the scope of topics covered by our activities. A program is being formulated for the 1982 meeting to help meet this goal.

In conclusion, I would like to formally thank all those who contributed their time and energy to make this years' program a success. Special thanks go to Burnaby Munson, Catherine Fenselau, Roger Upham, Judith Watson, and Tom Terwilliger for their help in staging the birthday celebration; and to the ASMS board for their support throughout the year.

Respectfully submitted,

Lura J. Powell
Chairman, Committee IV

COMMITTEE REPORT

Environmental Committee

SYMPOSIUM: HIGH RESOLUTION GC/MS IN ENVIRONMENTAL CHEMISTRY AND BIOCHEMISTRY

This symposium was organized in cooperation with the biochemistry committee and consisted of six lectures on the state-of-the-art in high performance capillary gas chromatography high performance mass spectrometry. Subjects discussed included: separation and identification of chiral myo-inositol phosphates using a chiral capillary liquid phase, W. Sherman; high resolution MID from capillary columns for precision quantitative identification of dioxins and other molecules, J.R. Hass; ultra-high resolution gas chromatography using thick films and hyperbaric inlet pressures for analysis of hydrocarbons and urinary components, P.A. Leclercq; high resolution capillary gc on Silar 10C for isomer specific analysis of dioxins and dibenzofurans in environmental samples, H.R. Buser; capillary gas chromatography mass spectrometry of fluoroacyl derivatives of indole amines for identification and quantitation at sub pg levels, P.L. Taylor; and capillary gc/MS with low resolution precision mass measurement for identification of humic acid components and humic acid degradation products, D.S. Millington. The symposium was very well received by the membership. During most of the symposium, there was standing room only in the auditorium. For the best attended talks there were more than 300 people in the room.

WORKSHOP: CHEMICAL STANDARDS AND METHODS VALIDATION

This workshop was attended by more than 125 people. There was standing room only for the duration of the workshop. The workshop panel consisted of: W. Budde, EPA, OH; H. Hertz, NBS, MD; D. Kuehl, EPA, MN; S. Markey, NIH, MD; J. McCloskey, U. Utah; R. Mitchum, NCTR, AR and J. Sphon, FDA, DC. The subjects discussed included: specific identification of compounds to be analyzed; requirements for procedural blanks; establishment of calibration for quantitative methods; chemical standards for both calibration and evaluation of instrument performance; and the presently available and soon to be available Standard Reference Materials for analysis of biological and environmental material. The discussion was lively and many points of view on the requirements for validation of methods of analysis for specific compounds were presented. Specific problems with artifacts that are developed from either background contamination or compounds generated in derivatization were discussed. The requirements for certainty in identification, numbers of ions in MID analysis, the use of high resolution MID and related topics were discussed. The virtue of monitoring a single ion to prove the lack of the presence of a given compound in a matrix was discussed. The utility of high temperature annealing of chemical glassware for the reduction of background contamination was discussed. Pitfalls in the use of isotope dilution for quantitation of specific compounds were presented. It was suggested that thorough calibration curves be prepared for high performance analysis. It was generally concluded that high performance capillary introduction is one of the best methods for reducing matrix effects on the results of the analysis. The relative utility of chemical standards like decafluorotriphenylphosphen and the fluorinated polymer "Ultramark 1600" were discussed. Standard Reference Materials are now available from the NBS for shale oil, polynuclear aromatic hydrocarbons in water and a number of compounds in human serum. Standard reference materials will soon be available for polynuclear aromatic hydrocarbons in dust, polychlorobiphenyls in oil and organic compounds in drinking water.

COMMITTEE MEETING:

Attendance at the annual environmental committee meeting was lower than it would have been had the meeting been held just after the workshop. Nonetheless, a number of very active people in the field were present and the discussion was lively. Suggestions for session topics for the 1982 meeting included: Organic Chemicals in Water; Toxic Residues; Precision and Accuracy in Analysis. Several individuals were suggested as candidates for "lead speakers" in the environmental sessions. Interest was expressed in two separate workshop topics for 1982. These topics were: Evaluation of Precision, Accuracy and Reliability; and Analytical Problems Addressed by Mass Spectrometry and Other Analytical Techniques with case studies. It was recommended that an introductory lecture be presented in 1982 on the subject of high performance capillary chromatography. A number of people were suggested as suitable for the presentation of that lecture.

ASMS COMMITTEE ON HIGH TEMPERATURE MASS SPECTROMETRY

D. L. Hildenbrand
SRI International
Menlo Park, CA 94025

At the 29th annual meeting of ASMS in Minneapolis, the committee organized and sponsored two events: a Symposium on High Temperature Mass Spectrometry, and a Workshop on Improved Methods for Measuring Appearance Potentials in High Temperature Beam Species. The Symposium consisted of five invited papers on diverse topics related to the energetics, ionization, and spectroscopy of high temperature species, and to new methods for characterizing these species. There were, in addition, ten contributed papers describing recent studies in the high temperature area. The response indicates that the Symposium served its intended purposes of highlighting some of the newer developments pertinent to the field, and of re-establishing communications between laboratories. Significantly, there were three foreign participants, representing Belgium, Great Britain, and West Germany.

The workshop on ionization and appearance potentials was organized by Dr. E. Murad, and was composed of several informal presentations and discussions concerned with photoelectron spectroscopy, electron impact measurements, and the use of reaction energetics and thermochemical cycles to evaluate ionization energies of radicals and unstable species. The combined symposium and workshop sessions provided the first such activity within ASMS in about a decade, and all agreed that continued activity of this type would be highly beneficial.

Future activities of the committee were discussed at a business meeting. In view of potential overlap with the Gordon Research Conference on High Temperature Chemistry and the International Conference on Mass Spectrometry in 1982, no specific activities are planned for the Honolulu meeting of ASMS. Activities for 1983 and beyond were discussed, but no formal recommendations will be made until several features are investigated further. In response to a suggestion by one of the participants, it was agreed that the inclusion of studies of the pyrolysis of biomass and other organic materials in committee activities would be desirable. Possibilities for coordinating our efforts with those of the European high temperature group were also explored.

The Chairman would like to take this opportunity to thank committee members for their input and assistance during the past year.

ASMS Committee on Good Laboratory Practices

The Good Laboratory Practices (GLP) committee meeting was held on Wednesday, May 27, 1981 at 3:00 p.m. Approximately 45 people were in attendance.

The meeting began with an overview of the GLP regulations and how they apply to mass spectrometry laboratories. Copies of the regulations (Federal Register, 43(247), 60013, 1978) were (and will be) distributed to those asking for them. The latest draft of the proposed ASTM guideline on GLP was discussed in some detail. It was noted that mass spectrometers fit into different organizations in very different ways, ranging from dedicated mass spectrometry laboratories to a small part of a group of analytical instruments dedicated to solving the problems of specific projects. This makes it virtually impossible to have a standardized sample handling or logging format. However, it is important in each case that appropriate operating and maintenance records are maintained for all instruments involved in GLP analyses.

The draft of the ASTM guideline is available to anyone interested. Comments are welcome and should be made by early fall, if possible. After the meeting Drs. J. Sphon (FDA, Washington) and R. Thompson (Battelle, Col.) offered to help work on the next draft of the guideline. Any other assistance is welcomed.

The last part of the meeting dealt with the recently published article, "Critical Evaluation of Class II and Class III Electron Impact Mass Spectra. Operating Parameters and Reporting Mass Spectra," J. G. Dillard, S. R. Heller, F. W. McLafferty, G. W. A. Milne and R. Venkataraghavan, Org. Mass Spectrom., 16(1), 48 (1981). This article provides specifications for the collection, reporting and evaluation of electron impact mass spectra. Spectra may be classified as Research Reference Spectra (Class II) or Analytical Reference Spectra (Class III) depending on the amount of care taken to ensure proper instrument operation, data reporting and sample purity.

This article provided impetus for a good deal of lively discussion regarding the quality of current and future spectra entered in the various libraries. Several people expressed their doubts about the quality of the various chemical ionization spectra now being accepted by some libraries and suggested that a document similar to this one would be useful for these spectra as well. Comments on this article or on assuring the quality of library spectra in general are invited. These should be addressed to Dr. McLafferty (Dept. of Chem., Cornell Univ., Ithaca, N.Y. 14853) or to the committee chairman (The Procter & Gamble Co., P.O. Box 39175, Cincinnati, OH 45247).

Respectfully submitted,

Anthony DeStefano

Anthony DeStefano
Chairman

st

WORKSHOP REPORT
ON
PYROLYSIS MASS SPECTROMETRY, PRACTICE AND TECHNIQUES

The Workshop on the Techniques and Practice of Pyrolysis Mass Spectrometry was held Monday, May 25, 1981, at 8:00 p.m. This Workshop was designed to highlight the differences and similarities; and the advantages and disadvantages of the different pyrolysis/mass spectrometric techniques presently in use. The panel members represented many of these different techniques. The Workshop began with each of the panel members presenting a brief description of the pyrolysis mass spectrometry techniques employed in their laboratories and the specific applications that they are put to.

Panel members included:

Dr. S.C. Israel
Polymer Science Program
Department of Chemistry
University of Lowell
Lowell, MA 01854
617-452-5000

Dr. H.L.C. Meuzelaar
Biomaterials Profiling Center
University of Utah
391 S. Chipeta Way
Salt Lake City, UT 84108
801-581-5841

Dr. C.M. Wong
Lawrence Livermore National Laboratory
P.O. Box 808, L-325
Livermore, CA 94550
415-422-0435

Dr. N.E. Vanderborgh
Los Alamos Scientific Laboratory
P.O. Box 1663, MS. 329
Los Alamos, N.M. 87545
505-667-2631

Dr. Meuzelaar opened the discussion with a description of his efforts in the application of direct pyrolysis mass spectrometry to the profiling of biomaterials and fossil fuels. The system described utilized a curie-point pyrolyzer interfaced directly to the ion source of a quadrapole mass spectrometer; the pyrolysis products being analyzed by low voltage electron impact ionization. The system is fully automated, permitting routine analysis of a large number of samples.

Dr. Israel presented his work in the determination of polymer structure and composition utilizing a specially constructed "pyroprobe" type pyrolyzer interfaced directly to the ion source of a double focussing mass spectrometer. The pyrolysis products are analyzed by chemical ionization.

Dr. Wong discussed the entry of her group into the analysis of oil shale and fossil fuels pyrolysis products by a computer controlled triple quadrapole mass spectrometer. Dr. Wong raised questions regarding instrumental interfacing and pyrolysis techniques and some of these questions served as the basis for much of the discussion that followed.

Dr. Vanderbourgh presented his work in the area of geochemical analysis by laser pyrolysis mass spectrometry. He discussed the apparatus and techniques necessary for these samples and presented some results that emphasized the utility of laser pyrolysis.

During and after the presentation there was extensive discussion among the panel members and members of the audience. Initially, the discussion centered on the advantages and disadvantages of each of the techniques with emphasis on the curie-point and pyroprobe. The discussion highlighted the differences in the sampling techniques and sample handling of each method. The catalytic effects of metals and sample residue on the pyrolysis process was discussed and many suggestions were made for treating and cleaning apparatus. A discussion of interlaboratory reproductability of pyrolysis results led to further discussion of the effect of pyrolysis temperature and temperature rise time on pyrolysis products and the problems involved in measurement of actual sample temperature.

At this point interest turned to a discussion of the differences between pyrolysis at the ion source and pyrolysis external to the mass spectrometer with transfer of pyrolysis products for analysis. Most of the discussion involved pyrolysis into a gas chromatographic inlet and possible trapping techniques for the pyrolysis products.

The final area to be discussed was the treatment of pyrolysis data by the techniques of factor analysis, mathematical mapping and use of the Arthur Computer Programs.

The Workshop was adjourned after about two hours of extensive discussion and participation by the panelists and audience alike, with noteable contribution from Drs. Soltys, Gritter, Grayson, Lattimer, Abbey, and other members of the audience.

Respectfully submitted,

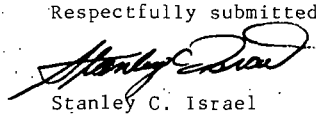

Stanley C. Israel
Chairman

ASMS COMMITTEE ON BIOMEDICAL APPLICATIONS

The Biomedical Applications Committee held a Workshop on Capillary GC and GCMS and, at the suggestion of Dr. Daniel Knapp of the Medical University of North Carolina, an inquiry into and discussion on the question of whether there is a need for a low cost MS detector for gas chromatography. The Committee also co-sponsored, with the Environmental Applications Committee, a symposium (MPMOA1-6) on "High Resolution GCMS in Environmental Chemistry and Biochemistry".

The workshop began at 8 PM on Tuesday, June 25. About two hundred people were present. Five discussants, Dr. Dennis Lin, Battelle Columbus, Dr. David Millington, University of North Carolina, Dr. Phillip L. Taylor, N.I.M.H., Rand Jenkins, J. & W. Scientific and the Committee Chairman gave brief presentations. The purpose of the workshop was to identify a few problem areas in capillary GC and GCMS and to discuss the solutions, if any, to the problems. It was hoped that audience participation would contribute to the solution of methodological difficulties and to clarify misinterpretations of results. Perhaps a greater effort could have been made to draw out the audience in the latter regard although a few spontaneous discussions occurred. The topics covered included: Lin, precision of quantitative analysis using fused silica columns where he has encountered significant problems with compounds which can be categorized as "polar". He pointed out the difficulties in obtaining precise data with these columns using the sampling times commonly available with many data systems. Millington showed the design of his direct fused silica column inlet into the VG-7070 and several schemes for direct on-column injection. Taylor commented that, in the connection of fused silica columns to a quadrupole via an open split interface, a phase-coated fused silica transfer line from the interface to the source gave him the best results with respect to adsorptive losses. There was comment about the difficulty in obtaining sizes of the silica transfer line which provided a restriction suitable to accommodate the sudden pressure drop from the column to the source. Sherman pointed out how seemingly small structural or derivative variations in inositol phosphates can result in large differences in adsorption by the column, and that this could be variable from column-to-column even from the same manufacturer. He also reported on an intramolecular phosphate migration which was enhanced at elevated temperatures and absent at reduced temperatures. In response to reports that fused silica capillary columns were occasionally being observed to fracture while in use, Jenkins described the changing nature of the industry and suggested that new methods of protecting fused silica columns will be forthcoming. MEANWHILE, USERS SHOULD BE WARNED OF THIS LIABILITY TO FRACTURE, ESPECIALLY WHEN USING H_2 AS CARRIER. One instance was reported (Markey and Taylor, NIMH) of a leak within the polymide coating of the column, visible only under pressure, submerged in water. This portion of the meeting ended at 9:30 when about 150 of the group departed for the hospitality suites.

A discussion was then held with the remaining 50 people of the question "Is there a need for a simple mass spectrometer designed for selected ion monitoring only?" The consensus of the group appeared to be that there was a need for such an instrument and some felt that one could be sold for well under $50,000. L.F. Herzog (Nuclide) suggested that such an instrument might be based on an existing permanent magnet isotope ratio instrument which he manufactures. There was a broad range of opinion as to what the capabilities of such an instrument should be. It was suggested that one should not even call it a mass spectrometer because doing so inevitably leads to an escalation in the desired capabilities. Although there was at least one vigorous proponent of a single ion instrument, most felt that it should have two or three ion capability. The mass range necessary in such an instrument was also a subject of broad opinion (see plot below).

A question sheet was distributed and 31 responses received. Twenty-three answered that there was a need. Of the eight negative replies, most expressed the opinion that it was impossible to build and sell an instrument for under $50,000 to adequately do the job. There was an equal opinion (11 each) as to whether it should be EI only or EI/CI. Three voted for CI only. Twenty felt that it should have capillary and packed column capability while 5 said capillary only. Eleven respondents saw a need for a probe inlet. The quadrupole type was preferred 21 to 6 over the magnetic type. The figure below shows the response to the questionnaire regarding the mass range of such an instrument.

William R. Sherman
Chairman, Biomedical Applications

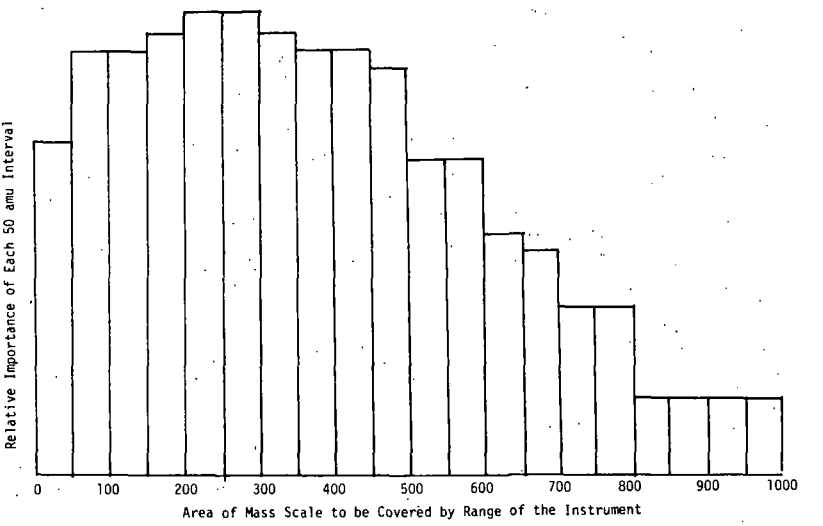

Report on Workshop

on

Improved Methods for Measuring

Appearance Potentials in High Temperature Beam Species

The workshop was held on Tuesday, 26 May 1981 at the Radisson Hotel. The panelists were:

J. L. Beauchamp, California Institute of Technology

D. L. Hildenbrand, SRI International

N. Jonathan, University of Southampton, England

R. F. Porter, Cornell University

19 persons attended this workshop.

Dr. Jonathan began by summarizing results which he and Dr. John Dyke obtained using photoelectron spectroscopy. The species discussed included CrO, SiO and a number of inorganic and organic free radicals such as NF, NCO, NH_2, PH, PH_2, HCO and FO. These species are generated by reacting F atoms with HX, where X is the radical in question. The spectra are obtained at room temperature. To make these measurements a density of about 10^{11} molecules/cc is needed.

Dr. Beauchamp described a different approach they have used in his laboratory to study the photoelectron spectra of simple organic free radicals. Simply, the free radicals are generated by the pyrolysis of organic nitrites at temperatures varying between 400 and 1100 C. He described ways of obtaining structural information about free radicals, and illustrated this by a discussion of the structure of $C_2H_5^+$.

Dr. Porter described a set of experiments they have performed to measure the electron affinities of positive ions of unstable neutrals, e.g. CH_5^+. In these experiments they measured the kinetic energy of the products of neutralization reactions such as:

$$X^+ + Na \rightarrow X + Na^+$$

where X^+ is NH_4^+, CH_5^+, H_3O^+, etc. They have also used other neutralizing metals such as K and Zn. These measurements yield the only information about the respective neutral molecules.

Dr. Hildenbrand described briefly how they measure appearance potentials by the extrapolated voltage difference method. He then presented a table showing a comparison between ionization potentials measured by electron impact and those measured subsequently by photoelectron spectroscopy. The agreement was excellent.

Edmond Murad

EDMOND MURAD
Chairman

WORKSHOP:

LASERS AND MASS SPECTROMETRY

The format of the workshop was to summarize current achievements and to explore future developments in three basic areas which combine lasers and mass spectrometry:

(1) Surface analysis, LAMMA, scanning milliprobes, etc.
(2) Multiphoton techniques, resonant and non-resonant absorption and two laser systems; and
(3) Laser desorption of non-volatile compounds.

Robert Conzemius from the Ames Laboratory (Iowa State) opened the discussion by noting the large number of laser/mass spectrometer techniques, which are designated by their acronyms: LMS (laser mass spectrometry), LEMS (laser evaporation mass spectrometry), LIMS (laser ionization mass spectrometry), and so forth. The techniques differ in several critical parameters, including: lager energy (10^{-7} to 10^{1} Joules), pulse widths (10^{-9} to 10^{-3} s), power (10 to 10^{8} watts), power density (10^{5} to 10^{12} W/cm^2) and wavelength (0.22 to 10.6 μM). Another important distinction is geometry, ϕ/θ, where ϕ is the laser/sample surface angle and θ is the surface/mass analyzer angle. A common geometry is $45^{o}/90^{o}$, and the LAMMA technique, which desorbs sample from the back of a foil, is designated as $-90^{o}/90^{o}$.

Results by Bykova, et al. (Sov. Tech. Phys. Lett., 1, 1980, 1975) show that at low laser powers, 10^{6} W/cm^2 and below, thermal events predominate, which are proportional to the laser power density. Neutrals and ions are desorbed which have low energy spreads. Above 10^{8} W/cm^2, non-linear phenomena predominate and visible plasmas can be observed. At 10^{9} W/cm^2, n^{+}/n^{o}, the ratio of ions to neutrals formed, approaches unity and 100% ionization can be achieved at even higher power densities. Such high densities are used for elemental analysis, cause cratering in the metal substrates and produce ions with considerable energy spread (100 to 1000 e.v.). However, good quantitative (as well as qualitative) analyses of metals can be achieved with high power density techniques.

Robert Dunbar, from Case Western, summarized current multiphoton techniques, which include multiphoton ionization of molecules in the gas phase, and dissociation of pre-formed ions. Visible multiphoton dissociation usually involves two visible photons in which the first photon is used to produce excited states, and the second to achieve dissociation of strongly bound ions. Continuous wave (CW) infra red techniques are used for weakly bound ions, and a combination of IR and visible photons can be used for IR enhancement of visible 2-photon dissociation.

Robert Cotter, from the Johns Hopkins University, presented a laser desorption chemical ionization instrumental configuration, which uses a pulsed CO_2 laser in combination with a scanning mass spectrometer. At 10^{6} W/cm^2, more neutrals than ions are produced which can be ionized in the isobutane reagent gas plasma. The ions which are formed are generally cationized species,

or molecular cations of salts such as tetra methyl ammonium chloride.

Ben Freiser of Purdue University reported experiments using a laser in conjunction with an ICR mass spectrometer, to generate metal ions as selective CI reagents. Franz Krueger, Inst. fuhr Biophysik, Frankfurt, described a 30°/90° LAMMA geometry and reported positive and negative spectra of glycine and L-leucine. Graham Cooks (Purdue) noted that a 10nS pulse from a YAG laser produced ion pulses for 10 microseconds, which produces problems in a time-of-flight mass spectrometer, even with a non-confined source. Krueger noted that peaks in his LAMMA spectra did not exhibit tails, and Cooks added that such time spreading was a direct function of the laser power density.

Franz Krueger pointed out that molecular cations from quaternary ammonium salts were the most easily desorbed at power densities of around 10^6 W/cm^2. Metal ions required 10^7 W/cm^2, and cationization occurred around 10^8 W/cm^2. Robert Day of the University of Pittsburgh stated that carbohydrates as large as 800 amu were easily cationized when mixed with methanol and sodium chloride. The cationization may be a chelation effect as observed in the laser desorption spectra of the crown ethers, since a non-cyclic analogue to glucose did not cationize. He also reported protonation of molecules containing carboxylic acid groups, using crystalline solids, which discourages cationization.

About 200 people attended the workshop.

Robert J. Cotter

Robert J. Cotter
Middle Atlantic Mass
Spectrometry Facility
Workshop Chairman

Acknowledgement: The author is grateful to Louis C. Frees of the Oak Ridge National Laboratory for assistance in preparing this report.

COMMITTEE ON COMPUTER APPLICATIONS

Report for 1980-81

Roger A. Upham
Chairman

Workshop: Reliability of GCMS Computer Identifications.

An audience of about 100 heard very brief presentations by Jim Robinson, Paul Dymerski, Larry Slivon, and Ged Tyror. All agreed that no one search algorithm is best for all compounds. Jim Robinson pointed out that the best searches are performed when the analyst has a good feel for the data base and the various methods of searching. One must choose between the n largest peaks or n in m peak method, in addition to a forward or reverse search. Ultimately the analyst should use chemical knowledge and mass spectral interpretation background to confirm identifications provided by the computer. Paul Dymerski addressed the question of the minimum number which can be successfully used to perform a library search. The point of increased sample complexity reducing the reliability of the search was discussed. When looking at a single scan, the more peaks on which one chooses to search, the more false positives one will be found; and, conversely, the use of fewer peaks will lead to more false negatives. Larry Slivon described a round-robin test of 57 analyses run by three different laboratories. The results showed a significant number of false identifications which were attributed to the operators attempting to push the system too hard and possible poor selection of search variables. He noted that care should be taken when using retention indices that the search window is not too large. The use of isotopically labeled internal standards for compounds of interest would cure this problem.

Ged Tyror stated again that no one search technique will work in every situation and that the experience of the analyst must be brought to bear. He described a search system he found to be quite powerful involving use of: a pre-search based on four masses; a reverse search of the pre-search results using 20 masses; Kovat's indices in the search algorithm; and a plot of the unknown against library hits with the analyst reviewing the results. He found that 20 masses is sufficient to permit reliable identification of the unknown. The use of ancillary data such as Kovat's indices should be stressed.

Further comments from the audience and panelists:

The difficulty arising from use of different columns when utilizing Kovat's indices was raised. The point being whether such data is totally reliable or simply obtained.

The only method of positive identification is to perform co-injection with the compound thought to be identified. It was noted several times that for installations with large through-puts this is impractical.

Several statements were made to the effect that it is not reasonable to expect complete and unambiguous identification of unknowns based on the results of one technique, rather other analytical tools such as IR, GC-IR, UV, and NMR should be applied.

The question of the number of masses necessary and sufficient for a satisfactory fit was the subject of considerable debate. The acceptable values range from 3-4 to 20 and sometimes greater than 20 for high molecular weight organometallic compounds.

The final two comments of the session clearly summarized the content of the workshop: (1) People perform identifications and analyses - computers are only tools for this purpose and should be so used; and (2) the art of interpretation of mass spectral data is not a dead art and should be exercised more frequently rather than less.

ASMS COMMITTEE SOLIDS AND SURFACE ANALYSIS
Chairman: Peter Williams

SIMS Round Robin

A round-robin evaluation of secondary ion mass spectrometry (SIMS) instrumentation was organized and the results were discussed in a workshop at the Minneapolis meeting. The aims of the initial study were to evaluate the relative sensitivities of different instrument types and to determine detection limits for hydrogen. Ion-implanted samples of boron (dose 10^{15} atom/cm^2) and hydrogen (dose 10^{16} atom/cm^2) were mailed to 56 laboratories in the U.S., Europe, Japan, and South Africa, including representatives of most instrument manufacturers, with a request to depth-profile both samples and determine (a) the "useful yield" of boron i.e. ions detected/atom sputtered, and (b) the "dynamic range", i.e. peak-to-background ratio for the hydrogen implant. If oxygen ion bombardment or oxygen spraying techniques were used for the boron, then the boron ion yield should be saturated, and the useful yield should give a measure of relative instrument transmission. Because the peak concentration of the hydrogen profile was calculable from the dose, the hydrogen background level in each instrument could be calculated from the dynamic range.

Eleven responses were received, from users of the two types of magnetic instruments in general use in the U.S. and Europe, and from three types of dedicated quadrupole-based systems. No manufacturers responded by the meeting deadline, although several promised results. The range of boron useful yield values spanned four decades. A magnetic instrument gave the highest value, and a quadrupole the lowest, but there was significant overlap, with some quadrupoles performing better than some magnetic instruments. Hydrogen backgrounds spanned the range from 2000 ppm to 25 ppm (bulk equivalent).

The round robin results demonstrated that dedicated SIMS instruments -- those with primary ion columns specifically designed for depth-profiling -- could perform boron and hydrogen analyses with good sensitivity. The exercise was generally felt to be useful by the participants.

The workshop was attended by several organic SIMS researchers. A discussion was held on the relationship that should exist between the solids/SIMS committee and organic mass spectroscopists who use SIMS as an ionization technique, particularly in view of the explosion of interest in SIMS of liquid samples (FAB). It was suggested that assessment of organic instrument transmission, along the lines of the round-robin study, would be useful, and the use of a shallow implant of Cs was suggested for organic mass spectrometer systems with low sputtering rates. We will investigate the possibility of obtaining and circulating such implants. There was a concensus that the sputtering of inorganic and organic materials had many common features, and that a broader interaction between workers in the two fields, covering both instrumental approaches and fundamental mechanisms, would be useful. It was agreed that an effort should be made to arrange a session in Hawaii in which these topics could be discussed jointly.

Respectfully submitted,

Pet—Will—

Peter Williams
Chairman, Committee VII

ASMS FUNDAMENTALS COMMITTEE

"Workshop of Mass Spectrometry/Mass Spectrometry"

This year a new workshop format was used. A group of panelists was asked to respond, without advance information, to a set of questions about mass spectrometry/mass spectrometry. Each question was put to two of five panel members and answers from the floor were also taken. This led in many cases to a consensus being reached.

Panel members, all representing compaines which produce MS/MS instrumentation, were Drs. Bill Davidson (Sciex), Mel Seigel (Extranuclear), Syd Evans (Kratos), Charles Smith (VG), and Mike Story (Finnigan). The questions dealt with the capabilities of MS/MS, the various instrumental configurations possible and with specific applications, especially in analysis of complex mixtures.

Some highlights of the discussion were:

(i) recognition that MS/MS spectra are reproducible to ca. 10% even without use of internal standards and to better than this with standards

(ii) data on sensitivity showing < 10 picogram detection limits for TCDD

(iii) information on the compatibility of MS/MS with the new desorption ionization methods, including molecular SIMS and fast atom bombardment

(iv) evidence that the anlytically useful charge inversion reactions - which lead to a characteristic spectrum of positively charged fragments from negatively charged precursors - can be accessed in low kinetic energy (quadrupole) MS/MS via charge transfer to SF_6 in a multi-collision sequence

(v) agreement that variation of the collision energy is an important ancillary means of structural characterization. (Sensitivity of the spectra to collision energy also requires that agreement be reached on conditions for taking MS/MS spectra and comparing them with libraries)

(vi) recognition that one of the weakest features of MS/MS is the need for ionization from a matrix where other constituents might influence the ionization efficiency.

R. Graham Cooks
Purdue University

ASMS COMMITTEE REPORT

QUALITATIVE ORGANIC TECHNIQUES

WORKSHOP ON NEWER ASPECTS OF ION CYCLOTRON RESONANCE (FOURIER TRANSFORM MASS SPECTROMETRY)

Participants in this workshop included the chairman, M. M. Bursey, and three discussion leaders, M. B. Comisarow, R. T. McIver, Jr., and C. L. Wilkins.

M. M. Bursey briefly reviewed the origins and development of the ion cyclotron resonance technique, describing commercial instruments but not identifying the contributions of individual workers.

M. B. Comisarow (University of British Columbia) outlined the basic principles of ion cyclotron resonance, and then described the Fourier transform ion cyclotron resonance experiment. He illustrated the high sensitivity and high resolution possible with FT-ICR, and also gave examples from his work with volatile transition metal complexes showing the greatly extended mass range of the ion cyclotron resonance spectrometer in the FT operation, and also the application of double resonance techniques and pressure variations to identify reaction mechanisms for the production of high-mass ions.

R. T. McIver, Jr. (University of California, Irvine) described some of his newest results with his large cell for trapping involatile species, illustrating with spectra and derived proton affinities for relatively involatile molecules which otherwise would require field desorption or one of the newer rapid heating or laser techniques for producing gaseous ions. In his ICR experiments ions are trapped for extended periods of time until enough evaporation has occurred to give enough ions to produce a good spectrum. He also described very recent experiments with his high-field large-cell instrument in which enough energy is imparted to ions on rf excitation to permit their collisional activation by argon atoms in the cell. Thus the MS/MS technique has now been carried out by ICR.

C. L. Wilkins (University of Nebraska, now University of California, Riverside) showed the extremely high resolution available even at relatively high mass, the ability to achieve a few ppm mass measurement accuracy, and the capability of applying this mass measurement accuracy to compounds eluting from a SCOT capillary GC column and therefore present in the cell for only a few seconds.

Ion cyclotron resonance seems about to pass from the province of the physical chemist who is not hampered by the former mass and data acquisition rate to the province of the analytical chemist with more serious constraints on his/her instrumental requirements. To avoid the analytical chemist's association of ion cyclotron resonance with these earlier problems preventing practical application, the term "Fourier transform mass spectrometry" has been proposed for the family of new techniques, though even within the small group of active investigators there is no agreement that this term is the most appropriate.

Approximately 70 persons attended this workshop and the brief business meeting which followed.

Maurice M. Bursey
University of North Carolina at Chapel Hill
Chairman

Minutes of the "Orphaned Instruments" Workshop
May 27, 1981, 5:00 P.M.

The meeting opened with the chairman asking for another description of "orphaned" instruments. The workshop was meant to convene those investigators who are working with mass spectrometers and data systems that are no longer supported (or only peripherally so) by their original supplier. We hope that by pooling resources within and across instrument lines, a few more years of life can be extracted from good systems. With existing government policies, it seems that our ranks can only increase.

A list was circulated for names and addresses of attendees; the chairman will arrange these by instrument and circulate copies to those present. Others may obtain the list by writing to the chairman. A show of hands revealed the presence of 54 individuals representing eighteen LKB 9000 and 2091 users, twenty-six CEC-DuPont 103, 104, 110, 490, 491, 492 and Dymaspec users, three Hitachi RMU, nine Varian (Finnigan) M-66, M-44, CH4 and 7, two Finnigan 1015, 3300, three AEI (Kratos) MS 9, 10, 12, 20, and 30, one Finnigan Alpha-16, and one Varian data system user. The oldest instrument represented appeared to be a CVC 102 made in 1945!

The chairman was surprised that some of these systems were considered abandoned, but those present insisted it to be true. The LKB group exhibited strong sentiment about the company(s) that are responsible for supplying repairs and parts. Technical advice and instrument repair is nonexistent and parts, especially large shipments, apparently take as much as a year to be delivered. Some talked of entering a suit against the companies involved because support for a number of years had been assured during purchase. Sten Wikstrom reported that some progress is being made in Sweden in assembling parts (Staffan Bornefelt, Remont AB, Box 307, S-198-00, Balsta, Sweden). He would be glad to help with technical advice as well. His address is Huddinge University Hospital Research Center, S-14186, Huddinge, Sweden. Bill Frasure reported Boehringer-Mannheim Diagnostics people in Houston and Indianapolis do have parts available now. I have called them (Mike Serricchio (713)782-6740) and was assured that over a half-million dollars in parts are available. Call the above number for parts, explaining in great detail what part is needed. If you have trouble identifying it, call M. Nicoletti (BMD) at 800-428-5074 for help. Attempts are being made by BMD to secure third party service. They also state that the Remont people in Sweden are glad to help with technical problems; write or call them.

Someone reminded us that Finnigan-MAT has announced that it will support all its systems for 5 years from the date they are discontinued.

A call for names of servicemen willing to repair older instruments yielded the following:

Mike D. Claus (M-66, CEC, CH-5) P.O. Box 751, Barnegat, NJ 08005
(609-698-1720)

Jim J. Wilder - (MS-9, CEC 110), 1474 Fieldcrest Circle, Pleasant Hill, CA 94523.

Bill Frasure- (LKB-9000, CH4, CEC 103, 104, 130, 110, quads, ICR)
326 Marion Ave., St. Louis, MO 63119 (314-962-8648 or
314-664-9800 x 170)

Bob Dutky, 14112 New Hampshire Ave., Colesville, MD, 301-284-5305
or 609-698-1720 (Data systems, LKB, MAT, Hitachi, Statos recorders)

Len Herzog of Nuclide Corporation mentioned that they have a series of CEC 110 and 103 update kits. They will also modernize vacuum systems on many instruments, including the LKB, and supply updated data systems for old instruments. Roger Upham (University of Minnesota) mentioned a probe retrofit kit for the MS-30 that he has available for $900. He also stated that VG has "VG Updates" to convert various VG systems to the 7070 - contact John Holmes there. Roger also noted that he has designs (and parts such as silver gaskets) for a revised pumping system for the Hitachi. He also mentioned an unusual technique for softening used copper gaskets. Simply plunge the red hot gasket (use a Meker burner, etc.) into a beaker of methanol! If the methanol ignites, just cover the dish with something to extinguish the flame (*Your reporter assumes no responsibility*). *The resulting gasket is bright* and soft.

Bill Sherman has available plans for a simple diverter valve for the LKB 9000 (and other systems) that does away with hard to get gold-lined compression seals and is nearly foolproof in operation.

Bill Frasure mentioned a technique of demagnetizing a multiplier head to increase sensitivity. Bring an external magnet near the multiplier housing and twist it around its axis as it is withdrawn from the vicinity of the multiplier.

Orville Mamer mentioned that compression valves on LKB and other interfaces can be recovered for use simply by filling the hole made in the copper surface with silver solder - be sure to use hard silver solder. Orville also remarked that when plates of his LKB-9000 magnet separated, he had simply drilled a hole and bolted them tight. I'd advise you to call him before you try it though. Help was sought for a replacement for the CEC 492 power resistor as well as the plastic ink holder for statos recorders. Any ideas?

Stan Israel, University of Lowell, Mass. will give away free a Perkin-Elmer 270 - any takers? T. Terwilliger will sell an old LKB-9000 for about $5,000. This statement brought up the question of how to get rid of old instruments. Herzog of Nuclide said he will take any CEC 103 or 104s. Someone noted that the metal in some machines is worth quite a lot at junk dealers if worse comes to worse.

Many present noted that quality control in commercially available filaments seems to be bad - failures of about 40% were noted.

Next year the group may want to break into smaller sections for that part of the discussion pertaining to specific instruments, and then reconvene for general comments.

H. Fales
(301)496-2135

FAST ATOM BOMBARDMENT MASS SPECTROMETRY WORKSHOP

Kenneth L. Rinehart, Jr., Moderator

University of Illinois at Urbana-Champaign, Urbana, IL 61801

The first fast atom bombardment mass spectrometry (FABMS) workshop attracted a large and spirited audience on Thursday evening, May 28, at 8 PM, with M. Barber, R. D. Sedgwick and R. S. Bordoli, three of the University of Manchester Institute of Science and Technology inventors of the FAB technique, as panelists. A number of participants had requested time for short presentations and the workshop was divided into three areas of interest--fundamental processes, mechanics of the technique, and examples of applications.

Fundamental Processes. Dr. Barber spoke first, noting initially that the theory of sputtered ions is in its infancy but that there is a considerable energy spread (ca. 8 volts half-width) in the ion source with sputtered ions. He also likened the mechanism of an argon atom striking the glycerol surface at a 20° angle to that of a billiard ball striking a plate of porridge, disrupting the lattice and peeling off the surface layer, producing a temperature spike and a dense gas in a very short time (0.37 psec). The overall ionization process, which perhaps involves a percussive mechanism, must resemble that of chemical ionization rather than electron ionization or field ionization, since the spectra look like CI spectra, with even-electron ions; ammonium chloride, for example, gives NH_4^+ and Cl^- adducts in the positive and negative ion modes. In the discussion, Dr. H. R. Morris, Imperial College, also argued for the similarity of FAB-produced peptide spectra to those from CI and Dr. R. J. Cotter, Johns Hopkins, noted the similarity between FAB spectra and thermal desorption spectra obtained in his laboratory.

In later discussion, one of the major questions centered on production of $M^{+\cdot}$ ions, as opposed to $(M + H)^+$ ions. True molecular ions appear to be rare, but do occur, especially with organometallic compounds, where the metals may be oxidized. On the other hand, Dr. Sedgwick noted that $M^{+\cdot}$ often can be shown by metastable ion studies to come from $(M + H)^+$. Another interesting point is that both multiply charged ions, e.g., $(M + H + H)^{++}$, and multimers $(M_n + H)^+$ are observed, with some fragment ions coming from the latter.

The second and third contributors, Dr. C. Magee, RCA Laboratories, and Dr. R. G. Cooks, Purdue University, provided background for the FAB technique in terms of SIMS (secondary ion mass spectrometry). Dr. Magee noted the early contributions of Honig at RCA and Satkiewicz at Johns Hopkins to SIMS and drew the following diagram relating the techniques, stating it

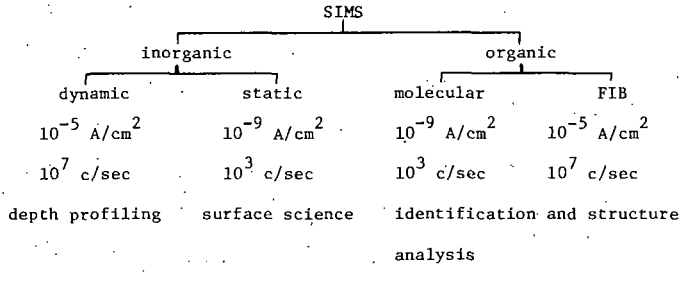

is the right hand, FIB, column which has given rise to FABMS.

Dr. Cooks noted the instrumental limits of quadrupole spectrometers, and agreed that the chief hindrance to use of SIMS on a magnetic sector instrument was the difficulty in bringing a 5-Kv ion beam into the ion source of a sector instrument operating a 3-10 Kv. Dr. Cooks argued for the primary contribution of molecular SIMS, then noted the work of Benninghoven at Muenster, Karasek at Waterloo, Rabalais at Houston, and Winograd at Purdue. He also noted that Devienne in France had earlier reported a neutral atom bombardment experiment on a solid surface but without a glycerol matrix. [Dr. Barber, who also has an extensive background in SIMS, noted that Devienne's experiment, in addition, lacked the rather critical low angle, ca. 20°, necessary to prevent excessive fragmentation.] Finally, Dr. Cooks argued for similarities in appearance of SIMS and FABMS spectra and attempted to link the SIMS and FABMS techniques by arguing for electron transfer to an approaching argon ion to give, effectively, atom bombardment in SIMS.

The fourth contributor, Dr. F. H. Field, Rockefeller University, noted the similarity of FABMS and plasma desorption (PDMS), a development of Macfarlane at Texas A & M. [This sentiment was echoed by Dr. Barber.] Dr. Field also noted the similarity in energy between "fast atoms" and the physicists' "slow ions". He then presented again instrumental improvements in his time-of-flight mass spectrometer which yield more useful PD spectra, as described elsewhere in this volume (TPMOC5).

Techniques. Dr. F. W. McLafferty, Cornell University, asked what the ultimate limit on FAB-produced masses might be. Dr. Sedgwick noted success with mellitin, with a molecular weight of 2843, and Dr. Morris reported seeing ions above m/z 3000.

Dr. W. L. Harrington, RCA, suggested neutral molecules with 10-12 atoms as a bombarding beam, but noted chemical effects of such a beam could be a problem. In this connection, Dr. Magee noted the virtues of a cesium ion gun and Dr. W. Eng, University of Manitoba,

described a FAB ion source, employing cesium atoms, in which the sample in methanol is electrosprayed onto a plate in the absence of glycerol.

Attention was devoted to the importance of the matrix in short presentations by W. M. Bone, University of Virginia, and Dr. Cotter. There was general consensus among the panelists that glycerol at present is the best medium and Dr. Sedgwick noted that the surface properties of glycerol are important as well as the concentration of substrate dissolved in glycerol. Dr. Cooks suggested polyphenyl ether, but Dr. Sedgwick reported far less success with this matrix.

"Reverse derivatization" to give more polar substrates is a useful concept. An interesting point is that preformed ions such as quaternary ammonium salts and sodium salts of organic phosphates and carboxylates work particularly well by FAB and may be seen at lower temperatures, with thermally produced ions at higher temperatures. On the other hand, the Moderator noted the similarity in spectra between otherwise identical neutral and acidic peptides. To effect ionization of the substrate, addition of acid (e.g., oxalic acid) can sometimes help, as can addition (or removal) of sodium or potassium ions.

Perhaps the most important areas for future developments are in the technique itself, i.a., alternative matrices, multichannel analysis for weak ions, high resolution, computerized data reduction.

Applications. Dr. Barber perhaps supplied the most telling comment at the outset, noting that the Wednesday morning oral session (WAMOA) had already provided an impressive array of applications in a very short time for such a new technique.

Among the proposed applications for FAB (suggested largely by Dr. Cooks on the basis of present SIMS capabilities) are direct use of chromatograms (already a reality in Dr. Morris's lab), surface analysis, including depth profiling, and microscopy of cellular constituents (an atom microprobe).

ASMS NOMENCLATURE COMMITTEE WORKSHOPS - Minneapolis, 1981

Two Workshops were held on Monday, May 25, 1981 and Thursday, May 28, 1981. 84 members attended the first Workshop and 35 members the second. A copy of the list of terms and definitions for use in mass spectrometry that had been prepared following last year's Workshop was distributed to each attendee. The list had already been circulated in advance to 50 people who had attended last year's Workshop or who had written requesting that the list be sent to them and their suggested modifications had been incorporated.

Each term on the list was considered in detail. A copy of the terms finally approved at the Workshops is attached.

Help was sought to prepare an additional list of terms for consideration at next year's Workshops. The following people volunteered to provide terms under the headings listed alongside their names :

M.S. Story, Finnegan Instruments	(Instrumentation; detectors)
C.R. Lagergren, Battelle	(Surface ionization; thermal ionization)
M. Elliott, V.G. Ltd.	(Isotope mass spectrometry)
F.A. Elder, Xerox Corporation	(Knudsen cell mass spectrometry)
C.M. Judson, University of Kansas	(Sample introduction)

Several other people offered to send additional terms (with or without definitions) for inclusion in next year's list.

(The deadline for receipt of terms by me is August 31, 1981. This will allow time for circulation of a new list of terms to the attendees at this year's Workshops so that their comments can be included, and preparation of an agreed list for discussion at the 1982 Meeting in Hawaii).

The following decisions were taken unanimously :

1. That the attached list of terms be submitted to the ASMS Board of Directors for their approval, with the following recommendations

   (i) That if the list is approved, it be considered 'provisional' for one more year so as to give all members a final opportunity of commenting upon it.

   (ii) That all comments received before December 31, 1981 be considered by the Chairman of the Nomenclature Committee who would then recommend to the Board, in the light of such comments, which terms should be issued as ASMS recommended terms.

   (iii) That terms issued under the headings 'Vacuum' and 'Data System' should be separated into an Appendix to the list of recommended terms.

   (iv) That the generosity of the American Vacuum Society in providing most of the terms under the heading 'Vacuum' should be acknolwedged in the list.

2. That the same procedure as was used this year should be followed again so that a further list of terms can be submitted to the Board in a year's time.

Royal Society Research Unit
University College of Swansea
Singleton Park, SWANSEA SA2 8PP, UK.

J.H. Beynon
Chairman

IONIZATION NOMENCLATURE

Electron Ionization This is the term used to describe ionization of any species by electrons. The process may, for example, be written

$$M + e^- \rightarrow M^{+\cdot} + 2e^- \quad \text{for atoms or molecules,}$$
$$\text{and} \quad M^{\cdot} + e^- \rightarrow M^{+} + 2e^- \quad \text{for radicals.}$$

Photo-Ionization This is the term generally used to describe ionization of any species by photons. The process may, for example, be written

$$M + h\nu \rightarrow M^{+\cdot} + e^-$$

[Note: Electrons and photons do not "impact" molecules or atoms. They interact with them in ways that result in various electronic excitations including ionization. For this reason it is recommended that the terms 'Electron impact' and 'Photon impact' be not used].

Field Ionization This term relates to the removal of electrons from any species by interaction with a high electrical field.

Field Desorption This term is used to describe the formation of ions in the gas phase from a material deposited on a solid surface (known as an 'emitter') in the presence of a high electrical field. 'Field desorption' is an ambiguous term because it implies that the electric field desorbs a material as an ion from some kind of emitter on which the material is deposited. There is growing evidence that some of the ions formed are due to thermal ionization, some to field ionization of vapor evaporated from material on the emitter. Because there is little or no ionization unless the emitter is heated by an electric current, 'field desorption' is a misnomer. The term is however firmly implanted in the literature and most users (by no means all) understand what is going on regardless of the implications of the term. In addition, no better simple term has been suggested to take its place and so, reluctantly, it is recommended that it be retained.

Chemi-ionization and chemical ionization are two terms which should not be used inter-changeably.
Chemi-ionization refers to a process whereby gaseous molecules are ionized when they interact with other internally excited gaseous molecules or molecular moieties.
Chemical ionization concerns the process whereby new ionized species are formed when gaseous molecules interact with ions. The process may involve transfer of an electron, proton or other charged species to or between the reactants. When a positive ion results from chemical ionization, the term may be used without qualification. When a negative ion results, the term negative ion chemical ionization should be used.

Surface Ionization takes place when an atom or molecule is ionized when it interacts with a solid surface. Ionization only occurs when the work function of the surface, the temperature of the surface, and the ionization energy of the atom or molecule have an appropriate relationship.

Thermal Ionization takes place when an atom or molecule interacts with a heated surface or is in a gaseous environment at high temperatures. [Examples of the latter may be a capillary arc plasma, a microwave plasma, or an inductively coupled plasma].

Atmospheric Pressure Ionization is an ambiguous term. In essence, it is used to describe chemical ionization at atmospheric pressure. It is recommended that use of the term should be discouraged.

Spark (Source) Ionization occurs when a solid sample is vaporized and partially ionized by an intermittent electric discharge. Further ionization occurs in the discharge when gaseous atoms and small molecular moieties interact with energetic electrons in the intermittent discharge. It is recommended that the word 'source' be dropped from this term.

Auto-ionization occurs when an internally supra excited atom or molecular moiety loses an electron spontaneously without further interaction with an energy source. (The state of the atom or molecular moiety is known as a pre-ionization state).

Associative Ionization occurs when two excited gaseous atoms or molecular moieties interact and the sum of their internal energies is sufficient to produce a single, additive ionic product.

Multi-photon Ionization occurs when an atom or molecule and their concomitant ions have energy states whereby the energy in two or more photons can be absorbed.

Penning Ionization occurs through the interaction of two or more neutral gaseous species at least one of which is internally excited.

Charge Exchange (Charge Transfer) Ionization occurs when an ion/atom or ion/molecule reaction takes place in which the charge on the ion is transferred to the neutral species without any dissociation of either.

Ion-Pair Formation involves an ionization process in which a positive fragment ion and a negative fragment ion are the only products.

Ionization Cross Section This is a measure of the probability that a given ionization process will occur when an atom or molecule interacts with an electron or a photon.

Electron Attachment A resonance process whereby an external electron is incorporated into an atomic or molecular orbital of an atom or molecule.

Ionization Energy This is the minimum energy of excitation of an atom, molecule or molecular moiety required to remove an electron in order to produce a positive ion.

Vertical Ionization This is a process whereby an electron is removed from a molecule in its ground or an excited state so rapidly that a positive ion is produced without change in the positions or momenta of the atoms. The resultant ion is often in an excited state.

Adiabatic Ionization A process whereby an electron is removed from the ground state of an atom or molecule producing an ion in its ground state.

Ionization A process which produces an ion from a neutral atom or molecule.

Dissociative Ionization An ionization process in which a gaseous molecule decomposes to form products, one of which is an ion.

Ionic Dissociation A decomposition of an ion into another ion of lower formula weight and one or more neutral species.

Ionization Efficiency is the ratio of the number of ions formed to the number of electrons or photons used.

An Ionization Efficiency Curve shows the number of ions produced as a function of the energy of the electrons or photons used to produce ionization.

Laser Ionization occurs when a sample is irradiated with a laser beam. In the irradiation of gaseous samples, ionization occurs via a single- or multi-photon process. In the case of solid samples, ionization occurs via a thermal process.

TYPES OF IONS

Positive Ion This is an atom, radical, molecule or molecular moiety which has lost one or more electrons thereby retaining an electrically positive charge. The use of the term cation as an alternative is not recommended. The use of mass ion is not recommended.

Negative Ion An atom, radical, molecule or molecular moiety in the vapor phase which has gained one or more electrons thereby acquiring an electrically negative charge. The use of the term anion as an alternative is not recommended.

Singly-, Doubly-, Triply- etc. Charged Ion These terms are used to describe an atom, molecule or molecular moiety which has gained or lost one, two, three or more electrons. The term multiply-charged ion is used to refer to ions that have gained or lost more than one electron where the number of electrons lost or gained is not designated.

Parent Ion An electrically charged molecular moiety which may dissociate to form fragments, one or more of which may be electrically charged, and one or more neutral species. A parent ion may be a molecular ion or an electrically charged fragment of a molecular ion.

Fragment Ion An electrically charged dissociation product of an ionic fragmentation. Such an ion may dissociate further to form other electrically charged molecular or atomic moieties of successively lower formula weight. (See also Daughter Ion).

Daughter Ion An electrically charged product of reaction of a particular parent ion. In general such ions have a direct relationship to a particular precursor ion and indeed may relate to a unique state of the precursor ion. The reaction need not necessarily involve fragmentation. It could, for example involve a change in the number of charges carried. Thus, all fragment ions are daughter ions but not all daughter ions are necessarily fragment ions.

Rearrangement Ion An electrically charged dissociation product, involving a molecular or parent ion, in which atoms or groups of atoms have transferred from one portion of a molecule or molecular moiety to another during the fragmentation process.

Stable Ion An ion which is not sufficiently excited to dissociate into a daughter ion and associated neutral fragment(s) or to react further in any other way.

Unstable Ion An ion which is sufficiently excited to dissociate within the ion source.

Metastable Ion An ion which is sufficiently excited to dissociate into a particular daughter ion and neutral species during the flight from the ion source to the detector. The dissociation is most readily observed when it takes place in one of the field-free regions in a mass spectrometer.

Precursor Ion This term is synonymous with Parent Ion.

Product Ion This term is synonymous with Daughter Ion.

Molecular Ion An ion formed by the removal (positive ions) or addition (negative ions) of one or more electrons from a molecule without fragmentation of the molecular structure. The mass of this ion corresponds to the sum of the masses of the most abundant naturally occurring isotopes of the various atoms that make up the molecule (with a correction for the masses of the electrons lost or gained). For example, the mass of the molecular ion of ethyl bromide, C_2H_5Br will be 2x12 plus 5x1.0078246 plus 78.91839 minus the mass of the electron (m_e). This is equal to 107.95751 u - m_e, u being the unit of atomic mass based on the standard that the mass of the isotope ^{12}C = 12u exactly.

Isotopic Molecular Ion A molecular ion containing one or more of the less abundant naturally occurring isotopes of the atoms that make up the molecular structure. Thus, for ethyl bromide there exist molecular isotope ions such as $^{13}CCH_5Br^{+\cdot}$, $C_2H_4D\ Br^{+\cdot}$, $C_2H_5{}^{81}Br^{+\cdot}$, $^{13}C_2H_5{}^{81}Br^{+\cdot}$ etc.

Isotopic Ion Any ion containing one or more of the less abundant naturally occurring isotopes of the elements that make up its structure.

Isotopically Enriched Ions When the abundance of a particular isotope is increased above the level at which it occurs in nature and is incorporated in a molecule the term "isotopically enriched ion" is used to describe any ion containing the enriched isotope.

Dimeric Ion An ion formed either when a chemical species exists in the vapor phase as a dimer and can be detected as such, or when a molecular ion can attach to a neutral molecule within the ion source to form an ion such as $[2M]^{+\cdot}$ where M represents the molecule.

Protonated Molecule An ion formed by interaction of a molecule with a proton abstracted from an ion, as often occurs in Chemical Ionization according to the reaction : $M + XH^+ \rightarrow MH^+ + X$. The symbolism $[M+H]^+$ may also be used to represent the protonated molecule.
[Note : The widely-used term 'protonated molecular ion' to describe the MH^+ ion is not recommended. It suggests an association product of a proton with a molecular ion].

Adduct Ion An ion formed by interaction of two species, usually an ion and a molecule, and often within the ion source, to form an ion containing all the constituent atoms of one species as well as an additional atom or atoms.

Cluster Ion An ion formed by the combination of two or more molecules of a chemical species often in association with a second species. For example, $[(H_2O)_nH]^+$ is a cluster ion.

Radical Ion An ion containing an un-paired electron which is thus both an ion and a free radical. The presence of the odd electron is denoted by placing a dot alongside the symbol for the charge. Thus, $C_2H_6^{+\cdot}$ and $SF_6^{-\cdot}$ are radical ions.

Odd-electron Ion This term is synonymous with Radical Ion.

Even-electron Ion An ion containing no un-paired electrons, for example CH_3^+ in its ground state.

OTHER TERMS

Mass Analysis A process by which a mixture of ionic or neutral species is identified according to the mass-to-charge (m/z) ratios (ions) or their aggregate atomic masses (neutrals). The analysis may be qualitative and/or quantitative.

Detection of Ions In mass spectrometry this concerns the observation of the arrival of particular ionic species, at a detector under conditions that preclude or minimize ambiguities due to interferences. Ions may be detected by photographic or suitable electrical means.

Scanning Method This term refers to the sequence of control over operating parameters of a mass spectrometer which results in a spectrum of masses, velocities, momenta or energies.

Sample Introduction This refers to the manner in which a material which is to be subject to analysis is placed in the ion source of a mass spectrometer before and/or during such an analysis.

Vacuum System Those components used to lower the pressure within a mass spectrometer are all parts of the vacuum system. This includes not only the various pumping components but also valves, gauges and associated electronic or other control devices, the chamber in which ions are formed and detected and the vacuum envelope.

Data System The components used to record and process information during the analysis of a sample are part of the data system. This includes electronic or other control devices, and recording storage and data manipulation devices.

Data Processing Once information is obtained with an appropriate data system, the information must be interpreted appropriate to the end use. Those steps which lead to this end use are of concern in data processing. Note that data processing does not necessarily include application of modern computer techniques.

Data Reduction The process of transforming the initial digital representation of a spectrometer output into a form which is amenable to interpretation; for example, a bar graph or a table of ion currents.

m/z This abbreviation is used to denote the dimensionless quantity formed by dividing the mass number of an ion by the number of charges carried by the ion. It has long been called the mass-to-charge ratio although m is not the ionic mass nor is z a multiple of the electronic charge, e^-. The abbreviation m/e is, therefore, not recommended. Thus, for example, for the ion $C_7H_7^{2+}$, m/z = 45.5.

ION/MOLECULE REACTIONS

Ion/Neutral Reaction A process wherein a charged species interacts with a neutral reactant to produce either chemically different species or changes in the internal energy of one or both of the reactants.
(NB. The term ion/neutral reaction is not ideal, simply because the word neutral is not a noun. However, any alternatives such as ion/neutral-species are so clumsy as to seem unlikely to be generally accepted).

Ion/Molecule Reaction An ion/neutral reaction in which the neutral species is a molecule.

Charge Inversion Reaction An ion/neutral reaction wherein the charge on the reactant ion is reversed in sign.

Charge Transfer Reaction An ion/neutral reaction wherein the total charge on the reactant ion is transferred initially to the reactant neutral species so that the reactant ion becomes a neutral entity.

Partial Charge Transfer Reaction An ion/neutral species reaction wherein the charge on a multiply-charged reactant ion is reduced.

Charge Stripping Reaction An ion/neutral reaction wherein the charge on the reactant ion is made more positive.

Charge Permutation Reaction This is a general term to describe an ion/neutral reaction wherein there is a change in the magnitude and/or sign of the charges on the reactants.

[Note : Considering some of the possible reactions of ions M^{2+}, M^+ and M^- with a neutral species N these would be categorised on the basis of the above definitions as follows :

$M^{2+} + N \rightarrow M^+ + N$ (Partial charge transfer)
$M^+ + N \rightarrow M^{2+} + N + e^-$ (Charge stripping)
$M^- + N \rightarrow M^+ + N + 2e^-$ (Charge stripping and charge inversion).

All are ion/neutral reactions and also charge permutation reactions].

Collision-induced Dissociation An ion/neutral process wherein the (fast) projectile ion is dissociated as a result of interaction with a target neutral species. This is brought about by conversion of part of the translational energy of the ion to internal energy in the ion during the collision.

Collisional Activation An ion/neutral process wherein excitation of a (fast) projectile ion is brought about by the same mechanism as in collision-induced dissociation. (The ion may decompose subsequently).

Collisional Excitation An ion/neutral process wherein there is an increase in the (slow) reactant ion's internal energy at the expense of the translational energy of either (or both) of the reacting species. The scattering angle may be large.

[Note : It is recommended that all three of the above terms should be retained].

Elastic Scattering An ion/neutral interaction wherein the direction of motion of the ion is changed, but there is no change in the total translational energy or internal energy of the collision partners.

Inelastic Scattering An ion/neutral interaction wherein the direction of motion of the ion is changed, and the total translational energy of the collision partners is reduced.

Elastic Collision A collision resulting in elastic scattering.

Inelastic Collision A collision resulting in inelastic scattering.

Superelastic Collision A collision in which the translational energy of the fast-moving collision partner is increased.

Ionizing Collision An ion/neutral reaction in which an electron or electrons are stripped from the ion and/or the neutral species in the collision. Generally, this term has come to be used to describe collisions of fast moving ions with a neutral species in which the neutral species is ionized with no change in the number of charges carried by the ion. Care should be taken when this term is used to emphasize if charge stripping of the ion has taken place.

Association Reaction (associative combination) The reaction of a (slow moving) ion with a neutral species wherein the reactants combine to form a single ionized species.

Ion/neutral Exchange Reaction In this reaction an Association Reaction is accompanied by the subsequent or simultaneous liberation of a different neutral species as product.

Translational Spectroscopy A technique to investigate the distribution of the velocity of product ions from ion/neutral reactions.

Ion Energy Loss Spectra Spectra that show the loss of translational energy of ions involved in ion/neutral reactions.

Impact Parameter The distance of closest approach of two particles if they had continued in their original direction of motion at their original speeds.

Interaction Distance The furthest distance of approach of two particles at which it is discernible that they will not pass at the impact parameter.

Charge Exchange Reaction This term is synonymous with Charge Transfer Reaction.

Partial Charge Exchange Reaction This term is synonymous with Partial Charge Transfer Reaction.

SCANNING OF SPECTRA

Mass Spectrum A spectrum obtained when a beam of ions is separated according to the mass-to-charge (m/z) ratios of the ionic species contained within it.

[Note : A quadrupole mass spectrometer achieves separation of the various ionic species in this way].

Momentum Spectrum A spectrum obtained when a beam of ions is separated according to the momentum-to-charge ratios of the ionic species contained within it.

[Note : A sector magnetic field achieves separation of the various ionic species in this way. If the ion beam is homogeneous in translational energy, as is the case with sector instruments, separation according to the m/z ratios is also achieved].

Ion Kinetic Energy Spectrum A spectrum obtained when a beam of ions is separated according to the translational energy-to-charge ratios of the ionic species contained within it.

[Note : A radial electric field achieves separation of the various ionic species in this way].

Magnetic Field Scan The usual method of producing a momentum (mass) spectrum in instruments.

Accelerating Voltage (High Voltage) Scan An alternative method of producing a momentum (mass) spectrum in magnetic deflection instruments. This scan can also be used, in conjunction with a fixed radial electric field to produce an ion kinetic energy spectrum.

Linked Scan A scan, in an instrument comprising two or more analysers, in which two or more of the analyser fields are scanned simultaneously so as to preserve a predetermined relationship between parameters characterising these fields. Often, these parameters are the field strengths, but may also be the frequencies in the case of analysers in which alternating fields are employed.

Linked Scan at Constant B/E A linked scan at constant B/E may be performed on a sector instrument incorporating at least one magnetic sector plus one electric sector. It involves scanning the magnetic sector field-strength B and the electric sector field-strength E simultaneously, holding the accelerating voltage V constant, so as to maintain the ratio B/E at a constant value. This constant value is determined by the ratio of the two field strengths which transmit main-beam ions of predetermined mass:charge ratio; these preselected main-beam ions are the precursor ions whose fragment-ion spectrum is required. The fragmentation reactions so observed occur in a field-free region traversed before the two sectors scanned in this way.

[Notes : This term should not be used without prior explanation of the meanings of B and E.

The term "B/E linked scan" is not recommended. It may suggest that the ratio B/E varies during the scan].

Linked Scan at Constant E^2/V A linked scan at constant E^2/V may be performed on a sector instrument incorporating at least one electric sector plus one magnetic sector. It involves scanning the electric sector field E and the accelerating voltage V simultaneously, so as to maintain the ratio E^2/V at a constant value, equal to the value of this ratio which transmits the main beam of ions through the electric sector. The magnetic sector field is set at a fixed value such that main-beam ions of a predetermined mass:charge ratio are transmitted by the magnet; these preselected main-beam ions are the precursor ions whose fragment-ion spectrum is required. The fragmentation reactions so observed occur in a field-free region traversed before the two sectors scanned in this way.

[Notes : This term should not be used without prior explanation of the meanings of E and V.

The term "E^2/V linked scan" is not recommended].

Linked Scan at Constant B^2/V A linked scan at constant B^2/E may be performed on a sector instrument incorporating at least one electric sector plus one magnetic sector. It involves holding the accelerating voltage fixed, and scanning the magnetic field B and the electric field E simultaneously so as to maintain the ratio B^2/E at a constant value. This constant value corresponds to the ratio of the two fields which transmit main-beam ions of predetermined mass:charge ratio; these preselected main-beam ions are the fragment ions whose precursor-ion spectrum is required. The fragmentation reactions thus observed occur in a field-free region traversed before the two sectors scanned in this way.

[Notes : This term should not be used without prior explanation of the meanings of B and E.

The term "B^2/E linked scan" is not recommended].

Linked Scan at Constant $B[1 - (E/E_o)]^{\frac{1}{2}}/E$ A linked scan at constant $B[1 - (E/E_o)]^{\frac{1}{2}}/E$ may be performed on a sector instrument incorporating at least one electric sector plus one magnetic sector. It involves holding the accelerating voltage fixed, and scanning the magnetic field B and electric field E simultaneously, so as to maintain the quantity $B[1 - (E/E_o)]^{\frac{1}{2}}/E$ at a constant value. This constant value is equal to B_3/E_o, where E_o and B_3 are respectively the electric sector field and magnetic sector field required to transmit m_3^+ ions in the main ion-beam; m_3 represents the mass $(m_1 - m_2)$ of the selected neutral fragment whose precursor ion spectrum is required. The fragmentation reactions so observed occur in a field-free region traversed before the two sectors scanned in this way.

[Note : This term should not be used without prior explanation of the meanings of B, E and E_o.

The term "$B[1 - (E/E_o)]^{\frac{1}{2}}/E$ linked scan" is not recommended].

The above three definitions are merely examples of the types of linked scan that might be used. Any other linked scans can readily be defined in a similar manner.

Fixed Precursor Ion Scans

1. Mass Selection followed by Ion Kinetic Energy Analysis

If a precursor (parent) ion is selected, for example by a magnetic sector, all product ions formed from it in the field-free region between the magnetic sector and a following electric sector can be identified by scanning an ion kinetic energy spectrum.

2. Linked Scan at Constant B/E or at Constant E^2/V

Both of these linked scans give a spectrum of all product (daughter) ions formed from a preselected precursor (parent) ion.

Fixed Product-Ion Scans

1. High Voltage Scan.

2. Linked Scan at Constant B^2/E.

Both 1. and 2. give a spectrum of all precursor (parent) ions that fragment to yield a pre-selected product (daughter) ion.

Fixed Neutral Fragment Scans

The linked scan at constant $B[1 - (E/E_o)]^{\frac{1}{2}}/E$ gives a spectrum of all product (daughter) ions that have been formed by loss of a pre-selected neutral fragment from any precursor (parent) ions.

[Note : The above definitions have all been given with reference to sector instruments; linked scans to give similar information have also been devised for instruments incorporating one or more quadrupoles].

2E Mass Spectrum Processes of the partial charge-transfer type :

$$m^{2+} + N \rightarrow m^{+} + N^{+}$$

occurring in a collision cell (containing a gas, N) located in a field-free region preceding a magnetic and electric sector combination placed in either order, may be detected as follows.

If the instrument slits are wide, and if the electric sector field E is set to twice the value required to transmit the main ion-beam, the only ions to be transmitted will be those with a kinetic energy/charge ratio twice, or almost exactly twice, that of the main ion-beam. The product ions of the process shown fulfill this condition. If the magnetic field B is scanned, a mass spectrum of such singly-charged product ions, and thus of their doubly-charged precursors, is obtained. Such a spectrum is called a 2E mass spectrum.

E/2 Mass Spectrum Processes of the charge-stripping type :

$$m^{+} + N \rightarrow m^{2+} + N + e^{-}$$

occurring in a collision cell (containing a gas N) located in a field-free region preceding a magnetic and electric sector combination placed in either order, may be detected as follows.

If the instrument slits are wide and if the electric sector field E is set to half the value required to transmit the main ion-beam, the only ions to be transmitted will be those with a kinetic energy/charge ratio half, or almost exactly half, that of the main ion-beam. The product ions of the charge-stripping process fulfill this condition. If the magnetic field B is scanned, a mass spectrum of such doubly-charged product ions, and thus of their singly-charged precursors, is obtained. Such a spectrum is called an E/2 mass spectrum.

[Note : Interference from product ions from processes of the type :

$$m_1^+ + N \rightarrow m_2^+ + N + (m_1 - m_2)$$

where $m_2 \simeq 0.5\ m_1$, can arise in E/2 mass spectra].

Charge Inversion Mass Spectrum. Charge inversion processes of the types :

$$m^+ + N \rightarrow m^- + N^{2+}$$

or $$m^- + N \rightarrow m^+ + N + 2e^-$$

respectively, occurring in a collision cell (containing a gas, N) located in a field-free region preceding a magnetic and electric sector combination placed in either order, may be detected as follows.

If the instrument slits are wide, and if the connections to the two sectors, appropriate to transmission of either positive or negative main-beam ions, are simply reversed, the negative or positive product ions of the two processes, respectively, will be transmitted. If the magnetic field is scanned, a spectrum of such product ions will be obtained, and this spectrum is called a charge-inversion mass spectrum. These spectra are sometimes referred to as -E and +E spectra, respectively.

[Note : The terms "2E, E/2, -E or +E mass spectrum" should not be used without prior explanation of the meaning of 2E, E, +E or -E].

APPENDIX

VACUUM

(The terms in this section have been contributed, almost entirely, by the American Vacuum Society, to whom grateful acknowledgment is made)

Adsorption The process by which gas or vapor is bonded on a solid or liquid surface.

Aperture Impedance The additional resistance encountered by gas flowing through a tube with an abrupt reduction in cross-section. For molecular flow, it is the product of the molecular effusion impedance of an orifice with a cross-sectional area A_2 and the aperture correction factor $(1 - A_2/A_1)$, where A_1 is the cross-sectional area of the larger tube and A_2 that of the smaller tube.

Background Spectrum A mass spectrum of residual gas species in a system. It is usually obtained before a sample of interest is introduced and analyzed in order to deduce by subtraction of spectra the true mass spectrum of the sample.

Backstreaming The flow of charged and/or neutral particles emanating from a pump and moving counter to the flow of the gases being pumped.

Baffle A series of surfaces placed in the line of gas or vapor flow to prevent straight line flow.

Collision Frequency The number of molecules or atoms striking a unit area of surface per unit time; also, the number of collisions between the molecules or atoms in a gas per unit volume and unit time. The collision frequency per molecule is equal to the probability per unit time that a molecule will collide with a surface or another molecule.

Collision Rate The collision probability per unit time for an atom or molecule travelling at a specified speed through a gas.

Conductance The ratio of throughput, under steady-state conservative conditions, to the pressure differential between two specified cross-sections inside a pumping system.

Critical Inlet Pressure The inlet pressure of a vapor pump above which an abrupt decrease in pumping speed occurs.

Cryopump A vacuum pump which operates by the condensation and/or sorption of gas at surfaces maintained at temperatures sufficiently low for the vapor pressures of the condensed gases to be insignificant.

Cryosorption Pump A vessel containing an adsorbent which can be refrigerated for the cryosorption pumping of gases.

Cryosorption Pumping A technique of producing vacuum by physical adsorption of gases on solid adsorbents cooled to low temperatures.

Diffusion Pump A vapor pump in which the pumped gas flows into a vapor stream under conditions in which molecular flow predominates. Momentum is transferred from the vapor to the gas, carrying it along in the direction of the stream. Pump fluid is heated in vacuum to generate the vapor which is directed through a nozzle. It expands freely in the stream before it reaches a cool wall where it condenses and is returned to the boiler to begin a new cycle.

Ejector Pump A vapor pump in which the pumped gas enters the pump and the vapor stream under predominantly viscous flow conditions.

Evaporation The conversion of a substance from the liquid state into the gaseous state by absorption of energy.

Exhaust Port An opening in a vacuum pump or stage from which gases are ejected either to a succeeding stage or to the atmosphere.

Feedthrough A device for transmitting electrical current, fluids or mechanical motion through the wall of a vacuum system.

Flange A (projecting) rim usually in the form of an annulus intended for fastening and sealing one part of the vacuum system to another.

Flapper Valve A thin gauge spring steel plate fastened on one end to the pump housing which seals the exhaust port of a mechanical pump from the oil reservoir or atmosphere. During the exhaust cycle, gas pressure is sufficient to deflect the plate away from its seat and gas is discharged from the pump. Syn: flutter reed valve.

Flow (Gas) The motion or passage of a gas. A description of gas flow may be characterized by the Knudsen number into three ranges.

Molecular Flow The flow of gas through a channel under conditions such that the mean free path is much greater than the largest dimension of a transverse section of the channel. At these pressures, the flow characteristics are determined by collisions of the gas molecules with the channel surfaces and flow effects from molecular collisions are insignificant.

Transition Flow The flow of a gas through a channel under conditions that the mean free path is of the same order as the transverse dimensions of the channel. In this pressure range, the flow characteristics are determined by collisions of the gas molecules with surfaces as well as with other gas molecules. Also called Knudsen flow.

Viscous Flow The flow of a gas through a channel under conditions such that the mean free path is very small in comparison with smallest dimension of a transverse section of the channel. At these pressures the flow characteristics are determined mainly by collisions between the gas molecules, i.e. the viscosity of the gas. The flow may be laminar or turbulent.

Fore Pump A vacuum pump for maintaining the forepressure of another pump below its critical value.

Forepressure The pressure measured downstream from the outlet or foreline of a vacuum pump.

Fractionating Pump A diffusion pump whose design allows the more volatile impurities in the pump fluid resulting from decomposition or contamination to be either ejected out of the foreline or trapped within the pump in such a manner as to effectively reduce their chance of escape out of the pump inlet.

Holding Time (Pump) The time required for the forepressure of an isolated vapor or diffusion pump to reach the limiting forepressure.

Hot Cathode Ionization Gauge An ionization gauge in which pressure is measured in terms of the current of positive ions produced by electrons emitted from a heated cathode.

Bayard-Alpert Gauge A hot cathode ionization gauge in which a fine wire ion collector is positioned on the axis of a cylindrical grid functioning as anode. The cathode is mounted outside the grid.

Impedance The reciprocal of conductance.

Incidence Rate The number of molecules striking a unit area of surface per unit time.

Inlet Pressure The gas pressure at the entrance to a pump.

Interstage Pressure The gas pressure at any point between the exhaust port of the low-pressure stage and high-pressure or roughing stage of a compound pump.

Ion Pump An electron device in which ionization produces a significant rate of gas removal.

Differential Sputter Pump A sputter-ion pump having two cathodes for which materials and sputtering rates differ.

Diode Pump An ion pump containing two uniquely shaped electrodes, viz. a cathode and anode. Two-electrode ion pumps are also referred to as diode getter and diode sputter ion pumps.

Electrostatic Pump An ion pump having only electrostatic fields rather than both electric and magnetic fields to generate the ionizing discharge. The getter material is sublimed by electron heating or by ohmic heating into the discharge space.

Electrostatic Getter Pump An electrostatic-ion pump in which a getter material is made to sublime.

Evaporation Pump A getter-ion pump in which the getter is evaporated from a molten surface rather than sublimed or sputtered from a solid source.

Getter Pump A pump which combines the pumping mechanisms used in the ion pump and the getter pump. (See sputter-ion pump and electrostatic pump).

Magnetic Pump An ion pump usually with multiple anode cells immersed in a magnetic field parallel to the cell axes with two cathode end plates of reactive material spaced from the ends of the anode cells which terminates the discharge space.

Noble Gas Pump A magnetic-ion pump with novel cathode geometries to enhance the pumping of noble gases.

Sputter Pump A getter-ion pump in which the getter surfaces are continuously renewed by sputtering.

Triode Pump An ion pump usually of the sputter-ion type, containing three uniquely shaped electrodes; an anode, a sputter cathode, and an ion collector electrode.

Triode Getter Pump A triode-ion pump in which gettering is a part of the pumping mechanism.

Knudsen Flow The flow of gas through a pump or system under transition flow conditions which are intermediate between viscous flow and molecular flow.

Knudsen Gauge A vacuum gauge which indicates pressure by responding to the net rate of transfer of momentum by molecules moving between two surfaces maintained at different temperatures and separated by a distance smaller than the mean free path of the gas molecules. Various types of Knudsen gauges differ mainly in the shape and method of suspension of the movable element.

Knudsen Number The ratio of the mean free path of a gas molecule to a characteristic dimension of the channel through which gas is flowing. For a cylindrical tube, the diameter is a characteristic dimension.

Leak A hole or permeable element through which leakage may occur under the action of a pressure difference. This includes a device used to introduce gas into a vacuum system at a controlled rate.

Calibrated Leak A leak which has a known leakage rate for a specific gas under specific conditions.

Capillary Leak A leak having a small cross section dimension and length many times its cross section dimension.

Membrane Leak A leak which permits gas flow by permeation through a thin nonporous wall.

Molecular Leak A leak of such a size that the leakage through it is predominantly molecular flow for a given pressure.

Variable Leak A leak with an adjustable leakage rate which can be controlled.

Virtual Leak An apparent leak because of the presence of contaminants which outgas very slowly within a vacuum system.

Viscous Leak A leak of such a size that the leakage through it is predominantly viscous flow for a given pressure.

Accumulation Leak Detection Technique A leak detection technique in which tracer gas (e.g. helium) enters the part under test and is allowed to accumulate within the part, or within a system containing the part, for a period of time. The part or system is then opened to the leak detector. The system may include the leak detector sensing element.

Backing Space Leak Detection Technique A leak detection technique in which the leak detector is connected to the forevacuum side of a pump attached to the vacuum system or element undergoing leak test. A tracer gas is sampled at a higher pressure after compression by the diffusion pump or other type of pump operating at high speed relative to its backing pump.

Bagging A jargon term for a leak detection technique in which the part under test is enclosed in a bag (or other enclosure) which is filled with a tracer gas to slightly more than atmospheric pressure. A tracer gas is applied to the entire surface of the part to determine the total leakage from all leaks in the part.

Diffusion Leakage A leakage resulting from the temperature dependent diffusion of a specific gas through a membrane. Examples are the diffusion of hydrogen through palladium and helium through glass.

Leakage (leak) Rate The quantity of gas passing through a leak in a given time divided by that time (see throughput).

Limiting Forepressure The pressure at the discharge side of a vacuum pump, at a stated throughput, above which the pumping action of the pump rapidly deteriorates, evidenced by a sudden increase of inlet pressure. Syn: critical backing pressure.

Load (Vapor Pump) The quantity of gas, not including pump fluid vapor, in mass units, flowing through the pump per unit time. It is also called capacity or mass flow.

Manometer An instrument for measuring the pressure of gases and vapors.

Maximum Pressure Ratio (Vacuum Pump) The maximum value of the ratio of forepressure to inlet pressure which a pump can maintain at zero gas flow. In vapor pumps, this term is usually significant only for light gases such as hydrogen and helium.

McLeod Gauge A liquid level manometer in which a known volume of the gas, whose pressure is to be measured, is compressed by the movement of a liquid column and confined in a small measurable volume. Corrections need to be made for any appreciable change in gas pressure in the system caused by the movement of the liquid.

Mean Free Path The average distance a particle travels between successive collisions with the other particles of an ensemble.

Mean Path The mean distance a particle travels between successive collisions with other particles or surfaces. When the pressure is high or the vessel dimensions are large, so that the mean path is small with respect to the vessel dimensions, the mean path and mean free path become numerically identical.

Mechanical Pump (Vacuum) A device with moving parts such as rotating vanes, a piston, or eccentric rotary members used for pumping gas or vapor.

Molecular Effusion The molecular flow of gas from a region at one pressure to one at a lower pressure through an orifice in a wall of negligible thickness and with a diameter much less than the mean free path of the molecules.

Molecular Flux The net number of gas molecules crossing a specified surface in unit time. Those having a velocity component in the same direction as the normal to the surface at the point of crossing are counted as positive and those having a velocity component in the opposite direction are counted as negative.

Molecular Velocity Distribution The average value of the fraction of the molecules in a small volume, dr, surrounding a given point, located by the radius vector r in a fluid medium, which have velocity vectors lying within an infinitesimal volume, dv, surrounding the point in velocity space. The averaging process is carried out over a time long enough to smooth statistical fluctuations in the molecular populations, but short compared with the time required for significant variations in the macroscopic properties. For a gas in equilibrium at rest, the distribution of the velocity vectors with a given magnitude is uniform over a sphere about the origin in velocity space. The distribution known as Maxwell's law of velocity distribution is $f_v\, dv = 4\pi v^2 (m/2\pi kT)^{3/2} \exp(-mv^2/2kT)dv$, where m is the mass of a molecule, T is the absolute temperature, k is the Boltzmann constant, and $4\pi v^2\, dv$ is the volume of a spherical shell of radius equal to the magnitude of v and of thickness dv equal to the increment in this magnitude and gives the fraction of molecules having speeds between v and v + dv. The function f_v is the Maxwellian distribution function.

Net Speed (Vacuum Pump) The throughput across a section remote from the pump inlet divided by the pressure as measured at that section. The net speed can be calculated when the pumping speed is known by adding to the sum of all the impedances between the pump inlet and the given cross section, the reciprocal of the measured pumping speed and then taking the reciprocal of the result.

Pascal The basic S.I. unit of pressure recommended for general use in vacuum technology. It is one newton per square meter. (see also : Torr).

Permeability Coefficient The rate of flow of gas through a unit area and a unit thickness of a solid barrier per unit differential pressure at a given temperature.

Permeation The passage of gas through a solid. The process always involves diffusion through the solid and may involve surface phenomena such as sorption, dissociation, migration and desorption.

Physical Adsorption An adsorption process caused by van der Waals forces between adsorbent and adsorbate. Typical binding energies are less than 10 kcal/mole. Syn: physisorption. (See adsorption.)

Positive Displacement Pump A mechanical vacuum pump in which the pumping action is provided by displacement or trapped volume of gases typically by a rotating or reciprocating piston, sliding vane, or intermeshing lobes.

Pressure (Gas) The average normal force per unit area exerted by gas molecules impacting on a surface.

Ultimate Pressure The limiting low pressure approached in a vacuum system after a sufficient pumping time has elapsed to establish that further reductions in pressure will be negligible. Sometimes called the ultimate vacuum, or blank-off pressure, or base pressure when referred to a pump under test.

Ultimate Partial Pressure The part of the ultimate pressure in a vacuum system caused by the partial pressure of a specific gas.

(Saturated) Vapor Pressure The pressure of a vapor in thermodynamic equilibrium with a condensed phase at a fixed temperature. The definition applies to single components as well as to multicomponent systems. In the latter case, it is necessary to distinguish between the total pressure over the condensed phase and the partial pressure of a given component. Syn : saturation pressure.

Pump Fluid A liquid, usually having a low vapor pressure, used as the working fluid in a mechanical or vapor pump.

Pumping Speed The ratio of the throughput of a given gas to the partial pressure of that gas at a specified point near the inlet port of a pump.

Seal (Vacuum) A joint between two elements of a vacuum system which is effective in maintaining leakage at or below a required level.

Bakeable Seal A seal which can be baked at elevated temperatures.

Break Seal A seal consisting of a thin glass membrane separating adjacent sections of a vacuum system. The membrane is broken to connect the two sections.

Demountable Seal A seal between two elements designed for disassembly without resort to cutting, fracturing, or melting, which is effective in maintaining the desired vacuum.

Gasket Seal A demountable seal which employs a closed loop of deformable material pressed between two harder members. It may be reuseable. The gasket may be fabricated from metal washers, wire rings, elastomers or other materials.

O-Ring A demountable, elastomer, gasket seal made with a toroidal gasket of circular cross section.

Pump Speed The volumetric rate of gas flow across a section at the pump inlet. It can be obtained from the ratio of the throughput of a gas to the partial pressure of that gas at a specific point near the inlet port of the pump. (Often called pumping speed.)

Speed Factor The ratio of the speed to the product of the vacuum pump inlet cross section area and the maximum flow rate per unit area as given by the effusion law. It is also called efficiency, or speed efficiency.

Speed of Exhaust The instantaneous rate of reduction of pressure in a system multiplied by its volume and divided by its pressure.

Sticking Coefficient The ratio of the number of molecules which are adsorbed on a surface for a finite period of time to the number of molecules striking that surface.

Sublimation The process of transition directly from the solid vapor phase without passing through the intermediate liquid phase by the absorption of energy. Syn: sublime.

Thermal Conductivity Gauge A vacuum gauge containing two surfaces at different temperatures between which heat can be transported by gas molecules. Changes in the temperatures, or in the heating power required to maintain constant temperature of one of the surfaces can be correlated with the gas pressure. Thermal conductivity gauges differ in the method of indicating the temperature change. (See : thermocouple gauge).

Thermistor Gauge A form of thermal conductivity gauge in which the temperature-sensitive elements are made of semiconducting material instead of metal.

Thermocouple Gauge A thermal conductivity gauge which contains a heated filament and a thermocouple for the measurement of filament temperature as a function of gas pressure.

Throat (Vacuum Component) (a) (Nozzle or Diffuser). The smallest cross section of an expanding nozzle, converging diffuser or converging/diverging nozzle or diffuser. (b) (Vapor Pump). The smallest clearance area between the pump casing and the nozzle nearest the inlet port.

Throughput The quantity of gas in pressure-volume units, at a specified temperature, flowing per unit time across a specified open cross section. Throughput may be referred to a specific constituent of a gas in which case the partial pressure of that constituent and the associated flow rate are the relevant quantities.

Torr A unit of pressure defined as 1/760 of a standard atmosphere. It replaced the term millimeter of mercury (mm of Hg), and has now been replaced by the Pascal as a preferred unit of pressure. (1 mm Hg = 1.000 000 14 Torr = 133.322 386 7 Pascal).

Trap (Vacuum System) A device used in a vacuum pumping line to reduce vapor pressure in a vacuum system or prevent backstreaming and migration of vacuum pump fluids such as mercury and/or oil.

Anti-Migration Trap A trap which includes a chilled surface or other means to prevent surface migration of oil from a source into the vacuum system.

Cold Trap A trap with a refrigerated surface used to condense various vapors present in the vacuum system.

Molecular Sieve Trap A trap containing molecular sieve material that has a high surface area and that adsorbs hydrocarbon and water vapors at or below room temperature.

U-Tube Trap A trap in the form of a U-shaped tube which is immersed in a coolant.

Turbomolecular Pump An axial flow turbine for operation in the molecular flow range consisting of a series of alternate circular rotor and stator disks both of which have inclined blades designed to impart momentum change to gas molecules in a preferential direction from the pump inlet to the outlet.

Vacuum The condition of a gaseous environment in which the gas pressure is below atmospheric pressure.

Low Vacuum A vacuum in which the pressure is less than 10^5 Pa (~750 Torr) and greater than 3.3×10^3 Pa (25 Torr).

Medium Vacuum A vacuum in which the pressure is less than or equal to 3.3×10^3 Pa (25 Torr) and greater than 10^{-1} Pa (7.5×10^{-4} Torr).

High Vacuum A vacuum in which the pressure is less than or equal to 10^{-1} Pa (7.5×10^{-4} Torr) and greater than 10^{-4} Pa (7.5×10^{-7} Torr).

Very High Vacuum A vacuum in which the pressure is less than or equal to 10^{-4} Pa (7.5×10^{-7} Torr) and greater than 10^{-7} Pa (7.5×10^{-10} Torr).

Ultrahigh Vacuum A vacuum in which the pressure is less than or equal to 10^{-7} Pa (7.5×10^{-10} Torr) and more than 10^{-10} Pa (7.5×10^{-13} Torr).

Extreme Ultrahigh Vacuum A vacuum in which the pressure is less than 10^{-10} Pa (7.5×10^{-13} Torr).

Vacuum Valve A mechanical device by which the flow of gas or vapor may be started, stopped, or regulated by a moving part which opens or obstructs a passage.

Angle Valve A valve in which the ports are not in line, as, for example, a right angle valve.

Vacuum Baffle A valve containing a shield which remains in line with the valve port and can thus act as a baffle.

Butterfly Valve A valve which is opened or closed by rotating a disk 90° about an axis through the center of the disk.

Diaphragm Valve A valve in which the valve stem is mounted in a bonnet which is isolated from the rest of the valve by using a diaphragm to divide the space inside the valve body. Either metal, elastomer or plastic is commonly used for the diaphragm. An elastomer or plastic diaphragm sometimes functions also as a gasket. In any case, motion is limited to avoid exceeding the elastic limit of the diaphragm material.

Leak Valve A valve for admitting air or gas at a precisely determined rate into a vacuum system.

Needle Valve A leak valve in which a tapered needle is moved along its axis against a seat which may also be tapered.

Relief Valve A valve which will automatically open when the pressure on the seat side rises above a specific pre-set valve. It is generally regarded as a safety device.

Sealed Bellows Valve A valve usually for high vacuum applications, in which the stem is sealed by a flexible metal bellows. One end of the bellows is attached to the valve body and the other end to the disk part of the valve stem.

Solenoid Valve A valve in which the movable member is actuated electrically by an electromagnet.

Straight Through Valve A valve in which the ports are in line, or coaxial, and for which the internal construction is such that line-of-sight flow occurs when the valve is open.

DATA SYSTEM

Data Acquisition The process of transforming representations of (spectrometer) signals from their original form into suitable representations, with or without modification, in conjunction with a computer system.

Real Time In data acquisition in Real Time the computer representations are generated within the same time frame as the original experiment.

Off-Line In this method of data acquisition there is some (time) discontinuity in the transfer or transformation of the representations.

Data Logging is a more specific term implying data collection from more than one relatively low frequency source with storage of the collected data for later processing.

Hardware The term used for the physical components of a computer system.

Software This term is used to describe computer programs, whether inside or outside a computer, and whether they are machine readable or normally legible.

Firmware Computer programs stored in a semi permanent form, usually semi conductor memory, and used repeatedly without modification. Firmware can be changed only by exchanging or removing hardware.

Pre-Processor A device in a data acquisition system which performs a significant amount of data reduction, extracting specific information from raw signal representations, in advance of the main processing operation.
A preprocessor may constitute the whole of a data acquisition interface, in which case it must also perform the data acquisition task (spectrometer signal to computer representation conversion), or it may specialise solely in data treatment.

Hard Wired A preprocessor may be hard wired, that is capable of performing only certain defined tasks and no others without major physical modification.

Pre-Programmed A preprocessor may be pre-programmed, that is, it can be a general purpose device incorporating specific but readily alterable instructions to perform a particular task.

Signal Conditioning The process of altering the relationship of a transducer (spectrometer) output with respect to time or other parameters (frequency, voltage or current).

Signal Processing The mechanism of analysing, routing, sampling or changing the representation of a signal.

Operational Amplifier A high gain DC voltage amplifer with high input impedance, low output impedance and the capability of producing a bipolar output from a bipolar input.

Amplifier Complex A number of operational amplifiers configured for a specific function, packaged as a single unit and used as such.

Amplifier Bandwidth The range of signal frequencies over which an amplifier is capable of undistorted or unattenuated transmission. An Operational Amplifier should transmit DC voltage accurately and the upper (bandwidth) limit is defined as the 3 db point (factor of 2 attenuation).
Bandwidth can vary with gain and hence Gain-Bandwidth Product can be a more useful parameter.

Amplifier Noise This can be of two kinds, White Noise which is random signal fluctuations whose power spectrum contains all frequencies equally over a specified bandwidth and Pink Noise where the frequencies diminish in a specified fashion over a specified range.

Differential Amplifier An (operational) amplifier which has two inputs of opposite sense gain polarity with respect to its output. Differential Ouput Amplifiers with two opposite sense outputs, also exist.

Single-ended Amplifier An (operational) amplifier with a single input (or output).

Analogue Signal This is a signal which can be expressed as a continuously variable mathematical function of time.

Digital Signal This is a signal which represents information in a computer-compatible form as a sequence of (binary) numbers which may describe discrete samples of an analogue signal.

MINUTES OF THE MEETING ON SECTION M ON
MASS SPECTROMETRY ASTM COMMITTEE D-2, RES. DIV. IV

The meeting of Section M was held on Monday, May 25, 1981 at 9:00 a.m. at the Radisson Hotel, Minneapolis, MN. A total of 22 persons attended, representing academic government and industrial organizations. A list of attendees is available from Thomas Aczel.

The meeting was opened with a call from the Chairman to intensify efforts in providing methods for the analysis of coal and shale derived liquids. This was agreed to.

Dr. T. Ashe of Exxon reported on the cooperative study on high resolution, high voltage MS. Aromatics from a blend of several crudes were distributed to five participating laboratories. Data tabulated from the runs show a good degree of similarity between raw spectra. More evaluation is needed, however, before a definitive method based on high resolution can be proposed.

Dr. G. Greenwood of Phillips Petroleum reported on the analysis of the saturates from the above blend. These results, from seven laboratories, show that the precision specifications in ASTM D-2786 are too lenient; the present data showed significantly better agreement. Final action to modify ASTM D-2786 accordingly will be initiated as soon as all eleven laboratories participating in this effort send in their data. A question was raised on the purity of the fractions; as monoaromatic content is high; this is being investigated.

New business included the formation of two Task Groups, one on coal liquids, with R. Lett of the PETC, Pittsburgh as Chairman and one on shale liquids with G. Greenwood and S. Scheppele of DOE, Bartlesville as Co-chairmen. Samples will be sent to be analyzed under conditions now being agreed to by the respective Chairmen. Eleven people requested samples initially; additional participants are invited. Inquiries can be sent to Thomas Aczel or Gil Greenwood. Details on the aromatics and saturates analyses are also available from Thomas Aczel.

The formal meeting was adjourned at 10:00 a.m. An informal meeting was held on the methodologies of shale oil analysis on Tuesday at 4:00 p.m. Deliberations are still continuing on the subject; suggestions are welcome.

Respectfully submitted,

Thomas Aczel
Chairman

Exxon Research and Engineering Co.
P. O. Box 4255
Baytown, TX 77520

MINUTES OF THE 1981 ASTM E-14 BUSINESS MEETING

The Business Meeting of ASTM Committee E-14 on Mass Spectrometry was held on May 25, 1981 in Minneapolis, Minnesota. Representatives of industrial, academic and government oranizations provided an attendance of 35.

The meeting was opened by the Chairman, M.C. Hamming, who introduced the current officers and the ASTM staff manager.

Chairman:	M.C. Hamming, CONOCO, Inc., Res. and Dev. Dept., Box 1267, Ponca City, OK 74601
Vice Chairman:	T. Aczel, Exxon Res. and Eng. Co., Box 4255, Baytown, TX 77520
Secretary-Treasurer:	B.N. Colby, Systems, Science and Software, Box 1620, La Jolla, CA 92038
Staff Manager:	Ken C. Pearson, ASTM, 1916 Race St., Philadelphia, PA 19103

The minutes of the previous meeting were presented by B.N. Colby and approved. This was followed by a brief discussion of ASTM E-14/ASMS joint projects by M.C. Hamming.

A report on Awards prepared by R. Pancirov was read by T. Ashe. It described results of a limited E-14 survey which supported the award concept. The discussion which followed culminated in a motion to have E-14 establish an award to be presented at the ASMS banquet at undefined intervals. This was ammended "to take place as soon as possible". Both ammendment and motion as ammended were passed by a show-of-hands vote.

T. Ashe, Chairman of Subcommittee E14.13 on GC/MS, gave an update on the GC/MS practice which is in preparation. Draft 1.3 had been distributed for vote and received several negatives; Sections 6.1, 6.2, 6.3 and 6.5 being the problem areas. J. McGuire and D. Parees agreed to organize a meeting during the week to determine appropriate action with respect to the GC/MS practice.

P. Price, Chairman of Subcommittee E14.14 on General Practices, gave our update on title changes for the two existing E-14 practices. The proposed new name for E137 was rejected. Discussion will be held with the individuals who voted negatively in order to determine if the objections are editorial. The revision to E304 was accepted as proposed.

Also discussed was the proposed "Good Laboratory Practices" practice which had received a 90 percent negative response on balloting. A decision was made to address this during the GC/MS meeting later in the week.

T. Aczel, Chairman of Subcommittee E14.91, Liaison, gave a very brief update on the activity of D2 where method precision is being reevaluated.

B. Colby, Chairman of Subcommittee E14.92 on Long Range Planning and Programs, mentioned the possibility of a symposium on oil shale for next years meeting. T. Aczel will be planning this activity. Also discussed was the possibility of preparing a questionaire for distribution to E-14 members with the intent of improved understanding of member interests. Mynard Hamming will prepare this.

The possibility of an E-14 STP (Standard Technical Publication) was discussed. T. Aczel suggested the Oil Shale Symposium as a potential target for an STP.

The Nominating Committee provided a brief report identifying candidates for the 82-83 term. They are:

Chairman:	Thomas Aczel
Vice Chairman:	Gil Greenwood Phil Price

Secretary-Treasurer: Bruce Colby
Ed Emery

Ken Pearson, ASTM Staff Manager, presented an "Award of Appreciation" to Mynard Hamming for outstanding work performed for ASTM.

Old Business was discussed. This primarily centered around subcommittee and task force chairmanships:

- Jacob Shen, has found it necessary to resign as Chairman of Task Force E14.13.02 on GC/MS Terminology and was replaced by Doug Cameron.
- There is still no chairman for Subcommittee E14.04 on Data and Information Problems.
- Terry Ashe indicated that he found it necessary to resign as Chairman of E14.13 on GC/MS.

New business consisted of a discussion of new mass spectrometry techniques. MS-MS was of particular interest. Subcommittee E14.15 on "New Instrumentation and Techniques" was established with Doug Cameron as Chairman.

The Business Meeting was then adjourned.

An informal executive committee meeting was held by the officers after the Business Meeting. They discussed the above topics with ASMS representatives.

Respectfully Submitted,

Bruce N. Colby

Bruce N. Colby
Secretary-Treasurer

OFFICERS

ASTM COMMITTEE E-14 AND THE AMERICAN SOCIETY FOR MASS SPECTROMETRY

Year	President	Vice President (Programs)	Vice President (Arrangements)	Vice President (Data & Stds.)
		ASTM E-14		
1961-2	V.H. Dibeler	R.E. Fox	R.A. Brown	-
1963-4	R.E. Fox	N.D. Coggeshall	A.G. Sharkey	-
1965-6	N.D. Coggeshall	H.M. Rosenstock	M.K. Testerman	-
1967-8	H.M. Rosenstock	J.L. Franklin	D.B. Harrington	-
1968-9	J.L. Franklin	R.E. Honig	C.E. Johannsen	-
		ASMS		
1970	J.L. Franklin	R.E. Honig	C.E. Johannsen	H.R. Harless
1971-2	R.E. Honig	F.H. Field	G.L. Kearns	H.R. Harless
1972-4	F.H. Field	H.J. Svec	A.H. Struck	E. Lumpkin
1974-6	H.J. Svec	J.H. Futrell	W.H. Brubaker	*
1976-8	J.H. Futrell	J.A. McCloskey	E.J. Bonelli	-
1978-9	J.A. McCloskey	B. Munson	E.J. Bonelli	-
1979-80	J.A. McCloskey	B. Munson	W.A. Wolstenholme	-
1980-1	B. Munson	C.C. Fenselau	W.A. Wolstenholme	-

Year	Secretary	Treasurer	Directors-at-Large	
		ASTM E-14		
1961	C.F. Crable	-	J.H. Beynon	C.F. Robinson
1963-4	H.E. Lumpkin	-	S. Meyerson	A.L. Wahrhaftig
1965-6	G.L. Cook	-	H.I. Schiff	W.M. Hickam
1967-8	A.B. King	-	E.E. Muschlitz	R.M. Teeter
1969	J.M. McCrea	-	R.F. Porter	J.T. Heron
		ASMS		
1970	J.M. McCrea	H.D. Cook	R.F. Porter	J.T. Herron
1971-2	F.E. Saalfeld	H.D. Cook	A.G. Sharkey	A.L. Wahrhaftig
1972-4	F.E. Saalfeld	M.T. Laug	J. Berkowitz	E.B. Owens
1974-6	J.A. McCloskey	M.T. Laug	P. Kebarle +E.M. Emery	J.L. Margrave
1976-7	K.E. McCulloh	M.T. Laug	H.M. Fales	A.G. Harrison
1977-8	H.M. Fales	M.A. Frisch	H.M. Fales +E.G. Carlson	A.G. Harrison
1978-9	H.M. Fales	M.A. Frisch	C.C. Fenselau +M.C. Hamming	A.G. Harrison
1979-80	H.M. Fales	M.A. Frisch	C.C. Fenselau +M.C. Hamming	W.L. Fite
1980-1	H.M. Fales	M.A. Frisch	J.T. Watson +M.C. Hamming	W.L. Fite

*ASTM E-14 Chairman was dropped as a Vice President and made a Director-at-Large in 1974.

+ASTM E-14 Chairman

AMERICAN SOCIETY FOR MASS SPECTROMETRY
1980 SALARY SURVEY

JONES AND FOXWELL
SURVEY CONSULTANTS

JANUARY 31, 1981

CONTENTS

SURVEY METHODOLOGY

On November 17, 1980, Dr. Burnaby Munson, president of the American Society for Mass Spectrometry, wrote to the Society's 1,436 members asking them to participate in the 1980 Membership Survey. The mailing included the questionnaire that appears as an appendix to this report and an unstamped envelope addressed to the survey firm engaged to analyze the survey results. By January 25, 1981, more than half the questionnnaires (54%) had been received. The responses were edited when necessary to eliminate inappropriate or nonsensical responses, and the edited responses were then entered into computer storage. Survey responses were anonymous, and no attempt was made to measure non-response bias.

The tables in the report were produced using an Alpha-Micro computer, with programs written by Harry Foxwell and John Robert Jones.

TECHNICAL NOTES

How to Read the Tables

This report contains two types of tables: cross-tabulations and salary tables. The format of each table is based on two questions from the survey questionnaire. One of these questions is associated with the rows, and the other question is associated with the columns. The possible answers to these questions determine the row headings and the column headings.

Cross-tabulations. Each "cell" of a cross-tabulation contains three items: the Count, the Row Percent, and the Column Percent. The count is the number of responses in that cell; the row percent is the cell count as a percent of the total in that row; and the column percent is the cell count as a percent of the total in that column.

Salary tables. Each cell of a salary table contains four items: the Median salary, the Mean salary, the Standard Deviation of the salaries, and the Count. The median salary divides all the salaries into two groups of equal size (that is, half the salaries are more and half are less than the median). The mean is the sum of the salaries divided by the number of salaries. The standard deviation is a measure of the variation among the salaries in that cell.

Item Non-response

Non-response to question E concerning the numbers of subordinates was interpreted to mean zero subordinates.

Estimates of Proportions

Estimates of the proportion of respondents falling into a given category are sample proportions, which are subject to sampling error. How large the sampling error is likely to be depends upon the observed values used both as the numerator and as the denominator of the proportion being estimated. The table below contains information that will approximate limits on the size of the sampling error.

Approximate Sampling Error for Percents
(Confidence level = 95%)

	n=50	n=100	n=200	n=500
p=10% or 90%	8.3%	5.9%	4.2%	2.6%
p=20% or 80%	11.1	7.8	5.5	3.5
p=30% or 70%	12.7	9.0	6.4	4.0
p=40% or 60%	13.6	9.6	6.8	4.3
p=50%	13.9	9.8	6.9	4.4

The values of p and n come from the sample data: n is the denominator of the fraction of interest, and p is that fraction, which appears in the table in the form of a percent.

As an example of how to use this table, consider Table XTAB.008, Highest degree by Profession. The proportion of organic chemists whose highest degree is the PhD is listed as 80.4%. The total number of organic chemists in this table is 56. Thus, n is 56 and p is 80.4%. If p and n are approximated as 80% and 50, the table indicates the sampling error is probably between -11.1% and +11.1%. Therefore, among full-time employed organic chemists, the proportion who are PhD-holders is probably between 70% and 92% (that is, within 11% of 81%). If this procedure were repeated many times on different samples from the same population, about 95% of the intervals obtained from the table would actually contain the true population percent.

Estimates of Medians

Estimates of median salaries are also subject to sampling error. Median salaries based on sample data is not useful if the number of observed salaries is very small. Thus, the tables in this report do not show median salaries for cells with fewer than 15 respondents.

Comparing salaries

The warnings in the previous two sections apply with greater force to comparisons between salaries of groups of respondents because sampling error affects each of the two numbers being compared.

LIST OF TABLES

1980 Salary Survey of
The American Society for Mass Spectrometry
Jones and Foxwell, Survey Consultants

A. Highest degree earned:
PhD 1[] MD 2[] Masters 3[] Bachelors 4[] Other 5[]
Year highest degree received: _____
Years of professional experience: _____
Years involved in mass spectrometry: _____

B. I consider my major profession to be (select one):

Chemist:	
Agriculture/Food . . . . . .1[]	Biologist . . . . . 8[]
Analytical . . . . . .2[]	Engineer . . . . . 9[]
Inorganic . . . . . .3[]	Physician . . . . . 10[]
Organic . . . . . .4[]	Physicist . . . . . 11[]
Physical . . . . . .5[]	Other . . . . . 12[]
Polymer . . . . . .6[]	
Pharmaceutical, Medicinal, Clinical 7[]	

C. Current or most recent full-time employer:

Private Industry:	Government
Manufacturing . . . 1[]	Federal . . . . . 4[]
Non-manufacturing . 2[]	State/Local . . . . . 5[]
College/University . 3[]	Self-employment . . . . . 6[]
	Other . . . . . 7[]

D. Present or most recent principal work function (select one only):

Teaching/Teaching and research . . . 1[]	Marketing/Sales . . . . . 7[]
Research and Development	Production/Quality control 8[]
Management/Administration of R&D . 2[]	Forensic Analysis . . . . 9[]
Basic Research . . . . . 3[]	Computer/Data processing .10[]
Applied research/Develop./Design . 4[]	Consulting . . . . . .11[]
General Management (other than R&D) . 5[]	Other. . . . . .12[]
Writing /Editing/Abstracting/Library 6[]	

E. Number of subordinates reporting to you directly or through others:
Professionals: _____ Technicians: _____ Others: _____

F. Age as of November 15, 1980: _____

G. Sex: Male . . 1[] Female . . 2[]

H. Racial or ethnic group:

White (not of Hispanic origin) . . . . . 1[]	White Hispanic . . 4[]
Black (not of Hispanic origin) . . . . . 2[]	Black Hispanic . . 5[]
Asian (including Subcontinental Indian) 3[]	American Indian . 6[]
	Other . . . . . 7[]

I. Employment status as of November 15:

Employed:		Not employed:	
Predoctoral student 1[]	full-time 3[]	seeking employment	5[]
Postdoctoral fellow 2[]	part-time 4[]	not seeking employment	6[]

Please continue ===>

J. Principal ANNUAL SALARY as of November 15, 1980.
(Do not include payments for summer teaching, overtime work, second job, or other supplemental employment.) $ _____ per year

If your main employment is with a college or university, skip to question L.

K. Job title: _____ Skip to question O.

L. Academic rank:

Professor . . . . . 1[]	Instructor/Lecturer . . . . . 4[]
Associate professor . . 2[]	Unranked faculty member . . . 5[]
Assistant professor . . 3[]	Non-faculty member . . . . . 6[]

M. Have you been granted tenure? Yes. 1[] No. 2[]

N. My basic annual salary covers service of: 9-10 months . . 1[]
11-12 months . . 2[]

O. How many employers have you had since receiving highest degree? _____

P. How many years have you been with your present employer? _____

Q.

	0-10%	10-30%	30-60%	60-80%	80-100%
What percent of your working time is devoted to "hands-on" operation of mass spectrometer or computer?	1[]	2[]	3[]	4[]	5[]
What percent of mass spectral data obtained with your mass spectrometers do you interpret for yourself or others?	1[]	2[]	3[]	4[]	5[]
What percent of the sample preparation (purification/derivatization) do you perform?	1[]	2[]	3[]	4[]	5[]
What percent of maintenance problems do you refer to the manufacturer through its service engineers?	1[]	2[]	3[]	4[]	5[]
Even though you may not repair equipment yourself, please indicate the percent of mechanical/electrical problems you have the ABILITY to correct.	1[]	2[]	3[]	4[]	5[]

OPTIONAL:

The officers of the ASMS seek your guidance regarding the Society's activities. Please use a separate sheet of paper if you wish to make any comments that you think might be helpful. (The reason for the separate paper concerns confidentiality: no one associated with the Society will see your completed questionnaire.) The officers especially seek your suggestions regarding:

a) Time of meetings
b) Location of meetings
c) Cost to attend meetings (hotel plus travel)
d) Bound volumes of proceedings or other publications
e) Program

Appendix B: Job Titles

Question K asked respondents employed in non-academic positions to indicate their job titles. The 513 responses to this question were distributed as follows:

199 Chemists
- --69 research chemists
- --43 chemists
- --21 senior research chemists
- --14 senior chemists
- -- 8 analytical chemists
- -- 3 principal cemists
- -- 3 senior analytical chemists
- -- 3 staff chemists

16 Engineers
- -- 4 senior engineers
- -- 3 engineers
- -- 2 marketing engineers

16 Physicists
- -- 7 physicists
- -- 3 research physicists
- -- 3 senior physicists

83 Scientists
- --15 research scientists
- --12 senior research scientists
- --11 scientists
- --11 senior scientists
- -- 5 staff scientists
- -- 3 advisory scientists

24 Mass spectrometrists
- -- 9 mass spectrometrists
- -- 4 senior mass spectrometrists

38 Managers
- -- 6 managers
- -- 4 sales managers
- -- 3 project managers
- -- 2 general managers
- -- 2 laboratory managers
- -- 2 marketing managers

15 Directors
9 Group leaders
9 Research associates
7 Supervisors
6 Presidents
5 Vice-presidents
4 Project leaders
4 Sales managers
4 Research group leaders
3 Research specialists
3 Senior research associates
3 Postdoctoral fellows
65 others

YEAR OF DEGREE by HIGHEST DEGREE
ALL RESPONDENTS
XTAB.001

HIGHEST DEGREE	YEAR OF DEGREE '79-'80	'76-'78	'73-'75	'68-'72	'63-'67	'58-'62	'53-'57	'48-'52	'43-'47	'38-'42	'30-'37	No Response	TOTAL	
Ph.D.	28	63	66	132	71	34	26	16	5	3	3	17	464	-Count
	6.0%	13.6%	14.2%	28.4%	15.3%	7.3%	5.6%	3.4%	1.1%	0.6%	0.6%	3.7%	100.0%	-% of Row
	75.7%	56.3%	66.7%	72.9%	66.4%	46.6%	57.8%	39.0%	35.7%	37.5%	100.0%	30.9%	59.9%	-% of Col
M.D.	1	1	0	0	2	1	2	0	0	0	0	0	7	
	14.3%	14.3%	0.0%	0.0%	28.6%	14.3%	28.6%	0.0%	0.0%	0.0%	0.0%	0.0%	100.0%	
	2.7%	0.9%	0.0%	0.0%	1.9%	1.4%	4.4%	0.0%	0.0%	0.0%	0.0%	0.0%	0.9%	
Masters	7	21	14	24	8	14	3	8	1	1	0	12	113	
	6.2%	18.6%	12.4%	21.2%	7.1%	12.4%	2.7%	7.1%	0.9%	0.9%	0.0%	10.6%	100.0%	
	18.9%	18.8%	14.1%	13.3%	7.5%	19.2%	6.7%	19.5%	7.1%	12.5%	0.0%	21.8%	14.6%	
Bachelors	1	25	18	22	26	22	12	15	8	4	0	15	168	
	0.6%	14.9%	10.7%	13.1%	15.5%	13.1%	7.1%	8.9%	4.8%	2.4%	0.0%	8.9%	100.0%	
	2.7%	22.3%	18.2%	12.2%	24.3%	30.1%	26.7%	36.6%	57.1%	50.0%	0.0%	27.3%	21.7%	
Other	0	0	1	2	0	1	2	2	0	0	0	8	16	
	0.0%	0.0%	6.3%	12.5%	0.0%	6.3%	12.5%	12.5%	0.0%	0.0%	0.0%	50.0%	100.0%	
	0.0%	0.0%	1.0%	1.1%	0.0%	1.4%	4.4%	4.9%	0.0%	0.0%	0.0%	14.5%	2.1%	
No Response	0	2	0	1	0	1	0	0	0	0	0	3	7	
	0.0%	28.6%	0.0%	14.3%	0.0%	14.3%	0.0%	0.0%	0.0%	0.0%	0.0%	42.9%	100.0%	
	0.0%	1.8%	0.0%	0.6%	0.0%	1.4%	0.0%	0.0%	0.0%	0.0%	0.0%	5.5%	0.9%	
TOTAL	37	112	99	181	107	73	45	41	14	8	3	55	775	
	4.8%	14.5%	12.8%	23.4%	13.8%	9.4%	5.8%	5.3%	1.8%	1.0%	0.4%	7.1%	100.0%	
	100.0%	100.0%	100.0%	100.0%	100.0%	100.0%	100.0%	100.0%	100.0%	100.0%	100.0%	100.0%	100.0%	

HIGHEST DEGREE by AGE LEVEL
ALL RESPONDENTS
XTAB.002

AGE LEVEL	HIGHEST DEGREE						
	Ph.D.	M.D.	Masters	Bachelor	Other	No Response	TOTAL
20-24	0 0.0% 0.0%	0 0.0% 0.0%	0 0.0% 0.0%	6 100.0% 3.6%	0 0.0% 0.0%	0 0.0% 0.0%	6 -Count 100.0% -% of Row 0.8% -% of Col
25-29	33 38.4% 7.1%	0 0.0% 0.0%	20 23.3% 17.7%	31 36.0% 18.5%	0 0.0% 0.0%	2 2.3% 28.6%	86 100.0% 11.1%
30-34	91 61.1% 19.6%	1 0.7% 14.3%	24 16.1% 21.2%	30 20.1% 17.9%	3 2.0% 18.8%	0 0.0% 0.0%	149 100.0% 19.2%
35-39	145 72.9% 31.3%	1 0.5% 14.3%	27 13.6% 23.9%	22 11.1% 13.1%	2 1.0% 12.5%	2 1.0% 28.6%	199 100.0% 25.7%
40-44	78 67.8% 16.8%	1 0.9% 14.3%	9 7.8% 8.0%	24 20.9% 14.3%	3 2.6% 18.8%	0 0.0% 0.0%	115 100.0% 14.8%
45-49	48 64.9% 10.3%	1 1.4% 14.3%	8 10.8% 7.1%	14 18.9% 8.3%	1 1.4% 6.3%	2 2.7% 28.6%	74 100.0% 9.5%
50-54	33 44.6% 7.1%	3 4.1% 42.9%	14 18.9% 12.4%	21 28.4% 12.5%	3 4.1% 18.8%	0 0.0% 0.0%	74 100.0% 9.5%
55-59	17 38.6% 3.7%	0 0.0% 0.0%	9 20.5% 8.0%	15 34.1% 8.9%	3 6.8% 18.8%	0 0.0% 0.0%	44 100.0% 5.7%
60-64	9 52.9% 1.9%	0 0.0% 0.0%	2 11.8% 1.8%	5 29.4% 3.0%	1 5.9% 6.3%	0 0.0% 0.0%	17 100.0% 2.2%
>=65	10 90.9% 2.2%	0 0.0% 0.0%	0 0.0% 0.0%	0 0.0% 0.0%	0 0.0% 0.0%	1 9.1% 14.3%	11 100.0% 1.4%
No Response	0 ***.*% 0.0%	0 ***.*% 0.0%	0 ***.*% 0.0%	0 ***.*% 0.0%	0 ***.*% 0.0%	0 ***.*% 0.0%	0 ***.*% 0.0%
TOTAL	464 59.9% 100.0%	7 0.9% 100.0%	113 14.6% 100.0%	168 21.7% 100.0%	16 2.1% 100.0%	7 0.9% 100.0%	775 100.0% 100.0%

HIGHEST DEGREE by SEX OF RESPONDENT
ALL RESPONDENTS
XTAB.003

SEX OF RESPONDENT	HIGHEST DEGREE Ph.D.	M.D.	Masters	Bachelor	Other	No Respose	TOTAL	
Male	429	7	96	143	16	6	697	-Count
	61.5%	1.0%	13.8%	20.5%	2.3%	0.9%	100.0%	-% of Row
	92.5%	100.0%	85.0%	85.1%	100.0%	85.7%	89.9%	-% of Col
Female	34	0	17	23	0	0	74	
	45.9%	0.0%	23.0%	31.1%	0.0%	0.0%	100.0%	
	7.3%	0.0%	15.0%	13.7%	0.0%	0.0%	9.5%	
No Response	1	0	0	2	0	1	4	
	25.0%	0.0%	0.0%	50.0%	0.0%	25.0%	100.0%	
	0.2%	0.0%	0.0%	1.2%	0.0%	14.3%	0.5%	
TOTAL	464	7	113	168	16	7	775	
	59.9%	0.9%	14.6%	21.7%	2.1%	0.9%	100.0%	
	100.0%	100.0%	100.0%	100.0%	100.0%	100.0%	100.0%	

HIGHEST DEGREE by RACE
ALL RESPONDENTS
XTAB.004

RACE OR ETHNICITY	HIGHEST DEGREE Ph.D.	M.D.	Masters	Bachelor	Other	No Respose	TOTAL	
White	422	6	106	155	15	6	710	-Count
	59.4%	0.8%	14.9%	21.8%	2.1%	0.8%	100.0%	-% of Row
	90.9%	85.7%	93.8%	92.3%	93.8%	85.7%	91.6%	-% of Col
Black	2	0	0	3	0	0	5	
	40.0%	0.0%	0.0%	60.0%	0.0%	0.0%	100.0%	
	0.4%	0.0%	0.0%	1.8%	0.0%	0.0%	0.6%	
Asian	29	1	3	4	0	0	37	
	78.4%	2.7%	8.1%	10.8%	0.0%	0.0%	100.0%	
	6.3%	14.3%	2.7%	2.4%	0.0%	0.0%	4.8%	
White Hisp	2	0	2	3	0	0	7	
	28.6%	0.0%	28.6%	42.9%	0.0%	0.0%	100.0%	
	0.4%	0.0%	1.8%	1.8%	0.0%	0.0%	0.9%	
Black Hisp	0	0	0	0	0	0	0	
	***.*%	***.*%	***.*%	***.*%	***.*%	***.*%	***.*%	
	0.0%	0.0%	0.0%	0.0%	0.0%	0.0%	0.0%	
Amer Ind	0	0	0	1	0	0	1	
	0.0%	0.0%	0.0%	100.0%	0.0%	0.0%	100.0%	
	0.0%	0.0%	0.0%	0.6%	0.0%	0.0%	0.1%	
Other	1	0	1	1	1	0	4	
	25.0%	0.0%	25.0%	25.0%	25.0%	0.0%	100.0%	
	0.2%	0.0%	0.9%	0.6%	6.3%	0.0%	0.5%	
No Response	8	0	1	1	0	1	11	
	72.7%	0.0%	9.1%	9.1%	0.0%	9.1%	100.0%	
	1.7%	0.0%	0.9%	0.6%	0.0%	14.3%	1.4%	
TOTAL	464	7	113	168	16	7	775	
	59.9%	0.9%	14.6%	21.7%	2.1%	0.9%	100.0%	
	100.0%	100.0%	100.0%	100.0%	100.0%	100.0%	100.0%	

HIGHEST DEGREE by EMPLOYMENT STATUS
ALL RESPONDENTS
XTAB.005

EMPLOYMENT STATUS	HIGHEST DEGREE Ph.D.	M.D.	Masters	Bachelor	Other	No Response	TOTAL	
Pre-Doc	1	0	9	19	0	2	31	-Count
	3.2%	0.0%	29.0%	61.3%	0.0%	6.5%	100.0%	-% of Row
	0.2%	0.0%	8.0%	11.3%	0.0%	28.6%	4.0%	-% of Col
Post-Doc	12	1	1	0	0	0	14	
	85.7%	7.1%	7.1%	0.0%	0.0%	0.0%	100.0%	
	2.6%	14.3%	0.9%	0.0%	0.0%	0.0%	1.8%	
Full-Time	439	6	101	146	16	4	712	
	61.7%	0.8%	14.2%	20.5%	2.2%	0.6%	100.0%	
	94.6%	85.7%	89.4%	86.9%	100.0%	57.1%	91.9%	
Part-Time	4	0	0	3	0	0	7	
	57.1%	0.0%	0.0%	42.9%	0.0%	0.0%	100.0%	
	0.9%	0.0%	0.0%	1.8%	0.0%	0.0%	0.9%	
Unemp-Seeking Employment	2	0	0	0	0	0	2	
	100.0%	0.0%	0.0%	0.0%	0.0%	0.0%	100.0%	
	0.4%	0.0%	0.0%	0.0%	0.0%	0.0%	0.3%	
Unemp-Not seeking Employment	4	0	2	0	0	0	6	
	66.7%	0.0%	33.3%	0.0%	0.0%	0.0%	100.0%	
	0.9%	0.0%	1.8%	0.0%	0.0%	0.0%	0.8%	
No Response	2	0	0	0	0	1	3	
	66.7%	0.0%	0.0%	0.0%	0.0%	33.3%	100.0%	
	0.4%	0.0%	0.0%	0.0%	0.0%	14.3%	0.4%	
TOTAL	464	7	113	168	16	7	775	
	59.9%	0.9%	14.6%	21.7%	2.1%	0.9%	100.0%	
	100.0%	100.0%	100.0%	100.0%	100.0%	100.0%	100.0%	

HIGHEST DEGREE by YEARS OF PROFESSIONAL EXPERIENCE
FULL-TIME EMPLOYED RESPONDENTS
XTAB.006

PROF EXPERIENCE	HIGHEST DEGREE						
	Ph.D.	M.D.	Masters	Bachelor	Other	No Response	TOTAL
0-1	5	0	1	1	0	0	7 -Count
	71.4%	0.0%	14.3%	14.3%	0.0%	0.0%	100.0% -% of Row
	1.1%	0.0%	1.0%	0.7%	0.0%	0.0%	1.0% -% of Col
2-4	43	0	10	10	0	0	63
	68.3%	0.0%	15.9%	15.9%	0.0%	0.0%	100.0%
	9.8%	0.0%	9.9%	6.8%	0.0%	0.0%	8.8%
5-7	59	0	11	17	0	0	87
	67.8%	0.0%	12.6%	19.5%	0.0%	0.0%	100.0%
	13.4%	0.0%	10.9%	11.6%	0.0%	0.0%	12.2%
8-12	114	0	25	23	3	0	165
	69.1%	0.0%	15.2%	13.9%	1.8%	0.0%	100.0%
	26.0%	0.0%	24.8%	15.8%	18.8%	0.0%	23.2%
13-17	71	0	15	24	4	0	114
	62.3%	0.0%	13.2%	21.1%	3.5%	0.0%	100.0%
	16.2%	0.0%	14.9%	16.4%	25.0%	0.0%	16.0%
18-22	53	0	14	18	3	1	89
	59.6%	0.0%	15.7%	20.2%	3.4%	1.1%	100.0%
	12.1%	0.0%	13.9%	12.3%	18.8%	25.0%	12.5%
23-27	29	2	4	15	1	0	51
	56.9%	3.9%	7.8%	29.4%	2.0%	0.0%	100.0%
	6.6%	33.3%	4.0%	10.3%	6.3%	0.0%	7.2%
28-32	15	1	15	15	2	1	49
	30.6%	2.0%	30.6%	30.6%	4.1%	2.0%	100.0%
	3.4%	16.7%	14.9%	10.3%	12.5%	25.0%	6.9%
33-37	8	0	3	5	1	0	17
	47.1%	0.0%	17.6%	29.4%	5.9%	0.0%	100.0%
	1.8%	0.0%	3.0%	3.4%	6.3%	0.0%	2.4%
38-42	3	0	0	4	1	0	8
	37.5%	0.0%	0.0%	50.0%	12.5%	0.0%	100.0%
	0.7%	0.0%	0.0%	2.7%	6.3%	0.0%	1.1%
> 42	37	3	3	13	1	2	59
	62.7%	5.1%	5.1%	22.0%	1.7%	3.4%	100.0%
	8.4%	50.0%	3.0%	8.9%	6.3%	50.0%	8.3%
No Response	2	0	0	1	0	0	3
	66.7%	0.0%	0.0%	33.3%	0.0%	0.0%	100.0%
	0.5%	0.0%	0.0%	0.7%	0.0%	0.0%	0.4%
TOTAL	439	6	101	146	16	4	712
	61.7%	0.8%	14.2%	20.5%	2.2%	0.6%	100.0%
	100.0%	100.0%	100.0%	100.0%	100.0%	100.0%	100.0%

HIGHEST DEGREE by YEARS IN MASS SPECTROMETRY
FULL-TIME EMPLOYED RESPONDENTS
XTAB.007

YEARS IN MASS SPEC	Ph.D.	M.D.	Masters	Bachelor	Other	No Response	TOTAL
	HIGHEST DEGREE						
0-1	3	0	2	5	0	0	10 -Count
	30.0%	0.0%	20.0%	50.0%	0.0%	0.0%	100.0% -% of Row
	0.7%	0.0%	2.0%	3.4%	0.0%	0.0%	1.4% -% of Col
2-4	42	0	22	22	0	1	87
	48.3%	0.0%	25.3%	25.3%	0.0%	1.1%	100.0%
	9.6%	0.0%	21.8%	15.1%	0.0%	25.0%	12.2%
5-7	81	0	21	30	2	0	134
	60.4%	0.0%	15.7%	22.4%	1.5%	0.0%	100.0%
	18.5%	0.0%	20.8%	20.5%	12.5%	0.0%	18.8%
8-12	129	2	19	31	7	0	188
	68.6%	1.1%	10.1%	16.5%	3.7%	0.0%	100.0%
	29.4%	33.3%	18.8%	21.2%	43.8%	0.0%	26.4%
13-17	88	1	13	17	2	1	122
	72.1%	0.8%	10.7%	13.9%	1.6%	0.8%	100.0%
	20.0%	16.7%	12.9%	11.6%	12.5%	25.0%	17.1%
18-22	34	0	8	8	2	1	53
	64.2%	0.0%	15.1%	15.1%	3.8%	1.9%	100.0%
	7.7%	0.0%	7.9%	5.5%	12.5%	25.0%	7.4%
23-27	15	0	5	10	1	0	31
	48.4%	0.0%	16.1%	32.3%	3.2%	0.0%	100.0%
	3.4%	0.0%	5.0%	6.8%	6.3%	0.0%	4.4%
28-32	4	0	6	3	0	0	13
	30.8%	0.0%	46.2%	23.1%	0.0%	0.0%	100.0%
	0.9%	0.0%	5.9%	2.1%	0.0%	0.0%	1.8%
33-37	5	0	1	5	1	0	12
	41.7%	0.0%	8.3%	41.7%	8.3%	0.0%	100.0%
	1.1%	0.0%	1.0%	3.4%	6.3%	0.0%	1.7%
38-42	0	0	0	1	1	0	2
	0.0%	0.0%	0.0%	50.0%	50.0%	0.0%	100.0%
	0.0%	0.0%	0.0%	0.7%	6.3%	0.0%	0.3%
> 42	37	3	3	13	0	1	57
	64.9%	5.3%	5.3%	22.8%	0.0%	1.8%	100.0%
	8.4%	50.0%	3.0%	8.9%	0.0%	25.0%	8.0%
No Response	1	0	1	1	0	0	3
	33.3%	0.0%	33.3%	33.3%	0.0%	0.0%	100.0%
	0.2%	0.0%	1.0%	0.7%	0.0%	0.0%	0.4%
TOTAL	439	6	101	146	16	4	712
	61.7%	0.8%	14.2%	20.5%	2.2%	0.6%	100.0%
	100.0%	100.0%	100.0%	100.0%	100.0%	100.0%	100.0%

HIGHEST DEGREE by PROFESSION
FULL-TIME EMPLOYED RESPONDENTS
XTAB.008

PROFESSION	HIGHEST DEGREE Ph.D.	M.D.	Masters	Bachelor	Other	No Response	TOTAL	
Chem-Agr/Food	6	0	3	1	0	0	10	-Count
	60.0%	0.0%	30.0%	10.0%	0.0%	0.0%	100.0%	-% of Row
	1.4%	0.0%	3.0%	0.7%	0.0%	0.0%	1.4%	-% of Col
Chem-Analy	219	2	61	101	8	1	392	
	55.9%	0.5%	15.6%	25.8%	2.0%	0.3%	100.0%	
	49.9%	33.3%	60.4%	69.2%	50.0%	25.0%	55.1%	
Chem-Inorg	4	0	2	2	0	0	8	
	50.0%	0.0%	25.0%	25.0%	0.0%	0.0%	100.0%	
	0.9%	0.0%	2.0%	1.4%	0.0%	0.0%	1.1%	
Chem-Org	45	0	3	8	0	0	56	
	80.4%	0.0%	5.4%	14.3%	0.0%	0.0%	100.0%	
	10.3%	0.0%	3.0%	5.5%	0.0%	0.0%	7.9%	
Chem-Phys	81	1	4	3	0	1	90	
	90.0%	1.1%	4.4%	3.3%	0.0%	1.1%	100.0%	
	18.5%	16.7%	4.0%	2.1%	0.0%	25.0%	12.6%	
Chem-Poly	2	0	0	0	0	0	2	
	100.0%	0.0%	0.0%	0.0%	0.0%	0.0%	100.0%	
	0.5%	0.0%	0.0%	0.0%	0.0%	0.0%	0.3%	
Chem-Pharmacuetical	32	1	8	5	1	0	47	
Medicinal	68.1%	2.1%	17.0%	10.6%	2.1%	0.0%	100.0%	
Clinical	7.3%	16.7%	7.9%	3.4%	6.3%	0.0%	6.6%	
Biologist	5	1	0	1	0	0	7	
	71.4%	14.3%	0.0%	14.3%	0.0%	0.0%	100.0%	
	1.1%	16.7%	0.0%	0.7%	0.0%	0.0%	1.0%	
Engineer	4	0	7	7	4	1	23	
	17.4%	0.0%	30.4%	30.4%	17.4%	4.3%	100.0%	
	0.9%	0.0%	6.9%	4.8%	25.0%	25.0%	3.2%	
Physician	1	1	0	0	0	0	2	
	50.0%	50.0%	0.0%	0.0%	0.0%	0.0%	100.0%	
	0.2%	16.7%	0.0%	0.0%	0.0%	0.0%	0.3%	
Physicist	18	0	10	13	0	0	41	
	43.9%	0.0%	24.4%	31.7%	0.0%	0.0%	100.0%	
	4.1%	0.0%	9.9%	8.9%	0.0%	0.0%	5.8%	
Other	18	0	3	4	2	1	28	
	64.3%	0.0%	10.7%	14.3%	7.1%	3.6%	100.0%	
	4.1%	0.0%	3.0%	2.7%	12.5%	25.0%	3.9%	
No Response	4	0	0	1	1	0	6	
	66.7%	0.0%	0.0%	16.7%	16.7%	0.0%	100.0%	
	0.9%	0.0%	0.0%	0.7%	6.3%	0.0%	0.8%	
TOTAL	439	6	101	146	16	4	712	
	61.7%	0.8%	14.2%	20.5%	2.2%	0.6%	100.0%	
	100.0%	100.0%	100.0%	100.0%	100.0%	100.0%	100.0%	

HIGHEST DEGREE BY EMPLOYER
FULL-TIME EMPLOYED RESPONDENTS
XTAB.009

EMPLOYER	HIGHEST DEGREE Ph.D.	M.D.	Masters	Bachelor	Other	No Response	TOTAL	
Mfg-Ind	103	3	44	59	7	1	217	-Count
	47.5%	1.4%	20.3%	27.2%	3.2%	0.5%	100.0%	-% of Row
	23.5%	50.0%	43.6%	40.4%	43.8%	25.0%	30.5%	-% of Col
Non-Mfg Industry	53	0	10	21	2	2	88	
	60.2%	0.0%	11.4%	23.9%	2.3%	2.3%	100.0%	
	12.1%	0.0%	9.9%	14.4%	12.5%	50.0%	12.4%	
Coll/Univ	174	2	15	16	4	1	212	
	82.1%	0.9%	7.1%	7.5%	1.9%	0.5%	100.0%	
	39.6%	33.3%	14.9%	11.0%	25.0%	25.0%	29.8%	
Govt-Fed	76	0	24	33	0	0	133	
	57.1%	0.0%	18.0%	24.8%	0.0%	0.0%	100.0%	
	17.3%	0.0%	23.8%	22.6%	0.0%	0.0%	18.7%	
Govt-State Local	4	1	1	9	0	0	15	
	26.7%	6.7%	6.7%	60.0%	0.0%	0.0%	100.0%	
	0.9%	16.7%	1.0%	6.2%	0.0%	0.0%	2.1%	
Self-Empl	2	0	0	1	0	0	3	
	66.7%	0.0%	0.0%	33.3%	0.0%	0.0%	100.0%	
	0.5%	0.0%	0.0%	0.7%	0.0%	0.0%	0.4%	
Other Empl	25	0	7	5	3	0	40	
	62.5%	0.0%	17.5%	12.5%	7.5%	0.0%	100.0%	
	5.7%	0.0%	6.9%	3.4%	18.8%	0.0%	5.6%	
No Response	2	0	0	2	0	0	4	
	50.0%	0.0%	0.0%	50.0%	0.0%	0.0%	100.0%	
	0.5%	0.0%	0.0%	1.4%	0.0%	0.0%	0.6%	
TOTAL	439	6	101	146	16	4	712	
	61.7%	0.8%	14.2%	20.5%	2.2%	0.6%	100.0%	
	100.0%	100.0%	100.0%	100.0%	100.0%	100.0%	100.0%	

HIGHEST DEGREE by WORK FUNCTION
FULL-TIME EMPLOYED RESPONDENTS
XTAB.010

WORK FUNCTION	HIGHEST DEGREE Ph.D.	M.D.	Masters	Bachelor	Other	No Response	TOTAL	
Tch/Res	121	1	4	2	1	1	130	-Count
	93.1%	0.8%	3.1%	1.5%	0.8%	0.8%	100.0%	-% of Row
	27.6%	16.7%	4.0%	1.4%	6.3%	25.0%	18.3%	-% of Col
R&D Mgt	38	2	7	11	0	0	58	
	65.5%	3.4%	12.1%	19.0%	0.0%	0.0%	100.0%	
	8.7%	33.3%	6.9%	7.5%	0.0%	0.0%	8.1%	
Bas Res	98	2	26	22	5	1	154	
	63.6%	1.3%	16.9%	14.3%	3.2%	0.6%	100.0%	
	22.3%	33.3%	25.7%	15.1%	31.3%	25.0%	21.6%	
Appl R&D	141	1	41	51	7	1	242	
	58.3%	0.4%	16.9%	21.1%	2.9%	0.4%	100.0%	
	32.1%	16.7%	40.6%	34.9%	43.8%	25.0%	34.0%	
Gen Mgt	11	0	6	14	0	0	31	
	35.5%	0.0%	19.4%	45.2%	0.0%	0.0%	100.0%	
	2.5%	0.0%	5.9%	9.6%	0.0%	0.0%	4.4%	
Writ/Edit	0	0	0	1	0	0	1	
	0.0%	0.0%	0.0%	100.0%	0.0%	0.0%	100.0%	
	0.0%	0.0%	0.0%	0.7%	0.0%	0.0%	0.1%	
Mkt/Sales	10	0	4	6	1	0	21	
	47.6%	0.0%	19.0%	28.6%	4.8%	0.0%	100.0%	
	2.3%	0.0%	4.0%	4.1%	6.3%	0.0%	2.9%	
Prod/QC	2	0	4	18	1	0	25	
	8.0%	0.0%	16.0%	72.0%	4.0%	0.0%	100.0%	
	0.5%	0.0%	4.0%	12.3%	6.3%	0.0%	3.5%	
Forens Ana	2	0	3	5	0	0	10	
	20.0%	0.0%	30.0%	50.0%	0.0%	0.0%	100.0%	
	0.5%	0.0%	3.0%	3.4%	0.0%	0.0%	1.4%	
Data Proc	2	0	2	0	0	0	4	
	50.0%	0.0%	50.0%	0.0%	0.0%	0.0%	100.0%	
	0.5%	0.0%	2.0%	0.0%	0.0%	0.0%	0.6%	
Consulting	5	0	1	3	1	0	10	
	50.0%	0.0%	10.0%	30.0%	10.0%	0.0%	100.0%	
	1.1%	0.0%	1.0%	2.1%	6.3%	0.0%	1.4%	
Other	5	0	3	10	0	1	19	
	26.3%	0.0%	15.8%	52.6%	0.0%	5.3%	100.0%	
	1.1%	0.0%	3.0%	6.8%	0.0%	25.0%	2.7%	
No Response	4	0	0	3	0	0	7	
	57.1%	0.0%	0.0%	42.9%	0.0%	0.0%	100.0%	
	0.9%	0.0%	0.0%	2.1%	0.0%	0.0%	1.0%	
TOTAL	439	6	101	146	16	4	712	
	61.7%	0.8%	14.2%	20.5%	2.2%	0.6%	100.0%	
	100.0%	100.0%	100.0%	100.0%	100.0%	100.0%	100.0%	

WORK FUNCTION by HANDS-ON EXPERIENCE
FULL-TIME EMPLOYED RESPONDENTS
XTAB.011

WORK FUNCTION	HANDS-ON OPERATION 0-10%	10-30%	30-60%	60-80%	80-100%	No Response	TOTAL	
Tch/Res	63	55	6	3	1	2	130	-Count
	48.5%	42.3%	4.6%	2.3%	0.8%	1.5%	100.0%	-% of Row
	26.6%	27.6%	4.8%	3.7%	1.5%	100.0%	18.3%	-% of Col
R&D Mgt	43	11	3	1	0	0	58	
	74.1%	19.0%	5.2%	1.7%	0.0%	0.0%	100.0%	
	18.1%	5.5%	2.4%	1.2%	0.0%	0.0%	8.1%	
Bas Res	31	49	29	30	15	0	154	
	20.1%	31.8%	18.8%	19.5%	9.7%	0.0%	100.0%	
	13.1%	24.6%	23.2%	37.0%	22.1%	0.0%	21.6%	
Appl R&D	50	55	65	34	38	0	242	
	20.7%	22.7%	26.9%	14.0%	15.7%	0.0%	100.0%	
	21.1%	27.6%	52.0%	42.0%	55.9%	0.0%	34.0%	
Gen Mgt	21	2	3	2	3	0	31	
	67.7%	6.5%	9.7%	6.5%	9.7%	0.0%	100.0%	
	8.9%	1.0%	2.4%	2.5%	4.4%	0.0%	4.4%	
Writ/Edit	1	0	0	0	0	0	1	
	100.0%	0.0%	0.0%	0.0%	0.0%	0.0%	100.0%	
	0.4%	0.0%	0.0%	0.0%	0.0%	0.0%	0.1%	
Mkt/Sales	11	7	3	0	0	0	21	
	52.4%	33.3%	14.3%	0.0%	0.0%	0.0%	100.0%	
	4.6%	3.5%	2.4%	0.0%	0.0%	0.0%	2.9%	
Prod/QC	6	8	5	4	2	0	25	
	24.0%	32.0%	20.0%	16.0%	8.0%	0.0%	100.0%	
	2.5%	4.0%	4.0%	4.9%	2.9%	0.0%	3.5%	
Forens Ana	1	3	1	3	2	0	10	
	10.0%	30.0%	10.0%	30.0%	20.0%	0.0%	100.0%	
	0.4%	1.5%	0.8%	3.7%	2.9%	0.0%	1.4%	
Data Proc	0	1	3	0	0	0	4	
	0.0%	25.0%	75.0%	0.0%	0.0%	0.0%	100.0%	
	0.0%	0.5%	2.4%	0.0%	0.0%	0.0%	0.6%	
Consulting	4	2	1	0	3	0	10	
	40.0%	20.0%	10.0%	0.0%	30.0%	0.0%	100.0%	
	1.7%	1.0%	0.8%	0.0%	4.4%	0.0%	1.4%	
Other	5	5	3	3	3	0	19	
	26.3%	26.3%	15.8%	15.8%	15.8%	0.0%	100.0%	
	2.1%	2.5%	2.4%	3.7%	4.4%	0.0%	2.7%	
No Response	1	1	3	1	1	0	7	
	14.3%	14.3%	42.9%	14.3%	14.3%	0.0%	100.0%	
	0.4%	0.5%	2.4%	1.2%	1.5%	0.0%	1.0%	
TOTAL	237	199	125	81	68	2	712	
	33.3%	27.9%	17.6%	11.4%	9.6%	0.3%	100.0%	
	100.0%	100.0%	100.0%	100.0%	100.0%	100.0%	100.0%	

WORK FUNCTION by INTERPRETATION
FULL-TIME EMPLOYED RESPONDENTS
XTAB.012

WORK FUNCTION	INTERPRETATION 0-10%	10-30%	30-60%	60-80%	80-100%	No Response	TOTAL
Tch/Res	18	27	26	17	40	2	130 -Count
	13.8%	20.8%	20.0%	13.1%	30.8%	1.5%	100.0% -% of Row
	15.4%	23.5%	25.0%	19.3%	14.2%	28.6%	18.3% -% of Col
R&D Mgt	24	15	8	3	8	0	58
	41.4%	25.9%	13.8%	5.2%	13.8%	0.0%	100.0%
	20.5%	13.0%	7.7%	3.4%	2.8%	0.0%	8.1%
Bas Res	12	19	16	21	85	1	154
	7.8%	12.3%	10.4%	13.6%	55.2%	0.6%	100.0%
	10.3%	16.5%	15.4%	23.9%	30.2%	14.3%	21.6%
Appl R&D	26	21	41	33	119	2	242
	10.7%	8.7%	16.9%	13.6%	49.2%	0.8%	100.0%
	22.2%	18.3%	39.4%	37.5%	42.3%	28.6%	34.0%
Gen Mgt	14	8	3	3	3	0	31
	45.2%	25.8%	9.7%	9.7%	9.7%	0.0%	100.0%
	12.0%	7.0%	2.9%	3.4%	1.1%	0.0%	4.4%
Writ/Edit	1	0	0	0	0	0	1
	100.0%	0.0%	0.0%	0.0%	0.0%	0.0%	100.0%
	0.9%	0.0%	0.0%	0.0%	0.0%	0.0%	0.1%
Mkt/Sales	10	6	1	1	3	0	21
	47.6%	28.6%	4.8%	4.8%	14.3%	0.0%	100.0%
	8.5%	5.2%	1.0%	1.1%	1.1%	0.0%	2.9%
Prod/QC	3	5	4	2	11	0	25
	12.0%	20.0%	16.0%	8.0%	44.0%	0.0%	100.0%
	2.6%	4.3%	3.8%	2.3%	3.9%	0.0%	3.5%
Forens Ana	1	4	0	2	3	0	10
	10.0%	40.0%	0.0%	20.0%	30.0%	0.0%	100.0%
	0.9%	3.5%	0.0%	2.3%	1.1%	0.0%	1.4%
Data Proc	2	1	0	0	0	1	4
	50.0%	25.0%	0.0%	0.0%	0.0%	25.0%	100.0%
	1.7%	0.9%	0.0%	0.0%	0.0%	14.3%	0.6%
Consulting	2	3	1	0	4	0	10
	20.0%	30.0%	10.0%	0.0%	40.0%	0.0%	100.0%
	1.7%	2.6%	1.0%	0.0%	1.4%	0.0%	1.4%
Other	4	3	4	3	4	1	19
	21.1%	15.8%	21.1%	15.8%	21.1%	5.3%	100.0%
	3.4%	2.6%	3.8%	3.4%	1.4%	14.3%	2.7%
No Response	0	3	0	3	1	0	7
	0.0%	42.9%	0.0%	42.9%	14.3%	0.0%	100.0%
	0.0%	2.6%	0.0%	3.4%	0.4%	0.0%	1.0%
TOTAL	117	115	104	88	281	7	712
	16.4%	16.2%	14.6%	12.4%	39.5%	1.0%	100.0%
	100.0%	100.0%	100.0%	100.0%	100.0%	100.0%	100.0%

WORK FUNCTION by PREPARATION
FULL-TIME EMPLOYED RESPONDENTS
XTAB.013

WORK FUNCTION	PREPARATION 0-10%	10-30%	30-60%	60-80%	80-100%	No Response	TOTAL
Tch/Res	75	23	11	4	14	3	130 -Count
	57.7%	17.7%	8.5%	3.1%	10.8%	2.3%	100.0% -% of Row
	19.6%	17.8%	19.3%	10.5%	14.7%	30.0%	18.3% -% of Col
R&D Mgt	50	3	2	1	2	0	58
	86.2%	5.2%	3.4%	1.7%	3.4%	0.0%	100.0%
	13.1%	2.3%	3.5%	2.6%	2.1%	0.0%	8.1%
Bas Res	64	28	11	13	36	2	154
	41.6%	18.2%	7.1%	8.4%	23.4%	1.3%	100.0%
	16.7%	21.7%	19.3%	34.2%	37.9%	20.0%	21.6%
Appl R&D	110	55	24	16	35	2	242
	45.5%	22.7%	9.9%	6.6%	14.5%	0.8%	100.0%
	28.7%	42.6%	42.1%	42.1%	36.8%	20.0%	34.0%
Gen Mgt	27	3	0	0	1	0	31
	87.1%	9.7%	0.0%	0.0%	3.2%	0.0%	100.0%
	7.0%	2.3%	0.0%	0.0%	1.1%	0.0%	4.4%
Writ/Edit	1	0	0	0	0	0	1
	100.0%	0.0%	0.0%	0.0%	0.0%	0.0%	100.0%
	0.3%	0.0%	0.0%	0.0%	0.0%	0.0%	0.1%
Mkt/Sales	16	2	1	0	2	0	21
	76.2%	9.5%	4.8%	0.0%	9.5%	0.0%	100.0%
	4.2%	1.6%	1.8%	0.0%	2.1%	0.0%	2.9%
Prod/QC	9	5	6	1	2	2	25
	36.0%	20.0%	24.0%	4.0%	8.0%	8.0%	100.0%
	2.3%	3.9%	10.5%	2.6%	2.1%	20.0%	3.5%
Forens Ana	4	2	2	0	2	0	10
	40.0%	20.0%	20.0%	0.0%	20.0%	0.0%	100.0%
	1.0%	1.6%	3.5%	0.0%	2.1%	0.0%	1.4%
Data Proc	4	0	0	0	0	0	4
	100.0%	0.0%	0.0%	0.0%	0.0%	0.0%	100.0%
	1.0%	0.0%	0.0%	0.0%	0.0%	0.0%	0.6%
Consulting	6	2	0	1	1	0	10
	60.0%	20.0%	0.0%	10.0%	10.0%	0.0%	100.0%
	1.6%	1.6%	0.0%	2.6%	1.1%	0.0%	1.4%
Other	10	6	0	2	0	1	19
	52.6%	31.6%	0.0%	10.5%	0.0%	5.3%	100.0%
	2.6%	4.7%	0.0%	5.3%	0.0%	10.0%	2.7%
No Response	7	0	0	0	0	0	7
	100.0%	0.0%	0.0%	0.0%	0.0%	0.0%	100.0%
	1.8%	0.0%	0.0%	0.0%	0.0%	0.0%	1.0%
TOTAL	383	129	57	38	95	10	712
	53.8%	18.1%	8.0%	5.3%	13.3%	1.4%	100.0%
	100.0%	100.0%	100.0%	100.0%	100.0%	100.0%	100.0%

WORK FUNCTION by REFER TO MANUFACTURER
FULL-TIME EMPLOYED RESPONDENTS
XTAB.014

WORK FUNCTION	REFER TO MFG 0-10%	10-30%	30-60%	60-80%	80-100%	No Response	TOTAL	
Tch/Res	67	34	14	7	5	3	130	-Count
	51.5%	26.2%	10.8%	5.4%	3.8%	2.3%	100.0%	-% of Row
	19.3%	21.3%	12.8%	14.3%	16.7%	17.6%	18.3%	-% of Col
R&D Mgt	24	18	8	3	3	2	58	
	41.4%	31.0%	13.8%	5.2%	5.2%	3.4%	100.0%	
	6.9%	11.3%	7.3%	6.1%	10.0%	11.8%	8.1%	
Bas Res	77	34	26	9	5	3	154	
	50.0%	22.1%	16.9%	5.8%	3.2%	1.9%	100.0%	
	22.2%	21.3%	23.9%	18.4%	16.7%	17.6%	21.6%	
Appl R&D	104	56	47	19	12	4	242	
	43.0%	23.1%	19.4%	7.9%	5.0%	1.7%	100.0%	
	30.0%	35.0%	43.1%	38.8%	40.0%	23.5%	34.0%	
Gen Mgt	19	5	3	3	1	0	31	
	61.3%	16.1%	9.7%	9.7%	3.2%	0.0%	100.0%	
	5.5%	3.1%	2.8%	6.1%	3.3%	0.0%	4.4%	
Writ/Edit	0	1	0	0	0	0	1	
	0.0%	100.0%	0.0%	0.0%	0.0%	0.0%	100.0%	
	0.0%	0.6%	0.0%	0.0%	0.0%	0.0%	0.1%	
Mkt/Sales	13	1	3	0	2	2	21	
	61.9%	4.8%	14.3%	0.0%	9.5%	9.5%	100.0%	
	3.7%	0.6%	2.8%	0.0%	6.7%	11.8%	2.9%	
Prod/QC	18	2	1	2	1	1	25	
	72.0%	8.0%	4.0%	8.0%	4.0%	4.0%	100.0%	
	5.2%	1.3%	0.9%	4.1%	3.3%	5.9%	3.5%	
Forens Ana	6	2	2	0	0	0	10	
	60.0%	20.0%	20.0%	0.0%	0.0%	0.0%	100.0%	
	1.7%	1.3%	1.8%	0.0%	0.0%	0.0%	1.4%	
Data Proc	2	2	0	0	0	0	4	
	50.0%	50.0%	0.0%	0.0%	0.0%	0.0%	100.0%	
	0.6%	1.3%	0.0%	0.0%	0.0%	0.0%	0.6%	
Consulting	6	0	0	3	0	1	10	
	60.0%	0.0%	0.0%	30.0%	0.0%	10.0%	100.0%	
	1.7%	0.0%	0.0%	6.1%	0.0%	5.9%	1.4%	
Other	7	5	3	2	1	1	19	
	36.8%	26.3%	15.8%	10.5%	5.3%	5.3%	100.0%	
	2.0%	3.1%	2.8%	4.1%	3.3%	5.9%	2.7%	
No Response	4	0	2	1	0	0	7	
	57.1%	0.0%	28.6%	14.3%	0.0%	0.0%	100.0%	
	1.2%	0.0%	1.8%	2.0%	0.0%	0.0%	1.0%	
TOTAL	347	160	109	49	30	17	712	
	48.7%	22.5%	15.3%	6.9%	4.2%	2.4%	100.0%	
	100.0%	100.0%	100.0%	100.0%	100.0%	100.0%	100.0%	

WORK FUNCTION by REPAIR ABILITY
FULL-TIME EMPLOYED RESPONDENTS
XTAB.015

WORK FUNCTION	REPAIR ABILITY 0-10%	10-30%	30-60%	60-80%	80-100%	No Response	TOTAL	
Tch/Res	10	23	29	37	28	3	130	-Count
	7.7%	17.7%	22.3%	28.5%	21.5%	2.3%	100.0%	-% of Row
	22.2%	19.8%	14.9%	20.7%	16.9%	25.0%	18.3%	-% of Col
R&D Mgt	3	12	16	13	14	0	58	
	5.2%	20.7%	27.6%	22.4%	24.1%	0.0%	100.0%	
	6.7%	10.3%	8.2%	7.3%	8.4%	0.0%	8.1%	
Bas Res	6	26	46	35	39	2	154	
	3.9%	16.9%	29.9%	22.7%	25.3%	1.3%	100.0%	
	13.3%	22.4%	23.7%	19.6%	23.5%	16.7%	21.6%	
Appl R&D	14	32	76	59	59	2	242	
	5.8%	13.2%	31.4%	24.4%	24.4%	0.8%	100.0%	
	31.1%	27.6%	39.2%	33.0%	35.5%	16.7%	34.0%	
Gen Mgt	6	2	7	9	6	1	31	
	19.4%	6.5%	22.6%	29.0%	19.4%	3.2%	100.0%	
	13.3%	1.7%	3.6%	5.0%	3.6%	8.3%	4.4%	
Writ/Edit	0	0	0	1	0	0	1	
	0.0%	0.0%	0.0%	100.0%	0.0%	0.0%	100.0%	
	0.0%	0.0%	0.0%	0.6%	0.0%	0.0%	0.1%	
Mkt/Sales	3	4	4	6	2	2	21	
	14.3%	19.0%	19.0%	28.6%	9.5%	9.5%	100.0%	
	6.7%	3.4%	2.1%	3.4%	1.2%	16.7%	2.9%	
Prod/QC	1	4	6	5	8	1	25	
	4.0%	16.0%	24.0%	20.0%	32.0%	4.0%	100.0%	
	2.2%	3.4%	3.1%	2.8%	4.8%	8.3%	3.5%	
Forens Ana	1	2	2	3	2	0	10	
	10.0%	20.0%	20.0%	30.0%	20.0%	0.0%	100.0%	
	2.2%	1.7%	1.0%	1.7%	1.2%	0.0%	1.4%	
Data Proc	0	1	0	1	2	0	4	
	0.0%	25.0%	0.0%	25.0%	50.0%	0.0%	100.0%	
	0.0%	0.9%	0.0%	0.6%	1.2%	0.0%	0.6%	
Consulting	0	4	2	1	2	1	10	
	0.0%	40.0%	20.0%	10.0%	20.0%	10.0%	100.0%	
	0.0%	3.4%	1.0%	0.6%	1.2%	8.3%	1.4%	
Other	1	5	3	6	4	0	19	
	5.3%	26.3%	15.8%	31.6%	21.1%	0.0%	100.0%	
	2.2%	4.3%	1.5%	3.4%	2.4%	0.0%	2.7%	
No Response	0	1	3	3	0	0	7	
	0.0%	14.3%	42.9%	42.9%	0.0%	0.0%	100.0%	
	0.0%	0.9%	1.5%	1.7%	0.0%	0.0%	1.0%	
TOTAL	45	116	194	179	166	12	712	
	6.3%	16.3%	27.2%	25.1%	23.3%	1.7%	100.0%	
	100.0%	100.0%	100.0%	100.0%	100.0%	100.0%	100.0%	

SALARY PERIOD by RANK
FULL-TIME EMPLOYED RESPONDENTS
XTAB.016

ACADEMIC RANK	SALARY PERIOD 9-10 months	11-12 months	No Response	TOTAL	
Full Prof	31	25	0	56	-Count
	55.4%	44.6%	0.0%	100.0%	-% of Row
	48.4%	12.7%	0.0%	7.9%	-% of Col
Assoc Prof	17	29	2	48	
	35.4%	60.4%	4.2%	100.0%	
	26.6%	14.7%	0.4%	6.7%	
Asst Prof	12	23	1	36	
	33.3%	63.9%	2.8%	100.0%	
	18.8%	11.7%	0.2%	5.1%	
Instr/Lec	2	7	0	9	
	22.2%	77.8%	0.0%	100.0%	
	3.1%	3.6%	0.0%	1.3%	
Unranked	0	19	0	19	
	0.0%	100.0%	0.0%	100.0%	
	0.0%	9.6%	0.0%	2.7%	
Non-Fac	1	43	2	46	
	2.2%	93.5%	4.3%	100.0%	
	1.6%	21.8%	0.4%	6.5%	
No Response	1	51	446	498	
	0.2%	10.2%	89.6%	100.0%	
	1.6%	25.9%	98.9%	69.9%	
TOTAL	64	197	451	712	
	9.0%	27.7%	63.3%	100.0%	
	100.0%	100.0%	100.0%	100.0%	

EXPERIENCE by NUMBER OF PROFESSIONAL SUBORDINATES
FULL-TIME EMPLOYED RESPONDENTS
XTAB.017

	PROF EXPERIENCE											
PROF SUBS	0-1	2-4	5-7	8-12	13-17	18-22	23-27	28-32	33-37	38-42	> 42	No Response	TOTAL
0	5 1.5% 71.4%	43 12.5% 68.3%	48 14.0% 55.2%	88 25.7% 53.3%	45 13.1% 39.5%	35 10.2% 39.3%	15 4.4% 29.4%	21 6.1% 42.9%	7 2.0% 41.2%	4 1.2% 50.0%	30 8.7% 50.8%	2 0.6% 66.7%	343 -Count 100.0% -% of Row 48.2% -% of Col
1-2	1 0.7% 14.3%	13 8.8% 20.6%	20 13.5% 23.0%	28 18.9% 17.0%	28 18.9% 24.6%	17 11.5% 19.1%	10 6.8% 19.6%	15 10.1% 30.6%	4 2.7% 23.5%	2 1.4% 25.0%	10 6.8% 16.9%	0 0.0% 0.0%	148 100.0% 20.8%
3-7	0 0.0% 0.0%	4 2.9% 6.3%	14 10.0% 16.1%	34 24.3% 20.6%	29 20.7% 25.4%	19 13.6% 21.3%	19 13.6% 37.3%	9 6.4% 18.4%	3 2.1% 17.6%	0 0.0% 0.0%	8 5.7% 13.6%	1 0.7% 33.3%	140 100.0% 19.7%
8-12	1 1.8% 14.3%	3 5.4% 4.8%	4 7.1% 4.6%	9 16.1% 5.5%	7 12.5% 6.1%	15 26.8% 16.9%	4 7.1% 7.8%	2 3.6% 4.1%	3 5.4% 17.6%	1 1.8% 12.5%	7 12.5% 11.9%	0 0.0% 0.0%	56 100.0% 7.9%
13-17	0 0.0% 0.0%	0 0.0% 0.0%	0 0.0% 0.0%	1 25.0% 0.6%	2 50.0% 1.8%	1 25.0% 1.1%	0 0.0% 0.0%	0 0.0% 0.0%	0 0.0% 0.0%	0 0.0% 0.0%	0 0.0% 0.0%	0 0.0% 0.0%	4 100.0% 0.6%
18-22	0 0.0% 0.0%	0 0.0% 0.0%	0 0.0% 0.0%	1 16.7% 0.6%	2 33.3% 1.8%	0 0.0% 0.0%	1 16.7% 2.0%	1 16.7% 2.0%	0 0.0% 0.0%	1 16.7% 12.5%	0 0.0% 0.0%	0 0.0% 0.0%	6 100.0% 0.8%
23-32	0 0.0% 0.0%	0 0.0% 0.0%	1 11.1% 1.1%	2 22.2% 1.2%	1 11.1% 0.9%	0 0.0% 0.0%	2 22.2% 3.9%	1 11.1% 2.0%	0 0.0% 0.0%	0 0.0% 0.0%	2 22.2% 3.4%	0 0.0% 0.0%	9 100.0% 1.3%
33-47	0 0.0% 0.0%	0 0.0% 0.0%	0 0.0% 0.0%	1 33.3% 0.6%	0 0.0% 0.0%	2 66.7% 2.2%	0 0.0% 0.0%	0 0.0% 0.0%	0 0.0% 0.0%	0 0.0% 0.0%	0 0.0% 0.0%	0 0.0% 0.0%	3 100.0% 0.4%
48-67	0 0.0% 0.0%	0 0.0% 0.0%	0 0.0% 0.0%	1 50.0% 0.6%	0 0.0% 0.0%	0 0.0% 0.0%	0 0.0% 0.0%	0 0.0% 0.0%	0 0.0% 0.0%	0 0.0% 0.0%	1 50.0% 1.7%	0 0.0% 0.0%	2 100.0% 0.3%
68-99	0 0.0% 0.0%	0 0.0% 0.0%	0 0.0% 0.0%	0 0.0% 0.0%	0 0.0% 0.0%	0 0.0% 0.0%	0 0.0% 0.0%	0 0.0% 0.0%	0 0.0% 0.0%	0 0.0% 0.0%	1 100.0% 1.7%	0 0.0% 0.0%	1 100.0% 0.1%
>=100	0 ***.*% 0.0%	0 ***.*% 0.0%	0 ***.*% 0.0%	0 ***.*% 0.0%	0 ***.*% 0.0%	0 ***.*% 0.0%	0 ***.*% 0.0%	0 ***.*% 0.0%	0 ***.*% 0.0%	0 ***.*% 0.0%	0 ***.*% 0.0%	0 ***.*% 0.0%	0 ***.*% 0.0%
TOTAL	7 1.0% 100.0%	63 8.8% 100.0%	87 12.2% 100.0%	165 23.2% 100.0%	114 16.0% 100.0%	89 12.5% 100.0%	51 7.2% 100.0%	49 6.9% 100.0%	17 2.4% 100.0%	8 1.1% 100.0%	59 8.3% 100.0%	3 0.4% 100.0%	712 100.0% 100.0%

EXPERIENCE by NUMBER OF PROFESSIONAL AND TECHNICAL SUBORDINATES
FULL-TIME EMPLOYED RESPONDENTS
XTAB.018

	PROF EXPERIENCE												
PROF+TECH SUBS	0-1	2-4	5-7	8-12	13-17	18-22	23-27	28-32	33-37	38-42	> 42	No Response	TOTAL
0	1 0.6% 14.3%	20 12.5% 31.7%	24 15.0% 27.6%	42 26.3% 25.5%	17 10.6% 14.9%	20 12.5% 22.5%	8 5.0% 15.7%	10 6.3% 20.4%	4 2.5% 23.5%	2 1.3% 25.0%	12 7.5% 20.3%	0 0.0% 0.0%	160 -Count 100.0% -% of Row 22.5% -% of Col
1-2	1 0.5% 14.3%	27 12.2% 42.9%	27 12.2% 31.0%	48 21.7% 29.1%	40 18.1% 35.1%	23 10.4% 25.8%	10 4.5% 19.6%	16 7.2% 32.7%	4 1.8% 23.5%	4 1.8% 50.0%	19 8.6% 32.2%	2 0.9% 66.7%	221 100.0% 31.0%
3-7	4 2.0% 57.1%	12 5.9% 19.0%	23 11.2% 26.4%	46 22.4% 27.9%	39 19.0% 34.2%	27 13.2% 30.3%	19 9.3% 37.3%	14 6.8% 28.6%	5 2.4% 29.4%	0 0.0% 0.0%	15 7.3% 25.4%	1 0.5% 33.3%	205 100.0% 28.8%
8-12	1 1.2% 14.3%	3 3.7% 4.8%	10 12.3% 11.5%	20 24.7% 12.1%	12 14.8% 10.5%	9 11.1% 10.1%	12 14.8% 23.5%	4 4.9% 8.2%	1 1.2% 5.9%	1 1.2% 12.5%	8 9.9% 13.6%	0 0.0% 0.0%	81 100.0% 11.4%
13-17	0 0.0% 0.0%	1 6.3% 1.6%	1 6.3% 1.1%	3 18.8% 1.8%	1 6.3% 0.9%	4 25.0% 4.5%	0 0.0% 0.0%	1 6.3% 2.0%	2 12.5% 11.8%	0 0.0% 0.0%	3 18.8% 5.1%	0 0.0% 0.0%	16 100.0% 2.2%
18-22	0 0.0% 0.0%	0 0.0% 0.0%	0 0.0% 0.0%	1 16.7% 0.6%	2 33.3% 1.8%	0 0.0% 0.0%	0 0.0% 0.0%	2 33.3% 4.1%	1 16.7% 5.9%	0 0.0% 0.0%	0 0.0% 0.0%	0 0.0% 0.0%	6 100.0% 0.8%
23-32	0 0.0% 0.0%	0 0.0% 0.0%	1 11.1% 1.1%	1 11.1% 0.6%	1 11.1% 0.9%	3 33.3% 3.4%	1 11.1% 2.0%	1 11.1% 2.0%	0 0.0% 0.0%	0 0.0% 0.0%	1 11.1% 1.7%	0 0.0% 0.0%	9 100.0% 1.3%
33-47	0 0.0% 0.0%	0 0.0% 0.0%	1 9.1% 1.1%	3 27.3% 1.8%	2 18.2% 1.8%	2 18.2% 2.2%	1 9.1% 2.0%	1 9.1% 2.0%	0 0.0% 0.0%	0 0.0% 0.0%	1 9.1% 1.7%	0 0.0% 0.0%	11 100.0% 1.5%
48-67	0 0.0% 0.0%	0 0.0% 0.0%	0 0.0% 0.0%	0 0.0% 0.0%	0 0.0% 0.0%	1 100.0% 1.1%	0 0.0% 0.0%	0 0.0% 0.0%	0 0.0% 0.0%	0 0.0% 0.0%	0 0.0% 0.0%	0 0.0% 0.0%	1 100.0% 0.1%
68-99	0 0.0% 0.0%	0 0.0% 0.0%	0 0.0% 0.0%	1 50.0% 0.6%	0 0.0% 0.0%	0 0.0% 0.0%	0 0.0% 0.0%	0 0.0% 0.0%	0 0.0% 0.0%	1 50.0% 12.5%	0 0.0% 0.0%	0 0.0% 0.0%	2 100.0% 0.3%
>=100	0 ***.*% 0.0%	0 ***.*% 0.0%	0 ***.*% 0.0%	0 ***.*% 0.0%	0 ***.*% 0.0%	0 ***.*% 0.0%	0 ***.*% 0.0%	0 ***.*% 0.0%	0 ***.*% 0.0%	0 ***.*% 0.0%	0 ***.*% 0.0%	0 ***.*% 0.0%	0 ***.*% 0.0%
TOTAL	7 1.0% 100.0%	63 8.8% 100.0%	87 12.2% 100.0%	165 23.2% 100.0%	114 16.0% 100.0%	89 12.5% 100.0%	51 7.2% 100.0%	49 6.9% 100.0%	17 2.4% 100.0%	8 1.1% 100.0%	59 8.3% 100.0%	3 0.4% 100.0%	712 100.0% 100.0%

EXPERIENCE by TOTAL NUMBER OF SUBORDINATES
FULL-TIME EMPLOYED RESPONDENTS
XTAB.019

TOTAL SUBORDINATES	PROF EXPERIENCE 0-1	2-4	5-7	8-12	13-17	18-22	23-27	28-32	33-37	38-42	> 42	No Resp	TOTAL
0	1	16	22	39	14	16	7	8	3	2	9	0	137 -Count
	0.7%	11.7%	16.1%	28.5%	10.2%	11.7%	5.1%	5.8%	2.2%	1.5%	6.6%	0.0%	100.0% -% of Row
	14.3%	25.4%	25.3%	23.6%	12.3%	18.0%	13.7%	16.3%	17.6%	25.0%	15.3%	0.0%	19.2% -% of Col
1-2	1	26	20	43	35	24	11	16	5	4	19	2	206
	0.5%	12.6%	9.7%	20.9%	17.0%	11.7%	5.3%	7.8%	2.4%	1.9%	9.2%	1.0%	100.0%
	14.3%	41.3%	23.0%	26.1%	30.7%	27.0%	21.6%	32.7%	29.4%	50.0%	32.2%	66.7%	28.9%
3-7	3	15	28	50	40	23	13	15	4	0	15	1	207
	1.4%	7.2%	13.5%	24.2%	19.3%	11.1%	6.3%	7.2%	1.9%	0.0%	7.2%	0.5%	100.0%
	42.9%	23.8%	32.2%	30.3%	35.1%	25.8%	25.5%	30.6%	23.5%	0.0%	25.4%	33.3%	29.1%
8-12	2	5	13	25	17	14	17	4	3	0	10	0	110
	1.8%	4.5%	11.8%	22.7%	15.5%	12.7%	15.5%	3.6%	2.7%	0.0%	9.1%	0.0%	100.0%
	28.6%	7.9%	14.9%	15.2%	14.9%	15.7%	33.3%	8.2%	17.6%	0.0%	16.9%	0.0%	15.4%
13-17	0	0	2	2	3	7	1	2	2	1	2	0	22
	0.0%	0.0%	9.1%	9.1%	13.6%	31.8%	4.5%	9.1%	9.1%	4.5%	9.1%	0.0%	100.0%
	0.0%	0.0%	2.3%	1.2%	2.6%	7.9%	2.0%	4.1%	11.8%	12.5%	3.4%	0.0%	3.1%
18-22	0	1	0	2	2	0	0	2	0	0	0	0	7
	0.0%	14.3%	0.0%	28.6%	28.6%	0.0%	0.0%	28.6%	0.0%	0.0%	0.0%	0.0%	100.0%
	0.0%	1.6%	0.0%	1.2%	1.8%	0.0%	0.0%	4.1%	0.0%	0.0%	0.0%	0.0%	1.0%
23-32	0	0	1	1	1	1	0	1	0	0	2	0	7
	0.0%	0.0%	14.3%	14.3%	14.3%	14.3%	0.0%	14.3%	0.0%	0.0%	28.6%	0.0%	100.0%
	0.0%	0.0%	1.1%	0.6%	0.9%	1.1%	0.0%	2.0%	0.0%	0.0%	3.4%	0.0%	1.0%
33-47	0	0	0	2	1	2	2	1	0	0	2	0	10
	0.0%	0.0%	0.0%	20.0%	10.0%	20.0%	20.0%	10.0%	0.0%	0.0%	20.0%	0.0%	100.0%
	0.0%	0.0%	0.0%	1.2%	0.9%	2.2%	3.9%	2.0%	0.0%	0.0%	3.4%	0.0%	1.4%
48-67	0	0	1	0	1	2	0	0	0	0	0	0	4
	0.0%	0.0%	25.0%	0.0%	25.0%	50.0%	0.0%	0.0%	0.0%	0.0%	0.0%	0.0%	100.0%
	0.0%	0.0%	1.1%	0.0%	0.9%	2.2%	0.0%	0.0%	0.0%	0.0%	0.0%	0.0%	0.6%
68-99	0	0	0	1	0	0	0	0	0	1	0	0	2
	0.0%	0.0%	0.0%	50.0%	0.0%	0.0%	0.0%	0.0%	0.0%	50.0%	0.0%	0.0%	100.0%
	0.0%	0.0%	0.0%	0.6%	0.0%	0.0%	0.0%	0.0%	0.0%	12.5%	0.0%	0.0%	0.3%
>=100	0	0	0	0	0	0	0	0	0	0	0	0	0
	***.*%	***.*%	***.*%	***.*%	***.*%	***.*%	***.*%	***.*%	***.*%	***.*%	***.*%	***.*%	***.*%
	0.0%	0.0%	0.0%	0.0%	0.0%	0.0%	0.0%	0.0%	0.0%	0.0%	0.0%	0.0%	0.0%
TOTAL	7	63	87	165	114	89	51	49	17	8	59	3	712
	1.0%	8.8%	12.2%	23.2%	16.0%	12.5%	7.2%	6.9%	2.4%	1.1%	8.3%	0.4%	100.0%
	100.0%	100.0%	100.0%	100.0%	100.0%	100.0%	100.0%	100.0%	100.0%	100.0%	100.0%	100.0%	100.0%

EMPLOYER by PROFESSION
FULL-TIME EMPLOYED RESPONDENTS
XTAB.020

PROFESSION	EMPLOYER								
	Mfg-Ind	Non-Mfg Ind	Coll/Uni	Govt-Fed	Govt-St Local	Self-Emp	Other Emp	No Response	TOTAL
Chem-Agr/Food	4	0	4	2	0	0	0	0	10 -Count
	40.0%	0.0%	40.0%	20.0%	0.0%	0.0%	0.0%	0.0%	100.0% -% of Row
	1.8%	0.0%	1.9%	1.5%	0.0%	0.0%	0.0%	0.0%	1.4% -% of Col
Chem-Analy	154	53	78	72	7	1	26	1	392
	39.3%	13.5%	19.9%	18.4%	1.8%	0.3%	6.6%	0.3%	100.0%
	71.0%	60.2%	36.8%	54.1%	46.7%	33.3%	65.0%	25.0%	55.1%
Chem-Inorg	2	1	3	2	0	0	0	0	8
	25.0%	12.5%	37.5%	25.0%	0.0%	0.0%	0.0%	0.0%	100.0%
	0.9%	1.1%	1.4%	1.5%	0.0%	0.0%	0.0%	0.0%	1.1%
Chem-Org	11	7	23	12	0	1	2	0	56
	19.6%	12.5%	41.1%	21.4%	0.0%	1.8%	3.6%	0.0%	100.0%
	5.1%	8.0%	10.8%	9.0%	0.0%	33.3%	5.0%	0.0%	7.9%
Chem-Phys	11	8	45	20	0	0	5	1	90
	12.2%	8.9%	50.0%	22.2%	0.0%	0.0%	5.6%	1.1%	100.0%
	5.1%	9.1%	21.2%	15.0%	0.0%	0.0%	12.5%	25.0%	12.6%
Chem-Poly	0	0	2	0	0	0	0	0	2
	0.0%	0.0%	100.0%	0.0%	0.0%	0.0%	0.0%	0.0%	100.0%
	0.0%	0.0%	0.9%	0.0%	0.0%	0.0%	0.0%	0.0%	0.3%
Chem-Pharmaceutical Medicinal Clinical	12	2	23	4	3	0	2	1	47
	25.5%	4.3%	48.9%	8.5%	6.4%	0.0%	4.3%	2.1%	100.0%
	5.5%	2.3%	10.8%	3.0%	20.0%	0.0%	5.0%	25.0%	6.6%
Biologist	0	0	6	1	0	0	0	0	7
	0.0%	0.0%	85.7%	14.3%	0.0%	0.0%	0.0%	0.0%	100.0%
	0.0%	0.0%	2.8%	0.8%	0.0%	0.0%	0.0%	0.0%	1.0%
Engineer	11	1	8	1	1	0	1	0	23
	47.8%	4.3%	34.8%	4.3%	4.3%	0.0%	4.3%	0.0%	100.0%
	5.1%	1.1%	3.8%	0.8%	6.7%	0.0%	2.5%	0.0%	3.2%
Physician	0	0	1	0	1	0	0	0	2
	0.0%	0.0%	50.0%	0.0%	50.0%	0.0%	0.0%	0.0%	100.0%
	0.0%	0.0%	0.5%	0.0%	6.7%	0.0%	0.0%	0.0%	0.3%
Physicist	6	12	7	11	0	1	3	1	41
	14.6%	29.3%	17.1%	26.8%	0.0%	2.4%	7.3%	2.4%	100.0%
	2.8%	13.6%	3.3%	8.3%	0.0%	33.3%	7.5%	25.0%	5.8%
Other	4	3	11	6	3	0	1	0	28
	14.3%	10.7%	39.3%	21.4%	10.7%	0.0%	3.6%	0.0%	100.0%
	1.8%	3.4%	5.2%	4.5%	20.0%	0.0%	2.5%	0.0%	3.9%
No Response	2	1	1	2	0	0	0	0	6
	33.3%	16.7%	16.7%	33.3%	0.0%	0.0%	0.0%	0.0%	100.0%
	0.9%	1.1%	0.5%	1.5%	0.0%	0.0%	0.0%	0.0%	0.8%
TOTAL	217	88	212	133	15	3	40	4	712
	30.5%	12.4%	29.8%	18.7%	2.1%	0.4%	5.6%	0.6%	100.0%
	100.0%	100.0%	100.0%	100.0%	100.0%	100.0%	100.0%	100.0%	100.0%

WORK FUNCTION by PROFESSION
FULL-TIME EMPLOYED RESPONDENTS
XTAB.021

PROFESSION	Tch/Res	R&D Mgt	Bas Res	Appl R&D	Gen Mgt	Writing Editing	Mkt/Sale	Prod/QC	Forens Analysis	Data Pro	Consult-ing	Other	No Response	TOTAL
Chem-Ag Food	3	0	3	2	0	0	1	1	0	0	0	0	0	10 -Coun
	30.0%	0.0%	30.0%	20.0%	0.0%	0.0%	10.0%	10.0%	0.0%	0.0%	0.0%	0.0%	0.0%	100.0% -% of
	2.3%	0.0%	1.9%	0.8%	0.0%	0.0%	4.8%	4.0%	0.0%	0.0%	0.0%	0.0%	0.0%	1.4% -% of
Chem-Analy	46	39	59	164	19	1	13	19	4	2	7	14	5	392
	11.7%	9.9%	15.1%	41.8%	4.8%	0.3%	3.3%	4.8%	1.0%	0.5%	1.8%	3.6%	1.3%	100.0%
	35.4%	67.2%	38.3%	67.8%	61.3%	100.0%	61.9%	76.0%	40.0%	50.0%	70.0%	73.7%	71.4%	55.1%
Chem-Inorg	3	0	1	1	1	0	0	2	0	0	0	0	0	8
	37.5%	0.0%	12.5%	12.5%	12.5%	0.0%	0.0%	25.0%	0.0%	0.0%	0.0%	0.0%	0.0%	100.0%
	2.3%	0.0%	0.6%	0.4%	3.2%	0.0%	0.0%	8.0%	0.0%	0.0%	0.0%	0.0%	0.0%	1.1%
Chem-Org	17	4	12	15	1	0	3	0	0	0	2	2	0	56
	30.4%	7.1%	21.4%	26.8%	1.8%	0.0%	5.4%	0.0%	0.0%	0.0%	3.6%	3.6%	0.0%	100.0%
	13.1%	6.9%	7.8%	6.2%	3.2%	0.0%	14.3%	0.0%	0.0%	0.0%	20.0%	10.5%	0.0%	7.9%
Chem-Phys	32	7	31	16	2	0	1	0	0	0	0	0	1	90
	35.6%	7.8%	34.4%	17.8%	2.2%	0.0%	1.1%	0.0%	0.0%	0.0%	0.0%	0.0%	1.1%	100.0%
	24.6%	12.1%	20.1%	6.6%	6.5%	0.0%	4.8%	0.0%	0.0%	0.0%	0.0%	0.0%	14.3%	12.6%
Chem-Poly	2	0	0	0	0	0	0	0	0	0	0	0	0	2
	100.0%	0.0%	0.0%	0.0%	0.0%	0.0%	0.0%	0.0%	0.0%	0.0%	0.0%	0.0%	0.0%	100.0%
	1.5%	0.0%	0.0%	0.0%	0.0%	0.0%	0.0%	0.0%	0.0%	0.0%	0.0%	0.0%	0.0%	0.3%
Chem-Pharmaceutical	12	0	22	10	0	0	0	0	3	0	0	0	0	47
Medicinal	25.5%	0.0%	46.8%	21.3%	0.0%	0.0%	0.0%	0.0%	6.4%	0.0%	0.0%	0.0%	0.0%	100.0%
Clinical	9.2%	0.0%	14.3%	4.1%	0.0%	0.0%	0.0%	0.0%	30.0%	0.0%	0.0%	0.0%	0.0%	6.6%
Biologist	2	0	4	1	0	0	0	0	0	0	0	0	0	7
	28.6%	0.0%	57.1%	14.3%	0.0%	0.0%	0.0%	0.0%	0.0%	0.0%	0.0%	0.0%	0.0%	100.0%
	1.5%	0.0%	2.6%	0.4%	0.0%	0.0%	0.0%	0.0%	0.0%	0.0%	0.0%	0.0%	0.0%	1.0%
Engineer	2	3	2	11	2	0	0	1	0	1	0	1	0	23
	8.7%	13.0%	8.7%	47.8%	8.7%	0.0%	0.0%	4.3%	0.0%	4.3%	0.0%	4.3%	0.0%	100.0%
	1.5%	5.2%	1.3%	4.5%	6.5%	0.0%	0.0%	4.0%	0.0%	25.0%	0.0%	5.3%	0.0%	3.2%
Physician	1	0	1	0	0	0	0	0	0	0	0	0	0	2
	50.0%	0.0%	50.0%	0.0%	0.0%	0.0%	0.0%	0.0%	0.0%	0.0%	0.0%	0.0%	0.0%	100.0%
	0.8%	0.0%	0.6%	0.0%	0.0%	0.0%	0.0%	0.0%	0.0%	0.0%	0.0%	0.0%	0.0%	0.3%
Physicist	4	4	12	13	5	0	1	1	0	0	1	0	0	41
	9.8%	9.8%	29.3%	31.7%	12.2%	0.0%	2.4%	2.4%	0.0%	0.0%	2.4%	0.0%	0.0%	100.0%
	3.1%	6.9%	7.8%	5.4%	16.1%	0.0%	4.8%	4.0%	0.0%	0.0%	10.0%	0.0%	0.0%	5.8%
Other	5	0	6	8	1	0	2	0	3	1	0	1	1	28
	17.9%	0.0%	21.4%	28.6%	3.6%	0.0%	7.1%	0.0%	10.7%	3.6%	0.0%	3.6%	3.6%	100.0%
	3.8%	0.0%	3.9%	3.3%	3.2%	0.0%	9.5%	0.0%	30.0%	25.0%	0.0%	5.3%	14.3%	3.9%
No Response	1	1	1	1	0	0	0	1	0	0	0	1	0	6
	16.7%	16.7%	16.7%	16.7%	0.0%	0.0%	0.0%	16.7%	0.0%	0.0%	0.0%	16.7%	0.0%	100.0%
	0.8%	1.7%	0.6%	0.4%	0.0%	0.0%	0.0%	4.0%	0.0%	0.0%	0.0%	5.3%	0.0%	0.8%
TOTAL	130	58	154	242	31	1	21	25	10	4	10	19	7	712
	18.3%	8.1%	21.6%	34.0%	4.4%	0.1%	2.9%	3.5%	1.4%	0.6%	1.4%	2.7%	1.0%	100.0%
	100.0%	100.0%	100.0%	100.0%	100.0%	100.0%	100.0%	100.0%	100.0%	100.0%	100.0%	100.0%	100.0%	100.0%

YEARS WITH CURRENT EMPLOYER by YEAR OF DEGREE
FULL-TIME EMPLOYED RESPONDENTS
XTAB.022

YEAR OF DEGREE	YRS WITH EMPLOYER 0-1	2-4	5-7	8-12	13-17	18-22	23-27	28-32	33-37	38-42	> 42	No Response	TOTAL
'79-'80	11	9	1	2	0	0	0	0	0	0	0	3	26 -Count
	42.3%	34.6%	3.8%	7.7%	0.0%	0.0%	0.0%	0.0%	0.0%	0.0%	0.0%	11.5%	100.0% -% of Row
	22.4%	4.7%	1.1%	1.4%	0.0%	0.0%	0.0%	0.0%	0.0%	***.*%	0.0%	15.8%	3.7% -% of Col
'76-'78	12	53	7	4	2	1	0	0	0	0	1	5	85
	14.1%	62.4%	8.2%	4.7%	2.4%	1.2%	0.0%	0.0%	0.0%	0.0%	1.2%	5.9%	100.0%
	24.5%	27.7%	7.4%	2.7%	2.2%	2.1%	0.0%	0.0%	0.0%	***.*%	20.0%	26.3%	11.9%
'73-'75	6	44	28	9	0	2	0	0	0	0	0	5	94
	6.4%	46.8%	29.8%	9.6%	0.0%	2.1%	0.0%	0.0%	0.0%	0.0%	0.0%	5.3%	100.0%
	12.2%	23.0%	29.5%	6.1%	0.0%	4.3%	0.0%	0.0%	0.0%	***.*%	0.0%	26.3%	13.2%
'68-'72	10	40	36	71	9	4	3	0	0	0	1	3	177
	5.6%	22.6%	20.3%	40.1%	5.1%	2.3%	1.7%	0.0%	0.0%	0.0%	0.6%	1.7%	100.0%
	20.4%	20.9%	37.9%	48.3%	10.1%	8.5%	10.0%	0.0%	0.0%	***.*%	20.0%	15.8%	24.9%
'63-'67	1	20	10	30	39	2	1	1	0	0	0	2	106
	0.9%	18.9%	9.4%	28.3%	36.8%	1.9%	0.9%	0.9%	0.0%	0.0%	0.0%	1.9%	100.0%
	2.0%	10.5%	10.5%	20.4%	43.8%	4.3%	3.3%	3.7%	0.0%	***.*%	0.0%	10.5%	14.9%
'58-'62	2	3	2	10	23	20	7	1	0	0	2	0	70
	2.9%	4.3%	2.9%	14.3%	32.9%	28.6%	10.0%	1.4%	0.0%	0.0%	2.9%	0.0%	100.0%
	4.1%	1.6%	2.1%	6.8%	25.8%	42.6%	23.3%	3.7%	0.0%	***.*%	40.0%	0.0%	9.8%
'53-'57	0	4	5	7	7	8	10	2	0	0	0	0	43
	0.0%	9.3%	11.6%	16.3%	16.3%	18.6%	23.3%	4.7%	0.0%	0.0%	0.0%	0.0%	100.0%
	0.0%	2.1%	5.3%	4.8%	7.9%	17.0%	33.3%	7.4%	0.0%	***.*%	0.0%	0.0%	6.0%
'48-'52	1	1	2	5	2	5	3	17	1	0	1	1	39
	2.6%	2.6%	5.1%	12.8%	5.1%	12.8%	7.7%	43.6%	2.6%	0.0%	2.6%	2.6%	100.0%
	2.0%	0.5%	2.1%	3.4%	2.2%	10.6%	10.0%	63.0%	7.7%	***.*%	20.0%	5.3%	5.5%
'43-'47	0	2	0	1	1	1	1	2	5	0	0	0	13
	0.0%	15.4%	0.0%	7.7%	7.7%	7.7%	7.7%	15.4%	38.5%	0.0%	0.0%	0.0%	100.0%
	0.0%	1.0%	0.0%	0.7%	1.1%	2.1%	3.3%	7.4%	38.5%	***.*%	0.0%	0.0%	1.8%
'38-'42	0	0	0	0	0	1	0	1	5	0	0	0	7
	0.0%	0.0%	0.0%	0.0%	0.0%	14.3%	0.0%	14.3%	71.4%	0.0%	0.0%	0.0%	100.0%
	0.0%	0.0%	0.0%	0.0%	0.0%	2.1%	0.0%	3.7%	38.5%	***.*%	0.0%	0.0%	1.0%
'30-'37	0	1	0	0	0	0	0	0	0	0	0	0	1
	0.0%	100.0%	0.0%	0.0%	0.0%	0.0%	0.0%	0.0%	0.0%	0.0%	0.0%	0.0%	100.0%
	0.0%	0.5%	0.0%	0.0%	0.0%	0.0%	0.0%	0.0%	0.0%	***.*%	0.0%	0.0%	0.1%
No Response	6	14	4	8	6	3	5	3	2	0	0	0	51
	11.8%	27.5%	7.8%	15.7%	11.8%	5.9%	9.8%	5.9%	3.9%	0.0%	0.0%	0.0%	100.0%
	12.2%	7.3%	4.2%	5.4%	6.7%	6.4%	16.7%	11.1%	15.4%	***.*%	0.0%	0.0%	7.2%
TOTAL	49	191	95	147	89	47	30	27	13	0	5	19	712
	6.9%	26.8%	13.3%	20.6%	12.5%	6.6%	4.2%	3.8%	1.8%	0.0%	0.7%	2.7%	100.0%
	100.0%	100.0%	100.0%	100.0%	100.0%	100.0%	100.0%	100.0%	100.0%	***.*%	100.0%	100.0%	100.0%

NUMBER OF EMPLOYERS by YEAR OF DEGREE
FULL-TIME EMPLOYED RESPONDENTS
XTAB.023

YEAR OF DEGREE	NUM OF EMPLOYERS 1	2	3	4-6	7-10	>10	No Response	TOTAL
'79-'80	23	3	0	0	0	0	0	26 -Count
	88.5%	11.5%	0.0%	0.0%	0.0%	0.0%	0.0%	100.0% -% of Row
	8.9%	1.3%	0.0%	0.0%	0.0%	0.0%	0.0%	3.7% -% of Col
'76-'78	43	30	9	1	0	0	0	83
	51.8%	36.1%	10.8%	1.2%	0.0%	0.0%	0.0%	100.0%
	16.7%	13.0%	6.9%	1.7%	0.0%	0.0%	0.0%	11.9%
'73-'75	40	35	12	7	0	0	0	94
	42.6%	37.2%	12.8%	7.4%	0.0%	0.0%	0.0%	100.0%
	15.6%	15.2%	9.2%	12.1%	0.0%	0.0%	0.0%	13.5%
'68-'72	54	61	40	16	4	0	0	175
	30.9%	34.9%	22.9%	9.1%	2.3%	0.0%	0.0%	100.0%
	21.0%	26.4%	30.5%	27.6%	30.8%	0.0%	0.0%	25.1%
'63-'67	30	35	25	10	3	2	0	105
	28.6%	33.3%	23.8%	9.5%	2.9%	1.9%	0.0%	100.0%
	11.7%	15.2%	19.1%	17.2%	23.1%	40.0%	0.0%	15.1%
'58-'62	20	26	17	3	1	0	0	67
	29.9%	38.8%	25.4%	4.5%	1.5%	0.0%	0.0%	100.0%
	7.8%	11.3%	13.0%	5.2%	7.7%	0.0%	0.0%	9.6%
'53-'57	10	15	10	5	2	1	0	43
	23.3%	34.9%	23.3%	11.6%	4.7%	2.3%	0.0%	100.0%
	3.9%	6.5%	7.6%	8.6%	15.4%	20.0%	0.0%	6.2%
'48-'52	15	7	6	5	1	1	1	36
	41.7%	19.4%	16.7%	13.9%	2.8%	2.8%	2.8%	100.0%
	5.8%	3.0%	4.6%	8.6%	7.7%	20.0%	50.0%	5.2%
'43-'47	3	4	4	1	0	0	0	12
	25.0%	33.3%	33.3%	8.3%	0.0%	0.0%	0.0%	100.0%
	1.2%	1.7%	3.1%	1.7%	0.0%	0.0%	0.0%	1.7%
'38-'42	1	1	1	4	0	0	0	7
	14.3%	14.3%	14.3%	57.1%	0.0%	0.0%	0.0%	100.0%
	0.4%	0.4%	0.8%	6.9%	0.0%	0.0%	0.0%	1.0%
'30-'37	0	0	0	0	0	1	0	1
	0.0%	0.0%	0.0%	0.0%	0.0%	100.0%	0.0%	100.0%
	0.0%	0.0%	0.0%	0.0%	0.0%	20.0%	0.0%	0.1%
No Response	18	14	7	6	2	0	1	48
	37.5%	29.2%	14.6%	12.5%	4.2%	0.0%	2.1%	100.0%
	7.0%	6.1%	5.3%	10.3%	15.4%	0.0%	50.0%	6.9%
TOTAL	257	231	131	58	13	5	2	697
	36.9%	33.1%	18.8%	8.3%	1.9%	0.7%	0.3%	100.0%
	100.0%	100.0%	100.0%	100.0%	100.0%	100.0%	100.0%	100.0%

TENURE by YEAR OF DEGREE
FULL-TIME EMPLOYED ACADEMIC PHD RESPONDENTS
XTAB.024

YEAR OF DEGREE	GRANTED TENURE ? Yes	No	No Response	TOTAL	
'79-'80	0	4	1	5	-Count
	0.0%	80.0%	20.0%	100.0%	-% of Row
	0.0%	4.9%	14.3%	2.9%	-% of Col
'76-'78	0	14	0	14	
	0.0%	100.0%	0.0%	100.0%	
	0.0%	17.3%	0.0%	8.0%	
'73-'75	3	23	0	26	
	11.5%	88.5%	0.0%	100.0%	
	3.5%	28.4%	0.0%	14.9%	
'68-'72	22	26	3	51	
	43.1%	51.0%	5.9%	100.0%	
	25.6%	32.1%	42.9%	29.3%	
'63-'67	27	9	1	37	
	73.0%	24.3%	2.7%	100.0%	
	31.4%	11.1%	14.3%	21.3%	
'58-'62	11	2	0	13	
	84.6%	15.4%	0.0%	100.0%	
	12.8%	2.5%	0.0%	7.5%	
'53-'57	8	0	1	9	
	88.9%	0.0%	11.1%	100.0%	
	9.3%	0.0%	14.3%	5.2%	
'48-'52	8	1	0	9	
	88.9%	11.1%	0.0%	100.0%	
	9.3%	1.2%	0.0%	5.2%	
'43-'47	2	0	0	2	
	100.0%	0.0%	0.0%	100.0%	
	2.3%	0.0%	0.0%	1.1%	
'38-'42	2	0	0	2	
	100.0%	0.0%	0.0%	100.0%	
	2.3%	0.0%	0.0%	1.1%	
'30-'37	0	0	0	0	
	***.*%	***.*%	***.*%	***.*%	
	0.0%	0.0%	0.0%	0.0%	
No Response	3	2	1	6	
	50.0%	33.3%	16.7%	100.0%	
	3.5%	2.5%	14.3%	3.4%	
TOTAL	86	81	7	174	
	49.4%	46.6%	4.0%	100.0%	
	100.0%	100.0%	100.0%	100.0%	

SALARIES of FULL-TIME EMPLOYED RESPONDENTS
by YEARS OF PROFESSIONAL EXPERIENCE and HIGHEST DEGREE
SAL.001

HIGHEST DEGREE	PROF EXPERIENCE 0-1	2-4	5-7	8-12	13-17	18-22	23-27	28-32	33-37	38-42	> 42	No Response	TOTAL	
Ph.D.	---	27,700	29,000	32,500	36,000	42,850	41,250	---	---	---	32,000	---	33,100	-Median
	26,600	27,447	29,683	32,450	36,569	40,665	41,518	43,729	46,050	43,900	33,663	36,400	34,564	-Mean
	6,580	4,084	5,888	7,090	7,430	8,643	12,641	9,063	9,390	8,890	8,180	4,808	9,017	-Std Dev
	5	43	59	114	71	52	28	14	8	3	35	2	434	-Count
M.D.	---	---	---	---	---	---	---	---	---	---	---	---	---	
	---	---	---	---	---	---	43,250	65,000	---	---	45,033	---	47,767	
	---	---	---	---	---	---	1,061	---	---	---	10,464	---	10,773	
	0	0	0	0	0	0	2	1	0	0	3	0	6	
Masters	---	---	---	27,000	31,000	---	---	35,400	---	---	---	---	29,700	
	25,900	19,590	28,418	27,696	31,647	34,657	32,750	35,220	31,833	---	24,733	---	29,858	
	---	3,245	6,223	6,162	7,086	6,045	4,272	6,928	7,147	---	6,408	---	7,495	
	1	10	11	25	15	14	4	15	3	0	3	0	101	
Bachelors	---	---	24,000	25,000	30,000	32,750	31,000	33,000	---	---	---	---	30,000	
	17,000	21,640	23,129	25,596	29,629	34,283	35,940	34,300	36,960	48,000	30,808	21,000	30,105	
	---	7,747	4,130	4,660	7,130	7,360	13,188	4,583	6,950	15,210	9,484	---	9,454	
	1	10	17	23	24	18	15	15	5	4	13	1	146	
Other	---	---	---	---	---	---	---	---	---	---	---	---	25,300	
	---	---	---	19,200	24,375	29,533	22,000	30,100	30,000	39,000	27,000	---	26,369	
	---	---	---	5,583	1,797	4,843	---	7,212	---	---	---	---	6,278	
	0	0	0	3	4	3	1	2	1	1	1	0	16	
No Response	---	---	---	---	---	---	---	---	---	---	---	---	---	
	---	---	---	---	---	36,000	---	42,900	---	---	28,250	---	33,850	
	---	---	---	---	---	---	---	---	---	---	2,475	---	7,197	
	0	0	0	0	0	1	0	1	0	0	2	0	4	
TOTAL	---	26,400	28,000	30,000	33,600	36,000	37,150	36,500	41,000	---	31,000	---	31,700	
	25,129	25,278	28,243	30,533	34,032	37,972	38,822	37,981	39,924	45,338	32,833	31,267	32,893	
	6,464	5,670	6,136	7,283	7,942	8,473	12,456	8,926	9,848	11,506	8,923	9,519	9,249	
	7	63	87	165	114	88	50	48	17	8	57	3	707	

SALARIES of FULL-TIME EMPLOYED NON-ACADEMIC RESPONDENTS
by YEARS IN MASS SPECTROMETRY and HIGHEST DEGREE
SAL.002

HIGHEST DEGREE	YEARS IN MASS SPEC 0-1	2-4	5-7	8-12	13-17	18-22	23-27	28-32	33-37	38-42	> 42	No Respo	TOTAL	
Ph.D.	---	30,000	31,500	34,000	40,000	---	---	---	---	---	33,000	---	34,350	-Median
	31,467	31,958	32,048	34,705	39,904	40,079	46,418	---	45,650	---	35,804	36,000	35,740	-Mean
	5,163	6,072	5,515	6,535	8,177	7,165	4,529	---	11,809	---	8,807	---	7,754	-Std Dev
	3	33	48	78	47	14	11	0	2	0	25	1	262	-Count
M.D.	---	---	---	---	---	---	---	---	---	---	---	---	---	
	---	---	---	54,500	---	---	---	---	---	---	42,500	---	48,500	
	---	---	---	14,849	---	---	---	---	---	---	13,435	---	13,478	
	0	0	0	2	0	0	0	0	0	0	2	0	4	
Masters	---	23,600	26,000	30,000	---	---	---	---	---	---	---	---	30,000	
	25,900	27,294	27,274	29,306	35,633	39,743	32,650	35,550	24,000	---	31,000	37,000	30,810	
	---	7,137	5,284	5,847	6,697	7,249	3,545	7,535	---	---	5,657	---	7,334	
	1	17	19	16	12	7	4	6	1	0	2	1	86	
Bachelors	---	23,000	26,500	32,000	---	---	---	---	---	---	---	---	30,000	
	20,167	22,514	26,679	32,711	34,955	38,075	36,820	38,933	42,400	44,000	32,045	30,000	30,791	
	4,252	4,623	5,581	7,006	5,098	8,414	13,838	5,478	16,471	---	9,756	---	9,482	
	3	21	29	27	11	8	10	3	5	1	11	1	130	
Other	---	---	---	---	---	---	---	---	---	---	---	---	---	
	---	---	33,000	25,120	22,000	27,000	35,200	---	27,000	39,000	---	---	27,983	
	---	---	---	740	---	4,243	---	---	---	---	---	---	5,209	
	0	0	1	5	1	2	1	0	1	1	0	0	12	
No Response	---	---	---	---	---	---	---	---	---	---	---	---	---	
	---	---	---	---	30,000	42,900	---	---	---	---	26,500	---	33,133	
	---	---	---	---	---	---	---	---	---	---	---	---	8,637	
	0	0	0	0	1	1	0	0	0	0	1	0	3	
TOTAL	---	28,000	29,000	33,000	38,500	38,050	37,500	---	---	---	33,000	---	32,500	
	25,829	28,048	29,518	33,545	38,050	38,775	40,177	36,678	39,367	41,500	34,661	34,333	33,492	
	6,844	7,151	5,998	7,394	7,951	7,672	10,505	6,771	14,742	3,536	9,152	3,786	8,639	
	7	71	97	128	72	32	26	9	9	2	41	3	497	

SALARIES of FULL-TIME EMPLOYED PHD RESPONDENTS
by YEARS OF PROFESSIONAL EXPERIENCE and EMPLOYER
SAL.003

EMPLOYER	PROF EXPERIENCE 0-1	2-4	5-7	8-12	13-17	18-22	23-27	28-32	33-37	38-42	> 42	No Respo	TOTAL	
Mfg-Ind	---	---	34,750	34,950	---	---	---	---	---	---	---	---	35,200	-Median
	30,000	28,800	33,422	36,023	41,992	40,718	44,000	43,250	47,500	---	38,071	---	36,533	-Mean
	---	3,788	4,367	6,265	5,418	10,625	2,828	10,436	9,192	---	11,002	---	8,005	-Std Dev
	1	14	18	30	12	11	2	4	2	0	7	0	101	-Count
Non-Mfg Ind	---	---	---	---	---	---	---	---	---	---	---	---	33,250	
	29,333	29,100	31,175	37,750	36,575	48,500	37,300	34,000	---	---	34,000	39,800	34,856	
	1,528	2,737	2,654	7,158	4,476	5,447	---	---	---	---	5,715	---	6,841	
	3	9	8	10	8	4	1	1	0	0	7	1	52	
Coll/Univ	---	---	24,400	26,000	34,600	40,700	---	---	---	---	---	---	30,000	
	---	22,711	25,186	27,680	34,717	38,921	43,382	45,400	43,325	40,850	32,757	---	32,772	
	---	1,978	5,461	5,872	7,116	8,770	18,668	9,545	12,474	10,112	9,225	---	10,429	
	0	9	21	45	35	24	11	7	4	2	14	0	172	
Govt-Fed	---	---	---	35,200	---	---	---	---	---	---	---	---	36,100	
	15,000	27,714	29,938	36,143	38,190	42,445	42,888	43,700	50,050	50,000	30,650	33,000	36,743	
	---	1,577	4,581	4,276	4,662	6,450	4,798	8,910	71	---	2,271	---	7,560	
	1	7	8	21	10	11	8	2	2	1	4	1	76	
Govt-St/Loc	---	---	---	---	---	---	---	---	---	---	---	---	---	
	---	22,000	---	27,200	---	---	32,000	---	---	---	32,500	---	28,425	
	---	---	---	---	---	---	---	---	---	---	---	---	4,905	
	0	1	0	1	0	0	1	0	0	0	1	0	4	
Self-Empl	---	---	---	---	---	---	---	---	---	---	---	---	---	
	---	---	---	---	46,000	---	---	---	---	---	---	---	46,000	
	---	---	---	---	19,799	---	---	---	---	---	---	---	19,799	
	0	0	0	0	2	0	0	0	0	0	0	0	2	
Other Empl	---	---	---	---	---	---	---	---	---	---	---	---	30,300	
	---	28,200	35,067	29,900	27,725	35,850	36,980	---	---	---	30,000	---	31,936	
	---	2,546	7,184	5,023	5,844	2,616	9,790	---	---	---	4,243	---	6,753	
	0	2	3	7	4	2	5	0	0	0	2	0	25	
No Response	---	---	---	---	---	---	---	---	---	---	---	---	---	
	---	38,300	26,700	---	---	---	---	---	---	---	---	---	32,500	
	---	---	---	---	---	---	---	---	---	---	---	---	8,202	
	0	1	1	0	0	0	0	0	0	0	0	0	2	
TOTAL	---	27,700	29,000	32,500	36,000	42,850	41,250	---	---	---	32,000	---	33,100	
	26,600	27,447	29,683	32,450	36,569	40,665	41,518	43,729	46,050	43,900	33,663	36,400	34,564	
	6,580	4,084	5,888	7,090	7,430	8,643	12,641	9,063	9,390	8,890	8,180	4,808	9,017	
	5	43	59	114	71	52	28	14	8	3	35	2	434	

SALARIES of FULL-TIME EMPLOYED BACHELORS DEGREE RESPONDENTS
by YEARS OF PROFESSIONAL EXPERIENCE and EMPLOYER
SAL.004

EMPLOYER	PROF EXPERIENCE 0-1	2-4	5-7	8-12	13-17	18-22	23-27	28-32	33-37	38-42	> 42	No Respo	TOTAL	
Mfg-Ind	---	---	---	---	---	---	---	---	---	---	---	---	30,000	-Median
	---	24,500	23,125	28,267	33,278	37,700	41,263	32,560	31,000	49,333	34,780	21,000	32,597	-Mean
	---	10,304	3,964	3,987	7,710	7,743	15,245	3,716	1,414	18,339	8,124	---	10,811	-Std Dev
	0	4	8	9	9	5	8	5	2	3	5	1	59	-Count
Non-Mfg Ind	---	---	---	---	---	---	---	---	---	---	---	---	26,500	
	---	21,500	22,850	28,000	27,750	35,000	26,467	33,200	34,000	---	24,750	---	27,029	
	---	---	4,240	5,657	3,182	---	5,464	3,704	---	---	7,425	---	5,702	
	0	1	6	2	2	1	3	3	1	0	2	0	21	
Coll/Univ	---	---	---	---	---	---	---	---	---	---	---	---	22,000	
	---	17,300	---	20,000	24,460	28,350	37,000	---	---	---	24,000	---	24,538	
	---	3,032	---	---	8,225	5,907	---	---	---	---	4,243	---	7,319	
	0	3	0	1	5	4	1	0	0	0	2	0	16	
Govt-Fed	---	---	---	---	---	---	---	---	---	---	---	---	30,700	
	---	15,000	26,500	25,329	31,600	36,967	26,000	34,683	43,800	44,000	42,850	---	32,082	
	---	---	4,950	3,325	2,408	7,312	5,657	4,419	---	---	1,626	---	7,821	
	0	1	2	7	5	6	2	6	1	1	2	0	33	
Govt-St/Loc	---	---	---	---	---	---	---	---	---	---	---	---	---	
	---	---	18,100	20,250	26,000	31,900	40,600	---	---	---	17,300	---	23,878	
	---	---	---	3,175	---	---	---	---	---	---	---	---	7,969	
	0	0	1	4	1	1	1	0	0	0	1	0	9	
Self-Empl	---	---	---	---	---	---	---	---	---	---	---	---	---	
	---	---	---	---	---	---	---	44,000	---	---	---	---	44,000	
	---	---	---	---	---	---	---	---	---	---	---	---	---	
	0	0	0	0	0	0	0	1	0	0	0	0	1	
Other Empl	---	---	---	---	---	---	---	---	---	---	---	---	---	
	17,000	30,000	---	---	30,000	26,500	---	---	---	---	26,100	---	25,920	
	---	---	---	---	---	---	---	---	---	---	---	---	5,320	
	1	1	0	0	1	1	0	0	0	0	1	0	5	
No Response	---	---	---	---	---	---	---	---	---	---	---	---	---	
	---	---	---	---	19,800	---	---	---	45,000	---	---	---	32,400	
	---	---	---	---	---	---	---	---	---	---	---	---	17,819	
	0	0	0	0	1	0	0	0	1	0	0	0	2	
TOTAL	---	---	24,000	25,000	30,000	32,750	31,000	33,000	---	---	---	---	30,000	
	17,000	21,640	23,129	25,596	29,629	34,283	35,940	34,300	36,960	48,000	30,808	21,000	30,105	
	---	7,747	4,130	4,660	7,130	7,360	13,188	4,583	6,950	15,210	9,484	---	9,454	
	1	10	17	23	24	18	15	15	5	4	13	1	146	

SALARIES of FULL-TIME EMPLOYED NON-ACADEMIC RESPONDENTS
by YEARS OF PROFESSIONAL EXPERIENCE and NUMBER OF PROFESSIONAL SUBORDINATES
SAL.005

PROF SUBS	PROF EXPERIENCE 0-1	2-4	5-7	8-12	13-17	18-22	23-27	28-32	33-37	38-42	> 42	No Respo	TOTAL	
0	---	27,000	28,000	28,600	31,000	34,500	---	32,000	---	---	30,000	---	30,000	-Median
	24,000	26,442	27,614	29,353	32,447	35,629	34,633	34,411	33,933	49,000	31,933	27,000	30,803	-Mean
	7,416	5,515	5,708	5,702	7,102	7,636	8,189	7,682	8,711	14,166	7,598	8,485	7,726	-Std Dev
	5	33	35	55	30	21	12	18	6	4	21	2	242	-Count
1-2	---	---	26,400	33,000	35,000	---	---	---	---	---	---	---	33,000	
	25,900	28,164	28,420	32,511	34,111	32,992	34,900	37,267	38,667	---	33,500	---	32,670	
	---	5,257	4,855	5,420	6,712	4,372	5,349	4,859	7,767	---	6,317	---	6,104	
	1	11	15	19	19	13	6	12	3	0	6	0	105	
3-7	---	---	---	34,100	---	---	---	---	---	---	---	---	36,750	
	---	27,700	32,855	33,792	39,108	45,170	41,731	39,814	43,800	---	32,960	39,800	37,341	
	---	1,838	6,209	6,432	6,891	4,111	12,602	13,293	---	---	13,899	---	9,383	
	0	2	11	26	12	10	13	7	1	0	5	1	88	
8-12	---	---	---	---	---	---	---	---	---	---	---	---	38,000	
	30,000	27,600	32,750	39,500	40,550	42,922	36,500	39,000	47,333	50,000	31,875	---	39,139	
	---	---	4,992	7,892	10,920	10,153	10,607	13,859	8,327	---	12,113	---	9,851	
	1	1	4	8	6	9	2	2	3	1	4	0	41	
13-17	---	---	---	---	---	---	---	---	---	---	---	---	---	
	---	---	---	50,000	42,200	46,300	---	---	---	---	---	---	45,175	
	---	---	---	---	4,525	---	---	---	---	---	---	---	4,573	
	0	0	0	1	2	1	0	0	0	0	0	0	4	
18-22	---	---	---	---	---	---	---	---	---	---	---	---	---	
	---	---	---	42,000	26,000	---	49,900	38,000	---	35,000	---	---	38,180	
	---	---	---	---	---	---	---	---	---	---	---	---	8,810	
	0	0	0	1	1	0	1	1	0	1	0	0	5	
23-32	---	---	---	---	---	---	---	---	---	---	---	---	---	
	---	---	43,000	48,500	---	---	44,000	44,000	---	---	44,350	---	45,243	
	---	---	---	707	---	---	---	---	---	---	3,748	---	2,753	
	0	0	1	2	0	0	1	1	0	0	2	0	7	
33-47	---	---	---	---	---	---	---	---	---	---	---	---	---	
	---	---	---	32,000	---	49,500	---	---	---	---	---	---	43,667	
	---	---	---	---	---	707	---	---	---	---	---	---	10,116	
	0	0	0	1	0	2	0	0	0	0	0	0	3	
48-67	---	---	---	---	---	---	---	---	---	---	---	---	---	
	---	---	---	18,500	---	---	---	---	---	---	---	---	18,500	
	---	---	---	---	---	---	---	---	---	---	---	---	---	
	0	0	0	1	0	0	0	0	0	0	0	0	1	
68-99	---	---	---	---	---	---	---	---	---	---	---	---	---	
	---	---	---	---	---	---	---	---	---	---	32,500	---	32,500	
	---	---	---	---	---	---	---	---	---	---	---	---	---	
	0	0	0	0	0	0	0	0	0	0	1	0	1	
>=100	---	---	---	---	---	---	---	---	---	---	---	---	---	
	---	---	---	---	---	---	---	---	---	---	---	---	---	
	---	---	---	---	---	---	---	---	---	---	---	---	---	
	0	0	0	0	0	0	0	0	0	0	0	0	0	
TOTAL	---	27,700	29,000	32,250	34,000	37,850	37,800	36,000	---	---	31,000	---	32,500	
	25,129	26,923	29,215	32,160	34,921	38,579	38,126	36,715	38,877	46,833	32,951	31,267	33,492	
	6,464	5,273	6,055	7,181	7,797	8,382	10,081	8,287	9,239	12,416	8,690	9,519	8,639	
	7	47	66	114	70	56	35	41	13	6	39	3	497	

SALARIES of FULL-TIME EMPLOYED NON-ACADEMIC RESPONDENTS
by YEARS OF PROFESSIONAL EXPERIENCE and NUMBER OF PROF AND TECH SUBORDINATE
SAL.006

PROF+TECH SUBS	PROF EXPERIENCE 0-1	2-4	5-7	8-12	13-17	18-22	23-27	28-32	33-37	38-42	> 42	No Respo	TOTAL	
0	---	---	29,000	28,000	---	---	---	---	---	---	---	---	29,000	-Median
	17,000	26,023	28,090	27,552	33,171	33,355	32,150	34,743	32,500	43,500	31,333	---	30,026	-Mean
	---	6,919	6,048	5,946	9,940	6,575	7,755	9,167	2,179	707	8,409	---	7,748	-Std Dev
	1	13	21	27	14	11	6	7	3	2	9	0	114	-Count
1-2	---	28,000	27,150	30,300	31,500	34,000	---	35,400	---	---	---	---	31,000	
	29,000	27,374	28,228	30,952	32,429	36,037	35,386	36,647	45,367	54,500	30,864	27,000	32,197	
	---	4,862	5,558	4,708	5,695	7,066	8,050	6,712	4,561	21,920	3,729	8,485	7,258	
	1	23	18	33	24	19	7	15	3	2	11	2	158	
3-7	---	---	26,850	34,000	36,000	---	---	---	---	---	---	---	33,100	
	24,975	26,990	27,969	33,453	36,886	41,229	36,925	39,270	33,267	---	35,580	39,800	34,367	
	6,972	4,332	5,817	6,510	6,601	7,434	6,932	11,162	9,961	---	11,824	---	8,515	
	4	10	16	32	21	14	12	10	3	0	10	1	133	
8-12	---	---	---	---	---	---	---	---	---	---	---	---	35,000	
	30,000	27,600	34,338	36,600	39,829	37,400	44,600	35,425	38,000	50,000	32,720	---	37,467	
	---	---	3,850	6,748	10,297	10,460	14,365	9,053	---	---	7,541	---	9,268	
	1	1	8	14	7	4	8	4	1	1	5	0	54	
13-17	---	---	---	---	---	---	---	---	---	---	---	---	---	
	---	---	29,000	41,000	45,400	45,150	---	36,000	40,000	---	27,750	---	38,018	
	---	---	---	12,728	---	1,626	---	---	14,142	---	14,496	---	10,261	
	0	0	1	2	1	2	0	1	2	0	2	0	11	
18-22	---	---	---	---	---	---	---	---	---	---	---	---	---	
	---	---	---	42,000	38,500	---	---	30,000	54,000	---	---	---	38,833	
	---	---	---	---	707	---	---	0	---	---	---	---	8,909	
	0	0	0	1	2	0	0	2	1	0	0	0	6	
23-32	---	---	---	---	---	---	---	---	---	---	---	---	---	
	---	---	36,000	48,000	---	47,567	49,900	38,000	---	---	47,000	---	45,200	
	---	---	---	---	---	11,369	---	---	---	---	---	---	7,973	
	0	0	1	1	0	3	1	1	0	0	1	0	8	
33-47	---	---	---	---	---	---	---	---	---	---	---	---	---	
	---	---	43,000	42,500	26,000	49,500	44,000	44,000	---	---	41,700	---	42,520	
	---	---	---	9,179	---	707	---	---	---	---	---	---	7,779	
	0	0	1	3	1	2	1	1	0	0	1	0	10	
48-67	---	---	---	---	---	---	---	---	---	---	---	---	---	
	---	---	---	---	---	50,000	---	---	---	---	---	---	50,000	
	---	---	---	---	---	---	---	---	---	---	---	---	---	
	0	0	0	0	0	1	0	0	0	0	0	0	1	
68-99	---	---	---	---	---	---	---	---	---	---	---	---	---	
	---	---	---	18,500	---	---	---	---	---	35,000	---	---	26,750	
	---	---	---	---	---	---	---	---	---	---	---	---	11,667	
	0	0	0	1	0	0	0	0	0	1	0	0	2	
>=100	---	---	---	---	---	---	---	---	---	---	---	---	---	
	---	---	---	---	---	---	---	---	---	---	---	---	---	
	---	---	---	---	---	---	---	---	---	---	---	---	---	
	0	0	0	0	0	0	0	0	0	0	0	0	0	
TOTAL	---	27,700	29,000	32,250	34,000	37,850	37,800	36,000	---	---	31,000	---	32,500	
	25,129	26,923	29,215	32,160	34,921	38,579	38,126	36,715	38,877	46,833	32,951	31,267	33,492	
	[illegible]	[illegible]	[illegible]	7,181	7,797	8,382	10,081	8,287	9,239	12,416	8,690	9,519	8,639	

SALARIES of FULL-TIME EMPLOYED NON-ACADEMIC RESPONDENTS
by YEARS OF PROFESSIONAL EXPERIENCE and TOTAL NUMBER OF SUBORDINATES
SAL.007

TOTAL SUBORDINATES	PROF EXPERIENCE 0-1	2-4	5-7	8-12	13-17	18-22	23-27	28-32	33-37	38-42	> 42	No Respo	TOTAL	
0	---	---	29,000	28,000	---	---	---	---	---	---	---	---	29,000	-Median
	17,000	26,608	28,090	27,552	32,631	33,355	30,480	34,743	31,750	43,500	30,100	---	29,796	-Mean
	---	6,883	6,048	5,946	10,129	6,575	7,366	9,167	2,475	707	7,560	---	7,606	-Std Dev
	1	12	21	27	13	11	5	7	2	2	7	0	108	-Count
1-2	---	28,000	27,150	30,000	31,000	34,000	---	35,400	---	---	---	---	31,000	
	29,000	26,443	27,881	30,393	32,143	36,037	36,025	36,647	42,525	54,500	30,483	27,000	32,057	
	---	4,690	5,390	4,593	5,644	7,066	7,669	6,712	6,795	21,920	3,792	8,485	7,395	
	1	21	16	29	23	19	8	15	4	2	12	2	152	
3-7	---	---	26,700	34,000	38,500	---	---	---	---	---	---	---	33,000	
	24,667	26,900	27,794	33,538	37,610	40,318	35,900	39,270	28,000	---	33,422	39,800	33,803	
	8,505	4,217	5,678	6,140	6,042	7,830	6,047	11,162	5,657	---	10,242	---	8,132	
	3	11	17	32	21	11	8	10	2	0	9	1	125	
8-12	---	---	---	35,000	---	---	---	---	---	---	---	---	36,250	
	27,950	31,633	34,213	36,642	38,089	42,913	44,064	30,967	45,267	---	36,433	---	38,039	
	2,899	5,816	3,729	7,094	10,183	10,775	12,409	1,914	8,100	---	11,324	---	9,519	
	2	3	8	19	9	8	11	3	3	0	6	0	72	
13-17	---	---	---	---	---	---	---	---	---	---	---	---	---	
	---	---	33,500	41,000	45,400	45,150	28,000	42,400	40,000	50,000	38,000	---	40,393	
	---	---	6,364	12,728	---	1,626	---	9,051	14,142	---	---	---	8,381	
	0	0	2	2	1	2	1	2	2	1	1	0	14	
18-22	---	---	---	---	---	---	---	---	---	---	---	---	---	
	---	---	---	42,000	38,500	---	---	30,000	---	---	---	---	35,800	
	---	---	---	---	707	---	---	0	---	---	---	---	5,495	
	0	0	0	1	2	0	0	2	0	0	0	0	5	
23-32	---	---	---	---	---	---	---	---	---	---	---	---	---	
	---	---	36,000	48,000	---	45,000	---	38,000	---	---	46,000	---	43,167	
	---	---	---	---	---	---	---	---	---	---	1,414	---	4,956	
	0	0	1	1	0	1	0	1	0	0	2	0	6	
33-47	---	---	---	---	---	---	---	---	---	---	---	---	---	
	---	---	---	40,500	26,000	43,350	46,950	44,000	---	---	29,600	---	39,080	
	---	---	---	12,021	---	7,990	4,172	---	---	---	17,112	---	10,842	
	0	0	0	2	1	2	2	1	0	0	2	0	10	
48-67	---	---	---	---	---	---	---	---	---	---	---	---	---	
	---	---	43,000	---	---	50,000	---	---	---	---	---	---	47,667	
	---	---	---	---	---	0	---	---	---	---	---	---	4,041	
	0	0	1	0	0	2	0	0	0	0	0	0	3	
68-99	---	---	---	---	---	---	---	---	---	---	---	---	---	
	---	---	---	18,500	---	---	---	---	---	35,000	---	---	26,750	
	---	---	---	---	---	---	---	---	---	---	---	---	11,667	
	0	0	0	1	0	0	0	0	0	1	0	0	2	
>=100	---	---	---	---	---	---	---	---	---	---	---	---	---	
	---	---	---	---	---	---	---	---	---	---	---	---	---	
	---	---	---	---	---	---	---	---	---	---	---	---	---	
	0	0	0	0	0	0	0	0	0	0	0	0	0	
TOTAL	---	27,700	29,000	32,250	34,000	37,850	37,800	36,000	---	---	31,000	---	32,500	
	25,129	26,923	29,215	32,160	34,921	38,579	38,126	36,715	38,877	46,833	32,951	31,267	33,492	
	6,464	5,273	6,055	7,181	7,797	8,382	10,081	8,287	9,239	12,416	8,690	9,519	8,639	
	7	47	66	114	70	56	35	41	13	6	39	3	497	

SALARIES of FULL-TIME EMPLOYED NON-ACADEMIC MALE RESPONDENTS
by YEARS OF PROFESSIONAL EXPERIENCE and HIGHEST DEGREE
SAL.008

HIGHEST DEGREE	PROF EXPERIENCE 0-1	2-4	5-7	8-12	13-17	18-22	23-27	28-32	33-37	38-42	> 42	No Respo	TOTAL	
Ph.D.	---	28,800	33,000	35,000	39,000	44,000	42,000	---	---	---	32,750	---	35,000	-Median
	26,600	28,770	32,286	36,019	38,700	42,640	40,312	42,057	51,367	50,000	35,311	36,400	36,001	-Mean
	6,580	3,572	4,519	6,063	7,423	7,744	6,921	8,964	2,281	---	7,569	4,808	7,748	-Std Dev
	5	33	37	62	34	25	17	7	3	1	18	2	244	-Count
M.D.	---	---	---	---	---	---	---	---	---	---	---	---	---	
	---	---	---	---	---	---	44,000	65,000	---	---	42,500	---	48,500	
	---	---	---	---	---	---	---	---	---	---	13,435	---	13,478	
	0	0	0	0	0	0	1	1	0	0	2	0	4	
Masters	---	---	---	28,000	---	---	---	35,400	---	---	---	---	31,000	
	---	20,133	29,800	28,486	35,767	35,382	32,500	35,220	31,833	---	22,250	---	31,641	
	---	231	6,799	6,190	5,626	6,634	2,121	6,928	7,147	---	6,718	---	7,326	
	0	3	8	21	9	11	2	15	3	0	2	0	74	
Bachelors	---	---	24,000	26,000	30,000	---	---	33,000	---	---	---	---	30,000	
	17,000	23,833	23,433	26,313	30,822	38,080	35,864	34,300	36,960	48,000	32,620	---	31,471	
	---	9,342	4,066	4,969	6,510	7,254	13,682	4,583	6,950	15,210	10,086	---	9,780	
	1	6	15	16	18	10	14	15	5	4	10	0	114	
Other	---	---	---	---	---	---	---	---	---	---	---	---	---	
	---	---	---	25,100	24,375	28,500	---	30,100	30,000	39,000	27,000	---	27,983	
	---	---	---	---	1,797	6,364	---	7,212	---	---	---	---	5,209	
	0	0	0	1	4	2	0	2	1	1	1	0	12	
No Response	---	---	---	---	---	---	---	---	---	---	---	---	---	
	---	---	---	---	---	---	---	42,900	---	---	28,250	---	33,133	
	---	---	---	---	---	---	---	---	---	---	2,475	---	8,637	
	0	0	0	0	0	0	0	1	0	0	2	0	3	
TOTAL	---	28,000	29,450	33,000	34,500	39,000	37,550	36,000	---	---	32,000	---	33,000	
	25,000	27,448	29,742	32,775	35,231	39,438	38,129	36,715	38,700	46,833	33,566	36,400	34,019	
	7,071	5,276	6,004	7,209	7,940	8,106	10,233	8,287	9,627	12,416	8,912	4,808	8,654	
	6	42	60	100	65	48	34	41	12	6	35	2	451	

SALARIES of FULL-TIME EMPLOYED NON-ACADEMIC FEMALE RESPONDENTS
by YEARS OF PROFESSIONAL EXPERIENCE and HIGHEST DEGREE
SAL.009

HIGHEST DEGREE	PROF EXPERIENCE 0-1	2-4	5-7	8-12	13-17	18-22	23-27	28-32	33-37	38-42	> 42	No Respo	TOTAL	
Ph.D.	---	---	---	---	---	---	---	---	---	---	---	---	32,000	-Median
	---	26,400	27,800	31,500	32,750	44,250	---	---	41,000	---	28,000	---	32,571	-Mean
	---	---	---	4,106	4,596	13,789	---	---	---	---	4,359	---	7,185	-Std Dev
	*	*	*	*	*	*	*	*	*	*	*	*	17	-Count
M.D.	---	---	---	---	---	---	---	---	---	---	---	---	---	
	---	---	---	---	---	---	---	---	---	---	---	---	---	
	---	---	---	---	---	---	---	---	---	---	---	---	---	
	*	*	*	*	*	*	*	*	*	*	*	*	0	
Masters	---	---	---	---	---	---	---	---	---	---	---	---	---	
	25,900	21,567	24,733	20,500	27,500	30,000	38,000	---	---	---	---	---	25,692	
	---	2,290	1,963	---	3,536	---	---	---	---	---	---	---	5,118	
	*	*	*	*	*	*	*	*	*	*	*	*	12	
Bachelors	---	---	---	---	---	---	---	---	---	---	---	---	26,300	
	---	21,500	20,850	24,440	34,000	30,725	---	---	---	---	26,300	21,000	25,973	
	---	---	5,445	3,907	---	1,539	---	---	---	---	---	---	5,083	
	*	*	*	5	*	4	*	*	*	*	*	*	15	
Other	---	---	---	---	---	---	---	---	---	---	---	---	---	
	---	---	---	---	---	---	---	---	---	---	---	---	---	
	---	---	---	---	---	---	---	---	---	---	---	---	---	
	*	*	*	*	*	*	*	*	*	*	*	*	0	
No Response	---	---	---	---	---	---	---	---	---	---	---	---	---	
	---	---	---	---	---	---	---	---	---	---	---	---	---	
	---	---	---	---	---	---	---	---	---	---	---	---	---	
	*	*	*	*	*	*	*	*	*	*	*	*	0	
TOTAL	---	---	---	---	---	---	---	---	---	---	---	---	27,100	
	25,900	22,520	23,950	27,938	30,900	34,486	38,000	---	41,000	---	27,575	21,000	28,445	
	---	2,707	3,827	5,535	4,278	8,800	---	---	---	---	3,659	---	6,730	
	*	5	6	13	5	7	*	*	*	*	4	*	44	

* fewer than 4 responses

SALARIES of FULL-TIME EMPLOYED ACADEMIC PHD RESPONDENTS
by YEARS OF PROFESSIONAL EXPERIENCE and RANK
SAL.010

ACADEMIC RANK	PROF EXPERIENCE 0-1	2-4	5-7	8-12	13-17	18-22	23-27	28-32	33-37	38-42	> 42	No Respo	TOTAL	
Full Prof	---	---	---	---	---	43,700	---	---	---	---	---	---	44,000	-Median
	---	---	---	35,600	40,117	42,471	51,900	48,083	49,233	33,700	46,000	---	43,873	-Mean
	---	---	---	7,621	5,159	7,750	18,535	6,989	4,895	---	11,605	---	10,060	-Std Dev
	0	0	0	3	12	17	7	6	3	1	3	0	52	-Count
Assoc Prof	---	---	---	---	31,500	---	---	---	---	---	---	---	31,250	
	---	---	32,750	32,400	32,860	32,500	27,000	29,300	25,600	---	31,725	---	32,066	
	---	---	5,500	4,991	5,686	1,842	4,243	---	---	---	3,586	---	4,880	
	0	0	4	13	15	4	2	1	1	0	4	0	44	
Asst Prof	---	---	---	---	---	---	---	---	---	---	---	---	25,550	
	---	23,880	25,155	26,667	30,000	---	---	---	---	---	27,233	---	25,869	
	---	1,949	2,509	3,950	---	---	---	---	---	---	3,995	---	3,299	
	0	5	11	12	1	0	0	0	0	0	3	0	32	
Instr/Lec	---	---	---	---	---	---	---	---	---	---	---	---	---	
	---	---	---	20,000	32,000	---	---	---	---	---	---	---	24,800	
	---	---	---	4,583	1,414	---	---	---	---	---	---	---	7,362	
	0	0	0	3	2	0	0	0	0	0	0	0	5	
Unranked	---	---	---	---	---	---	---	---	---	---	---	---	---	
	---	---	21,300	24,300	34,300	26,050	---	---	---	---	26,000	---	26,318	
	---	---	---	2,080	990	2,758	---	---	---	---	---	---	4,462	
	0	0	1	5	2	2	0	0	0	0	1	0	11	
Non-Fac	---	---	---	---	---	---	---	---	---	---	---	---	22,000	
	---	21,250	19,980	23,717	18,900	30,000	---	---	---	---	28,667	---	22,905	
	---	500	3,978	1,877	1,273	---	---	---	---	---	4,933	---	4,311	
	0	4	5	6	2	1	0	0	0	0	3	0	21	
No Response	---	---	---	---	---	---	---	---	---	---	---	---	---	
	---	---	---	24,600	40,400	---	29,950	---	---	48,000	---	---	31,729	
	---	---	---	1,778	---	---	71	---	---	---	---	---	9,175	
	0	0	0	3	1	0	2	0	0	1	0	0	7	
TOTAL	---	---	24,400	26,000	34,600	40,700	---	---	---	---	---	---	30,000	
	---	22,711	25,186	27,680	34,717	38,921	43,382	45,400	43,325	40,850	32,757	---	32,772	
	---	1,978	5,461	5,872	7,116	8,770	18,668	9,545	12,474	10,112	9,225	---	10,429	
	0	9	21	45	35	24	11	7	4	2	14	0	172	

SALARIES of FULL-TIME EMPLOYED NON-ACADEMIC RESPONDENTS
by YEARS OF PROFESSIONAL EXPERIENCE and NUMBER OF EMPLOYERS
SAL.011

NUM OF EMPLOYERS	PROF EXPERIENCE 0-1	2-4	5-7	8-12	13-17	18-22	23-27	28-32	33-37	38-42	> 42	No Respo	TOTAL	
1	---	27,600	29,700	32,750	36,000	36,850	---	33,000	---	---	---	---	31,000	-Median
	25,129	26,376	30,250	32,017	36,724	39,244	37,754	35,568	38,667	---	30,231	---	32,879	-Mean
	6,464	4,560	6,599	7,888	6,571	9,221	5,811	9,550	7,767	---	5,778	---	8,269	-Std Dev
	7	25	24	42	25	18	13	22	3	0	13	0	192	-Count
2	---	28,400	29,450	34,050	30,000	37,000	---	---	---	---	---	---	33,500	
	---	29,769	28,971	33,718	30,589	37,505	41,133	39,120	43,220	43,000	36,800	36,400	33,795	
	---	5,013	6,237	6,541	7,473	8,504	8,542	6,422	12,310	---	9,945	4,808	8,204	
	0	16	28	34	19	20	6	10	5	1	10	2	151	
3	---	---	---	30,000	---	---	---	---	---	---	---	---	32,000	
	---	20,740	27,500	30,975	36,064	39,845	35,238	38,000	34,825	50,000	37,500	21,000	33,390	
	---	4,302	3,797	5,581	8,924	8,122	9,234	---	6,153	---	10,821	---	8,747	
	0	5	7	24	14	11	8	1	4	1	6	1	82	
4-6	---	---	---	---	---	---	---	---	---	---	---	---	33,000	
	---	---	28,000	31,367	36,300	38,400	43,467	37,533	---	47,000	29,767	---	34,986	
	---	---	5,292	9,439	10,182	6,748	28,268	10,929	---	15,769	9,977	---	12,282	
	0	0	4	12	6	4	3	3	0	4	6	0	42	
7-10	---	---	---	---	---	---	---	---	---	---	---	---	---	
	---	---	31,750	27,650	41,500	26,000	40,250	37,400	---	---	---	---	34,570	
	---	---	7,425	1,485	2,121	---	13,647	---	---	---	---	---	8,177	
	0	0	2	2	2	1	2	1	0	0	0	0	10	
>10	---	---	---	---	---	---	---	---	---	---	---	---	---	
	---	---	---	---	36,000	---	---	30,700	---	---	33,000	---	33,740	
	---	---	---	---	0	---	---	---	---	---	0	---	2,267	
	0	0	0	0	2	0	0	1	0	0	2	0	5	
No Response	---	---	---	---	---	---	---	---	---	---	---	---	---	
	---	---	---	---	---	---	40,000	---	---	---	28,000	---	34,000	
	---	---	---	---	---	---	---	---	---	---	---	---	8,485	
	0	0	0	0	0	0	1	0	0	0	1	0	2	
TOTAL	---	27,650	29,000	32,250	34,000	36,850	37,300	35,300	---	---	31,000	---	32,000	
	25,129	27,509	29,665	32,160	35,949	40,007	40,436	39,613	42,117	46,833	33,818	31,267	34,392	
	6,464	3,459	4,867	7,181	5,014	3,829	3,409							

SALARIES of FULL-TIME EMPLOYED NON-ACADEMIC RESPONDENTS
by YEARS OF PROFESSIONAL EXPERIENCE and YEARS WITH PRESENT EMPLOYER
SAL.012

YRS WITH EMPLOYER	PROF EXPERIENCE 0-1	2-4	5-7	8-12	13-17	18-22	23-27	28-32	33-37	38-42	> 42	No Respo	TOTAL	
0-1	---	---	---	---	---	---	---	---	---	---	---	---	28,000	-Median
	25,129	26,771	27,208	30,714	---	48,000	40,000	---	---	---	28,000	---	28,356	-Mean
	6,464	2,144	5,457	8,200	---	---	---	---	---	---	---	---	6,920	-Std Dev
	7	7	12	7	0	1	1	0	0	0	1	0	36	-Count
2-4	---	28,600	29,400	31,150	33,500	---	---	---	---	---	29,800	---	30,000	
	---	27,435	29,152	32,325	34,229	37,750	29,800	34,900	---	---	31,883	27,000	30,794	
	---	5,568	6,054	6,623	8,277	12,065	1,131	7,889	---	---	10,856	8,485	7,807	
	0	37	25	28	17	6	2	3	0	0	18	2	138	
5-7	---	---	29,400	34,000	---	---	---	---	---	---	---	---	33,000	
	---	---	30,519	32,330	36,625	38,000	52,500	---	---	---	33,667	---	33,273	
	---	---	6,080	6,605	12,724	6,595	31,820	---	---	---	4,041	---	8,972	
	0	0	21	20	4	5	2	0	0	0	3	0	55	
8-12	---	---	---	32,000	36,000	---	---	---	---	---	---	---	34,000	
	---	23,400	28,000	31,778	36,586	40,180	40,600	37,700	34,000	---	36,500	39,800	34,053	
	---	---	9,626	7,601	6,042	7,421	6,317	424	---	---	6,576	---	7,683	
	0	1	4	51	22	5	6	2	1	0	5	1	98	
13-17	---	---	---	---	33,100	36,000	---	---	---	---	---	---	35,000	
	---	---	---	42,400	33,996	37,573	37,200	38,900	50,100	---	30,475	---	36,035	
	---	---	---	10,748	8,405	7,856	8,290	6,655	---	---	5,457	---	8,239	
	0	0	0	2	24	15	6	5	1	0	4	0	57	
18-22	---	---	---	---	---	36,000	---	---	---	---	---	---	38,000	
	---	---	---	---	24,000	37,791	47,233	40,520	30,000	---	40,567	---	38,611	
	---	---	---	---	---	8,190	3,530	9,431	---	---	2,228	---	8,321	
	0	0	0	0	1	22	3	5	1	0	3	0	35	
23-27	---	---	---	---	---	---	---	---	---	---	---	---	34,000	
	---	---	---	34,000	---	---	35,236	32,457	33,500	50,000	38,500	---	35,192	
	---	---	---	---	---	---	7,883	2,849	---	---	7,778	---	6,971	
	0	0	0	1	0	0	14	7	1	1	2	0	26	
28-32	---	---	---	---	---	---	---	36,000	---	---	---	---	36,500	
	---	---	---	---	---	---	28,000	36,717	40,600	41,500	---	---	37,238	
	---	---	---	---	---	---	---	10,275	15,254	3,536	---	---	10,285	
	0	0	0	0	0	0	1	18	3	2	0	0	24	
33-37	---	---	---	---	---	---	---	---	---	---	---	---	---	
	---	---	---	---	---	---	---	---	39,333	49,333	26,550	---	39,736	
	---	---	---	---	---	---	---	---	7,633	18,339	636	---	12,607	
	0	0	0	0	0	0	0	0	6	3	2	0	11	
TOTAL	---	27,700	29,000	32,250	34,000	37,850	37,800	36,000	---	---	31,000	---	32,500	
	25,129	26,923	29,215	32,160	34,921	38,579	38,126	36,715	38,877	46,833	32,951	31,267	33,492	
	6,464	5,273	6,055	7,181	7,797	8,382	10,081	8,287	9,239	12,416	8,690	9,519	8,639	
	7	47	66	114	70	56	35	41	13	6	39	3	497	

SALARIES of *FULL-TIME EMPLOYED NON-ACADEMIC RESPONDNTS*
by YEARS OF PROFESSIONAL EXPERIENCE and HANDS-ON OPERATION
SAL.013

HANDS-ON OPERATION	PROF EXPERIENCE 0-1	2-4	5-7	8-12	13-17	18-22	23-27	28-32	33-37	38-42	> 42	No Respo	TOTAL	
0-10%	---	---	32,500	35,000	39,000	44,000	---	---	---	---	---	---	36,500	-Median
	31,000	25,975	32,794	35,311	37,409	42,852	40,536	39,582	36,700	51,667	39,092	---	37,845	-Mean
	---	7,883	6,140	7,093	6,795	8,382	12,073	11,057	10,952	17,559	9,895	---	9,399	-Std Dev
	1	4	16	35	23	25	14	11	5	3	13	0	150	-Count
10-30%	---	---	30,500	34,100	34,000	---	---	---	---	---	---	---	32,000	
	24,667	26,592	30,075	33,859	36,444	33,350	36,591	37,900	36,900	44,000	29,160	39,800	33,231	
	8,386	6,750	5,457	6,643	8,648	5,191	5,703	8,069	9,758	---	2,569	---	7,461	
	3	12	16	27	16	10	11	14	2	1	10	1	123	
30-60%	---	29,000	26,400	32,750	32,500	---	---	---	---	---	---	---	31,400	
	28,000	28,375	27,379	31,804	32,681	38,655	42,860	33,633	41,050	39,000	39,000	---	32,418	
	---	3,699	4,942	6,794	7,379	8,466	7,540	5,615	12,799	---	7,000	---	7,563	
	1	16	19	24	16	11	5	9	2	1	3	0	107	
60-80%	---	---	---	28,000	---	---	---	---	---	---	---	---	29,750	
	25,900	26,156	30,260	27,853	36,188	33,500	34,350	35,467	41,500	43,000	24,820	27,000	30,731	
	---	4,846	5,706	4,795	7,377	4,359	17,466	7,714	8,505	---	7,518	8,485	7,706	
	1	9	5	17	8	5	2	3	4	1	5	2	62	
80-100%	---	---	---	---	---	---	---	---	---	---	---	---	27,000	
	17,000	25,500	25,080	25,391	26,943	32,580	27,133	32,550	---	---	30,525	---	27,407	
	---	5,338	6,179	5,403	4,859	5,083	6,801	3,504	---	---	5,203	---	5,916	
	1	6	10	11	7	5	3	4	0	0	8	0	55	
No Response	---	---	---	---	---	---	---	---	---	---	---	---	---	
	---	---	---	---	---	---	---	---	---	---	---	---	---	
	---	---	---	---	---	---	---	---	---	---	---	---	---	
	0	0	0	0	0	0	0	0	0	0	0	0	0	
TOTAL	---	27,700	29,000	32,250	34,000	37,850	37,800	36,000	---	---	31,000	---	32,500	
	25,129	26,923	29,215	32,160	34,921	38,579	38,126	36,715	38,877	46,833	32,951	31,267	33,492	
	6,464	5,273	6,055	7,181	7,797	8,382	10,081	8,287	9,239	12,416	8,690	9,519	8,639	
	7	47	66	114	70	56	35	41	13	6	39	3	497	

SALARIES of FULL-TIME EMPLOYED NON-ACADEMIC RESPONDENTS
by YEARS OF PROFESSIONAL EXPERIENCE and MS DATA INTERPRETATION
SAL.014

INTERPRETATION	PROF EXPERIENCE 0-1	2-4	5-7	8-12	13-17	18-22	23-27	28-32	33-37	38-42	> 42	No Respo	TOTAL	
0-10%	---	---	---	36,000	---	---	---	---	---	---	---	---	35,200	-Median
	30,500	30,000	31,625	36,178	34,408	43,800	37,750	37,833	41,833	35,000	37,170	---	36,807	-Mean
	707	11,314	8,032	8,973	8,103	9,887	16,746	7,118	10,774	---	9,453	---	10,058	-Std Dev
	2	2	12	18	12	14	8	6	3	1	10	0	88	-Count
10-30%	---	---	---	33,250	---	---	---	---	---	---	---	---	33,000	
	---	29,800	27,425	32,994	40,127	41,157	41,180	34,150	35,933	---	31,333	39,800	35,014	
	---	4,868	4,653	7,549	9,808	6,181	10,333	9,242	7,100	---	1,528	---	8,548	
	0	5	8	18	11	7	5	4	3	0	3	1	65	
30-60%	---	---	---	32,000	---	---	---	---	---	---	---	---	32,500	
	21,500	27,000	24,717	30,418	38,345	48,333	40,386	38,200	32,000	---	35,125	---	33,445	
	9,192	4,636	5,488	7,703	7,256	6,658	4,799	7,904	---	---	9,750	---	9,112	
	2	9	6	17	11	3	7	7	1	0	4	0	67	
60-80%	---	---	---	28,400	---	---	---	---	---	---	---	---	30,000	
	---	26,967	30,857	28,940	32,586	31,186	33,483	36,000	---	---	28,760	21,000	30,016	
	---	3,888	8,528	5,816	6,968	2,541	8,196	---	---	---	12,030	---	6,799	
	0	9	7	15	7	7	6	1	0	0	5	1	58	
80-100%	---	27,700	28,000	32,000	32,000	35,000	---	34,700	---	---	30,000	---	31,500	
	23,967	26,343	29,000	31,991	32,424	35,832	38,100	36,155	40,017	49,200	31,476	33,000	32,674	
	6,229	5,510	4,608	5,938	6,105	6,296	6,877	9,174	10,807	12,276	7,360	---	7,834	
	3	21	31	45	29	25	9	22	6	5	17	1	214	
No Response	---	---	---	---	---	---	---	---	---	---	---	---	---	
	---	17,500	33,000	30,300	---	---	---	42,900	---	---	---	---	31,340	
	---	---	5,657	---	---	---	---	---	---	---	---	---	9,536	
	0	1	2	1	0	0	0	1	0	0	0	0	5	
TOTAL	---	27,700	29,000	32,250	34,000	37,850	37,800	36,000	---	---	31,000	---	32,500	
	25,129	26,923	29,215	32,160	34,921	38,579	38,126	36,715	38,877	46,833	32,951	31,267	33,492	
	6,464	5,273	6,055	7,181	7,797	8,382	10,081	8,287	9,239	12,416	8,690	9,519	8,639	
	7	47	66	114	70	56	35	41	13	6	39	3	497	

SALARIES of FULL-TIME EMPLOYED NON-ACADEMIC RESPONDENTS
by YEARS OF PROFESSIONAL EXPERIENCE and SAMPLE PREPARATION
SAL.015

PREPARATION	PROF EXPERIENCE 0-1	2-4	5-7	8-12	13-17	18-22	23-27	28-32	33-37	38-42	> 42	No Respo	TOTAL	
0-10%	---	28,000	29,000	33,550	38,250	41,000	40,500	36,000	---	---	33,000	---	34,800	-Median
	30,000	28,462	30,010	33,227	36,876	40,535	41,371	37,021	37,288	51,667	36,688	31,267	35,322	-Mean
	1,000	4,735	6,446	7,923	8,769	8,816	12,089	7,367	9,187	17,559	8,046	9,519	9,181	-Std Dev
	3	21	31	66	38	37	17	19	8	3	17	3	263	-Count
10-30%	---	---	---	32,500	---	---	---	---	---	---	---	---	30,000	
	26,950	25,230	27,223	30,562	33,730	34,600	37,086	33,775	47,550	---	26,144	---	30,717	
	1,485	5,096	5,419	5,511	5,049	5,983	8,437	4,402	3,606	---	5,408	---	6,944	
	2	10	13	21	10	5	7	8	2	0	9	0	87	
30-60%	---	---	---	---	---	---	---	---	---	---	---	---	31,950	
	15,000	29,860	26,050	34,570	34,575	35,580	29,333	32,133	32,000	41,500	31,150	---	31,966	
	---	4,995	6,828	5,459	8,496	4,456	2,082	6,407	---	3,536	5,424	---	6,776	
	1	5	6	10	4	5	3	3	1	2	4	0	44	
60-80%	---	---	---	---	---	---	---	---	---	---	---	---	30,000	
	---	25,200	30,633	29,250	31,400	36,100	36,667	47,900	---	43,000	22,900	---	32,507	
	---	5,020	5,154	1,038	1,817	7,709	4,619	17,150	---	---	4,808	---	9,191	
	0	5	3	4	5	3	3	3	0	1	2	0	29	
80-100%	---	---	---	---	---	---	---	---	---	---	---	---	30,000	
	17,000	24,520	29,918	28,582	32,300	33,567	34,700	35,529	40,000	---	36,529	---	31,791	
	---	5,969	5,423	6,604	6,355	7,606	6,221	8,230	14,142	---	9,390	---	7,771	
	1	5	11	11	12	6	5	7	2	0	7	0	67	
No Response	---	---	---	---	---	---	---	---	---	---	---	---	---	
	---	17,500	33,350	27,150	23,000	---	---	42,900	---	---	---	---	29,200	
	---	---	5,162	4,455	---	---	---	---	---	---	---	---	8,683	
	0	1	2	2	1	0	0	1	0	0	0	0	7	
TOTAL	---	27,700	29,000	32,250	34,000	37,850	37,800	36,000	---	---	31,000	---	32,500	
	25,129	26,923	29,215	32,160	34,921	38,579	38,126	36,715	38,877	46,833	32,951	31,267	33,492	
	6,464	5,273	6,055	7,181	7,797	8,382	10,081	8,287	9,239	12,416	8,690	9,519	8,639	
	7	47	66	114	70	56	35	41	13	6	39	3	497	

SALARIES of FULL-TIME EMPLOYED NON-ACADEMIC RESPONDENTS
by YEARS OF PROFESSIONAL EXPERIENCE and MAINTENANCE REFERAL
SAL.016

REFER TO MFG	PROF EXPERIENCE 0-1	2-4	5-7	8-12	13-17	18-22	23-27	28-32	33-37	38-42	> 42	No Respo	TOTAL	
0-10%	---	28,500	28,000	33,000	33,200	36,850	38,650	35,200	---	---	30,000	---	32,500	-Median
	30,500	26,638	28,848	32,992	34,468	37,947	38,761	36,648	38,600	42,000	33,044	39,800	34,200	-Mean
	707	4,272	6,354	6,985	8,388	8,649	12,915	8,716	10,938	6,481	8,929	---	8,922	-Std Dev
	2	16	27	51	31	34	18	25	9	4	18	1	236	-Count
10-30%	---	---	30,000	32,500	34,000	---	---	---	---	---	---	---	33,250	
	29,000	28,400	29,280	31,550	34,176	38,740	38,018	37,550	---	56,500	31,667	---	33,375	
	---	5,327	6,466	8,154	6,295	7,188	5,825	9,742	---	19,092	7,878	---	8,449	
	1	13	15	24	17	10	11	6	0	2	9	0	108	
30-60%	---	---	---	28,600	---	---	---	---	---	---	---	---	30,000	
	15,000	25,175	27,543	29,961	39,450	43,000	36,100	34,000	39,500	---	32,550	21,000	31,723	
	---	4,491	4,900	6,615	8,050	10,789	7,947	---	7,778	---	9,532	---	8,896	
	1	12	14	23	12	6	5	1	2	0	6	1	83	
60-80%	---	---	---	---	---	---	---	---	---	---	---	---	32,000	
	22,500	28,467	31,167	32,443	33,071	36,000	38,000	30,800	41,000	---	31,600	33,000	31,959	
	7,778	8,891	2,858	7,327	5,419	7,550	---	6,239	---	---	6,618	---	6,340	
	2	3	6	7	7	3	1	3	1	0	5	1	39	
80-100%	---	---	---	---	---	---	---	---	---	---	---	---	37,400	
	25,900	27,000	33,500	35,380	33,550	38,933	---	39,480	38,000	---	---	---	35,695	
	---	---	10,332	8,878	11,384	6,424	---	7,166	---	---	---	---	7,907	
	1	1	3	5	2	3	0	5	1	0	0	0	21	
No Response	---	---	---	---	---	---	---	---	---	---	---	---	---	
	---	27,750	37,000	33,325	23,000	---	---	40,000	---	---	52,000	---	34,080	
	---	14,496	---	3,867	---	---	---	---	---	---	---	---	9,574	
	0	2	1	4	1	0	0	1	0	0	1	0	10	
TOTAL	---	27,700	29,000	32,250	34,000	37,850	37,800	36,000	---	---	31,000	---	32,500	
	25,129	26,923	29,215	32,160	34,921	38,579	38,126	36,715	38,877	46,833	32,951	31,267	33,492	
	6,464	5,273	6,055	7,181	7,797	8,382	10,081	8,287	9,239	12,416	8,690	9,519	8,639	
	7	47	66	114	70	56	35	41	13	6	39	3	497	

SALARIES of FULL-TIME EMPLOYED NON-ACADEMIC RESPONDENTS
by YEARS OF PROFESSIONAL EXPERIENCE and REPAIR ABILITY
SAL.017

REPAIR ABILITY	PROF EXPERIENCE 0-1	2-4	5-7	8-12	13-17	18-22	23-27	28-32	33-37	38-42	> 42	No Respo	TOTAL	
0-10%	---	---	---	---	---	---	---	---	---	---	---	---	36,250	-Median
	25,900	26,400	39,250	34,000	36,500	45,150	59,500	34,500	---	52,500	36,250	---	39,013	-Mean
	---	---	3,889	9,644	7,062	7,930	21,920	6,455	---	24,749	9,159	---	11,720	-Std Dev
	1	1	2	3	7	4	2	4	0	2	6	0	32	-Count
10-30%	---	---	---	34,000	---	---	---	---	---	---	---	---	32,000	
	20,667	27,960	27,529	32,129	36,563	34,183	32,600	36,486	44,333	---	27,467	33,000	31,917	
	8,145	6,350	6,165	8,391	10,479	6,625	7,266	7,352	8,505	---	7,938	---	8,555	
	3	5	14	17	8	12	5	7	3	0	6	1	81	
30-60%	---	27,850	29,550	32,000	32,000	---	---	---	---	---	---	---	31,700	
	29,500	26,655	29,750	31,609	34,716	41,967	40,888	35,560	34,000	43,500	31,114	---	32,695	
	2,121	4,454	5,384	7,161	6,925	8,734	6,822	9,168	---	707	5,496	---	7,827	
	2	22	18	35	19	12	8	5	1	2	14	0	138	
60-80%	---	---	---	29,600	34,000	36,000	---	---	---	---	---	---	31,000	
	29,000	26,030	28,062	30,293	32,442	37,168	37,773	34,029	37,700	---	34,188	21,000	32,394	
	---	6,938	5,101	5,911	7,285	7,633	7,724	7,417	7,795	---	10,156	---	7,801	
	1	10	13	30	19	19	11	7	4	0	8	1	123	
80-100%	---	---	29,250	34,200	36,900	---	---	36,600	---	---	---	---	34,200	
	---	26,813	29,278	34,908	37,344	39,978	34,422	38,661	37,520	44,500	37,175	39,800	35,150	
	---	4,309	6,617	7,691	7,815	9,399	8,581	9,349	11,932	7,778	12,890	---	8,911	
	0	8	18	25	16	9	9	18	5	2	4	1	115	
No Response	---	---	---	---	---	---	---	---	---	---	---	---	---	
	---	38,000	37,000	32,550	23,000	---	---	---	---	---	45,000	---	34,150	
	---	---	---	2,774	---	---	---	---	---	---	---	---	6,528	
	0	1	1	4	1	0	0	0	0	0	1	0	8	
TOTAL	---	27,700	29,000	32,250	34,000	37,850	37,800	36,000	---	---	31,000	---	32,500	
	25,129	26,923	29,215	32,160	34,921	38,579	38,126	36,715	38,877	46,833	32,951	31,267	33,492	
	6,464	5,273	6,055	7,181	7,797	8,382	10,081	8,287	9,239	12,416	8,690	9,519	8,639	
	7	47	66	114	70	56	35	41	13	6	39	3	497	

SALARIES of FULL-TIME EMPLOYED ACADEMIC PHD RESPONDENTS
by YEARS OF PROFESSIONAL EXPERIENCE and SALARY PERIOD
SAL.018

SALARY PERIOD	PROF EXPERIENCE 0-1	2-4	5-7	8-12	13-17	18-22	23-27	28-32	33-37	38-42	> 42	No Respo	TOTAL	
9-10 mo	---	---	---	---	---	---	---	---	---	---	---	---	32,750	-Median
	---	22,967	25,840	27,890	35,160	39,357	36,267	39,100	39,650	33,700	37,657	---	34,178	-Mean
	---	1,976	1,713	6,572	5,471	9,128	7,228	8,487	19,870	---	10,578	---	9,188	-Std Dev
	0	3	5	10	10	14	3	3	2	1	7	0	58	-Count
11-12 mo	---	---	23,500	26,000	34,600	---	---	---	---	---	---	---	30,000	
	---	22,583	24,981	27,620	34,743	38,310	51,417	50,125	47,000	48,000	27,857	---	32,092	
	---	2,154	6,229	5,759	7,696	8,687	22,272	8,045	4,243	---	4,059	---	11,117	
	0	6	16	35	23	10	6	4	2	1	7	0	110	
No Response	---	---	---	---	---	---	---	---	---	---	---	---	---	
	---	---	---	---	32,200	---	29,950	---	---	---	---	---	31,075	
	---	---	---	---	11,597	---	71	---	---	---	---	---	6,820	
	0	0	0	0	2	0	2	0	0	0	0	0	4	
TOTAL	---	---	24,400	26,000	34,600	40,700	---	---	---	---	---	---	30,000	
	---	22,711	25,186	27,680	34,717	38,921	43,382	45,400	43,325	40,850	32,757	---	32,772	
	---	1,978	5,461	5,872	7,116	8,770	18,668	9,545	12,474	10,112	9,225	---	10,429	
	0	9	21	45	35	24	11	7	4	2	14	0	172	

Deaths

The Society regrets the untimely death of one of its charter members, Peter Brown, on March 25, 1981.

Prof. Brown was born in Lincoln, England, September 12, 1938, educated at the University of Southampton, and received postdoctoral training with Carl Djerassi at Stanford from 1964-7. He then joined the faculty at Arizona State University where he became Professor of Organic Chemistry in 1977. He has published extensively in the areas of cycloaddition reactions, photochemistry and organic mass spectrometry where his interests included alkyl migrations, field ion kinetics and structure determination of natural products.

ASSELIN MICHEL	DEFENCE RES ESTAB	VALCARTIER	PO BOX 8500	COURCELETTE, PQ	G0A 1R0
AU M K	UNIV OF WINDSOR	CHEMISTRY DEPT		WINDSOR,ONTARIO	N9B 3P4
BARBER ROBERT C	UNIV OF MANITOBA	PHYSICS DEPT		WINNIPEG, MANITOBA	R3T 2N2
BAUER G	HEWLETT PACKARD	17500 TRANSCANADA S		KIRKLAND,PQ	H9R 4R6
BEAVIS RONALD C	75 HAZELDELL AVE			WINNIPEG, MANITOBA	R2K 0P3
BENOIT F M	HEALTH-WELFARE DEPT	ENVIRONMENTAL HEALTH	TUNNEYS PASTURE	OTTAWA, ONTARIO	K1A 0L2
BERTRAND M J	UNIV OF MONTREAL	CHEMISTRY DEPT	C.P. 6210 SUK.A	MONTREAL, QUEBEC	H3C 3U1
BOHME D K	YORK UNIVERSITY	CHEMISTRY DEPT		DOWNSVIEW, ONTARIO	M3J 1P3
BONNER R F	MINISTRY ENVIRONMENT	PO BOX 213		REXDALE, ONTARIO	M9W 5L1
BOULANGER PIERRE	1790 SHEPPARD			SILLERY, QUEBEC	G1S 1K7
BOYD R K	UNIV OF GUELPH	CHEMISTRY DEPT		GUELPH, ONTARIO	N1G 2W1
BUCKLEY J A	SCIEX INC	55 GLENCAMERON RD	SUITE 202	THORNHILL, ONTARIO	L3T 1P2
CASHMORE J M	TRENT UNIV	CHEMISTRY DEPT		PETERBOROUGH, ONTARI	K9J 7B8
COMISAROW M B	UNIV BRIT COLUMBIA	CHEMISTRY DEPT	2036 MAIN MALL	VANCOUVER, BC	V6T 1Y6
COULOMBE P L	ANALYTECH	742 MOONEY'S BAY PL		OTTAWA, ONTARIO	;
CROCKER I H	ATOMIC ENERGY CANADA	STATION 320C		CHALK RIVER, ONTARIO	K0J 1J0
DANYLEWYCH-MAY L L	SCIEX, INC	55 GLENCAMERON RD		THORNHILL, ONTARIO	L3T 1P2
DAVIDSON W R	SCIEX INC	55 GLENCAMERON RD	SUITE 202	THORNHILL, ONTARIO	L3T 1P2
DAWSON P H	NAT RESEARCH COUNCIL	PHYSICS DEPT		OTTAWA, ONTARIO	K1A 0R6
DOUGLAS D J	SCIEX INC	55 GLENCAMERON RD	SUITE 202	THORNHILL, ONTARIO	L3T 1P2
DURDEN DAVID A	PSYCHIATRIC RES DIV	508A UNIV HOSP		SASKATOON,SASK	S7N 0X0
EIGENDORF G K	UNIV BRIT COLUMBIA	CHEMISTRY DEPT		VANCOUVER, BC	V6T 1Y6
ENS WERNER E	UNIV OF MANITOBA	PHYSICS DEPT		WINNIPEG, MANITOBA	R3T 2N2
FLINN CHRISTOPHER G	ATLANTIC RES LAB	NAT'L RES COUNCIL	1411 OXFORD ST	HALIFAX, NOVA SCOTIA	B3H 3Z1
FOSTER M G	MINISTRY ENVIRONMENT	OTC	PO BOX 213	REXDALE, ONTARIO	M9W 5L1
FRENCH J B	UNIV OF TORONTO	INST FOR AEROSPACE S	4925 DUFFERIN ST	DOWNSVIEW ONTARIO	M3H 5T6
GODSE D D	CLARKE INST PSYCHIAT	250 COLLEGE STREET		TORONTO, ONTARIO	M5T 1R8
GORDON M	MERCK-ISOTOPES	612-1209 RICHMOND ST		LONDON, ONTARIO	N6A 3L7
HARRISON A G	UNIV OF TORONTO	CHEMISTRY DEPT		TORONTO, ONTARIO	M5S 1A1
HOGG A M	UNIV OF ALBERTA	CHEMISTRY DEPT		EDMONTON, ALBERTA	T6G 2G2
HOGGE L	PRARIE REGIONAL LAB			SASKATOON, SASK	S7N 0W8
HOLMES J L	UNIV OF OTTAWA	CHEMISTRY DEPT		OTTAWA, ONTARIO	K1N 9B4
JAMIESON W D	NRC	1411 OXFORD ST		HALIFAX, NOVA SCOTIA	B3H 3Z1
KALLOO M	MERCK SHARP & DOHME	PO BOX 899		POINTE CLAIRE QUEBEC	H9R 4P7
KAZDAN EVA	3615 RIDGEWOOD	NO. 402		MONTREAL, QUEBEC	H3V 1B4
KEBARLE P	UNIV OF ALBERTA	CHEMISTRY DEPT		EDMONTON, ALBERTA	T6G 2G2
LANE D A	31 DE VERE GDNS			TORONTO, ONTARIO	M5M 3E6
LAO R C	ENVIRONMENT CANADA	CHEMISTRY DIV	APCD	OTTAWA, ONTARIO	K1A 1C8
LAU BENJAMIN P	HEALTH & WELFARE CAN	FOOD RESEARCH	TUNNEY'S PASTURE	OTTAWA,ONTARIO	K1A 0L2
LOVETT A M	SCIEX INC	55 GLENCAMERON RD	SUITE 202	THORNHILL, ONTARIO	L3T 1P2
MAMER ORVAL	MCGILL UNIV	1130 PINE AVE WEST		MONTREAL, QUEBEC	H3A 1A3
MARCH R E	TRENT UNIVERSITY			PETERBOROUGH, ONT	K9J 7B8
MCGILLIVRAY D L	UNIV OF VICTORIA	CHEMISTRY DEPT		VICTORIA, BC	V8W 2Y2
MESSIER F Y	MCMASTER UNIVERSITY	CHEMISTRY DEPT	1280 MAIN ST WEST	HAMILTON, ONTARIO	L8S 4M1
MILES W F	PLANT PRODUCTS	LAB SERVICES DIV	BLDG #22, C.E.F.	OTTAWA, ONTARIO	K1A 0C6
MOIR R T	IMPERIAL OIL LTD	RESEARCH DEPT	PO BOX 3022	SARNIA, ONTARIO	N7T 7M1
OLTHETEN J B	2710	BRABANT MARINEAU		MONTREAL, QUEBEC	H4S 1L1
QUILLIAM M A	MCMASTER UNIVERSITY	CHEMISTRY DEPT		HAMILTON, ONTARIO	L8S 4M1
RAMALEY L	DALHOUSIE UNIVERSITY	CHEMISTRY DEPT		HALIFAX, NOVA SCOTIA	B3H 4J3
ROBINSON J R	CAN AGRICUL RESEARCH	UNIVERSITY POST OFF		LONDON, ONTARIO	N6A 5B7
SADLIER R W	10 WOODMAN SR	NO. 402		HAMILTON, ONTARIO	L8K 4E1
SCHMIT J P	SHERBROOKE UNIV	CHEMISTRY DEPT		SHERBROOKE,	J1K 2R1
SHUSHAN B I	UNIV OF GUELPH	CHEMISTRY DEPT		GUELPH, ONTARIO	N1G 2W1
STANDING K	UNIV OF MANITOBA	PHYSICS DEPT		WINNIPEG, MANITOBA	R3T 2N2
STRAIN PETER	DALHOUSIE UNIV	OCEANOGRAPHY DEPT		HALIFAX, NOVA SCOTIA	B3H 3Z1

SUN W F	UNIV OF WINDSOR	CHEMISTRY DEPT		WINDSOR,ONTARIO	N9B 3P4
TANNER SCOTT D	SCIEX INC	55 GLENCAMERON RD		THORNHILL, ONTARIO	L3T 1P2
THOMSON ROD	CAN CTR FOR INLAND	WWATER QUAL BRAN	867 LAKESHORE RD	BURLINGTON, ONTARIO	L7R 4A6
THOMSON B	SCIEX INC	55 GLENCAMERON RD	SUITE 202	THORNHILL, ONTARIO	L3T 1P2
VALLERAND PIERRE	LE CENTRE HOSP UN.	L2705 BOUL. LAURIER	LOCAL S-1	STE-FOY, PQ	G1V 4G2
WESTMORE J B	UNIV OF MANITOBA	CHEMISTRY DEPT		WINNIPEG, MANITOBA	R3T 2N2
WOOD G W	UNIV OF WINDSOR	CHEMISTRY DEPT		WINDSOR, ONTARIO	N9B 3P4
YAMDAGNI R	UNIV OF CALGARY	CHEMISTRY DEPT		CALGARY, ALBERTA	T2N 1N4
ZAMECNIK J	CTR OF FORENSIC SCI	25 GROSVENOR ST		TORONTO,ONTARIO	M7A 2G8

AYALA JORGE	APARTADO POSTAL 475			CUERNAVACA, MOR	MEXICO
BARBER MICHAEL	U.M.I.S.T.	CHEMISTRY DEPT	SACKVILLE STREET	MANCHESTER M60 1QD	ENGLAND
BEAUGRAND CLAUDE	NERMAG	49 QUAI DU HALAGE		92500 RUEIL MALMAISO	FRANCE
BEYNON JOHN H	UNIVERSITY COLLEGE	ROYAL SOC RES UNIT		SWANSEA SA2 8PP	WALES
BILL JOHN C	VG ANALYTICAL LTD	4 TAXMERE CLOSE	SANDBACH	CHESHIRE	ENGLAND
BOTTER RENE N	CEN SACLAY	DPC-SPP-SP	91191 GIF SUR YVETTE CEDEX		FRANCE
BRACHMANN KLAUS	NECKAR STR 26			2805 STUHR 1	W GERMANY
BRENTON GARETH	KRATOS LTD	BARTON DOCK ROAD		MANCHESTER M31 2LD	UNITED KINGD
BRUNNEE C	VARIAN MAT GMBH	BARKHAUSENSTR 2	POSTFACH 14 4062	D-2800 BREMEN 10	WEST GERMANY
BUSER H R	SWISS FEDERAL RESEAR			WADENSWIL	SWITZERLAND
CANTLE JOHN	VG ISOTOPES	ION PATH ROAD 3		WINSFORD CHESHIRE	UNITED KINGD
CHATILLON CHRISTIAN	E.N.S.E.E.G.	PP 44		38401 ST MARTIN D'HE	FRANCE
COVENEY D	KRATOS SCIEN APP LTD	BARTON DOCK ROAD	URMSTON	MANCHESTER, M31 2LD	ENGLAND
DE LEENHEER A P	LAB MED BIOCHEMIE	DE PINTELAAN 135		B-9000 GENT	BELGIUM
DELL A	IMPERIAL COLLEGE	BIOCHEMISTRY DEPT		LONDON, SW7	ENGLAND
DOLIVA GILLES	INST OF PHYSICAL CHE	EPFL-ECUSIENS		1015 LAUSANNE	SWITZERLAND
DROWART J D	VRIJE UNIV BRUSSELS	PLEINLAAN 2		B-1050 BRUSSELS	BELGIUM
EDDY MICHIELS	CBNM	STEENWEG NAAR RETIE		B-9440 GEEL	BELGIUM
ELLIOTT MARTIN	VG ISOTOPES	ION PATH	ROAD THREE	WINSFORD, CHESHIRE	UNITED KINGD
EPPLER HANS P	BALZERS			BALZERS FL9496	LIECHTENSTEI
EVANS S	KRATOS SCIEN APP LTD	BARTON DOCK ROAD	URMSTON	MANCHESTER, M3I 2LD	ENGLAND
FERREIRA M A	FACULTY OF SCIENCES	CHEMISTRY DEPT		1294 LISBON CODEX	PORTUGAL
FITCHES H J	KRATOS SCIEN APP LTD	BARTON DOCK ROAD	URMSTON	MANCHESTER, M3I 2LD	ENGLAND
FRASER-MONTEIRO LUIS	UNIV NOVA DE LISBOA	SEMIN. OLIVAIS		LISBON	PORTUGAL
FRASER-MONTEIRO MARIA	FISICA MOLECULAR	I.S.T. AV.	R. PAIS	1000 LISBON	PORTUGAL
FRIESEN M D	IARC/CIRC	150 COURS A THOMAS		69372 LYON	FRANCE
GAMES D E	UNIVERSITY COLLEGE	CHEMISTRY DEPT	PO BOX 78	CARDIFF, CF1 1XL	WALES
GASKELL S J	TENOVUS INSTITUTE	WELSCH NAT'L SCH OF		CARDIFF CF4 4XX	UNITED KINGD
GOWER J L	BEECHAM PHARMACEUTIC	BROCKHAM PARK	BETCHWORTH	SURREY	ENGLAND
HABFAST K E	VARIAN MAT GMBH	BARKHAUSENSTR 2	POSTFACH 14 4062	D-2800 BREMEN 10	WEST GERMANY
HAEGELE K D	MERRELL INTL	RESEARCH CENTER		67084 STRASBOURG	FRANCE
HAINES R C	VG ISOTOPES LTD	ROAD 3	WINSFORD	CHESHIRE	ENGLAND
HARAGUCHI S I	KURUME UNIVERSITY	RESEARCH INST GC-MS	SCHOOL OF MEDICINE	FUKUOKA, 830	JAPAN
HARRISON A	VG MICROMASS LTD	ION PATH	WINSFORD	CHESHIRE	ENGLAND
HARVEY D J	OXFORD UNIVERSITY	PHARMACOLOGY DEPT	SOUTH PARKS RD	OXFORD, OX1 3QT	ENGLAND
HOLMES JOHN M	VG ANALYTICAL	TUDOR ROAD	ALTRINCHAM	CHESHIRE WA14 5RZ	ENGLAND
HUA SU H	PO BOX 914			BEIJING	CHINA
HWANG CHANG-SHI	TAIWAN NORMAL UNIV	CHEMISTRY DEPT	88 ROOSEVELT RD.	TAIPEI, TAIWAN	REP OF CHINA
IHLE HANS R	PO BOX 1913			517 JULICH	W GERMANY
ISHIBASHI MASATAKA	NIPPON KAYAKU CO	3-31 SHIMO	KITA-KU	TOKYO 115	JAPAN
JANSSON MARGITH	KAROLINSKA INSTITUTE	MASS SPECTROMETRY LA		S-10401 STOCKHOLM	SWEDEN
JENCKEL LUDOLT	MUHLENTAL 15			282 BREMEN 77	GERMANY
JENNINGS K R	UNIV OF WARWICK	CHEMISTRY &MOLECULAR	SCIENCES DEPT	COVENTRY, CV4 7AL	ENGLAND
JONATHAN NEVILLE	SOUTHAMPTON UNIV	CHEMISTRY DEPT		SOUTHAMPTON SO5NH	ENGLAND
JONCKHEERE J A	BRANDSTRAAT 49 G			B-9131 BEERVELDE	BELGIUM
KEMP TREVOR R	VG ANALYTICAL LTD	TUDOR ROAD	ALTRINCHAM	CHESHIRE	UK
KING GRAHAM S	QUEEN CHARLOTTES HOS	CHEMICAL PATHOLOGY		LONDON W6 0XG	ENGLAND
KONDO MASAAKI	TORAY RESEARCH CTR	3-2-1 SONOYAMA OTSU-		SHIGA. PREF. 525	JAPAN
KOPRIO JURG	BALZERS	DEPT ECA		9496 BALZERS	LIECHTENSTEI
KRUEGER FRANZ	MESSELER STR. 24			D-61 DARMSTADT 12	W GERMANY
LANDI-MAURO M L	DOW LEPETIT	DURANDO 38		20158 MILANO	ITALY
LAUWERS L W	JANSSEN PHARMACEUTIC	TURNHOUTSE BAAN		B-2340 BEERSE	BELGIUM
LECLERCQ P A	EINDHOVEN UNIV TECH	PO BOX 513		5600-MB EINDHOVEN	NETHERLANDS
LIFSHITZ CHAVA	HEBREW UNIV	PHYSICAL CHEM DEPT	MAIL CODE 91904	JERUSALEM	ISRAEL
LUEG V	VARIAN MAT	BARKHAUSENSTR 2		D-2800 BREMEN	WEST GERMANY

MARNELA K M	TAMPERE UNIV	PO BOX 607		33101 TAMPERE 10	FINLAND
MATSUMOTO I M	KURUME UNIVERSITY	RESEARCH INST GC-MS	SCHOOL OF MEDICINE	FUKUOKA, 830	JAPAN
MCDOWELL R A	IMPERIAL COLLEGE	BIOCHEMISTRY DEPT		LONDON, SW7 2AZ	ENGLAND
MILLINGTON D S	VG ORGANIC LTD	TUDOR ROAD	ALTRINCHAM	CHESIRE, WA14 5RZ	ENGLAND
MITSUTAKE K M	KURUME UNIVERSITY	RES INST OF GC/MS		FUKUOKA, 830	JAPAN
MOCHIZUKI KOHEI	HITACHI LTD	NAKA WORKS	882 ICHIGE	KATSUTA, IBARAKI	JAPAN
MORGAN ROGER	THORNTON RESEARCH CTR	PO BOX 1		CHESTER	UNITED KINGD
MORRIS H R	IMPERIAL COLLEGE	BIOCHEMISTRY DEPT		LONDON	ENGLAND
PANICO M	IMPERIAL COLLEGE	BIOCHEMISTRY DEPT		LONDON	ENGLAND
PHILP PAUL	CSIRO	PO BOX 136		N RYDE 2113	AUSTRALIA
PLATZNER T I	NRC NEGEV	CHEMISTRY DEPT	PO BOX 9001	BEER-SHEVA	ISRAEL
PORTER CHRIS J	SWANSEA UNIV	ROY SOC RESEARCH UNIS	INGLETON PARK	SWANSEA, S WALES	UNITED KINGD
POWERS PATRICK	296 BRAMHALL LN SOUT	BRAMHALL		CHESHIRE SK7 3DJ	ENGLAND
PRZYBYLSKI M P	UNIV MAINZ	INST ORG CHEMIE		D-6500 MAINZ	WEST GERMANY
RADDATZ H	VARIAN MAT-GMBH	BARKHAUSENSTR 2		D-2800 BREMEN	WEST GERMANY
RAPP U	VARIAN GMBH	BARKHAUSENSTR 2		D-2800 BREMEN	WEST GERMANY
ROBINSON J D	VG DATA SYSTEMS	TRIBUNE ROAD		ALTRINCHAM, CHESHIRE	ENGLAND
RYAN P A	KRATOS SCIEN APP LTD	BARTON DOCK ROAD	URMSTON	MANCHESTER, M31 2LD	ENGLAND
SAITO K	KANSAI MEDICAL SCH	DEPT MEDICAL CHEM	MORIGUCHI	OSAKA 570	JAPAN
SAKAI I	TORRAY RESEARCH CTR	1111 TEBIRO		KAMAKURA	JAPAN
SCHLUNEGGER U P	UNIVERSITAT BERN	INSTIT ORGAN CHEMIE	FREIESTRASSE 3	CH-3012 BERN	SWITZERLAND
SCHMIDT GUNTER	REMBRANDT STR. 12			2872 HUDE	W GERMANY
SCHMIDT MIKE P	FINNIGAN MAT	BARKHAUSEN STR. 2		D-2800 BREMEN	W GERMANY
SEDGWICK R D	U.M.I.S.T.	CHEMISTRY DEPT	SACKVILLE ST	MANCHESTER M60 1QD	UNITED KINGD
SELF R	AGR RES COUNCIL	FOOD RES INSTITUTE		NORWICH, NR4 7UA	ENGLAND
SHINKA T S	KURUME UNIVERSITY	RES INST OF MED MS		FUKUOKA, 830	JAPAN
SMITH CHARLES	VG ANALYTICAL	TUDOR ROAD	ALTRINCHAM	CHESHIRE	ENGLAND
SUZUKI M	MEIJO UNIVERSITY	PHARMACY FACULTY	TEMPAKU	NAGOYA, 468	JAPAN
SZABO I	UNIVERSITY OF LUND	CHEMICAL CENTER	PO BOX 740	S-22007 LUND 7	SWEDEN
TATEMATSU A	MEIJO UNIVERSITY	PHARMACY FACULTY	TEMPAKU	NAGOYA, 468	JAPAN
TAYLOR LESTER	KRATOS LTD	BARTON DOCK ROAD	URMSTON	MANCHESTER	UNITED KINGD
TSUCHIYA M	4 37 27 KUGAYAMA	SUGINIMI KU		TOKYO, 168	JAPAN
UENO TAMIO	KYOTO UNIV	PESTICIDE RESEARCH I		606 KYOTO	JAPAN
VIGNY PAUL	INSTITUTE CURIE	11 PIERRE ET MARIE		75231 PARIS	FRANCE
VINCZE A	ISRAEL INST BIOL RES	PO BOX 19		NESS ZIONA, 70400	ISRAEL
WANG XIE Q	PO BOX 914			BEIJING	CHINA
WIKSTROM S A	HUDDINGE UNIV HOSP	RESEARCH CENTER F61		S-14186 HUDDINGE	SWEDEN
WILLIAMS DUDLEY H	UNIV OF CAMBRIDGE	CHEMICAL LAB	LENSFIELD RD	CAMBRIDGE LB2 1EW	ENGLAND
YINON J	WEIZMANN INS SCIENCE			REHOVOT	ISRAEL
ZARETSKII Z V	WEIZMANN INS SCIENCE	PO BOX 26		REHOVOT	ISRAEL
ZMORA HAZAI	SOREG RESEARCH CTR			YAVNEH 70600	ISRAEL

ABAJIAN H B	HOFFMANN-LAROCHE,INC	BLDG 71, RM 108	340 KINGSLAND RD	NUTLEY	NJ	07110
ABBEY L E	GEORGIA TECH	CHEMISTRY DEPT		ATLANTA	GA	30332
ABBOTT ROBERT C	SUNY MED SCHOOL	BIOPHYSICS DEPT	118 CARY HALL	BUFFALO	NY	14214
ABERNATHEY R M	120 MONTE REY DR N			LOS ALAMOS	NM	87544
ABERNATHY R N	PENN STATE UNIV	152 DAVEY LAB		UNIVERSITY PARK	PA	16802
ABERTH W	440 PAGE MILL RD			PALO ALTO	CA	94306
ABRAHAM ROBERT T	MAYO CLINIC	PHARMACOLOGY DEPT		ROCHESTER	MN	55901
ABRAMSON F P	GEORGE WASHINGTON UN	PHARMACOLOGY DEPT		WASHINGTON	DC	20037
ACZEL T	EXXON R/E	PO BOX 4255		BAYTOWN	TX	77520
ADAMS R A	3480 TANBARK CT NE			ATLANTA	GA	30319
AICHELE DANIEL	BATTELLE COLS	505 KING AVE		COLUMBUS	OH	43001
ALDOUS K M	NY STATE HEALTH DEPT	TOXICOLOGY INST	TOWER BLDG	ALBANY	NY	12201
ALFORD E D	B/W RES	PO BOX 35090		LOUISVILLE	KY	40232
ALKALAY D	CIBA-GEIGY CORP	444 SAWMILL RIVER RD		ARDSLEY	NY	10502
ALLEN R H	R H ALLEN CO	PO BOX 27		BOULDER	CO	80306
ALLISON J	MICHIGAN STATE UNIV	CHEMISTRY DEPT		EAST LANSING	MI	48824
ALTEMOSE V D	CORNING GLASS WORKS			CORNING	NY	14830
ALWAN A K	536 S. CLARK ST.			CHICAGO	IL	60605
ANBAR M	181 HALWILL DR			SNYDER	NY	14226
ANDEREGG R J	UNIV OF MAINE	473 AUBERT HALL		ORONO	ME	04469
ANDERSON F W	IBM CORP	Z41 C		HOPEWELL JUNCTION	NY	12533
ANDERSON LAWRENCE	NIH,NCI	BLDG 37	ROOM 5A01	BETHESDA	MD	20805
ANDREWS P A	1121 GLENEAGLE RD			BALTIMORE	MD	21239
ANDRZEJEWSKI D A	4114 DAVIS PLACE NW	APT 303		WASHINGTON	DC	20007
ANICICH V G	8036 GRAYSTONE			SUNLAND	CA	91040
ASHE T R	EXXON R/E	PO BOX 121		LINDEN	NJ	07036
AULD J W	37748 SUNNYDALE			LIVONIA	MI	48154
AUSLOOS P J	700 NEW HAMPSHIRE AV			WASHINGTON	DC	20037
AVERY M J	IOWA STATE UNIV	9 GILMAN		AMES	IA	50011
AYERS R J	1560 E JEFFERSON			DETROIT	MI	48207
BACZYNSKYJ L	THE UPJOHN CO	301 HENRIETTA		KALAMAZOO	MI	49001
BAER T	UNIV NORTH CAROLINA	CHEMISTRY DEPT		CHAPEL HILL	NC	27514
BAFUS D A	4114 CLOVERNOOK LANE			SEABROOK	TX	77586
BAILLIE T A	UNIV OF CALIFORNIA	PHARMACEUTICAL CHEM		SAN FRANCISCO	CA	94143
BAKKE JEROME E	METABOLISM & RAD. RES	TATE U. STATION		FARGO	ND	58105
BALLARD J M	UNIV OF VIRGINIA	CHEMISTRY DEPT		CHARLOTTESVILLE	VA	22901
BALU K	CIBA-GEIGY CORP	AGRICULTURE DIV	SWING ROAD	GREENSBORO	NC	27409
BARBALAS M P	CORNELL UNIV	BAKER LAB		ITHACA	NY	14853
BARLAK T M	7400 VERNON SQ DR	APT 303		ALEXANDRIA	VA	22306
BAROFSKY D F	OREGON GRAD CENTER	19600 NW WALKER RD		BEAVERTON	OR	97005
BARRON R P	FDA	HFD-420	200 C ST SW	WASHINGTON	DC	20204
BARTHOLOMEW D R	CORNELL UNIVERSITY	G-24 URIS HALL		ITHACA	NY	14853
BARTMESS J E	INDIANA UNIV	CHEMISTRY DEPT		BLOOMINGTON	IN	47405
BARTNER P J	SCHERING CORP	60 ORANGE		BLOOMFIELD	NJ	07003
BASILE B P	UNIV OF UTAH	MEDICINAL CHEMISTRY	SKAGGS HALL	SALT LAKE CITY	UT	84112
BAUER MARK	MICHIGAN STATE UNIV	CHEMISTRY DEPT		EAST LANSING	MI	48824
BEAUCHAMP JESSE L	CALTECH	NOYES LAB 127-72		PASADENA	CA	91125
BECK MARY D	FOREMOST MCKESSON	DUBLIN RES & DEV	6363 CLARK AVE	DUBLIN	CA	94566
BEGGS D P	HP SCIENTIFIC INSTR	1601 CALIFORNIA AVE		PALO ALTO	CA	94304
BEIER BARBARA	EXXON RES & ENGIN	PO BOX 4255		BAYTOWN	TX	77520
BEIMER R G	TRW SYSTEMS 01/2020	ONE SPACE PARK		REDONDO BEACH	CA	90646
BENCSATH F A	430 E. 63RD ST	APT 3 G		NEW YORK	NY	10021
BENDORAITIS J G	MOBIL RESEARCH & DEV			PAULSBORO	NJ	08066
BENZ W	HOFFMANN-LAROCHE,INC			NUTLEY	NJ	07110
BERG PETER J	MAYO CLINIC	ENDO. RESEARCH	200 1ST, S.W.	ROCHESTER	MN	55901

BERGER P S	TEKNIVENT CORP	9261 OLD BONHOMME RD		ST LOUIS	MO	63132
BETOWSKI L D	EPA-EMSL	QUAL ASSURANCE DIV	PO BOX 15027	LAS VEGAS	NV	89114
BEZUK STEVE J	UNIV OF MINNESOTA	CTR FOR PLASMA CHEM	100 UNION ST, SE	MINNEAPOLIS	MN	55108
BHATTACHARYA A K	MOBIL CHEMICAL CO	PO BOX 240		EDISON	NJ	08817
BIEMANN K	MIT	CHEMISTRY, 56-010		CAMBRIDGE	MA	02139
BIGLEY M J	VARIAN MAT	205 W TOUHEY RD		PARK RIDGE	IL	60068
BINIAKEWITZ R C	25 WARDWELL ST			STAMFORD	CT	06902
BLAKLEY C R	UNIV OF HOUSTON	CHEMISTRY DEPT		HOUSTON	TX	77004
BLUETT LYNN J	154 BIRCHWOOD DR			ROCHESTER	NY	14622
BOAL JIM R	UPJOHN	301 HENRIETTA ST		KALAMAZOO	MI	49001
BOCKHOFF FRANK M	STANDARD OIL CO	4440 WARRENSVILLE CT		CLEVELAND	OH	44128
BOETTGER H G	5346 N STARDUST RD			LA CANADA	CA	91011
BOGDAN M R	SUPELCO, INC	SUPELCO PARK		BELLEFONTE	PA	16823
BOITNOTT CHARLES A	FINNIGAN INST	845 W. MAUDE		SUNNYVALE	CA	94062
BONDAROVICH HENRY A	5 CASALE DR			WARREN	NJ	07060
BONE L J	DOW CHEMICAL	B-1226		FREEPORT	TX	77541
BONE WILLIAM M	UNIV OF VIRGINIA	CHEMISTRY DEPT	MC CORMICK RD	CHARLOTTESVILLE	VA	22903
BONNELL DAVID W	NATL BUR OF STANDARDS	A329 223		WASHINGTON	DC	20234
BORDOLI R S	UMIST	PO BOX88	SACKVILLE ST.	MANCHESTER M60 1QD		
BOSTWICK DAVID	GEORGIA INST OF TECH	CHEMISTRY DEPT		ATLANTA	GA	30332
BOWERS LARRY D	UNIV OF MINNESOTA	LABORATORY MEDICINE	BOX 198 MAYO	MINNEAPOLIS	MN	55455
BOWERS M T	UNIV OF CALIFORNIA	CHEMISTRY DEPT		SANTA BARBARA	CA	93106
BRADFORD DON C	FINNIGAN MAT	845 W MAUDE AVE		SUNNYVALE	CA	94086
BRADLEY J C	KOR ISOTOPES	56 ROGERS		CAMBRIDGE	MA	02142
BRAIN D K	PROCTOR & GAMBLE	IVORYDALE TECH CENTR		CINCINNATI	OH	45217
BRENT D A	BURROUGHS WELLCOME	3030 CORNWALLS		RESEARCH TRIANGLE PK	NC	27709
BRIGGS P R	29 AUSTIN LANE			HOLLISTON	MA	01746
BRIGGS ROBERT G	NY ST DEPT OF HEALTH	TOWER BLDG, ESP	MASS SPECTROMETRY	ALBANY	NY	12201
BRILLANTE S M	CROWN ZELLERBACH	904 NW DRAKE ST		CAMAS	WA	98607
BRITTEN R A	84 WEST MARIPOSA ST			ALTADENA	CA	91001
BROTHERTON S A	MICHIGAN TECH UNIV	CHEMISTRY & CHEM ENG		HOUGHTON	MI	49931
BROUSEK L M	IITRI	ANALYTICAL CHEMISTRY	10 WEST 35TH ST	CHICAGO	IL	60616
BROWN C L	CALIFORNIA STATE UN	CHEMISTRY DEPT		LOS ANGELES	CA	90032
BROWN H L	UTI	325 N MATHILDA AVE	PO BOX 519	SUNNYVALE	CA	94086
BROWN JOHNIE C	196 ROCK AVENUE			PARK RIDGE	NJ	07656
BROWNAWELL MARILYN L	320 ROBERTS LN			SCOTCH PLAINS	NJ	07076
BRUBAKER W M	1954 HIGHLAND OAKS			ARCADIA	CA	91006
BRUNFELDT ROBERT J	2721 EVERGREEN DR			BARTLESVILLE	OK	74003
BRYANT WILLIAM F	NATL CTR TOX RES	HFT 154		JEFFERSON	AR	71029
BUDDE W L	EPA	26 W ST CLAIR ST		CINCINNATI	OH	45268
BUFF RANDY D	NATL BUR OF STANDARDS	BLDG 222, A158		WASHINGTON	DC	2023
BURINSKY D J	PURDUE UNIVERSITY	CHEMISTRY DEPT	BOX 321	WEST LAFAYETTE	IN	47907
BURLINGAME A L	UNIV OF CALIFORNIA	PHARMCEUTICAL CHEM		SAN FRANCISCO	CA	94143
BURR P H	286 S ROOSEVELT AVE			PASADENA	CA	91107
BURROWS D G	NORTHWEST & ALASKA	FISHERIES CENTER	2725 MONTLAKE BLVD E	SEATTLE	WA	98112
BURSEY M M	UNIV NORTH CAROLINA	CHEMISTRY DEPT 045A		CHAPEL HILL	NC	27514
BUSCH K L	WOODFIELD ACRES #6			WEST LAFAYETTE	IN	47906
BUSH E D	3645 WHITMAN AVE N	#204		SEATTLE	WA	98103
BUTLER G F	PPG INDUSTRIES	PO BOX 4026		CORPUS CHRISTI	TX	78408
BUTLER J J	UNIV NORTH CAROLINA	VENABLE LABS 045A		CHAPEL HILL	NC	27514
BUTTERWORTH BRIAN	US EPA	ENVIR RES LAB	6201 CONGDON BLVD	DULUTH	MN	55804
BUTTRILL S E	SRI INTERNATIONAL	333 RAVENSWOOD AVE	RM 204A	MENLO PARK	CA	94025
BYRD G D	PURDUE UNIV	CHEMISTRY BLDG		WEST LAFAYETTE	IN	47907
CAFARELLA JOHN	BALZERS	8 SAGAMORE PARK RD		HUDSON	NH	03057
CALDECOURT VICTOR	DOW CHEMICAL CO	1603 BLDG		MIDLAND	MI	48640

CALDWELL GARY	INDIANA UNIV	CHEMISTRY DEPT		BLOOMINGTON	IN	47401
CALLERY P S	UNIV OF MARYLAND	636 W LOMBARD ST		BALTIMORE	MD	21201
CALLIS E L	ARGONNE NATIONAL LAB	BLDG 200	9700 S CASS AVE	ARGONNE	IL	60439
CAMERON DOUGLAS	UNION OIL CO OF CA	SCI & TECH DIV		BREA	CA	92621
CAMPANA JOSEPH E	NAVAL RES LAB	CHEMISTRY DIV	CODE 6110	WASHINGTON	DC	20375
CAMPBELL GARY L	NORTH CARO ST UNIV	PO BOX 5995	BURLINGTON LABS	RALEIGH	NC	27650
CAMPBELL SCOTT	SHELL DEV CO	PO BOX 4248		MODESTO	CA	95352
CANADA DAVID C	UNION CARBIDE	PO BOX P	K1004B	OAK RIDGE	TN	37830
CAPELLEN J M	IOWA STATE UNIV	AMES LAB		AMES	IA	50011
CAPP R J	3611 ECHODALE AVE			BALTIMORE	MD	21214
CAPRIOLI R M	UNIV OF TEXAS HSC	PO BOX 20708		HOUSTON	TX	77030
CARDACIOTTO STANLEY	AMER CYANAMID CO	PO BOX 400		PRINCETON	NJ	08540
CARLIN DIANA	105-B MARRIED ST CTS			W LAFAYETTE	IN	47906
CARLIN J R	MERCK SHARP & DOHME	RESEARCH LABORATORY	PO BOX 2000	RAHWAY	NJ	07065
CARLIN T J	PURDUE UNIV	BOX 347	CHEMISTRY DEPT	WEST LAFAYETTE	IN	47907
CARLSEN STEPHEN	CIBA-GEIGY CORP			ARDSLEY	NY	10502
CARLSON MARK	1107 GIBRALTER AVE			FARGO	ND	58102
CARNEY THOMAS E	UNIV OF N CAROLINA	CHEMISTRY DEPT		CHAPEL HILL	NC	27514
CARR STEVEN A	LHRRB RM B-08	45 SHATTUCK ST		BOSTON	MA	02115
CARROLL DAVID I	BAYLOR COLL MEDICINE	INST LIPID RESEARCH	TEXAS MEDICAL CENTER	HOUSTON	TX	77030
CARTER G T	CIBA-GEIGY CORP	OLD MILL RD		SUFFERN	NY	10901
CARTER MIKE H	US EPA	WH-552	401 M STREET SW	WASHINGTON	DC	20460
CARY ALLEN M	FINNIGAN MAT	845 W MAUDE AVE		SUNNYVALE	CA	94086
CASSADY C J	400 N RIVER RD	NO 303		WEST LAFAYETTE	IN	47906
CATTRAN L C	HEWLETT PACKARD	1601 CALIFORNIA AVE		PALO ALTO	CA	94304
CEPA STEVEN	FINNIGAN MAT	666 INDUSTRIAL DR		ELMHURST	IL	60126
CHAI J W	MICHIGAN STATE UNIV	CHEMISTRY DEPT		EAST LANSING	MI	48824
CHAIT B T	ROCKEFELLER UNIV	1230 YORK AVE		NEW YORK	NY	10021
CHAKEL J A	MICHIGAN STATE UNIV	CHEMISTRY DEPT		EAST LANSING	MI	48824
CHAMBERLIN W S	2183-B 36TH ST			LOS ALAMOS	NM	87544
CHAN KELVIN	50 RAL	BOX 88	1209 W CALIFORNIA AV	URBANA	IL	61801
CHANG C	WRIGHT STATE UNIV	BREHM LAB		DAYTON	OH	45431
CHANG S Y	MCNEIL PHARMACEUTICAL	WELSH & MCKEAN RD		SPRING HOUSE	PA	19477
CHANG T L	AMERICAN CYANAMID	1937 W MAIN ST		STAMFORD	CT	06904
CHARKOWSKI DENNIS M	UNIV OF IOWA	PHARMACOLOGY DEPT	TOXICOLOGY CTR	IOWA CITY	IA	52242
CHASTAGNER P	E I DUPONT	SAVANNAH RIVER LAB		AIKEN	SC	29801
CHEN TUNG-HO	ARRADCOM	EMD, BLDG 407		DOVER	NJ	07801
CHENG MICHAEL T	CORNELL UNIV	BAKER LAB	BOX 396	ITHACA	NY	14850
CHEPLEN MARK	ICI AMERICAS	PO BOX 208		GOLDSBORO	NC	27530
CHESS E K	UNIV OF NEBRASKA	CHEMISTRY DEPT	BOX 715	LINCOLN	NE	68588
CHHEDA G B	ROSWELL PRK INSTITUT	666 ELM STREET		BUFFALO	NY	14263
CHIANG T C	JOHNSON & JOHNSON	RESEARCH CENTER	RT 1	NORTH BRUNSWICK	NJ	08903
CHINN D M	UNIV OF UTAH	CTR HUMAN TOXICOLOGY	SKAGGS HALL 38	SALT LAKE CITY	UT	84112
CHO D K	SYNTEX RESEARCH	3401 HILLVIEW AVE		PALO ALTO	CA	94304
CHOU F E	334 OVERBROOK RD			BALTIMORE	MD	21212
CHURCHILL L B	UOP INC	TEN UOP PLAZA	ALGONQUIN/MT PRSPECT	DES PLAINES	IL	60016
CIUPEK JAMES D	PURDUE UNIV	CHEMISTRY DEPT	BOX 360	W LAFAYETTE	IN	47907
CLARK E E	ORNL, UNION CARBIDE	PO BOX P	MS 458	OAK RIDGE	TN	37830
CLARK JUSTIN	UNIV OF UTAH	BIOPHYSICS DEPT	320 12TH AVE	SALT LAKE CITY	UT	84103
COATES M L	824-D CABELL AVE			CHARLOTTESVILLE	VA	22903
COHEN A I	SQUIBB INST MED RES	PO BOX 4000		PRINCETON	NJ	08540
COLBY BRUCE N	SYSTEMS,SCI. & SOFTW	PO BOX 1260		LA JOLLA	CA	92037
COLLINS G J	STAUFFER CHEM CO			DOBBS FERRY	NY	10522
COMPSON K R	26A FRANKLIN AVE			MONTVALE	NJ	07645
CONNELL JOHN D	603 ROSE CT			LISLE	IL	60532

CONNOLLY MICHAEL	MONTANA STATE UNIV	CHEMISTRY DEPT		BOZEMAN	MT	59715
CONWAY D C	TEXAS A&M UNIVERISTY	CHEMISTRY DEPT		COLLEGE STATION	TX	77843
CONZEMIUS R J	1211 GARFIELD AVE			AMES	IA	50010
COOK J C	UNIV OF ILLINOIS	CHEMICAL SCIENCES		URBANA	IL	61801
COOK KELSEY D	UNIV OF ILLINOIS	44 ROGER ADAMS LAB,8	1209 W CALIFORNIA	URBANA	IL	61801
COOKS R G	PURDUE UNIVERSITY	CHEMISTRY DEPT		WEST LAFAYETTE	IN	47907
COOPER D A	DEA SPECIAL TESTING	7704 OLD SPRINGHOUSE		MCLEAN	VA	22101
CORY H T	OREGON GRAD CENTER	19600 NW WALKER RD		BEAVERTON	OR	97005
COSTELLO C E	MIT	CHEMISTRY, 56-029	77 MASS AVE	CAMBRIDGE	MA	02139
COSULICH D B	LEDERLE LABORATORIES			PEARL RIVER	NY	10965
COTTER R J	JOHNS HOPKINS UNIV	MID ATLANTIC MS LAB	725 N WOLFE ST	BALTIMORE	MD	21205
COUTANT J E	DOW CHEMICAL	PO BOX 68511		INDIANAPOLIS	IN	46268
CRAIN PAMELA F	UNIV OF UTAH	310 SKAGGS HALL		SALT LAKE CITY	UT	84112
CRANDALL R K	350 JOHN ST			ROCHESTER	NY	14623
CRAWFORD D W	US DEPT OF ENERGY	9800 S CASS AVE		ARGONNE	IL	60439
CRAWFORD RICHARD W	LLNL	PO BOX 808	L 310	LIVERMORE	CA	94550
CROW F W	UNIV OF NEBRASKA	CHEMISTRY DEPT	MCMS	LINCOLN	NE	68588
CROWLEY JAN R	UNIV OF FLORIDA	RADIOLOGY DEPT	BOX J374	GAINESVILLE	FL	32601
CRUMP JOY A	MAR, INC	EPA CEN REG LAB	536 S CLARK ST	CHICAGO	IL	60605
CURRY Z F	51 OAKHURST CIRCLE			PITTSBURGH	PA	15238
CURTIS H M	HALLIBURTON SERVICES	CHEMISTRY DEPT		DUNCAN	OK	73533
CURTIS TOMMIE G	MONSANTO CO	800 N LINDBERGH		ST LOUIS	MO	63166
CZUCZWA J	INDIANA UNIV	CHEMISTRY DEPT		BLOOMINGTON	IN	47401
DANACEAU M S	7 BROOKES AVE			GAITHERSBURG	MD	20760
DANIELSON JAMES	FD & DRUG ADMIN	MCMI	240 HENNEPIN	MINNEAPOLIS	MN	55401
DANNACHER J D	NATL BUR OF STAN	225-C313		GAITHERSBURG	MD	20760
DASS CHHABIL	UNIV OF NEBRASKA	CHEMISTRY DEPT	30 HAMILTON HALL	LINCOLN	NE	68588
DAS PRADIP R	UNIV OF NEBRASKA	CHEMISTRY DEPT	541 HAMILTON HALL	LINCOLN	NE	68588
DAVES G D	OREGON GRAD CENTER	19600 NW WALKER ROAD		BEAVERTON	OR	97005
DAVIDSON WALTER	HALCON	PHILLIPS PKWY		MONTVALE	NJ	07643
DAVIS DEAN V	PURDUE UNIVERSITY	CHEMISTRY DEPT		WEST LAFAYETTE	IN	47907
DAVIS WILLIAM S	18200 W HIGHWAY 72			GOLDEN	CO	80401
DAY R A	UNIV OF CINCINNATI	CHEMISTRY DEPT		CINCINNATI	OH	45221
DAY ROBERT J	235 VESTAL AVE			ENDICOTT	NY	13760
DEAL D E	34 WAWONA ST			SAN FRANCISCO	CA	94127
DECORPO J J	NRL	CODE 6110		WASHINGTON	DC	20375
DEINZER MAX L	OREGON STATE UNIV	AGRICUL CHEM DEPT		CORVALLIS	OR	97331
DEJONGH DON C	FINNIGAN INST	11 TRIANGLE PARK DR		CINCINNATI	OH	45246
DELMORE J E	ACC	ANALYTICAL DIV	550 2ND ST	IDAHO FALLS	ID	83401
DERODS F L	BATTELLE LABS	505 KING AVE		COLUMBUS	OH	43201
DESIDERIO D M	UNIV OF TENNESSEE	STOUT NEUROSCIENCE	800 MADISON AVE	MEMPHIS	TN	38163
DE STEFANO A J	PROCTER & GAMBLE	MIAMI VALLEY LAB	PO BOX 39175	CINCINNATI	OH	45239
DINO J J	NEW YORK UNIVERSITY	INST OF ENV MEDICINE	LONGMEADOW RD	TUXEDO	NY	10987
DINWIDDIE DUANE E	MERICHEM CO	1503 CENTRAL		HOUSTON	TX	77012
DOLCATER DAVE L	AMOCO PROD CO	PO BOX 591		TULSA	OK	74102
DOLE M	BAYLOR UNIVERSITY	CHEMISTRY DEPT		WACO	TX	76703
DORN STEVEN B	RALTECH SCIEN. SERVI	3301 KINSMAN BLVD		MADISON	WI	53704
DOUCET R J	VACUMETRICS INC	2261-#1 PALMA DR		VENTURA	CA	93003
DOUGHERTY R C	FLORIDA STATE UNIV	CHEMISTRY DEPT		TALLAHASSEE	FL	32306
DRAWBAUGH R B	8800 STARCREST DR	NO 39		SAN ANTONIO	TX	78217
DUBAY G R	COLUMBIA NATIONAL	FISHERIES RESEARCH	ROUTE 1	COLUMBIA	MO	65201
DUGGER D L	114 LEOLEIS DR			MARLBORO	MA	01752
DUHOLKE W K	THE UPJOHN CO	7171 PORTAGE RD		KALAMAZOO	MI	49001
DUNBAR R C	CASE WESTERN RESERVE	CHEMISTRY DEPT		CLEVELAND	OH	44106
DUTKY R C	14112 NEW HAMP AVE			COLESVILLE	MD	20904

DYER ROBERT	ACUREX CORP	405 CLYDE AVE	BLDG 12	MT VIEW	CA	94042
DYMERSKI P P	OH MATERIALS	PO BOX 1022		FINDLAY	OH	45840
EADON G A	NYS DEPT OF HEALTH	DIV OF LABORATORIES AND RESEARCH, E.S.P.		ALBANY	NY	12201
EBY R E	ORNL, UNION CARBIDE	PO BOX Y		OAK RIDGE	TN	37830
ECHO M W	EXXON NUCLEAR	PO BOX 536		IDAHO FALLS	ID	83401
EDMONDS C G	UNIV OF UTAH	COLLEGE OF PHARMACY	MEDICINAL CHEM DEPT	SALT LAKE CITY	UT	84112
EDELSON MARTIN C	IOWA STATE UNIV	AMES LABORATORY		AMES	IA	50011
EDWARDS J G	UNIV OF TOLEDO	CHEMISTRY DEPT		TOLEDO	OH	43606
EHRESMAN DAVID J	ST PAUL RAMSEY HOSP	640 JACKSON ST		ST PAUL	MN	55101
EIDNES MARTHA	HENKEL CORP	2010 E HENNEPIN		MINNEAPOLIS	MN	55413
EINOLF W N	PHILIP MORRIS USA	RESEARCH CENTER	PO BOX 26583	RICHMOND	VA	23261
ELDER F A	237 JUDSON ST			WEBSTER	NY	14580
ELLEFSON R E	MRC	MOUND LAB R171		MIAMISBURG	OH	45342
ELLENBERGER MARK R	UNIV OF MINNESOTA	CHEMISTRY DEPT 165	207 PLEASANT ST, SE	MINNEAPOLIS	MN	55455
ELLIOTT W H	ST LOUIS UNIV	BIOCHEMISTRY DEPT	1402 S GRAND	ST LOUIS	MO	63104
ELLIS ROBERT H	HEWLETT PACKARD	SCIEN INSTR DIV	1601 CALIFORNIA AVE	PALO ALTO	CA	94304
ENG J F	PRINCETON UNIV	CHEMISTRY DEPT		PRINCETON	NJ	08544
ENKE C G	MICHIGAN STATE UNIV	CHEMISTRY DEPT		EAST LANSING	MI	48824
ERNIE DOUGLAS	UNIV OF MINNESOTA	CTR OF PLASMA CHEMIS	100 UNION ST, SE	MINNEAPOLIS	MN	55455
ESKEW T J	NUCLIDE CORP	642 E COLLEGE AVE		STATE COLLEGE	PA	16801
ESPINOSA-LENIZ R	NATL BUR OF STAN	BLDG 222,RM A113		WASHINGTON	DC	20234
EVANS JAMES E	E KENNEDY SHRIVER CT	200 TRAPELO RD		WALTHAM	MA	02254
EVANS J V	MILES LABORATORIES	CHEMISTRY DEPT	PO BOX 40	ELKHART	IN	46515
FALES H M	6502 STONEHAM RD			BETHESDA	MD	20034
FARNETH WILLIAM E	UNIV OF MINNESOTA	CHEMISTRY DEPT		MINNEAPOLIS	MN	55455
FASSETT J D	NBS	BLDG 221, RM A21		WASHINGTON	DC	20234
FATLAND CHARLOTTE	ESDA-SEA	META & RAD RES LAB	ST UNIV STATION BOX	FARGO	ND	58105
FAULL K F	STANFORD UNIVERSITY	PSYCHIATRY DEPT	MEDICAL SCHOOL	STANFORD	CA	94305
FEIL V J	1438 3RD ST N			FARGO	ND	58102
FENNESSEY P V	UNIV OF COLORADO	MEDICAL CENTER, C233	4200 E 9TH AVE	DENVER	CO	80262
FENSELAU C C	JOHNS HOPKINS UNIV	PHARMACOLOGY DEPT	725 N WOLFE ST	BALTIMORE	MD	21205
FERGUSON ELDON	AERONOMY LAB	NOAA		BOULDER	CO	80303
FERREIRO LUIS M	UNIV OF MINNESOTA	CHEMISTRY DEPT	207 PLEASANT ST, SE	MINNEAPOLIS	MN	55455
FIELD F H	ROCKEFELLER UNIV	1230 YORK AVE		NEW YORK	NY	10021
FIES W J	155 CHEROKEE WAY			PORTOLA VALLEY	CA	94025
FINNIGAN R E	FINNIGAN CORP	845 W MAUDE AVE		SUNNYVALE	CA	94086
FINNEY RAYMOND J	MONSANTO RES CORP	MOUND FACILITY, R-2		MIAMISBURG	OH	45342
FISH FRED P	2220 GREAT ROCK RD			BIRMINGHAM	AL	35216
FITE WADE L	EXTRANUCLEAR LAB	100 BETA DR	PO BOX 11512	PITTSBURGH	PA	15238
FLEMING R H	SRI INTERNATIONAL	333 RAVENSWOOD		MENLO PARK	CA	94025
FLESCH G D	IOWA STATE UNIV	AMES LAB	USDOE	AMES	IA	50011
FLYNN YVONNE H	US EPA	CRL 10TH FLOOR	536 S CLARK ST	CHICAGO	IL	60605
FOLTZ R L	UNIV OF UTAH	CTR HUMAN TOXICOLOGY		SALT LAKE CITY	UT	84112
FORD CECIL	INDIANA UNIV	GEOLOGY DEPT	SPEA LAB, RM541	BLOOMINGTON	IN	47401
FORD H T	CONTINENTAL OIL CO	RESEARCH & DEVELOP	PO DRAW 1267	PONCA CITY	OK	74601
FOSS G O	3001 B KAISER DR			SANTA CLARA	CA	95051
FRALEY DAVID F	5407 KINGSWAY W			CINCINNATI	OH	45215
FRANKLIN J L	RICE UNIVERSITY	CHEMISTRY DEPT	PO BOX 1892	HOUSTON	TX	77005
FRASURE W	ST LOUIS UNIV	MEDICAL SCHOOL	1402 S GRAND	ST LOUIS	MO	63104
FRAZIER DARRELL E	845 W MAUDE AVE			SUNNYVALE	CA	94086
FREAS ROY B	11-2 THORN LANE			NEWARK	DE	19711
FREES LOUIS C	OAK RIDGE NAT'L LAB	4500 S, H 151	BOX X	OAK RIDGE	TN	37830
FREISER B S	PURDUE UNIVERSITY	CHEMISTRY DEPT		WEST LAFAYETTE	IN	47907
FREY CARL	459 GRANITE SPRINGS			YORKTOWN HEIGHTS	NY	10598
FRIEDMAN L	BROOKHAVEN NATL LAB	CHEMISTRY DEPT		UPTON	NY	11973

FRIESEN R D	LLL	PO BOX 808, L-230		LIVERMORE	CA	94550
FRISCH M A	IBM RESEARCH CENTER	PO BOX 218		YORKTOWN HEIGHTS	NY	10598
FU EMIL W	SANDOZ, INC	59 ROUTE 10	BLDG 404, RM 376	E. HANOVER	NJ	07936
FUHRMAN J D	MONSANTO	800 N LINDBERGH BLVD		ST LOUIS	MO	63166
FUHRHOP RALPH W	MONSANTO	800 N LINDBERGH BLVD		ST LOUIS	MO	63166
FUJII TOSHIHIRO	UNIV OF NEBRASKA			LINCOLN	NE	68588
FUJIWARA H	MONSANTO CO	800 N LINDBERGH BLVD		ST LOUIS	MO	63166
FUNKE P T	E R SQUIBB	PO BOX 4000		PRINCETON	NJ	08540
FURNISH T S	391 NEWMAN AVE			CLARKSVILLE	IN	47130
FUTRELL J H	UNIV OF UTAH	CHEMISTRY DEPT		SALT LAKE CITY	UT	84112
FREGIEN KELLY D	ST PAUL RAMSEY HOSP	640 JACKSON		ST PAUL	MN	55101
GALE P J	RCA	DAVID SARNOFF RES CT		PRINCETON	NJ	08540
GALLAHER KENNETH L	SOHIO	4440 WARRENSVILLE RD		CLEVELAND	OH	44128
GALLEGOS E J	CHEVRON	PO BOX 1627		RICHMOND	CA	94804
GARDNER RUSSELL D	CONOCO, INC	PO BOX 1267		PONCA CITY	OK	74601
GARLAND W A	HOFFMAN-LAROCHE, INC	BIOCHEMISTRY DEPT		NUTLEY	NJ	07110
GARRETT JOHN H	WRIGHT STATE UNIV	3640 COLONEL GLENN H		DAYTON	OH	45435
GARTY KENNETH T	UNION CARBIDE CORP	RIVER ROAD		BOUND BROOK	NJ	08805
GAUL MICHAEL D	1119 ROOSEVELT			AMES	IA	50010
GEELHAAR L	UNIV OF MARYLAND	636 W LOMBARD ST		BALTIMORE	MD	21201
GEIGERT J	CETUS CORP	600 BANCROFT WAY		BERKELEY	CA	94710
GELIJKENS C F	UNIV OF UTAH	MEDICINAL CHEM DEPT		SALT LAKE CITY	UT	84112
GELLENE G	CORNELL UNIV	BAKER LAB, BOX 168		ITHACA	NY	14853
GENTRY W R	UNIV OF MINNESOTA	CHEMISTRY DEPT		MINNEAPOLIS	MN	55455
GHADERI SAHBA	NICOLET INST CO	5225 VERONA RD		MADISON	WI	53711
GIBLIN D E	4526 PRESCOTT			LINCOLN	NE	68506
GIBSON B	MIT	CHEMISTRY DEPT		CAMBRIDGE	MA	02138
GILBERT L	CVC PRODUCTS	525 LEE RD		ROCHESTER	NY	14603
GILLES P W	UNIV OF KANSAS	CHEMISTRY DEPT		LAWRENCE	KS	66045
GILMAN J P	UNIV OF NEBRASKA	CHEMISTRY DEPT		LINCOLN	NE	68588
GINGERICH K A	TEXAS A&M UNIVERSITY	CHEMISTRY DEPT		COLLEGE STATION	TX	77843
GIORDANI ANNE B	2480 BOWEN ROAD			HOWELL	MI	48843
GIRDAUKAS G G	UNIV OF WISCONSIN	PHARMACY DEPT		MADISON	WI	53706
GLISH G L	OAK RIDGE NATIONAL L	PO BOX Y	BLDG 9735	OAK RIDGE	TN	37830
GOLDICH S S	US GEOLOG SURVEY	ISOTOPE GEOLOGY	FEDERAL CTR	DENVER	CO	80225
GOODLEY PAUL C	HEWLETT PACKARD	SCI INST DIV	1601 CALIFORNIA AVE	PALO ALTO	CA	94304
GOODLOE G W	AVON PRODUCTS INC	DIVISION ST		SUFFERN	NY	10901
GORETSAS GWEN D	STATE LAB OF HYGIENE	465 HENRY MALL		MADISON	WI	53706
GORMAN L A	VARIAN	134 JUNEDALE DR		CINCINNATI	OH	45218
GRADE H	GENERAL ELECTRIC CO	R&D CENTER	BLDG K-1, PO BOX 8	SCHENECTADY	NY	12301
GRADE M M	GENERAL ELECTRIC	R&D CENTER	BLDG K-1, PO BOX 8	SCHENECTADY	NY	12301
GRANLUND K	HEWLETT-PACKARD	1601 CALIFORNIA AVE		PALO ALTO	CA	94022
GRAVES P W	LAKE RD			BROOKFIELD	MA	01506
GRAYSON M A	427 GLENMEADOW DR			BALLWIN	MO	63011
GREEN L A	MOBIL RESEARCH & DEV			PAULSBORO	NJ	08066
GREEN M M	CHEMISTRY DEPT	POLYTECHNIC INST	OF NEW YORK	BROOKLYN	NY	11201
GREENE F T	MIDWEST RESRCH INST	425 VOLKER BLVD		KANSAS CITY	MO	64110
GREENHOUSE S H	21 OAK TERRACE	APT IA		SOMERVILLE	NJ	08876
GREENWOOD G J	PHILLIPS PETROLEUM	224 RESEARCH, BLDG 1		BARTLESVILLE	OK	74003
GREGG H R	MICHIGAN STATE UNIV	CHEMISTRY DEPT		EAST LANSING	MI	48824
GRIFF STANLEY P	DART N KRAFT IND, INW	115 CENTURY RD		PARAMUS	NJ	07652
GRIFFIN D A	OREGON STATE UNIV	AGRICULTURAL CHEM		CORVALLIS	OR	97331
GRIGSBY RONALD D	DEPT OF ENERGY	PO BOX 1398		BARTLESVILLE	OK	74003
GRIMSRUD E P	MONTANA STATE UNIV	CHEMISTRY DEPT		BOZEMAN	MT	59715
GRINDSTAFF Q G	BARTLESVILLE ENERGY	TECHNOLOGY CENTER	BOX 1398, DOE	BARTLESVILLE	OK	74003

GRITTER ROY J	40 W BROKAW RD			SAN JOSE	CA	95110
GROENEWOLD G S	UNIV OF NEBRASKA	720 HAMILTON HALL		LINCOLN	NE	68588
GROSS M L	UNIV OF NEBRASKA	CHEMISTRY DEPT		LINCOLN	NE	68588
GRUENKE L D	UNIV OF CALIFORNIA	PHARMCEUTICAL CHEM	926S	SAN FRANCISCO	CA	94143
GRUVER ROBERT M	PENN STATE UNIV	BORLAND BLDG		UNIVERSITY PARK	PA	16802
GUIDOBONI RICHARD J	NORTHERN ANAL LAB	7 TOPSFIELD DR		NASHUA	NH	03062
GUTHRIE J W	SANDIA NATIONAL LAB	ORG 1551	PO BOX 5800	ALBUQUERQUE	NM	87185
HADDON W F	USDA	WESTERN REG LAB		ALBANY	CA	94710
HAGEMAN LYNN R	MON ST DEPT OF AG	MC CII HALL	MONTANA STATE UNIV	BOZEMAN	MT	59717
HALE R J	TENNESSEE EASTMAN CO	B-150		KINGSPORT	TN	37662
HAMMING MYNARD C	CONOCO INC			PONCA CITY	OK	74601
HAMPTON C V	38017 MEADOWHILL DR			NORTHVILLE	MI	48167
HANSEN G E	JOHNS HOPKINS UNIV	PHARMACOLOGY DEPT	725 N WOLFE ST	BALTIMORE	MD	21205
HANSON ROY L	708 LANDMAN PLACE NE			ALBUQUERQUE	NM	87123
HARDIN E D	DEPT OF CHEMISTRY	UNIV OF HOUSTON		HOUSTON	TX	77004
HARPER TIMOTHY W	845 S DEXTER	NO 303		DENVER	CO	80221
HARPOLD D N	GODDARD SPC FLT CTR	CODE 962		GREENBELT	MD	20771
HARRINGTON W L	RCA LABORATORIES			PRINCETON	NJ	08540
HARRISON W W	UNIV OF VIRGINIA	CHEMISTRY DEPT		CHARLOTTESVILLE	VA	22901
HARVAN D J	NIEHS	PO BOX 12233		RESEARCH TRIANGLE PK	NC	27709
HARVEY MICHAEL M	PO BOX 5323			CHARLOTTESVILLE	VA	22905
HASS J R	NIEHS	PO BOX 12233		RESEARCH TRIANGLE PK	NC	27709
HATCH F W	BOEHRINGER INGELHEIM	90 EAST RIDGE	PO BOX 368	RIDGEFIELD	CT	06877
HATTOX SUSAN E	UNIV OF COLORADO	MEDICAL SCHOOL		DENVER	CO	80220
HAYES J M	INDIANA UNIV	CHEMISTRY DEPT		BLOOMINGTON	IN	47405
HAYES TIMOTHY L	BATTELLE COLS LABS	505 KING AVE		COLUMBUS	OH	43201
HAYES TODD R	3121 UNIVERSITY AVE			MINNEAPOLIS	MN	55414
HAYS J D	CASE WESTERN RESERVE	CHEMISTRY DEPT		CLEVELAND	OH	44106
HAZLITT LONNIE G	DOW CHEMICAL TX DIV	B 1219		FREEPORT	TX	77547
HEATH EUGENE C	HARRIS LABS	624 PEACH ST		LINCOLN	NE	68501
HECK H D	CIIT	PO BOX 12137		RESEARCH TRIANGLE PK	NC	27709
HEIKES D L	FDA	1009 CHERRY		KANSAS CITY	MO	64106
HEIMARK LARRY	UNIV OF WASHINGTON	MED CHEMISTRY	BG-20	SEATTLE	WA	98195
HEIMERMANN WAYNE	HORMEL INSTITUTE	801 16TH AVE, NE		AUSTIN	MN	55912
HEIN R E	NICOLET INSTRUMENTS	5225 VERONA RD		MADISON	WI	53711
HELLER D N	JOHN HOPKINS UNIV	B-6 BIOHPYSICS DEPT	725 N WOLFE ST	BALTIMORE	MD	21205
HELLER S R	2413 LILLIAN DRIVE			SILVER SPRING	MD	20902
HELLMANN ROBERT	NLO, INC	PO BOX 39158		CINCINNATI	OH	45239
HEMBERGER PHIL	UNION CARBIDE	NUCLEAR DIV	X-12 PLANT BLDG 9995	OAK RIDGE	TN	37830
HENDERSON T R	5609 DON FELIPE CT S			ALBUQUERQUE	NM	87105
HENION J D	CORNELL UNIVERSITY	NYS COL VET MEDICINE	132 DIAGNOSTIC LAB	ITHACA	NY	14853
HENIS NEIL B	UNIV OF MINNESOTA	CHEMISTRY DEPT		MINNEAPOLIS	MN	55455
HENKEL PAUL R	GALILEO ELECTRO OPT	GALILEO PARK		STURBRIDGE	MA	01518
HEPPNER R A	LARAMIE ENERGY TECH	UNIVERSITY STATION	PO BOX 3395	LARAMIE	WY	82071
HER G R	MICH STATE UNIV	CHEMISTRY DEPT	PO BOX 178	EAST LANSING	MI	48824
HEROLD D A	UNIV OF VIRGINIA	PATHOLOGY DEPT	MEDICAL CENTER	CHARLOTTESVILLE	VA	22901
HERON E J	HP SCIENTIFIC INSTR	1601 CALIFORNIA AVE		PALO ALTO	CA	94304
HERRIN C B	1702 QUEENS			PONCA CITY	OK	74601
HERTZ H S	NBS	A113 CHEMISTRY		WASHINGTON	DC	20234
HERZOG L F	NUCLIDE CORP	642 E COLLEGE AVE		STATE COLLEGE	PA	16801
HESS W B	E I DUPONT	SAVANNAH RIVER LAB	BLDG 232-H	AIKEN	SC	29801
HIDY B J	BATTELLE LABS	505 KING AVE		COLUMBUS	OH	43201
HIERL P M	UNIV OF KANSAS	CHEMISTRY DEPT		LAWRENCE	KS	66044
HIGNITE C E	VETERANS ADMIN HOSP	4801 LINWOOD BLVD		KANSAS CITY	MO	64128
HILDENBRAND D L	SRI INTERNATIONAL			MENLO PARK	CA	94025

HILKER D R	HIGHLAND HILLS	APT 2601		EAST GREENBUSH	NY	12061
HILPERT L R	NBS	BLDG 222, RM B124		WASHINGTON	DC	20234
HITES R A	INDIANA UNIV	400 E SEVENTH ST		BLOOMINGTON	IN	47405
HOAD LYAL	1301 CONSTITUTION AV			WASHINGTON	DC	20222
HOFF JOHN J	US TOBACCO	PO BOX 22029		NASHVILLE	TN	37202
HOFFBAUER MARK A	UNIV OF MINNESOTA	CHEMISTRY DEPT	207 PLEASANT ST, SE	MINNEAPOLIS	MN	55455
HOFFMAN H T	AMERICAN CAN CO	PO BOX 50		PRINCETON	NJ	08540
HOFFMAN M K	USDA-FSQS			BELTSVILLE	MD	20705
HOLKEBOER D H	231 WINDCREST DR			CAMILLUS	NY	13031
HOLLAND J F	MICHIGAN STATE UNIV	BIOCHEMISTRY DEPT		EAST LANSING	MI	48824
HOLLER J S	CENTER DISEASE CNTRL	TOXICOLOGY BRANCH		ATLANTA	GA	30333
HONOVICH J P	CASE WESTERN RESERVE	CHEMISTRY DEPT	MILLIS SCIENCE CENTR	CLEVELAND	OH	44106
HOPPESCH J P	BORG-WARNER RESEARCH	WOLF & ALGONQUIN RDS		DES PLAINES	IL	60018
HOUR ROBERT S	IOWA STATE UNIV	CHEMISTRY DEPT		AMES	IA	50011
HRIBAR J D	G D SEARLE & CO	PO BOX 5110		CHICAGO	IL	60680
HSIEH TACHENG	VELSICAL CHEM CORP	ANAL RESEARCH	341 E OHIO ST	CHICAGO	IL	60611
HSU C S	EXXON R/E	P O BOX 121		LINDEN	NJ	07036
HUANG S	MICH STATE UNIV	CHEMISTRY DEPT	BOX 184	EAST LANSING	MI	48824
HUANG W Y	SUNMARK EXPLORATION	600 N CENTRAL EXPWAY		RICHARDSON	TX	75080
HUDSON C E	MARINE BIOMEDICAL	200 UNIVERSITY BLVD		GALVESTON	TX	77550
HUDSON J E	UNIV OF TEXAS	CHEMISTRY DEPT	103W WELCH HALL	AUSTIN	TX	78712
HUNG H L	CHEMISTRY DEPT	NORTHWESTERN UNIV	2145 SHERIDAN RD	EVANSTON	IL	60201
HUNT D F	UNIV OF VIRGINIA	CHEMISTRY DEPT		CHARLOTTESVILLE	VA	22901
HUNTRESS W T	JET PROPULSION LAB	SSD		PASADENA	CA	91103
HURST H E	UNIV OF LOUISVILLE	PHARMACOLOGY DEPT		LOUISVILLE	KY	40292
HYDE PAUL M	LSUMC	BIOCHEMISTRY DEPT	1542 TULANE AVE	NEW ORLEANS	LA	70112
HYDE W G	IOWA STATE UNIV	VET DIAG LAB		AMES	IA	50011
IDEN CHARLES R	SUNY-STONY BROOK	PHARMACOLOGY DEPT		STONY BROOK	NY	11794
ILLIES ANDREAS J	UC-SANTA BARBARA	CHEMISTRY DEPT		SANTA BARBARA	CA	93105
INSALACO S E	PO BOX 551			FINDLAY	OH	45840
IRVING PHILIP	BALZERS	8 SAGAMORE PARK RD		HUDSON	NH	03051
ISRAEL S C	UNIV OF LOWELL	CHEMISTRY DEPT		LOWELL	MA	01854
ISSACHAR D	MICHIGAN STATE UNIV	BIOCHEMISTRY DEPT		EAST LANSING	MI	48824
JACKSON T J	1614 RICHFOREST			RICHARDSON	TX	75081
JACOBS M L	COMMERICAL TESTING	AND ENGINEERING	490 ORCHARD ST	GOLDEN	CO	80401
JARDINE I	MAYO CLINIC	PHARMACOLOGY DEPT		ROCHESTER	MN	55901
JARROLD MARTIN F	UNIV OF CALIFORNIA	CHEMISTRY DEPT		SANTA BARBARA	CA	93106
JELUS-TYROR B L	LABS & RESEARCH	TOXICOLOGY INSTITUTE	NY DEPT OF HEALTH	PLAZA TOWER BLDG	NY	12201
JENKINS E E	1617 MAPLE AVE			SALT LAKE CITY	UT	84106
JENKINS RAND G	6180 TERRACE DR			POLLOCK PINES	CA	95726
JENSEN T E	INDIANA UNIV	SPEA	541 GEOLOGY BLDG	BLOOMINGTON	IN	47405
JENSON FRED	662 ARBOR VALLEY			CAMPBELL HALL	NY	10916
JEROLAMON D	ALLIED CHEMICAL CORP	PO BOX 1021-R		MORRISTOWN	NJ	07960
JEROME B A	2326 KNAPP			AMES	IA	50010
JOHNSON KENNETH L	1027 S. LAKE AVE			DULUTH	MN	55802
JOHNSON P E	HUMAN NUTRITION LAB	BOX 7166 UNIV STATN		GRAND FORKS	ND	58202
JOHNSON R L	5933 FARMGATE RD			RALEIGH	NC	27606
JONES G G	STANDARD OIL INDIANA	PO BOX 400		NAPERVILLE	IL	60540
JONES LOUIS A	NORTH CAROLINA ST UN	CHEMISTRY DEPT		RALEIGH	NC	27650
JUDSON CHARLES M	UNIV OF KANSAS	CHEMISTRY DEPT		LAWRENCE	KS	66044
JUNGCLAUS G A	281 PRINCE OF WALES			GAHANNA	OH	43230
JUNK G A	IOWA STATE UNIV	AMES LAB	USDOE	AMES	IA	50011
JURUSIK J J	RD NO 6			AMSTERDAM	NY	12010
KAGAN MORTON R	IBM INSTRUMENTS INC	ORCHARD PARK	PO BOX 332	DANBURY	CT	06810
KAIER R J	E I DUPONT	EXPERIMENTAL STATION	BLDG 336/6	WILMINGTON	DE	19898

KALBRON J J	MCNEIL LABORATORIES	RD 3	ACORN DRIVE	VINCENTOWN	NJ	08088
KALEY R G	MONSANTO	800 N LINDBERGH		ST LOUIS	MO	63141
KALLOS GEORGE J	DOW CHEMICAL CO	BLDG 574		MIDLAND	MI	48640
KALMBACH K A	260 ELKTON RD, G 2			NEWARK	DE	19711
KANANEN G E	HEWLETT PACKARD CO	ROUTE 41		AVONDALE	PA	19311
KEARNS G L	58 BUCKINGHAM DR			STAMFORD	CT	06902
KEEFE R	UNIV OF VIRGINIA	CHEMISTRY DEPT	MCCORMICK RD	CHARLOTTESVILLE	VA	22901
KELLEY J A	NIH	NCI, DRUG DESIGN	BLDG 37, RM 6D23	BETHESDA	MD	20205
KELLEY PAUL E	FINNIGAN CORP	845 W MAUDE AVE		SUNNYVALE	CA	94086
KELLY WILLIAM R	NATL BUR OF STANDARDS	BLDG 222, A355		WASHINGTON	DC	20234
KELNER LEONID	12274 GREENLEAF AVE			POTOMAC	MD	20854
KEMP D L	1813 RIDGE ROAD			MARTINSVILLE	NJ	08836
KENNISH J M	UNIV OF ALASKA	CHEMISTRY DEPT	3221 PROVIDENCE DR	ANCHORAGE	AK	99504
KENYON C N	HP SCIENTIFIC INSTR	1601 CALIFORNIA AVE		PALO ALTO	CA	94304
KEOUGH T W	8557 CAVALIER DR			CINCINNATI	OH	45231
KERFOOT E G	13483 W OREGON CT			LAKEWOOD	CO	80228
KIMBLE B J	UNIV OF CALIFORNIA	LEHR		DAVIS	CA	95616
KING J D	DFC	MS977	PO BOX 25046	DENVER	CO	80225
KING J W	3850 GAVOTA AVE			SAN JOSE	CA	95124
KING R W	UNIV OF FLORIDA	CHEMISTRY DEPT		GAINESVILLE	FL	32611
KINGSTON H M	NATL BUR OF STANDARDS	BLDG 222	CHEMISTRY	WASHINGTON	DC	20234
KINOSHITA T	UNIV OF UTAH	DEPT OF MED CHEM	COLL OF PHARMACY	SALT LAKE CITY	UT	84112
KINSER R D	PHILIP MORRIS USA	RESEARCH CENTER	PO BOX 26583	RICHMOND	VA	23261
KINSINGER J A	RALTECH SCIENTIFIC	SERVICES	PO BOX 7545	MADISON	WI	53707
KIRK M C	SOUTHERN RES INST	K-MEYER LAB	2000 NINTH AVE SOUTH	BIRMINGHAM	AL	35205
KISER R W	781 GLENDOVER ROAD			LEXINGTON	KY	40502
KITSON F G	3 HARTFORD PLACE			NEWARK	DE	19711
KLEINSCHMIDT P D	LOS ALAMOS NATL LAB	MS 730, CMB-5		LOS ALAMOS	NM	87545
KNAPP D R	MED UNIV SO CAROLINA	PHARMACOLOGY DEPT		CHARLESTON	SC	29403
KNIGHTON W B	MONTANA STATE UNIV	CHEMISTRY DEPT		BOZEMAN	MT	59717
KNOWLES MICHAEL H	FINNIGAN MAT	845 W MAUDE	PO BOX 459	SUNNYVALE	CA	94086
KNOX J M	1011 FETTERMAN			LARAMIE	WY	82070
KNUDSEN T P	FINNIGAN CORP	845 W MAUDE AVE		SUNNYVALE	CA	94086
KOHL F J	NASA LEWIS RES CTR	MS 106-1		CLEVELAND	OH	44135
KOLOR M G	GENERAL FOODS CORP	555 SO BROADWAY		TARRYTOWN	NY	10591
KORNEL ALFRED	UNIV OF CINCINNATI	CHEMISTRY DEPT		CINCINNATI	OH	45221
KREEK MARY J	ROCKEFELLER UNIV	1230 YORK AVE		NEW YORK	NY	10021
KRICK T	UNIV OF MINNESOTA	BIOCHEMISTRY DEPT		ST PAUL	MN	55108
KRISHNAMURTHY T	JTC ENVIRONMENTAL	CONSULTANTS, INC	7979 OLD GEORGETOWN	BETHESDA	MD	20014
KUEHL D W	6201 CONDON BLVD			DULUTH	MN	55804
KURZWEG LUTZ	EXTRANUCLEAR LAB	100 BETA DR	PO BOX 11512	PITTSBURGH	PA	15238
KUYKENDALL PHIL A	FINNIGAN MAT	666 INDUSTRIAL DR		ELMHURST	IL	60126
LABELLE GILLES	KOR ISOTOPES	56 ROGERS		CAMBRIDGE	MA	02142
LAGERGREN C R	2110 HOWELL AVE			RICHLAND	WA	99352
LAINE R A	UNIV OF KENTUCKY	BIOCHEMISTRY DEPT	MEDICAL SCHOOL	LEXINGTON	KY	40506
LAMOUREUX CAROLE J	METAB & RAD RES LAB	STATE UNIV STATION		FARGO	ND	58105
LAMPARSKI L	2754 K-BAR-L DR			MIDLAND	MI	48640
LAMPE F W	PENN STATE UNIV	150 DAVEY LAB		UNIVERSITY PARK	PA	16802
LANE DOROTHY C	ATHENS ENVIR RES LAB	ANAL CHEMISTRY	COLLEGE STATION RD	ATHENS	GA	30613
LANG RUSSELL F	9430 NW 20 STREET			PEMBROKE PINES	FL	33024
LAPP RICK	UNIV OF NEBRASKA	16 HAMILTON HALL		LINCOLN	NE	68580
LATTIMER R P	B F GOODRICH R & D	9921 BRECKSVILLE RD		BRECKSVILLE	OH	44141
LATVEN R K	MICHIGAN STATE UNIV	CHEMISTRY DEPT		EAST LANSING	MI	48824
LAWRENCE D L	10826 WEST RD			HARRISON	OH	45030
LAWRENCE J L	ANALOG TECHNOLOGY	15859 E EDNA PLACE		IRWINDALE	CA	91706

LAY J O	1431 D STREET	APT 9		LINCOLN	NE	68502
LEGEL MARGARET A	US-DOE	NEW BRUNSWICK LAB	BLDG 350	ARGONNE	IL	60439
LEHMAN T A	PO BOX 435			NORTH NEWTON	KS	67117
LEHOTSKY R B	PERKIN-ELMER CORP	AEROSPACE DIVISION	PO BOX 2801	POMONA	CA	91766
LEICH DOUGLAS A	LAWRENCE LIVERMORE	NPO BOX 808		LIVERMORE	CA	94550
LEIKER T J	UNIV OF COLORADO	MEDICAL CENTER	4200 E 9TH AVE	DENVER	CO	80220
LEONARD EDWARD N	ERL-D	6201 CONGDON BLVD		DULUTH	MN	55804
LETT RICHARD G	PETC-DOE	ANALYTICAL CHEM DIV	PO BOX 10940	PITTSBURGH	PA	15236
LEV N B	CASE WESTERN RESERVE	CHEMISTRY DEPT		CLEVELAND	OH	44106
LEVINE F	VANDERBILT UNIV	PHARMACOLOGY DEPT		NASHVILLE	TN	37232
LEWIS DAVID A	NORTHEASTERN UNIV	360 HUNTINGTON AVE		BOSTON	MA	02115
LEWIS S G	UNIV OF CALIFORNIA	SPACE SCIENCES LAB		BERKELEY	CA	94720
LEWIS W T	MOBIL CHEMICAL CO	PO BOX 240		EDISON	NJ	08817
LIAS S G	NBS			WASHINGTON	DC	20234
LIN D C	BATTELLE LABS	505 KING AVE		COLUMBUS	OH	43201
LIN K C	UTI	325 N MATHILDA AVE		SUNNYVALE	CA	94086
LIN S N	UNIV OF TEXAS HSC	ANALYTICAL CHEMISTRY	PO BOX 20708	HOUSTON	TX	77030
LINEBERGER W C	UNIV OF COLORADO	JILA BOX 440		BOULDER	CO	80309
LIPPSTREU D L	UNIV OF NEBRASKA	CHEMISTRY DEPT		LINCOLN	NE	68588
LITRENTI JIM	VOP, INC	TEN VOP PLAZA		DES PLAINES	IL	60016
LITTLE DAVID	KRATOS			RESTON	VA	22091
LITTON J F	OCC RESEARCH	PO BOX 19601		IRVINE	CA	92713
LIU NORMAN W	SEARLE RES LAB	PO BOX 5110		CHICAGO	IL	60680
LLOYD J R	1230 YORK AVE	BOX 253		NEW YORK	NY	10021
LO H H	EXTRANUCLEAR LABS,	PO BOX 11512		PITTSBURGH	PA	15238
LOMBARSKI MICHAEL	MICH STATE UNIV	CHEMISTRY DEPT		EAST LANSING	MI	48824
LOPEZ-AVILA V	MIDWEST RESRCH INST	425 VOLKER BLVD		KANSAS CITY	MO	64110
LOUGHRAN EDWARD D	LOS ALAMOS NAT'L LAB	PO BOX 1663	MS 920	LOS ALAMOS	NM	87545
LOVING T J	UNIV OF VIRGINIA	CHEMISTRY DEPT		CHARLOTTESVILLE	VA	22901
LYON PHILIP A	CAPSULE LABS	840 SIBLEY MEM HWY		ST PAUL	MN	55118
LYTLE LESLIE T	3843 HILLTOP DR			GIBSONIA	PA	15044
MACDONALD J L	RALSTON PURINA CO	3RS CHECKERBOARD SQ		ST LOUIS	MO	63188
MACH M H	AEROSPACE CORP	PO BOX 92957		LOS ANGELES	CA	90009
MACKELLAR FORREST A	WARNER LAMBERT	PHARM RES DIV	2800 PLYMOUTH RD	ANN ARBOR	MI	48105
MADDEN ROBERT J	UNIV OF LOUISVILLE	PHARMACOLOGY DEPT		LOUISVILLE	KY	40292
MAGEE C W	RCA LABORATORIES			PRINCETON	NJ	08540
MAGIN DON E	PHILIP MORRIS RES CT	BOX 26583		RICHMOND	VA	23261
MALIK J M	MONSANTO	U2G	800 N LINDBERGH	ST LOUIS	MO	63141
MANNION J J	DIAMOND SHAMROCK RES	PO BOX 348		PAINESVILLE	OH	44077
MARASCO JOSEPH M	H-11 UNIVERSITY	GARDENS APTS		CHARLOTTESVILLE	VA	22901
MARCONI M A	3219 W 54TH ST			CHICAGO	IL	60632
MARCUS ALVIN B	6 BAYARD ROAD	APT 859		PITTSBURGH	PA	15213
MARCUS MARK	STAUFFER CHEMICAL	400 FARMINGTON AVE		FARMINGTON	CT	06032
MARKEY SANFORD P	NIH	NIMH	BLDG 10 - 3N322	BETHESDA	MD	20205
MARKS MATTHEW L	5205 MESA RD			MONONA	WI	53716
MARRIOTT T D	RICE UNIVERSITY	CHEMISTRY DEPT		HOUSTON	TX	77005
MARSH PHILIP G	UNION CARBIDE CORP	CEN. SCIENTIFIC LAB		TARYYTOWN	NY	10591
MARSHALL D J	PO BOX 315			ACTON	MA	01720
MARTIN S A	MIT	BLDG 56-035	77 MASSACHUSETTS AVE	CAMBRIDGE	MA	02139
MARTINSEN DAVID	302 SOPHIA COURT			BALTIMORE	MD	21208
MARUSHIA P C	ACC	ANALYTICAL DIV	550 2ND ST	IDAHO FALLS	ID	83401
MASUCCI JOHN A	UNIV OF VIRGINIA	CHEMISTRY DEPT		CHARLOTTESVILLE	VA	22901
MATHEWS W R	773 EUDORA			DENVER	CO	80220
MATTHEWS D E	WASHINGTON UNIV	METABOLIC DIV	SCHOOL OF MEDICINE	ST LOUIS	MO	63110
MAULDIN R K	CELANESE	PO BOX 32414		CHARLOTTE	NC	28232

MAYER W J	5803 SONOMA ROAD			BETHESDA	MD	20034
MCADAMS DON R	EXXON	BOX 2226		BATON ROUGE	LA	70821
MCADOO D J	62 LE BRUN COURT W			GALVESTON	TX	77551
MCCAMAN M W	CITY OF HOPE MED CTR			DUARTE	CA	91010
MCCARRICK T A	313 WILLOW AVE			ITHACA	NY	14850
MCCARTHY E R	ALLIED CHEMICAL CORP	PO BOX 1021-R		MORRISTOWN	NJ	07950
MCCLOSKEY J A	UNIV OF UTAH	COLLEGE OF PHARMACY	MEDICINAL CHEM DEPT	SALT LAKE CITY	UT	84112
MCCLURE C R	FINNIGAN CORP	845 W MAUDE AVE		SUNNYVALE	CA	94086
MCCLUSKY G A	FREDERICK CANCER	RES CTR, BLDG 538	PO BOX B	FREDERICK	MD	21701
MCCLUSKEY RICK J	CLARKSON COLLEGE	CHEMICAL ENGIN		POTSDAM	NY	13676
MCCREA J M	PO BOX 172			MONROEVILLE	PA	15146
MCCRERY D A	1201 S 24TH ST			LINCOLN	NE	68502
MCDONALD R N	KANSAS STATE UNIV	CHEMISTRY DEPT		MANHATTAN	KS	66506
MCEWEN C N	24 COACHLIGHT CT			NEW CASTLE	DE	19720
MCFARLAND MARGARET B	MICHIGAN STATE UNIV	CHEMISTRY DEPT		EAST LANSING	MI	48824
MCGUIRE J M	ATHENS ENVIRONMENTAL	RESEARCH LABORATORY	COLLEGE STATION RD	ATHENS	GA	30605
MCINTOSH D J	UNIV OF ALASKA	INST MARINE SCIENCE		FAIRBANKS	AK	99701
MCIVER R T	UNIV OF CALIFORNIA	CHEMISTRY DEPT		IRVINE	CA	92717
MCKEEN L W	E I DUPONT	3500 GRAYS FERRY AVE		PHILADELPHIA	PA	19146
MCKEOWN MICHAEL C	EXTRANUCLEAR LAB	100 BETA DR	PO BOX 11512	PITTSBURGH	PA	15238
MCLAFFERTY F W	CORNELL UNIVERSITY	CHEMISTRY DEPT	BAKER LABORATORY	ITHACA	NY	14853
MCLUCKEY S A	PURDUE UNIVERSITY	CHEMISTRY DEPT	PO BOX 600	WEST LAFAYETTE	IN	47907
MCNAUGHT RICHARD	GENERAL FOODS CORP	TECHNICAL CTR		WHITE PLAINS	NY	10625
MCREYNOLDS J H	SUNY MEDICAL SCHOOL	BIOPHYSICAL SCIENCE	118 CARY HALL	BUFFALO	NY	14214
MCVEETY B D	INDIANA UNIV	CHEMISTRY DEPT	BOX 215	BLOOMINGTON	IN	47401
MEHNERT H H	US GEOLOGICAL SURVEY	ISOTOPE GEOLOGY		DENVER	CO	80225
MEIKLEJOHN R A	3M CO	3M CENTER	CRL 201-BS	ST PAUL	MN	55144
MEISELS G G	UNIV OF NEBRASKA	CHEMISTRY DEPT	HAMILTON HALL	LINCOLN	NE	68588
MERRILL G L	24 SOUTHBURY RD			CLIFTON PARK	NY	12065
MERRITT C	FOOD SCIENCE LAB	CHEMISTRY	US ARMY NATICK LABS	NATICK	MA	01760
MESCHER-SMITH J A	UNIV OF DAYTON	RESEARCH INST		DAYTON	OH	45469
MEUZELAAR H L	BIOMAT PROFILING CTR	391 S CHIPETA WAY		SALT LAKE CITY	UT	84108
MEYER V D	GTE LIGHTING PROD	100 ENDICOTT ST		DANVERS	MA	01923
MEYERSON SEYMOUR	STANDARD OIL INDIANA	RESEARCH DEPT	PO BOX 400	NAPERVILLE	IL	60566
MIGNANO JOHN E	BOX 114	RD1		TUXEDO	NY	10987
MICKE M A	UNIV OF WISCONSIN	BIOCHEMISTRY DEPT	420 HENRY MALL	MADISON	WI	53706
MILBERG RICHARD M	UNIV OF ILLINOIS	SCH OF CHEM SCIENCES	31 NOYES LAB	URBANA	IL	61801
MILLEN W G	CYANAMID	PO BOX 400		PRINCETON	NJ	08540
MILLER DENNIS A	MICH TECH UNIV	CHEM & CHEM ENGIN		HOUGHTON	MI	49931
MILLER D J	D O E GFETC			GRAND FORKS	ND	58201
MILLER D L	UNIV OF NEBRASKA	DEPT OF CHEMISTRY		LINCOLN	NE	68588
MILNE T A	SERI	1536 COLE BLVD		GOLDEN	CO	80401
MINARD R D	PENN STATE UNIV	152 DAVEY LAB		UNIVERSITY PARK	PA	16802
MINTZ D M	FINNIGAN CORP	845 W MAUDE AVE		SUNNYVALE	CA	94086
MITCHUM RONALD K	NAT'L CTR TOXICOLOGI			JEFFERSON	AR	72079
MO S H	CORNELL UNIV	BAKER LAB		ITHACA	NY	14853
MOL G J	IBM CORP	5600 COTTLE ROAD		SAN JOSE	CA	95193
MONCUR J G	FINNIGAN CORP	2334 WALSH AVE		SANTA CLARA	CA	95050
MONSON K R	ICI AMERICAS INC	BIOMEDICAL RES LAB		WILMINGTON	DE	19897
MOORE A	MARATHON OIL CO	PO BOX 269		LITTLETON	CO	80210
MOORE J A	DOW CORNING CORP	3901 S SAGINAW RD	BOX 1592 MO 27	MIDLAND	MI	48640
MUELLER S L	ABBOTT LABS	D-417		NORTH CHICAGO	IL	60064
MUN IN K	CORNELL UNIV	BAKER LAB	BOX 231	ITHACA	NY	14853
MUNSON B	UNIV OF DELAWARE	CHEMISTRY DEPT		NEWARK	DE	19711
MURAD E	AFGL-LKD			HANSCOM AFB	MA	01731

MURAKAMI AKI A	MILLER BREWING CO	3939 W HIGHLAND BLVD		MILWAUKEE	WI	53201
MURPHY R C	UNIV OF COLORADO	MEDICAL CENTER	PHARMCOLOGY DEPT	DENVER	CO	80262
MUSSELMAN BRIAN D	MICH STATE UNIV	BIOCHEMISTRY DEPT	MASS SPEC FACIL	EAST LANSING	MI	48824
MYERHOLTZ CARL A	MICHIGAN STATE UNIV	CHEMISTRY DEPT		EAST LANSING	MI	48824
MYERS LES C	MASON & HANGER	PO BOX 30020		AMARILLO	TX	79177
NAITO Y	JEOL CORP	235 BIRCHWOOD AVE		CRANFORD	NJ	07016
NARASIMHACHARI N	MEDICAL COL VIRGINIA	PSYCHIATRY DEPT		RICHMOND	VA	23298
NARINE DEOA J	RED BUD HILL	APT 307		BLOOMINGTON	IN	47401
NAYAR B	UNIV OF MARYLAND	MEDICINAL CHEMISTRY & PHARMACOGNOSY DEPT		BALTIMORE	MD	21201
NERO VINCENT P	TEXACO INC	BOX 509		BEACON	NY	12508
NESTRICK T	DOW CHEMICAL COMPANY	ANALYTICAL LABS	BLDG 574	MIDLAND	MI	48640
NEWTON A S	1665 THOUSAND OAKS			BERKELEY	CA	94707
NG K T	CIBA-GEIGY CORP			ARDSLEY	NY	10502
NGUYEN T L	UCSF MED CTR			SAN FRANCISCO	CA	94143
NICHOLS BILL	EASTMAN KODAK	KODAK PARK	BLDG 339	ROCHESTER	NY	14650
NIER A O	UNIV OF MINNESOTA	PHYSICS/ASTRONOMY		MINNEAPOLIS	MN	55455
NIKORA J A	B F GOODRICH CENTER	CHEMISTRY DIVISION	PO BOX 122	AVON LAKE	OH	44012
NISHIOKA MARCIA G	BATTELLE COLUMBUS LAB	RM 6306	505 KING AVE	COLUMBUS	OH	43201
NJUGUNA H	44 CENTER GROVE RD	D 33		RANDOLPH	NJ	07869
NOEL D L	INTERNATIONAL PAPER	CORPORATE RESEARCH	PO BOX 797	TUXEDO PARK	NY	10987
NORMAN E J	1044 SUNWOOD CT			CINCINNATI	OH	45231
NORWOOD DANIEL L	UNIV OF NORTH CAROLI	ENVIRON SCI ENG DEPT	SCH OF PUB HEALTH	CHAPEL HILL	NC	27514
NYSTROM J A	UNIV NORTH CAROLINA	CHEMISTRY DEPT		CHAPEL HILL	NC	27514
OCCOLOWITZ J L	ELI LILLY RES LABS			INDIANAPOLIS	IN	46285
O'CONNELL V P	TEKNIVENT CORP	10774 TRENTON AVE		ST LOUIS	MO	63132
ODOM R W	4331 PEMBROKE DR			CONCORD	CA	94521
ODONNELL A D	9216 S HOYNE AVE			CHICAGO	IL	60620
OHASHI M	FDA	DDC HFD-420	501 FIRST ST, SE	WASHINGTON	DC	20204
OLDHAM JAMES H	COMMERCIAL TESTING	490 ORCHARD ST		GOLDEN	CO	80401
OLDHAM R G	RADIAN CORP	PO BOX 9948		AUSTIN	TX	78766
OLIVARES J A	163-E UNIVERSITY VIL			AMES	IA	50010
OLSON EDWIN S	GRAND FORKS ENER TEC			GRAND FORKS	ND	58202
OLSON K L	13747 ADAMS DR			WARREN	MI	48093
O'MALLEY REBECCA M	UNIV OF S FLORIDA	CHEMISTRY DEPT		TAMPA	FL	33620
ORR DENNIS J	FINNIGAN MAT	2334 G WALSH AVE		SANTA CLARA	CA	95050
ORTH R G	2630 STRINGHAM AVE	APT 310		SALT LAKE CITY	UT	84109
OTTO CHARLES H	LLNL	Z-310	BOX 808	LIVERMORE	CA	94550
OXBORROW GORDON S	US FDA	240 HENNEPIN AVE		MINNEAPOLIS	MN	55401
PAGE R P	A/R CO	400 E SIBLEY BLVD		HARVEY	IL	60426
PAREES D M	AIR PRODUCTS & CHEM	PO BOX 538		ALLENTOWN	PA	18105
PARKER C E	PO BOX 232	ROUTE 3		APEX	NC	27502
PARR A C	NBS	BLDG 221, RM A251		WASHINGTON	DC	20234
PARSONS N H	GENERAL ELECTRIC CO	PO BOX 11508	N D DEPT	ST PETERSBURG	FL	33733
PATTERSON D G	CENTER DISEASE CNTRL	TOXICOLOGY BRANCH	BLDG 31, ROOM 8	ATLANTA	GA	30333
PATTON JERRY R	PCR, INC	PO BOX 1466		GAINESVILLE	FL	32607
PAUL THOMAS D	SUNY AT BUFFALO	BIOPHYSICAL SCIENCE	132 CARY HALL	BUFFALO	NY	14214
PAULSEN P J	NBS	BLDG 221, RM A25		WASHINGTON	DC	20234
PAULSON JOSEPH F	12 MILES RD			CLAYMONT	DE	19703
PEARCE D S	HEWLETT PACKARD CO	1601 CALIFORNIA AVE		PALO ALTO	CA	94304
PEELE G L	VACUMETRICS INC	2261-#1 PALMA DR		VENTURA	CA	93003
PENA H E	215 RIO VISTA DR			ST CHARLES	MO	63301
PERRIN R E	LOS ALAMOS SCIEN LAB	MS 514		LOS ALAMOS	NM	87544
PETERMAN P H	WISC LAB HYGIENE	465 HENRY MALL		MADISON	WI	53706
PETTERSON ROGER C	FOREST PROD LAB	PO BOX 5130		MADISON	WI	53705
PFOST R B	P P G INDUSTRIES	PO BOX 31		BARBERTON	OH	44203

PHINNEY M J	139 LAUREL VALLEY DR	COLUMBIA LAKES			WEST COLUMBIA	TX	77486
PINKSTON J D	MICH STATE UNIV	CHEMISTRY DEPT	BOX250		EAST LANSING	MI	48824
PIRONE A J	10 KENLEIGH CT				WILMINGTON	DE	19808
PLASHKO BRUCE E	A E STALEY CO	3200 ELDORADO			DECATUR	IL	62525
PLATTNER R D	NOR REGIONAL LAB	1815 N UNIVERSITY ST			PEORIA	IL	61604
POEPPEL M O	3 HOLLYHOCK WAY				MERCERVILLE	NJ	08619
POON B T	WALTER REED ARMY	INST OF RESEARCH	EXPTL THERAPEUTICS		WASHINGTON	DC	20012
PORTER R F	CORNELL UNIVERSITY	CHEMISTRY DEPT			ITHACA	NY	14853
POWELL LURA P	NBS	BLDG 221, RM A21			WASHINGTON	DC	20234
POWELL MARK L	SCHERING-PLOUGH	DRUG METAB. & PHARMO			BLOOMFIELD	NJ	07003
PRAMANIK B N	SCHERING CORP	60 ORANGE ST			BLOOMFIELD	NJ	07003
PRESCOTT CHARLES L	4305 FLAGSTAFF CIRCL				AUSTIN	TX	78759
PRICE P C	UNION CARBIDE	TECHNICAL CENTER	PO BOX 8361		SOUTH CHARLESTON	WV	25303
RADECKI BARBARA D	MICH STATE UNIV	CHEMISTRY DEPT	BOX252		EAST LANSING	MI	48824
RADOLOVICH G R	7300 BELLEVIEW				KANSAS CITY	MO	64114
RADUS T P	BROOKHAVEN NATL LAB				UPTON	NY	11973
RAMJIT H G	MERCK INSTITUTE OF	THERAPEUTIC RESEARCH	DEPT 805		WEST POINT	PA	19486
RAPP LARRY A	ARCO, HTC	400 E SIBLEY BLVD			HARVEY	IL	60426
RAYFORD WARREN E	1815 N UNIVERSITY				PEORIA	IL	61604
RECHSTEINER C E	2906 STEARNS HILL RD				WALTHAM	MA	02154
REENTS W D	425 HAWTHORNE AVE				MIDDLESEX	NJ	08846
REINHOLD V N	HARVARD MEDICAL SCH	LHRRB	45 SHATTUCK ST		BOSTON	MA	02115
REISER R W	E I DUPONT	EXPERIMENTAL STATION	B10CHEM, BLDG 324		WILMINGTON	DE	19898
REMLING DON K	7622 S JOHNSON ST				LITTLETON	CO	80127
RENNEKAMP M E	ASHLAND OIL INC	MS LAB	PO BOX 2458		COLUMBUS	OH	43216
REYNOLDS T P	PO BOX 314				BETHEL	CT	06801
RHODES GERALD R	UNIV OF VIRGINIA	CHEMISTRY DEPT			CHARLOTTESVILLE	VA	22901
RICHARDSON JOHN	PHILLIPS PETROLEUM	152 PL PRC			BARTLESVILLE	OK	74004
RIDGE D P	UNIV OF DELAWARE	CHEMISTRY DEPT			NEWARK	DE	19711
RILEY JIM L	SCI RESEARCH LAB	S3061	BOX 2053		DEARBORN	MI	48121
RINEHART K L	UNIV OF ILLINOIS	454 ROGER ADAMS LAB			URBANA	IL	61801
RING R D	1609 BIDDLE AVE				WYANDOTTE	MI	48192
RINGES GEOFFREY	BEAM DYNAMICS, INC	708 E 56 STREET			MINNEAPOLIS	MN	55417
RIZZO D J	GENERAL FOODS CORP	555 SO BROADWAY			TARRYTOWN	NY	10591
ROACH J A	FDA	HFF-459	200 C ST SW		WASHINGTON	DC	20204
ROBBINS EUGENE F	UNIV OF IL MED CTR	RESEARCH RESOURCES C	1940 W TAYLOR ST		CHICAGO	IL	60612
ROBERTS G D	691 CRESSMAN RD				HARLEYVILLE	PA	19438
ROBERTSON GARY L	UNIV OF IOWA	HYGIENIC LAB			IOWA CITY	IA	52242
ROBOZ JOHN	MT SINAI SCH OF MED	1 GUSTAVE LEVY PL			NEW YORK	NY	10029
ROKOP DONALD J	LAWL				LOS ALAMOS	NM	87545
ROSA SUSAN D	METRO WATER QUALITY	TPPS LAB	410 W HARRISON		SEATTLE	WA	98119
ROSECRANCE A E	SAI	1200 PROSPECT			LA JOLLA	CA	92037
ROSEN R T	FMC CORP	PO BOX 8			PRINCETON	NJ	08540
ROSENBLATT G M	PENN STATE UNIV	CHEMISTRY DEPT	152 DAVEY LAB		UNIVERSITY PARK	PA	16802
ROSENSTOCK H M	NBS	RADIATION PHYSICS DV	NATL BUR STANDARDS		WASHINGTON	DC	20234
ROTHBERG J L	RALSTON PURINA CO	3RS CHECKERBOARD SQ			ST LOUIS	MO	63188
ROTTSCHAEFER S	1195 HART LANE				HARTSVILLE	PA	18974
ROY TIM	98 W BROAD ST				HOPEWELL	NJ	08525
RUDAT M A	DUPONT	RES & DEV	EXP STATION 228-101		WILMINGTON	DE	19898
RUSSELL D H	TEXAS A&M UNIV	CHEMISTRY DEPT			COLLEGE STATION	TX	77843
RUSSELL JOHN W	MEAD COMPUCHEM	PO BOX 12652			RES TRI PARK	NC	27709
RYAN P W	COLORADO STATE UNIV	CHEMISTRY DEPT			FORT COLLINS	CO	80523
RYBA R J	STANDARD OIL INDIANA	PO BOX 400			NAPERVILLE	IL	60566
SAAD F M	MICHIGAN PUB HEALTH	3500 N LOGAN ST			LANSING	MI	48909
SAADY JOSEPH J	MED COLLEGE OF VA	MCV STATION BOX 597			RICHMOND	VA	23298

SAALFELD F F	NRL	CODE 6100		WASHINGTON	DC	20375
SAMSON P C	112 E BARRETT LANE			SCHAUMBURG	IL	60193
SANDERS R A	1900 WILTSHIRE BLVD			FAIRFIELD	OH	45014
SATOH PAUL	UPJOHN CO	301 HENRIETTA ST		KALAMAZOO	MI	49001
SAVICKAS P J	UNIV OF VIRGINIA	CHEMISTRY DEPT		CHARLOTTESVILLE	VA	22901
SCAMUFFA M D	HEWLETT-PACKARD	5201 TOLLVIEW DR		ROLLING MEADOWS	IL	60008
SCANLAN GALE F	MAYO CLINIC	734 GUGG		ROCHESTER	MN	55901
SCANLON M D	SUNY	BIOPHYSICS DEPT		BUFFALO	NY	14214
SCHEEL R H	MICH PUBLIC HEALTH	ENVIRON EPIDEMIOLOGY	PO BOX 30035	LANSING	MI	48909
SCHELLING F J	UNIV OF COLORADO	CHEMISTRY DEPT	BOX 215	BOULDER	CO	80309
SCHEPPELE S E	BARTLESVILLE ENERGY	TECHNOLOGY CENTER	PO BOX 1398, DOE	BARTLESVILLE	OK	74003
SCHKUTA A	MIT	BLDG 56-022	77 MASSACHUSETTS AVE	CAMBRIDGE	MA	02139
SCHNUTE W C	FINNIGAN CORP	845 W MAUDE AVE		SUNNYVALE	CA	94086
SCHOELLER D A	UNIV OF CHICAGO	BH-BOX 243		CHICAGO	IL	60637
SCHOEN A E	PURDUE UNIVERSITY	CHEMISTRY DEPT	PO BOX 737	WEST LAFAYETTE	IN	47907
SCHOENGOLD D M	2305 EASTON			RICHLAND	WA	99352
SCHRAM K H	UNIV OF ARIZONA	COLLEGE OF PHARMACY		TUCSON	AZ	85721
SCHROEPFER JOSEPH N	3M	3M CENTER	BLDG 201-1W	ST PAUL	MN	55144
SCHRONK LEONARD R	CITIES SERVICE TECH	PO BOX 3908		TULSA	OK	74102
SCHUETTE G E	PHILLIPS PETROLEUM	PHILLIPS RES	CL-T	BARTLESVILLE	OK	74004
SETHI S K	UNIV OF UTAH	MEDICINAL CHEM DEPT	331 SKAGGS HAL	SALT LAKE CITY	UT	84112
SETTINE R L	UNIV OF ALABAMA	GCMS CENTER		BIRMINGHAM	AL	35294
SHABANOWITZ J	UNIV OF VIRGINIA	CHEMISTRY DEPT		CHARLOTTESVILLE	VA	22901
SHADOFF L A	DOW CHEMICAL CO	574 BLDG		MIDLAND	MI	48640
SHOUP RONALD	BIOANALYTICAL SYSTEM	1205 KENT AVE		W LAFAYETTE	IN	47906
SHARP T E	LOCKHEED RES LAB	3251 HANOVER	D52-35 B204	PALO ALTO	CA	94304
SHAW C J	12 RUTGERS DRIVE			DELRAN	NJ	08075
SHEARER P W	HERCULES INC	RESEARCH CENTER		WILMINGTON	DE	19899
SHERMAN W R	WASHINGTON UNIV	PSYCHIATRY DEPT	SCHOOL OF MEDICINE	ST LOUIS	MO	63110
SHERRILL N D	US GEOL SURVEY	MS-18	345 MIDDLEFIELD RD	MENLO PARK	CA	94025
SHUM Y Y	WARNER LAMBERT	/PARKE DAVIS	2800 PLYMOUTH RD	ANN ARBOR	MI	48105
SIDES G D	1732 TAHITI LANE			ALABASTER	AL	35007
SIEGEL M M	39 - 24 GRANT ST	F		FAIRLAWN	NJ	07410
SIEGEL MELVIN W	EXTRANUCLEAR LAB	100 BETA DR	PO BOX 11512	PITTSBURGH	PA	15238
SIGSBY M L	1400 HIGHLAND DRIVE	APT 705		ST ALBANS	WV	25177
SILVERMAN R W	UNIV OF CALIFORNIA	PHARMACOLOGY DEPT	CENTER HEALTH SCIENC	LOS ANGELES	CA	90024
SISAK M E	UNIV OF VIRGINIA	CHEMISTRY DEPT		CHARLOTTESVILLE	VA	22901
SIZEMORE EVERETTE H	161 W CLIFF ST			SOMERVILLE	NJ	08874
SKOOG EDWARD W	GENERAL ELECTRIC	VALLECITOS RD		PLEASANTON	CA	94596
SKOTNICKI PEGGY A	HOOKER CHEM CO	PO BOX 8		NIAGARA FALLS	NY	14302
SLEPUKHOF HOLLY R	10304 MEDALLION DR			SAN ANTONIO	TX	78245
SLIVON L E	BATTELLE LABS	505 KING AVE		COLUMBUS	OH	43201
SMITH DANNE E	44 CENTER GROVE RD	APT T 12		DOVER	NJ	07801
SMITH DAVID E	960 JUNESONG WAY			SAN JOSE	CA	95133
SMITH D H	ORNL, UNION CARBIDE	PO BOX Y, BLDG 9735		OAK RIDGE	TN	37830
SMITH D J	ROUTE 1	PO BOX 12194		RESEARCH TRIANGLE PK	NC	27709
SMITH D L	UNIV OF UTAH	311 SKAGGS HALL		SALT LAKE CITY	UT	84112
SMITH JACK L	MERCK & CO	PO BOX 2000		RAHWAY	NJ	07065
SMITH J S	ALLIED CHEMICAL CORP	PO BOX 1021-R		MORRISTOWN	NJ	07960
SMITH LARELL K	1155TH TCHOS MCLP			MCCLELLAN AFB	CA	95652
SMITH R D	BATTELLE-NW	BLDG 329, AREA 300		RICHLAND	WA	99352
SNELLING C R	UNIV OF ILLINOIS	PO BOX 101	RAL	URBANA	IL	61801
SNIATECKI J J	NUCLEAR FUEL SERVICE			ERWIN	TN	37650
SOKOLOW STEVE	1901 VALPARAISO			MENLO PARK	CA	94025
SOLCH J G	4967 TANNER DRIVE			DAYTON	OH	45424

SOLKA B H	7813 W ROSEDALE			CHICAGO	IL	60631
SOLOMON J J	NEW YORK UNIV	ENVIRON MEDICINE	MEDICAL CENTER	TUXEDO PARK	NY	10987
SOLSTEN R T	130 1/2 N SANTA RITA			TUCSON	AZ	85719
SOLTYS MICHAEL N	SERI	1617 COLE BLVD		GOLDEN	CO	80401
SPARKMAN O D	1657 LUIKA PLACE			CAMPBELL	CA	95008
SPENCER R B	5121 FLAMBEAU RD			MADISON	WI	53705
SPHON J A	FDA	HFF-459	200 C ST SW	WASHINGTON	DC	20204
SPINDT C A	SRI INTERNATIONAL	333 RAVENSWOOD AVE		MENLO PARK	CA	94025
SPRATLEY A W	UNION CARBIDE	PO BOX 50		HAHNVILLE	LA	70057
SPREEN R C	UNIV OF DELAWARE	BROWN LABORATORY		NEWARK	DE	19711
SQUIRES ROBERT R	UNIV OF COLORADO	CHEMISTRY DEPT	CAMPUS BOX 215	BOULDER	CO	80309
STACEY J S	749 GILPIN ST			DENVER	CO	80218
STAFFORD G C	1463 ILIKAI AVE			SAN JOSE	CA	95118
STALEY R H	MIT	CHEMISTRY, 6-128A		CAMBRIDGE	MA	02139
STAUFFER DOUGLAS B	CORNELL UNIV	BAKER LAB	BOX 68	ITHACA	NY	14853
STAUFFER J L	ARTHUR D LITTLE INC	ACORN PARK		CAMBRIDGE	MA	02140
STEBBINGS W L	3M COMPANY	PO BOX 33221		ST PAUL	MN	55133
STEINHAUS JIM F	325 N MATHILDA AVE			SUNNYVALE	CA	94086
STOGNIEW M	UNIV OF MARYLAND	MEDICINAL CHEM &	PHARMACOGNOSY	BALTIMORE	MD	21201
STORK JOSEPH R	FINNIGAN INSTITUTE	11 TRIANGLE PK DR		CINCINNATI	OH	45246
STORY M S	15745 WOODACRES RD			LOS GATOS	CA	95030
STOUT S J	AMERICAN CYANIMID	AGRICULTURAL DIV	PO BOX 400	PRINCETON	NJ	08540
STRONG J M	13103 BLUHILL RD			SILVER SPRINGS	MD	20906
STULTS JOHN T	MICH STATE UNIV	CHEMISTRY DEPT		EAST LANSING	MI	48824
STURM G P	BARTLESVILLE ENERGY	TECHNOLOGY CENTER	PO BOX 1398, DOE	BARTLESVILLE	OK	74003
STYRIS DAVID L	205 CRAIGHILL			RICHLAND	WA	99352
SUGNAUX F R	STANFORD UNIV	CHEMISTRY DEPT	MASS SPEC LAB	PALO ALTO	CA	94305
SULFRIDGE C	158 WADDELL CIRCLE			OAK RIDGE	TN	37830
SVEC H J	IOWA STATE UNIV	CHEMISTRY DEPT		AMES	IA	50011
SWANSON A R	UNIV OF MINNESOTA	PHARMACOLOGY DEPT	435 DELAWARE ST SE	MINNEAPOLIS	MN	55455
SWEELEY C C	MICHIGAN STATE UNIV	BIOCHEMISTRY DEPT		EAST LANSING	MI	48824
SWEETMAN B J	VANDERBILT UNIV	PHARMACOLOGY DEPT		NASHVILLE	TN	37232
SWIJTER D J	327 N. 8TH ST			ALLENTOWN	PA	18102
SWIMS J C	RALSTON PURINA CO	900 CHECKERBOARD SQ		ST LOUIS	MO	63188
SZYBIST J	NUCLIDE CORP	642 E COLLEGE AVE		STATE COLLEGE	PA	16801
TALLEY C R	E I DUPONT	EXPERIMENTAL STATION	PETRO CHEM, BLDG 336	WILMINGTON	DE	19898
TAN Y L	DOE	ENVIRON MEAS LAB	376 HUDSON ST	NEW YORK	NY	10014
TANAKA CALVIN	RADIAN CORP	3401 LA GRANDE BLVD		SACRAMENTO	CA	95823
TANNER D P	12664 MARKAIRE			ST LOUIS	MO	63141
TAYLOR A R	CONOCO INC	1000 SOUTH PINE		PONCA CITY	OK	74601
TAYLOR M L	WRIGHT STATE UNIV	CHEMISTRY DEPT	BREHM LAB	DAYTON	OH	45431
TAYLOR P A	2503 BUENO DR			DAVIS	CA	95616
TAYLOR PHILIP L	NIH	BLDG 10, RM 315	9000 ROCKVILLE PK	BETHESDA	MD	20205
TECON P	3064 SCOTT BLVD			SANTA CLARA	CA	95050
TEMPLETON J L	UNIV OF FLORIDA	PESTICIDE RES LAB		GAINESVILLE	FL	32611
TERWILLIGER D T	29 CHETWYND RD			PAOLI	PA	19301
THOMAS D W	SRI INTERNATIONAL	333 RAVENSWOOD AVE	B-011	MENLO PARK	CA	94025
THOMPSON R M	BATTELLE LABS	505 KING AVE		COLUMBUS	OH	43201
THOMSON M L	AMERICAN CYANIMID	AGRICULTURAL DIV	PO BOX 400	PRINCETON	NJ	08540
THORP J R	3111 WINDMILL			SUGAR LAND	TX	77478
TIERNAN T O	WRIGHT STATE UNIV	BREHM LAB		DAYTON	OH	45431
TINDALL G W	TENNESSEE EASTMAN CO	BLDG 54		KINGSPORT	TN	37662
TOKES L	SYNTEX RESEARCH	3401 HILLVIEW AVE	STANFORD INDUST PARK	PALO ALTO	CA	94304
TOMER K B	RES TRIANGLE INST	PO BOX 12194	CLSD	RESEARCH TRIANGLE PK	NC	27709
TONDEUR Y	NIEHS	PO BOX 12233		RESEARCH TRIANGLE PK	NC	27709

TONG S L	UNIV OF VIRGINIA	CHEMISTRY DEPT		CHARLOTTESVILLE	VA	22901
TOU J C	DOW CHEMICAL CO	ANALYTICAL LAB	B-574	MIDLAND	MI	48640
TRAN V T	PO BOX 109			CEREDO	WV	25507
TREWELLA J J	MOBIL R&D CORP			PAULSBORO	NJ	08066
TSAI B P	UNIV OF MINNESOTA	CHEMISTRY DEPT		DULUTH	MN	55812
TSERNG K Y	17006 BEAVER CIRCLE			STRONGSVILLE	OH	44136
TURBETT JERRY R	1278 VAN DYCK DR			SUNNYVALE	CA	94087
TWAY P C	MERCK SHARP & DOHME	RESEARCH LABORATORY	PO BOX 2000	RAHWAY	NJ	07065
TYROR G	25 WEST MEADOW DR			ALBANY	NY	12203
TYSON B J	HEWLETT PACKARD	1003 SCOTT BLVD		SANTA CLARA	CA	95050
UDSETH H R	UNIV OF OF UTAH	CHEMISTRY DEPT	PO BOX 43	SALT LAKE CITY	UT	84112
ULBRICHT W H	NEW BRUNSWICK LAB	DEPT OF ENERGY, D3509800	S CASS AVE	ARGONNE	IL	60439
ULLMAN ALAN H	PROCTOR & GAMBLE	11530 REED HARTMAN H		CINCINNATI	OH	45241
UNDERWOOD DENNIS	ROCKEFELLER UNIV	1230 YORK AVE		NEW YORK	NY	10021
UNGER S E	150 ARNOLD DR	APT #4		WEST LAFAYETTE	IN	47906
UPHAM R A	UNIV OF MINNESOTA	CHEMISTRY DEPT		MINNEAPOLIS	MN	55455
VALLON PAUL P	ESTEE LAUDER INC	210 MARCUS BLVD		HAUPPAUGE	NY	11787
VANDERBORGH NICK E	LOS ALAMOS NATL LAB	GEOSCIENCE DIV	MS 570	LOS ALAMOS	NM	87545
VANDER HAAR ROY W	STANDARD OIL INDIANA	PO BOX 400		NAPERVILLE	IL	60566
VANDER VELDE G	1109 IRONWOOD DR			FINDLAY	OH	45840
VANE F M	HOFFMANN-LAROCHE, INC			NUTLEY	NJ	07110
VAN NESS G F	1983 REDSTONE DR			FAIRBORN	OH	45324
VERMA SUNITA	PURDUE UNIV	CHEMISTRY DEPT		W LAFAYETTE	IN	47906
VESTAL M L	UNIV OF HOUSTON	CHEMISTRY DEPT	4800 CALHOUN	HOUSTON	TX	77004
VESTLING M M	SUNY	CHEMISTRY DEPT		BROCKPORT	NY	14420
VEYSEY STEVE W	IOWA STATE UNIV	85 A GILMAN HALL		AMES	IA	50011
VOUROS P	NORTHEASTERN UNIV	INST CHEMICAL ANAL		BOSTON	MA	02115
VOYKSNER R D	203-A BRANSON ST			CHAPEL HILL	NC	27514
VRBANAC JIM J	MICHIGAN STATE UNIV	BIOCHEMISTRY DEPT		EAST LANSING	MI	48824
VU V T	JOHNS HOPKINS UNIV	PHARMACOLOGY DEPT	725 N WOLFE ST	BALTIMORE	MD	21205
WADSWORTH P A	SHELL DEVELOPMENT CO	WESTHOLLOW RESEARCH	PO BOX 1380	HOUSTON	TX	77001
WAHRHAFTIG A L	UNIV OF UTAH	CHEMISTRY DEPT		SALT LAKE CITY	UT	84112
WALKER R W	MERCK SHARP & DOHME	RESEARCH LABORATORY	PO BOX 2000	RAHWAY	NJ	07065
WALLER G R	OKLAHOMA STATE UNIV	BIOCHEMISTRY DEPT		STILLWATER	OK	74074
WALLS F C	UNIV OF CALIFORNIA	SPACE SCIENCES LAB		BERKELEY	CA	94720
WALSH B C	WESTINGHOUSE	BETTIS LAB	PO BOX 79	WEST MIFFLIN	PA	15122
WALTON J R	ORNL, UNION CARBIDE	PO BOX Y, BLDG 9735		OAK RIDGE	TN	37830
WANG JULIE C	WWTP	CITY OF NIAG FALLS		NIAGARA FALLS	NY	14302
WANG J S	93 SHADOW RIDGE RD			STAMFORD	CT	06905
WANG S I	ABBOTT LABS	DEPT 417		NORTH CHICAGO	IL	60064
WARREN J L	FRITO LAY, INC	900 N LOOP 12	DOCK R	IRVING	TX	75061
WARREN P L	FINNIGAN CORP	845 W MAUDE AVE		SUNNYVALE	CA	94086
WARREN ROBERT W	SUNTECH INC	BOX 1135		MARCUS HOOK	PA	19061
WATSON J T	DEPT BIOCHEMISTRY	MICHIGAN STATE UNIV		EAST LANSING	MI	48824
WATT J G	FINNIGAN CORP	845 W MAUDE AVE		SUNNYVALE	CA	94086
WEBB G W	770 STIMSON			IDAHO FALLS	ID	83401
WEDDLE G H	FAIRFIELD UNIV	CHEMISTRY DEPT		FAIRFIELD	CT	06430
WEGMANN A	STANFORD UNIV	CHEMISTRY DEPT	MASS SPEC LAB	PALO ALTO	CA	94305
WEIBEL L A	RALTECH SCIENTIFIC	SERVICES	PO BOX 7545	MADISON	WI	53707
WEIBLEN DON G	3M COMPANY	3M CENTER		ST PAUL	MN	55144
WEIL DAVID A	3347 15TH AVE SOUTH			MINNEAPOLIS	MN	55407
WEINKAM R J	PURDUE UNIVERSITY	MEDICINAL CHEMISTRY		WEST LAFAYETTE	IN	47907
WEINTRAUB SUSAN T	UT HEALTH SCI CTR	7703 FLOYD CURL DR		SAN ANTONIO	TX	78284
WEISS M	124 FOXWOOD			PORTOLA VALLEY	CA	94025
WELCH K J	SC JOHNSON & SON, INC	ANAL R&D STA #56	1525 HOWE ST	RACINE	WI	53403

WELCH MICHAEL J	NAT'L BUR OF STANDARD	RM A-113,BLDG 222		WASHINGTON	DC	20234
WERNESS STEVE	UNIV OF MICHIGAN	CHEMISTRY DEPT	930 N UNIVERSITY	ANN ARBOR	MI	48104
WESTMORELAND D G	ROHM & HAAS CO			SPRING HOUSE	PA	19477
WESTON A F	HOOKER CHEMICALS	GRAND ISLAND COMPLEX	LONG ROAD	GRAND ISLAND	NY	14072
WHITE E	NBS	A113 CHEMISTRY		WASHINGTON	DC	20234
WHITE E L	PO BOX 12137			RES TRI PARK	NC	27709
WHITE F A	RENSSELAER POLY INST	NUCLEAR ENG DEPT		TROY	NY	12181
WHITE JAMES M	HENKEL CORP	2010 E HAMPTON AVE		MINNEAPOLIS	MN	55413
WHITE R H	VIRGINIA POLYTECH	BIOCHEMISTRY DEPT		BLACKSBURG	VA	24061
WHITE ROBERT L	UNIV OF CALIFORNIA	CHEMISTRY DEPT		RIVERSIDE	CA	92506
WHITNEY J O	131 TERESITA BLVD			SAN FRANCISCO	CA	94127
WHITTAKER N F	NIH	BLDG 4, RM B2-37		BETHESDA	MD	20205
WHITTAKER STEVE	MEAD JOHNSON & CO	2404 PENNSYLVANIA AV		EVANSVILLE	IN	47721
WILKES B E	UNION CARBIDE	PO BOX 8361	BLDG 770-318	SOUTH CHARLESTON	WV	25303
WILKES P S	FDA	60 EIGHTH ST NE		ATLANTA	GA	30309
WILKINS C L	UNIV OF NEBRASKA	CHEMISTRY DEPT		LINCOLN	NE	68588
WILKINSON JOANN E	SYSTEM SCI & SOFTWARE	PO BOX 1620		SAN DIEGO	CA	92038
WILLIAMS C M	UNIV OF FLORIDA	RADIOLOGY DEPT	JHMHC	GAINESVILLE	FL	32611
WILLIAMS P	UNIV OF ILLINOIS	MATERIALS RES LAB		URBANA	IL	61801
WILLIAMS R M	RESEARCH CORP	405 LEXINGTON AVE		NEW YORK	NY	10174
WILSON B W	BATTELLE-NW	BLDG 329, AREA 300		RICHLAND	WA	99352
WINMILL D L	HERCULES INC	RESEARCH CENTER		WILMINGTON	DE	19899
WISHNOK JOHN S	MIT	56-315		CAMBRIDGE	MA	02139
WITTSTRUCK T A	NUCLIDE CORP	AGV DIV	916 MAIN ST	ACTON	MA	01720
WNUK RICHARD J	UPJOHN CO	7255-209-017	301 HENRIETTA ST	KALAMAZOO	MI	49007
WOBSCHALL D C	STATE UNIV OF NY	4232 RIDGE LEA		AMHERST	NY	14221
WOLFE MARTA H	MASS GENERAL HOSP	MASS SPEC LAB	51 BLOSSOM ST	BOSTON	MA	02114
WOLSTENHOLME W A	13840 W OAK GLEN RD			VALLEY CENTER	CA	92082
WONG CURT A	GENERAL MOTORS RES LDEPT 22		12 MILE & MOUND RDS	WARREN	MI	48090
WONG C M	LLL	PO BOX 808, L-325		LIVERMORE	CA	94550
WONG DANIEL	UNIROYAL CHEM CO	ELM ST	BLDG 81	NAUGATUCK	CT	06770
WONG L K	UNIV OF PITTSBURGH	SCHOOL OF PHARMACY	721 SALK HALL	PITTSBURGH	PA	15261
WONG WILLIAM W	BAYLOR COLL OF MEDICINE	MED TOWERS BLDG RM 56	608 FANNIN ST	HOUSTON	TX	77030
WONG WINSTON	BAYLOR COLL OF MED	6608 FANNIN	NO 519	HOUSTON	TX	77030
WOOD D	19 HILLCREST AVE			DARIEN	CT	06820
WOOD G M	2 LITTLE BLUFF RD			NEWPORT NEWS	VA	23606
WOOD KARL V	PURDUE UNIV	FUELS ANAL LAB	CHEMISTRY BLDG	WEST LAFAYETTE	IN	47907
WOOD NEVILLE	BASF WYANDOTTE	140 NEW DUTCH LN		FAIRFIELD	NJ	07869
WOODS J W	8 RICHARDS RD			LYNNFIELD	MA	01940
WOZNIAK T J	INDIANA UNIV	CHEMISTRY DEPT		BLOOMINGTON	IN	47401
WRIGHT J	UNIV OF MARYLAND	SCHOOL OF PHARMACY	636 W LOMBARD ST	BALTIMORE	MD	21201
WRONKA J	5011 GARFIELD AVE			PENNSAUKEN	NJ	08109
WU R L	WRIGHT STATE UNIV	BREHM LABORATORY		DAYTON	OH	45431
WYATT J R	NRL	CODE 6110		WASHINGTON	DC	20375
YAMADA S	UNIV OF TENN	STOUT LAB	800 MADISON AVE	MEMPHIS	TN	38163
YELTON R O	116 WALDEN FARM CIR			UNION	OH	45322
YERGEY ALFRED L	NIH	BLDG 6, RM 136		BETHESDA	MD	20205
YOST R A	UNIV OF FLORIDA	CHEMISTRY DEPT		GAINESVILLE	FL	32611
YOUNG G W	R J REYNOLDS TOBACCO	RESEARCH DEPT		WINSTON-SALEM	NC	27102
YOUNGLESS TIM L	GULF RES & DEV	PO DRAWER 2138		PITTSBURGH	PA	15230
YOUSSEFI M	UNION CARBIDE	ONE RIVER RD		BOUND BROOK	NJ	08854
YU C T	UNIV OF UTAH	MEDICINAL CHEM		SALT LAKE CITY	UT	84112
YU CHI	AFWAL-MLU-ACG	WPAFB		DAYTON	OH	45433
YU K O	AFAMRL-THT			WRIGHT PATT AFB	OH	45433
ZABIELSKI SR M	UNITED TECH RES CTR	SILVER LANE		EAST HARTFORD	CT	06108

ZACCHEI A G	MERCK SHARP & DOHME	RESEARCH LABORATORY		WEST POINT	PA	19486
ZADIG MICHAEL S	RDS-NERMAG	1020 CORPORATION WAY		PALO ALTO	CA	94303
ZAKETT D	PURDUE UNIVERSITY	CHEMISTRY DEPT	POX 835	WEST LAFAYETTE	IN	47907
ZARE RICHARD N	STANFORD UNIV	CHEMISTRY DEPT		STANFORD	CA	94305
ZIRROLLI J A	AFESC/RDVC			TYNDALL AFB	FL	32403
ZUBYK R M	19 ATTERBURY DR			MALVERN	PA	19355
ZUMBERGE J E	CITIES SERVICE CO	PO BOX 3908	4500 S 129 E AVE	TULSA	OK	74102

NOTES